Surgical Research in Implant Dentistry

Michel M. Dard

Editor

Springer

Surgical Research in Implant Dentistry

Michel M. Dard

Editor

Surgical Research in Implant Dentistry

Editor
Michel M. Dard
New York, USA

Foreword

Endosseous dental implants have revolutionized the practice of dentistry in the last 40 years. No other development, technology, or material has had such an effect on the dental profession in our lifetime. Such a sea change in a health profession requires extensive scrutiny and massive scientific investigation. The concept that a foreign body could integrate with the tissues of the oral cavity and establish a functional equilibrium was unthinkable just a few decades ago. This is particularly true given the dynamic complexities in the oral cavity such as the microbial challenges, the immune responses, multiple tissue interaction and turnover, the flow of salvia and all of its components, and the functional needs of food and liquid intake, chewing, speaking, and swallowing. Given this situation, it is remarkable that endosseous dental implants today are a routine dental procedure with very high success rates both in the placement and maintenance of the implant itself, as well as of the prosthesis fabrication and usage. This remarkable success story has occurred through extensive scientific investigation that has accompanied the use of dental implants at first mainly in edentulous patients but then evolved with developments into partially edentulous patients. This fascinating story has now enhanced and influenced millions of lives daily and has evolved because of serious and comprehensive scientific investigations. This outstanding book has managed to bring together incredible information that exhaustively and very comprehensively explains how the science of dental implantology has supported the translational application of this remarkable treatment for our patients. It covers scientific research over the entire spectrum of dental implantology from various in vitro and animal models for investigation to translational studies for clinical success.

The editor nicely sets the tone for the book by suggesting that dental implant researchers are "knowledge explorers" and that their mission as surgical researchers is the "generation of knowledge, transmitting it, and adding clinical value." The book then begins with insights into various animal model systems and the advantages and disadvantages of the many species of animals that researchers have used to evaluate tissue interactions with the implanted foreign body. The structural, functional, and compositional components of various animal species offer a wide array of tissue reaction for the evaluation of the implant. For example, some animal models offer osseous tissue comprised of mainly cortical bone and little cancellous bone while other models offer a more balanced composition of cortical and cancellous bone tissue for evaluation. The authors of these chapters have complied in this one resource

an incredibly comprehensive documentation when one is deciding what animal model might be applicable for further scientific investigation.

These chapters exhaustively describe preclinical study designs in a number of animal models including rodents, rabbits, swine, canine, ovine, and caprine animals. These are well-written chapters that describe advantages and limitations of each model, the particular locations that have been typically utilized for implant studies, systemic conditions possible in the species, how outcomes can be evaluated, and furthermore describe some major studies that have utilized the model in the literature. I believe these chapters are one of the only places that one can turn to in order to have all the information you might need to learn about all the possible animal models to use for implant research and have the information needed to evaluate how the models can best be utilized.

The next series of chapters comprehensively explain how animal preclinical research is translated into clinical investigations in implant dentistry. This information again exhaustively covers a broad range of topics in an extremely comprehensive fashion and defines and describes the components of different kinds of studies that are usually performed in implant dentistry. Levels of evidence are explained and standard guidelines for the reporting of results and quality control practices are also included. A plea is also made for standardization for data collection and evaluation methods including data from private practice to reflect what goes on in the so-called real world.

These chapters are followed with extensive discussions on other crucial aspects of implant dentistry research including biomechanics and testing in vitro and then in vivo for various materials including finite element analyses; a really excellent, comprehensive, and up-to-date review of the biological events that take place at the interface of the implant and bone including five phases of osseointegration, and material influences and surface characteristics of the implant and their significance on implant integration. Also included are comprehensive chapters on radiographic imaging, the mechanics of the implant-abutment connection, and prosthetic rehabilitation and the factors relevant for the prosthesis to be successful in the long term.

Implant dentistry often involves the use of various bone graft materials. Each of these materials has advantages and disadvantages so a thorough understanding of bone grafts is essential and is included in the book. Several chapters discuss bone substitute materials including non-resorbable and resorbable grafts as well as the biology of low substitution bone materials, calcium-phosphate, and polymer-based bone substitutes. An emphasis is also placed on the various techniques for imaging these materials and evaluating their effectiveness as a bone promoting material, the host tissue reaction to the material, and the degradation of the bone substitute. The use of membranes and soft tissue grafting goes hand in hand with bone grafting, and these materials are additionally covered.

Three additional chapters are included in the book that round out current research in implant dentistry. These include how biomarkers have been examined to monitor tissue health around the implant including the use of saliva and peri-implant crevicular fluid composition. A second chapter provides a comprehensive examination of the state-of-the-art use of computer-assisted

concepts and digital technologies and how these have been incorporated and influenced diagnosis, planning, and evaluation of implant therapy for patients. Exciting new digital technologies like photogrammetry are explained; CAD/CAM use and static and dynamic guidance for implant placement are also explored and discussed. Lastly, a chapter is included on hypothesis testing, sample size determination, probability distributions, data collection, and how statistical analyses are typically performed with the incorporation of a statistician who has the mathematical and statistical knowledge to use appropriate techniques to get the most out of your experimental and clinical dental implant studies.

As you can see, this book is a unique resource in implant dentistry that is comprehensive in the field and extensive in its breath and depth in all areas of dental implant research. The contents of this book confirm that the placement of foreign bodies into the jaw bones has revolutionized dentistry as a profession. The scientific investigation of all aspects of this procedure is outlined here, and it has demonstrated the evolution of this therapy to its highly successful outcome that it enjoys today. Achieving the goal of replacing and supporting teeth with endosseous implants has required enormous scientific discovery, and this book provides an outstanding resource for appreciating and understanding the tremendous scientific advancements and evolution that have taken place in implant dentistry.

David L. Cochran
Department of Periodontics
University of Texas Health Science Center San Antonio
San Antonio, TX, USA

Contents

The Method Sets the Tone

1

Michel M. Dard

Fragments of truth constitute science

Claude Bernard

1.1 Introduction

This textbook finds its roots in the reading of some of the most knowledgeable thinkers, scientists, and philosophers in the field of methodology, and it represents a modest illustration of their remarkable reflections applied to implant dentistry, this being analyzed and reported in the most possible humble manner.

The word method appeared in the early fifteenth century from Latin "methodus" borrowed from Greek "methodos" formed by juxtaposition of "meta" (μετά) and "hodos" (ὁδός), which can literally be translated into "beyond the way."

Referring to Collins and Cambridge dictionaries, a methodology is a system or a set of methods and principles for practicing in a defined domain, by instance for operating, studying, or carrying out research. A method itself is a systematic, recognized, and established procedure within a professional community of practice.

Methodology is also the branch of philosophy dealing with the science of procedures or orderly arrangement and the branch of logic concerned with the application of the principles of reasoning to scientific and philosophical inquiry.

Methodology broadly corresponds to the fusion of an ordered approach and a philosophical quest by following the way and looking forward ("beyond the way").

Methodology is inherent to research, and a methodologist attitude implies being well-versed in the international literature and fixing collegially the goal and priorities of the study. It consists in identifying the population of interest, sampling the comprising elements before designing the study, making sure that the accuracy of data can be reached, and finally, analyzing them.

Research studies are two-dimensional. The first dimension consists in laboratory research, which provides data, outcomes, and conclusions on materials and devices with the help of physicochemical and mechanical tests, cells, tissues, and animal models. The second dimension inheres clinical research, which must be practice-

M. M. Dard (✉)
New York, USA
e-mail: mmd2190@cumc.columbia.edu

oriented and implement methods to reduce the burden of patient discomfort and, eventually, illness in the real world.

Preclinical research enjoys very high internal validity because the investigator actively decides on independent variables and randomly assigns subjects to experimental and control groups, as demonstrated further in this book. Preclinical research constitutes the first step to conscious clinical research; both being strongly linked by similar methodological approaches and an incremental knowledge acquisition towards understanding of human oral health and resolution of diseases.

In this context, the Academy of Surgical Research (Wayzata, MN, United States) defines its expertise field as examining and evaluating innovative and conventional ideas related to surgery through scholarship analysis of data and the generation and investigation of hypotheses.

This definition fully applies to dentistry, including implant dentistry which accomplished major progress during the last 50 years, signing up the evolution from a carnival attraction to an academic profession and science [1]. Implant dentistry research gained more and more attention and interest and greatly advanced the profession, consequently influencing the patients' welfare and well-being.

1.2 The Heroes

We are all building up on Aristotle (384–322 bc), who was one of the greatest philosophers who ever lived and the first genuine scientist in history. He made pioneering contributions to all fields of philosophy and science, he discovered and substantified the formal logic format, and he identified the various scientific disciplines and explored their relationships.

The process of logical deduction was invented by Aristotle (he has been called the "father of logic"), and perhaps lies at the heart of all his famous achievements in biology, political science, zoology, embryology, scientific method, rhetoric, and psychology. He was the first person to come up with an authentic and logical procedure to conclude a statement based on the propositions at hand, and he exerted a unique influence on almost every form of knowledge and knowledge acquisition in the Occident.

During his life, René Descartes (1596–1650) imbricated his talents as a mathematician, a natural scientist or "natural philosopher," and a metaphysician. He was heralded as the first modern philosopher. He offered a new vision of nature that continues to shape our thought today: a world of matter possessing a few fundamental properties and interacting according to a few universal laws. This world included an immaterial mind that, in human beings, was directly related to the brain; in this way, Descartes formulated the modern version of the mind–body interactions.

He claimed early on to have developed a special method, which can variously be applied in mathematics, natural philosophy, and metaphysics, and which, in the latter part of his life, was supplemented by a method of doubt.

Descartes presented his results in "Discours de la Méthode Pour bien conduire sa raison, et chercher la vérité dans les sciences" (1637, in English: "Discourse on the Method of Rightly Conducting One's Reason and of Seeking Truth in the Sciences"). This book is best known as the source of the famous quotation "Je pense, donc je suis" ("I think, therefore I am," or "I am thinking, therefore I exist") and remains one of the most influential works in the history of modern philosophy, and development of natural sciences.

He proposed to apply the four following precepts:

– Doubt everything.
– Break every problem into smaller parts.
– Solve the simplest problems first.
– Be thorough in the sense of making enumerations so complete and reviews so general that nothing becomes omitted.

The historian B. Cohen (Harvard University) called Claude Bernard (1813–1878) "one of the greatest of all men of science."

In his major discourse on the scientific method "Introduction à l'étude de la médecine expérimentale" (1865, in English: "An Introduction to the Study of Experimental Medecine"), C. Bernard described what makes a scientific theory good and what makes a scientist a true discoverer. C. Bernard was obsessed with ensuring the objectivity of scientific observations. He recommended to consider thoroughly the following eight quotations:

– Only the unknown is the playground for true researchers.
– Experimental methods and observable reality represent the only authority, not the dogmatic scholastic sources.
– Reasoning from the particular to the general (induction) and reasoning from the general to the particular (deduction) act synergically.
– Exploring a relation between cause and effect is founded on a hypothesis formulation. A proven hypothesis becomes a scientific theory.
– A valuable theory is one which can be verified by the most facts considering that best efforts must be made to disprove theories. Theories are never final.
– In biology, qualitative analysis must always precede quantitative analysis, although the application of mathematics to every aspect of science remains a major goal.
– Insufficient or neglected observations always correlate with questionable results.
– The "ardent desire for knowledge which is the sole torment and sole happiness" of investigators corresponds to the true scientific spirit, which shall always prevail.

Knowledge development was addressed by Jean Piaget (1896–1980) who postulated fundamental distinctions among three kinds of knowledge: social knowledge, physical knowledge, and logico-mathematical knowledge.

Piaget's theory is based on the idea that knowledge acquisition is a process of continuous self-construction shaped by interactions of the child with the surrounding world; we can assume that this process persists all along our life.

The association of physical and logico-mathematical knowledges renders the observable world understandable to us by incorporating the rules of basic logical inference in everyday activities.

The masterpiece of Donald Brunette, "Critical Thinking. Understanding and Evaluating Dental Research" [2], crystallizes decades of reflections on methodology and applies them specifically to the dental research field.

This fascinating book covers rhetoric and logic, methodology, research strategies, probability and statistics, experimental designs, scientific publications, diagnostic and clinical decision. It represents a decisive contribution to dental surgical research that everybody in the area should read and reflect upon.

It is worth mentioning the team around Hans Troidl et al. [3] and Wiley Souba and Douglas Wilmore [4] for their respective almost unbeatable classic books which brushed the broad landscape of Surgical Research in medicine.

1.3   The Endless Revolution

Producing new knowledge or identifying new ways of making existing knowledge accessible to the surgical/medical community, patients, and stakeholders is the ultimate purpose of Surgical Research. A genuine systematic approach of reasoning, documenting, analyzing, and reporting preclinical and clinical observations must occupy our daily working sphere and participate in a surgical revolution encouraging surgeons to become better researchers by intertwining surgical research and daily practice.

The word revolution covers here two different senses: a movement in a circle or curve around a central point and a far-reaching and drastic change in ideas, methods, and understanding.

The never-ending circumvolution of this Archimedean screw (Fig. 1.1) applies to the generation of knowledge and, consequently to the revolutionary research process itself.
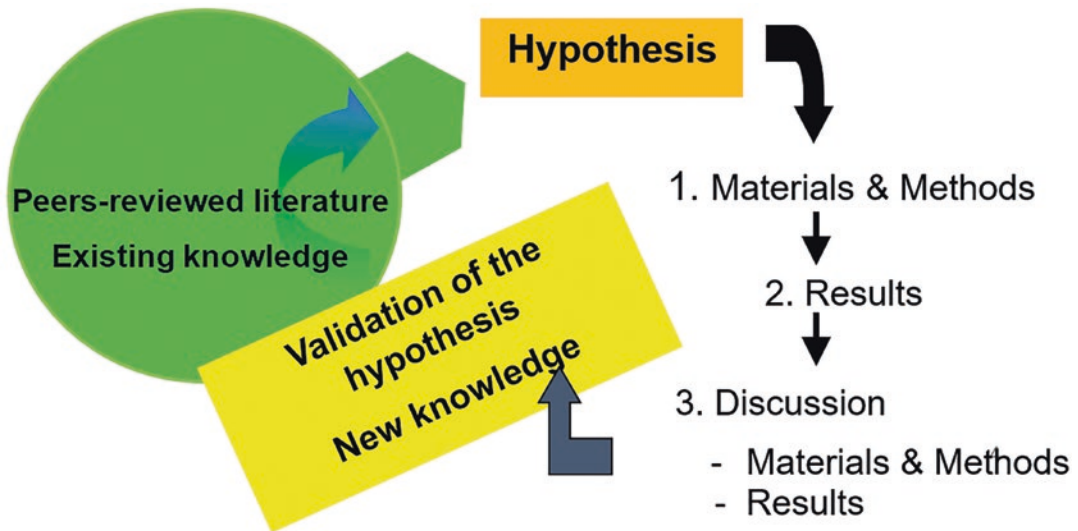
Fig. 1.1 Surgical Research Archimedean screw: the spires which shape the nonending thread

At this stage of our demonstration, two decisive elements must be outlined:

– the importance of the hypothesis and,
– the study design.

1.3.1 The Hypothesis

To guide this process, methodologists pay attention to the process of defining the population of interest, the options/interventions under consideration, the outcomes that will sustain the decision, and the settings where the options would be implemented, always prioritizing a population or system-level perspective.

But prior to choosing the study design, a valid research question which will be eventually formulated as a hypothesis, must clearly emerge.

The research question aims at focusing on one primary issue only.

A well-built research question should encounter four parts, referred to as the PICO format/framework/model, which considers Patient/Population (clinical or experimental situation), Intervention (diagnosis, treatment, procedure, and product), Comparison (alternative), and Outcomes (measurements and results).

The PICO format is used to explore the causation of disease, diagnosis of a disease or therapy, and prognosis of a particular condition.

Although developed to answer a clinical or healthcare-related question [5], it was argued that PICO might be useful for every scientific endeavor, even beyond clinical settings, if applied to interventional and experimental designs.

1.3.2 The Design

In vitro, preclinical and clinical study designs for various questions arising from dental clinical practice or knowledge are presented in the 20 following chapters of this book.

It is to be kept in mind the usefulness of a pilot phase before starting with any large study. A pilot phase can efficiently contribute to making the investigator(s) and his/her staff familiar with the work to be performed, refine the design and save time, re-evaluate, and control costs.

1.3.3 Evidence-Based Dentistry

The definition of evidence-based medicine or dentistry is victim of the occurrence which con-

sists in defining a term by using the same wording as within the term itself. Thereby it can be found written that evidence-based medicine or dentistry relates to "available evidence" or "best evidence" or "relevant evidence" or "evidence appraisal" or "sufficient evidence" or "clinical evidence" or "research evidence". This reverts to a vague or even non-understandable definition. The expression "evidence-based dentistry" deserves a much more accurate and precise definition.

Nowadays, it remains that making clinical decisions about the proper use of devices, materials, technology, and procedures in daily dental practice (clinical expertise pillar) involves the correct interpretation of scientific data (research pillar) for the benefit of the patients in a conscious and responsible way (patient value pillar).

1.4 Conclusion

Without denying the pivotal role of the research question, the main engine triggering a researcher forward is his/her research interest which covers different aspects such as passion, intellectual excitement, desire to serve a community and even human-being, own knowledge acquisition and world comprehension, corporate, or academic career development and finances.

Avenues for researchers' accomplishment in surgical research are unfolding in multiple directions like getting results published in international peer-reviewed literature, translated into patents, developed into new perspectives for surgical procedures and treatments and building the framework of training and education programs.

The above elements shall not only benefit the professionals but also influence the patients' welfare serving his/her dental and general health.

Although methodology in surgical research is not questionable one wonders why modern research is still confounded by opinion, ambiguity, and deference to experts. René Descartes, in his time, already fought against such spurious behaviors, comments, and speculations. He rejected that everything could be determined by logical analysis and sometimes speculations, without recourse to observation or experiment.

The mission of Surgical Research in Implant Dentistry consists of and will remain in generating knowledge, transmitting it, and adding clinical value.

We are and we shall remain the Knowledge Explorers.

References

1. Jansen J. Developments in dental and maxillofacial surgical research. J Invest Surg. 1995;8:327–9.
2. Brunette D. Critical thinking. Understanding and evaluating dental research. 3rd ed. Batavia: Quintessence Publishing; 2020, 406p.
3. Troidl H, McKneally M, Mulder D, Wechsler A, McPeek B, Spitzer W. Surgical research. Basic principles and clinical practice. 3rd ed. New York: Springer; 1998, 695p.
4. Souba WW, Wilmore DW. Surgical research. 1st ed. New York: Academic Press; 2001, 1460p.
5. Huang X, Lin J, Demner-Fushman D. Evaluation of PICO as a knowledge representation for clinical questions. AMIA Annu Symp Proc. 2006;2006:359–63.

Evidence-Based Dentistry Related References

Richards D, Lawrence A. Evidence based dentistry. Br Dent J. 1995;179:270.
Rubin A, Bellamy J. Practitioner's guide to using research for evidence-based practice. Hoboken: Wiley; 2012.
Sackett DL, Rosenberg WM, Gray JM, Haynes RB, Richardson WS. Evidence based medicine: what it is and what it isn't. Br Med J. 1996;1996(312):71–2.
Sadaf D. How to apply evidence-based principles in clinical dentistry. J Multidiscip Healthc. 2019;12:131–6.

Preclinical Studies Design and Place of Rodents

2

Shiwen Zhang, Weiqing Liu, and Quan Yuan

2.1 Experimental Animal Model

2.1.1 Animal Species: Naturally-Occurring, Purpose-Bread, and/or Genetically Modified

There are many species of mice or rats, such as C57BL/6 mice, CD1 mice, BALB/c mice, Sprague-Dawley (SD) rats, and Wistar rats for biomedical research. The most widely used mouse and rat strains are C57BL/6 mice and SD rats in dental implant studies. C57BL/6 mice, also called "C57 black 6," have the advantages of strain stability and easy breeding. The mouse genome has been sequenced, and many mouse genes have human homologues. The genetically modified mouse models could simulate human disease to provide new insights into the mechanism of osseointegration at the dental implant surface [1]. In addition, C57BL/6 mice are used as a background strain for generating congenic with both spontaneous and induced mutations. Sprague-Dawley rat is a hybrid albino strain with a high reproduction rate and low incidence of spontaneous tumors. Its calm temperament and easy handling are welcome features to scientists. Compared to large animals, the easy breeding and handling, as well as the genetic modification of mouse and rat make them an ideal complementary model for dental implant research.

2.1.2 General Use in Medical Devices Research

In general, rodents are more convenient for disease-associated research. Systematic disease models, such as osteoporosis, diabetes, and chronic kidney disease, have been created on mouse or rat to evaluate the implant osseointegration in compromised conditions and the treatment effect [2, 3]. In addition, the fast turnover rate of bone reconstruction and the rapid occurrence of biological processes make the small-animal model very suitable for pretesting experiments before moving to large animals or human trials. More importantly, the sequencing

S. Zhang · Q. Yuan (✉)
State Key Laboratory of Oral Diseases, National Clinical Research Center for Oral Diseases, West China Hospital of Stomatology, Sichuan University, Chengdu, China

Department of Oral Implantology, West China Hospital of Stomatology, Sichuan University, Chengdu, China
e-mail: sw.zhang2018@scu.edu.cn; yuanquan@scu.edu.cn

W. Liu
State Key Laboratory of Oral Diseases, National Clinical Research Center for Oral Diseases, West China Hospital of Stomatology, Sichuan University, Chengdu, China

Department of Prosthodontics, West China Hospital of Stomatology, Sichuan University, Chengdu, China
e-mail: weiqing_liu@scu.edu.cn

of mouse and rat genomes smoothed the progress of transgenic and knockout models, contributing to the knowledge of the function and modulation of specific genes in implant osseointegration.

2.1.3 Financial Considerations

Laboratory rodents such as mouse and rat are often used before larger animals. Because they are comparatively more cost-effective and easier to house and handle, they yield larger sample numbers and the availability of molecular and cellular biological reagents [4–6].

2.2 Surgical Model

2.2.1 Surgical Anatomical Site and Surgical Procedures for Implant Dentistry

2.2.1.1 Surgical Locations

Extraoral

Anatomy and Histology
The most often chosen location for implant insertion in mouse or rat is the anterior-distal surface of femur metaphysis and the medial-proximal surface of metaphysis in tibia, since there is more trabecular bone in these sites, which partially resembles the situation in alveolar bone [7]. Femoral condyle is selected when investigating the impact of the osteoporotic condition on bone-implant integration [8] (Fig. 2.1).

The anterior-distal flat surface of femur metaphysis instead of the midshaft or femoral condyle was chosen for several reasons. First, in view of anatomy, the cortical bone becomes thicker toward diaphysis while the diameter of the femur progressively decreases [9], therefore if we insert an implant at diaphysis, it is very likely that the implant will be supported by bicortical bones, or the implant need to be miniature. Second, the flat area of the anterior-distal surface of femur metaphysis is much larger than we

could find in the diaphysis part of the femur, thus providing sufficient bone tissue to surround the implant. Still, reduced-sized dental implants are used (2 mm in length, around 1 mm in width). Third, implant inserted into this site avoids damaging the epiphyseal growth plate, where cartilage proliferates to cause the elongation of the bone. Thus eliminates the possibility of interfering with normal femur growth, which is common when implant is placed via femoral condyle. Considering the fact that bone growth in rats continues much longer after sexual maturity than in humans [10].

Once an implant is placed, cortical bone, which is thick and dense, provides primary stability. Next, cancellous bone is actively involved during bone-implant integration by forming new bone around the implant. Bone marrow, which contains numerous blood vessels and capillaries and the multipotent progenitor cells plays an important role in implant osseointegration.

Function and Physiology (Movement, Loading)
In general, dental implants are osseointegrated to withstand loading pressure. However, the implants are not loading if inserted into extraoral sites, like femur or tibia.

Inserting implant into hindlimbs itself introduce potential complications for disabled rodents, so it is recommended to perform surgery on only one side of the hindlimbs while leaving the other side intact to ensure minimal impact on motion. However, especially in femoral condyle model, in which the implant was inserted into the knee joint, and interrupted the growth plate, thus interfering with normal movement and bone growth. Therefore, femoral condyle is not recommended for animal farewell reasons.

Unlike human, rodents have limited cortical remodeling or secondary osteon formation, but they can still model cancellous bone responses in lumbar vertebral bodies and the distal femoral and proximal tibial metaphyses [11].

Long and alveolar bones are derived from different embryonic stem cell populations. The mesoderm gives rise to the long bone, while neu-
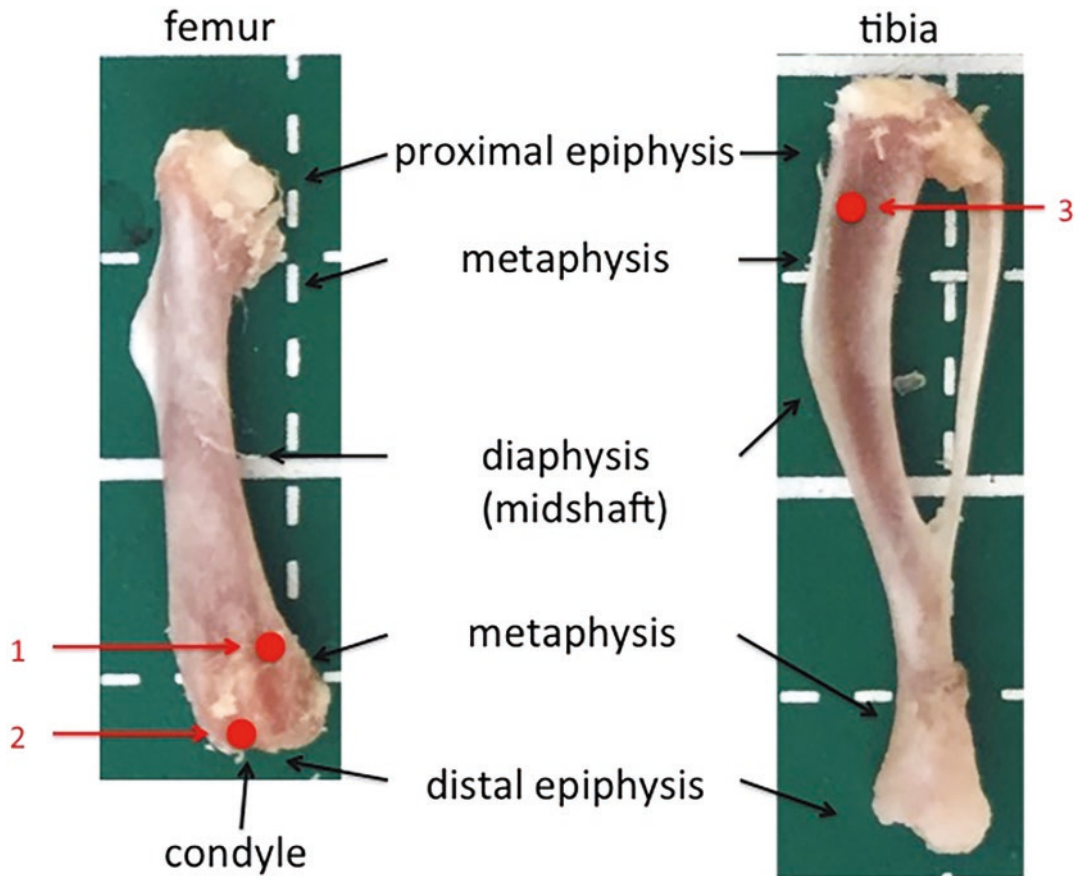
Fig. 2.1 Anatomy of the mouse femur and tibia, and three most commonly used implant insertion spots. (9-week-old C57Bl/6 mouse). The following three points, as indicated by round red dots, were usually chosen for implant insertion. (1) the anterior-distal surface of femur metaphysis; (2) femoral condyle; (3) the medial-proximal surface of tibia metaphysis

ral crest-derived skeletal progenitor cells produce the bones and cartilages of the craniofacial bones.

With regard to bone development, femur and tibia are formed by endochondral ossification, while calvaria is derived from cranial neural crest and formed by intramembranous ossification in which bone forms directly from an immature fibrous stroma.

The detailed response of the periosteum to injury coupled with implant insertion was reported by Leuchit et al. [12]. A majority of progenitor cells that resides in the cambial layer of periosteum differentiated into chondrocytes, which were then removed and replaced by bone through the program of endochondral ossification.

Advantages/Inconveniences in Implant Dentistry

The main advantage of extraoral implant sites in rodents is the easy access to operation compared to microsurgery in small oral cavities in mice or rats.

Another advantage is that long bone heals faster than analogous injuries to the craniofacial bones. The marrow space in the tibia or femur contains abundant osteoprogenitor cells, a robust blood supply, and stem cell niche signals, all of which are essential for new bone formation. The

maxillary bone, however, has little or no marrow space and presumably lacks the stem cell populations that reside in the marrow cavity. However, this advantage could also be viewed as an inconvenience at the same time when considering clinical relevance.

Possible inconveniences are that implant osseointegration in craniofacial bones is substantially different from that in long bones. For example, preosteoblasts are derived from the cranial neural crest in the maxilla peri-implant, whereas in the tibia peri-implant, osteoblasts are derived from mesoderm. In the maxilla, new osteoid arises from the periosteal of the maxillary bone, but in the femur or tibia, the new osteoid arises from the marrow space.

Another limitation is that rodents do not have a haversian system, thus disabling the mouse and rat model to simulate the Haversian remodeling process during human healing [13].

Although experimental factors, such as age, race, sex, pathogenic mechanism, and living environment, are well controlled in rodent animal models, their biological response may differ from that of humans.

Recommendations

The choice of different implant sites is mainly determined by the research question of the study.

Overall, the extraoral sites (i.e., tibia and femur) are used more often than intraoral sites, considering the small size of the oral cavity to operate, which makes the implant surgery highly technically sensitive. In addition, there is a significantly smaller bone to accommodate the implant in rodent's maxilla or mandible compared to their long bones, which, accordingly, it requires a much smaller implant, which is hard to prepare and inconvenient to handle.

Among the commonly used extraoral sites, the femur metaphysis was the most suitable location for implant placement due to its relatively larger embedded bone volume than the tibia, and it is much easier to operate than the femoral condyle. When investigating the bone-implant integration in osteoporotic bones, rat femoral condyle is suggested [14]. Since osteoporosis occurs most significantly in the trabecular bone, the femoral

condyle is rich in trabecular bone. Since osteoporosis occurs most significantly in the trabecular bone, and the femoral condyle is rich in trabecular bone. However, one should notice that surgery in this site would result in joint destruction, which compromised animal movement.

Intraoral

Anatomy and Histology

The rat maxillary alveolar bone [15], the first or second maxillary molar site [16, 17], as well as the above sites in mandible [18] were all ever been used for implant placement. At the same time, the most often used was located at first maxillary molar. The alveolar bone at this site was obviously protuberant on the buccal side to accommodate the anatomy of the roots. There was no obvious boundary between the maxillary sinus and nose cavity, and they appeared to merge to form a single cavity (Fig. 2.2a). Micro-CT analysis demonstrated that the first molar in the rat maxilla has five roots, the largest of which was the mesial root (Fig. 2.2d, e). The vertical and horizontal dimensions of the alveolar bone in this region were approximately 2.5 mm (Fig. 2.2d, e). For mice, the often-used site was the maxillary alveolar bone area of the first maxillary molar after being extracted for several weeks [19]. A 1–1.5 mm site in the front of the first maxillary molar along the crest bone (Fig. 2.3a) has also been used [20]. The reason for choosing this site rather than the first molar is probably the technical difficulty in extracting and preparing the implant bed in the first molar area. Since the mesial root of the first molar is mesial tilting (Fig. 2.3c), enough safe space should be reserved to avoid root injury. There is a relatively flat crest bone area with about 1 mm in diameter for implant placement (Fig. 2.3b). However, the thickness is only 0.6 mm for most areas (Fig. 2.3c–e), which means limited primary stability.

The soft tissue at these two implant sites, like other areas of the oral cavity, is heavily orthokeratinized, as indicated in Fig. 2.3g. The hard palate extends from the incisors to the posterior of the third molars, composed of dense connective
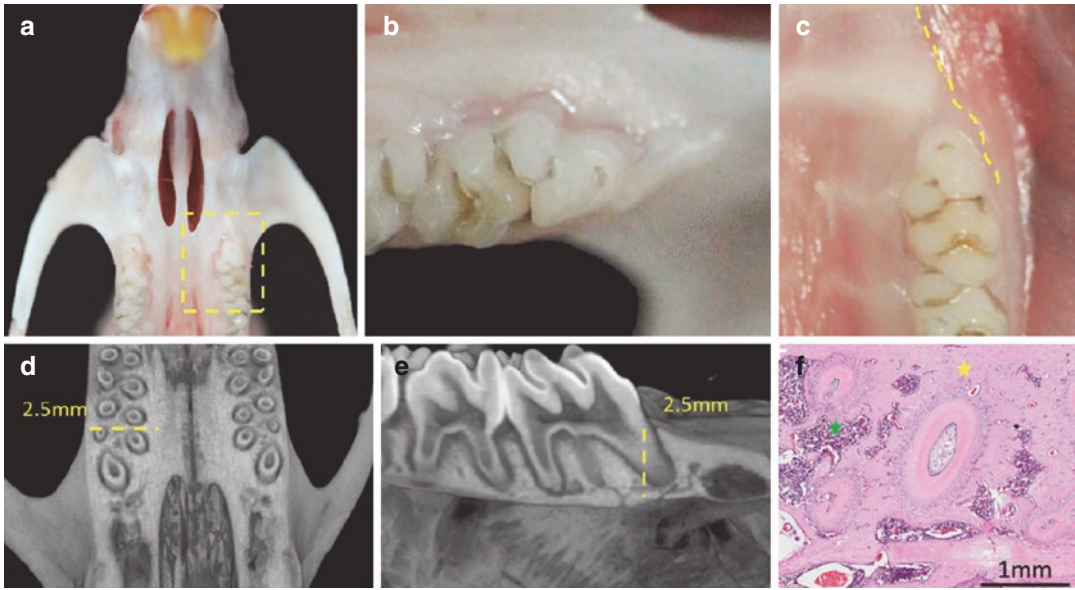
Fig. 2.2 Anatomy and histology of adult rat maxilla. (**a**) Shows outline of the maxilla. (**b**) Shows the magnification picture of the first molar area. (**c**) Shows the soft tissue. The yellow dotted line indicates the junction of the palate and buccal mucosa. (**d**) Micro-CT image of the maxilla in the coronal section shows the five roots of the first molar, and the yellow dotted line indicates the horizontal distance in this area is about 2.5 mm. (**e**) Longitudinal micro-CT image of the first molar area. The vertical dimension is about 2.5 mm. (**f**) HE staining in the coronal section of the first molar area is horizontal. The yellow star indicates the cortical bone; the green star indicates the bone marrow

tissue that blends with the periosteum of the palatine process of the maxillary (Figs. 2.2c and 2.3f). The oral soft tissue has a quite fast healing speed, while a suture is still needed to cover the implant to avoid infection. The periodontal ligament fibers attach to the bone lining the socket (Fig. 2.2f). These ligament fibers will compromise implant osseointegration if the root remains in the socket after tooth extraction.

Long and alveolar bones are derived from different embryonic stem cell populations. Neural crest-derived skeletal progenitor cells give rise to the bones and cartilages of the upper and lower jaws, and the mesoderm gives rise to the long bone [21]. Different from a long bone, which contains larger numbers of osteoprogenitor cells and a robust blood supply, the maxilla has limited bone marrow and presumably lacks the stem cell populations that reside in the marrow cavity [20, 22], as shown in Figs. 2.2f and 2.3g. For mice, there is a reduced amount of trabecular (cancellous) bone in the implant site, and in place of this trabecular framework is cortical bone (Fig. 2.3c, e).

Cortical bone provides primary stability for implants.

Function and Physiology (Movement, Loading, and Occlusion)

The main functions of the oral cavity are prehension and mastication of food. The occlusion force will generate an effect on the healing of the implant. Nowadays, early or immediate loading of implants has also become feasible because of improved surface characteristics and placement techniques. However, it is still true that loading during the bone healing period will more readily cause the failure of osseointegration and that occlusal overloading might lead to implant failure, even after osseointegration has been established [16]. Therefore, the intraoral animal model, which can mimic the human oral environment, is more suitable for studying the mechanical effect on implant osseointegration [23, 24]. However, almost all the implant occlusion model was created on a large animal. The lack of a small-animal experimental model may also
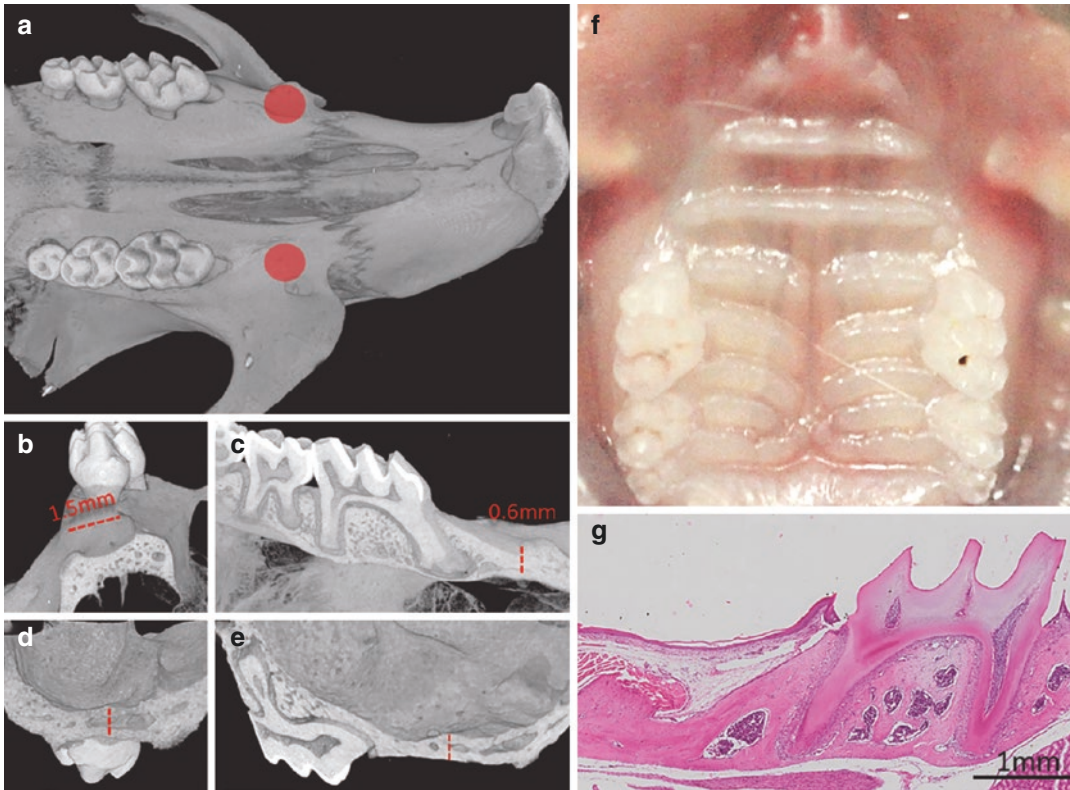
Fig. 2.3 Anatomy and histology of adult mouse maxilla. (**a**) Micro-CT image shows the outline of maxilla. Red circles indicate the potential implant sites. (**b–e**) Micro-CT images from different views (front and rear sides) in different sections (sagittal and longitudinal) show the potential implant location. (**f**) Shows the mouse mucosa in the oral cavity. (**g**) HE staining in the longitudinal section of the first molar and implant site area

explain why few studies discuss the loading effect.

Alveolar bone is among mammals' most physiologically active bone, perhaps the bone that can be resorbed at the fastest rate. Alveolar bone displays a 6-day cycle of formation and resorption consisting of resorption for 1.5 days, a reversal phase for 3.5 days, and deposition for 1 day [25]. The fast remodeling process determines the short observation time of implant healing, usually 1 or 2 weeks, for healthy conditions.

Advantages/Inconveniences in Implant Dentistry Anatomy and Histology

The most advantage of intraoral site is the possibility to simulate the oral environment, such as oral bacteria, masticatory and saliva, which cannot be achieved in the long bone model.

Furthermore, it is impossible to create peri-implantitis model, smoking model, or other models related to oral cavity in the long bone. In contrast, the biggest inconvenience is the small bone size which makes visualization and operation challenging. For mice, the surgical microscope was required for implant bed preparation. And the bone volume is quite limited to embed some of the commercial, experimental implants used in long bone.

Recommendations

The rat or mouse jaw-bones have been used to mimic many human clinical situations, such as periodontitis, orthodontic tooth movement, and periodontal regeneration. However, there is inadequately published literature describing the use of the rat or mouse jaw bone in dental implant

research because the jaw bone is small and difficult to operate on. While there a number of studies were performed in intraoral sites to investigate the effect of systematic diseases, such as osteoporosis and diabetes, on the healing of dental implants. When healthy animals were used, the predominant implant sites were extraoral. However, the intraoral site is the only choice to create peri-implantitis model, smoking model, or other models related to the oral cavity.

2.2.1.2 Surgical Procedures

Extraoral: Description of the Procedures

Animal Welfare, Preparation for Survival
Surgery, and Anesthesia (General, Local)
All research involving rodents must have approval from the researchers' Institutional Animal Care and Use Committee (IACUC) or equivalent ethics committee(s) and must have been conducted according to applicable national and international guidelines. Approval must be received prior to beginning research.

The animals should be kept under climate-controlled conditions (25 °C; 55% humidity; 12 h of light alternating with 12 h of darkness). Bottled tap water and standard food are available ad libitum. Animals need to be acclimatized to the study conditions for 14 days before the implant surgery.

Measures should be taken to minimize pain and distress in animals undergoing major surgery—appropriate perioperative care, including administration of effective anesthetic and analgesic drugs.

All surgery needs to be performed under proper anesthesia. Inhalation (isofluorane in nitrous oxide and oxygen, induction at 5%, maintenance at 2–2.5%) is the preferred anesthesia method. Only when inhalation anesthesia equipment is not available at your own institute intraperitoneal injection of a combination of ketamine (100 mg/kg) and xylazine (10 mg/kg) should be used. In addition, buprenorphine (0.05 mg/kg) should be given both pre- and postoperatively (every 12 h for 48 h) for analgesia to minimize suffering and pain.

Surgical Step by Step: Anterior-Distal Surface
of Femur Metaphysis
1. Position of the animal: Mouse was immobilized supine with the knee joint in a maximally flexed position.
2. Skin preparation: the corresponding skin region, delineated by the red box in Fig. 2.4a, need to be shaved and disinfected with 7.5% povidone-iodine professional veterinary use surgical scrub (Betadine, Stamford, CT, USA)—all the following procedures needed to be done under aseptic conditions.
3. Skin incision (Fig. 2.4b): A 1.5 cm-long skin incision was made longitudinally to the femur just above the knee joint.
4. Exposure and immobilization the operating field (Fig. 2.4c): After careful exposure via muscle blunt dissection, the anterior-distal surface of mouse femur was chosen as the implant insertion site.
5. Preparation of the implant site: Implant site was prepared by sequential drilling with 0.7 mm round bur and 1.0 mm surgical stainless steel twist drills (Fig. 2.4d); laboratory handpiece driven by the NSK MIO electric dental micromotor (Fig. 2.4e). Drilling should be strictly perpendicularly to the surface of the cortical bone on the designated implant insertion surface. At the same time, drilling should also be under ample cooled sterile saline irrigation, and the speed should not exceed 1500 rpm to avoid thermal bone necrosis. The final hole appears as it is shown in Fig. 2.4g.
6. Experimental implant (Fig. 2.4f): Institut Straumann AG (Basel, Switzerland) provides researchers with the experimental titanium implant 1 mm in diameter and 2 mm in length (sterile, ready to insert, unthreaded cylindrical, SLA surface).
7. Implant insertion (Fig. 2.4h): The implant was press fitted into the drilled hole by hand.
8. Wound closure (Fig. 2.4i): Muscles were carefully sutured with 6-0 silk to cover the implant and further guaranteed the stability of the implant and its protection in the biological environment. The skin was closed with 5-0 silk.
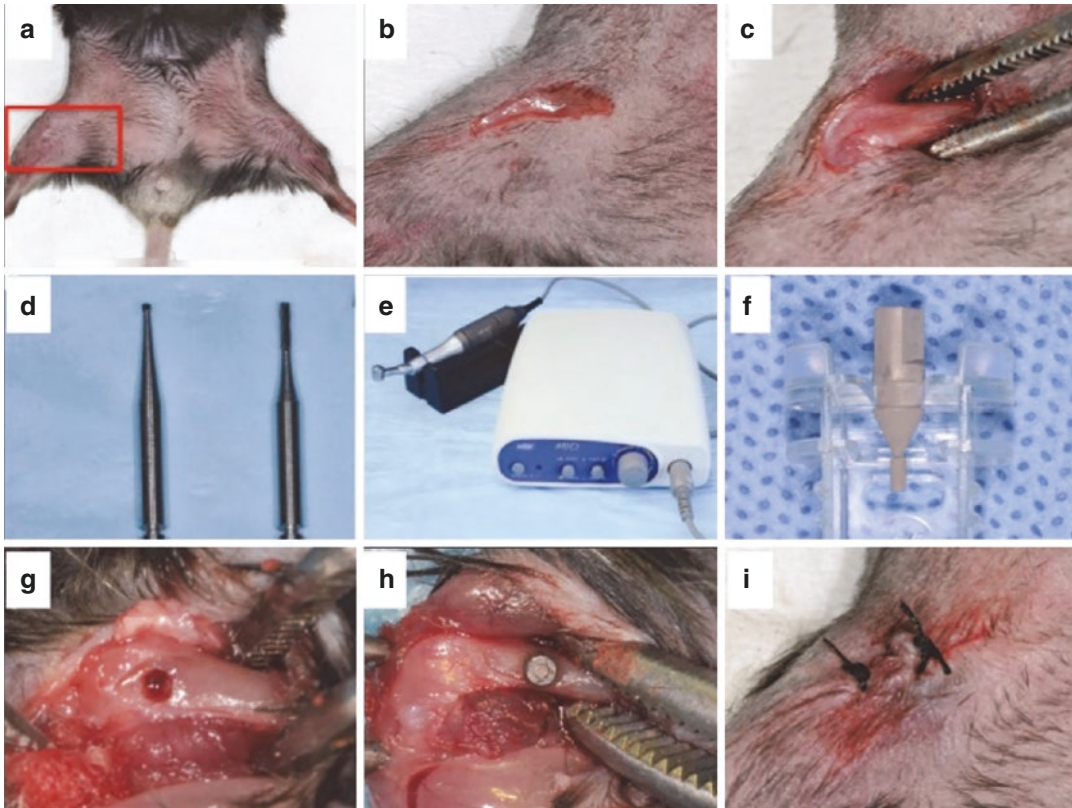
Fig. 2.4 Implant surgery procedure in mouse. (**a**) Skin preparation, red box indicates the corresponding skin region of implant site. (**b**) Skin incision. (**c**) Exposure and immobilization the operating field. (**d**) 0.7 mm round bur and 1.0 mm twist drills. (**e**) Laboratory handpiece for implant insertion. (**f**) Experimental implant. (**g**) Implant sites prepared in the distal end of femur. (**h**) Implant insertion. (**i**) Wound closure

9. Allow the animal to recover on an appropriately heated surgical pad and closely monitor the mobilization of the hind limbs. Only when the mouse or rat starts to move around freely, you can return the mice to the cage in the animal facility.

In rats, the surgical steps are principally similar to that in mice. Given the larger size of the rat, the bigger implant is possible; therefore, accordingly, wider and deeper implant holes were drilled. The rat femur could hold the implant 2.5 mm in length and 1.2 mm in diameter, while the rat tibia was able to accommodate a screw-shaped implant 4.0 mm in length and 2.2 mm in diameter [26–29] or 4.1 mm in length and 1.0 mm in diameter [30–32].

Surgical Step-by-Step:Femoral Condyle

Generally, placement of the implant at femoral condyle is similar to that of aforesaid. The differences are listed as followings:

1. Incise the knee joint capsule longitudinally.
2. Fully expose the knee joint by lifting the patellar ligament gently and moving it laterally, which could be facilitated by a slight extension of the knee.
3. At the intercondylar notch, a cylindrical hole was prepared parallel to the long axis of the femur [8].

After exposure to femoral medullary cavity, there is an alternative way to create the hole and insert the implant. One group expands the bone cavity with electroporation until it is large enough to hold the implant. After implantation of the Ti

rods, the surgical site was closed layer by layer after the opening hole in the femur condyle was sealed with bone wax [33].

Surgical Step by Step: Medial-Proximal Surface of Tibia Metaphysis

For the tibia, the proximal medial aspect of the metaphysis was usually chosen as the designated implant site. The proximal limit of the entry point was delimited by a virtual line perpendicular to the long axis of the tibia and crossing the anterior edge of the growth plate centrally, which is curved in this central region anteriorly and inferiorly. A second anatomical landmark was a virtual line going from the inferior border of the tendinous insertion on the proximal anterior tibial crest to a medial tendinous insertion probably corresponding to the pes anserinus in humans; the point of implantation was mid-way between these two tendinous insertions. With such landmarks X-ray examination demonstrated the implant to be in contact with the trabecular bone of the proximal tibial metaphysis, at a distance of 2 mm from the growth plate proximally along the axis of the tibia [31]. The depth of the inserted part of the implant into the bone corresponded to the length of the nonthreaded part of the implant. Only the threaded part remained outside the bone for prehension for the pull-out test.

Follow-up and Termination

Rodents are euthanized by carbon dioxide inhalation. If blood tests are required, blood could be collected by cheek pouch puncture prior to euthanasia. Femurs or tibias carrying the implant are harvested and dissected carefully by removing adhering soft tissues and fixed in 10% buffered formalin for 1 day at 4 °C.

Recommendations

The general stages of implant healing in mouse tibia resembled those in larger animal models and supported the use of this model as a test bed for studying cellular and molecular responses to different biomaterial and biomechanical conditions [34].

Generally, we would recommend the use of the anterior-distal surface of femur metaphysis as the implant insertion site.

Femoral condyle might also be a suitable location to evaluate the osseointegration of bone implants placed in an osteoporotic condition [8]. However, for animal welfare reasons mentioned before, femoral condyle is not routinely recommended.

Intraoral: Description of the Procedures

Animal Welfare, Preparation for Survival Surgery and Anesthesia (General, Local)

Animal welfare is the same as extraoral procedures. For the intraoral site, the anesthesia was performed through intraperitoneal injection of Ketamine–Xylazine solution. After anesthesia, the mouth was rinsed using a povidone-iodine solution before the surgery. A stereomicroscope was needed to magnify and illuminate the surgery area.

Surgical Step-by-Step: Rat

1. Oral cavity exposure: The rat maxillary area was fully exposed to facilitate tooth extraction after being anesthetized and the oral cavity cleaned (Fig. 2.5a).
2. Tooth extraction: The first molar was extracted using a modified probe and toothed forceps, and the mesial root socket was then inspected to ensure no broken root remained (Fig. 2.5b).
3. Implant site preparation: A 1.8 mm diameter drill was used to create the osteotomy to a depth of 2.5–3.0 mm with a speed of 1000 rpm (Fig. 2.5c).
4. Implant placement: An implant of 2 mm in diameter and length was placed into the mesial socket until the most coronal parts of the implant coincided with the bone crest, and primary stability was achieved (Fig. 2.5d).
5. The flap was then closed with 6-0 sutures, and the implant was fully submerged (Fig. 2.5e).

Surgical Step-by-Step: Mouse

1. Exposure of operation field: the mouse was laid down on a foam board, and the four arms were fixed with adhesive tape. A custom-made mouth gag was used to fully explore the surgery sites (Fig. 2.6a).
2. Flap: a transverse incision was made from the maxillary first molar to the mid-point on the
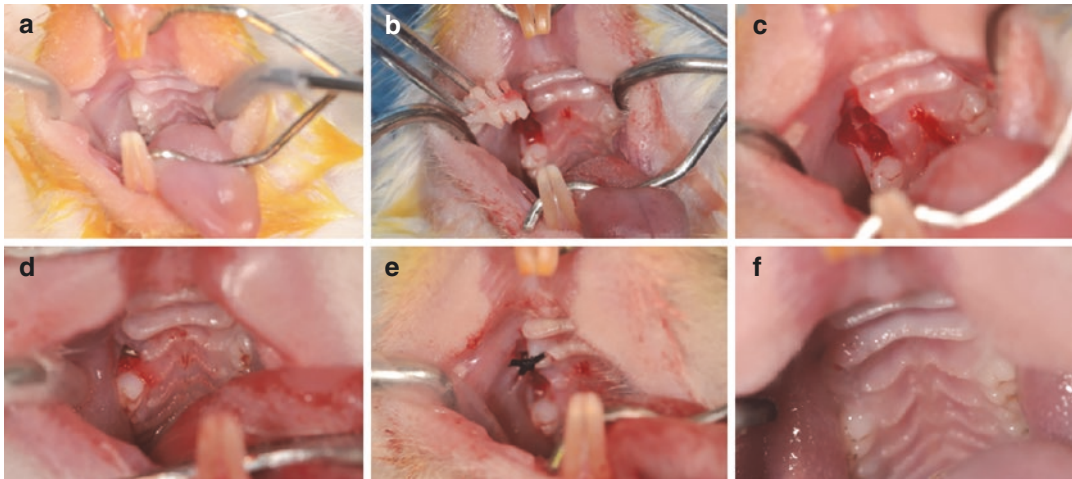
Fig. 2.5 Surgery procedure of rat. (**a**) The rat's oral cavity was fully exposed to facilitate tooth extraction. (**b**) Extraction of the maxillary first molar. (**c**) A 1.8 mm hole is prepared in the mesial socket. (**d**) The 2 mm diameter titanium screw-type implant is placed manually, followed by careful rinsing. (**e**) Wounds are closed with nonabsorbable single interrupted sutures. (**f**) Soft tissue covered the healing implant 1 week after surgery
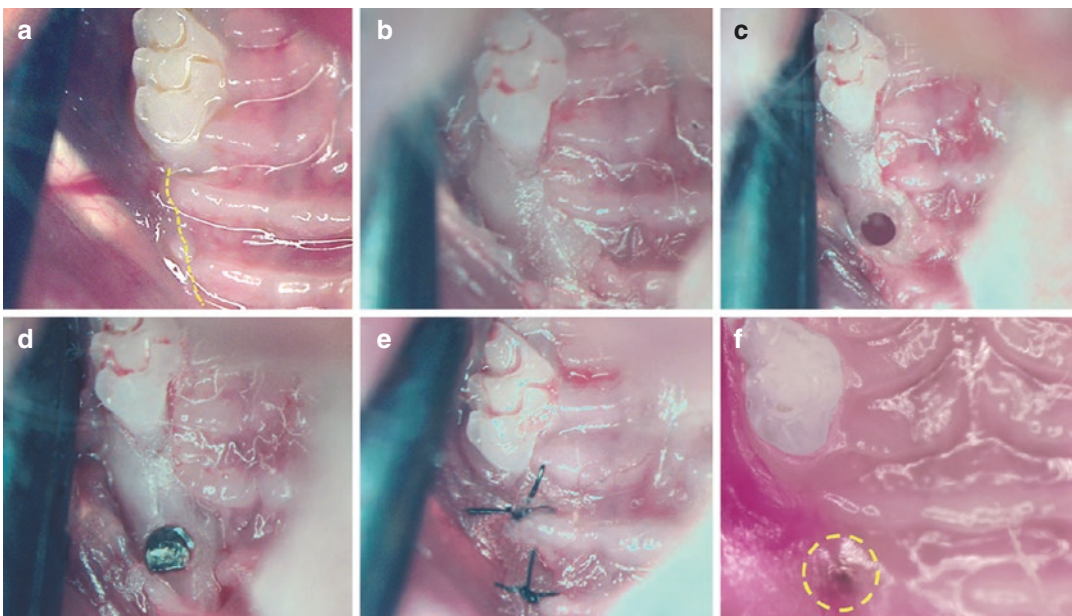
Fig. 2.6 Surgery procedure of mouse. (**a**) Preoperative photograph of the alveolar crest, anterior to the maxillary first molar; yellow dotted line indicates incision. (**b**) A full-thickness flap is elevated to expose the alveolar bone. (**c**) A 0.45 mm hole is prepared on the crest, 1.5 mm anterior of the first maxillary molar. (**d**) The 0.6 mm diameter titanium screw-type implant is placed manually, followed by careful rinsing. (**e**)Wounds are closed with nonabsorbable single interrupted sutures. (**f**) Soft tissue covered the healing implant 2 weeks after surgery. A yellow dotted circle indicated the implant site
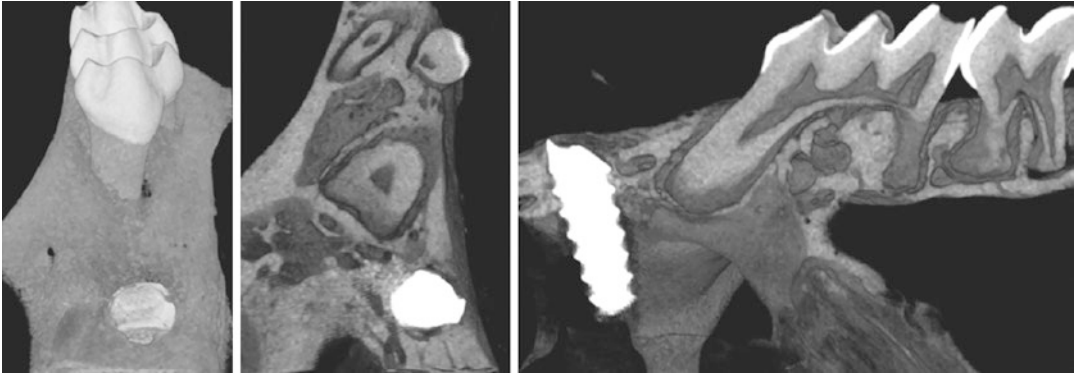
Fig. 2.7 Micro-CT images of implant in maxilla in different directions after 2 weeks of healing

alveolar crest until behind the incisor, followed by a full-thickness flap. The entire extent of the bone where the implants are to be placed was exposed (Fig. 2.6b).

3. Creating the pilot hole for the implant: an implant site was made on the crest 1.5 mm in front of the first molar using a bur drill, and then a 0.45 mm pilot drill was used to prepare the implant hole (Fig. 2.6c).

4. Implant placement: After implant bed preparation, a 0.6 mm titanium implant at length of 1.5 mm was screwed down into the implant bed, maintained by a needle holder. A small part of implant was left exposed above the crest bone (Fig. 2.6d).

5. Suture: The flap was closed using nonabsorbable single interrupted sutures (7-0) (Fig. 2.6e).

Follow-Up and Termination
The animals were kept warm using a heating pad, hot water bottle, or heat lamp after surgery. Animals should be checked frequently, preferably every 10–15 min, turning from side to side until recovered. Soft food was administrated for 2 or 3 days after recovery from anesthesia before changed to hard food. The weight was monitored daily to determine if there were any complications in feeding as a result of the bilateral molar extraction and implant placement. Following postoperative care, the animal is allowed to mature and will then be sacrificed (Fig. 2.7).

Recommendations
1. For rats, fracturing of the tooth roots is a common observation. If the implant is placed in contact with the remaining roots, there is a possibility of forming an encapsulation from the periodontal ligament, thus reducing the degree of osseointegration. So, make sure that an intact root has been extracted.

2. There is thinner bone on the palatal side compared to the buccal side for rat first molar. Hence, when preparing the implant socket, the drill position should be slightly more toward the buccal than the palatal side, at least 0.5 mm away from the mesial root extraction socket, rather than just following the direction of the extraction socket.

3. A shorter implant is recommended to avoid the incidence of sinus perforation for rats.

4. For mice, a drill smaller than the implant and screw-type implant was often recommended to increase the primary stability of implant.

5. Sometimes, especially for mice, a stereomicroscope is required for the surgery process.

2.3   Investigative Methods of Evaluation

2.3.1   X-Rays

X-ray examination is the easiest and quickest method, mainly as the preliminary analysis of extraoral sites, but it may not be suitable for

intraoral sites. X-ray could show whether the implants were surrounded with bone without any notable radio translucent gap or not. The X-ray can also be used to confirm that the implants were free from cortical bone support from the bottom sides of the implants.

Before submission to X-ray examination, femur or tibia needs to be fully dissected from surrounding muscles and soft tissue. Mouse or rat hindlimbs can be analyzed with a Faxitron MX-20 specimen radiography system (Faxitron X-ray Corp., Buffalo Grove, IL).

2.3.2 Micro-CT

Although histological analyses provide unique information on cellularity and dynamic indices of bone remodeling, they have inherent limitations by presuming that the bone microarchitecture is plate-like. To this end, high-resolution 3D imaging like micro-CT allows direct 3D measurement of trabecular morphology, such as trabecular thickness and separation. However, it has to be noted that metallic scattering artifacts of X-rays could prevent accurate evaluation of trabecular bone around the implant.

Micro-CT can be used to characterize trabecular bone morphology, which contributes substantially to bone quality. Parameters such as bone volume fraction (BV/TV), trabecular number (Tb.N), trabecular thickness (Tb.Th), and trabecular separation (Tb.Sp) are commonly compared between experimental and control groups. Some researchers also reported connectivity density (Conn.D) and the structure model index (SMI).

An important issue that should be considered when assessing bone morphology in long bones of small animals like rodents is that not all trabecular bone sites show equally rapid alterations in bone structures by establishing the disease model (e.g., hypogonadism [35]). Based on this knowledge, the region of interest needs to be well-defined [8].

When choosing the region of interest, it is recommended to refer to your histomorphometric measurements on H&E-stained sections in the same experiment. Only the area new bone was formed around the implant needs to be included.

The titanium implant and bone were segmented individually using two distinct threshold values [31] because of their different densities.

Assessment of bone morphology by micro-CT scanning is nondestructive, thus samples can be used subsequently for histology or mechanical testing.

2.3.3 Histology (Remove Implant or Not)

Histological analysis was the most commonly used method, including different qualitative and quantitative methods to assess the implant–bone interface.

The femur or tibia carrying the implant can be processed either undecalcified or decalcified.

The undecalcified histological preparation allows the implant to remain in situ, thus enables the evaluation of the intimate contact of trabecular bone at the implant surface.

Specimens were dehydrated and embedded in light-curing epoxy resin (Technovit 7200VLC, Hereaus Kulzer, Wehrheim, Germany). Embedded specimens were sawed perpendicular to the longitudinal axis of the implants at a site 0.5 mm from its apical end. Then the specimen was grounded to about 50 µm thickness with a grinding system (Exakt Apparatebau, Norderstedt, Germany). Subsequently, the sections are usually stained with Stevenel's blue and Van Gieson's picro fusin stain [36–40], toluidine blue [28], or Goldner's trichrome stain [41]. It should be noted that for undecalcified samples if immunohistochemistry is required, Technovil 9100 (Heraeous Kulzer) must be used instead of Technovil 7100 used in standard histology [42].

On the other hand, decalcification removes the calcium ions from the bone, thereby making the bone flexible and easy for pathological investigation.

After decalcification, the implants were gently removed, and then the sample could be processed like any other soft tissue, i.e., dehydrated in an ascending series of ethanol, cleared in xylene, and embedded in paraffin, sectioned using microtome to a thickness of 5 μm, and finally mounted on a glass slide [43]. Immunohistochemical staining [12, 43] and in situ hybridization [12, 34] can be routinely performed on these decalcified paraffin-embedded sections like ordinary soft tissue.

The embedded block could be sectioned in two directions, transverse [36–39, 43] or longitudinal to the long axis of the implant [12].

In general, it is recommended to cut the block perpendicularly, thus resulting in a section with the cylindrical implant in the middle with surrounding newly formed bone, which yields more consistent results.

Longitudinal sections are often employed to show the bone formed between each screw; however, in order to be consistent, you need to confirm that the selected section crosses the diameter of the implant. Only one section representative of the implant mid-portion was used for subsequent histometric analyses.

2.3.4 Optics and Electronic Histology-Histomorphometry (Including Immunohistolabeling)

Bone labeling facilitated several analytic time points throughout the study without an increase in the number of animals being used. Bone-seeking fluorochromes provide a useful tool for analyzing bone formation sites, time, and amount of bone deposition. The administration of several fluorochrome colors provides spatiotemporal information on the dynamics of bone regeneration in the vicinity of the implant surface over single labels. Considering the fact that bone-implant integration takes place within the first few weeks in rodents, a shorter period between the injections of markers is recommended.

Images of the implant and peri-implant–bone tissues were digitized and histomorphometrically analyzed with NIH Image J (National Institutes of Health, USA). Bone-implant contact (BIC) was calculated as the linear percentage of direct bone-to-implant contact to the total surface of the implant; and the bone volume (BV/TV) in the circumferential zone within 100 μm of the implant surface was calculated. The following formulas were used for analysis (Fig. 2.8).

For the threaded implant, the percentage of bone-to-implant contact (BIC), bone area (BA) within the threads of the implant, and the percentages of bone density (BD) proportion of mineralized tissue in a 500 μm-wide zone adjacent to the implants [26, 29] were obtained bilaterally.

2.3.5 Biomechanics

Biomechanical characterization is an important evaluation parameter of bone as supporting tissue [44], which can be evaluated by push-in test, pull-out test, push-out test, and reverse torque test [9].

2.3.5.1 Push-in Test

The push-in test was developed as a rapid, sensitive assay system for assessing bone-implant integration rather than the strength of the surrounding bone, which provides clinically and functionally relevant information [9].

Femurs carrying implant were embedded into auto-polymerizing resin with the top surface of the implant level. To prevent the auto-polymerizing resin from infiltrating into the areas where there is no contact between bone and implant, soft wax was used to seal the 3 mm area around the bone-implant interface. It should be noted that the orientation of the implant when embedding is critical for the reproducibility and accuracy of the push-in test.

The crosshead was moved as close to the specimen as possible without touching it with the push-in rod. Thereafter, a vertical force (parallel to a long axis of implant) with a displacement
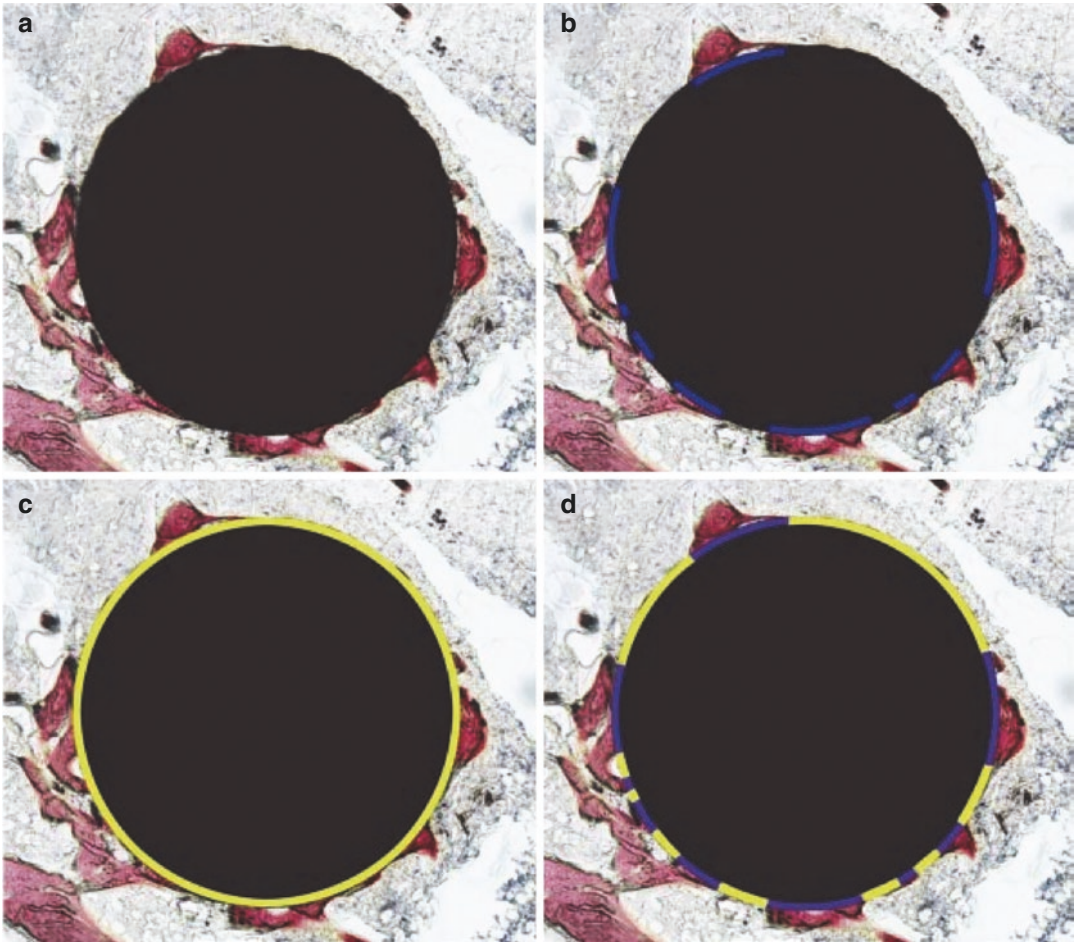
Fig. 2.8 Bone-implant contact (BIC) calculation. (**a**) transversal undecalcified section of implant and surrounding bone; (**b**) blue lines represent the length of bone-implant contact; (**c**) yellow lines represent the circumference length of the implant; (**d**) blue lines represent the length of bone-implant contact, while yellow lines represent the length of implant surface without direct contact with bone

$$BV/TV = \frac{\text{bone area in 100 μm zone}}{\text{area of 100 μm zone}} \times 100\%$$

$$BIC = \frac{\text{sum of the length of bone/implant contact}}{\text{circumference of the implant}} \times 100\%$$
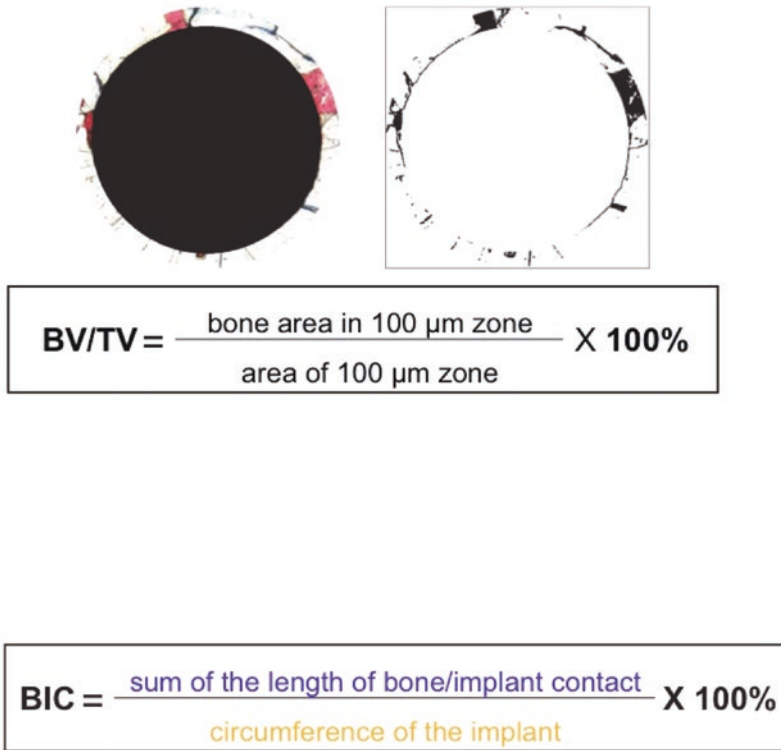
Fig. 2.8 (continued)

speed of 1 mm/min was applied to the implant. The test was stopped when the peak force was reached (representing implant loosening) and was recorded in Newton (N). The push-in value was determined by measuring the peak of the load–displacement curve [36–39].

2.3.5.2 Pull-Out Test

For pull-out test, the implant needs to be customized to leave specific threaded part outside of the implanted bone for prehension. A specifically designed metal device, with two flat supports set at a distance of 5.6 mm from each other on which the medial zone of the proximal tibae was laid, and another metal piece was screwed onto the threaded part of the implant. The pull-out strength was determined as the peak force applied to fully loosen the implant from the bone as measured with an electromechanical system (Instron 5566; Instron Corp., High Wycombe, UK) with the actuator displaced at 2 mm/min [30, 45].

2.3.6   Bacteriology

Bacteria dwelling around the implant and within surrounding bone tissue can be analyzed quantitatively by the spread plate method, and results are reported in colony-forming units (CFUs) [33]. Bacteriology test was mainly performed in the intraoral model of peri-implantitis studies.

2.3.7   Genomics

Overall, it should be noted that biomechanical evaluation of implant osseointegration is not necessarily correlated with histomorphometric measurements [46]. By means of a combination of histomorphometric and biomechanical evaluation, implant in rodents provides a simple and valid in vivo model for research on implant osseointegration.

2.4   Flag Ship Results from the Literature Using These Experimental-Surgical Models (Outlining Your Own Results): Critical Mini-Review

Over the last few decades, dental implants have been a common treatment alternative for missing teeth replacement with a remarkably low failure rate. The widespread acceptance of dental implants has driven significant research activity aimed at improving their effectiveness. To this end, modification of the implant surface [47] and local or systemic treatments [48, 49] have all been explored to improve osseointegration or shorten the implant healing process. The undesirable effects of systemic diseases (e.g., diabetes and osteoporosis) on the osseointegration of implants have also been examined. In order to assess the effects of these parameters on osseointegration and bone regeneration, various animal models have been routinely used before proceeding to human clinical trials [50]. The use of animal models is an essential step in the testing of dental implants prior to clinical use and evaluating the effect of different kinds of diseases on bone–implant interactions [51]. Large animals, especially dogs, are the most often used in the study of dental implants for their similarity in bone composition and density, as well as similar bone remodeling and bone turnover with human [52, 53]. However, these models are large, expensive, number limited and difficult to handle. Furthermore, the genetic background of many of these animals has not been established [54]. Small animals, such as mouse and rat are often

used before moving to larger animals, not only because of their cost-effectiveness, easy to housing and handling, and larger sample numbers, but also because they can be used to mimic human systematic diseases, such as osteoporosis and diabetes [20]. Although possessing these advantages, there are significant limitations to consider when extrapolating implant findings from small animals to human, including significant differences in bone structure, rates of growth, and size [50].

There are several factors to consider when selecting rat or mouse model for dental implant research. The first challenge is the identification of a suitable implant site. Historically, the predominant implant sites for dental implant placement in mouse or rat models are extraoral, that is, femur or tibia, as these sites are relatively easy to perform surgery and have sufficient bone tissue to embed implant [53]. The tibia, mainly at the proximal metaphyseal region and the femur at posterior-lateral aspect, was the most often chosen location [55, 56], because there is more trabecular bone in these sites, which partially resembles the situation in alveolar bone [7]. However, several issues need to be considered when choosing extraoral sites for the study of dental implant osseointegration other than intraoral ones. The long bones have a different development origin and ossification mechanism from the craniofacial bone [21, 57]. In addition, it is impossible to simulate the oral environment, such as oral bacteria, masticatory and saliva, which may have important influences on the osseointegration process [20]. For example, studies that have used long bones showed that osteoporosis negatively influenced osseointegration. However, similar studies when repeated in alveolar bone found that there was no effect on osseointegration [58]. Although having these disadvantages, it comes as that the majority of experimental studies on oral implant osseointegration are conducted in long bones, rather than on the maxilla or mandible for small-animal models. The most often quoted reasons are the bone size in intraoral sites, usually the first maxillary molar area, is relatively small making visualization challenging. Sometimes, especially for

mice, a stereomicroscope is required for surgery process [17]. And the bone volume is quite low to embed the commercial, experimental implant. In addition, compared with alveolar bone, long bone contains a very large and pro-osteogenic marrow cavity, which facilitates rapid bone formation around the implant [9, 10]. Overall, there are no ideal implant sites for rat or mouse that can fulfill all the requirements and one must know the limitations of these sites. Very recently, Matthieu Renaud et al. reported a rat tail vertebrae model for implant osseointegration study, which permits 4 or 5 implants placement with a great stability in the same animal at the same time. Thereby, a decreased number of rats can be involved. Furthermore, live animals can be easily monitored by micro-CT to investigate for bone–implant contact and bone formation in the vicinity of implants [59]. Another implant site, like hard palate [60], was also investigated.

As for the implant type and size, the common implant designs used in animal models are either screw-type (threaded) or cylindrical (rod-shaped). Based on the size of animal and bone chosen and on the implant design, cylindrical implants placed into rat tibial and femoral bone are usually 2 mm in diameter, 1.5–2 mm in length and 1 mm in diameter for mouse femur or tibia. As for intraoral site, the implant sizes are smaller, usually 1 mm in width and 2 mm in length for rat and approximately 0.5 mm in diameter for mouse. There is no consensus suggestion for the implant size. However, no matter what size is chosen, there should be enough bone surrounding implant in order to avoid pathological fracture of the test site.

The commonly used methods for evaluating the healing condition of dental implant are histological, biomechanical and radiological analyses. Histological analysis was the most commonly used method, including different qualitative and quantitative methods for assessing the implant–bone interface, such as percentage of bone-to-implant contact (% BIC) and different staining for evaluating newly formed bone [53]. Common mechanical testing used on tissue harvested from in vivo studies include torque removal test, pull-out test, and push-out test. These tests are used to evaluate the strength of the interaction between the bone and implant surface. High-resolution 3D methods via the micro-CT could provide further insight into the trabecular bone structure around implant. However, it has to be emphasized that metallic scattering artifact of X-ray prevents an accurate evaluation of trabecular bone in the close vicinity to the implant surface. Other assay methods like microbiological techniques were used mainly in studies on peri-implant diseases.

Using the rat or mouse model (mainly divided into healthy animal models and those with systematic diseases), a large number of preclinical studies has been performed to reduce the healing period and acquire more stable osseointegration between implant and bone. Buser et al. reported that, among many factors affecting osseointegration of implant, surface property of implant itself plays a key role in the speed of osseointegration [6, 7]. Numerous surface modifications which including topography modification [61–63], surface coating [64, 65] and local treatment [66–71], as well as systemic treatment [72] have been performed on rat models to investigate the dental bone-implant interface action. Although rat models and a few mouse models have been created to assay the osseointegration of dental implant, the most frequently used animal models for dental bone-implant interface studies in healthy condition are dog and mini-pig [73]. The clear advantage of such animal models is the similar size of the jaw-bones compared with human, thus permitting the use of commercially available implant. This infers that the results obtained are more likely to mimic those expected in human [74]. Implant biomaterials are often analyzed in rat or mouse models for the screening of various parameters, and different surface treatments, for example, before entering the second stage of animal experiments in larger animal models. Another concern for choosing rat or mouse model is that it offers physiologically shorter bone healing periods and the ability to use a large number of animals, and it can be readily manipulated to invoke physiologic changes in the animal by surgical or pharmacologic intervention.

The most applications of rat or mice models for implant research are the experiments on the

healing of systemically compromised animals. A consensus of the eighth European workshop reported that the dog was the most commonly utilized animal model in studies on tissue integration. Rodents were mainly used in studies on tissue integration to implant in systemically compromised animals [53]. Osteoporosis and diabetes mellitus are the most common systemic diseases that are considered risk factors for compromised implant osseointegration [3, 68, 75]. Rat models of osteoporosis and diabetes have contributed significantly to the pathophysiologic understanding of these clinical challenges with regard to bone turnover, bone regeneration, and pharmacologic therapies. Osteoporosis rat models were almost all induced by ovariectomized, which has been recommended by Food and Drug Administration (FDA) as the preclinical animal model for testing osteoporotic medications [76]. Since osteoporotic conditions occur significantly most in trabecular bone, the femoral condyle and the tibia, mainly at the proximal metaphyseal region, rich in trabecular bone, were suggested as a suitable location for studying bone-implant interface [7, 8]. Type 1 diabetic rat models which induced by a single dose of streptozotocin were more often used, although type 2 diabetes mellitus is more common in human. An explanation is that both types of diabetes have a high blood glucose level in common, which negatively influences physiologic pathways. With regard to implant position, 10 mm below the knee joint on the tibia and the posterior-lateral aspect of the femur were considered suitable [7]. Overall, there is a negative effect of osteoporosis and diabetes on the osseointegration of dental implant [7, 8, 77]. Treatment strategies including implant coating [78] and systemic therapies, such as treatment with bisphosphonates [79], parathyroid hormone [80], calcitonin [81, 82], or insulin [83, 84], have also been studies to improve bone-implant interface using the above disease models. Chronic kidney disease (CKD), as another common systematic disease, could profoundly influence bone remolding and the structure of the mandible. Our group have created CKD mouse models and generated a series of studies about the effect of CKD on the healing of dental

implants. The reason to choose mouse model is the easy generation of CKD model, and fast turnover rate of mouse bone, which could shorten the experimental period. The CKD mice were established by a two-step 5/6 nephrectomy and titanium implants with SLA surface (1 mm in diameter and 2 mm in length) were placed in distal aspects of the femur 8 weeks after the second surgery of renal ablation. Using this model, we have demonstrated that CKD negatively affects the osseointegration of titanium implants at the early stage [37]. Treatment strategies, such as vitamin D supplementation [36] and FGF23 neutralization were also investigated to enhance the osseointegration of titanium implants in chronic kidney disease mice [38].

Despite that, the general principles for studying osseointegration in these disease models are similar. However, different from healthy animal models, the researchers should consider several factors, such as implant location, the time of disease induction and implant placement, as well as the observation period, when choosing these models. Different research questions have led to a diversity of animal models to evaluate the impact of systematic diseases on the process of osseointegration. For example, the main effects of OVX on osseointegration were observed in the medullary but not in the cortical compartment, suggesting that the region of interest must be considered. Implants being inserted prior to, simultaneous, and after OVX surgery was performed in different studies, which may result in variation of the final conclusion. The selection of the observation period is also very important for animal models with systematic diseases. For example, no statistically significant difference in bone-to-implant contact was reported between diabetic and nondiabetic rats 10 days after implant placement. However, 3 weeks following implant installation, diabetic rats exhibited a 50% lower bone-to-implant contact [84]. Another study reported that "little osteogenic activity occurred during the initial period of study (second and third weeks)" and "the period of highest osteogenic activity was at the beginning of the fourth week and at the end of the fifth week" [85]. Our group demonstrated that the chronic

kidney disease impaired BIC ratio and strength of bone-implant integration at 2 weeks of healing. However, there is no significant difference between the two groups after a longer healing period (4 weeks). Usually, the observation period after implantation was longer in OVX rats than in diabetic rats. Because osteoporosis is an age-related disease that is better represented by adult animals, while untreated type 1 diabetes has a severe impact on metabolism, for which younger animals are more suitable. Researchers should know the variations and design the protocol carefully before choosing the suitable model.

Another common disease that influences the osseointegration of dental implant is peri-implantitis. Peri-implantitis has become a global clinical problem with a prevalence rate of up to 56% [86]. The pathogenesis of peri-implant lesions remains poorly understood due to the nonavailability of inexpensive animal models for peri-implantitis. Most animal studies have been performed using dogs [87, 88]. Although a large number of studies used rat model for periodontitis investigation, there are few studies using rat model for peri-implantitis probably because of the technical difficulties. Dr. Homayoun Zadeh et al. [60] developed a peri-implantitis rat model by placing aggregatibacter actinomycetemcomitans biofilm-inoculated implant into rat hard palate or alveolar ridge. Greater inflammatory response was observed around the biofilm-inoculated implant, and greater bone volume loss was found by micro-CT after 6 weeks of implant insertion. Very recently, Theofilos Koutouzis et al. [89] induced a novel intraoral peri-implantitis rat model utilizing a polymicrobial infection. The amount of bone resorption observed for implants subjected to polymicrobial infection was greater compared with control implants. However, due to the limitation of a small sample size of this study, it needs to be confirmed with further studies. Treatment study was also reported to prevent peri-implantitis through immobilizing bacitracin on titanium for prophylaxis of infection [33].

Smoking is one of the factors often discussed in relation to implant failure. Stefani et al. [90] and Nociti Jr. et al. [91] have investigated the effects of nicotine administration on osseointegration and bone density around dental implants in rabbit. A slight negative effect of nicotine on the bone-to-implant contact around implants with machined surfaces was observed. Nociti Junior, F. H. et al. have carried out a series of histological studies in rat model to investigate the influence of cigarette consumption and/or its compounds on bone healing around titanium implants [26, 27, 29, 92, 93]. A cigarette smoke exposure chamber, which consisted of a clear acrylic chamber, an air pump and two inflow/outflow tubes, was designed to create the smoke model. Their results demonstrated a negative influence of smoking on bone healing around titanium implants. Systemic administration of nicotine was also used to mimic the smoke model in rat [40], and a similar result was observed.

Rat has also been used to evaluate peri-implant–bone reactions under local conditions such as excessive loading [16] and controlled moderate loading [94]. The choice of the rat model presents a study limitation, since rat lacks the haversian bone system. Other rat models, such as radiation [95–98], hyperlipidemia [99], and osteonecrosis [49], hepatic osteodystrophy [100], vitamin D deficiency [101], magnesium deficiency [102], protein deficiency [32], aging [103] models have also been studied. Although these disease models are relatively rare, they present a reference to your future related studies.

Among the small-animal models, rabbit and rat are the most frequently used for dental implant studies. In comparison, mice have the advantage of more molecular tools and reagents available than rats [104]. The availability of a broad spectrum of antibodies and gene-targeted animals caused an increasing interest in mouse models to study molecular mechanisms of dental implant osseointegration. However, few studies suggested that this model is suitable for implant placement [34, 43]. Implants can either be removed during processing or remain in situ for further analysis to reveal the level and mechanism of osseointegration. Nowadays, studies employing transgenic and knockout mouse models have also provided new insights into the mechanism of osseointegration at the dental implant surface. J.Chen et al.

used two different retroviral gene delivery systems to achieve local overexpression of SATB2 after dental implant placement. They demonstrated that in vivo overexpression of SATB2 significantly accelerates osseointegration of titanium implants and SATB2 can serve as a potent molecule in promoting tissue regeneration [105]. Takato. T et al. used a knockout mice to examine the effect of cyclooxygenase (COX)-2 on bone response after implant placement in the femur. They found that new bone formation was minimal in COX-2−/− mice which suggested that COX-2 plays an essential role in osseointegration [106]. Gong. P's group have demonstrated that implant osseointegration significantly decreased in the α-CGRP−/− mice and α-CGRP overexpression resulted in greater gains in osseointegration [107]. These data imply that lentiviral vector system might have a potential application in enhancing the osseointegration of dental implants in an effective, appropriate and sustained manner. With the rapid development of transgenic mice, there will be more and more mouse models for the mechanism study of osseointegration at the dental implant surface.

2.5   Expert Opinion: Balancing Models (Experimental and Surgical) Validation and Validity

Despite dogs or other large animals being the most commonly used animal model to study implant integration, rodents provide a more rapid and economical alternative. In addition, it is more convenient to study the effect of systematic diseases, such as osteoporosis, diabetes, and chronic kidney disease, using the small-animal model. And the easier generation of gene-modified animals for dental implant research is also their remarkable advantage.

In general, for small animals, considering the size of the recipient bone tissue and the convenience to operate, the extraoral sites are mainly chosen for implant insertion, and the anterior-distal flat surface of femur metaphysis was the

most cited location. For intraoral sites, the first maxillary molar was the most often used for rat. However, there was no consensual suggestion site for mouse owing to the relatively few studies.

References

1. Beppu K, Kido H, Watazu A, Teraoka K, Matsuura M. Peri-implant bone density in senile osteoporosis-changes from implant placement to osseointegration. Clin Implant Dent Relat Res. 2013;15(2):217–26.
2. Alsaadi G, Quirynen M, Komarek A, van Steenberghe D. Impact of local and systemic factors on the incidence of oral implant failures, up to abutment connection. J Clin Periodontol. 2007;34(7):610–7.
3. Mombelli A, Cionca N. Systemic diseases affecting osseointegration therapy. Clin Oral Implants Res. 2006;17(Suppl 2):97–103.
4. Histing T, Garcia P, Holstein JH, Klein M, Matthys R, Nuetzi R, et al. Small animal bone healing models: standards, tips, and pitfalls results of a consensus meeting. Bone. 2011;49(4):591–9.
5. Karimbux NY, Sirakian A, Weber HP, Nishimura I. A new animal model for molecular biological analysis of the implant-tissue interface: spatial expression of type XII collagen mRNA around a titanium oral implant. J Oral Implantol. 1995;21(2):107–13; discussion 14–5.
6. Ferris DM, Moodie GD, Dimond PM, Gioranni CW, Ehrlich MG, Valentini RF. RGD-coated titanium implants stimulate increased bone formation in vivo. Biomaterials. 1999;20(23–24):2323–31.
7. Glosel B, Kuchler U, Watzek G, Gruber R. Review of dental implant rat research models simulating osteoporosis or diabetes. Int J Oral Maxillofac Implants. 2010;25(3):516–24.
8. Alghamdi HS, van den Beucken JJ, Jansen JA. Osteoporotic rat models for evaluation of osseointegration of bone implants. Tissue Eng Part C Methods. 2014;20(6):493–505.
9. Ogawa T, Ozawa S, Shih JH, Ryu KH, Sukotjo C, Yang JM, et al. Biomechanical evaluation of osseous implants having different surface topographies in rats. J Dent Res. 2000;79(11):1857–63.
10. Kilborn SH, Trudel G, Uhthoff H. Review of growth plate closure compared with age at sexual maturity and lifespan in laboratory animals. Contemp Top Lab Anim Sci. 2002;41(5):21–6.
11. Recker RR, Kimmel DB, Dempster D, Weinstein RS, Wronski TJ, Burr DB. Issues in modern bone histomorphometry. Bone. 2011;49(5):955–64.
12. Leucht P, Kim JB, Wazen R, Currey JA, Nanci A, Brunski JB, et al. Effect of mechanical stimuli

on skeletal regeneration around implants. Bone. 2007;40(4):919–30.

13. Nunamaker DM. Experimental models of fracture repair. Clin Orthop Relat Res. 1998;(355 Suppl):S56–65.

14. Giavaresi G, Fini M, Gnudi S, De Terlizzi F, Carpi A, Giardino R. The femoral distal epiphysis of ovariectomized rats as a site for studies on osteoporosis: structural and mechanical evaluations. Clin Exp Rheumatol. 2002;20(2):171–8.

15. Fujii N, Kusakari H, Maeda T. A histological study on tissue responses to titanium implantation in rat maxilla: the process of epithelial regeneration and bone reaction. J Periodontol. 1998;69(4):485–95.

16. Nagasawa M, Takano R, Maeda T, Uoshima K. Observation of the bone surrounding an overloaded implant in a novel rat model. Int J Oral Maxillofac Implants. 2013;28(1):109–16.

17. Du Z, Lee RS, Hamlet S, Doan N, Ivanovski S, Xiao Y. Evaluation of the first maxillary molar post-extraction socket as a model for dental implant osseointegration research. Clin Oral Implants Res. 2016;27(12):1469–78.

18. Siqueira CR, Semenoff TA, Palma VC, Borges AH, Silva NF, Segundo AS. Effect of chronic stress on implant osseointegration into rat's mandible. Acta Cir Bras. 2015;30(9):598–603.

19. Wang L, Wu Y, Perez KC, Hyman S, Brunski JB, Tulu U, et al. Effects of condensation on peri-implant bone density and remodeling. J Dent Res. 2017;96(4):413–20.

20. Mouraret S, Hunter DJ, Bardet C, Brunski JB, Bouchard P, Helms JA. A pre-clinical murine model of oral implant osseointegration. Bone. 2014;58:177–84.

21. Helms J, Schneider R. Cranial skeletal biology. Nature. 2003;423(6937):326.

22. Yin T, Li L. The stem cell niches in bone. J Clin Investig. 2006;116(5):1195.

23. Yi Y, Men Y, Jing D, Luo W, Zhang S, Feng JQ, et al. 3-Dimensional visualization of implant-tissue interface with the polyethylene glycol associated solvent system tissue clearing method. Cell Prolif. 2019;52(3):e12578.

24. Yi Y, Stenberg W, Luo W, Feng JQ, Zhao H. Alveolar bone marrow Gli1+ stem cells support implant osseointegration. J Dent Res. 2021;101:73.

25. Hall BK. Bones and cartilage: developmental and evolutionary skeletal biology. Academic Press; 2005.

26. Lima LL, Cesar Neto JB, Cayana EG, Nociti FH Jr, Sallum EA, Casati MZ. Parathyroid hormone (1-34) compensates the negative effect of smoking around implants. Clin Oral Implants Res. 2013;24(9):1055–9.

27. Nociti Junior FH, Cesar Neto JB, Carvalho MD, Sallum EA, Sallum AW. Intermittent cigarette smoke inhalation may affect bone volume around titanium implants in rats. J Periodontol. 2002;73(9):982–7.

28. Cesar-Neto JB, Duarte PM, Sallum EA, Barbieri D, Moreno H Jr, Nociti FH Jr. A comparative study on the effect of nicotine administration and cigarette smoke inhalation on bone healing around titanium implants. J Periodontol. 2003;74(10):1454–9.

29. Correa MG, Gomes Campos ML, Cesar-Neto JB, Casati MZ, Nociti FH, Sallum EA. Histometric evaluation of bone around titanium implants with different surface treatments in rats exposed to cigarette smoke inhalation. Clin Oral Implants Res. 2009;20(6):588–93.

30. Maimoun L, Brennan TC, Badoud I, Dubois-Ferriere V, Rizzoli R, Ammann P. Strontium ranelate improves implant osseointegration. Bone. 2010;46(5):1436–41.

31. Dayer R, Rizzoli R, Kaelin A, Ammann P. Low protein intake is associated with impaired titanium implant osseointegration. J Bone Miner Res. 2006;21(2):258–64.

32. Dayer R, Badoud I, Rizzoli R, Ammann P. Defective implant osseointegration under protein undernutrition: prevention by PTH or pamidronate. J Bone Miner Res. 2007;22(10):1526–33.

33. Nie B, Ao H, Long T, Zhou J, Tang T, Yue B. Immobilizing bacitracin on titanium for prophylaxis of infections and for improving osteoinductivity: an in vivo study. Colloids Surf B Biointerfaces. 2017;150:183–91.

34. Colnot C, Romero DM, Huang S, Rahman J, Currey JA, Nanci A, et al. Molecular analysis of healing at a bone-implant interface. J Dent Res. 2007;86(9):862–7.

35. Lelovas PP, Xanthos TT, Thoma SE, Lyritis GP, Dontas IA. The laboratory rat as an animal model for osteoporosis research. Comp Med. 2008;58(5):424–30.

36. Liu W, Zhang S, Zhao D, Zou H, Sun N, Liang X, et al. Vitamin D supplementation enhances the fixation of titanium implants in chronic kidney disease mice. PLoS One. 2014;9(4):e95689.

37. Zou H, Zhao X, Sun N, Zhang S, Sato T, Yu H, et al. Effect of chronic kidney disease on the healing of titanium implants. Bone. 2013;56(2):410–5.

38. Sun N, Guo Y, Liu W, Densmore M, Shalhoub V, Erben RG, et al. FGF23 neutralization improves bone quality and osseointegration of titanium implants in chronic kidney disease mice. Sci Rep. 2015;5:8304.

39. Zhang S, Guo Y, Zou H, Sun N, Zhao D, Liu W, et al. Effect of estrogen deficiency on the fixation of titanium implants in chronic kidney disease mice. Osteoporos Int. 2015;26(3):1073–80.

40. Yamano S, Berley JA, Kuo WP, Gallucci GO, Weber HP, Sukotjo C. Effects of nicotine on gene expression and osseointegration in rats. Clin Oral Implants Res. 2010;21(12):1353–9.

41. Ozawa S, Ogawa T, Iida K, Sukotjo C, Hasegawa H, Nishimura RD, et al. Ovariectomy hinders the early stage of bone-implant integration: histomorphomet-

ric, biomechanical, and molecular analyses. Bone. 2002;30(1):137–43.

42. Goldschlager T, Abdelkader A, Kerr J, Boundy I, Jenkin G. Undecalcified bone preparation for histology, histomorphometry and fluorochrome analysis. J Vis Exp. 2010;(35):1707.

43. Xu B, Zhang J, Brewer E, Tu Q, Yu L, Tang J, et al. Osterix enhances BMSC-associated osseointegration of implants. J Dent Res. 2009;88(11):1003–7.

44. Turner CH, Burr DB. Basic biomechanical measurements of bone: a tutorial. Bone. 1993;14(4):595–608.

45. Takahashi T, Watanabe T, Nakada H, Tanimoto Y, Kimoto S, Mijares DQ, et al. Effect of a dietary supplement on peri-implant bone strength in a rat model of osteoporosis. J Prosthodont Res. 2016;60(2):131–7.

46. Wong M, Eulenberger J, Schenk R, Hunziker E. Effect of surface topology on the osseointegration of implant materials in trabecular bone. J Biomed Mater Res. 1995;29(12):1567–75.

47. Yeo IS. Reality of dental implant surface modification: a short literature review. Open Biomed Eng J. 2014;8:114–9.

48. Carcuac O, Derks J, Charalampakis G, Abrahamsson I, Wennstrom J, Berglundh T. Adjunctive systemic and local antimicrobial therapy in the surgical treatment of peri-implantitis: a randomized controlled clinical trial. J Dent Res. 2016;95(1):50–7.

49. Abtahi J, Agholme F, Sandberg O, Aspenberg P. Effect of local vs. systemic bisphosphonate delivery on dental implant fixation in a model of osteonecrosis of the jaw. J Dent Res. 2013;92(3):279–83.

50. Pearce AI, Richards RG, Milz S, Schneider E, Pearce SG. Animal models for implant biomaterial research in bone: a review. Eur Cell Mater. 2007;13:1–10.

51. Alzarea BK. Selection of animal models in dentistry: state of art, review article. J Anim Vet Adv. 2014;13(18):1080–5.

52. Wancket LM. Animal models for evaluation of bone implants and devices: comparative bone structure and common model uses. Vet Pathol. 2015;52(5):842–50.

53. Berglundh T, Stavropoulos A, Working Group 1 of the VIII European Workshop on Periodontology. Preclinical in vivo research in implant dentistry. Consensus of the eighth European workshop on periodontology. J Clin Periodontol. 2012;39(Suppl 12):1–5.

54. Kantarci A, Hasturk H, Van Dyke TE. Animal models for periodontal regeneration and peri-implant responses. Periodontology 2000. 2015;68(1):66–82.

55. Liu W, Zhou L, Xue H, Li H, Yuan Q. Growth differentiation factor 11 impairs titanium implant healing in the femur and leads to mandibular bone loss. J Periodontol. 2020;91(9):1203–12.

56. Xue H, Guo Y, Zhang S, Xu T, Wen J, Kang N, et al. The role of USP34 in the fixation of titanium implants in murine models. Eur J Oral Sci. 2020;128(3):211–7.

57. Chai Y, Maxson RE Jr. Recent advances in craniofacial morphogenesis. Dev Dyn. 2006;235(9):2353–75.

58. Giro G, Coelho PG, Sales-Pessoa R, Pereira RM, Kawai T, Orrico SR. Influence of estrogen deficiency on bone around osseointegrated dental implants: an experimental study in the rat jaw model. J Oral Maxillofac Surg. 2011;69(7):1911–8.

59. Renaud M, Farkasdi S, Pons C, Panayotov I, Collart-Dutilleul PY, Taillades H, et al. A new rat model for translational research in bone regeneration. Tissue Eng Part C Methods. 2015;22:125.

60. Freire MO, Sedghizadeh PP, Schaudinn C, Gorur A, Downey JS, Choi JH, et al. Development of an animal model for Aggregatibacter actinomycetemcomitans biofilm-mediated oral osteolytic infection: a preliminary study. J Periodontol. 2011;82(5):778–89.

61. Abron A, Hopfensperger M, Thompson J, Cooper LF. Evaluation of a predictive model for implant surface topography effects on early osseointegration in the rat tibia model. J Prosthet Dent. 2001;85(1):40–6.

62. Marinho VC, Celletti R, Bracchetti G, Petrone G, Minkin C, Piattelli A. Sandblasted and acid-etched dental implants: a histologic study in rats. Int J Oral Maxillofac Implants. 2003;18(1):75–81.

63. Mendes VC, Moineddin R, Davies JE. The effect of discrete calcium phosphate nanocrystals on bone-bonding to titanium surfaces. Biomaterials. 2007;28(32):4748–55.

64. Haimov H, Yosupov N, Pinchasov G, Juodzbalys G. Bone morphogenetic protein coating on titanium implant surface: a systematic review. J Oral Maxillofac Res. 2017;8(2):e1.

65. Bhattarai G, Lee YH, Lee MH, Yi HK. Gene delivery of c-myb increases bone formation surrounding oral implants. J Dent Res. 2013;92(9):840–5.

66. Wermelin K, Tengvall P, Aspenberg P. Surface-bound bisphosphonates enhance screw fixation in rats--increasing effect up to 8 weeks after insertion. Acta Orthop. 2007;78(3):385–92.

67. Wermelin K, Suska F, Tengvall P, Thomsen P, Aspenberg P. Stainless steel screws coated with bisphosphonates gave stronger fixation and more surrounding bone. Histomorphometry in rats. Bone. 2008;42(2):365–71.

68. Tengvall P, Skoglund B, Askendal A, Aspenberg P. Surface immobilized bisphosphonate improves stainless-steel screw fixation in rats. Biomaterials. 2004;25(11):2133–8.

69. Chang PC, Seol YJ, Cirelli JA, Pellegrini G, Jin Q, Franco LM, et al. PDGF-B gene therapy accelerates bone engineering and oral implant osseointegration. Gene Ther. 2010;17(1):95–104.

70. Schliephake H, Rublack J, Forster A, Schwenzer B, Reichert J, Scharnweber D. Functionalization of titanium implants using a modular system for binding and release of VEGF enhances bone-implant contact in a rodent model. J Clin Periodontol. 2015;42(3):302–10.

71. Dunn CA, Jin Q, Taba M Jr, Franceschi RT, Bruce Rutherford R, Giannobile WV. BMP gene delivery for alveolar bone engineering at dental implant defects. Mol Ther. 2005;11(2):294–9.

72. Kim JH, Park YB, Li Z, Shim JS, Moon HS, Jung HS, et al. Effect of alendronate on healing of extraction sockets and healing around implants. Oral Dis. 2011;17(7):705–11.

73. Stadlinger B, Pourmand P, Locher MC, Schulz MC. Systematic review of animal models for the study of implant integration, assessing the influence of material, surface and design. J Clin Periodontol. 2012;39:28–36.

74. Meng HW, Chien EY, Chien HH. Dental implant bioactive surface modifications and their effects on osseointegration: a review. Biomark Res. 2016;4:24.

75. Salvi GE, Carollo-Bittel B, Lang NP. Effects of diabetes mellitus on periodontal and peri-implant conditions: update on associations and risks. J Clin Periodontol. 2008;35(8 Suppl):398–409.

76. Thompson D, Simmons H, Pirie C, Ke H. FDA guidelines and animal models for osteoporosis. Bone. 1995;17(4):S125–S33.

77. Javed F, Romanos GE. Impact of diabetes mellitus and glycemic control on the osseointegration of dental implants: a systematic literature review. J Periodontol. 2009;80(11):1719–30.

78. Takeshita F, Iyama S, Ayukawa Y, Kido MA, Murai K, Suetsugu T. The effects of diabetes on the interface between hydroxyapatite implants and bone in rat tibia. J Periodontol. 1997;68(2):180–5.

79. Tokugawa Y, Shirota T, Ohno K, Yamaguchi A. Effects of bisphosphonate on bone reaction after placement of titanium implants in tibiae of ovariectomized rats. Int J Oral Maxillofac Implants. 2003;18(1):66–74.

80. Shirota T, Tashiro M, Ohno K, Yamaguchi A. Effect of intermittent parathyroid hormone (1-34) treatment on the bone response after placement of titanium implants into the tibia of ovariectomized rats. J Oral Maxillofac Surg. 2003;61(4):471–80.

81. Duarte PM, Cesar-Neto JB, Sallum AW, Sallum EA, Nociti FH Jr. Effect of estrogen and calcitonin therapies on bone density in a lateral area adjacent to implants placed in the tibiae of ovariectomized rats. J Periodontol. 2003;74(11):1618–24.

82. Nociti FH Jr, Sallum AW, Sallum EA, Duarte PM. Effect of estrogen replacement and calcitonin therapies on bone around titanium implants placed in ovariectomized rats: a histometric study. Int J Oral Maxillofac Implants. 2002;17(6):786–92.

83. Kwon PT, Rahman SS, Kim DM, Kopman JA, Karimbux NY, Fiorellini JP. Maintenance of osseointegration utilizing insulin therapy in a diabetic rat model. J Periodontol. 2005;76(4):621–6.

84. Siqueira JT, Cavalher-Machado SC, Arana-Chavez VE, Sannomiya P. Bone formation around titanium implants in the rat tibia: role of insulin. Implant Dent. 2003;12(3):242–51.

85. Ottoni CE, Chopard RP. Histomorphometric evaluation of new bone formation in diabetic rats submitted to insertion of temporary implants. Braz Dent J. 2004;15(2):87–92.

86. Smeets R, Henningsen A, Jung O, Heiland M, Hammacher C, Stein JM. Definition, etiology, prevention and treatment of peri-implantitis--a review. Head Face Med. 2014;10:34.

87. Berglundh T, Lindhe J, Marinello C, Ericsson I, Liljenberg B. Soft tissue reaction to de novo plaque formation on implants and teeth. An experimental study in the dog. Clin Oral Implants Res. 1992;3(1):1–8.

88. Berglundh T, Gotfredsen K, Zitzmann NU, Lang NP, Lindhe J. Spontaneous progression of ligature induced peri-implantitis at implants with different surface roughness: an experimental study in dogs. Clin Oral Implants Res. 2007;18(5):655–61.

89. Koutouzis T, Eastman C, Chukkapalli S, Larjava H, Kesavalu L. A novel rat model of polymicrobial peri-implantitis: a preliminary study. J Periodontol. 2017;88(2):e32–41.

90. Stefani CM, Nogueira F, Sallum EA, de TS, Sallum AW, Nociti FH Jr. Influence of nicotine administration on different implant surfaces: a histometric study in rabbits. J Periodontol. 2002;73(2):206–12.

91. Nociti FH Jr, Stefani CM, Sallum EA, Duarte PM, Sallum AW. Nicotine and bone density around titanium implants: a histometric study in rabbits. Implant Dent. 2002;11(2):176–82.

92. Nociti FH Jr, Cesar NJ, Carvalho MD, Sallum EA. Bone density around titanium implants may be influenced by intermittent cigarette smoke inhalation: a histometric study in rats. Int J Oral Maxillofac Implants. 2002;17(3):347–52.

93. Getulio da R Nogueira-Filho, Cadide T, Rosa BT, Neiva TG, Tunes R, Peruzzo D, et al. Cannabis sativa smoke inhalation decreases bone filling around titanium implants: a histomorphometric study in rats. Implant Dent. 2008;17(4):461–70.

94. Zhang X, Duyck J, Vandamme K, Naert I, Carmeliet G. Ultrastructural characterization of the implant interface response to loading. J Dent Res. 2014;93(3):313–8.

95. Nyberg J, Hertzman S, Svensson B, Johansson CB. Osseointegration of implants in irradiated bone with and without hyperbaric oxygen treatment: an experimental study in rat tibiae. Int J Oral Maxillofac Implants. 2013;28(3):739–46.

96. de Oliveira JA, do Amaral Escada AL, Alves Rezende MC, Mathor MB, Alves Claro AP. Analysis of the effects of irradiation in osseointegrated dental implants. Clin Oral Implants Res. 2012;23(4):511–4.

97. Khadra M. The effect of low level laser irradiation on implant-tissue interaction. In vivo and in vitro studies. Swed Dent J Suppl. 2005;172:1–63.

98. Renou SJ, Guglielmotti MB, de la Torre A, Cabrini RL. Effect of total body irradiation on peri-implant tissue reaction: an experimental study. Clin Oral Implants Res. 2001;12(5):468–72.

99. Keuroghlian A, Barroso AD, Kirikian G, Bezouglaia O, Tintut Y, Tetradis S, et al. The effects of hyperlipidemia on implant osseointegration in the mouse femur. J Oral Implantol. 2015;41(2):e7–e11.

100. Gorustovich A, de los Esposito M, Guglielmotti MB, Giglio MJ. Periimplant bone healing under experimental hepatic osteodystrophy induced by a choline-deficient diet: a histomorphometric study in rats. Clin Implant Dent Relat Res. 2003;5(2):124–9.

101. Kelly J, Lin A, Wang CJ, Park S, Nishimura I. Vitamin D and bone physiology: demonstration of vitamin D deficiency in an implant osseointegration rat model. J Prosthodont. 2009;18(6):473–8.

102. Del Barrio RA, Giro G, Belluci MM, Pereira RM, Orrico SR. Effect of severe dietary magnesium deficiency on systemic bone density and removal torque of osseointegrated implants. Int J Oral Maxillofac Implants. 2010;25(6):1125–30.

103. Mair B, Tangl S, Feierfeil J, Skiba D, Watzek G, Gruber R. Age-related efficacy of parathyroid hormone on osseointegration in the rat. Clin Oral Implants Res. 2009;20(4):400–5.

104. Elefteriou F, Yang X. Genetic mouse models for bone studies--strengths and limitations. Bone. 2011;49(6):1242–54.

105. Yan SG, Zhang J, Tu QS, Ye JH, Luo E, Schuler M, et al. Enhanced osseointegration of titanium implant through the local delivery of transcription factor SATB2. Biomaterials. 2011;32(33):8676–83.

106. Chikazu D, Tomizuka K, Ogasawara T, Saijo H, Koizumi T, Mori Y, et al. Cyclooxygenase-2 activity is essential for the osseointegration of dental implants. Int J Oral Maxillofac Surg. 2007;36(5):441–6.

107. Xiang L, Ma L, Wei N, Wang T, Yao Q, Yang B, et al. Effect of lentiviral vector overexpression alpha-calcitonin gene-related peptide on titanium implant osseointegration in alpha-CGRP-deficient mice. Bone. 2017;94:135–40.

Preclinical Studies Design and Place of Rabbits

3

R. Sandgren

3.1 Experimental Animal Model

3.1.1 Animal Species: Naturally-Occurring, Purpose-Bred and/or Genetically Modified

Rabbits are small mammals from the family *Leporidae* and the order *Lagomorpha.* Initially, they were classified in the same order as rodents, but later they were separated into their own order because of anatomical differences described by Gidley 1912 [1]. These include that the rabbit has two pairs of incisors in the upper jaw with its additional peg teeth, compared to rodents with only one pair [1]. There are differences in the dental formula, and in addition, there are also differences in the chewing pattern, with only lateral chewing in the rabbit but anteposterior and lateral in rodents [1].

Rabbits used in research originate from the European rabbit, *Oryctolagus cuniculus*, which was spread from their native habitat, the Iberian Peninsula, and now exists almost all over the world [2].

There are many breeds that display a wide range of different features such as size, ear formation, and color. The most common breed used in the laboratory is the New Zealand white [3], which has a bodyweight of 2–5 kg [4].

Other popular breeds are the Flemish Giant (≥9 kg) and the Dutch Belted (1–2 kg) [5], as well as the Polish and the Lop rabbits, commonly used in implant research [6].

Laboratories have developed different strains and lines for research, some of them inbred [2]. Since 1985 it is also possible to get a transgenic rabbit model [7].

Rabbits can be purchased for research from commercial animal breeding facilities and local breeders. Local breeders usually do not have the same health status as commercial breeders, which usually produce specific pathogen-free animals and follow a health-monitoring program. The commercial animal breeding facilities also have standardized breeding programs, housing, and handling of the animals. This entails the production of high-quality animals.

3.1.1.1 Animal Welfare
Animal welfare should be thoroughly considered when performing research. If the welfare of the laboratory animal is compromised, the results from the experiment may be compromised as well.

The welfare of an animal has many dimensions, such as type of housing, health status, access to enrichment, outlining of the research procedures, mentioning a few. Foundational principles regarding animal research ethics and ani-

R. Sandgren (✉)
Centre for Comparative Medicine, CCM, Lunds Universitet, Lund, Sweden
e-mail: rebecca.sandgren@med.lu.se

mal welfare can be found in Russel and Burch's description of the three Rs (3Rs), replacement, reduction, and refinement [8], which should always be fulfilled.

Animals are covered by a national federal animal protection act that varies between countries. These regulations are minimum standards that must be followed. The animals should be handled and treated in the best possible way. The environment should mimic natural but still allow standardization.

3.1.1.2 Handling and Husbandry

For handling and husbandry, it is important to have knowledge about natural behavior and needs of the rabbit.

Rabbits are herbivores [2] and nocturnal animals that grace in groups [9]. They are very social and territorial [9]. They mark their territory with scent glands and feces [9]. The rabbit is a reserved and anxious animal in unfamiliar territory because it is a prey species [10]. This behavior can make them difficult to handle and examine because they can either become immobile or struggle with stress when being handled [9]. In the wild, rabbits dig burrows in the ground to hide away from predators and heat.

The national regulations concerning housing must be followed but should, if possible, be better. Housing properties should make room for natural behavior, with an elevated area, a place to hide, and sufficient space. The space should not only be large enough to contain a rabbit but should provide the ability for the rabbit to move around and stretch out its long body. This will prevent obesity and stereotypic behavior.

For laboratory rabbits, there are specially designed cages that fulfill many of the housing conditions. These cages give the possibility of a single housing. If rabbits are alone in their cages, it is important that they can see and smell other rabbits [3]. This is important from a welfare aspect, since rabbits live in large groups in nature.

If possible, social housing should be chosen, which gives them the possibility of interacting with other rabbits and a larger space to move around [3]. However, in case of surgery and implantation in the legs of the rabbit, it can be

preferable with initial single housing, to reduce the risk of fractures. Sexual mature males should not be housed together, because of severe fighting [3]. Female rabbits also fight, although generally less so and with less severe consequences.

The rabbits should also be provided environmental enrichment. This can be accomplished with hay and straw. It can even be toys to play with. Food items can also be enriching, like a piece of apple, banana, or carrot. However, the risk of infection from bringing these items into the animal facility must be considered.

Diets should be adapted for laboratory rabbits and meet their nutritional needs. The amount should be limited to prevent obesity, which is a common problem in laboratory settings [4]. Diets most often come in the form of a pellet; therefore, the rabbits should also be offered hay, straw, or a woodblock for the wear of the incisors. High-fiber content is important for a healthy gastrointestinal canal. They should be provided ad libitum fresh water.

Most laboratory animals are transported between animal facilities before the experiments. This very stressful situation can increase the risk of disease [11] and affect physiologic parameters [12]. Since the rabbit is anxious in new environments, time should be given, for acclimatization in the new animal facility, before an experiment starts [13]. If the animal is not acclimatized enough, it will be stressed and unsuitable for experimentation.

The duration of the acclimatization period depends on several factors, the experimental procedure being one of them, and is therefore difficult to determine. There are recommendations that it should be at least 7 days, but preferably it should be 14 days [14].

The anxious behavior of the rabbit and the fact that it is a prey animal should be considered during handling. This will prevent injury to the rabbit as well as to the researcher. During acclimatization, the rabbits can get familiar with the environment and handling. When the experiment starts, they will be less prone to stress.

Common signs of pain can be anorexia, immobility, and aggressiveness [9]. A rabbit can also scream from pain and fear [9].

There are different techniques for handling, and these should be trained before contact with the rabbits. Rabbits should not be grabbed by their ears; instead, they should be grabbed by the skin on their neck. Also, the backlegs must be supported to prevent spine fractures and prevention from being scratched. See Fig. 3.1 for the holding technique. For fixation, different devices can be used, and an example is displayed in Fig. 3.2, although wrapping them in a cloth is also useful.

Fig. 3.1 Handling techniques where the legs and body of the rabbit are supported

Fig. 3.2 Fixation box

3.1.1.3 Health Status

From the animal welfare point of view, it is important to know the health status of the animals. Rabbits with unknown health status can appear healthy but have subclinical infections that can manifest themselves during stress or during anesthesia [14].

Individuals that are free from agents that can interfere with the research and animal welfare should be selected. Known health status also makes it easier to reproduce the results of a study [15]. There are recommendations available for which agents to test for in rabbits [15].

3.1.2   General Use in Medical Devices Research

Animal research is needed for in vivo testing of new materials for biocompatibility and mechanical evaluation. The rabbit as an animal model is common in medical device research because of its many advantages compared to other species.

The rabbit is suitable for implant research where dental implants and different forms of biomaterials can be tested [16]. Because of its bone properties, it serves mainly as a screening model before implants are tested in larger animals [17]. However, it should not be used as a routine and must be well-motivated before being chosen as a model.

Osseointegration is dependent on two main parameters, which form the basis for most research on dental implants and bone substitute implants [6]. These are; the surface characteristics of an implant and the implant design [18]. Interaction between the implant and the biology of the host is of clinical importance both in human and veterinary medicine [19]. Animal models allow testing of the tissue close to the implant but also for studying wear particle debris in other locations of the body [19].

Research in implant dentistry is important for solutions regarding esthetical and functional problems in patients with tooth loss [18]. The volume of bone available at the implant site is

crucial for the placement of a dental implant [20]. Severe bone loss can lead to rejection of an implant [20]. To increase bone volume, there are different options for bone augmentation, like onlay bone grafting and guided bone regeneration [21]. The desirable outcome of dental implant research is shorter treatment time and less surgery-trauma to human patients [22]. This can be achieved with early or immediate loading of the implants [23] and bone-stimulating characteristics of implants.

Implants can be of different materials and shapes, with surface treatments and with coatings [24]. Titanium is still considered the gold standard and is widely used in orthopedic and dental implants [25]. Yet advances in dental implantation are ongoing to find characteristics that will stimulate bone healing and increase osseointegration. Grafting material is subject to research and newer technology, tissue engineering [26].

Biomaterials can be put in bone defects, usually a critical size defect (CSD). CSD is a defect that has been described by Hollinger and Kleinschmidt [27] as a defect that does not regenerate more than 10% of its prior bone during the lifetime of an animal.

Medical devices can also be tested in rabbits, where the model mimics different bone diseases and characteristics of bone found in humans. These are characteristics like; bone loss—since rabbits have endosteal bone loss throughout life [28]; irradiated bone, as often the case in clinical situations [29]. Also osteoporosis, induced in ovariectomized rabbits as monotherapy [30] or with either glucocorticoid treatment [31] or a low-calcium diet, can be applied with similar histologic changes as in the human diet [32].

Diabetic rabbits can also be used in implantation models. Hou et al. [33] investigated the effect of insulin on grafting in the maxillary sinus. In their study they induced type I diabetes in rabbits with intravenous monohydrated alloxan to impair the pancreatic beta cells. They then compared diabetic rabbits receiving insulin with nontreated individuals and showed several significant differences including the observation that insulin promotes bone formation in diabetic rabbits [33].

In a review by Tsolaki et al. [34], the outcome of dental implants in osteoporotic individuals in animals and human patients is summarized, showing the varying results of implants in jaws and other skeletal sites, but without controversy in osteoporotic patients. Therefore the osteoporotic rabbit model can be applicable, with the awareness that the effects of osteoporosis on different bone sites, cortical versus trabecular bone, can be different [35].

As with all other animal models, it is important to have knowledge of anatomy and physiology to know where the model is different from the human and how to interpret and extrapolate research results. When choosing the rabbit for research, one must consider the advantages and disadvantages of the model. This chapter highlights these differences and guides why and when to choose this model.

3.1.3 Financial Considerations

Although cost is always an important parameter when setting up a study, the scientific value of the research must be prioritized. The most suitable model must be chosen, including the correct choice of species, proper study design, and animal welfare. Otherwise, the study would be unethical.

Rabbits are easy to breed and, therefore, easy to acquire. Individuals can be more cost-effective compared to larger animal models [36], although specific pathogen-free animals can be more costly. For example, the fast bone turnover makes the healing periods shorter, leading to shorter experimental time and, therefore, less housing costs.

Using an animal of intermediate size can be advantageous. The number of animals needed for a study can be reduced since their size makes it possible to place multiple implants and have

internal controls [37], compared with the rat, where the number of implants is limited due to size [17].

3.2 Surgical Model: Surgical Anatomical Site and Surgical Procedures for Implant Dentistry

3.2.1 Surgical Locations, Anatomy, and Histology

Following information is anatomical facts and comparisons with humans that are important for the suitability of the rabbit as a surgical subject for the study of dental implants.

3.2.1.1 General Anatomical Information

General anatomical features of the rabbit should be mentioned, such as their fragile skeleton [38], weak spine, and strong muscles, which make them prone to fractures [39]. This information is important to bear in mind during the handling of the animals.

At about 6 months, the rabbit is sexually mature, and a peak in bone density occurs [40]. Up to 6 months, mineral deposition is continued, cortical thickness is increased, and bone mechanical properties are enhanced [41]. Masoud et al. studied the bones of New Zealand white rabbits and found that skeletal growth was complete at 28 weeks [42]. Ossification processes and size of the rabbit are determined by the same race-specific genes [43].

Similar to humans, throughout the rabbits life, the bone continues to remodel, with positive bone balance on the periosteal bone surface and negative balance on the endosteal surface, which with aging, results in expansion of the bone marrow [28]. Also, the toughness of rabbit bone is similar to human bone [44].

When looking at remodeling, the sigma value (time of remodeling cycle) in humans is 3–4 months [45], compared to 6 weeks in rabbits and the appositional rate of 2 μm per day in the rabbit [46]. Roberts et al. concluded that 6 weeks

is an adequate preloading and healing time, as indicated by histology and biomechanical testing [46]. These facts make it possible to extrapolate the healing time of bone to clinical studies, where rabbit has about three times faster bone formation, remodeling, and maturation than humans [46].

The rabbit skeleton comprises 70–80% of cortical bone [40]. It is distributed in longbones making up the diaphyses and on the surface of the epiphyses. Also, the surface of the shortbones and outer and inner layer of the skull is made up of cortical bone [47].

Trabecular bone is found inside the longbones and between the cortical layers of the skull [47]. Bone marrow is found between the trabeculae in trabecular bone [47]. Trabecular bone is more metabolically active than cortical bone [47].

3.2.1.2 Extraoral

Femur and Tibia
Tibia and femur are long bones, like all mature mammalian bones they consist of lamellar bone. Rabbit cortical bone has a primary vascular longitudinal structure [48], a different microstructure compared to humans, with a secondary osteonal bone structure [44].

The different layers of femur cortical bone were investigated by Martiniaková et al. [49], and their microstructure was described. There are four layers as follows:

- the innermost layer is built up by primary longitudinal canals,
- the next layer shows scarce Haversian systems and dense Haversian remodeling,
- the next is primary vascular radial but mostly longitudinal bone tissue,
- the outer layer, close to the periosteum, consists of primary vascular longitudinal bone.

The morphology of the cortical bone is determined by the size and shape of the bone-forming units [50]. The rabbit has short primary vascular canals in the primary osteons with a mean value of 12.49 μm in diameter, and the mean diameter of the Haversian canals of the secondary osteon

is 17.49 μm [49]. Compared to humans and larger mammals (pigs, cows, and sheep), these structures are the smallest in rabbits [51].

Also, the microstructure within the same species can be dependent on several factors such as age [52], genetics [53], environmental factors [47], and length of the bone [50]. Also, diet has a great effect on bone regarding function and development [47].

Longitudinal growth of the long bones, dependent on endochondral ossification, stops when the rabbit is about 6 months of age [50]. Kaweblum et al. [54] performed a radiographic and histologic study determining the closure of growth plates in the New Zealand white rabbit and found that the distal femur closes, histologically and radiographically 19–24/20–23 weeks, respectively, growth plates in the proximal tibia close at 25–32/22–27 weeks [54].

The formation of new bone in the tibia has been shown to be the way mature tibial bone is arranged, with cortical layers with bone marrow in between [55].

Comparing juvenile and adult bone shows primary vascular longitudinal structure in both [52]. However, juvenile bone has shown to differ in from adult bone with lower density of secondary osteons and measured variables of primary osteon vascular canals, the Haversian canals and the secondary osteons were higher [52].

Macroscopically there are differences compared to humans in both size and shape. The thickness of the tibial cortex of diaphysis and metaphyses is thin, about 1.5 mm [56].

Skull

The calvaria is a flat bone, the membranous part of the skull formed by intramembranous ossification [57]. Embryologic development of the rabbit calvaria is similar to the of human [58]. Also, the embryology of the maxillofacial bones is the same as well as the morphology in the calvaria [59].

The bones of the skull consist of cortical bone in the inner and outer layer with thin trabecular bone in between [47]. Slotte et al. studied the morphology of the skull, and they found natural hollow connections in the cortex, and that the right and left bones of the skull have symmetrical vessels, bone proportions, and density; thus, the bilateral use in research is, therefore, reliable [60].

The frontalbones also show age-related changes in qualitative and quantitative microscopic structures [61].

3.2.1.3 Intra Oral

Maxilla and Mandible

Rabbits have teeth that are hypsodont [3]. The permanent teeth of the rabbit erupt continuously [62]. A crown and root do not separate the teeth and have open apexes [63]. Other characteristics are their peg teeth and the diastema between the incisors and premolars [3].

The edentulous diastema in the maxilla has been described by Lundgren et al. [64]; it consists of a compartment of trabecular bone with cortical bone around it. Lateral cortex has been described as thick and dense with a vaulted and even shape. The medial cortex plate is much straighter than the lateral. Together with the lateral plate, the medial fuse at the ridge where the cortex is the thickest. The trabecular bone of this area contains little trabeculae and is, therefore, almost filled with bone marrow.

In the mandible, described by Campillo et al. [63], the posterior area with teeth has low bone volume, and the roots take up a significant part of the mandibular bone. It should also be mentioned that the alveolar nerve runs in the alveolar canal and passes by the apexes. In the anterior area, between incisors and premolars, the bone volume is larger and contains trabecular bone.

Sinuses

The maxillary sinus in the rabbit is just like in humans, covered on the inside with the Schneiderian membrane. The air pressure in the rabbit maxilla is the same as in humans-isobaric [65], and the air pressure will keep the bony wall of the sinus in place [66].

3.2.1.4 Function and Physiology (Movement, Loading)

Implants in rabbits will not be loaded the way they will in human jaws. This is because they will never be connected with an abutment and prosthesis used for chewing, whether it is placed in the oral cavity or not. Even if they were to be used for chewing, rabbits do not have the same chewing pattern as humans [1].

However, there can be a load on the implants from the rabbit, affected by the posture and movement of the rabbit, movement of muscles, and other overlying tissue. Also, an applied load from attached devices can be used [46, 67]. Extraoral sites are easily accessed for daily loading [68].

3.2.2   Surgical Procedures

3.2.2.1 Description of the Procedures; Preparation to Survival Surgery and Anesthesia (General, Local)

Antibiotics

Antibiotics are sometimes administered as prophylactics as a part of the research protocol to avoid infections. It can even be administered in case of postsurgical infections. Postsurgical infections can inhibit healing and can lead to the termination of the animal before the endpoint is reached. However, the use of antibiotics should be restricted to avoid contribution to the development of antibiotic resistance. Instead, sterile surgical techniques should be used. Also, the rabbit is sensitive to antibiotics, with administration leading to gastrointestinal disturbances [36]. A veterinarian should be consulted to evaluate a postsurgical infection and medication with antibiotics.

Preoperative Care

Preoperative preparations and treatments are very important for the course of good anesthesia, including the choice of drugs and handling of animals [14]. Rabbits are very prone to stress, and in combination with anesthesia, it can lead to cardiac and respiratory arrest [69].

Rabbits should not have fasted for the avoidance of gastrointestinal disturbances, and neither can they vomit [69].

There are many anesthesia protocols available for rabbits. The most important aspect of anesthesia is to use a refined protocol that the user is familiar with. It should be a suitable protocol for the procedure that provides a sufficient duration and level of anesthesia [14]. A protocol with all equipment and techniques should be described for the possibility of reproducing a study and increase scientific value.

Intraoperative Care

The anesthesia required for any procedure depends on the level of pain. For surgical procedures, pain perception must be suppressed either by general, local, or regional anesthesia [14]. For managing anesthesia and evaluating the required level, skills and training in the field is necessary. Therefore including a veterinarian prior to and/or during the procedure is preferable. Different equipment for monitoring physiologic parameters can help the management, but it is not always necessary if the clinical assessment of sufficient vital parameters can be done. Control of temperature and oxygen saturation in the blood are examples of parameters that are recommended to be monitored, except for pulse and number of breaths, which can be monitored without equipment.

Other intraoperative considerations apart from the anesthesia are factors that can help maintain balanced physiology and welfare, such as heatpads, intravenous fluids, eye moisture, and oxygen supply.

Despite many different rabbit anesthesia protocols, none are specifically made for implant dentistry. The only requirement is general anesthesia. General anesthesia can be achieved through intramuscular injection, intravenous route, and inhalation anesthesia, with a row of different compounds, alone or in combination.

Flecknell lists different regimes that can be used for rabbits in laboratory settings including tranquilizers like fentanyl/fluanison, medetomidine, xylazine, acepromazine, diazepam, ketamine, alfaxalone/alphadolone [69]. Flecknell

also mentions that fentanyl/fluanison with diazepam or midazolam is a good choice for anesthesia in rabbits. In addition, combinations like; ketamine with medetomidine, fentanyl with medetomidine, thiopentone, and propofol can be administered [69].

Inhalant agents can be used in rabbits but should be avoided as induction agents because it induces aversive reactions in rabbits [70, 71]. It should always be administered after premedication with an injectable drug [69].

When inhalant agents are being used, the rabbit can preferably be intubated. Intubation is also important for maintaining the airway. The technique is not easy on the rabbit and should be practiced before the experiment starts [72]. Intubation is also required where the animal needs mechanical ventilation. In the case of apnea, artificial breathing and the placement of a larynx mask can be lifesaving.

Postoperative Care

Postoperative monitoring is just as important as monitoring preoperative and during surgery. It is the most common time for an animal to die [73]. Animals should be monitored during this time until they are fully awake. When they have recovered from anesthesia, they can return to their homecage.

Local Anesthesia

Local anesthesia is useful as preemptive analgesia and reduces postoperative pain [74]. Common drugs are lidocaine and bupivacaine, which can both be administered as an anesthetic cream for topical use [75]. Drugs can also be injected epidurally [76], subcutaneously, and for local nerve blocks [14].

Pain Management

Pain should be avoided in all possible events; pain relief is important in animal welfare. For complete refinement, pain should be recognized and treated; however, in rabbits, it can be difficult to recognize and demands an understanding of the behavior and physiology of the rabbit [72]. Though pain management awareness is increasing in clinical and laboratory animal medicine [10], Coultier et al. present data showing that rabbits undergoing surgical procedures, especially orthopedic, are not sufficiently pain relieved [77]. This is a welfare problem that needs to be addressed [77]. In the case of survival surgery, multi-modal, preemptive, intra-, and postoperative analgesia should be used [78, 79].

A grimace pain face scale can help the rabbit evaluate and recognize pain [80]. Other indicators of pain are anorexia and weightloss [78], teeth grinding, reduced growth of fur, and reduced motility [72].

For analgesia, opioids as well as nonsteroidal anti-inflammatory (NSAIDs) agents, can be used. Common opioids are butorphanol, buprenorphine, morphine, hydromorphone, oxymorphone, and fentanyl [10]. When using these agents, one must be aware of the side effects. Especially fentanyl can cause adverse effects like as anorexia and ileus; however, pain-induced ileus can also occur and is much more difficult to treat [10]. Buprenorphine and butorphanol are commonly used to treat mild to moderate pain [10].

NSAIDs are commonly used analgesics and have anti-inflammatory and antipyretic effects and few side effects [10]. Meloxicam is the most common one used in rabbits [72].

NSAIDs and Their Effect on Bone Healing

NSAIDs can inhibit bone healing because inflammation is important to healing [81]. They are thought to inhibit by reducing the level of prostaglandins [82] that play an important role in the regulation of bone formation [83]. The effects on bone healing are various [84]. The various effects on bone healing, when different studies are compared, are probably due to differences in dosage and the length of treatment [85]; also, the type of surgery and bone defects have been different, and results are difficult to compare.

3.2.2.2 Description of the Procedures; Surgical Step by Step

Anesthesia and animal preparations should be done with an emphasis on animal welfare and suitable anesthesia and analgesia, as previously discussed in this chapter. For all surgical sites, the preparation is the same; the fur is shaved, the skin cleaned, disinfected, and covered in a sterile manner. Local anesthesia is then injected subcutaneously. During

drilling, irrigation with sterile saline should be used to prevent damage to the bone from heat. The procedures that are being described can be modified to their own need. After implantation, the periosteum and muscles are sutured, followed by subcutaneous and cutaneous sutures. A size 15, scalpel blade in the following sites can be used for incision. Sutures of size 4/0-3/0 are suitable. Absorbable sutures in tissues other than the cutis should be used. In the cutis, nonabsorbable sutures can be used. Generally, the number of implants recommended in the rabbit model is a maximum of 6, with three tests and three controls, in each rabbit [86].

3.2.2.3 Extraoral

The size of the implants that can be placed into tibia and femur are 8–10 mm in mean length and with a mean diameter of 4 mm [16].

Tibia

In the tibia, screws can be placed [87], as well as coin-shaped implants [88]. Also, defects for bone augmenting biomaterials can be made and evaluated using a critical size defect of 6 mm in longbones [89]. In this area also, bicortical implants can be placed [90].

Below follows a description of the procedure in the **proximal tibial metaphysis/diaphysis area** as previously described [91]:

- During the procedure, the rabbit should lie on its back. Keep the knees slightly bent.
- Make an incision on the medial side, along the leg, about 5 cm long, starting about 0.5 cm from the joint.
- With blunt dissection of the muscles and gentle lifting of the periosteum, the bone is exposed. Once the bone is uncovered, implantation/making of the defect is possible, see Fig. 3.3.
- To access the lateral side, the rabbit can lie on its side. The lateral side of the proximal tibia can be accessed like described above for the medial side.

In the proximal tibia, implantation can also be done with coin-shaped implants; Ronold and Ellingsen [88] presented the use of a coin-shaped titanium implant that was put in a leveled platform.
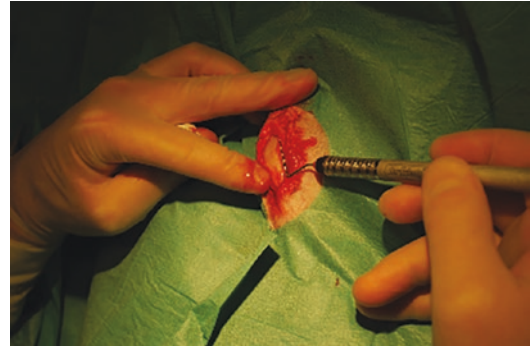
Fig. 3.3 Exposure of the metaphysis/diaphysis area
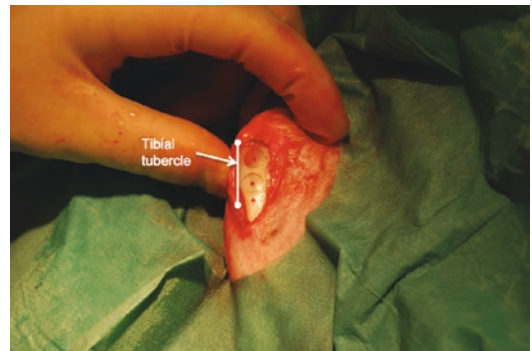
Fig. 3.4 Two circular defects on the flat area of the proximal tibia. Tibial tubercle is marked for orientation

In the previously mentioned study, the procedure was performed, described in detail in the following text, after the exposure of the proximal tibial area:

- Four guide holes are made, using a 1.0 mm twiat drill, with a guide for correct positioning. It is important to adjust the holes so that the placement of the implants does not involve any soft tissue. They should also be adjusted so that they fit on the flat area of the proximal tibia, usually along the tibial tubercle, as shown in Fig. 3.4.
- Make a leveled platform, see Fig. 3.4, with a 7.05 mm bur, slow speed, and saline irrigation.
- Place the implants, with a plastic cap on, 6.25 mm diameter and 1.95 mm height.
- Place a retainer (0.2 mm titanium maxillofacial retainer) to hold the implants in place, with one proximal and one distal 1.23 mm titanium screw, see Fig. 3.5.

Instead of titanium implants, other coin-shaped materials can also be placed in the same manner.

Femur

Locations in the femur for implantation include the knee joint [87], distal femoral lateral condyle [92], distal femoral medial condyle [93], and diaphysis [94]:

Knee Joint

- Skin is incised on the lateral side over the knee, followed by an incision in the fascia and capsule, to access the cartilage, see Fig. 3.6. Make sure not to damage the tendon of the extensor digitorum longus.

- The patella can be medially dislocated, and the cartilage implanted, see Fig. 3.7.
- Capsule, fascia, and skin are then sutured in separate layers.

Distal Femoral Lateral Condyle

- About 1 cm skin incision made on the lateral side of the knee, toward the femoral condyle.
- Dissect muscles to make the periosteum available. Dissection of muscles should, if possible, be done between the muscles, M. Vastus lateralis and M. Biceps femoris, instead of through them, as shown in Fig. 3.8.
- Periosteum elevated for bone exposure.
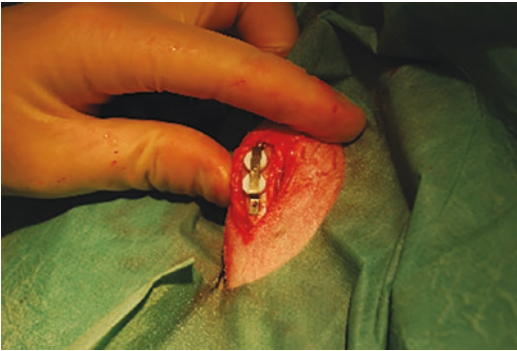
Fig. 3.5 Implants have been placed, and the white plastic caps can be seen with a titanium retainer on top for fixation

Fig. 3.6 Lateral view of the knee with the incision in the fascia. Note that skin has been removed for visibility of underlying structures

Fig. 3.7 Medial dislocation of the patella with exposure of the trochlear cartilage where defects can be made. Tip of forceps pointing at the groove were the patella glides between the medial and lateral ridges. Tendon of extensor digitorum longus marked with the black arrow. M. Biceps femoris marked with white text for orientation

M. Biceps femoralis

Tendon of extensor digitorum longus
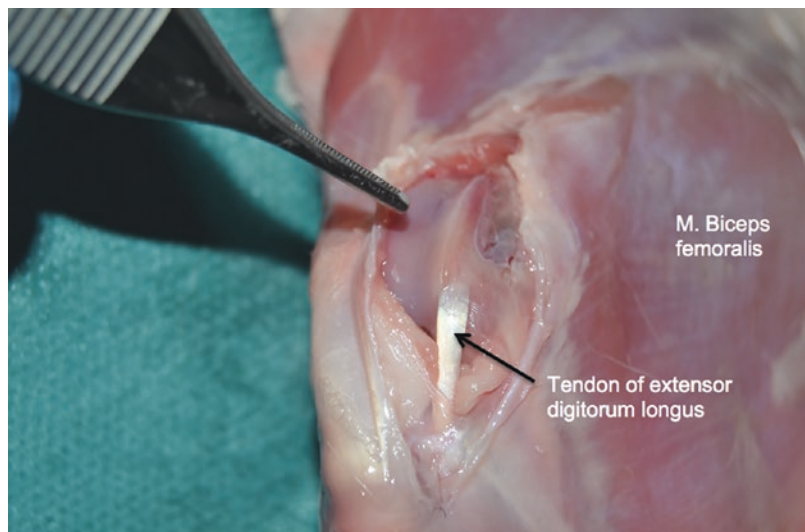
Fig. 3.8 Figure showing the separation of muscles M. Vastus lateralis and M. Biceps for access to the lateral femoral condyle. Bone exposure of the condyle is seen between the two needles. M. Tensor fascia marked for orientation
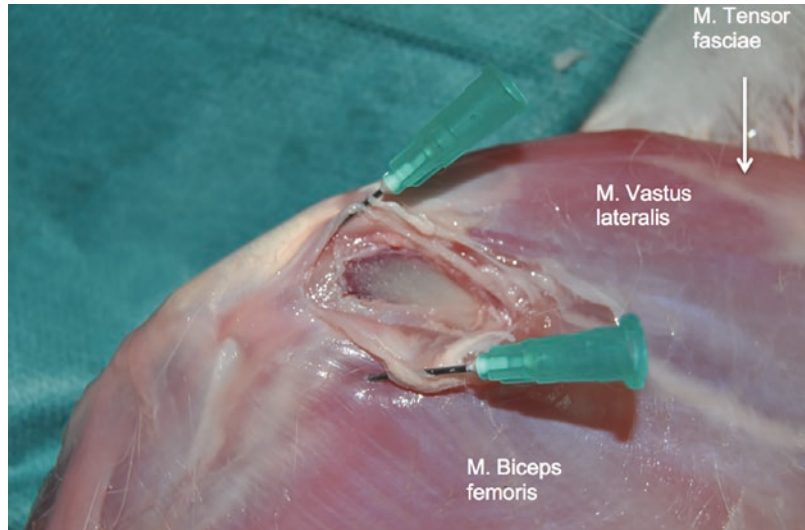
Fig. 3.9 Medial view of the knee with medial condyle visible and the area for implantation and making of the defect. For access to this area, M. Vastus medialis (white arrow) has been dissected
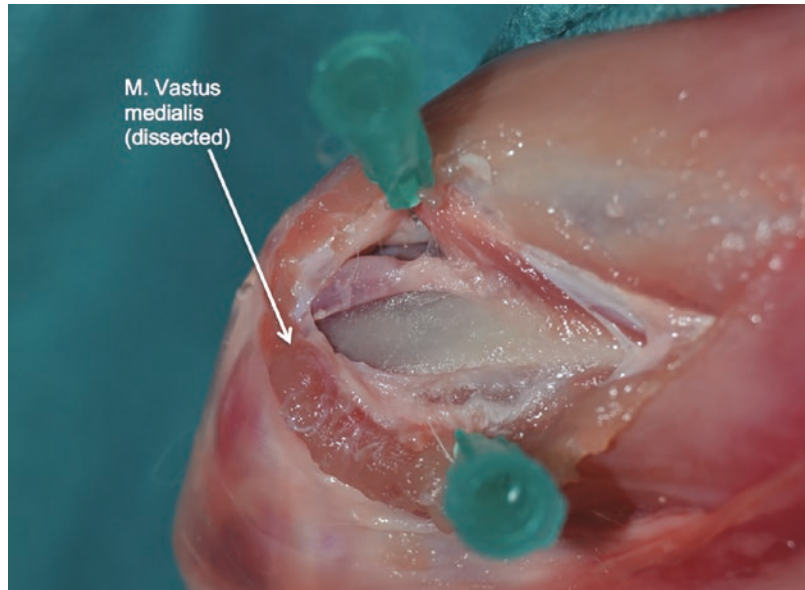
- Implantation made on the central area of the condyle.
- Care must be taken not to incise the joint capsule.

Distal Femoral Medial Condyle
- Skin insicion, about 3 cm, on the medial side of the knee, followed by blunt dissection of muscles and reflection of periosteum.

- The medial aspect of the condyle should be exposed as a flat area where drilling or making of a defect can be done, see Fig. 3.9.
- Care must be taken not to incise the joint capsule.

Diaphysis
- Anteromedial incision and dissection to expose the bone of the shaft. Try to dissect

between the muscles instead of through them for minimum trauma.

- Implantation can be made along the middle of the shaft.

Skull

The calvarium (parietal bone, frontal bone, and occipital bone) is easily accessed through only a thin layer of tissue. For surgery of the skull, the rabbit should be in a ventral position.

- Skin incision in the midline.
- Reflection of tissue to expose the calvarial bones, see Fig. 3.10.

After exposure of the skull, defects can be created, and implantation performed in different sizes, and numbers, depending on the hypothesis being investigated. Commonly defects are done by drilling 1–4 cylindrical holes [6], as a critical size defect of 15 mm [95]. A trephine bur can be used for making the defect. While transosseous defects are made, care must be taken not to damage the dura mater nor to include sagittal and coronal sutures [96]. Therefore the depth of the defect should be controlled continuously during drilling, for example with a neural elevator, and stopped just before completely penetrating the inner cortex [97].

Hopper et al. used full-thickness cranial defect for orthotopic grafting, in cylindrical holes 15 mm in diameter, between the coronal and lambdoid suture [98]. In the previously mentioned study a silicone sheet was placed to isolate the dura, hence making the graft dependent on the calvarial bone edges for vascularization and bone remodeling cells [98]. A barrier device in the form of a titanium cylinder can also be used as a barrier to evaluating wall influence on augmented bone [99].

Calvarial bone can also be used for implant assessment through loading of the implants and transcutaneous measurements, and this was investigated with the implantation of two titanium implants in the midsagittal suture, 11 mm apart, and connection with a wire between the abutments on the two implants [67].

Assessment of implant stability through transcutaneous investigations has also been described in the nasal bone [100]. Access to the nasal bone has proceeded similarly to the calvarial bone but incision along the back of the nose. These implants were also evaluated by applying a loading force.

3.2.2.4 Intraoral

Intraoral investigation and application of loading forces are not as common as investigation in the

Fig. 3.10 Anatomical landmarks of the rabbit calvarial bones for orientation
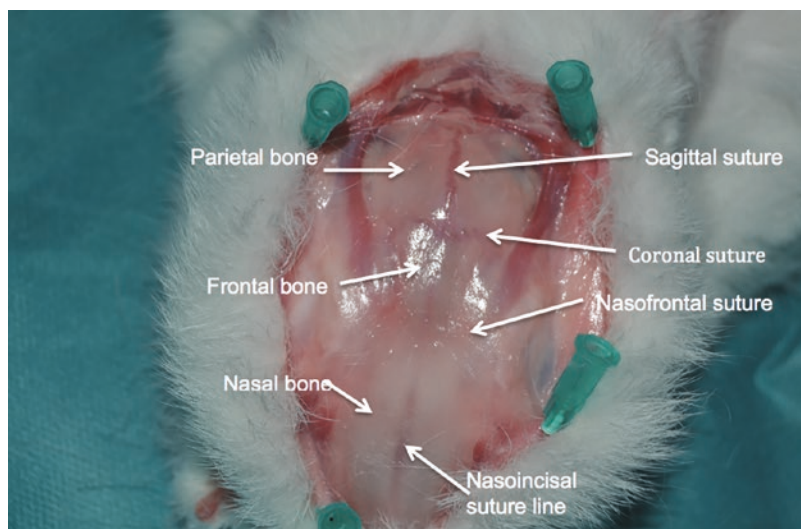
extraoral sites due to technical issues and animal compliance [16].

Maxillary Sinus
The rabbit sinus model is used to evaluate various grafting materials and implants [101].

The maxillary sinus can be reached through different sites; transcutaneously through the nasal dorsum [66], through lateral antral wall of maxilla [102], and more seldomly through the oral cavity [103].

Asai et al. [66] established a model for **maxillary sinus augmentation**, a procedure described in detail as follows;

• Incision in the midline about 5 cm long, on the nasal dorsum.
• Elevate skin and periosteum for exposure of the bone.
• For identification of the nasoincisal suture line, see Fig. 3.10.
• A circular window is made, about 5 mm in diameter, 20 mm anterior to the nasofrontal suture line and 10 mm lateral to the midline, without damaging the sinus mucosa.
• The mucosa is stripped off to make a hollow space.

Sinus lift, lateral antral wall, described by Watanabe et al. [102]:

• Insicion a few millimeters above the inferior border of incisive bones and the maxilla.
• Subcutaneous tissue and muscles were dissected to expose periost.
• Periost elevated dorsally.
• Trap door in the lateral antral wall of maxilla, see Fig. 3.11, is made with a diamond bur, without perforating the antral membrane.
• After fracturing the trap door into the sinus cavity, the antral membrane was elevated from the sinus floor.
• Autologous bone is placed in the cavity.

Rabbit sinus model was previously a two-stage sinus floor elevation. Young-Sung et al. introduced a one-stage sinus floor lift with a simultaneous implant in the rabbit model, where they placed mini-implants on the edentulous alveolar ridge [101]. A one-stage sinus lift is clinically preferred since it reduces the treatment time [101].

Sinus lift, oral cavity, described by Rahmani et al. [103]:

• One centimeter incision in the mucosa, overlying the alveolar ridge below the sinus, starting with a distance of 4 mm from the mesial of the maxillary first molar tooth.
• Make a full-thickness mucoperiosteal flap.
• Osteotomy for the placement of both grafting material and an implant, 3 mm long. The

Fig. 3.11 Blue circle showing the anatomical location of the trap door just in front of the infraorbital nerve and artery (white arrow)
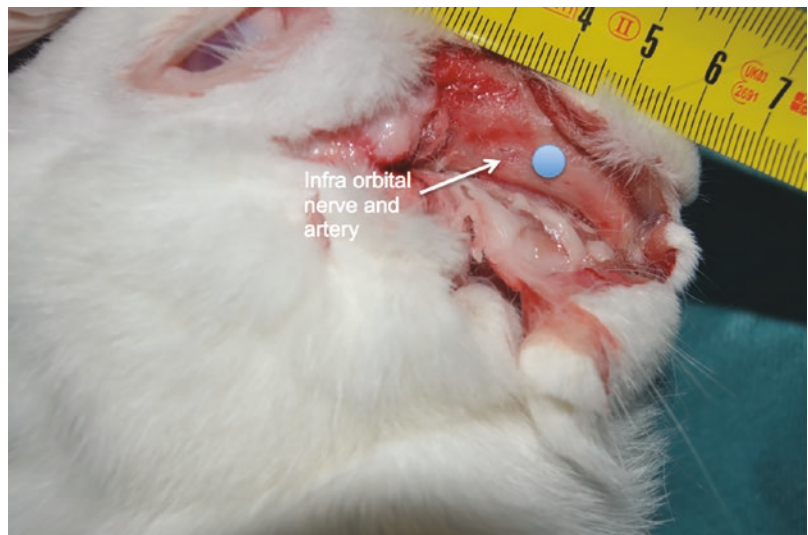
implant extends 1 mm into the sinus cavity, since the bone below the sinus is approximately 2 mm thick.

Maxilla

The edentulous space that rabbits have between the incisors and molars in the maxilla, diastema, has been used as a model to test the healing of the jaw bone defects [63, 103] and can be described in detail as follows:

- About 1.5 cm incision, either on the alveolar crest or lateral to the crest between the incisor and the first premolar; see Fig. 3.12 for maxillar edentulous bone.
- A mucoperiosteal flap is raised to expose the buccal bone of the maxilla.
- Implantation/alveolar ridge augmentation.
- Suturing of the flap.

Mandible

Extraoral access to the mandibular bone can be made through the skin in the submandibular region, see Fig. 3.13. CSD in the mandible is 5 mm [104].

Inferior Border Defect [104]
- Incision in the submandibular midline.
- Dissection through subcutaneous tissue and muscles to expose the inferior border of the mandible, both medial and lateral walls. Avoid damaging the fascial artery on the medial side along the mandibular angle.

Fig. 3.12 Figure showing maxillary edentulous bone exposed. Note that the cheek has been incised only to make the diastema visible

Fig. 3.13 Exposure of mandibular bone where implantation can take place

- A periosteal flap is raised, exposing the area where defects can be made without one or both cortical walls.

Posterior Mandible Placement [105, 106]
- Insicion above the mandibular angle.
- Dissection of subcutaneous tissue and muscles to expose the lateral area of the posterior mandible.
- In the posterior mandible, implantation can take place. It has been described that a scaffold retention screw can be placed as an umbrella when implants and biomaterial scaffold are placed simultaneously, to protect the scaffold from external influences.

Placement in Mandible Body
This can be made as a partial-thickness or full-thickness defect with or without intraoral communication, with similarities to clinical conditions, such as trauma, infection, and developmental bony defects where periosteum is retained [107].

In detail, as described by Shah et al. [108]

- Incision in the submandibular region.
- Dissection through subcutaneous tissue and muscles, until the lateral wall of the mandible is exposed.
- The defect can be made in the molar/premolar area of the mandible.
- A trephine bur can be made to drill through the lateral cortex. The cortex plate can then be lifted with a periosteal elevator, thereby expos-

ing the teeth roots. Three roots should be visible.

- Drill through the roots and remove them. Implantation could be made here if a partial-thickness defect is the aim.
- For full-thickness defect: use a trephine bur to drill through the lateral cortex and lift the cortex plate and carefully dissect the periosteum.
- Implantation can be made here.
- For intraoral communication: this is done by removing the tooth/crown of which the whole root was removed, usually the central one. Drilling should be made using the margins of the tooth as a guide. Remove the tooth/crown when it is loose.

Implantation can now be done. A fixation plate can be used across the implant for fixation or along the inferior border of the mandible for the prevention of fractures. Muscle fascia and skin are sutured.

In the study of Young et al., they describe that the partial-thickness defect will contain endosteum and periodontal ligament cells since the roots are still present, leaving a potential osteogenic stem cell population available for the healing process, unlike the full-thickness defect [107].

Yazan et al. placed two customized implants in the molar area with enough distance from molar teeth apices for intramembranous ossification [109].

Alveolar Ridge Augmentation [110]
- Extraction of one of the lateral incisors and socket left to heal for 2 weeks.
- Incision in the gingiva down to the periosteum in front of the first molar, which is the area where a full-thickness defect can be made and filled with bone augmenting material in accordance with the individual research protocol.
- Gingiva is then sutured.

Tooth Extraction Socket Model
This model has been used by Lalani et al. where the incisors in both the mandible and maxilla were extracted, and the healing of the sockets was investigated with several timepoints [111].

Osteoporosis Model
Ovariectomy-induced osteoporosis was described in a procedure where both tibia and femur were implanted in the same surgical procedure [112]. Osteoporosis was induced in female rabbits by surgical bilateral removal of the ovaries from the dorsal side of the rabbit and fed on a low-calcium diet (0.15% calcium and 0.59% of phosphorus) [112]. The control group in the study was sham-operated, where the ovaries were lifted and exposed but put back in place afterward [112].

3.2.3 Follow-Up and Termination

After surgery, the animals should be evaluated for pain and infection. In orthopedic surgery, it can be recommended that a first treatment is given before surgery begins and a second if the surgery is prolonged. Pain should be monitored and treated, as discussed previously in this chapter. Also, treatment with antibiotics should be in line with the information previously presented in this chapter.

Pain relief can be important for other aspects than animal welfare. For implantation in limbs, pain can affect the outcome of a study, and reproducibility is affected if the animal is not using its legs for movement because of pain.

When the desired time point of an experiment has been reached, the experiment is terminated. Humane methods of euthanasia should follow for animal welfare. The animals can be sedated prior to intravenous injection, usually with an overdose of a barbiturate, although other methods of euthanasia can also be used.

The time points for the termination of the experiment should be selected based on the work of Roberts et al. [46]. Who showed that the rabbit is approximately three times faster in bone formation and remodeling than humans. Also, the best tissue quality should be achieved quickly [113].

Different time points have been described in the literature and are dependent on the hypothesis that is being investigated. Research on dental implants is trying to achieve a shorter healing time, contributing to timepoints earlier than nor-

mal. Also, the repair rate depends on the defect size [114]; consequently, the time for termination varies between studies.

3.2.4 Advantages and Inconveniences

3.2.4.1 General
Advantages

- Compared to larger laboratory animals handling and housing is easier, due to the intermediate size.
- Early skeletal maturity.
- High bone turnover.
- Easy to breed and get hold of.
- Have short gestation, lactation, and puberty cycles.
- Genetic standardization is possible.
- The environment can be standardized.

Limitations and Inconveniences

- The bone structure is the least similar to humans compared to dogs, sheep, goats, and pig.
- Faster bone turnover and differences in remodeling make preclinical results difficult to extrapolate to the clinical response in humans.
- Neither intra- nor extra orally implants can be loaded, by chewing, as in humans.
- The size brings limitations regarding the size and number of implants that can be placed compared to larger animals. The recommendation for an individual rabbit is to have six implants in total (three tests and three controls) [62], which is less than in bigger animal models like sheep, pigs, goats, and pigs [115]. For cylindrical implants, the recommendation in size is 2 mm in diameter and 6 mm in length [86].
- Human implants for clinical use cannot be placed intraorally because the mouth of the rabbit is too small; they can only be placed into jaws (maxillla and mandible) and knees (distal femur and proximal tibia).

3.2.4.2 Femur and Tibia

Femur and tibia are extraoral bone sites, and the advantages as surgical sites are that they contain a satisfactory available amount of bone volume and are more accessible for surgery than in the rabbit jaws [16]. Implants of the same size placed in the human mandible and maxilla can also be placed in the rabbit femur and tibia. Two layers of cortex can be implanted. Both sites can easily be accessed for loading.

Anatomical disadvantages in the tibial model have been highlighted by the authors Stübinger and Dard [16]. The shape of the tibia makes it difficult to drill and fixate the implant without partly ending up in the cis-cortex. To avoid this, using only distal femur and proximal tibia is recommended.

Research on grafting material in cortical bone like femur and tibia should be extrapolated to the clinical intraoral situations with care because of the differences in anatomy and physiology [16].

There are risks for fractures in tibia and femur after surgery [116]. They are also easily accessible for the rabbits to gnaw on the sutures, leading to the opening of the operation sites and increasing the risk for postoperative infection.

3.2.4.3 Maxilla and Mandible

The maxilla of the rabbit is a good model for intramembranous bone healing that resembles clinical jaw defects [16]. The edentulous area in the maxilla has the advantage that mastication can cause some mechanical stress on the bone [117]. One should consider that the masticatory forces can also cause damage to tissue structures [16].

It is also suitable for investigating guided bone regeneration in alveolar ridge augmentation because of the high amount of trabecular bone [118]. Implantation of both cortical layers is also possible in both mandible and maxilla.

Although there are a lot of advantages to surgery in the mandible and maxilla, there are many advantages and limitations, making it difficult to do surgery on these bones. The complexity of the human intraoral environment, an important factor

for implant reliability [18], is impossible to simulate in rabbits. The limited access to the oral cavity of rabbits makes implantation difficult and human dental implants impossible. Also, only small defects can be made [16].

3.2.4.4 Skull

It is formed by intramembranous ossification [57] and has similar embryologic development to humans [58]. Also, the embryology of the maxillofacial bones is the same as the morphology in the calvaria [59], making them easier to compare.

The calvaria is easily accessed, and the surgical procedure is simple. However, only mini-implants can be placed [6].

There is a risk of damaging the dura if surgery is not carefully performed.

3.2.5   Recommendations

For the handling of animals and anesthesia, training is crucial. In some animal facilities, the researcher can choose to perform every step of the study by him/herself, or to use animal technicians and veterinarians in place. The latter usually have more experience, which will reduce stress in the animals and contribute to a more standardized procedure.

The surgical procedures are not all clearly described in the literature. For example, the exact placement and anatomy of the different available sites are not always described. Surgery in animals is different compared to surgery in humans. For these reasons, it is important for the surgeon to practice on cadavers before doing surgery on live animals for the recognition of anatomical structures and for refinement of the procedures. It is recommended to contact the person who developed the technique for direct instruction and training.

For surgery in the hindlimbs, it is recommended to use skeletally mature animals due to the increased risk of fracture in younger animals [113].

When implantation is done with cylindrical implants in the tibiae, it is important to try to adjust the placement so that the leveled platform is without soft tissue around the edges. Also, the flat area of the diaphysis/metaphysis area can be different between animals and not always being completely flat. Making of the platform should be done where this area is the flattest.

When choosing the mandible as the surgery site, it is important to keep in mind that there might be damage to the surgical site because of mastication causing soft tissue to be torn and implants to be dislocated [60].

Since rabbits have small jawbones with low bone volume, they are unsuitable for placing dental implants or creating wider bone defects in the alveolar ridge [16, 119]. In the mandible, the anterior part is best suited for implantation due to the higher bone volume and presence of trabecular bone compared to the rest of the mandible [63].

3.3   Investigative Methods of Evaluation

The methods used for investigating a study result are often the same that is being used both in clinical and preclinical cases. With nondestructive methods, evaluation of different healing periods in the same individual is possible.

3.3.1   Imaging

Imaging techniques such as X-ray and CT are widely used in human dentistry for the assessment of bone and implants [20]. They are both noninvasive and can be used in vivo throughout the healing phase.

X-ray and CT are also common in veterinary medicine and can be used in laboratory animals like rabbits for the evaluation of bone mineral content (BMC) and bone mineral density (BMD) [120].

In three dimensions with micro-computed tomography (micro-CT), bone structure can be assessed and quantified with high accuracy, with a voxel size <10 μm [121]. It only gives a small field of view and high radiation dose, which

makes it suitable for preclinical animal studies [121]. Bone-implant contact (BIC) and bone-implant volume (BIV) can be assessed [122].

3.3.2 Optic and Electronic Histology-Histomorphometry (Including Immunohistolabelings)

Qualitative assessment can be done by histology by identifying the structural pattern and quantitatively by counting and measuring structural characteristics, such as primary osteons, Haversian canals, and secondary osteons [47].

Electron microscopy can also be used for bone-implant assessment [123].

Different labeling techniques can be used for the investigation of bone. Bigham-Sadegh and Oryan [97] listed several staining methods for the evaluation of bone healing in their review.

Tetracycline can be used as a safe marker for bone turnover for histomorphometrical investigation, as the tetracycline will deposit at the calcification front where active mineralization takes place, and the bone growth rate can be obtained in micrometers per day looked at in fluorescence microscopy [45]. It should be injected into the animal at different intervals to distinguish different time points [45]. Labeled bone cannot be decalcified before investigation, and then the tetracycline will be lost [45].

In an article by van Gaalen and colleagues [124], they concluded that the administration of fluorochromes is a standard method but lacks a standardized protocol. They presented different fluorochromes and gave examples of protocols suitable for use in laboratory animals, including rabbits.

3.3.3 Biomechanics

Biomechanical tests are used to evaluate the strength of the bone and implant interaction where high forces correspond to good integration and ingrowth of porous materials [19]. Common tests are pull-out and push-out tests, used on screw and cylindrical implants. Removal torque tests (RTQ) are used on screw-type implants [19] and reverse torque tests (RTT) [125], and tensile tests [126].

Mechanical tests should be carried out at 37 °C [41]. The type of test and the direction and type of force applied to the implant will affect the result's stability [127].

Torque tests are destructive tests, where the torque necessary to loosen the implant is registered and gives a value in the newton-centimeter that reflects the interfacial shear strength [128] and reflects BIC [127]. Inherent bone can rupture if the implant is strongly integrated [129]. They do not give information about bone-bonding properties and attachment because friction and the growth of bone correlate with torque results [88].

The moment of force can come from hand-controlled devices and electronic equipment, where electronic equipment is superior because it ensures a fixed rotation rate, has high reproducibility, and gives a lower operator sensitivity [129]. There are different equipment that can be used that is based on the same principle, where a torsion rig is connected to the implant, the torque given by a motor, and the maximum value for loosening the implant is recorded [128].

RTT measures the torque where bone–implant contact is destroyed and gives indirect information about the BIC in an implant [125].

Pull-out and push-out tests are also destructive tests and used preclinically [130], for evaluation of the implant stiffness, by applying a force along the longitudinal axis of the implant and visualizing it with a force-displacement curve [131]. The implants tested this way are usually placed transcortical or intramedullary [132]. The maximum force is divided with the bone-implant contact for the calculation of shear strength [130]. Ii is very important that the force is aligned with the implant not to obscure the result [133].

Tensile test is used to detach the implant from the surrounding bone [126].

Other nondestructive, biomechanical tests like resonance frequency analysis (RFA), Periotest®, and cutting resistance/ insertional torque, are tests that are more common clinically [132].

3.3.4 Biologic Fluids Analysis (Blood, Saliva, etc.)

The rabbit model can be subject to investigation of local and /or systemic accumulation of metal-derived products. In a study by Bianco et al. [134], levels of titanium were measured in blood serum and urine. In their chapter, other locations for metal derivatives are discussed, such as lymphatic tissue, feces, and tissue distal to the implant. For this reason, such material can also be investigated. Also, inflammatory marker measurements have been done after implantation, by looking at hematology and blood biochemistry [135].

3.3.5 Genomics

Genome transcriptional analysis can be used to look at genes expressed in certain tissues. For example, gene expression involved in bone healing can be investigated with polymerase chain reaction (PCR) and used as biomarkers [136]. Upregulation of bone extracellular matrix (ECM)-genes, such as osteopontin, osteocalcin, and integrins, can be found during the healing of an implant site [137]. Genes expressed in the tissue around implants can play an important role in osseointegration [138], and their expression can be analyzed with DNA microarrays and qRT-PCR in rabbits [139]. Kim et al. [139] used microarrays to analyze the gene expression to evaluate the tissue response at different timepoints after implantation.

3.4 Discussion and Expert Opinion: Balancing Models (Experimental and Surgical) Validation and Validity

3.4.1 General Considerations

Similarities between the rabbit and humans are unfortunately limited. The surgical site chosen for implantation in the rabbit does not always resemble the human anatomy. It is important to know that implantation sites may differ in bone macro- and microarchitecture. Therefore leading to differences in healing and biomechanic factors. These differences are reasons for the rabbit being mainly a screening model.

3.4.1.1 Choosing Animals

When choosing the rabbit breed, it is preferable if it is a large strain; this will make the implantation sites larger and easier to access. Preferably individuals should be purchased from a commercial breeder giving more standardized animals. Whether to choose young or adult-skeletally mature animals should be determined and depends on the hypothesis that is being investigated. In immature animals, bone growth can interfere when looking at bone healing [113] and should be avoided when bone defect repair is being studied. Compositional and mechanical properties change during the rabbits first 3–6 months of age [41]. Older rabbits can be studied, with the physiology of aging as an object [16].

If the study should include both males and females are difficult to conclude. Throughout literature, both a mix of genders and either females or males have been used, without reference to why. If it is not expected that the result should be affected by gender, females can be chosen from a welfare point of view for the ability of social housing.

3.4.1.2 Implantation

Throughout the literature, the surgical methods for implantation in the rabbit, are described in variable detail levels, with or without pictures, and very often without any reference. This gives the impression that there is no standardized method. For example, implantation in the tibia could be done all along the tibia; however, the anatomy differs between the epiphysis, metaphysis, and diaphysis, which is why it should be stated exactly where on the tibia the implant was inserted.

The implantation sites and surgical methods are both important considerations for the ability to reproduce an experiment. The standardization and validation of animal models make it possible

to compare results between studies and can help to reduce the number of animals that is needed for an experiment.

Choosing between the implantation sites, the anatomical and surgical advantages and inconveniences should be considered. It is preferable to implant in a site that resembles the human site, with an implant that can be used in a clinical setting. There must be enough place for the desired defect size to implant biomaterial. The most common implantation sites are the rabbit's hindleg and skull. These are bones that heal in both endochondral ways when it comes to longbones and intramembranous ways when talking about the skull. Mini-implants, all kinds of biomaterials as well as customized implants, can be implanted in these bones [16].

The loading force applied in human implants is impossible to mimic anywhere in the rabbit, which is a major drawback.

Bone grafting is preferably used with autologous bone but is not always taken from a similar anatomical site. Endochondral bone from a rabbit radius that was transplanted into an intraoral, membranous bone site resulted in bone volume as a result [140], which is why the anatomical structure must be kept in mind. The healing properties of different bone grafts vary significantly. For example, the oral cavity should be grafted with bone of intramembranous origin [141].

Also, investigative methods are not always the same. For comparison between studies, it would be easier if the same methods were used.

3.4.2 Surgical Model

3.4.2.1 Femur and Tibia
The rabbit knee, including the distal femur and proximal tibia, is common [16] and a good site for placing both implants and grafting material in cortical bone [87] for following evaluation with biomechanical measurements combined with histological observations and measurements [6].

The placement in the proximal tibia is a good site because the area is relatively flat and large, where number, size, and possible randomization

of implants meet the requirements for a standardized screening model [16, 88]. Implantation can also be bicortical in this site for the investigation of two layers of the cortex. It can be used as a model resembling the more cortical structure of the mandible [142].

Loading forces in the longbones come from the movement of muscles and the weight-bearing force and are different from loading in the mouth that comes from mastication. This affects healing, and it has been shown that the tibia resembles the healing and remodeling time of the mandible, both being faster than in the maxilla [143, 144].

Biomechanical testing can be affected by the microstructure of the tibia. Interlocking and friction can mask the implant-bone interaction from chemical bonding [16]. To evaluate biomaterial in the proximal tibia, cylindrical implants can be placed in a leveled platform, giving maximum contact between bone and implant surfaces. This way of implantation will make it possible to evaluate tissue-implant surface interaction without the mechanical forces affecting the bone-bonding result [88].

The femoral epiphysis in the knee joint can be used for the resemblance of the trabecular architecture in the maxilla [142]. Implantation in both the lateral and medial condyle is possible.

The risk of fractures in femur and tibia increases with surgical intervention and should be considered when choosing these surgical sites [36].

The hindlegs are easily accessible for the rabbit to gnaw on the sutures. Consequently, leading to the risk of opening surgical wounds and a greater risk of infection. To prevent this, a good suturing technique is crucial. Some surgeons prefer simple interrupted sutures for the increased likelihood of sutures remaining in place than continuous sutures. Some prefer continuous intracutaneous sutures for the reason that they do not extend above the skin. The choice of suture material can be discussed for many reasons. Absorbable versus nonabsorbable, monofilament versus multi-filament, and whether the material will interact with the research.

3.4.2.2 Skull

The calvaria has been used commonly to test allografts, xenografts, and autogenous or synthetic bone grafts [6]. The thickness of the calvaria usually inhibits the placement of dental implants [16].

Compared to other extraoral sites, the calvarial bone site is not easily manipulated by the rabbit [16]. It is without muscle attachments, leg movement and not easily accessible for gnawing of the rabbit. Comparing the anatomy with smaller laboratory animals, the skull is larger, giving the possibility of greater surgical control and precision [16]. In addition, it is easily accessible for surgery. Also, the embryology of the maxillofacial bones is the same and has the same morphology as the calvaria, making implantation in the calvaria comparable to implantation in the maxilla [59]. The healing time and remodeling of the calvaria are also similar to that of the maxilla, which is slower than in the mandible [143, 144]. These facts conclude that the calvaria is a better model for implantation in the maxilla than in the mandible.

3.4.2.3 Maxilla and Mandible

Implantation in the maxilla and mandible are the same bone sites for implantation as in humans. However, the model does not allow the same kind of implantation procedures as in humans. As described in "surgical step by step" sinus lift and alveolar ridge augmentation can be performed similarly to humans. Sinus lift in the rabbit is one of the most common sites, and as reviewed by Stübinger and Dard [16], different biomaterials, scaffolds, and cell-based procedures can be investigated in this site, even if their anatomy, function, and physiology are different compared to humans. What makes these procedures difficult is the limited access to the rabbit mouth because of its small oral opening. It enables the implantation of human implants and only allows a limited sample number [16]. Loading forces from mastication is not possible. Mastication, however, can lead to soft tissue damage.

Implanting grafting material in the sinuses for sinus elevation needs to have enough mechanical strength to keep the height elevated from the bone surface [145].

3.4.3   Ethical Considerations

Validation of a model with limited similarities is more difficult than other more similar models. In such a model, like a rabbit, it is more important to balance the possible outcome of a study with the welfare of the animals. Their welfare should be a primary consideration for the use of laboratory animals. The benefit of any model should exceed the risk and suffering that the animal is exposed to. A minimum number of animals and refined procedures should always be used.

Since the ethical point of view in animal research is not the same in every country, different procedures can be allowed in one place but not another.

When more than one implant is put in one limb or when large defects are made, the rabbit must be from a large strain to reduce the risk of fracture [36].

Sennerby et al.. [87, 146] described implantation in the joint cartilage of the distal femur. This requires opening the joint capsule, which will increase the risk of systemic infection and decreased welfare. Joint surgery should be performed with strict asepsis to minimize the risk of infection. Antibiotics can also be administered prophylactic to minimize the risk. However, the use of antibiotics, especially prophylactic, should be avoided.

Extraction of rabbit teeth can be used for making defects. It has been described by Lalani et al. were incisors in both the mandible and maxilla got extracted [111]. Rabbits can manage without their incisors [147]. Extraction of both the lower incisors for grafting material and implantation after a period of healing was done by Munhoz et al. [119]. However, This procedure should be done with care, since the lower incisors play an important role in chewing and tearing the upper incisors. In this case, if the upper incisors are not extracted as well, they need to get cut regularly to prevent them from getting overgrown.

There is also a description in the literature of implantation in the socket after extraction of the first premolar in the mandible, where a 5 cm long incision through the cheek was made to access the premolar area [148]. That large incision in a rabbit's cheek is an invasive procedure that will compromise animal welfare.

These procedures were not described in the section "surgery step by step" because of the great risk of compromised animal welfare, and therefore not considered valid surgery models.

References

1. Gidley JW. The lagomorphs an independent order. Science (80-). 1912;36:285–6.
2. Naff KA, Craig S. The domestic rabbit, oryctolagus cuniculus: origins and history. In: Lab. Rabbit. Guinea pig, hamster, other rodents; 2012. p. 157–63.
3. Suckow M, Stevens K, Wilson R. The laboratory rabbit, guinea pig, hamster, and other rodents. In: Lab rabbit guinea pig, hamster, other rodents; 2012. https://doi.org/10.1016/C2009-0-30495-X.
4. Yanni AE. The laboratory rabbit: an animal model of atherosclerosis research. Lab Anim. 2004;38:246–56.
5. Brewer NR. Biology of the rabbit. J Am Assoc Lab Anim Sci. 2006;45:8–24.
6. Dard MM. Animal models for experimental surgical research in implant dentistry. In: Implant dentistry research guide. Basic, translational and clinical research; 2012. p. 167–90.
7. Hammer RE, Pursel VG, Rexroad CE, Wall RJ, Bolt DJ, Ebert KM, Palmiter RD, Brinster RL. Production of transgenic rabbits, sheep and pigs by microinjection. Nature. 1985;315:680–3.
8. Russell WMS, Burch RL. The principles of humane experimental technique. London: UFAW; 1992. http://altweb.jhsph.edu/.
9. Sohn J, Couto AM. Anatomy, physiology, and behavior. In: Suckow MA, Stevens KA, Wilson RP, editors. Laboratory rabbit, guinea pig, hamster, other rodents. Amsterdam: Elsevier; 2012. p. 195–215.
10. Johnston MS. Clinical approaches to analgesia in ferrets and rabbits. Semin Avian Exot Pet Med. 2005;14:229–35.
11. Swallow J, Anderson D, Buckwell AC, et al. Guidance on the transport of laboratory animals. Lab Anim. 2005;39:1–39.
12. Toth L. Physiological stabilization of rabbits after shipping. Lab Anim Sci. 1990;40:384–7.
13. Obernier JA, Baldwin RL. Establishing an appropriate period of acclimatization following transportation of laboratory animals. ILAR J. 2006;47:364–9.
14. Flecknell P. Preparing for anaesthesia. In: Flecknell P, editor. Laboratory animal anaesthesia. Burlington: Elsevier; 2009. p. 1–17.
15. Mähler M, Berar M, Feinstein R, Gallagher A, Illgen-Wilcke B, Pritchett-Corning K, Raspa M. FELASA recommendations for the health monitoring of mouse, rat, hamster, Guinea pig and rabbit colonies in breeding and experimental units. Lab Anim. 2014;48:178–92.
16. Stübinger S, Dard M. The rabbit as experimental model for research in implant dentistry and related tissue regeneration. J Investig Surg. 2013;26:266–82.
17. Pearce AI, Richards RG, Milz S, Schneider E, Pearce SG. Animal models for implant biomaterial research in bone: a review. Eur Cells Mater. 2007;13:1–10.
18. Shemtov-Yona K, Rittel D. An overview of the mechanical integrity of dental implants. Biomed Res Int. 2015;2015:1. https://doi.org/10.1155/2015/547384.
19. Arora H, Nafria A, Kanase A. Rabbits as animal models in contemporary implant biomaterial research. World J Dent. 2011;2:129–34.
20. Zohrabian VM, Sonick M, Hwang D, Abrahams JJ. Dental Implants. Semin Ultrasound CT MRI. 2015;36:415–26.
21. Abrahams JJ. Augmentation procedures of the jaw in patients with inadequate bone for dental implants: radiographic appearance. J Comput Assist Tomogr. 2000;24:152–8.
22. Javed F, Romanos GE. The role of primary stability for successful immediate loading of dental implants. A literature review. J Dent. 2010;38:612–20.
23. Slaets E, Naert I, Carmeliet G, Duyck J. Early cortical bone healing around loaded titanium implants: a histological study in the rabbit. Clin Oral Implants Res. 2009;20:126–34.
24. Binon PP. Implants and components: entering the new millennium. Int J Oral Maxillofac Implants. 2000;15:76–94.
25. Marco F, Milena F, Gianluca G, Vittoria O. Peri-implant osteogenesis in health and osteoporosis. Micron. 2005;36:630–44.
26. Oryan A, Bigham-Sadegh A, Abbasi-Tesnizi F. Effects of osteogenic medium on healing of the experimental critical bone defect in a rabbit model. Bone. 2014;63:53–60.
27. Hollinger JO, Kleinschmidt JC. The critical size defect as an experimental model to test bone repair materials. J Craniofac Surg. 1990;1:60–8.
28. Stoker NG, Epker BN. Age changes in endosteal bone remodeling and balance in the rabbit. J Dent Res. 1971;50:1570–4.
29. Ocaña RP, Rabelo GD, Sassi LM, Rodrigues VP, Alves FA. Implant osseointegration in irradiated bone: an experimental study. J Periodontal Res. 2017;52:505–11.
30. Wanderman NR, Mallet C, Giambini H, Bao N, Zhao C, An KN, Freedman BA, Nassr A. An ovariectomy-induced rabbit osteoporotic model: a new perspective. Asian Spine J. 2018;12:12–7.

31. Baofeng L, Zhi Y, Bei C, Guolin M, Qingshui Y, Jian L. Characterization of a rabbit osteoporosis model induced by ovariectomy and glucocorticoid. Acta Orthop. 2010;81:396–401.

32. Mori H, Manabe M, Kurachi Y, Nagumo M. Osseointegration of dental implants in rabbit bone with low mineral density. J Oral Maxillofac Surg. 1997;55:351–62.

33. Hou CJ, Liu JL, Li X, Bi LJ. Insulin promotes bone formation in augmented maxillary sinus in diabetic rabbits. Int J Oral Maxillofac Surg. 2012;41:400–7.

34. Tsolaki IN, Madianos PN, Vrotsos JA. Outcomes of dental implants in osteoporotic patients. A literature review. J Prosthodont. 2009;18:309–23.

35. Bono CM, Einhorn TA. Overview of osteoporosis: pathophysiology and determinants of bone strength. Eur Spine J. 2003;12:S90. https://doi.org/10.1007/s00586-003-0603-2.

36. Mapara M, Thomas BS, Bhat KM. Rabbit as an animal model for experimental research. Dent Res J (Isfahan). 2012;9:111–8.

37. Muschler GF, Raut VP, Patterson TE, Wenke JC, Hollinger JO. The design and use of animal models for translational research in bone tissue engineering and regenerative medicine. Tissue Eng Part B Rev. 2010;16:123–45.

38. Cruise L, Brewer N. The biology of the rabbit. In: Manning P, Ringler D, editors. Biology of the laboratory rabbit. San Diego: Academic Press; 1994. p. 483.

39. Suckow M, Douglas F. The laboratory rabbit. 2nd ed. Boca Raton: CRC Press; 1997.

40. Gilsanz V, Roe TF, Gibbens DT, Schulz EE, Carlson ME, Gonzalez O, Boechat MI. Effect of sex steroids on peak bone density of growing rabbits. Am J Phys. 1988;255:E416–21.

41. Isaksson H, Harjula T, Koistinen A, Iivarinen J, Seppänen K, Arokoski JPA, Brama PA, Jurvelin JS, Helminen HJ. Collagen and mineral deposition in rabbit cortical bone during maturation and growth: effects on tissue properties. J Orthop Res. 2010;28:1626–33.

42. Masoud I, Shapiro F, Kent R, Moses A. A longitudinal study of the growth of the New Zealand white rabbit: cumulative and biweekly incremental growth rates for body length, body weight, femoral length, and tibial length. J Orthop Res. 1986;4:221–31.

43. CRARY DD, SAWIN PB. Genetic differences in the ossification pattern of the rabbit. Anat Rec. 1947;97:327.

44. Wang X, Mabrey JD, Agrawal CM. An interspecies comparison of bone fracture properties. Biomed Mater Eng. 1998;8:1–9.

45. Frost HM. Tetracycline-based histological analysis of bone remodeling. Calcif Tissue Res. 1969;3:211–37.

46. Roberts WE, Smith RK, Zilberman Y, Mozsary PG, Smith RS. Osseous adaptation to continuous loading of rigid endosseous implants. Am J Orthod. 1984;86:95–111.

47. Martiniaková M, Omelka R, Chrenek P. Compact bone structure of unmodified and genetically modified rabbits. Anim Sci. 2010;43:166–71.

48. Enlow DH, Brown SO. A comparative histological study of fossil and recent bone tissues. Part III. Texas J Sci. 1956;10:210–1.

49. Martiniaková M, Vondráková M, Fabiš M. Investigation of the microscopic structure of rabbit compact bone tissue. Scr Med (Brno). 2003;76:215–20.

50. Jowsey J. Studies of Haversian systems in man and some animals. J Anat. 1966;100:857–64.

51. Martiniaková M, Grosskopf B, Omelka R, Vondráková M, Bauerová M. Differences among species in compact bone tissue microstructure of mammalian skeleton: use of a discriminant function analysis for species identification. J Forensic Sci. 2006;51:1235–9.

52. Martiniaková M, Omelka R, Chrenek P, Vondráková M, Bauerová M. Age-related changes in histological structure of the femur in juvenile and adult rabbits: a pilot study. Bull Vet Inst Pulawy. 2005;49:227–30.

53. Beamer WG, Shultz KL, Donahue LR, Churchill GA, Sen S, Wergedal JR, Baylink DJ, Rosen CJ. Quantitative trait loci for femoral and lumbar vertebral bone mineral density in C57BL/6J and C3H/HeJ inbred strains of mice. J Bone Miner Res. 2001;16:1195–206.

54. Kaweblum M, Aguilar MDC, Blancas E, Kaweblum J, Lehman WB, Grant AD, Strongwater AM. Hisotological and radiographic determination of the age of physeal closure of the distal femur, proximal tibia, and proximal fibula of the New Zealand white rabbit. J Orthop Res. 1994;12:747–9.

55. Lundgren AK, Sennerby L, Lundgren D, Taylor A, Gottlow J, Nyman S. Bone augmentation at titanium implants using autologous bone grafts and a bioresorbable barrier An experimental study in the rabbit tibia. Clin Oral Implants Res. 1997;8:82–9.

56. Cho LR, Kim DG, Kim JH, Byon ES, Jeong YS, Park CJ. Bone response of Mg ion-implanted clinical implants with the plasma source ion implantation method. Clin Oral Implants Res. 2010;21:848–56.

57. Jin SW, Sim KB, Kim SD. Development and growth of the normal cranial vault: an embryologic review. J Korean Neurosurg Soc. 2016;59:192–6.

58. Bruce J. Time and order of appearance of ossification centres and their development in the skull of the rabbit. Am J Anat. 1941;68:41–67.

59. Frame JW. A convenient animal model for testing bone substitute materials. J Oral Surg. 1980;38:176–80.

60. Slotte C, Lundgren D, Sennerby L. Bone morphology and vascularization of untreated and guided bone augmentation-treated rabbit calvaria: evaluation of an augmentation model. Clin Oral Implants Res. 2005;16:228–35.

61. Copping RR. Microscopic age changes in the frontal bone of the domestic rabbit. J Morphol. 1978;155:123–30.

62. Hirschfeld Z, Weinreb MM, Michaeli Y. Incisors of the rabbit: morphology, histology, and development. J Dent Res. 1973;52:377–84.

63. Campillo VE, Langonnet S, Pierrefeu A, Chaux-Bodard AG. Anatomic and histological study of the rabbit mandible as an experimental model for wound healing and surgical therapies. Lab Anim. 2014;48:273–7.

64. Lundgren D, Lundgren AK, Sennerby L. The effect of mechanical intervention on jaw bone density. An experimental study in the rabbit. Clin Oral Implants Res. 1995;6:54–9.

65. Scharf KE, Lawson W, Shapiro JM, Gannon PJ. Pressure measurements in the normal and occluded rabbit maxillary sinus. Laryngoscope. 1995;105:570–4.

66. Asai S, Shimizu Y, Ooya K. Maxillary sinus augmentation model in rabbits: effect of occluded nasal ostium on new bone formation. Clin Oral Implants Res. 2002;13:405–9.

67. Majzoub Z, Finotti M, Miotti F, Giardino R, Aldini NN, Cordioli G. Bone response to orthodontic loading of endosseous implants in the rabbit calvaria: early continuous distalizing forces. Eur J Orthod. 1999;21:223–30.

68. Slaets E, Carmeliet G, Naert I, Duyck J. Early cellular responses in cortical bone healing around unloaded titanium implants: an animal study. J Periodontol. 2006;77:1015–24.

69. Flecknell P. Anaesthesia of common laboratory species: special considerations. In: Flecknell P, editor. Laboratory animal anaesthesia. Burlington: Elsevier; 2009. p. 181–241.

70. Flecknell PA, Cruz IJ, Liles JH, Whelan G. Induction of anaesthesia with halothane and isof lurane in the rabbit: a comparison of the use of a face-mask or an anaesthetic chamber. Lab Anim. 1996;30:67. https://doi.org/10.1258/002367796780744910.

71. Flecknell PA, Roughan JV, Hedenqvist P. Induction of anaesthesia with sevoflurane and isoflurane in the rabbit. Lab Anim. 1999;33:41–6.

72. Varga M. Analgesia and pain management in rabbits. Vet Nurs J. 2016;31:149–53.

73. Brodbelt D. Perioperative mortality in small animal anaesthesia. Vet J. 2009;182:152–61.

74. Hawkins MG. The use of analgesics in birds, reptiles, and small exotic mammals. J Exot Pet Med. 2006;15:177–92.

75. Flecknell P. Analgesia in small mammals. Semin Avian Exot Pet Med. 1998;7:41–7.

76. Kero P, Thomasson B, Soppi AM. Spinal anaesthesia in the rabbit. Lab Anim. 1981;15:347–8.

77. Coultier C, Flecknell P, Matthew C, Claire A. Reported analgesic administration to rabbits undergoing experimental surgical procedures. BMC Vet Res. 2011;7:1–6.

78. Weaver LA, Blaze CA, Linder DE, Andrutis KA, Karas AZ. A model for clinical evaluation of perioperative analgesia in rabbits (Oryctolagus cuniculus). J Am Assoc Lab Anim Sci. 2010;49:845–51.

79. Barter LS. Rabbit analgesia. Vet Clin North Am Exot Anim Pract. 2011;14:93–104.

80. Keating SCJ, Thomas AA, Flecknell PA, Leach MC. Evaluation of EMLA cream for preventing pain during tattooing of rabbits: changes in physiological, behavioural and facial expression responses. PLoS One. 2012;7:e44437. https://doi.org/10.1371/journal.pone.0044437.

81. Harder AT, An YH. The mechanisms of the inhibitory effects of nonsteroidal anti-inflammatory drugs on bone healing: a concise review. J Clin Pharmacol. 2003;43:807–15.

82. Barry S. Non-steroidal anti-inflammatory drugs inhibit bone healing: a review. Vet Comp Orthop Traumatol. 2010;23:385–92.

83. Kawaguchi H, Pilbeam CC, Harrison JR, Raisz LG. The role of prostaglandins in the regulation of bone metabolism. Clin Orthop Relat Res. 1995;313:36.

84. Radi ZA, Khan NK. Effects of cyclooxygenase inhibition on bone, tendon, and ligament healing. Inflamm Res. 2005;54:358–66.

85. Cottrell J, O'Connor JP. Effect of non-steroidal anti-inflammatory drugs on bone healing. Pharmaceuticals. 2010;3:1668–93.

86. Upman PJ. ISO 10993-6 : tests for local effects after implantation; 2006.

87. Sennerby L, Thomsen P, Ericson LE. Early tissue response to titanium implants inserted in rabbit cortical bone - part I light microscopic observations. J Mater Sci Mater Med. 1993;4:240–50.

88. Rønold HJ, Ellingsen JE. The use of a coin shaped implant for direct in situ measurement of attachment strength for osseointegrating biomaterial surfaces. Biomaterials. 2002;23:2201–9.

89. Benfu C, Xueming T. Ultrastructural investigation of experimental non-union of fractures. A transmission electron microscopic study. Chin Med J (Engl). 1986;99:207–14.

90. Ivanoff CJ, Sennerby L, Lekholm U. Influence of mono- and bicortical anchorage on the integration of titanium implants. A study in the rabbit tibia. Int J Oral Maxillofac Surg. 1996;25:229–35.

91. Kim Y-H, Koak J-Y, Chang I-T, Wennerberg A, Heo S-J. A histomorphometric analysis of the effects of various surface treatment methods on osseointegration. Int J Oral Maxillofac Implants. 2003;18:349–56.

92. Kim J-R, Kim S-H, Kim I-R, Park B-S, Kim Y-D. Low-level laser therapy affects osseointegration in titanium implants: resonance frequency, removal torque, and histomorphometric analysis in rabbits. J Korean Assoc Oral Maxillofac Surg. 2016;42:2–8.

93. Chen HH, Lai WY, Chee TJ, Chan YH, Feng SW. Monitoring the changes of material properties at bone-implant interface during the healing process in vivo: a viscoelastic investigation. Biomed Res Int. 2017;2017:1945607. https://doi.org/10.1155/2017/1945607.

94. Itälä A, Koort J, Ylänen HO, Hupa M, Aro HT. Biologic significance of surface microroughing in bone incorporation of porous bioactive glass implants. J Biomed Mater Res A. 2003;67:496–503.

95. Hollinger JO, Schmitz JP, Mizgala JW, Hassler C. An evaluation of two configurations of tricalcium phosphate for treating craniotomies. J Biomed Mater Res. 1989;23:17–29.

96. Alberius P, Klinge B, Isaksson S. Management of craniotomy in young rabbits. Lab Anim. 1989;23:70–2.

97. Bigham-Sadegh A, Oryan A. Selection of animal models for pre-clinical strategies in evaluating the fracture healing, bone graft substitutes and bone tissue regeneration and engineering. Connect Tissue Res. 2015;56:175–94.

98. Hopper RA, Zhang JR, Fournasier VL, Morova-Protzner I, Protzner KF, Pang CY, Forrest CR. Effect of isolation of periosteum and dura on the healing of rabbit calvarial inlay bone grafts. Plast Reconstr Surg. 2001;107:454–62.

99. Lundgren AK, Lundgren D, Wennerberg A, Hammerle CH, Nyman S. Influence of surface roughness of barrier walls on guided bone augmentation: experimental study in rabbits. Clin Implant Dent Relat Res. 1999;1:41–8.

100. Inaba M. Evaluation of primary stability of inclined orthodontic mini-implants. J Oral Sci. 2009;51:347–53.

101. Kim YS, Kim SH, Kim KH, Jhin MJ, Kim WK, Lee YK, Seol YJ, Lee YM. Rabbit maxillary sinus augmentation model with simultaneous implant placement: differential responses to the graft materials. J Periodontal Implant Sci. 2012;42:204–11.

102. Watanabe K, Niimi A, Ueda M. Autogenous bone grafts in the rabbit maxillary sinus. Oral Surg Oral Med Oral Pathol Oral Radiol Endod. 1999;88:26–32.

103. Rahmani M, Shimada E, Rokni S, Deporter DA, Adegbembo AO, Valiquette N, Pilliar RM. Osteotome sinus elevation and simultaneous placement of porous-surfaced dental implants: a morphometric study in rabbits. Clin Oral Implants Res. 2005;16:692–9.

104. Kahnberg KE. Restoration of mandibular jaw defects in the rabbit by subperiosteally implanted Teflon® mantle leaf. Int J Oral Surg. 1979;8:449–56.

105. Freilich M, Shafer D, Wei M, Kompalli R, Adams D, Kuhn L. Implant system for guiding a new layer of bone. Computed microtomography and histomorphometric analysis in the rabbit mandible. Clin Oral Implants Res. 2009;20:201–7.

106. Wen B, Li Z, Nie R, Liu C, Zhang P, Miron RJ, Dard MM. Influence of biphasic calcium phosphate surfaces coated with enamel matrix derivative on vertical bone growth in an extra-oral rabbit model. Clin Oral Implants Res. 2016;27:1297–304.

107. Young S, Bashoura AG, Borden T, Baggett LS, Jansen JA, Wong M, Mikos AG. Development and characterization of a rabbit alveolar bone nonhealing defect model. J Biomed Mater Res Part A. 2008;86:182–94.

108. Shah SR, Young S, Goldman JL, Jansen JA, Wong ME, Mikos AG. A composite critical-size rabbit mandibular defect for evaluation of craniofacial tissue regeneration. Nat Protoc. 2016;11:1989–2009.

109. Yazan M, Atil F, Gonen ZB, Kocyigit IDTU. A novel experimental model for dental implant research. Int J Exp Dent Sci. 2018;7:43–7.

110. Jegoux F, Aguado E, Cognet R, Malard O, Moreau F, Daculsi G, Goyenvalle E. Alveolar ridge augmentation in irradiated rabbit mandibles. J Biomed Mater Res Part A. 2010;93:1519–26.

111. Lalani Z, Wong M, Brey EM, Mikos AG, Duke PJ, Miller MJ, Johnston C, Montufar-Solis D. Spatial and temporal localization of FGF-2 and VEGF in healing tooth extraction sockets in a rabbit model. J Oral Maxillofac Surg. 2005;63:1500–8.

112. Wen B, Zhu F, Li Z, Zhang P, Lin X, Dard M. The osseointegration behavior of titanium-zirconium implants in ovariectomized rabbits. Clin Oral Implants Res. 2014;25:819–25.

113. Cacchioli A, Spaggiari B, Ravanetti F, Martini FM, Borghetti P, Gabbi C. The critical sized bone defect: morphological study of bone healing. Ann Fac Med Vet di Parma. 2006;26:97–110.

114. Schmitz JP, Hollinger JO. The critical size defect as an experimental model for craniomandibulofacial nonunions. Clin Orthop Relat Res. 1986;(205):299–308.

115. Wancket LM. Animal models for evaluation of bone implants and devices: comparative bone structure and common model uses. Vet Pathol. 2015;52:842–50.

116. Zehnder A, Kapatkin AS. Orthopedics in small mammals. In: Ferrets, rabbits, and rodents: clinical medicine and surgery. St. Louis: Saunders; 2012. p. 472–84.

117. Lundgren AK, Sennerby L, Lundgren D. An experimental rabbit model for jaw-bone healing. Int J Oral Maxillofac Surg. 1997;26:461–4.

118. Lundgren AK, Sennerby L, Lundgren D. Guided jaw-bone regeneration using an experimental rabbit model. Int J Oral Maxillofac Surg. 1998;27:135–40.

119. Munhoz EA, Bodanezi A, Cestari TM, Taga R, De Carvalho PSP, Ferreira O. Long-term rabbits bone response to titanium implants in the presence of inorganic bovine-derived graft. J Biomater Appl. 2012;27:91–8.

120. Castañeda S, Largo R, Calvo E, Rodríguez-Salvanés F, Marcos ME, Díaz-Curiel M, Herrero-Beaumont G. Bone mineral measurements of subchondral and trabecular bone in healthy and osteoporotic rabbits. Skelet Radiol. 2006;35:34–41.

121. Campbell GM, Sophocleous A. Quantitative analysis of bone and soft tissue by micro-computed tomography: applications to ex vivo and in vivo studies. Bonekey Rep. 2014;3:1–12.

122. Bernhardt R, Kuhlisch E, Schulz MC, Eckelt U, Stadlinger B. Comparison of bone-implant contact and bone-implant volume between 2D-histological sections and 3D-SRµCT slices. Eur Cells Mater. 2012;23:237–48.

123. Linder L, Albrektsson T, Branemark PI, Hansson HA, Ivarsson B, Jonsson U, Lundström I. Electron microscopic analysis of the bone-titanium interface. Acta Orthop. 1983;54:45–52.

124. van Gaalen SM, Kruyt MC, Geuze RE, de Bruijn JD, Alblas J, Dhert WJA. Use of fluorochrome labels in in vivo bone tissue engineering research. Tissue Eng Part B Rev. 2010;16:209–17.

125. Atsumi M, Park S-H, Wang H-L. Methods used to assess implant stability: current status. Int J Oral Maxillofac Implants. 2007;22:743–54.

126. Kitsugi T, Nakamura T, Oka M, Yan WQ, Goto T, Shibuya T, Kokubo T, Miyaji S. Bone bonding behavior of titanium and its alloys when coated with titanium oxide (TiO2) and titanium silicate (Ti5Si3). J Biomed Mater Res. 1996;32:149–56.

127. Sennerby L, Meredith N. Implant stability measurements using resonance frequency analysis: biological and biomechanical aspects and clinical implications. Periodontol 2000. 2008;47:51–66.

128. Wennerberg A, Albrektsson T, Lausmaa J. Torque and histomorphometric evaluation of c.p. titanium screws blasted with 25- and 75-μm-sized particles of Al2O3. J Biomed Mater Res. 1996;30:251–60.

129. Sul YT, Johansson CB, Jeong Y, Wennerberg A, Albrektsson T. Resonance frequency and removal torque analysis of implants with turned and anodized surface oxides. Clin Oral Implants Res. 2002;13:252–9.

130. Berzins A, Shah B, Weinans H, Sumner DR. Nondestructive measurements of implant-bone interface shear modulus and effects of implant geometry in pull-out tests. J Biomed Mater Res. 1997;34:337–40.

131. Brunski JB, Puleo DA, Nanci A. Biomaterials and biomechanics of oral and maxillofacial implants: current status and future developments. Int J Oral Maxillofac Implants. 2000;15:15–46.

132. Chang PC, Lang NP, Giannobile WV. Evaluation of functional dynamics during osseointegration and regeneration associated with oral implants: a review. Clin Oral Implant Res. 2011;21:1–12.

133. Kangasniemi IMO, Verheyen CCPM, van der Velde EA, De Groot K. In vivo tensile testing of fluorapatite and hydroxylapatite plasma-sprayed coatings. J Biomed Mater Res. 1994;28:563–72.

134. Bianco P, Ducheyne P, Cuckler J. Titanium serum and urine levels in rabbits with a titanium implant in the absence of wear. Biomaterials. 1996;17:1937–42.

135. Chakraborty A, Kundu B, Basu D, Pal TK, Nandi SK. In vivo bone response and interfacial properties of titanium-alloy implant with different designs in rabbit model with time. Indian J Dent Res. 2011;22:277–84.

136. Faot F, Deprez S, Vandamme K, Camargos GV, Pinto N, Wouters J, Van Den Oord J, Quirynen M, Duyck J. The effect of L-PRF membranes on bone healing in rabbit tibiae bone defects: micro-CT and biomarker results. Sci Rep. 2017;7:1–10.

137. Ogawa T, Sukotjo C, Nishimura I. Modulated bone matrix-related gene expression is associated with differences in interfacial strength of different implant surface roughness. J Prosthodont. 2002;11:241–7.

138. Kojima N, Ozawa S, Miyata Y, Hasegawa H, Tanaka Y, Ogawa T. High-throughput gene expression analysis in bone healing around titanium implants by DNA microarray. Clin Oral Implants Res. 2008;19:173–81.

139. Kim EC, Leesungbok R, Lee SW, Hong JY, Ko EJ, Ahn SJ. Effects of static magnetic fields on bone regeneration of implants in the rabbit: micro-CT, histologic, microarray, and real-time PCR analyses. Clin Oral Implants Res. 2017;28:396–405.

140. Salata LZ, Rasmusson L, Kahnberg KE. Effects of a mechanical barrier on the integration of cortical onlay bone grafts placed simultaneously with endosseous implant. Clin Implant Dent Relat Res. 2002;4:60–8.

141. Wong RWK, Rabie ABM. A quantitative assessment of the healing of intramembranous and endochondral autogenous bone grafts. Eur J Orthod. 1999;21:119–26.

142. Sennerby L, Thomsen P, Ericson LE. A morphometric and biomechanic comparison of titanium implants inserted in rabbit cortical and cancellous bone. Int J Oral Maxillofac Implants. 1992;7:62–71.

143. Slotte C, Lundgren D, Sennerby L, Lundgren AK. Surgical intervention in enchondral and membranous bone: intraindividual comparisons in the rabbit. Clin Implant Dent Relat Res. 2003;5:263–8.

144. Najjar TA, Kahn D. Comparative study of healing and remodeling in various bones. J Oral Surg. 1977;35:375–9.

145. Jiang XQ, Sun XJ, Lai HC, Zhao J, Wang SY, Zhang ZY. Maxillary sinus floor elevation using a tissue-engineered bone complex with β-TCP and BMP-2 gene-modified bMSCs in rabbits. Clin Oral Implants Res. 2009;20:1333–40.

146. Sennerby L, Thomsen P, Ericson LE. Early tissue response to titanium implants inserted in rabbit cortical bone - part II ultrastructural observations. J Mater Sci Mater Med. 1993;4:494–502.

147. Harcourt-Brown F. Dental disease in pet rabbits: diagnosis and treatment. In Pract. 2009;31:432–45.

148. Pinheiro FAL, de Almeida Barros Mourão CF, Diniz VS, Silva PC, Meirelles L, Santos Junior E, Schanaider A. In-vivo bone response to titanium screw implants anodized in sodium sulfate. Acta Cir Bras. 2014;29:376–82.

149. Masago H, Shibuya Y, Munemoto S, Takeuchi J, Umeda M, Komori T, Kuboki Y. Alveolar ridge augmentation using various bone substitutes -a web form of titanium fibers promotes rapid bone development. Kobe J Med Sci. 2007;53:257–263.

150. Turri A, Dahlin C. Comparative maxillary bone-defect healing by calcium-sulphate or deproteinized bovine bone particles and extra cellular matrix membranes in a guided bone regeneration setting: an experimental study in rabbits. Clin Oral Implants Res. 2015;26:501–6.

Preclinical Studies Design and Place of Swine

4

Nikos Mardas, Elena Calciolari, and Xanthippi Dereka

4.1 Experimental Animal Model

4.1.1 Animal Species

Among other large experimental animal models, like the dog, the sheep or the monkey, swine has a long history in translational biomedical research as well as for procedural training in different surgical disciplines [1–3]. In recent years, swine has attracted attention in musco-skeletal surgery and in oral, maxillofacial bone surgery related research [4, 5]. This chapter will specifically discuss the place of swine as an experimental model for dental implant rehabilitation.

Farm or miniature breeds of *Sus scrofa domestica* are the main experimental pig models used in biomedical research. Commercial breeds of the domestic pig differ from the miniature breeds in size and sexual maturity. Mini-pigs reach skeletal and dental maturity at 2 years of age compared to 3 years of age in farm pigs [6, 7]. Mini-pigs, at maturity, weigh approximately 30–60 kg, while domestic farm breeds can weigh between 100 and 200 kg [8, 9]. However, it takes ~2.4 times as long to grow to 40% of their mature weight as it does for intensely fed domestic breeds [7]. In dental implant research, where jaw bone and skeletal maturity is a requirement, miniature swine are more suitable since the increased weight of the domestic breeds at maturity could be an issue in terms of handling, housing, anesthesia, food, and medication costs. Despite their smaller size, mini-pigs are large enough to receive dental implants or other devices that can be harvested with surrounding tissues at termination. Mini-pigs are also less aggressive, and their genetic code is better described than the larger nonbarrier farm breeds, which also present a higher risk for infections and disease transmission [6, 9, 10].

The most commonly used strains in preclinical dental implant research are the Yucatan (mini-pig and micro-pig), Göttingen, Hanford, and the Sinclair Hormel (also known as Minnesota). Other strains like the Bama, Yorkshire, Pitman-Moore, Kangaroo Island, Ohmini, Lee Sung, and Morini have also been considered [3–5].

N. Mardas (✉)
Centre for Oral Clinical Research, Institute of Dentistry, Barts and The London School of Medicine and Dentistry, Queen Mary University of London (QMUL), London, UK
e-mail: n.mardas@qmul.ac.uk

E. Calciolari
Centre for Clinical Oral Research, Institute of Dentistry, Barts and The London School of Medicine and Dentistry, Queen Mary University of London (QMUL), London, UK

X. Dereka
Department of Periodontology, National and Kapodistrian University of Athens, Athens, Greece

4.1.2 General Use in Medical Research

Domestic and especially miniature swine have become established animal models for physiology, pharmacology, toxicology, radiology, surgery, organ transplantation, traumatology, pathology, embryology, gastroenterology, nephrology, immunology, and pediatric research [1, 2, 6, 11–13]. Because of their anatomical (e.g., body weight, skin, bone, cardiovascular system, and urinary system) and functional (gastrointestinal system and immune system) similarities to humans, the translation of research findings in pigs is more representative of human conditions in comparison to other experimental models like the mouse, rat or rabbit [11, 13–15]. These anatomical and physiologic similarities have facilitated, for example, investigations on the metabolism and pharmacokinetic profiles of drugs [6, 14–16], on toxicity testing of new medicines and chemicals [14, 17], or on susceptibility to a variety of risk factors for cardiovascular disease [18]. In addition, swine has been selected as a model of induced pathological conditions in the case of diabetes [19–21], osteoporosis [22], or peptic ulcers [23] following and for healing liver transplant studies [24] and plastic surgery procedures [25]. Furthermore, the development of genetically modified pigs has increased their usefulness as transgenic disease models, complementing the widely used rodent models [26, 27]. Finally, swine models have been extensively used recently for the evaluation of orthopedic and craniomaxillofacial osseous defect healing utilizing a great array of bone grafts, substitutes, devices, or orthopedic and dental implants [3–5, 28, 29].

4.1.3 Financial and Ethical Considerations

Besides their apparent similarity to human, swine has been considered as an experimental model in biomedicine due to economic but also ethical reasons. The assumption, however, that because pigs are not companion animals, like dogs, cats, or rabbits, and are positioned much lower in the phylogenetic order from humans than monkeys, has largely contributed to their higher acceptance as an animal model in biomedical research [12, 15, 30] has been recently challenged [31].

Although swine—especially the larger domestic breeds—are characterized by a unique behavior and have specific housing requirements, diet and socialization needs are relatively cheaper and easily available in regular laboratory settings. Furthermore, swine are able to produce large litters of new-borns, obtain a larger volume of blood or tissue biopsies, and allow the implantation of multiple test and control devices/implants of similar dimensions to what is already available in the market in the same animal, reducing the total number of animal necessary and the cost of customization, respectively [12, 15, 30].

4.2 Anatomical and Histological Characteristics of Porcine Bone

Swine have been chosen as experimental models for skeletal research due to their similarities in bone anatomy, morphology, healing, and remodeling, with human bone [3, 9, 15, 29, 32, 33]. Pigs, in contrast with other big animals (sheep and cows), are monogastric animals like humans and dogs [2]; this has affected their oral and dental anatomy and their masticatory system, which is closer to that of humans [3].

The cranial and mandibular bones are massive, but their shape differs between domestic and miniature breeds. For example, the snout of the Yucatan and Sinclair strains is shorter, and their calvaria is rounder than that of the farm breeds [2]. These differences should be taken into consideration in oral and maxillofacial research. On the other hand, their tempo-mandibular joint is similar to that of humans and presents comparable masticatory function making them more relevant models for dental implant research than rodents, rabbits, and carnivores [30, 34].

Although pig skeleton has a higher bone mass and thicker trabecular bone than that of humans,

porcine bone has a similar collagen matrix organization [33], lamellar structure, and remodeling rate to humans [22, 32, 33, 35]. The bone regeneration rate of the mini-pig mandible (1.2–1.5 μm/day) is comparable to that of humans (1.0–1.5 μm/day) and less than that of dogs (1.5–2.0 μm/day) [36, 37]. On the other hand, interspecies comparison of posterior maxillae in humans, mice, rats, and mini-pigs, demonstrated equivalencies among the animal species in terms of bone mineral density, osteocyte density, and bone remodeling appositional rates [33]. The authors found no evidence of pig models' superiority over rodent models in representing human bone biology. Similarly, adult mini-pigs and rats presented similar mineral apposition and remodeling rates following a tooth extraction, although the duration of the healing process was four times faster in rats [38].

In recent years, the development of "osteopenia" [5, 9, 22] or "diabetes" [5, 19] mini-pig models provided opportunities to investigate the impact of these metabolic conditions on osseous healing and mineralization following different osseous reconstructive and implant treatments. Miniature swine do not usually develop spontaneous diabetes; therefore, it is induced by a combination of either a slow infusion (130 mg/kg) or by a single dosage of streptozotocin (90 mg/kg body weight) and an enriched in lipids diet [39–42]. Utilizing these diabetic models, we could expect similar metabolic alterations and histopathological hard and soft tissues changes to those observed in diabetic humans [41, 42]. In a similar way, osteoporosis is induced in mini-pigs by ovariectomy and a calcium-deficient diet [9, 22] in combination with glucocorticoids [43].

Several extra and intraoral anatomic locations models have been used in domestic and mini-pig breeds to evaluate (a) osseous healing following treatment with different biomaterials for bone regeneration, (b) osseointegration of dental implants and recently, and (c) the treatment of peri-implantitis. The following chapters will present the most commonly used and established in dental implant research, swine surgical models according to their anatomic location and clinical indication.

4.3   Intraoral Surgical Models

Intraoral surgical models are more clinical relevant for studies evaluating dental implant osseointegration or osseous regeneration of various alveolar and peri-implant defects. The most common intraoral locations are the posterior mandible and maxilla, while models simulating sinus augmentation procedures have also been developed [5].

4.3.1   Anatomy of Mandible and Maxilla

The gross anatomy of the maxillofacial bones in pigs is similar to that of humans [30]. The most important anatomic characteristics in pig mandible and maxilla are illustrated in Figs. 4.1, 4.2, and 4.3.

The facial nerve and mental nerve distribution is different from that of humans. Pigs have also 3–5 mental foramina in the lateral mental region because the mental nerve comprises four distinct nerves something that makes local anesthesia more difficult than with humans (Fig. 4.4) [44]. Another anatomic characteristic of mini-pigs is the fact that the volume, length, and depth of the mandibular canal, which is relevant for implant placement, is age dependent. The increase in the volume of the mandibular canal in relation to the decreased alveolar bone height reduces the available space for dental implantation and increases the risk for neurovascular trauma during surgery in older than 12 months mini-pigs [45]. In 12-month-old Göttingen mini-pigs, the average alveolar bone height was 17.7 ± 2.8 mm,
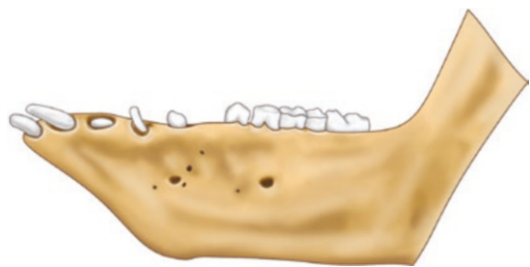
Fig. 4.1   Buccal view of a macerated pigs mandible
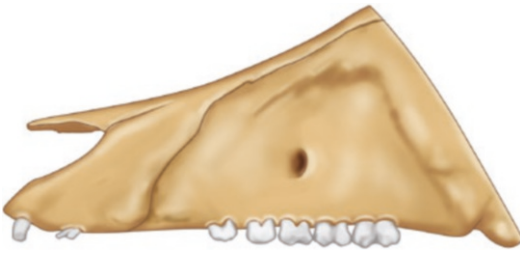
Fig. 4.2 Buccal view of a part of a macerated pigs maxilla

Fig. 4.3 A young pigs' macerated mandible cut in the medial sagittal plane, lingual view

Fig. 4.4 Buccal view of a fresh cadaveric mandibular specimen. Three mental foramina with the associated branches of the mental nerve can be identified in the lateral mental region of the mandible
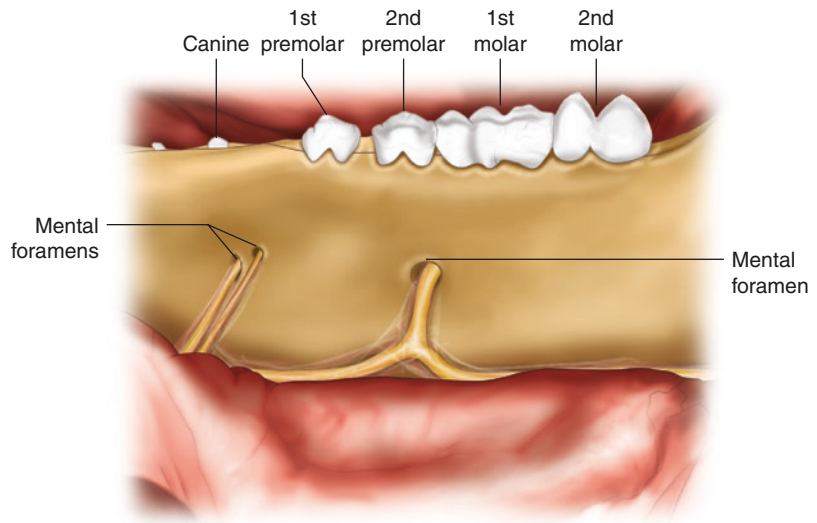
significantly higher than the 17 and 21 months old animals, which had an average of 13.9 ± 1.8 mm and 14.3 ± 1.2 mm, respectively [45].

The dentition in swine shares a lot of morphological similarities with the human one and has a deciduous and permanent dentition with three and four types of teeth, respectively. Their deciduous dentition comprises three incisors, one canine and three premolars and the permanent of three incisors, one canine and three to four premolars and four molars, with one premolar usually smaller or absent [46]. The deciduous dentition in the pig is completed at 6–8 months of age, and the permanent teeth eruption starts at 3 months and is completed at 22 months after birth [47] (Table 4.1), although there are distinct

Table 4.1 Gingival emergence timing of permanent teeth in domestic pigs [46]

	Overall range of domestic pig (in months after birth)
First incisor	11–17
Second incisor	14–20
Third incisor	6–12
Canine	6–12
First premolar	3.5–8
Second premolar	12–16
Third premolar	12–16
Fourth premolar	12–16
First molar	4–8
Second molar	7–13
Third molar	16–22

differences between domestic and the different miniature breeds. This means that in most of the experimental models used in dental implant research, part of the deciduous dentition may be present at the age when usually the experimental surgery is taken place.

The histological characteristics of the oral mucosa and gingival epithelium follow a similar pattern to that of humans [47]. In mini-pigs, the squamous dental epithelium covers a significant part of the crown and similar to humans, is made of a stratified in-layer epithelium over a lamina propria of connective tissue. It is characterized by epithelial pegs, which are long and thin in the free gingiva and shorter in the crevicular epithelium [30, 47]. The width of the attached gingiva is similar to that in humans [30].

4.3.2 Intraoral Osseous Defects for Bone Regeneration

Full or partial-thickness intraoral defects with a circular, oval, or rectangular configuration have been suggested to evaluate osseous healing following treatment with different bone grafts, substitutes, and biologics [5]. Although the vast majority of these defects are located in the mandible, the location, configuration, and dimensions of the ideal intraoral critical size defect in swine have not been determined yet [5].

4.3.2.1 Mandibular Bone Defects
Mandibular, cylindrical defects of standardized dimensions, made with trephine drills of specific diameters, are easily reproducible and comparable. Fuerst et al. treated 8 mm in diameter and 6 mm in depth trephine mandibular defects in Minnesota mini-pigs with fibrin sealant with or without PRP [48] and with platelet-released growth factors (PRGF) and collagen type [49] and followed up the healing for a period of 4 and 8 weeks. The authors reported that neither the fibrin sealant nor the PRGF combine or not with the collagen increased the amount of newly formed bone when compared to untreated defect controls. Jensen et al. [50] used 7 mm in diameter and 4 mm in depth trephine defects in the lateral

surface of the ramus of Göttingen mini-pigs to compare three different bio-ceramic formulations with autogenous bone under Teflon membranes for guided bone regeneration (GBR) and evaluated histomorphometrically the healing after 2, 4, 8, and 24 weeks. Pieri et al. [51] created trephine cylindrical bone defects (3.5 mm in diameter and 8 mm in depth) in the postextraction area of the second and fourth mandibular premolar, 2 months after their extraction and grafted each defect with combinations of mesenchymal stem cells (MSCs), platelet-rich plasma (PRP) incorporated into a fluorohydroxyapatite (FHA) scaffold or autogenous bone under collagen barrier. Histometric analysis showed that autogenous bone and the MSCs enhanced combination graft significantly increased bone formation after 3 months of healing. However, the lack of untreated control defects in these studies does not allow any conclusion regarding the dimensions of cylindrical critical size defects in the mandible.

In an alternative model, similar standardized cylindrical defects of 6–7 mm in diameter and depth were created bilaterally on the surgically reduced and flattened mandibular alveolar ridge, 3 months after the extraction of second, third fourth premolar and first molar. This model allowed the investigators to evaluate histologically the influence of different biomaterials on promoting new bone formation at 3 and 8 weeks' postgrafting [52] and the osseointegration of the subsequently placed titanium implants at 8 weeks postimplantation [53]. The defects in these studies were not intended to be of critical size.

Besides the trephine cylindrical defect, other defect configurations of different dimensions have also been used in various mandibular locations [54–61]. Buser et al. [54] suggested an experimental model where several grafts could be tested in the same animal by making three partial thickness rhomboid defects (width at the base ~12 mm, width at top ~10 mm, height ~12 mm, and defect depth ~5–6 mm) in each mandibular angle site of adult miniature pigs. In the specific study, one defect (control) was filled only with blood clots while the rest were treated with either a collagen sponge or demineralized freeze-dried

bone allograft (DFDBA), or tricalcium phosphate (TCP), coral-derived hydroxyapatite (HA) or autogenous bone grafts. All defects were covered with an e-PTFE membrane for GBR. Histological specimens at 4, 12, and 24 weeks showed the highest bone fill in the autograft-treated sites, while TCP resulted in significantly more bone fill among the other bone substitutes at 24 weeks postoperatively. This type of defect, however, may not have been of critical size dimensions since significant new bone formation was obtained in the empty but still membrane-protected control defects. Therefore, more demanding, chronic, one- or two-wall defects may be necessary for further evaluation of materials/techniques for mandibular bone reconstruction. Henkel et al. claimed that oval-shaped, full-thickness, critical size defects (CSD) (>5 cm^3) in the anterior mandibular ridge of 12-month-old Göttingen mini-pigs were of critical size dimensions. The defects were filled with a ceramic graft (60% HA, 40% b-TCP) alone or in combination with cultures autologous osteoblasts but reported less bone formation in the combination group than the untreated the control where 54% new bone formation was recorded at only 5 weeks postoperatively [55]. Similarly, Sun et al. concluded that 5 cm^3 defects in the mandibular angle of growing domestic pigs (4 months) fulfill the criteria for CSD in contrast with similar defects in the anterior mandible [56]. The validity of this 5 cm^3 CSD has been questioned before by Ruehe et al. [57] who reported using CT scan 87.2% and 75.5% new bone formation in 4.2 cm^3 and 10.1 cm^3 alveolar ridge defects at 6 weeks of healing in even older (3 years old) Göttingen mini-pigs. Differences in age, breed and anatomic location may have played role in these discrepancies.

4.3.2.2 Maxillary Bone Defects

Maxillary bone defects in domestic and miniature pigs have also been used for the evaluation of bone regeneration treatment protocols. Becker et al. [62] restored the resected sinus wall in Göttingen mini-pigs with collagen membrane and HA blocks and Chang et al. [63] infraorbital rim defects of 3 × 1.2 cm^2 with mesenchymal cells as carriers of BMP-2 gene.

Henkel et al. [64] estimated that the CSD in the palate of young and older domestic pigs should be larger than 4 mm.

4.3.2.3 Alveolar Ridge Augmentation

Göttingen mini-pigs have been used as model for alveolar horizontal and vertical ridge augmentation with onlay block grafts [65–67]. Schliephake et al. created block shaped defect (~7 × 10 × 25 mm) through an extraoral incision and compared HA blocks of different porosity to autogenous cortical iliac bone graft for vertical ridge augmentation [65], or evaluated the effect of polylactic membranes over similar block grafts for lateral ridge augmentation [66]. Although the blocks were fixed with titanium screw implants, loss or fracture of the blocks in the vicinity of the titanium implants was a common problem and resulted in loss of graft. In another study, they reported a similar amount of horizontal bone augmentation following subperiosteal implantation of prefabricated autogenous bone grafts cultivated in bovine bone blocks [67] with or without the use of a GBR barrier. The authors discussed the high osteogenic potential of the periosteum in mini-pigs, in contrast to humans, where the osteogenic activity of the periosteum is reduced with age.

Aluden et al. [68, 69] developed a new model for lateral ridge augmentation in the lateral surface of the posterior mandible in 18 months old Göttingen mini-pigs, which allowed direct comparison of four different combinations of grafting materials in the same animal. The lateral and inferior mandibular border was exposed through a submandibular skin incision, and the soft lateral surface of the mandible was exposed and divided into four recipient sites. The first recipient site was positioned 15 mm from the posterior border of the mandibular ramus with an inter-recipient site distance of 10 mm. Following perforation of the lateral cortex, osteosynthesis screws were placed close to the inferior border of the mandible, corresponding to the midline of each augmented area, as a reference landmark for

orientation at the later histological preparation. A fabricated stainless-steel frame ($10 \times 10 \times 5$ mm) was used to ensure a standardized quantity of the graft material at each recipient site. Changes in augmentation height and volume were assessed on CT, and new bone formation and graft consolidation was evaluated histologically at 10, 20, and 30 weeks postoperatively. The authors discussed the possibility of periosteal-driven bone formation since lateral augmentation was performed outside the skeletal envelope; however, this was equally distributed between the respective groups. Another possible side effect was the animals' postoperative behavior, which may cause difficulties in controlling pressure on the augmented areas.

4.3.3   Intraoral Implant Osseointegration Models

Due to the anatomic similarities, intraoral models are more relevant for evaluating dental implant osseointegration and have been extensively used in swine in the last 20 years [3, 5]. Most of these studies evaluated histologically the effect of various implant surfaces surgical placement protocols and timings or bone augmentation materials for the treatment of peri-implant defects on bone-to-implant contact (BIC).

Although earlier attempts to use intraoral jaw locations for the integration of dental implants have been reported in the literature [70], the first intra-alveolar model for titanium root-form dental implants osseointegration in swine was developed by Hale et al. in 1991 [71]. They placed ten implants in the posterior edentulous mandible and evaluated their osseointegration histologically after 18 weeks of healing. The authors emphasized the suitability of the mini-pig mandible as an experimental model in dental implantology due to the anatomical similarities and the dimensions of the porcine mandible that allow the placement of similar size dental implants with what we use in clinical practice.

Three studies [72–74] from the University of Goteborg used an osseointegration model where three implants were placed in the mesial socket of the second deciduous premolar, the mesial socket of the contralateral first deciduous premolar and the canine region and one implant in the maxillary deciduous lateral incisor in 12-week-old, growing Pigham pigs. The authors concluded that proper implant osseointegration models should be performed in skeletally mature animals because osseointegrated implants behave more like ankylosed rather than normal erupting teeth during the period of active growth of the maxillofacial area and developing dentition. The authors also reported an elevated failure rate, probably due to the immediate implantation that resulted in residual defects around the implants, facilitating fibrous tissue down growth, thus preventing osseointegration of the fixture in these growing animal models [73].

In a later study, Stadlinger et al. examined the osseointegration of different dental implant surfaces (type I collagen (coll), coll/chondroitin sulfate (CS), and coll/CS/rhBMP-4) in young, 1-year-old miniature pigs [75]. Because the animals were young, they had to extract both deciduous premolars and the nonerupted tooth germs 8 months before implant placement. The authors discussed the increased risk for unintentional implant placement into the alveolar canal due to the large extent of it, especially in adult pigs [45] or on the canine root whose crown is buccally located with a root crossing through the mandibular body toward a lingual position.

Similar osseointegration models in the posterior mandible of adult Göttingen mini-pigs have been used to evaluate the effect on osseointegration of diagnostic radiation [76], thermal exposure during drilling sequence [77], immediate loading [78–82], platelet-rich plasma application [83, 84], to assess the influence of different implant surface modifications or materials on BIC [85–91], different implant designs [92, 93] and to evaluate the accuracy of a computer-aided surgical navigation system [94].

The mandible has been used as a location for models of immediate (type I) implant placement into fresh extraction sockets [95, 96]. Rimondini et al. inserted 13 mm long and 4.5 mm wide implants into the interradicular septum of mandibular premolar fresh extraction sockets in adult

mini-pigs to evaluate osseointegration rate and the remodeling of soft and hard tissues around implants at 7, 15, 30, and 60 days postoperative. The results revealed that the immediately placed implants were osseointegrated after 60 days, even without an initial bone contact [95]. Linares et al. also used a mandibular model in 14–16 months old female Göttingen mini-pigs to investigate the possible effect of immediate implant placement and loading on buccal bone crest levels and BIC on implants with a hydrophilic moderately rough surface [96]. Three months after the extraction of first molar and second premolar in one hemi-mandible, they immediately installed two implants in the distal sockets of the third and fourth premolar, which left to heal without any loading for 1 month period. One month later, two more implants were placed immediately into the same extraction sockets in the other hemi-mandible and loaded immediately with long (4.5 mm) single healing abutments. According to the authors, functional loading occurred immediately, as it was indicated by the abrasions on the surface of the long-healing abutments that have a similar height to that of the neighboring teeth cusps.

The maxilla of adult mini-pigs (>2 years old) has been used as an alternative to the mandible model to study the influence of different implant surface modifications on osseointegration. Buser et al. [97] inserted six implants with different surface micro-topography and surface treatment at 6 months after extraction of the anterior maxillary teeth. After 4, 8, and 12 weeks of healing, removal torque testing was performed to evaluate the interfacial shear strength of each implant type. The results revealed that the interfacial shear strength of titanium implants was significantly influenced by their surface characteristics, whereby the machined titanium surface demonstrated significantly lower removal torque in the maxilla as compared to the rougher surfaces. The same animal model was used to evaluate the osseointegration of chemically modified SLA titanium surface [98] or zirconia implants [99].

Finally, Clockie & Bell suggested an alternative model that allows to study of dental implants in the jaw bone and reduces the risk of early fail-

ure due to premature loading. For this reason, they performed a submandibular skin/muscle incision to access the inferior border of the mandible and placed four implants in each hemi-mandible of male Yucatan mini-pigs. They reported that this model was reliable for osseointegration and allowed them to test the effect of recombinant human transforming growth factor beta-1 on bone-to-implant conduct [100].

4.3.4 Treatment of Peri-Implant Defects

Intraoral experimental models simulating dehiscence and/or fenestration defects around dental implants, immediate implant placement into fresh extraction sockets, and peri-implantitis-like osseous defects have been used in recent years in swine [5]. The effect of functional loading on the amount of newly formed bone and osseointegration at dehiscence-type defects around implants with a hydrophilic surface, following bone grafting and GBR, has been histologically evaluated in 12, 20-month-old Göttingen mini-pigs [101]. Chronic defects were created on both sides of the mandible by tooth extraction and resection of the buccal plate on a length of 40 mm and a height of 6 mm, leaving the lingual cortical plate intact. After 3 months, dental implants were inserted into the reduced thickness alveolar ridge, and new standardized dehiscence defects (2× 6× 12, see Fig. 4.5) were treated either with a synthetic bone substitute (SBS) or with SBS and a polyethylene glycol membrane. In total, 48 implants were placed in 12 animals (four implants/animal), two in each hemi-mandible. The histological analysis performed after 2 months revealed that the use of barrier membranes with appropriate occlusive properties is strongly recommended in order to avoid interference with the healing and that the short-term loading of implants with a hydrophilic SLActive surface inserted in the dehiscence defects may have a positive influence on osseointegration. The double, acute—chronic nature of this type of defect recreated much closer the clinical reality and provided a model for osseous healing around implants that com-
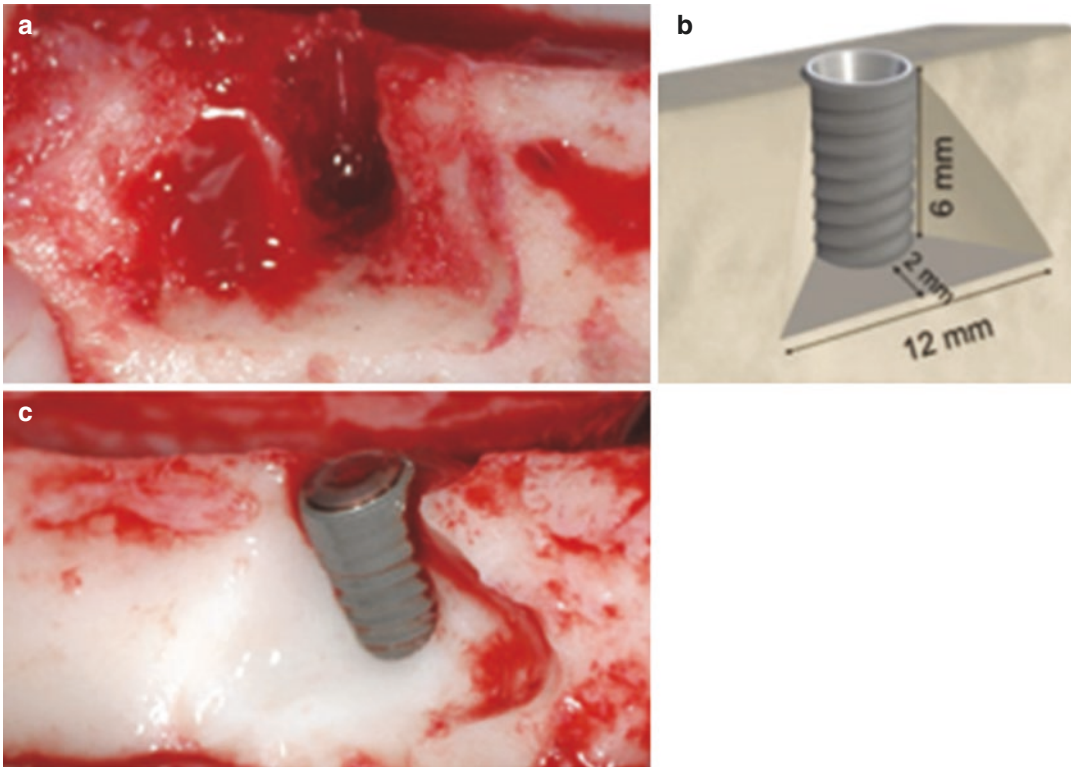
Fig. 4.5 Three months after baseline: Creation of standardized acute dehiscence-type defect. (**a**) Standardized defects were created around the osteotomy by removing part of the buccal bone. (**b**) The resulting dehiscence defects presented a triangular-shaped base and the following dimensions: 6 mm apicocoronally, 12 mm mesiodistally, and 2 mm bucco-lingually. (**c**) Schematic representation of the dehiscence defect. (With permissions from [101])

bined the reduced healing potential of a chronic defect and the standardized dimensions of an acute defect.

Similar dehiscence [102] or circumferential [103, 104] defects have been used as experimental models for the evaluation of other biomaterials for simultaneous GBR around dental implants. It is worth mentioning, however, that the circumferential defects described in the above studies are not of critical size dimensions, and a significant amount of spontaneous osseous healing should be expected.

Similar to Clockie and Bell [79], Almansoori et al. [105] placed three implants in the inferior border of each hemi-mandible of miniature pigs and created standardized half-round bony defects with a diameter of 8 mm, depth of 2 mm, and height of 4 mm in the buccal aspect of implants to evaluate with μCT and histology the bone regeneration capacity of a composite scaffold loaded with stem cells and platelet-rich plasma.

Intraoral peri-implant defects simulating those found in peri-implantitis have also been presented in mini-pigs. Hickey et al. [106] successfully induced peri-implantitis 45 days following 4-0 silk suture ligature placement around 12 implants placed in the edentulous mandibular premolar region of two micro swine. Singh et al. [107] used the same model of experimental peri-implantitis to report that peri-implantitis-induced osseous defects could be regenerated by Teflon GBR barriers. However, only 35.6% of the regenerated bone fill was re-osseointegrated since a soft tissue interface was observed between bone and fixture in the remaining 64.4% of the regenerated bone. Both studies concluded that mini-

pigs could be used as peri-implantitis models where both the pathogenesis and treatment of the disease could be investigated in a reproducible way.

4.3.5 Sinus Augmentation

Animal models of sinus augmentation models are not always simple because of the anatomical differences between the different species and the human. The ideal sinus augmentation model should have a similar cortical thickness of the lateral sinus wall, morphology, and thickness of the Schneiderian membrane and should allow an intraoral approach [108, 109]. In pigs, the maxillary sinus is located caudally, close to the zygomatic bone and the infraorbital nerve in adult animals and is smaller than in sheep and goats. Because the projection field of the sinus in pigs, is 2 cm dorsally and 2 cm caudally from the oral cleft, the approach from the oral cavity, like in humans, needs an extensive enlargement of the buccal vestibule [108]. In addition, the cortical bone thickness of the pig lateral sinus wall averages 2.8 mm, significantly thicker than that of humans [108]. On the contrary, the sinuses in miniature pigs are of comparable size and shape to human sinuses, and the sinus membrane is similar to that of humans [110]. For this reason, an extraoral access of the maxillary sinus where the implants could be inserted from the lateral sinus wall rather than the alveolar process has been suggested [109–111]. Terheyden et al. [109] used this approach in Göttingen mini-pigs to examine whether the combination of rhOP-1 with natural bovine bone mineral (NBBM) would improve ossification and the BIC in a sinus floor augmentation with simultaneous placement of implants. He reported significantly higher BIC in the augmented with rhOP-1 sinus was 80.0% after 6 months of healing. The same model was used to investigate the effect of grafting the sinus cavity with autogenous osteoblast-like cells on an NBBM carrier [112], beta-tricalcium phosphate (β-TCP) with recombinant human growth and differentiation factor-5 with or autogenous bone [113] autologous and NBBM bone grafts with

platelets derivatives [114] and MSCs and PRP on a HA scaffold [115]. In all these studies, the lateral sinus wall was exposed through an extraoral sagittal skin incision, and the implants were inserted from the lateral wall.

4.4 Extraoral Surgical Models

Extraoral locations in swine were used in a limited number of studies for the investigation of implant osseointegration. The most common extraoral locations are: (a) calvarial and facial bones, (b) long bones, and (c) other locations like scapula and iliac crest.

4.4.1 Calvarial and Facial Bones

Critical size calvarial defects in mini-pigs have been mainly suggested as a model for the investigation of bone regeneration materials [37, 116], although this anatomical area has also been used for the study of implant osseointegration in conjunction with bone regeneration [117].

Schlegel et al. (2003) developed a model for implant osseointegration in 12-month-old pigs. Following intravenous injection of ketamine hydrochloride and local anesthesia, a full-thickness sagittal incision was made to reflect skin, muscles, and periosteum. Four implants were placed into the frontal bone, in a sagittal row from left to right, and each one was assigned to one of the four experimental groups according to different osteotomy preparation protocols: (a) manufacturer's guidelines, (b) implant surface conditioning with bovine collagen, (c) PRP placement into the osteotomy, and (d) osteotomy widening bone condensers. The soft tissues were readapted and closed by resorbable sutures. Streptomycin (0.5 g/day) was administered for the first 3 postoperative days. The animals were sacrificed by an overdose of pentobarbital at 2, 4, and 8 weeks. The authors concluded that bone bed conditioning with bone condensation, bovine collagen, or PRP might enhance the osseointegration of implants in the frontal skull of the pigs only at the early phase of healing [117].

Poort et al. (2016) developed a similar model in miniature pigs to evaluate the effect of implant surface treatment and irradiation on osseointegration of implants by means of resonance frequency analysis and removal torques [118]. In 16 adult Göttingen, mini-pigs, a U-shaped incision was performed over the frontal bone to obtain a broad vascular base skin-muco-periosteal flap, and nine implants were placed in the frontal bone of each animal 13 weeks after irradiation. Three groups of four pigs received radiation of 25, 50, and 70 Gy; one group served as control. During implant placement, four pilot holes were drilled in the left side of the frontal irradiated bone, and another five holes were drilled in the nonirradiated bone caudally of the irradiated field. Three different implant surfaces were compared: (a) machined, (b) sandblasted and etched, and (c) sandblasted, etched and hydroxy-apatite-vapor-deposition (HAVD) coated. Antibiotic prophylaxis and pain medication were given for 3 days. The authors reported that irradiated bone does not influence implant stability and osseointegration, especially when HAVD surfaces are used, considering, however, that in this model, the radiation dose was given in two major fractions, while in humans radiotherapy is given in daily small fractions [118].

4.4.2 Long Bones

Dental implants have been placed in the femur, tibia, fibula, scapula, and iliac crest [119–121] to evaluate the possible effect of placement protocols, surface modifications, and regeneration materials on their osseointegration rate and characteristics.

Buser et al. [119] designed a model in the tibial and femoral metaphysis of 12-month-old miniature pigs to evaluate the influence of different surface characteristics on osseointegration of hollow-cylinder implants. After 3 and 6 weeks, the histological examination showed that the extent of BIC is positively correlated with the increasing roughness of the implant surface.

The femur of Göttingen mini-pigs has also been used to evaluate histologically and biome-

chanically and with micro-CT the osseointegration rate of poly(L-lactide-*co*-glycolide) (PLGA) implants compounded with either nanostructured or microsized β-TCP particles [122] and of titanium plasma-spray (TPS) chromo-sulfuric acid etched (CSA) coated implants [123].

The tibia of mini-pigs has been used as a model for the evaluation of different surface modifications on implant osseointegration. Kalemaj et al. (2016) evaluated histomorphometrically four implant surface modifications (1) Kohno Straight dual-engineered surface (DES); (2) SLActive (Straumann); (3) SM Biotite-H coated with Brushite (DIO); and (4) UF hybrid sandblasted and acid-etched (HAS) (DIO)], following insertion into both tibias of six Göttingen mini-pigs. Biocompatibility and bone healing were characterized equal and satisfactory for all surfaces, but the hybrid sandblasted and acid-etched surface resulted in higher bone-to-implant conduct values [124]. In a similar model, after 56 days of healing, alumina-toughened zirconia implants showed higher osseointegration indexes compared to phosphate-enriched titanium oxide implants [125] when inserted into mini-pig tibia and electrochemical oxidation led to significantly higher bone apposition on SLAffinity-Ti implants placed into the tibia of Lanyu small-ear pigs after 2 and 8 weeks of healing [126].

Tibia models have also been used for the evaluation of different surgical placement protocols and regenerative materials. Buchter et al. (2005) observed decreased implant stability and osseointegration when implants were placed in the cranial and caudal tibia condyle of Göttingen mini-pigs using the osteotome technique, in comparison to implants placed with the convectional osteotomy protocol [127]. Furthermore, a collagenous disc-shaped scaffold (ICBM = Insoluble Collagenous Bone Matrix) containing rhBMP-2 (Bone Morphogenetic Protein-2) and/or VEGF (Vascular Endothelial Growth Factor) was applied around the coronal part of dental implants inserted into tibia of 12 mini-pigs to investigate the possible synergistic effect of rhBMP-2 and VEGF on vertical bone augmentation [128].

4.4.3 Other Locations

Other extraoral skeletal locations that have been used are the scapula and the iliac crest. Rohner et al. investigated the potential biomechanical benefits of bi-cortical anchorage of dental implants placed, besides long bones (fibula), into the scapula and iliac crest of Yorkshire pigs. They showed that the quality of bone, the type of anchorage, and the length of the implant determine the biomechanical fit and the biologic bone–implant interface [120, 121]. Recently, Lee et al. developed a block-type ilium and an intervertebral cage-type spine model in 12 adult male Yucatan mini-pigs for the BIC quantitative measure and histological evaluation of HA-coated PEEK implants. They demonstrated that the fusion rate of the implant and the regeneration of bone tissue were improved after HA coating on PEEK implants [129].

4.5 Description of Presurgical and Surgical Procedures

4.5.1 Presurgical

All surgical procedures should be performed under aseptic conditions in order to avoid infections. Prior to the surgery, the animals could be prescribed 1 g amoxicillin IM [119, 122].

4.5.2 Induction, General, and Local Anesthesia

Protocols for general anesthesia are also well-established [123, 130]. The animals could be sedated and subsequently anesthetized by one of the following:

1. Ketamine, induced and orally intubated with Pentobarbitane and maintained with 1% Halothane [120].
2. Ketamine (10 mg/kg), atropine (0.06 ml/kg), and Stresnil (0.03 ml/kg) [127].

3. 2% Xylazine (2.3 mg/kg) and Tiletamine/Zolazepam (3 mg/kg) prior to intubation anesthesia with Isoflurane/Halothane and O_2 [125]
4. Zoletil 100 (Tiletamine hydrochloride + Zolazepam hydrochloride) at a dose of 6 mg/kg IM and maintained with Isoflurane at 2/2.5% in oxygen [124].
5. Intramuscular injection of Azaperone (3–4 mg/kg) and Atropine (0.04–0.05 mg/kg) and the anesthesia was maintained with 2% Halothane gas inhalation via a facemask [126].
6. 10 mg/kg Ketamin and 5 mg/kg Azaperon (Stresnil®) by endotracheal intubation. [128]

Local infiltration with 3% lignocaine or 2% lidocaine with 12.5 mg/ml epinephrine could be used [120, 127]. For intraoperative pain management, 0.5 ml piritramid and articainhydrochloride have been suggested [128].

4.5.3 Postoperative Pain Control and Coverage

After the first few postoperative days, all animals should be monitored for signs of wound infection and assessed for good health. Postoperatively, animals are prescribed standard postoperative pain medication and oral antibiotic coverage [119, 120, 122, 124, 127, 128] and given ad libitum access to food and water for the duration of the study.

An overdose of pentobarbital intravenously is the most common protocol for sacrifice [124, 126, 128].

4.5.4 Description of the Extraoral Procedure

In general, tibial and femoral bone is exposed after the incision of the skin and the subcutaneous tissue. Relevant arteries such as the tibial artery could be ligated in advance. Mono- or bicortical osteotomies are prepared, in a parallel

sagittal row, into the anterior cortex of the femur or in the diaphysis of the tibia under saline irrigation following sequential drilling according to manufacturer's guidelines [126]. A maximum of two implants in the femur and three to six implants in the tibia, with similar dimensions to those used in the clinic, have been placed in the majority of the studies [119, 122]. The correct implant insertion could be confirmed by postoperative radiographs, and a multi-layered wound closure to completely cover the implants using resorbable sutures is performed [125, 128]. Some authors have underlined the importance of allocating the different type of implants in such a way as to avoid placement of a certain type of implant only in the mesial or distal part of the tibia, where anatomically bone is narrower, and the probability of bi-cortical contact is higher.

In the porcine models using the fibula, the surgical area is dissected through a lateral approach, and the implants are inserted perpendicular to the lateral surface of the middle third of the fibula trying to achieve bi-cortical fixation. Because of the limited bone thickness (7 mm) in that region, only 6–8 mm implants can be inserted [120, 121]. The iliac crest is dissected through a skin crestal incision starting from the anterior superior to the posterior spine, and the implants are placed perpendicular to the superior crest. The lateral border of the scapula is exposed by skin incision and via muscle flaps, and up to four implants could be inserted mono-cortically along the axis of the scapula at the lateral crest.

4.5.5   Conclusions

The optimum location for implant placement is rather determined by the specific scientific question, the hypothesis under investigation, and the number and nature of the control groups. The advantage of using a mini-pig femur might be that the shaft of the femur could accommodate five conical implants for equal healing conditions [122].

Both the frontal skull and long bone of mini-pigs provide comparable implant placement sites for inter- and intra-individual analysis. The pub-

lished data referred to these surgical locations demonstrated no complications such as infections or other clinical concerns [119, 126, 127]. However, the intramembranous ossification with a similar mineralization rate between human and the porcine calvarial bones [4], the absence of central blood vessel supply, and the class 2 or 3 bone quality [117] make calvaria models a more representative model for implant dentistry. Besides that, the extrapolation of the results of the studies on implants inserted into extraoral locations should be made with caution as bone recovery differs compared to intraoral bone, the exposure to oral environment microorganisms is missing, and the implants are not loaded [124, 128].

4.6   Investigative Methods of Evaluation

In light of the refinement principle in animal research, it is of outmost importance to choose the best investigative methods so that reliable and relevant data can be extrapolated and meaningful conclusions can be drawn.

4.6.1   Radiographic Analyses

4.6.1.1 2D Radiographs

Intraoral radiographs are of limited value for documenting interval bone healing and implant osseointegration in animal models, as they are two-dimensional images which demonstrate bone formation only after the regenerated tissue is densely calcified. Moreover, evaluations on intraoral radiographs might be impaired by anatomical superposition and geometric distortion, which could hide unfavorable marginal bone level loss or absence of osseointegration. Nevertheless, intraoral radiographic measures could estimate marginal peri-implant bone level in mini-pigs, with a significant correlation between peri-implant bone level assessments performed on intraoral radiographs, CBCT images, and histological slices [131]. On average, CBCT and intraoral radiograph images

deviated 1.2 and 1.17 mm from the histological bone level.

Some studies have suggested using contact radiography (CR) as a fast and economical method to assess osseointegration. Unlike conventional radiography, CR is performed by direct contact between the X-ray film and the object, thus reducing blurring artifacts. Bissinger et al. [132] showed that only moderate differences in terms of BIC (0.6%) and BV/BT (1.3%) could be observed when histology slices of implants placed in the maxilla of mini-pigs were analyzed with CR or Giemsa-eosin stain and conventional histomorphometry.

4.6.1.2 3D Radiographic Examinations

Computed tomography (CT) is a well-documented methodology for the 3D evaluation of calcified anatomical structures such as bone and teeth, and it has been used for the assessment of bone geometry, volume, and density values through Hounsfield units (HU). The linear relationship between mean CT-values and calcium content has been well documented for several bones in humans [133, 134], including the mandible [135].

Few studies in mini-pigs have successfully employed serial CT scans to evaluate the mean percentage of bone volume and/or radiographic bone fill in bone defect models [57, 136] and distraction osteogenesis models [137] or to perform bone density measurements in the jawbones [138]. In a study comparing conventional radiography, CT, and magnetic resonance imaging (MRI) in the head region of pigs, Kyllar et al. [139] showed that radiography is only suitable for a general assessment of bone structures and CT shows excellent spatial definition of bony structure, while MRI is able to return fine soft tissue details. Recently, it was indicated that the primary stability of implants placed in porcine femoral heads could be quantitatively estimated using the CT value preoperatively, since it was correlated with removal torque value, insertion torque value, and implant stability quotient [140].

The cone-beam computed tomography (CBCT) was introduced in the late Nineties in medical imaging, and since then, its indications and applications in dentistry have consistently grown due to its image quality, the relatively low radiation exposure, and the reduced costs compared to CT [141]. Grobe et al. [142] reported that the accuracy of bone measurements performed in the vicinity of titanium implants placed in mini-pigs with CBCTs was comparable to histological measurements. Likewise, Kropil et al. [143] reported a positive correlation between histological bone regeneration of tibial bone defects in mini-pigs and the extent of bone regeneration measured with CBCT and suggested that CBCT allowed for reliable, noninvasive quantitative monitoring of bone healing.

While the use of HUs derived from MSCTs is well-established to assess bone quality, the use of gray values in CBCTs for bone quality assessment is more controversial [144]. Recently, Kang et al. reported that dental implant stability in mini-pig bone measured by impact response frequency was highly correlated with 3D trabecular micro-structural parameters recorded using CBCT and μ-CT and it was suggested that the combination of bone density and architectural parameters measured using CBCT could predict the implant stability more accurately than the density alone [145].

Another relevant technique to visualize complex 3D structures is μ-CT. It offers the possibility for qualitative 3D recording of the bone–implant system and for nondestructive evaluation of bone architecture and mineral density [146, 147]. In addition, when combined with a perfused contrast agent in vivo, μ-CT can show 3D vascular architecture within the bone compartment [148]. μ-CT requires the definition of a volume of interest (VOI) around the implant and that a threshold is chosen to detect voxels representing bone. The following measurements are commonly obtained from μ-CT scanning for both trabecular and cortical bone:

- the total volume (TV) of tissue enclosed by the contours;
- bone volume (BV); the volume of the voxels that are above the threshold chosen to indicate bone tissue;

– BV/TV: bone volume fraction is the ratio of BV to TV (this parameter is described as a percentage of the TV that is bone);
– BMD: the average mineral density of only those voxels above the threshold;
– BMC: the average mass of bone mineral above the threshold.

In addition, can also be measured, as well as parameters such as trabecular number (Tb.N), trabecular thickness (Tb.Th), trabecular separation (Tb.Sp), connectivity density (Conn.D), and structure mode index (SMI).

The accuracy of μ-CT-based quantitative evaluation may be affected by unavoidable metal scatter surrounding the titanium implant due to the implant material. Nevertheless, a constrained three-dimensional Gaussian filter can be used to partially suppress image noise [149, 150], and preclinical studies in mini-pig reported a positive correlation between μ-CT and histomorphometry outcomes [151, 152], thus suggesting that μ-CT should be used as a complementary method to histomorphometry.

Recently, Pilawski et al. analyzed specimens of posterior mandibles from humans, mini-pigs, rats, and mice via μ-CT imaging, followed by quantitative analyses coupled with histology and immunohistochemistry [33]. These analyses demonstrated that bone volume differed among the species while bone mineral density was equal. All species showed a similar density of alveolar osteocytes, with a highly conserved pattern of collagen organization.

4.6.2 Histology-Histomorphometry

Histology and histomorphometry probably remain the most accurate technology to quantify implant integration. Specimens of the implant and surrounding tissue can be fixed and embedded in a plastic resin (methyl methacrylate, MMA), which allows cut sections of approximately 150 μm, according to the EXAKT Cutting & Grinding Technology. The sections can then be placed on a high-resolution X-ray film or digitized plate to yield contact radiographs (CR).

Otherwise, sections can be stained with toluidine blue (or other stains, such as von Kossa for mineralized tissue) and analyzed under a light microscope for histomorphometry analysis. Undecalcified sections can be further ground to <100 μm; however, in the presence of an implant, this should be done carefully as it might result in implant detachment.

Alternatively, bone samples (without implants) can also be fixed, decalcified, dehydrated, and embedded into paraffin for traditional decalcified histology.

Performing undecalcified bone histology is technically more challenging, particularly with large-size specimens; it is more time-consuming and expensive. Moreover, enzyme and immunohistochemistry analyses of MMA-embedded sections remain far more challenging and not completely validated. However, undecalcified histology offers the major advantage of maintaining the structural integrity of bone and preserving information about bone mineralization; furthermore, it is the technique of choice in the presence of a hard, nonmineralized structure like dental implants.

When assessing implant integration, it is important to compare sections cut along the same direction. The histomorphometric parameters that are most commonly evaluated in implant studies include:

– bone to-implant contact (BIC); this intuitively represents the direct contact between bone and the implant threads. Each implant thread needs to be evaluated under light microscope and image analysis tools are employed to assess BIC.
– bone area (BA); this parameter is employed to quantify the area of bone in a thread region or preselected region of interest (ROI). While BIC reflects more osseointegration, BA reflects the remodeling activity in the threaded region as a whole. The ratio of bone area to total area (BATA) around the implant can also be assessed [89].
– percentage of bone area on the total area (BA/TA). It is a planar measurement in histology, in contrast to the volumetric value of the entire ROI in μCT.

– marginal bone loss (MBL), representing the linear distance from the top of the implant to the first bone contact.

Other parameters that can be evaluated are trabecular number (Tb.N), trabecular thickness (Tb. Th), and trabecular separation (Tb.Sp).

Furthermore, the sequential administration of fluorescent polychrome labeling while the animal is alive can be employed to estimate the rate of new bone formation in the animals [153]. There is, however, a lack of standardized procedures for using this technique. In addition, many types of fluorochromes exist and different results can be obtained in relation to the type, concentration, route of administration, and methods of visualization [154].

Immunohistochemistry (IHC) and immunofluorescence (IF) are widely applied techniques that allow to identify specific molecules of interest within the histological tissue analyzed. In implant dentistry research, they can be employed, for instance, to identify bone markers (e.g., osteocalcin, alkaline phosphatase, osteonectin, osteopontin, etc.), inflammatory markers (e.g., cytokines), or angiogenesis markers (VEGF, CD31, etc.).

Both techniques rely on the specificity of the antigen–antibody reaction to detect the distribution of a target molecule, but the methods for detecting the target output signals are different and require different equipment. In IHC, the target molecule(s) is visualized with visible light through chromogenic dyes with enzymatic reactions, while IF staining uses fluorescence probes conjugated either with the primary or secondary antibody against the target. IHC is more suitable for detecting the distribution of marker-positive cells in a large area, while IF is more suitable for the subcellular localization of target molecules [155]. Although IHC and IF are conventionally applied to decalcified bone specimens, specific protocols have been developed for undecalcified bone sections [156].

4.6.3 Biomechanics

Mechanical strength of the bone–implant interface in mini-pigs is commonly tested through the *removal torque testing* (RTQ), which has been described in details by Buser et al. [157]. Each maxilla where implants have been placed is embedded in a fast-curring dental cement to facilitate handling and provide adequate temperature isolation. RTQ testing is then performed on a servo-hydraulic biaxial testing machine. The alignment of the dental implant axis with that of the hydraulic actuator is essential to ensure the application of pure axial torsion to the specimens. The implants are, therefore, attached to the hydraulic actuator via the custom-machined square interface, thus guaranteeing alignment of the implant and actuator. The implant–bone–cement composite specimen is then lowered into a metal container, which is rigidly attached to the loading frame of the machine. The space surrounding the specimen should be filled with a low-melting temperature metal alloy, and the cooling of the alloy rigidly fixes the specimen in the machine. RTQ is performed by rotating the implant counter clockwise at a rate of 0.1°/s while simultaneously collecting angle and torque data at a sampling rate of 10 Hz. Specimens should be kept moist throughout testing by spraying with saline solution. A torque rotation curve, showing RTQ as a function of degrees of rotation, needs to be recorded during each removal process of the analyzed implants, and the RTQ value is eventually defined as the maximum torque measured.

Other mechanical evaluations that can be recorded and can provide useful information on the osseointegration process and stability of the implants include the insertion torque, the pull-out test, the resistance to fracture on insertion, the flexural strength, and fracture resonance frequency analysis (RFA). The latter is a noninvasive test that relates to the "implant stability as a function of the stiffness" [158]. RFA requires the

connection of a metal peg (transducer) with a magnet top to the implant. Magnetic pulses (alternating sine waves of uniform amplitude) cause the peg to vibrate, increasing steadily in pitch until the implant resonates. More specifically, RFA returns an Implant Stability Quotient (ISQ), whose scale runs from 1 to 100. The higher the resonant frequency, the more stable the implant. Garamanzini et al. [146] showed a significant positive correlation between insertion torque and RFA in implants placed in mini-pigs' tibiae, while studies in orthodontic mini-implants placed in pigs showed a correlation between RFA and insertion depth, radiographic bone density, cortical bone thickness and percussion test values [159, 160].

Most of the available studies have investigated the mechanical properties of implants placed in mini-pigs at 4, 8, and 12 weeks [157, 161–163], so these healing points should also be recommended in future studies in order to make the outcomes comparable.

4.6.4 Biologic Fluids Analysis

The mechanism by which inflammatory and bone biomarkers are released during osseointegration has not yet been identified, and the analysis of biological fluids, such as blood, saliva, and peri-implant crevicular fluid (PICF), might offer new insights. In particular, saliva and peri-implant fluid are attractive sources of biomarkers, as their collection is noninvasive, quick, cost-effective, and can be performed at optimal time points during the osseointegration process. Recent systematic reviews have highlighted that PICF contains inflammatory mediators that can be used as additional criteria for a more robust diagnosis of peri-implant infection [164, 165].

Limited literature is currently available on the characterization of porcine saliva, and it mainly relates to the identification of stress biomarkers or disease markers [166, 167]. Recently, Carlisle et al. [168] assessed the concentration of rh-BMP-2 and inflammatory markers in serum and surgery-site drain effluent in a study evaluating the efficacy of rhBMO-2-loaded scaffolds to treat

mandibular fractures. To our knowledge, no study has used PICF in implant studies in mini-pigs.

Future studies are therefore needed to investigate the potential of biomarkers noninvasively retrieved in biological fluids like saliva and PICF to monitor the osseointegration process in animal models.

4.6.5 Bacteriology

Dental implants like natural teeth are colonized by microorganisms. Microbiology analysis of supra and subgingival plaque samples associated with dental implants is important to study the transition from a health peri-implant mucosa to mucositis and to peri-implantitis. In recent years, next-generation sequencing technologies have dramatically improved sequencing capabilities and have been successfully applied for oral microbial analysis in a high-throughput manner [169].

An advantage of using pigs as a model for bacterial infections is that they present an immune response comparable to that of humans [170]. As a matter of fact, there is a 78% similarity, both structurally and functionally, between human and porcine immune-related proteins [171]. The population of immune cells in humans and pigs is also alike similar to humans, and pigs also have a large percentage of PMNs in the peripheral blood [170].

As such, Hickey et al. proposed to collect plaque samples in ligature-induced peri-implantitis models in min-pigs to study microbiological changes [106].

4.6.6 Omics Analyses

Advances in molecular biology are progressively improving our understanding of complex biological processes such as bone formation and osseointegration [172]. The main omics platforms that have been employed to study bone tissue are transcriptomics, proteomics, and epigenomics. Omics technologies can be applied to biological fluids and bone samples, though protein

extraction from bone specimens is still considered a challenging task [173, 174]. Genomic analyses comprise the conventional reverse transcription polymerase chain reaction (PCR) to detect the expression of specific genes and the more complex microarray analyses and whole genome sequencing. Moreover, in recent years epigenetic changes in gene expression that do not imply a modification in nucleotide sequence have attracted significant attention. These involve DNA methylation and histone modifications that modulate gene transcription and mRNA regulation by noncoding RNAs (ncRNAs) called microRNAs (miRNAs). The available knowledge on epigenetics related to implant dentistry is weak. Future studies are warranted to identify which implant surface features can upregulate or downregulate genes related to osseointegration or how different systemic conditions can impact osseointegration via epigenetic modifications.

The study of the proteome complements the study of the genome. While the genome of each individual is constant, the proteome varies and is dynamic. The goal of proteomics is, therefore, to analyze the varying proteomes of an organism at different time points in order to highlight differences between them and signaling pathways differentially expressed. While traditional ELISA, Western blot, or immunofluorescence analyses only focus on specific antibodies and do not allow to gain a wide picture of how different biomolecules interact, and crosstalk, two-dimensional gel electrophoresis followed by mass spectrometry and the more recent shotgun gun proteomics can be successfully employed to identify the proteome expressed during complex biological processes such as bone regeneration and osseointegration.

All omics technologies require the support of bioinformatic tools to interpret the large amount of data obtained and identify the signaling pathways differently regulated.

In the future, the identification of genes and proteins that play a key role during the establishment of osseointegration will be of particular importance as they could be targeted with the aim of shortening the healing time around implants

and to increase the clinical outcomes in patients with local or systemic conditions impairing bone metabolism [172, 175].

4.7   Recommendations and Conclusion

The selection of a suitable animal and experimental model largely depends on whether its anatomical and physiological characteristics are close enough to human ones and meet the specific research demands [5]. Small animal models are suitable for basic screening and concept evaluation, but larger animals are more suitable in cases where the focus of the study is the evolution of a surgical technique or the evaluation of a new biomaterial performance in terms of biomechanical properties or healing response because of their anatomical and physiological proximity to humans and their useful size [3, 5, 176].

Swine is a reliable preclinical research model in the area of implant dentistry due to its similar physical, anatomical, and biological characteristics to humans. Its physiological functions and bone metabolism are extensively documented and the closest to humans with the exception of nonhuman primates. Mini-pigs are particularly suitable for long-term studies because of their convenient size, ease of handling, relatively low cost, and their availability. Therefore, they represent the animal model of choice to implement experimental models on implant osseointegration and bone regeneration. Intraoral mini-pig models are the most clinically relevant to evaluate the effect of various surface treatments and implant placement protocols on osseointegration outcomes and for the repair and regeneration of peri-implant defects using various grafting materials and techniques.

In conclusion, swine provides a preclinical model allowing various translational research considerations in different clinical indications in implant dentistry. At the same time provides an animal experimental platform fully compatible with the 3Rs principles (replacement, reduction, and refinement).

References

1. McAnulty PA, Dayan AD, Ganderup N, Hastings KL. The minipig in biomedical research. Boca Raton: CRC Press; 2011.

2. Swindle M. Swine as models in biomedical research. Ames: Iowa State University Press; 1992.

3. Pearce AI, Richards RG, Milz S, Schneider E, Pearce SG. Animal models for implant biomaterial research in bone: a review. Eur Cell Mater. 2007;13:1–10.

4. Dard MM. Animal models for experimental surgical research in implant dentistry. In: Ballo A, editor. Implant dentistry research guide: basic, translational and experimental clinical research. Hauppauge: Nova Science Publishers; 2012. p. 167–90.

5. Mardas N, Dereka X, Donos N, Dard M. Experimental model for bone regeneration in oral and cranio-maxillo-facial surgery. J Investig Surg. 2014;27(1):32–49.

6. Bollen P, Ellegaard L. The Gottingen minipig in pharmacology and toxicology. Pharmacol Toxicol. 1997;80(Suppl 2):3–4.

7. Kohn F, Sharifi AR, Simianer H. Modeling the growth of the Goettingen minipig. J Anim Sci. 2007;85(1):84–92.

8. Smith AC, Swindle MM. Preparation of swine for the laboratory. ILAR J. 2006;47(4):358–63.

9. Reinwald S, Burr D. Review of nonprimate, large animal models for osteoporosis research. J Bone Miner Res. 2008;23(9):1353–68.

10. Rydhmer L, Zamaratskaia G, Andersson HK, Algers B, Guillemet R, Lundström K. Aggressive and sexual behaviour of growing and finishing pigs reared in groups, without castration. Acta Agric Scand A. 2006;56(2):109–19.

11. Brown DR, Terris JM. Swine in physiological and pathophysiological research. In: Tumbleson ME, Schook LB, editors. Advances in swine in biomedical research. 1st ed. New York: Plenum Press; 1996.

12. Almond GW. Research applications using pigs. Vet Clin North Am Food Anim Pract. 1996;12(3):707–16.

13. Kaser T. Swine as biomedical animal model for T-cell research-success and potential for transmittable and non-transmittable human diseases. Mol Immunol. 2021;135:95–115.

14. van der Laan JW, Brightwell J, McAnulty P, Ratky J, Stark C, Steering Group of the RETHINK Project. Regulatory acceptability of the minipig in the development of pharmaceuticals, chemicals and other products. J Pharmacol Toxicol Methods. 2010;62(3):184–95.

15. Ribitsch I, Baptista PM, Lange-Consiglio A, Melotti L, Patruno M, Jenner F, et al. Large animal models in regenerative medicine and tissue engineering: to do or not to do. Front Bioeng Biotechnol. 2020;8:972.

16. Swindle MM, Smith AC, Goodrich JA. Chronic cannulation and fistulization procedures in swine: a review and recommendations. J Investig Surg. 1998;11(1):7–20.

17. Forster R, Bode G, Ellegaard L, van der Laan JW. The RETHINK project on minipigs in the toxicity testing of new medicines and chemicals: conclusions and recommendations. J Pharmacol Toxicol Methods. 2010;62(3):236–42.

18. Bocan TM. Animal models of atherosclerosis and interpretation of drug intervention studies. Curr Pharm Des. 1998;4(1):37–52.

19. Larsen MO, Rolin B. Use of the Gottingen minipig as a model of diabetes, with special focus on type 1 diabetes research. ILAR J. 2004;45(3):303–13.

20. Kobayashi K, Kobayashi N, Okitsu T, Yong C, Fukazawa T, Ikeda H, et al. Development of a porcine model of type 1 diabetes by total pancreatectomy and establishment of a glucose tolerance evaluation method. Artif Organs. 2004;28(11):1035–42.

21. Stump KC, Swindle MM, Saudek CD, Strandberg JD. Pancreatectomized swine as a model of diabetes mellitus. Lab Anim Sci. 1988;38(4):439–43.

22. Mosekilde L, Weisbrode SE, Safron JA, Stills HF, Jankowsky ML, Ebert DC, et al. Evaluation of the skeletal effects of combined mild dietary calcium restriction and ovariectomy in Sinclair S-1 minipigs: a pilot study. J Bone Miner Res. 1993;8(11):1311–21.

23. Bertram TA, Krakowka S, Morgan DR. Gastritis associated with infection by Helicobacter pylori: comparative pathology in humans and swine. Rev Infect Dis. 1991;13(Suppl 8):S714–22.

24. Dent DM, Hickman R, Uys CJ, Saunders S, Terblanche J. The natural history of liver alloone and autotransplantation in the pig. Br J Surg. 1971;58(6):407–13.

25. Kerrigan CL, Zelt RG, Thomson JG, Diano E. The pig as an experimental animal in plastic surgery research for the study of skin flaps, myocutaneous flaps and fasciocutaneous flaps. Lab Anim Sci. 1986;36(4):408–12.

26. Dehoux JP, Gianello P. The importance of large animal models in transplantation. Front Biosci. 2007;12:4864–80.

27. Perleberg C, Kind A, Schnieke A. Genetically engineered pigs as models for human disease. Dis Model Mech. 2018;11(1):dmm030783.

28. An YH, Friedman RJ. Animal models of orthopedic implant infection. J Investig Surg. 1998;11(2):139–46.

29. Meng X, Ziadlou R, Grad S, Alini M, Wen C, Lai Y, et al. Animal models of osteochondral defect for testing biomaterials. Biochem Res Int. 2020;2020:9659412.

30. Wang S, Liu Y, Fang D, Shi S. The miniature pig: a useful large animal model for dental and orofacial research. Oral Dis. 2007;13(6):530–7.

31. Webster J, Bollen P, Grimm H, Jennings M, Steering Group of the RETHINK Project. Ethical implications of using the minipig in regulatory toxicology studies. J Pharmacol Toxicol Methods. 2010;62(3):160–6.

32. Martiniakova M, Grosskopf B, Omelka R, Vondrakova M, Bauerova M. Differences among species in compact bone tissue microstructure of

mammalian skeleton: use of a discriminant function analysis for species identification. J Forensic Sci. 2006;51(6):1235–9.

33. Pilawski I, Tulu US, Ticha P, Schupbach P, Traxler H, Xu Q, et al. Interspecies comparison of alveolar bone biology, part I: morphology and physiology of pristine bone. JDR Clin Trans Res. 2021;6(3):352–60.

34. Bermejo A, Gonzalez O, Gonzalez JM. The pig as an animal model for experimentation on the temporomandibular articular complex. Oral Surg Oral Med Oral Pathol. 1993;75(1):18–23.

35. Martinez-Gonzalez JM, Cano-Sanchez J, Campo-Trapero J, Gonzalo-Lafuente JC, Diaz-Reganon J, Vazquez-Pineiro MT. Evaluation of minipigs as an animal model for alveolar distraction. Oral Surg Oral Med Oral Pathol Oral Radiol Endod. 2005;99(1):11–6.

36. Glowacki J, Shusterman EM, Troulis M, Holmes R, Perrott D, Kaban LB. Distraction osteogenesis of the porcine mandible: histomorphometric evaluation of bone. Plast Reconstr Surg. 2004;113(2):566–73.

37. Schlegel KA, Lang FJ, Donath K, Kulow JT, Wiltfang J. The monocortical critical size bone defect as an alternative experimental model in testing bone substitute materials. Oral Surg Oral Med Oral Pathol Oral Radiol Endod. 2006;102(1):7–13.

38. Pan J, Pilawski I, Yuan X, Arioka M, Ticha P, Tian Y, et al. Interspecies comparison of alveolar bone biology: tooth extraction socket healing in mini pigs and mice. J Periodontol. 2020;91(12):1653–63.

39. Franconi F, Seghieri G, Canu S, Straface E, Campesi I, Malorni W. Are the available experimental models of type 2 diabetes appropriate for a gender perspective? Pharmacol Res. 2008;57(1):6–18.

40. Larsen MO, Rolin B, Wilken M, Carr RD, Svendsen O. High-fat high-energy feeding impairs fasting glucose and increases fasting insulin levels in the Gottingen minipig: results from a pilot study. Ann N Y Acad Sci. 2002;967:414–23.

41. Koopmans SJ, Mroz Z, Dekker R, Corbijn H, Ackermans M, Sauerwein H. Association of insulin resistance with hyperglycemia in streptozotocin-diabetic pigs: effects of metformin at isoenergetic feeding in a type 2-like diabetic pig model. Metabolism. 2006;55(7):960–71.

42. Coelho PG, Pippenger B, Tovar N, Koopmans SJ, Plana NM, Graves DT, et al. Effect of obesity or metabolic syndrome and diabetes on osseointegration of dental implants in a miniature swine model: a pilot study. J Oral Maxillofac Surg. 2018;76(8):1677–87.

43. Liao YJ, Tang PC, Chen YH, Chu FH, Kang TC, Chen LR, et al. Porcine induced pluripotent stem cell-derived osteoblast-like cells prevent glucocorticoid-induced bone loss in Lanyu pigs. PLoS One. 2018;13(8):e0202155.

44. Sasaki R, Watanabe Y, Yamato M, Aoki S, Okano T, Ando T. Surgical anatomy of the swine face. Lab Anim. 2010;44(4):359–63.

45. Corte GM, Plendl J, Hunigen H, Richardson KC, Gemeinhardt O, Niehues SM. Refining experimen-

tal dental implant testing in the Gottingen Minipig using 3D computed tomography-A morphometric study of the mandibular canal. PLoS One. 2017;12(9):e0184889.

46. Bull G, Payne S. Tooth eruption and epiphyseal fusion in pigs and wild boar ageing and sexing animal bones from archaeological sites, vol. 109. Oxford: BAR British Series; 1982.

47. Wong JW, Gallant-Behm C, Wiebe C, Mak K, Hart DA, Larjava H, et al. Wound healing in oral mucosa results in reduced scar formation as compared with skin: evidence from the red Duroc pig model and humans. Wound Repair Regen. 2009;17(5):717–29.

48. Fuerst G, Gruber R, Tangl S, Sanroman F, Watzek G. Effects of fibrin sealant protein concentrate with and without platelet-released growth factors on bony healing of cortical mandibular defects. An experimental study in minipigs. Clin Oral Implants Res. 2004;15(3):301–7.

49. Fuerst G, Reinhard G, Tangl S, Mittlbock M, Sanroman F, Watzek G. Effect of platelet-released growth factors and collagen type I on osseous regeneration of mandibular defects. A pilot study in minipigs. J Clin Periodontol. 2004;31(9):784–90.

50. Jensen SS, Yeo A, Dard M, Hunziker E, Schenk R, Buser D. Evaluation of a novel biphasic calcium phosphate in standardized bone defects: a histologic and histomorphometric study in the mandibles of minipigs. Clin Oral Implants Res. 2007;18(6):752–60.

51. Pieri F, Lucarelli E, Corinaldesi G, Fini M, Aldini NN, Giardino R, et al. Effect of mesenchymal stem cells and platelet-rich plasma on the healing of standardized bone defects in the alveolar ridge: a comparative histomorphometric study in minipigs. J Oral Maxillofac Surg. 2009;67(2):265–72.

52. Dahlin C, Obrecht M, Dard M, Donos N. Bone tissue modelling and remodelling following guided bone regeneration in combination with biphasic calcium phosphate materials presenting different microporosity. Clin Oral Implants Res. 2015;26(7):814–22.

53. Mihatovic I, Schwarz F, Obreja K, Becker J, Sader R, Dard M, et al. Staged implant placement after defect regeneration using biphasic calcium phosphate materials with different surface topographies in a minipig model. Clin Oral Investig. 2020;24(9):3289–98.

54. Buser D, Hoffmann B, Bernard JP, Lussi A, Mettler D, Schenk RK. Evaluation of filling materials in membrane--protected bone defects. A comparative histomorphometric study in the mandible of miniature pigs. Clin Oral Implants Res. 1998;9(3):137–50.

55. Henkel KO, Gerber T, Dorfling P, Gundlach KK, Bienengraber V. Repair of bone defects by applying biomatrices with and without autologous osteoblasts. J Craniomaxillofac Surg. 2005;33(1):45–9.

56. Sun Z, Kennedy KS, Tee BC, Damron JB, Allen MJ. Establishing a critical-size mandibular defect model in growing pigs: characterization of spontaneous healing. J Oral Maxillofac Surg. 2014;72(9):1852–68.

57. Ruehe B, Niehues S, Heberer S, Nelson K. Miniature pigs as an animal model for implant research: bone regeneration in critical-size defects. Oral Surg Oral Med Oral Pathol Oral Radiol Endod. 2009;108(5):699–706.

58. Pogrel MA, Regezi JA, Fong B, Hakim-Faal Z, Rohrer M, Tran C, et al. Effects of liquid nitrogen cryotherapy and bone grafting on artificial bone defects in minipigs: a preliminary study. Int J Oral Maxillofac Surg. 2002;31(3):296–302.

59. Mai R, Reinstorf A, Pilling E, Hlawitschka M, Jung R, Gelinsky M, et al. Histologic study of incorporation and resorption of a bone cement-collagen composite: an in vivo study in the minipig. Oral Surg Oral Med Oral Pathol Oral Radiol Endod. 2008;105(3):e9–14.

60. Zheng Y, Liu Y, Zhang CM, Zhang HY, Li WH, Shi S, et al. Stem cells from deciduous tooth repair mandibular defect in swine. J Dent Res. 2009;88(3):249–54.

61. Abukawa H, Zhang W, Young CS, Asrican R, Vacanti JP, Kaban LB, et al. Reconstructing mandibular defects using autologous tissue-engineered tooth and bone constructs. J Oral Maxillofac Surg. 2009;67(2):335–47.

62. Becker J, Neukam FW, Schliephake H. Restoration of the lateral sinus wall using a collagen type I membrane for guided tissue regeneration. Int J Oral Maxillofac Surg. 1992;21(4):243–6.

63. Chang SC, Chuang HL, Chen YR, Chen JK, Chung HY, Lu YL, et al. Ex vivo gene therapy in autologous bone marrow stromal stem cells for tissue-engineered maxillofacial bone regeneration. Gene Ther. 2003;10(24):2013–9.

64. Henkel KO, Ma L, Lenz JH, Jonas L, Gundlach KK. Closure of vertical alveolar bone defects with guided horizontal distraction osteogenesis: an experimental study in pigs and first clinical results. J Craniomaxillofac Surg. 2001;29(5):249–53.

65. Schliephake H, Neukam FW. Bone-replacement with porous hydroxyapatite blocks and titanium screw implants - an experimental-study. J Oral Maxillofac Surg. 1991;49(2):151–6.

66. Schliephake H, Neukam FW, Hutmacher D, Becker J. Enhancement of bone ingrowth into a porous Hydroxylapatite-matrix using a resorbable polylactic membrane - an experimental pilot-study. J Oral Maxillofac Surg. 1994;52(1):57–63.

67. Schliephake H, Aleyt J. Mandibular onlay grafting using prefabricated bone grafts with primary implant placement: an experimental study in minipigs. Int J Oral Maxillofac Implants. 1998;13(3):384–93.

68. Aludden H, Mordenfeld A, Dahlin C, Hallman M, Starch-Jensen T. Histological and histomorphometrical outcome after lateral guided bone regeneration augmentation of the mandible with different ratios of deproteinized bovine bone mineral and autogenous bone. A preclinical in vivo study. Clin Oral Implants Res. 2020;31(10):1025–36.

69. Aludden H, Mordenfeld A, Cederlund A, Dahlin C, Spin-Neto R, Veiss-Pedersen P, et al. Radiographic changes in height and volume after lateral GBR procedures with different ratios of deproteinized bovine bone mineral and autogenous bone at different time points. An experimental study. Clin Oral Implants Res. 2021;32(2):167–79.

70. Atkinson PJ, Powell K, Woodhead C. Cortical structure of the pig mandible after the insertion of metallic implants into alveolar bone. Arch Oral Biol. 1977;22(6):383–91.

71. Hale TM, Boretsky BB, Scheidt MJ, McQuade MJ, Strong SL, Van Dyke TE. Evaluation of titanium dental implant osseointegration in posterior edentulous areas of micro swine. J Oral Implantol. 1991;17(2):118–24.

72. Odman J, Grondahl K, Lekholm U, Thilander B. The effect of osseointegrated implants on the dento-alveolar development. A clinical and radiographic study in growing pigs. Eur J Orthod. 1991;13(4):279–86.

73. Sennerby L, Odman J, Lekholm U, Thilander B. Tissue reactions towards titanium implants inserted in growing jaws. A histological study in the pig. Clin Oral Implants Res. 1993;4(2):65–75.

74. Thilander B, Odman J, Grondahl K, Lekholm U. Aspects on osseointegrated implants inserted in growing jaws. A biometric and radiographic study in the young pig. Eur J Orthod. 1992;14(2):99–109.

75. Stadlinger B, Pilling E, Huhle M, Mai R, Bierbaum S, Scharnweber D, et al. Evaluation of osseointegration of dental implants coated with collagen, chondroitin sulphate and BMP-4: an animal study. Int J Oral Maxillofac Surg. 2008;37(1):54–9.

76. Basquill PJ, Steflik DE, Brennan WA, Horner J, Van Dyke TE. Evaluation of the effects of diagnostic radiation on titanium dental implant osseointegration in the micropig. J Periodontol. 1994;65(9):872–80.

77. Heuzeroth R, Pippenger BE, Sandgren R, Bellon B, Kuhl S. Thermal exposure of implant osteotomies and its impact on osseointegration-a preclinical in vivo study. Clin Oral Implants Res. 2021;32(6):672–83.

78. Ko CC, Douglas WH, DeLong R, Rohrer MD, Swift JQ, Hodges JS, et al. Effects of implant healing time on crestal bone loss of a controlled-load dental implant. J Dent Res. 2003;82(8):585–91.

79. Meyer U, Wiesmann HP, Fillies T, Joos U. Early tissue reaction at the interface of immediately loaded dental implants. Int J Oral Maxillofac Implants. 2003;18(4):489–99.

80. Neugebauer J, Traini T, Thams U, Piattelli A, Zoller JE. Peri-implant bone organization under immediate loading state. Circularly polarized light analyses: a minipig study. J Periodontol. 2006;77(2):152–60.

81. Nkenke E, Lehner B, Weinzierl K, Thams U, Neugebauer J, Steveling H, et al. Bone contact, growth, and density around immediately loaded implants in the mandible of mini pigs. Clin Oral Implants Res. 2003;14(3):312–21.

82. Semez G, Cescato A, Luca RE, Tonetti L, Todea DC. A comparative analysis regarding the osseointegration of immediate loaded implants

using two different implant site preparations: erbium:yttrium-aluminum-garnet laser versus surgical conventional way-An in vivo and histological animal study. Photobiomodul Photomed Laser Surg. 2021;39(1):70–80.

83. Fuerst G, Gruber R, Tangl S, Sanroman F, Watzek G. Enhanced bone-to-implant contact by platelet-released growth factors in mandibular cortical bone: a histomorphometric study in minipigs. Int J Oral Maxillofac Implants. 2003;18(5):685–90.

84. Zechner W, Tangl S, Tepper G, Furst G, Bernhart T, Haas R, et al. Influence of platelet-rich plasma on osseous healing of dental implants: a histologic and histomorphometric study in minipigs. Int J Oral Maxillofac Implants. 2003;18(1):15–22.

85. Dostalova T, Himmlova L, Jelinek M, Grivas C. Osseointegration of loaded dental implant with KrF laser hydroxylapatite films on Ti6Al4V alloy by minipigs. J Biomed Opt. 2001;6(2):239–43.

86. Perrin D, Szmukler-Moncler S, Echikou C, Pointaire P, Bernard JP. Bone response to alteration of surface topography and surface composition of sandblasted and acid etched (SLA) implants. Clin Oral Implants Res. 2002;13(5):465–9.

87. Zechner W, Tangl S, Furst G, Tepper G, Thams U, Mailath G, et al. Osseous healing characteristics of three different implant types. Clin Oral Implants Res. 2003;14(2):150–7.

88. Kammerer T, Lesmeister T, Palarie V, Schiegnitz E, Schroter A, Al-Nawas B, et al. Calcium phosphate-coated titanium implants in the mandible: limitations of the in vivo minipig model. Eur Surg Res. 2020;61(6):177–87.

89. Thome G, Sandgren R, Bernardes S, Trojan L, Warfving N, Bellon B, et al. Osseointegration of a novel injection molded 2-piece ceramic dental implant: a study in minipigs. Clin Oral Investig. 2021;25(2):603–15.

90. Susin C, Finger Stadler A, Musskopf ML, de Sousa RM, Ramos UD, Fiorini T. Safety and efficacy of a novel, gradually anodized dental implant surface: a study in Yucatan mini pigs. Clin Implant Dent Relat Res. 2019;21(Suppl 1):44–54.

91. Chappuis V, Maestre L, Burki A, Barre S, Buser D, Zysset P, et al. Osseointegration of ultrafine-grained titanium with a hydrophilic nano-patterned surface: an in vivo examination in miniature pigs. Biomater Sci. 2018;6(9):2448–59.

92. Francisco H, Finelle G, Bornert F, Sandgren R, Herber V, Warfving N, et al. Peri-implant bone preservation of a novel, self-cutting, and fully tapered implant in the healed crestal ridge of minipigs: submerged vs. transgingival healing. Clin Oral Investig. 2021;25(12):6821–32.

93. El Chaar E, Puisys A, Sabbag I, Bellon B, Georgantza A, Kye W, et al. A novel fully tapered, self-cutting tissue-level implant: non-inferiority study in minipigs. Clin Oral Investig. 2021;25(11):6127–37.

94. Meyer U, Wiesmann HP, Runte C, Fillies T, Meier N, Lueth T, et al. Evaluation of accuracy of insertion of dental implants and prosthetic treatment by computer-aided navigation in minipigs. Br J Oral Maxillofac Surg. 2003;41(2):102–8.

95. Rimondini L, Bruschi GB, Scipioni A, Carrassi A, Nicoli-Aldini N, Giavaresi G, et al. Tissue healing in implants immediately placed into postextraction sockets: a pilot study in a mini-pig model. Oral Surg Oral Med Oral Pathol Oral Radiol Endod. 2005;100(3):e43–50.

96. Linares A, Mardas N, Dard M, Donos N. Effect of immediate or delayed loading following immediate placement of implants with a modified surface. Clin Oral Implants Res. 2011;22(1):38–46.

97. Buser D, Nydegger T, Oxland T, Cochran DL, Schenk RK, Hirt HP, et al. Interface shear strength of titanium implants with a sandblasted and acid-etched surface: a biomechanical study in the maxilla of miniature pigs. J Biomed Mater Res. 1999;45(2):75–83.

98. Buser D, Broggini N, Wieland M, Schenk RK, Denzer AJ, Cochran DL, et al. Enhanced bone apposition to a chemically modified SLA titanium surface. J Dent Res. 2004;83(7):529–33.

99. He X, Reichl FX, Milz S, Michalke B, Wu X, Sprecher CM, et al. Titanium and zirconium release from titanium- and zirconia implants in mini pig maxillae and their toxicity in vitro. Dent Mater. 2020;36(3):402–12.

100. Clokie CM, Bell RC. Recombinant human transforming growth factor beta-1 and its effects on osseointegration. J Craniofac Surg. 2003;14(3):268–77.

101. Zambon R, Mardas N, Horvath A, Petrie A, Dard M, Donos N. The effect of loading in regenerated bone in dehiscence defects following a combined approach of bone grafting and GBR. Clin Oral Implants Res. 2012;23(5):591–601.

102. Wang E, Han J, Zhang X, Wu Y, Deng XL. Efficacy of a mineralized collagen bone-grafting material for peri-implant bone defect reconstruction in mini pigs. Regen Biomater. 2019;6(2):107–11.

103. Verket A, Lyngstadaas SP, Tiainen H, Ronold HJ, Wohlfahrt JC. Impact of particulate deproteinized bovine bone mineral and porous titanium granules on early stability and osseointegration of dental implants in narrow marginal circumferential bone defects. Int J Oral Maxillofac Surg. 2018;47(8):1086–94.

104. Catros S, Sandgren R, Pippenger BE, Fricain JC, Herber V, El Chaar E. A novel xenograft bone substitute supports stable bone formation in circumferential defects around dental implants in minipigs. Int J Oral Maxillofac Implants. 2020;35(6):1122–31.

105. Almansoori AA, Kwon OJ, Nam JH, Seo YK, Song HR, Lee JH. Mesenchymal stem cells and platelet-rich plasma-impregnated polycaprolactone-beta tricalcium phosphate bio-scaffold enhanced bone regeneration around dental implants. Int J Implant Dent. 2021;7(1):35.

106. Hickey JS, O'Neal RB, Scheidt MJ, Strong SL, Turgeon D, Van Dyke TE. Microbiologic characterization of ligature-induced peri-implantitis

in the microswine model. J Periodontol. 1991;62(9):548–53.

107. Singh G, O'Neal RB, Brennan WA, Strong SL, Horner JA, Van Dyke TE. Surgical treatment of induced peri-implantitis in the micro pig: clinical and histological analysis. J Periodontol. 1993;64(10):984–9.

108. Estaca E, Cabezas J, Uson J, Sanchez-Margallo F, Morell E, Latorre R. Maxillary sinus-floor elevation: an animal model. Clin Oral Implants Res. 2008;19(10):1044–8.

109. Terheyden H, Jepsen S, Moller B, Tucker MM, Rueger DC. Sinus floor augmentation with simultaneous placement of dental implants using a combination of deproteinized bone xenografts and recombinant human osteogenic protein-1. A histometric study in miniature pigs. Clin Oral Implants Res. 1999;10(6):510–21.

110. Furst G, Gruber R, Tangl S, Zechner W, Haas R, Mailath G, et al. Sinus grafting with autogenous platelet-rich plasma and bovine hydroxyapatite. A histomorphometric study in minipigs. Clin Oral Implants Res. 2003;14(4):500–8.

111. Roldan JC, Jepsen S, Schmidt C, Knuppel H, Rueger DC, Acil Y, et al. Sinus floor augmentation with simultaneous placement of dental implants in the presence of platelet-rich plasma or recombinant human bone morphogenetic protein-7. Clin Oral Implants Res. 2004;15(6):716–23.

112. Liu Y, Springer IN, Zimmermann CE, Acil Y, Scholz-Arens K, Wiltfang J, et al. Missing osteogenic effect of expanded autogenous osteoblast-like cells in a minipig model of sinus augmentation with simultaneous dental implant installation. Clin Oral Implants Res. 2008;19(5):497–504.

113. Gruber RM, Ludwig A, Merten HA, Pippig S, Kramer FJ, Schliephake H. Sinus floor augmentation with recombinant human growth and differentiation factor-5 (rhGDF-5): a pilot study in the Goettingen miniature pig comparing autogenous bone and rhGDF-5. Clin Oral Implants Res. 2009;20(2):175–82.

114. Roldan JC, Knueppel H, Schmidt C, Jepsen S, Zimmermann C, Terheyden H. Single-stage sinus augmentation with cancellous iliac bone and anorganic bovine bone in the presence of platelet-rich plasma in the miniature pig. Clin Oral Implants Res. 2008;19(4):373–8.

115. Pieri F, Lucarelli E, Corinaldesi G, Iezzi G, Piattelli A, Giardino R, et al. Mesenchymal stem cells and platelet-rich plasma enhance bone formation in sinus grafting: a histomorphometric study in minipigs. J Clin Periodontol. 2008;35(6):539–46.

116. Dau M, Kammerer PW, Henkel KO, Gerber T, Frerich B, Gundlach KK. Bone formation in mono cortical mandibular critical size defects after augmentation with two synthetic nanostructured and one xenogenous hydroxyapatite bone substitute -

in vivo animal study. Clin Oral Implants Res. 2016;27(5):597–603.

117. Schlegel KA, Kloss FR, Kessler P, Schultze-Mosgau S, Nkenke E, Wiltfang J. Bone conditioning to enhance implant osseointegration: an experimental study in pigs. Int J Oral Maxillofac Implants. 2003;18(4):505–11.

118. Poort LJ, Kiewiet CC, Cleutjens JP, Houben R, Hoebers FJ, Kessler PA. Osseointegration and implant stability of extraoral implants in Gottingen minipigs after irradiation. J Craniomaxillofac Surg. 2016;44(11):1842–8.

119. Buser D, Schenk RK, Steinemann S, Fiorellini JP, Fox CH, Stich H. Influence of surface characteristics on bone integration of titanium implants. A histomorphometric study in miniature pigs. J Biomed Mater Res. 1991;25(7):889–902.

120. Rohner D, Meng CS, Hutmacher DW, Tsai KT. Bone response to unloaded titanium implants in the fibula, iliac crest, and scapula: an animal study in the Yorkshire pig. Int J Oral Maxillofac Surg. 2003;32(4):383–9.

121. Rohner D, Tay A, Chung SM, Hutmacher DW. Interface of unloaded titanium implants in the iliac crest, fibula, and scapula: a histomorphometric and biomechanical study in the pig. Int J Oral Maxillofac Implants. 2004;19(1):52–8.

122. Kulkova J, Moritz N, Suokas EO, Strandberg N, Leino KA, Laitio TT, et al. Osseointegration of PLGA implants with nanostructured or microsized beta-TCP particles in a minipig model. J Mech Behav Biomed Mater. 2014;40:190–200.

123. Seidling R, Lehmann LJ, Lingner M, Mauermann E, Obertacke U, Schwarz ML. Analysis of the osseointegrative force of a hyperhydrophilic and nanostructured surface refinement for TPS surfaces in a gap healing model with the Gottingen minipig. J Orthop Surg Res. 2016;11(1):119.

124. Kalemaj Z, Scarano A, Valbonetti L, Rapone B, Grassi FR. Bone response to four dental implants with different surface topographies: a histologic and histometric study in minipigs. Int J Periodontics Restorative Dent. 2016;36(5):745–54.

125. Schierano G, Mussano F, Faga MG, Menicucci G, Manzella C, Sabione C, et al. An alumina toughened zirconia composite for dental implant application: in vivo animal results. Biomed Res Int. 2015;2015:157360.

126. Ou KL, Hsu HJ, Yang TS, Lin YH, Chen CS, Peng PW. Osseointegration of titanium implants with SLAffinity treatment: a histological and biomechanical study in miniature pigs. Clin Oral Investig. 2016;20(7):1515–24.

127. Buchter A, Kleinheinz J, Wiesmann HP, Kersken J, Nienkemper M, Weyhrother H, et al. Biological and biomechanical evaluation of bone remodelling and implant stability after using an osteotome technique. Clin Oral Implants Res. 2005;16(1):1–8.

128. Schorn L, Sproll C, Ommerborn M, Naujoks C, Kubler NR, Depprich R. Vertical bone regeneration using rhBMP-2 and VEGF. Head Face Med. 2017;13(1):11.

129. Lee JH, Jang HL, Lee KM, Baek HR, Jin K, Noh JH. Cold-spray coating of hydroxyapatite on a three-dimensional polyetheretherketone implant and its biocompatibility evaluated by in vitro and in vivo minipig model. J Biomed Mater Res B Appl Biomater. 2017;105(3):647–57.

130. Ettrup KS, Glud AN, Orlowski D, Fitting LM, Meier K, Soerensen JC, et al. Basic surgical techniques in the Gottingen minipig: intubation, bladder catheterization, femoral vessel catheterization, and transcardial perfusion. J Vis Exp. 2011;52:2652.

131. Corpas Ldos S, Jacobs R, Quirynen M, Huang Y, Naert I, Duyck J. Peri-implant bone tissue assessment by comparing the outcome of intra-oral radiograph and cone beam computed tomography analyses to the histological standard. Clin Oral Implants Res. 2011;22(5):492–9.

132. Bissinger O, Gotz C, Jeschke A, Haller B, Wolff KD, Kaiser P, et al. Comparison of contact radiographed and stained histological sections for osseointegration analysis of dental implants: an in vivo study. Oral Surg Oral Med Oral Pathol Oral Radiol. 2018;125(1):20–6.

133. Husby T, Hoiseth A, Haffner F, Alho A. Quantification of bone mineral measured by single-energy computed tomography. Acta Orthop Scand. 1989;60(4):435–8.

134. Bradley JG, Huang HK, Ledley RS. Evaluation of calcium concentration in bones from CT scans. Radiology. 1978;128(1):103–7.

135. Lindh C, Petersson A, Klinge B, Nilsson M. Trabecular bone volume and bone mineral density in the mandible. Dentomaxillofac Radiol. 1997;26(2):101–6.

136. Fu J, Xiang Y, Ni M, Qu X, Zhou Y, Hao L, et al. In vivo reconstruction of the acetabular bone defect by the individualized three-dimensional printed porous augment in a swine model. Biomed Res Int. 2020;2020:4542302.

137. Zimmermann CE, Harris G, Thurmuller P, Troulis MJ, Perrott DH, Rahn B, et al. Assessment of bone formation in a porcine mandibular distraction wound by computed tomography. Int J Oral Maxillofac Surg. 2004;33(6):569–74.

138. Poort LJ, Bittermann GK, Bockmann RA, Hoebers FJ, Houben R, Postma AA, et al. Does a change in bone mineral density occur in the mandible of Gottingen minipigs after irradiation in correlation with radiation dose and implant surgery? J Oral Maxillofac Surg. 2014;72(11):2149–56.

139. Kyllar M, Stembirek J, Putnova I, Stehlik L, Odehnalova S, Buchtova M. Radiography, computed tomography and magnetic resonance imaging of craniofacial structures in pig. Anat Histol Embryol. 2014;43(6):435–52.

140. Howashi M, Tsukiyama Y, Ayukawa Y, Isoda-Akizuki K, Kihara M, Imai Y, et al. Relationship between the CT value and cortical bone thickness at implant recipient sites and primary implant stability with comparison of different implant types. Clin Implant Dent Relat Res. 2016;18(1):107–16.

141. Tyndall DA, Price JB, Tetradis S, Ganz SD, Hildebolt C, Scarfe WC, et al. Position statement of the American Academy of Oral and Maxillofacial Radiology on selection criteria for the use of radiology in dental implantology with emphasis on cone beam computed tomography. Oral Surg Oral Med Oral Pathol Oral Radiol. 2012;113(6):817–26.

142. Grobe A, Semmusch J, Schollchen M, Hanken H, Hahn M, Eichhorn W, et al. Accuracy of bone measurements in the vicinity of titanium implants in CBCT data sets: a comparison of radiological and histological findings in minipigs. Biomed Res Int. 2017;2017:3848207.

143. Kropil P, Hakimi A, Jungbluth P, Riegger C, Rubbert C, Miese F, et al. Cone beam CT in assessment of tibial bone defect healing: an animal study. Arcad Radiol. 2012;19(3):320–5.

144. Pauwels R, Jacobs R, Singer SR, Mupparapu M. CBCT-based bone quality assessment: are Hounsfield units applicable? Dentomaxillofac Radiol. 2015;44(1):20140238.

145. Kang S, Bok SC, Choi SC, Lee SS, Heo M, Huh K, et al. The relationship between dental implant stability and trabecular bone structure using cone-beam computed tomography. J Periodont Implant Sci. 2016;46(2):116–27.

146. Garamanzini M, Gargiuli S, Zarone F, Megna R, Apicella A, Aversa R, et al. Combined microcomputed tomography, biomechanical and histomorphometric analysis of the peri-implant bone: a pilot study in minipig model. Dent Mater. 2016;32(6):794–806.

147. Rendenbach C, Fischer H, Kopp A, Schmidt-Bleek K, Kreiker H, Stumpp S, et al. Improved in vivo osseointegration and degradation behavior of PEO surface-modified WE43 magnesium plates and screws after 6 and 12 months. Mater Sci Eng C Mater Biol Appl. 2021;129:112380.

148. Kotsougiani D, Hundepool C, Bulstra LF, Friedrich P, Shin A, Bishop A. Bone vascularized composite allotransplantation model in swine tibial defect: evaluation of surgical angiogenesis and transplant viability. Microsurgery. 2019;39:160.

149. Hasturk H, Kantarci A, Ghattas M, Dangaria SJ, Abdallah R, Morgan EF, et al. The use of light/chemically hardened polymethylmethacrylate, polyhydroxylethylmethacrylate, and calcium hydroxide graft material in combination with polyanhydride around implants and extraction sockets in minipigs: part II: histologic and micro-CT evaluations. J Periodontol. 2014;85(9):1230–9.

150. Elian N, Bloom M, Dard M, Cho SC, Trushkowsky RD, Tarnow D. Radiological and micro-computed tomography analysis of the bone at dental implants inserted 2, 3 and 4 mm apart in a minipig model with

platform switching incorporated. Clin Oral Implants Res. 2014;25(2):e22–9.

151. Bissinger O, Probst F, Wolff K, Jeschke A, Weitz J, Deppe H, et al. Comparative 3D micro-CT and 2D histomorphometry analysis of dental implant osseointegration in the maxilla of minipigs. J Clin Periodontol. 2017;44(4):418–27.

152. Bernhardt R, Kuhlisch E, Schulz M, Eckelt U, Stadlnger B. Comparison of bone-implant contact and bone-implant volume between 2D-histological sections and 3D-SRµCT slices. Eur Cell Mater. 2012;10(23):237–47.

153. Hung CC, Fu E, Chiu HC, Liang HC. Bone formation following sinus grafting with an alloplastic biphasic calcium phosphate in Lanyu Taiwanese mini-pigs. J Periodontol. 2020;91(1):93–101.

154. van Gaalen SM, Kruyt MC, Geuze RE, de Bruijn JD, Alblas J, Dhert WJ. Use of fluorochrome labels in in vivo bone tissue engineering research. Tissue Eng Part B Rev. 2010;16(2):209–17.

155. Mori H, Cardiff RD. Methods of immunohistochemistry and immunofluorescence: converting invisible to visible. Methods Mol Biol. 2016;1458:1–12.

156. Knabe C, Kraska B, Koch C, Gross U, Zreiqat H, Stiller M. A method for immunohistochemical detection of osteogenic markers in undecalcified bone sections. Biotech Histochem. 2006;81(1):31–9.

157. Buser D, Nydegger T, Hirt HP, Cochran DL, Nolte LP. Removal torque values of titanium implants in the maxilla of miniature pigs. Int J Oral Maxillofac Implants. 1998;13(5):611–9.

158. Meredith N, Alleyne D, Cawley P. Quantitative determination of the stability of the implant-tissue interface using resonance frequency analysis. Clin Oral Implants Res. 1996;7(3):261–7.

159. Nienkemper M, Santel N, Hoscheid R, Drescher D. Orthodontic mini-implant stability at different insertion depths : sensitivity of three stability measurement methods. J Orofac Orthop. 2016;77(4):296–303.

160. Su Y, Wilmes B, Honscheid R, Drescher D. Application of a wireless resonance frequency transducer to assess primary stability of orthodontic mini-implants: an in vitro study in pig ilia. Int J Oral Maxillofac Implants. 2009;24(4):647–54.

161. Bormann KH, Gellrich NC, Kniha H, Dard M, Wieland M, Gahlert M. Biomechanical evaluation of a microstructured zirconia implant by a removal torque comparison with a standard Ti-SLA implant. Clin Oral Implants Res. 2012;23(10):1210–6.

162. Gahlert M, Gudehus T, Eichhorn S, Steinhauser E, Kniha H, Erhardt W. Biomechanical and histomorphometric comparison between zirconia implants with varying surface textures and a titanium implant in the maxilla of miniature pigs. Clin Oral Implants Res. 2007;18(5):662–8.

163. Li D, Ferguson SJ, Beutler T, Cochran DL, Sittig C, Hirt HP, et al. Biomechanical comparison of the sandblasted and acid-etched and the machined and acid-etched titanium surface for dental implants. J Biomed Mater Res. 2002;60(2):325–32.

164. Faot F, Nascimento GG, Bielemann AM, Campao TD, Leite FR, Quirynen M. Can peri-implant crevicular fluid assist in the diagnosis of peri-implantitis? A systematic review and meta-analysis. J Periodontol. 2015;86(5):631–45.

165. Duarte PM, Serrao CR, Miranda TS, Zanatta LC, Bastos MF, Faveri M, et al. Could cytokine levels in the peri-implant crevicular fluid be used to distinguish between healthy implants and implants with peri-implantitis? A systematic review. J Periodontal Res. 2016;51(6):689–98.

166. Gutierrez AM, De La Cruz-Sanchez E, Montes A, Sotillo J, Gutierrez-Panizo C, Fuentes P, et al. Easy and non-invasive disease detection in pigs by adenosine deaminase activity determinations in saliva. PLoS One. 2017;12(6):e0179299.

167. Gutierrez A, Ceron JJ, Razzazi-Fazeli E, Schlosser S, Tecles F. Influence of different sample preparation strategies on the proteomic identification of stress biomarkers in porcine saliva. BMC Vet Res. 2017;13(1):375.

168. Carlisle P, Guda T, Silliman DT, Burdette AJ, Talley AD, Alvarez R, et al. Localized low-dose rhBMP-2 is effective at promoting bone regeneration in mandibular segmental defects. J Biomed Mater Res B Appl Biomater. 2019;107(5):1491–503.

169. Metzker ML. Sequencing technologies - the next generation. Nat Rev Genet. 2010;11(1):31–46.

170. Meurens F, Summerfield A, Nauwynck H, Saif L, Gerdts V. The pig: a model for human infectious diseases. Trends Microbiol. 2012;20(1):50–7.

171. Jensen LK, Johansen ASB, Jensen HE. Porcine models of biofilm infections with focus on pathomorphology. Front Microbiol. 2017;8:1961.

172. Calciolari E, Donos N. The use of omics profiling to improve outcomes of bone regeneration and osseointegration. How far are we from personalized medicine in dentistry? J Proteomics. 2018;188:85.

173. Calciolari E, Mardas N, Dereka X, Anagnostopoulos AK, Tsangaris GT, Donos N. The effect of experimental osteoporosis on bone regeneration: part 2, proteomics results. Clin Oral Implants Res. 2017;28(9):e135–e45.

174. Calciolari E, Mardas N, Dereka X, Anagnostopoulos AK, Tsangaris GT, Donos N. Protein expression during early stages of bone regeneration under hydrophobic and hydrophilic titanium domes. A pilot study. J Periodontal Res. 2018;53(2):174–87.

175. Calciolari E, Donos N. Proteomic and transcriptomic approaches for studying bone regeneration in health and systemically compromised conditions. Proteomics Clin Appl. 2020;14(3):e1900084.

176. Heino TJ, Alm JJ, Moritz N, Aro HT. Comparison of the osteogenic capacity of minipig and human bone marrow-derived mesenchymal stem cells. J Orthop Res. 2012;30(7):1019–25.

Preclinical Studies Design in the Canine Model

5

Ivan Darby, Wayne Fitzgerald, Helen Davies, and Stephen Chen

5.1 Introduction

The canine model has been widely used for pre-clinical studies in dental implantology and related tissue regeneration since the 1970s [1, 2]. It is a widely available and important model and has had broad applications for research in this field.

5.2 Experimental Animal Model

5.2.1 The Canine

An experimental model should, as closely as possible, mimic the anatomy, inflammatory responses and healing of the human. In this regard, the canine model fits most requirements, as these dental definitions demonstrate:

Brachydont. Teeth do not continually erupt and have well-formed roots with closed apices (*c.f. hypsodont* as in the herbivores such as the horse).

Isognathic. Jaws of a similar size.

Heterodont. Different forms: Incisors, canines, premolars and molars.

Diphyodont. Temporary and permanent dentitions.

The study design often requires detail such as histopathology at the level of the bone-implant interface and thus requires sacrifice of the study model. In these cases, both medical and humane care of the dog patient is mandatory and understood. The source and the ongoing care of the study animals are of concern to the ethics committees, the researchers as well as the general public.

The canine model is accessible and does not provide handling or husbandry obstacles. However, there are social and emotive arguments against their use since they are sentient companion animals. The issue of professional and animal ethics should be addressed at the initial study design stage and are of paramount consideration. The most common breed for dental implant and regenerative studies is the Beagle [3–6], with other breeds such as the Labrador [7, 8], American Fox Hound [9] and Greyhound [10] also used. Mongrels [11] have also been utilized. There is no need to genetically modify the canine 'model'.

I. Darby (✉) · S. Chen
Periodontics, Melbourne Dental School, University of Melbourne, Parkville, VIC, Australia
e-mail: idarby@unimelb.edu.au;
schen@periomelbourne.com.au

W. Fitzgerald
Melbourne Veterinary Dentistry, Melbourne, Australia

H. Davies
Department of Veterinary BioSciences, University of Melbourne, Melbourne, Australia

5.2.2 General Use in Medical Devices Research

The canine model has been widely used in medical research, in diverse fields such as cancer research [12], bone tissue engineering and regenerative medicine [13], orthopedic research [14] and cardiovascular research [15]. The most relevant of these to dental implantology are in the fields of bone biology, bone tissue engineering and orthopedics. There are obvious differences in the size and morphological characteristics of canine bones compared to humans, which varies depending upon the breed and size of the dog. There are also microstructural differences, with human bone comprised of secondary osteons (and their associated central vascular structures) with cement lines between adjacent lamellae, compared to canine bone which has a mixed microstructure comprising secondary osteonal structures and laminar bone. Additionally, the mineral density of canine bone is higher than that of human bone [16]. Notwithstanding these differences, it has been reported that canine bone most closely resembles human bone when comparison are made with other species [17]. It has also been reported that bone regeneration and bone remodeling has a higher rate in dogs compared to humans [18].

5.2.3 Financial Considerations

The canine model is readily available, inexpensive to house and easy to care for. Animals are available from specialized breeders or unwanted strays to be put down. Recent changes in public opinion have reduced the availability of suitable canines for research, thus increasing costs.

5.3 Surgical Anatomy and Surgical Procedures for Implant Dentistry

5.3.1 Surgical Locations

5.3.1.1 Extraoral
Extraoral considerations are of little relevance to research in dental implantology, other than with respect to analgesia. In veterinary medicine, the distal mandibular nerve block (of the inferior alveolar nerve as it enters the mandibular canal's distal foramen) is most frequently accessed externally. In the dog, the site of the injection involves placing the drug over the mandibular foramen using all or some of these landmarks:

- Halfway along a line between the angular process of the mandible and the last molar tooth (M3 or tooth #311 or 411). The injection site is the medial (or lingual) aspect of the mandible; and/or
- Using the mandible's distal ventral notch as a landmark (present in the dog's mandible), place the needle at its mid-curvature, to a depth equal to half of the distance from the mandible's ventral margin to the gingival edge of the first molar (tooth #309 or 409).

Either of these will place the needle in the same area. As the injection is close to but not necessarily onto the nerve itself, this involves the drug diffusing at the site to encompass the nerve and as such, the volume of agent is larger than it would be if placed in direct contact with the nerve.

In all cases, a fine needle no coarser than a 25 g 5/8-in needle should be used. The technique is to always withdraw on the syringe before injecting the drug to ensure it has not been inadvertently placed intravenously or intra-arterially.

Intraoral
Although there is some breed variation, a dog's mouth can open widely to effect grasping of prey and allowing penetration by the canine teeth. The small digastricus muscle is the main muscle responsible for opening the mouth, with the powerful temporal and masseter muscles being the main closing muscles. There is some lateral excursion possible via the masseter and pterygoid muscles but this is not significant in the dog. This has implications for loading studies which attempt to create laterally directed rather than vertically directed forces on dental implants [19].

The maxillary bones that include the incisive bone that holds the incisor teeth and the maxillary and palatine bones that hold the cheek teeth

are all significantly less dense than the mandible.

The evolution of the mammal allows for a total of 44 permanent teeth, with the dog having 42 (Fig. 5.1) and the human 32. Notably, the dog has six incisors compared to the human's four; they have the same number of canines (four, one in each quadrant). The dog has four premolars in both quadrants, all being two-rooted except for the maxillary fourth premolar that has three roots.

All of the dog's mandibular teeth are two-rooted; there is more space in the maxilla and like the maxillary fourth premolar, the (two) upper molars are three-rooted.

The tooth structures are similar in that the crown is covered by enamel albeit thicker in the human; the greater mass of the tooth structure is dentine-containing dentinal tubules. Cementum covers the roots being the attachment for the periodontal ligament attachment fibers. The roots in the canine are general larger than in the human and, in 2 or 3-rooted teeth, usually diverge forming significant mechanical attachment to the alveolar bone.

The apex of the canine's tooth usually has multiple canals, up to 60 that form a 'delta', and lateral canals are not unusual. This has significant implications with endodontic procedures.

The eruption of a dog's permanent dentition is usually complete by 6 months of age but complete apexogenesis takes more than another 6 months or so. There are breed and individual variations in this timing.

The dog's "cheek" teeth (premolars and molars) should interdigitate (forming a pinking shear arrangement) but this has significant variation considering the malocclusion breeds such as in the brachycephalics. The dog's mandibular teeth lie inside the maxillary arcade allowing for a scissor or cutting effect supported by the form of the dental crowns.

The massive root-to-crown ratio suggests that these teeth can be a challenge to extract and this affects the instrumentation and techniques used in their extraction.

The choice between maxilla or mandible is decided in large by the nature of the study.
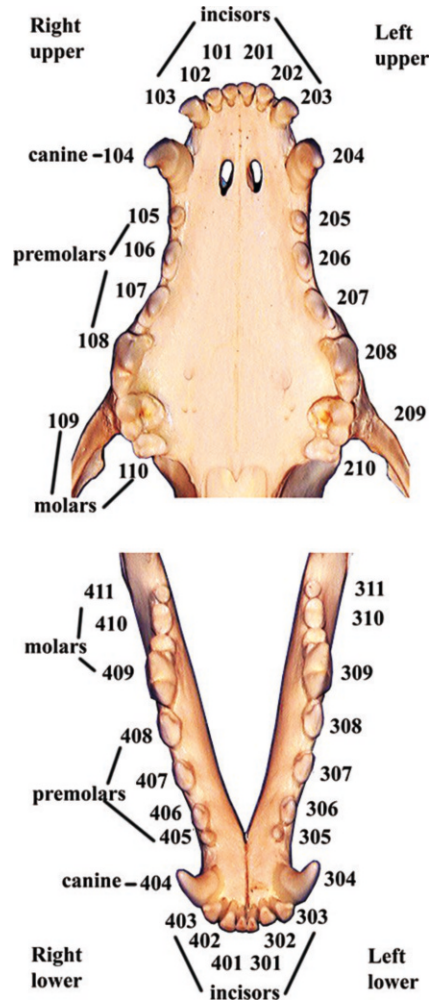
Fig. 5.1 Tooth numbers of the canine dentition

The most common site are the mandibular premolars and molars. All of the mandibular premolar teeth in the dog have two roots, usually of regular divergence but significantly longer than seen in the human because of the higher loads placed upon them. The dog has four premolars, the second and third are most commonly selected for involvement in studies. The mandibular first molar is a large and significant tooth, being a 'carnassial tooth' a term that describes its function for crushing bone/food material and cutting soft tissue. The opposing carnassial tooth in the maxilla is the fourth premolar but this tooth is three-rooted, as are the maxillary molars.

As the dog has six upper and lower incisor teeth, the single-rooted, straight second incisor may be selected, as the central incisors lie adjacent to the mandibular symphysis or the maxillary fissure/suture-line. The third maxillary incisor is a large tooth with a significant curve and is unlike any human tooth, and therefore not a suitable site. As the dog has six upper and lower incisor teeth, the single-rooted, straight second incisor may be selected, as the central incisors lie adjacent to the mandibular symphysis or the maxillary fissure/suture-line. The third maxillary incisor is a large tooth with a significant curve and is unlike any human tooth, and therefore not a suitable site.

5.3.2 Surgical Procedures

5.3.2.1 Extraoral
Extraoral locations are generally not used in the canine model. They would include lower border of mandible and calvarium.

5.3.2.2 Intraoral
The ethics committees are provided with a detailed plan of the proposed study, the reasons for it and expected outcomes as well as details of the procedural and technical plan. The surgical procedures are performed under general anesthesia as per other routine surgeries; analgesia is always provided independently of the anesthesia allowing for a minimal depth of anesthesia and hence minimizing risk to the animal.

Examination/Recordkeeping/Sedation
All dogs should be well-socialized and clinically examined to ensure good health prior to the commencement of the study. Premedication using acepromazine (ACP) administered a half hour prior to induction is recommended. The purpose of the premedication is to smooth both induction and recovery. ACP is a psychotropic drug that acts to calm down the animal and smooth out the induction and recovery. All findings and medications should be recorded on a standard anesthetic chart throughout the procedures.

Anesthetic Protocol
The administration of perioperative fluids and administration of the induction agent is via a 22 g I/V catheter placed into a foreleg cephalic vein; the anesthetic agent is also introduced through this catheter, usually as a slow full bolus. Alfaxalone at 2 mg/kg is the most commonly used induction agent; induction with this drug is expected to be smooth and uneventful, without cardiac or respiratory depression. Alfaxalone has only a brief duration of effect but allows intubation and a smooth transition to gaseous anesthesia. A cuffed endotracheal tube allows a secure connection to the gaseous anesthetic machine and isolation of the oral cavity from the respiratory system; oxygen is delivered at two liters/min. Once the tube cuff is inflated, isoflurane is delivered initially at 2% concentration; maintenance is usually satisfactory at 1–1.5% concentration due to the effective analgesia provided. Anesthetic delivery in these dogs, of about 30–35 kg, is via a semi-circle rebreathing system with an out-of-circle vaporizer.

Isotonic saline fluids are delivered I/V via the cephalic catheter up to 300 ml/h; approximating surgical rates (10 × body weight). The anesthetic is monitored using an automatic monitoring system (Cardell) but supported manually by a dedicated assistant as well; readings of mean, systolic and diastolic blood pressures, oxygen saturation (%SPO$_2$), pulse and respiratory rates are recorded every 5 min.

Analgesia
Preemptive analgesia is provided via an appropriate nerve block, usually using plain lignocaine. In routine veterinary oral procedures, as these studies generally are, it is not beneficial to the dog to be allowed to recover with a locally anesthetized muzzle or tongue. Their lack of appreciation of the local analgesia or of the hypersensitive phase that occurs as the local analgesia wears off has been recorded as a cause of self-trauma, especially to the tongue, as a bilateral block of the inferior alveolar nerve may inadvertently also include the lingual nerve. The problems with bupivacaine are twofold: firstly, the long time

after application to effect (in the order of half an hour) and the duration of effect (in the order of 5–6 h). This can be compared with plain lignocaine which may take 10 min to effect and lasts for 1–2 h. Of course, these timings are not only dose-dependent but also dependent on local tissue diffusion. Considering these pharmacological differences, lignocaine is the most common agent used in routine veterinary dentistry.

Peri and/or postsurgical analgesia can be provided by an opioid or a nonsteroidal analgesic (NSAID). Carprofen or Meloxicam are commonly used NSAIDs in veterinary medicine being administered subcutaneously for postrecovery analgesia, and this ensures at least 24 h of effective analgesia in the dog. Oral supplementary administration can be used for longer postsurgical analgesia.

Distal maxillary (intraorally administered) or distal mandibular blocks (administered extraorally) are used routinely but the infraorbital block may be used if only the rostral maxilla is involved.

Drug list:

– Acepromazine (ACP).
– Alfaxalone.
– Isoflurane.
– Lignocaine.
– Carprofen or Meloxicam.

Follow-Up and Termination

In experiments that require the dogs to be maintained for a length of time, they should be housed in runs with appropriate daily social interaction and exercised daily on the lead and allowed free exercise in runs with playthings such as water baths, rubber balls, and so on. In general softened food is provided for the first week, although the surfaces over the extracted teeth have generally healed uneventfully well within that time. Gingival and tooth/implant cleaning with dilute chlorhexidine solution and tooth brushing with appropriate chicken or beef flavored toothpaste is applied daily as required. Where investigation of tissue reactions to implant placement is a necessary end-point, the dogs are euthanized. This is done by the normal handlers within the dog's familiar housing in order to minimize any stress to the animals. An intravenous overdose of phenobarbitone (20 ml Lethobarb, Valobarb for a 30–35 kg dog) is administered through the cephalic vein with a 21 gauge needle. Care is taken that the needle is cleanly within the vein before administration of the euthanasia solution as it is very irritant if allowed to enter the tissues around the vein.

5.3.2.3 Surgical Step-by-Step

Two areas have primarily been used in the canine, the posterior mandible and, more recently, the anterior maxilla. Dental implant and regenerative investigations usually require the extraction of teeth as a precursor to the experimental procedure.

General Principles

It is a requirement that the teeth are extracted with minimal trauma to the alveoli and that the extracted teeth are delivered completely without leaving root fragments behind. This is the challenge to the operator as extraction of a pathologically affected tooth would normally be a surgical procedure. A mucogingival flap would be raised, some buccal bone removed using a high-speed carbide bur and the furcation (in two or three-rooted teeth) identified so that the tooth can be sectioned into its individual root segments that are then extracted individually. However, for dental implant trials, it is usually a requirement that the teeth are removed, leaving intact alveoli.

Following an appropriate nerve block and an intraoral radiograph to determine any root anomalies, a fine luxator is inserted into either the mesial or distal periodontal space. The instrument is then carefully but firmly rotated in order to detect resistance that would be expected if the instrument is correctly positioned. This force is held isometrically for a period of about 10 s. The aim is to stretch and then fatigue the periodontal ligament allowing some tearing of its fibers and consequent bleeding to occur. At this time, it is unlikely that any noticeable movement or progress will be observed. The instrument is then

placed into the opposite (mesial or distal) peri-odontal space and the process is repeated.

It is recommended that an inward-curved luxator is used for this initial procedure. This is because the curved tip tends to enter and follow the periodontal ligament space quite well. A heavier or straight instrument is less likely to do this.
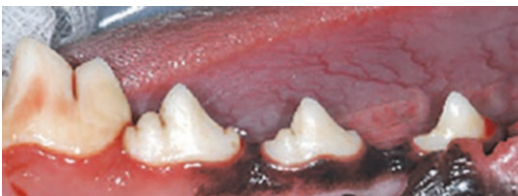
The above luxation procedure is repeated; it might be noted that the instrument penetrates into the PD space further each time. It is important to not rush this or apply excessive force, as the likely result will be either instrument or bone damage or fracture of the tooth's crown or root.

If/when the luxator becomes too small, a larger instrument is selected and the procedure continued. Eventually, some movement will be detected, but the luxation procedure should be persisted with until the movement is significant. At this time, elevator forceps may be used to attempt a 'corking' force: the jaws of the instrument are placed onto the tooth at the level of the cementoenamel junction, being careful not to crush the tooth, and a rotational force applied, firstly in one direction and then held for 10 s, then the other direction and again, held.

The aim is to further fatigue the remaining PD ligament fibers, allowing further tearing and bleeding of the fibers. If extraction does not occur, then again the luxator instrument is used to further effect. Once delivered, the tooth is examined for an intact apex, however, a postsurgical intraoral radiograph is taken to confirm the desired result.

Mandible

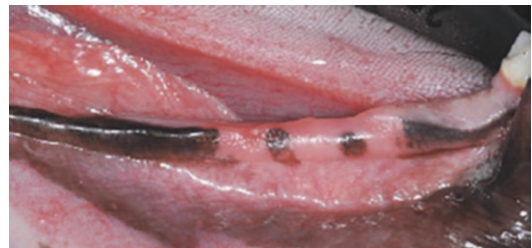Commonly all premolars and first carnassial teeth are extracted which provides space for up to four implants (Fig. 5.2). Space is limited by the distal extension of the root of the canine tooth and the positions of the mental foramina. Generally, the soft tissue around the teeth is elevated and the teeth sectioned to facilitate their removal.

When the protocol calls for extraction without flap elevation, intracrevicular incisions need to be made beforehand to free the marginal gingivae from the teeth. Careful inspection and probing are required to identify the location of the furcation entrance. Separation of the tooth into individual roots should be performed from the crown to the furcation (not the reverse) before luxation is started. As described previously, luxators and elevators are used in mesodistal movement, followed by removal with dental forceps (Fig. 5.3). Extraction of the more posterior teeth, especially the first carnassial, is very difficult. Bone removal is not undertaken. Healing is often characterized by a narrow zone of keratinized tissue and narrow ridges(Fig. 5.4).

In study designs that require a single root socket, one-half of the hemisected premolar (usually the mesial) may be retained. It is necessary to perform endodontic treatment on the retained

Fig. 5.3 Extracted premolars and first molar. Note that the double rooted second, third and fourth premolars, as well as the first molar have been divided into 2 prior to extraction. The first premolar has a single root

Fig. 5.2 Buccal view of right mandibular premolars and first molar in the dog. From right to left—second premolar (or #406), third premolar (#407), fourth premolar (#408) and first molar (#409)

Fig. 5.4 Buccal view of the right mandible 2 months after extraction of premolars and first molar teeth
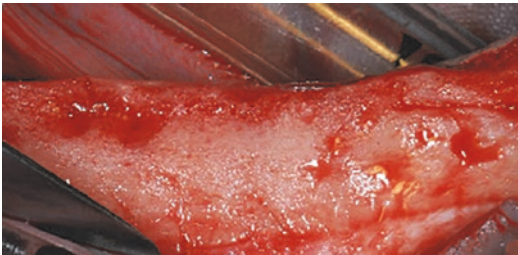
root and to provide an effective coronal seal with an appropriate restorative material. Incomplete root canal obturation may lead to peri-apical infection affecting the proposed implant sites.

Postextraction healing of 2–4 months has typically been used prior to the insertion of implants into the mandibular jaw, either with a submerged or transmucosal technique (Fig. 5.5). The height of the ridge is limited by the position of the inferior alveolar nerve. Reduced diameter and short implants are placed following standard protocols according to the implant manufacturer (Fig. 5.6). The breed of dog determines the ridge dimensions and usefulness in implant studies. Patterns of resorption following extraction vary between breeds. Implant placement is usually submerged as chewing may dislodge healing abutments with transmucosal placement and interfere with osseointegration. Following integration, healing abutments can be attached or peri-implantitis may be induced by applying ligatures to the integrated implants. Depending on breed and cooperation, plaque removal by standard oral hygiene meth-

ods and/or chlorhexidine is possible each day (procedure described previously). This greatly facilitates healing and is representative of the postoperative care in humans.

Anterior Maxilla

Extraction of the second incisor in the maxilla provides a socket that is similar to a small human single-rooted extraction socket and is more representative of healing in the anterior maxilla in humans than the posterior mandible (Figs. 5.7 and 5.8). Infraorbital blocks and local infiltrations are used to gain analgesia. Utilizing simple extraction techniques, the second incisors are extracted using luxators, elevators and forceps to deliver the whole tooth (Fig. 5.9). Careful extraction and good technique will prevent damage to the thin buccal plate. The extraction of incisor teeth is not as difficult as the mandibular poste-

Fig. 5.7 Occlusal view of the six maxillary incisors in a dog. From left to right, the teeth are #103. #102, #101, #201, #202 and #203. The right and left second incisors are teeth #102 and #202 respectively

Fig. 5.5 Intraoperative view following elevation of full thickness mucoperiosteal flaps at the buccal and lingual aspects of the alveolar ridge

Fig. 5.6 Four dental implants have been placed following flattening of the ridge crest and creation of experimental buccal defects

Fig. 5.8 Occlusal view following extraction of the right and left second incisors (#102 and #202). The teeth were extracted following intracrevicular incisions to release the gingival attachment from the teeth. The teeth were extracted by careful luxation and without elevation of surgical flaps
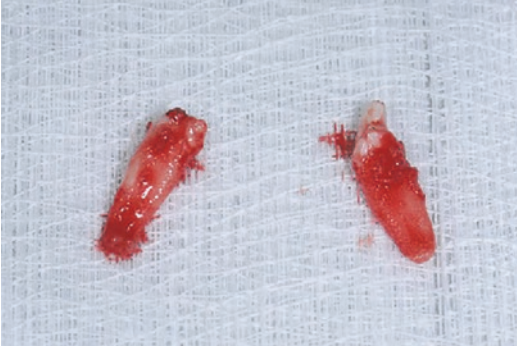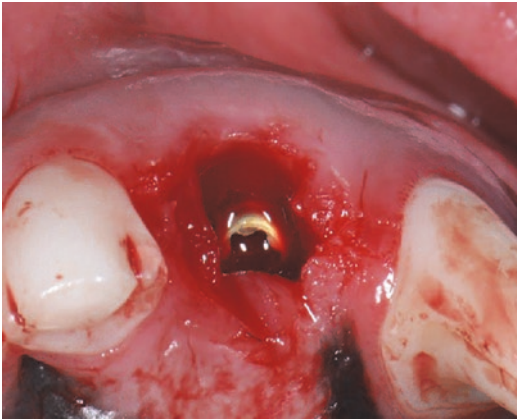
Fig. 5.9 The second maxillary incisors are following extraction. They are dimensionally similar to small lateral incisors in humans

Fig. 5.11 The residual defect on the buccal aspect of the implant has been grafted with particulate bovine bone mineral (BioOss, Geistlich Pharma, Switzerland) to test the efficacy of the material in this indication

Fig. 5.10 The second maxillary incisor socket may be utilised for immediate implant placement studies. Here a reduced diameter implant (3.3 mm bone level Roxolid Bone Level implant; Straumann AG, Basel, Switzerland) has been inserted. Note the marginal gap on the buccal aspect of approximately 2 mm which is similar to the marginal gap following immediate implants placed into maxillary incisor sites in humans
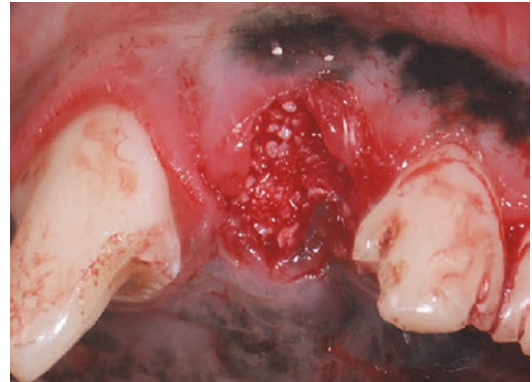
Fig. 5.12 The right second incisor socket has been grafted with bovine bone mineral (BioOss Collagen; Geistlich Pharma, Wolhusen, Switzerland) to test the efficacy of ridge preservation procedures utilising this biomaterial

rior teeth. The other incisor teeth are left in place to protect the site and composite resin bridges between the first and third incisors have been used to provide further protection [20]. The second incisors have curved roots pointing posteriorly and distally and need to be removed along this path.

Implant placement can be immediate (type 1) placement [10] (Figs. 5.10 and 5.11) or after 6–8 weeks of healing according to early implant placement (type 2) protocol. These time frames represent those used in humans. Ridge dimen-

sions at 6–8 weeks still allow implants to be placed. Short and reduced-diameter implants are placed, such as 8 mm in length. Longer implants may perforate the cortical plate or nasal floor. The angulation of implants in socket follows that of the roots, posteriorly and distally. Incorrect alignment may result in damage to the neighboring teeth. Ridge preservation studies using standard bone graft materials and membranes to fill and cover the socket can easily be undertaken [21] (Figs. 5.12 and 5.13). Elevation of the soft tissue is possible to allow grafting procedures and coronal advancement to submerge implants,
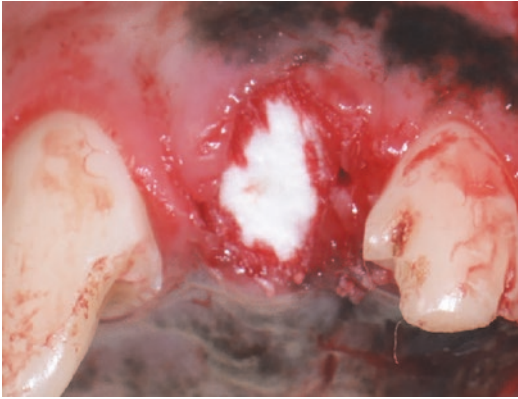
Fig. 5.13 The graft within the socket has been covered with a resorbable collagen membrane (Mucograft Seal: Geistlich Pharma, Wolhusen, Switzerland) to promote soft tissue healing

Fig. 5.14 Following 3 months of healing, the soft tissues have healed with complete regeneration and gingival coverage of the graft

but elevation beyond the mucogingival junction can result in degloving of the anterior maxilla once the dog recovers and starts to bite and chew again. Healing protocols with immediate implant placement may include nonsubmerged, partially or semi-submerged, and fully submerged healing (Fig. 5.14). To facilitate soft tissue closure over the sockets, resorbable membranes may be use.

Buccal dehiscence defects can be created with surgical instruments or burs, creating a situation similar to that in the anterior maxilla in humans. These can be grafted, covered with a membrane and submerged with delayed implant placement. Again, chewing can dislodge healing abutments and interfere with integration. Depending on breed and cooperation, daily plaque removal by standard oral hygiene methods and/or chlorhexidine is possible.

Recommendations

Both models have their advantages and disadvantages. The posterior mandible provides a very representative model for use in preclinical implant research. It is suited for analysis of osseointegration, the effect of implant design and surface treatments on integration, simultaneous or staged augmentation with or without defects, bone regeneration, such as removal of the buccal wall, implant loading, orthodontic loading, biofunctional research, ridge preservation, soft tissue healing around implants, and peri-implantitis studies. It is, however, not representative of socket healing in the anterior maxilla in humans. The second incisor extraction socket model in the maxilla provides a better extraction socket model and can be used for ridge preservation, socket healing studies, bone regeneration, and immediate and/or delayed implant placement with or without grafting.

5.4   Investigative Methods of Evaluation

There have been a wide variety of investigations performed in the canine model. Initially, the majority of studies investigated the osseointegration of titanium implants into jawbone and the factors that might influence this process. Studies of osseointegration also investigated the influence of dental implant surface topography [22, 23], coating materials and bioactive molecules incorporated in or applied to the implant surface [24]. Tissue and histomorphometric analyses have usually been undertaken on undecalcified sections created by the cutting/grinding process and light microscopy [25] (Fig. 5.15).

Flurochrome labeling of bone, polarized light microscopy, scanning electron microscopy and microCT have also been employed as analytical tools. Resonance frequency analysis has been used as an indirect measure of osseointegration. The most common oral sites for studies of osseo-
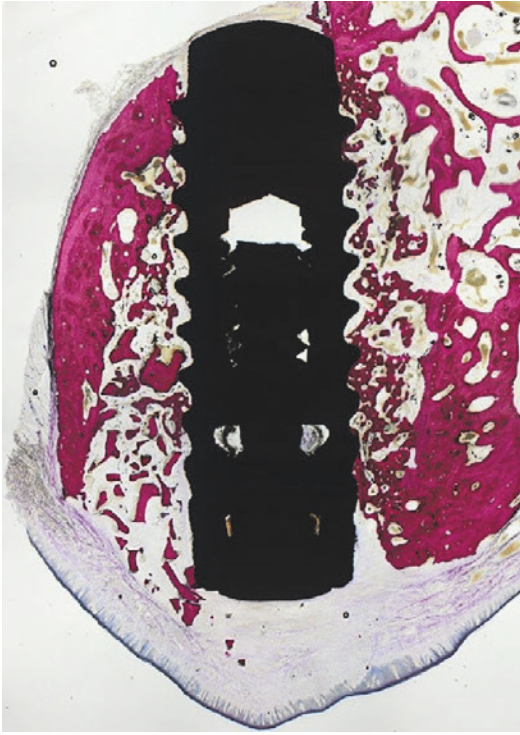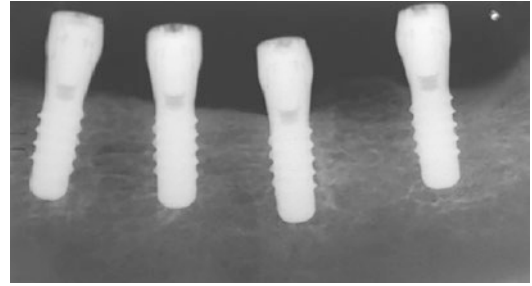
Fig. 5.15 Histomorphometric analysis is the most common evaluation undertaken for preclinical studies in dental implantology utilising the canine model. Non-decalcified sections are prepared by the cutting and grinding technique [25] followed by staining with Paragon (toludine blue and basic fuchsine). This image illustrates a dental implant placed immediately into the maxillary second incisor socket and grafted with a biomaterial

Fig. 5.16 Intraoral radiograph for implants placed into the posterior mandible. Intraoral radiography is useful for evaluating changes in crestal bone position around dental implants

integration have been the mandibular premolar and first molar regions. Postextraction healing of 2–4 months has typically been used prior to the insertion of implants into the mandibular jaw, either with a submerged or transmucosal technique [3, 5, 7, 8, 26, 27].

5.4.1 Intraoral Radiography

Intraoral radiography is an invaluable diagnostic and investigative tool. Diagnostic radiographs will demonstrate the local anatomy that includes the alveolar bone, the periodontal ligament space, the dentine and enamel, and also the crown-root ratio and the shape of the root/s can be determined.

The dog has a flat palate, unlike the vaulted palate in humans and as such, the parallel technique for taking intraoral radiographs is not pos-

sible for maxillary teeth. In fact the only position that parallel technique is possible in the dog is for the distal mandible (molar and distal premolar teeth). In all other areas, the bisecting angle technique is used.

Presurgical radiographs are taken to document the individual's anatomy, as variations from 'normal' are not uncommon: ankylosis (of the PD ligament), root dilacerations and even supernumerary or twinning of roots can be encountered. The radiographs are repeated postextraction and after the placement of the implant (Fig. 5.16).

In veterinary dentistry, the hand-held mobile dental X-ray machine is more common than the wall-mounted units; likewise, the use of film and wet chemistry has largely been replaced by digital technology.

5.5 Flagship Results

The canine model has a long history of use in implant research.

5.5.1 Socket Healing

Socket healing studies include two classic papers by Cardaropoli and co-workers [28] and Araujo and Lindhe [29]. Cardaropoli et al. sequentially extracted teeth and followed the healing of the sockets over 180 days, providing the first really detailed evidence of the changes in the socket walls and stages of healing with the blood clot, granulation tissue, woven and lamellar bone. Araujo and Lindhe [29] investigated the healing of

the lingual and buccal sockets walls following extraction reporting the greater loss of the buccal plate. They attributed this to the greater proportion of bundle bone in the buccal wall, which is a tooth-derived structure. This seminal paper has changed the way implant dentistry is undertaken.

5.5.2 Implant Loading

Heitz-Mayfield et al. [19] studied the effect of occlusal overload on integrated implants placed in the posterior mandible. Crowns were placed such that they occluded with the opposing natural teeth and received substantial loading. They showed that axial overloading of the implant did not affect the integration.

5.5.3 Biologic Width at Implants

The effect of implant design on the biologic width was reported by Hermann and coworkers in their classic paper [30]. In the posterior mandible they placed six different implant designs, both submerged and nonsubmerged, above, at, or below bone level to determine the effect of the position of the rough/smooth border or implant/abutment interface on the peri-implant soft tissues. Two-piece implant designs resulted in more apical bone levels.

5.5.4 Guided Bone Regeneration (GBR)

Schenk et al. [31] investigated the healing of bone produced by guided bone regeneration in the posterior mandible [31]. After extracting the posterior teeth, they created a series of defects which were then covered by membranes. Histologic evaluation showed the new bone occurred in similar stages to that of normal bone growth and deposition.

5.5.5 Peri-implantitis

Two studies from Gothenberg compared the periodontal and peri-implant tissues following plaque buildup. The first [32] showed that peri-implant mucosa reacts similarly to gingival tissues. The second [33] reported greater clinical and radiographic destruction in the peri-implant tissues compared to the periodontal tissues following induction of peri-implantitis, that the soft tissue inflammatory infiltrate was bigger around implants, and lastly, that the peri-implant inflammatory lesion extended into the bone where the periodontal lesion did not.

5.5.6 Immediate Implants

The use of the anterior maxilla has provided a leap forward as it closely resembles that of humans and our group has been instrumental in its development. Immediate implant placement in the anterior maxilla was reported by Mellati et al. [10]. The effect of submerged versus nonsubmerged healing was compared around implants placed in fresh extraction sockets and grafted with deproteinized bovine bone mineral and a collagen membrane with coronal advancement of the soft tissue to submerge half the implants. The histological analysis showed no difference between the two groups.

5.5.7 Bone Healing Around Implants

By adding a circumferential trough in the preparation of the implant, Berglundh et al. [34] added an experimental chamber for the study of early wound healing. Using 160 implants placed in 20 dogs they showed using very clear histology the stages of implant healing from coagulum to lamellar and then woven bone. They also showed the remodeling of bone lateral to the threads.

5.5.8 Alveolar Ridge Preservation

The mandible has been the most commonly used area for ridge preservation studies with a mix of second, third, fourth premolars and first molars selected. Classically these teeth are sectioned and one root is used as the test site, usually the distal

root. Control sites, usually the mesial root, are either the healing socket of the extracted second root or the second root left in situ, which should be root canal treated.

The use of the maxillary second incisor provides a healing socket more similar to a human socket. Raveendiran et al. [21] analyzed the socket dimensions of maxillary second incisors with natural healing or ridge preservation using histomorphometric measurements, CBCT and superimposition of 3D scanned models. They clearly showed less horizontal resorption at the crestal mid-buccal in the ridge preserved sites.

In both models, grafting of the sockets provided greater ridge dimension, but did not prevent the resorption of the buccal wall completely.

5.6   Conclusions

The canine is a versatile preclinical model for studies on postextraction healing, dental implantology and related tissue regeneration. It continues to be an important model for research in these fields.

References

1. Grenoble DE, Melrose RJ, Markle DH. Histologic evaluation of vitreous carbon endosteal implants in occlusion in dogs. Biomater Med Devices Artif Organs. 1975;3:245–58.
2. Mazzocco DM, Ceravolo FJ, Baumhammers A, Vaughn RL, Molinari JA, Verbin R, Ruskin PF. Quantitation of retention of endosseous dental blade implants in dogs. J Periodontol. 1978;49:39–42.
3. Lee D, Sohn B, Kim KH, Kim S, Koo KT, Kim TI, Seol YJ, Lee YM, Rhyu IC, Ku Y. Effects of untreated periodontitis on osseointegration of dental implants in a beagle dog model. J Periodontol. 2016;87:1141–8.
4. Kim MY, Choi H, Lee JH, Kim JH, Jung HS, Park YB, Moon HS. UV photofunctionalization effect on bone graft in critical one-wall defect around implant: a pilot study in beagle dogs. Biomed Res Int. 2016;2016:4385279.
5. Carral C, Munoz F, Permuy M, Linares A, Dard M, Blanco J. Mechanical and chemical implant decontamination in surgical peri-implantitis treat-
ment: preclinical "in vivo" study. J Clin Periodontol. 2016;43:694–701.
6. Discepoli N, Vignoletti F, Laino L, de Sanctis M, Munoz F, Sanz M. Fresh extraction socket: spontaneous healing vs. immediate implant placement. Clin Oral Implants Res. 2015;26:1250–5.
7. Rea M, Botticelli D, Ricci S, Soldini C, Gonzalez GG, Lang NP. Influence of immediate loading on healing of implants installed with different insertion torques--an experimental study in dogs. Clin Oral Implants Res. 2015a;26:90–5.
8. Rea M, Lang NP, Ricci S, Mintrone F, Gonzalez Gonzalez G, Botticelli D. Healing of implants installed in over- or under-prepared sites--an experimental study in dogs. Clin Oral Implants Res. 2015b;26:442–6.
9. Lozano-Carrascal N, Delgado-Ruiz RA, Gargallo-Albiol J, Mate-Sanchez JE, Hernandez Alfaro F, Calvo-Guirado JL. Xenografts supplemented with pamindronate placed in postextraction sockets to avoid crestal bone resorption. Experimental study in fox hound dogs. Clin Oral Implants Res. 2016;27:149–55.
10. Mellati E, Chen S, Davies H, Fitzgerald W, Darby I. Healing of bio-Oss grafted marginal gaps at implants placed into fresh extraction sockets of incisor teeth in dogs: a study on the effect of submerged vs. non-submerged healing. Clin Oral Implants Res. 2015;26:553–62.
11. Ferrari DS, Piattelli A, Iezzi G, Faveri M, Rodrigues JA, Shibli JA. Effect of lateral static load on immediately restored implants: histologic and radiographic evaluation in dogs. Clin Oral Implants Res. 2015;26:e51–6.
12. Khanna C, Lindblad-Toh K, Vail D, London C, Bergman P, Barber L, Breen M, Kitchell B, McNeil E, Modiano JF, Niemi S, Comstock KE, Ostrander E, Westmoreland S, Withrow S. The dog as a cancer model. Nat Biotechnol. 2006;24:1065–6.
13. Muschler GF, Raut VP, Patterson TE, Wenke JC, Hollinger JO. The design and use of animal models for translational research in bone tissue engineering and regenerative medicine. Tissue Eng Part B Rev. 2010;16:123–45.
14. Pearce AI, Richards RG, Milz S, Schneider E, Pearce SG. Animal models for implant biomaterial research in bone: a review. Eur Cell Mater. 2007;13:1–10.
15. Rashid ST, Salacinski HJ, Hamilton G, Seifalian AM. The use of animal models in developing the discipline of cardiovascular tissue engineering: a review. Biomaterials. 2004;25:1627–37.
16. Wang X, Mabrey JD, Agrawal CM. An interspecies comparison of bone fracture properties. Biomed Mater Eng. 1998;8:1–9.
17. Aerssens J, Boonen S, Lowet G, Dequeker J. Interspecies differences in bone composition, density, and quality: potential implications for in vivo bone research. Endocrinology. 1998;139:663–70.
18. Laiblin C, Jaeschke G. [Clinical chemistry examinations of bone and muscle metabolism under stress in

the Gottingen miniature pig--an experimental study]. Berl Munch Tierarztl Wochenschr. 1979;92:124–8.

19. Heitz-Mayfield LJ, Schmid B, Weigel C, Gerber S, Bosshardt DD, Jonsson J, Lang NP. Does excessive occlusal load affect osseointegration? An experimental study in the dog. Clin Oral Implants Res. 2004;15:259–68.

20. De Santis E, Botticelli D, Pantani F, Pereira FP, Beolchini M, Lang NP. Bone regeneration at implants placed into extraction sockets of maxillary incisors in dogs. Clin Oral Implants Res. 2011;22:430–7.

21. Raveendiran N, Chen S, Davies H, Fitzgerald W, Darby I. The influence of BioOss® collagen on dimensional changes of the maxillary lateral incisor socket. Clin Oral Implants Res. 2019;30:670–81.

22. Wennerberg A, Albrektsson T. Effects of titanium surface topography on bone integration: a systematic review. Clin Oral Implants Res. 2009;20(Suppl 4):172–84.

23. Wennerberg A, Albrektsson T, Andersson B. Design and surface characteristics of 13 commercially available oral implant systems. Int J Oral Maxillofac Implants. 1993;8:622–33.

24. Fiorellini JP, Glindmann S, Salcedo J, Weber HP, Park CJ, Sarmiento HL. The effect of osteopontin and an osteopontin-derived synthetic peptide coating on osseointegration of implants in a canine model. Int J Periodontics Restorative Dent. 2016;36:e88–94.

25. Donath K, Breuner G. A method for the study of undecalcified bones and teeth with attached soft tissues. The Sage-Schliff (sawing and grinding) technique. J Oral Pathol. 1982;11:318–26.

26. Nevins M, De Angelis N, Ghaffari S, Bassir H, Kim DM. Comparative clinical and histologic assessments of dental implants delivered with a manual torque lim-

iting wrench versus with an electronically controlled torque limiting device. Int J Periodontics Restorative Dent. 2015;35:819–23.

27. Mainetti T, Lang NP, Bengazi F, Favero V, Soto Cantero L, Botticelli D. Sequential healing at implants installed immediately into extraction sockets. An experimental study in dogs. Clin Oral Implants Res. 2016;27:130–8.

28. Cardaropoli G, Araujo M, Lindhe J. Dynamics of bone tissue formation in tooth extraction sites. An experimental study in dogs. J Clin Periodontol. 2003;30:809–18.

29. Araujo MG, Lindhe J. Dimensional ridge alterations following tooth extraction. An experimental study in the dog. J Clin Periodontol. 2005;32:212–8.

30. Hermann JS, Buser D, Schenk RK, Schoolfield JD, Cochran DL. Biologic width around one- and two-piece titanium implants. Clin Oral Implants Res. 2001;12:559–71.

31. Schenk RK, Buser D, Hardwick WR, Dahlin C. Healing pattern of bone regeneration in membrane-protected defects: a histologic study in the canine mandible. Int J Oral Maxillofac Implants. 1994;9:13–29.

32. Berglundh T, Lindhe J, Marinello C, Ericsson I, Liljenberg B. Soft tissue reaction to de novo plaque formation on implants and teeth. An experimental study in the dog. Clin Oral Implants Res. 1992;3:1–8.

33. Lindhe J, Berglundh T, Ericsson I, Liljenberg B, Marinello C. Experimental breakdown of peri-implant and periodontal tissues. A study in the beagle dog. Clin Oral Implants Res. 1992;3:9–16.

34. Berglundh T, Abrahamsson I, Lang NP, Lindhe J. De novo alveolar bone formation adjacent to endosseous implants. Clin Oral Implants Res. 2003;14:251–62.

Preclinical Studies Design and Place of Ovine and Caprine

6

Stefan Stübinger and Brigitte von Rechenberg

6.1 Experimental Animal Model

6.1.1 Animal Species and Animal Model

For preclinical studies of dental implantology, one has to clearly ask the appropriate question before deciding on an animal model and or species. What exactly needs to be tested—and in which order? Is the same animal model appropriate for each of these questions, or do we need separate and different animal studies to answer questions in an adequate fashion.

As a general rule, small animal rodents do not qualify to be used as animal models in dental implantology simply due to size. Rabbits could be used for testing biocompatibility alone but not for biomimetic substances since they produce bone at almost any stimulus. However, results often cannot be repeated in larger animals. In this case, sheep or goats would be more accurate. If weighing sheep against goats, one must consider

that sheep are more robust, which is an advantage in long-term experiments. Goats are more sensitive to diseases, especially slow virus infections that may be missed in an early stage. In addition, goats may prove to be difficult to live in a herd, since they attack each other quite frequently, being more individualistic than sheep.

Apart from size of implants other factors require similar decisions.

Let us take an example: a new dental implant has been developed, where a new implant design and implant material were chosen. In addition, the surface of the implant is specially coated with a bone-inducing agent that is expected to facilitate osseointegration of the new implant. With a new implant like this, at the end, safety, biocompatibility, efficacy, and functionality have to be assessed and proven to the regulatory authorities.

Each of these questions needs a different approach. While safety is the sum of all others, biocompatibility is related to the implant material. Efficacy has to be proven for the bone-inducing agent, and functionality has to be shown with the final implant in situ, mimicking most accurately the clinical situation in humans before clinical trials (phase I–III) in humans can be initiated.

The most severe mistake often done in preclinical research is that, mainly for cost reasons, all questions are jammed into one experiment. If too many questions are combined, usually, none

S. Stübinger (✉)
Hightech Research Center of Cranio-Maxillofacial Surgery, University of Basel, Allschwil, Switzerland
e-mail: stefan.stuebinger@unibas.ch

B. von Rechenberg
Musculoskeletal Research Unit (MSRU), Competence Center for Applied Biotechnology (CABMM), Vetsuisse Faculty ZH, University of Zurich, Zurich, Switzerland
e-mail: bvonrechenberg@vetclinics.uzh.ch

of the answers will be gained due to the complex situation of an in vivo experiment. In the case of dental implantology, several factors within the environment play a role. There is the mandibular or maxillary bone to consider, but also the surrounding soft tissue and mucosa, the mechanism of teeth, resp. implant fixation and as a major factor the oral contamination with commensal bacteria. If the implant described above needs testing, the first step should be related to biocompatibility. This should be done in an environment without biomechanical or infectious stress. There, a pelvic model in sheep (see Sect. 6.2.1) serves well. Osseointegration can be tested easily, such that bone–implant interface can be determined standardized without interferences. Furthermore, biomechanical tests can be performed in the same sheep model. Lastly, bone-inducing substances can be tested in the same model, since results can be directly transferred to human beings. Once these questions are clarified, functionality can finally be tested in an oral cavity model, possibly even in another species, such as mini-pigs.

6.1.2 General Use in Medical Device Research

Implants need to be tested in preclinical studies before they can be used in human beings. For this, regulatory affairs need to be respected for implant production (good manufacturing practice (GMP)) as well as for conducting the animal experiments under Good Laboratory Practice (GLP) conditions. Both are needed to get accreditation through the official regulatory authorities, such as the FDA in the United States, TÜV in Europe, or PMDA in Japan. For a long time, medical devices were required to be tested only after OECD guidelines. However, as of January 1, 2018, medical devices also need to be tested in preclinical experiments according to GLP as pharmaceuticals. Only then, implants can be taken for clinical trials (phase I–III) according to Good Clinical Practice (GCP).

6.1.3 Financial Consideration

Financial considerations are often the basis of why too many questions are combined in one single animal experiment. However, saving money does not work, if no answers can be given at the end. A classic of this problematic approach is the role of mucosal membranes if new dental implants are to be tested in the oral cavity. If a new implant has to be tested for biocompatibility and the implant is tested directly in the oral cavity, in case of failure, it is impossible to draw valid conclusions. If they fail and become loose—is it because implants are not biocompatible or because contamination with commensurate bacteria leads to infection, ultimately leading to implant loosening? Or worse, in many cases, membranes to protect the alveolar bed from the ingrowth of fibrous tissue are added as well without having been separately tested. At the end of the day, all costs were for nothing. Therefore, costs should never be at the forefront of study design. Taking a solid step-by-step approach and answering one question at a time may seem to drive costs considerably in the beginning. But then, when clear answers were obtained, the costs were worthwhile in their effort.

6.2 Surgical Model

In oral and maxillofacial as well as in orthopedic surgery, there is an increasing demand for reliable animal models to resemble human bone remodeling and biomechanics. In this respect, the number of skeletally mature female sheep included in animal trials for dental implantology and orthopedic problems is becoming more and more popular [1].

Generally, animal models provide substantial data for three fundamental issues of implant dentistry: appraisal of toxicity, assessment of biocompatibility, and refinement of implant material and design [2]. In each of these areas, different animal species are of special importance and offer decisive suitability for the later intended

clinical use. Yet beneath following the 3R (reduce, replace, refine) concept, it is also of pivotal importance for any experimental in vivo trial to have an economically valuable model offering adequate quantities and qualities of tissue exhibiting an approximation to the human situation.

According to international standards regarding species suitability for testing implants in bone, rats, rabbits, dogs, mini-pigs, coats, and sheep represent important preclinical models. Although especially dogs and rabbits are one of the most frequently used models, they offer certain drawbacks and constraints, e.g., significant differences in bone composition, healing, and anatomy as well as ethical issues. In contrast, sheep are a reliable and suitable large animal model for bone research because of similar bone metabolism to humans, availability, animal cost, ease of handling/housing, and overall acceptability to society [3]. Furthermore, for large animals like sheep and goats the International Organization for Standardization (ISO) recommends dimensions of cylindrical implants of 4 mm in diameter and 12 mm in length for implantation that ideally fit the general design of dental implants [4].

6.2.1   Surgical Locations

6.2.1.1   Extraoral
Sheep and goats are usually recruited for extraoral implantation experiments in implant dentistry. Vignoletti and coworkers [5] record that in 71.4% of all goat and sheep studies which they included in their analysis, an extraoral location was chosen. The most common reasons for this choice are obviously surgical accessibility and available bone volume. Adult sheep have comparable body weight, bone size, and bone healing potential to humans. Thus the transferability of any biological or functional results to humans exhibits a much more sound basis than in comparison to smaller species like mice or rabbits [6]. As sheep and goats show sufficient bone mass serial sampling and multiple experimental procedures are possible. Thereby also a differentiation between endochondral and intramembranous bone remodeling in long bones, respectively, the skull is feasible.

According to the study of Aerssens and coworkers [7] about interspecies differences in bone composition, humans and sheep disclose some similarities in trabecular bone and less in cortical bone regarding ash, hydroxyproline, and extractable protein content.

In addition to these findings, Ravaglioli et al. [8] demonstrated that bone mineral composition does not strikingly differ between humans and sheep. Yet sheep exhibit an overall higher bone density (mass/volume) and consequently strength than humans. Nafei et al. [9] observed a density of 0.61 g/cm^3 for sheep trabecular bone taken from the proximal tibia. Thus, in contrast to humans, the trabecular bone density is 1.5–2 times higher [10]. However, such measurements and results from the literature have to be interpreted very critically. On the one hand, they account not for all anatomical sites in the same way, and on the other hand, also, age, season, and food have a vital influence [11, 12].

Interestingly, seasonal influences on sheep iliac crest biopsies exhibited the same trends: increasing bone mass in summer and decreasing bone mass in winter [13].

However, while differences in bone structure and composition between sheep and humans are often inconsistent in literature, one pivotal issue for choosing an extraoral implantation site in sheep is certainly the bone remodeling process. Several studies have proven that both trabecular and cortical endochondral bone remodeling of sheep are very similar to humans [1]. Yet for the sake of completeness, it has to be mentioned that there are also some reports in the literature that object to this statement. Objections include the fact that sheep possess less Haversian canals than humans and primarily show off a primary bone structure, whereas humans have a large component of secondary bone at maturity [14].

In general, the characteristics of bone macro-, microstructure, and bone remodeling of sheep also apply to goats [15]. In this respect, a qualitative evaluation of goat iliac crest bone revealed a well-defined trabecular structure, with a different orientation of the trabeculae in the center of the

iliac crest compared with the peripheral borders [16]. The trabecular network in the center of the goat's iliac crest disclosed a rather porous architecture with a bone volume fraction substantially lower than in the goat femoral condyle. Hillier et al. [17] demonstrated that the cortex of long bones in mature goats consists of both plexiform and Haversian bone tissue. Whereas near the periosteal surface, mainly pelxiform bone, with scattered areas of Haversian tissue could be seen, the endosteal surface disclosed a dense Haversian tissue.

Based on the described anatomical and histological findings nowadays in mostly either the pelvic bone or the tibia and femur are chosen for extraoral implant sites in sheep and goats. Especially, the pelvic bone of sheep offers sufficient quantity and quality of cancellous as well as cortical bone distribution for a comparison with the human mandible according to the Lekholm and Zarb index [18]. The pelvic bone structures allow for a separate and distinct evaluation and analysis of the influence of characteristic implant features, e.g., implant macro design or implant surface modifications. In particular, the histological interpretation of the Bone-to-Implant-Contact (BIC) can be meticulously analyzed with respect to trabecular bone or dense bone. In combination with an additional torque, push, or pull-out test, this approach provides a comprehensive biological and biomechanical assessment. Also, a clear distinction and evaluation of a possible press-fit effect with marginal bone condensation and crack formation in cancellous or cortical bone is possible in sheep as well as in goats [19].

The sheep pelvis model allows the implantation of a relatively high number (up to $n = 18$) of implants in one animal. With the possibility to place implants of a length of up to 10 mm under aseptic conditions, the model is ideal for a direct comparison to the human situation with a clear focus on the osseointegration properties. A similar approach in the goat pelvic bones also offers the possibility of inserting up to $n = 10$ implants per animal.

In both models, the high number of comparable test sites allows for a good standardization and reasonable statistical evaluation with very high statistical power. Furthermore, this animal model is recognized and accredited by regulatory authorities to test safety and biocompatibility, although the numbers if implants per pelvic site are limited to six implants each.

Yet the pelvic model also shows off one major drawback. Like with any extraoral implant site an analysis of peri-implant soft tissues structures or the biological width is not possible. Thus the vital influence of these important parameters on the initial bone healing phase or the long-term stability cannot be assessed. Likewise, any microbiological examinations or biofilm formation are excluded from this specific extraoral surgical location.

In contrast to the pelvic bone, the tibia or femur offers less comparable advantages with regard to cancellous and cortical bone distribution. Interpretation of data is often challenging due to the high amount of plexiform cortical bone histological and biomechanical. The central medullary cavity even aggravates this situation, especially in the tibia of sheep and goats, where almost no trabecular area is present except at the proximal metaphysis. In the latter, even the trabecular bone is very dense and does not match well with the bone structure of the mandibula. An accidental bi-cortical placement of too long implants can produce misleading histological and biomechanical results. Also, in case of close vicinity, the opposite cortical bone often induces growth toward the apices of the implants and consequently fosters bone remodeling. Furthermore, the amount of cancellous bone in the femoral condyle is more compact and dense in comparison to the human mandible [20]. With four to six implant sites per limb also sample size is restricted and thus hamper standardization and statistical evaluation. Postoperatively, there is a possible risk for occasionally transient swollen knees due to edema or hematoma. However, the model is often chosen because of its uncomplicated surgical access with less muscular trauma.

Except for the pelvic bone or the tibia and femur there are only a few isolated studies in the literature that also tried a different extraoral location in sheep or goats. Schopper et al. [21] described a costal sheep model. Thereby ribs of

skeletally mature female sheep were exposed via a straight lateral approach of the right hemithorax. Five implants per rib were spaced at least 10 mm apart from each other. Although the authors did not report any severe problems by using this model, there are no further studies available to support the advantages of this model.

In conclusion, especially extraoral sheep models are increasingly used in many biomedical studies because of their similarity in bone remodeling, as well as for economic, and ethical reasons. Both sheep and goats are valuable preclinical animal models that can be widely used in oral and craniofacial research.

Yet even though results derived from extraoral surgical sites in sheep and goats provide sound experimental data, the models must always be viewed with caution because of the differences between species, biomechanical loading situation, and missing vital intraoral soft tissue structures.

6.2.1.2 Intraoral

Sheep have their specific and intensive biomechanical chewing patterns inherent to their constant ruminant activity. This makes tooth extractions seem highly questionable and need a profound ethical clearance. Nevertheless, there were some attempts to use sheep as a potential animal model for immediate implant placement in fresh extraction sockets. Whereas tooth extraction and implant placement techniques do not relevantly different from mini-pigs, implant osseointegration is massively disturbed. Vlaminck and coauthors [22] report cumulative implant failure rates of 45.5%, 63.6%, and 77.3% at 30, 90, and 180 days. Due to this high failure rate, this procedure currently cannot be supported for implant research.

Another option is the naturally edentulous region between the canine and molars. This region can be used for either direct implant placement or an augmentation procedure. Even though this area may work for some specific procedures, e.g. distraction osteogenesis [23], in many cases, this approach leads to adverse results. Likewise, attempts to resemble an atrophied alveolar ridge by surgical resection of the mandible caused

postoperative complications. Mainly wound infection, severe sepsis, or even pathologic fractures restricted any further utilization of this anatomical site [24].

Other authors also supported the adverse effects of placing implants in the lower alveolar ridge. Gatti et al. [25] reported a retarded and incomplete bone healing in the mandibular bone, albeit using transcutaneous access. After 4, 8, and even 12 months, the empty reference hole in this area disclosed an incomplete bone repair with only a little bone ingrowth into the defect.

In contrast, an approach to the mandibular ramus of sheep via cutaneous access from the posterior edge of the ramus revealed much more promising results with respect to wound healing and risk of infection [26]. Notwithstanding, it has to be mentioned that in this study, not a primary bone healing respectively, osseointegration, but the resorption rate of ultrasound-activated pins was evaluated. Huasong [27] and coworkers used similar access in goats. Again the mandibular angle was approached by an extraoral incision to insert two implants in the ramus region. For them, the wide variance of cortical thickness among different goats and/or locations compromised the global practicability of the model.

In contrast to the mandible and the maxilla, respectively, a lateral sinus elevation procedure apically of the roots of the upper molars is much more popular. On the one hand no tooth extraction is necessary, and on the other side, the enclosed cavity of the maxillary sinus is less prone to wound infection. Furthermore, sinus studies predominantly look for the behavior and healing of bone grafting materials in a predefined hollow space in the sinus. Thus, host bone composition and distribution not play the same important role as in implant osseointegration studies, as implants are finally placed into an augmented (mostly biomaterial) area. For this reason, there are also no specific clinical data available about the macro- or microstructure of maxillary bone. Generally, however, basic bone parameters, e.g. mineral composition, do not significantly differ from extraoral sites.

One major experimental disadvantage of the approach to the maxillary sinus is that it requires

either an extraoral approach or a previous enlargement of the buccal vestibule. This access does not resemble the clinical situation in humans, where access to the sinus is performed from the oral cavity. The appearance and orientation of the sinus are a bit different from humans, even though some authors also report that sheep are a useful animal model because both the general nasal anatomy and the paranasal sinus anatomy are similar to humans [28].

Clearly, profound differences exist at the intraoral anatomic, functional, and microbiological levels between humans and sheep and goats. These differences must be critically assessed before extrapolating the results of a given study to the human clinical situation.

6.2.2 Surgical Procedures

From an ethical standpoint considering animal welfare and protection, sheep and goat are commonly well-accepted animal models. Surgery of the pelvis or femoral condyle does not interfere significantly with normal ambulation of the animals, and housing can be easily provided appropriate to the species and handling. As the resultant pain and stress for the animals are rather low, and the recovery time of the animals is relatively quick, both species become more and more relevant for a qualitative and quantitative analysis of osseointegration.

For all extra and intraoral surgical interventions in sheep and goats, general anesthesia with corresponding analgesia under sterile conditions is necessary. Generally, an experienced professional in veterinary anesthesia should conduct the anesthesia. Thereby full monitoring during the whole procedure with a combined systemic administration of analgesia and.

loco-regional anesthetic techniques is advisable. This approach by the authors has proven to be highly successful over several years in more than 7000 different orthopedic and maxillofacial surgical interventions in sheep.

6.2.2.1 Extraoral Description of the Procedures

Pelvic Bone
The pelvic sheep model was developed and introduced by the authors to provide a similar remodeling rate, bone structure, and bone proportions to the human mandible. The surgical approach takes place in the following way.

Initially, sheep are placed in lateral recumbency with the pelvis slightly inclined (ca. 15%) toward the surgeon. An about 13–18 cm long curved skin incision is performed more or less parallel and in the middle of the iliac wing reaching the acetabular region. The fascia is incised, and a blunt approach to the pelvis bone is performed between the middle gluteal and the tensor fasciae latae muscle. With a scalpel, the deep and middle gluteal muscles are incised and carefully separated close to the iliac wing in the lower third of the muscle insertions at the iliac crest.

In stepwise approach, the gluteal muscles are retracted dorsally using appropriate retractors, and the iliac wing is exposed. The periosteum is incised and removed ventrally, resp. dorsally exposing the entire iliac crest. Then a customized aluminum template with up to nine drill hole markers is meticulously contoured to the linea glutea of the iliac wing, with the template end joining and being fixed with a clamp right at the insertion of the gluteal muscles. Depending on the overall amount of implants, drill holes are prepared. Generally, a maximum of $n = 9$ implants can be placed per wing. The implant positions are distributed on alternating sides along the linea glutea, with position 1 being the most caudal and position 9 being the most cranial in the iliac shaft. Care has to be taken that drill holes do not reach more caudal than the broad part of the iliac bone, since otherwise, fracture of the small part of the ileac bone proximal to the acetabulum will occur due to the brittle bone of the sheep (Fig. 6.1). In addition, drill holes have to be at 90° angle to the pelvic bone such that implants can be inserted into the deepest part of the ileac bone and do not
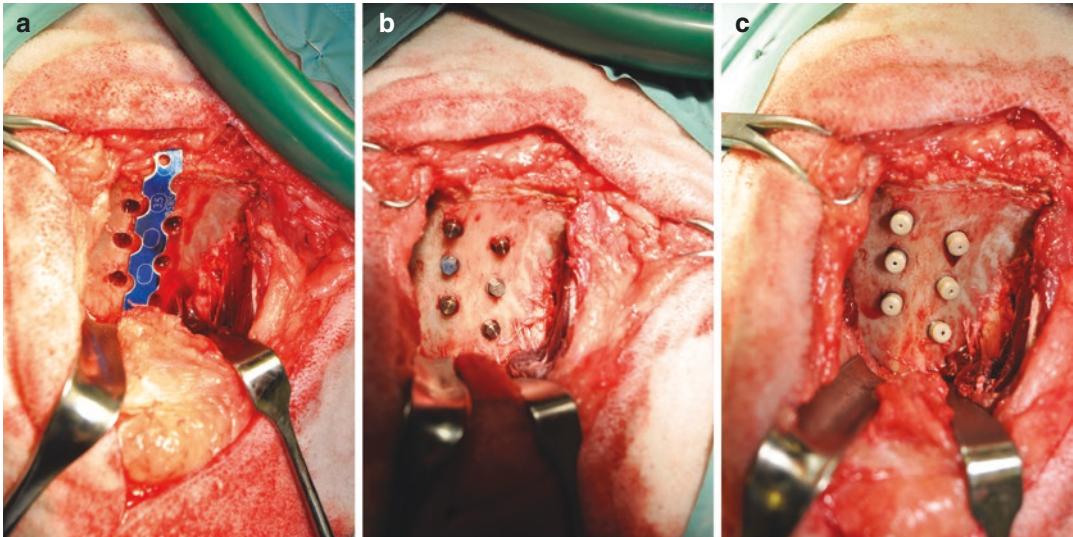
Fig. 6.1 (**a**) The template is placed on the linea glutea and drill holes have been prepared. (**b**) Implants are inserted and (**c**) caps have been placed on implants to avoid ingrowth. Note that implants were set at both sides of the linea glutea and were set relatively straight at 90° to the pelvic surface

Fig. 6.2 Radiograph of the dental implants in situ at sacrifice. Both ileal wings of the sheep were used

penetrate the trans-cortex (Fig. 6.2). After implant installation muscles are repositioned and the muscle insertions refixed with sutures to the original insertion place. Fascia and subcutaneous skin are closed with resorbable sutures while the skin usually is closed with staples. Finally, a gauze is applied as protection.

In the hands of the authors, the insertion of implants into the top of the iliac crest, such that the implants are inserted parallel to the pelvic bone did not work out. The iliac crest maintains its cartilaginous structure up to the age of 2–4 years, also in sheep and goats.

Postoperatively sheep should be kept in small boxes for 2 weeks and then transferred to larger stalls for the remaining time of the study.

By analogy with this approach, especially in goats but also some sheep, a slightly different access respectively implantation regime in the pelvic bone is outlined in the literature [29]. Schouten et al. described the course of action of their goat iliac crest model in the following way: Goats were immobilized in a ventral position. A transverse skin incision was made from the intermediate zone of the iliac crest until the anterior superior iliac spine on both sides of the vertebral column. The incision also included the underlying tissue layers down to the periosteum. The periosteum was undermined and lifted carefully aside to fully expose the iliac crest. By this approach and finally based on the anatomical

dimensions of the iliac crest, five up to a maximum of ten implants per goat are possible. The overall distance between implants is said to be 4 mm.

Tibia and Femur

Depending on the amount of implants as well as the investigative methods, there are slightly different approaches to the tibia and femur. For access to the tibial proximal epiphysis Rodriguez et al. [30] described the following approach. In their study, animals were positioned in lateral recumbency. Then a curved anterolateral incision was made over the stifle joint. A lateral parapatellar incision of the capsula articularis and the alar ligament was also performed. In the following, an area of a few centimeters of the vastus lateralis of the quadriceps was dissected in the proximal direction to completely expose the external surface of the metaphysis of the femur. Beneath the patellae, a rectangular area was exposed for implant installation. This area allowed for the insertion of three to five implants.

For access to the shaft of the tibia Bacchelli et al. [31] used the following technique: The medial approach to the shaft of the tibia was performed directly above the bone. From the distal aspect of the stifle to the hock joint, the medial fascia of the tibia was incised, and the medial aspect of the tibia was exposed without disturbing the medial collateral ligament. The periosteum was incised and reflected at the implant site. After complete exposure of the bony area, six implants were installed in the mid-diaphysis cortical bone. Implants had about 1.5 cm distance from each other.

Access to the sheep femur is usually gained via exposure by a classic lateral approach from the great trochanter to the distal epiphysis [32]. A longitudinal incision over the medial or lateral surface of the femoral condyle allows the placement of the implants in a perpendicular direction to the long axis of the femur [33]. Thereby a first implant can be placed at the base of the great trochanter and three others in the femoral distal metaphysis. A more elegant approach would be a keyhole approach to the proximal and distal femur, as described by Nuss et al., to avoid an unnecessary and large wound extending over the entire length of the femur [34].

6.2.2.2 Intraoral Description of the Procedures

Maxillary Sinus

Surgical access to the maxillary sinus in sheep and goats usually requires a previous surgical incision and preparation of the skin. The small size of the mouth with tight soft tissue structures hampers direct access via the oral cavity.

After shaving and washing the skin of the maxillary sinus area, the lateral maxillary sinus wall is exposed over a skin incision. Thereby surgical procedures and techniques differ slightly between authors. Haas et al. [35] gained access to the sinus wall by exposure over a 6-cm-long paramedian sagittal skin incision. The authors detached one-third of the masseter muscle. Rostrally, they created a 1 cm × 1 cm bone window with a dental drill. After the removal of the resultant bone plate, they elevated the antral membrane from the buccal bony wall and displaced it dorsocranially with variably bent blunt dissectors. Then holes for implants were drilled under the careful protection of the antral membrane with an elevator. The holes for the two implants were drilled distally to the bony window. Finally, the authors filled the newly formed hollow space with different augmentation materials and installed the implants.

In contrast, Estaca et al. [36] describe access via a 2-cm skin incision led caudally from the angle of the mouth to the second molar. Then an additional perpendicular, dorsal, 2 cm incision was connected at the end of the other one. A complete mucocutaneous flap was raised after incision, and the outer surface of the maxilla and the origin of the masseter muscle were fully exposed. Afterward, they detached the masseter muscle at the site of origin and created a bone window of 1 cm × 1 cm to expose the Schneiderian membrane.

Overall, most study protocols in current literature follow these approaches to the maxillary sinus. The only points where surgical procedures differ from each other are the size of the window, choice of the bone graft material, on-stage or two-stage approach, number of implants, and healing time. As the extraoral surgical access to the lateral sinus wall is very simple and additionally allows a very clear sight onto the alveolar ridge and sinus membrane, this model offers some advantages over an intraoral approach. In particular, soft tissue trauma by massive retraction forces as well as the risk of an infection triggered off by oral bacteria is reduced.

Mandible

Even though this surgical location has to be ranked rather critically, especially with respect to tooth extractions and direct implant placement, a short description will be provided for the sake of completeness. The procedure is based only on studies using the edentulous area between the canine and molars. Any description of tooth extractions, respectively, direct implant placement into fresh extraction sockets will not be provided due to the dubiousness of this approach by the authors.

After disinfection of the operation site, a midcrestal incision is performed in the edentulous area between the canine and molars. Mesial and/or distal releasing incisions are possible. A full mucoperiosteal flap is prepared. After complete elevation of the flap the underlying bone can be either used or an augmentation technique or implant placement. Frisken et al. [37] describe the insertion of implants (10 mm long and 3.75 mm diameter) into the mandibular bone 5 mm mesial to the first molar using the standard technique recommended by the manufacturer. Due to the study design, the authors implanted just one implant per edentulous area. Yet up to three implants are possible. Afterward, the mucoperiosteal flap is repositioned and fixed with a resorbable suture. Albeit the authors concluded that this access to the edentulous location in sheep is reasonable, they lost each implant after 4 weeks and the other at 12 weeks postoperatively.

6.3   Investigative Methods of Evaluation

Whenever bone research is done, different methods need to be employed to receive valuable answers by combining them all. When working with permanent implants seated in bone, the normal "working horses" to assess outcomes are clinical macroscopic evaluation, radiographs, computed tomography, histology with nondecalcified bone specimens in situ, biomechanical tests, and analysis of implant surfaces. In special cases, biological analysis of fluids, including blood saliva or fluids accumulated within mucosal pockets, may be warranted, and in very basic questions, investigations into genomics may give answers.

6.3.1   Clinical Macroscopic Evaluation

During this examination, the firm seat of the implants needs to be confirmed. Depending on the initial insertion, coverage of the implants in case of subgingival and adherence of the mucosa in case of transgingival insertion has to be assessed. In addition, the quality of the mucosa (smooth versus cobblestone-like), state of inflammation, signs of pocket formation around the implants, and signs of infection (pus, debris, and food remnants) within mucosal pockets need scoring.

6.3.2   Radiographs

Radiographs of the mandible or maxilla are very reliable and effective tools to assess changes within the bone and around the implants. It is recommended to use special high-grade technology films to demonstrate the fine details of trabecular bone, possible sclerosis, and signs of bone resorption, resp. interface membrane formation around the implant. In order to get good-quality radiographs, animals require full anesthesia and open-mouth techniques. The mandible can be

radiographed through an oblique technique through the open mouth coming from the cranial aspect for both sides with the animal in ventral recumbency, while the lateral view needs to be taken from both sides separately with the site of interest laying directly on the plate and the animals positioned in lateral recumbency. The same techniques are appropriate for the maxilla, except that for the open-mouth technique the animals have to be placed in dorsal recumbency. It is recommended to use gauze wrapped around the mandibular and maxillary bone to keep the mouth open, since metal spacers may obscure the view.

6.3.3 Microradiography

For microradiographs, the luxury version is to use a fixation equipment (Fig. 6.3). Nowadays, there are only few providers for this equipment
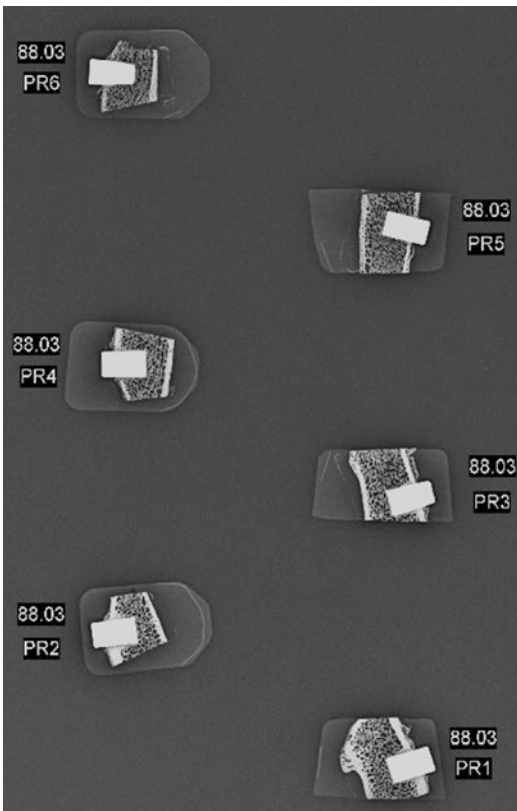
Fig. 6.3 Miroradiographs of each implant after individual blocks were cut with the implant in situ

with variable quality. The problem is to have enough fine details of bone structure while having enough power to also have large specimens as an entire femur analyzed. It also requires good equipment not to have artifacts produced between a metal implant in situ and surrounding bone. This quality can be achieved in our hands using the new equipment produced by FAXITRON BIOPTICS, LLC, 3440 E Britannia Drive, Suite 150, Tucson, Arizona. The downside of this equipment is the prize, which is only worthwhile to purchase if a laboratory uses this equipment routinely. However, collaborations with other laboratories may be possible. If this is not possible, the use of normal X-ray equipment and mammary high-grade detail films may be a satisfactory surrogate.

6.3.4 Computer Tomography (CT)

CT pictures allow three-dimensional reconstruction of the mandibular and maxillar bones. The technology also permits calculating volumes, density, and width of trabecular bone and cortical bone; however, in conjunction with metal implants, artifacts obscure the assessment of the transition from bone to implant. There, CT is of less value compared to radiographs.

6.3.5 Micro-CT

The techniques of Micro-CTs have improved in recent years and are reported to show less artifacts between implants and surrounding bone. However, Micro-CTs can only be performed with small samples and obviously only after sacrifice. The same measurements can be made as mentioned for regular CT, although more details can be expected.

6.3.6 Histology

In case of dental implantology histology of non-decalcified bone specimens with implants in situ is still the most reliable and classic way to inves-
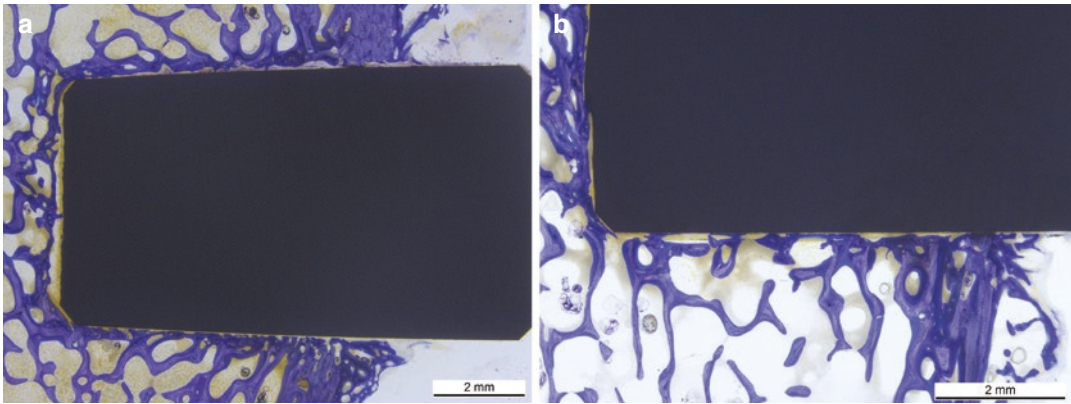
Fig. 6.4 (**a**) Ground section of a dental implant in situ shows good osseointegration and new bone formation in the environment of the implant. (**b**) Magnification: Dark blue staining indicates new woven, light blue older lamellar bone (ground section, PMMA embedding, staining with toluidine blue)

tigate osseointegration (Fig. 6.4). For this, specimens need to be embedded in methylmethacrylate, and ground sections have to be prepared using special saws with diamond-coated saw bands (EXAKT). This special equipment allows surface staining with toluidine blue, gives excellent results, and allows distinguishing different stages of bone formation. Lamellar bone (light blue) can be distinguished from woven bone (dark blue) and osteoid (turquoise). The regularity of lamellar bone can be assessed, as well as the area of new bone formation and the extent of the bone–implant contact. Computer programs are available, which make it possible to measure these features quantitatively and highly accurately. The formation of a fibrous interface membrane between bone and implant can be demonstrated, which can be related to biomechanical stability. Furthermore, the biocompatibility of implants and their coatings can be assessed. The time frame of the latter is possible within 2 months after implantation as well as primary osseointegration. Long-term osseointegration should be demonstrated for at least 6 and optimally for 12 months after implantation to make sure that no osteolysis along with aseptic loosening is occurring. Thereby, the native fluorescence section can further help to disclose peri-implant bone remodeling (Fig. 6.5).
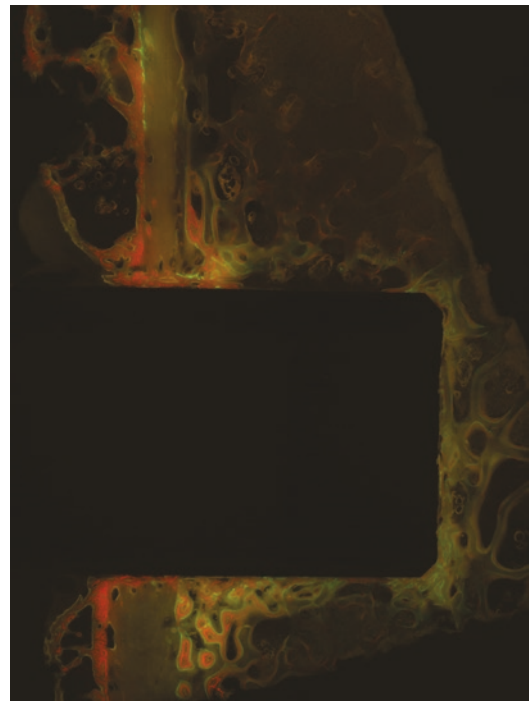
Fig. 6.5 Native fluorescence section shows calcium deposition at 4, 6 and 8 weeks (green = calcein green; red = xylenol orange; ocre = tetracyclin)

6.3.7 Biomechanics

Biomechanical tests are required to prove adequate fixation and osseointegration of the

implants. The most accurate for testing osseointegration is the "removal torque test." There, implants are tested using an Instron materials testing machine that is equipped with an appropriate screwdriver, resp. adapter, fitting the implant head. Measured is the force that is required to loosen the implant in a reverse direction. The curve of the torque is recorded until the implant breaks away from its surrounding. Apart from the actual peak of force recorded, the type of curve is also important, since it may reveal where the brake occurs. If the curve increases steadily, the peak is high, and then the curve drops suddenly; the brake most likely occurs at the materials interface to the bone. Instead, the curve may have a plateau, which decreases more slowly. If the force is high, it may be that the trabecular bone is attached firmly and gets torn with the implant; if the force is low, this indicates fibrous tissue formation.

"Pull-out tests" are another option to assess osseointegration. This makes sense, if implants are not round or are round but without threads. In the latter case, the removal torque tests provide better information about the connection between the implant and bone.

In some instances, push-out tests are also recommended. However, the problem with push-out tests is that specimens need to be specially prepared. This includes normally removing the (cortical) bone at the tip of the threads or even cutting a bone sample with the implant in situ in half, which is only possible using a saw. Since this procedure involves the implant, it may already loosen the implant beforehand, and thus, values may be inaccurate. These tests are not recommended by the authors to test osseointegration.

6.3.8 Biologic Analysis of Fluids (Blood, Saliva, etc.)

Biologic analysis of fluids, resp. saliva makes sense, if specific enzymes, macromolecules, or concentrations of pharmacological substances need investigation. In this case, most often, swabs are taken using a sterile cotton tip, or even rolls, mostly out of the pockets at the site of peri-implantitis. Swabs are taken and should be placed immediately in sterile tubes. Dilution may be achieved with a standardized amount of NaCl. Depending on the enzyme to be investigated, special inhibitors may have to be added immediately after harvesting the sample. Later appropriate laboratory tests (mostly commercial kits) may be used to analyze the target enzyme of the macromolecule.

6.3.9 Bacteriology

As with biological fluids samples for bacteriological analysis are taken with special swabs that are commercially available for this type of analysis. It has to be kept in mind that the oral cavity is overwhelmed with different bacteria and it may be very difficult to get results that allow interpretation of results. The classic bacterial tests on agar may also be difficult depending on best culture standard of different bacterial strains (gram positive, gram negative).

6.3.10 Genomics

Modern molecular analysis using genomics may be done for several factors by either determining the presence of DNA in case of bacteria, or by studying up- and down-regulation of mRNA after certain events. While the determination of bacterial DNA may obliterate problems encountered with bacterial cultures of the intraoral cavity, the quantification of mRNA may be only useful in selected cases of basic research as performed in small laboratory rodents (mice and rats). Its value may be limited in applied research using large animals, such as sheep or goats, especially since contamination may be a problem. In addition, it may be difficult to find suitable molecular probes for these animals.

6.4   Flagship Results

1. Both intra and extraoral surgical sites in sheep or goats do not provide the same associated anatomic, biochemical, physiologic, and biological characteristics as those found in the human oral cavity. Whereas all extraoral sites do not provide any surrounding mucosal tissue or physiological biting forces, intraoral sites show off a different gross anatomy and healing pattern.
2. The specific oral biomechanics inherent to the constant ruminant activity exclude sheep and goats for tooth extractions with secondary implant placement.
3. In terms of surgical approach, anatomy, and implant positioning, extraoral sites are preferable to intraoral sites. Thereby the iliac crest is advantageous over the femoral condyle due to bone composition and the number of implants.
4. For s separate analysis of just the safety, biocompatibility, and osseointegrative properties of a dental implant, the sheep pelvic model turns out to be very suitable.
5. A precise and comprehensive clarification of the research hypothesis is mandatory to select the suitable location and avoid overseeing specific limitations of each model.

6.5   Expert Opinion

Sheep and goats are reliable and suitable large animal models for bone research because of their similar bone metabolism to humans and overall acceptability to society. Yet, in contrast to the literature [3], the authors see issues, e.g. availability, animal cost, and ease of handling/housing more critical, as animal welfare is more complex and requires profound knowledge.

For all extra and intraoral surgical interventions in sheep and goats, general anesthesia with corresponding analgesia under sterile conditions is mandatory.

Even though sheep and goats offer a wide range of different anatomical sites for implant testing, the pelvic sheep model discloses to be the most reliable with respect to the evaluation of osseointegration. With its histological features, the pelvic sheep model allows a clinically reflective assessment of dental implants in an anatomical site similar to the jaw, where both cortical and cancellous bone integration is required. Yet for the assessment of peri-implant hard and soft tissue reactions under special loading conditions, an additional analysis in a suitable animal model is necessary.

References

1. Martini L, Fini M, Giavaresi G, Giardino R. Sheep model in orthopedic research: a literature review. Comp Med. 2001;51:292–9.
2. Stübinger S, Dard M. The rabbit as experimental model for research in implant dentistry and related tissue regeneration. J Investig Surg. 2013;26:266–82.
3. Turner AS. Experiences with sheep as an animal model for shoulder surgery: strengths and shortcomings. J Shoulder Elb Surg. 2007;16:158–63.
4. Pearce AI, Richards RG, Milz S, Schneider E, Pearce SG. Animal models for implant biomaterial research in bone: a review. Eur Cell Mater. 2007;13:1–10.
5. Vignoletti F, Abrahamsson I. Quality of reporting of experimental research in implant dentistry. Critical aspects in design, outcome assessment and model validation. J Clin Periodontol. 2012;39:6–27.
6. Reichert JC, Saifzadeh S, Wullschleger ME, Epari DR, Schütz MA, Duda GN, et al. The challenge of establishing preclinical models for segmental bone defect research. Biomaterials. 2009;30:2149–63.
7. Aerssens J, Boonen S, Lowet G, Dequeker J. Interspecies differences in bone composition, density, and quality: potential implications for in vivo bone research. Endocrinology. 1998;139:663–70.
8. Ravaglioli A, Krajewski A, Celotti GC, Piancastelli A, Bacchini B, Montanari L, et al. Mineral evolution of bone. Biomaterials. 1996;17:617–22.
9. Nafei A, Danielsen CC, Linde F, Hvid I. Properties of growing trabecular ovine bone. Part I: mechanical and physical properties. J Bone Joint Surg Br. 2000;82:910–20.
10. Liebschner MA. Biomechanical considerations of animal models used in tissue engineering of bone. Biomaterials. 2004;25:1697–14.
11. Bonucci E, Ballanti P. Osteoporosis—bone remodeling and animal models. Toxicol Pathol. 2014;42:957–69.
12. Wancket LM. Animal models for evaluation of bone implants and devices: comparative bone structure and common model uses. Vet Pathol. 2015;52:842–50.

13. Arens D, Sigrist I, Alini M, Schawalder P, Schneider E, Egermann M. Seasonal changes in bone metabolism in sheep. Vet J. 2007;174:585–91.
14. Eitel F, Klapp F, Jacobson W, Schweiberer L. Bone regeneration in animals and in man. Arch Orthop Traum Surg. 1981;99:59–64.
15. Spaargaren DH. Metabolic rate and body size: a new view on the 'surface law' for basic metabolic rate. Acta Biotheor. 1994;42:263–9.
16. Schouten C, Meijer GJ, van den Beucken JJ, Spauwen PH, Jansen JA. A novel implantation model for evaluation of bone healing response to dental implants: the goat iliac crest. Clin Oral Implants Res. 2010;21:414–23.
17. Hillier ML, Bell LS. Differentiating human bone from animal bone: a review of histological methods. J Forensic Sci. 2007;52:249–63.
18. Langhoff JD, Voelter K, Scharnweber D, Schnabelrauch M, Schlottig F, Hefti T, Kalchofner K, Nuss K, von Rechenberg B. Comparison of chemically and pharmaceutically modified titanium and zirconia implant surfaces in dentistry: a study in sheep. Int J Oral Maxillofac Surg. 2008;37:1125–32.
19. Tabassum A, Meijer GJ, Walboomers XF, Jansen JA. Biological limits of the undersized surgical technique: a study in goats. Clin Oral Implants Res. 2011;22:129–34.
20. Stübinger S, Biermeier K, Bächi B, Ferguson SJ, Sader R, von Rechenberg B. Comparison of Er:YAG laser, piezoelectric, and drill osteotomy for dental implant site preparation: a biomechanical and histological analysis in sheep. Lasers Surg Med. 2010;42:652–61.
21. Schopper C, Moser D, Goriwoda W, Ziya-Ghazvini F, Spassova E, Lagogiannis G, et al. The effect of three different calcium phosphate implant coatings on bone deposition and coating resorption: a long-term histological study in sheep. Clin Oral Implants Res. 2005;16:357–68.
22. Vlaminck L, Gorski T, Huys L, Saunders J, Schacht E, Gasthuys F. Immediate postextraction implant placement in sheep's mandibles: a pilot study. Implant Dent. 2008;17:439–50.
23. Rachmiel A, Aizenbud D, Peled M. Enhancement of bone formation by bone morphogenetic protein-2 during alveolar distraction: an experimental study in sheep. J Periodontol. 2004;75:1524–31.
24. Arvier J, Scott J, Goss A, Wilson D, Tideman H. Biological and clinical evaluation of the transmandibular implant. Aust Dent J. 1989;34:524–9.
25. Gatti AM, Zaffe D. Long-term behaviour of active glasses in sheep mandibular bone. Biomaterials. 1991;12:345–50.
26. Pilling E, Mai R, Theissig F, Stadlinger B, Loukota R, Eckelt U. An experimental in vivo analysis of the resorption to ultrasound activated pins (Sonic weld) and standard biodegradable screws (ResorbX) in sheep. Br J Oral Maxillofac Surg. 2007;45:447–50.
27. Liu H, Klein CP, van Rossen IP, de Groot K. A model for the evaluation of mandibular bone response to implant materials. J Oral Rehabil. 1995;22:283–7.
28. Brumund KT, Graham SM, Beck KC, Hoffman EA, McLennan G. The effect of maxillary sinus antrostomy size on xenon ventilation in the sheep model. Otolaryngol Head Neck Surg. 2004;131:528–33.
29. Orsini E, Giavaresi G, Trirè A, Ottani V, Salgarello S. Dental implant thread pitch and its influence on the osseointegration process: an in vivo comparison study. Int J Oral Maxillofac Implants. 2012;27:383–92.
30. Rodriguez y Baena R, Zaffe D, Pazzaglia UE, Rizzo S. Morphology of peri-implant regenerated bone, in sheep's tibia, by means of guided tissue regeneration. Minerva Stomatol. 1998;47:673–87.
31. Bacchelli B, Giavaresi G, Franchi M, Martini D, De Pasquale V, Trirè A, Fini M, Giardino R, Ruggeri A. Influence of a zirconia sandblasting treated surface on peri-implant bone healing: an experimental study in sheep. Acta Biomater. 2009;5:2246–57.
32. Grizon F, Aguado E, Huré G, Baslé MF, Chappard D. Enhanced bone integration of implants with increased surface roughness: a long term study in the sheep. J Dent. 2002;30:195–203.
33. Nikolidakis D, Meijer GJ, Oortgiesen DA, Walboomers XF, Jansen JA. The effect of a low dose of transforming growth factor beta1 (TGF-beta1) on the early bone-healing around oral implants inserted in trabecular bone. Biomaterials. 2009;30:94–9.
34. Nuss K, Auer J, Boos A, von Rechenberg B. An animal model in sheep for biocompatibility testing of biomaterials in cancellous bones. BMC Musculoskelet Disord. 2006;7:67.
35. Haas R, Donath K, Födinger M, Watzek G. Bovine hydroxyapatite for maxillary sinus grafting: comparative histomorphometric findings in sheep. Clin Oral Implants Res. 1998;9:107–16.
36. Estaca E, Cabezas J, Usón J, Sánchez-Margallo F, Morell E, Latorre R. Maxillary sinus-floor elevation: an animal model. Clin Oral Implants Res. 2008;19:1044–8.
37. Frisken KW, Dandie GW, Lugowski S, Jordan G. A study of titanium release into body organs following the insertion of single threaded screw implants into the mandibles of sheep. Aust Dent J. 2002;47:214–7.

Clinical Investigations in Implant Dentistry: Experimentation Versus Observation and the Future of Merging Data

D. French and Michel M. Dard

7.1 Introduction

The term "clinical investigation" has to be considered generic as it includes a wide range of options for clinical protocols, patient profiles, treatment types, evaluation methods and forms of reporting. In general, clinical investigations are usually considered to address different aspects of a treatment or of a surgical intervention, e.g. investigate the mechanism of action, assess the safety and/or efficacy, compare the safety/efficacy of a new versus an established procedure or treatment, and answer specific questions related to these topics.

These types of studies, which can be qualified as observational or investigative, are both important; however, these traditional types of clinical investigation have significant limitations, particularly the potential for bias. As such, most top-ranked dental journals favor experimental investigations (prospective controlled studies) over clinical observations and retrospective studies. A new approach to clinical retrospective observational study is therefore required, one that centers on patient outcomes, using modern data

D. French (✉)
Faculty of Dentistry, University of British Columbia, Vancouver, Canada

M. M. Dard
New York, USA

systems collecting large representative samples to better reflect a real-world setting.

In dentistry, there is a lack of consensus about appropriate clinical investigations due to a lack of consistent guidelines, lack of objective validity, the relevance of outcome measurements, and differing opinions on levels of evidence among the professional community. There is also confusion about the various types of clinical study and the different ways to describe them, which can be misleading [1]. Terms used in the literature include randomized controlled trials/studies; adaptive trials; nonrandomized studies (e.g., interrupted time-series studies); cohort studies (prospective or retrospective); case–control studies; case series studies; cross-sectional studies; ecological studies; superiority, equivalence, and noninferiority studies; crossover studies; longitudinal studies; and postmarketing studies [1–3]. Many of these terms are used inappropriately, for example "cohort studies" and "case series" have been used to describe the same type of study [1, 2, 4–6].

Randomized controlled trials (RCTs) in the field of dentistry are considered superior in the hierarchy of evidence in therapy, since they limit bias by randomly assigning groups to intervention vs. nonintervention (placebo or control), potentially minimizing known and unknown confounding variables. However, RCTs may offer no advantage, or may not even be possible in areas of study that respond to multifactorial outcomes

such as those typically seen in clinical practice. Observational studies can be of value in the multifactorial reality of clinical practice but their power is limited by a lack of randomization and control group. Furthermore, the assignment of subjects to various treatments in various environments over various time points introduces significant confounding factors and consequently known and unknown bias [7].

RCTs and the systematic reviews that utilize them are therefore generally agreed to be more valuable. Control over variables including subject allocation and blinded observer are proven ways to remove bias from a study. However, it is a falsehood to presume that bias is not present in RCTs and their related reviews. Prospective controlled studies have inherent bias, since the very design of a prospective study restricts certain conditions, such as number and type of subjects, with strict inclusion/exclusion criteria that are often chosen to create ideal parameters. This can bias the study toward a more favorable outcome than might otherwise be achieved in the reality of a noncontrolled environment of clinical practice. Furthermore, performing clinical investigations in implant dentistry brings a unique set of challenges, as it is impossible to perform traditional placebo-controlled RCTs in the same way as for pharmaceutical interventions. "Controlled trials" often have questionable validity, since the control treatments (i.e. other implants) are not evaluated against a comparator but rather against implants that have become the "standard(s)" over the years. Consequently, the majority of clinical trials in implant dentistry are therefore observational. In addition, patient population and procedure for "controlled" studies may not always be well defined and may vary between clinicians and patients, particularly in different countries. As such, the same intervention using the same implant system may suffer from a lack of "calibration" between clinicians or uniformity between patients. It is worth noting that some standard classifications have been proposed but are rarely consistently followed [2].

Meta-analyses and systematic reviews are of value in summarizing and providing state-of-the-art conclusions, but their quality depends largely on how the included controlled studies are conducted and reported. Furthermore, meta-analyses and systematic reviews select narrow criteria for study inclusion in a review, which again represents bias. Additionally, only certain types of research papers (typically RCTs) or specific areas of interest are published, so publication bias may exist.

It has to be also considered that RCTs are intended to determine efficacy, while observational studies are used to measure the effectiveness of treatment/intervention in real-world scenarios. According to Anglemeyer et al. [4] and Song and Chung [8], there is little evidence for significant differences in the estimation of effect between RCTs and observational studies, regardless of study design or heterogeneity of studies. In the near future, with the advent of electronic patient records, the quality and quantity of data available for retrospective observational studies may rival that of prospective controlled studies.

Observational studies, therefore, remain a valuable part of the landscape in dental implant research and perform a critical function in the dental literature. Because they can cover long time periods and respond to multiple factors, they offer researchers and clinicians the chance for postmarketing surveillance. This kind of long-term follow-up, in particular outcomes of interventions or devices used in daily practice, can help clinicians' understanding and allow them to achieve better outcomes in real world scenarios. Observational studies can further complement prospective studies in that they can generate novel hypotheses that can then be tested in pilot studies and RCTs. Similarly, they can guide the design of future studies by evaluating multiple variables simultaneously and may better reflect the "uncontrolled" reality of clinical practice.

7.2   Systematic Reviews and Meta-Analyses

The top level in the hierarchy of evidence is considered to be systematic reviews and meta-analyses (Fig. 7.1). Indeed, such reviews are very useful to describe the state-of-the-science and

RESEARCH HIERARCHY OF EVIDENCE
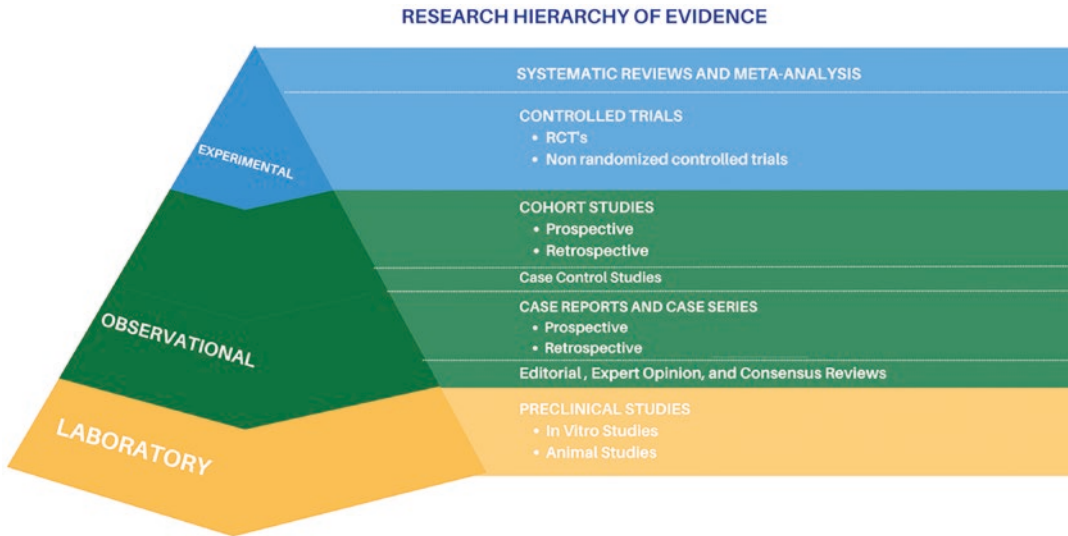
Fig. 7.1 Hierarchy of evidence in clinical research

understanding of a given topic. They are designed to deliver definitive answers based on currently available evidence [9, 10], and can give clinicians a good overview of the latest literature, including how findings may be applied in general practice [9, 10]. They look for evidence across a number of studies, as opposed to providing conclusions based on a single study [9]. Conclusions from systematic reviews and meta-analyses can theoretically be more reliable and robust than those of individual studies [9, 11], but only if most forms of bias are minimized [12].

Systematic reviews in theory consist of a deep analysis of all available evidence on a particular intervention or clinical question, performed according to well-defined guidelines, protocol, and inclusion/exclusion criteria [11–14]. They are superior to narrative literature reviews [9–11] and contribute to estimating the size of an effect or intervention [11]. Systematic reviews also help to improve generalisability and reduce subjective influence [9], and are efficient with regard to resource allocation and preparation costs, compared to generating novel data in clinical trials with associated high cost of subject enrollment and follow-up.

Meta-analyses are subsets of systematic reviews – they are "studies of studies" that combine data from several primary studies that exam-

ine the same research question to produce a single estimate based on aggregate data [9–11]. This requires the statistical analysis of results from many individual studies [11], which can help to develop guidelines and plan future research [9]. They can be amended over time as new published data become available, so that accuracy and statistical power can theoretically be improved [12]. Although "quantitative," the results should still be interpreted with a degree of caution since they assume a common truth behind conceptually similar studies and that sources of bias are controlled [10, 11]. The quality of the meta-analysis is therefore dependent on the quality of the included studies [9, 10, 13].

Systematic reviews and related meta-analyses have some disadvantages because restricting inclusion to published data only may reduce the reliability of the conclusions, i.e. publication bias, where the published literature may not be adequately representative of all completed studies [9, 10, 13, 14]. Furthermore, due to potential publication bias, neutral or negative results may be suppressed or harder to find [9, 11]. A systematic review is thus limited by the quality and quantity of research that is available for analysis, often with novel, controversion or nonconventional studies being excluded. As such, users of systematic reviews need to evaluate whether

certain methodology and evidence base has been performed using established tools such as PRISMA (Preferred Reporting Items for Systematic Reviews and Meta-Analyses) guidelines, which consists of a 27-item checklist that can assist in evaluating transparency [13, 14].

An increasing problem with systematic reviews and meta-analyses is a trend by clinicians, opinion leaders, and speakers at scientific forums to over-utilize reviews and rely solely on the conclusions without covering the underlying data in each study. This often provides a simple take-home message, but since the quality of the review is dependent on the quality of the included studies [9, 10, 13], it is incumbent on the clinicians who present such conclusions to evaluate and describe the studies within the review and explain potential shortcomings in the concluding statements.

An example of "state-of-the-science review" that, despite much research, still provides uncertain clinical validity is extraction socket preservation. This increasingly popular recommendation occupies much lecture time at implant conferences of the European Association for Osseointegration (EAO) and the Academy of Osseointegration (AO), with the potential to increase biomaterial use if the procedure is adopted and the concept spread out. Not surprisingly, there has been an expansion of publications on socket preservation. A search for "extraction socket grafting or ridge preservation" returns over 2000 articles on Pubmed.gov (*US National Library of Medicine National Institutes of Health*), but these are heavily weighted toward animal studies and short-term case reports. Indeed, a recent systematic review found only nine articles that met the requirement of RCT or controlled clinical trial (CCT) with unassisted socket healing as controls in humans [15]. A similar review found there were few 1-year follow-up studies and, as of 2012, only one 3-year controlled study [16]. Though animal studies are useful in describing ridge healing and the impact of socket graft on dimensional preservation, these do not provide sufficient evidence for long-term clinical applications in humans. Nevertheless,

many clinicians accept socket preservation as a required procedure and given the numerous systematic reviews and speaker time allocated to socket grafting, it might even be assumed to be a "standard of care."

Systematic reviews on ridge preservation, do indeed provide evidence of vertical and horizontal crestal bone "preservation" in the order of 1.5 mm [16, 17].

However, there is minimal evidence for superiority of any particular biomaterial and no data on long-term outcomes [16] and the research is limited by systematic errors of publication bias, conflicts of interest and structural and methodological variability [17].

When performed appropriately, systematic reviews and meta-analyses can be very efficient tools to summarize current understanding and state-of-the-science, and are accepted to represent the highest level of clinical evidence [18]. The research question and eligibility criteria need to be well defined, however, and risk of bias needs to be assessed and addressed [9, 12, 13]. The reader must evaluate the studies, both included and excluded, and remember that the conclusions are only as good as the data on which they are based; otherwise, they are at risk for vague guidance or, at worst, can risk generating garbage in–garbage out summaries or erroneous conclusions.

7.3 Types of Clinical Investigations in Implant Dentistry

7.3.1 Experimental Studies

Experimental studies such as RCTs (Randomized Controlled Trials) and CCTs (Controlled Clinical Trials) measure the outcome of the effect of an intervention. A CCT is similar to an RCT with treatment and control groups but not necessarily randomized. These clinical trials are next on the hierarchy after meta-analysis and are the highest form of clinical research. RCTs were initially developed to assess drug treatments but are more

difficult to conduct for surgical interventions [8, 19]. The comparative placebo routinely used in drug evaluation is not conceivable in medical devices for technical and ethical reasons. One more limitation consists in the fact that some RCTs investigator(s) directly involved as operators placing the devices under investigation cannot be blinded, as investigator(s) analyzing imaging data where the device appears and can be identified.

Studies with two or more interventions, possibly including control or no intervention, are compared through random allocation of participants [20, 21]. Mostly, there is one intervention to one individual, but it is also possible to assign one intervention to a group (e.g., a household) or different interventions within an individual, e.g., different areas or parts of the body. As stated by Levin (2007), RCTs have the advantage that they allow for causal associations to be inferred, since all factors other than intervention are considered equal [20].

RCTs typically must be tailored to answer a specific question. Since they are prospective by design, they require knowledge of the planned intervention and the expected outcome in order to properly set up the study, otherwise may risk an inability to control variables or a lack of power in sample. Furthermore, without an understanding of the degree of the expected outcome, the study may provide a statistically significant result but not a clinically significant outcome. Sample size, valid hypothesis, statistical power calculations, and significance level all need to be considered; thus, preparatory work is typically done with pilot studies [2, 20].

Certain criteria have been proposed to assist in the design of pilot studies [22–24],e.g.:

1. evaluate the integrity of a study protocol for a larger study;
2. acquire preliminary estimates for sample size computation;
3. test data collection questionnaires;
4. test the randomization technique(s);
5. estimate the recruitment and consent rates;
6. test the acceptability of the intervention;
7. choose the most suitable outcome measure(s).

Fundamentally RCTs are designed to minimize bias, which may include allocation bias (difference in effect due to subject selection), performance bias (difference in response due to knowledge of group assignment or different means of administration), assessment bias (assessment of outcomes influenced by knowledge of group assignment), or attrition bias (loss-to-follow-up bias) [20, 25]. RCTs ought to comply with reporting guidelines such as CONSORT (Consolidated Standards Of Reporting Trials) [26], which defines the minimum recommendations on how randomized trials should be reported. A checklist and flow diagram allows standardized reporting of randomized trials, which reduces bias and makes interpretation of the results easier.

RCTs are randomized with regard to subject allocation and controlled by use of a control treatment such as placebo or sham surgery. However, unless they are double-blind with both subject and observer blind to intervention strategy, RCTs remain prone to selection and observer bias as well as subject performance bias. It is often implausible or impossible to utilize RCT evidence for many study designs, particularly in implant dentistry. In some instances, a given treatment may be so well accepted clinically that it may be difficult to have a control group where such treatment is withheld. In other cases, it may be impossible to test the result of treatment in a blinded, randomized manner.

One example demonstrating the lack of RCT evidence in the dental literature is flossing. Recent media headlines revealed no data to support dental flossing as a routine to avoid tooth loss [27]. The US government health guidelines, which recommended flossing since 1979, required this to be based on scientific evidence. The Associated Press reviewed 25 studies comparing tooth brushing with or without flossing, and the evidence for flossing was deemed weak, unreliable, and with bias. The Associated Press then challenged the department responsible for the guidelines, but since flossing efficacy had not been fully researched, the recommendation was removed. The dental community, in response, completed systematic reviews but fared no better,

since the reviews were all based on the same weak data; hence they also concluded there was a lack of evidence to support flossing [28].

The problem lies not in the absence of benefit of flossing, rather in the failure of the scientific community to properly design a study to evaluate the benefits, and also the scientific community discounting of clinical observation and experience in preference for blinded RCTs. It is, of course, impossible to develop a proper RCT to study flossing since the "subject" will be aware of the act of flossing. It is also very difficult to get long-term outcomes on flossing as there will be a selection bias, since those who floss long-term are more likely to value flossing, so may have other health-oriented behaviors such as healthy diet. There is nonetheless good short-term clinical evidence that flossing reduces decay and gingival inflammation, and it remains an advised procedure in the opinion of most dental professional organizations including the American Academy of Periodontology [29].

External validity is another important consideration or potential limitation of RCT. It is defined as the "degree that the result of a study can be generalized to other conditions or populations" [30]. In general, external validity is *poor* if multiple variables are tested in a small sample but *good* if a single variable is tested on a large sample (Fig. 7.2). External validity is made difficult by the design requirements for a RCT, where the high trial running costs and follow-up of subjects limits sample size. Similarly, focusing on controlled variables, particularly in the subject sample, limits the ability of the sample to represent real world clinical practice outcomes. Furthermore, RCTs may suffer external validity in that actively enrolled subjects must themselves accept being allotted to treatment or control so may not reflect normal population.

One of the major drawbacks to RCTs is the high cost; given this, there is a potential for corporate sponsorships to introduce bias in the literature on a given topic. High costs stem from enrollment and follow-up which often limits patient enrollment to a number that is "just sufficient" to reach statistical power and also limits the time of follow-up to periods, so may miss longer-term unexpected outcomes [20]. With a sample just large enough for statistical validity, any drop-outs can have a dramatic effect on the results, potentially missing the threshold for meaningful analysis. Furthermore, a high drop-out rate can mask undesirable effects, including the introduction of bias, and may also render the whole study ethically questionable. Cairo et al. (2012) added that variation in levels of improvement may make calculation of sample size different for clinically meaningful results [31]. Operator and institution experience may also be low, especially where surgical procedures are involved, which is always the case in implant

Fig. 7.2 Interaction of sample size and treatment complexity on validity
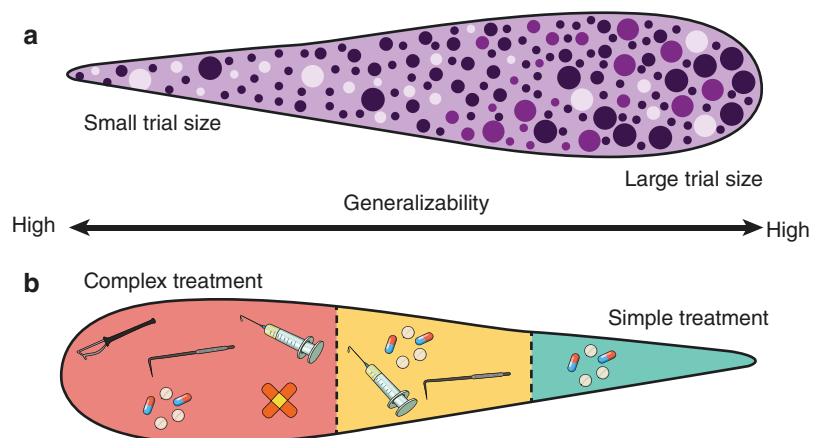
dentistry. As noted by Marx (2014), the lack of standardized terms may lead to different definitions of the same clinical observation [32].

A well-designed RCT should ideally test one variable on subjects that are random and equal with all other variables being known and controlled for. An example of a well-designed RCT is the series of 1–3-5 year study of TiZr vs. Ti 3.3 mm diameter implants in edentulous mandibles [33–35]. It is a double-blind, multicentre, split-mouth RCT that included 91 edentulous mandibles, two different implants of the same designs (Straumann BL 3.3 mm) but differing in only one variable, the implant material, which was either TiZr (Roxolid®) or Ti Grade IV (control). The 3-year results in 75 patients showed a cumulative survival rate of 98.7% for TiZr and 97.3% for Ti. There was also no significant difference between the groups where mean marginal bone loss was 0.78 mm for TiZr and 0.60 mm for Ti [34]. This RCT stands out as an example of a well-controlled RCT, but the question of the utility of the study to clinicians remains. The purpose of this study was to evaluate a single focused question, i.e. will TiZr perform as well as Ti Grade IV, but does this matter? The answer is yes, to prove equivalency for market approval of the device. However, does this affect clinical decisions in the uncontrolled environment of daily practice? No, because the study did not evaluate any risk factors, nor did it evaluate various methods to improve outcomes. The exclusion criteria make this RCT well-controlled, but it provides minimal utility to complex multifactorial risks seen in broad clinical usage. The device was proven equivalent, but since TiZr is stronger than Ti Grade IV; it may be superior to load resistance and perhaps able to be used in higher load scenarios such as narrow dimensions supporting a bicuspid or even a molar. The stronger TiZr may also be utilized in sites where bone width is compromised, therefore avoiding bone graft by using a reduced-diameter implant. The outcomes of the aforementioned RCT's could suggest that TiZr may be used in the above-described higher load scenarios, but this cannot be stated since the device was not tested in any load-challenging cases. For this type of analysis, we need postmar-

keting surveillance and clinical observation studies whereby clinicians who use the new device in novel applications track and report their outcome.

In summary, RCTs are restricted to answer a single question in a controlled environment, so they do not necessarily reflect the more complex environment of clinical implant dentistry. Furthermore, the high costs limit the size of samples and duration of follow-up and also introduce the potential for publication bias in favor of the sponsor since the studies must be funded.

7.3.2 Observational Studies

This category of clinical study design is important, but sometimes neglected or under-used design [8] (Fig. 7.1). To evaluate the complex multifactorial reality of clinical practice over long periods of time, we rely on observational studies while recognizing that such studies have both observer and subject bias and are not randomized or controlled. Given these inherent limitations, it is not surprising that they tend to over-report effects by about 20–40% [36].

Despite the potential utility of clinical observational studies, there remains a large disparity in funding. Although 90% of dental care is provided in a clinical setting and 2% is provided in a research setting, only 7% of dental research funding is spent in the clinical setting; the majority of funding goes to research facilities and controlled trials [36]. An additional barrier is the recruitment of dentists and patients with a minimum interruption and cost to a clinical practice. The advent of digital practice management may improve the ease of data collection, particularly if the treatment parameters data can be entered with field search capability so that it can be more reliably retrieved than historical chart reviews.

The lack of recognition and support for clinical practice studies overlooks the strengths and benefits of observational studies, in that they can gain insight into the complex, poorly controlled reality of the clinical environments. Observational studies are also ethically sound since there is no withholding of treatment in a control group and

the interventions are usually part of routine clinical procedures. Such studies are relatively inexpensive, especially if they are retrospective and the data collection is incorporated into daily practice routine. Observational studies can be qualitative as well as quantitative, and can assess the strength of an effect as well as the type of effect. Observational studies can also generate new hypotheses or novel discoveries that can subsequently be tested in controlled studies.

An example of this kind of novel discovery is the retrospective case series on a drug side effect, whereby bisphosphonate was linked to refractory bone exposures based on a retrospective observation of 119 osteonecroses of the jaw (ONJ) complications [37]. This was a straightforward retrospective observational report that has since led to hundreds of studies, position papers, and, eventually systematic reviews.

One of the main limitations of observational studies is that, being uncontrolled, they are prone to numerous forms of bias, as outlined below:

- *Observer bias,* where researchers notice or record more reliably what they want to see or "know" when looking at restrospective or clinical outcomes.
- *Sample bias,* especially in retrospective studies where subject and treatment allocation is not randomized and may not be representative of a larger population set. Lack of randomization of treatment allocation is a core issue with observational studies whereby the groups that receive treatment may be different with regard to risk. One potential tool used to manage sample bias is a multivariate analysis which adjusts for the difference in risk exposure of the subjects.
- *Measurement & recording bias*, for example, not including or missing certain data in records. An example of this may be a risk factor such as selective serotonin reuptake inhibitor (SSRI) antidepressant medications and their potential effect on implant outcomes. This was not commonly considered a risk 10 years ago, so it may or may not have been included in data collection at the time and thus

represents an unknown confounding variable due to incomplete data [38].

- *Contextual and temporal bias*, which may or may not apply to different circumstances, locations, or time periods such as a comparison of implant complications in smokers when looking at different countries, groups with different socio-economic status, or even differing time periods with vastly different smoking prevalences that could make the data less meaningful to broader populations. For example, one clinical retrospective study reported a 7-year implant survival of >98% but the subjects were high SES Canadians with low smoking prevalence [39, 40]. Whereas a similar retrospective study in a Japanese population reported <94% 10-year implant survival [41]. Although in the Japan study smoking rate was not reported, it is possible that the difference in failure was partly influenced by smoking in Japan where the consumption rate of cigarettes per person per year is 1841 with Japan being one of the world's largest tobacco markets.

Observational studies can be adapted to evaluate outcomes at the treatment level such as "implant-level" vs. "patient-level" analysis of failure, whereby the patient is a unit and within a given patient, there may be more than one treatment. One example is a study on implant survival where the implant-level survival rate at 7 years was 98.4% but at the patient level was 95.9% [39]. This kind of patient-centered outcome is important to clinical practice in that nearly 1/20 patients were exposed to a failure event and patient experience is critical to private practice success. The above are both examples of clinician-reported outcomes, but observational studies can also evaluate patient-reported outcomes such as improvement of QOL after implant-supported denture by means of standardized patient surveys [42].

Observational studies may be in the form of case reports, case series, case–control studies, cross-sectional studies, and cohort studies. The simplest of these are case reports and case series.

Reporting guidelines are also in place for observational studies in the form of STROBE (STrengthening the Reporting of OBservational Studies in Epidemiology), which covers cohort, case–control and cross-sectional studies, and CARE (CAse REport) for case reports [43, 44].

One new field of investigation in the form of observational studies opened recently with the need for *usability studies*. Usability studies look at the interactions between human operators and the medical device and how the user interacts with a device and forms a key component of overall risk management and safety.

User experience (UX) evaluation and assessment should be conducted on and with anyone who plays a role in operating the device, from patients to healthcare professionals, including staff members responsible for shipping, storing, sterilizing, and maintaining it.

It has to be noticed that usability standards are not clearly specified yet. There is little knowledge and information about the impact of the context of use and especially by the characteristics of its users on the usability outcome.

Nowadays, it is critical to consider the following NORMS: (1) IEC 62366-1:2015, which is the overlapping standard for FDA, the European Commission, and other regulatory bodies. IEC specifies that the standard covers assessment and mitigation of risk associated with normal use and use errors of the device and to (2) ISO 9241-11, 2018 which provides a framework for understanding the concept of usability and applying it to situations where people use interactive systems and other types of systems, products, and services.

Furthermore, the recent publication of Bitkina et al. [45] provides an overview on the current state, analysis methodologies, and future challenges when it comes to the usability of medical devices.

The full usability is difficult to address and to assess because medical devices are used in a broad range of settings: clinical (practice, hospital, alongside many other devices) or home-use which will require a potentially unskilled patient or caregiver serving as the operator of the device.

For these reasons, medical device usability testing demands a detailed analysis by researchers/engineers/practitioners/patients to understand the interactions between the device and the end user within the intended use environment. This allows for the creation of realistic risk acceptability models.

Data from the FDA shows that up to 50% of medical device failures can be attributed to design issues, while 36% of product recalls are initiated due to design. The design of the medical device, along with its labeling, packaging, and instructions for use, should always promote safe and effective use. This type of issue requires sound studies to be properly designed before the device reaches the operation suite and along with its use to collect and evaluate usability data as part of a manufacturer's postmarket monitoring and surveillance.

7.3.2.1 Case Reports

Case reports are useful for identifying novel or rare clinical outcomes or scenarios but rely on one subject treated and carefully observed for the outcome. The subject is not random, there is no control, and they are prone to examiner bias. They are also descriptive and do not allow for hypothesis validation and educated conclusion.

7.3.2.2 Case Series

Case series are often incorrectly referred to as "cohort studies" [1, 2, 4–6]. They can be prospective or retrospective, and consecutive or nonconsecutive [1, 6], but they do not include comparison to a control element [1, 2, 5]. Outcomes are described in a group of patients who all received the same intervention [1, 46]. A case series follows a d*escriptive* study design (compared to RCTs, cohort studies, and case–control studies, all of which have an *analytical* study design). Generally, no hypothesis is developed for case series, but they can be useful to help develop hypotheses for further analytical studies [2].

A retrospective case series corresponds to retrospective review of multiple case records (typically the lower limit is set at five cases) [6]. These can be used to describe unique cases, discover

new diseases, or report unexpected risk associations. As such, case series are useful for analyzing trends, generating hypotheses and healthcare planning [2, 43]. They can be prepared quickly and can efficiently describe unexpected outcomes in clinical practice scenarios, and so can function well as postmarketing surveillance reports.

However, the lack of comparison or control group means that it is not possible to infer any conclusions about possible associations, causal or otherwise [1, 42, 47]. Additionally, the results from case series are not to be used to examine associations between exposure and outcomes, so there is no way to discern if time alone affects the result [2].

Another limitation is that typically the sample is small and nonrandom so is not representative of larger populations; they may therefore be prone to selection bias [6]. The typically retrospective nature of case reports means that missing data is another limitation, since chart records may not be complete enough to provide thorough analysis of confounding factors. Finally, since there is no active enrollment or follow-up, patient drop-out rate may be an issue in case series.

An excellent example of a retrospective case series study in implant dentistry is the report by Sennerby et al. (2008) that served as a valuable postmarketing surveillance report [48]. The authors evaluated the survival rate and marginal bone conditions around 117 Nobel Direct one-piece implants in 43 consecutive patients. Calculations of radiographic marginal bone loss were performed at placement and after an average of 10 months of loading. Marginal bone loss (>3 mm) was reported around more than one third of the implants, therefore quickly providing clinicians with a cautionary conclusion that Nobel Direct implants for immediate, multi-unit constructions and flapless surgery may be at potentially greater risk for failure [47, 48].

7.3.2.3 Case–Control Studies

Case series can be combined with a control to develop a case–control study that can overcome some of the limitations of case reports in determining cause and effect. Case–control studies are therefore designed to examine associations

between exposure to risk factors and disease/condition [8, 49]. Unlike cohort studies, subjects with the condition of interest are entered into the study at the outset, and risk factor information is collected retrospectively [8, 49]. Diagnosis and eligibility criteria need to be explicitly defined, however [49, 50]. The inclusion of a control element is feasible, but needs careful consideration to reduce bias [49, 50].

Case–control studies are typically retrospective observational studies that look back to earlier "exposures" of individuals, a common tool in epidemiology. The cases are identified as subjects with the particular outcome or disease in question, while "controls" are identified as subjects without the outcome or disease. Researchers then compare the proportion of cases exposed to a particular risk condition to the proportion of controls exposed to the same risk condition. This design *assumes* that cases differ from controls *only* in having the particular outcome or disease and that this is increased by more risk exposure.

The advantage of case–control studies is that they can cover long periods in a cost-effective manner to identify effects of variables that have long latency periods, e.g. lung cancer in smokers or the effect of diabetes on peri-implantitis. Such studies have the additional advantages that they are quick and relatively inexpensive to perform [8, 50]. They may also be useful for rare or uncommon conditions [8, 50, 51]. However, this design has numerous limitations, such as unknown or hidden variables may affect outcome. For example, sample selection of the control subjects may not be representative of the general population, in that they may be "related" to case subjects by such variables as nationality, background and socio-economic status, or by hidden or unknown variables that potentially act as confounding factors, making it difficult to overcome potential bias [8, 49, 50]. Successful selection of appropriately representative cases and controls can therefore be challenging [8, 50, 51].

Typically in case–control retrospective reports, insufficient data is collected to identify potential confounding factors. Additionally, changes may occur over time such as standards

of care or societal perspectives that can affect both measurement and reporting. For example, consider a potential study on alcohol in relation to spousal abuse, whereby both socially accepted levels of alcohol consumption and the definition or even recognition of spousal abuse can change over time as well as in different geographical regions. An example by Ashraf et al. (2012) examined oral health and coronary artery disease, where cases consisted of subjects with CAD while controls had no CAD [52]. Oral health was assessed in both sets of subjects (e.g. using number of missing teeth, periodontal index, etc.). In subjects matched for socio-economic status, the authors found a significant association between poor oral health and CAD (odds ratio 5.04 at 95%).

7.3.2.4 Cross-Sectional Studies

This type of observational study relates two or more variables at a single time point with no manipulation of variables. Subjects are grouped by those with or without the variable and then compared according to outcome. These provide an odds ratio that represents the probability of the outcome if the variable is present; for example, the relationship between presence of *P. gingivalis(+)* and bone loss. The advantage of this design is that is quick and relatively inexpensive since there no follow-up or time period requirements. As such there is also no confounding elements introduced over time.

The studies are generally straightforward and ethical, in that the subject is not exposed to a known risk or condition. One limitation is that, since the data are collected at one time point with no follow-up over time, all data are derived from a single time point, which negates the potential to evaluate cause and effect. An example may be the question "Does sedentary life cause obesity, or does obesity lead to sedentary life?"

These studies are also prone to concomitant variation, whereby extraneous factors may be the reason for any relationships observed, and varying one condition can unknowingly alter another. An example from the dental literature is a cross-sectional study of food impaction relative to implant embrasure space of 150 fixed dental prostheses (FDPs) in 100 patients [53]. Radiographic embrasure dimensions and radiographic implant bone loss were measured, and larger embrasure was found to be related to greater peri-implant bone loss. This study reveals the limitation of concomitant variation, i.e., bone loss may be a function of time alone; both bone loss and open embrasure may occur independently over time, but there was no analysis of the time that FDPs had been in service to account for the effect of time alone. Since embrasure space and bone loss may both increase over time, embrasure space may only represent concomitant variation.

7.3.2.5 Cohort Studies

Cohort studies are considered to provide the highest level of evidence of all observational studies [5, 8]. These studies consider a group of subjects over time and collect information about the outcomes of interest [54, 55]. They are designed to examine associations between exposure to risk factors and disease/condition [51, 54, 55], and may include a control or comparative element [3, 55]. They can be "closed" (no variation in subjects, and drop-outs are not replaced) or "open" (new subjects can enter the study) [54], but the analysis of the data must include a comparison of risk factors between subjects [54, 55].

A cohort is described as subjects with specific and common characteristics [56]. A common feature of cohort studies is the observation of large numbers over a long time (typically years), comparing incidence rates in groups that differ in exposure levels [6]. One example in line with the above definition would be dental implant placement in a specific clinic over a period of time, such as in the open cohort reported by French et al. (2015), with 4591 implants in 2060 patients over a period of 10 years [39]. Other definitions of cohort studies exist, however. For example, one definition is a "study in which a group of subjects, selected to represent the population of interest, is studied over time." This has a slightly different meaning to the previous definition, so there remains the potential for the discrepancy in what is deemed a cohort study [54].

Advantages

Cohort studies are cost-effective if they can be performed using existing records and if this retrospective collection of existing clinical records is readily suitable for ethical approval. Retrospective cohort studies can evaluate long follow-up periods and collect large samples, which makes them suitable for seeking rare events or events with long time horizons (e.g. implant loss, implant fractures, etc.), as well as evaluating exposure to risks with long latencies.

Cohort studies can efficiently establish the frequency of a disease or complications and can be designed to study multiple outcomes following a single intervention/treatment [8, 54, 55] or evaluate multiple input variables. By analyzing associations between risk indicators and outcomes through multivariate analysis, they allow for calculation of incidence rates, relative risks, and 95% confidence intervals [55] and enable absolute risk estimates for the outcomes; however, they can show only association [5, 8].

Evaluated over time, cohort studies can provide correlation and "guidance" of cause and effect by measuring change in exposures and the incidence of outcomes; however, in the absence of interventional experiments, they cannot provide evidence for cause and effect [8, 51, 54]. Instead, causal hypotheses can be implied since the longitudinal nature of these studies allows evaluation of exposure relative to the outcome, i.e. if levels of exposure over time relate to levels of the outcome it may reveal a dose–response relationship that supports potential causality. An example is smoking and the relationship to implant loss; one can report smoking habits (the predictor variable), then in a retrospective cohort study evaluate patients who received a dental implant. Patients with a failed implant (outcome variable) can then be compared to patients with no implant loss.

Cohort studies can evaluate multiple risks at once and, with sufficiently comprehensive records, may identify "novel" risks. Comparing complication rates relative to various risks can be done initially by univariate analysis to determine the relationship to complications, then by selecting those that were significant, and then performing a multivariate analysis to evaluate the effect of confounding factors. An example is a cohort study on Straumann implant survival [39]. Male gender or autoimmune disease were not expected to be factors, but the retrospective analysis found these risk indicators to be related to progressive bone loss. These risk indicators had not previously been reported in the literature as risk indicators for implant bone loss. This type of novel finding may therefore warrant future prospective controlled studies. Another example of this type of analysis may be an investigation of complication rates with bone grafting at the time of implant placement. Firstly, data could be extracted from other implant procedures where a bone graft was also performed, followed by an examination of other data from the health record such as smoking, diabetes, penicillin allergy, etc., data on the type of graft (e.g. autogenous bone vs. allograft bone usage) can be taken from the patient's chart, and finally data on any recorded complications of the procedure could be evaluated.

Another example of a novel finding from a retrospective cohort study is the possible relationship of proton pump inhibitors (PPIs) to dental implant outcomes [57]. The authors noted that PPIs can negatively affect bone accrual, and investigated the possible association between PPIs and the risk of osseointegrated implant failure in a retrospective cohort of 1773 dental implants in 799 patients treated in a single center from 2007 to 2015. They reported a novel risk indicator in that subjects using PPIs had a higher risk of dental implant failure (HR = 2.73; 95% CI = 1.10–6.78).

A final and major advantage of cohort studies is that they represent the uncontrolled complex multifactorial environment of clinical reality. Dental implant failure is potentially a multifactorial phenomenon, so it is very difficult to model in a controlled study. Figure 7.3 shows the multiple factors and interactions between them that may affect a given outcome such as implant failure. Only by evaluating all variables and their interactions on implant failure can a true picture of implant failure be constructed (Fig. 7.3).
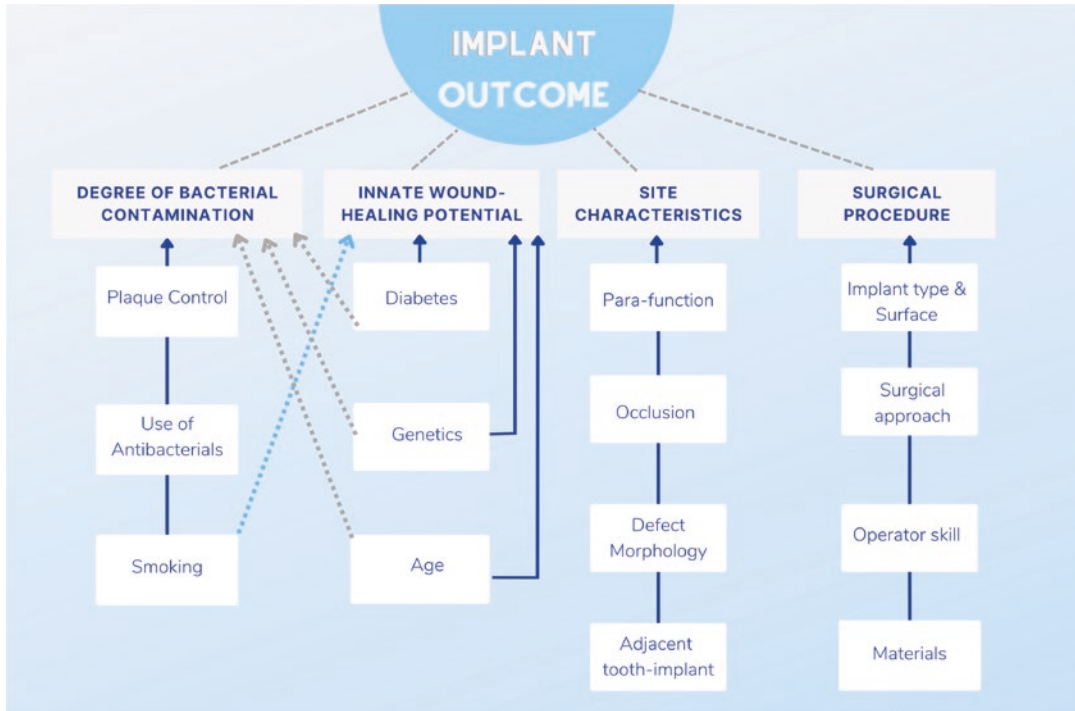
Fig. 7.3 The complex multivariable environment of clinical implant outcomes

Limitations

Cohort studies are prone to numerous forms of bias such as selection, reporting and performance bias, and they are also prone to confounding errors. Since there is no control to evaluate the effect of no treatment or alternate treatment, there is the added difficulty that the selected comparison groupings in cohort studies are often not sufficiently similar to the treatment group [51]. Selection bias in such studies is exemplified by a study on the effectiveness of implants in a Swedish population [58], where smoking, periodontitis, implant length $\leq$ 10 mm, and certain implant brands, showed higher odds ratios for early implant loss. However, the following need to be considered; how well do the subjects chosen under national dental care in Sweden represent the more commercial market place population in the US dental implant market?; and importantly, were the subjects evenly distributed between general dentists and specialists within this cohort such that the effect of brand could be explained by surgical experience?

With reporting bias, clinicians "see what we already know," so examiners may record or report findings that align with their beliefs. Performance bias can also exist, since subjects are not blinded, and the examiner may present the expected outcome to the subject in a biased manner. For example, the clinician may use language such as "we now use this improved implant design," so a subject may expect and then report better outcomes.

Confounding errors in such studies are unknown factors that may develop over the duration of the study. For example, a study of implant design evolution and its relationship to peri-implantitis may fail to pick up a reduction of smoking in the general population over the same time frame, so may ascribe the improved outcomes related to the newer implant design and not to background factors that elevated overall outcomes.

The treatment applied is usually nonrandom and thus prone to allocation bias. An example of this kind of nonrandom allocation is seen as men-

tioned above in the [58] Derks study, where it is possible that dental specialists chose different brands of implants than general dentists. The reports indicated that the brands used by specialists had a better outcome, but this may be due to nonrandom application of different brands rather than any actual limitation of the implant system itself.

The potential confounders and biases, and also the uncontrolled multifactorial nature of cohort studies, mean that large-sized cohorts are typically required depending on the prevalence of various factors. Furthermore, with the long time periods typically required, cohort studies are prone to higher drop-out rates, especially in open cohort studies where the population is not well defined, and the follow-up periods may be poorly defined or enforced. As such, a difference in outcome incidence between those who continue to participate and those who drop out would also introduce bias [25, 54].

Sample Size

Sample size (N) in cohort studies can be either advantageous or disadvantageous. Larger samples are required if the examiners want to do subgroup analyses, since this further reduces the N of a particular group. Large sample sizes are usually required, particularly if investigating uncommon, rare outcomes, as smaller sample sizes are less likely to find significant outcomes [8, 54]. An example where a large sample is beneficial is implant failure and subgroup analysis. Implant failure rate is typically <5% over a 10-year period; therefore if the sample is small and there are multiple subgroups, the study will lack sufficient power to find a given variable related to the failure. A good example of limited power is a recent study that evaluated implant survival in patients with or without chronic periodontal disease in a cohort treated by a single clinician from 2002 to 2011 [59]. The sample of 202 patients and 689 implants are small, so unsurprisingly, they found no significant difference in survival rate (93.1% vs. 95.8% in patients with and without periodontal disease, respectively; $p \geq 0.05$). Furthermore, most implants (54.9%) were lost before loading so the long-term effect of peri-

odontal disease on implant loss was evaluated in less than half the cohort. The authors further divided the cohort into subclasses of implant types, length, and prosthesis design, further reducing the N within the study; unsurprisingly there was no significant difference between subclasses. In such a small cohort over a long period other unknown variables such as evolution of surgical techniques, and skill set changes, may have affected outcomes. Given the multiple variables, both known and unknown, and the small sample size of the study it is clear that there was insufficient power to show any significant outcomes. Therefore, the conclusion that it is safe to proceed in patients with a history of periodontal disease history may not be justified.

A large sample size has advantages in that it best reflects the general population, and thus real world outcomes, and can increase precision of the result. Large samples are also required to find long latency outcomes such as peri-implantitis or rare outcomes such as implant fractures. One such example is a study of incidence and factors associated with implant fracture, which evaluated 18,700 implants [60]. Indeed, such a large cohort was required because even with this large sample size there were only 37 fractures. Clearly with a fracture rate of 0.002% a large cohort is required, so this would be impossible to evaluate in a prospective or controlled trial. The study was also able to show that relative risk for implant fractures was greater in posterior sites than anterior sites and for screw-retained crowns vs. cemented crowns.

Prospective or Retrospective Cohort Studies

Cohort studies can be either prospective or retrospective (Figs. 7.4 and 7.5). An important feature is that cohort studies followed from the present into the future are prospective and can therefore be tailored to collect specific data or outcomes [8, 54, 55], while retrospective cohort studies look at events from a past time point up to the present [8, 54, 55]. One major difference is that prospective designs can look for causal relationships (risk factors) and retrospective designs can only look for correlation relationships (risk indicators).
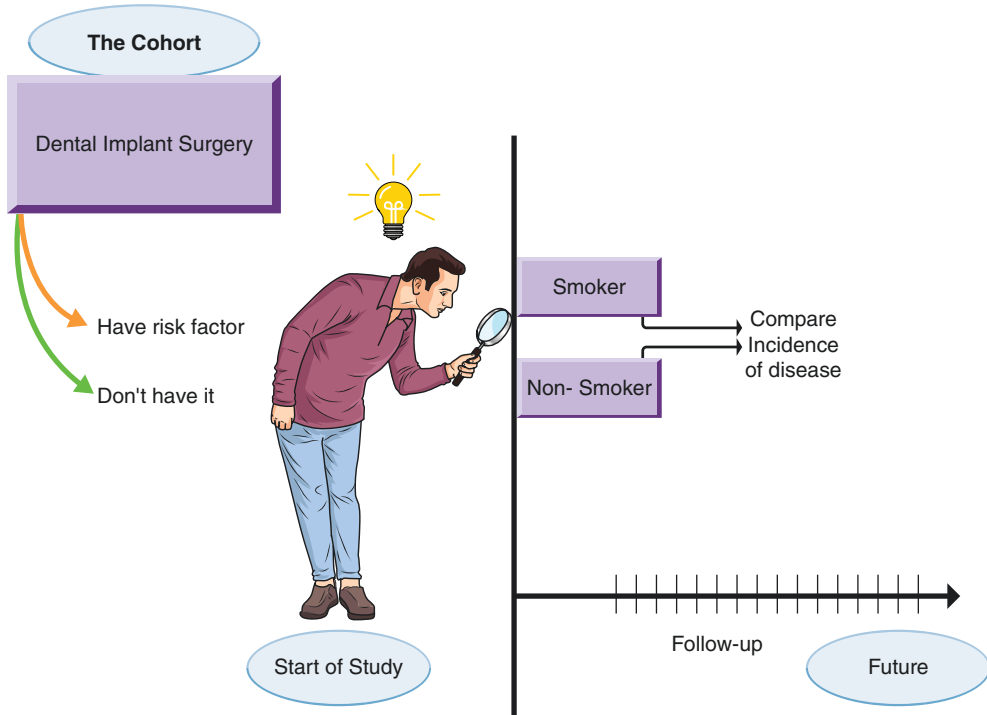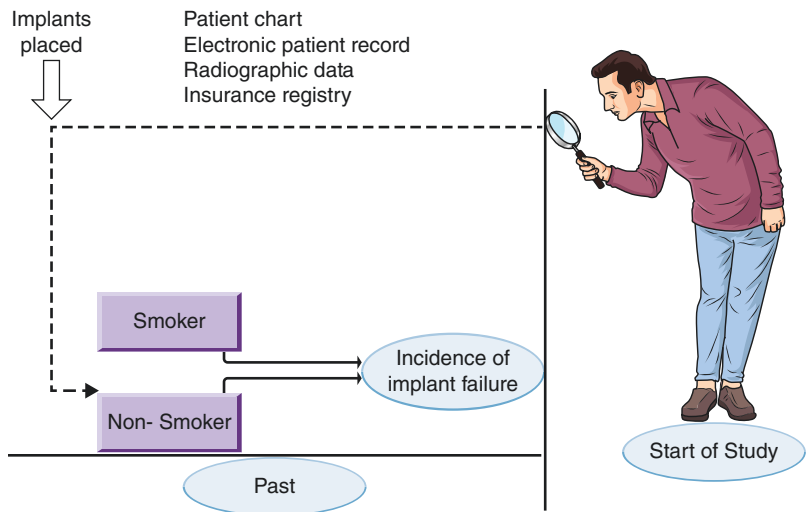
Fig. 7.4 Prospective cohort observational study design

Fig. 7.5 Retrospective cohort observational study design

In a prospective cohort study, investigators conceive the study design, recruit subjects, collect baseline data, and follow subjects into the future to record outcomes (Fig. 7.4). Investigators have well-designed inclusion and exclusion criteria which, in some cases, can be designed to limit known risk factors so as to reduce failure rates such as not treating smokers or diabetics. Investigators must also decide beforehand what data to collect and how. If the rates of some outcomes are low then prospective studies must continue for long periods to observe a sufficient number of cases to reliably estimate incidence. Because there is closer follow-up in prospective

studies vs. retrospective studies there is a higher cost to provide follow-up. As such, these studies are typically of shorter duration so may miss rare and late-stage complications such as implant fracture. They may also not fully reflect compliance-related problems with long latencies such as peri-implantitis.

By comparison, retrospective cohort studies are more time- and cost-efficient. They are typically done by "chart review," whereby examiners review and extract nonstandardized data from existing patient records (Fig. 7.5). Because the documentation is sought from existing records retrospectively, the retrieval of data is often less reliable, with potentially missing or unreliable data. Electronic patient records (EPRs) have become more commonplace in private practice and have the potential to improve the quality of retrospective observational studies and may elevate them to be nearly equal to prospective cohort studies. EPRs allow multiple parameter entries and deep data mining, resulting in less missing or unreliable data and, thus, potential blurring of the lines between prospective and retrospective studies. A hybrid design potentially exists, termed a "historical prospective cohort," and is already in common usage in medical clinical evaluations where detailed electronic patient records have been implemented. All treated subjects may now represent a potential cohort, and the data can be easily entered for every scenario in an easily retrievable manner. Analysis can therefore be made at multifactorial levels with the precision of a prospective study.

Two examples that provide a good comparison of a prospective cohort vs. a retrospective study can be seen in the prospective study by Van Velzen et al. [61] and the retrospective study by French et al. (2015) study [39], where the studies were similar, and the statistical methodology and analysis were by the same author (Dr. Ofec).

In the study by van Velzen et al., implant surgery was performed by the same surgeon in 95% of cases. Records were retrieved from 250 partially and fully edentulous patients who were enrolled in the study at the outset and received treatment with SLA dental implants from 1997 to 2001. The study evaluated patient factors (smok-ing, periodontitis, age, gender, and medical status), and also recorded implant-related parameters such as type, length, and width. They reported a 10-year survival rate of 99.7% and success rate of 92.7% [61], based on the Buser (1997) implant success criteria [62].

In the French et al. study, implant surgery was performed by the same periodontist in all cases, and similar patient factors were evaluated, including smoking, periodontitis, age, gender, and medical status. As with van Velzen et al., implant-related parameters such as type, length, and width were also collected. The report was up to 10 years, but the volume of data was limited at 8- to 10-year period, so survival outcome was reported at 7 years with implant-level and patient-level survival of 98.4% and 95.9%, respectively. These two studies essentially differ only in the fact that patient selection and data collection were made prospectively from the outset in the former study whereas data were retrospectively gathered from standardized chart records from patients included throughout the period of review in the latter.

In summary, retrospective cohort studies are less expensive to run and can follow long time periods, but are more prone to incomplete data compared to prospective cohort studies, which define the cohort and variables at outset and mobilize resources over a considerable amount of time [54]. However, both types of cohort studies are prone to attrition rate (loss to follow-up), which can increase over time [8, 51, 55].

7.3.2.6 Data Collection, Standardization, and Evaluation for Observational Studies

Data collection is often difficult to plan in a retrospective study, since some data collected may relate to endpoints that are not yet known or understood. In any case, It is critical to establish as much standardization as possible in the method of collection, within reasonable time limits and efficiency, to assist with later data extraction and to reduce missing data.

A cohort study of implant therapy analyzed in a Swedish population is an excellent example of

a large-scale retrospective cohort study with multiple variables evaluated that is representative for the given population [58]. The cohort is described as patients who received dental implant therapy provided by the Swedish Social system in 2003. This cohort was then evaluated by risk exposures and outcomes. Multiple risks exposures were evaluated simultaneously using multivariate analysis, e.g. the impact of smoking vs. non-smoking could be evaluated, as well as the existence of periodontal disease history. Retrospective cohorts can also allow multiple combined predictor variables to be evaluated, such as implant failure in patients with both diabetes and smoking. Furthermore, multiple outcomes were evaluated, such as failure, bone loss, and technical complications, provided the records were complete. Completeness of data is an issue, however; complete data collection is critical in retrospective studies, and one of the main weaknesses is missing data.

For all its strength, however, the Derks study has significant areas of missing data, which may not have been recorded or retrievable. The authors were transparent about this, and some examples where data were missing are listed below:

- patent-related data,
  - periodontal disease history (missing data from 53% of patients)
  - diabetes status (missing data from 54% of patients)
- implant-related data,
  - bone augmentation (missing data from 14% of implants)
  - implant length (missing data from 9% of implants).

Standardized data collection is advocated to increase quantity and quality of data retrieval over time and from multiple locations. This is made easier by EPRs, but this increases the need for security as the database is more accessible and from remote sources than a comparable paper entry system. So-called "back doors" exist in the majority of computer softwareHackers use such flaws (mistakes written into the lines of code) to obtain access, making full data protection nearly impossible [63]. Known examples of data breaches are epidemic, so it is not enough to try to secure data behind passwords or firewalls. Nowadays, best practices require that data collection and data entry is anonymized by use of clinical reference numbers that is separate from name or other personal identifiers.

7.3.2.7 Analysis and Interpretation

#### Data Quality, Missing, or Incomplete Data
Electronic data collection is inescapable. Electronic Patient Records (EPRs) provide several advantages, such as improving data entry reliability and recovery. The potential to merge standardized data across multiple centers also outweighs the risk of data breach provided it is done safely and appropriately.

How can it be done? In the French et al. (2015) cohort study the EPR was initiated in 2004 by a simple question from a patient, namely "*How many of implants have been done by the clinician, and how many have failed?*". The answer was not immediately available so the literature on general outcomes was given, as most clinicians would do. However, such broad general quotations do not provide any understanding of outcomes for the procedure under consideration in a given practice, by a specific clinician using a specific procedure with a specific implant system [39]. The question led to the establishment of an EPR listing all implant placements using Microsoft Access. This was made possible since, in 1997, the practice converted to digital radiographs, thus enabling screening of all digital X-rays from 1997 to 2004 for implant surgery images from this a perform a conventional chart review was performed, and data were then entered retrospectively for all implant patients. A standardized data entry format was thus created, which later became part of the electronic patient record from 2005 onward (in addition to the conventional chart).

Certain standardized input data were, and continue to be, applied using an anonymized identifier, i.e. patient factors such as age, medical systemic factors (e.g. smoking, penicillin allergy), medications; implant factors such as

implant type, length, and width; surgical factors such as insertion torque, timing of placement, timing of loading, graft or sinus lift (including both type of procedure and materials used), adjunctive or adjacent procedures and date of placement; prosthetic factors such as single vs. multiple units, screw- vs. cement-retained, stock vs. custom abutment, and abutment materials. Time output variables are also recorded, such as time of stage 2 test, failure (loss of implant), radiographic bone scores at all recall opportunities, soft tissue score using the novel implant mucosal index that evaluates degree of bleeding and suppuration [64], gingival recession, and other negative outcomes such biological or technical complications (Fig. 7.6). From this standardized data entry, real-time analysis of any input or outcome is available to assist evidence-

based decisions from real data from within the practice. For example, a patient allergic to penicillin may ask how many immediate implants with bone graft have been completed and whether the outcome is different than with nonallergic patients. A field search of EPR for immediate placement, penicillin allergy, infection, failure, as well as screening any other negative outcome files, provides an instant report that is not only evidence-based but created from data within the actual clinic where the patient will receive treatment. This also helps the clinician form their own evidence-based opinion to counter or corroborate certain "trends" and expert opinions that may be heard at scientific dental implant congresses. One published example using the EPR to evaluate a "question" is the effect of reported penicillin allergy on implant outcomes. In this study by
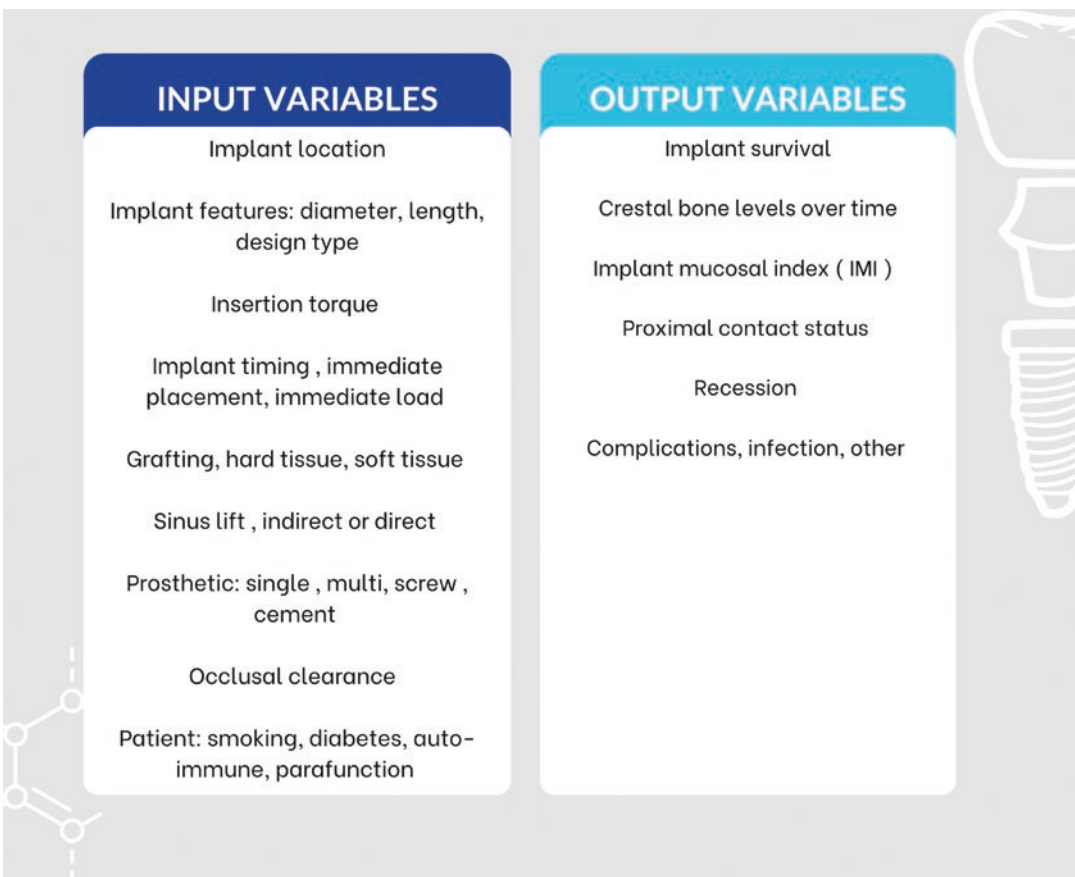
Fig. 7.6 Example of input and output variable evaluation

French and colleagues, outcomes in penicillin-allergic patients were evaluated from 5576 implant surgeries. It was found that for immediate implant placement, penicillin-allergic patients had ten-fold higher failure rates than nonallergic patients. Most failures were early postsurgical failures related to infection, since penicillin-allergic patients had a higher infection rate of 3.4% compared to 0.6% in the nonallergic group ($P < 0.05$) [65].

The same data can be evaluated more broadly using the entire cohort to assess multiple variables and multiple outcomes. This kind of detailed electronic patient record made possible a four-part research series on dental implants placed over a 10-year period, as reported in a multivariate survival analysis [39], a bleeding and bone score analysis [64]. Data collection which was completed efficiently as part of daily practice routine, and with minimal effort provided the base for one of the largest comprehensive multivariate survival analysis reports from a single center in private practice [39]. The study was comprehensive in terms of the investigated explanatory variables, which were grouped into the following categories: implant-related; surgery-related; prosthesis-related; and, patient-related. A visual description of investigated variables can be seen as extracted from the study [39].

7.3.3 Going Forward: A Proposal for Data Collection Standardization and Protocols

There is a need to standardize and facilitate data collection from private practice. This could allow for large comprehensive observational clinical studies conducted in the form of an "in-line case series" collected from clinical centers in cities and countries worldwide [66].

To reflect the realities of clinical practice, the inclusion criteria should be broad. The following broad inclusion criteria is therefore suggested for in-line case series: males or females at least 18 years old, who have signed an informed consent form and implant placement in a center that is enrolled and trained as part of the in-line case series and who voluntarily consent to anonymous data collection and are willing to attend follow-up appointments. Similarly, to provide the most valuable and broad clinical outcomes analysis, the exclusion criteria should be limited to: pregnant women or systemic disease that precludes dental implant therapy such as ASA class 3 or 4 [67], alcohol or drug abuse, and conditions or circumstances that would, in the opinion of the investigator, prevent completion of study participation. Patients who are smokers, or who have inadequate oral hygiene or periodontal disease history, physical or mental handicaps, parafunctional bruxism, clenching or apnea, can and should all be included; however, this additional information should be recorded under patient-related parameters to allow multifactorial evaluation on outcomes. Similarly, local exclusion criteria should be limited to areas with untreated endodontic or otherwise infected sites, and history of local irradiation therapy in area. Periodontal disease patients with probing pocket depth of ≥ 5 mm adjacent to the dental implant, bone augmentation procedure at the implant site, or immediate or early placement should also be included and recorded for any potential effect on outcomes. If there is no implant primary stability, this too can be included and tracked accordingly.

There is no currently accepted standard for minimum data that should be collected, nor is there a standard for outcomes analysis such as measurements or indices used. Most offices do not collect *any* systematic implant outcomes, and the few that do usually only record such events and implant placement and implant loss. As a minimum, more detailed outcomes than implant failure would be beneficial. We therefore propose a minimum input collection for centers who wish to collect data. These can be broken down to patient, implant, surgical and restorative parameters.

Patient parameters should include anonymous patient identifier and date of birth or age at time of placement, and basic medical parameters that are already established as risk factors, including diabetes, prior periodontal disease, smoking (duration and amount). Certain other medical

conditions could be evaluated depending on the depth of the study; these may include medications of bisphosphonates, SSRI antidepressants, steroids for autoimmune conditions, and PPI antacid medications. Implant parameters should include implant brand, type and dimensions (length and width). Surgical parameters should include implant location (FDI number), insertion torque, timing of placement (e.g. immediate vs. conventional), implant loading (e.g. immediate, early or conventional delayed [68].

Minimum follow-up data should include outcomes after time of implant placement, such as infection or membrane exposure. Stage 2 parameters should then be recorded including implant stability and bone score. Restorative data can be entered at this time with a minimum recording of splinted vs. nonsplinted, cement- vs. screw-retained, and abutment type. Subsequently, after a minimum of 1 year after placement, recorded outcomes should include survival and as well as success criteria at yearly intervals. Success criteria can be partly based on the Buser et al. 1990 classification [69], i.e. successful if all of the following success criteria are met: absence of persistent subjective discomfort such as pain, foreign body perception and or dysaesthesia (painful sensation); absence of a recurrent peri-implant infection with suppuration; absence of implant mobility on manual palpation and absence of any continuous peri-implant radiolucency.

Bone score data (bone loss) on periapical radiographs should also be included with standardized reference points as per French et al. [64] or bone level or tissue level designs. To assess changes in interproximal bone levels, standardized periapical radiographs of the treated areas will be taken. Standardization of the radiographs will be achieved as a minimum using a parallel technique with Rinn holders and, if possible, individual silicon bite registrations [70]. Radiographs must be of high enough quality and definition to identify the bone contours in question. It is not essential that the apical end of the implant is visible on the radiograph, but at least two threads of the implant should be visible. Evaluation of radiographs should be performed using a computer image analysis software (e.g.

Image J, National institutes of Health (NIH), Bethesda, MD, USA) or similar digital measurement system, calibrated to the known distance between the implant threads or implant length.

Bleeding on probing should use an ordinal scale such as the proposed *Implant Mucosal Index* [64] instead of a binary yes/no analysis, since implants are prone to false positive bleeding [71]. Suppuration is already included in this index so is not then reported separately. Pocket depth can vary based on abutment type and tissue biotype so baseline data at stage 2 and annually can use a threshold value such as <5 vs. ≥5 mm to facilitate ease of data entry and comparison rather than recording each depth value at each recall [72].

Today, most offices only record very limited data. The reasons for this are several fold:

1. The collection of standardized data can be very time-consuming exceeding the time of surgery.
2. In private practices the cost of data collection is not remunerated with the implant treatment fee.
3. Data exchange across offices is typically limited to treatment data and not outcome data.
4. Finally, little consensus which data to collect exists.

To assist in achieving a minimum of standardized data collection and to facilitate the enrollment of centers, a series of analog or digital forms have been developed.

Another very promising solution is a specialized software that records and shares standardized clinical data. Standardized parameters and logical checks can ensure data quality and comparability of data sets. Using QR scanners to scan the product codes reduces errors as well as the time to enter data. The fact that data a stored in a central register allows more efficient data exchange between practices. Once the center is enrolled and standard training on the recording process has been completed, data can be collected and is immediately available.

Using a cloud set up like this reduces the liability for (local) software maintenance, allows

sharing of patient records, provides real-time analysis of postmarket research, collaboratively answers questions that require large datasets, identifies trends in terms of treatment variation and geographic or subject variations, and create internal benchmarking of different individuals.

Such a system is at an advanced stage of development at the Straumann Group (Basel, Switzerland) and can already be accessed by dental professionals: https://www.straumann.com/myregistry

In the future, data entry systems can and will be more integrated into the flow of daily practice, and with this, the quality of data entry will increase, and cost of data entry will decrease compared to chart reviews that are currently used. With the aim of patient safety, most dental offices in the next few years will merge their patient records with state healthcare systems to provide better knowledge of general patient health, disease status, and medications used. This will be combined with ever-increasing dental EPRs that include more than just treatment performed and fee allocated, but also outcomes and standardized outcome analysis. All this can then be field searched and evaluated for relationships. In a solo practice, this will greatly increase the ability to understand clinical outcomes and provide clinicians with real-time measures of their performance, but if multiple centers use the same systems and then merge their data, this will provide massive datasets from which to improve statistical power and increase external validity by removing the confound of "one provider's" skill, environment or habits [73].

7.4   Conclusion: A New Paradigm for Clinical Investigations in Implant Dentistry—Real-World Evidence

Between the scientific measurements based on RCTs and the benefit measurements at two levels of cost in the community there is a gulf which has been much underestimated—Archie Cochrane, *Effectiveness and Efficacy: Random Reflections on Health Services, 1972*

Real-world evidence is generated not from data collected in conventional clinical trials, but from personal medical records and other electronic health records, disease registries, insurance company databases (e.g. as reported by Derks et al. (2015) [55]) clinical databases in hospitals and private practices, healthcare agencies, pharmacies, laboratories, pharmaceutical and medical device companies or national and patient surveys.

The use and importance of this type of data has dramatically increased in recent years and has become more and more critical to answer new questions and support decisions by e.g. regulatory agencies because they are collected from many different kinds of patients and can therefore provide a robust longitudinal cross-section of outcomes and issues with a particular intervention. However, it should be borne in mind that such data may be incomplete, especially regarding outcome measurements. It should also be remembered that diagnosis data, for example, may not be completely accurate, and depends on the source. Nevertheless these data allow for an analysis of "real world outcomes," i.e. patients experiencing a therapeutic outcome (dental implant) in a real-world setting (private dental practice).

A wider adoption of such outcomes and evidence depends on a number of factors, not least of which are alignment on outcomes and access/generation of data. Tonetti and Palmer proposed several outcome domains that could be used to help align standardized outcomes in implant dentistry [1]: patient-reported outcomes, e.g. health-related quality of life, general satisfaction, peri-implant tissue health, e.g. marginal bone level, tissue inflammation, probing depth, and performance of implant-supported restorations, e.g. longevity (survival), function/occlusion outcomes, technical complications.

The future could be to elaborate study designs including usability testing based on the new concept of an "in-line standardized clinical case series," which is foreseen to provide real-world evidence in implant dentistry but in a more standardized form [66]. In a nutshell, patients at a

small group of geographically close clinics receive the same treatment/intervention for the same indication in a short space of time. Unlike clinical trials, patients can be treated by expert implant surgeons but also by more general dental practitioners because surgeons and surgical teams are "calibrated" so that all preparation and surgical procedures are carried out the same way in all clinics, with standardized follow-up and outcomes measurement. Thus providing real-time evaluation of large-scale clinical outcomes.

References

1. Tonetti M, Palmer R, On behalf of Working Group 2 of the VIII European Workshop on Periodontology. Clinical research in implant dentistry: study design, reporting and outcome measurements: consensus report of Working Group 2 of the VIII European Workshop on Periodontology. J Clin Periodontol. 2012;39(Suppl 12):73–80. https://doi.org/10.1111/j.1600-051X.2011.01843.x.
2. Berglundh T, Giannobile WV. Investigational clinical research in implant dentistry. Beyond observational and descriptive studies. J Dent Res. 2013;92(12 Suppl):107S–8S. https://doi.org/10.1177/0022034513510531.
3. Grimes DA, Schulz KF. An overview of clinical research: the lay of the land. Lancet. 2002a;359:57–61. https://doi.org/10.1016/S0140-6736(02)07283-5.
4. Anglemeyer A, Horvath HT, Bero L. Healthcare outcomes assessed with observational study designs compared with those assessed in randomized clinical trials. Cochrane Database Syst Rev. 2014;(4):MR000034. https://doi.org/10.1002/14651858.MR000034.pub2.
5. Dekkers OM, Egger M, Altman DG, Vandenbroucke JP. Distinguishing case series from cohort studies. Ann Intern Med. 2012;156:37–40. https://doi.org/10.7326/0003-4819-156-1-201201030-00006.
6. Meijer HJA, Raghoebar GM. Quality of reporting of descriptive studies in implant dentistry. Critical aspects in design, outcome assessment and clinical relevance. J Clin Periodontol. 2012;39(Suppl 12):108–13. https://doi.org/10.1111/j.1600-051X.2011.01834.x.
7. Fletcher R, Fletcher S. Clinical epidemiology. The essentials. Philadelphia: Lippincott Williams & Wilkins; 2005, 252p.
8. Song JW, Chung K. Observational studies: cohort and case-control studies. Plast Reconstr Surg. 2010;126:2234–42. https://doi.org/10.1097/PRS.0b013e3181f44abc.
9. Gopalakrishnan S, Ganeshkumar P. Systematic reviews and meta-analysis: understanding the best evidence in primary healthcare. J Family Med Prim Care. 2013;2:9–14. https://doi.org/10.4103/2249-4863.109934.
10. Feldstein DA. Clinician's guide to systematic reviews and meta-analyses. WMJ. 2005;104:25–9.
11. Bartolucci AA, Hillegass WB. Overview, strengths, and limitations of systematic reviews and meta-analyses. In: Chiappelli F, et al., editors. Evidence-based practice: toward optimizing clinical outcomes. Berlin: Springer; 2010.
12. Higgins JPT, Green S. Cochrane handbook for systematic reviews of interventions. 2011. http://handbook.cochrane.org.
13. Moher D, Liberati A, Tetzlaff J, Altman DG, PRISMA Group. Preferred reporting items for systematic reviews and meta-analyses: the PRISMA statement. BMJ. 2009;339:b2700. https://doi.org/10.1136/bmj.b2700.
14. Liberati A, Altman DG, Tetzlaff J, Mulrow C, Gøtzsche PC, Ioannidis JPA, et al. The PRISMA statement for reporting systematic reviews and meta-analyses of studies that evaluate healthcare interventions: explanation and elaboration. BMJ. 2009;339:b2700. https://doi.org/10.1136/bmj.b2700.
15. MacBeth N, Trullenque-Eriksson A, Donos N, Mardas N. Hard and soft tissue changes following alveolar ridge preservation: a systematic review. Clin Oral Implants Res. 2017;28(8):982–1004. https://doi.org/10.1111/clr.12911.
16. Vignoletti F, Matesanz P, Rodrigo D, Figuero E, Martin C, Sanz M. Surgical protocols for ridge preservation after tooth extraction. A systematic review. Clin Oral Implants Res. 2012;23(Suppl 5):22–38. https://doi.org/10.1111/j.1600-0501.2011.02331.x.
17. De Buitrago JG, Avila-Ortiz G, Elangovan S. Quality assessment of systematic reviews on alveolar ridge preservation. J Am Dent Assoc. 2013;144(12):1349–57.
18. Krithikadatta J. Research methodology in dentistry: part 1- the essentials and relevance of research. J Conserv Dent. 2012;15:5–11. https://doi.org/10.4103/0972-0707.92598.
19. Blencowe NS, Brown JM, Cook JA, Metcalfe C, Morton DG, Nicholl J, et al. Interventions in randomised controlled trials in surgery: issues to consider during trial design. Trials. 2015;16:392. https://doi.org/10.1002/14651858.MR000034.pub2.

20. Levin KA. Study design VII: randomised controlled trials. Evid Based Dent. 2007;8:22–3. https://doi.org/10.1038/sj.ebd.6400473.
21. Schulz KF, Grimes DA. Generation of allocation sequences in randomised trials: chance, not choice. Lancet. 2002;359:515–9. https://doi.org/10.1016/S0140-6736(02)07683-3.
22. Thabane L, Ma J, Chu R, Cheng J, Ismaila A, Rios LP, et al. A tutorial on pilot studies: the what, why and how. BMC Med Res Methodol. 2010;10:1. https://doi.org/10.1186/1471-2288-10-1.
23. Lancaster GA, Dodd S, Williamson PR. Design and analysis of pilot studies: recommendations for good practice. J Eval Clin Pract. 2004;10(2):307–12. https://doi.org/10.1111/j.2002.384.doc.x.
24. Arnold DM, Burns KE, Adhikari NK, Kho ME, Meade MO, Cook DJ, McMaster Critical Care Interest Group. The design and interpretation of pilot trials in clinical research in critical care. Crit Care Med. 2009;37(1 Suppl):S69–74. https://doi.org/10.1097/CCM.0b013e3181920e33.
25. Grimes DA, Schulz KF. Bias and causal associations in observational research. Lancet. 2002;359:248–52. https://doi.org/10.1016/S0140-6736(02)07451-2.
26. Schulz KF, Altman DG, Moher D, CONSORT Group. CONSORT. Statement: updated guidelines for reporting parallel group randomised trials. BMJ. 2010;2010(340):c332. https://doi.org/10.1136/bmj.c332.
27. Donn J. Medical benefits of flossing teeth unproven. The Globe and Mail. 2016. https://www.theglobeandmail.com/life/health-and-fitness/health/medical-benefits-of-flossing-teeth-unproven/article31229865/. Accessed 30 Sept 2018.
28. Sambunjak D, Nickerson JW, Poklepovic T, Johnson TM, Imai P, Tugwell P, et al. Flossing for the management of periodontal diseases and dental caries in adults. Cochrane Database Syst Rev. 2011;7(12):CD008829. https://doi.org/10.1002/14651858.CD008829.pub2.
29. AAP Advisory, American Academy of Periodontology continues to recommend flossing as essential in maintaining healthy teeth and gums. 2016. Perio.org.
30. Brunette DM. Critical thinking: understanding and evaluating dental research. 1st ed. Chicago: Quintessence Publishing; 1996.
31. Cairo F, Sanz I, Matesanz P, Nieri M, Pagliaro U. Quality of reporting of randomized clinical trials in implant dentistry. A systematic review on critical aspects in design, outcome assessment and clinical relevance. J Clin Periodontol. 2012;39(Suppl):81–107. https://doi.org/10.1111/j.1600-051X.2011.01839.x.
32. Marx RE. The deception and fallacies of sponsored randomized prospective double-blinded clinical trials: the bisphosphonate research example. Int J Oral Maxillofac Implants. 2014;29:e37–44. https://doi.org/10.11607/jomi.te40.
33. Al-Nawas B, Brägger U, Meijer HJ, Naert I, Persson R, Perucchi A, et al. A double-blind randomized controlled trial (RCT) of Titanium-13 zirconium versus titanium grade IV small-diameter bone level implants in edentulous mandibles--results from a 1-year observation period. Clin Implant Dent Relat Res. 2012;14(6):896–904. https://doi.org/10.1111/j.1708-8208.2010.00324.x.
34. Quirynen M, Al-Nawas B, Meijer HJ, Razavi A, Reichert TE, Schimmel M, et al. Small-diameter titanium grade IV and titanium-zirconium implants in edentulous mandibles: three-year results from a double-blind, randomized controlled trial. Clin Oral Implants Res. 2015;26(7):831–40. https://doi.org/10.1111/clr.12367.
35. Müller F, Al-Nawas B, Storelli S, Quirynen M, Hicklin S, Castro-Laza J, et al. Small-diameter titanium grade IV and titanium-zirconium implants in edentulous mandibles: five-year results from a double-blind, randomized controlled trial. BMC Oral Health. 2015;15(1):123. https://doi.org/10.1186/s12903-015-0107-6.
36. Clarkson J. Experience of clinical trials in general dental practice. Adv Dent Res. 2005;18(3):39–41. https://doi.org/10.1177/154407370501800302.
37. Marx RE, Sawatari Y, Fortin M, Broumand V. Bisphosphonate-induced exposed bone (osteonecrosis/Osteopetrosis) of the jaws: risk factors, recognition, prevention, and treatment. J Oral Maxillofac Surg. 2005;63(11):1567–75. https://doi.org/10.1016/j.joms.2005.07.010.
38. Wu X, Al-Abedalla K, Rastikerdar E, Abi Nader S, Daniel NG, Nicolau B, et al. Selective serotonin reuptake inhibitors and the risk of osseointegrated implant failure: a cohort study. J Dent Res. 2014;93(11):1054–61. https://doi.org/10.1177/0022034514549378.
39. French D, Larjava H, Ofec R. Retrospective cohort study of 4591 Straumann implants in private practice setting, with up to 10-year follow-up. Part 1: multivariate survival analysis. Clin Oral Implants Res. 2015;26(11):1345–54. https://doi.org/10.1111/clr.12463.
40. Reid JL, Hammond D, Driezen P. Socio-economic status and smoking in Canada, 1999–2006: has there been any progress on disparities in tobacco use? Can J Public Health. 2010;101:73–8.
41. Kaneda K, Kondo Y, Masaki C, Mukaibo T, Tsuka S, Tamura A, Aonuma F, Shinmyouzu K, Iwasaki M, Ansai T, Hosokawa R. Ten-year survival of immediate-loading implants in fully edentulous mandibles in the Japanese population: a multilevel analysis. J Prosthodont Res. 2019;63:35–9.
42. Feine J, et al. Outcome assessment of implant-supported prostheses. J Prosthet Dent. 1998;79(5):575–9. https://doi.org/10.1016/S0022-3913(98)70179-9.

43. von Elm E, Altman DG, Egger M, Pocock SJ, Gøtzsche PC, Vandenbroucke JP, STROBE Initiative. Strengthening the reporting of observational studies in epidemiology (STROBE) statement: guidelines for reporting observational studies. BMJ. 2007;335:806–8. https://doi.org/10.1136/bmj.39335.541782.AD.

44. Gagnier JJ, Kienle G, Altman DG, Moher D, Sox H, Riley D, CARE Group. The CARE guidelines: consensus-based clinical case reporting guideline development. BMJ Case Rep. 2013;2013:bcr2013201554. https://doi.org/10.1136/bcr-2013-201554.

45. Bitkina O, Kim HK, Park J. Usability and user experience of medical devices: an overview of the current state, analysis methodologies, and future challenges. Int J Ind Ergon. 2020;76:102932.

46. Kooistra B, Dijkman B, Einhorn TA, Bhandari M. How to design a good case series. J Bone Joint Surg Am. 2009;91(Suppl 3):21–6. https://doi.org/10.2106/JBJS.H.01573.

47. Grimes DA, Schulz KF. Descriptive studies: what they can and cannot do. Lancet. 2002;359:145–9. https://doi.org/10.1016/S0140-6736(02)07373-7.

48. Sennerby L, Rocci A, Becker W, Jonsson L, Johansson L-A, Albrektsson T. Short-term clinical results of Nobel Direct implants: a retrospective multicentre analysis. Clin Oral Implants Res. 2008;19(3):219–26. https://doi.org/10.1111/j.1600-0501.2007.01410.x.

49. Schulz KF, Grimes DA. Case control studies: research in reverse. Lancet. 2002;359:431–4.

50. Levin KA. Study design V. Case-control studies. Evid Based Dent. 2003;7:83–4.

51. Rocchietta I, Nisand D. A review assessing the quality of reporting of risk factor research in implant dentistry using smoking, diabetes and periodontitis and implant loss as an outcome: critical aspects in design and outcome assessment. J Clin Periodontol. 2012;39(Suppl 12):114–21. https://doi.org/10.1111/j.1600-051X.2011.01829.x.

52. Ashraf J, Hussain Bokhari SA, Manzoor S, Khan AA. Poor oral health and coronary artery disease: a case-control study. J Periodontol. 2012;83(11):1382–7. https://doi.org/10.1902/jop.2012.110563.

53. Jeong J-S, Chang M. Food impaction and periodontal/peri-implant tissue conditions in relation to the embrasure dimensions between implant-supported fixed dental prostheses and adjacent teeth: a cross-sectional study. J Periodontol. 2015;86(12):1314–20. https://doi.org/10.1902/jop.2015.150322.

54. Levin KA. Study design IV. Cohort studies. Evid Based Dent. 2003;7:51–2.

55. Grimes DA, Schulz KF. Cohort studies: marching towards outcomes. Lancet. 2002;359:341–5.

56. Brunette. Critical thinking. 2nd ed. Chicago: Quintessence Publishing; 2007. ISBN: 978-0-86715-426-9.

57. Wu X, Al-Abedalla K, Abi-Nader S, Daniel NG, Nicolau B, Tamimi F. Proton pump inhibitors and the risk of osseointegrated dental implant failure: a cohort study. Clin Implant Dent Relat Res. 2017;19(2):222–32. https://doi.org/10.1111/cid.12455.

58. Derks J, Håkansson J, Wennström JL, Tomasi C, Larsson M, Berglundh T. Effectiveness of implant therapy analyzed in a Swedish population: early and late implant loss. J Dent Res. 2015;3 Suppl:44S–51S. https://doi.org/10.1177/0022034514563077.

59. Correia F, Gouveia S, Felino AC, Costa AL, Almeida RF. Survival rate of dental implants in patients with history of periodontal disease: a retrospective cohort study. Int J Oral Maxillofac Implants. 2017;32(4):927–34. https://doi.org/10.11607/jomi.3732.

60. Tabrizi R, Behnia H, Taherian S, Hesami N. What are the incidence and factors associated with implant fracture? J Oral Maxillofac Surg. 2017;75(9):1866–72. https://doi.org/10.1016/j.joms.2017.05.014.

61. van Velzen FJ, Ofec R, Schulten EA, Ten Bruggenkate CM. 10-year survival rate and the incidence of peri-implant disease of 374 titanium dental implants with a SLA surface: a prospective cohort study in 177 fully and partially edentulous patients. Clin Oral Implants Res. 2015;26(10):1121–8. https://doi.org/10.1111/clr.12499.

62. Buser D, Mericske-Stern R, Bernard JP, Behneke A, Behneke N, Hirt HP, et al. Long-term evaluation of non-submerged ITI implants. Part 1: 8-year life table analysis of a prospective multi-center study with 2359 implants. Clin Oral Implants Res. 1997;8(3):161–72.

63. Economist why everything is hackable. Computer security is broken from top to bottom. The Economist. 2017. https://www.economist.com/science-and-technology/2017/04/08/computer-security-is-broken-from-top-to-bottom. Accessed 3 Oct 2018.

64. French D, Cochran DL, Ofec R. Retrospective cohort study of 4,591 Straumann implants placed in 2,060 patients in private practice with up to 10-year follow-up: the relationship between Crestal bone level and soft tissue condition. Int J Oral Maxillofac Implants. 2016;31(6):e168–78. https://doi.org/10.11607/jomi.4932.

65. French D, Noroozi M, Shariati B, Larjava H. Clinical retrospective study of self-reported penicillin allergy on dental implant failures and infections. Quintessence Int. 2016;47(10):861–70. https://doi.org/10.3290/j.qi.a36887.

66. Dard M. The standardised in-line clinical case series: a new concept for real-world evidence in dentistry J Dent Oral Health. 2017. http://scientonline.org/fulltext/the-standardised-in-line-lase-series-a-new-concept-for-real-world-evidence-in-dentistry/21455. Accessed 3 Oct 2018.

67. Owens WD, Felts JA, Spitznagel EL Jr. ASA physical status classifications: a study of consistency of ratings. Anesthesiology. 1978;49(4):239–43.

68. Ganeles J, Zöllner A, Jackowski J, ten Bruggenkate C, Beagle J, Guerra F. Immediate and early loading of Straumann implants with a chemically modified surface (SLActive) in the posterior mandible and

maxilla: 1-year results from a prospective multicenter study. Clin Oral Implants Res. 2008;19(11):1119–28.

69. Buser D, Weber HP, Lang NP. Tissue integration of non-submerged implants. 1-year results of a prospective study with 100 ITI hollow-cylinder and hollow-screw implants. Clin Oral Implants Res. 1990;1(1):33–40.

70. Wadhwani CP, Schuler R, Taylor S, Chen CS. Intraoral radiography and dental implant restoration. Dent Today. 2012;31(8):66, 68, 70–1; quiz 72–3.

71. Gerber JA, Tan WC, Balmer TE, Salvi GE, Lang NP. Bleeding on probing and pocket probing depth in relation to probing pressure and mucosal health around oral implants. Clin Oral Implants Res. 2009;20(1):75–8.

72. Heitz-Mayfield LJ. Peri-implant diseases: diagnosis and risk indicators. J Clin Periodontol. 2008;35(8 Suppl):292–304.

73. Joda T. Big data in dental research and oral health care. Basel: MDPI; 2021.

74. Sutherland SE. Evidence-based dentistry: part IV. Research design and levels of confidence. J Can Dent Assoc. 2001;67:375–8.

Translational Aspects in Living Mammalian Organisms

8

J. Blanco-Carrion, A. Liñares, and F. Muñoz

8.1 General Definition of Translation

It is necessary to understand and not confuse concepts such as *translation, translational research, translational medicine and translational dentistry.*

The *translation*, or more correctly the translability, corresponds to the degree of correlation between preclinical study outcomes and clinical situations in humans. It refers to the clinical predictability [1].

Translational Research is considered a priority for the National Institutes of Health (NIH). But what do we mean by translational research? For many, the term refers to the "bench-to-bedside" taking advantage of knowledge from basic sciences to produce new products, drugs, devices and treatment possibilities for the patients. In this field of research the main outcome is the generation of a promising new treatment that can be used in clinical practice or commercialized ("brought to market") [2]. This initiative is crucial and has been characterized as follows: "effective translation of the new knowledge, mechanisms and techniques generated by advances in basic science research into new

approaches for prevention, diagnosis and treatment of disease is essential for improving health" [3]. For others—particularly health services researchers and public health investigators whose studies focus on health care and health as the primary outcome—translational research refers to translating research into practice, i.e., ensuring that new treatments and research knowledge reach the patients or populations for whom they are intended and are implemented correctly. The production of a new drug, an end point for "bench-to-bedside" translational research, is only the starting point for this second area of research [2]. The difference between these two concepts of translational research was articulated by the Institute of Medicine's Clinical Research Roundtable [4], which described two "translational blocks" in the clinical research work and which some now label as T1 and T2. The first roadblock (T1) was described by the roundtable as "the transfer of new understandings of disease mechanisms gained in the laboratory into the development of new methods for diagnosis, therapy and prevention and their first testing in humans." The roundtable described the second roadblock (T2) as "the translation of results from clinical studies into everyday clinical practice and health decision making."

Another concept that emerges in the literature is *Translational Medicine*, which primary goal is to integrate the corresponding findings and capabilities for optimizing patient outcomes, preven-

J. Blanco-Carrion (✉) · A. Linares · F. Munoz
University of Santiago de Compostela,
Santiago de Compostela, Galicia, Spain
e-mail: juan.blanco@usc.es; antonio.linares@usc.es;
fernandom.munoz@usc.es

tion, screening and therapy of disease and improving health policy altogether [5]. The historical "benchside" concept of translational medicine emphasized translating laboratory discoveries into practical clinical applications that would benefit the patient [6]. Such a unilateral concept focused on benchside expertise only and missed the crucial feedback from bedside, which is as equally important as benchside. Translational medicine next evolved into a "two-way bridge" concept [7]. In addition to historical benchside concept, the benchside–bedside–benchside concept involves returning the clinical findings to research labs to redefine or create new hypothesis-driven research efforts which might result in innovative discoveries. Since many clinicians are often overburdened or unfamiliar with research techniques and infrastructure, there can be a considerable communication and even cultural gap between clinicians and basic scientists. In addition to clinical trial data (when they are available), clinical publications in the form of case reports constitute a good resource to transmit bedside findings back to the bench, but this process is often difficult and case reports remain isolated in their clinical fields. While this two-way bridge terminology (bedside to benchside and back) is currently quite popular, it still misses an important aspect of the health care cycle, the community, represented by healthy populations and patients as well as by medical practitioners. From the start, the European Society for Translational Medicine (EUSTM) realized the need for a clear, comprehensive and concise definition of Translational Medicine (TM) that would also apply globally, across nations, markets and disciplines. Accordingly, EUSTM defines Translational Medicine as an interdisciplinary branch of the biomedical field supported by three main pillars: benchside, bedside and community. The goal of TM is to combine disciplines, resources, expertise and techniques within these pillars to promote enhancements in prevention, diagnosis and therapies. While benchside and bedside are already well understood, EUSTM puts an equal emphasis on the "community" pillar, as community is the

actual end user for all TM interventions and thus, a key stakeholder [5].

Embedded within its fundamental tenets, Patient Protection and Affordable Care Act [8] argues in favor of *translational health care*. The translational perspective in the health sciences consists of two independent yet intertwined facets of the same coin: the concerted and complementary contribution of translational research and translational effectiveness in improving the health care process [9].

Evidence-based dental practice, as one essential component of translational healthcare, is a patient-centered, effectiveness-focused and evidence-based endeavor, which commences with the patient-clinician encounter at the diagnostic stage and culminates in the patient-clinician encounter during the entirety of the treatment prognostic and follow-up stages [10–13]. As a translational science of healthcare, evidence-based dental practice consists of two primary facets:

1. *Translational research*: emerging from the initial patient-clinician encounter, biopsies and clinical tests are obtained to define and characterize the fundamental biological pathways that underlie the observed physiopathology.

2. *Translational effectiveness*: also emerging from the initial patient-clinician encounter, fundamental criteria are isolated by the clinician to discern the clinical literature that pertains specifically to the type of patient affliction (P), the possible interventions (I) and comparators (C), the desired clinical outcome (O), within the timeline under consideration (T) and the selected clinical settings (S). The crafted PICOTS question reveals the medical subject headings (MeSH) and keywords needed to uncover the pertinent clinical trials, observational studies and systematic reviews. Once obtained, the peer-reviewed evidence is assessed and evaluated for level (i.e., type of study) and quality (i.e., risk of bias). The consensus of the best evidence base results from a cogent analysis of the evidence ranked by level and quality.

We cannot forget another important pillar in the way of developing a new material or technique. When one of these are to be introduced successfully, efficiently and effectively across a wide range of geographical and professional settings, there must be careful consideration of how dental education (across the range from the dental graduate, the dental team and continuing education) can equip new and current practitioners with the information and skills to best use these new materials as they are introduced and evolve.

8.2   Importance of Parallel and Complementary Study Designs

Nowadays, practical contemporary medicine follows stringently the scientific method in the process of validating efficacy and effectiveness of new or improved modes of treatment intervention. These complementary or alternative interventions must be validated by stringent research before they can be reliably integrated into medicine.

Evidence-based research (EBR) in medicine, as conceived by A. Cochrane, must not be confused with medicine based on research evidence. EBR is a research movement in the medical sciences based on the application of the scientific method. It seeks the conscientious, explicit and judicious identification, evaluation and use of the best evidence currently available. It is a systematic process whose purpose is to congeal the best available research findings with patient history and laboratory test results in order to optimize the process of making decisions about the care of each individual patient. Medicine based on the evidence, in contrast, is the traditional approach to medical treatment. It rests on long-established existing medical traditions, supplemented by individual pieces of evidence provided by the medical exam (e.g., history, test results), which may or may not have undergone adequate or sufficient scientific scrutiny.

The use of animals in scientific research remains a vital tool in improving our understanding of how biological systems work both in health and disease, and in the development of new medicines, treatments and technologies. Underpinning this research is a strong commitment to maintaining a rigorous regulatory system that ensures that animal research is carried out only where no practicable alternative exists and under controls that keep suffering to a minimum. This is achieved through robustly applying the principles of the 3Rs (replacement, reduction and refinement) to all research proposals involving the use of animals.

Replacement refers to technologies or approaches which directly replace or avoid the use of animals in experiments where they would otherwise have been used.

Reduction refers to methods that minimize the number of animals used per experiment or study consistent with the scientific aims.

Refinement refers to methods that minimize the pain, suffering, distress or lasting harm that may be experienced by research animals, and which improve their welfare.

Study designs are implemented in order to produce new evidence, and depending of the kind of studied outcome different designs are applied.

Parallel studies on animals and humans have been conducted for years in order to prove that translational research works. However, in many occasions, results achieved in animal research are no corroborated in human studies.

8.2.1   Observational Human Clinical Studies vs. Observational Animal Studies

An observational study is a nonexperimental trial where current behavior is simply observed without intervention. A clear example of humans is to assess the effect of smoking on implant patients.

Two major observational studies are case-control and cohort trials. Cohort studies can be prospective or retrospective. Prospective studies are carried out from the present time into the future. Because prospective studies are designed with specific data collection methods, it can be tailored to collect specific exposure data and may be complete. The disadvantage of a prospective

Experimental peri-implantitis model
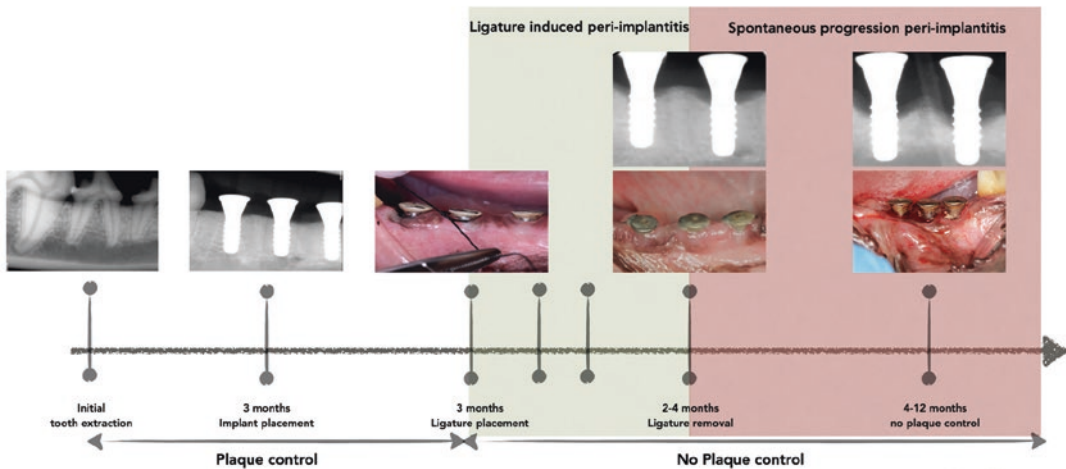
Fig. 8.1 Peri-implantitis model in beagle dogs

cohort study may be the long follow-up period while waiting for events or diseases to occur. Thus, prospective cohort studies are difficult to implement on animals, unless disease initiation and/or progression can occur early. This may appear in the peri-implantitis animal model studies, since early disease can be initiated by the application of ligatures around implant necks.

Retrospective cohort studies, also known as historical cohort studies, are carried out at the present time and look to the past to examine medical events or outcomes. This can be designed on humans, and may bring up new scientific hypothesis; however, retrospective cohort studies in animals are rare due to mainly ethical issues, short lifespan, care and cost.

Lindhe & Berglundh developed, in 1992, the peri-implantitis model in beagle dogs [14]. This model assesses the effect of plaque on initiation and progression of peri-implantitis. This design is proof of the principle that infection leads to peri-implant bone loss. Briefly, this model applies ligatures (i.e., 3-0 silk) after normal implant healing (2–3 months). These ligatures will accumulate plaque and will induce inflammation in the soft tissues surrounding the implant. This inflammation will turn later into the bone loss. Some designs replace ligatures every month until around 30% of bone loss has been achieved. This

is what it is known as ligature-induced peri-implantitis, since this is not a "normal" infection but also a foreign body reaction. To assimilate what occurs in natural progression on humans, these ligatures are removed and leave a normal progression or remission of the established disease without any plaque control. This period may last from 4 to 12 months. The following image represents this model and the potential outcomes over time (Fig. 8.1).

Observational studies on human clearly show that peri-implantitis occurs in a high number of patients [15], and the role of plaque and bacteria has a major impact on this disease [16]. However, time is needed in order disease occurrence. This issue is sorted in animal studies applying that kind of ligature to speed up the initiation of the disease.

8.2.2 Experimental Human Clinical Studies vs. Experimental Animal Studies

Although observational studies can be applied to animal research, nowadays due to ethical issues, animals are used mainly to test treatment outcomes rather than observational designs. This turns into the category of experimental studies.

An experiment is a procedure carried out to support, refute, or validate a hypothesis. Experiments provide insight into cause and effect by demonstrating what outcome occurs when a particular factor is manipulated.

Experiments typically include controls, which are designed to minimize the effects of variables other than the single independent variable. This increases the reliability of the results, often through a comparison between control measurements and the other measurements.

In example, continuing with peri-implantitis, once the model mentioned above is applied, an experimental study can be performed in order to test treatment options.

In implant therapy, human studies evaluated the effect of immediate impact placement after tooth extraction [17]. It was thought that after extraction, an implant could counteract the bone resorption process if the device is applied at the same moment of tooth removal. Later on, a model was designed to test if the implant could prevent the normal bone resorption process after tooth extraction [18]. This experimental study showed clearly that the dynamics of bone resorption after tooth extraction occur in a similar manner if the implant is placed into a socket immediately or no placement. In fact, clinical studies on humans clearly show that this process also occurs [19].

Thus, it seems that animal experiments may be extended to human trials in a parallel way, and last ones bearing out the outcomes achieved in preclinical studies. Implant dentistry has evolved dramatically in the last two decades, thanks to animal research trials feeding up evidence-based healthcare approaches.

8.3   Choice of the Experimental Model in Implant Dentistry

8.3.1   Introduction

Development of an optimal interface between bone and orthopedic or dental implants has taken place for many years. Schmidt et al. defined an ideal bone–implant material as having a biocompatible chemical composition to avoid adverse tissue reactions, excellent corrosion resistance in the physiologic milieu, acceptable strength, a high resistance to wear, and a modulus of elasticity similar to that of bone to minimize bone resorption around the implant [20].

In vitro tests of toxicity and cytocompatibility have been widely used, avoiding the indiscriminate use of animals. However, in vitro characterization is not able to demonstrate the tissue response to materials or the loading conditions. This means that in vitro studies can be difficult to extrapolate to the in vivo situation [20]. That is because animal models play an indispensable step in the testing of implants and biomaterials for understanding their characteristics related to osteoconductivity, biocompatibility, mechanical properties, degradation and interaction with host tissues [21].

8.3.2   Animal Selection

No particular animal model of a usage test for dental implant systems has yet been validated as relevant to the human situation [1]. Various factors have to be considered for selecting a specific animal model. Firstly, the model should demonstrate physiological and pathological analogies in comparison to humans. Second, it must be able to operate and observe numerous subjects over a short period of time. Finally, details as cost for acquisition, care, availability, acceptance for society, tolerance to captivity and ease of housing are important in the selection of the model [20, 21].

In other words, the researcher must establish a series of points before definitively decide what animal use as model in implant dentistry: (1) ethics, (2) genetics, (3) transport, housing and related animal behavior, (4) anesthesia procedure and cardiovascular stability, (5) bone anatomy and structure, (6) jaw and mouth anatomy, (7) alimentation and chewing process, (8) periodontium and soft tissues histology, (9) oral hygiene, (10) type of defect: induced (acute or chronic) or spontaneously occurring [1].

Although the specific anatomy is quite different between these species and humans, the tissue response to periodontal disease and gingival recession is quite similar [22]. However, it is important to keep in mind that the results obtained from an animal trial do not allow any direct correlations and conclusions concerning human situations or treatments to be drawn [1].

Dog, sheep, goat, pig and rabbit models are commonly used to evaluate bone–implant interactions (Fig. 8.2). The most used models for implantation are the miniature pig maxilla and the rabbit femur [23]. In many situations, multiple model systems will be required to establish a broad body of knowledge [20].

It is important to consider the size of the implants to test, number per animal, duration of the test and expected biological differences [21]. Guidelines are provided for the dimensions of implants for in vivo studies, based on the size of animal and bone chosen and on the implant design, in order to avoid pathological fractures [20]. We recommend the use of ISO 10993-6 as reference guide.

8.3.3 Remarks and Recommendations

1. Handling animals is difficult and complications may occur. The most frequent are during anesthesia and the infection of the wound.
2. The use of young animals may bring serious complications, covering the implant totally and finally placed inside the bone marrow. If the oral approach is used, the definitive teeth will displace or remove the implants with fatal results for the study.
3. Older animals or miniature pigs with a slower rate of growth are recommended [23].
4. It is extremely important that control implants should be of a material already in clinical use and should allow the outcome data to be related to existing products [20].
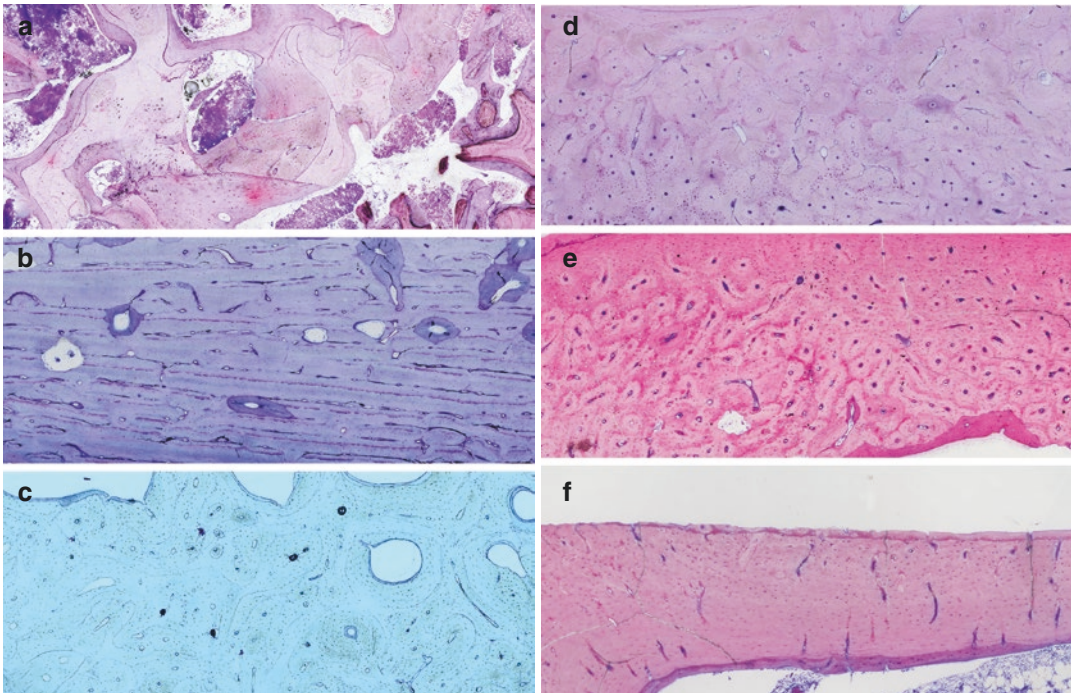
Fig. 8.2 Bone structure of different species used in dental research. (**a**) human, (**b**) pig, (**c**) sheep, (**d**) dog, (**e**) rabbit and (**f**) rat

5. About bone composition, density and function, the dog and pig are the species most closely to human situation [20].
6. Katranji studied the thickness of the cortical bone in different regions of maxillary and mandibular bone in human cadavers, observing great differences in the edentulous or dentate maxilla and mandible [24]. Based on the differences of bone–implant contact (BIC) between cortical and trabecular bone, studies should be accompanied by details on the ratio between compact and spongy bone at the site of implantation [23].

8.3.4 Animal Species and Bones Used in Experimental Dental Implantology

8.3.4.1 Rodents
One of the most used models thanks to its size, easy handle and cost. Recently, mice were used to evaluate the effects of condensation on peri-implant bone density and remodeling, showing very interesting results [25]. In addition, rats are the most used animals for studying tooth movement [26].

Transgenic technologies are critical to identifying the function of a specific gene that may participate in bone development, remodeling, repair and diseases. Mice have a well-developed transgenic system, which provides a powerful tool for researchers to study the molecular mechanisms. That makes mice very useful for evaluating the early stage tissue response of biomaterials [27].

The main limitations of model are the small size of the long bones and thin and fragile cortices, making rodents unsuitable for testing multiple implants simultaneously or the evaluation of commercial human-size implants [20].

In addition, rodents have significant dissimilarities with the human bone. Alveolar bone is denser and does not show Haversian-type remodeling in the cortex [21]. The osteoid tissue along the alveolar bone surface in rats is less, and the calcium concentration is more controlled by intestinal absorption [26].

The most used models in rodents have been the distal femur (rat, 2 mm diameter; mice, 0.8 mm) and calvarial defects (rat, 8 mm; mice, 4 mm) [21, 27].

8.3.4.2 Rabbits
Rabbits are one of the most commonly used animal models, mainly for studies of biocompatibility of implants and biomaterials. Rabbits offer advantages over large animal models by reaching skeletal maturity at a relatively early age (6 months) and advantages over rodents by undergoing more secondary osteonal remodeling [28]. In addition, are easily available and handling.

However, this species shows the least similarities to human bone [20, 23] and its small size limits the assessment of multiple defect evaluations [21]. Rabbits also have relatively fatty bone marrow which is not ideal for autogenous bone grafts [28].

About bone remodeling, in comparison with other species, the rabbit has faster skeletal change and bone turnover. This makes difficult to extrapolate the results, but are very used for screening implant materials prior to testing in a larger animal model [21].

8.3.4.3 Canine
The dog is one of the more used large animal models for dental research. There is a considerable amount of literature about a comparison between canine and human bone. However, there are increasing ethical issues relating to the use of dogs in medical research due to their status as companion animals [20, 23].

Regarding macrostructure, there may be some discrepancy in the size, but the dimensions of dental implants and equipment fits well to the size of the most utilized breeds. As differences, the masticatory movements are limited to vertical direction.

While adult human bone has a secondary osteonal structure, canine bone is found to have a mixed microstructure comprising predominantly secondary osteonal bone in the center of cortical bone, but with, what is called plexiform or lami-

nar bone in the areas adjacent to the periosteum and endosteum. It is formed more rapidly than secondary osteonal tissue, but provides greater mechanical support than woven bone. The mineral density of canine bone is higher than human bone and supports better compression than human [20].

About remodeling, we can find important differences. Usually humans have a lower rate of remodeling, but there is highly variable between bone sites. With regards to cortical bone, we can find an 18% of annual turnover rate in ribs and less than 1% in long bones, and varies with age, showing an age related decrease in bone remodeling activity [20]. In dogs, the bone regeneration rate runs faster than in humans (dog, 1.5–2.0 mm/day; human, 1.0–1.5 mm/day).

The dog presents a natural susceptibility to accumulate biofilm and suffer from periodontitis, being the model of choice for research in periodontal surgery [1].

8.3.4.4 Pigs
Swine constitutes one of the major animal species used in translational research, surgical models and procedural training and is increasingly being recruited as an alternative to the dog or monkey in biomedical research. Since the early 1990s has been established as a standard for studies on bone regeneration around dental implants or bone substitutes [1] because of their heterodont dentition with incisors and molars only slightly larger than humans [29].

Commercial breeds of pigs are difficult to handle, mainly for its large size, noisy and sometimes aggressive. The development of miniature breeds has made possible its use [20, 21]. Adult miniature pigs generally weight about 40 kg [1] and have a complete knowledge of the anatomy of the skull focused on the dental research [29].

Pigs are considered to be close representative models of human bone regeneration processes with regard to bone anatomy, morphology, healing capacity, remodeling, mineral density and concentration [21]. While having a denser trabecular network, the pigs have a lamellar bone structure and mineralization rate similar to humans [20]. In addition, pigs mimic the masti-

catory movements of humans. Its bone regeneration rate (1.2–1.5 mm/day) is comparable to that of humans (1.0–1.5 mm/day). However, recently has been observed that Göttingen Minipigs younger than 21 months have not ended the development of the bones of the jaw [29]. That fact should be taken into account and use animals older than 21 months of age.

8.3.4.5 Sheep/Goats
Since the 2000s, sheep and goats have increased its use as a model, probably related to the ethical issues and negative public perception of using companion animals for medical research [20]. The sheep are considered the ideal model for sinus lift elevation research [30].

Adult sheep and goat offer the advantage of possesses a body weight similar to adult humans. This makes them especially suitable for testing human orthopedic implants and prostheses [21]. Goats are reported to be more tolerant to ambient conditions than other species such as sheep [20].

Mineral composition is similar to human, except in young animals [20]. About bone structure, sheep have similar macrostructure to human [21], and the repair rate is comparable to humans [28]. However, the rate at which a bone graft is vascularized and converted into a vital trabecular structure is found to be faster in the goat, occurring at approximately 3 months in comparison to 8 months in humans [20]. Histologically is very different, having a significantly higher trabecular bone density and more strength compared to humans. Adult sheep have a plexiform bone structure comprising a combination of woven and lamellar bone within which vascular plexuses are sandwiched. Remodeling becomes more prevalent with age [20, 21]. It is important to be cautious because the age differences may make comparisons between studies difficult [22].

8.3.4.6 Nonhuman Primates
The nonhuman primate (NHP) is considered as the most accurate and reliable model in implant dentistry research. In particular, the baboon was a model exceptionally suitable for dental research [1].

In European Union (EU), the use of nonhuman primates for scientific purposes is governed by Directive 2010/63/EU on the protection of animals used for scientific purposes [31]. The directive sets the standards for the use of animals for scientific purposes across the EU. The use of nonhuman primates should be permitted only in those biomedical areas essential for the benefit of human beings, such a potentially life-threatening conditions or debilitating conditions. Testing the safety of medical devices in animals such as NHPs before they are introduced in human clinical trials is required for both ethical and legal reasons. However, very few medical devices need to be tested in NHPs. Researchers should provide an accurate description of the benefits, harms to animals and limitations of such research and be realistic about the potential outputs and impacts [32].

8.3.5   Ethical

Dental implant surgery in animals is a surgery that penetrates and exposes a body cavity, or produces substantial impairment of physical or physiological functioning, or involves extensive tissue dissection, or has the potential to produce a permanent handicap in an animal. Therefore, the highest awareness must be raised by all involved parties [1].

Evaluating surgical methods or implants in animals is a relatively recent concept in medicine. For centuries new surgical procedures or medical treatments were tried immediately in patients and, therefore, became a sacrifice to the goal of medical progress. From the eighteenth century, the use of animals was rapidly standardized, mainly for the study of anatomy and physiology. However, human experimentation followed until the mid-twentieth century. One of the causes was the modern warfare that created the needed of replacement or repair of major body parts [22]. After the Second World War, Nuremberg Code (1947) [33] and later the Declaration of Helsinki (1964) [34] established the bases for the use of animals and humans as experimental subjects. In the case of humans is firstly considered the "Voluntary Consent" as mandatory and consider that all experiment should be designed and based on the results of animal experimentation. In these years, many advances were made in the surgical disciplines and many devices were tested on animals, prolonging and improving the quality of life in many millions of patients.

In recent years, professional efficacy and general safety rules generated scientific and governmental efforts to formalize bench trials and animal testing as a prerequisite for the use of implantable materials and devices in patients. This made the development of regulations and reports to protect the animals and humans used as subjects of research.

All this regulations were developed, in the case of the animals, thanks to the efforts of people involved in the cause of the animal rights. The first steps were given in the own scientific community. These were the principles of replacement, refinement and reduction that were published in 1959 by Russell and Burch [35]. Later appeared a movement emerged among the people headed from Departments of Philosophy of the Universities in the 70s. The argument is based in that the boundary between human and animal is completely arbitrary and that the animals have to be treated with respect. This fact makes not ethically acceptable the investigation on animals in most cases. The most renowned authors of the movement were Peter Singer [36] and Tom Regan [37]. Its ideas were gaining widespread in society and the scientific community. The supporters have got that the governments changed the regulations for the use of animals in research to follow the principles of 3Rs.

8.3.6   Regulatory Affairs

Before any dental implantable device reaches the marketplace and thereafter must be evaluated to protect the public from unsafe and ineffective products, once done, regulatory agencies will approve the use before it can be marketed and used clinically.

Two major regulatory schemes dominate the global requirements: CE certification (EU) and FDA registration (510k, USA). Regulations of other countries are based on these and often have additional requirements [38]. The Food and Drug Administration (FDA) and the European Medicines Agency (EMA) are the national agencies that are in charge of the regulations on these categories.

US Federal agencies related to dental implants and biomaterials include FDA (Food and Drug Administration), NIST (National Institute of Standards and Technology) and NIDCR (National Institute of Dental and Craniofacial Research, Department of Health and Human Services, National Institute of Health).

In Europa, directive 93/42/EEC covers the placing on the market and putting into service medical devices, including dental materials and implants. In the United States, most devices follow the abbreviated premarket notification process, also known as 510k.

The time required to generate a new product and bring it to market was estimated between 2 and 10 years, depending on the novelty. Taking a totally new material to market can take a very long time, and costs may be seen as prohibitive.

In order to determine whether a newly developed implant or material conforms to the requirements of biocompatibility, osseointegration, mechanical stability, and safety, it must undergo rigorous testing both in vitro and in vivo [20]. Really these tests are considered as a pretranslational model because they lack clinical direct application. These preclinical studies may be conducted in laboratories at universities and in industry according to established procedures and standards. It should be noted that all tests must be conducted according to carefully constructed protocols that have to include appropriate controls [39].

The biocompatibility of a dental material can be evaluated following the guidance and methods described in the ISO 10993 series of documents (Biological evaluation of medical devices) and ISO 7405 (Dentistry–Preclinical evaluation of biocompatibility of medical devices used in dentistry–Test methods for dental materials).

Usually, the animals used are rodents or rabbits, suitable for an evaluation of biocompatibility. The guides cover all the aspects related to the procedure, preparation of samples, size of implants and maximum number of implants placed in each animal depending on the specie.

In addition, to evaluate the influence of functional stress to a dental implant system may be useful to work with the ISO/TS 22911 (Dentistry–Preclinical evaluation of dental implant systems–Animal test methods). According to ISO 22911, the selected animal species should meet the following criteria [1]:

- Oral hygiene can be maintained, either naturally or artificially.
- The jaws are of sufficient size to allow normal surgical access and to accommodate the dental implant system in its form intended for use in humans.
- The site where the dental implant system is to be placed should have opposing teeth.
- The animals should be skeletally mature if appropriate for its intended use.
- Animals having a nonherbivorous pattern of masticatory jaw movement are preferable.

If these recommendations are followed, then the only models suitable for the evaluation of ISO 22911 would be the adult swine, canines and nonhuman primates. These can mimic human physiology. If the functional loading is not evaluated, the adult sheep and goats may be an interesting option.

In resume, first we will evaluate our device in aspects as cytotoxicity and fatigue using physical methods and cellular cultures. If the device passes this test, we will evaluate the biocompatibility over animal species like rodents or rabbits. Finally may be necessary to evaluate the function in an oral environment.

8.3.7 Main Experimental Models

These studies are focused on resolving a clinical problem or on the knowledge of the biological facts that surround a pathologic process. We will

try to reflect the nature of the human disease in an animal or experimental model.

Over the years, it has been found that human systems resemble similar systems in various animal species. However, no species fulfills all requirements of an ideal model [23]. The animal model should have consistently reproducible features that simulate an analogous homologous condition where the biomaterial would be used in man.

The decision regarding which animal model to use for a specific study must come from an extensive review of the literature based on evidence-based preclinical and clinical data. This review must be related not only to the intended application of the new device to be implanted or technique developed but also to the physiology and comparative animal anatomy of the studied species. All this must refer to its final relation and applicability to the target species: humans [1, 22]. It has to be clearly stated that the intended study should not duplicate an already existing one [1].

In all cases (regulatory or experimental models), all protocols should adhere to ISO 10993-1 and to 3R international protocols. In the United States of America, the welfare and housing of animals is usually covered by a Federal Animal Protection Act. Researchers should use the "Guide for the care and use of Laboratory Animals" [40]. In European Union, all procedures are mandatory to follow the directive 2010/63/EU [31]. These rules may slightly vary between countries, usually being more restrictive in European Union, in terms of space available per animal. These guides include rules for:

- The replacement and reduction of the use of animals in procedures and the refinement of the breeding, accommodation care and use of animals in procedures.
- The origin, breeding, marking, care and accommodation and killing the animals.
- The operations of breeders, suppliers and users and the specific requirements for personnel.
- The evaluation and authorization of projects involving the use of animals in procedures.

- Minimum requirements in terms of housing dimensions, lighting, flooring, etc.

The main experimental models used in animal research in terms of implants therapy and applied into Translational Research are:

- Implant osseointegration process.
- Immediate implant placement.
- Peri-implantitis therapy.
- Bone regeneration around implants.

8.3.7.1 Implant Osseointegration Process

Implantology has evolved in the last 60 years. Clinicians placed dental implants according to standard protocols based on few histological studies and observational studies; however, the dynamics of early bone healing after implant placement were unknown. Berglundh et al. [41] established a beagle model that assessed early healing events after implant placements in healed sites. Basically, lower premolars were removed, and implants were placed after 3 months of healing. Sacrifice of animals was performed after different time points, showing that after 2 months of healing, the bone-to-implant contact was around 80%, and then the prosthetic loading could be delivered. This study translated to clinicians waiting shorter times for loading, challenging the classic loading protocols with longer healing times for loading. Thus, patients were acknowledged due to shorter times for function and esthetics. With this model, later on different implant surfaces could be tested in terms of osseointegration. In fact, it was shown that rougher implant surfaces osseointegrate faster and reach higher levels of bone-to-implant contact in comparison to smooth surfaces [42], so they shortened treatment times. With basic science proof, studies were conducted in humans in order to assess the impact of these new rough surfaces on early implant loading. In fact, experimental studies in humans corroborated the animal findings. Early and immediate loading could be provided to patients if a minimum level of primary stability was achieved. This is a clear example of experi-

mental animal research translated to experimental human research and consequently to daily practice.

8.3.7.2 Immediate Implant Placement

The animal model on immediate implant placement was developed by Araujo et al. [43] in order to study if an implant could prevent the normal bone resorption process that occurs after tooth extraction. This hypothesis comes from patient preferences for shorter treatment times on implantology as potentially improved esthetic outcomes. This experiment conducted primarily in large animal as beagle dogs consists in removing the lower premolars 3 and 4 after flap elevation and teeth hemisection. After that, the implants are placed into the sockets (mainly distal sockets), and flaps are repositioned in a nonsubmerged healing approach. After 6 months of healing, the animals are sacrificed, and buccolingual sections are prepared for histological analysis. This study showed that after that period of time, buccal bone is lost partially, thus, implants are not able to prevent bone loss. In fact, cohort studies in humans [19] showed that immediate implant placement might lead to buccal bone loss and soft tissue recession with unsightly outcomes. Thus these parallel and similar outcomes lead researchers to search for improved results with these kinds of procedures. Similar animal models were used to study the effect of flapless [44], immediate loading [45, 46], implant diameter [47], the use of grafting materials [48] or connective tissue grafts [49]. The most important factors of those investigations that led to the almost prevention of the alveolar bone resorption on immediate implant placements were placing a small diameter implant and filling the resulting buccal gap defect with a bone graft. In fact, a randomized clinical trial in humans showed that filling the buccal gap with a bone replacement graft reduced the horizontal bone resorptive changes occurring in the buccal bone after the immediate implantation in fresh extraction sockets [50]. Thus, it seems that animal models on immediate implant placement show good parallelism with experimental human stud-

ies and are therefore implemented in daily clinical practice.

8.3.7.3 Peri-Implantitis Therapy

The peri-implantitis animal model established by Lindhe & Berglundh in 1992 has been used extensively with small modifications in order to test therapeutic approaches to this disease [14]. Two main research fields have been performed. The first was to treat the infection surgically and disinfect the implant surface. The second model was developed more toward bone reconstruction techniques in infected peri-implant defects. Nowadays, it is an increasing problem with peri-implantitis lesions, and no high levels protocols of treatment have been advocated. Moreover, difficulties in designing good experimental human studies may lead to low level of evidence with this challenging problem. Recruitment of high number of patients is a tough task. Thus, clinicians rely on experimental studies performed so far. Since this is an infection problem, and daily mechanical plaque control is unusual in animals, no promising results are expected in animal research. The peri-implantitis model is good for testing different implant systems and/or surfaces on the behavior once peri-implantitis. In fact, it was clearly shown that rough surfaces speed up the progression of peri-implantitis with also inferiority treatment outcomes with respect to smooth surfaces [51–53]. Animal studies are urgently needed to test therapeutic disinfection approaches as reconstructive. Basically, the experimental model can be used to establish the disease and then surgical procedures in order to test antiseptic agents on the implant surfaces and bone grafting materials with or without membranes in order to assess the level of reosseointegration.

8.3.7.4 Bone Regeneration Around Implants

Implant placement can be a challenge in many circumstances due to alveolar bone loss. Clinicians try to augment this bone loss in width and/or height simultaneously or before implant placement. Principal Guided Bone Regeneration (GBR) was tested in the late 80s [54]. After that,

different animal models have been designed in order to assess bone regeneration in vertical and/or horizontal dimension. One of the first animal experiments developed was the capsule model. In this mainly, in the calvarial or the lower border of the mandible in rats, the Teflon capsule was placed to leave an empty space between the bone and the soft tissue. With this experiment, it was demonstrated that bone could grow extra skeletally. This is the principle of membrane applications, but this kind of trail cannot be tested in humans. The most common model applied in animal research for bone regeneration and applied also in humans is the dehiscence model. This imitates what occurs in clinical practice when after implant placement, a dehiscence bone defect appears at the coronal aspect of the implant. Controlled clinical studies showed GBR procedures may successfully promote bone formation in dehiscence and fenestrations around one and two-stage implants [55, 56]. The biological principles of this kind of defect have been tested in animals, mainly in dogs and mini pigs models, where dehiscence, contained and noncontained can also be regenerated in a different manner when facing different implant surfaces [57, 58]. This kind of implant defect can be acute; this is produced at the same time as implant placement, or chronic defects, where in early surgery, most of the buccal bone plate is removed in order to create later on a dehiscence defect that is chronic. The acute defects show self-regenerated areas after some healing time; thus, the dehiscence chronic defect is the most acceptable one and resembles what occurs in clinical situations.

8.3.8 Quality Control (GLP, GCP, GCLP)

The formal, regulatory, concept of "Good Laboratory Practice" (GLP) originated in the USA in the 1970s because of concerns about the validity of nonclinical safety data submitted to the Food and Drug Administration (FDA) in the context of New Drug Applications (NDA). The inspection of studies and test facilities revealed instances of inadequate planning and incompetent execution of studies, insufficient documentation of methods and results, and even cases of fraud. The GLP regulations provided the basis for assurance that reports on studies submitted to FDA would reflect faithfully and completely the experimental work carried out.

The GLP are ruled that all the assays have to follow to keep the quality and reproducibility of the procedures. They may evaluate a part of the procedure or the complete assay and are independent of the site where studies are performed. They apply to studies planned and conducted in a manufacturer's laboratory, at a contract or subcontract facility, or in a university or public sector laboratory.

On the international level, the Organization for Economic Cooperation and Development (OECD) assembled an expert group to formulate the first OECD Principles of GLP [59]. A number of OECD Member Countries have incorporated these Principles into their national legislation, notably the amendment of the European Union in Commission Directive 1999/11/EC to the Council Directive 87/18/EEC, where GLP had first been introduced formally into European legislation. Internationally, compliance with GLP is a prerequisite for the mutual acceptance of data.

The purpose of the Principles of Good Laboratory Practice is to promote the development of quality test data and provide a tool to ensure a sound approach to the management of laboratory studies, including conduct, reporting and archiving. The Principles may be considered as a set of standards for ensuring the quality, reliability and integrity of studies, the reporting of verifiable conclusions and the traceability of data. The Principles require institutions to assign roles and responsibilities to staff in order to ensure good operational management of each study and to focus on those aspects of study execution (planning, monitoring, recording, reporting and archiving) that are of special importance for the reconstruction of the whole study.

Depending on national legal situations, the GLP requirements for nonclinical laboratory studies conducted to evaluate drug safety, includ-

ing medical devices for human use, cover the following classes of studies:

- Single dose toxicity.
- Repeated dose toxicity (subacute and chronic).
- Reproductive toxicity (fertility, embryo-fetal toxicity and teratogenicity, peri-/postnatal toxicity).
- Mutagenic potential.
- Carcinogenic potential.
- Toxicokinetics (pharmacokinetic studies which provide systemic exposure data for the above studies).
- Pharmacodynamic studies designed to test the potential for adverse effects (Safety pharmacology).
- Local tolerance studies, including phototoxicity, irritation and sensitization studies, or testing for suspected addictive and/or withdrawal effects of drugs.

Good Clinical Practice (GCP) is an international ethical and scientific quality standard for designing, conducting, recording and reporting trials that involve the participation of human subjects. Compliance with this standard provides public assurance that the rights, safety and well-being of trial subjects are protected, consistent with the principles that have their origin in the Declaration of Helsinki [60].

Good Clinical Laboratory Practice (GCLP) applies those principles established under GLP for data generation used in regulatory submissions relevant to the analysis of samples from a clinical trial. At the same time, it ensures that the objectives of the GCP principles are carried out. This ensures the reliability and integrity of data generated by analytical laboratories [61].

8.3.9 Economic Aspects

It has to take into account that the procedures that involve any assay have a high cost, and that has three main facts. First, all procedures that involve the use of animals usually ended with the dead or serious malfunctions of them; second, the instal-

lations and handling of the animals are expensive because they have to cover strict conditions of temperature, humidity and isolation. Finally, complementary tests may be as expensive as animal experiments.

A laboratory evaluation of bone-tissue processing has unique characteristics, such as a more demanding fixation, the need for heavy-duty microtomes, saws for tissue sectioning and grinders for improve the final result. The existence of implants adds complexity to the process. Actually, histology and histomorphometry are the gold standards for evaluating the biocompatibility of a biomaterial or dental implant. In addition, it is a time-consuming technique with a cost more expensive than the decalcified preparation of samples.

Bone-tissue evaluation using microCT has been recently introduced in dentistry. This technique offers the evaluation of the bone–implant interface automatically. This reduces work times. However, the perpendicular position of the implant during the scanning has to be very accurate. In addition, some biomaterials are not easily detected because their radiographic density is very similar to the surrounding bone. The high cost of the equipment makes difficult its use as a routine technique, but it will become a standard in the future years.

Other methods used for the evaluation of samples involved in animal studies are microbiological (cultures and PCR assays), the detection of proteins and other substances involved in the mechanisms related to bone healing and inflammation.

8.3.10 Publications

In recent years, most of the indexed publications requires authors of preclinical animal studies submit with their manuscript the ARRIVE guidelines checklist [62]. These guidelines consist of a checklist of 20 items describing the minimum information that all scientific publications reporting research using animals should include, such as the number and specific characteristics of ani-

mals used, details of housing and husbandry; and the experimental, statistical and analytical methods. These guidelines were developed to maximize the output from research and should be enough information to allow the experiment to be repeated. Anesthesia practice and specific surgical protocol should be included in the publications to make sure that animal welfare is well established.

Editors should carefully evaluate whether these items were reported at an adequate level that allows the evaluation of bias without contacting the authors of the studies to get the "extra" information.

8.4   Management of the Translational Chain

8.4.1   Successive and/or Complimentary Investigations (In Vitro, In Vivo, Human)

The evaluation procedure of a new medical device starts by examining the device with isolated cells in vitro, and continues by implanting it into multi-cellular organism's in vivo [1]. It is clear, however, that in vivo models compared with in vitro studies provide distinct advantages in the understanding of the complex molecular, cellular and tissue reactions that occur in response to the device. This development is based on the understanding of the etiology of the disease, its progression and the general principles of tissue healing. However, knowledge in these areas does not necessarily allow conclusions about safety and efficacy of the device investigated. This situation is reflected by the regulatory approval agencies such as the European Medicines Agency, the US Food and Drug Administration, and other international bodies that demand a sequence of preclinical evaluations before clinical studies can be conducted. Based on these demands, preclinical studies pave the way for clinical studies that lead to the approvals for new medical devices [63].

Strategically positioned between materials science and clinical research, preclinical research offers a necessary field of expertise to investigate the device behavior in contact with living organisms (cell or animals) in order to assess and understand the host response. Preclinical studies, particularly in animals, constitute a prerequisite to accumulate knowledge under reproducible and standardized biological conditions, progressing to human trials at a larger stage. These evaluations end up, therefore, with long-term prospective and controlled-randomized clinical trials.

It is important, however, to keep in mind that the results, as they stand, obtained from an animal trial, although translational, do not allow any direct correlations and conclusions concerning human situations or treatments to be drawn [1, 64]. Nevertheless, well-designed animal studies, and consequently properly implemented animal/experimental reproducible models, will enhance translational prospects for the corresponding human surgical treatment of interest. Planning a preclinical study to test a new medical device requires decisions about animal species, the defect type, study endpoint and study duration. An animal study finds its strength if correlated in advance with other animal trails belonging to the same synergic program. This implies a progressive, complimentary, successive and incremental approach including studies with different animal and experimental models that complement each other and allow discrimination through comparison. The selection of preclinical models usually takes the phylogenetic tree into consideration; however this can be hampered by the differences in anatomy and healing characteristics between small and larger animals.

Very important is to distinguish between animal and experimental model, where animal model refers to a nonhuman living animal with an inherited, naturally acquired, or induced pathology process or lesion, and beyond the animal model itself, but part of it, is the experimental model. This is defined as the association of an animal type used for a particular surgical procedure that is to elicit a particular defect at a specific anatomical site [1].

Furthermore Sah and Ratcliffe [65] claimed that there is a substantial need for improved and standardized animal models for tissue engineering and regenerative medicine, and that animal model, especially large animal models, are critical to the preclinical step of translating research from bench to chair-side.

8.4.2   Speed and Efficiency (from the Bench to the Dental Chair)

Despite a major interest in translational research, development of new, effective medical interventions is difficult. Of 101 very promising claims of new discoveries with clear clinical potential that were made in major basic science journals between 1979 and 1983, only five resulted in interventions with licensed clinical used by 2003 and only had extensive clinical use [66]. In an analysis done by Contopoulos-Ioannidis and co-workers [67], they examined key milestones in the life cycle of translational research, for interventions claimed to be effective in at least one study that received over 1000 citations in the literature in 1990–2004, on the basis of the Web of Science. Out of 49 articles with more than 1000 citations, they selected 32 interventions for specific indications, and they could place the milestone of when their first highly cited clinical study was published. They considered this an important time point in the translational process and estimated how long ("translation lag") it had taken from the initial discovery of each intervention to reach that point. Highly cited status does not necessarily mean that these interventions continue to be considered as effective as proposed in the original highly cited papers. By the end of 2006, the effectiveness of 19 interventions had been replicated by other subsequent studies ($n = 14$) or had remained unchallenged ($n = 5$), whereas the other 13 had been either contradicted ($n = 5$) or found to have had initially stronger effects ($n = 8$) when larger or better controlled subsequent studies were performed. To place each discovery in time, they identified the year when the earliest journal publication on preparation, isolation, or synthesis appeared or the earli-

est patent was awarded (whichever occurred first). Overall, the median translation lag was 24 years (interquartile range, 14–44 years) between first description and earliest highly cited article. This was longer on average (median 44 vs. 17 years) for those interventions that were fully or partially "refuted" (contradicted or having initially stronger effects) than for nonrefuted ones (replicated or remaining unchallenged). Their analysis clearly documents the long length of time that passes between discovery and translation.

More recently McNamee and co-workers [68] addressed the long path from initiation of research on novel drug targets, to approval of drugs based on this research. They examined timelines of translational science for 138 drugs and biologicals approved by the FDA from 2010 to 2014 using an analytical model of technology maturation. Research on targets for 102 products exhibited a characteristic maturation pattern with exponential growth between statistically defined technology initiation (calculated as the date of maximum acceleration of publication activity, corresponding to the beginning of a period of exponential growth) and established points (calculated as the point where exponential growth ends, and there is maximum slowing of publication activity). The median initiation was 1974, with a median of 25 years to the established point, 28 years to first clinical trials, and 36 years to FDA approval No products were approved before the established point, and development timelines were significantly longer when the clinical trials began before this point (11.5 vs. 8.5 years, $p < 0.0005$). Technological maturation represents the longest stage of translation, and significantly impacts the efficiency of drug development. The evidence suggests that the inefficiency in the early stages may be limiting the pace of translational science. This work emphasizes the importance of considering the complete timeline of translational science from the initial insights or inventions that give rise to a new technology, through to the launch of new products based on these technologies. The observation that the median time from target technology initiation to first clinical entry was 3–4 times longer than

the timeline of clinical development, suggests that initiatives aimed at strategies for accelerating technology maturation could have a proportionally greater effect on the rate of translational science tan those aimed exclusively at clinical development. Thus, research aimed at understanding the dynamic nature of technology maturation and its relationship to successful product development should be a high priority. The present observations point to the critical importance of consistent funding for nascent stage technologies to ensure their continued, unimpeded maturation; and also, to the need for closer alignment between the basic and applied science that contributes to the maturity of technologies, and the strategic needs of the product development [68].

References

1. Dard M. Methods and interpretation of performance studies for dental implants. In: Boutrand J, editor. Biocompatibility and performance of medical devices. Hoboken: Wiley; 2012. p. 308–44.

2. Woolf SH. The meaning of translational research and why it matters. JAMA. 2008;299(2):211–3. https://doi.org/10.1001/jama.2007.26.

3. Fontanarosa PB, DeAngelis CD. Basic science and translational research in JAMA. JAMA. 2002;287(13):1728. https://doi.org/10.1001/jama.287.13.1728.

4. Sung NS, Crowley WF Jr, Genel M, Salber P, Sandy L, Sherwood LM, Johnson SB, Catanese V, Tilson H, Getz K, Larson EL, Scheinberg D, Reece EA, Slavkin H, Dobs A, Grebb J, Martinez RA, Korn A, Rimoin D. Central challenges facing the national clinical research enterprise. JAMA. 2003;289(10):1278–87. https://doi.org/10.1001/jama.289.10.1278.

5. Cohrs RJ, Martin T, Ghahramani P, Bidaut L, Higgins PJ, Shahzad A. Translational medicine definition by the European Society for Translational Medicine. New Horiz Transl Med. 2015;2(3):86–8. https://doi.org/10.1016/j.nhtm.2014.12.002.

6. Goldblatt EM, Lee W-H. From bench to bedside: the growing use of translational research in cáncer medicine. Am J Transl Res. 2010;2(1):1–18.

7. Chan JYH, Chang AYW, Chan SHH. New insights on brain stem death: from bedside to bench. Prog Neurobiol. 2005;77(6):396–425. https://doi.org/10.1016/j.pneurobio.2005.11.004.

8. U. S. Centers for Medicare @ Medicaid services. Patient Protection and Affordable Care Act (PPACA), Baltimore. 2010. https://www.healthcare.gov/glossary/patient-protection-and-affordable-care-act/. Accessed 3 Dec 2021.

9. Chiappelli F, Kasar VR, Hwang JM, Cajulis OS. Translational dentistry: the new frontier in dental practice. Transl Biomed. 2015;6:4. https://doi.org/10.21767/2172-0479.100034.

10. Chiappelli F. Fundamentals of evidence-based health care and translational science. Heidelberg: Springer; 2014. https://doi.org/10.1007/978-3-642-41857-0.

11. Institute of Medicine. Initial national priorities for comparative effectiveness research. Washington, DC: The National Academies Press; 2009. https://doi.org/10.17226/12648.

12. Chiappelli F. Methods, fallacies and mplications of comparative effectiveness research (CER) for healthcare in the 21st century. In: Chiappelli F, editor. Comparative Effectiveness Research (CER): new methods, challenges and health implications. New York: Nova Science; 2015.

13. Chiappelli F. Involving community dentists in evidence based dentistry: a hypothetical quest for the next frontier. Dent Hypotheses. 2015;6(4):127–8. https://doi.org/10.4103/2155-8213.170630.

14. Lindhe J, Berglundh T, Ericsson I, Liljenberg B, Marinello C. Experimental breakdown of peri-implant and periodontal tissues. A study in the beagle dog. Clin Oral Implants Res. 1992;3(1):9–16. https://doi.org/10.1034/j.1600-0501.1992.030102.x.

15. Derks J, Schaller D, Håkansson J, Wennstrom JL, Tomasi C, Berglundh T. Peri-implantitis – onset and pattern of progression. J Clin Periodontol. 2016;43:383–8. https://doi.org/10.1111/jcpe.12535.

16. Leonhardt Å, Berglundh T, Ericsson I, Dahlen G. Putative periodontal and teeth in pathogens on titanium implants and teeth in experimental gingivitis and periodontitis in beagle dogs. Clin Oral Implants Res. 1992;3(3):112–9. https://doi.org/10.1034/j.1600-0501.1992.030303.x.

17. Paolantonio M, Dolci M, Scarano A, d'Archivio D, di Placido G, Tumini V, Piattelli A. Immediate implantation in fresh extraction sockets. A controlled clinical and histological study in man. J Periodontol. 2001;72:1560–71. https://doi.org/10.1902/jop.2001.72.11.1560.

18. Araújo MG, Lindhe J. Dimensional ridge alterations following tooth extraction. An experimental study in the dog. J Clin Periodontol. 2005;32(2):212–8. https://doi.org/10.1111/j.1600-051X.2005.00642.x.

19. Chen S, Buser D. Esthetic outcomes following immediate and early implant placement in the anterior maxilla—a systematic review. Int J Oral Maxillofac Implants. 2014;29(Suppl):186–215. https://doi.org/10.11607/jomi.2014suppl.g3.3.

20. Pearce AI, Richards RG, Milz S, Schneider E, Pearce SG. Animal models for implant biomaterial research in bone: a review. Eur Cell Mater. 2007;13:1–10. https://doi.org/10.22203/ecm.v013a01.

21. Li Y, Chen SK, Li L, Qin L, Wang XL, Lai YX. Bone defect animal models for testing efficacy of bone sub-

stitute biomaterials. J Orthop Translat. 2015;3:95–104. https://doi.org/10.1016/j.jot.2015.05.002.

22. Mendenhall HV. Animal selection. In: von Recum AF, editor. Handbook of biomaterials evaluation: scientific, technical and clinical testing of implant materials. Philadelphia: Taylor & Francis; 1999. p. 475–9.

23. Babuska V, Moztarzadeh O, Kubikova T, Moztarzadeh A, Hrusak D, Tonar Z. Evaluating the osseointegration of nanostructured titanium implants in animal models: current experimental methods and perspectives (review). Biointerphases. 2016;11(3):030801. https://doi.org/10.1116/1.4958793.

24. Katranji A, Misch K, Wang H. Cortical bone thickness in dentate and edentulous human cadavers. J Periodontol. 2007;78(5):874–8. https://doi.org/10.1902/jop.2007.060342.

25. Wang L, Wu Y, Perez KC, Hyman S, Brunski JB, Tulu U, Bao C, Salmon B, Helms JA. Effects of condensation on peri-implant bone density and remodeling. J Dent Res. 2017;96(4):413–20. https://doi.org/10.1177/0022034516683932.

26. Di Domenico M, D'apuzzo F, Feola A, Cito L, Monsurrò A, Pierantoni GM, Berrino L, De Rosa A, Polimeni A, Perillo L. Cytokines and VEGF induction in orthodontic movement in animal models. J Biomed Biotechnol. 2012;2012:201689. https://doi.org/10.1155/2012/201689.

27. Liu W, Dan X, Wang T, Lu WW, Pan H. A bone-implant interaction mouse model for evaluating molecular mechanism of biomaterials/bone interaction. Tissue Eng Part C Methods. 2016;22(11):1018–27. https://doi.org/10.1089/ten.TEC.2016.0250.

28. Wancket LM. Animal models for evaluation of bone implants and devices: comparative bone structure and common model uses. Vet Pathol. 2015;52(5):842–50. https://doi.org/10.1177/0300985815593124.

29. Corte GM, Plendl J, Hünigen H, Richardson KC, Gemeinhardt O, Niehues SM. Refining experimental dental implant testing in the Göttingen Minipig using 3D computed tomography. A morphometric study of the mandibular canal. PLoS One. 2017;12(9):e0184889. https://doi.org/10.1371/journal.pone.0184889.

30. Valbonetti L, Berardinelli P, Scarano A, Piatelli A, Mattioli M, Barboni B, Podaliri M, Muttini A. Translational value of sheep as animal model to study sinus augmentation. J Craniofac Surg. 2015;26:737–40. https://doi.org/10.1097/SCS.0000000000001785.

31. European Union. Directive 2010/63/EU of the European Parliament and of the Council on 22 September 2010 on the protection of animals used for scientific purposes. 2010. http://data.europa.eu/eli/dir/2010/63/oj. Accessed 5 Dec 2021.

32. SCHEER (Scientific Committee on Health Environmental and Emerging Risks). Final opinion on the need for non-human primates in biomedical research, production and testing of products and devices. 2017. http://ec.europa.eu/environment/chemicals/lab_animals/pdf/Scheer_may2017.pdf.

33. Nuremberg Code. U.S. Department of Health & Human Services. https://history.nih.gov/research/downloads/nuremberg.pdf.

34. World Medical Association. Declaration of Helsinki. Ethical principles for medical research involving human subjects. 1964. https://www.wma.net/policies-post/wma-declaration-of-helsinki-ethical-principles-for-medical-research-involving-human-subjects/. Accessed 3 Dec 2021.

35. Tannenbaum J, Bennett BT. Russell and Burch's then and now: the need for clarify in definition and purpose. J Am Assoc Lab Anim Sci. 2015;54(2):120–32.

36. Singer P. Animal liberation: a new ethics for our treatment of animals. New York: Harper Collins; 1975.

37. Regan T. The case for animal rights. California: University of California Press; 1983.

38. Pitts NB, Drummond J, Guggenberger R, Ferrillo P, Johnston S. Incorporating new materials and techniques into clinical practice. Adv Dent Res. 2013;25(1):33–40. https://doi.org/10.1177/0022034513502209.

39. Dee KC, Puleo DA, Bizios R. An introduction to tissue-biomaterial interactions. Cambridge: Woodhead Publishers; 2002.

40. National Research Council. Guide for the care and use of laboratory animals. The National Academies Press. 2011. http://nap.edu/12910. Accessed 5 Dec 2021.

41. Berglundh T, Abrahamsson I, Lang NP, Lindhe J. De novo alveolar bone formation adjacent to endosseous implants. A model study in the dog. Clin Oral Implants Res. 2003;14:251–62. https://doi.org/10.1034/j.1600-0501.2003.00972.x.

42. Abrahamsson I, Berglundh T, Linder E, Lang NP, Lindhe J. Early bone formation adjacent to rough and turned endosseous implant surfaces. An experimental study in the dog. Clin Oral Implants Res. 2004;15:381–92. https://doi.org/10.1111/j.1600-0501.2004.01082.x.

43. Araujo MG, Sukekava F, Wennström JL, Lindhe J. Ridge alterations following implant placement in fresh extraction sockets: an experimental study in the dog. J Clin Periodontol. 2005;32:645–52. https://doi.org/10.1111/j.1600-051X.2005.00726.x.

44. Blanco J, Nuñez V, Aracil L, Muñoz F, Ramos I. Ridge alterations following immediate implant placement in the dog: flap versus flapless surgery. J Clin Periodontol. 2008;35:640–8. https://doi.org/10.1111/j.1600-051X.2008.01237.x.

45. Blanco J, Liñares A, Villaverde G, Perez J, Muñoz F. Flapless immediate implant placement with or without immediate loading. A histomorphometric study in beagle dog. J Clin Periodontol. 2010;37:937–42. https://doi.org/10.1111/j.1600-051X.2010.01608.x.

46. Blanco J, Liñares A, Perez J, Muñoz F. Ridge alterations following flapless immediate implant placement with or without immediate loading. Part II: a histometric study in the Beagle dog. J Clin Periodontol. 2011;38:762–70. https://doi.org/10.1111/j.1600-051X.2011.01747.x.

47. Caneva M, Salata LA, de Souza SS, Bressan E, Botticelli D, Lang NP. Hard tissue formation adjacent to

implants of various size and configuration immediately placed into extraction sockets: an experimental study in dogs. Clin Oral Implants Res. 2010;21:885–90. https://doi.org/10.1111/j.1600-0501.2010.01931.x.

48. Araújo MG, Linder E, Lindhe J. Bio-Osss collagen in the buccal gap at immediate implants: a 6-month study in the dog. Clin Oral Implants Res. 2011;22:1–8. https://doi.org/10.1111/j.1600-0501.2010.01920.x.

49. Caneva M, Botticelli D, Vigano P, Morelli F, Rea M, Lang NP. Connective tissue grafts in conjunction with implants installed immediately into extraction sockets. An experimental study in dogs. Clin Oral Implants Res. 2013;24:50–6. https://doi.org/10.1111/j.1600-0501.2012.02450.x.

50. Sanz M, Lindhe J, Alcaraz J, Sanz-Sanchez I, Cecchinato D. The effect of placing a bone replacement graft in the gap at immediately placed implants: a randomized clinical trial. Clin Oral Implants Res. 2017;28:902–10. https://doi.org/10.1111/clr.12896.

51. Albouy J-P, Abrahamsson I, Persson LG, Berglundh T. Spontaneous progression of peri-implantitis at different types of implants. An experimental study in dogs. I: clinical and radiographic observations. Clin Oral Implants Res. 2008;19:997–1002. https://doi.org/10.1111/j.1600-0501.2008.01589.x.

52. Albouy J-P, Abrahamsson I, Persson LG, Berglundh T. Implant surface characteristics influence the outcome of treatment of peri-implantitis: an experimental study in dogs. J Clin Periodontol. 2011;38:58–64. https://doi.org/10.1111/j.1600-051X.2010.01631.x.

53. Albouy J-P, Abrahamsson I, Berglundh T. Spontaneous progression of experimental peri-implantitis at implants with different surface characteristics. An experimental study in dogs. J Clin Periodontol. 2012;39:182–7. https://doi.org/10.1111/j.1600-051X.2011.01820.x.

54. Dahlin C, Linde A, Gottlow J, Nyman S. Healing of bone defects by guided tissue regeneration. Plast Reconstr Surg. 1988;81(5):672–6. https://doi.org/10.1097/00006534-198805000-00004.

55. Mayfield L, Skoglund A, Nobréus N, Attström R. Clinical and radiographic evaluation, following delivery of fixed reconstructions, at GBR treated titanium fixtures. Clin Oral Implants Res. 1998;9:292–302. https://doi.org/10.1034/j.1600-0501.1998.090502.x.

56. Sanz-Sánchez I, Ortiz-Vigón A, Sanz-Martín I, Figuero E, Sanz M. Effectiveness of lateral bone augmentation on the alveolar crest dimension: a systematic review and meta-analysis. J Dent Res. 2015;9(Suppl):128S–42S. https://doi.org/10.1177/0022034515594780.

57. Schwarz F, Sager M, Kadelka I, Ferrari D, Becker J. Influence of titanium implant surface characteristics on bone regeneration in dehiscence-type defects: an experimental study in dogs. J Clin Periodontol. 2010;37(5):466–73. https://doi.org/10.1111/j.1600-051X.2010.01533.x.

58. Zambon R, Mardas N, Horvath A, Petrie A, Dard M, Donos N. The effect of loading in regenerated bone in dehiscence defects following a combined approach of bone grafting and GBR. Clin Oral Implants Res. 2012;23:591–601. https://doi.org/10.1111/j.1600-0501.2011.02279.x.

59. WHO (World Health Organization). Handbook: good laboratory practice (GLP). 2009. https://www.who.int/tdr/publications/training-guideline-publications/good-laboratory-practice-handbook/en. Accessed 3 Dec 2021.

60. European Medicines Agency. ICH harmonised guideline integrated addendum to ICH E6(R2): guideline for good clinical practice. 2021. https://www.ema.europa.eu/en/ich-e6-r2-good-clinical-practice. Accessed 3 Dec 2021.

61. WHO (World Health Organization). Good clinical laboratory practice (GCLP). 2009. https://www.who.int/tdr/publications/documents/gclp-web.pdf. Accessed 3 Dec 2021.

62. Kilkenny C, Browne WJ, Cuthill IC, Emerson M, Altman DG. Improving bioscience research reporting: the ARRIVE guidelines for reporting animal research. PLoS Biol. 2010;8(6):e1000412. https://doi.org/10.1371/journal.pbio.1000412.

63. Pellegrini G, Seol YJ, Gruber R, Giannobile WV. Pre-clinical models for oral and periodontal reconstructive therapies. J Dent Res. 2009;88(12):1065–76. https://doi.org/10.1177/0022034509349748.

64. Perel P, Roberts I, Sena E, Wheble P, Briscoe C, Sandercock P, Macleod M, Mignini LE, Jayaram P, Khan KS. Comparison of treatment effects between animal experiments and clinical trials: systematic review. BMJ. 2007;334(7586):197. https://doi.org/10.1136/bmj.39048.407928.BE.

65. Sah R, Ratcliffe A. Translational models for musculo-skeletal tissue engineering and regenerative medicine. Tissue Eng Part B Rev. 2010;16(1):1–3. https://doi.org/10.1089/ten.TEB.2009.0726.

66. Contopoulos-Ioannidis DG, Ntzani E, Ioannidis JP. Translation of highly promising basic science. Research into clinical applications. Am J Med. 2003;114(6):477–84. https://doi.org/10.1016/s0002-9343(03)00013-5.

67. Contopoulos-Ioannidis DG, Alexiou GA, Gouvias TC, Ioannidis JP. Medicine. Life cycle of translational research for medical interventions. Science. 2008;321(5894):1298–9. https://doi.org/10.1126/science.1160622.

68. McNamee LM, Walsh MJ, Ledley FD. Timelines of translational science: From technology initiation to FDA approval. PLoS One. 2017;12(5):e0177371. https://doi.org/10.1371/journal.pone.0177371.

Biomechanics of the Radicular Component of Endosteal Implants

9

E. A. Bonfante, D. Bordin, E. T. P. Bergamo,
I. S. Ramalho, S. Soares, and P. G. Coelho

9.1 Introduction

Variables in implant reconstructions often involve so many combinations of implant materials and dimensions, abutment designs, and restorative options that are designing sound randomized controlled clinical trials (RCTs) to answer specific questions regarding osseointegration and survival of restored implants represents a significant challenge due to the need of large population samples for statistical significance and longer follow-ups than commonly presented. In addition, if one considers the prolificacy of the dental implant literature, it has been shown that 63% of published clinical trials in this field have been found as having a risk of bias for not presenting funding source, and of major concern is that industry sponsored trials do present significantly lower (4.8 times) annual failure probability when compared with nonindustry sponsored trials [1]. Although very unfortunate, such outcome was expected some point after the acknowledgment, over 20 years ago, of a shift in implant dentistry from a science-oriented field to commodity development [2]. With the increasing number of competing dental implant companies, some traded in the stock exchange, and dental implant/restorative market anticipated to reach U$17 billion in 2025 [3], efforts have been directed not only in the standardization of the success criteria in implant dentistry [4] but also in comprehensively reporting the results from RCTs [5]. Lastly, the fact that most clinical studies in the dental implant literature commonly report simple success rates (usually upwards of 95%), instead of cumulative survival rates, becomes alarming given that such rates are inflated and not truly representative of the real outcomes [6].

As expectations that trial design in implant dentistry will continue to develop, as it did in medicine, with challenges for improvement already presented elsewhere [7], well-designed preclinical assessments of dental implants become paramount when more rapid responses are demanded. However, preclinical studies from virtual to in vitro and in vivo simulations also demand robust effort in designing and selecting reproducible models. A Nature's survey recently alarmed that 70% of experiments, in general,

E. A. Bonfante (✉) · E. T. P. Bergamo
I. S. Ramalho · S. Soares
Department of Prosthodontics and Periodontology, Bauru School of Dentistry, University of São Paulo, Bauru, SP, Brazil

D. Bordin
Department of Periodontology and Implant Dentistry, University of Guarulhos, Guarulhos, SP, Brazil

University São Judas Tadeus, Sao Paulo, SP, Brazil

P. G. Coelho
Division of Plastic Surgery, DeWitt Daughtry Family Department of Surgery, University of Miami Miller School of Medicine, Miami, FL, USA

Department of Biochemistry and Molecular Biology, University of Miami, Miami, FL, USA

could not be reproduced, leading to what is currently called as "reproducibility crisis" [8]. What the majority of respondents believed to be the solution for improved reproducibility included: (1) more robust experimental design, (2) better statistics and (3) better mentorship. Therefore, in implant dentistry, it is important that besides these three factors, research groups create an informed database with robust and standardized methodology so accurate and sound comparisons can be performed for system's improvement to eventually benefit the patient population.

Interestingly, whereas commercially pure titanium and its alloys as well as ceramic dental implants have all been shown to osseointegrate, the interplay between dental implant bulk design and related surgical instrumentation dimension (hardware) will dictate healing pathways, eventually altering bone remodeling and long-term mechanical properties [9]. However, the methodology used to assess variations from macro to nano features in the implantable device as well as the surgical technique, can seriously overlook outcomes and underestimate short and long-term results.

The in vitro biomechanical assessment of implant systems has endeavored to serve as a preclinical assessment of their performance in some methodologies. As previously suggested, if research data from standardized testing is gathered under the same methodological approach, then bona fide comparisons between restored implants can be made. In the dental implant scenario, once restored, the implant system becomes a complex comprised by prostheses and abutments that can be of a variety of materials and configurations where different combinations eventually affect performance [10]. Within this context, biomechanical evaluations should ideally be made in systems that simulate the final restored dental implant. Since titanium and its alloy failures are mainly derived from fatigue [11], this chapter will concentrate on such methods. Also, considering that norms (e.g., ISO 14801) serve in general as invaluable tools for industry for regulatory and even marketing purposes, eventually increasing population welfare,

its use to move forward original cutting-edge research may be complementary rather than essential.

9.2 In Vitro Mechanical Testing Methods

Mechanical testing should be designed either to characterize material's properties or to simulate the performance of implants, prostheses, and prosthetic components, where clinically relevant failures can be reproduced [12]. Therefore, it is important that the testing equipment simulates mandibular movements and that applied load ranges are compatible with the ones reported in the literature in different regions of the mouth [13]. During jaw closure two phases are observed in the early chewing stages prior to swallowing: (1) Fast closure until teeth come into contact with the food bolus; and (2) Slow closure phase where resistance is provided by the food, increasing the masticatory muscle activity according to bolus consistency [14, 15]. A masticatory cycle takes approximately 1 s (1 Hz) [16]. Although maximum voluntary bite force varies depending on type of prosthesis, antagonist, gender, age, and location in the mouth [13], its value may predict worst-case loading conditions.

The most commonly used mechanical in vitro testing methods and analysis are described in the following sections.

9.2.1 Single Load to Failure (SLF)

In the single-load-to-failure method, a sample failure is analyzed by applying increasing static load until fracture. A force/displacement curve is acquired for an individual specimen and the maximum load at failure is reported. Controlled specimen preparation and geometry may lead to SLF testing where invaluable information can be gathered for understanding of materials properties such as strength and fracture toughness (e.g., ISO 6872, ASTM C 1161 - 02). However, a robust body of dental literature has used the SLF test,

where the calculation of surface contact stresses at failure is commonly not presented. Considering that "strength" is defined as the stress at which failure occurs, the reported load at failure data is seldom related to the stresses resulting in the failure itself [17]. Moreover, restorations are subjected to repeated lower intensity loads during function that lead to cumulative damage, and not to a ramping force until fracture, usually resulting in higher failure values in SLF compared to fatigue [18], which should not be correlated with bite forces available in the literature for survival predictions. In function, forces could vary from 150 to 800N [19]. Most critical is that SLF testing does not simulate clinical failures [18].

One important use of SLF is as a tool for initial screening and designing of fatigue tests, as subsequently discussed. However, its use solely to report load at failure data is highly discouraged since almost 20 years [17, 20].

9.2.2 Initial Concepts on Fatigue

Fatigue is the process of progressive localized permanent structural change occurring in a material subjected to conditions that produce fluctuating stresses and strains at some point or points and that may culminate in cracks or complete fracture after a sufficient number of fluctuations [21]. The mode of stress or strain may be static (remains constant with time), dynamic (applied at some constant rate), or cyclic (stress or strain magnitude varying with time) [22]. Considering that drawing stress cycle diagrams (*S-N*, Wöhler curves) for a large number of samples to ensure safety at use level may be exceedingly time-consuming, alternative methods have been developed, as discussed in this chapter.

The flaws present in implants and prostheses materials act as stress raisers with far-field stresses concentrated, at a microscopic scale, near the edge of each flaw [23]. A certain stress intensity factor is associated with each flaw and is dependent on the far field stresses and the degree of stress concentration:

$$K_I = Y\sigma\sqrt{a} \qquad (9.1)$$

where K_I is the stress intensity factor (MPa m$^{1/2}$), Y is the stress intensity shape factor related to the location and shape of the crack (unitless), σ is the far-field stress (MPa), and a is the flaw size (μm). The implant-prosthesis complex will fracture when the stress intensity factor surpasses a critical level. The inherent property of materials to resist propagation of an existing crack or flaw is known as fracture toughness [24].

Given that fractures of the implant-prostheses complex may be expected at some point [25], demanding maintenance, it becomes evident that the strength and reliability of restored systems degrade over time after being installed. Fatigue failure usually consists of crack initiation, growth, and ultimate failure. This process is known as *subcritical crack growth* (SCG) where flaws grow over time under the presence of a stress intensity factor below the critical level until both flaw size and stress level result in a stress intensity factor that exceeds the fracture toughness of the material. Two subcritical crack growth mechanisms, namely stress corrosion and cyclic fatigue, may run simultaneously or individually [26, 27]. In most biomedical ceramics, SCG has been attributed to stress corrosion at the crack tip, or at any preexisting defect in the ceramic, associated with cyclic fatigue. Stresses at the crack tip and the presence of water or body fluid molecules, temperature, and other extraneous variables (reducing surface energy at the crack tip), results in the rupture of the metallic oxide bonds of the material, with the subsequent formation of hydroxides [28–30]. Thus, as a consequence of stress corrosion, a defect may reach its critical size and result in fast fracture [31]. Specific features during slow crack growth have been comprehensively presented in a crack velocity (*V*) versus K_I diagram describing three stages, each with a distinct power law that can fit the speed at which a crack propagates when stressed [28]. In region I, the environmental species react with the ceramic bonds at the crack tip leading to stable crack propagation. Region II, which is insensitive to applied stress, is associated with increasing crack velocities and environment species being unable to reach the crack front-tip. Region III is associated with fast fracture and then with K_{IC}

[28]. Since cyclic fatigue is a mechanical phenomenon that refers to load oscillation leading to crack propagation [32], it is paramount that mechanical testing also simulates the environment condition (water or artificial saliva) to more accurately provide information regarding slow crack growth and fatigue life or limit.

Cyclic fatigue predominates in alpha titanium (Ti) alloys grades 1 and 2 (ASTM F67), whereas variations in Ti composition, such as the increased oxygen interstitial weight concentration, increases the susceptibility of grade 4 to stress corrosion cracking in aqueous media [33–35]. Failure analysis of human retrieved samples corroborate the main role of fatigue in Ti and its alloys [36], as subsequently discussed. When subjected to cyclic fatigue, the fluctuating stress intensity factor degrades the fracture resistance of the material in front of or in the wake of the crack tip [37]. Therefore, strength degradation in metals is elicited from cold working leading to increased brittleness at the atomic scale, and the velocity of slow crack growth caused by cyclic fatigue is determined by the crack shape and size, range of stress fluctuation, ratio of minimum to maximum stress and frequency of cycling [38, 39]. Commercially pure titanium implants, for instance, have a higher probability of fracture when fatigued at 2 Hz compared to 30 Hz for up to 10^6 cycles [40]. According to the ISO-14801, testing frequency should be no more than 15 Hz, which corroborates with literature findings that a loading frequency of up to 15 Hz does not influence the number of cycles to failure relative to 2 Hz [39]. A detailed characterization of the effect of cycling frequency in the lifetime and failure of existing and upcoming implant materials is warranted to support fatigue testing parameters.

Efforts to understand failures through analyses of human-retrieved titanium fractured samples are modest but increasing. Analysis of fractured retrieved commercially pure Ti and Ti-6Al-4V dental implants unequivocally showed that fatigue is the main failure mechanism leading to failure where corrosion processes are likely involved in the crack formation and/or propagation process [41]. A large retrieval study of implants removed due to peri-implantitis showed that 62% of them presented several flaws in the thread and neck region, evidenced by the presence of full cracks (over 0.5 mm crack extension) and crack-like defects (25–100 μm length) [36]. Those cracks predominated in commercially pure titanium grade 2 compared to Ti-6Al-4V implants and have been reported to be the embryos for fatigue crack nucleation that eventually leads to implant fracture [41].

Regarding the role of corrosion and fatigue on the failure of Ti dental implants, it has been shown that Ti-6Al-4V implants had fatigue performance reduced when tested in artificial saliva compared to testing in a dry environment. However, even after testing up to five million cycles, there was no evidence of corrosion in the fractographic analysis which suggested that the shorter fatigue life was likely due to crack growth acceleration due to the saliva-like environment acting at the crack tip [42]. Therefore, although ISO 14801:2016 indicates testing in water or normal saline only when the chosen frequency is ≤2 Hz and cycles total two million cycles, testing in a water or saliva-like environment may be encouraged to simulate the clinical environment and accelerate failures since a wet environment has shown to reduce the fatigue strength of different metal alloys [43].

Each fatigue method presented herein provides or hinders certain deliverables and should be selected according to the study aims and capabilities of the fatigue armamentarium. When testing dental implants as restored single-units, calculation of the bending moment (M) is required, as follows:

$$M = y \times F \tag{9.2}$$

where y is the moment arm, defined as $l \times \sin \theta$ (for most dental setting tests $\theta = 30°$), where l is the distance from the center of the crown to the clamping plane. Since force is expressed in N, bending moment is typically reported in $N \cdot mm$. For the determination of stress leading to failure (MPa), subsequent calculation includes:

$$\sigma_{Stress} = \frac{My}{I} \tag{9.3}$$

where M represents the bending moment, y is the perpendicular distance from the center of the

inertia moment and I is the area moment of inertia, described by the area of the abutment cross-section as:

$$I_{circular} = \frac{\pi \cdot d^4}{64} \quad \text{or} \quad I_{cylindrical} = \frac{\pi \cdot (d_o - d_i)^4}{64}$$

(9.4)

where d is the circle diameter, d_o is the outside diameter, and d_i is the inside diameter.

Data analysis of fatigue methods should acknowledge that variation in lifetime cannot usually be properly modeled by a Gaussian distribution. It is the largest flaw, not the average flaw, that commands the lifetime of a restorative system. The lifetime for a given stress state can be predicted when the velocity of crack growth, the initial size of the crack, and the size of the crack which surpasses the fracture toughness are known [38]. Therefore, considering that the distribution of preexisting flaws of different sizes within any implant/restorative system vary randomly, results may vary proportionally.

9.2.2.1 Fatigue Life (Constant Stress)

Fatigue life is the number of cycles a sample can resist, prior to failure, when cycled between fixed upper and lower limits [44]. Cycles can be virtually infinite for samples to fail under constant stress fatigue when the selected load is low or when the material presents low susceptibility to subcritical crack growth and/or a high-stress intensity factor threshold (K_{I0}), which represents the stress level at which cracks start to grow stably. Ceramic prostheses with high K_{I0} present higher reliability and longer service life [45]. Conversely, a reduction in fatigue life has previously been associated with high-stress ratios [46]. Hence, if the selected load be way above K_{I0}, early failures could be misinterpreted as materials egregious flaws. No consensus exists on the ideal parameters for stress amplitude and frequency.

The use of 1.2 million cycles to represent 5 years of service (continuous 50N load) has been suggested [47]. In contrast, 500,000 cycles have been credited to simulate 10 years [48]. In another study, 1 year was simulated by 800,000 cycles [49]. Another example adding to the contradiction is the empirical determination of 1,000,000 cycles (at 800N) to represent 1 year of bruxism [20]. One million cycles at 1 Hz has been roughly estimated to correspond to 1 year of function based on the assumption that subjects complete three 15-min meals resulting in 2700 chews per day [50]. Whereas correlations between cycles and years of service have been attempted, such simplistic mathematical translation cannot be supported by current evidence of differences in chewing paces across individuals [51], and the complex nature of oral function.

One shortcoming of fatigue life is the high sample size and associated budget increase, and the unforeseen time to failure of the sample that can overextend the study deadline. To overcome this, research groups have used constant stress fatigue to a predetermined amount of cycles and then subjected samples to SLF testing [52, 53]. This approach is highly discouraged considering the limitations discussed for SLF testing, and that fatigue damage information is lost.

Unless several machineries are available, fatigue life testing is seldom time and cost-effective. Complexity levels are low, and analysis can be made by either Kaplan—Meier [54] or Weibull statistics [55, 56].

9.2.2.2 Fatigue Limit/Resistance

Fatigue limit or fatigue resistance is the value of stress that a sample can survive for a given number of stress cycles [57]. In the staircase method, samples are tested sequentially to determine the median value of a fatigue limit. Each specimen is tested for a determined lifetime corresponding to the infinite life. The number of cycles should be guided by previous experience and based on the expected number of cycles to which the component is likely to be subjected during its intended life [58, 59]. In dentistry, 10^6 cycles have been empirically used, which corresponds to 1 year of clinical use [50], as well as 1.2 million cycles have been suggested to correspond to 5 years which corroborates the lack of consensus [60].

In the staircase, if the specimen fails prior to the preset unlimited endurance, the next specimen will be tested at a predetermined decrement

in stress level. If the specimen does not fail within this life of interest, the subsequent sample will be tested at an equal amount of the predetermined stress level that will be incremented. Therefore, specimens are tested one at a time, each test dependent on the previous result, with the stress level being increased or decreased by selected increments (1–2 standard deviations). Without pretests, 20 samples are deemed necessary for the evaluation of a fracture probability of 50%, 40 specimens for the probabilities of 10 and 90%, and 50 specimens for the probabilities of 1 and 99% [61].

Data reduction techniques, such as the Dixon and Mood method or that of Zhang and Kececioglu, must be applied to determine the statistical distribution of the results. The Dixon and Mood method is based on the maximum likelihood estimation (MLE) and calculates the mean and standard deviation of a fatigue limit that follows a normal distribution. This approach considers either only the failures or only the survivals to determine the statistical properties and is dependent on the least frequent event. To consider only half of the tested samples for statistical evaluation implies in low efficiency, reducing the economic feasibility of the technique. The Zhang and Kececioglu method considers the suspended items and the MLE for the data. It is usually applied if the Dixon and Mood method is not indicated; that is, when the fatigue limit is not normal, the stress increments are not identical, and the stress increment is greater than twice the standard deviation [58]. Improved statistical assessments have been suggested [62] and the use of lifetime distributions (e.g., Weibull) is possible when proper sample size and failure to survival ratio is adequately observed throughout testing. Also, an alternative for better estimation of the confidence bounds based on binomial probability has been presented, and conclusion was that the staircase test cannot be used to estimate the scatter in fatigue strength and should not be used to develop lower bound fatigue threshold estimates [63].

Although the staircase is a straightforward, "up-and-down" sequential technique for estimat-

ing the fatigue resistance, the test is not conducted in a wide force range or to extreme stress values, which could mask the performance under worst scenarios. In addition, the number of cycles to determine the failure or survival of each specimen is preset, avoiding long-term performance simulations.

For certification purposes, ISO 14801, a standardized dental implant fatigue testing protocol, was developed [64]. It was not designed to predict long-term clinical performance. Samples are tested in a 30° inclination and under worst-case scenarios. Testing is limited to wet at 2 Hz until failure or two million cycles, which would take virtually 12 days for each runout. Although the standard allows testing up to 15 Hz until failure or five million cycles for dry conditions, the dry environment does not simulate physiological conditions. Moreover, failures beyond one million cycles followed a different failure probability distribution, indicating a different failure mechanism [40]. The standard states that "a multi-part endosseous dental implant shall be tested as assembled according to its intended use." However, it recommends a hemispherical device to simulate a crown, which is not close in anatomy to dental prostheses. The ISO 14801:2007(E) is a valid certification tool for industry and continues under development as it has been created under limited experimental data [65].

9.2.2.3 Step-Stress Accelerated Life Testing (SSALT)

In accelerated life fatigue testing, the engineer extrapolates a product's failure behavior at normal conditions from life data obtained at accelerated stress levels. Since materials fail more quickly at higher stress levels, this strategy allows the engineer to obtain reliability information (e.g., mean life, probability of failure at a specific time, etc.) in a shorter time. These tests require preventing any modification of the damaging mode from the low level to the higher levels chosen.

In SSALT, a specimen is subjected to successively higher levels of stress. First, each specimen

is submitted to constant stress during a predetermined length of time. The stress on this specimen is then increased step-by-step until its failure or suspension. SSALT has been widely applied to characterize a plethora of materials, because industrial competition requires speedy testing and designing of mechanical components. Similarly, it has been used for dental biomaterials, such as ceramic and composite restorations, and implants.

Previous work using SSALT in dentistry has utilized SLF as the first step to determine step-stress accelerated life-testing profiles (usually three: mild, moderate, and aggressive) [66]. The use of at least three profiles for this type of testing reflects the need to distribute failure across different step loads and allows better prediction statistics, narrowing confidence intervals. Mild, moderate, and aggressive refer to the increasingly stepwise rapidity with which a specimen is fatigued to reach a certain level of load meaning that specimens assigned to a mild profile will be cycled longer to reach the same load of a specimen assigned to either a moderate or aggressive profile. These profiles usually begin at a load that is approximately 30% of the mean value of SLF and end at a load of roughly 60% of the same value [10].

Investigations published from our lab and others have demonstrated that 18 specimens are usually enough to obtain good linear regression fits. Three additional samples were subjected to SLF, and 18 were then assigned to mild ($n = 9$), moderate ($n = 6$), and aggressive ($n = 3$) fatigue profiles—a ratio of 3:2:1 (4:2:1 has also been used for distribution of 21 specimens) [67]. The reason for using the three step-stress profiles is that the accuracy of estimates from such a test is inversely proportional to its length; therefore, nine samples are favored in the mild relative to three in the aggressive. Following the parameters of loading for each predetermined profile, the specimens are fatigued until failure or suspension (no failure at the end of step-stress profiles), where maximum loads are applied up to a limit previously established based on SLF mean value (N).

The life-stress relationship model used to analyze data from SSALT, which include time-varying-stresses, must consider the cumulative effect of the applied stresses and is known as cumulative damage model. Based upon the step-stress distribution of the failures, a cumulative damage model that best fits the data (Weibull, Lognormal, or Exponential) is then chosen for data analysis. In the early 50 s, Waloddi Weibull showed in his hallmark paper that an extreme value distribution can properly and meaningfully model such data sets [56]. Considering the many shapes that the Weibull distribution can attain for various values of beta (slope), it became one of the most applied distributions in reliability engineering. It can model a variety of data and life characteristics that makes it an all-purpose distribution.

The SSALT data are then analyzed using an underlying life distribution to describe the life data collected at different stress levels and a life-stress relationship to quantify the manner in which the life distribution changed across different stress levels [10, 68–70]. Thus, the Weibull distribution is usually chosen, as explained above, to fit the life data collected in SSALT, and its probability density functions (pdfs) are given by [70]:

$$f(T) = \frac{\beta}{\eta}\left(\frac{T}{\eta}\right)^{\beta-1} e^{-(T/\eta)^{\beta}} \qquad (9.5)$$

where $f(T) \geq 0$, $T \geq 0$, $\beta > 0$, $\eta > 0$, and η = scale parameter; β = shape parameter (or slope).

Considering the time-varying stress model ($x(t)$), the inverse power law relationship (IPL) is selected to extrapolate a use level condition considering the cumulative effect of the applied stresses, referred as the cumulative damage model as mentioned above. In such a model, the IPL would be given by:

$$L(x(t)) = (\alpha / x(t))^{\eta} \qquad (9.6)$$

where L = life data, and $x(t)$ = stress. Then, the IPL-Weibull pdf (where η is replaced by the IPL) would be given by:

$$f(t, x(t)) = \beta \left(\frac{x(t)}{\alpha}\right)^{n} \left(\int_0^t \left(\frac{x(t)}{\alpha}\right)^{n} du\right)^{\beta-1} e^{-\left(\left(\frac{x(t)}{\alpha}\right)^{n} du\right)^{\beta}} \qquad (9.7)$$

From the extrapolated use level pdf, a variety of functions can be derived, including reliability:

$$R\left(t, x(t)\right) = e^{-\left(\left(\frac{x(t)}{\alpha}\right)^n du\right)^\beta} \qquad (9.8)$$

The model provides the use level probability Weibull curves and a beta (β) value, which is the slope of the regressed line in a probability plot. This parameter describes the failure rate behavior over time, where $\beta < 1$ indicates that failure rate decreases over time, commonly associated with "early failures" or failures that occur due to egregious flaws; $\beta \sim 1$ demonstrates that the failure rate does not vary over time, associated with failures of a random nature; and $\beta > 1$ indicates that failure rate increases over time, associated with failures related to damage accumulation [71]. When the calculated beta (β) is <1 for any tested group, meaning that the implant-abutment connection or restorative material failure is controlled by materials strength rather than damage accumulation from fatigue testing, a Weibull two-parameter calculation of Weibull modulus (m) and characteristic strength (η), which indicates the load at which 63.2% of the specimens of each group would fail) may be presented using the final load at failure or suspensions during fatigue as input, disregarding the number of cycles [69, 72]. The calculated Weibull modulus (m) and characteristic strength values are utilized to determine the confidence bounds through the maximum likelihood ratio method utilizing a chi-squared value at a 90% level of significance and 1 degree of freedom.

An instructive graphical method to determine whether these data sets are significantly different through the nonoverlap of confidence bounds) is the utilization of a Weibull 2-parameter contour plot (Weibull modulus vs. characteristic strength). Each contoured region represents possible values given by both parameters combination and difference at 90% level is detected if contour overlap between groups does not exist (in such case, samples will be considered to be from different populations) [69, 72]. Weibull modulus m ("modulus" means absolute value or number, from the Latin, a (small) measure) is a unitless parameter that measures the variability of the results. A higher m indicates smaller and/or fewer defects (greater structural reliability); a lower m is evidence of greater variability of the strength, reflecting more flaws in the system and a decrease in reliability [31].

A reliability calculation (with two-sided confidence bounds that can be calculated by a variety of methods, including the MLE) is then mathematically estimated for the completion of a given number of cycles (mission) at a specific load level. For the mission reliability and β parameters calculated, the 90% confidence interval range is calculated as follows:

$$\text{IC} = E(G) \pm Z\alpha \, \text{sqrt}\left(\text{Var}(G)\right) \qquad (9.9)$$

where IC is the confidence bound (CB), $E(G)$ is the mean estimated reliability for the mission calculated from Weibull statistics, $Z\alpha$ is the z value concerning the given IC level of significance, and Var(G) is the value calculated by the Fisher information matrix [69, 72].

To characterize the implant-prostheses complex, the SSALT method has been employed using a servo-all-electric system, where the indenter contacts the specimen surface, applies the prescribed load within the step profile, and lifts off of the material surface. However, the step-stress method can also be conducted with an electrodynamic testing machine to simulate mouth-motion fatigue (MMSSALT, where the indenter contacts, applies the load, slides, and then lifts off the sample simulating the masticatory motion described under Sect. 9.2) [73, 74]. Thus, specimens can be tested in either axial or off-axis loading orientation. Such equipment must allow precise control of load magnitude, frequency, and displacement, especially of vertical (approach and retract rates, contact, loading and unloading rates) and horizontal actuator adjustment of the drag and retract rates, starting and end points.

The applicability of SSALT has been demonstrated by several studies using different restorative materials. Of special interest is that testing performed by MMSSALT has thus far been shown to be the only testing method able to reproduce in vitro the fracture modes observed clinically [18, 73, 74], providing dental ceramics

developers with an informed platform, one that is currently being utilized to improve dental ceramic systems for the future.

The use of SSALT for reliability and failure mode analysis of several implant restorative scenarios has been reported by our group and others. An example involving a compilation of data collected in our laboratory on narrow dental implants from a variety of manufacturers is shown in Fig. 9.1. The aim is to present the main effect of implant bulk material (C.P. Titanium grades 2 and 4, Ti-6Al-4V, and TiZr alloys), connection design and diameter on the probability of survival of narrow implants. The criteria to include narrow implants was a diameter between 3 mm and 3.75 mm [75], although our analysis included diameters from 3.3 to 3.5 mm. For the 18 tested groups, reliability calculation for a mission of 200,000 cycles at 180N showed a trend of lower survival for C.p. Ti grade 2 compared to other implant bulk materials. Also, internal conical implant-abutment connections generally showed higher survival compared to others, with some 3.4 mm diameter conical Ti-6Al-4V implants

presenting equal or superior performance than 3.5 mm diameter nonconical internal connections.

The main advantage of SSALT is that it quickly yields failures ensured by the increasing stress levels. However, quick failures do not guarantee more accurate estimates, which in SSALT is inversely proportional to the profile length. For instance, a constant fatigue test with a few specimen failures usually yields greater accuracy than a shorter step-stress test in which all specimens fail. It is the total time on the test (summed over all specimens), not the number of failures, that determines accuracy [69]. One disadvantage of step-stress tests is that under clinical conditions, most specimens run at constant stress, not step-stress. Thus, the tested model must properly take into account the cumulative effect of exposure to successive stresses. Moreover, the model must also provide an estimate of life under constant stress that should not exceed three to four times the average number of cycles employed throughout the test for all groups [69].
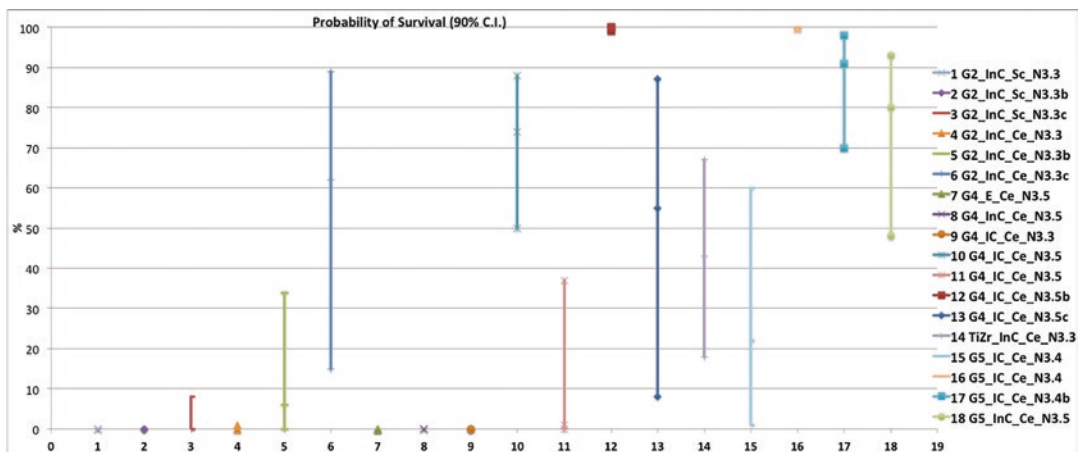
Fig. 9.1 Probability of survival of narrow implants with upper and lower confidence intervals for a mission of 200,000 cycles at 180N. Names of groups shown on the right side mean implant bulk material, connection type, crown fixation mode, and diameter in mm. Implant bulk materials: G2 and G4—commercially pure titanium grade 2 and grade 4, respectively; G5—Ti-6Al-4V; *TiZr* titanium-zirconium alloy, Connection type: *E* external hexagon, *InC* Internal nonconnical, *IC* internal connical; Fixation mode: *Sc* screwed, *Ce* cemented

9.3 Fractographic Analysis of Failed Implants and Prostheses

Fractographic analysis involves the systematic observation and pattern recognition of failed parts that can provide information regarding failure origin and loading conditions. It should be performed in every sample that failed under laboratory-controlled conditions and compared to those retrieved from the service. Robust fractography work has been performed on ceramic restorations either retrieved or replicated, allowing sound comparison of clinical versus laboratory failure modes [76, 77]. Design, fabrication, and handling features must be considered in the fractographic analysis. The nomenclature and a vast array of examples of the analysis of brittle materials is freely available [78] as well as guidance to conduct it [79].

Fractographic analysis of retrieved commercially pure Ti prosthetic screw has shown several shear cracks (50–100 μm extension) along the inner diameter portion of several threads and one of them related to the fracture origin. The fractured surface of the screw showed transgranular stress corrosion cracking, i.e., ductile fracture and fluted steps. Whereas plastic deformation may take place during tightening at the recommended torque, marks in the surface layer were compatible with brittle fracture consistent with hydrogen absorption [80], reported to cause a reduction in the ductility of titanium [81, 82].

A set of nomenclature is used for the fractography of titanium [83]. Fatigue striations (marks left during crack growth where a striation result from a single stress cycle) may predict the lifetime of the implants and estimate the cleavage and dimple fracture of implants [84]. As in ceramics and composites, mechanical, environmental, and microstructural factors should be considered in the analysis of failed dental implants and parts. Continuous effort in the construction of a database for comparison of clinical and laboratory failure modes in metallic implants is encouraged.

9.4 In Vivo Testing

Once tested for general safety through in vitro assays, dental implant's next analyses comprise animal testing. To the present date, if one considers the variations employed in in vivo testing including the various animal models, surgical protocols, temporal evaluations, implant designs, evaluation methods, and many others, it becomes reasonable to suspect that comparisons between studies lead to a heuristic interpretation of the current dental implant literature. For the most investigated implant design variable, i.e., implant surface engineering, directions for in vivo study design have already been suggested [85] and while subsequent work pointed that measurement and evaluation techniques still lack standardization the majority of studies still rarely present essential information which is proper implant surface characterization [86]. Comprehensive physicochemical characterization including implant surface spatial and hybrid parameters are paramount. Considering that such differences in methodology lead to serious difficulties in comparison between studies, as is the case discussed in the in vitro mechanical testing section of this chapter, researchers questing for reliable comparisons between implant systems and their variables are encouraged to create their own database under strictly standardized methodological approaches. Also, round robin tests are not common whatsoever in the field. With that in mind, this section is targeted at overviewing some trends currently shown to improve the characterization and interpretation of the host-to-biomaterial interface, but it is definitely not intended to serve as guidelines for in vivo study design.

Animal models frequently used for dental implant research include rats, rabbits, dogs, sheep, pigs, and nonhuman primates. Rabbits and rats are the most commonly used due to their low cost and ease of handling, despite their size limitation that hinders comparison of multiple implant/surgical factors per sample [87]. Although choosing an animal model is chal-

lenged by several factors such as cost, society acceptability, availability, countries specific animal protection act, housing, etc. researchers should attempt to consider the similarity of bone macro and microstructure, modeling and remodeling kinetics of the selected model to most closely simulate the intended region of biomaterial use and human response. Despite differences in mineral apposition rates, dogs and pigs have similar bone composition to humans [88] and as long as well controlled animal studies with temporal evaluations are designed, valuable comparisons can be obtained. Sheep is a large animal model and its ilium has been successfully utilized to evaluate bone response to surgical techniques and implant surfaces in a relevant simulation of low-density bone [89]. Nonhuman primates (NHP) have also been used to evaluate alveolar ridge dimensional changes [90], the regenerative potential of growth factors on periodontal defects [91, 92] and loaded implant bulk biomaterials responses [93]. Regardless of selected animal model, approval from animal committees is mandatory and report of results according to Arrive guidelines is encouraged. Differences in the pathophysiology of animal models and humans must be acknowledged prior to extrapolations.

Regarding in vivo evaluation methods, the largest possible number should be selected to establish comparisons of biological responses between biomaterials systems. Methods include static and dynamic histomorphometric parameters evaluated through 2 and 3D measurement tools in combination with biomechanical testing. Some histometric 2D parameters have shown to correlate well with 3D parameters obtained through microcomputed tomography with benefits observed for the latter technique when temporally observing bone density evolution and reaction to implants [94]. Bone-to-implant contact (BIC) and sometimes bone area fraction occupancy (BAFO) are typically evaluated 2D histometric parameters. They may both be of limited value if not temporally reported or if not combined with biomechanical evaluations such as torque to interface failure or nanoindentation testing [85]. Also, very high insertion torque values could be correlated with the early observation of high values of BIC and BAFO which commonly decrease as bone remodeling takes place and vary primarily due to variations on surgical instrumentation technique and implant macrogeometry, regardless of surface treatment [95, 96].

For nanoindentation testing, a loading profile is commonly developed (e.g., peak load of 300 μN at a rate of 60 μN/s, holding time of 10 s and an unloading time of 2 s) as detailed elsewhere [97]. A load–displacement curve is obtained after each indentation usually subdivided into bone quadrants. From each analyzed load–displacement curve, reduced modulus (GPa) and hardness (GPa) of bone tissue are computed, and elastic modulus Eb (GPa) is calculated as follows:

$$\frac{1}{E_r} = \frac{1-v^2}{E} + \frac{1-v_i^2}{E_i} \tag{9.10}$$

where E_r is the reduced modulus (GPa). $v(0.3)$ is the Poisson's ratio for cortical bone (if that is the case), and E_i (1140 GPa) and v_i (0.07) are the elastic modulus and Poisson's ratio for the indenter, respectively [98–100].

Each method poses its own advantages and limitations that should be acknowledged. For instance, rougher implants will tend to present higher early torque to interface failure relative to their smoother counterparts, regardless of biological performance. Histometric 2D parameters should also be interpreted with caution since high values of BIC in low biomechanical competence bone may not be preferred over much lower BIC values in high biomechanical competence bone, especially in implant high load-bearing scenarios [85]. Continued efforts to increase the database on human retrieved implants with long-term evaluations (≥10 years) along with biomechanical evaluations are warranted, as presented previously [101–104].

9.5 Digital Simulation: In Silico Analysis

The success of dental implants osseointegration lies not only on the biological integration but also on the biomechanical equilibrium between bone

and implant's threads contact [105–107]. Therefore, the implants must be able to receive the forces from chewing loading and transfer them to the surrounding bone tissues at the physiological load-bearing capacity of the organism [108]. The stress/strain at the bone-implant interface might acts as a mechanical stimulus to bone, in which bone response may vary per intensity and frequency of the stimulus. According to Rieger et al. [109], stress about 1.4–5.0 GPa seems to be desirable for bone health maintenance, although precise mechanisms are not fully understood; at the time the mechanical stimulus exceeds the physiological limit, bone overloading might be leading to the pathological bone loss and consequently implant failure [105, 110, 111]. Also, the functionality of the prosthetic components and dental implants involves the biomechanical stress distribution and the respective materials strength limits, which might support the load effects [112–116].

Experimental studies have failed to effectively determine these parameters since the literature has reported only bone mechanical properties such as stiffness, strength, and elastic modulus. The finite element analysis (FEA) was developed over 80 years ago to solve complex problems in the civil and aeronautical field; the applications of the method have spread through the orthopedic biomechanics [117] and ventricular systems [118].

The finite element analysis (FEA) is a powerful computer methodology that helps researchers to predict the stress and strain distribution around dental implants in contact with cortical and trabecular bone and among prosthetic components. The FEA is a technique used to obtain a solution to a complex mechanical problem by dividing a heavy geometry into smaller elements using a virtual mesh. An overall solution for the problem is achieved according to the given studied variables such as implant design, bone type and prosthetic connection.

The major challenge using FEA is the human bone reproducibility and its response interpretation given simulated chewing loadings. Some parameters influence the data interpretation such

as model construction, materials properties, boundary conditions, and bone–implant interface [119].

9.5.1   Model Construction

The first step of a FEA is the model design, where a virtual model will be constructed based on such specific dimensions. The models can comprise two-dimensions (2D) or three-dimensions (3D). The 2D model is a simplified model, which does not consider the geometry's volume. Consequently, a decreased accuracy can be expected, and the data interpretation must be carefully evaluated. In contrast, 3D models should be preferably used since they offer accurate data through full geometry representation at a virtual level. Additionally, 3D computer tomography images can be used as reference to create accurate models of bone defects or atrophic maxilla/mandible, for example [120]. However, due to the model complexity, mesh refinements can be difficult to achieve and require high-performance computers to the mathematical analysis. Some studies have reported that even simplified models might show reliable data, enhanced performance and efficiency of comparative strain analysis relative to the complex models [121, 122].

The virtual geometries can be obtained by manual or automatic methods. While the former consists of manually modeling the real or literature-based geometry dimensions, the latter uses 3D images obtained through laser scans which are converted into a wireframes structure and later into a solid model using CAD software, i.e., SolidWorks (Corp., Concord, MA, USA), AutoCAD (Autodesk, San Rafael, USA), Pro/ Engineer (Wildfire, PTC, Needham, MA, USA), Rhinoceros (Robert McNeel & Associates, Seattle, USA), etc.

Additionally, medical topographies can be used as a helpful tool to obtain bitmapped images regarding different bone sections and later transformed into a solid model. Mimics (Materlialise, Leuven, Belgium) and InVesalius (CTI,

Fig. 9.2 The complete mandibular model reproduces all anatomic structures based on tomography slices. Although a realistic and detailed model was obtained, the mathematical solution can be hardly achieved

Fig. 9.3 A segmented model reproduces a detailed region, which can be helpful to single or multiple implant's perimeter bone stress study. In this scenario, lower elements numbers are generated during the mesh creation that facilitates the mathematical solution achievement

Campinas, Brazil) are some examples of specific software programs used to work with tomography images using gray scale tons. Nataly et al. [123], showed that model design affects stress pattern distribution by about 30%. Because of detailed modeling at the bone-implant interface, it was possible to evaluate the stress/strain at the peri-implant area where bone stiffness affected the stress distribution pattern and the total displacement due to variation of the modeled cortical thickness [123, 124] (Figs. 9.2 and 9.3).

9.5.2 The Analysis

After model creation, the files are imported by some analysis software that use the geometry and the material's properties to calculate the structure stress when subjected to a given load application. The most common software packages used for finite element analysis are ANSYS (Swanson Analysis Systems, Houston, Pa), ABAQUS (Pawtucket, RI, USA), COSMOS (Structural Research and Analysis Corp., Los Angeles, CA, USA) and MSC PATRAN (Santa Ana, CA).

9.5.3 Materials Properties

Materials properties influence the stress and strain distribution in a model. Most of software require the material's Young modulus, which is defined as the material stress/strain measured at the extension or compression. In another word is defined as the material's deformation measured by a given applied load [123, 125]. Materials properties are usually considered as homogeneous, isotropic, and linearly elastic to simplify the analysis. The isotropic property indicates that the material mechanical response is similar in all directions. The literature has reported that bone should be considered as anisotropic, since it has different mechanical properties when measured in different directions [125]. In addition, the mechanical properties are dependent on several factors such as porosities, mineralization level, and collagens fibers orientation [126, 127]. The anisotropic bone property might increase the ten-

sile stress and strain by 20–30% at the cortical crest level compared to isotropic bone, while decrease by 40% the shear stress at the cancellous bone as reported by O'Mahony [125]. The bone anisotropy property has a significant potential to modify the stress levels and should take into consideration while designing the analysis.

There is a variety of bone mechanical properties reported in the literature. It has been reported that the lower the bone density, the higher the implant failure probability. Thus, some FEA studies have been focused on the peri-implant stress behavior of patients with reduced bone properties due to osteopenia or osteoporosis [128–133].

Additionally, the Poisson ratio is also used and represents the lateral strain divided by the axial strain. This parameter represents the material behavior (extension or compression) to maintain the volume when underwent to a given load and usually is based on the literature.

9.5.4 Boundaries and Bone-Implant Interface

Most of studies have considered the bone-implant interface as ideal osseointegration, and the contact is defined as "bonded" (linear analysis). Such condition is valid when the material shows a linear stress-strain relationship up to a stress level known as the proportional limit, meaning that the strain is linearly proportional to the magnitude of the given load. In another words, the higher the loading, the higher the stress/strain. Nonetheless, this type of contact does not occur in an intraoral scenario.

The partial contact modeling between implant's threads and bone should be carefully evaluated to avoid mathematical errors during the analysis since it increases the complexity of the analysis. To solve this, friction coefficients can be previously measured by experimental studies and be simulated among surfaces using numerical algorithms (nonlinear analysis) [134–137]. It has been commonly used the 0.3 friction coefficient between bone-implant [138–140] to simu-

late an immediate loading condition; however, there is no clinical evidence to support it.

Clinically, the presence of as saliva, mainly composed of water, and abundant proteins, serum albumin, prolactin-inducible protein, filaggrin, and desmoglein-1, as isoform 1, has the ability to shift the friction coefficient between prosthetic surfaces in vitro [136]; the friction coefficient between two titanium surfaces under dry (0.23) or saliva conditions (0.19) and between titanium and zirconia under dry (0.14) or saliva conditions (0.19) to simulate de prosthetic contact among implant-abutment and screw [136]. Additionally, the friction coefficient can also be used to simulate the preload stress resultant from the screw tightening using different surface coatings [137, 141] which approaches the clinical scenario of stress distribution and mechanical performance [116].

Materials nonlinearity allows structure stiffness changes according to different load-levels, which is expressed by a nonlinear stress/strain. Nonlinear contacts have become a powerful tool to simulate a more realistic scenario and help to predict the stress and strain behavior of studied structures [134].

9.5.5 Loading Conditions

There is a consensus in the literature that the location and the magnitude of the loading influence the stress and strain in all implant joint components [106, 142]. When the biological response is considered, it is essential to determine if the complex loading is due to internal (preload) [143] or external source (chewing or traumatic occlusion) [144, 145]. In all external scenarios, the occlusal loading is first applied on the crown and later distributed to prosthetic components, implant, and surrounding bone. Factors such as prosthesis retention (screwed or cemented), prosthesis material (all-ceramic, metal-ceramic), implant and prosthetic design (prosthetic connection, diameter and length) and bone quality can affect the loading distribution to peri-implant–bone [146–149].

Literature findings have reported a widespread range of bite forces according to different regions of the mouth, usually around 150N [150–152] for anterior teeth and 250–500N for posteriors [138, 153–157]. Additionally, even higher values have been demonstrated for maximum bite force (up to 650N) [13]. To reproduce a more accurate scenario for FEA, it has been suggested the combination of axial and oblique loading considering the implant longitudinal axis. Nevertheless, additional attention must be drawn since the resultant stress due to oblique forces is amplified [158, 159]. Some studies have considered oblique loading as parafunctional or traumatic occlusion depending on its magnitude [111, 158–160].

9.5.6 Mesh Generation and Output

To calculate the solution, the software needs to split a heavy geometry into small elements; each element is tree-dimensionally connected through nodes to create a 3D mesh [119]. Since de geom-

etry of the element do influences the stress output, quadratic tetrahedral elements are usually preferable since they better adapt into curved surfaces as anatomic structures.

The mesh refinement means to reduce the element size and create a smoother transition between the contacted surfaces. Also, it helps to identify any "element aberrations" which might compromise the solution. As the lower the element size, the higher the number of elements necessary to fill the geometry, and consequently, the complexity of the solution is increased. The consensus among several studies have adopted convergence criteria set as 5% [114, 140, 147, 161, 162]; it means that the output difference (stress, strain, etc.) between a selected element size (i.e., 0.5 mm) and a refined one (i.e., 0.4 mm) is up to 5% (Fig. 9.4).

Lastly, the FEA is an unequivocally valid tool to evaluate the impact of modifications involving implant geometry, bone properties and morphologies and prototypes testing [163, 164]. Data output is usually evaluated considering the tensile
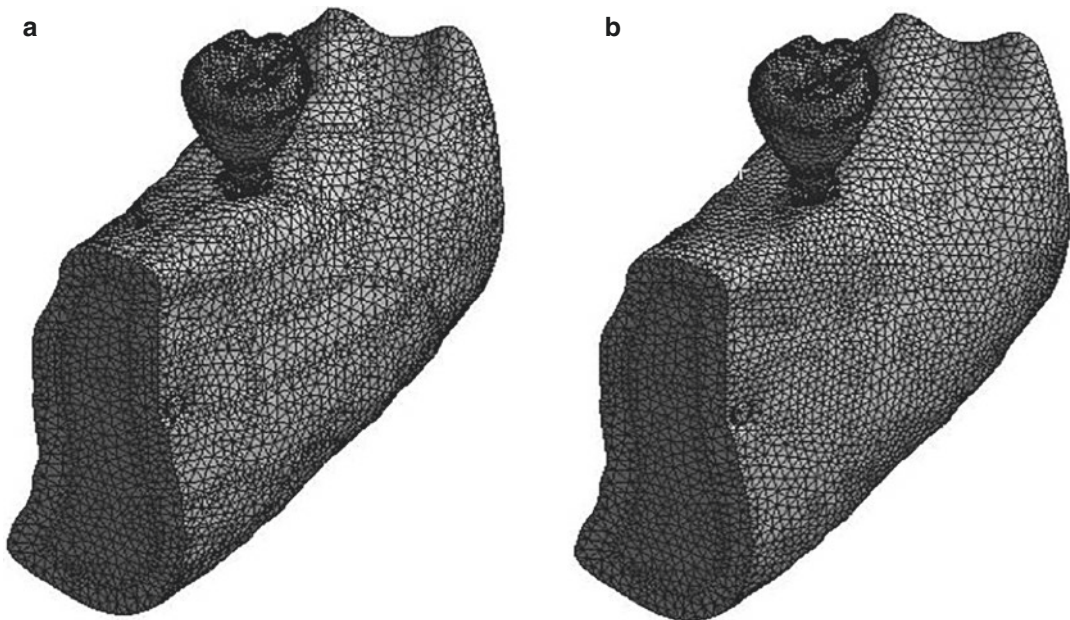
Fig. 9.4 The mesh refinement at the implant–bone interface is an important step to achieve reliable data. (**a**) shows a 0.5 mm element-mesh, which the STL model lines were automatically used to guide the mesh creation. The mesh quality will directly influence the stress dissipa-

tion through the model. Additionally, the nonlinearity can be hardly achieved, and the results might not represent the data reliability. (**b**) shows a refined model with 0.5 mm element-mesh, which all elements are contacting each other, without any line interference
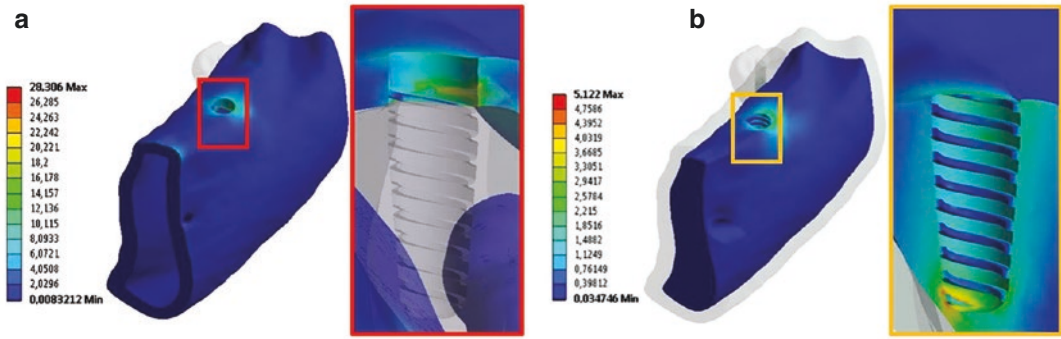
Fig. 9.5 shows the cortical (**a**) and medullar (**b**) shear stress distribution after an FEA simulation. The red box shows the cross-section area at the cortical level, in which the peak stress concentration (28.30 MPa) was located at the implant crest level. The yellow box shows the medul-

lar cross-section, in which the stress peak (5.12 MPa) was located at implant apex. The stress data did not represent the osseointegration success or failure just by itself. Data interpretation should be carefully conducted and compared with clinical findings

(maximum stress), compression (minimum stress) and/or strain. The group of ductile materials (metals or alloys, i.e., titanium) is usually evaluated by the von-Mises stress since this criterion is associated with fatigue failure [113, 165] (Fig. 9.5).

Nonetheless, the data interpretation must be always supported by clinical and experimental findings. The FEA should not be considered itself as the only factor used for data extrapolation to the clinical scenario since there is still a lack of information regarding biological parameters, which are not considered in mechanical simulations.

9.6 Expert Opinion

Along with well-designed long-term randomized controlled trials addressing questions that are especially important to the patient population welfare, in silico, in vitro and in vivo testing of the dental implant system will continue to provide relevant information that can improve even further the outcomes of implant therapy. It is desired that new methods are developed and that existing ones improved, but more importantly, that robust study design and report, statistical evaluation, equipment and personnel calibration continue to be endeavored, so the literature becomes more friendly when comparisons are to be made.

References

1. Popelut A, Valet F, Fromentin O, et al. Relationship between sponsorship and failure rate of dental implants: a systematic approach. PLoS One. 2010;5:e10274.
2. Henry PJ. Implant hardware--science or commodity development? J Dent Res. 1995;74:301–2.
3. Market Ra: global dental implants and prothestics market analysis & trends - product - forecast to 2025; 2017.
4. Papaspyridakos P, Chen CJ, Singh M, et al. Success criteria in implant dentistry: a systematic review. J Dent Res. 2012;91:242–8.
5. Moher D, Schulz KF, Altman DG. The CONSORT statement: revised recommendations for improving the quality of reports of parallel-group randomised trials. Lancet. 2001;357:1191–4.
6. Griggs JA. Dental Implants. Dent Clin N Am. 2017;61:857–71.
7. Berglundh T, Giannobile WV. Investigational clinical research in implant dentistry: beyond observational and descriptive studies. J Dent Res. 2013;92:107S–8S.
8. Baker M. Is there a reproducibility crisis? A nature survey lifts the lid on how researchers view the 'crisis rocking science and what they think will help. Nature. 2016;533:452–5.

9. Coelho PG, Jimbo R. Osseointegration of metallic devices: current trends based on implant hardware design. Arch Biochem Biophys. 2014;561:99–108.
10. Bonfante EA, Coelho PG. A critical perspective on mechanical testing of implants and prostheses. Adv Dent Res. 2016;28:18–27.
11. Morgan MJ, James DF, Pilliar RM. Fractures of the fixture component of an osseointegrated implant. Int J Oral Maxillofac Implants. 1993;8:409–14.
12. Rekow D, Zhang Y, Thompson V. Can material properties predict survival of all-ceramic posterior crowns? Compend Contin Educ Dent. 2007;28:362–8; quiz 369, 386.
13. van der Bilt A. Assessment of mastication with implications for oral rehabilitation: a review. J Oral Rehabil. 2011;38:754–80.
14. Agrawal KR, Lucas PW, Bruce IC, et al. Food properties that influence neuromuscular activity during human mastication. J Dent Res. 1998;77:1931–8.
15. Hiiemae K. Mechanisms of food reduction, transport and deglutition: how the texture of food affects feeding behavior. J Texture Stud. 2004;35:171–200.
16. Woda A, Foster K, Mishellany A, et al. Adaptation of healthy mastication to factors pertaining to the individual or to the food. Physiol Behav. 2006;89:28–35.
17. Kelly JR, Benetti P, Rungruanganunt P, et al. The slippery slope: critical perspectives on in vitro research methodologies. Dent Mater. 2012;28:41–51.
18. Coelho PG, Bonfante EA, Silva NR, et al. Laboratory simulation of Y-TZP all-ceramic crown clinical failures. J Dent Res. 2009;88:382–6.
19. DeLong R, Douglas WH. Development of an artificial oral environment for the testing of dental restoratives: bi-axial force and movement control. J Dent Res. 1983;62:32–6.
20. Kelly JR. Clinically relevant approach to failure testing of all-ceramic restorations. J Prosthet Dent. 1999;81:652–61.
21. ASTM: ASTM E 1150-1987, standard definitions of fatigue. Annual Book of Standards. ASTM; 1995.
22. Baran G, Boberick K, McCool J. Fatigue of restorative materials. Crit Rev Oral Biol Med. 2001;12:350–60.
23. Griffith AA. The phenomena of rupture and flow in solids. Philos Trans R Soc Lond Ser A. 1921;221:163–98.
24. Mustafa A, Matinlinna J. Materials in dentistry. In: Matinlinna JP, editor. Handbook of oral biomaterials. Boca Raton: CRC Press; 2014.
25. Pjetursson BE, Thoma D, Jung R, et al. A systematic review of the survival and complication rates of implant-supported fixed dental prostheses (FDPs) after a mean observation period of at least 5 years. Clin Oral Implants Res. 2012;23(Suppl 6):22–38.
26. Paris P, Erdogan F. A critical analysis of crack propagation laws. J Basic Eng. 1963;85:528–34.
27. Wiederhorn S. Subcritical crack growth in ceramics. Fracture mechanics of ceramics. Berlin: Springer; 1974.
28. De Aza AH, Chevalier J, Fantozzi G, et al. Crack growth resistance of alumina, zirconia and zirconia toughened alumina ceramics for joint prostheses. Biomaterials. 2002;23:937–45.
29. Anusavice KJ, Lee RB. Effect of firing temperature and water exposure on crack propagation in unglazed porcelain. J Dent Res. 1989;68:1075–81.
30. Chevalier J, Olagnon C, Fantozzi G. Subcritical crack propagation in 3Y-TZP ceramics: static and cyclic fatigue. J Am Ceram Soc. 1999;82:3129–38.
31. Ritter JE. Predicting lifetimes of materials and material structures. Dent Mater. 1995;11:142–6.
32. Qiao GJ, Wang HJ, Jin ZH. Comparison between fatigue behavior of some ceramics: a new concept of intrinsic stress-corrosion exponent n(0). Int J Fatigue. 2002;24:499–508.
33. Judy RW, Caplan IL, Bogar FD: Effects of oxygen and iron on the environmental and mechanical-properties of unalloyed titanium. In: Titanium '92: science and technology, vols. 1–3, 92; 1993. p. 2073–80.
34. Judy Jr R, Rath B, Caplan I. Stress corrosion cracking of pure titanium as influenced by oxygen content. In: Sixth world conference on titanium IV; 1988.
35. Bundy KJ, Zardiackas LD. Corrosion fatigue and stress-corrosion cracking in metallic biomaterials. In: ASM handbook: corrosion: environments and industries materials. Park: ASM International; 2006. p. 853–90.
36. Shemtov-Yona K, Rittel D. On the mechanical integrity of retrieved dental implants. J Mech Behav Biomed Mater. 2015;49:290–9.
37. Knehans R, Steinbrech R. Memory effect of crack resistance during slow crack growth in notched Al 2 O 3 bend specimens. J Mater Sci Lett. 1982;1:327–9.
38. Griggs J. Lifetime prediction of dental implants and prostheses. In: Proceedings of the International Dental Materials Congress. Seoul: International Dental Materials Congress; 2011.
39. Duan Y, Griggs JA. Effect of loading frequency on cyclic fatigue lifetime of a standard-diameter implant with an internal abutment connection. Dent Mater. 2018;34:1711–6.
40. Karl M, Kelly JR. Influence of loading frequency on implant failure under cyclic fatigue conditions. Dent Mater. 2009;25:1426–32.
41. Shemtov-Yona K, Rittel D. Identification of failure mechanisms in retrieved fractured dental implants. Eng Fail Anal. 2014;38:58–65.
42. Zavanelli RA, Guilherme AS, Pessanha-Henriques GE, et al. Corrosion-fatigue of laser-repaired commercially pure titanium and Ti-6Al-4V alloy under different test environments. J Oral Rehabil. 2004;31:1029–34.
43. Lassila LV, Vallittu PK. Effect of water and artificial saliva on the low cycle fatigue resistance of cobalt-chromium dental alloy. J Prosthet Dent. 1998;80:708–13.

44. Llobell A, Nicholls JI, Kois JC, et al. Fatigue life of porcelain repair systems. Int J Prosthodont. 1992;5:205–13.

45. Yoshimura HN, Cesar PF, Soki FN, et al. Stress intensity factor threshold in dental porcelains. J Mater Sci Mater Med. 2008;19:1945–51.

46. de Krijger J, Rans C, Van Hooreweder B, et al. Effects of applied stress ratio on the fatigue behavior of additively manufactured porous biomaterials under compressive loading. J Mech Behav Biomed Mater. 2017;70:7–16.

47. Rosentritt M, Siavikis G, Behr M, et al. Approach for valuating the significance of laboratory simulation. J Dent. 2008;36:1048–53.

48. Zahran M, El-Mowafy O, Tam L, et al. Fracture strength and fatigue resistance of all-ceramic molar crowns manufactured with CAD/CAM technology. J Prosthodont. 2008;17:370–7.

49. Rosentritt M, Behr M, Gebhard R, et al. Influence of stress simulation parameters on the fracture strength of all-ceramic fixed-partial dentures. Dent Mater. 2006;22:176–82.

50. Wiskott HW, Nicholls JI, Belser UC. Fatigue resistance of soldered joints: a methodological study. Dent Mater. 1994;10:215–20.

51. Po JM, Kieser JA, Gallo LM, et al. Time-frequency analysis of chewing activity in the natural environment. J Dent Res. 2011;90:1206–10.

52. Rosentritt M, Rembs A, Behr M, et al. In vitro performance of implant-supported monolithic zirconia crowns: influence of patient-specific tooth-coloured abutments with titanium adhesive bases. J Dent. 2015;43:839–45.

53. Senyilmaz DP, Canay S, Heydecke G, et al. Influence of thermomechanical fatigue loading on the fracture resistance of all-ceramic posterior crowns. Eur J Prosthodont Restor Dent. 2010;18:50–4.

54. Kaplan EL, Meier P. Nonparametric-estimation from incomplete observations. J Am Stat Assoc. 1958;53:457–81.

55. Lorenzoni FC, Martins LM, Silva NR, et al. Fatigue life and failure modes of crowns systems with a modified framework design. J Dent. 2010;38:626–34.

56. Weibull W. A statistical distribution function of wide applicability. J Appl Mech Trans ASME. 1951;18:293–7.

57. Asmussen E, Jorgensen KD. Fatigue strength of some resinous materials. Scand J Dent Res. 1982;90:76–9.

58. Lin SK, Lee YL, Lu MW. Evaluation of the staircase and the accelerated test methods for fatigue limit distributions. Int J Fatigue. 2001;23:75–83.

59. Song J, Mourelatos Z, Gu R, et al. Sensitivity study of staircase fatigue tests using Monte Carlo simulation. SAE technical paper; 2005.

60. Kern M, Strub JR, Lu XY. Wear of composite resin veneering materials in a dual-axis chewing simulator. J Oral Rehabil. 1999;26:372–8.

61. Handbook A. Fatigue and fracture. ASM Int. 1996;19:18.

62. Castillo E, Ramos A, Koller R, et al. A critical comparison of two models for assessment of fatigue data. Int J Fatigue. 2008;30:45–57.

63. Wallin KRW. Statistical uncertainty in the fatigue threshold staircase test method. Int J Fatigue. 2011;33:354–62.

64. ISO-14801: Dentistry — Implants — Dynamic fatigue test for endosseous dental implants. 2nd ed. 2007-11-15. ISO International Standard. Switzerland: ISO.

65. Lee CK, Karl M, Kelly JR. Evaluation of test protocol variables for dental implant fatigue research. Dent Mater. 2009;25:1419–25.

66. Bonfante EA, Coelho PG, Navarro JM Jr, et al. Reliability and failure modes of implant-supported Y-TZP and MCR three-unit bridges. Clin Implant Dent Relat Res. 2010;12:235–43.

67. Guess PC, Zhang Y, Kim JW, et al. Damage and reliability of Y-TZP after cementation surface treatment. J Dent Res. 2010;89:592–6.

68. Bergamo ETP, Bordin D, Ramalho IS, et al. Zirconia-reinforced lithium silicate crowns: effect of thickness on survival and failure mode. Dent Mater. 2019;35:1007–16.

69. Nelson W. Accelerated testing: statistical models, test plans and data analysis. Chichester: Wiley; 2004.

70. Zhao W, Elsayed EA. A general accelerated life model for step-stress testing. IIE Trans. 2005;37:1059–69.

71. Reliasoft: a high value of beta is not necessarily cause for concern; 2010.

72. Abernethy R. The new Weibull handbook. 5th ed. North Palm Beach: Dr. Robert B. Abernethy; 2006.

73. Guess PC, Bonfante EA, Silva NR, et al. Effect of core design and veneering technique on damage and reliability of Y-TZP-supported crowns. Dent Mater. 2013;29:307–16.

74. Silva NR, Bonfante EA, Martins LM, et al. Reliability of reduced-thickness and thinly veneered lithium disilicate crowns. J Dent Res. 2012;91:305–10.

75. Al-Johany SS, Al Amri MD, Alsaeed S, et al. Dental implant length and diameter: a proposed classification scheme. J Prosthodont. 2016;26:252.

76. Moraguez OD, Wiskott HW, Scherrer SS. Three- to nine-year survival estimates and fracture mechanisms of zirconia- and alumina-based restorations using standardized criteria to distinguish the severity of ceramic fractures. Clin Oral Investig. 2015;19:2295–307.

77. Scherrer SS, Quinn JB, Quinn GD, et al. Fractographic ceramic failure analysis using the replica technique. Dent Mater. 2007;23:1397–404.

78. Quinn G. Fractography of ceramics and glasses. A NIST recommended practice guide; special publication 960-16. Washington, DC: National Institute of Standards and Technology; 2007. http://www.ceramics.nist.gov/pubs/practice.htm.

79. Scherrer SS, Lohbauer U, Della Bona A, et al. ADM guidance-ceramics: guidance to the use of fractog-

raphy in failure analysis of brittle materials. Dent Mater. 2017;33:599–620.

80. Yokoyama K, Ichikawa T, Murakami H, et al. Fracture mechanisms of retrieved titanium screw thread in dental implant. Biomaterials. 2002;23:2459–65.

81. Williams D. The hydrogen embrittlement of titanium alloys. J Inst Met. 1962;91:147–52.

82. Tal-Gutelmacher E, Eliezer D. The hydrogen embrittlement of titanium-based alloys. JOM. 2005;57:46–9.

83. Joshi V. Titanium alloys: an atlas of structures and fracture features. Boca Raton: CRC Press; 2006.

84. Kim RW, Kim HS, Choe HC, et al. Microscopic analysis of fractured dental implant surface after clinical use. In: 11th international conference on the mechanical behavior of materials (Icm11), vol. 10; 2011. p. 1955–60.

85. Coelho PG, Granjeiro JM, Romanos GE, et al. Basic research methods and current trends of dental implant surfaces. J Biomed Mater Res B Appl Biomater. 2009;88:579–96.

86. Wennerberg A, Albrektsson T. Effects of titanium surface topography on bone integration: a systematic review. Clin Oral Implants Res. 2009;20(Suppl 4):172–84.

87. Liebschner MA. Biomechanical considerations of animal models used in tissue engineering of bone. Biomaterials. 2004;25:1697–714.

88. Aerssens J, Boonen S, Lowet G, et al. Interspecies differences in bone composition, density, and quality: potential implications for in vivo bone research. Endocrinology. 1998;139:663–70.

89. Lahens B, Neiva R, Tovar N, et al. Biomechanical and histologic basis of osseodensification drilling for endosteal implant placement in low density bone. An experimental study in sheep. J Mech Behav Biomed Mater. 2016;63:56–65.

90. Min S, Liu Y, Tang J, et al. Alveolar ridge dimensional changes following ridge preservation procedure with novel devices: Part 1--CBCT linear analysis in non-human primate model. Clin Oral Implants Res. 2016;27:97–105.

91. Jimbo R, Tovar N, Janal MN, et al. The effect of brain-derived neurotrophic factor on periodontal furcation defects. PLoS One. 2014;9:e84845.

92. Jimbo R, Singer J, Tovar N, et al. Regeneration of the cementum and periodontal ligament using local BDNF delivery in class II furcation defects. J Biomed Mater Res B Appl Biomater. 2017;106:1611.

93. Kohal RJ, Weng D, Bachle M, et al. Loaded custom-made zirconia and titanium implants show similar osseointegration: an animal experiment. J Periodontol. 2004;75:1262–8.

94. Jimbo R, Coelho PG, Vandeweghe S, et al. Histological and three-dimensional evaluation of osseointegration to nanostructured calcium phosphate-coated implants. Acta Biomater. 2011;7:4229–34.

95. Campos FE, Gomes JB, Marin C, et al. Effect of drilling dimension on implant placement torque and early osseointegration stages: an experimental study in dogs. J Oral Maxillofac Surg. 2012;70:e43–50.

96. Gomes JB, Campos FE, Marin C, et al. Implant biomechanical stability variation at early implantation times in vivo: an experimental study in dogs. Int J Oral Maxillofac Implants. 2013;28:e128–34.

97. Jimbo R, Coelho PG, Bryington M, et al. Nano hydroxyapatite-coated implants improve bone nanomechanical properties. J Dent Res. 2012;91:1172–7.

98. Oliver WC, Pharr GM. An improved technique for determining hardness and elastic modulus using load and displacement sensing indentation experiments. J Mater Res. 1992;7:1564–83.

99. Hoffler CE, Guo XE, Zysset PK, et al. An application of nanoindentation technique to measure bone tissue lamellae properties. J Biomech Eng. 2005;127:1046–53.

100. Hoffler CE, Moore KE, Kozloff K, et al. Heterogeneity of bone lamellar-level elastic moduli. Bone. 2000;26:603–9.

101. Baldassarri M, Bonfante E, Suzuki M, et al. Mechanical properties of human bone surrounding plateau root form implants retrieved after 0.3-24 years of function. J Biomed Mater Res B Appl Biomater. 2012;100:2015–21.

102. Coelho PG, Bonfante EA, Marin C, et al. A human retrieval study of plasma-sprayed hydroxyapatite-coated plateau root form implants after 2 months to 13 years in function. J Long-Term Eff Med Implants. 2010;20:335–42.

103. Coelho PG, Marin C, Granato R, et al. Histomorphologic analysis of 30 plateau root form implants retrieved after 8 to 13 years in function. A human retrieval study. J Biomed Mater Res B Appl Biomater. 2009;91:975–9.

104. Gil LF, Suzuki M, Janal MN, et al. Progressive plateau root form dental implant osseointegration: a human retrieval study. J Biomed Mater Res B Appl Biomater. 2014;103:1328.

105. Adell R, Eriksson B, Lekholm U, et al. Long-term follow-up study of osseointegrated implants in the treatment of totally edentulous jaws. Int J Oral Maxillofac Implants. 1990;5:347–59.

106. Isidor F. Loss of osseointegration caused by occlusal load of oral implants. A clinical and radiographic study in monkeys. Clin Oral Implants Res. 1996;7:143–52.

107. Jemt T, Pettersson P. A 3-year follow-up study on single implant treatment. J Dent. 1993;21:203–8.

108. Duyck J, Ronold HJ, Van Oosterwyck H, et al. The influence of static and dynamic loading on marginal bone reactions around osseointegrated implants: an animal experimental study. Clin Oral Implants Res. 2001;12:207–18.

109. Rieger MR, Mayberry M, Brose MO. Finite element analysis of six endosseous implants. J Prosthet Dent. 1990;63:671–6.

110. Bertolini MM, Del Bel Cury AA, Pizzoloto L, et al. Does traumatic occlusal forces lead to peri-implant

bone loss? A systematic review. Braz Oral Res. 2019;33:e069.

111. de Calais CD, Bordin D, Piattelli A, et al. Lateral static overload on immediately restored implants decreases the osteocyte index in peri-implant bone: a secondary analysis of a pre-clinical study in dogs. Clin Oral Investig. 2021;25:3297–303.

112. Bordin D, Bergamo ETP, Bonfante EA, et al. Influence of platform diameter in the reliability and failure mode of extra-short dental implants. J Mech Behav Biomed Mater. 2018;77:470–4.

113. Bordin D, Bergamo ETP, Fardin VP, et al. Fracture strength and probability of survival of narrow and extra-narrow dental implants after fatigue testing: in vitro and in silico analysis. J Mech Behav Biomed Mater. 2017;71:244–9.

114. Bordin D, Cury A, Faot F. Influence of abutment collar height and implant length on stress distribution in single crowns. Braz Dent J. 2019;30:238–43.

115. Bordin D, Witek L, Fardin VP, et al. Fatigue failure of narrow implants with different implant-abutment connection designs. J Prosthodont. 2018;27:659–64.

116. Fardin VP, Bergamo ETP, Bordin D, et al. Effect of different tightening protocols on the probability of survival of screw-retained implant-supported crowns. J Mech Behav Biomed Mater. 2021;126:105019.

117. Huiskes R, Chao EY. A survey of finite element analysis in orthopedic biomechanics: the first decade. J Biomech. 1983;16:385–409.

118. Yin FC. Applications of the finite-element method to ventricular mechanics. Crit Rev Biomed Eng. 1985;12:311–42.

119. Erdemir A, Guess TM, Halloran J, et al. Considerations for reporting finite element analysis studies in biomechanics. J Biomech. 2012;45:625–33.

120. Bordin D, Castro MB, Carvalho MA, et al. Different treatment modalities using dental implants in the posterior maxilla: a finite element analysis. Braz Dent J. 2021;32:34–41.

121. Okumura N, Stegaroiu R, Nishiyama H, et al. Finite element analysis of implant-embedded maxilla model from CT data: comparison with the conventional model. J Prosthodont Res. 2011;55:24–31.

122. Winter W, Steinmann P, Holst S, et al. Effect of geometric parameters on finite element analysis of bone loading caused by nonpassively fitting implant-supported dental restorations. Quintessence Int. 2011;42:471–8.

123. Natali AN, Pavan PG, Ruggero AL. Analysis of bone-implant interaction phenomena by using a numerical approach. Clin Oral Implants Res. 2006;17:67–74.

124. Chandran V, Maquer G, Gerig T, et al. Supervised learning for bone shape and cortical thickness estimation from CT images for finite element analysis. Med Image Anal. 2019;52:42–55.

125. O'Mahony AM, Williams JL, Spencer P. Anisotropic elasticity of cortical and cancellous bone in the posterior mandible increases peri-implant stress and strain under oblique loading. Clin Oral Implants Res. 2001;12:648–57.

126. Asgari M, Abi-Rafeh J, Hendy GN, et al. Material anisotropy and elasticity of cortical and trabecular bone in the adult mouse femur via AFM indentation. J Mech Behav Biomed Mater. 2019;93:81–92.

127. Morgan EF, Unnikrisnan GU, Hussein AI. Bone mechanical properties in healthy and diseased states. Annu Rev Biomed Eng. 2018;20:119–43.

128. Camargos GV, Bhattacharya P, van Lenthe GH, et al. Mechanical competence of ovariectomy-induced compromised bone after single or combined treatment with high-frequency loading and bisphosphonates. Sci Rep. 2015;5:10795.

129. Bala Y, Depalle B, Farlay D, et al. Bone micromechanical properties are compromised during long-term alendronate therapy independently of mineralization. J Bone Miner Res. 2012;27:825–34.

130. Alghamdi HS, van den Beucken JJ, Jansen JA. Osteoporotic rat models for evaluation of osseointegration of bone implants. Tissue Eng Part C Methods. 2014;20:493–505.

131. Xiao JR, Kong L, Chen YX, et al. Selection of optimal expansion angle and length of an expandable implant in the osteoporotic mandible: a three-dimensional finite element analysis. Int J Oral Maxillofac Implants. 2013;28:e88–97.

132. Xiao JR, Li YF, Guan SM, et al. The biomechanical analysis of simulating implants in function under osteoporotic jawbone by comparing cylindrical, apical tapered, neck tapered, and expandable type implants: a 3-dimensional finite element analysis. J Oral Maxillofac Surg. 2011;69:e273–81.

133. Ward J, Wood C, Rouch K, et al. Stiffness and strength of bone in osteoporotic patients treated with varying durations of oral bisphosphonates. Osteoporos Int. 2016;27:2681–8.

134. Wakabayashi N, Ona M, Suzuki T, et al. Nonlinear finite element analyses: advances and challenges in dental applications. J Dent. 2008;36:463–71.

135. Geng JP, Tan KB, Liu GR. Application of finite element analysis in implant dentistry: a review of the literature. J Prosthet Dent. 2001;85:585–98.

136. Bordin D, Cavalcanti IM, Jardim Pimentel M, et al. Biofilm and saliva affect the biomechanical behavior of dental implants. J Biomech. 2015;48:997–1002.

137. Bordin D, Coelho PG, Bergamo ETP, et al. The effect of DLC-coating deposition method on the reliability and mechanical properties of abutment's screws. Dent Mater. 2018;34:e128–37.

138. Huang HL, Hsu JT, Fuh LJ, et al. Bone stress and interfacial sliding analysis of implant designs on an immediately loaded maxillary implant: a non-linear finite element study. J Dent. 2008;36:409–17.

139. Horita S, Sugiura T, Yamamoto K, et al. Biomechanical analysis of immediately loaded implants according to the "all-on-four" concept. J Prosthodont Res. 2017;61:123–32.

140. Dos Santos MBF, Meloto GO, Bacchi A, et al. Stress distribution in cylindrical and conical implants under

rotational micromovement with different boundary conditions and bone properties: 3-D FEA. Comput Methods Biomech Biomed Engin. 2017;20:893–900.

141. Peixoto HE, Bordin D, Del Bel Cury AA, et al. The role of prosthetic abutment material on the stress distribution in a maxillary single implant-supported fixed prosthesis. Mater Sci Eng C Mater Biol Appl. 2016;65:90–6.

142. Al Jabbari YS, Fournelle R, Ziebert G, et al. Mechanical behavior and failure analysis of prosthetic retaining screws after long-term use in vivo. Part 4: failure analysis of 10 fractured retaining screws retrieved from three patients. J Prosthodont. 2008;17:201–10.

143. Burguete RL, Johns RB, King T, et al. Tightening characteristics for screwed joints in osseointegrated dental implants. J Prosthet Dent. 1994;71:592–9.

144. Kayumi S, Takayama Y, Yokoyama A, et al. Effect of bite force in occlusal adjustment of dental implants on the distribution of occlusal pressure: comparison among three bite forces in occlusal adjustment. Int J Implant Dent. 2015;1:14.

145. Katona TR, Eckert GJ. The mechanics of dental occlusion and disclusion. Clin Biomech (Bristol, Avon). 2017;50:84–91.

146. Balik A, Karatas MO, Keskin H. Effects of different abutment connection designs on the stress distribution around five different implants: a 3-dimensional finite element analysis. J Oral Implantol. 2012;38 Spec No:491–6.

147. Bacchi A, Consani RL, Mesquita MF, et al. Effect of framework material and vertical misfit on stress distribution in implant-supported partial prosthesis under load application: 3-D finite element analysis. Acta Odontol Scand. 2013;71:1243–9.

148. Dittmer MP, Kohorst P, Borchers L, et al. Influence of the supporting structure on stress distribution in all-ceramic FPDs. Int J Prosthodont. 2010;23:63–8.

149. Aradya A, Kumar UK, Chowdhary R. Influence of different abutment diameter of implants on the peri-implant stress in the crestal bone: a three-dimensional finite element analysis--in vitro study. Indian J Dent Res. 2016;27:78–85.

150. Caglar A, Bal BT, Karakoca S, et al. Three-dimensional finite element analysis of titanium and yttrium-stabilized zirconium dioxide abutments and implants. Int J Oral Maxillofac Implants. 2011;26:961–9.

151. de Carvalho NA, de Almeida EO, Rocha EP, et al. Short implant to support maxillary restorations: bone stress analysis using regular and switching platform. J Craniofac Surg. 2012;23:678–81.

152. Lee JS, Lim YJ. Three-dimensional numerical simulation of stress induced by different lengths of osseo-integrated implants in the anterior maxilla. Comput Methods Biomech Biomed Engin. 2012;16:1143.

153. Chang CL, Chen CS, Yeung TC, et al. Biomechanical effect of a zirconia dental implant-crown system: a three-dimensional finite element analysis. Int J Oral Maxillofac Implants. 2012;27:49–57.

154. Kunavisarut C, Lang LA, Stoner BR, et al. Finite element analysis on dental implant-supported prostheses without passive fit. J Prosthodont. 2002;11:30–40.

155. Anchieta RB, Machado LS, Bonfante EA, et al. Effect of abutment screw surface treatment on reliability of implant-supported crowns. Int J Oral Maxillofac Implants. 2014;29:585–92.

156. Bates JF, Stafford GD, Harrison A. Masticatory function - a review of the literature. III. Masticatory performance and efficiency. J Oral Rehabil. 1976;3:57–67.

157. Kim ES, Shin SY. Influence of the implant abutment types and the dynamic loading on initial screw loosening. J Adv Prosthodont. 2013;5:21–8.

158. Cheng HC, Peng BY, Chen MS, et al. Influence of deformation and stress between bone and implant from various bite forces by numerical simulation analysis. Biomed Res Int. 2017;2017:2827953.

159. Verri FR, Batista VE, Santiago JF Jr, et al. Effect of crown-to-implant ratio on peri-implant stress: a finite element analysis. Mater Sci Eng C Mater Biol Appl. 2014;45:234–40.

160. Torcato LB, Pellizzer EP, Verri FR, et al. Effect of the parafunctional occlusal loading and crown height on stress distribution. Braz Dent J. 2014;25:554–60.

161. Moreira de Melo EJ Jr, Francischone CE. Three-dimensional finite element analysis of two angled narrow-diameter implant designs for an all-on-4 prosthesis. J Prosthet Dent. 2020;124:477–84.

162. Lopez CAV, Vasco MAA, Ruales E, et al. Three-dimensional finite element analysis of stress distribution in zirconia and titanium dental implants. J Oral Implantol. 2018;44:409–15.

163. Lima de Andrade C, Carvalho MA, Bordin D, et al. Biomechanical behavior of the dental implant macrodesign. Int J Oral Maxillofac Implants. 2017;32:264–70.

164. Manea A, Baciut G, Baciut M, et al. New dental implant with 3D shock absorbers and tooth-like mobility-prototype development, finite element analysis (FEA), and mechanical testing. Materials (Basel). 2019;12:3444.

165. Yemineni BC, Mahendra J, Nasina J, et al. Evaluation of maximum principal stress, Von Mises stress, and deformation on surrounding mandibular bone during insertion of an implant: a three-dimensional finite element study. Cureus. 2020;12:e9430.

Radiographic Imaging in Implant Dentistry

10

Andreas Stavropoulos, Kristina Bertl, Florian Beck,
Paolo Cattaneo, and Ann Wenzel

10.1 Introduction

Radiographic imaging is key in all phases of dental implant therapy, i.e., diagnosis, planning and assessment of treatment, and long-term monitoring, both in terms of clinical practice and in implant research. Traditionally two-dimensional (2-D) imaging has been the standard in clinical

A. Stavropoulos (✉)
Department of Periodontology, Faculty of Odontology, Malmö University, Malmö, Sweden

Division of Conservative Dentistry and Periodontology, University Clinic of Dentistry, Medical University of Vienna, Vienna, Austria
e-mail: andreas.stavropoulos@mau.se

K. Bertl
Department of Periodontology, Faculty of Odontology, Malmö University, Malmö, Sweden

Division of Oral Surgery, University Clinic of Dentistry, Medical University of Vienna, Vienna, Austria

Department of Periodontology, Dental Clinic, Faculty of Medicine, Sigmund Freud University, Vienna, Austria

F. Beck
Division of Oral Surgery, University Clinic of Dentistry, Medical University of Vienna, Vienna, Austria

P. Cattaneo
Division of Orthodontics, Department of Dentistry and Oral Health, Aarhus University, Aarhus, Denmark

Melbourne Dental School, Faculty of Medicine, Dentistry and Health Sciences, Melbourne, Australia

A. Wenzel
Division of Oral Radiology, Department of Dentistry and Oral Health, Aarhus University, Aarhus, Denmark

practice and research; however, recent technological advances and increased access to new technologies have made three-dimensional (3-D) imaging quite common in both clinical practice and research (e.g., cone-beam computed tomography; CBCT). Considering potential health risks due to radiation exposure, it is important to understand the possibilities and the limitations of the various radiographic techniques and technologies to assess the recipient bone for implant planning and the bone-to-implant interface and peri-implant bone level after installation.

10.2 Periapical Radiographs

Periapical radiographs can be used for treatment planning in straightforward cases, but they are most commonly used for assessing the marginal peri-implant bone levels at follow-up. Evaluation of the marginal peri-implant bone level, i.e., the distance from the most coronal bone crest to a specific implant landmark—commonly the margin of the implant collar—is relevant in implant research when assessing the effect of various implant macro-designs and surface technologies on the physiological bone remodeling occurring after implant installation and loading, or when assessing various surgical techniques, as the goal is to have the entire implant body within the bone. Further, monitoring the marginal peri-implant bone level and assessing possible

changes (i.e., bone loss) between different time points is essential, as stability of the marginal peri-implant bone level is considered the most reliable sign of peri-implant health [1]. In this context, various cut-off values of bone level have been suggested and employed among studies and classification systems to discriminate between a healthy implant and an implant with peri-implantitis [2, 3]. Nevertheless, it is accepted that there is some variation in crestal bone level distances that is compatible with peri-implant health. This variation depends, among other factors, on the implant system, i.e., different implant systems experience a different amount of crestal bone loss due to initial bone remodeling after implant installation and/or loading. It is thus obvious, that dimensional accuracy of the depicted/registered anatomical structures around implants is very important.

10.2.1 Distortion

Periapical radiographs of good quality provide high spatial and contrast resolution and thus sharp images but may show some degree of image magnification depending on the relative focal spot-to-film and object-to-film distance [4]. In general, an average magnification of 5% is usually accepted for periapical radiographs recorded with the paralleling technique [5], irrespective of the site within the mouth. Nevertheless, studies comparing measurements/distances of structures recorded in periapical radiographs with direct measurements showed that the range of differences may be quite large. For example, Sonick et al. [6] compared the localization of the mandibular canal with the clinically measured distances and those made in periapical images obtained by a long-cone paralleling technique, with a film holder attached to the tube of the X-ray unit; the difference in absolute values between clinical and radiographical measurements was only 1.9 mm on average, however, a range of 0.5 to 5.5 mm was observed, which in turn translated into a magnification ranging from 8% to 24% (14% on average). Similarly, Schropp

et al. [7] observed an average magnification of 6% when evaluating the distortion of metal calibration balls recorded in periapical radiographs, however, the range was from 1% to 12%. Although the dimensional distortion in periapical radiographs may not constitute a major problem in everyday clinical work, estimation of the true magnification is necessary for studies on the prevalence of peri-implant biological complications and differential diagnosis (i.e., mucositis and peri-implantitis), and/or for early detection of peri-implantitis to allow timely therapeutic interventions. Indeed, studies assessing the prevalence and/or incidence of peri-implantitis require not only the presence of clinical signs of disease but also the presence of bone loss beyond the crestal bone level changes resulting from initial bone remodeling, taking also a measurement error in periapical radiographs of 0.5 mm, on average, into account [8]. In this context, estimation of the true magnification in periapical radiographs appears imperative for research purposes.

Several methods have been suggested for calibration purposes of periapical images, for example, the use of cylindrical metal markers [9] or of a metal ball with a standardized diameter [7] (Fig. 10.1). Autoclavable cylinder metal markers, used often as indicators for implant angulation during treatment planning, can also be used for calibration purposes. However, despite the fact that no information on the implant angulation can be obtained by means of a metal ball, this method offers the advantage that projection geometry does not influence the radiographic image due to the symmetrical shape of the ball, and thus, is to be preferred. In context, in periapical images depicting implants, it is most often not necessary to include a reference marker, since the implant itself can be used for calibration purposes, provided that information on implant dimensions is retrievable or the distance between the peaks of the implant threads is known. Obviously, using the peaks of the implant threads for calibration purposes requires that radiographs show an optimal projection geometry in the vertical plane, i.e., the image displays sharp threads with no overlaps on both sides of the implant.
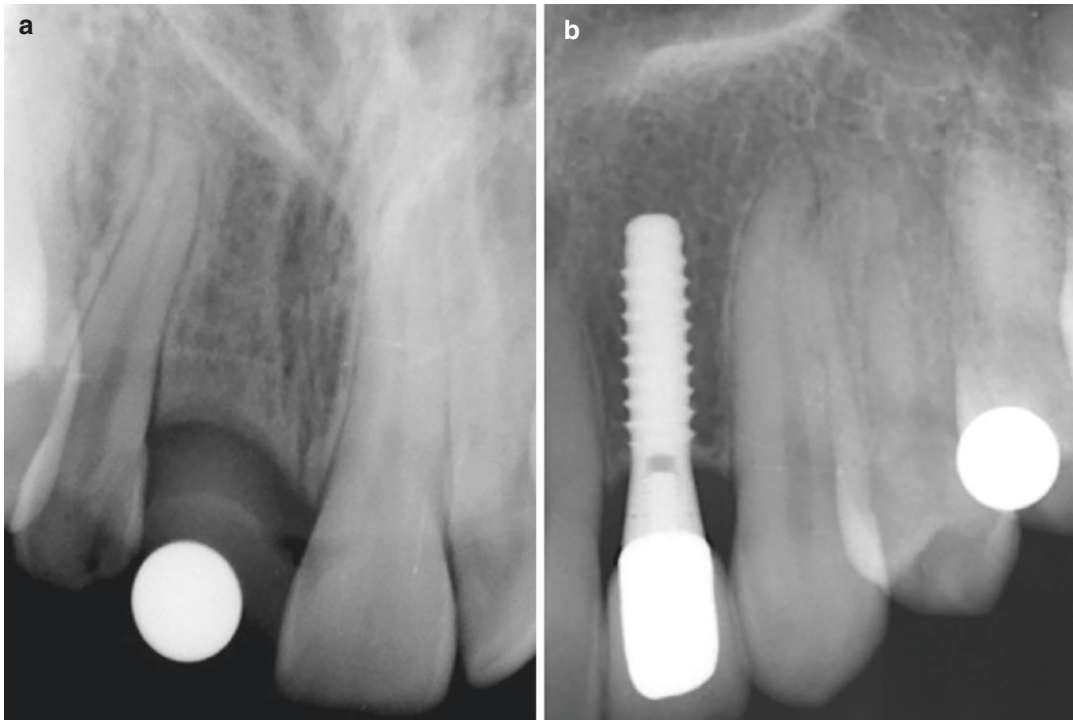
Fig. 10.1 A metal ball (5 mm diameter) can be used for calibration purposes in periapical radiographs, during treatment planning where no implant is included (**a**), but also when an implant of unknown dimensions is registered (**b**)

Nevertheless, in cases where pre-surgical radiographs (i.e., without an implant) are included in the analysis, a metal ball or other reference marker should be used.

10.2.2 Projection Geometry

Proper projection geometry in the vertical plane, so that the implant displays sharp threads with no overlaps on both sides, is important not only for calibration purposes but also to facilitate proper assessment of the marginal peri-implant bone level at follow-ups. For example, in a radiograph taken with the radiation beam being not perpendicular to the long axis of the implant, the threads of a screw-type implant appear blurred on either side of the implant; this may not allow for properly define the most coronal bone-to-implant contact (BIC). On the other hand, with an optimal projection angle in the vertical plane, i.e., the

film/digital receptor is positioned parallel to the implant axis, and the radiation beam is directed perpendicular to this axis, the implant image displays sharp threads with no overlaps on either side allowing proper evaluation and recording of the peri-implant bone levels (Fig. 10.2).

Proper projection geometry in periapical radiographs is also crucial for controlling for possible risk factors for technical or biological complications, e.g., the misfit between implant and/or prosthetic components, component fracture, or cement remnants (Fig. 10.3). Obtaining implant images with optimal projection geometry may be challenging due to the fact that implants are often not inserted with an inclination corresponding to that of the alveolar process or neighboring teeth. This might especially be the case in fully edentulous patients, but also in single tooth gaps in agenesis sites where variable amounts of alveolar bone may be missing. Thus, correct alignment of the radiation beam is often difficult
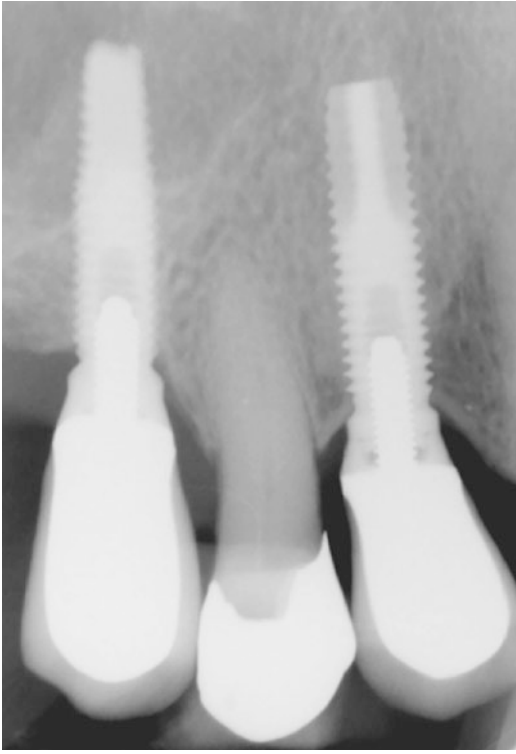
Fig. 10.2 The left implant image presents with threads blurred on either side, which makes it difficult or impossible to properly define the most coronal radiographic BIC. In contrast, the right implant presents with sharp threads and no overlaps on either side of the implant, making identification of the most coronal radiographic BIC easy. Due to differences in the implant inclination within the jaw, the radiation beam was not perpendicular to the long axis of the implant and the sensor for the left implant, but it was for the right one

to predict when the implant is still submerged or before the prosthetic restoration has been mounted; but even in cases including the prosthetic restoration, correct determination of the implant axis by clinical examination might be impaired as the abutment and restoration may be angulated.

Depending on the direction of the radiation beam, i.e., the beam has either an obtuse or an acute angle in relation to the long axis of the implant, the implant threads of a screw-type implant appear on the radiograph mostly blurred on the left or right side, respectively [10]; this is irrespective of whether the implant is placed in the upper or lower jaw. In the case of radiographs

with blurred implant threads, the "RB-RB/LB-LB" mnemonic rule, suggested by Schropp et al. [11], can be applied in order to correct the inclination of the X-ray tube and obtain a second image with sharp implant threads. RB/RB means, "if Right Blur, then Raise Beam" (Fig. 10.4), i.e., if the threads are mostly blurred at the right side of the implant image, the X-ray beam direction must be raised towards the ceiling to obtain sharper threads on both sides. Accordingly, LB/LB means, "if Left Blur, then Lower Beam," i.e., if the implant threads are mostly blurred at the left side of the implant image, the X-ray beam direction must be lowered towards the floor to obtain sharper threads on both sides.

The degree of beam correction needed can be roughly estimated by the degree of implant thread overlapping; i.e., if the threads on one side of the implant image are still rather clearly discernible, a correction of the radiation beam of up to about 10° is needed, while if the threads in both sides of the implant image are poorly discernible, a correction of the radiation beam of about 20° is needed (Fig. 10.5) [12]. Obviously, a prerequisite for the RB-RB/LB-LB mnemonic rule to properly function is that the film/sensor is also repositioned so that the radiation beam is kept perpendicular to the film/sensor, e.g., by means of a holder, while the position of patient's head remains stable during the repeated exposures.

Implementation of the RB-RB/LB-LB mnemonic rule has been proven rather easy, since even operators inexperienced in radiography (third-year dental students), after a short instruction in the use of the rule, were able to record higher quality implant images in 2/3 of the cases by changing the vertical projection angle in the correct direction from one exposure to the next [11]. Specifically, in this in vitro study, after an average of only 2 exposures, images either perfectly sharp or only with slightly blurred threads, were obtained, even in cases of extreme—compared to the neighboring teeth—implant inclinations. In another in vitro study, after a maximum of 2 exposures, no significant differences were observed between the use of the RB-RB/LB-LB mnemonic rule or the use of customized rigid imaging guides (acrylic splints) in terms of effi-
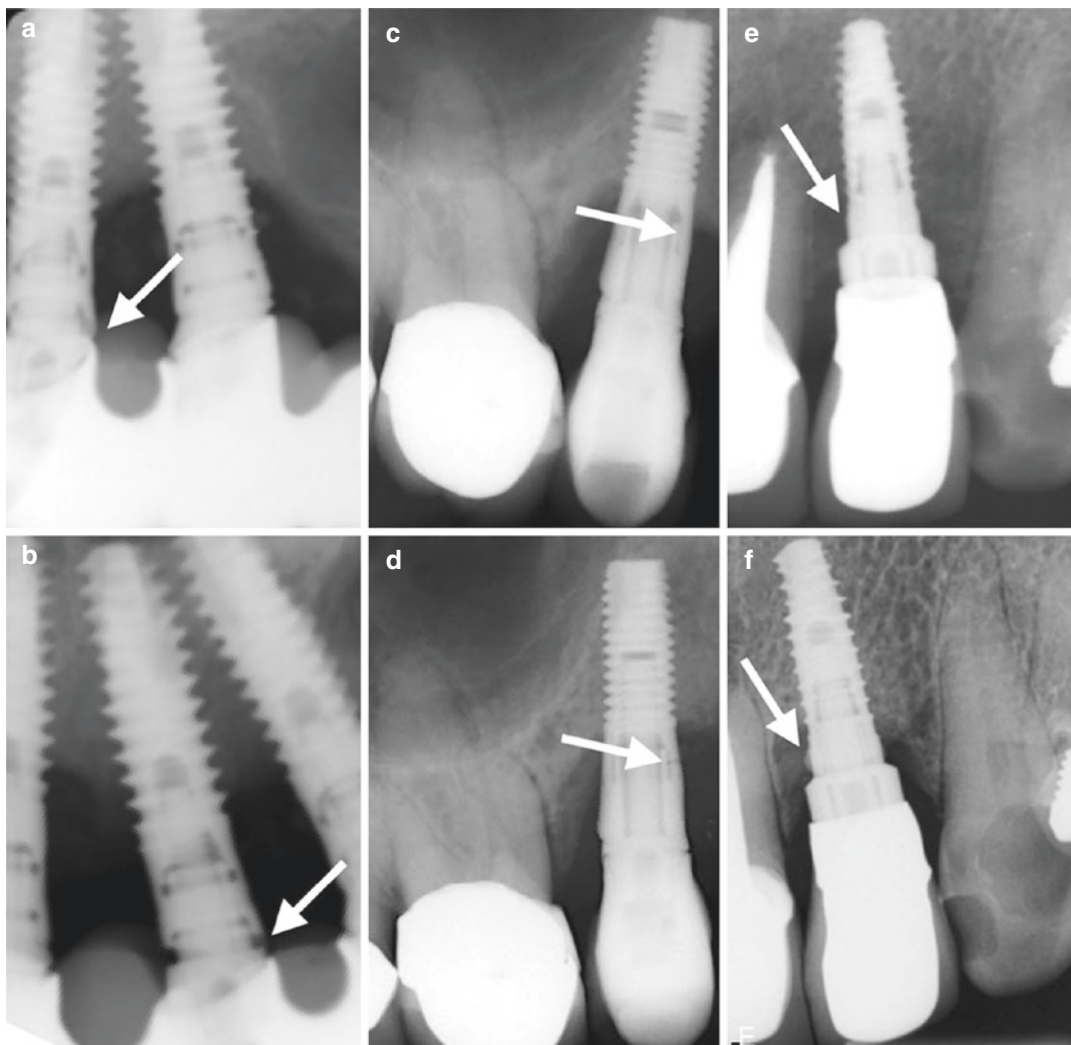
Fig. 10.3 Examples of radiographs with improper (**a**, **c**, **e**) and proper (**b**, **d**, **f**) projection geometry. Proper projection geometry, i.e., the radiograph is taken with the radiation beam being perpendicular to the long axis of the implant, facilitates proper diagnosis of technical and biological complications, e.g., misfit of prosthetic components (**a** vs. **b**), fracture of the implant neck (**c** vs. **d**), and cement remnants (**e** vs. **f**)

cacy of obtaining images with perfectly sharp threads or images with only slightly blurred threads, i.e., more than 70% of the cases were judged acceptable or perfect [13]. In perspective, considering the relatively limited added benefit and the much larger effort needed for constructing a customized imaging guide, it is reasonable to suggest that for monitoring purposes in the clinic or in large field studies the RB-RB/LB-LB mnemonic rule is sufficient.

10.2.3 Reliability of Measurements

For standard monitoring of implants in the clinic, a crude method of evaluating the stability of peri-implant bone levels in consecutive periapical radiographs is by simply comparing the level of marginal peri-implant bone to a reference landmark; for example, counting the number of implant threads with no BIC in radiographs taken at different time points is an easy way to assess
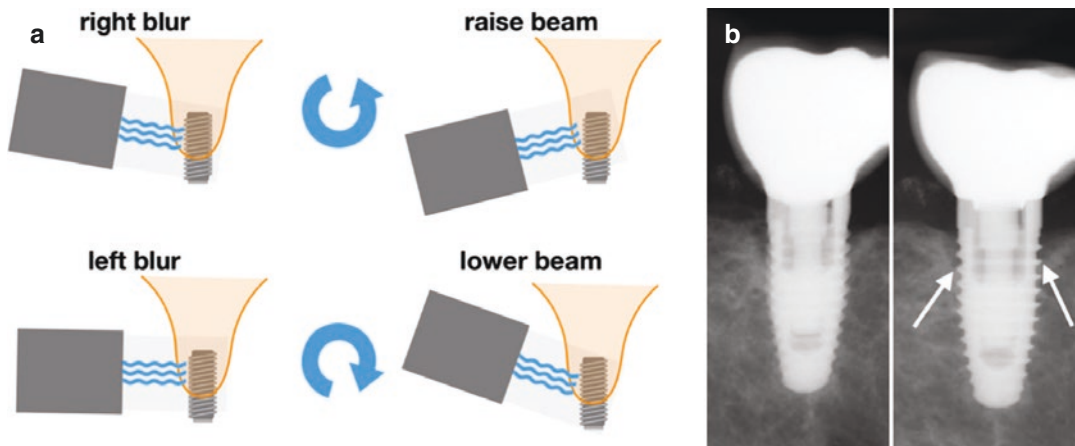
Fig. 10.4 Graphic presentation of the RB-RB/LB-LB mnemonic rule (**a**), with an implant inserted in the upper jaw. If the implant threads are mostly blurred at the right side of the implant image, the radiation beam direction must be raised towards the ceiling to obtain sharper threads on both implant sides. If the implant threads are mostly blurred at the left side of the implant image, the radiation beam direction must be lowered towards the floor to obtain sharper threads on both implant sides. (**b**) An implant in position 45 is registered with blurred threads, mostly at its left side; to the right, a new exposure with the beam lowered by about 15° results in an implant image with sharp threads at both sides allowing identification of the radiographic BIC. It is noteworthy that the RB-RB/LB-LB mnemonic rule applies irrespective of whether the implant is placed in the upper or lower jaw
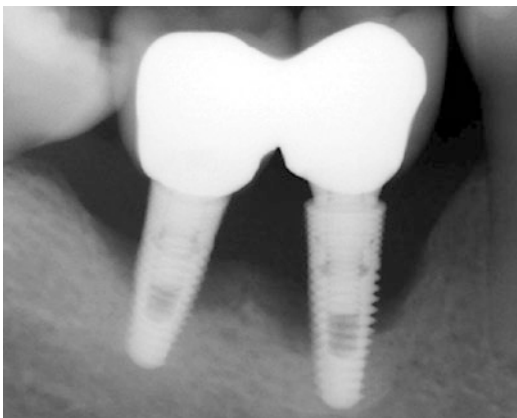
Fig. 10.5 For screw-type (threaded) implants, a deviation of the radiation beam of up to about 10° from the right angle to the axis of the implant, results in an implant image with threads at either side still rather clearly discernible (right implant); when the deviation of the radiation beam is about 20° or more, the threads are poorly discernible at both sides of the implant image (left implant)

progressive bone loss. For research purposes, however, where high data precision is mandatory, peri-implant bone levels may be evaluated by measuring the distance from a reference land-mark to the most coronal radiographic BIC by means of image analysis software. Usually, the shoulder of the implant is used as the fixed reference landmark, as it most often corresponds to the level of the bone at insertion (for bone-level implants) and is generally readily recognizable (Fig. 10.6).

Depending on the type of implant connection and/or abutment or prosthetic material type, identification of the fixture-abutment margin can be sometimes difficult; in such cases the margin of the prosthetic restoration or the apex of the implant can be used as a fixed landmark (Fig. 10.7). However, in such cases, only relative changes in bone levels (e.g., between two time points) should be considered, as the level of the bone at insertion cannot be determined.

In this context, the accuracy of radiographic recordings of marginal bone levels in terms of representing the true (histological) marginal peri-implant bone levels has been assessed in pre-clinical in vivo studies using clinical-type implants. Most of the studies showed that radiography underestimates peri-implant bone level
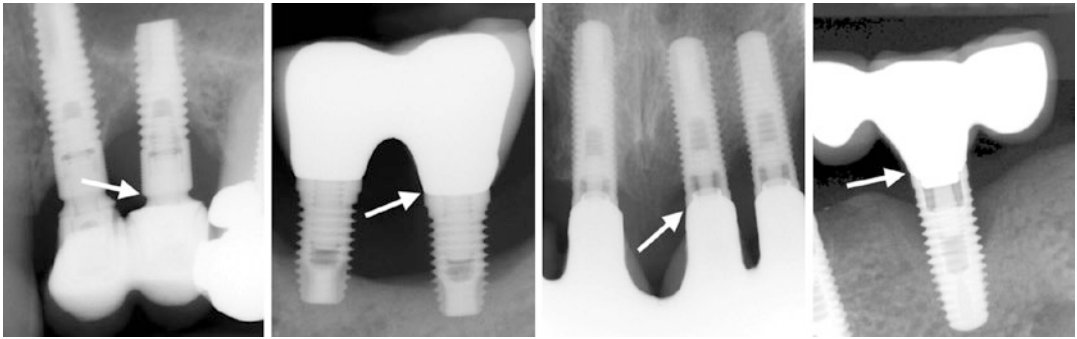
Fig. 10.6 The implant shoulder (indicated by the arrows) is usually quite easily identified and is commonly used as the reference landmark because it most often corresponds to the level of the bone at insertion (for bone-level implants)
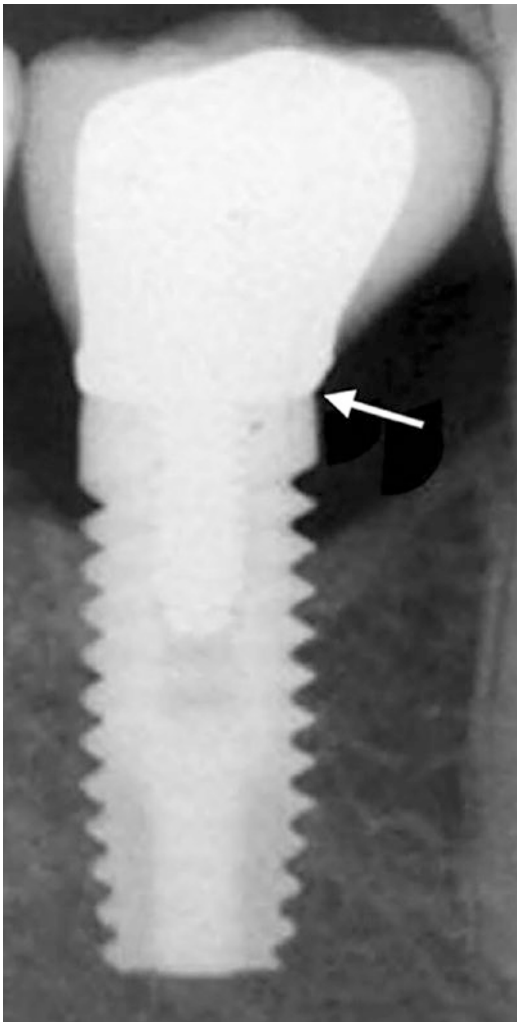
Fig. 10.7 When the implant shoulder cannot be identified, the margin of the prosthetic restoration (arrow) or the apex of the implant can be used as the fixed landmark for assessing relative changes in bone levels

in the majority of cases with about 0.5 mm [14–18]. For example, one study in dogs showed a correlation of 0.7 ($p < 0.01$) between bone level measurements made in digital intraoral radiographs and in histological sections, while the differences were 0.5 mm or less in half of the cases, but the average difference between radiographic and histological measurements was 1.17 mm. Similarly, another study showed that the radiographic evaluation underestimated the bone level by 0.6–1.4 mm [17, 18]. These observations imply that radiography may indeed in some cases fail in diagnosing a considerable amount of bone loss. In perspective, it has been demonstrated that probing pocket depth measurements (with or without standardized probing force) at implant sites do not necessarily correlate well with the bone level either. Specifically, depending on the degree of inflammation in the peri-implant tissues, the probe tip is farther from or closer to the bone level (in healthy and in inflamed tissues, respectively) [19, 20], and additionally, the prosthetic reconstruction often interferes with proper probe positioning/angulation [21] (Fig. 10.8).

Thus, the marginal peri-implant bone level can be estimated more precisely in periapical radiographs than with clinical probing, while no significant differences have been reported between conventional and digital periapical radiography (i.e., sensors or photostimulable phosphor plate systems) regarding the diagnostic accuracy in detecting and estimating the size of peri-implant defects [22–26]. It is however important to keep in mind that radiographic evi-
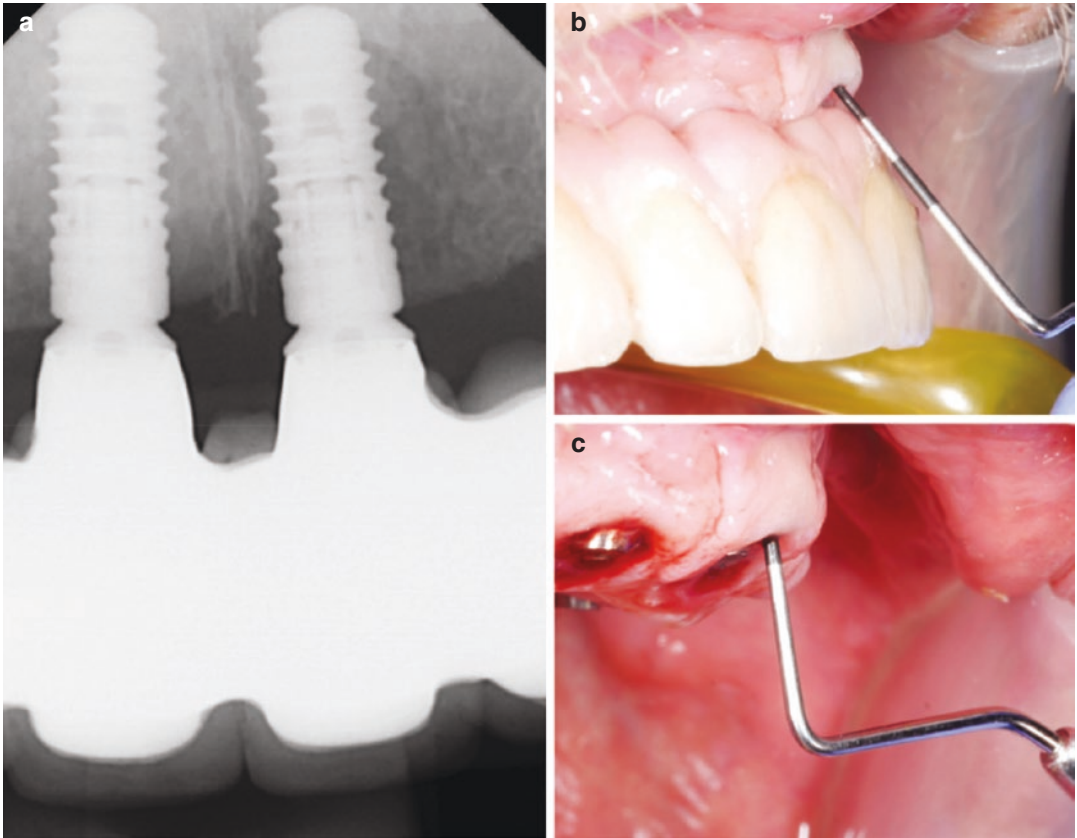
Fig. 10.8 The implant in position 21 has completely lost osseointegration (**a**) and harbors a very deep pocket which cannot be properly probed (**b**) due to the configuration of the prosthetic reconstruction interfering with a proper probe angulation (**c**)

dence of BIC does not necessarily imply osseointegration on the histological level [27].

A limitation of periapical images is that they display only a limited part of the alveolar process and consequently may in some instances register only part of an implant; e.g., in situations where extensive bone loss due to disease and/or physiological remodeling after long periods of edentulism has resulted in the implant placed "too deep" in comparison with the neighboring alveolar crest (Fig. 10.9) or cases with a flat palate impeding proper placement of the sensor (Fig. 10.10). In most cases, this poses no problem, as it is more important to display the coronal part of the implant with sharp threads for optimal bone level estimation than to image the apical part of the implant.
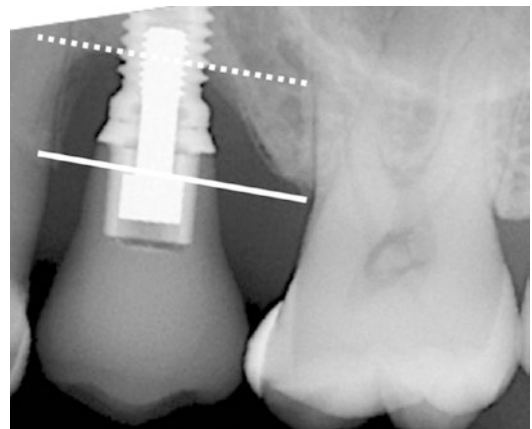
Fig. 10.9 The implant in position 25 is placed "too deep" in comparison with the neighboring alveolar crest and thus, it is difficult to register the entire implant length with proper projection geometry

Fig. 10.10 In the case of a flat palate (**a**), proper placement of the film holder/sensor is not possible (**b**), resulting in recording only a part of the implant (**c**); in this particular case, the peri-implant bone level is at the normal level for this specific type of implant, hence not displaying the entire implant does not pose a diagnostic problem
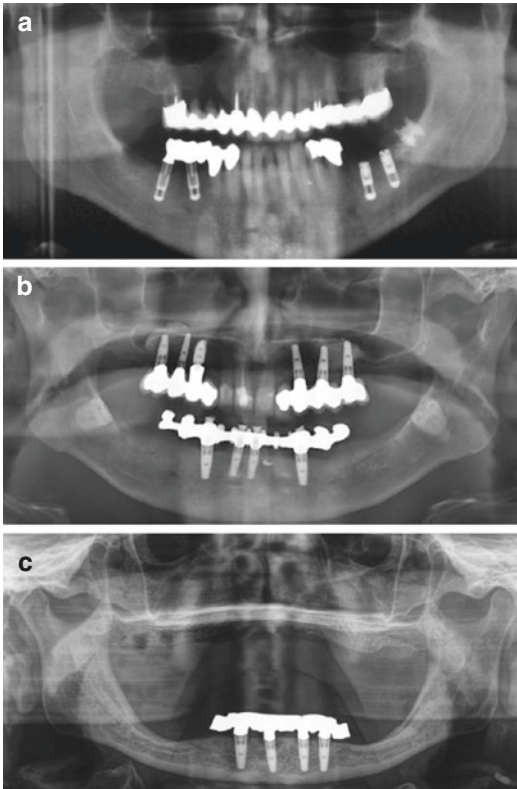
10.3 Panoramic Radiographs

Panoramic radiography provides an overview of the jaws and the overall status of the teeth and surrounding periodontal and periapical conditions, including the interrelations of the various neighboring anatomical structures. Panoramic radiographs are cheap and highly available, and the radiation dose of digital equipment is comparable to approximately 4 periapical radiographs. On the other hand, due to the projection technique panoramic radiographs also display an overlap of non-dental anatomic structures (e.g., the spine) or among neighboring teeth (particularly among the premolars in the upper jaw). Additionally, the lower spatial resolution and the enlargement factor must be considered; such issues may negatively influence measurement precision and accuracy.

In studies evaluating the periodontal bone level in panoramic or periapical images in comparison with direct intra-surgical measurements, panoramic images had a significantly lower accuracy than periapical images in terms of detecting bone loss and estimating the bone level (i.e., mostly underestimating the bone level) [4, 27, 28]. Thus, up-to-now panoramic radiography cannot be considered the method of choice for research purposes for evaluating details regarding the outcome of treatment or for monitoring the peri-implant bone level as measuring precision is required. Panoramic examination has been used, however, for evaluating the outcome of maxillary sinus augmentation procedures, because the entire sinus including the apical portion of the implant can be more easily visualized in these images compared to the smaller-field periapical radiography [29, 30]. In general, a panoramic image is often used when more than one implant are to be installed, for selecting the appropriate implant size and position during treatment planning in straightforward cases where the bucco-lingual dimension of the alveolar process can be clinically judged. Nevertheless, the distortion and enlargement of structures in the image have to be taken into consideration by a calibration procedure.

Panoramic images are not considered appropriate for evaluating marginal peri-implant bone conditions in the clinic, although, in specific clinical situations, panoramic radiographs may be preferred to periapical radiographs. For example, in cases with many implants, where proper radiographic registration of implants is cumbersome or even not possible with periapical radiography due to the anatomical situation; e.g., in cases of highly atrophied mandibles, where the residual alveolar process is close to or at the level of the floor of the mouth. In this context, it has to be noted that the image quality, including the frontal regions, has substantially improved during recent years due to technically controlled, more penetrating radiation given to this region during the exposure that blurs the shadow of the spine in the image (Fig. 10.11). Further, new-generation radiographic devices allow for registering segmented panoramic images in the vertical or horizontal plane, which de facto reduces the radiation

Fig. 10.11 The evolvement of the quality of panoramic radiographs from analog (**a**) to different generations of digital images (**b**, **c**)

burden to the patient and often results in sharper images. Thus, the usefulness of panoramic radiography may increase in the future.

10.3.1 Distortion

In general, a rather large magnification is inherent in panoramic images and depends on several factors, such as patient position/malposition, mandibular angulation, and equipment [31–34].

Magnification moreover varies among the regions of the mouth in the same image, as well as in the horizontal and vertical plane. In a clinical study involving patients to receive implants in various regions of the mouth [7], the true magnification in panoramic images was estimated by measuring the dimensions of a standardized metal ball of known size that was placed close to the anticipated implant site during exposure; although the average magnification was 22%, a great variation in magnification existed, ranging from −10 to 90%. Furthermore, it was observed that a larger variation in magnification was found in the horizontal plane than in the vertical plane (i.e., distortion), and the largest deviation from the standard magnification factor of 25% was seen in the horizontal plane and was most pronounced in the maxillary anterior region [7]. Furthermore, in another ex vivo evaluation (unpublished data), 25 metal balls 5 mm in diameter were placed buccally at the height of the crown and of the apex in the upper and lower jaw of a dry human skull, and at the occlusal plane in the molar, premolar, and anterior region (Fig. 10.12); the images of the spheres presented often as an ellipse with different orientation and magnification depending on the position of the sphere, with the maximum and minimum diameter of these ellipses ranging between 4.58–5.85 mm and 3.11–5.03 mm, respectively. In perspective, based on the fact that large variation in panoramic image distortion exists, depending on the region in the mouth as well as on the equipment, it seems reasonable to suggest that for research purposes a reference marker of known dimensions, like the metal ball mentioned before, should be placed on top of the alveolar process in the area of interest during exposure and used for calibration to true size measurements [35].
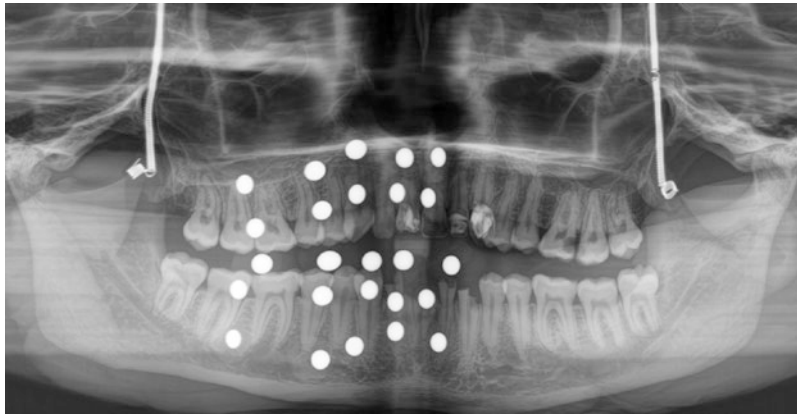
Fig. 10.12 Panoramic radiograph of a dry human skull with 25 metal balls (each 5 mm in diameter) placed buccally at the height of the crown and apex in the upper and lower jaw, and at the occlusal plane in the molar, premolar, and anterior region. Depending on the region, the metal balls were displayed as ellipses in different orientations and magnifications with up to almost 1 and 2 mm differences from the actual diameter of 5 mm if the maximum and minimum diameter, respectively, was measured

10.4   3-D Radiography

10.4.1   CBCT

An obvious disadvantage of both periapical and panoramic radiography is that a 2-D image of 3-D structures is displayed. The missing buccolingual dimension can be captured with cross-sectional radiography, such as conventional computed tomography (CT) or CBCT. All 3-D radiographic techniques have in most studies been found superior to intraoral and panoramic radiography in visualizing anatomical structures, e.g., the mandibular canal [6, 36–44]. 3-D radiographic techniques (i.e., CT and CBCT) have also been found superior to periapical radiography in identifying various types of artificially created bone defects (including periapical defects) [45–49] or bone lesions of endodontic origin [50, 51]. In a study comparing the image quality and visibility of anatomical structures in the mandible among five CBCT scanners and one multi-slice CT system (MSCT), CBCT was found to be comparable or even superior to MSCT [52]. CT and CBCT offer also the advantage, compared with periapical and panoramic images, of practically no dimensional distortion, as well as the possibility of visualizing 3-D reconstructions of the registered hard tissues. Due to the considerably lower radiation dose of CBCT compared to CT, the constantly increasing quality, smaller fields-of-view, and lately affordable prices, CBCT is a prevailing technology [53].

CBCT may be used in implant dentistry for implant treatment planning, for example, in cases where clinical examination or conventional radiographic techniques may indicate inadequate bone volume for implant installation or anatomical aberrations are suspected that may require special attention or modification of the surgical technique, e.g., a narrow residual alveolar ridge or a deep submandibular fossa, or the presence of septa when a sinus lift augmentation procedure is planned [54]. In this context, studies have assessed how the additional information from the third dimension, i.e., the bucco-oral bone width, changes the selection of the implant size when compared with planning based on information from a panoramic image [55–58]. For example, in one study involving 121 single implant sites, the implant size selected based on only panoramic images differed in almost 90% of the cases in width and/or length from that selected with CBCT, having access to additional information on the bucco-oral width [58]. Further, approximately

50% of the anterior implants planned based on information from CBCT were narrower compared to those planned based on a panoramic radiograph. Similarly, in another study on 71 patients with 103 implant sites, planning based on CBCT re-categorized the majority of cases into a narrower or shorter implant size compared with planning based solely on panoramic radiographs [55]. With regard to sinus lift, although in most cases a panoramic radiograph is considered sufficient for planning a sinus augmentation procedure, a preoperative CBCT scan increased surgical confidence and detection rate of sinus septa and mucosal hypertrophy [59–61]. In fact, a study involving 101 patients judged in need of a sinus lift procedure based on periapical and/or panoramic radiographs showed that in about 65% of the cases, an implant of at least 8 mm could be placed without sinus augmentation when planning was based on CBCT [62]. Indeed, a recent study demonstrated that due to the high variability

of the dimensions of the maxillary sinus, both in-between patients but also in-between tooth regions within the same patient, the bucco-oral sinus width cannot be assumed based on the residual bone height or standard values [63]. Thus, although there is no evidence that implant treatment planning or sinus lift procedures based on a CBCT examination result in better treatment results than those based on panoramic images, one may consider that knowing the proper implant size prior to surgery may be advantageous for the surgeon in order to be as well prepared as possible (e.g., alternative implant sizes in stock, instrumentation and material necessary for additional procedures like lateral bone augmentation, etc.), and of course for the patient in case that a more invasive procedure can be avoided.

Except treatment planning, CBCT has been used for the diagnosis of symptoms of unclear etiology associated with implants (e.g., paresthesia) (Fig. 10.13) and/or of bone defects associ-

Fig. 10.13 The paresthesia reported by the patient since the time of implant placement could not be explained based on the information provided by the panoramic radiograph (**a**), but was easy to explain with the bucco-oral section provided by the CBCT (**b**); the implant apex is violat- ing the coronal/lingual aspect of the mandibular canal (arrow)

ated with implants, for assessing the marginal bone level around implants—in particular that of the buccal bone—and for assessing the outcome of bone regenerative procedures [49, 55, 58, 64–72]. For instance, the outcome of lateral bone augmentation with autogenous and allogenic bone blocks was compared based on CBCT recorded post-operatively and after 6 months [72]. Specifically, bucco-oral cross-sections were generated at the center of the fixation screw, ensuring spatial reproducibility of the sections from the two observation periods; one mask overlapping the bone block and one the pristine bone were generated on the post-operative CBCT, where the boundaries of the block were clearly recognizable. Then the sum of these two regions was subtracted from the region of a single mask overlapping the bone tissues in the 6-month CBCT, where the interface of the bone block and the pristine bone was not recognizable anymore. Based on the assumption that the volume of the pristine bone is not really changing during the observation period, bone block resorption could be estimated (Fig. 10.14).

Although CBCT has indeed been proven to be very accurate in terms of distance measurements of anatomical landmarks and dimensions of bone defects [49, 55, 58, 65, 68], there are concerns regarding the diagnostic accuracy of CBCT to assess peri-implant bone defects and the marginal peri-implant bone level. In a methodological study, a good correlation between the measurements of bone levels in CBCT scans and histological sections was shown, but the radio-graphic peri-implant bone level estimated with CBCT was on average 1.12 mm higher than the true histological bone level [73]. Similar results have been shown in other studies with mean differences up to 2.6 mm between CBCT estimates and true bone levels [74–76]. The discrepancies between CBCT and true measurements can be explained by the variations in image sectioning and display settings, such as section thickness and mapping of scalar values stored within the displayed image (e.g., windowing/contrast control), which are shown to have a large impact on the characteristics of the final image [77], but also by the questionable image quality of CBCT in close proximity to dental implants, due to beam-hardening artifacts from the metal of the implants and/or reconstruction [78]. The beam-hardening artifacts within the reconstructed images are cupping and streak artifacts. Cupping artifacts occur when the multi-energetic radiation beam passes through a round or oval object with a high atomic number, e.g., metal. The softer part of the radiation beam is absorbed in the object, and the part of the beam that has succeeded in penetrating the center of the object will be harder when it reaches the receptor than the part passing through the edges. Streak artifacts appear as dark bands between two dense objects, such as two dental implants in the same jaw (Fig. 10.15).

Several factors seem to influence the diagnostic accuracy of CBCT with regard to buccal bone measurements at implant sites [79–86]. For example, in an ex vivo study with implants inserted flush to the alveolar crest of human man-
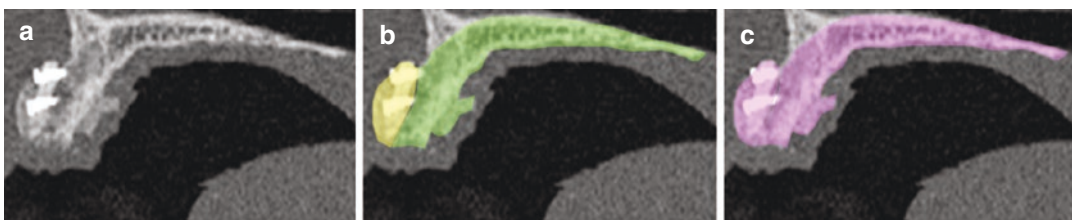
Fig. 10.14 Using the center of the fixation screw as a reference, spatial reproducibility of the sections between different observation periods is ensured; on the post-operative CBCT (**a**), where the boundaries of the block are clearly recognizable, masks overlapping the bone block and the pristine bone can be generated (**b**). The sum of the 2 regions is then subtracted from the region of a single mask overlapping the bone tissues in a later CBCT (**c**), where the interface of the bone block and the pristine bone is not recognizable anymore, to estimate bone block resorption
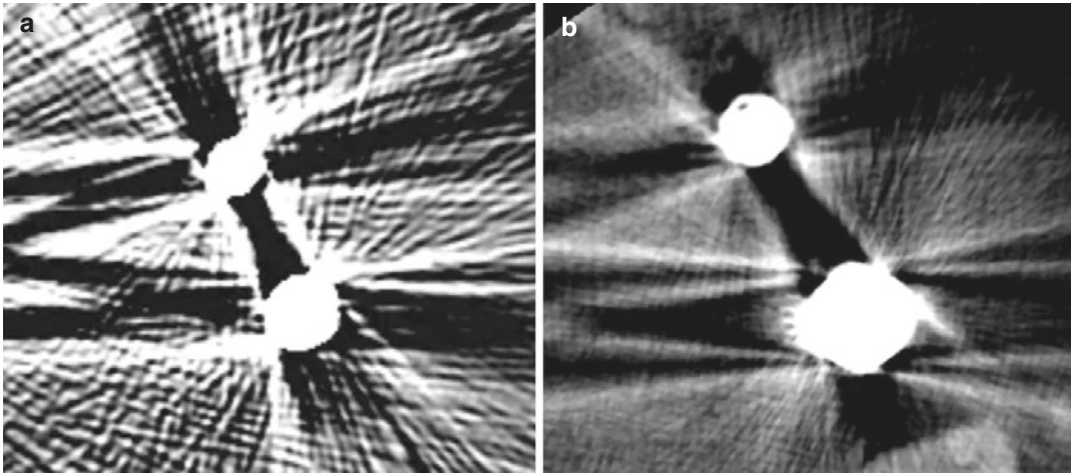
Fig. 10.15 Example of extreme beam-hardening artifacts between 2 dental implants in a CT (**a**) and CBCT (**b**) scan

dibles and harboring rectangular bone defects of varying dimensions at their buccal aspect, small volume defects (i.e., <3 × 3 mm) were much more frequently missed, compared with larger defects [82]. In two recently published in vitro evaluations in dry pig mandibles, it was demonstrated that various modifiable (e.g., the resolution and the image reconstruction thickness, the CBCT unit) and non-modifiable (e.g., the implant-abutment material, the number of implants in the field of view, the thickness of the buccal bone wall) factors influence the diagnostic accuracy of CBCT when assessing the buccal bone at implant sites [83, 84]. For instance, a high number of implants in the field-of-view, a low image resolution and reconstruction thickness, and the presence of a zirconium implant impair the correct diagnosis and/or measurements [83]. Further, a buccal bone wall less than 1 mm thick at implant sites was shown to significantly interfere with the ability of expert evaluators to discern whether or not a bone was present [83]. In another recently published ex vivo study [87], 9 out of 10 times a dehiscence was diagnosed although it did not exist when the buccal bone thickness was less than 1 mm, while when the buccal bone thickness was 1 mm or more, the presence of a dehiscence was wrongly attributed only in 20–30% of the cases (Fig. 10.16). In this

context, previous reports indicate that the majority of extraction sites in the anterior regions of the mouth present a thin buccal wall; thus, such sites experience larger dimensional changes, i.e., volume loss in terms of "buccal collapse," compared with posterior sites where the buccal bone is often thicker (> 1 mm) [88, 89]. It may be expected therefore that also anterior implants often present with a buccal wall less than 1 mm thick at the crestal aspect. It appears therefore, reasonable to suggest that CBCT should not be used to assess the buccal bone level at implants inserted in narrow alveolar ridges, especially in the anterior regions of the mouth (Fig. 10.17).

CBCT has also been suggested as a method to assess bone quality, i.e., more or less dense trabecular bone, as an analog to conventional CT. Although the judgment of bone quality based on Hounsfield Unit values is well accepted for conventional CT imaging [90, 91], a similar correlation between gray values in CBCT scans and bone quality cannot be assumed. Several studies have tested the possibility to correlate quantitatively gray values of CBCT scans to bone quality [90, 92–94]. However, gray values of CBCT scans are strongly affected by the CBCT device, positioning of the patient, artifacts, and imaging parameters, which do not allow any meaningful use of CBCT for assessing bone quality.
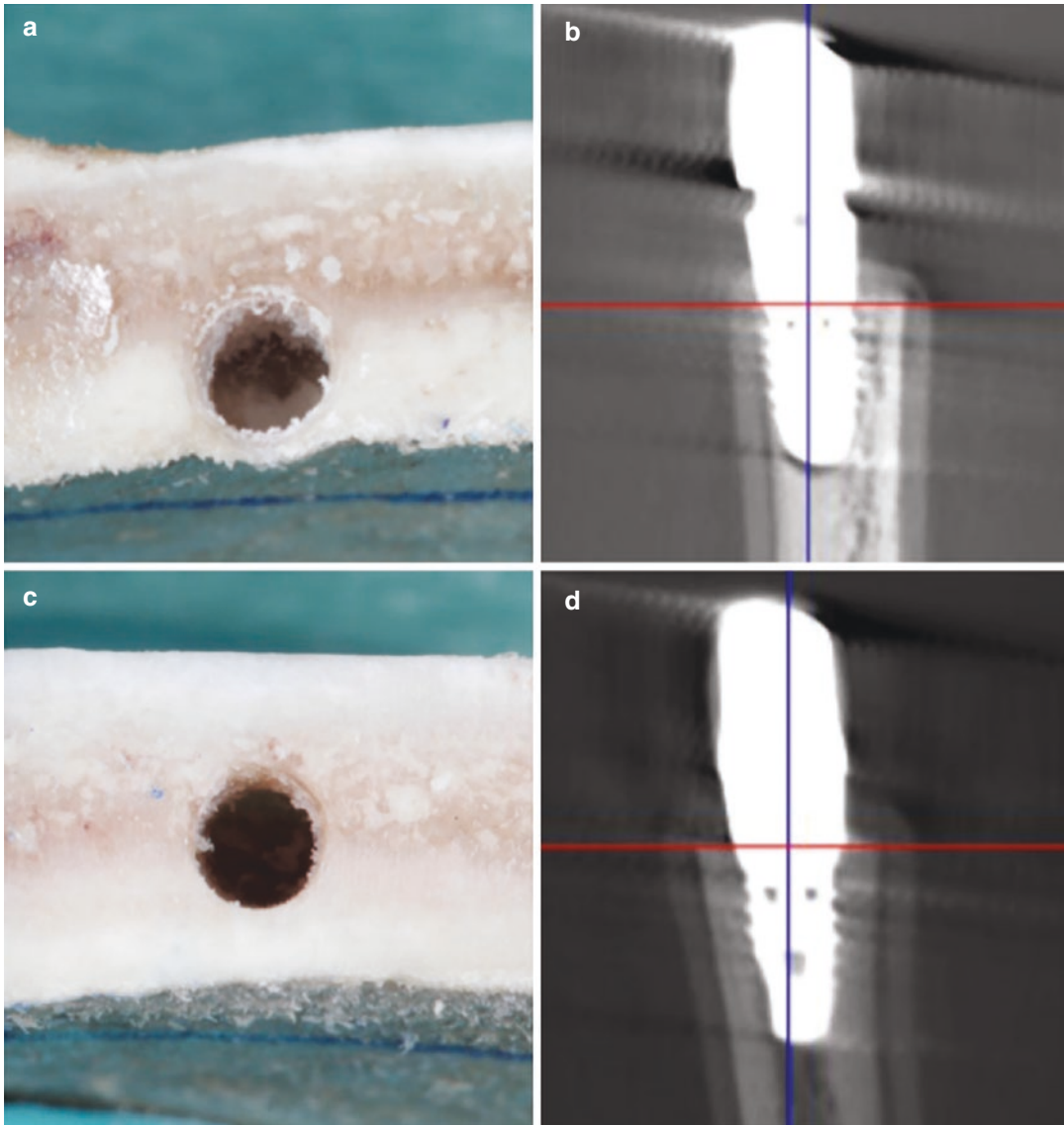
Fig. 10.16 A buccal bone thickness less than 1 mm (**a**) significantly interferes with the ability to discern whether the bone is present or absent in a CBCT scan (**b**), while a buccal bone >1 mm thick (**c**) is easier to identify (**d**). Note that the extra layer visible in the CBCT scans on the outside of the bone is a layer of pink wax imitating the soft tissue during the scan

In perspective, the use of CBCT is not recommended as a routine imaging technique for implant cases according to the European Guideline: Radiation Protection No. 172 [95]. Nevertheless, a recent study from Finland indicated a possible association between the reduced frequency of compensable malpractice claims related to dental implants and the increasing availability of CBCT technology [96].
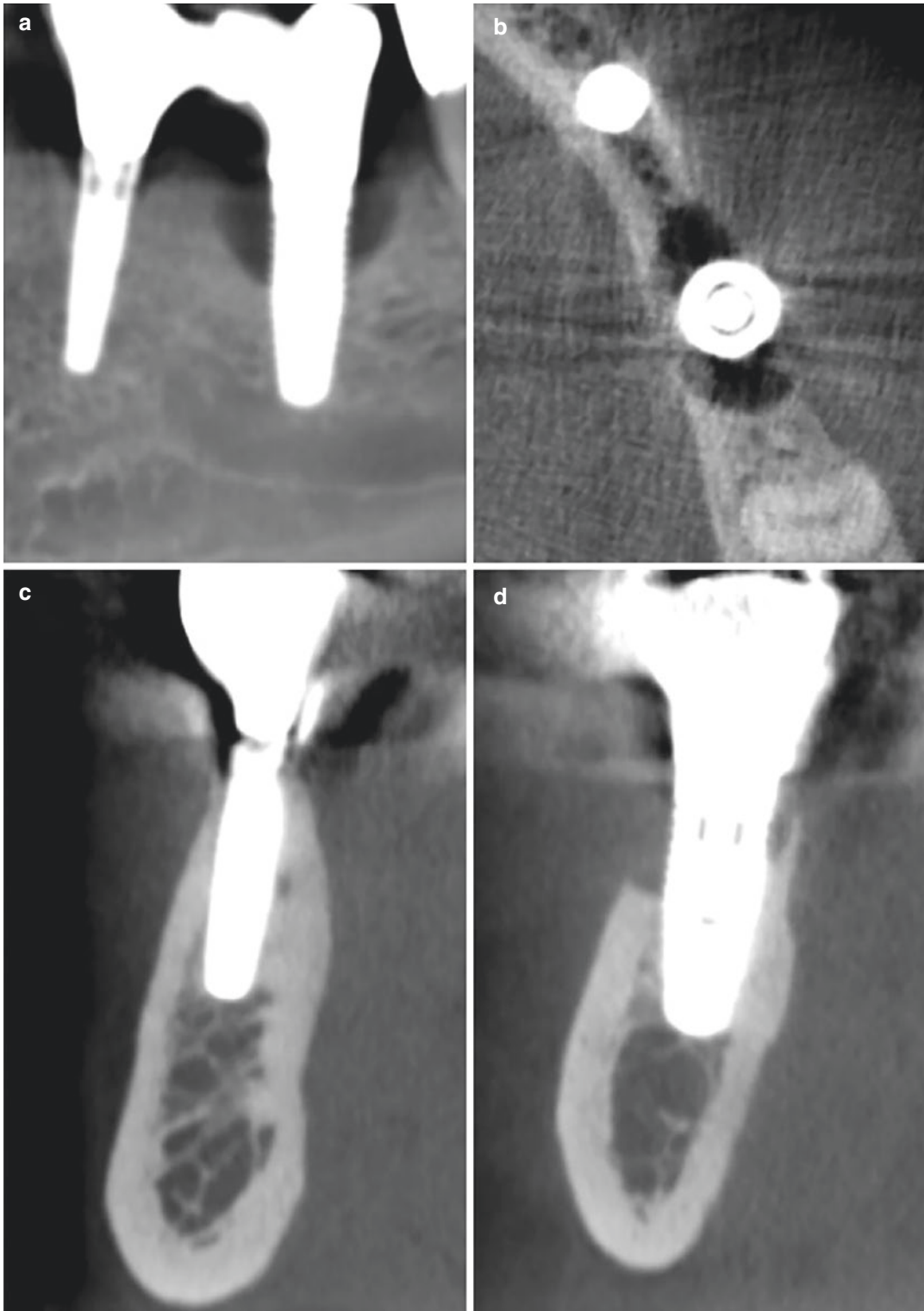
Fig. 10.17 Panoramic view (**a**), axial view (**b**), and cross-sectional view of the mesial (**c**; left implant in **a**) and distal (**d**; right implant in **a**) implant. Note that the level of the buccal bone at the mesial implant, where the bone is thin, cannot be clearly discerned, compared with that in the distal implant where the buccal bone is thick

10.4.2 MRI

Magnetic resonance imaging (MRI) provides an imaging modality free of ionizing radiation in contrast to conventional radiography or computed tomography (CT or CBCT), and it has been used for a long time in dentistry for imaging of temporomandibular joint (TMJ) disorders [97] REF SHOULD BE 96. The basic principle of MRI relies on the possibility of magnetizing atomic nuclei (protons), i.e., hydrogen atoms, which are found in different amounts in the human body. Hydrogen atoms are randomly orientated; however, they align parallel in the longitudinal axis of the body if an external magnetic field is turned on (resting alignment). This alignment can be disturbed by external radiofrequency (RF) waves. If the RF impulse is turned off, the protons return to their resting alignment by emission of RF energy, which is then captured by specific sensors and finally displayed as a grayscale image. Different relaxation times result in T1-weighted (longitudinal relaxation time) and T2-weighted (transverse relaxation time) images. They can be distinguished by, e.g., the cerebrospinal fluid, which appears dark (T1) or light (T2) [98].

Advances in MRI technology and the development of ultra-short or zero echo time sequences have broadened its spectrum for imaging, including hard tissues, e.g., bones, which have short T2 relaxation rates [99, 100], and thus the use of MRI is currently explored also within implant dentistry. MRI allows the visualization of cortical and trabecular bone of the maxilla/mandible, maxillary sinus, teeth, pulp chamber, periodontal space, and critical structures, including the lingual nerve and inferior alveolar nerve (IAN), mental foramen, and the incisive nerve (Fig. 10.18) [99, 101–104].

A clear depiction of bone and teeth is crucial if MRI should be considered a reasonable diagnostic method for the planning, placing, and monitoring of implants in dentistry. The appearance of bone in MRI is entirely different from CT and CBCT imaging, e.g., cortical bone consists by its nature of a relatively low number of nuclei (protons in water) that can be magnetized. As a result, cortical bone is displayed as a dark region corresponding to a signal void (Fig. 10.19) [105].

Recent studies considered MRI as an option for preoperative implant planning and even the fabrication of surgical guides. A comparison of virtually planned implants in MRI and CBCT datasets demonstrated no significant differences relating to the apical and coronal position of the implant. However, when comparing the distance from the alveolar crest to the mandibular canal (visualized in CBCT) with that to the inferior alveolar nerve (visualized in MRI), it was found
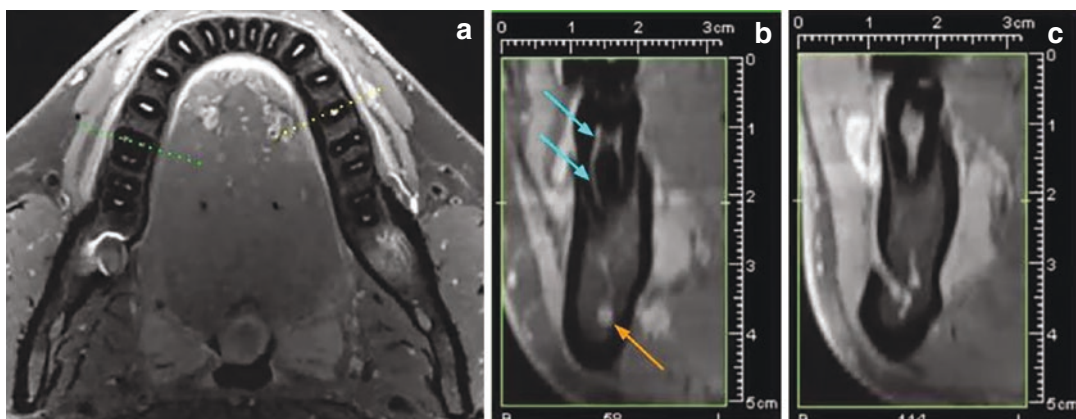
Fig. 10.18 Axial view of the mandible (**a**). Note the hypointense signal of the cortical bone and teeth in contrast to the hyperintense signal of the pulp. (**b**) The pulp and the root canals of the mesial root (first molar) are clearly depicted (turquoise arrows). The inferior alveolar nerve/neurovascular bundle can be directly visualized (orange arrow). (**c**) Visualization of the mental foramen in MRI
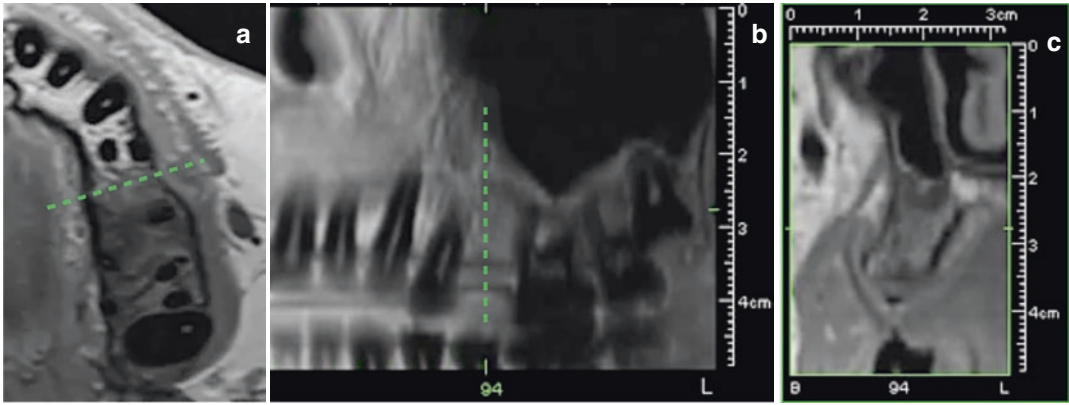
Fig. 10.19 Preoperative axial view of the implant planning site (**a**), the green dotted line on the panoramic-view (**b**) indicates the slice of orthoradial reconstruction (**c**) which allows measuring of the bone quantity

that it was significantly larger (by 1.3 ± 0.81 mm) in the MRI, i.e., implant planning by means of MRI would accept the installation of longer implants [106]. Nevertheless, there is no verification of the true distance from the alveolar crest to the inferior alveolar nerve, in vivo or in vitro.

MRI-based implant planning can be verified when this information is transferred to surgical guides and ultimately used for implant placement. Fully guided implant placement based on information from MRI has been successfully performed in vivo in five patients [107] and in vitro involving 16 human cadaver hemi-mandibles [108]. Planning and printing of the surgical guides were based solely on MRI data and optical surface scans. The in-vitro study design allowed comparison of the planned (MRI) and the final implant position (hemi-mandible) by postoperative CBCT and optical scans: deviations were 1.34 ± 0.84 and 1.03 ± 0.46 mm at the implant shoulder and 1.41 ± 0.88 and 1.28 ± 0.52 mm at the implant apex, respectively. Angular deviations of the implant axis were $4.84 \pm 3.18°$ and $4.21 \pm 2.01°$, respectively [108]. Despite the feasibility of using MRI for preoperative planning, it is evident that MRI (still) requires an additional optical scan for virtual implant planning. Teeth surfaces are depicted with insufficient accuracy, and alignment is basically based on soft tissue (e.g., keratinized mucosal surface) and/or radio-opaque markers [108]. A lower accuracy for MRI compared to CBCT for tooth surface reconstruc-

tion has been demonstrated: geometric deviations were 0.26 ± 0.08 and 0.1 ± 0.04 RMS, [1] respectively [109].

In this context, artifacts may occur in MRI similarly to CT and CBCT and can strongly impair the diagnostic value of the image. They can be classified according to their origin as patient (e.g., motion, metal artifact), signal-processing (e.g., chemical shift artifact, partial volume artifact), or hardware-related (e.g., external magnetic field inhomogeneity, gradient field artifacts) [110]. Metal artifacts result from the different magnetic susceptibility of adjacent tissues, e.g., the interface between a dental implant and bone, which can lead to (total) signal loss. Furthermore, the prosthetic restoration material also induces susceptibility artifacts. Resin as a crown material hardly produced any artifacts, while precious metal-ceramic, ceramic, and zirconia demonstrated minor artifacts. Furthermore, the number of crowns significantly affects the extension of the artifacts measured by area [111]. Similar results have been reported for implants restored with various types of crowns: monolithic zirconia crowns attached to zirconia implants demonstrated the least artifacts, followed by porcelain-fused-to-zirconia and monolithic zirconia crowns on titanium implants. Most artifacts were reported for titanium implants in combination with non-precious alloys [112]. Therefore,

---

[1]*RMS* root mean square.

patients considered for dental MRI should be screened for metal-containing fillings/restorations, orthodontic wires, or dental implants that may interfere with the region of interest.

The obvious advantage of having no ionizing radiation makes MRI a reasonable alternative for monitoring dental implants and 3D defect imaging in case of peri-implant diseases. However, the use of MRI appears more relevant for zirconia implants (Fig. 10.20), which are depicted more clearly, compared to titanium or titanium-zirconia implants, both demonstrating signal voids due to susceptibility artifacts [113] (Fig. 10.21). The distribution of artifacts is smaller for zirconia than titanium implants, irrespective of the implant's geometry or the site of measurement
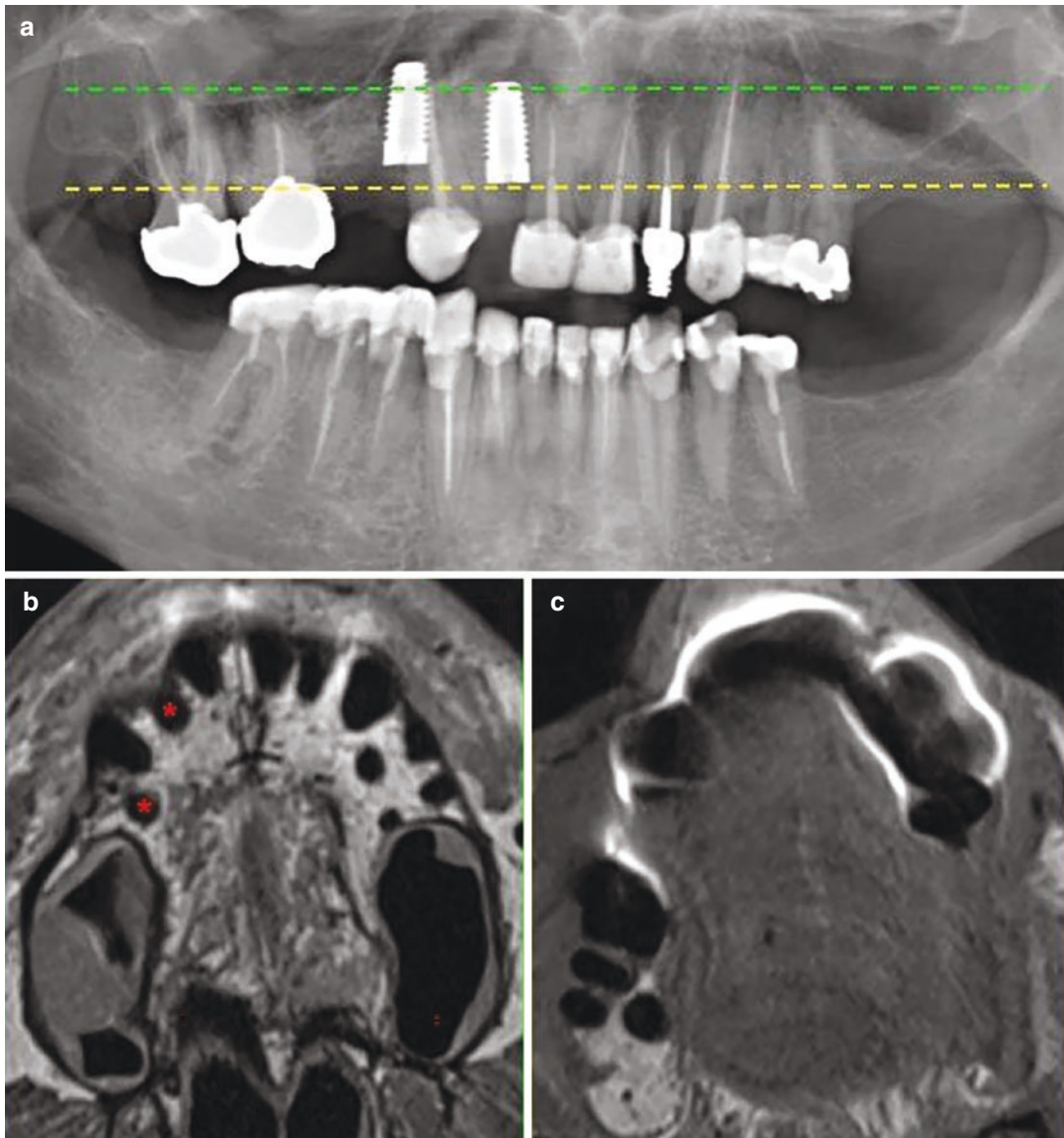
Fig. 10.20 Postoperative panoramic X-ray (**a**) and MRI (**b**, **c**) following placement of two zirconia implants. Note, MRI verifies that zirconia implants (red asterisks) do not interfere with adjacent teeth, despite the presence (**c**) of susceptibility artifacts
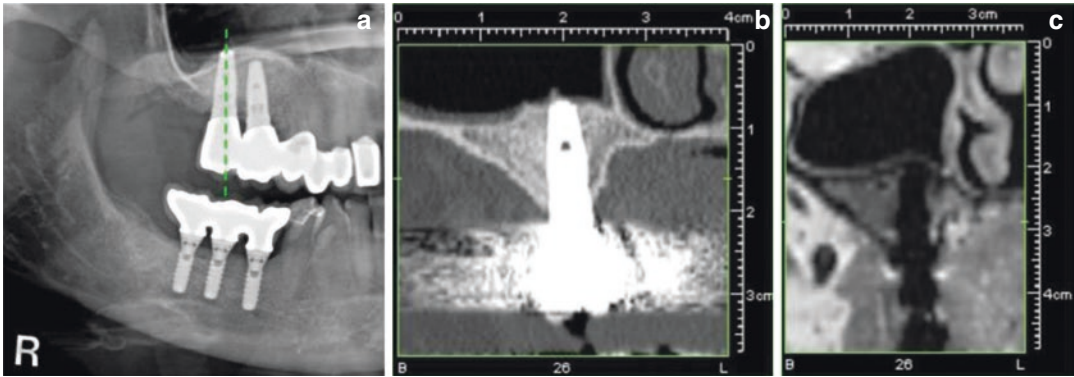
Fig. 10.21 Panoramic X-ray indicating titanium implants with zirconia crowns (**a**); the green dotted line demonstrates the orthoradial view in CT (**b**) and MRI (**c**) of implant #16. Note the strong and minor artifacts induced by the zirconia crown in CT (**b**) and MRI (**c**), respectively. In addition, the titanium implant appears slightly distorted in MRI (**c**) in comparison to CT (**b**) imaging

(e.g., buccal vs. lingual) [114]. Distance measurements of zirconia implants indicated a high correlation between MRI and CBCT, which is also reflected by the longitudinal and transversal accuracy of the actual implant's size, i.e., 0.8% and 2.3%, respectively. In contrast, the size of titanium implants was overestimated by 29.7% and 36.9%, respectively [115]. Both zirconia and titanium implants appear as hypointense structures, i.e., signal voids; however, artifacts were more significant on T2- than T1-weighted images [116]. However, similar results for MRI and CBCT have been demonstrated for the judgment of large peri-implant defects (i.e., 3 mm) around zirconia implants in-vitro, both outperforming intraoral radiographs. Nevertheless, intraoral radiographs performed better in detecting small defect sizes (i.e., 1 mm) [117].

Besides inherent artifacts, MRI remains a valuable diagnostic tool if an injury of the infe-rior alveolar nerve following implant placement is clinically suspected. MRI allows direct visualization of the inferior alveolar nerve in contrast to CT/CBCT, which may miss the protrusion of an implant into the mandibular canal if its corticalization is insufficient [103, 118]. MRI has also been investigated for the evaluation of bone augmentations, particularly maxillary sinus floor augmentations (MSFA) and onlay grafts. Vertical bone height changes following MSFA can be assessed safely using MRI (Fig. 10.22) [119]. Furthermore, the healing of autologous onlay bone grafts in their early stages was visualized by MRI in combination with an intraoral coil. Cortical and cancellous bone could be differentiated, and the volume of the block graft was calculated. Osteosynthesis screws were displayed as signal voids encircled by a thin fringe [120].
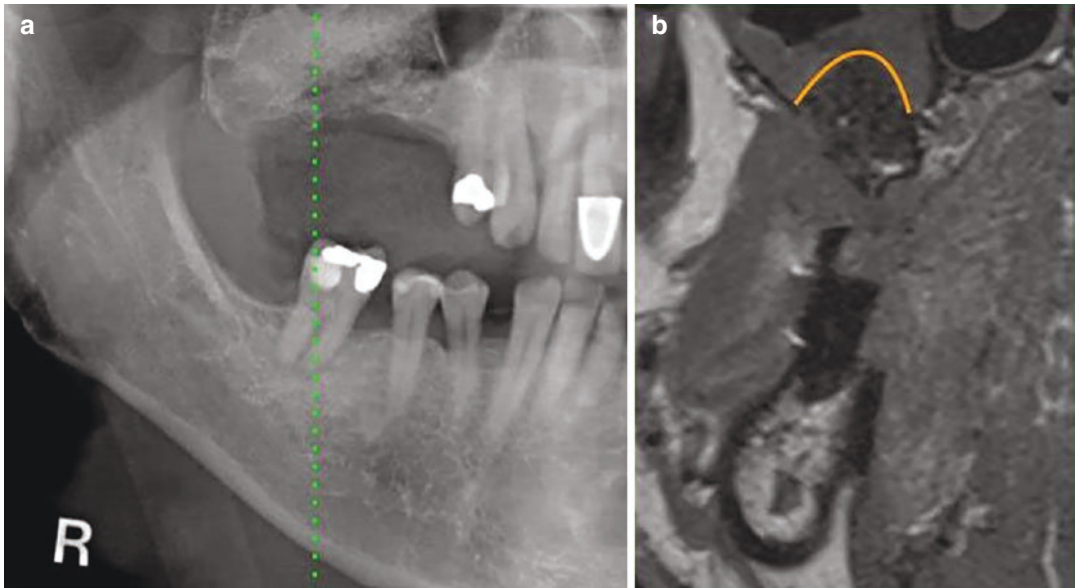
Fig. 10.22 Panoramic X-ray following MSFA (**a**) and MRI 1 day postoperatively to verify possible dislocation of the graft into the maxillary sinus (**b**). Note: the green dotted line (**a**) indicates the coronal view (**b**) of the MRI, the orange line indicates the upper border of the graft

10.5   Subtraction Radiography

Subtraction radiography was introduced in the 1930s and is a well-established method for the detection of bone changes in serial radiographs. During the 1990s subtraction radiography has also been used in dental research, including assessment of morphologic changes and bone formation and remodeling of extraction sites [121] as well as for the follow-up evaluation of implants [122–126].

Manual, semi-, or fully-automated systems for subtraction radiography exist. Briefly, subtraction radiography is based on the principle that a computer program simply calculates the pixel-pixel difference between two digital radiographs. Some systems are more advanced and, based on contrast adaption, subtract the gray shade value of each pixel in one image from the corresponding pixel value in another image, resulting in the subtraction image that represents the differences in gray shades between the pixels values in two radiographs. Provided that the two radiographs to be subtracted are recorded with standardized projection geometry and properly aligned, the differ-ences in gray shades in the bone may be interpreted as differences in bone mineral content. For example, Reddy et al. [126] demonstrated high repeatability of a semi-automated computer-assisted method used for measuring bone loss around implants. In another study, Brägger et al. [122] demonstrated peri-implant density changes during the early healing phase and ligature-induced peri-implantitis in an animal model, as well as cases documenting the loss of peri-implant bone density associated with infection or increase in density caused by remodeling after functional loading of an implant with a single crown.

Despite the fact that subtraction radiography has been advocated for the detection of minor bone changes, one must be aware of the shortcomings of this technique. The major limitation of subtraction radiography when analyzing changes in a given bone defect is that the visualization depends on the bucco-oral width of this defect. Total bone fill with uniform density in a bowl- or cone-shaped defect, as in an augmented peri-implantitis defect or an immediate implant placed in an extraction socket, respectively, may

be visualized only in the coronal part. This is because the width of the defect at that point makes up a larger fraction of the total width of the alveolar bone at its coronal aspect as compared with the apical aspect. Likewise, one must bear in mind that the subtraction image is a product of remodeling of the bone walls on the buccal and lingual/palatal aspect of the defect on one hand and bone formation/resorption within the defect on the other; obviously, it may not be possible to distinguish among these biological phenomena.

In perspective, due to the above shortcomings, together with the high costs associated with dedicated software and the cumbersome training needed, as well as the time-consuming use of the technique and the fact that the new digital systems give better possibilities for direct visualization of shades of gray, subtraction radiography has not achieved widespread use in implant research.

10.6   Micro CT

Histomorphometry, i.e., the quantitative assessment of histological sections from non-decalcified samples containing the implant and surrounding tissues, is commonly used to assess the amount/extent of osseointegration, i.e., the direct BIC; this method allows also the assessment of the bone type and mineralization level and is considered the gold standard [127–129]. However, histomorphometry—and histology in general—is a destructive technique, and once the sections are cut, it is not possible anymore to analyze the sample in any other direction than that of the section plane. Further, non-decalcified sections have the additional drawback that a rather significant volume of the specimen/implant is lost during the cutting process, due to the physical thickness of the cutting knife itself and the subsequent grinding/polishing of the section. Thus, from standard-size implants, only 1–2 sections are usually available for histomorphometric evaluation, which does not allow an accurate 3-D assessment of bone architecture.

In this context, microcomputed tomography (μCT) is a high-resolution 3-D imaging technique and is an established tool to assess bone ex vivo, as an alternative method to bone histomorphometry [130–136]. μCT offers the main advantages—compared to histomorphometry—of non-destructive assessment of bone morphology, and that relatively large volumes of interest can be analyzed in a truly 3-D way. In addition, the whole process of analysis can start immediately after the tissue samples are available and thus a faster analysis can be achieved. μCT has also been suggested to assess BIC [137–140]. A few studies have shown a good correlation between BIC estimates from μCT and from histomorphometry with relatively small discrepancies—either showing under- or overestimation of BIC with μCT [139, 141]. Other studies, however, have observed large differences between BIC values from μCT and histomorphometry, which are attributed to the presence of similar type—but of less magnitude—of artifacts, as those described above for CBCT (i.e., beam-hardening artifacts) [142, 143] (Fig. 10.23).

Conventional μCT devices are limited by the maximum current of the X-ray tube; this in turn is limited by physical constraints and the integration time that is directly related to the total scanning time. A way to improve resolution, voxel information content, and to limit drastically the beam-hardening effect is to use synchrotron radiation (SR) as the X-ray source. The beam generated from an SR source is very brilliant, characterized by a high flux of photons; it is, therefore, possible to filter the beam using a monochromator so that only a specific, narrow range of energies is utilized. As the intensity of the original beam is very high, the remaining monochromatic flux has enough photons, all characterized by the same energy level, to generate an excellent signal-to-noise ratio (SNR) with virtually the absence of beam hardening. Further, in contrast with conventional μCT, where the beam has either a fan shape or a cone shape, the incident beam of SR is long, the source divergence is small, and, the X-rays are nearly parallel. These characteristics of SRμCT scanning
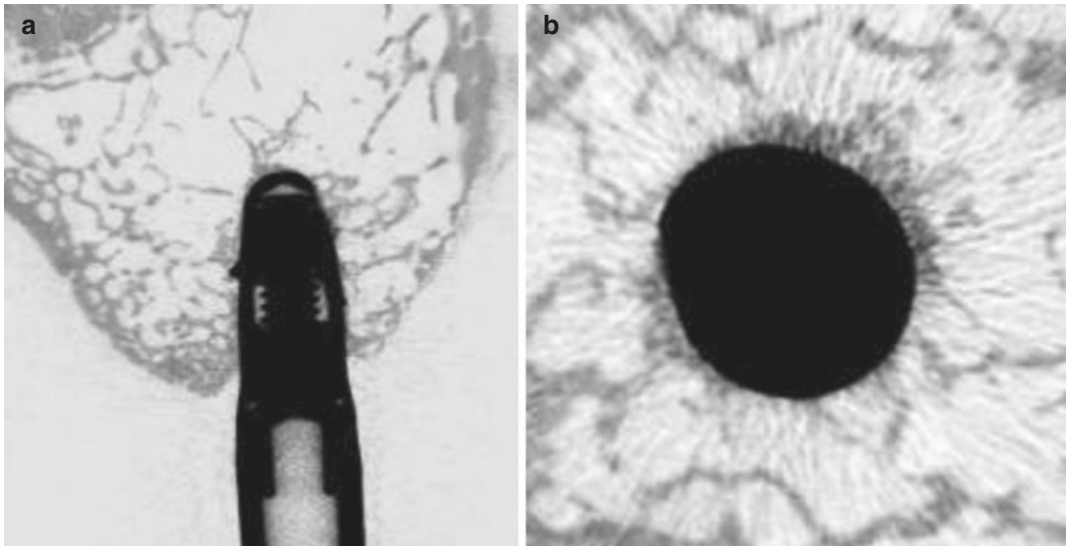
Fig. 10.23 Bucco-palatal (**a**) and axial (**b**) section from the maxilla of a macaca fascicularis monkey, containing a titanium dental implant scanned with conventional µCT. Precise BIC estimation appears compromised due to the presence of beam-hardening artifacts
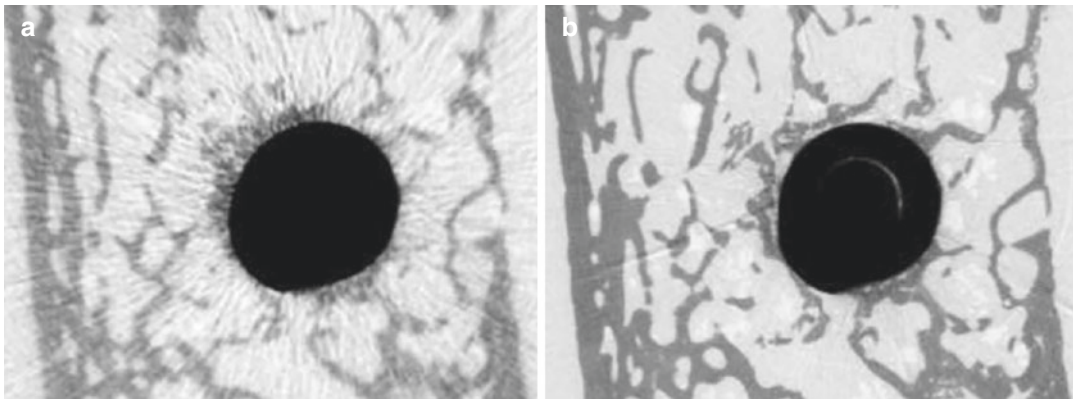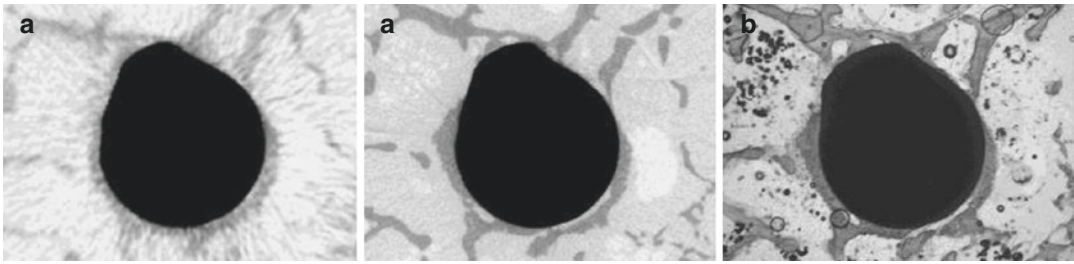

Fig. 10.24 Cross-sections from the maxilla of a macaca fascicularis monkey containing a titanium dental implant scanned with conventional µCT (**a**) and SRµCT. Note the extent of beam-hardening artifacts in the µCT image (**a**), that are almost absent in the image from the SR-based scanner (**b**)

allow for higher resolution, which can be up to 1/10 of the 1 µm range [144]. Consequently, the images obtained from SRµCT scanning are less noisy and the bony edges are sharper than the ones generated by the conventional µCT (Fig. 10.24).

Thus, with limited beam-hardening artifacts in SRµCT scans, better visualization of the relationship of the bone tissue to the implant is possible (Fig. 10.25). Nevertheless, and although it may

seem reasonable that a better estimation of BIC would also be possible with SRµCT compared with conventional µCT, a recent study showed a discrepancy of 5–15% between SRµCT and histology in terms of BIC [145]. In perspective, µCT and SRµCT facilitate improved visualization and understanding of tissues and implants in 3-D (Fig. 10.26) but are still not considered as precise as classic histomorphometry using light microscopy to assess osseointegration [146].

Fig. 10.25 Assessment of BIC is clearly compromised due to beam-hardening artifacts in a section from a conventional μCT (**a**), while BIC in a section from a SRμCT (**b**) seems to correspond well to that estimated in a non-decalcified histological section (**c**)
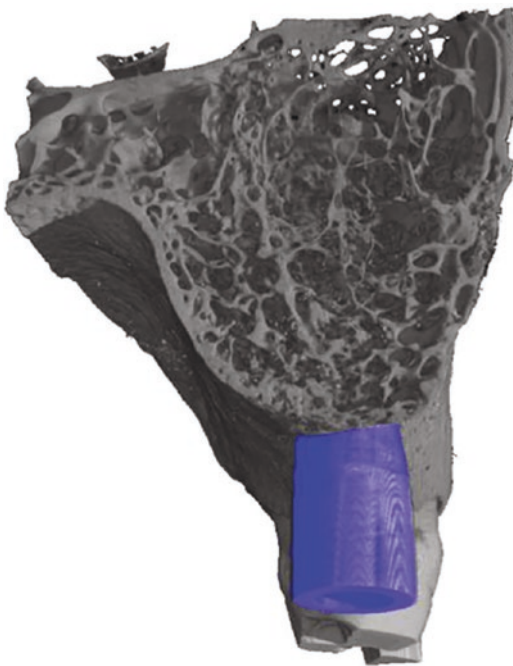
Fig. 10.26 3-D reconstruction of an aspect of the maxilla of a macaca fascicularis monkey containing a titanium dental implant scanned with SRμCT, where even some of the smallest trabeculae are clearly visible

10.7 Conclusion

Intraoral periapical radiographs provide the best spatial resolution and are recommended for implant planning in simple implant cases where clinical measures suffice to estimate bone thickness and no challenges exist with respect to interference with anatomic structures, e.g., the mandibular canal. Periapical radiography is most often the method of choice for clinical monitoring and research purposes when assessing the peri-implant bone level. A pre-requisite for assessing the peri-implant bone level with relatively good precision in periapical radiographs is that images are calibrated and that sharp threads on both sides of the implant are displayed. This can readily be achieved with the RB-RB/LB-LB mnemonic rule. Panoramic images are often appropriate for treatment planning, i.e., for selecting the implant size and position, in most of the cases where more than one implant is planned or in cases with a risk for interference with anatomic structures; the distortion and magnification of the panoramic image should be taken into consideration by a calibration procedure. However, when a clinical examination or the panoramic radiograph may indicate inadequate bone volume for implant installation or anatomical aberrations, which may require special attention or modification of the surgical technique, a CBCT should be obtained. However, panoramic images and CBCT are not appropriate for routine monitoring or for research purposes for assessing the peri-implant bone level, because the bone-to-implant interface is not clearly visualized. Similarly, although μCT and SRμCT are precise for bone volume estimations, the technology cannot yet be used to assess BIC as precisely as with histomorphometry.

References

1. Coli P, Christiaens V, Sennerby L, Bruyn H. reliability of periodontal diagnostic tools for monitoring peri-implant health and disease. Periodontol 2000. 2017;73:203–17. https://doi.org/10.1111/prd.12162.

2. Koldsland OC, Scheie AA, Aass AM. Prevalence of peri-implantitis related to severity of the disease with different degrees of bone loss. J Periodontol. 2010;81:231–8. https://doi.org/10.1902/jop.2009.090269.

3. Fuglsig JMCES, Thorn JJ, Ingerslev J, Wenzel A, Spin-Neto R. Long term follow-up of titanium implants installed in block-grafted areas: a systematic review. Clin Implant Dent Relat Res. 2018;20:1036–46. https://doi.org/10.1111/cid.12678.

4. Pepelassi EA, Diamanti-Kipioti A. Selection of the most accurate method of conventional radiography for the assessment of periodontal osseous destruction. J Clin Periodontol. 1997;24:557–67.

5. Larheim TA, Eggen S. Determination of tooth length with a standardized paralleling technique and calibrated radiographic measuring film. Oral Surg Oral Med Oral Pathol. 1979;48:374–8.

6. Sonick M, Abrahams J, Faiella RA. A comparison of the accuracy of periapical, panoramic, and computerized tomographic radiographs in locating the mandibular canal. Int J Oral Maxillofac Implants. 1994;9:6.

7. Schropp L, Stavropoulos A, Gotfredsen E, Wenzel A. Calibration of radiographs by a reference metal ball affects preoperative selection of implant size. Clin Oral Investig. 2009;13:375–81. https://doi.org/10.1007/s00784-009-0257-5.

8. Berglundh T, Armitage G, Araujo MG, et al. Peri-implant diseases and conditions: consensus report of workgroup 4 of the 2017 world workshop on the classification of periodontal and Peri-implant diseases and conditions. J Clin Periodontol. 2018;45(Suppl 20):S286–91. https://doi.org/10.1111/jcpe.12957.

9. Borrow JW, Smith JP. Stent marker materials for computerized tomograph-assisted implant planning. Int J Periodontics Restorative Dent. 1996;16:60–7.

10. Gröndahl K, Ekestubbe A, Gröndahl H. Postoperative radiographic examinations. In: Gröndahl K, Ekestubbe A, Gröndahl H, editors. Radiography in oral endosseous prosthetics; 1996. p. 111–26.

11. Schropp L, Stavropoulos A, Spin-Neto R, Wenzel A. Evaluation of the RB-RB/LB-LB mnemonic rule for recording optimally projected intraoral images of dental implants: an in vitro study. Dentomaxillofac Radiol. 2012;41:298–304. https://doi.org/10.1259/dmfr/20861598.

12. Sewerin I. Device for serial intraoral radiography with controlled projection angles. Tandlaegebladet. 1990;94:613–7.

13. Schropp L, Stavropoulos A, Spin-Neto R, Wenzel A. Implant image quality in dental radiographs recorded using a customized imaging guide or a standard film holder. Clin Oral Implants Res. 2012;23:55–9. https://doi.org/10.1111/j.1600-0501.2011.02180.x.

14. Abrahamsson I, Berglundh T, Moon IS, Lindhe J. Peri-implant tissues at submerged and non-submerged titanium implants. J Clin Periodontol. 1999;26:600–7.

15. Gotfredsen K, Berglundh T, Lindhe J. Bone reactions at implants subjected to experimental peri-implantitis and static load. A study in the dog. J Clin Periodontol. 2002;29:144–51.

16. Duyck J, Corpas L, Vermeiren S, et al. Histological, histomorphometrical, and radiological evaluation of an experimental implant design with a high insertion torque. Clin Oral Implants Res. 2010;21:877–84. https://doi.org/10.1111/j.1600-0501.2010.01895.x.

17. Albouy JP, Abrahamsson I, Persson LG, Berglundh T. Spontaneous progression of peri-implantitis at different types of implants. An experimental study in dogs. I: clinical and radiographic observations. Clin Oral Implants Res. 2008;19:997–1002. https://doi.org/10.1111/j.1600-0501.2008.01589.x.

18. Albouy JP, Abrahamsson I, Persson LG, Berglundh T. Spontaneous progression of ligatured induced peri-implantitis at implants with different surface characteristics. An experimental study in dogs II: histological observations. Clin Oral Implants Res. 2009;20:366–71.

19. Lang NP, Wetzel AC, Stich H, Caffesse RG. Histologic probe penetration in healthy and inflamed peri-implant tissues. Clin Oral Implants Res. 1994;5:191–201.

20. Schou S, Holmstrup P, Stoltze K, Hjørting-Hansen E, Fiehn NE, Skovgaard LT. Probing around implants and teeth with healthy or inflamed peri-implant mucosa/gingiva. A histologic comparison in cynomolgus monkeys (Macaca fascicularis). Clin Oral Implants Res. 2002;13:113–26.

21. Serino G, Turri A, Lang NP. Probing at implants with peri-implantitis and its relation to clinical peri-implant bone loss. Clin Oral Implants Res. 2013;24:91–5. https://doi.org/10.1111/j.1600-0501.2012.02470.x.

22. Borg E, Gröndahl K, Persson LG, Gröndahl HG. Marginal bone level around implants assessed in digital and film radiographs: in vivo study in the dog. Clin Implant Dent Relat Res. 2000;2:10–7.

23. De Smet E, Jacobs R, Gijbels F, Naert I. The accuracy and reliability of radiographic methods for the assessment of marginal bone level around oral implants. Dentomaxillofac Radiol. 2002;31:176–81. https://doi.org/10.1038/sj/dmfr/4600694.

24. Kavadella A, Karayiannis A, Nicopoulou-Karayianni K. Detectability of experimental peri-implant cancellous bone lesions using conventional and direct digital radiography. Aust Dent J. 2006;51:180–6.

25. Matsuda Y, Hanazawa T, Seki K, Sano T, Ozeki M, Okano T. Accuracy of Digora system in detecting artificial peri-implant bone defects. Implant Dent. 2001;10:265–71.

26. Mörner-Svalling AC, Tronje G, Andersson LG, Welander U. Comparison of the diagnostic potential of direct digital and conventional intraoral radiography in the evaluation of peri-implant conditions. Clin Oral Implants Res. 2003;14:714–9.

27. Akesson L, Håkansson J, Rohlin M. Comparison of panoramic and intraoral radiography and pocket probing for the measurement of the marginal bone level. J Clin Periodontol. 1992;19:326–32.

28. Hämmerle CH, Ingold HP, Lang NP. Evaluation of clinical and radiographic scoring methods before and after initial periodontal therapy. J Clin Periodontol. 1990;17:255–63.

29. Ferreira CE, Novaes AB, Haraszthy VI, Bittencourt M, Martinelli CB, Luczyszyn SM. A clinical study of 406 sinus augmentations with 100% anorganic bovine bone. J Periodontol. 2009;80:1920–7. https://doi.org/10.1902/jop.2009.090263.

30. Lai HC, Zhuang LF, Lv XF, Zhang ZY, Zhang YX, Zhang ZY. Osteotome sinus floor elevation with or without grafting: a preliminary clinical trial. Clin Oral Implants Res. 2010;21:520–6. https://doi.org/10.1111/j.1600-0501.2009.01889.x.

31. Batenburg RH, Stellingsma K, Raghoebar GM, Vissink A. Bone height measurements on panoramic radiographs: the effect of shape and position of edentulous mandibles. Oral Surg Oral Med Oral Pathol Oral Radiol Endod. 1997;84:430–5.

32. Gomez-Roman G, Lukas D, Beniashvili R, Schulte W. Area-dependent enlargement ratios of panoramic tomography on orthograde patient positioning and its significance for implant dentistry. Int J Oral Maxillofac Implants. 1999;14:248–57.

33. Riecke B, Friedrich RE, Schulze D, et al. Impact of malpositioning on panoramic radiography in implant dentistry. Clin Oral Investig. 2015;19:781–90. https://doi.org/10.1007/s00784-014-1295-1.

34. Sadat-Khonsari R, Fenske C, Behfar L, Bauss O. Panoramic radiography: effects of head alignment on the vertical dimension of the mandibular ramus and condyle region. Eur J Orthod. 2012;34:164–9. https://doi.org/10.1093/ejo/cjq175.

35. Jacobs R, van Steenberghe D. Radiographic indications and contra-indication for implant placement. In: Jacobs R, van Steenberghe D, editors. Radiographic planning and assessment of endosseous oral implants; 1998. p. 45–58.

36. Angelopoulos C, Thomas SL, Thomas S, et al. Comparison between digital panoramic radiography and cone-beam computed tomography for the identification of the mandibular canal as part of presurgical dental implant assessment. J Oral Maxillofac Surg. 2008;66:2130–5. https://doi.org/10.1016/j.joms.2008.06.021.

37. Bolin A, Eliasson S, von Beetzen M, Jansson L. Radiographic evaluation of mandibular posterior implant sites: correlation between panoramic and tomographic determinations. Clin Oral Implants Res. 1996;7:354–9.

38. Bou Serhal C, Jacobs R, Flygare L, Quirynen M, van Steenberghe D. Perioperative validation of localisation of the mental foramen. Dentomaxillofac Radiol. 2002;31:39–43. https://doi.org/10.1038/sj/dmfr/4600662.

39. Lam EW, Ruprecht A, Yang J. Comparison of two-dimensional orthoradially reformatted computed tomography and panoramic radiography for dental implant treatment planning. J Prosthet Dent. 1995;74:42–6.

40. Lindh C, Petersson A. Radiologic examination for location of the mandibular canal: a comparison between panoramic radiography and conventional tomography. Int J Oral Maxillofac Implants. 1989;4:249–53.

41. Lindh C, Petersson A, Klinge B. Visualisation of the mandibular canal by different radiographic techniques. Clin Oral Implants Res. 1992;3:90–7.

42. Lindh C, Petersson A, Klinge B. Measurements of distances related to the mandibular canal in radiographs. Clin Oral Implants Res. 1995;6:96–103.

43. Madrigal C, Ortega R, Meniz C, López-Quiles J. Study of available bone for interforaminal implant treatment using cone-beam computed tomography. Med Oral Patol Oral Cir Bucal. 2008;13:E307–12.

44. Tal H, Moses O. A comparison of panoramic radiography with computed tomography in the planning of implant surgery. Dentomaxillofac Radiol. 1991;20:40–2. https://doi.org/10.1259/dmfr.20.1.1884852.

45. Fuhrmann R, Bücker A, Diedrich P. Radiological assessment of artificial bone defects in the floor of the maxillary sinus. Dentomaxillofac Radiol. 1997;26:112–6. https://doi.org/10.1038/sj.dmfr.4600223.

46. Fuhrmann RA, Wehrbein H, Langen HJ, Diedrich PR. Assessment of the dentate alveolar process with high resolution computed tomography. Dentomaxillofac Radiol. 1995;24:50–4. https://doi.org/10.1259/dmfr.24.1.8593909.

47. Fuhrmann RA, Bücker A, Diedrich PR. Furcation involvement: comparison of dental radiographs and HR-CT-slices in human specimens. J Periodontal Res. 1997;32:409–18.

48. Langen HJ, Fuhrmann R, Diedrich P, Günther RW. Diagnosis of infra-alveolar bony lesions in the dentate alveolar process with high-resolution computed tomography. Experimental results. Invest Radiol. 1995;30:421–6.

49. Stavropoulos A, Wenzel A. Accuracy of cone beam dental CT, intraoral digital and conventional film radiography for the detection of periapical lesions. An ex vivo study in pig jaws. Clin Oral Investig. 2007;11:101–6. https://doi.org/10.1007/s00784-006-0078-8.

50. Tammisalo T, Luostarinen T, Vähätalo K, Tammisalo EH. Comparison of periapical and detailed narrow-beam radiography for diagnosis of periapical bone

lesions. Dentomaxillofac Radiol. 1993;22:183–7. https://doi.org/10.1259/dmfr.22.4.8181644.

51. Velvart P, Hecker H, Tillinger G. Detection of the apical lesion and the mandibular canal in conventional radiography and computed tomography. Oral Surg Oral Med Oral Pathol Oral Radiol Endod. 2001;92:682–8. https://doi.org/10.1067/moe.2001.118904.

52. Liang X, Jacobs R, Hassan B, et al. A comparative evaluation of cone beam computed tomography (CBCT) and multi-slice CT (MSCT) part I. on subjective image quality. Eur J Radiol. 2010;75:265–9. https://doi.org/10.1016/j.ejrad.2009.03.042.

53. Nardi C, Talamonti C, Pallotta S, et al. Head and neck effective dose and quantitative assessment of image quality: a study to compare cone beam CT and multislice spiral CT. Dentomaxillofac Radiol. 2017;46:20170030. https://doi.org/10.1259/dmfr.20170030.

54. Harris D, Horner K, Gröndahl K, et al. E.a.O. guidelines for the use of diagnostic imaging in implant dentistry 2011. A consensus workshop organized by the European Association for Osseointegration at the Medical University of Warsaw. Clin Oral Implants Res. 2012;23:1243–53. https://doi.org/10.1111/j.1600-0501.2012.02441.x.

55. Correa LR, Spin-Neto R, Stavropoulos A, Schropp L, da Silveira HE, Wenzel A. Planning of dental implant size with digital panoramic radiographs, CBCT-generated panoramic images, and CBCT cross-sectional images. Clin Oral Implants Res. 2014;25:690–5. https://doi.org/10.1111/clr.12126.

56. Diniz AF, Mendonça EF, Leles CR, Guilherme AS, Cavalcante MP, Silva MA. Changes in the pre-surgical treatment planning using conventional spiral tomography. Clin Oral Implants Res. 2008;19:249–53. https://doi.org/10.1111/j.1600-0501.2007.01475.x.

57. Schropp L, Wenzel A, Kostopoulos L. Impact of conventional tomography on prediction of the appropriate implant size. Oral Surg Oral Med Oral Pathol Oral Radiol Endod. 2001;92:458–63. https://doi.org/10.1067/moe.2001.118286.

58. Schropp L, Stavropoulos A, Gotfredsen E, Wenzel A. Comparison of panoramic and conventional cross-sectional tomography for preoperative selection of implant size. Clin Oral Implants Res. 2011;22:424–9. https://doi.org/10.1111/j.1600-0501.2010.02006.x.

59. Baciut M, Hedesiu M, Bran S, Jacobs R, Nackaerts O, Baciut G. Pre- and postoperative assessment of sinus grafting procedures using cone-beam computed tomography compared with panoramic radiographs. Clin Oral Implants Res. 2013;24:512–6. https://doi.org/10.1111/j.1600-0501.2011.02408.x.

60. Lang AC, Schulze RK. Detection accuracy of maxillary sinus floor septa in panoramic radiographs using CBCT as gold standard: a multi-observer receiver operating characteristic (ROC) study. Clin Oral Investig. 2019;23:99–105. https://doi.org/10.1007/s00784-018-2414-1.

61. Pommer B, Ulm C, Lorenzoni M, Palmer R, Watzek G, Zechner W. Prevalence, location and morphology of maxillary sinus septa: systematic review and meta-analysis. J Clin Periodontol. 2012;39:769–73. https://doi.org/10.1111/j.1600-051X.2012.01897.x.

62. Fortin T, Camby E, Alik M, Isidori M, Bouchet H. Panoramic images versus three-dimensional planning software for oral implant planning in atrophied posterior maxillary: a clinical radiological study. Clin Implant Dent Relat Res. 2013;15:198–204. https://doi.org/10.1111/j.1708-8208.2011.00342.x.

63. Bertl K, Mick RB, Heimel P, Gahleitner A, Stavropoulos A, Ulm C. Variation in bucco-palatal maxillary sinus width does not permit a meaningful sinus classification. Clin Oral Implants Res. 2018;29:1220–9. https://doi.org/10.1111/clr.13387.

64. Chappuis V, Rahman L, Buser R, Janner SFM, Belser UC, Buser D. Effectiveness of contour augmentation with guided bone regeneration: 10-year results. J Dent Res. 2018;97:266–74. https://doi.org/10.1177/0022034517737755.

65. Fokas G, Vaughn VM, Scarfe WC, Bornstein MM. Accuracy of linear measurements on CBCT images related to presurgical implant treatment planning: a systematic review. Clin Oral Implants Res. 2018;29(Suppl 16):393–415. https://doi.org/10.1111/clr.13142.

66. Jung RE, Benic GI, Scherrer D, Hämmerle CH. Cone beam computed tomography evaluation of regenerated buccal bone 5 years after simultaneous implant placement and guided bone regeneration procedures—a randomized, controlled clinical trial. Clin Oral Implants Res. 2015;26:28–34. https://doi.org/10.1111/clr.12296.

67. Kaminaka A, Nakano T, Ono S, Kato T, Yatani H. Cone-beam computed tomography evaluation of horizontal and vertical dimensional changes in buccal Peri-implant alveolar bone and soft tissue: a 1-year prospective clinical study. Clin Implant Dent Relat Res. 2015;17(Suppl 2):e576–85. https://doi.org/10.1111/cid.12286.

68. Mengel R, Kruse B, Flores-de-Jacoby L. Digital volume tomography in the diagnosis of peri-implant defects: an in vitro study on native pig mandibles. J Periodontol. 2006;77:1234–41. https://doi.org/10.1902/jop.2006.050424.

69. Sbordone L, Toti P, Menchini-Fabris GB, Sbordone C, Piombino P, Guidetti F. Volume changes of autogenous bone grafts after alveolar ridge augmentation of atrophic maxillae and mandibles. Int J Oral Maxillofac Surg. 2009;38:1059–65. https://doi.org/10.1016/j.ijom.2009.06.024.

70. Schropp L, Wenzel A, Spin-Neto R, Stavropoulos A. Fate of the buccal bone at implants placed early, delayed, or late after tooth extraction analyzed by cone beam CT: 10-year results from a randomized, controlled, clinical study. Clin Oral Implants Res. 2015;26:492–500. https://doi.org/10.1111/clr.12424.

71. Smolka W, Eggensperger N, Carollo V, Ozdoba C, Iizuka T. Changes in the volume and density of calvarial split bone grafts after alveolar ridge augmentation. Clin Oral Implants Res. 2006;17:149–55. https://doi.org/10.1111/j.1600-0501.2005.01182.x.

72. Spin-Neto R, Stavropoulos A, Dias Pereira LA, Marcantonio E, Wenzel A. Fate of autologous and fresh-frozen allogeneic block bone grafts used for ridge augmentation. A CBCT-based analysis. Clin Oral Implants Res. 2013;24:167–73. https://doi.org/10.1111/j.1600-0501.2011.02324.x.

73. Corpas LS, Jacobs R, Quirynen M, Huang Y, Naert I, Duyck J. Peri-implant bone tissue assessment by comparing the outcome of intra-oral radiograph and cone beam computed tomography analyses to the histological standard. Clin Oral Implants Res. 2011;22:492–9. https://doi.org/10.1111/j.1600-0501.2010.02029.x.

74. Golubovic V, Mihatovic I, Becker J, Schwarz F. Accuracy of cone-beam computed tomography to assess the configuration and extent of ligature-induced peri-implantitis defects. A pilot study. Oral Maxillofac Surg. 2012;16:349–54. https://doi.org/10.1007/s10006-012-0320-2.

75. Ritter L, Elger MC, Rothamel D, et al. Accuracy of peri-implant bone evaluation using cone beam CT, digital intra-oral radiographs and histology. Dentomaxillofac Radiol. 2014;43:20130088. https://doi.org/10.1259/dmfr.20130088.

76. Wang D, Künzel A, Golubovic V, et al. Accuracy of peri-implant bone thickness and validity of assessing bone augmentation material using cone beam computed tomography. Clin Oral Investig. 2013;17:1601–9. https://doi.org/10.1007/s00784-012-0841-y.

77. Spin-Neto R, Marcantonio E, Gotfredsen E, Wenzel A. Exploring CBCT-based DICOM files. A systematic review on the properties of images used to evaluate maxillofacial bone grafts. J Digit Imaging. 2011;24:959–66. https://doi.org/10.1007/s10278-011-9377-y.

78. Schulze R, Heil U, Gross D, et al. Artefacts in CBCT: a review. Dentomaxillofac Radiol. 2011;40:265–73. https://doi.org/10.1259/dmfr/30642039.

79. Benic GI, Sancho-Puchades M, Jung RE, Deyhle H, Hämmerle CH. In vitro assessment of artifacts induced by titanium dental implants in cone beam computed tomography. Clin Oral Implants Res. 2013;24:378–83. https://doi.org/10.1111/clr.12048.

80. Bohner LOL, Tortamano P, Marotti J. Accuracy of linear measurements around dental implants by means of cone beam computed tomography with different exposure parameters. Dentomaxillofac Radiol. 2017;46:20160377. https://doi.org/10.1259/dmfr.20160377.

81. Gröbe A, Semmusch J, Schöllchen M, et al. Accuracy of bone measurements in the vicinity of titanium implants in CBCT data sets: a comparison of radiological and histological findings in Minipigs. Biomed Res Int. 2017;2017:3848207. https://doi.org/10.1155/2017/3848207.

82. Kamburoğlu K, Murat S, Kılıç C, et al. Accuracy of CBCT images in the assessment of buccal marginal alveolar peri-implant defects: effect of field of view. Dentomaxillofac Radiol. 2014;43:20130332. https://doi.org/10.1259/dmfr.20130332.

83. Liedke GS, Spin-Neto R, da Silveira HED, Schropp L, Stavropoulos A, Wenzel A. Factors affecting the possibility to detect buccal bone condition around dental implants using cone beam computed tomography. Clin Oral Implants Res. 2017;28:1082–8. https://doi.org/10.1111/clr.12921.

84. Liedke GS, Spin-Neto R, da Silveira HED, Schropp L, Stavropoulos A, Wenzel A. Accuracy of detecting and measuring buccal bone thickness adjacent to titanium dental implants-a cone beam computed tomography in vitro study. Oral Surg Oral Med Oral Pathol Oral Radiol. 2018;126:432–8. https://doi.org/10.1016/j.oooo.2018.06.004.

85. Raskó Z, Nagy L, Radnai M, Piffkó J, Baráth Z. Assessing the accuracy of cone-beam computerized tomography in measuring thinning Oral and buccal bone. J Oral Implantol. 2016;42:311–4. https://doi.org/10.1563/aaid-joi-D-15-00188.

86. Razavi T, Palmer RM, Davies J, Wilson R, Palmer PJ. Accuracy of measuring the cortical bone thickness adjacent to dental implants using cone beam computed tomography. Clin Oral Implants Res. 2010;21:718–25. https://doi.org/10.1111/j.1600-0501.2009.01905.x.

87. Domic D, Bertl K, Ahmad S, Schropp L, Hellén-Halme K, Stavropoulos A. Accuracy of cone-beam computed tomography is limited at implant sites with a thin buccal bone: a laboratory study. J Periodontol. 2021;92:592–601. https://doi.org/10.1002/JPER.20-0222.

88. Ferrus J, Cecchinato D, Pjetursson EB, Lang NP, Sanz M, Lindhe J. Factors influencing ridge alterations following immediate implant placement into extraction sockets. Clin Oral Implants Res. 2010;21:22–9. https://doi.org/10.1111/j.1600-0501.2009.01825.x.

89. Huynh-Ba G, Pjetursson BE, Sanz M, et al. Analysis of the socket bone wall dimensions in the upper maxilla in relation to immediate implant placement. Clin Oral Implants Res. 2010;21:37–42. https://doi.org/10.1111/j.1600-0501.2009.01870.x.

90. Pauwels R, Jacobs R, Singer SR, Mupparapu M. CBCT-based bone quality assessment: are Hounsfield units applicable. Dentomaxillofac Radiol. 2015;44:20140238. https://doi.org/10.1259/dmfr.20140238.

91. Turkyilmaz I, Ozan O, Yilmaz B, Ersoy AE. Determination of bone quality of 372 implant recipient sites using Hounsfield unit from computerized tomography: a clinical study. Clin Implant Dent Relat Res. 2008;10:238–44. https://doi.org/10.1111/j.1708-8208.2008.00085.x.

92. Nackaerts O, Maes F, Yan H, Couto Souza P, Pauwels R, Jacobs R. Analysis of intensity variability in multislice and cone beam computed tomogra-

phy. Clin Oral Implants Res. 2011;22:873–9. https://doi.org/10.1111/j.1600-0501.2010.02076.x.

93. Pauwels R, Nackaerts O, Bellaiche N, et al. Variability of dental cone beam CT grey values for density estimations. Br J Radiol. 2013;86:20120135. https://doi.org/10.1259/bjr.20120135.

94. Spin-Neto R, Gotfredsen E, Wenzel A. Variation in voxel value distribution and effect of time between exposures in six CBCT units. Dentomaxillofac Radiol. 2014;43:20130376. https://doi.org/10.1259/dmfr.20130376.

95. European Commission. Radiation protection no. 172. Evidence based guidelines based on cone beam CT for dental and maxillofacial radiology. Luxembourg: Office for Official Publications of the European Communities; 2012.

96. Marinescu Gava M, Suomalainen A, Vehmas T, Ventä I. Did malpractice claims for failed dental implants decrease after introduction of CBCT in Finland. Clin Oral Investig. 2019;23:399–404. https://doi.org/10.1007/s00784-018-2448-4.

97. Aiken A, Bouloux G, Hudgins P. MR imaging of the temporomandibular joint. Magn Reson Imaging Clin N Am. 2012;20:397–412. https://doi.org/10.1016/j.mric.2012.05.002.

98. Currie S, Hoggard N, Craven IJ, Hadjivassiliou M, Wilkinson ID. Understanding MRI: basic MR physics for physicians. Postgrad Med J. 2013;89:209–23. https://doi.org/10.1136/postgradmedj-2012-131342.

99. Gaudino C, Cosgarea R, Heiland S, et al. MR-imaging of teeth and periodontal apparatus: an experimental study comparing high-resolution MRI with MDCT and CBCT. Eur Radiol. 2011;21:2575–83. https://doi.org/10.1007/s00330-011-2209-0.

100. Kang Y, Hua C, Wu B, et al. Investigation of zero TE MR in preoperative planning in dentistry. Magn Reson Imaging. 2018;54:77–83. https://doi.org/10.1016/j.mri.2018.07.007.

101. Al-Haj Husain A, Valdec S, Stadlinger B, Rücker M, Piccirelli M, Winklhofer S. Preoperative visualization of the lingual nerve by 3D double-echo steady-state MRI in surgical third molar extraction treatment. Clin Oral Investig. 2022;26:2043–53. https://doi.org/10.1007/s00784-021-04185-z.

102. Assaf AT, Zrnc TA, Remus CC, et al. Evaluation of four different optimized magnetic-resonance-imaging sequences for visualization of dental and maxillo-mandibular structures at 3 T. J Craniomaxillofac Surg. 2014;42:1356–63. https://doi.org/10.1016/j.jcms.2014.03.026.

103. Burian E, Probst FA, Weidlich D, et al. MRI of the inferior alveolar nerve and lingual nerve-anatomical variation and morphometric benchmark values of nerve diameters in healthy subjects. Clin Oral Investig. 2020;24:2625–34. https://doi.org/10.1007/s00784-019-03120-7.

104. Hilgenfeld T, Kästel T, Heil A, et al. High-resolution dental magnetic resonance imaging for planning palatal graft surgery-a clinical pilot study.

J Clin Periodontol. 2018;45:462–70. https://doi.org/10.1111/jcpe.12870.

105. de Carvalho E, Silva Fuglsig JM, Wenzel A, Hansen B, Lund TE, Spin-Neto R. Magnetic resonance imaging for the planning, execution, and follow-up of implant-based oral rehabilitation: systematic review. Int J Oral Maxillofac Implants. 2021;36:432–41. https://doi.org/10.11607/jomi.8536.

106. Grandoch A, Peterke N, Hokamp NG, Zöller JE, Lichenstein T, Neugebauer J. 1.5 T MRI with a dedicated dental signal-amplification coil as noninvasive, radiation-free alternative to CBCT in presurgical implant planning procedures. Int J Oral Maxillofac Implants. 2021;36:1211–8. https://doi.org/10.11607/jomi.8103.

107. Flügge T, Ludwig U, Hövener JB, Kohal R, Wismeijer D, Nelson K. Virtual implant planning and fully guided implant surgery using magnetic resonance imaging-proof of principle. Clin Oral Implants Res. 2020;31:575–83. https://doi.org/10.1111/clr.13592.

108. Flügge T, Ludwig U, Winter G, Amrein P, Kernen F, Nelson K. Fully guided implant surgery using magnetic resonance imaging—an in vitro study on accuracy in human mandibles. Clin Oral Implants Res. 2020;31:737–46. https://doi.org/10.1111/clr.13622.

109. Hilgenfeld T, Juerchott A, Deisenhofer UK, et al. In vivo accuracy of tooth surface reconstruction based on CBCT and dental MRI-A clinical pilot study. Clin Oral Implants Res. 2019;30:920–7. https://doi.org/10.1111/clr.13498.

110. Erasmus LJ, Hurter D, Naudé M, Kritzinger HG, Acho S. A short overview of MRI artefacts. S Afr J Radiol. 2004;8:13.

111. Gao X, Wan Q, Gao Q. Susceptibility artifacts induced by crowns of different materials with prepared teeth and titanium implants in magnetic resonance imaging. Sci Rep. 2022;12:428. https://doi.org/10.1038/s41598-021-03962-w.

112. Hilgenfeld T, Prager M, Schwindling FS, et al. Artefacts of implant-supported single crowns—impact of material composition on artefact volume on dental MRI. Eur J Oral Implantol. 2016;9:301–8.

113. Demirturk Kocasarac H, Ustaoglu G, Bayrak S, et al. Evaluation of artifacts generated by titanium, zirconium, and titanium-zirconium alloy dental implants on MRI, CT, and CBCT images: a phantom study. Oral Surg Oral Med Oral Pathol Oral Radiol. 2019;127:535–44. https://doi.org/10.1016/j.oooo.2019.01.074.

114. Bohner L, Meier N, Gremse F, Tortamano P, Kleinheinz J, Hanisch M. Magnetic resonance imaging artifacts produced by dental implants with different geometries. Dentomaxillofac Radiol. 2020;49:20200121. https://doi.org/10.1259/dmfr.20200121.

115. Duttenhoefer F, Mertens ME, Vizkelety J, Gremse F, Stadelmann VA, Sauerbier S. Magnetic resonance imaging in zirconia-based dental implantology. Clin Oral Implants Res. 2015;26:1195–202. https://doi.org/10.1111/clr.12430.

116. Smeets R, Schöllchen M, Gauer T, et al. Artefacts in multimodal imaging of titanium, zirconium and binary titanium-zirconium alloy dental implants: an in vitro study. Dentomaxillofac Radiol. 2017;46:20160267. https://doi.org/10.1259/dmfr.20160267.

117. Hilgenfeld T, Juerchott A, Deisenhofer UK, et al. Accuracy of cone-beam computed tomography, dental magnetic resonance imaging, and intraoral radiography for detecting peri-implant bone defects at single zirconia implants-an in vitro study. Clin Oral Implants Res. 2018;29:922–30. https://doi.org/10.1111/clr.13348.

118. Wanner L, Ludwig U, Hövener JB, Nelson K, Flügge T. Magnetic resonance imaging-a diagnostic tool for postoperative evaluation of dental implants: a case report. Oral Surg Oral Med Oral Pathol Oral Radiol. 2018;125:e103–7. https://doi.org/10.1016/j.oooo.2018.01.005.

119. Senel FC, Duran S, Icten O, Izbudak I, Cizmeci F. Assessment of the sinus lift operation by magnetic resonance imaging. Br J Oral Maxillofac Surg. 2006;44:511–4. https://doi.org/10.1016/j.bjoms.2006.02.004.

120. Flügge T, Ludwig U, Amrein P, et al. MRI for the display of autologous onlay bone grafts during early healing-an experimental study. Dentomaxillofac Radiol. 2021;50:20200068. https://doi.org/10.1259/dmfr.20200068.

121. Schropp L, Wenzel A, Kostopoulos L, Karring T. Bone healing and soft tissue contour changes following single-tooth extraction: a clinical and radiographic 12-month prospective study. Int J Periodontics Restorative Dent. 2003;23:313–23.

122. Brägger U, Bürgin W, Lang NP, Buser D. Digital subtraction radiography for the assessment of changes in peri-implant bone density. Int J Oral Maxillofac Implants. 1991;6:160–6.

123. Jeffcoat MK. Digital radiology for implant treatment planning and evaluation. Dentomaxillofac Radiol. 1992;21:203–7. https://doi.org/10.1259/dmfr.21.4.1299635.

124. Jeffcoat MK, Reddy MS, van den Berg HR, Bertens E. Quantitative digital subtraction radiography for the assessment of peri-implant bone change. Clin Oral Implants Res. 1992;3:22–7.

125. Reddy MS, Jeffcoat MK, Richardson RC. Assessment of adjunctive flurbiprofen therapy in root-form implant healing with digital subtraction radiography. J Oral Implantol. 1990;16:272–6.

126. Reddy MS, Mayfield-Donahoo TL, Jeffcoat MK. A semi-automated computer-assisted method for measuring bone loss adjacent to dental implants. Clin Oral Implants Res. 1992;3:28–31.

127. Garetto LP, Chen J, Parr JA, Roberts WE. Remodeling dynamics of bone supporting rigidly fixed titanium implants: a histomorphometric comparison in four species including humans. Implant Dent. 1995;4:235–43.

128. Gotfredsen K, Budtz-Jörgensen E, Jensen LN. A method for preparing and staining histological sections containing titanium implants for light microscopy. Stain Technol. 1989;64:121–7.

129. Sennerby L, Ericson LE, Thomsen P, Lekholm U, Astrand P. Structure of the bone-titanium interface in retrieved clinical oral implants. Clin Oral Implants Res. 1991;2:103–11.

130. Cattaneo PM, Dalstra M, Melsen B. The finite element method: a tool to study orthodontic tooth movement. J Dent Res. 2005;84:428–33. https://doi.org/10.1177/154405910508400506.

131. Dalstra M, Cattaneo PM, Beckmann F. Synchrotron radiation-based microtomography of alveolar support tissues. Orthod Craniofac Res. 2006;9:199–205. https://doi.org/10.1111/j.1601-6343.2006.00376.x.

132. Bouxsein ML, Boyd SK, Christiansen BA, Guldberg RE, Jepsen KJ, Müller R. Guidelines for assessment of bone microstructure in rodents using micro-computed tomography. J Bone Miner Res. 2010;25:1468–86. https://doi.org/10.1002/jbmr.141.

133. Elliott JC, Dover SD. X-ray microtomography. J Microsc. 1982;126:211–3.

134. Feldkamp LA, Goldstein SA, Parfitt AM, Jesion G, Kleerekoper M. The direct examination of three-dimensional bone architecture in vitro by computed tomography. J Bone Miner Res. 1989;4:3–11. https://doi.org/10.1002/jbmr.5650040103.

135. Layton MW, Goldstein SA, Goulet RW, Feldkamp LA, Kubinski DJ, Bole GG. Examination of subchondral bone architecture in experimental osteoarthritis by microscopic computed axial tomography. Arthritis Rheum. 1988;31:1400–5.

136. Odgaard A. Three-dimensional methods for quantification of cancellous bone architecture. Bone. 1997;20:315–28.

137. Kiba H, Hayakawa T, Oba S, Kuwabara M, Habata I, Yamamoto H. Potential application of high-resolution microfocus X-ray techniques for observation of bone structure and bone-implant interface. Int J Oral Maxillofac Implants. 2003;18:279–85.

138. Sennerby L, Wennerberg A, Pasop F. A new microtomographic technique for non-invasive evaluation of the bone structure around implants. Clin Oral Implants Res. 2001;12:91–4.

139. Van Oossterwyck H, Duyck J, Vander Sloten J, et al. Use of microfocus computerized tomography as a new technique for characterizing bone tissue around oral implants. J Oral Implantol. 2000;26:5–12. https://doi.org/10.1563/1548-1336(2000)026<0005:TUOMCT>2.3.CO;2.

140. Yip G, Schneider P, Roberts EW. Micro-computed tomography: high resolution imaging of bone and implants in three dimensions. Semin Orthod. 2004;10:174–87.

141. Vandeweghe S, Coelho PG, Vanhove C, Wennerberg A, Jimbo R. Utilizing micro-computed tomography to evaluate bone structure surrounding dental implants: a comparison with histomorphometry. J Biomed

Mater Res B Appl Biomater. 2013;101:1259–66. https://doi.org/10.1002/jbm.b.32938.

142. Schouten C, Meijer GJ, van den Beucken JJ, Spauwen PH, Jansen JA. The quantitative assessment of peri-implant bone responses using histomorphometry and micro-computed tomography. Biomaterials. 2009;30:4539–49. https://doi.org/10.1016/j.biomaterials.2009.05.017.

143. Stoppie N, van der Waerden JP, Jansen JA, Duyck J, Wevers M, Naert IE. Validation of microfocus computed tomography in the evaluation of bone implant specimens. Clin Implant Dent Relat Res. 2005;7:87–94.

144. Neldam CA, Pinholt EM. Synchrotron μCT imaging of bone, titanium implants and bone sub- stitutes - a systematic review of the literature. J Craniomaxillofac Surg. 2014;42:801–5. https://doi.org/10.1016/j.jcms.2013.11.015.

145. Neldam CA, Sporring J, Rack A, et al. Synchrotron radiation μCT and histology evaluation of bone-to-implant contact. J Craniomaxillofac Surg. 2017;45:1448–57. https://doi.org/10.1016/j.jcms.2017.05.019.

146. Arvidsson A, Sarve H, Johansson CB. Comparing and visualizing titanium implant integration in rat bone using 2D and 3D techniques. J Biomed Mater Res B Appl Biomater. 2015;103:12–20. https://doi.org/10.1002/jbm.b.33168.

Biological Events at the Interface Between the Radicular Part of a Dental Implant and Bone

11

Barbara D. Boyan, Ethan M. Lotz,
Michael B. Berger, Jingyao Deng,
D. Joshua Cohen, and Zvi Schwartz

Abbreviations

$1\alpha,25(OH)_2D_3$	1α,25-dihydroxyvitamin D3
BMP	Bone morphogenetic protein
BSA	Bovine serum albumin
CCR	C chemokine receptor
CD	Cluster of differentiation
ELISA	Enzyme-linked immunosorbent assay
ERK	Extracellular regulated kinase
FAK	Focal adhesion kinase
FBGC	Foreign body giant cell
FBS	Fetal bovine serum
FITC	Fluorescein isothiocyanate
FTIR	Fourier-transform infrared spectroscopy
GFOGER	Glycine-phenylalanine-hydroxyproline-glycine-glutamic acid-arginine
HLA-DR	Human leukocyte antigen—antigen D related
IGF	Insulin-like growth factor
IL	Interleukin
IL-1ra	Interleukin 1 receptor antagonist
ILK	Integrin-linked kinase
LPS	Lipopolysaccharide
MALDI-ToF-MS	Matrix-assisted laser desorption/ionization time of flight mass spectroscopy
MAPK	Mitogen-activated protein kinase
MCP-1	Monocyte chemoattractant protein 1
M-CSF	Macrophage colony-stimulating factor
MIP-1α	Macrophage inflammatory protein 1 alpha
MMP	Matrix metalloproteinase
MSC	Mesenchymal stem cell
NET	Neutrophil extracellular trap
NO	Nitric oxide

B. D. Boyan (✉)
Department of Biomedical Engineering, College of Engineering, Virginia Commonwealth University, Richmond, VA, USA

Wallace H. Coulter Department of Biomedical Engineering, Georgia Institute of Technology, Atlanta, GA, USA
e-mail: bboyan@vcu.edu

E. M. Lotz · M. B. Berger · J. Deng · D. J. Cohen
Department of Biomedical Engineering, College of Engineering, Virginia Commonwealth University, Richmond, VA, USA
e-mail: lotzem@vcu.edu; bergermb@vcu.edu; dengj3@vcu.edu; djcohen@vcu.edu

Z. Schwartz
Department of Biomedical Engineering, College of Engineering, Virginia Commonwealth University, Richmond, VA, USA

Department of Periodontics, University of Texas Health Science Center at San Antonio, San Antonio, TX, USA
e-mail: zschwartz@vcu.edu

NOS2	Nitric oxide synthase 2
OB	Osteoblasts
OC	Osteoclasts
OCN	Osteocalcin
OCP	Osteoclast precursors
OPG	Osteoprotegerin
OPN	Osteopontin
PBMC	Peripheral blood mononuclear cell
PGE_1	Prostaglandin E_1
PGE_2	Prostaglandin E_2
PHA	Phytohemagglutinin
PLXN	Plexin
PMN	Polymorphonuclear leukocytes
RANK	Receptor activator of nuclear factor kappa B
RANKL	Receptor activator of nuclear factor kappa B ligand
RGD	Arginine-glycine-aspartic acid
RUNX2	Runt-related transcription factor 2
SEM	Scanning electron microscopy
SEMA	Semaphorin
SLM	Selective laser melting
STAT	Signal transducer and activator of transcription
TGFβ1	Transforming growth factor beta 1
TNAP	Tissue non-specific alkaline phosphatase
TNF-α	Tumor necrosis factor-alpha
TUNNEL	Terminal deoxynucleotidyl transferase (TdT) dUTP nick-end labeling
VEGF	Vascular endothelial growth factor
WNT	Wingless-related integration site

11.1 Definition of the Interface

The radicular portion of an endosseous implant derives its name from the location of implant placement within the alveolar bone and its similarity in function to that of an intact tooth root. It acts as the interface between the dental prosthesis and bone, stabilizing the implant within a native bone. This interface between the radicular surface and bone develops through the process of osseointegration, in which appositional bone is regulated both directly by surface parameters and distally through cellular signaling mechanisms to anchor the implant. In order to define this biological interface, it is essential to understand the underlying steps of osseointegration, while also describing the effects of implant surface design on each step and the methods by which this interface can be analyzed.

Osseointegration is the structural and functional connection between organized living bone and the surface of a load-carrying implant. The overall process of osseointegration involves osteogenesis from the surrounding bone as well as osteogenesis on the implant material [1–3]. It is measured histologically in vivo as the bone-to-implant contact, typically covering roughly 30–70% of the implant surface, and has been shown to be dependent on topography [4–6]. The process of osseointegration can be categorized into 5 phases: hemostasis, osteoconduction, primary bone formation, modeling/remodeling, and functional integration.

During implantation, destruction of native bone and blood vessel rupture initiate a clotting cascade and hematoma formation. The radicular surface serves as the initial contact point for cellular and biological fluid interaction, which is initiated by the exudation of blood into the implant micro-environment from drilling trauma. The resulting fibrinogen polymerization and adsorption of plasma proteins like fibronectin and albumin, along with local factor release from the platelets that enter the implant micro-environment, provide the first provisional extracellular matrix around the implant (Fig. 11.1).

Implant surface designs can modulate this protein deposition via bulk chemistry, wettability, and topography. Plasma proteins possess specific affinities for adsorption to the implant surface, dependent upon amino acid composition, protein size and shape, and plasma concentration. Altering the wettability and topography of the implant can create differences in the profile
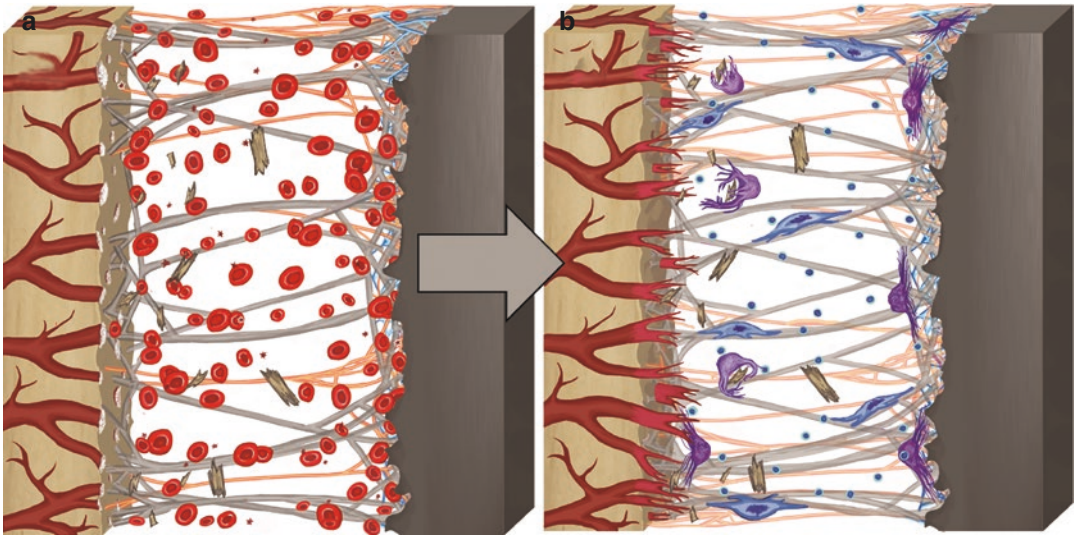
Fig. 11.1 Resolution of the clot. Implant placement causes the exudation of blood into the implant microenvironment. Through the process of surgical trauma growth factors, fibrinogen, and soluble blood proteins adsorb onto the implant surface. Neutrophils migrate into the wound bed and begin attacking any resident bacteria through the complement system and growth factors such as TNF-α, initiating the migration of monocytes and macrophages towards the implant, migrating across the fibronectin pro-visional matrix. Macrophages phagocytose debris and foreign bodies and dependent upon implant surface properties exhibit either an M1 or M2 inflammation resolution. M2 regeneration increases the production of IL-10, IL-4, and TGF-β1, which supports the migration of MSCs to the implant, decreases the response of T and B lymphocytes, and maintains immature dendritic cells to prevent adaptive immune response

of proteins that adsorb onto the surface, and the overall conformation of the proteins once adsorbed [4, 7, 8]. Thus, the process of hemostasis is a key organizing phase of the overall integration, as initial protein deposition dictates the biological response of the surrounding alveolar bone through cell attachment and activation.

Inflammatory pathway activation occurs after the development of the hematoma around the implant. Immune cells such as neutrophils, dendritic cells, monocytes, and macrophages migrate into the wound site following chemical gradients of chemoattractants, mitogens, and growth factors, including tumor necrosis factor-alpha (TNF-α) and a range of Interleukins (ILs). Neutrophils have not been studied extensively until recently. They have been shown to alter immediate implant response by regulating toll-like receptors and through the creation of DNA fiber networks termed neutrophil extracellular traps (NETs) that have dual regulation of inflammation depending on the environment [9, 10]. These extracellular

modulators have also been shown to regulate the most potent immunoregulatory cell within the implant microenvironment, macrophages [9, 10]. Within the first 2 days of implantation, resident tissue and migratory macrophages are present around the implant. Macrophages are responsible for debris phagocytosis, production of tissue remodeling enzymes, and secretion of regenerative cytokines, making them important regulators of implant integration during the inflammatory phase (Figs. 11.1 and 11.2a) [4, 6, 8].

Macrophage response is dependent upon the activation profile present within the wound environment. The classical M1 pro-inflammatory profile is characterized by high levels of interferon-γ, IL-6, monocyte chemoattractant protein-1 (MCP-1), and TNF-α. These induce high levels of reactive oxygen species and nitric oxide (NO) via nitric oxide synthase 2 (NOS2) in order to destroy resident bacteria [11–13]. However, persistent M1 activation by excessive and prolonged bacterial contamination can create
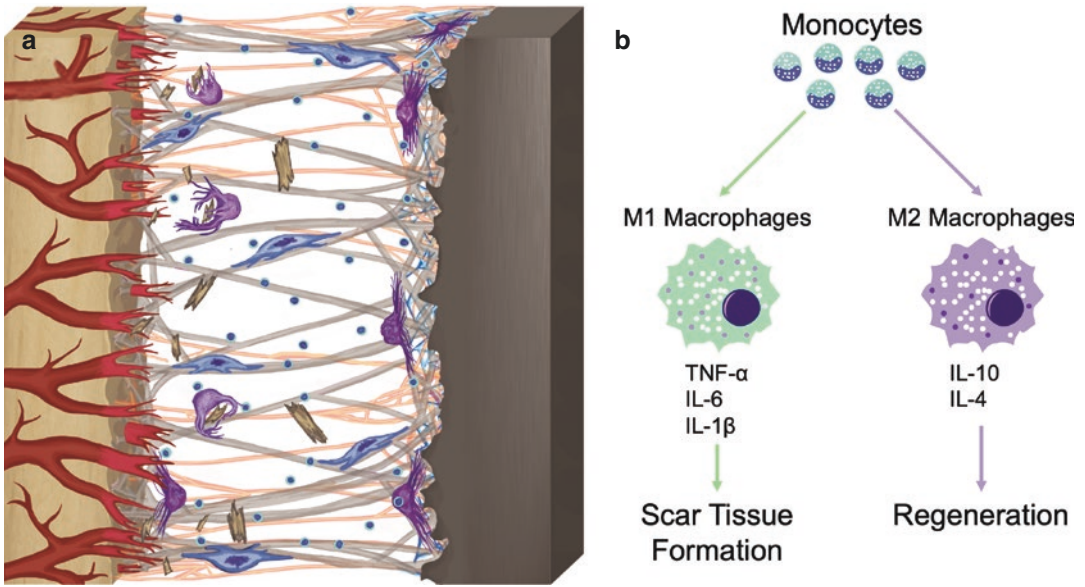
Fig. 11.2 Diagram of the interface during the inflammatory phase of osseointegration. (**a**) Inflammatory response is characterized by the migration of monocytes, macrophages, and MSCs into the implant microenvironment. (**b**) Macrophage activation determines local immune resolution. M1 activation is pro-inflammatory and promotes fibrous tissue formation through TNF-α, IL-6, and IL-1β, while M2 macrophage activation promotes regeneration and implant integration through elevated production of IL-10 and IL-4

a toxic wound environment, preventing integration by the stimulation of foreign body giant cells and fibrous encapsulation (Fig. 11.2b). Surface design and proper aseptic implant placement can facilitate an alternative M2 activation, which is more regenerative in nature. IL-10 and IL-4 are highly expressed during a regenerative macrophage response and pro-inflammatory cytokine production is down-regulated (Fig. 11.2b).

Dendritic cells also contribute to the overall integration of an implanted synthetic implant. These cells primarily direct adaptive immunity through cytokine production and are characterized by a maturation state. Immunological studies and in vitro analysis on clinically relevant titanium (Ti) surfaces demonstrate that immature dendritic cells promote a more tolerance-based adaptive immune response through IL-10-secreting T-cells and CD4+ T-regulator (T-reg) cells (Fig. 11.1) [14]. The maturation of dendritic cells increases local inflammation through IL-12 and activation of T-cells and B-cells of the adaptive immune lineage [4, 15].

This regenerative resolution to implant placement promotes the migration of progenitor cells from the distal bone bed toward the implant micro-environment, using the provisional matrix created by the blood clot. Clinically, the success of implanted materials in orthopedics and dentistry is dependent not only on bone apposition at the implant–tissue interface but also on the establishment of a vascular supply in the peri-implant bone to allow delivery of oxygen and nutrients, as well as systemic hormones and osteoblast-progenitor cells (Fig. 11.1). Angiogenesis, the formation of new capillary blood vessels from the preexisting vasculature, is also initiated in a regenerative micro-environment. This is a critical process during the formation of new bone and bone fracture healing [16, 17], as well as during bone regeneration and osseointegration of implanted materials [18].

Progenitor cells migrating to the peri-implant microenvironment from the bone bed and progenitor cells on the implant surface secrete modulatory proteins that support the creation of an

osteogenic environment during inflammation resolution. Growth factors and cytokines promote osteoblast (OB) lineage-commitment of MSCs and osteoprogenitor cells and later on, further OB maturation, enhance angiogenesis, and modulate osteoclast (OC) mediated bone-resorption around the implant [19]. This transition from an inflammatory response to primary bone formation occurs 1–2 weeks post-implantation.

OBs are responsible for secreting and mineralizing the initial unorganized collagen matrix to form primary bone. In addition to the primary bone formation by OBs migrating toward the implant from the distal native bone bed, contact osteogenesis also occurs directly proximal to the implant surface. Progenitor cells differentiate into OBs based on chemical and topographical cues of the implant surface. The initially adsorbed proteins from the hematoma remain important as the cells do not directly adhere to the surface of the implanted material. Mediated by integrins, MSCs on the implant surface differentiate into OBs via soluble Wnt and bone morphogenetic protein (BMP) signaling [20–24].

Cells interact with proteins on the implant surface through integrin complexes composed of one alpha and one beta subunit. Integrin complexes demonstrate specificity for binding motifs in proteins present in the extracellular environment and then interact with cytoskeletal elements to link the cell to its matrix. OBs express mRNAs for a number of integrin subunits including alpha 1 (α1), alpha 2 (α2), alpha 5 (α5), alpha v (αv), beta1 (β1), and beta 3 (β3) [20]. Fibronectin adsorbed to the implant surface or within the hematoma has arginine-glycine-aspartic acid (RGD) motifs that interact with the α5β1 integrin complex, enabling cells to attach and proliferate [25]. As these cells produce extracellular matrix, they express the α2β1 and α1β1 integrin complexes, which recognize glycine-phenylalanine-hydroxyproline-glycine-glutamic acid-arginine (GFOGER) motifs on type 1 collagen [26]. Topographical cues from cell-surface interactions can change the conformation of the adsorbed proteins, resulting in a change in the conformation of the integrin complex, and a corresponding change in the cytoskeleton. This results in activation of cytoskeletal-based signal cascades, usually acting through phosphorylation of integrin-linked kinase (ILK) and focal adhesion kinase (FAK), and their respective downstream signals [26, 27].

Binding of α2β1 to collagen type 1 further enhances OB differentiation by upregulation of Wnt/BMP signaling to alter cell shape from a more flatted and spread morphology typical of MSCs to a more columnar shape typical of a secretory OB [28]. This is accompanied by increased expression of mRNAs for tissue non-specific alkaline phosphatase (TNAP) and increased alkaline phosphatase-specific activity, followed by increased expression and secretion of osteocalcin (BGLAP, OCN) (Fig. 11.3). Production of transforming growth factor beta 1 (TGFβ1), as well as BMPs 2 and 4 and their inhibitors is also increased [29]. Disruption of these integrin complexes has been shown to inhibit OB differentiation, demonstrating the importance of these attachment proteins in cell sensing and response [20, 28].

Wnt signaling proteins have been shown to be involved throughout the bone modeling phase of osseointegration [30–32]. The Wnt cascade works through two pathways: canonical and non-canonical, defined by the involvement of β-catenin. Canonical Wnt (Wnt1/3/3a/8) signaling increases the concentration of β-catenin in the nucleus and alters the transcriptional activity of T-cell specific transcription factor/lymphoid enhancer-binding factor 1 (TCF/LEF) family of transcription factors and transcriptional activation of Wnt target genes (RUNX2, BGLAP, TNAP, and OPG) [31, 32]. Non-canonical Wnt signaling works independently of β-catenin to enhance bone formation through Ca^{2+}-dependent signaling, protein kinase C (PKC), and calcineurin [24, 33]. Moreover, non-conical Wnt5a, together with protein disulfide isomerase A3 (PDIA3), a cell membrane-associated receptor for the vitamin D metabolite 1α,25-dihydroxy vitamin D_3 [1α,25($OH)_2D_3$], signal through PKC and enhance expression of BMP2 and BMP4 in MSCs (Fig. 11.3) [24, 31, 34, 35]. This mechanism contributes to the enhanced OB differentia-
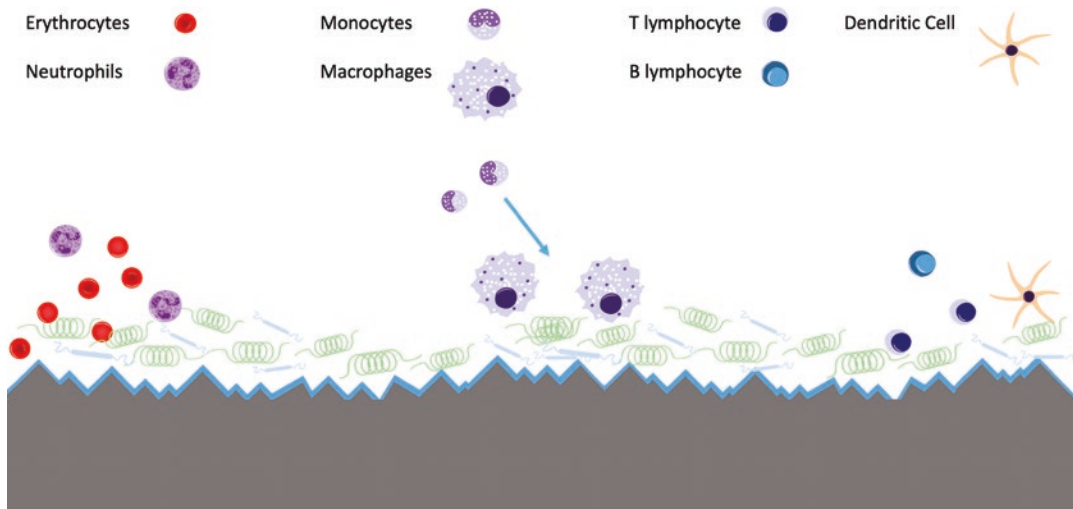
Fig. 11.3 Diagram of protein adsorption onto a titanium implant and the subsequent migration of neutrophils and erythrocytes onto the fibrin network within the first few minutes of implantation. Subsequently followed by migration of monocytes which differentiate into M1 or M2 macrophages dependent on the implant microenviron- ment. Late immune maintenance by adaptive immune cells such as T and B lymphocytes and regulated by dendritic cells. Immature dendritic cells help maintain implant integration whereas sensitive dendritic cells can leave to late-stage inflammation

tion observed in MSCs cultured on microstructured Ti surfaces [36].

BMP signaling also activates SMAD signaling pathways and causes the upregulation of the RUNX2 transcription factor and osteoblastic gene expression [37]. BMP signaling is not only SMAD dependent; additional signaling pathways via ERK MAPK can also be upregulated to enhance the expression of osteoblastic genes. Downstream targets of these pathways are alkaline phosphatase, osteopontin, osteocalcin, and collagen type I, which work in tandem to create primary bone appositionally to the implant surface [38, 39] and local factor production that regulates distal bone formation (Fig. 11.3) [40].

The first bone present following implantation is the primary woven bone. Woven bone is characterized by randomly oriented collagen fibrils in the bone trabeculae and is unable to sustain the load. Mineralization of primary bone involves extracellular matrix vesicles. Implant surface designs to increase surface roughness have also been suggested to increase matrix vesicle density surrounding the implant, but it is not

known if this is due to the surface or load transfer around the implant [4, 41].

The random organization of primary woven bone must be remodeled into load-sustaining secondary bone [3]. The remodeling phase is characterized by the first appearance of OCs around 14 days post-implantation. OCs function by tightly connecting to the mineralized bone matrix using integrins, creating a sealed space that is acidic, enabling the dissolution of the bone mineral. Proteolytic enzymes within the space include acidic matrix metalloproteinases (MMPs) and cysteine proteinases, including cathepsin K. These enzymes degrade the bone matrix, resulting in the formation of an OC resorption pit [42, 43]. OCs also coat the demineralized bone surface with proteins that provide binding sites for osteoprogenitor cells that migrate onto the newly generated surfaces of the resorption pits. These cells differentiate into OBs and synthesize and mineralize new bone. Thus, the primary bone is reorganized into a load-sustaining orientation by the cyclical action of OBs secreting and mineralizing matrix and OCs resorbing bone. This

communication is reciprocal in nature and is due to tightly regulated paracrine signaling. The end result is stress-oriented haversian bone [44, 45].

Paracrine signaling between OBs and OCs involves the interaction of receptor activator of nuclear factor kappa B ligand (RANKL) with RANK on OC precursors (OCPs), stimulating their differentiation into mature OCs. OBs and immune cells secrete macrophage colony-stimulating factor (M-CSF) as a chemoattractant for monocytes of the hematopoietic stem cell lineage, to form OCPs expressing the RANK receptor [46]. OBs can hinder OC differentiation via OPG, which is a decoy receptor for RANKL. OPG binding to RANKL sequesters the activating ligand and prevents differentiation of OCs, decreasing the rates of resorption. This has the result of enabling net peri-implant bone deposition and ensuring appropriate rates of remodeling primary bone.

OBs are in turn stimulated via bone matrix proteins that are released during OC-mediated resorption. BMPs, insulin-like growth factors (IGFs), and transforming growth factors (TGFs) stimulate OB differentiation and maturation and increase matrix deposition [4, 6, 46]. TGFβ1 stimulates the proliferation of mesenchymal cells and enhances the production of extracellular matrix, particularly type I collagen [19]. It is synthesized in latent form and stored in the extracellular matrix together with a binding protein termed latent TGFβ binding protein (LTBP). The amount of TGFβ1 produced by OBs cultured on Ti is modulated in a surface-dependent manner. Most of the growth factor is produced in latent form and stored in the extracellular matrix, although there is also an increase in active TGFβ1 in cultures grown on microstructured Ti. The active growth factor acts in an autocrine/paracrine manner to upregulate the production of OPG [47]. Surface designs to increase OPG and decrease the RANKL/OPG ratio are known to increase net bone formation, increase bone-to-implant contact, and better implant survival rates through the regulation of OC fusion and activity.

A robust vascular network is important for bone health. There is now a growing awareness that blood vessels are associated with nerves. The importance of neural regulation of bone homeostasis has been addressed primarily by revealing bone innervation at the anatomical level [48]. The direct neural regulation in titanium implant osseointegration has been inferred by contrasting a model that imposes both direct denervation and diminished muscle activity with a model of diminished muscle activity [49]. Semaphorins, originally as identified as nerve-derived factors, have been implicated in the regulation of bone remodeling [50, 51].

The crosstalk regulation between OBs and OCs can also occur through the semaphorin signaling system, including their receptors, plexins (PLXNs), and non-ribosomal peptides (NRPs) [52–54]. Semaphorins are a class of membrane-bound and soluble proteins whose functions were first validated in the nervous system. The semaphorin-plexin system has been reported in the involvement of various biological events, including angiogenesis [55], immune response [56], oncogenesis [57], and bone homeostasis [58, 59]. Of the eight classes of semaphorin families, SEMA3A and SEMA4D have been shown to be involved in the bone remodeling process. SEMA4D is a membrane-associated protein but acts as a soluble factor after proteolytic shedding [60]. SEMA4D is expressed in OCPs and mature OCs, but not in OBs [61, 62]. Its receptor PLXNB1 is detected in OBs, which indicates its potential role as a coupling factor. SEMA4D-PLXNB1 inhibits bone formation by activating RhoA and inhibiting the IGF-1 signaling pathway [61, 63]. Deficiency in SEMA4D and PLXNB1 or blocking SEMA4D with antibodies in mice causes the trabecular bone mass increase. Fc-SEMA4D treatment inhibits osteoblast differentiation by reducing alkaline phosphatase activity and osteocalcin production [61].

SEMA3A is a secreted protein that exerts its biological activity through interactions with NRP1 and subsequent complex formation with PLXNA1 [64, 65]. The dual regulation of SEMA3A on stimulating bone formation and suppressing bone resorption indicates its importance in the bone remodeling process. Regulation via SEMA3A has the potential to overcome the side effect of traditional humoral factors, which

simultaneously reduce bone formation and resorption [53, 66]. The synthetic SEMA3A treatment of OBs activates Rac1 through FARP2, which leads to the accumulation of β-catenin in the cytoplasm and the translocation of β-catenin into the nucleus [53]. The complex of SEMA3A and NRP1 also competes with the binding between PLXNA1 and TREM2/DAP12 complex, which is a co-stimulator of RANKL-induced osteoclast differentiation [53].

SEMA3A is produced by osteoblastic lineage cells, including MSCs and OBs. Its production is regulated by titanium surface properties via signaling by integrins α2 and β1 [67]. Exogenous SEMA3A increases the osteoblastic differentiation of MSCs on microrough titanium surfaces, and this effect is further enhanced when the cells are cultured on microrough and hydrophilic titanium surfaces. Increased production of OPN and OPG in response to SEMA3A treatment supports an important role for SEMA3A as a coupling factor capable of regulating bone remodeling occurring with the presence of titanium surfaces [67].

Over time sufficient bone is remodeled and the implant gains what is known as secondary stability. Following repeated cycles of OB–OC interaction in a load-sustaining fashion over 2–3 months, the implant becomes stably integrated into haversian bone. Haversian bone is characterized by tree trunk-like ring structures, or osteons, which are concentric circles of new bone with blood vessels and innervation at the center. The haversian bone then is controlled internally via mechano-sensing osteocytes, which sense load and microfluidic movement through nanopores within the bone, and modulate the reciprocal action of OBs and OCs [68]. Osteocytes are terminally differentiated OBs that are embedded within the mineralized matrix and form a network of cell processes throughout the haversian bone system. They decrease net bone formation by producing a soluble protein called sclerostin, which inhibits Wnt and BMP-induced OB differentiation and action [69]. Osteocytes can also signal using nitric oxide and prostaglandins to recruit OCs, thereby stimulating new bone formation in response to micro-trauma from load-

ing. Ultimately, the end result is bone capable of remodeling and realigning to sustain cyclical loading transduced by the implant [4, 6].

Instances of poor implant integration can be attributed to a number of issues during implant placement and the subsequent biological response. If an implant does not achieve primary stability, the micro and possible macro-movement of the implant can disrupt primary bone formation, leading to fibrous encapsulation with fibronectin and collagen types I and III [70]. There are also compromised situations in which an implanted endosseous dental implant will have a higher degree of failure due to alveolar ridge deficiency [71]. Alveolar ridge deficiency occurs after natural teeth are lost and the alveolar bone around the socket of the tooth becomes unloaded. Additionally, patients who have undergone natural or surgical menopause can have estrogen-deficient bone loss. Therefore, some treatment options require bone augmentation prior to implant placement [71, 72].

Post-integration there are still some major issues plaguing the field of dental implantology such as peri-implantitis and metal ion leaching. Osseointegrated implants can undergo site-specific prolonged infectious disease due to one or a combination of causation factors such as excessive loading, implant resident bacteria, soft tissue morphology changes or degradation, and implant design. The result is a gradual recession of bone height, fibrous encapsulation, infection, pain, and implant failure [4, 6, 70, 73].

11.2 Material and Surface Designs

The ability of an implant surface to dictate cellular response is a fundamental principle of modern implantology. Therefore, there are key parameters when considering surface design for a dental implant. The implant material should be highly biocompatible. The surface must also be corrosion-resistant and wear-resistant to sustain structural integrity and reduce metal debris throughout the life of the implant under cyclic loading. Ti and Ti alloys like titanium-aluminum-

vanadium (Ti6Al4V) and titanium-zirconium (TiZr) fit these requirements because the Ti oxide that forms on the surface is biocompatible, corrosion-resistant, and wear-resistant. In addition, the material surface should be osteoconductive to enable peri-implant osteogenesis and it should provide sufficient physical and chemical information that supports OB differentiation of osteoprogenitor cells.

The osteoconductive/osteogenic properties of the material surface are essential for specific protein adsorption profiles on the implant surface, which determines available binding domains of adsorbed proteins. Overall wettability further facilitates these protein-surface interactions. As a result, materials that readily interact with water through intermolecular forces can have superior behavior post-implantation through the adsorption and homogeneous spreading of proteins across the surface during implant placement. The concentration of fibronectin on the surface increases with increasing surface roughness, and the increase in available binding sites for cells contributes to enhanced osseointegration [74]. It is important to note that any one parameter is not sufficient to account for the osteogenic properties of a surface design. Fibronectin can also lead to fibroblastic differentiation of progenitor cells, and ultimately fibrous connective tissue formation. Thus, it is the totality of the surface properties that elicit chemical and biological outcomes and not one single parameter.

Various methods currently exist to modify the surface parameters and alter protein adsorption onto the surface; subsequently, these altered protein profiles dictate cellular response. The microscale mesoscale and nanoscale topographic features of the implant surface are important parameters for modulating biological response. The surface roughness of commercially available implants is usually generated through varying degrees of grit-blasting, acid-etching, or a combination of the two processes [20, 24, 35, 47, 75, 76], although other methods exist, such as Ti plasma spraying (TPS), anodization, cold plasma treatment, and synthetic biochemical surface coatings [77–80].

Novel manufacturing methods for medical devices have also impacted the development of metal-based orthopedic and dental implants. Additive manufacturing (AM) has been used in the aerospace industry to create lightweight but durable parts and is being used in the medical field with increasing prevalence. Many methods exist to create 3D metal implants with complex geometries, and each method has its strengths and drawbacks [81]. The method used can determine build time, resolution of the implant geometries, material selection, and mechanical properties. Additional macro and microscale roughness can be the result of the manufacturing method. AM implants possess microroughness due to the sintering of micrometer-diameter particles. However, AM implants that have not undergone further processing by grit-blasting and/or acid-etching do not possess meso or nanostructures and may result in loose particle wear from partially sintered metallic particles, metal hypersensitivity, and prolonged inflammation. AM implants can also be further processed by heat treatment to improve the fatigue properties of the metal, but this may further alter the surface morphology of the construct and affect cellular response. The effect of these heat treatments on cellular response is just beginning to be examined. Guidelines for further investigation have been implemented by the United States Food and Drug Administration (FDA), the American Society for Testing and Materials International (ASTM), and the American National Standards Institute (ANSI), among others to address the concerns regarding differences in material manufacturing and post-processing of medical devices [82–86].

Ti and its alloys have been the gold standard for dental implant materials as the ceramic Ti oxide surface they possess has a high affinity for appositional bone formation, biocompatibility, and good corrosion resistance. Additionally, Ti also has an excellent strength-to-weight ratio. Ti has more similar mechanical properties to bone when compared to other metals and alloys. However, its elastic modulus ranges from 90 to 110 GPa, which is still much higher than the

20 GPa reported for cortical bone. These properties are tunable through the post-manufacturing modifications mentioned above [87, 88].

Other ceramics possess similar mechanical properties as Ti with respect to fatigue properties and strength and offer some advantages, such as tooth-like coloring and biocompatibility. The limitations of ceramics are their weak resistance to shear and tensile loading, leaving ceramic implants with a higher chance of fracture and implant failure. Recently, dental implant manufacturers have begun investigating the use of zirconium ceramics. The major ceramic used currently in non-metal dental implants is zirconia (ZrO_2), which is a white crystalline oxide of zirconium and possesses an elastic modulus of 200 GPa. However, zirconia is sensitive to temperature changes, and rapid cooling from higher temperatures can cause the implant to fail, necessitating the use of additional oxides to help maintain its tetragonal crystal structure. The advantages of zirconia implants are the biocompatible bulk chemistry of the implant and the low possibility for ion leaching, compared to Ti and its alloys. Zirconia also possesses better mechanical properties compared to aluminum oxide, previously used in ceramic dental implants. This is due to tetragonal zirconia polycrystals, which give zirconia a higher fractural resilience and higher flexural strength. Unfortunately, zirconia is still limited by the difficulty to produce tunable surface designs to facilitate enhanced osseointegration. Therefore, Ti is still the choice material for dental applications [89–92].

11.3 Protein-Surface Interactions

The initial interaction of an inserted implant with biological tissue is the interaction of soluble proteins in blood flowing into the wound bed during surgical trauma. Methods to assess the concentration and homogeneity of specific proteins at the interface can offer insights into the overall biologic response to the implant. In order to assess the interface of implant surface design in a laboratory setting assays have been developed for determining the mechanisms of protein adsorp-

tion, clot formation, and the quantity of soluble ions in the peri-implant space. In the section below, the methods for quantifying the initial interfacial interaction are described, as well as a description of the expected outcomes and context for the implications of these outcomes during osseointegration.

Assessment of the peri-implant interface and the effects of surface design on the initial biologic mechanisms of integration of a dental implant require specific testing specifications. Discs that have undergone the same manufacturing and post-processing methods are used to determine the interfacial behavior of the specified treatments. A common format for material coupons is a disk that is cut into 15 mm × 1 mm discs post-processed usually by grit-blasting and/or acid-etching, and stored in comparable packaging conditions used clinically [93].

One method to examine protein adsorption behavior uses fluorescence intensity to qualitatively and quantitatively assess the effect of surface treatments on protein conformation. In one example, discs were incubated with 1 μM fibrinogen Alexa Fluor 546 conjugate solution in a buffer solution (0.1 M Na_2CO_3) at a pH of 8.3. The solution was incubated on the disc and covered with a microscope coverslip [20-40 μL] in the dark for 5 min. Discs were then rinsed in the buffer solution three times for 5 min each and dried with nitrogen gas and examined with fluorescence microscopy. Using this qualitative method, there large areas of non-uniform protein adsorption are seen. Also, hydrophobic areas were present that lacked coverage. In contrast, surfaces treated to increase the wettability and hydrophilicity demonstrated increased coverage homogeneity. Quantitative image analysis of the areas of non-coverage as a percentage of total disc surface was correlated with surface cavities. Fluorescence intensity analysis of hydrophilic surfaces by this method demonstrated that hydrophilic surfaces decreased average intensity compared to hydrophobic surfaces, suggesting more uniform coverage and lower areas of clumping or disunity [93].

Additional methods to quantify protein adsorption use smaller discs (5 mm × 1 mm) in 96 wells, and a similar method can be undertaken

using fluorescent isothiocyanate (FITC) conjugated to albumin or RGD peptide incubated for 5 min and measured by microplate spectrofluorometric reader to determine the amount of adsorbed protein at a higher throughput [94].

Adsorption of bovine serum albumin (BSA) is often used as a model for human serum proteins. Samples are incubated in a known concentration of BSA. Non-adherent BSA remaining in the solution is determined using a standard curve. While this method can discern macroscale protein adsorption affinity, it does not provide specificity or conformation of the proteins on the substrate surface [95].

Enzyme-linked immunosorbent assays (ELISAs) can be used to quantify the concentration of specific proteins adsorbed onto the substrate. Samples are incubated in solutions containing proteins of interest. BSA is incubated on the substrate surface at 37 °C for an hour to block any sites not occupied by the test protein(s). Antibodies that target the proteins of interest, such as vitronectin or fibronectin, can be used to quantify their respective concentrations using a horseradish peroxidase secondary antibody. Colorimetric changes in absorbance are then read using a microplate reader [95].

Matrix-assisted laser desorption/ionization time of flight mass spectroscopy (MALDI-ToF-MS) can be used to determine the size of proteins adsorbed on the surface. Laser light is used to vaporize the protein at a resolution of 100 nm. The time of flight of the vaporized samples through the mass spectrometer determines the mass-to-charge ratio. Results are mapped onto known protein sizes in order to determine the adsorption profile of the surface [96]. Analysis by this method has demonstrated the ability of surface treatments to alter the profile of proteins and peptides under roughly 25 kDa. However, the complex interaction of these altered profiles in the context of osseointegration has not been elucidated.

Fourier transform infrared spectroscopy (FTIR) is used to further characterize the crystallinity of the proteins adsorbed onto the surface of substrates. 10% FBS or purified proteins (albumin or fibronectin) are commonly used as models. Samples are incubated for varying time points (1 to 4 h) in solutions of the proteins, rinsed, and analyzed for peak intensities of the amide I and amide II groups. In this method, amide I correlate to randomized orientations or turns in adsorbed proteins, while secondary protein structures such as α-helix or β-sheets are seen in amide II peaks. Surfaces that increase the FTIR peak for amide I have shown increased cell spreading and proliferation in vitro. This method is not sufficient to quantify the concentration of proteins adsorbed but can give predictive confirmation information of surface treatments [97].

Following initial protein adsorption, blood clot formation and extension is an important indicators of surface properties and their effects during implant integration. The methodology is rather simple. Whole human blood (50–200 μL) is pipetted onto the surface of the substrates and allowed to clot for 5–20 min. The surfaces are subsequently rinsed and fixed using paraformaldehyde, dehydrated by serial ethanol dilutions and desiccation, and imaged by SEM. Digital images can then be mapped for the extension of the clot over the surface of the substrate, using software like ImageJ (National Institutes of Health, Maryland, United States). Studies have shown that increased microroughness increases clot extension, and wettability may contribute to extension [77, 98, 99].

Cell attachment, proliferation, and migration have been used to analyze the impact of surface design on clot formation. Clots in whole blood are allowed to form on implant surfaces for 10 min. Cells are cultured on the clotted surface for 1, 3, or 5 days, fixed, and imaged by SEM. Surfaces that possess microroughness have been shown to increase the proliferation of precursor cells in a rat blood model. Another approach is to condition cell culture media with whole blood clots produced by incubating whole blood for 10 min on substrates of interest. This method enables examination of the effects of clot adsorption of local soluble factors. Again, microroughened surfaces were shown to increase the concentration of VEGF, MCP-1, and other soluble blood proteins, which increase the motility of precursor cells in a scratch test and transwell

migration analyses [100]. These assessment methods are similar to protein adsorption but more specific to non-soluble fibrin scaffolds. Expected outcomes for increased biological integration are increased adsorption of fibrin and fibronectin, and increased homogeneity of protein coating appositional to the surface. These factors can impact cell attachment, morphology, and differentiation.

Studies to determine the bonding strength of proteins to the substrate surface using atomic force microscopy. Tips are functionalized with monoclonal antibodies for specific cell attachment points or functional proteins. These methods have been undertaken to determine platelet adhesion and density across substrate surfaces [101, 102].

Collectively, these in vitro methods for determining protein adsorption onto implant surfaces can provide insights into the expected behavior of immune and progenitor cells that migrate into the implant microenvironment. Some studies are limited in the number of proteins being examined and are low throughput, while others are capable of using biologically relevant whole blood but differences in donor blood profiles have not been examined. In the scope of surface design, implant surfaces that possess microroughness and hydrophilic properties create more homogenous protein coating and alter the concentrations of the adsorbed proteins that have been shown to enhance integration in vivo [92, 103, 104].

11.4 Immune Response at the Interface

Immediately following the initial protein adsorption on the surface of the implant and the formation of the blood clot, the innate immune system responds to bacterial contaminants and tissue debris. Initial investigations to examine the interaction of immune cells with the implant surface used peripheral blood mononuclear cells (PBMCs) and polymorphonuclear leukocytes (PMNs). Experiments have assessed cell migration, adhesion, activation, signaling, and apoptosis, providing information on the peri-implant microenvironment during the resolution of the inflammatory phase of osseointegration. PBMCs include lymphocytes (T cells, B cells, and NK cells) and monocytes. PMNs include neutrophils, eosinophils, and basophils.

11.4.1 Neutrophils

Methods to examine the behavior of the initial interaction of a metal implant surface with the immune system use mononuclear cells and neutrophil leukocytes separately or in co-culture on discs with the properties of interest. This experimental method measures cytokines produced by these cells to predict the in vivo response to implant insertion. More recent analyses have evaluated the response of neutrophils isolated by flow cytometry (CD11b+/Ly6G+) by assessing cell spreading and overall NET formation via confocal microscopy, as well as by analyzing gene expression [9]. ELISAs are used to measure anti-inflammatory (IL-1 receptor antagonist, IL-4, IL-10) and pro-inflammatory (IL-8, IL-6, IL-1β, IL-12, IL-17, TNF-α) cytokine production. Neutrophil activity markers for inflammation like neutrophil elastase and myeloperoxidase are also evaluated by ELISA and have been shown to be regulated by surface properties [9].

To do these studies, mononuclear and neutrophil leukocytes are separated from human donor blood by centrifugation and cultured on metallic disc substrates. Conditioned media are collected and analyzed using LPS treatment as the positive control for inflammation [105, 106].

In addition to measuring cytokine production, conditioned media from these cultures are used to assess effects on macrophage regulation, bacterial killing, phagocytosis, and chemotaxis. Of particular interest is the effect of the conditioned media on macrophage phenotype based on the presence of pro- and anti-inflammatory surface receptors on macrophages [9]. The ability of the conditioned media to induce mononuclear leukocytes to kill *Staphylococcus aureus is used to indicate the effectiveness of an implant surface to direct a pro-healing immune response* [105]. Another approach is to examine the endocytosis

ability of myeloid leukocytes to take up fluorescently labeled *Escherichia coli* [105]. Another important indicator of a well-designed surface with respect to immunomodulation is the ability to attract neutrophils. This is assessed by assessing the migration of neutrophils through a membrane in response to a gradient generated by conditioned media [105].

Apoptosis is another process that can be monitored to determine the effect of surface topography and chemical makeup on the immune response. PMNs have relatively short life spans during osseointegration and prolonged activity can create high levels of reactive oxygen species. A method used to test the apoptotic affinity of the PMNs is described below. Conditioned media (500 μL) from either PMNs or PBMCs on the surfaces of the test substrates are mixed with 500μL of PMNs in cell suspension and cultured for 24 h. The cells are subsequently imaged using SEM and quantified for DNA fragmentation through flow cytometry by the TUNEL method [106]. TUNEL uses an enzyme (terminal deoxynucleotidyl transferase) to attach fluorescent labels to the end fragments of apoptotic DNA. Fluorescence intensity is then quantified as apoptosis. PMNs undergoing apoptosis exhibit blebbing morphology (tiny circular vesicles), condensation and separation of DNA, vacuole formation in the cytoplasm, and mitochondrial degradation. These changes can be assessed by SEM and bright field imaging [107].

Surface designs that enhance integration are expected to increase the production of anti-inflammatory factors by PBMCs and PMNs cultured on the material surface. It has been shown that increasing surface roughness increases the production of these cytokines, which could be attributed to extended PMN residence due to an inhibition of apoptosis signaling by cell-material interactions [105–108]. In the scope of peri-implant tissue repair there is no defined threshold for the extended residence of the PMNs. It is known these immune cells are necessary signaling mediators to remove bacterial/inflammatory agents and promote wound healing; however, in vitro assays are unable to determine if pro-

longed activity can be detrimental to osseointegration [106].

An important consideration to make in this experimental setup is the diameter of the material substrates. If the disc being used has a smaller diameter than the culture well, cells will be interacting with the tissue culture polystyrene (TCPS) surfaces in all experimental cases, which can dilute some of the effects of the material differences or surface designs.

11.4.2 Macrophages

Macrophages are also key regulators of the host immune response during the osseointegration of a dental implant. Much like PMNs, macrophages secrete cytokines and modulate phagocytosis, to control cell migration, proliferation, and activation. Methods to analyze these cells differ from PMNs in that macrophages are also dependent on their activation state when it comes in contact with the surface-adsorbed proteins. Studies into the morphological behavior of macrophages on differing substrates through bright field microscopy, confocal microscopy, and SEM imaging have demonstrated an affinity for macrophages to adhere and elongate on rough surface topographies [109–112].

To examine the behavior of macrophages at the interface, cells are often incubated with bacterial lipopolysaccharide (LPS) or IL-4 to activate the macrophages to either an M1 pro-inflammatory type or M2 regenerative type. Previous studies used only LPS to activate macrophages and compared the response to non-activated macrophages. In one study, inactivated and LPS-activated RAW264.7 mouse macrophages were cultured at 500,000 cells per mL per well for up to 48 h prior to media collection on substrates (15 mm × 1 mm) of differing combinations of grit-blasting and acid-etching. It is important to note these substrates fit and covered the entire well bottom of a 24-well plate, preventing cells from adhering to the TCPS surface. The macrophage-conditioned media were analyzed for cytokine production (TNF-α, IL-1β, IL-6,

MCP-1, and MIP-1α) by ELISA. Substrates that were grit blasted and acid etched enhanced the production of TNF-α, IL-1β, and IL-6 in a time-dependent manner in both activated and non-activated macrophage populations compared to the other surfaces. However, the chemokines MCP-1 and MIP-1α were decreased on the substrates treated by both grit-blasting and acid-etching for non-activated macrophages and were increased when cells were activated by LPS. These results suggest that specific topographic features can modulate the immune resolution and that surface treatments differentially affect chemokine production depending on the activation state of the macrophages in contact with the surface [113].

More recent investigations into macrophage-implant behavior have assessed surface hydrophilicity as a determining factor of macrophage activation and response. Similar to previous studies, primary non-activated macrophages were harvested from mice and cultured on clinically relevant metal-based implant substrates for 24 to 72 h to determine the cytokine production profiles. ELISA quantification of TNF-α, IL-1β, IL-6, IL-4, and IL-10 was used to predict the likely immune resolution process the macrophages would undergo. An M2 response was defined as increased production of the anti-inflammatory cytokines IL-4 and IL-10 and decreased levels of TNF-α, IL-1β, and IL-6. Substrates that had increased wettability produced higher levels of anti-inflammatory cytokines than hydrophobic roughness-matched substrates, and a combination of microroughness and hydrophilicity increased the anti-inflammatory cytokines, compared to smooth hydrophilic substrates [80, 112].

There is also evidence the bulk chemistry of an implant material can influence the macrophage resolution during osseointegration. Using a similar experimental design to the one described above, TiZr SLA was shown to be capable of producing an enhanced anti-inflammatory environment similar to the hydrophilic Ti SLA surfaces, even though the TiZr SLA surface is hydrophobic. This study also highlights another quantification method for macrophage response through

the examination of mRNA levels for anti-inflammatory genes (Il10,Tgfb, Chil3, and Rentla) and pro-inflammatory genes typical of M1 activation (Il1b, Il6, and Tnfa) 24 h after culture on the surfaces [114]. The results demonstrate a transcriptional control of macrophage response by surface properties, in addition to the regulation of protein production, which is important since macrophages play a vital role in initial innate implant tolerance and wound repair following surgical trauma.

11.4.3 Foreign Body Giant Cells

Foreign body giant cells (FBGCs) are large multinucleated cells formed through the fusion of macrophages. These cells are found on implant surfaces and are important for maintaining the equilibrium of osseointegration. Persistence at an implant site is defined as a "foreign body reaction," which occurs when there is a breakdown of this equilibrium. Reactivation of these cells can contribute to bone resorption, macrophage reactivation, and chronic inflammation [115–118].

FBGCs have been differentiated in vitro (from macrophages) with the addition of IL-4, and fuse through E-cadherin and STAT6 pathways [116]. However, it is still extremely difficult to model the complex immunological response required to activate fusion and examine the effects of FBGCs on an implant surface. Co-culture experiments using trans-wells and primary cells (fibroblasts and macrophages) have provided better predictions of in vivo cell interactions, compared to monoculture. This is attributed to the ability of cells to communicate through contact and non-contact signaling pathways in real time [119]. Further characterization of FBGC has demonstrated these cells are implant-resident and are differentiated from tartrate-resistant acid phosphatase (TRAP) positive OCs by expression of cell surface markers: integrin β2 for FBGCs and integrin β3 for OCs [115]. There are few analyses focused on FBGC behavior peri-implant; instead, studies focus on macrophage signaling and immune resolution within the innate immune system prior to FBGC formation.

11.4.4 Dendritic Cells

Dendritic cells are immunomodulatory cells that help organize the immune response around a foreign object and have been implicated with inflammatory osteoclastogenesis and osteolysis via upregulation of RANKL. Upon inflammation, the dendritic cells mature and increase production of pro-inflammatory cytokines. Therefore, a biomaterial that maintains the immature phenotype can decrease inflammatory response and accentuate osseointegration.

Methods to examine the maturation state and activation levels of dendritic cells peri-implant assess protein production and morphology. In order to test the effects of varying surface properties on dendritic cell maturation, in one example, adherent cells from PBMC whole blood isolations were cultured with dendritic cell media for 5 days in granulocyte-macrophage colony-stimulating factor (GM-CSF) and IL-4 to induce differentiation of monocytes into immature dendritic cells. At 5 days these immature dendritic cells were cultured on Ti substrates of clinical relevance at 500,000 cells per mL in a 24-well plate. Positive control for mature dendritic cells were TCPS wells treated with LPS, or untreated for negative control. Cells were harvested after 24 h and assessed for cytokine production in the cell culture supernatant, and detached from the surfaces to quantify CD83, CD86, and HLA-DQ, which are known maturation markers for dendritic cells. In order to determine morphological differences between dendritic cells on smooth Ti (PT), acid-etched/grit blasted Ti (SLA), and hydrophilic Ti (modSLA) surfaces, cells were imaged by SEM after serial dehydration in acetone, critical point dried, and sputter coated. Additionally, a multiplex magnetic bead analysis was undertaken to quantify the common immune markers (TNF-α, IL-6, IL-1 receptor antagonist, MIP-1α, MCP-1, IL-1β, IL-10, and IL-8). Results demonstrated that dendritic cells retained their immature phenotype on the modSLA surface [14]. Cells on SLA exhibited similar phenotypic maturation to dendritic cells cultured on polished Ti and TCPS, indicating that microroughness alone is not capable of modulating the immune response of dendritic cells for Ti substrates. Maturation of the dendritic cell phenotype resulted in increased production of MCP-1 and expression of cluster of differentiation 86 (CD86), potentially resulting in the recruitment of a variety of immune cells including monocytes, CD4+, and CD8+ memory T-cells.

In addition to implant surface interactions dendritic cells are also involved in hypersensitization to peri-implant metal ions. To test this, differentiated dendritic cells were treated with soluble Ti ions for up to 3 days, then analyzed for viability using a mitochondrial metabolism assay and BrdU incorporation assay for proliferation. The study also used flow cytometry to assess the surface marker expression of CD80, CD86, HLA-DR, CD54, and CCR6. Additionally, the production of IL-1β, IL-4, IL-6, IL-10, IL-12p70, and TNF-α was determined using a magnetic bead multiplex [120].

Exposure to Ti ions affected dendritic cell response, altering surface expression of HLA-DR, CD80, CD86, and CCR6, resulting in increased maturation and direction towards a Th1 hypersensitivity. However, preventing hydrocarbon deposition onto the microrough Ti substrates created a hydrophilic microrough surface, which prevented the maturation of the dendritic cell phenotype. Moreover, maintenance of the immature phenotype and non-stimulatory response of the dendritic cells did not inhibit their ability to respond to implant-associated infections [14].

11.4.5 B Cells, T Cells

The adaptive immune response relies primarily on antigen-presenting cells (macrophages and neutrophils) activating proliferation and maturation pathways for B and T cells. There is evidence that implanted metals can inhibit the adaptive immune system. When PBMCs, T cells that have been differentiated via treatment with phytohemagglutinin (PHA), or B cells differentiated by treatment with LPS were cultured on Ti, chromium, and cobalt, there were decreases in prolif-

eration, production of IL-2 and IL-6, and altered interferon-gamma production that depended on the bulk chemical properties of the metal [121].

The overall goal of the implantation of biocompatible materials is to prevent the cascade of adaptive immunity involving B cells, T helper cells, T cytotoxic cells, and mature dendritic cells. Therefore, less focus has been placed on the response of B and T cells to the implant surface, but rather on the response of the innate immune system and signaling molecules that prevent the development and incorporation of the adaptive immune system. Animal studies investigating the response of B cell formation and activity have demonstrated that after implantation, population numbers fluctuate but do not alter FBGC formation, and Ti implants have shown strong integration or immune tolerance by B cells.

PBMCs harvested from patients possessing successfully integrated Ti dental implants constitutively produced IL-10, which could counteract the upregulation of IL-1β, IL-6, and TNF-α during the innate immune response to Ti materials [122]. These analyses show bulk chemical properties influence cellular response, but there have not been studies to determine the effects of surface microroughness and free wettability on the cellular activity of adaptive immune cells. The overall response of the immune system has shown that hydrophilic microrough surfaces alter protein adsorption, which in turn changes how innate immune cells respond. Neutrophils and macrophages have been shown in an in vitro setting to create a microenvironment that fosters tissue remodeling, immune resolution, and removal of debris and contaminants. This microenvironment can be attributed to the downregulation of pro-inflammatory cytokines and increases in IL-10 and IL-4. These factors work in an autocrine/paracrine manner to prevent adaptive immune response through B and T cell activation, expediting the resolution of the inflammatory phase of osseointegration, and creating migratory signals for OB progenitor cells to start the osteogenesis phase of implant integration.

11.5   Assessment of Osteogenesis

Following the resolution of the inflammatory phase of osseointegration, the migration of MSCs and osteoprogenitor cells and the differentiation of these precursors into OBs create an environment that supports the formation and mineralization of bone in response to chemical, physical, and biological cues. In vitro models have been successfully used to assess the contributions surface properties have to different aspects of osteogenesis. Many of the in vitro studies employed to understand the bone–implant interface are based on cell attachment and the ability of the implant surface to facilitate an osteogenic environment. Most studies examining the osteogenic potential of implant surfaces in vitro have used cells that are either immature OBs or OB cell lines. However, the first group of cells to colonize the implant surface must be able to migrate through the peri-implant clot and are likely to be multipotent progenitor cells.

The attachment of MSCs to implant materials and their subsequent proliferation, extracellular matrix synthesis, and differentiation are sensitive to properties of the surface. Attachment is reduced on microrough surfaces compared with TCPS or smooth Ti substrates [123]. Moreover, those cells that do attach exhibit reduced proliferation. In contrast, these cells show increased markers of osteoblastic differentiation [124]. When cultured on implant surfaces MSCs produce markers of OB differentiation, including increased alkaline phosphatase-specific activity and production of osteocalcin, osteoprotegerin, osteopontin, TGFβ1, and RUNX2 [40]. Their differentiation is further increased when cultured on substrates that have been grit blasted and acid etched compared to smooth substrates. The stimulatory effect of the topographical features of the substrate is enhanced when the hydrophilicity of the surface is retained post-processing [82]. Moreover, MSC differentiation is accelerated from 21 days in cultures on TCPS grown in osteogenic media to within 4 days on Ti implant substrates without any osteogenic factors being

added to the cultures. OB phenotypic markers and the levels of regulatory factors in the conditioned media are modulated by $1\alpha,25(OH)_2D_3$ and in a manner that is synergistic with surface roughness [125].

The change in phenotypic markers is accompanied by a change in cell shape, suggesting that the physical environment elicits some of its effects via mechanical signals [28]. Cells that are attachment dependent interact with their substrate through a number of mechanisms, including specific binding of integrins to components of the extracellular matrix, as well as to proteins adsorbed on the substrate surface. The transition from MSC to OB is dependent on a change in integrin expression from predominantly $\alpha5\beta1$, which binds fibronectin, to $\alpha2\beta1$ and $\alpha1\beta1$, which bind collagen type 1 [126]. Inhibition of integrin signaling by silencing individual subunits revealed that the effect of the surface microstructure is mediated through $\alpha2\beta1$, whereas surface chemistry is mediated by $\alpha1\beta1$ [127]. Furthermore, inhibition of $\alpha5\beta1$ signaling results in reduced cell attachment to the surface and reduced proliferation indicating its importance for initial cell attachment [25], while cells silenced for $\alpha2\beta1$ fail to undergo changes in cell shape associated with the shift from proliferation to a columnar morphology associated with a secretory OB [28]. This failure to undergo cytoskeletal rearrangement is also followed by decreased production of osteoblastic markers like OCN, PGE_2, OPG, active and latent TGFβ1, and decreased alkaline phosphatase enzyme activity [20].

The distinct columnar morphology assumed by differentiated MSCs and mature OBs is dependent on the architectural features of their substrates. Microrough surfaces with peak-to-peak distances less than the length of the cell body drive the cells to become a more cuboidal shape with anchorage to the surface via long dendritic filopodia [128, 129]. This shift in cell shape by microrough topographies has been confirmed by experiments employing focused ion beam microscopy. The establishment of planar cell polarity correlates with the physiological behavior of the cells. On smooth surfaces, production of the OB markers, prostaglandin, TGFβ1, alkaline phosphatase-specific activity, and OCN is low [19]. Furthermore, proliferation rates are relatively high compared with cells cultured on rougher surfaces, and the morphology of cells appears more flattened and spread, resulting in a fibroblastic appearance. Moreover, these parameters are either not affected by $1\alpha,25(OH)_2D_3$ or the effect of the hormone is minimal, supporting a fibroblastic phenotype as opposed to a more mature secretory OB phenotype observed on rougher surfaces [130, 131].

In addition to modulating the cell shape, integrin binding to their extracellular matrix ligands initiates a signaling cascade resulting in new gene expression and protein synthesis. These signaling cascades include PKC-dependent phosphorylation and regulation of phospholipase D (PLD), culminating in mitogen-activated protein kinase (MAPK) activation [132]. Rough surfaces facilitate increased PLD activity of MG63 cells [133], suggesting that PLD may also play a role in OB differentiation on rough Ti substrates via interactions with PKC. Inhibition of PLD activity using siRNAs for the PLD isoforms PLD1 and PLD2 reduced surface-mediated OB differentiation and reduced PKC activity, suggesting that PLD is upstream of PKC in mediating OB response to surface microstructure. Furthermore, it was shown that PLD2 is the primary isoform involved in this process [134]. Part of the effect of $1\alpha,25(OH)_2D_3$ on OBs is also mediated via this signaling pathway [132], which may explain why the osteoblast-like MG63 cell line responds in a synergistic manner to $1\alpha,25(OH)_2D_3$ when they are cultured on microrough topographies.

In addition to altered intracellular signaling, surface-dependent changes in OB physiology can result in changes in local factor production and regulation in peri-implant tissues. Of these factors, prostaglandin plays an important role in mediating the effects of surface microtopography on OB physiology. As surface microroughness increases, levels of PGE_1 and PGE_2 produced by MG63 cells in the conditioned medium also increase [19]. The amount of PGE_2 produced also appears to be sensitive to the method used to fabricate microtextured surfaces [135] and to the

osteoblast-like cell model [136]. The elevated prostaglandins that are seen in cultures grown on rough surfaces appear to be required for enhanced osteogenesis as blocking prostaglandin production with the general cyclooxygenase (Cox) inhibitor indomethacin also blocks the increase in markers typical of mature OBs. Both constitutive Cox-1 and inducible Cox-2 are involved, as inhibitors specific to only one form of the enzyme fail to block all prostaglandin-dependent responses [137]. Moreover, $1\alpha,25(OH)_2D_3$ stimulates PGE_2 production by MG63 cells only when they are grown on rougher surfaces and this stimulatory effect is dose-dependent and synergistic with the surface effect [138].

Other interacting pathways may contribute to altered phenotypic expression due to surface microtopography. Recent studies have shown crosstalk between non-canonical Wnt and BMP signaling pathways during MSC commitment to the OB lineage. Wnt5a and Wnt11 are both non-canonical Wnts that work with some redundancy to promote osteoblast gene expression (*RUNX2*, *Col1A1*, *BGLAP*, and *TNAP*) and local factor production (BMP2, BMP4, OCN, OPG, FGF2, and VEGF) on plastic and Ti substrates. These effects are also increased in a surface roughness-dependent fashion, and the combination of Wnt and BMP contributes to OB differentiation of progenitor cells on microtextured Ti surfaces. Furthermore, stable suppression of *WNT11* gene expression decreases OB response and delays cytoskeletal changes seen in wildtype MSCs cultured on Ti surfaces possessing micro and mesoscale roughness and hydrophilicity, while treatment with either recombinant Wnt5a or Wnt11 reverses the effect of silencing. This mechanism is the opposite of that seen on TCPS, where Wnt3a-treated MSCs on TCPS underwent suppression of osteogenic markers, such as decreased TNAP expression and alkaline phosphatase activity [139]. However, on Ti surfaces, the effects of Wnt3a are suppressed and inhibition of Wnt3a signaling increases production of BMP2 and BMP4 by MSCs on microtextured Ti [24].

Downstream of non-canonical Wnt signaling the expression of BMP has been shown to be important for OB differentiation on microtextured Ti surfaces. BMP2 signaling is tightly regulated during surface-mediated osteogenesis, and modulation of these signals can enhance or inhibit this process [22]. Autocrine and paracrine actions (BMPs) are known to be involved in several cellular functions such as cell proliferation, differentiation, and apoptosis [140]. Among these proteins, BMPs 2, 4, and 7 are the most important in bone formation, healing, and regeneration. These osteoinductive factors provide molecular evidence of the increased osteoblastogenesis seen in vitro and for reduced time to loading and healing times seen clinically. Cells cultured on microstructured substrates display temporal upregulation of BMPs with increases of BMP2 and BMP4 occurring as early as 4 days [22], suggesting that they are early regulators of surface-mediated osteogenesis. Their presence could also serve as the impetus for the commitment of MSCs to the OB lineage when cultured on microstructured substrates, as they are known to regulate embryonic skeletal development. Furthermore, they also provide a mechanism for the differentiation of MSCs distal to the implant surface, as they are capable of multidirectional signaling. When MSCs were silenced for BMP2, the production of osteoblastic markers decreased when cultured on microstructured surfaces [22]. In contrast, increased production was observed when exogenous BMP2 was added to wild-type MSCs.

Recently, studies have examined paracrine signaling by local soluble factors produced by MSCs in contact with implant surfaces possessing complex architecture at the macro−/micro−/nano-scale. The results show that the production of factors necessary to induce osteogenesis in vitro is increased. The addition of blocking antibodies for BMP2 reduce this effect, indicating that BMP2 is responsible for the autocrine/paracrine stimulation of osteoblast differentiation that is observed. Conditioned media from these cultures causes osteoblast differentiation of naïve MSCs (OCN, OPN, OPG) [141].

Co-culture cell plates with adjustable heights can also be employed to evaluate the paracrine signaling of MSCs cultured on hierarchical Ti

surfaces. Recent work using these co-culture plates allows researchers to study the effect of local factors produced by MSCs cultured on Ti surfaces during surface-mediated differentiation on MSCs cultured above the surface on cell culture insert plastic. In this two-directional signaling assay, we see that the local factors produced by MSCs on the surface increase the differentiation of MSCs away from the surface and that these distal cells also produce local factors necessary for osteogenesis (OCN, OPN, OPG, BMP2, VEGFA) when all cells are cultured in fresh growth media separately for the last 24 h before assaying. Employing antibodies for BMP2 and altering culture times also allows the cell maturation stage and temporal signaling to be assessed. Results thus far indicate that biomimetic surfaces increase osteogenesis in vitro much more quickly compared to TCPS and osteogenic media [141]. Modification of the specifics of the experimental design may include allowing more mature MSCs to respond to the surface before beginning co-culture or altering the soluble factors in the co-culture to understand the differentiation process, as well as examining the interaction of various cell types.

Although BMP2 has been used to induce bone formation clinically, adverse effects including osteolysis, bone resorption, swelling, and seroma formation are concerning [142, 143]. Many of these adverse effects are attributed to the pro-inflammatory environment stimulated by high doses of BMP2 as well as its ability to induce apoptosis [140, 144]. This can be particularly problematic during the acute inflammatory response triggered in the early periods after injury associated with implantation. MSCs on microtextured surfaces produce lower levels of pro-inflammatory IL-6 and IL-8 and higher levels of anti-inflammatory IL-10 compared to MSCs on smooth substrates or TCPS [144]. While they produce BMPs locally, they also produce factors involved in their regulation, including Noggin [145] and they express BMP2 receptors [146]. This is important because the endogenous supply of BMP2 is modulated in a physiologically relevant way, and cells are able to respond to BMP2

when it is available. However, the addition of exogenous BMP2 reversed or blocked the effect of surface microtopography, increasing IL-6 and IL-8 and decreasing anti-inflammatory IL-10 [22]. Mitigating inflammatory co-stimulation is one of the main advantages of a substrate-induced activation of endogenous BMP2 compared to exogenous BMP2.

Implant roughness also modulates the production of angiogenic factors by OBs [147], suggesting materials that support peri-implant bone formation may support both angiogenesis and osteogenesis. Both MG63 cells and OBs secrete several angiogenic growth factors into their conditioned medium, including VEGF-A, basic fibroblast growth factor (FGF-2), and epidermal growth factor (EGF) [147]. When these cells were cultured on smooth substrates, secretions of VEGF-A, FGF-2, and EGF were increased compared to cells cultured on TCPS. On microrough substrates, there was a further increase in the secretion of these proangiogenic growth factors. The production of angiopoietin-1 (Ang-1), a marker of later stages of angiogenesis, was not affected by implant microtopography in vitro. The increased production of proangiogenic growth factors by MG63 cells cultured on substrates with a rough microtopography resulted in increased endothelial tubule formation in both Matrigel® and fibrin gel angiogenesis assays [147], suggesting that implant surface roughness may directly enhance neovascularization as well, potentially resulting in the greater clinical success of implanted materials.

The effect of supplementing microtopography with macro porosity on additively manufactured constructs alters the osteoblastic behavior as seen in MG63s and OBs. MG63s decreased proliferation and alkaline phosphatase-specific activity compared to surface microtopography alone. These early differentiation markers decreased with increasing porosity but are countered strongly by the significant increase in late maturation markers for OB differentiation, osteocalcin, and the OC modulatory protein OPG. Additionally, VEGF-A and BMPs 2 and 4 increased with increasing porosity [148]. Similar

effects are seen with OBs cultured on selective laser melting (SLM) constructs suggesting an enhanced differentiation capability [86].

There is evidence that the mechanisms by which cells sense microroughness on constructs with macro porosity are the same as those mediating cell response to microroughness on two-dimensional substrates. SLM has been used to examine the effects of varying pore size with Ti SLM constructs with 300–900 μm diameters in a rabbit tibia model, and demonstrated 600 μm increased implant fixation at an earlier time-point than the 300 and 900 μm pore diameter constructs [149].

Additional concepts have been tested to determine the ability to create implants with antibiotic-eluting drugs to help prevent peri-implant infection. Results showed that the orientation of the eluting channel can impact the area of coverage by the antibiotic [150], showing the need for further analysis of implants possessing macro porosity. It is important to highlight the need for post-manufacturing modifications such as grit-blasting and acid-etching to remove partially fused particles and decrease the likelihood of ion leaching into the area surrounding the implant.

To obtain a better understanding of the long-term effects of metal-based implants, an examination of ion concentrations has been undertaken to look at the effects of peri-implant ion leaching and metallic particles after platform-matched and platform-switched dental implants are inserted. Metal ion standards for titanium, aluminum, vanadium, and cobalt, chromium, molybdenum can be added to culture media to match ion concentrations around an implant for in vitro analysis. These analyses demonstrate that platform-matched implants decrease OB cell viability, and metal ions increase the expression of pro-inflammatory and osteoclastic cytokines (IL-6, IL-8, and Cox-2) compared to untreated media. Methods to reduce peri-implant metal ion implant byproducts therefore could increase net bone and reduce implant-associated bone loss after placement [151].

Although it has been understood for some time that micro-rough implants outperform their smooth counterparts, there exists an increasing body of evidence implicating a favorable cell response to submicron and nanoscale features. OBs and MSCs have consistently been shown to produce higher mRNA and protein levels of OB markers, such as osterix, alkaline phosphatase, and osteocalcin. Furthermore, morphological evaluations of cells growing on nanomodified substrates compared to smooth controls show more filopodia extensions and actin cytoskeletal alignment [152, 153], as well as enhanced cell adhesion [154].

Image analysis at the interface has been used to determine the OB response to microroughened Ti alloy that was produced by AM. Calvarial OBs from 2BalRrrc transgenic rats, which constitutively express a green fluorescent protein (GFP), were cultured for 2 days to determine cellular adhesion and morphological changes (Fig. 11.4a). A novel imaging approach was taken to correlate confocal fluorescent imaging with high-resolution SEM images taken at location-matched positions. To do this, cells were fixed in 4% para-formaldehyde for 15 min and stained in a 500 μL PBS solution containing 1:80 dilutions of phalloidin 594 and 1:1000 dilutions of Hoechst for 20 min in the dark. Cells were subsequently rinsed three times in PBS [155]. Next, a unique microscope mount was used to allow the translation of position between different microscopes. After sample calibration, confocal imaging was done to examine the cytoskeletal morphology of the OBs on the AM surfaces (Fig. 11.4b). Subsequently, the samples were dehydrated using serial step incubations in ethanol and critically dried using hexamethyldisilazane prior to image analysis with an SEM. Samples were sputter coated with platinum and high-magnification images of the cell attachment points were taken to look at the effects of submicron architecture on cell adhesion (Fig. 11.4c). Location-matched images of the surface by SEM could be correlated to confocal fluorescent images to give high-resolution surface details and cellular response at the same time (Fig. 11.4d) [155].

Responses to the surface also depend on the state of maturation of the cell in the OB lineage.
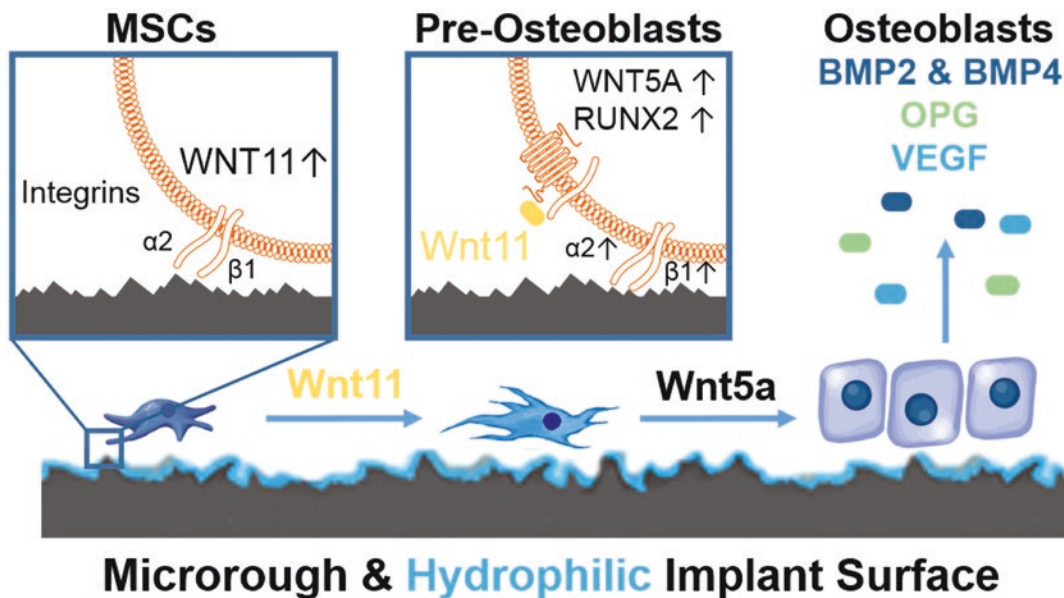
Fig. 11.4 Proposed mechanism for osteoblastic differentiation of MSCs on microtextured Ti surfaces. MSCs migrate into the implant microenvironment and adhere to the provisional matrix peri-implant through Integrin α2β1. MSCs upregulate the expression and production of Wnt11. Pre-osteoblasts produce Wnt11 which signals through the non-canonical Wnt signaling pathway to increase expression and production of Wnt5a, in turn modulating PKC activity. Crosstalk between Wnt11 and Wnt5a signaling enhances the maturation of pre-osteoblasts into osteoblasts and increases the production of soluble BMP2, BMP4, OPG, and VEGF to create an osteogenic microenvironment

Numerous cell lines and primary cell cultures have been examined in this model including multipotent MSCs, fetal rat calvarial cells, and osteocyte cell line MLO-Y4 [156, 157]. These experiments indicate that as cells become more mature, the stimulatory effect of the microrough surface on differentiation becomes attenuated. However, it is only on rough surfaces and only in the presence of BMP2 that fetal rat calvarial cells are able to establish three-dimensional nodules that form apatite minerals in a physiologically relevant manner [156]. Why this is the case is not yet clear. The results support in vivo observations that a material can affect cells directly on the surface as well as cells distal to the biomaterial [158], indicating that the extracellular signaling factors released by the cells in direct contact with the material are sensed by other cells in the microenvironment, and potentially systemically as well.

11.6 Bone Remodeling and the Importance of Osteoclasts

Bone remodeling is a continuous process that occurs throughout adulthood. Its purpose is to maintain bone strength, remove damaged bone, and replace soft, cartilaginous primary bone during osseointegration of implanted materials. The remodeling process is carried out by a balance of bone resorption by OCs and lamellar bone deposition by OBs. These cells as well as MSCs, OCPs, and osteocytes form the basic metabolic unit (BMU; Fig. 11.5). Within the BMU, cellular and molecular reciprocal communication is key to successful bone remodeling. This process is also involved in the process of "modeling" that reconstructs primary bone to haversian bone thereby providing biomechanical stability between the implant and surrounding tissues.
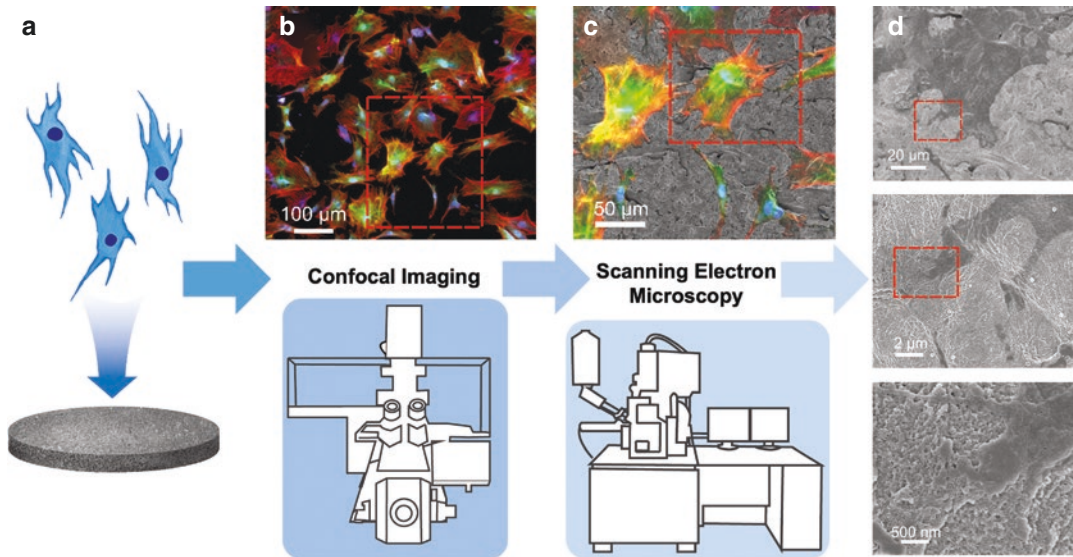
Fig. 11.5 Process of correlative microscopy to examine the cellular morphology at the interface. (**a**) Osteoprogenitor cells are cultured for 7 days on Ti implant surfaces. (**b**) After cells are fixed and stained, the cells are mounted on a unique microscope slide and calibrated to give (x,y) positioning during confocal imaging to determine the cytoskeletal morphology. (**c**) Cells are then fur-

ther processed by dehydration and sputter coated with platinum for SEM imaging. SEM images can be taken of specific interaction locations with increased resolution. (**d**) SEM Images can be overlaid with location-matched confocal images to give cytoskeletal and surface information

Any dysregulation in this coupling process may result in micro-damage accumulation, fractures, reduced bone healing, and implant failure [69].

Cells of the BMU maintain healthy communication through locally regulated factors and environmental cues. The remodeling phase of osseointegration is initiated once the OCs begin resorbing primary bone, leaving behind a uniquely prepared surface with a complex topographical and chemical structure. This surface has been shown to be chemotactic for OB lineage cells, which migrate onto the surface where they will differentiate, mature, and produce osteoid consisting of extracellular matrix proteins such as type I collagen as well as osteonectin [159, 160]. Mineralization of the osteoid is promoted through the regulation of local concentrations of calcium and phosphate and tailoring of the extracellular matrix components, including osteocalcin and various growth factors. This is demonstrated by studies investigating the response of MG63 cells cultured on surfaces of bone wafers that were preconditioned by OCs.

These cells preferentially colonized the resorption pits increasing their alkaline phosphatase activity as well as augmenting their production of osteocalcin and PGE_2. The effect of the bone surface was enhanced the longer it was conditioned by OCs [131]. Interestingly, prostaglandins are known to regulate bone remodeling by differentially affecting OBs and OCs. PGE_2 stimulates OC activity at high levels, but it is required at low levels for OB activity as previously described [161, 162].

Research of this nature was the impetus for designing dental and orthopedic implant surfaces containing complex topographical features and chemistries. Furthermore, these biologically inspired implant surfaces have been shown to influence the remodeling phase of osseointegration in vitro [45, 67]. To study BMU communication, a novel system was developed allowing examination of the effects surface-mediated MSC and OB factor production have on OCs (Fig. 11.6). OCs treated for 2d with media collected from MSCs and OBs cultured on micro-
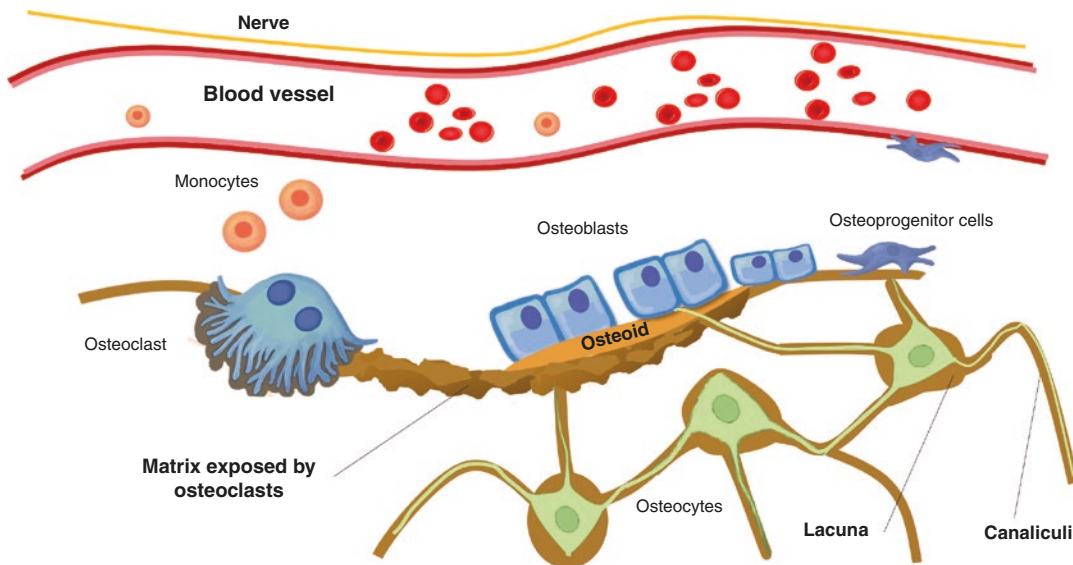
Fig. 11.6 Interaction of cells comprising the basic metabolic unit (BMU) during the remodeling phase of osseointegration. Monocytes differentiate into bone-resorbing osteoclasts by macrophage colony-stimulating factor (M-CSF) and receptor activator of NFκB ligand (RANKL). Bone marrow stromal cells are present near the vasculature and migrate to the bone surface and respond to the topographical and chemical cues of the bone surface, differentiating into osteoblasts that produce matrix. Osteoblasts embedded in an inorganic mineralized matrix are terminally differentiated and become mechano-sensitive osteocytes

structured surfaces were shown to have their resorptive activity reduced. This reduction was sensitive to the specific surface properties present on the implant surface. Furthermore, mRNA levels for OC fusion (*OCSTAMP*) and OC activity (*CSTB*, *CA2*) decreased while the expression of *ITGAV*, *ITGB3*, and *CTSK* remained largely unchanged [163].

These results demonstrate that implant surface properties can impact downstream events during the process of osseointegration including bone modeling. This is achieved without killing the OCs suggesting that the OCs have the capacity to return once the regulatory stimulus favors bone resorption. Others have shown that implant surfaces can impact other cells of the BMU. Osteocytes make direct contact with the implant surface, suggesting their importance in maintaining healthy bone remodeling as well as the longevity of implant osseointegration [164].

The rate and extent of OC resorption are controlled through a variety of mechanisms, but most notably through the release of active TGFβ1 and the production of OPG by neighboring cells. The regulation of TGFβ1 production on Ti surfaces depends on the cell model used [135, 136]. When MG63 cells are cultured on Ti surfaces, most of the TGFβ1 produced is in latent form and the amount increases on surfaces with rough microtopographies [19]. $1\alpha,25(OH)_2D_3$ does not alter TGFβ1 levels in cultures grown on smooth Ti, but it increases TGFβ1 levels in the media of cells grown on rougher surfaces and the effect is dose-dependent [125]. Furthermore, the distribution of TGF β1 between the matrix and the conditioned media of the cells is affected. On rougher surfaces, there is greater incorporation of TGFβ1 into the matrix [165]. This is important for later bone remodeling because OCs release TGFβ1 during the resorption phase where it is subsequently activated. Once activated, TGFβ1 can act on OCs to downregulate their activity, in part by regulating the production of OPG [47].

As previously stated, when RANKL binds its receptor RANK on OCPs, osteoclastogenesis is activated. To control this phenomenon, OBs produce OPG, which serves as a decoy receptor for RANKL [46]. By binding to RANKL, it prevents
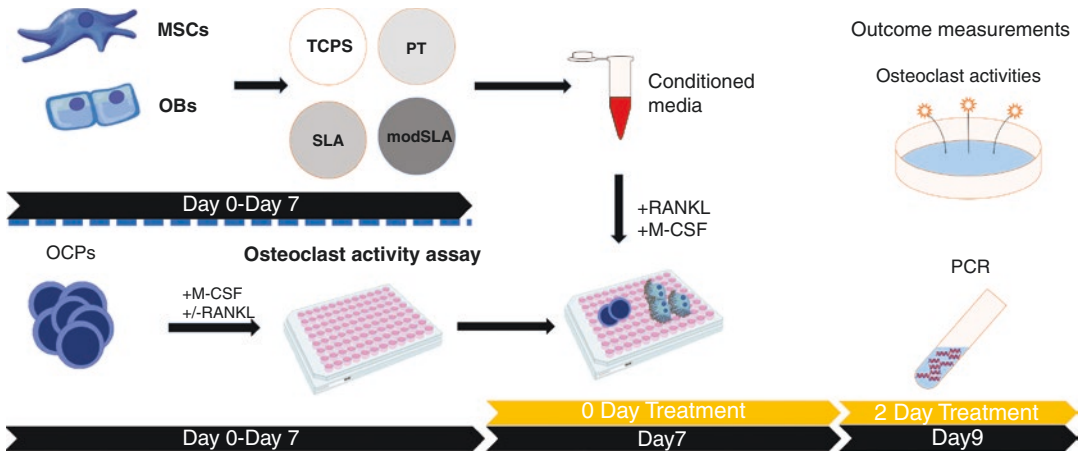
Fig. 11.7 Schematic of the process of evaluating bone remodeling interactions in vitro. MSCs or osteoblasts (OBs) are cultured for a duration of 7 days on titanium-based implant surfaces with distinct surface properties. Simultaneously osteoclast precursor cells (OCPs) are cultured in a 96-well plate with growth media containing macrophage colony-stimulating factor (M-CSF) and receptor activator of NFκB ligand (RANKL) for 7 days. Conditioned media collected from MSCs or OBs is then supplemented with equal amounts of M-CSF and RANKL and added to matured osteoclasts in the 96-well plate. Activity can be measured after 48 h of interaction by image analysis of bone resorption area, molecularly through PCR gene expression, or through conjugation of fluorophores to collagen substrates if not using bone wafers

OC differentiation by preventing its interaction with RANK. However, OBs also produce soluble RANKL to deplete excess OPG from their environment if the regulatory stimulus favors the formation of new OCs. When grown on substrates with rough microtopographies, MSCs, OBs, and MG63 cells produce higher levels of OPG, but mRNA for RANKL and levels of soluble RANKL protein do not change. Levels of OPG are further increased by $1\alpha,25(OH)_2D_3$ in a synergistic manner, but no change occurs in the expression of soluble RANKL. Thus, the net effect is bone formation without bone resorption. Interestingly, OPG levels are influenced by BMP2, as made evident from its decreased production by MSCs silenced for BMP2 suggesting it may also impact bone remodeling [141, 166] (Fig. 11.7).

11.7   Expert Opinion

Osseointegration is a complex cascade of events that leads to the structural and functional connection between bone and an implant. Greater bone apposition to implant materials results in func-tional stability, thus reducing the risk of failure while maintaining implant longevity. Although this is the desired clinical outcome, in vitro models have been successfully employed to assess the contributions surface properties have on the different phases and cell types involved with osseointegration. Many of these studies that attempt to understand the bone–implant interface are based on cell attachment and the ability of the implant surface to facilitate an osteogenic environment. Although important, this research has narrowed much of the focus of dental and orthopedic implantology to the development of modification techniques that are assessed only through their ability to support a favorable OB response. Vital knowledge of the impact implant surfaces have on the cellular and molecular events of osseointegration and how implant surface features alter the dynamics of wound healing can be ascertained by broadening the focus of implantology research. Advances in implantology will promote the development of patient-specific implants designed to trigger healthy bone formation despite any adverse health issues the patient may present.

References

1. Goriainov V, Cook R, Latham M, Dunlop D, Oreffo ROC, Latham JM, et al. Bone and metal: an orthopaedic perspective on osseointegration of metals. Acta Biomater. 2014;10:4043–57. https://doi.org/10.1016/j.actbio.2014.06.004.

2. Bosshardt DD, Stadlinger B, Terheyden H. Cell-to-cell communication—periodontal regeneration. Clin Oral Implants Res. 2015;26:229–39. https://doi.org/10.1111/clr.12543.

3. Davies J. Understanding peri-implant endosseous healing. J Dent Educ. 2003;67:932–49.

4. Terheyden H, Lang NP, Bierbaum S, Stadlinger B. Osseointegration - communication of cells. Clin Oral Implants Res. 2012;23:1127–35. https://doi.org/10.1111/j.1600-0501.2011.02327.x.

5. Joos U, Wiesmann HP, Szuwart T, Meyer U. Mineralization at the interface of implants. Int J Oral Maxillofac Surg. 2006;35:783–90. https://doi.org/10.1016/j.ijom.2006.03.013.

6. Branemark PI, Adell R, Albrektsson T, Lekholm U, Lundkvist S, Rockler B. Osseointegrated titanium fixtures in the treatment of edentulousness. Biomaterials. 1983;4:25–8.

7. Schwartz Z, Raines AL, Boyan BD. The effect of substrate microtopography on Osseointegration of titanium implants. Compr Biomater. 2011;7:343–52. https://doi.org/10.1016/B978-0-08-055294-1.00221-X.

8. Thevenot W, Tang P, Hu L. Surface chemistry influence implant biocompatibility. Curr Top Med Chem. 2008;8:11. https://doi.org/10.1016/j.nano.2008.04.001.SURFACE.

9. Abaricia JO, Shah AH, Olivares-Navarrete R. Substrate stiffness induces neutrophil extracellular trap (NET) formation through focal adhesion kinase activation. Biomaterials. 2021;271:120715. https://doi.org/10.1016/j.biomaterials.2021.120715.

10. Abaricia JO, Farzad N, Heath TJ, Simmons J, Morandini L, Olivares-Navarrete R. Control of innate immune response by biomaterial surface topography, energy, and stiffness. Acta Biomater. 2021;133:58. https://doi.org/10.1016/j.actbio.2021.04.021.

11. Snyder RJ, Lantis J, Kirsner RS, Shah V, Molyneaux M, Carter MJ. Macrophages: a review of their role in wound healing and their therapeutic use. Wound Repair Regen. 2016;24:613–29. https://doi.org/10.1111/wrr.12444.

12. Ginhoux F, Jung S. Monocytes and macrophages: developmental pathways and tissue homeostasis. Nat Rev Immunol. 2014;14:392–404. https://doi.org/10.1038/nri3671.

13. Varol C, Mildner A, Jung S. Macrophages: development and tissue specialization. Annu Rev Immunol. 2015;33:643. https://doi.org/10.1146/annurev-immunol-032414-112220.

14. Kou PM, Schwartz Z, Boyan BD, Babensee JE. Dendritic cell responses to surface properties of clinical titanium surfaces. Acta Biomater. 2011;7:1354–63. https://doi.org/10.1016/j.actbio.2010.10.020.

15. Franz S, Rammelt S, Scharnweber D, Simon JC. Immune responses to implants—a review of the implications for the design of immunomodulatory biomaterials. Biomaterials. 2011;32:6692–709. https://doi.org/10.1016/j.biomaterials.2011.05.078.

16. Duvall CL, Taylor WR, Weiss D, Wojtowicz AM, Guldberg RE. Impaired angiogenesis, early callus formation, and late stage remodeling in fracture healing of osteopontin-deficient mice. J Bone Miner Res. 2007;22:286–97. https://doi.org/10.1359/jbmr.061103.

17. Geris L, Gerisch A, Vander SJ, Weiner R, Van OH. Angiogenesis in bone fracture healing: a bioregulatory model. J Theor Biol. 2008;251:137–58. https://doi.org/10.1016/j.jtbi.2007.11.008.

18. Abshagen K, Schrodi I, Gerber T, Vollmar B. In vivo analysis of biocompatibility and vascularization of the synthetic bone grafting substitute NanoBone®. J Biomed Mater Res Pt A. 2009;91:557–66. https://doi.org/10.1002/jbm.a.32237.

19. Kieswetter K, Schwartz Z, Hummert TW, Cochran DL, Simpson J, Dean DD, et al. Surface roughness modulates the local production of growth factors and cytokines by osteoblast-like MG-63 cells. J Biomed Mater Res Pt A. 1996;32:55–63.

20. Olivares-Navarrete R, Raz P, Zhao G, Chen J, Wieland M, Cochran DL, et al. Integrin α2β1 plays a critical role in osteoblast response to micron-scale surface structure and surface energy of titanium substrates. Proc Natl Acad Sci U S A. 2008;105:15767–72. https://doi.org/10.1073/pnas.0805420105.

21. Boyan BD, Cheng A, Schwartz Z. Implant surface design regulates mesenchymal stem cell differentiation and maturation. Adv Dent Res. 2016;28:10–7. https://doi.org/10.1177/0022034515624444.

22. Olivares-Navarrete R, Hyzy SL, Haithcock DA, Cundiff CA, Schwartz Z, Boyan BD. Coordinated regulation of mesenchymal stem cell differentiation on microstructured titanium surfaces by endogenous

bone morphogenetic proteins. Bone. 2015;73:208–16. https://doi.org/10.1016/j.bone.2014.12.057.

23. Gittens RA, Scheideler L, Rupp F, Hyzy SL, Geis-Gerstorfer J, Schwartz Z, et al. A review on the wettability of dental implant surfaces II: biological and clinical aspects. Acta Biomater. 2014;10:2907–18. https://doi.org/10.1016/j.actbio.2014.03.032.

24. Olivares-Navarrete R, Hyzy SL, Hutton DL, Dunn GR, Appert C, Boyan BD, et al. Role of non-canonical Wnt signaling in osteoblast maturation on microstructured titanium surfaces. Acta Biomater. 2011;7:2740–50. https://doi.org/10.1016/j.actbio.2011.02.030.

25. Keselowsky BG, Wang L, Schwartz Z, Garcia AJ, Boyan BD. Integrin a5 controls osteoblastic proliferation and differentiation responses to titanium substrates presenting different roughness characteristics in a roughness independent manner. J Biomed Mater Res Pt A. 2007;80:700–10. https://doi.org/10.1002/jbm.a.

26. Barczyk M, Carracedo S, Gullberg D. Integrins. Cell Tissue Res. 2010;339:269–80. https://doi.org/10.1007/s00441-009-0834-6.

27. Askari JA, Buckley PA, Mould AP, Humphries MJ. Linking integrin conformation to function. J Cell Sci. 2009;122:165–70. https://doi.org/10.1242/jcs.018556.

28. Lai M, Hermann CD, Cheng A, Olivares-Navarrete R, Gittens RA, Bird MM, et al. Role of A2B1 integrins in mediating cell shape on microtextured titanium surfaces. J Biomed Mater Res Pt A. 2015;103:564–73. https://doi.org/10.1002/jbm.a.35185.

29. Olivares-Navarrete R, Hyzy SL, Chaudhri RA, Zhao G, Boyan BD, Schwartz Z. Sex dependent regulation of osteoblast response to implant surface properties by systemic hormones. Biol Sex Differ. 2010;1:4. https://doi.org/10.1186/2042-6410-1-4.

30. Lin GL, Hankenson KD. Integration of BMP, Wnt, and notch signaling pathways in osteoblast differentiation. J Cell Biochem. 2011;112:3491–501. https://doi.org/10.1002/jcb.23287.

31. Yavropoulou MP, Yovos JG. The role of the Wnt signaling pathway in osteoblast commitment and differentiation. Hormones. 2007;6:279–94.

32. Lerner UH, Ohlsson C. The WNT system: background and its role in bone. J Intern Med. 2015;277:630–49. https://doi.org/10.1111/joim.12368.

33. Sheldahl LC, Slusarski DC, Pandur P, Miller JR, Kühl M, Moon RT. Dishevelled activates Ca2+ flux, PKC, and CamKII in vertebrate embryos. J Cell Biol. 2003;161:769–77. https://doi.org/10.1083/jcb.200211094.

34. Doroudi M, Olivares-navarrete R, Boyan BD, Schwartz Z. A review of 1a,25(OH)2D3 dependent Pdia3 receptor complex components in Wnt5a noncanonical pathway signaling. J Steroid Biochem Mol Biol. 2015;152:84–8. https://doi.org/10.1016/j.jsbmb.2015.04.002.

35. Olivares-Navarrete R, Hyzy SL, Park JH, Dunn GR, Haithcock DA, Wasilewski CE, et al. Mediation of osteogenic differentiation of human mesenchymal stem cells on titanium surfaces by a Wnt-integrin feedback loop. Biomaterials. 2011;32:6399–411. https://doi.org/10.1016/j.biomaterials.2011.05.036.

36. Olivares-Navarrete R, Lee EM, Smith K, Hyzy SL, Doroudi M, Williams JK, et al. Substrate stiffness controls osteoblastic and chondrocytic differentiation of mesenchymal stem cells without exogenous stimuli. PloS One. 2017;12:e0170312. https://doi.org/10.1371/journal.pone.0170312.

37. Linkhart TA, Mohan S, Baylink DJ. Growth factors for bone growth and repair: IGF, TGFβ and BMP. Bone. 1996;19:1S. https://doi.org/10.1016/S8756-3282(96)00138-X.

38. Lai CF, Chaudhary L, Fausto A, Halstead LR, Ory DS, Avioli LV, et al. Erk is essential for growth, differentiation, integrin expression, and cell function in human osteoblastic cells. J Biol Chem. 2001;276:14443–50. https://doi.org/10.1074/jbc.M010021200.

39. Greenblatt MB, Shim J-H, Glimcher LH. Mitogen-activated protein kinase pathways in osteoblasts. Annu Rev Cell Dev Biol. 2013;29:63–79. https://doi.org/10.1146/annurev-cellbio-101512-122347.

40. Olivares-Navarrete R, Hyzy SL, Hutton DL, Erdman CP, Wieland M, Boyan BD, et al. Direct and indirect effects of microstructured titanium substrates on the induction of mesenchymal stem cell differentiation towards the osteoblast lineage. Biomaterials. 2010;31:2728–35. https://doi.org/10.1016/j.biomaterials.2009.12.029.

41. Annunziata M, Guida L. The effect of titanium surface modifications on dental implant Osseointegration. Front Oral Biol. 2015;17:62–77. https://doi.org/10.1159/000381694.

42. Everts V, Korper W, Hoeben KA, Jansen IDC, Bromme D, Cleutjens KBJM, et al. Osteoclastic bone degradation and the role of different cysteine proteinases and matrix metalloproteinases: differences between calvaria and long bone. J Bone Miner Res. 2006;21:1399–408. https://doi.org/10.1359/jbmr.060614.

43. Troen BR. The regulation of cathepsin K gene expression. Ann N Y Acad Sci. 2006;1068:165–72. https://doi.org/10.1196/annals.1346.018.

44. Raghavendra S, Wood MC, Taylor TD. Early wound healing around endosseous implants: a review of the literature. Int J Oral Maxillofac Implants. 2005;20:425–31. https://doi.org/10.1016/S0084-3717(08)70105-3.

45. Boyan BD, Lotz EM, Schwartz Z. (*) Roughness and hydrophilicity as osteogenic biomimetic surface properties. Tissue Eng Pt A. 2017;23:1479–89. https://doi.org/10.1089/ten.TEA.2017.0048.

46. Boyce BF, Xing L. The RANKL/RANK/OPG pathway. Curr Osteoporos Rep. 2007;5:98–104. https://doi.org/10.1007/s11914-007-0024-y.

47. Schwartz Z, Olivares-Navarrete R, Wieland M, Cochran DL, Boyan BD. Mechanisms regulating increased production of osteoprotegerin by osteo-

blasts cultured on microstructured titanium surfaces. Biomaterials. 2009;30:3390–6. https://doi.org/10.1016/j.biomaterials.2009.03.047.

48. Brazill JM, Beeve AT, Craft CS, Ivanusic JJ, Scheller EL. Nerves in bone: evolving concepts in pain and anabolism. J Bone Miner Res. 2019;34:1393–406. https://doi.org/10.1002/jbmr.3822.

49. Deng J, Cohen DJ, Redden J, McClure MJ, Boyan BD, Schwartz Z. Differential effects of Neurectomy and Botox-induced muscle paralysis on bone phenotype and titanium implant Osseointegration. Bone. 2021;153:116145. https://doi.org/10.1016/j.bone.2021.116145.

50. Verlinden L, Vanderschueren D, Verstuyf A. Semaphorin signaling in bone. Mol Cell Endocrinol. 2016;432:66–74. https://doi.org/10.1016/j.mce.2015.09.009.

51. Negishi-Koga T, Takayanagi H. Bone cell communication factors and Semaphorins. Bonekey Rep. 2012;1:183. https://doi.org/10.1038/bonekey.2012.183.

52. Fukuda T, Takeda S, Xu R, Ochi H, Sunamura S, Sato T, et al. Sema3A regulates bone-mass accrual through sensory innervations. Nature. 2013;497:490–3. https://doi.org/10.1038/nature12115.

53. Hayashi M, Nakashima T, Taniguchi M, Kodama T, Kumanogoh A, Takayanagi H. Osteoprotection by semaphorin 3A. Nature. 2012;485:69–74. https://doi.org/10.1038/nature11000.

54. Kim BJ, Koh JM. Coupling factors involved in preserving bone balance. Cell Mol Life Sci. 2019;76:1243–53. https://doi.org/10.1007/s00018-018-2981-y.

55. Serini G, Valdembri D, Zanivan S, Morterra G, Burkhardt C, Caccavari F, et al. Class 3 semaphorins control vascular morphogenesis by inhibiting integrin function. Nature. 2003;424:391–8.

56. Takamatsu H, Kumanogoh A. Diverse roles for semaphorin-plexin signaling in the immune system. Trends Immunol. 2012;33:127–35. https://doi.org/10.1016/j.it.2012.01.008.

57. Rehman M, Tamagnone L. Semaphorins in cancer: biological mechanisms and therapeutic approaches. Semin Cell Dev Biol. 2013;24:179–89. https://doi.org/10.1016/j.semcdb.2012.10.005.

58. Chen X, Wang Z, Duan N, Zhu G, Schwarz EM, Xie C. Osteoblast–osteoclast interactions. Connect Tissue Res. 2018;59:99–107. https://doi.org/10.1080/03008207.2017.1290085.

59. Huang S, Li Z, Liu Y, Gao D, Zhang X, Hao J, et al. Neural regulation of bone remodeling: identifying novel neural molecules and pathways between brain and bone. J Cell Physiol. 2019;234:5466–77. https://doi.org/10.1002/jcp.26502.

60. Delaire S, Billard C, Tordjman R, Chédotal A, Elhabazi A, Bensussan A, et al. Biological activity of soluble CD100. II. Soluble CD100, similarly to H-SemaIII, inhibits immune cell migration. J Immunol. 2001;166:4348–54. https://doi.org/10.4049/jimmunol.166.7.4348.

61. Negishi-Koga T, Shinohara M, Komatsu N, Bito H, Kodama T, Friedel RH, et al. Suppression of bone formation by osteoclastic expression of semaphorin 4D. Nat Med. 2011;17:1473–80. https://doi.org/10.1038/nm.2489.

62. Dacquin R, Domenget C, Kumanogoh A, Kikutani H, Jurdic P, Machuca-Gayet I. Control of bone resorption by semaphorin 4D is dependent on ovarian function. PloS One. 2011;6:6. https://doi.org/10.1371/journal.pone.0026627.

63. Deb Roy A, Yin T, Choudhary S, Rodionov V, Pilbeam CC, Wu YI. Optogenetic activation of Plexin-B1 reveals contact repulsion between osteoclasts and osteoblasts. Nat Commun. 2017;8:8. https://doi.org/10.1038/ncomms15831.

64. Takahashi T, Fournier A, Nakamura F, Wang LH, Murakami Y, Kalb RG, et al. Plexin-neuropilin-1 complexes form functional semaphorin-3A receptors. Cell. 1999;99:59–69. https://doi.org/10.1016/S0092-8674(00)80062-8.

65. Tamagnone L, Artigiani S, Chen H, He Z, Ming GL, Song HJ, et al. Plexins are a large family of receptors for transmembrane, secreted, and GPI-anchored semaphorins in vertebrates. Cell. 1999;99:71–80. https://doi.org/10.1016/S0092-8674(00)80063-X.

66. Li Z, Hao J, Duan X, Wu N, Zhou Z, Yang F, et al. The role of Semaphorin 3A in bone remodeling. Front Cell Neurosci. 2017;11:1–8. https://doi.org/10.3389/fncel.2017.00040.

67. Lotz EM, Berger MB, Boyan BD, Schwartz Z. Regulation of mesenchymal stem cell differentiation on microstructured titanium surfaces by semaphorin 3A. Bone. 2020;134:115260. https://doi.org/10.1016/j.bone.2020.115260.

68. Aarden EM, Burger EH, Nijweide PJ, Biology C, Leiden AA. Function of osteocytes in bone. J Cell Biochem. 1972;299:287–99.

69. Compton JT, Lee FY. Current concepts review: a review of osteocyte function and the emerging importance of sclerostin. J Bone Jt Surg Am. 2014;96:1659–68. https://doi.org/10.2106/JBJS.M.01096.

70. Chrcanovic BR, Albrektsson T, Wennerberg A. Reasons for failures of oral implants. J Oral Rehabil. 2014;41:443–76. https://doi.org/10.1111/joor.12157.

71. Barone A, Varanini P. Deep-frozen allogeneic Onlay bone grafts for reconstruction of atrophic maxillary alveolar ridges: a preliminary study. J Oral Maxillofac Surg. 2009;67:1300–6. https://doi.org/10.1016/j.joms.2008.12.043.

72. Schwartz Z, Hyzy SL, Moore MA, Hunter SA, Ronholdt CJ, Sunwoo M, et al. Osteoinductivity of demineralized bone matrix is independent of donor bisphosphonate use. J Bone Jt Surg. 2011;93:2278–86.

73. Gittens RA, Olivares-Navarrete R, Schwartz Z, Boyan BD. Implant osseointegration and the role of microroughness and nanostructures: lessons for

spine implants. Acta Biomater. 2014;10:3363–71. https://doi.org/10.1016/j.actbio.2014.03.037.

74. Pešáková V, Kubies D, Hulejová H, Himmlová L. The influence of implant surface properties on cell adhesion and proliferation. J Mater Sci Mater Med. 2007;18:465–73. https://doi.org/10.1007/s10856-007-2006-0.

75. Olivares-Navarrete R, Raines AL, Hyzy SL, Park JH, Hutton DL, Cochran DL, et al. Osteoblast maturation and new bone formation in response to titanium implant surface features are reduced with age. J Bone Miner Res. 2012;27:1773–83. https://doi.org/10.1002/jbmr.1628.

76. Zhang R, Geoffroy V, Ridall AL, Karsenty G, Tracy T, Bonner AS, et al. Bone resorption by osteoclasts. Science (80-). 2000;289:1504–8. https://doi.org/10.1126/science.289.5484.1504.

77. Le Guéhennec L, Soueidan A, Layrolle P, Amouriq Y. Surface treatments of titanium dental implants for rapid osseointegration. Dent Mater. 2007;23:844–54. https://doi.org/10.1016/j.dental.2006.06.025.

78. Kim K-H, Ramaswamy N. Electrochemical surface modification of titanium in dentistry. Dent Mater J. 2009;28:20–36. https://doi.org/10.4012/dmj.28.20.

79. Wennerberg A, Albrektsson T. Effects of titanium surface topography on bone integration: a systematic review. Clin Oral Implants Res. 2009;20:172–84. https://doi.org/10.1111/j.1600-0501.2009.01775.x.

80. Berger MB, Bosh KB, Cohen DJ, Boyan BD, Schwartz Z. Benchtop plasma treatment of titanium surfaces enhances cell response. Dent Mater. 2021;37:690–700. https://doi.org/10.1016/j.dental.2021.01.026.

81. Wang X, Xu S, Zhou S, Xu W, Leary M, Choong P, et al. Topological design and additive manufacturing of porous metals for bone scaffolds and orthopaedic implants: a review. Biomaterials. 2016;83:127–41. https://doi.org/10.1016/j.biomaterials.2016.01.012.

82. Zhao G, Schwartz Z, Wieland M, Rupp F, Geis-Gerstorfer J, Cochran DL, et al. High surface energy enhances cell response to titanium substrate microstructure. J Biomed Mater Res Pt A. 2005;74:49–58. https://doi.org/10.1002/jbm.a.30320.

83. Cohen DJ, Cheng A, Sahingur K, Clohessy RM, Hopkins LB, Boyan BD, et al. Performance of laser sintered Ti – 6Al – 4V implants with bone-inspired porosity and micro / nanoscale surface roughness in the rabbit femur. Biomed Mater. 2017;12:25021.

84. Cheng A, Cohen DJ, Kahn A, Clohessy RM, Sahingur K, Newton JB, et al. Laser sintered porous Ti–6Al–4V implants stimulate vertical bone growth. Ann Biomed Eng. 2017;45:2025–35. https://doi.org/10.1007/s10439-017-1831-7.

85. Cheng A, Cohen DJ, Boyan BD, Schwartz Z. Laser-sintered constructs with bio-inspired porosity and surface micro/nano-roughness enhance mesenchymal stem cell differentiation and matrix mineralization in vitro. Calcif Tissue Int. 2016;99:625–37. https://doi.org/10.1007/s00223-016-0184-9.

86. Hyzy SL, Cheng A, Cohen DJ, Yatzkaier G, Whitehead AJ, Clohessy RM, et al. Novel hydro-philic nanostructured microtexture on direct metal laser sintered Ti–6Al–4V surfaces enhances osteoblast response in vitro and osseointegration in a rabbit model. J Biomed Mater Res Pt A. 2016;104:2086–98. https://doi.org/10.1002/jbm.35739.

87. Rho JY, Ashman RB, Turner CH. Young's modulus of trabecular and cortical bone material: ultrasonic and microtensile measurements. J Biomech. 1993;26:111–9. https://doi.org/10.1016/0021-9290(93)90042-D.

88. Wieding J, Wolf A, Bader R. Numerical optimization of open-porous bone scaffold structures to match the elastic properties of human cortical bone. J Mech Behav Biomed Mater. 2014;37:56–68. https://doi.org/10.1016/j.jmbbm.2014.05.002.

89. Assal PA. The osseointegration of zirconia dental implants. Schweiz Monatsschr Zahnmed. 2013;123:644–54.

90. Özkurt Z, Kazazoğlu E. Zirconia dental implants: a literature review. J Oral Implantol. 2011;37:367–76. https://doi.org/10.1563/AAID-JOI-D-09-00079.

91. Steinemann G. Titanium—the material of choice? Periodontol 2000. 1998;17:7–21.

92. Gottlow J, Dard M, Kjellson F, Obrecht M, Sennerby L. Evaluation of a new titanium-zirconium dental implant: a biomechanical and histological comparative study in the mini pig. Clin Implant Dent Relat Res. 2012;14:538–45. https://doi.org/10.1111/j.1708-8208.2010.00289.x.

93. Tugulu S, Löwe K, Scharnweber D, Schlottig F. Preparation of superhydrophilic microrough titanium implant surfaces by alkali treatment. J Mater Sci Mater Med. 2010;21:2751–63. https://doi.org/10.1007/s10856-010-4138-x.

94. Cei S, Karapetsa D, Aleo E, Graziani F. Protein adsorption on a laser-modified titanium implant surface. Implant Dent. 2015;24:134–41. https://doi.org/10.1097/id.0000000000000214.

95. Divya Rani VV, Manzoor K, Menon D, Selvamurugan N, Nair SV. The design of novel nanostructures on titanium by solution chemistry for an improved osteoblast response. Nanotechnology. 2009;20:195101. https://doi.org/10.1088/0957-4484/20/19/195101.

96. Boyd AR, Burke GA, Duffy H, Holmberg M, O'Kane C, Meenan BJ, et al. Sputter deposited bioceramic coatings: surface characterisation and initial protein adsorption studies using surface-MALDI-MS. J Mater Sci Mater Med. 2011;22:74–84. https://doi.org/10.1007/s10856-010-4180-8.

97. Buchanan LA, El-Ghannam A. Effect of bioactive glass crystallization on the conformation and bioactivity of adsorbed proteins. J Biomed Mater Res Pt A. 2010;93:537–46. https://doi.org/10.1002/jbm.a.32561.

98. Ota-Tsuzuki C, Datte CE, Nomura KA, Gouvea Cardoso LA, Shibli JA. Influence of titanium surface treatments on formation of the blood clot extension. J Oral Implantol. 2011;37:641–7. https://doi.org/10.1563/AAID-JOI-D-09-00125.1.

99. Di Iorio D, Traini T, Degidi M, Caputi S, Neugebauer J, Piattelli A. Quantitative evaluation of the fibrin

clot extension on diffferent implant surfaces: an in vitro study. J Biomed Mater Res Pt B Appl Biomater. 2005;74:636–42. https://doi.org/10.1002/jbm.b.30251.

100. Yang J, Zhou Y, Wei F, Xiao Y. Blood clot formed on rough titanium surface induces early cell recruitment. Clin Oral Implants Res. 2015;27:1031–8. https://doi.org/10.1111/clr.12672.

101. Browne MM, Lubarsky GV, Davidson MR, Bradley RH. Protein adsorption onto polystyrene surfaces studied by XPS and AFM. Surf Sci. 2004;553:155–67. https://doi.org/10.1016/j.susc.2004.01.046.

102. Cullen DC, Lowe CR. AFM studies of protein adsorption. 1. Time-resolved protein adsorption to highly oriented pyrolytic graphite. J Colloid Interface Sci. 1994;166:102–8. https://doi.org/10.1006/jcis.1994.1276.

103. Lang NP, Salvi GE, Huynh-Ba G, Ivanovski S, Donos N, Bosshardt DD. Early osseointegration to hydrophilic and hydrophobic implant surfaces in humans. Clin Oral Implants Res. 2011;22:349–56. https://doi.org/10.1111/j.1600-0501.2011.02172.x.

104. Kopf BS, Ruch S, Berner S, Spencer ND, Maniura-Weber K. The role of nanostructures and hydrophilicity in osseointegration: in-vitro protein-adsorption and blood-interaction studies. J Biomed Mater Res Pt A. 2015;103:2661–72. https://doi.org/10.1002/jbm.a.35401.

105. Schildhauer TA, Peter E, Muhr G, Koller M. Activation of human leukocytes on tantalum trabecular metal in comparison to commonly used orthopedic metal implant materials. J Biomed Mater Res Pt A. 2009;88:332–41. https://doi.org/10.1002/jbm.a.31850.

106. Bogdanski D, Esenwein SA, Prymak O, Epple M, Muhr G, Köller M. Inhibition of PMN apoptosis after adherence to dip-coated calcium phosphate surfaces on a NiTi shape memory alloy. Biomaterials. 2004;25:4627–32. https://doi.org/10.1016/j.biomaterials.2003.12.001.

107. Häcker G. The morphology of apoptosis. Cell Tissue Res. 2000;301:5–17. https://doi.org/10.1007/s004410000193.

108. Köller M, Esenwein SA, Bogdanski D, Prymak O, Epple M, Muhr G. Regulation of leukocyte adhesion molecules by leukocyte/biomaterial-conditioned media: a study with calcium-phosphate-coated and non-coated NiTi-shape memory alloys. Materwiss Werksttech. 2006;37:558–62. https://doi.org/10.1002/mawe.200600037.

109. Rich A, Harris AK. Anomalous preferences of cultured macrophages for hydrophobic and roughened substrata. J Cell Sci. 1981;50:1–7.

110. Salthouse TN. Some aspects of macrophage behavior at the implant interface. J Biomed Mater Res. 1984;18:395–401. https://doi.org/10.1002/jbm.820180407.

111. Wójciak-Stothard B, Madeja Z, Korohoda W, Curtis A, Wilkinson C. Activation of macrophage-like cells by multiple grooved substrata. Topographical con- trol of cell behaviour. Cell Biol Int. 1995;19:485–90. https://doi.org/10.1006/cbir.1995.1092.

112. Hotchkiss KM, Reddy GB, Hyzy SL, Schwartz Z, Boyan BD, Olivares-Navarrete R. Titanium surface characteristics, including topography and wettability, alter macrophage activation. Acta Biomater. 2016;31:425–34. https://doi.org/10.1016/j.actbio.2015.12.003.

113. Refai AK, Textor M, Brunette DM, Waterfield JD. Effect of titanium surface topography on macrophage activation and secretion of proinflammatory cytokines and chemokines. J Biomed Mater Res. 2004;70A:194–205. https://doi.org/10.1002/jbm.a.30075.

114. Hotchkiss KM, Ayad NB, Hyzy SL, Boyan BD, Olivares-Navarrete R. Dental implant surface chemistry and energy alter macrophage activation in vitro. Clin Oral Implants Res. 2016;28:1–10. https://doi.org/10.1111/clr.12814.

115. Barbeck M, Booms P, Unger R, Hoffmann V, Sader R, Kirkpatrick CJ, et al. Multinucleated giant cells in the implant bed of bone substitutes are foreign body giant cells—new insights into the material-mediated healing process. J Biomed Mater Res Pt A. 2017;105:1105–11. https://doi.org/10.1002/jbm.a.36006.

116. Moreno JL, Mikhailenko I, Tondravi MM, Keegan AD. IL-4 promotes the formation of multinucleated giant cells from macrophage precursors by a STAT6-dependent, homotypic mechanism: contribution of E-cadherin. J Leukoc Biol. 2007;82:1542–53. https://doi.org/10.1189/jlb.0107058.

117. Trindade R, Albrektsson T, Tengvall P, Wennerberg A. Foreign body reaction to biomaterials: on mechanisms for buildup and breakdown of osseointegration. Clin Implant Dent Relat Res. 2016;18:192–203. https://doi.org/10.1111/cid.12274.

118. Sheikh Z, Brooks PJ, Barzilay O, Fine N, Glogauer M. Macrophages, foreign body giant cells and their response to implantable biomaterials. Materials (Basel). 2015;8:5671–701. https://doi.org/10.3390/ma8095269.

119. Holt DJ, Chamberlain LM, Grainger DW. Cell-cell signaling in co-cultures of macrophages and fibroblasts. Biomaterials. 2010;31:9382–94. https://doi.org/10.1016/j.biomaterials.2010.07.101.

120. Chan EP, Mhawi A, Clode P, Saunders M, Filgueira L, et al. Effects of titanium(iv) ions on human monocyte-derived dendritic cells. Metallomics. 2009;1:166–74. https://doi.org/10.1039/b820871a.

121. Wang JY, Tsukayama DT, Wicklund BH, Gustilo RB. Inhibition of T and B cell proliferation by titanium, cobalt, and chromium: role of IL-2 and IL-6. J Biomed Mater Res. 1996;32:655–61.

122. Thomas P, Iglhaut G, Wollenberg A, Cadosch D, Summer B. Allergy or tolerance: reduced inflammatory cytokine response and concomitant il-10 production of lymphocytes and monocytes in symptom-free titanium dental implant patients. Biomed Res Int. 2013;2013:539834. https://doi.org/10.1155/2013/539834.

123. Martin JY, Schwartz Z, Hummert TW, Schraub DM, Simpson J, Lankford J Jr, et al. Effect of titanium surface roughness on proliferation, differentiation, and protein synthesis of human osteoblast-like cells (MG63). J Biomed Mater Res. 1995;29:389–401. https://doi.org/10.1002/jbm.820290314.

124. Schwartz Z, Lohmann CH, Oefinger J, Bonewald LF, Dean DD, Boyan BD. Implant surface characteristics modulate differentiation behavior of cells in the osteoblastic lineage. Adv Dent Res. 1999;13:38–48. https://doi.org/10.1177/08959374990130011301.

125. Boyan BD, Batzer R, Kieswetter K, Liu Y, Cochran DL, Szmuckler-Moncler S, et al. Titanium surface roughness alters responsiveness of MG63 osteoblast-like cells to 1 alpha,25-(OH)2D3. J Biomed Mater Res. 1998;39:77–85.

126. Moursi AM, Globus RK, Damsky CH. Interactions between integrin receptors and fibronectin are required for calvarial osteoblast differentiation in vitro. J Cell Sci. 1997;110:2187–96.

127. Park JH, Wasilewski CE, Almodovar N, Olivares-Navarrete R, Boyan BD, Tannenbaum R, et al. The responses to surface wettability gradients induced by chitosan nanofilms on microtextured titanium mediated by specific integrin receptors. Biomaterials. 2012;33:7386–93. https://doi.org/10.1016/j.biomaterials.2012.06.066.

128. Brunette DM. The effects of implant surface topography on the behavior of cells. Int J Oral Maxillofac Implants. 1988;3:231–46.

129. Brunette DM. Spreading and orientation of epithelial cells on grooved substrata. Exp Cell Res. 1986;167:203–17. https://doi.org/10.1016/0014-4827(86)90217-X.

130. Boyan BD, Lossdörfer S, Wang L, Zhao G, Lohmann CH, Cochran DL, et al. Osteoblasts generate an osteogenic microenvironment when grown on surfaces with rough microtopographies. Cells Mater. 2003;6:22–7.

131. Boyan BD, Schwartz Z, Lohmann CH, Sylvia VL, Cochran DL, Dean DD, et al. Pretreatment of bone with osteoclasts affects phenotypic expression of osteoblast-like cells. J Orthop Res. 2003;21:638–47. https://doi.org/10.1016/S0736-0266(02)00261-9.

132. Schwartz Z, Lohmann CH, Vocke AK, Sylvia VL, Cochran DL, Dean DD, et al. Osteoblast response to titanium surface roughness and 1α,25-(OH)2D3 is mediated through the mitogen-activated protein kinase (MAPK) pathway. J Biomed Mater Res. 2001;56:417–26. https://doi.org/10.1002/1097-4636(20010905)56:3<417::AID-JBM1111>3.0.CO;2-K.

133. Kim MJ, Choi MU, Kim CW. Activation of phospholipase D1 by surface roughness of titanium in MG63 osteoblast-like cell. Biomaterials. 2006;27:5502–11. https://doi.org/10.1016/j.biomaterials.2006.06.023.

134. M. Fang R, Olivares-Navarrete, Wieland M, Cochran DL, Boyan BD, Schwartz Z. The role of phospholipase D in osteoblast response to titanium surface microstructure Mimi. J Biomed Mater Res Pt A. 2010;93:897–909. https://doi.org/10.1016/j.neuron.2009.10.017.A.

135. Mustafa K, Rubinstein J, Lopez BS, Arvidson K. Production of transforming growth factor beta1 and prostaglandin E2 by osteoblast-like cells cultured on titanium surfaces blasted with TiO2 particles. Clin Oral Implants Res. 2003;14:50–6.

136. Lohmann CH, Dean DD, Bonewald LF, Schwartz Z, Boyan BD. Nitric oxide and prostaglandin E2 production in response to ultra-high molecular weight polyethylene particles depends on osteoblast maturation state. J Bone Jt Surg. 2002;84:411–9.

137. Boyan BD, Lohmann CH, Sisk M, Liu Y, Sylvia VL, Cochran DL, et al. Both cyclooxygenase-1 and cyclooxygenase-2 mediate osteoblast response to titanium surface roughness. J Biomed Mater Res. 2001;55:350–9. https://doi.org/10.1002/1097-4636(20010605)55:3<350::AID-JBM1023>3.0.CO;2-M.

138. Schwartz Z, Dennis R, Bonewald L, Swain L, Gomez R, Boyan BD. Differential regulation of prostaglandin E2 synthesis and phospholipase A2 activity by 1,25-(OH)2D3 in three osteoblast-like cell lines (MC-3T3-E1, ROS 17/2.8, and MG-63). Bone. 1992;13:51–8. https://doi.org/10.1016/8756-3282(92)90361-Y.

139. Boland GM, Perkins G, Hall DJ, Tuan RS. Wnt 3a promotes proliferation and suppresses osteogenic differentiation of adult human mesenchymal stem cells. J Cell Biochem. 2004;93:1210–30. https://doi.org/10.1002/jcb.20284.

140. Hyzy SL, Olivares-Navarrete R, Schwartz Z, Boyan BD. BMP2 induces osteoblast apoptosis in a maturation state and noggin-dependent manner. J Cell Biochem. 2012;113:3236–45. https://doi.org/10.1002/jcb.24201.

141. Berger MB, Bosh KB, Jacobs TW, Joshua Cohen D, Schwartz Z, Boyan BD. Growth factors produced by bone marrow stromal cells on nanoroughened titanium–aluminum–vanadium surfaces program distal MSCs into osteoblasts via BMP2 signaling. J Orthop Res. 2020;39:1908. https://doi.org/10.1002/jor.24869.

142. Oetgen ME, Richards BS. Complications associated with the use of bone morphogenetic protein in pediatric patients. J Pediatr Orthop. 2010;30:192–8. https://doi.org/10.1097/BPO.0b013e3181d075ab.

143. Smoljanovic T, Cimic M, Bojanic I. Aggressive end plate decortication as a cause of osteolysis after rhBMP-2 use in cervical spine interbody fusion. Spine J. 2010;10:187–8. https://doi.org/10.1016/j.spinee.2009.10.001.

144. Hyzy SL, Olivares-navarrete R, Hutton DL, Tan C, Boyan BD, Schwartz Z. Microstructured titanium regulates interleukin production by osteoblasts, an effect modulated by exogenous BMP-2. Acta Biomater. 2013;9:5821–9. https://doi.org/10.1016/j.actbio.2012.10.030.

145. Abe E. Function of BMPs and BMP antagonists in adult bone. Ann N Y Acad Sci. 2006;1068:41–53. https://doi.org/10.1196/annals.1346.007.

146. Salazar VS, Gamer LW, Rosen V. BMP signalling in skeletal development, disease and repair. Nat Rev Endocrinol. 2016;12:203–21. https://doi.org/10.1038/nrendo.2016.12.

147. Raines AL, Olivares-Navarrete R, Wieland M, Cochran DL, Schwartz Z, Boyan BD. Regulation of angiogenesis during osseointegration by titanium surface microstructure and energy. Biomaterials. 2010;31:4909–17. https://doi.org/10.1016/j.biomaterials.2010.02.071.

148. Cheng A, Humayun A, Cohen DJ, Boyan BD, Schwartz Z. Additively manufactured 3D porous Ti-6Al-4V constructs mimic trabecular bone structure and regulate osteoblast proliferation, differentiation and local factor production in a porosity and surface roughness dependent manner. Biofabrication. 2014;6:45007. https://doi.org/10.1088/1758-5082/6/4/045007.

149. Taniguchi N, Fujibayashi S, Takemoto M, Sasaki K, Otsuki B, Nakamura T, et al. Effect of pore size on bone ingrowth into porous titanium implants fabricated by additive manufacturing: an in vivo experiment. Mater Sci Eng C. 2016;59:690–701. https://doi.org/10.1016/j.msec.2015.10.069.

150. Cox SC, Jamshidi P, Eisenstein NM, Webber MA, Hassanin H, Attallah MM, et al. Adding functionality with additive manufacturing: fabrication of titanium-based antibiotic eluting implants. Mater Sci Eng C. 2016;64:407–15. https://doi.org/10.1016/j.msec.2016.04.006.

151. Alrabeah GO, Brett P, Knowles JC, Petridis H. The effect of metal ions released from different dental implant-abutment couples on osteoblast function and secretion of bone resorbing mediators. J Dent. 2017;66:91–101. https://doi.org/10.1016/j.jdent.2017.08.002.

152. Biggs MJP, Richards RG, Gadegaard N, Wilkinson CDW, Dalby MJ. The effects of nanoscale pits on primary human osteoblast adhesion formation and cellular spreading. J Mater Sci Mater Med. 2007;18:399–404. https://doi.org/10.1007/s10856-006-0705-6.

153. Webster TJ, Ejiofor JU. Increased osteoblast adhesion on nanophase metals: Ti, Ti6Al4V, and CoCrMo. Biomaterials. 2004;25:4731–9. https://doi.org/10.1016/j.biomaterials.2003.12.002.

154. Khang D, Lu J, Yao C, Haberstroh KM, Webster TJ. The role of nanometer and sub-micron surface features on vascular and bone cell adhesion on titanium. Biomaterials. 2008;29:970–83. https://doi.org/10.1016/j.biomaterials.2007.11.009.

155. Cheng A, Chen H, Schwartz Z, Boyan BD. Imaging analysis of the interface between osteoblasts and microrough surfaces of laser-sintered titanium alloy constructs. J Microsc. 2017;270:41. https://doi.org/10.1111/jmi.12648.

156. Boyan BD, Bonewald LF, Paschalis EP, Lohmann CH, Rosser J, Cochran DL, et al. Osteoblast-mediated mineral deposition in culture is dependent on surface microtopography. Calcif Tissue Int. 2002;71:519–29. https://doi.org/10.1007/s00223-001-1114-y.

157. Lohmann CH, Bonewald LF, Sisk MA, Sylvia VL, Cochran DL, Dean DD, et al. Maturation state determines the response of osteogenic cells to surface roughness and 1,25-Dihydroxyvitamin D3. J Bone Miner Res. 2000;15:1169–80. https://doi.org/10.1359/jbmr.2000.15.6.1169.

158. Braun G, Kohavi D, Amir D, Luna M, Caloss R, Sela J, et al. Markers of primary mineralization are correlated with bone-bonding ability of titanium or stainless steel in vivo. Clin Oral Implants Res. 1995;6:1–13. https://doi.org/10.1034/j.1600-0501.1995.060101.x.

159. Ritter NM, Farach-Carson MC, Butler WT. Evidence for the formation of a complex between osteopontin and osteocalcin. J Bone Miner Res. 1992;7:877–85. https://doi.org/10.1002/jbmr.5650070804.

160. Glowacki J, Rey C, Glimcher MJ, Cox KA, Lian J. A role for osteocalcin in osteoclast differentiation. J Cell Biochem. 1991;45:292–302. https://doi.org/10.1002/jcb.240450312.

161. Atkin I, Dean DD, Muniz OE, Agundez A, Castiglione G, Cohen G, et al. Enhancement of osteoinduction by vitamin D metabolites in rachitic host rats. J Bone Miner Res. 1992;7:863–75. https://doi.org/10.1002/jbmr.5650070803.

162. Dean DD, Schwartz ZVI, Muniz OE, Gomez R, Swain LD, Howell DS, et al. Matrix vesicles contain metalloproteinases that degrade proteoglycans. Bone Miner. 1992;17:172–6. https://doi.org/10.1016/0169-6009(92)90731-R.

163. Lotz EM, Berger MB, Schwartz Z, Boyan BD. Regulation of osteoclasts by osteoblast lineage cells depends on titanium implant surface properties. Acta Biomater. 2018;68:296–307. https://doi.org/10.1016/j.actbio.2017.12.039.

164. Shah FA, Wang X, Thomsen P, Grandfield K, Palmquist A. High-resolution visualization of the osteocyte Lacuno-Canalicular network juxtaposed to the surface of nanotextured titanium implants in human. ACS Biomater Sci Eng. 2015;1:1. https://doi.org/10.1021/ab500127y.

165. Schwartz Z, Lohmann CH, Sisk M, Cochran DL, Sylvia VL, Simpson J, et al. Local factor production by MG63 osteoblast-like cells in response to surface roughness and 1,25-(OH)2D3 is mediated via protein kinase C- and protein kinase A-dependent pathways. Biomaterials. 2001;22:731–41.

166. Lossdörfer S, Schwartz Z, Wang L, Lohmann CH, Turner JD, Wieland M, et al. Microrough implant surface topographies increase osteogenesis by reducing osteoclast formation and activity. J Biomed Mater Res Pt A. 2004;70A:361–9. https://doi.org/10.1002/jbm.a.30025.

Mechanics of the Implant-Abutment-Connection

Katja Nelson, Alexander Rack, Bernhard Hesse, and Tobias Fretwurst

When investigating the interaction between implant and abutment in a dental implant system three essential features can be considered: **design** characteristics, **material** classification, and (bio)**mechanical properties**. Although described independently within this chapter, it should be apparent that an intimate relationship exists between these features. The investigation of the material properties and mechanics of the implant and abutment is essential to assess the performance and longevity of dental implants in the oral environment. It might also help understand the biological behavior of the peri-implant tissue. Mainly experimental studies and/or mathematical models, a priori resembling different approaches but sometimes used complementary, allow us to gain insights into the biomechanics of dental implants.

12.1 Design of the Implant-Abutment Connection

12.1.1 Types and Classification of the Implant-Abutment Complex

Predominantly two-piece implant systems are used in dentistry. Two-piece dental implants consist of an implant body, which is placed into the bone, and an abutment, which is fixed by an abutment screw on the implant (Fig. 12.1).

The connection between both components (implant and abutment) is called the **implant-abutment connection** (**IAC**) and is usually connected with an abutment screw making it a screwed joint. In contrast to a two-piece implant, a one-piece implant has no IAC since the implant body and the abutment are one piece. Irrespective of how many parts (one-piece vs. two-piece) the implant system consists of the prosthetic superstructure can be fixed on the abutment. In one-piece implants the superstructure can only be cemented onto the abutment in two-piece implants it can either be cemented or screw-retained. Further descriptions mainly focus on methods used for the evaluation of two-piece implants.

K. Nelson (✉)
Universitätsklinikum Freiburg, Klinik für MKG-Chirurgie, Freiburg, Germany
e-mail: katja.nelson@uniklinik-freiburg.de

A. Rack
X-Ray Imaging Group European Synchrotron Radiation Facility, BP 220, Grenoble Cedex, France
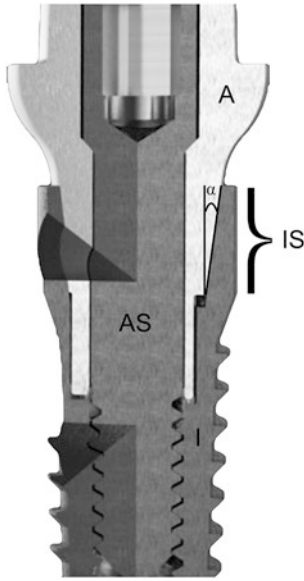e-mail: alexander.rack@esrf.fr

B. Hesse
ESRF, The European Synchrotron, CS 40220, Grenoble Cedex, France

Xploraytion GmbH, Berlin, Germany

T. Fretwurst
Department of Oral and Maxillofacial Surgery, Medical Center - University of Freiburg, University of Freiburg, Freiburg im Breisgau, Germany
e-mail: tobias.fretwurst@uniklinik-freiburg.de

Fig. 12.1 Cross-sectional view of conical implant. *I* implant, *IS* implant shoulder, *A* abutment, *AS* abutment screw, *a* angle of implant-abutment mating zone

The IAC is a joint that serves two purposes: (1) to ensure the **position stability** of the prosthetic components during the restorative phase (scan body, impression copings, abutments). The static position stability defines the spatial relationship between the abutment, impression coping or any other prosthetic part, and the implant. The precision of fit between the components ensures the accuracy of the transfer of the spatial position of the implant into a cast/virtual model or the precise re-positioning of prosthetic components in clinical use. The re-positioning of prosthetic parts has to be stable in three dimensions as the masticatory system involves a somatosensory system with a sensitivity that can detect occlusal deviations down to 8 μm [1–3].

The IAC and its precision are also essential for the (2) functional stability or **mechanical joint stability** defining the behavior during **dynamic loading**. In recent years increasing scientific focus has been laid on the mechanical properties of the IAC and its biological impact on the peri-implant tissue.

12.1.2 Position Stability of IAC

In the 1960s, the Brånemark implant was released, one of the first two-piece implants with extensive scientific documentation [4]. The initial Brånemark implant has a type of IAC defined as an external hexagonal butt-joint connection. The following years of research revealed mechanical complications with external hexagonal butt-joint implants such as an increased risk of abutment screw loosening [5]. The conical implant-abutment connection was introduced with the ITI (International Team of Implantology) implant 20 years later in the 1980s [6]. Initially, the ITI implant had no anti-rotational index. Its anti-rotational index was introduced using the geometric design of an octagon in the 1990s [7]. All two-piece implant systems are based on two principles: either having a **butt-joint** or **conical** connection. These terms describe the design of the implant-abutment-interface precisely the angulation of the corresponding contact surface (**mating zone**) between the implant and the abutment. Conical connections can exhibit friction fit (interference fit) if the angle (a) of the mating zone is between 1 and 8°, if the angle is greater than 8° it is not a conical connection based on friction fit. Butt-joint connections (clearance fit) depend on the preload of the abutment screw (Figs. 12.1 and 12.2).

The vertical position stability of butt-joint connections varies within a maximum of 10 μm whereas the conical connections can show a variation from 15 to 144 μm due to the property of the function of friction fit [1, 2, 8–10].

To ensure a rotation-safe positioning of the abutment an anti-rotation index is necessary. In external connections this index is positioned outside the implant body (e.g., Brånemark implant = external hexagonal butt-joint connection), and internal connections have their anti-rotation index inside the implant (Fig. 12.2). Today mainly internal connections are used, please regard, this is independent of the design of the mating zone. To minimize rotational freedom,
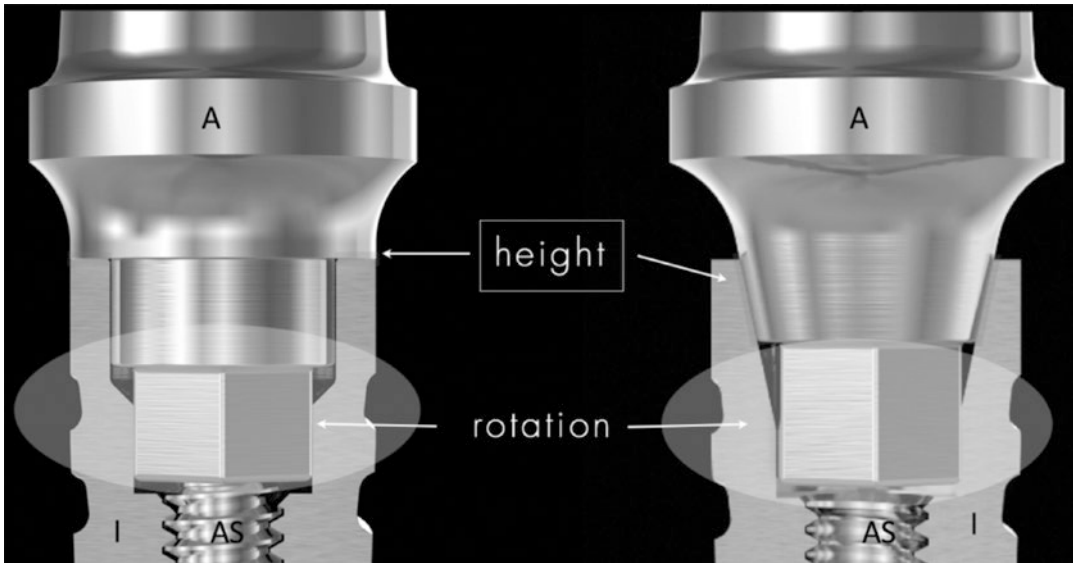
Fig. 12.2 Two-piece implant systems. Longitudinal section through the implant-abutment connection of two-piece implant systems: Butt-joint connection (left) and conical connection (right). The butt-joint connection is defined by two surfaces (abutment on implant shoulder) joining horizontally or almost horizontally (marked red). In conical connections, the abutment and the implant join on an angled surface inside the implant body (marked red). *I* implant, *A* abutment, *AS* abutment screw

three geometric designs of the anti-rotation index are mainly used in current implant systems. These designs are based on one of three geometric shapes/principles: polygon, polygon-profile, or cam-groove (Fig. 12.3) [11–13]. The different designs of the anti-rotation index have an impact on the rotational freedom IAC exhibits. Influencing factors on the amount of rotational freedom, which varies between 1.5 and 7.2° in current implant systems, are the geometric design and the engineering tolerance [1, 2, 8–10, 14].

To investigate the geometry of the anti-rotation index of a dental implant and its impact on rotational freedom Scanning Electron Microscopy (SEM) (Fig. 12.3) and geometric analysis can be used [1, 2, 8–10, 14–16].

After the design characterization of the implant-abutment-connection, e.g., mode of IAC, anti-rotation index, the precision of fit of the implant, and abutment can be evaluated.

Measurement of the position stability of the abutment in the implant can be performed using **optical** (digital image correlation, digital holography, stereo microscope) or **mechanical** (tactile) methods and sometimes they are combined. The science of measurement is termed metrology and the **metrologic methods** used in dental implant research to quantify the precision of fit between the implant and abutment are discussed. These methods are not only used for the evaluation of unloaded implant-abutment-connections but also when the load is applied to the IAC.

12.1.3 Metrologic Methods in Research Evaluating the IAC

Tactile measurements are usually performed using coordinate measuring machines **(CMM)** with very high accuracy in the sub-micron order [17]. CMMs measure the geometry of a physical object by sensing distinct points on the surface of the object with a probe. The object's position or displacement is measured in a 3D Cartesian coordinate system (*XYZ* axes). In each axis measurement, points are sensed resulting in a point cloud allowing the micrometer precise reproduction of the 3D-position of the object (Fig. 12.4). The
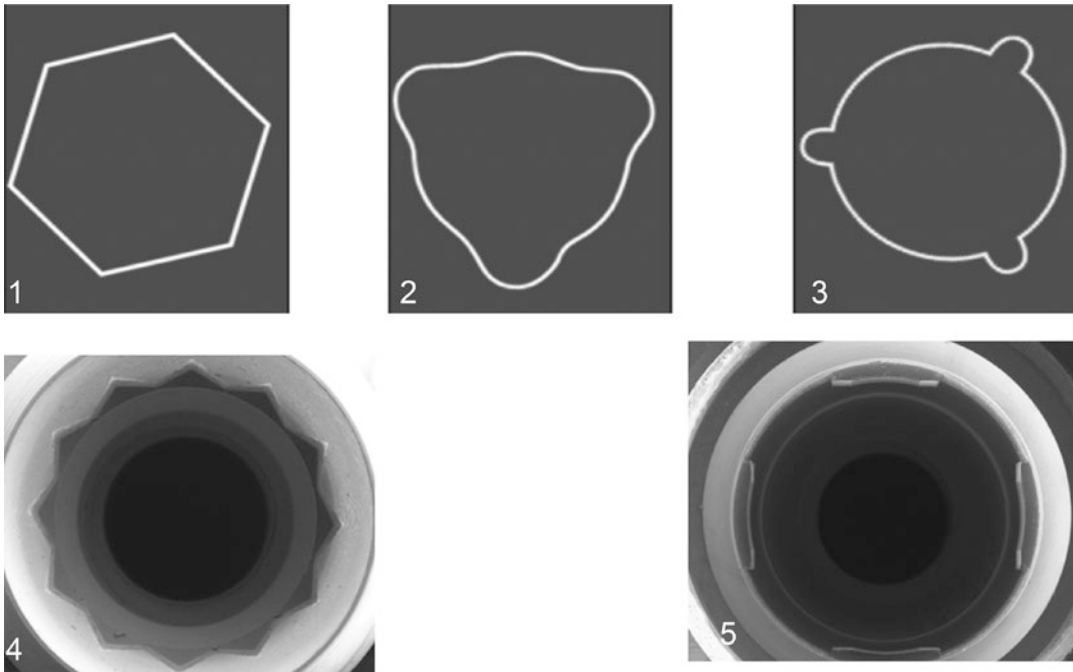
Fig. 12.3 Design of the anti-rotation index. The most common three geometric forms currently used in implants (polygonal (1) polygon profile (2) and cam groove (3)) whereas the polygonal and cam-groove designs are the most common. Scanning electron microscopic images can help evaluate anti-rotational indices the image of a polygonal (4) index design and a cam groove (5) design

CMM can be operated manually or computer controlled. Today CMMs can not only be operated with touch probes but combined with laser or light sensors.

**Optical measurements** can be performed using photometry and/or radiometry.

Digital image correlation (DIC) is a non-contact optical technique that employs image registration techniques for accurate 2D or 3D measurements of changes in images providing deformation field data. The gray value pattern of image datasets is matched and analyzed to extract shape, deformation, and/or motion, which are quantified using correlation-based measurements. Due to specialized algorithms and enhancement of the optical system's high resolution, this method also allows accurate measurement of the stress-strain curve of materials in motion. The DIC is often used to validate finite element analysis [18, 19].

Digital Holography (DH) describes the concept of digital holographic recording of a plane reference wave and the wave reflected from the object interferes at the surface of an electronic sensor array (e.g., Charged Coupled Device [CCD] or Complementary Metal Oxide Semiconductor [CMOS]). The resulting hologram is electronically recorded and stored in a computer. The object is, in general, a 3-dimensional body with diffusely reflecting surfaces, located at a distance d from the sensor (measured to some representative plane). This is the classical off-axis geometry of photographic holography but in which the recording medium is an electronic sensor array capturing diffracted waves rather than photographic film, which can only capture intensity [20–22].

These digital methods can be combined to increase the information value within one investigation or realize the evaluation of micro- and nano-sized objects.

The following methods are not only used for metrologic measurements but also for **material analysis**.
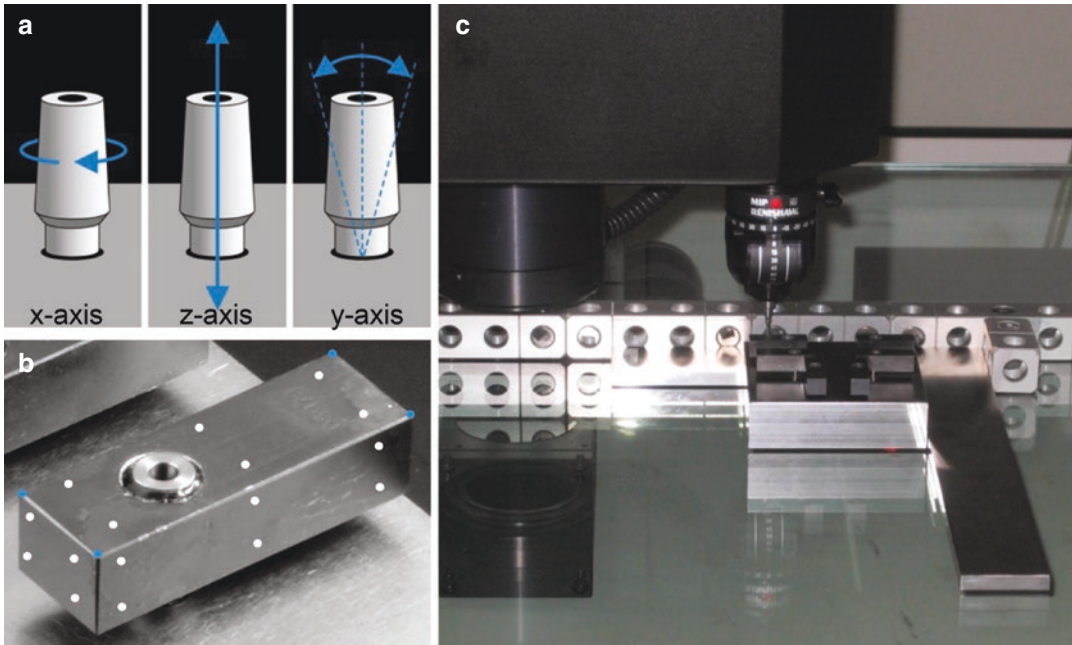
Fig. 12.4 The 3-dimensional displacement of the abutment (**a**) after re-positioning can be measured in a defined experimental set-up with a standardized measuring environment (temperature, formstabile embedding material, original parts), and multiple measuring points (white/blue dots) on standardized test bodies (**b**). Tactile measuring devices (**c**) have proven reliable

Stereo Microscope (SM) A stereo microscope is an optical instrument used to make objects larger in order to view their details. It uses light to illuminate the objects under view. The maximum magnification is 1250× and the resolving power is approximately ≥0.25 μm (250 nm). The light microscope is mainly used for thin light-transmitting objects (e.g., tissue biopsies). For solid objects, a reflected light microscope can be utilized. Its use for surface analysis or internal details of dental implants is restricted respectively not possible.

Applications: **Light microscopy (LM)** is predominantly utilized to study the contact zone of implant and peri-implant tissue using histologic sections [23].

The use of reflected light microscopes to quantify gaps (size ≥0.25 μm) between two objects has been described [24]. Its use for microstructural analysis will be discussed in the material section.

Electron Microscopy (EM) Electron microscopy uses a beam of accelerated electrons to illuminate and produce images of specimens. Using electron microscopy, higher magnification levels and resolution can be achieved compared to a light microscope because the wavelength of electrons is shorter than that of photons.

The first electron microscope was developed in 1931 by the German scientists Ernst Ruska and Max Knoll. Today, electron microscopy comprises a wide range of different methods that use the various signals arising from the interaction of the electron beam with the sample to obtain information about the structure, morphology, and composition of the sample. It can provide high-resolution information about cells, tissues, biopsy samples, and metals (Table 12.1).

Atomic Force Microscopy (AFM) Describes a scanning probe microscopy with probes mechanically "touching" the surface. It has a few

Table 12.1 Details about the specimen requirements and indications for the use of electron microscopic techniques

Electron microscopic method/abbreviation		Type/area of specimen	Indication
SEM Scanning electron microscopy	Morphology Topology	Compact/thin specimen down to 1 nm	– To study thin surfaces – Higher resolution than LM – 3D-imaging
TEM Transmission electron microscopy	Structure Composition	Thin specimen <100 nm	Detection of crystalline areas, defects and grain boundaries, phase analysis, particle size
ED Electron diffraction Usually combined with TEM	Structure	Surface of specimen	Determination of lattice parameter, crystal symmetry and orientation, phase analysis
EDX Usually combined with SEM or TEM	Chemical Composition	Surface of specimen	Allows qualitative and quantitative element analysis of materials or tissue biopsies up to a tissue depth of 5 μm/<0.1 mass%/element atomic no. >4

advantages over optical or electronic microscopy (1) it is not limited in spatial resolution due to diffraction or aberration, (2) it allows the measurement of forces, e.g., mechanical properties of a sample and (3) it enables the mechanical manipulation of a sample. These features are usually important in solid-state physics, surface chemistry, or molecular engineering as atoms at a surface can be identified, interactions between atoms can be evaluated and (c) the changes in physical properties arising from changes in an atomic arrangement through atomic manipulation can be studied.

Application: AFM technique is capable of revealing chemical information from the implant surface and bone-implant interface in 3D on an atomic level [25].

12.1.4 Implant Material

Besides the biological properties of implanted materials as described in Chap. 12 material properties are essential for the long-term survival of dental implants, these material properties comprise the microstructure of the implant and its surface composition. The material used should be biocompatible and exhibit adequate mechanical features [26]. In addition to the element's macroscopic properties (geometric properties), such as their length, width, thickness, and mechanical properties of materials, the microstructures are important for the mechanical performance and longevity of the implant.

The chemical composition of dental implants is either metal, ceramic, or polymer. The elemental composition of the materials can be evaluated using ICP-MS (Inductively Coupled Plasma Mass Spectrometry) and ICP-OES (inductively coupled plasma optical emission spectrometry), details of the methods are given in Table 12.4 [28].

Metals can be commercially pure titanium (Cp Ti) or titanium alloys. According to the American Society for Testing and Materials (ASTM), there are distinct types of titanium available as implant biomaterials. Four grades of commercially pure titanium (CpTi) and various titanium (Ti) alloys are being used for dental implants while today ceramic implants are made of yttrium-stabilized tetragonal polycrystalline zirconia (Y-TZP) [29]. PMMA, PEEK, and PU-Polymers are also used for the fabrication of dental implant bodies, but their dissemination is very low (Table 12.2) [30].

The American Society for Testing and Materials (ASTM), the British Standards Institute (BSI), and International Standards Organization (ISO) rationalize the various testing methods and parameters for biomaterials.

To characterize the material properties **hardness** and **strength** are measured. Ductile materials such as metallics or polymers will plastically deform until a fracture initiation, whereas brittle

Table 12.2 Overview of common materials for endosseous dental implants adopted and modified from Osman and Swain [30]

1. Metals	Titanium CpTi
	Titanium alloys: Ti-6A1-4V extra low interstitial (ELI) Ti-6A1-4V Ti-6Al-7Nb Ti-5Al-2.5Fe Ti-15 Zr-4Nb-2Ta-0.2Pd Ti-29Nb-13Ta-4.6Zr Roxolid (83%–87%Ti-13%–17%Zr)
2. Ceramics	Yttrium-stabilized tetragonal polycrystalline zirconia (Y-TZP)
3. Polymers	Polymethylmethacrylate (PMMA)
	Polyether ether ketone (PEEK)
	Polyurethane (PU)

materials, like ceramics, will fracture under very low strain [30, 31]. When a material breaks without significant plastic deformation it is termed brittle, even those of high strength [32].

Strength In general strength means the maximum stress the material can withstand. The strength of material in implant dentistry can be quantified by using the measurement of **Tensile Strength**. Tensile strength describes the force needed until the fracture of the material when pulled. By measuring the material while it is being pulled, we can obtain a stress/strain curve which shows how the material reacts to the forces being applied. The point of break or failure is of much interest, but other important properties include the modulus of elasticity, yield strength, and strain.

The **yield strength** defines the amount of stress a material can withstand before plastic deformation of the material occurs. For most materials, the initial portion of the test will exhibit a linear relationship between the applied force or load and the elongation exhibited by the specimen. In this linear region, the line obeys the relationship defined as "Hooke's Law" where the ratio of stress to strain is a constant also called "**Modulus of Elasticity**" or "Young's Modulus " it's SI unit is Pascal. Within this linear region, the tensile load can be removed from the specimen and the material will return to the exact same condition it had been in prior to the load being
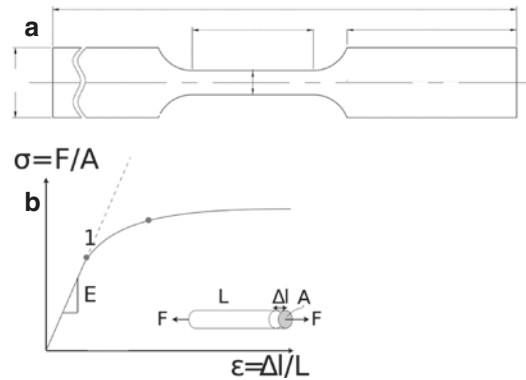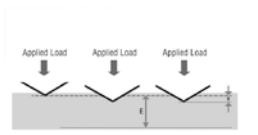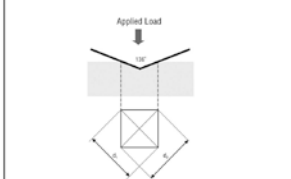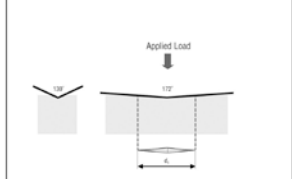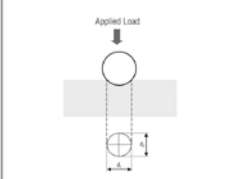

Fig. 12.5 (**a**) Sketch of a standard test specimen for tensile strength testing according to ISO 6892-1:2016 and ASTM E8:2016. (**b**) Depiction of a stress-strain curve for non-ferrous metals according to ISO 6892-1:2016 and ASTM E8:2016. Below this point (1) the amount of stress σ is proportional to strain ϵ (Hooke's law), defining the elastic modulus of the material. After point (1) plastic deformation of the material begins

applied. Beyond this point, plastic deformation occurs.

The tensile and yield strength of a metal is usually determined using a standardized testing method according to ISO 6892-1 and ASTM E8 [33, 34] (Fig. 12.5).

For materials with high modulus of elasticity (Young's Modulus) like zirconia, the methods based on resonance frequencies [35, 36] are the most practical and accurate choice because of the low stress and strain involved. **Flexural Strength** gives information about the resistance of a material against deformation, i.e. flexural strength indicates how much force is required to break a test sample of a defined diameter. It is usually evaluated when working with ceramic materials [37, 38].

Hardness Hardness is a surface property of a material. In general, a material is hard if it has a high tensile strength which might increase resistance to permanent deformation and wear. Different hardness tests exist, they are typically performed by pressing a specifically dimensioned and loaded object (indenter) into the surface of the material you are testing (Fig. 12.6). The hardness is determined by measuring the depth of indenter penetration or by measuring

Fig. 12.6 Standard test methods for hardness testing
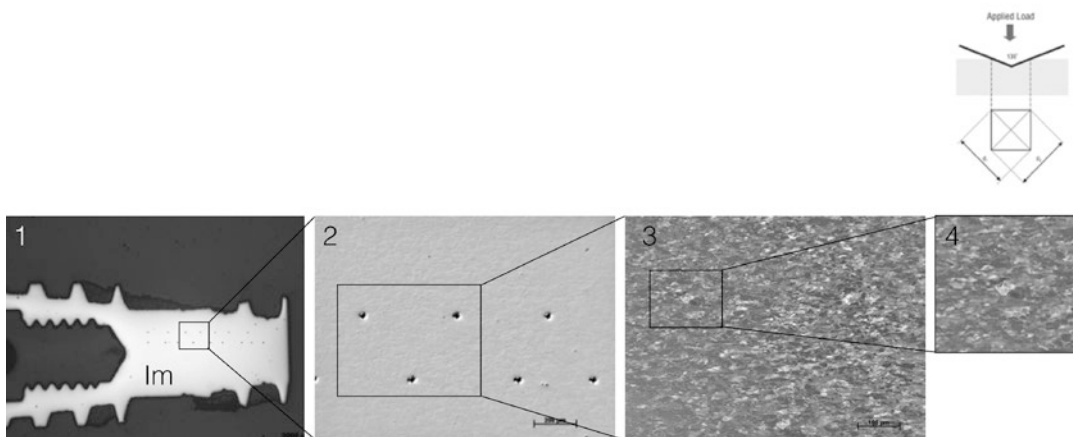
Fig. 12.7 (1) Light microscopic image of the cross-section of a dental implant prepared for microstructure analysis. Throughout the implant body (Im) various indentations are performed for the measurement of the hardness according to Vickers hardness test (HV). (2) The squared area of (1) is magnified, (3) further magnification reveals the microstructure of the material and the diamond pyramid indent becomes visible (4). All of the indentations will be electronically measured using the diagonals of the diamond pyramid indent which is seen in the middle of the picture (4)

the size of the impression left by an indenter [39] (Fig. 12.7).

Microstructure Describes the structure of a material that can only be revealed by a microscope on a nm-cm length scale. The microstructure of a material (metals, polymers, or ceramics) influences the physical properties such as strength, ductility, hardness, corrosion resistance, or wear resistance (Fig. 12.8).

The **crystal structure** of a material describes the average positions of atoms within the unit cell and is specified by the lattice type and the fractional coordinates of the atoms using X-ray diffraction. The crystal structure describes the appearance of the material on an atomic (or Å) length scale.

The examination of these properties is essential to acquire complete knowledge of existing and new materials.
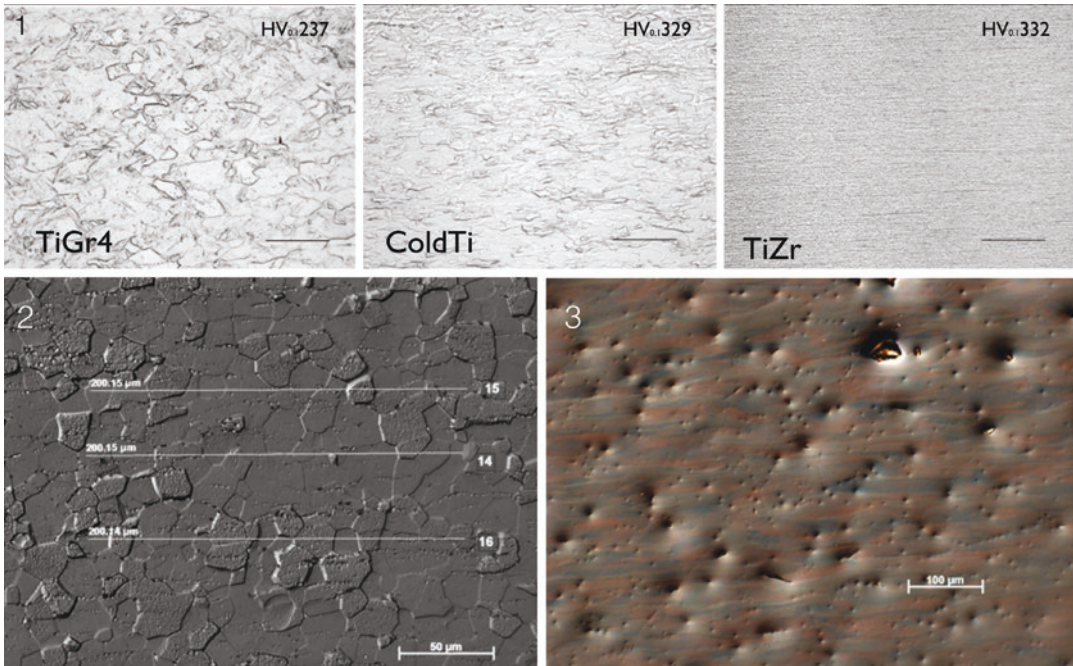
Fig. 12.8 (1) Light microscopic images of the microstructure and the Vickers hardness value (HV) of different implant materials. Pure titanium grade 4 (TiGr4), cold-worked titanium (ColdTi), and titanium-zirconia alloy (TiZr). (2) Measurement of the grain size of a titanium grade 4 metal. (3) At the light microscopic level flaws (air inclusion) of the material can be detected, the knowledge of these is essential as they have a negative impact on the material properties and therefore the wear resistance of an implant

12.2 Mechanical Properties of the IAC

12.2.1 Mechanical Joint Stability

To study the behavior of dental implants under load various methods are available usually comprising in vitro studies or theoretical approaches. In vivo studies are limited to animal studies and have been applied to study the influence of loading of dental implants on the peri-implant tissue [40, 41]. The mechanical behavior of the implant-abutment connection has been studied in in-vitro experiments and using numerical methods. Besides the geometric design features and material properties of the implant and the abutment the surrounding parameters (bone, mastication forces, and direction) of the implant are of importance for numerical (in silico studies) and in vitro studies [26]. The pseudo-latin term in silico describes the use of computational or mathematical simulation or modeling of a natural or laboratory process [42].

12.2.2 Finite Element Analysis

Finite element analysis (FEA) is a numerical method used for the prediction of how a part or assembly behaves under given conditions. It helps predict the performance of a workpiece with complicated geometry, loadings, and material properties where analytical solutions cannot be obtained. In implant dentistry, finite element analysis (FEA) has been applied to investigate the implant's design, the structure and material of the superstructure, and its influence on the surrounding bone. To date, FEA, in contrast to

in vivo studies, allows the measurement of stress distribution inside the peri-implant bone. Since the introduction of FEA in the field of implantology this form of analysis has been increasingly used [43, 44].

FEA is a technique that divides one complex mechanical problem into smaller and simpler elements with different field variables which can be interpolated by using shape functions. Various components and different forms of numerical analysis of the mechanical behavior of the dental implant in bone exist. Parameters that influence the numerical analysis for the evaluation of the biomechanical behavior of implant-abutment assemblies comprise the modeling of the implant (geometry, material properties, surface structure), loading details, properties of the human bone, boundary conditions and modeling of the interface [45]. When performing FEA the biological and mechanical data used for numerical analysis need to be described precisely including the parameters listed in Table 12.3.

With the increasing complexity of the numerical method the chances of the representation of realistic conditions become greater [44, 46]. To determine the degree of accurate representation of a real situation of a numerical analysis different validation models (in vivo human > in vivo animal > in vitro cadaver bone > in vitro animal bone > in vitro artificial material) in a hierarchical manner can be used [43, 44]. Due to the complexity of oral biology and ethical considerations human in vivo studies validating FEA data are scarce [47].

FEA can be validated in vitro using DIC, strain gauge measurements, and synchrotron radiography, to date only 10% of the FEA studies have used the mentioned validation methods [48–50].

To examine the mechanical durability and behavior under functional load application mechanical implant testing is mandatory.

12.2.3 Mechanical Testing

Mechanical testing of dental implants is performed in vitro using a reproducible set-up often

Table 12.3 Essential parameters and methods used in finite element analysis

Biological and mechanical parameters	Methods of finite element analysis
Implant: Geometry (length, diameter, design), material properties *Abutment*: Mode of fixation to the implant, geometry, material properties, abutment screw *Peri-implant environment*: Bone/material structure, bone/material quantity, bone/material to implant contact zone (BIC) *Suprastructure*: Geometry, material, mode of fixation on the abutment *Load*: Direction of application and amount	– 2-dimensional or 3-dimensional – Homogeneous isotropic linear elasticity – Inhomogeneous anisotropic linear elasticity
The fundamental assumptions for **linear elasticity** are small strains and linear relationships between the components of stress and strain For an **isotropic** medium, the applied force will give the same displacements (relative to the direction of the force) no matter the direction in which the force is applied (two constants). **Anisotropy** refers to the directional dependence of material properties which describes a material having different properties when measured in different directions (>2 constants). The degree of anisotropy can vary which influences the number of constants of a calculation (transversely isotropic, orthotropic)	

regarding regulatory aspects (FDA and/or CE-marking) [51]. The mechanical static and fatigue tests of dental implants are not only required for regulatory reasons they are also useful for the research explaining biological and technical complications encountered. Biological complications comprise inflammatory reactions of the peri-implant tissue (peri-implantitis) which can occur in up to 20% of the osseointegrated implants and technical complications, like implant fracture, abutment screw loosening in up to 40% of the implants after 5 years of loading [52–54]. Dental implants are subject to multi-axial loading during mastication (1 Hz) [55] and maximum mean loading forces in dental implants have been quantified to be up to 450 N [56].

Maximum mean voluntary bite force in the natural dentition shows varying forces up to

650 N depending on type of prosthesis, antagonist, sex, age, and location in the mouth [57, 58].

When in vitro analysis is performed, a detailed description of the implant, abutment, and abutment screw including material properties, geometry should be given as well as the parameters of the loading conditions (number of cycles, magnitude of force, angle, and medium) [48, 59]. Implant dimension and geometry should not only comprise the parameters diameter and length of the implant but also the implant wall thickness and the geometry of the implant-abutment-interface [48, 60].

In vitro mechanical testing methods used in dental implant testing, are **maximum static load-bearing capacity** or **single load to failure (SLF)** [61]. A load is applied to an individual specimen, and the maximum load at failure is reported. Failure is defined as the load value at which a sharp drop in the load occurs after the main part of deformation and energy absorption. Usually, a force/displacement curve documents the course to failure (Fig. 12.9).

The force at which the load–displacement curve first deviated by 10% from the regression line can be used as an indicator for the beginning of plastic deformation. In clinical reality implants are prone to repeated lower-intensity loads during function which can lead to cumulative damage [62]. Considering that "strength" is defined as the stress at which failure occurs, the reported load-to-failure data are seldom related to the stresses resulting in the failure itself [26, 63].

This method is helpful for the initial screening and designing of fatigue tests, however, this test does not give any information on the resistance of an implant-abutment assembly to fatigue loading [26, 63, 64].

Fatigue describes the process of weakening of a material caused by cyclic loading leading to progressive and localized structural damage it is characterized by crack initiation, slip band crack growth, crack growth on planes of high tensile stress, and ultimate ductile failure [65]. **Fatigue life**, as defined by ASTM, is the number of stress cycles with a specific character (static, dynamic, or cyclic) that the implant-abutment assembly will sustain before it fails in a defined manner [66, 67]. Engineering fatigue data is usually performed by constructing an $S-N$ curve (S = normalized engineering stress (stress/max(stress) and N = cycles to failure) which involves the cyclic loading of specimens at a high level of stress (2/3 of the tensile strength of the material)

Fig. 12.9 Load to failure test is performed using a universal testing machine (1), the specimen (↑) is placed in a holding device (★) and loaded at 30°. The results are displayed as a force-displacement curve (2) extracted from testing four different specimens
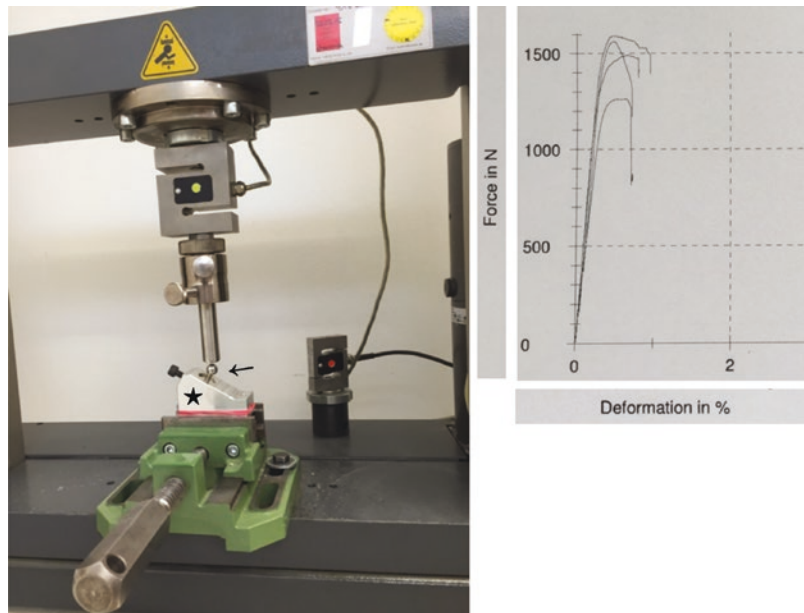
then carrying on at lower levels of stress until runout. Considering that producing $S–N$ diagrams (Wöhler curves) a large number of samples is necessary which may be time-consuming, therefore alternative methods have been implemented in dental implant research.

To provide failure data and/or degradation data in a limited test duration reliability testing, reliability estimation, and prediction models are commonly used [68]. It also presents approaches for the design of test plans for accelerated testing. In implant dentistry the step-stress accelerated life testing (SSALT) as proposed by Bonfante and Coelho might serve as an alternative to the time-consuming Wöhler curve [26, 69]. The SSALT is a reliability test in which specimens are tested at a high stress level successively increasing in a predefined time regimen. This test method is associated with a complex analysis to extrapolate the test data [26, 70].

No consensus exists on the ideal parameters for stress amplitude and cycling frequency. A variety of contradictory testing scenarios have been suggested to mimic the natural masticatory cycle over years ranging from one million to five million cycles and loads from 50 N to 800 N [26, 71]. The frequency of load application (Hz) in commercially pure titanium implants, has been shown to influence the fatigue limit with a higher probability of fracture at low frequency (2 Hz) within 10^6 cycles [64]. According to ISO 14801:2016, the testing frequency should not exceed 15 Hz.

ISO 14801:2016 is a standardized dental implant testing protocol for certification purposes. It allows testing up to 15 Hz until failure or five million cycles in dry conditions, which circumscribes a wide operational field. Synchrotron X-ray evaluation has revealed that testing of standard diameter implants at 15 Hz at 120 N for 5×10^6 cycles induces plastic deformation of the implant shoulder and wear at the implant-abutment interface can already be seen after 200,000 cycles at 98 N with 2 Hz [62, 72].

12.3 Visualization of the Micromechanics of the IAC

12.3.1 Micro-Mechanics of Two-Piece Dental Implants and Synchrotron Radiation

Similar to the experimental techniques outlined in the previous section, the use of hard synchrotron radiation (SRX) bears enormous potential for X-ray imaging [73]. The substantially higher photon flux density with respect to laboratory-based X-ray sources allows one to achieve excellent signal-to-noise ratios with short exposure times and even at high spatial resolution up to the micrometer range. When polychromatic radiation is applied for illumination, the exposure times can be short enough to progress towards the study of dynamic processes: either in two dimensions (radiography) or in three dimensions by tomographic techniques (cine-tomography). Another advantage of synchrotron light is the quasi-parallel beam propagation which allows for drastically increased sample-source distances of up to several 100 m. A long distance between the sample and the source with a comparable short distance between the sample and detector suppresses the influence of the finite source size on the image formation. Hence, effects like refraction at interfaces (so-called fringes) or interference effects (so-called X-ray phase contrast) can be exploited as contrast modality with drastically increased sensitivity. In the phase contrast regime, the grey levels in the images do not present anymore the physical density but rather are related to the local electron density: orders of magnitude more sensitive [74].

Both aspects, i.e. short acquisition times for time-resolved studies as well as high sensitivity have been exploited to study the micro-mechanical behavior of two-piece dental implants under static or dynamic load, respectively. For two-piece dental implants with a butt-joint con-

nection at the implant-abutment interface, it is well-known that microgap formation occurs and these gaps can be visualized using laboratory-based X-ray sources [72, 75–77]. Understanding and predicting these gaps may be important for the long-term performance and success of different implant designs. Depicting microgaps in two-piece dental implants with a conical connection is more challenging as the gap is inside a dense metal implant body and the size of the gap can be as small as a few micrometer down to submicrometer and metals such as zirconia or titan are highly attenuating objects making the use of laboratory-based X-ray sources for quantitative analysis impossible [78]. To date, laboratory-based X-ray sources do not allow the use of phase-contrast propagation at the required high photon energies to transmit dental implants, exploiting contrast formation by free wave propagation between sample and detector. The possibility to partially translate the capabilities of SR phase-contrast tomography to the laboratory is now emerging by using nearly monochromatic X-ray photons which might minimize the drawbacks created by the typical polychromatic illumination of laboratory X-ray sources especially

in highly attenuating objects like titanium or zirconia implants [79].

The contrast modulation in classical radiography by means of density contrast is frequently below the detection limit of X-ray imaging. The use of the above-mentioned edge enhancement or edge contrast is easy to implement at a synchrotron light source as only a finite drift space between sample and detector is needed, i.e. also perfectly suited for in-vitro studies involving sample environments. When combining the more sophisticated contrast modes with forward simulations, gap sizes can be estimated way below the resolution limit of the detector system used [80].

Synchrotron radiation allows the visualization of microgaps between the abutment and implant body which are greater than 0.1 μm (Fig. 12.10). It also allows the visualization of the micromovement of the abutment during load application involving a chewing simulator specially designed for in-situ microtomography applications which can be performed at the European Synchrotron Radiation Facility (ESRF) in Grenoble, France. Furthermore, the availability of a wiggler insertion device gives access to the required high pho-
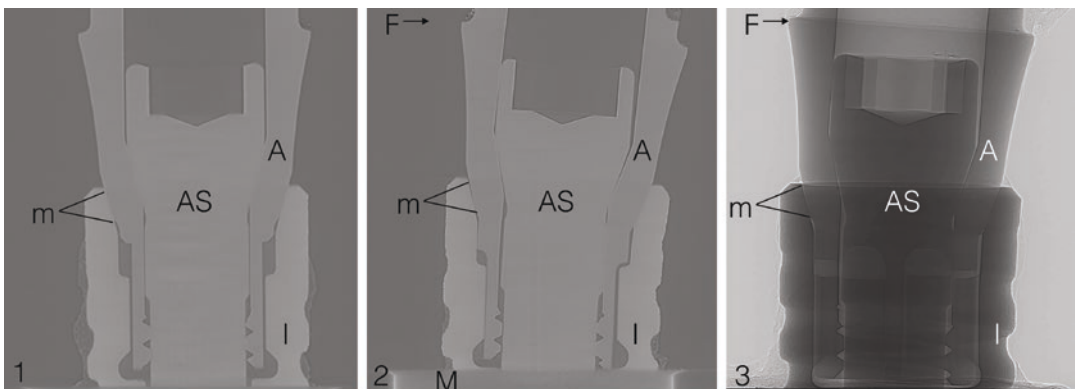
1: sagittal reconstruction of tomographic image (unloaded virgin implant); 2: sagittal reconstruction of tomographic image, 3: radiographic image based on synchrotron x-rays of a dental implant under load application: I=implant, A=abutment, AS=abutment screw, m=mating zone, M=metal cylinder, F=direction of load application

Fig. 12.10 Synchrotron-based tomography or radiography of the implant-abutment connection of dental implants embedded in a metal cylinder according to the DIN ISO standard 14801:2016. The high resolution of this method allows the visualization of the mechanical behavior of the

implant and abutment under load while allowing a submicrometer quantification of the micro-movement of the implant and abutment and the gap-formation in the mating zone (implant-abutment-interface) between these two components
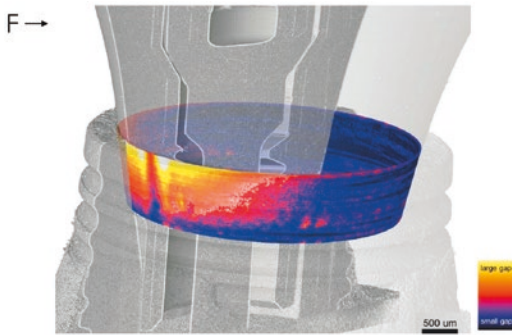
Fig. 12.11 Three-dimensional visualization of a micro-gap map at the implant-abutment connection (colored) of a loaded dental implant superimposed on the CT scan of the dental implant. The IAC map is calculated following Zabler et al. [82] and [76]. F: direction of load application

ton flux and hard X-ray energies around 60 keV (polychromatic) [76, 81]. An example result for the data sets acquired in situ is shown in Fig. 12.11.

The results found by the in situ microtomography approach under different loads are in accordance with the results from other ex situ studies with static load application [72, 82]. Synchrotron radiography and tomography not only allow the quantification of the microgap in the IAC but also the visualization of the micromovement of the abutment during loading [60, 62, 76]. Further examination of specimens evaluated with synchrotron using SEM and EDX revealed that the micromovement of the abutment during loading induces extensive wear and wear debris at the implant-abutment-interface [62]. The following section will elucidate the impact of the existence of wear particles and their analysis in vivo.

12.3.2 Metal and Ceramic Ions and Particles in Peri-Implant Tissue

Numerous orthopedic studies of the last decades demonstrated that arthroplasties especially of the hip and knee can be affected by so-called *aseptic loosening*. Local peri-prosthetic osteolysis is triggered by wear debris derived from metal, ceramic, or polyethylene joint replacement

material which is released by mechanical loading of hip and knee prostheses. Nanometer- to micrometer-sized particles with different chemical compositions have been detected in the tissue around orthopedic implants [83]. It is assumed that the particle composition and the configuration, such as size and shape are influencing parameters of the local immune response [83]. Lymphocyte- and macrophage-directed immune responses are assumed and it is known that a cascade of proinflammatory cytokines and mediators are involved in peri-implant bone lysis [84–86]. In dental Implantology, little evidence is available concerning particles and ions in the vicinity of implant material and their potential influence on peri-implant bone loss [87, 88]. However, titanium, ceramic ion, and particles were detected in inflamed peri-implant tissue. The local density was calculated to be as high as ~40 million particles/mm^3 in recent research [89]. Several plausible causes for ion and particle release into peri-implant tissue are discussed in the literature: wear debris from the implant-abutment connection, mechanical stripping from the implant surface during the implant placement, biocorrosion, particle release from dental restorations, or manipulations during implant surface treatment [90, 91]. Several techniques have been proposed for the detection of chemical elements in human tissue around dental implants [87, 89].

12.3.3 Techniques for Chemical Element Detection in Human Tissue Around Dental Implants

Initially, light microscopy was used for the histologic evaluation of peri-implant tissue [92]. Although tissue and cellular mapping is easily applicable and accessible with light microscopy, its resolution is limited to about 1 μm, and discrimination of element composition is not possible. If microscopy is combined with Energy-dispersive X-ray Spectroscopy (EDX) the elemental composition can be determined with limitations (Table 12.4). EDX allows the

Table 12.4 Techniques for the detection of chemical elements in human biopsies or implant materials (modified according to [27])

	Spatially resolved detection in tissue	Spatially resolved detection in cell	Identification of chemical elements	Chemical structure of the element	Destruction of tissue/specimen
Optical microscopy	+	+	−	−	−
ICP-MS	−	−	+	−	+
Laser ablation ICP-MS	+	−	+	−	+
ICP-OES	−	−	+	−	+
μ-XRF with XAS	+	−	+	+	+/−
TEM	−	+	+	+	+
SEM/EDX	−	+	+	−	+

identification of elements; however, no conclusions can be drawn concerning the chemical structure of the elements. Further, EDX is commonly coupled with SEM and can reach a spatial resolution of a few nm. However, the penetration depth of electrons is only about 1 μm [93].

μ-XRF synchrotron micro X-ray fluorescence, *μ-XAS* synchrotron absorption spectroscopy, *ICP-MS* inductively coupled plasma mass spectrometry, *ICP-OES* inductively coupled plasma optical emission spectrometry, *TEM* transmission electron microscopy, *SEM/EDX* scanning electron microscopy with energy-dispersive X-ray spectroscopy.

A further established technique with high sensitivity and high spatial resolution is laser ablation inductively coupled plasma mass spectrometry (LA-ICP-MS). LA-ICP-MS enables quantitative information about the elemental composition of metals and several nonmetals at sub-ppm concentrations [94]. The spatial resolution ranges from about 10–200 μm and is thus well suited for mapping metals in biological tissues [95].

Briefly described, a flat sample surface is exposed to a Laser beam. The Laser beam ablates the sample and the released particles are subsequently transported to the ICP-MS system by a carrier gas. The ablated particles are ionized with inductively coupled plasma. Subsequently, those ions are separated and quantified using a mass spectrometer. Single-particle ICP-MS is a powerful tool to assess nanoparticle size distribution in

an element-specific manner in biological tissues and materials [96, 97]. Recently, single particles (SP) ICP-MS coupled to Laser ablation was applied to gold nanoparticle investigation in mouse liver [98]. Thus SP-LA-ICP-MS enables 2D assessment of nanoparticle composition and size distribution in biological tissues.

Synchrotron micro and nano-X-ray fluorescence (μXRF/nanoXRF) is so far seen as the golden standard since XRF is characterized by high spatial resolution in combination with high elemental sensitivity and the possibility for chemical speciation by X-ray absorption spectroscopy using one single instrument [99]. In X-ray fluorescence spectroscopy atoms are excited by an X-ray beam and subsequently emit element characteristic radiation. This radiation is called X-ray fluorescence. The energy of the emitted radiation depends on the binding energy of the electrons involved in the electronic transitions. The intensity of the emitted radiation mainly depends on the amount of the respective atoms in the probing volume, the matrix composition, the energy of the exiting radiation, and the binding energy of the electrons involved in the electronic transitions.

Because of the extremely high flux of X-rays generated by Synchrotron sources the exciting beam can be focused to very small spot sizes of only tens of nm and a very narrow energy band can be selected. Scanning the X-ray energy of the exciting radiation around absorption edges of atoms of interest in the probing volume and col-
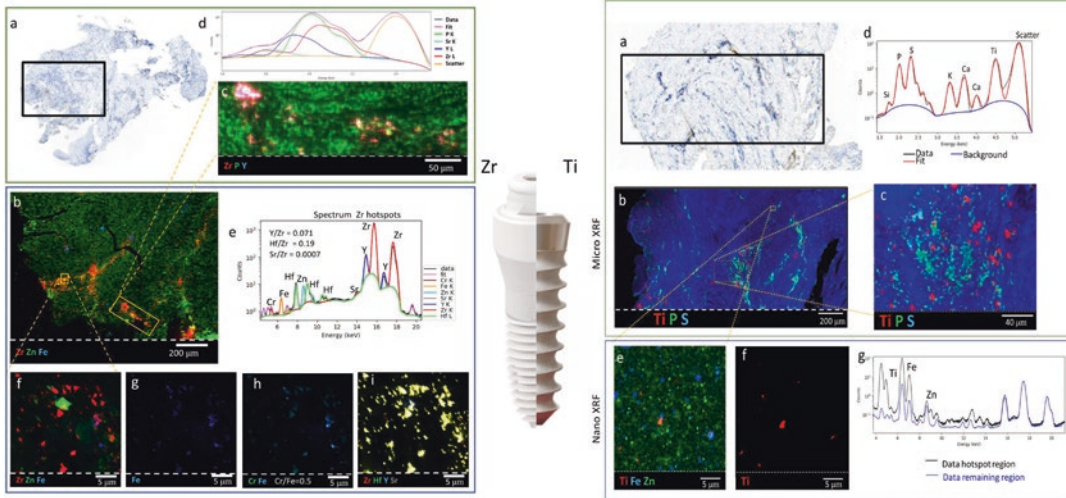
Fig. 12.12 Left figure. Ceramic Sample. (**a**): Histological image of a section of sample WGAM 6 (anti-CD68,1:200 (macrophage, clone PG-M1, DakoCytomation A/S, Glostrup, Denmark); counterstaining with hematoxylin). µXRF maps are shown in (**c**) at 4 µm step size. The average spectrum of Zr-rich regions of map (**c**) is shown in (**d**) including its de-convolution. Subsequently, nano XRF analysis was performed on the same section at 60 nm step size. (**b**) is a fast overview scan to identify regions of interest. An inset within (**b**) of Zr, Zn, Fe, Hf, Y, Sr, and Cr fluorescence intensities is shown in (**f**–**i**). In (**i**), it can be seen that Zr, Hf, Y, and Sr are co-localized. Their spectrum and relative mass fractions are shown in (**e**). (**h**) shows the presence of a few Fe-Cr particles, probably stainless steel with a mass-fraction ratio of Cr to Fe of 0.5. Right figure. Titanium Sample. (**a**) Histological image of a section of sample WGAM 14 (anti-CD68,1:200 (macrophage, clone PG-M1, DakoCytomation A/S, Glostrup, Denmark); counterstaining with hematoxylin). µXRF maps are shown in (**b**) and (**c**) at 10 and 4 µm step width, respectively. The average spectrum of Ti-rich regions of map (**c**) is shown in (**d**). Subsequently, nanoXRF analysis was performed on the same section at 60 nm step size. Ti, Fe, and Zn fluorescence intensities are shown in the overlay (**e**) after spectral de-convolution. The distribution of Ti is shown in (**f**). The spectra collected from Ti hotspots and the remaining regions are shown in (**g**) in black and blue, respectively. The mass fractions of Zn hotspots compared to Ti hotspots are 10,000 times smaller; those of Fe are 100 times smaller. (Figure from [89] with kind permission of ACS Publications)

lecting the emitted X-ray fluorescence as a function of exciting energy allows for assessing the chemical speciation of elements. This technique is called X-ray absorption near-edge structure spectroscopy. Thus, Synchrotron X-ray spectroscopy is a unique tool to assess elemental composition, chemical speciation, and the sizes of nanoparticles (NP) in complex matrixes, e.g., human tissues [89, 100, 101].

The synchrotron XAS technique X-ray absorption near edge structure (XANES) in combination with focusing optics is utilized to determine the chemical speciation of specific elements of interest at the same resolution. The main crystalline phases of TiO_2 nanoparticles (e.g., rutile and anatase) are the focus of current research. In peri-implant tissue, titanium and zirconia ceramic particles in local densities of several ten million per mm^3 can be detected via XANES. Titanium particles consist mainly of metallic and titanium dioxide (TiO_2) [89]. Figure 12.12 shows data collected from human peri-implant tissue. The spectra are de-convoluted and the different element-specific X-ray fluorescence emissions are shown. These data illustrate the use of Synchrotron micro- and nanoXRF analysis as well as XANES to assess implant-related particle release in human tissues. The influence of particle characteristics in peri-implant disease dynamics is a field of future research.

All of the methods and parameters mentioned within this chapter help investigate and understand existing and new implant materials and designs and the biomechanics of dental implants.

We, the authors of this chapter would like to thank all of the unmentioned helpers and co-workers, collaborators, and other researchers in our institutes and throughout the world to make this chapter become what it is.

References

1. Semper W, Heberer S, Mehrhof J, et al. Effects of repeated manual disassembly and reassembly on the positional stability of various implant-abutment complexes: an experimental study. Int J Oral Maxillofac Implants. 2010a;25(1):86–94.
2. Semper W, Kraft S, Mehrhof J, Nelson K. Impact of abutment rotation and angulation on marginal fit: theoretical considerations. Int J Oral Maxillofac Implants. 2010b;25(4):752–8.
3. Siirilä HS, Laine P. The tactile sensibility of the parodontium to slight axial loadings of the teeth. Acta Odontol Scand. 1963;21(5):415–29.
4. Brånemark PI, Hansson BO, Adell R, et al. Osseointegrated implants in the treatment of the edentulous jaw. Experience from a 10-year period. Scand J Plast Reconstr Surg Suppl. 1977;16:1–132.
5. Adell R, Eriksson B, Lekholm U, et al. Long-term follow-up study of osseointegrated implants in the treatment of totally edentulous jaws. Int J Oral Maxillofac Implants. 1990;5(4):347–59.
6. Sutter F, Schroeder A, Buser DA. The new concept of ITI hollow-cylinder and hollow-screw implants: Part 1. Engineering and design. Int J Oral Maxillofac Implants. 1988;3(3):161–72.
7. Sutter F, Weber HP, Sorensen J. The new restorative concept of the ITI dental implant system: design and engineering. Int J Periodontics Restorative Dent. 1993;13(5):408–31.
8. Semper W, Kraft S, Krüger T, Nelson K. Theoretical considerations: implant positional index design. J Dent Res. 2009a;88(8):725–30.
9. Semper W, Kraft S, Krüger T, Nelson K. Theoretical optimum of implant positional index design. J Dent Res. 2009b;88(8):731–5.
10. Semper-Hogg W, Kraft S, Stiller S, et al. Analytical and experimental position stability of the abutment in different dental implant systems with a conical implant-abutment connection. Clin Oral Investig. 2013;17(3):1017–23.
11. Binon PP. Implants and components: entering the new millennium. Int J Oral Maxillofac Implants. 2000;15(1):76–94.
12. Nelson K, Zabler S, Wiest W, et al. Die Implantat-Abutment-Verbindung. Implantologie. 2013a;21(4):355–63.
13. Nelson K, Semper-Hogg W, Kirsch A. Implant-abutment connection. In: Ewers R, Lambrecht T, editors. Oral implants bioactivating concepts. 1st ed; 2013b. p. 157–62.
14. Hogg WS, Zulauf K, Mehrhof J, et al. The influence of torque tightening on the position stability of the abutment in conical implant-abutment connections. Int J Prosthodont. 2015;28(5):538–41.
15. Garine WN, Funkenbusch PD, Ercoli C, et al. Measurement of the rotational misfit and implant-abutment gap of all-ceramic abutments. Int J Oral Maxillofac Implants. 2007;22(6):928–38.
16. Karl M, Taylor TD. Parameters determining micro-motion at the implant-abutment interface. Int J Oral Maxillofac Implants. 2014;29(6):1338–47.
17. Schwenke H, Wäldele F, Weiskirch C, et al. Opto-tactile sensor for 2D and 3D measurement of small structures on coordinate measuring machines. CIRP Ann. 2001;50(1):361–4.
18. Ghosh R, Gupta S, Dickinson A, et al. Experimental validation of finite element models of intact and implanted composite hemipelvises using digital image correlation. J Biomech Eng. 2012;134(8):081003.
19. Sutton MA, Orteu JJ, Schreier H. Image correlation for shape, motion and deformation measurements: basic concepts, theory and applications. New York: Springer; 2009.
20. Kim MK. Digital holographic microscopy. New York: Springer; 2011.
21. Schnars U. Direct phase determination in hologram interferometry with use of digitally recorded holograms. JOSA A. 1994;11(7):2011–5.
22. Schnars U, Jüptner W. Direct recording of holograms by a CCD target and numerical reconstruction. Appl Opt. 1994;33(2):179–81.
23. Ruehe B, Heberer S, Bayreuther K, et al. Effect of dehiscences to the bone response of implants with an acid-etched surface: an experimental study in miniature pigs. J Oral Implantol. 2011;37(1):3–17.
24. Nawafleh NA, Mack F, Evans J, et al. Accuracy and reliability of methods to measure marginal adaptation of crowns and FDPs: a literature review. J Prosthodont. 2013;22(5):419–28.
25. Sundell G, Dahlin C, Andersson M, Thuvander M. The bone-implant interface of dental implants in humans on the atomic scale. Acta Biomater. 2017;48:445–50.
26. Bonfante EA, Coelho PG. A critical perspective on mechanical testing of implants and prostheses. Adv Dent Res. 2016;28(1):18–27.
27. Swiatkowska I, Mosselmans JFW, Geraki T, et al. Synchrotron analysis of human organ tissue exposed to implant material. J Trace Elem Med Biol. 2018;46:128–37.
28. Gross C, Bergfeldt T, Fretwurst T, Rothweiler R, Nelson K, Stricker A. Elemental analysis of commercial zirconia dental implants-Is "metal-free" devoid of metals? Journal of the Mechanical Behavior of Biomedical Materials. 2020;107:103759.

29. Pieralli S, Kohal RJ, Jung RE, Vach K, Spies BC. Clinical outcomes of zirconia dental implants: a systematic review. J Dent Res. 2017;96(1):38–46.

30. Osman R, Swain M. A critical review of dental implant materials with an emphasis on titanium versus zirconia. Materials. 2015;8(3):932–58.

31. Rack HJ, Qazi JI. Titanium alloys for biomedical applications. Mater Sci Eng C. 2006;26(8):1269–77.

32. Li J, Zhang XH, Cui BC, Lin YH, Deng XL, Li M, Nan CW. Mechanical performance of polymer-infiltrated zirconia ceramics. J Dent. 2017a;58:60–6.

33. ASTM-E8/E8M—16a: Standard test methods for tension testing of metallic materials; metallic materials.

34. ISO/DIS 6892–1:2014 Metallic materials—Tensile testing—Part 1: Method of test at room temperature (ISO/DIS 6892-1:2014), DIN German Institute for Standardization, Beuth Verlag GmbH, Düsseldorf.

35. ASTM-E1875–13: Standard test method for dynamic Young's modulus, Shear modulus, and Poisson's ratio by Sonic resonance.

36. ASTM-E1876: Standard test method for dynamic Young's modulus, Shear modulus, and Poisson's ratio by impulse excitation of vibration.

37. Della Bona A, Corazza PH, Zhang Y. Characterization of a polymer-infiltrated ceramic-network material. Dent Mater. 2014;30(5):564–9.

38. Schatz C, Strickstrock M, Roos M, Edelhoff D, Eichberger M, Zylla IM, Stawarczyk B. Influence of specimen preparation and test methods on the flexural strength results of monolithic zirconia materials. Materials. 2016;9(3):180.

39. ASM International, Chandler H. Hardness testing. 2nd ed. Detroit, MI: ASM International; 1999. p. 06671G.

40. Duyck J, Vandamme K. The effect of loading on peri-implant bone: a critical review of the literature. J Oral Rehabil. 2014;41(10):783–94.

41. Kan JP, Judge RB, Palamara JE. In vitro bone strain analysis of implant following occlusal overload. Clin Oral Implants Res. 2014;25(2):e73–82.

42. Sieburg HB. Physiological studies in silico. Studies in the Sciences of Complexity. 1990;12(2):321–42.

43. Chang Y, Tambe AA, Maeda Y, et al. Finite element analysis of dental implants with validation: to what extent can we expect the model to predict biological phenomena? A literature review and proposal for classification of a validation process. Int J Implant Dent. 2018;4(1):7.

44. Geng JP, Tan KB, Liu GR. Application of finite element analysis in implant dentistry: a review of the literature. J Prosthet Dent. 2001;85(6):585–98.

45. Van Staden RC, Guan H, Loo YC. Application of the finite element method in dental implant research. Computer Methods in Biomechanics and Biomedical Engineering. 2006;9(4):257–70.

46. Ün K, Çalık A. Relevance of inhomogeneous–anisotropic models of human cortical bone: a tibia study using the finite element method. Biotechnology & Biotechnological Equipment. 2016;30(3):538–47.

47. Heckmann SM, Karl M, Wichmann MG, et al. Loading of bone surrounding implants through three-unit fixed partial denture fixation: a finite-element analysis based on in vitro and in vivo strain measurements. Clin Oral Implants Res. 2006;17(3):345–50.

48. Bordin D, Bergamo ETP, Fardin VP, Coelho PG, Bonfante EA. Fracture strength and probability of survival of narrow and extra-narrow dental implants after fatigue testing: in vitro and in silico analysis. J Mech Behav Biomed Mater. 2017;71:244–9.

49. de la Rosa CG, Guevara Perez SV, Arnoux PJ, et al. Mechanical strength and fracture point of a dental implant under certification conditions: a numerical approach by finite element analysis. J Prosthet Dent. 2018;119(4):611–9.

50. Wiest W, Rack A, Zabler S, Schaer A, Swain M, Nelson K. Validation of finite-element simulations with synchrotron radiography—a descriptive study of micromechanics in two-piece dental implants. Heliyon. 2018;4(2):e00524.

51. Marchetti E, Ratta S, Mummolo S, et al. Mechanical reliability evaluation of an oral implant-abutment system according to UNI EN ISO 14801 fatigue test protocol. Implant Dent. 2016;25(5):613–8.

52. Berglundh T, Persson L, Klinge B. A systematic review of the incidence of biological and technical complications in implant dentistry reported in prospective longitudinal studies of at least 5 years. J Clin Periodontol. 2002;29(Suppl 3):197–212.

53. Bozini T, Petridis H, Garefis K, Garefis P. A meta-analysis of prosthodontic complication rates of implant-supported fixed dental prostheses in edentulous patients after an observation period of at least 5 years. Int J Oral Maxillofac Implants. 2011;26(2):304–18.

54. Derks J, Tomasi C. Peri-implant health and disease. A systematic review of current epidemiology. J Clin Periodontol. 2015;42(S16):S158–71.

55. Woda A, Foster K, Mishellany A, Peyron MA. Adaptation of healthy mastication to factors pertaining to the individual or to the food. Physiol Behav. 2006;89(1):28–35.

56. Duyck J, Van Oosterwyck H, Vander Sloten J, De Cooman M, Puers R, Naert I. Magnitude and distribution of occlusal forces on oral implants supporting fixed prostheses: an in vivo study. Clin Oral Impl Res. 2000;11(5):465–75.

57. van der Bilt A, Tekamp A, van der Glas H, et al. Bite force and electromyograpy during maximum unilateral and bilateral clenching. Eur J Oral Sci. 2008;116(3):217–22.

58. van der Bilt A. Assessment of mastication with implications for oral rehabilitation: a review. J Oral Rehabil. 2011;38(10):754–80.

59. Rojo R, Prados-Privado M, Reinoso A, Prados-Frutos J. Evaluation of fatigue behavior in dental implants from in vitro clinical tests: a systematic review. Metals. 2018;8(5):313.

60. Nelson K, Schmelzeisen R, Taylor TD, Zabler S, Wiest W, Fretwurst T. The impact of force transmission on narrow-body dental implants made of commercially pure titanium and titanium zirconia alloy with a conical implant-abutment connection: an experimental pilot study. Int J Oral Maxillofac Implants. 2016;31(5):1066–71.

61. Dittmer S, Dittmer MP, Kohorst P, Jendras M, Borchers L, Stiesch M. Effect of implant-abutment connection design on load bearing capacity and failure mode of implants. J Prosthodont. 2011;20(7):510–6.

62. Blum K, Wiest W, Fella C, et al. Fatigue induced changes in conical implant-abutment connections. Dent Mater. 2015;31(11):1415–26.

63. Kelly JR, Benetti P, Rungruananunt P, et al. The slippery slope: critical perspectives on in vitro research methodologies. Dent Mater. 2012;28(1):41–51.

64. Karl M, Kelly JR. Influence of loading frequency on implant failure under cyclic fatigue conditions. Dent Mater. 2009;25(11):1426–32.

65. Karl M, Taylor TD. Effect of cyclic loading on micromotion at the implant-abutment Interface. Int J Oral Maxillofac Implants. 2016;31(6):1292–7.

66. ASM International, Davis JR. Handbook of materials for medical devices. Detroit, MI: ASM International; 2003.

67. Stephens RI, Fuchs HO. Metal fatigue in engineering. 2nd ed. Hoboken, NJ: Wiley; 2001.

68. Elsayed EA. Overview of reliability testing volume. IEEE Trans Reliab. 2012;61(2):282–91.

69. Coelho PG, Bonfante EA, Silva NR, Rekow ED, Thompson VP. Laboratory simulation of Y-TZP all-ceramic crown clinical failures. J Dent Res. 2009;88(4):382–6. https://doi.org/10.1177/0022034509333968. PMID: 19407162; PMCID: PMC3144055.

70. Nelson W. Accelerated life testing—step-stress models and data analyses. IEEE Transactions of Reliability. 1980;29(2):103–8.

71. Rosentritt M, Siavikis G, Behr M, Kolbeck C, Handel G. Approach for valuating the significance of laboratory simulation. J Dent. 2008;36(12):1048–53.

72. Rack T, Zabler S, Rack A, et al. An in vitro pilot study of the abutment stability during loading in new and fatigue-loaded conical dental implants using synchrotron-based radiography. Int J Oral Maxillofac Implants. 2013;28(1):44–50.

73. Maire E, Withers PJ. Quantitative X-ray tomography. Int Mater Rev. 2014;59(1):1–43.

74. Rack A, Tafforeau P, Stiller M, et al. Developments in high-resolution CT: Studying bioregeneration by hard X-ray synchrotron-based microtomography. In: Ducheyne P, Healy KE, Hutmacher DE, Grainger DW, Kirkpatrick CJ, editors. Comprehensive biomaterials II. Amsterdam: Elsevier; 2017.

75. Rack A, Rack T, Stiller M, et al. In vitro synchrotron-based radiography of micro-gap formation at the implant-abutment interface of two-piece dental implants. J Synchrotron Radiat. 2010;17(2):289–94.

76. Wiest W, Zabler S, Rack A, et al. In situ microradioscopy and microtomography of fatigue-loaded dental two-piece implants. J Synchrotron Radiat. 2015;22(6):1492–7.

77. Zipprich H, Weigl P, Ratka C, Lange B, Lauer HC. The micromechanical behavior of implant-abutment connections under a dynamic load protocol. Clin Implant Dent Relat Res. 2018;20(5):814–23.

78. Maire E, Babout L, Buffiere JY, Fougeres V. Recent results on 3D characterisation of microstructure and damage of metal matrix composites and a metallic foam using X-ray tomography. Mater Sci Eng A. 2001;319–321:216–9.

79. Gradl R, Dierolf M, Hehn L, Günther B, Yildirim A, Gleich B, Achterhold K, Pfeiffer F, Morgan KS. Propagation-based phase-contrast X-ray imaging at a compact light source. Sci Rep. 2017;7(1):4908.

80. Zabler S, Rack T, Rack A, et al. Quantitative studies on inner interfaces in conical metal joints using hard x-ray inline phase contrast radiography. Rev. Sci Instrum. 2010;81(10):103703.

81. Weitkamp T, Tafforeau P, Boller E, et al. Status and evolution of the ESRF beamline ID19. AIP Conf Proc. 2010;1221(1):33–8.

82. Zabler S, Rack T, Rack A, et al. Fatigue induced deformation of taper connections in dental Titanium implants. Int J Mater Res. 2012;103(2):207–16.

83. Bitar D, Parvizi J. Biological response to prosthetic debris. World J Orthop. 2015;6(2):172–89.

84. Lohmann CH, Singh G, Willert HG, et al. Metallic debris from metal-on-metal total hip arthroplasty regulates periprosthetic tissues. World J Orthop. 2014;5(5):660–6.

85. Obando-Pereda GA, Fischer L, Stach-Machado DR. Titanium and zirconia particle-induced proinflammatory gene expression in cultured macrophages and osteolysis, inflammatory hyperalgesia and edema in vivo. Life Sci. 2014;97(2):96–106.

86. Vasconcelos DM, Santos SG, Lamghari M, Barbosa MA. The two faces of metal ions: from implants rejection to tissue repair/regeneration. Biomaterials. 2016;84:262–75.

87. Fretwurst T, Nelson K, Tarnow D, et al. Is metal particle release associated with peri-implant bone destruction? An emerging concept. J Dent Res. 2018;97(3):259–65.

88. Suárez-López del Amo F, Garaicoa-Pazmiño C, Fretwurst T, et al. Dental implants-associated release of titanium particles: a systematic review. Clinical Oral Implants Research. 2018;29:1085; Epub ahead of print.

89. Nelson K, Hesse B, Addison O, Morrell AP, Gross C, Lagrange A, Suárez VI, Kohal R, Fretwurst T. Distribution and chemical speciation of exogenous micro- and nanoparticles in inflamed soft tissue

adjacent to titanium and ceramic dental implants. Anal Chem. 2020;92(21):14432–43.

90. Apaza-Bedoya K, Tarce M, Benfatti CAM, et al. Synergistic interactions between corrosion and wear at titanium-based dental implant connections: a scoping review. J Periodontal Res. 2017;52(6):946–54.

91. Fretwurst T, Buzanich G, Nahles S, et al. Metal elements in tissue with dental peri-implantitis: a pilot study. Clin Oral Implants Res. 2016;27(9):1178–86.

92. Olmedo D, Fernández MM, Guglielmotti MB, et al. Macrophages related to dental implant failure. Implant Dent. 2003;12(1):75–80.

93. Shindō D, Oikawa T. Analytical electron microscopy for materials science. Tokyo: Springer; 2002.

94. Moraleja I, Mena ML, Lázaro A, et al. An approach for quantification of platinum distribution in tissues by LA-ICP-MS imaging using isotope dilution analysis. Talanta. 2018;178:166–71.

95. Sabine BJ. Imaging of metals in biological tissue by laser ablation inductively coupled plasma mass spectrometry (LA-ICP-MS): state of the art and future developments. J Mass Spectrom. 2013;48(2):255–68.

96. Gray EP, Coleman JG, Bednar AJ, et al. Extraction and analysis of silver and gold nanoparticles from biological tissues using single particle inductively coupled plasma mass spectrometry. Environ Sci Technol. 2013;47(24):14315–23.

97. Schoon J, Geißler S, Traeger J, et al. Multi-elemental nanoparticle exposure after tantalum component failure in hip arthroplasty: in-depth analysis of a single case. Nanomedicine. 2017;13(8):2415–23.

98. Li Q, Wang Z, Mo J, et al. Imaging gold nanoparticles in mouse liver by laser ablation inductively coupled plasma mass spectrometry. Sci Rep. 2017b;7(1):2965.

99. Martínez-Criado G, Villanova J, Tucoulou R, et al. ID16B: a hard X-ray nanoprobe beamline at the ESRF for nano-analysis. J Synchrotron Radiat. 2016;23(1):344–52.

100. Schoon J, Hesse B, Rakow A, et al. Metal-specific biomaterial accumulation in human Peri-implant bone and bone marrow. Adv Sci (Weinh). 2020;7(20):2000412.

101. Schreiver I, Hesse B, Seim C, et al. Synchrotron-based ν-XRF mapping and μ-FTIR microscopy enable to look into the fate and effects of tattoo pigments in human skin. Sci Rep. 2017;7(1):11395.

Mechanics of the Prosthetic Rehabilitation

13

Lei Zhang, Yongsheng Zhou, and Qian Ding

13.1 Part I: Relevant Factors of Mechanics of the Prosthetic Rehabilitation

13.1.1 Passive Fit and Misfit

Passive fit is defined as the simultaneous and even contact of all the fitting surfaces, without the development of strains prior to functional loading [1, 2]. Better-fitting implant frameworks are associated with lower stresses within the framework, implants, abutments, and retaining screws [3]. Because of inevitable clinical and laboratory errors, misfits could exist at the interface between implants and prosthetic compo-

nents, leading to a lack of passive fit (Fig. 13.1). Compromised fit is thought to introduce uncontrolled stress into the bone-implant-framework complex, thus leading to biological and technical complications.

For instance, this stress may impact the stability of screw joints, risking long-term screw loosening [4]. In normal situations, when the retaining screw is tightened, the preload subjects the screw threads to tension. The elastic recovery of the screw creates a clamping force, which keeps the prosthesis and the abutment or implant in contact. In misfit situations, part of the preload is used to approximate the surfaces between the prosthesis and the abutment or implant. Further, the screws will be subjected to abnormal elonga-

L. Zhang · Y. Zhou (✉) · Q. Ding
Department of Prosthodontics, Peking University School and Hospital of Stomatology, Beijing, China

National Center of Stomatology, Beijing, China

National Clinical Research Center for Oral Diseases, Beijing, China

National Engineering Laboratory for Digital and Material Technology of Stomatology, Beijing, China

Beijing Key Laboratory of Digital Stomatology, Beijing, China

Research Center of Engineering and Technology for Computerized Dentistry Ministry of Health, Beijing, China

NMPA Key Laboratory for Dental Materials, Beijing, China
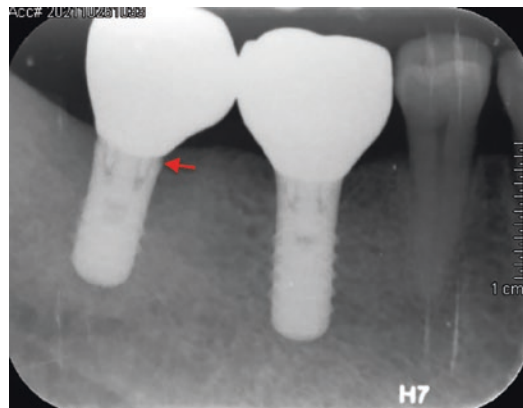
Fig. 13.1 A periapical radiograph can be used to detect misfits (red arrow) at the implant-abutment interface

tion (in the case of a vertical misfit) or binding and bending (in the case of a horizontal and angular misfit). The pre-stressed screw situation will be exacerbated further by functional loading, rendering the screws more susceptible to fatigue fracture, thread wear, plastic deformation, or loosening [3]. A misfit between restoration and the supporting implant is likely to cause compressive as well as tensile stress within the implant components and/or the frameworks. For metal-ceramic prostheses, areas, where tensile stress is concentrated, are potential crack-initiation sites and are prone to fracture, as ceramics are ill-equipped to tolerate tensile forces. Therefore, a misfit between a restoration and the supporting implant may increase the risk of cracking and/or chipping of the veneering porcelain [5]. A recent systematic review [6] concluded that the misfit was found related to the induced strain/stress in vitro studies, while the in vivo studies indicated the correlation between the misfit and the clinical consequences, including marginal bone loss, screw-related adverse events, and implant/prostheses failure, was weak.

Studies have shown that absolute passive fit is not clinically possible to achieve [7]. When attempting to fabricate a prosthesis with zero tolerance for error, too many variables are out of the dentist's control, including impression materials shrinkage, dental stone expansion, wax patterns distortion, investment material expansion, and dimensional changes during metalwork fabrication. But there is a biological and mechanical tolerance to implant framework misfit, while the degree of tolerable misfit remains a matter of debate [8]. Therefore, the goal will be to achieve the least misfit possible, and a clinically acceptable fit which reduces the possibility for mechanical complications. This can be achieved by following meticulous steps in the prosthetic procedures, including precise impression technique, creation of a verification cast, accurate manufacture of a framework using conventional or CAD/CAM technologies, and strict quality control of the restoration at the laboratory stage prior to intraoral try-in.

13.1.2 Fabrication Techniques and Fit

Implant abutments can be either prefabricated or custom, the latter including cast custom and CAD/CAM custom abutments. According to the fabrication technique, implant frameworks are of four types: (1) conventional cast frameworks, (2) frameworks made from carbon/graphite fiber-reinforced polymethylmethacrylate, (3) laser-welded titanium frameworks, and most recently, (4) CAD/CAM milled frameworks. Inaccuracies in the multiple fabrication steps can introduce distortions of prosthetic frameworks that compromise the implant-abutment interface fitting [9]. In order to enhance the fit of implant frameworks, the addition of a fit refinement step has been proposed, including sectioning and soldering/laser welding, and bonding of the framework body to prefabricated abutments.

The manufacturing technique is also a variable that influences the presence of a microgap, probably because of the different surface roughness produced by each manufacturing method. A rough contact surface inevitably produces a microgap between the implant and abutment and hinders the achievement of a passive fit [10]. Milled surfaces have been reported to show a better fit and a larger number of contacts with the implant mating surface than cast and sintered surfaces, which allows a better closure of the microgap between implant components [11, 12].

CAD/CAM is capable of producing implant frameworks with a precision of fit. Titanium and zirconia implant frameworks can be fabricated with a high level of accuracy with the aid of CAD/CAM [13]. They are not susceptible to distortion or casting porosity and have improved marginal fit when compared to cast gold frameworks [14]. Screw-retained zirconia implant-supported complete-arch CAD/CAM frameworks for fixed dental prostheses was recently reported to have a fit well within the range of 30 μm in the horizontal plane and 10 μm in the vertical plane, which was thought to be clinically acceptable [15]. Digital restorations had a better fit on the

control cast, and angulation of more than 10° between the implants could negatively affect the passive fit of the digitally fabricated restorations intraorally [16]. However, the accuracy of a CAD/CAM framework is still dependent on the accuracy of the cast model, the scanning technique, and the computer-based designing capabilities of the dental technician.

13.1.3 Material of the Prosthesis

Stress in either fixed or removable prostheses differs according to materials, implant distribution, and restoration design. The distribution of forces to the implants may differ on the basis of the material, but the total force on the combined implant-supporting system is the same [17]. Materials do, however, behave differently relative to the dissipation of impact forces. Stiffer materials, such as ceramics, will transmit forces to the implants more rapidly, while more resilient materials, such as acrylic resins, transmit forces more slowly, which is sometimes described as a dampening of the forces [18]. Besides, stiffer frameworks are expected to distort to a lesser extent than less rigid frameworks, then the stresses within the frameworks will be different. This was confirmed by an FEA study [19] that illustrated that, at a similar level of misfit, stiffer framework materials experienced significantly greater stress than more flexible materials. But when the accurate fit is assumed, other studies found that stiffer framework materials led to a more even distribution of stress [20].

Crowns with a zirconia core show more fracture of the veneering porcelain than metal ceramic crowns [21]. To prevent this, monolithic restorations made entirely of zirconia are used. Monolithic zirconia prostheses are demonstrated to have the highest fracture load, flexural strength, and elastic modulus compared with lithium disilicate, conventional veneered ceramic prostheses, and composite resin prostheses [22]. For fixed complete implant prostheses, zirconia fixed implant prostheses presented higher initial costs

than metal-acrylic hybrids, however, with satisfactory outcomes, reduction of overall complications, and superior survival rates at 8.7 years' mean follow-up [23]. In contrast to ceramics, resin-based restorative materials are more elastic and appear to compensate for the absence of the damping effect of the periodontal ligament in implant-supported prostheses. And resin-based restorative materials can be modified easily on the chair-side. Therefore, composite resins have been widely and successfully used as a provisional restorative material in implant prostheses. When using resin-based restorative materials, the use of metal or fiber reinforcement is advisable, only except for single crowns, in order to avoid frequent base fracture because of the reduced strength of resin.

13.1.4 Prosthetic Plan

Implant treatment is prosthetic-driven. Therefore, preliminary prosthetic planning is essential in order to prescribe an appropriate implant position. The use of a surgical guide is recommended for implant placement, whenever possible. The proper number, length, and diameter of implants should be selected based on the prosthetic plan, according to individual local conditions and patient's needs. The number, length, diameter, and positioning of implants can have an influence on functional force transfer and subsequent stress distribution around implants. The increase in the number, length, and diameter of implants improves the biomechanical behavior of implants, especially when subjected to bending forces.

It is a consensus [24] that short implants (≤6 mm) are a valid option in situations of reduced bone height; however, they reveal a higher variability and lower predictability in survival rates. Time in function may reduce the survival rate of short implants more than that of longer implants. And the presence of a single crown was associated with an increasing rate of short implant loss [25]. Reducing implant diameter brings an increased risk of the implant or

component fracture. Therefore caution is recommended for the use of narrow-diameter (≤3.5 mm) implants in patients with parafunctional habits and malocclusions [24]. Ti-Zr alloy has higher tensile strength than commercially pure titanium. Narrow-diameter Ti-Zr dental implants show survival and success rates comparable to regular diameter titanium implants in the short term, in both anterior and posterior areas [26]. Long-term clinical outcomes are needed to confirm. The proper number of implants to use must be determined according to the number of teeth to be replaced, available space for the prosthesis, local bone condition, and patient-related factors. Combining the restorative needs with the surgical options will allow the best prosthodontic plan to develop. Since 10-year survival rates of a fixed prosthesis supported by four or six implants [27] or three wide-diameter implants are quite high [28], the number of implant support may not have a remarkable effect on treatment outcome. But a minimum number of 4 appropriately distributed implants are recommended to support a one-piece full-arch fixed prosthesis [29]. And additional implants can provide options for fixed full-arch segmented prostheses.

Torques or bending moments imposed on implants because of excessively long cantilever bridge may result in interface break-down, bone resorption, prosthetic screw loosening, or bridge fracture [30, 31]. For posterior implant fixed partial dentures (FDPs) and implant single crowns, the maximum horizontal cantilever (the distance the crown or prosthesis extends laterally to the implant) should not exceed the diameter of the implant. For anterior FDPs, the maximum horizontal cantilever should not exceed twice the implant diameter [32]. For implant-supported fixed full-arch prosthesis, many influences including anterior-posterior (AP) spread, cantilever size, number and distribution of placed implants, prosthetic materials, and framework design, need to be considered when determining the cantilever length [33]. To avoid overloading, the length of the cantilever bridge is recommended to be less than 15 mm in the mandible and 10–12 mm in the maxilla [31].

13.1.5 Retention: Screw-Retained and Cement-Retained Prostheses

Implant-supported prostheses can be screw-retained, cement-retained, or a combination of both, where a metal or ceramic framework is screwed to the implants, and crowns are individually cemented to it. Different types of retention mechanisms also may influence the outcomes as the mechanical stability of prostheses relies on the structure and precision of implant-abutment interfaces. Both cementation and screw retention seem to have their benefits and shortcomings in their clinical application. Clinical criteria such as prosthesis retrievability and maintenance, esthetics, occlusion, the position of the implant, interarch occlusal space, and ease of fabrication may influence the retention mechanism decision of fixed implant prostheses.

13.1.5.1 Screw-Retained Implant Prostheses

Retrievability is one of the major advantages of screw-retained implant prostheses because it provides clinicians with the accessibility to retrieving these restorations if needed for repairs, remakes, hygiene, and abutment-screw tightening. Retrievability becomes more important in a complex case or involves more implants. In addition, because there is no cement interface required to retain a crown, a screw-retained crown can be used when interarch occlusal space is limited. Furthermore, when the reconstruction exhibits a good fit, biological problems are rather unlikely to occur [34].

The horizontal and angular positioning of the implant, however, is more delicate than cement-retained prostheses when using screw-retained prostheses, because non-ideal implant angulation may affect the final esthetic result if the screw access opening is visible. If implants are improperly positioned, screw-access holes may compromise aesthetics and occlusion because of the wear of restorative materials used to cover the screw-access channel. On the other hand, mechanical complications like loosening of

retaining screws or fracture of the veneering ceramic at the screw-access channel have been reported [35].

13.1.5.2 Cement-Retained Implant Prostheses

Cement-retained implant prostheses clinically and technically resemble the procedures used for tooth-borne prostheses. These restorations may be simpler to fabricate, and provide easier insertion in posterior areas of the mouth for patients with limited jaw openings. A cement-retained implant prosthesis and the implant body may be loaded axially, thus decreasing crestal bone strain [36]. In contrast, the axial occlusal load on a screw-retained prosthesis must load the occlusal screw region, which is usually representing 30% or more of the total occlusal surface of posterior teeth. For an implant-supported fixed prosthesis, the potential for achieving a passive fit is higher with cement-retained restorations, because the cement space may compensate for a lack of passive fit and serve as a shock absorber [37, 38].

The main drawbacks of cement-retained restorations are the difficult retrievability of excess cement, especially when the restoration margins are placed subgingivally or the implants are deeply placed. Diligence in cement removal at the time of cementation is critical. The presence of cement residue was proven to cause peri-implant inflammation associated with swelling, soreness, deeper probing depths, bleeding, and/or exudation on probing, with radiographic evidence of marginal bone loss, and may eventually result in implant loss [39]. Excess cement was associated with signs of peri-implant disease in 81% of cases investigated [40]. It is demonstrated that when the restorative margins of the abutments are placed 1.5–3 mm subgingival, the excess cement leaving is almost inevitable [41]. Use of screw-retained restorations or custom abutments for cement restorations with higher margins may be used to avoid cement-related complications in situations where implants are deeply placed (Fig. 13.2).

Besides, the minimum abutment height for the use of cement-retained restorations with

Fig. 13.2 A zirconia customized abutment to obtain a higher margin for cement restoration

predictable retention was documented as 5 mm [41]. Therefore, screw-retain restorations may be advisable in these instances when the interocclusal space is less than 4 mm. Another significant shortcoming of the cemented restorations is that, in case of problems, they are difficult or impossible to remove without destruction, for example, in cases of technical complications.

13.1.5.3 Retention Control

Several systematic reviews [42, 43] reported that cemented restorations exhibited less technical, but more biological problems like implant failures or marginal bone loss than screw-retained restorations. The screw-retained restorations, in contrast, exhibited more technical problems and higher rates for restoration loss, but fewer implant failures and less serious biological complications. Consensus statements from the third consensus conference of the European Association for Osseointegration concluded that both types of restorations influenced the clinical outcomes, but none of the fixation methods was clearly advantageous [44]. Cemented and screw-retained single-unit restorations had similar survival and complication rates for their supporting implants [45], whereas cemented multiunit restorations had lower survival rates than the screw-retained multiunit restorations for their supporting implants [46].

At single crowns, both types of retention mechanisms can be recommended. In the case of

cementation of the restorations, proper removal of cement excess is crucial to prevent biological complications. The radiographic examination could be a supplementary method for the detection of excess cement. Screw-retained restorations seem to be preferable from a biological perspective. In recent years, a hybrid cement- and screw-retained crown on implants has been used commonly. The concept is that a completely finished restoration is cemented to a titanium base on the cast and then screw-retained intraorally (Fig. 13.3), which combines the features and advantages of both cemented and screw-retained restorations.

Clinicians should weigh the advantages and disadvantages of cement-retained and screw-retained types of restorations, so as to select the most appropriate for a given clinical situation. Based on previous systematic review [47] and a consensus review paper [48], screw retention may be recommended

- in the presence of minimal interarch space (4 mm)
- for FDPs with a cantilever design
- for long-span FDPs, as the complications of these restorations are more frequent [49]
- to avoid an additional risk factor with the use of cement and a possible cement remnant
- for provisional prostheses to enable shaping of the emergence and mucosal profile in the esthetic zone
- when retrievability is desired.

Cement retention may be recommended

- for short-span prostheses with margins at or above the mucosa level
- to compensate for improper implant angle that cannot be corrected to conceal the access hole
- for cases where an easier control of occlusion without an access hole is desired, for example, with narrow-diameter crowns.
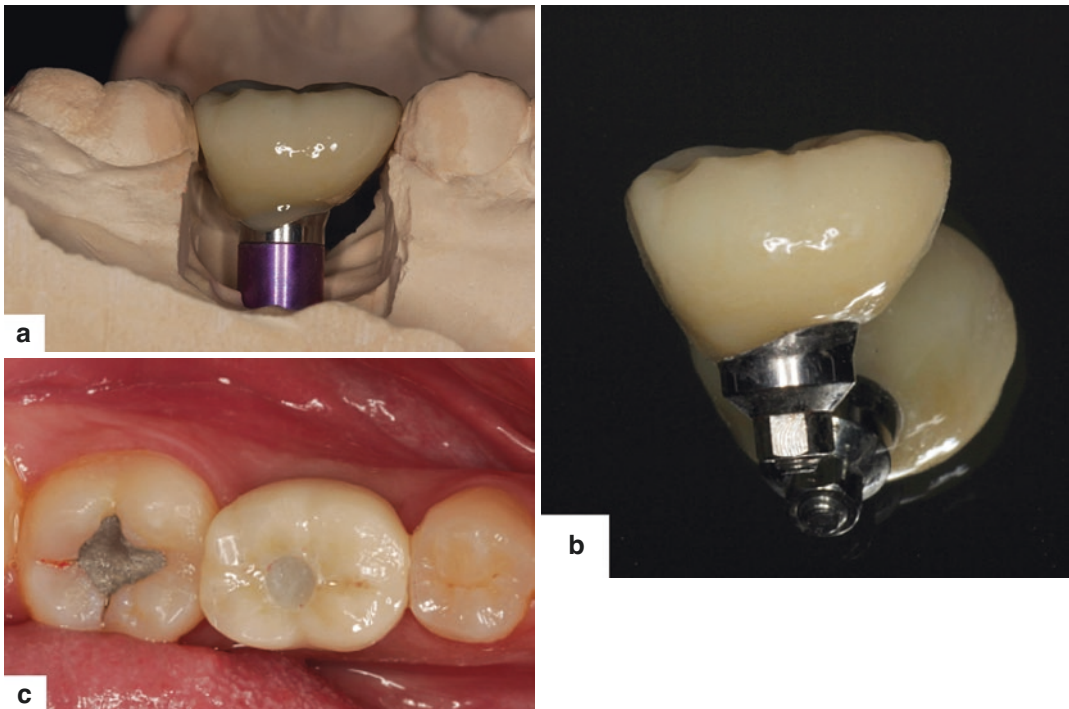
Fig. 13.3 Hybrid cement- and screw-retained implant-supported single crown. (**a**) The crown is cemented to a titanium base on the cast; (**b**) Remove the excess cement; (**c**) Screw-retained intraorally

13.1.6 Occlusal Loading of Implant Prosthesis

13.1.6.1 Occlusal Overloading Factors

When placed in function, dental implants are subjected to occlusal loads, which may vary dramatically in magnitude, frequency, and duration, depending on the patient's parafunctional activities and diet habits. As a result of the absence of the periodontal ligament and limited tactile sensitivity, osseointegrated implants react biomechanically to occlusal force in a manner distinct from natural teeth. All the structures subject to occlusal forces can be exposed to physiological loading or overloading. In the case of physiological loading, forces could be dissipated through the occlusal surfaces, prosthetic structure, implant-abutment connection, retention screw, implant body, implant-bone interface, and peri-implant supporting bone. While overloading might affect the weakest part of the system, producing implant osseointegration failure and mechanical complications such as screw loosening and fracture, prosthesis fracture, and implant fracture, eventually compromising implant longevity [50, 51].

Various factors and situations that can give rise to occlusal overloading have been reported [51], including:

1. Overextended cantilever
2. Parafunctional habits/Heavy bite force
3. Excessive premature contacts and interferences
4. Large occlusal table
5. Steep cusp inclination
6. Poor bone density/quality
7. Inadequate number of implants
8. Excessive crown-to-implant length ratio
9. Unfavorable direction of axial forces

Proper design of the prosthesis is the key factor of proper occlusion, which must include consideration of the magnitude of the occlusal force and its delivery. The duration of a high-magnitude force may affect the ultimate outcome of an implant system. Relatively low-magnitude forces applied repetitively over a long time, may result in fatigue failure of an implant or prosthesis. Stress concentrations and, ultimately, failure may develop if insufficient cross-sectional area is present to dissipate high-magnitude forces adequately. Insufficient osseointegration, narrow-diameter implant, inadequate thickness or misfit in implant-abutment connection, framework, and veneering material with poor design or manufacturing deficiency, may become the weakest part of the system when loaded with high-magnitude forces and ultimately lead to biological or mechanical complications.

13.1.6.2 Control and Maintenance of Implant Occlusion

The control and maintenance of implant occlusion may reduce mechanical and biological complications, thus increasing the longevity of prostheses [52]. Occlusal forces, like all forces, can be described and controlled in four ways: magnitude, duration, distribution, and direction [53].

Several researchers have proposed that the occlusion of FDPs should be designed to reduce their exposure to occlusal forces and evenly distribute loads between implants and adjacent teeth during forceful biting [54, 55]. To minimize excessive force, light contact during forceful biting and no contact in the maximum intercuspal position is considered a reasonable approach. The occlusal schemes of implant prostheses can result in a quantifiable time delay such that the natural teeth occlude in advance of the implant prostheses by fractions of seconds [56]. But the Kennedy Class I case should be an exception. In this case, contacts should be established on the implant in low- and medium-intensity occlusion at the maximum intercuspal position, and the incisors should be left without contact or with only slight contact.

In considering the direction of the occlusal forces, it is recommended to reduce shear forces and aim for compressive forces. In doing so, occlusion should create axial forces, rather than lateral or horizontal forces. Bone is stronger under compressive forces than shear forces [57]. Nonaxial loading causes higher stress and ten-

sion around the crestal bone. Rangert et al. [58] found that a deviation of 15° in a buccolingual direction contributed to occlusal overloading. A reduced cuspal inclination can protect the tooth from shear forces while decreasing force magnitude [59]. A narrow occlusal table can ensure that forces will be directed axially, prevent cantilever effects and bending moments, and reduce the magnitude of forces [60].

However, previous studies [61, 62] have reported that the occlusion of implant prostheses would not remain light with use. Natural dentition may exhibit continued tooth eruption and movement due to occlusal abrasion, periodontal disease, temporomandibular diseases, or orthodontic treatment, which all can cause changes in occlusion force distribution and occlusal contacts. While implants maintain their position integrating with bone under the change of natural teeth. Therefore, the occlusion of implant-supported fixed partial prostheses could change over time. Current scientific evidence as to occlusion variation of implant-supported prostheses is relatively rare, and most of them are cross-section studies or prospective studies with a short-term follow-up [61–63]. Our research group has published a 3-year prospective study to analyze the longitudinal variation of occlusion in posterior implant-supported single crowns using the computerized occlusal analysis system and found the initial light occlusion of implant-supported single crown changes over time, which is mainly reflected in the increasing relative occlusal force and occlusal contact time [61] (Fig. 13.4).

Continuous eruption of the opposing teeth and the occlusal wear of the remaining natural teeth were considered to play an important role in the increase of relative occlusal force and earlier occlusal contact of implant prostheses. The positions of natural teeth in dental arches are constantly changing as a consequence of continued slow tooth eruption and mesial tooth movement of about 0.1–0.2 mm annually [64, 65]. Because of the light occlusion after the implant-supported prostheses delivery, the implant-opposing natural dentition may be liable to erupt [62]. Occlusal wear of the natural teeth may facilitate these changes to some extent, especially before occlu-
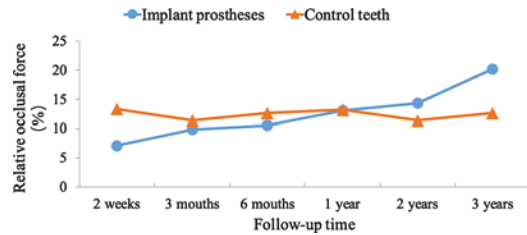
Fig. 13.4 Line graph of the 3-year longitudinal variation of occlusion in posterior implant-supported single crowns and control natural teeth

sal contacts were established in implant prostheses. A clinical study reported that the occlusal wear of natural enamel opposing natural enamel was 17.3 ± 1.88 μm in the premolar region and 35.1 ± 2.6 μm in the molar region after a year of function [66]. Although passive eruption could compensate for the occlusal wear of natural teeth to some extent, there was inconsistency between the rate of wear and continuous eruption, which had significant individual differences.

This demonstrates that, even after achieving a light contact occlusion, reducing the diameter of implant prostheses, and modifying the occlusal table, the occlusion of implant-supported fixed prostheses may not remain light indefinitely. The increase in occlusal force indicated that a higher percentage of occlusal force was attributed to the implant prosthesis, which means that the overloading risk of the implant prosthesis could increase. The occlusion of implant prostheses should be carefully monitored during follow-up examinations, and occlusal adjustment should be considered when potential overloading occurs, or if premature or interferences develop.

13.1.7 Patient-Related Variables

Patients exhibit different levels of occlusal and parafunctional forces. In some patients, the forces will exceed the strength of prosthetic materials and will cause screw loosening, fractures, and other mechanical complications [67]. Patients with poor osteointegration, uncontrolled periodontal disease, heavy occlusal wear in natural teeth, parafunctional habits, and special dietary

habits may have a high risk of overloading and complications in implant-supported prostheses. Therefore, it may be more appropriate for patients in these categories to consider a greater number of implants to share in the functional load and to consider implants of larger diameter, thereby making the implant more resistant to the forces that could cause implant fracture and other mechanical problems [1]. It is important to diagnose patients with parafunctional habits ahead of time and prescribe occlusal splints for night or day use as needed [68]. Patients with high risk need to be under routine periodic dental examinations and maintenance to address complications in time.

13.2 Part II: Mechanical Complications

Mechanical complications occur when the capacity of the prosthesis to withstand applied forces is exceeded. The precise complication will depend upon the magnitude and the direction of the applied force. Commonly reported mechanical complications associated with implant-supported fixed prostheses include implant fracture, prosthesis or framework fracture, screw loosening, screw fracture, fracture of the veneering material, and loss of retention. Primary complications that have difficulty in prevention and treatment, and have close relations with the mechanics of implant prosthetic rehabilitation are introduced below in detail.

13.2.1 Implant Fractures

Implant fracture (Fig. 13.5) is the most serious but rare mechanical complication that can occur after implant restoration, which usually manifests as implant loosening, peri-implant inflammation, and showing implant fracture and bone absorption around the crack on the radiograph. Implant fractures have occurred as a result of heavy occlusal loading, improper surgical placement of implants, improper implant design and manufacture, and lack of passive fit in restorations. Owing to metal fatigue, the longer the implant functions, the higher the fracture rate of the implant will be. When excessive force is used to insert an implant as a self-tapping device into dense bone, the implant or the components used to place the implant can also fracture.

13.2.1.1 Prevention
During surgical planning and placement, the bone density should be carefully assessed to determine whether bone tapping is needed or a self-tapping protocol can be followed.
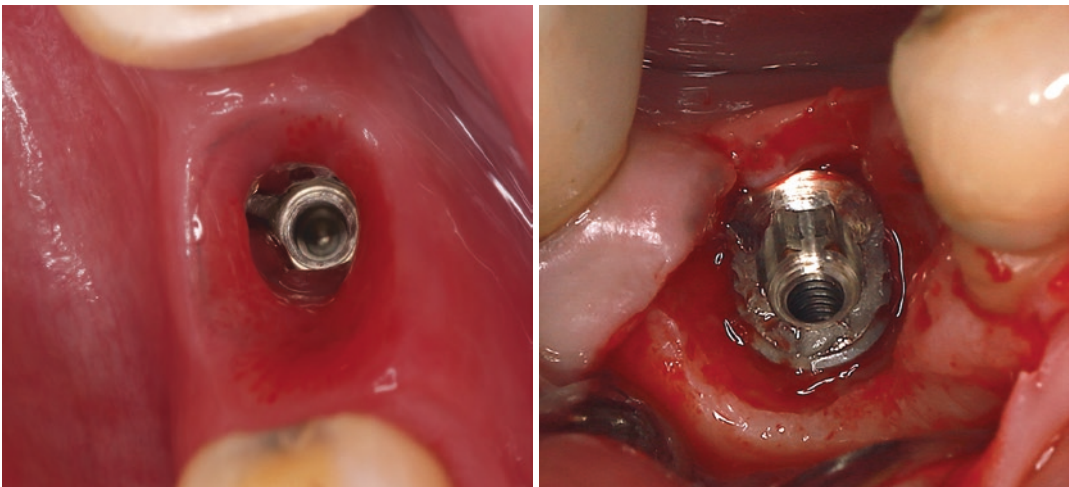
Fig. 13.5 Implant fracture after loading for only 1 year because of heavy occlusal loading

During prosthodontic planning, implant fracture is best avoided by the following means [1]: (1) limiting the extent and occlusal force of cantilevers; (2) using an adequate number of implants; (3) creating a staggered alignment of the implants for an FDP (not placing them in a straight line); (4) creating an appropriate symmetric curved arrangement of the implants for an implant fixed complete denture; (5) ensuring the passive fit of prostheses; (6) using wider diameter (≥4 mm) implants for the replacement of single molars, especially when the patient has high risk of overloading; (7) controlling occlusal loading; and (8) splinted superstructure has a lower risk of implant fracture [69].

13.2.1.2 Treatment
When an implant fractures, it should be removed if the reservation of the remaining part would affect the prosthetic effect or if the reservation was not accepted by the patient. There are trephine drills fitting over the implant available that can be used to remove the implant. The trephine drill removes a bony core that includes the fractured implant. Other methods of implant removal include the use of a thin drill or piezoelectric surgical tip to cut a channel around the implant so it can be removed using reverse torque. After the implant has been removed, a graft material and membrane barrier can be used to fill in the defect. The clinician can also choose to allow new bone formation eventually to fill the area without a graft being used. Following healing, another implant can be placed. It may also be possible immediately to place an implant with a larger diameter than the one removed.

When an implant fractures, if there is no significant effect on the current prosthesis, the clinician can remove the loose fragment, trim the part above the bone, make the necessary debridement, and submerge the remaining part with surrounding bone into the mucosa, making the fractured implant "sleep". If the remaining part of the fractured implant has proper location, diameter, length, and no serious peri-implant inflammation, there is an alternative method to consider, which is trimming the fracture surface and forming internal thread when necessary using special tools, then connecting the abutment, fabricating a new restoration.

13.2.2 Screw Loosening and Fractures

From the perspective of structure and mechanics, the screw is one of the weakest structures in the whole implant-prosthesis system. Screw loosening and/or fracture could result in slight or obvious mobility of the prosthesis, often accompanied by inflammation of peri-implant mucosa (Fig. 13.6). Screw loosening happens when micro-movement occurs in the interface of connection, which leads to the destruction of preload. Screw loosening and/or fractures can occur with inappropriate implant designs, a lack of specified torque during screw tightening, poorly fitting prostheses, and long crowns or abutments. Occlusal overloads and cantilevers also contribute to screw loosening and fracture.

13.2.2.1 Prevention
Preventing screw loosening and fractures is best accomplished by ensuring screws are tightened using either a hand or electronic torque device and making sure prostheses fit properly. Some implant systems suggest retightening of bridge screws a few weeks after the initial delivery of the prosthesis. A recent in-vitro study [70] found that the reverse tightening was higher when the

Fig. 13.6 Screw loosening accompanied by inflammation of peri-implant mucosa

screws were tightened, counter-tightened, and then tightened again, compared with that of tightening the abutment screw 2 times with a 10-min interval time, no interval time, or tightening it one time only. Research and manufacturing enhancements have resulted in surface coating and screw designs that improve fit, increase preload, and help prevent loosening [1]. Internal connection implants with Morse taper should be preferred over external connection implants. Reducing prosthesis cantilevers when possible, and aligning implants so they are centered beneath occluding surfaces and perpendicular to the occlusal plane also helps prevent the loosening of screws and/or fractures. Ensure to insert the implants in a reasonable position and orientation, and take appropriate measures to control the occlusal force, especially the non-axial force.

13.2.2.2 Treatment

When screws loosen, they can be retightened. If the screw has been in service for some time, it is advisable to replace the screw with a new one. When an abutment screw has come loose, cement-retained crowns or FDPs have to be removed. One method presented in the literature involves fabricating the crowns with threaded tubes designed for turning small screws, which can be used to unseat the crown via contact between the end of the screw and the underlying abutment [71].

When screws fracture, it can be a challenge to remove the screw fragment. However, many older screws were such that they did not incorporate frictional fit with the implant threads, thus permitting an explorer or other dental instrument to be used to manipulate the fragment slowly in a counterclockwise direction. When a screw breaks at the top of its threaded section, it may be accessible to a dental instrument and the screw can be rotated counterclockwise until it can be grasped with an instrument and removed.

Methods of removing screw fragments that cannot be rotated with a hand instrument or grasped by a hand instrument have included running a drill in reverse to grasp and remove the fragment, drilling into the screw fragment so it

can be grasped, grinding a slot into the top of the screw fragment and modifying some instrument so it fits into the slot and the fragment can thereby be unscrewed [72]. When a fractured abutment screw fragment is located inside an implant, there are manufactured retrieval instruments that can aid in the process. Screw taps are also manufactured to refresh implant threads should they become disturbed during the screw fragment removal.

13.2.3 Prosthesis or Framework Fractures

The reasons for fractures of prosthesis or framework may be, the heavy occlusal force, the stress concentration produced when retentive mechanisms are incorporated, fabricating defects, improper design of prosthesis or framework, porous and/or inadequate soldered connections, and inadequate thickness of prosthesis or framework that is not sufficient to resist the forces placed on the prosthesis. Even adequately thick resin and metal can fatigue over time and fracture (Fig. 13.7).

13.2.3.1 Prevention

Material selection and structure design should be based on specific clinical characteristics. Ensure the adequate thickness of the framework to resist the forces. Internal bubbles and poor welding of metal, milling defects in zirconia, and other processing defects should be avoided. Preventing implant overdenture fractures and resin base fractures is best accomplished by maintaining an adequate resin thickness of at least 2 mm over retentive devices and using metal frameworks or fiber reinforcement. The incorporation of metal palates, metal reinforcing meshes, or woven or fiberglass-impregnated meshes may be necessary for some patients.

13.2.3.2 Treatment

When resin base fractures occur, the prosthesis should be repaired and the resin thickness increased, if possible. It may also be prudent to incorporate a metal mesh into the repair site [1].

Fig. 13.7 Fracture in the inadequate thick part of the prosthesis

Fig. 13.8 Full-arch monolithic zirconia fixed prostheses

The fracture of a metal framework in a full-arch fixed prosthesis is best resolved by fabricating a new framework with thicker metal. Occasionally, it may be possible to remove overlying teeth/resin and solder the metal framework. Zirconia is suggested as a suitable material for frameworks in FPDs and full-arch fixed prostheses (Fig. 13.8) when there is sufficient prosthetic space [73]. Fractures of FDPs frameworks require the fabrication of a new prosthesis.

13.2.4 Fracture of the Veneering Material

Fracture of the veneering material is one of the most common mechanical complications. Implant-supported prostheses are particularly susceptible to fracture of the veneering material because implants have limited proprioceptive innervation and adaptive capacity. But is largely caused by unsupported veneering material or

occlusal overloading (Fig. 13.9). Manufacturing defects and insufficient restorative space can also contribute to the fracture of the veneering material. Superstructures may be veneered with porcelain, acrylic, or composite resin. Porcelain is the least likely to fracture and is often considered to be veneering material [74].

13.2.4.1 Prevention

To prevent veneering material fractures, sufficient support should be provided by the framework, with rational veneer thickness. Usually, a coping (manually or digitally) that closely reflects the final contour and volume of the anticipated final restoration should be fabricated. Then by manually trimming back the customized full contour of the final restoration by 1.5–2 mm before casting in metal, a 1.5–2 mm veneering space of even thickness can be accomplished. Strict polishing and glazing procedures are recommended to reduce surface defects that could cause fractures. Another method of preventing veneering material fractures is to avoid using metal alloys base and use monolithic zirconia restorations instead. For high-risk patients, a metal or zirconia occlusal surface is recommended (Fig. 13.10), and the cantilever should be avoided or shortened. The occlusion of implant prostheses should be carefully adjusted and monitored. Wearing a nightguard for a patient with bruxism could decrease the risk chipping of the prosthetic material [75].

13.2.4.2 Treatment

When a fracture of the veneering material occurs, small fractures in non-aesthetic areas can be smoothed while larger fractures usually require repair. Minor fractures can be repaired intraorally using resin or metal-ceramic repair systems. It is usually preferable to remove fractured superstructures and repair them in the laboratory. This process is facilitated when restorations are screw-retained. Porcelain absorbs water intraorally and may crack when re-introduced into a creaming furnace. Therefore, superstructures veneered with porcelain must be thoroughly dried in a low-temperature desiccator before attempting repair. When recurrent veneer fracture occurs occlusal and palatal surfaces may be constructed in metal or zirconia.

13.2.5 Incidence of Mechanical Complications: Related Clinical Studies

Previous studies have clearly pointed out that mechanical complications do actually occur frequently after relatively long follow-up time periods, which means they occur significantly later and more frequently than biological complica-

Fig. 13.9 Fracture of the veneering material because of occlusal overloading
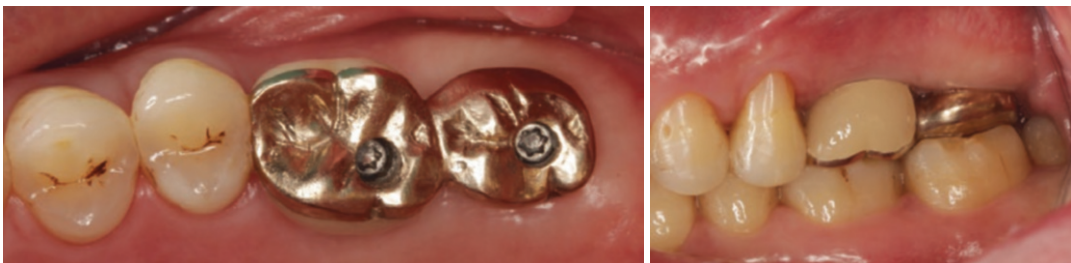
Fig. 13.10 Metal occlusal surface is recommended for a case with insufficient prosthetic space

tions [76, 77]. Dhima et al. [76] carried out a long-term retrospective study on the status of 1325 implants, after a follow-up time of 29 years. It is reported that more mechanical complications occur than biological ones. According to this study, more than half (58%) of the implants experienced at least one mechanical complication. Another long-term (9–15 years) retrospective study [78] assessed survival and complication rates of 376 patients treated with 1095 implants, and reported the occurrence of biological and technical complications at least once during the follow-up period was 52% and 32%, respectively.

Recent systematic reviews based on clinical studies of at least 5 years have reported abutment screw fracture percentages of 1.3–9.3% and screw loosening percentages of 5.3–10.4% [75, 79–82]. A systematic review of edentulous patients with fixed implant restorations reported that the most frequent mechanical complications were screw fracture and screw loosening. Each one of these complications alone presented a 5-year complication rate of approximately 10% and a 10-year complication rate of approximately 20% [83].

Kreissl et al. [84] reported, after an observation period of 5 years, a cumulative incidence of screw loosening of 6.7%; in addition, screw fracture occurred in 3.9% of cases, fracture of the veneering porcelain occurred in 5.7% of cases, and fracture of the supra-structure framework was rare (<1%). Jung et al. [85] performed a meta-analysis of the 5-year survival of implant-supported crowns and reported that the cumulative incidence of implant fractures was 0.14%. After 5 years, the cumulative incidence of screw or abutment loosening was 12.7%, and screw or abutment fracture occurred in 0.35% of cases. For suprastructure-related complications, the cumulative incidence of ceramic or veneer fractures was reported to have an incidence as high as 30% over 3 years [86] in an early study, although this incidence has reduced to 4.5–13.2% [87]. For implant-supported fixed complete prostheses, a cohort study concluded that fracture of the prosthetic material was the most frequent major complication with the estimated 5-year dental unit-based rate of 9.5% [75].

The fracture of osseointegrated implants is a relatively rare occurrence with an incidence range from 0.08% to 0.74%. However, once encountered, it is a catastrophic event. A meta-analysis [88] on the incidence of implant fracture, reviewing clinical studies that reported such fractures, concluded that the incidence of implant fracture comes to 2.8% after a follow-up time of 8.3 years. Yet, most implant fracture cases reported in this study occurred just after 4.1 ± 3.5 years.

A systematic review [89] of implant-supported cantilevered fixed dental rehabilitations in partially edentulous patients reported a cumulative 5–10 years complications rate of 0.31% for implant fractures, 1.57% for abutment screw fracture, 5.33% for screw loosening, and 13.93% for veneer fracture. In another systematic review [90] based on implant-supported cantilevered fixed dental rehabilitations in fully edentulous patients, the cumulative 5–10 years complications rate was reported to be 6.91% for abutment or screw fracture, 5.01% for screw loosening, 2.83% for framework fracture, and 25.66% for veneer fracture, with a 5-year veneer fracture rate of 37.32% on metal-resin full-arch cantilever restorations.

Clinicians providing implant treatment should be aware of these potential complications and the strategies by which they can be prevented and managed. Potential complications should be communicated to the patient before commencing treatment as part of the informed consent process.

References

1. Froum SJ. Dental implant complications: etiology, prevention, and treatment. New York, NY: John Wiley & Sons, Inc.; 2016.
2. Branemark PI. Osseointegration and its experimental background. J Prosthet Dent. 1983;50(3):399–410.
3. Abduo J, Judge RB. Implications of implant framework misfit: a systematic review of biomechanical sequelae. Int J Oral Maxillofac Implants. 2014;29(3):608–21.

4. Al-Turki LE, Chai J, Lautenschlager EP, Hutten MC. Changes in prosthetic screw stability because of misfit of implant-supported prostheses. Int J Prosthodont. 2002;15(1):38–42.

5. Lofgren N, Larsson C, Mattheos N, Janda M. Influence of misfit on the occurrence of veneering porcelain fractures (chipping) in implant-supported metal-ceramic fixed dental prostheses: an in vitro pilot trial. Clin Oral Implants Res. 2017;28(11):1381–7. https://doi.org/10.1111/clr.12997.

6. Pan Y, Tsoi J, Lam W, Pow E. Implant framework misfit: a systematic review on assessment methods and clinical complications. Clin Implant Dent Relat Res. 2021;23(2):244–58. https://doi.org/10.1111/cid.12968.

7. Paniz G, Stellini E, Meneghello R, et al. The precision of fit of cast and milled full-arch implant-supported restorations. Int J Oral Maxillofac Implants. 2013;28(3):687–93.

8. Katsoulis J, Takeichi T, Sol GA, Peter L, Katsoulis K. Misfit of implant prostheses and its impact on clinical outcomes. Definition, assessment and a systematic review of the literature. Eur J Oral Implantol. 2017;10(Suppl 1):121–38.

9. Zervas PJ, Papazoglou E, Beck FM, Carr AB. Distortion of three-unit implant frameworks during casting, soldering, and simulated porcelain firings. J Prosthodont. 1999;8(3):171–9.

10. Khraisat A, Stegaroiu R, Nomura S, Miyakawa O. Fatigue resistance of two implant/abutment joint designs. J Prosthet Dent. 2002;88(6):604–10. https://doi.org/10.1067/mpr.2002.129384.

11. Fernandez M, Delgado L, Molmeneu M, Garcia D, Rodriguez D. Analysis of the misfit of dental implant-supported prostheses made with three manufacturing processes. J Prosthet Dent. 2014;111(2):116–23. https://doi.org/10.1016/j.prosdent.2013.09.006.

12. Arroyo-Cruz G, Orozco-Varo A, Dominguez-Cardoso P, Jimenez-Castellanos E. A comparison of the passive fit of a 3-unit implant-supported fixed partial denture fabricated by lost-wax casting, milling soft metal blocks, or direct metal laser sintering: an in vitro study. J Prosthet Dent. 2022;128:1055. https://doi.org/10.1016/j.prosdent.2021.02.019.

13. Abduo J. Fit of CAD/CAM implant frameworks: a comprehensive review. J Oral Implantol. 2014;40(6):758–66. https://doi.org/10.1563/AAID-JOI-D-12-00117.

14. Torsello F, di Torresanto VM, Ercoli C, Cordaro L. Evaluation of the marginal precision of one-piece complete arch titanium frameworks fabricated using five different methods for implant-supported restorations. Clin Oral Implants Res. 2008;19(8):772–9.

15. Svanborg P, Norstrom SV, Stenport V, Eliasson A. Fit of 3Y-TZP complete-arch implant-supported fixed dental prostheses before and after porcelain veneering. J Prosthet Dent. 2019;122:137. https://doi.org/10.1016/j.prosdent.2018.12.021.

16. Rutkunas V, Larsson C, Vult VSP, Mangano F, Gedrimiene A. Clinical and laboratory passive fit assessment of implant-supported zirconia restorations fabricated using conventional and digital workflow. Clin Implant Dent Relat Res. 2020;22(2):237–45. https://doi.org/10.1111/cid.12885.

17. Mericske-Stern R, Venetz E, Fahrlander F, Burgin W. In vivo force measurements on maxillary implants supporting a fixed prosthesis or an overdenture: a pilot study. J Prosthet Dent. 2000;84(5):535–47. https://doi.org/10.1067/mpr.2000.110264.

18. Jemt T, Carlsson L, Boss A, Jorneus L. In vivo load measurements on osseointegrated implants supporting fixed or removable prostheses: a comparative pilot study. Int J Oral Maxillofac Implants. 1991;6(4):413–7.

19. Bacchi A, Consani RL, Mesquita MF, Dos SM. Effect of framework material and vertical misfit on stress distribution in implant-supported partial prosthesis under load application: 3-D finite element analysis. Acta Odontol Scand. 2013;71(5):1243–9. https://doi.org/10.3109/00016357.2012.757644.

20. Rubo JH, Souza EA. Finite element analysis of stress in bone adjacent to dental implants. J Oral Implantol. 2008;34(5):248–55. https://doi.org/10.1563/1548-1336(2008)34[249:FEAOSI]2.0.CO;2.

21. Schwarz S, Schroder C, Hassel A, Bomicke W, Rammelsberg P. Survival and chipping of zirconia-based and metal-ceramic implant-supported single crowns. Clin Implant Dent Relat Res. 2012;14(Suppl 1):e119–25. https://doi.org/10.1111/j.1708-8208.2011.00388.x.

22. de Kok P, Kleverlaan CJ, de Jager N, Kuijs R, Feilzer AJ. Mechanical performance of implant-supported posterior crowns. J Prosthet Dent. 2015;114(1):59–66. https://doi.org/10.1016/j.prosdent.2014.10.015.

23. Barootchi S, Askar H, Ravida A, et al. Long-term clinical outcomes and cost-effectiveness of full-arch implant-supported zirconia-based and metal-acrylic fixed dental prostheses: a retrospective analysis. Int J Oral Maxillofac Implants. 2020;35(2):395–405. https://doi.org/10.11607/jomi.7833.

24. Jung RE, Al-Nawas B, Araujo M, et al. Group 1 ITI consensus report: the influence of implant length and design and medications on clinical and patient-reported outcomes. Clin Oral Implants Res. 2018;29(Suppl 16):69–77. https://doi.org/10.1111/clr.13342.

25. Chen L, Yang T, Yang G, et al. Retrospective clinical analysis of risk factors associated with failed short implants. Clin Implant Dent Relat Res. 2020;22(1):112–8. https://doi.org/10.1111/cid.12879.

26. Iegami CM, Uehara PN, Sesma N, et al. Survival rate of titanium-zirconium narrow diameter dental implants versus commercially pure titanium narrow diameter dental implants: a systematic review. Clin Implant Dent Relat Res. 2017;19(6):1015–22. https://doi.org/10.1111/cid.12527.

27. Branemark PI, Svensson B, van Steenberghe D. Ten-year survival rates of fixed prostheses on four or six

implants ad modum Branemark in full edentulism. Clin Oral Implants Res. 1995;6(4):227–31.

28. Branemark PI, Engstrand P, Ohrnell LO, et al. Branemark Novum: a new treatment concept for rehabilitation of the edentulous mandible. Preliminary results from a prospective clinical follow-up study. Clin Implant Dent Relat Res. 1999;1(1):2–16.

29. Morton D, Gallucci G, Lin WS, et al. Group 2 ITI consensus report: prosthodontics and implant dentistry. Clin Oral Implants Res. 2018;29(Suppl 16):215–23. https://doi.org/10.1111/clr.13298.

30. Quirynen M, Naert I, van Steenberghe D. Fixture design and overload influence marginal bone loss and fixture success in the Branemark system. Clin Oral Implants Res. 1992;3(3):104–11.

31. Shackleton JL, Carr L, Slabbert JC, Becker PJ. Survival of fixed implant-supported prostheses related to cantilever lengths. J Prosthet Dent. 1994;71(1):23–6.

32. Rangert B, Jemt T, Jorneus L. Forces and moments on Branemark implants. Int J Oral Maxillofac Implants. 1989;4(3):241–7.

33. Walter L, Greenstein G. Utility of measuring anterior-posterior spread to determine distal cantilever length off a fixed implant-supported full-arch prosthesis: a review of the literature. J Am Dent Assoc. 2020;151(10):790–5. https://doi.org/10.1016/j.adaj.2020.06.016.

34. Keith SE, Miller BH, Woody RD, Higginbottom FL. Marginal discrepancy of screw-retained and cemented metal-ceramic crowns on implants abutments. Int J Oral Maxillofac Implants. 1999;14(3):369–78.

35. Torrado E, Ercoli C, Al MM, et al. A comparison of the porcelain fracture resistance of screw-retained and cement-retained implant-supported metal-ceramic crowns. J Prosthet Dent. 2004;91(6):532–7. https://doi.org/10.1016/S0022391304001398.

36. Clelland NL, van Putten MC. Comparison of strains produced in a bone simulant between conventional cast and resin-luted implant frameworks. Int J Oral Maxillofac Implants. 1997;12(6):793–9.

37. Michalakis KX, Hirayama H, Garefis PD. Cement-retained versus screw-retained implant restorations: a critical review. Int J Oral Maxillofac Implants. 2003;18(5):719–28.

38. Karl M, Taylor TD, Wichmann MG, Heckmann SM. In vivo stress behavior in cemented and screw-retained five-unit implant FPDs. J Prosthodont. 2006;15(1):20–4. https://doi.org/10.1111/j.1532-849X.2006.00064.x.

39. Gapski R, Neugeboren N, Pomeranz AZ, Reissner MW. Endosseous implant failure influenced by crown cementation: a clinical case report. Int J Oral Maxillofac Implants. 2008;23(5):943–6.

40. Wilson TJ. The positive relationship between excess cement and peri-implant disease: a prospective clinical endoscopic study. J Periodontol. 2009;80(9):1388–92. https://doi.org/10.1902/jop.2009.090115.

41. Agar JR, Cameron SM, Hughbanks JC, Parker MH. Cement removal from restorations luted to titanium abutments with simulated subgingival margins. J Prosthet Dent. 1997;78(1):43–7.

42. Sailer I, Muhlemann S, Zwahlen M, Hammerle CH, Schneider D. Cemented and screw-retained implant reconstructions: a systematic review of the survival and complication rates. Clin Oral Implants Res. 2012;23(Suppl 6):163–201. https://doi.org/10.1111/j.1600-0501.2012.02538.x.

43. Ma S, Fenton A. Screw- versus cement-retained implant prostheses: a systematic review of prosthodontic maintenance and complications. Int J Prosthodont. 2015;28(2):127–45.

44. Gotfredsen K, Wiskott A. Consensus report - reconstructions on implants. The Third EAO Consensus Conference 2012. Clin Oral Implants Res. 2012;23(Suppl 6):238–41. https://doi.org/10.1111/j.1600-0501.2012.02549.x.

45. Wolfart S, Rittich A, Gross K, et al. Cemented versus screw-retained posterior implant-supported single crowns: a 24-month randomized controlled clinical trial. Clin Oral Implants Res. 2021;32(12):1484–95. https://doi.org/10.1111/clr.13849.

46. Chaar MS, Att W, Strub JR. Prosthetic outcome of cement-retained implant-supported fixed dental restorations: a systematic review. J Oral Rehabil. 2011;38(9):697–711. https://doi.org/10.1111/j.1365-2842.2011.02209.x.

47. Wittneben JG, Joda T, Weber HP, Bragger U. Screw retained vs. cement retained implant-supported fixed dental prosthesis. Periodontol. 2017;73(1):141–51. https://doi.org/10.1111/prd.12168.

48. Wismeijer D, Bragger U, Evans C, et al. Consensus statements and recommended clinical procedures regarding restorative materials and techniques for implant dentistry. Int J Oral Maxillofac Implants. 2014;29(Suppl):137–40. https://doi.org/10.11607/jomi.2013.g2.

49. Thalji G, Bryington M, De Kok IJ, Cooper LF. Prosthodontic management of implant therapy. Dent Clin N Am. 2014;58(1):207–25. https://doi.org/10.1016/j.cden.2013.09.007.

50. Schwarz MS. Mechanical complications of dental implants. Clin Oral Implants Res. 2000;11(Suppl 1):156–8.

51. Kim Y, Oh TJ, Misch CE, Wang HL. Occlusal considerations in implant therapy: clinical guidelines with biomechanical rationale. Clin Oral Implants Res. 2005;16(1):26–35. https://doi.org/10.1111/j.1600-0501.2004.01067.x.

52. Yuan JC, Sukotjo C. Occlusion for implant-supported fixed dental prostheses in partially edentulous patients: a literature review and current concepts. J Periodontal Implant Sci. 2013;43(2):51–7. https://doi.org/10.5051/jpis.2013.43.2.51.

53. Michalakis KX, Calvani P, Hirayama H. Biomechanical considerations on tooth-implant supported fixed partial dentures. J Dent Biomech. 2012;3:1555642423. https://doi.org/10.1177/1758736012462025.

54. Lundgren D, Laurell L. Biomechanical aspects of fixed bridgework supported by natural teeth and endosseous implants. Periodontol. 1994;4:23–40.

55. Schulte W. Implants and the periodontium. Int Dent J. 1995;45(1):16–26.

56. Kerstein RB. Nonsimultaneous tooth contact in combined implant and natural tooth occlusal schemes. Pract Proced Aesthet Dent. 2001;13(9):751–5.

57. Hoshaw S. Mechanical loading of Brånemark implants affects interfacial bone modeling and remodeling. Int J Oral Maxillofac Implants. 1994;9:345–60.

58. Rangert B, Krogh PH, Langer B, Van Roekel N. Bending overload and implant fracture: a retrospective clinical analysis. Int J Oral Maxillofac Implants. 1995;10(3):326–34.

59. Rilo B, Da SJ, Mora MJ, Santana U. Guidelines for occlusion strategy in implant-borne prostheses. A review. Int Dent J. 2008;58(3):139–45. https://doi.org/10.1111/j.1875-595x.2008.tb00189.x.

60. Sheridan RA, Decker AM, Plonka AB, Wang HL. The role of occlusion in implant therapy: a comprehensive updated review. Implant Dent. 2016;25(6):829–38. https://doi.org/10.1097/ID.0000000000000488.

61. Luo Q, Ding Q, Zhang L, Xie Q. Analyzing the occlusion variation of single posterior implant-supported fixed prostheses by using the T-scan system: a prospective 3-year follow-up study. J Prosthet Dent. 2020;123(1):79–84. https://doi.org/10.1016/j.prosdent.2018.12.012.

62. Madani AS, Nakhaei M, Alami M, Haghi HR, Moazzami SM. Post-insertion posterior single-implant occlusion changes at different intervals: a T-scan computerized occlusal analysis. J Contemp Dent Pract. 2017;18(10):927–32. https://doi.org/10.5005/jp-journals-10024-2151.

63. Graves CV, Harrel SK, Nunn ME, et al. The association between occlusal status and the soft and hard tissue conditions around single-unit dental implants. Int J Periodontics Restorative Dent. 2019;39(5):651–6. https://doi.org/10.11607/prd.4184.

64. Heij DG, Opdebeeck H, van Steenberghe D, et al. Facial development, continuous tooth eruption, and mesial drift as compromising factors for implant placement. Int J Oral Maxillofac Implants. 2006;21(6):867–78.

65. Bondevik O. Changes in occlusion between 23 and 34 years. Angle Orthod. 1998;68(1):75–80. https://doi.org/10.1043/0003-3219(1998)068<0075:CIOBAY>2.3.CO;2.

66. Mundhe K, Jain V, Pruthi G, Shah N. Clinical study to evaluate the wear of natural enamel antagonist to zirconia and metal ceramic crowns. J Prosthet Dent. 2015;114(3):358–63. https://doi.org/10.1016/j.prosdent.2015.03.001.

67. Dittmer S, Dittmer MP, Kohorst P, et al. Effect of implant-abutment connection design on load bearing capacity and failure mode of implants. J Prosthodont. 2011;20(7):510–6. https://doi.org/10.1111/j.1532-849X.2011.00758.x.

68. Chrcanovic BR, Kisch J, Larsson C. Retrospective clinical evaluation of 2- to 6-unit implant-supported fixed partial dentures: mean follow-up of 9 years. Clin Implant Dent Relat Res. 2020;22(2):201–12. https://doi.org/10.1111/cid.12889.

69. Murakami H, Igarashi K, Fuse M, et al. Risk factors for abutment and implant fracture after loading. J Oral Sci. 2020;63(1):92–7. https://doi.org/10.2334/josnusd.20-0443.

70. Alnasser AH, Wadhwani C, Schoenbaum TR, Kattadiyil MT. Evaluation of implant abutment screw tightening protocols on reverse tightening values: an in vitro study. J Prosthet Dent. 2021;125(3):486–90. https://doi.org/10.1016/j.prosdent.2020.02.035.

71. Chee WW, Torbati A, Albouy JP. Retrievable cemented implant restorations. J Prosthodont. 1998;7(2):120–5.

72. Williamson RT, Robinson FG. Retrieval technique for fractured implant screws. J Prosthet Dent. 2001;86(5):549–50. https://doi.org/10.1067/mpr.2001.118922.

73. Rojas VF. Retrospective 2- to 7-year follow-up study of 20 double full-arch implant-supported monolithic zirconia fixed prostheses: measurements and recommendations for optimal design. J Prosthodont. 2018;27(6):501–8. https://doi.org/10.1111/jopr.12528.

74. Pjetursson BE, Thoma D, Jung R, Zwahlen M, Zembic A. A systematic review of the survival and complication rates of implant-supported fixed dental prostheses (FDPs) after a mean observation period of at least 5 years. Clin Oral Implants Res. 2012;23(Suppl 6):22–38. https://doi.org/10.1111/j.1600-0501.2012.02546.x.

75. Papaspyridakos P, Bordin TB, Kim YJ, et al. Technical complications and prosthesis survival rates with implant-supported fixed complete dental prostheses: a retrospective study with 1- to 12-year follow-up. J Prosthodont. 2020;29(1):3–11. https://doi.org/10.1111/jopr.13119.

76. Dhima M, Paulusova V, Lohse C, Salinas TJ, Carr AB. Practice-based evidence from 29-year outcome analysis of management of the edentulous jaw using osseointegrated dental implants. J Prosthodont. 2014;23(3):173–81. https://doi.org/10.1111/jopr.12084.

77. Shemtov-Yona K, Rittel D. An overview of the mechanical integrity of dental implants. Biomed Res Int. 2015;2015:547384. https://doi.org/10.1155/2015/547384.

78. Adler L, Buhlin K, Jansson L. Survival and complications: a 9- to 15-year retrospective follow-up of dental implant therapy. J Oral Rehabil. 2020;47(1):67–77. https://doi.org/10.1111/joor.12866.

79. Aglietta M, Siciliano VI, Zwahlen M, et al. A systematic review of the survival and complication rates of implant supported fixed dental prostheses with cantilever extensions after an observation period of at least 5 years. Clin Oral Implants Res. 2009;20(5):441–51. https://doi.org/10.1111/j.1600-0501.2009.01706.x.

80. Salvi GE, Bragger U. Mechanical and technical risks in implant therapy. Int J Oral Maxillofac Implants. 2009;24(Suppl):69–85.

81. Jung RE, Zembic A, Pjetursson BE, Zwahlen M, Thoma DS. Systematic review of the survival rate and the incidence of biological, technical, and aesthetic complications of single crowns on implants reported in longitudinal studies with a mean follow-up of 5 years. Clin Oral Implants Res. 2012;23(Suppl 6):2–21. https://doi.org/10.1111/j.1600-0501.2012.02547.x.

82. Romeo E, Storelli S. Systematic review of the survival rate and the biological, technical, and aesthetic complications of fixed dental prostheses with cantilevers on implants reported in longitudinal studies with a mean of 5 years follow-up. Clin Oral Implants Res. 2012;23(Suppl 6):39–49. https://doi.org/10.1111/j.1600-0501.2012.02551.x.

83. Papaspyridakos P, Chen CJ, Chuang SK, Weber HP, Gallucci GO. A systematic review of biologic and technical complications with fixed implant rehabilitations for edentulous patients. Int J Oral Maxillofac Implants. 2012;27(1):102–10.

84. Kreissl ME, Gerds T, Muche R, Heydecke G, Strub JR. Technical complications of implant-supported fixed partial dentures in partially edentulous cases after an average observation period of 5 years. Clin Oral Implants Res. 2007;18(6):720–6. https://doi.org/10.1111/j.1600-0501.2007.01414.x.

85. Jung RE, Pjetursson BE, Glauser R, et al. A systematic review of the 5-year survival and complication rates of implant-supported single crowns. Clin Oral Implants Res. 2008;19(2):119–30. https://doi.org/10.1111/j.1600-0501.2007.01453.x.

86. Goodacre CJ, Kan JY, Rungcharassaeng K. Clinical complications of osseointegrated implants. J Prosthet Dent. 1999;81(5):537–52.

87. Vere J, Bhakta S, Patel R. Prosthodontic complications associated with implant retained crowns and bridgework: a review of the literature. Br Dent J. 2012;212(6):267–72. https://doi.org/10.1038/sj.bdj.2012.225.

88. Pommer B, Bucur L, Zauza K, et al. Meta-analysis of oral implant fracture incidence and related determinants. J Oral Implants. 2014;2014:1–7.

89. Storelli S, Del FM, Scanferla M, Palandrani G, Romeo E. Implant supported cantilevered fixed dental rehabilitations in partially edentulous patients: systematic review of the literature. Part I. Clin Oral Implants Res. 2018;29(Suppl 18):253–74. https://doi.org/10.1111/clr.13311.

90. Storelli S, Del FM, Scanferla M, Palandrani G, Romeo E. Implant-supported cantilevered fixed dental rehabilitations in fully edentulous patients: systematic review of the literature. Part II. Clin Oral Implants Res. 2018;29(Suppl 18):275–94. https://doi.org/10.1111/clr.13310.

Imaging of Non-resorbable Bone Substitutes

J. Fleiner and A. Stricker

14.1 Introduction

14.1.1 Guided Bone Regeneration

Nowadays, bone grafts are widely accepted in reconstructive dental surgery due to their availability and utility [1]. Bone grafts promote new bone formation and bone healing while providing an ideal scaffold for these processes. To avoid misinterpretation of a non-resorbable bone graft on radiographic images with residual disease, radiologists need to be familiar with the main imaging features of such materials. This article is aiming to describe the different radiographic features of various non-resorbable bone graft materials, with an emphasis on the appearance of each material type on radiographs and other radiologic images.

14.1.2 Principles of Bone Grafting

The elementary role of NRBS is to support the physiological healing process of intraoral osseous defects by promoting new bone formation

J. Fleiner (✉) · A. Stricker
Center of Implantology, Periodontology and 3D Head-and-Neck Imaging, Konstanz, Germany
e-mail: fleiner@stricker-fleiner.de;
stricker@stricker-fleiner.de;
andres.stricker@uniklinik-freiburg.de

and structural support. The bone graft material provides a scaffold to enhance the ingrowth of vessels and the migration of host cells with subsequent osteogenesis. During the formation of the new bone, the inserted graft may be partially or completely resorbed by creeping substitution [2].

Successful incorporation of bone graft material in any site is based on new bone formation, structural incorporation of the graft, and adaptive bony remodeling due to mechanical loading. The sequential phases of the bony remodeling until the complete incorporation of the graft can be monitored by the radiographic follow-up [2].

14.1.3 Graft Materials

Bone grafts are widely used in dental surgical procedures, particularly in Periodontology [3–7], Implantology [4, 8–16], Endodontics [5, 17] and Oral Surgery [18, 19]. Despite the fact that autogenous bone can still be regarded as the "Gold Standard" in bone substitution [20–28], its major limitations comprise restricted general availability and the need for a second surgical site including increased postoperative morbidity [29]. In this context, other alternatives have been developed, and several types of filling biomaterials like allografts (human from tissue banks), xenografts (from animals), and numerous synthetic materials [22, 23, 25, 26, 30–34] have been eval-

uated for bone regeneration. The selection of the biomaterial mostly depends on its features and the therapeutic application [11, 31, 35] whereas all of them have merits and limitations [20–27]. The ultimate decision is based on many factors, including the size and location of the bone tissue defect as well as the structural, biological, and biomechanical properties of the graft itself and potential surgical graft prevention [27, 34, 36].

14.1.3.1 Heterologous Grafts (Xenografts)

Heterologous materials are obtained from bones of different animal species; bovine, equine, and porcine bone being the most common sources [37–40]. Xenografts have different properties depending on their origin, constitution, and processing [41], and their use might lead to increased general complications [42]. They have been used in different types of bone defects with quite promising results [2, 41]. These biomaterials are made of reticular apatite crystals, inducing coagulum synthesis and stability of the blood clot [43]. Although numerous authors have confirmed the osteoconductive properties [44–48], there might be a possible risk of transmission of CJD or Bovine Spongiform Encephalopathy [49, 50] by xenografts according to the Food and Drug Administration (FDA). Furthermore, low reabsorption is mainly seen for these biomaterials: after many years the material is still between 20% and 40% [51]. As collagen contributes to mineral deposition, vascular ingrowth, and growth factor binding, a trend towards collagen-based xenografts was observed within the last decade. It has to be mentioned that collagen could induce allergic responses, 3% of the population is allergic to collagen and has a predisposition to develop diseases such as polymyositis and dermatomyositis [44].

14.1.3.2 Alloplastic Grafts

Alloplastic grafts represent synthetic bone substitutes in various sizes, forms, and textures [12, 35, 41]. Bauer and Mischler reported this type of bone graft promotes stable bonds with neo-synthetized bone [6], while the internal structuring of the alloplastic grafts can be regarded as

similar to bone tissue [52]. Some types of synthetic grafts such as bioactive ceramics may even induce natural bone binding, due to their similarity with mineral bone tissue.

Hydroxyapatite Allografts

Hydroxyapatite is a natural component of hard tissue (65% in bone tissue, 98% in enamel). Synthetic hydroxyapatite is available in different forms (porous, non-porous, ceramic, and non-ceramic) and has been widely used for regenerative therapy in dental implantology, due to its osseointegrative capabilities [12, 53, 54].

Hydroxyapatite is bioinert and biocompatible, but it shows poor reabsorption and does not induce significant bone regeneration. Histomorphometric analysis could show a percentage of 41% of neo-synthetized bone, 30% of medullary spaces, and 31% of residual hydroxyapatite graft [55].

Tricalcic Phosphate Grafts

Tricalcic phosphate (TCP) grafts are pre-treated with naphthalene and then are compacted at high temperatures for obtaining a diameter porosity of 100–300 μm. During the process of reabsorption, TCP provides ionic calcium and magnesium to bone tissue promoting an ionic environment, which activates alkaline phosphatase, a fundamental element for further bone synthesis [56, 57].

Bioglass Grafts

Synthetic glass ceramics are made of silicon dioxide (45%), sodium oxide (24.5%), and phosphorus pentoxide [12, 58]. The bioglass particles show an average diameter of 300 μm. Bioglass has osteoconductive properties and its solubility is directly dependent on sodium oxide [12]. Histomorphometric analysis has given a percentage of 40% of new bone, 43% of medullary spaces, and 17% of bioglass particles surrounded by neo-synthetized bone [58].

Coralline Hydroxyapatite Grafts

Coralline hydroxyapatite is largely composed of calcium carbonate (87–98%), strontium, fluoride, magnesium, sodium and potassium (2–13%) [12,

59]. It has a porous structure (over 45%) with a diameter between 150 and 500 μm. The coralline hydroxyapatite has osteoconductive properties and underlies reabsorption by the carbonic anhydrases of osteoblasts. Histomorphometric analysis has shown 42% of neo-synthesized bone, 40% of medullary spaces, and 18% of residue biocoral [55, 60].

Polylactic Acid and Polyglycolic Acid

The combination of polymeric lactic acid and polyglycolic acid improves graft compatibility and degradability [58, 61, 62]. The insertion of polylactic and polyglycolic acid biopolymers could induce correct bone regeneration [63–65]. Histological analyses demonstrated almost complete reabsorption with 43% of mineral bone, 56% of medullary spaces, and only 1% of residual graft [55]. Although biological degradation and reabsorption (between 4 and 8 months) of this material is slow and progressive, it reveals a correct bone regeneration.

14.2   Imaging Characteristics of Non-resorbable Bone Substitutes

The potential influence of the up-above mentioned physical properties and characteristics of the graft material on the biological response cannot be easily generally predicted as the published data contains different types of hydroxyapatite (natural and synthetic), different particle sizes, and therefore varying physicochemical properties. In this context, bone substitutes of the same origin may differ with regard to their radiographic appearance.

14.2.1 Non-resorbable Bone Substitutes

Non-resorbable bone substitutes are mainly composed of calcium sulfate, hydroxyapatite, tricalcium phosphate, or a combination. NRBS provide an osteoconductive lattice on which host osteogenesis can take place, but they lack osteoinduc-

tive properties. As NRBS are available in a variety of forms, including pellets, cement, and injectable paste, they are radiopaque and designed for use in spaces that are not intrinsic to the stability of the bone structure. These products allow so-called "creeping substitution", which implies the resorption of the ceramic and its subsequent replacement by new bone during the healing process.

On radiographs, NRBS appear denser than the neighboring native bone. In the initial postoperative period, a lucent band is identifiable at the graft-host junction, and the margins and internal architecture of the graft are sharply outlined. Osseous integration starts right after surgery, with subsequent obliteration of the translucent area originally surrounding the implant. Furthermore, subsequent loss of definition of the implant margins can be radiographically observed. These changes in appearance are likely to result from osteoclastic activity and osseous ingrowth [66]. Generally, calcium sulfate ceramic shows quite similar radiographic attenuation in CT scans as observed for cortical bone immediately after surgical insertion; however, a near-complete radiolucency is seen after 3 months because of rapid resorption. As the ceramic bone substitutes contain calcium sulfates appearing hypointense and masslike, potential pitfalls may exist in MR imaging, regardless of the MR sequence used, leading physicians to mistake the graft for residual or recurrent tumor.

14.2.2 Composite Grafts

Composite grafts include the appreciated osteoconductive attributes of ceramics and osteoinductive characteristics of a demineralized bone matrix in a single compound. As is the case with other mineral-containing synthetic bone grafts, the composite grafts appear radiopaque on postoperative radiographs and CT scans and over time may be incorporated into the skeletal structure. Demineralized bone matrix putty also may be combined with a bone auto- or allograft to obtain both osteoconductive and osteoinduc-

tive properties. On both immediate postoperative and subsequent radiographs, the combination of putty and bonegraft components appears to have a density in the range of 500–1000 HU, thus representing a density between medullary and cortical bone. Diffuse signal enhancement in the postoperative area is a typical finding on MR images, most likely because of the calcium content of bone graft material and the ingrowth of vascularized granulation tissue.

14.3 Imaging Modalities for the Visualization of Non-resorbable Bone Substitutes and Peri-Implant Bony Interface

Radiographic analyses are commonly used in implant dentistry as an important diagnostic tool for treatment planning and follow-up. These analyses principally allow the evaluation of implant stability, marginal bone level, and bone–implant contact. They also serve for assessing the trabecular bony microstructure, bone quantity, and quality [67, 68], thus helping to evaluate the osseointegration or failing integration of implants and bone grafting material at an early stage already.

14.3.1 Intraoral Film Radiography/ Extraoral Panoramic Image

Intraoral radiography has been widely used to reveal changes around dental implants [69], mainly due to their considerable advantages, such as low costs, widespread availability, good patient tolerance, user-friendliness, and the ability to provide high-resolution images for accurate measurements at the implant sites [70, 71].

With regard to the radiological assessment of continuous bone loss, e.g., after a regenerative surgical procedure, intraoral radiographs suffer from their inherent two-dimensional (2D) character. On 2D images, the detection of the marginal bone level, the clear delineation of intra-osseous defects, and their changes over time may be negatively influenced by anatomical superimposition, overlay, and geometric distortion [70]. Furthermore, potential evaluation of the buccal and lingual bone levels is limited because of the two-dimensional character of the radiographic modality.

14.3.2 Micro-Computed Tomography (In-Vitro Assessment)

X-ray microtomography (micro-CT) can be considered a miniaturized form of conventional tomography, performing three-dimensional images with a high spatial resolution (<10-μm pixel size) in order to analyze the internal structures of small objects [72, 73]. As micro-CT is a non-invasive and non-destructive technique, samples need not be altered or treated in any way prior to scanning, in biomaterial studies and tissue engineering, this microtomographic technique shows very promising in vitro results and helps to characterize morphometric features of human bone tissue and biomaterials. Yet it has to be emphasized, that its use is limited to small ex vivo bone samples and cannot be employed for the clinical patient.

Micro-CT allows a precise three-dimensional (3D) reconstruction of jaw bone samples and the assessment of the cancellous bone [74], in this way contributing to measure histomorphometric variables, e.g. bone volume, total volume, bone volume fraction, trabecular thickness, trabecular number, and trabecular separation [75].

Compared to clinically relevant slice-imaging modalities such as high-resolution CBCT, microCT could confirm the correlation between

radiographic bone density basing on and bone density [76–82], however, the overestimation of morphometric parameters and acquisition settings in CBCT must be taken into account [83, 84].

14.3.3 Magnetic Resonance Imaging (MRI)

MR appearance of non-resorbable bone substitutes is quite variable [66]. Non-resorbable bone substitutes show high opacity and attenuation on initial postoperative radiographs and CT scans, while their opacity or attenuation gradually decreases over time, as graft incorporation takes place [66]. During radiographic follow-up controls, the inserted material will remain somewhat opaque and highly attenuating, followed by a degree of lucency as creeping substitution, resorption, and osseous healing or incorporation continue.

NRBS show hyperintense signals on T1-weighted images and hypointense response on T2-weighted images as the bone substitutes appear denser than the adjacent native bone [66]. Possible alterations during follow-up imaging may result due to infection and pathologic appearance of bony osteolytic changes after unsuccessful surgery. As new synthetic materials are developed, the recognition of their imaging characteristics will be further challenging in order to avoid diagnostic pitfalls.

14.3.4 Multispiral-Computed Tomography (MSCT)

Computed tomography (CT) allows precise three-dimensional evaluation of anatomic structures [85, 86] and direct measurements of bone density prior to dental implant surgery and regenerative treatment [87–91]. Bone density measurements are expressed by Hounsfield units (HU), representing the relative density of body tissues according to a calibrated gray-level scale, based on values for air (−1000 HU), water (0

HU), and bone density (+1000 HU) [92]. HU-based evaluation of the bone density seems to be a useful method to analyze the jaw bone, however high radiation doses associated with CT imaging have to be taken into account [68, 91, 93, 94].

14.3.5 Cone-Beam CT (CBCT)

The introduction of CBCT has led to a more widespread use of three-dimensional (3D) imaging in dentistry in recent years [95] allowing clinicians to view the craniofacial structures in three dimensions at a relatively high spatial resolution.

The inherent 3D nature of the surgical site has moved pre-surgical planning towards the use of dental CBCT, as it can offer high-quality 3D images at relatively low radiation doses and costs. Apart from the radiodiagnostic possibilities, dental CBCT offers peri- and postsurgical potential, explaining the success of CBCT in the fields of dental implantology and oral surgery while increasingly replacing multislice CT (MSCT) [96, 97] for the visualization of high-contrast structures of the oral region (bone, teeth, air cavities).

Traditionally, bone quality parameters and classifications were primarily based on HU representation derived from MSCT datasets. It has to be emphasized that there are crucial differences between MSCT and CBCT, which complicates the use of quantitative gray values (GV) for the latter [96–103]. Both experimental as well as clinical studies have shown that great variability of GVs may occur for CBCT images because of various reasons that are inherently associated with this technique. The imprecise and variable intensity values for CBCT may be attributed i.e. the limited field size, cone angle, high amount of scattered radiation, and limitations of image reconstruction algorithms resulting in inaccurate calculations [91, 104]. Numerous attempts were made to compare CBCT GVs with clinical bone parameters and to calibrate GVs along a density scale by various authors [67, 91, 105–113]. While the presented

results often seem promising, it must be stated that the intensity values in CBCT images are not entirely reliable, because they are influenced by the device, the imaging parameters, and the position of the area being evaluated [92]. In summary, conventional HU-representation of CT does not directly apply to CBCT [92, 114–120], the use of quantitative GV remains essential, therefore CBCT images should at least be acquired with identical exposure time and field-of-view to reduce GV variability [120]. As a consequence, recent research and clinical findings have shifted the paradigm of bone quality from a density-based analysis to a structural evaluation of the bone [94, 121–123].

In this context, it has to be emphasized that precise identification of corresponding landmarks and defined borders within consecutive (CB-)CT scans is regarded crucial for reliable assessment of bony remodeling and recontouring changes of the grafted augmentation material. Therefore further scientific attempts will have to be based on automated image registration and geometric alignment of consecutive datasets for a more consistent and precise evaluation, thus allowing the definition of identical ROI prior to the evaluation of bone grafts in images of different time points [124].

14.3.5.1 Accuracy of CBCT Measurements in Bone Regeneration Procedure Using NRBS

Modern CBCT technology has validated its usefulness and high measurement accuracy for several diagnostic purposes [125–135]. Compared to MSCT CBCT is related to a considerable radiation dose reduction [70, 136, 137]. In any way, the evaluation of the peri-implant bone including peri-implant bone regeneration requires three-dimensional radiological investigation on a high level of diagnostic precision [131]. Accuracy of CBCT measurements at the peri-implant tissues including bone defects after regenerative rehabilitation using NRBS has therefore to be compared to the golden standard of histological measurements or micro-CT [117–119, 138, 139]. Even if linear measurements using CBCT can provide values at a sub-millimeter accuracy level

[69, 127, 140, 141], it has to be emphasized that any distance or volume measurement might contain unavoidable errors of at least the selected voxel size. Additionally, a low contrast range and low image resolution are further limiting the precision of the modality by unavoidable artifact occurrence [140, 141]. The existence of radiodense objects like implants causes different types of artifacts [142], and might complicate the visualization of the bone–implant interface [130]. In normal clinical settings, the presence of metallic restorative materials with high atomic numbers hardens the X-ray beam while causing streaking artifacts, extinction, and beam-hardening artifacts [104]. Resulting artifacts degrade the quality of images and affect the gray scales of normal anatomical structures close to foreign bodies such as regenerative bone substitute materials. The severity of the mentioned effects is also dependent on the energy of the applied X-ray beam, density, and geometry of artifact-inducing materials [142]. In this context, it might be of interest whether and to what extent NRBS could cause beam hardening artifacts. Preliminary tests showed the radiopacities of the BAM used being only slightly or not above the radiopacities of human bone or dog bone [140, 141]. This is what can be expected as the NRBS used is of the bone origin or is composed of the same chemical elements as bone. Even if NRBS show as high-density radiopaque granule structures, significant beam hardening artifacts by the incorporated NRBS are unlikely, as they can normally be found in homogenous contact with the adjacent bone or completely integrated into living bone. Often there is some doubt or error because it is difficult to distinguish newly formed bone and bone substitute granules in CBCT images.

In conclusion, it has to be emphasized that current research study activities indicate that modern high-resolution CBCT systems allow measurements of peri-implant bone thickness at accuracy in the sub-millimeter range, and—within some limits—assessing the existence of NRBS and its integration into the bone, but the evaluation of complete hard-tissue covering of the implant surface still remains a diagnostic challenge for the above-mentioned reasons [124].

References

1. Rodella LF, Favero G, Labanca M. Biomaterials in maxillofacial surgery: membranes and grafts. Int J Biomed Sci. 2011;7(2):81–8.

2. Carlino P, Pepe V, Pollice G, Grassi FR. Immediate transmucosal implant placement in fresh maxillary and mandibular molar extraction sockets: description of technique and preliminary results. Minerva Stomatol. 2008;57:471.

3. Al Ghamdi AS, Shibly O, Ciancio SG. Osseous grafting part II: xenografts and alloplasts for periodontal regeneration--a literature review. J Int Acad Periodontol. 2010;12(2):39.

4. Baldini N, De Sanctis M, Ferrari M. Deproteinized bovine bone in periodontal and implant surgery. Dent Mater. 2011;27:61–70.

5. Bashutski JD, Wang HL. J Endod. 2009;35:321–8.

6. Stavropoulos F, Dahlin C, Ruskin JD, Johansson C. A comparative study of barrier membranes as graft protectors in the treatment of localized bone defects. An experimental study in a canine model. Clin Oral Implants Res. 2004;15:435.

7. Windisch P, Szendrői-Kiss D, Horváth A, Suba Z, Gera I, Sculean A. Reconstructive periodontal therapy with simultaneous ridge augmentation. A clinical and histological case series report. Clin Oral Investig. 2008;12(3):257–64. https://doi.org/10.1007/s00784-008-0194-8.

8. Buser D, Dahlin C, Schenk RK. Guided bone regeneration in implant dentistry. 1st ed. Chicago, IL: Quintessence Publishing; 1994. p. 101.

9. Cordaro L, Bosshardt DD, Palatella P, Rao W, Serino G, Chiapasco M. Maxillary sinus grafting with Bio-Oss or Straumann Bone Ceramic: histomorphometric results from a randomized controlled multicenter clinical trial. Clin Oral Implants Res. 2008;19:796–803.

10. Ferri J, Dujoncquoy J-P, Carneiro JM, Raoul G. Maxillary reconstruction to enable implant insertion: a retrospective study of 181 patients. Head Face Med. 2008;4:31. https://doi.org/10.1186/1746-160X-4-31.

11. Garofalo GS. Autogenous, allogenetic and xenogenetic grafts for maxillary sinus elevation: literature review, current status and prospects. Minerva Stomatol. 2007;56:373.

12. Kao ST, Scott DD. A review of bone substitutes. Oral Maxillofac Surg Clin N Am. 2007;19:513.

13. Nyström E, Ahlqvist J, Gunne J, Kahnberg K. 10-Year follow-up of onlay bone grafts and implants in severely resorbed maxillae. Int J Oral Maxillofac Surg. 2004;33:258–62.

14. Ramírez Fernández MP, Mazón P, Gehrke SA, Calvo-Guirado JL, De Aza PN. Comparison of two xenograft materials used in sinus lift procedures: material characterization and in vivo behavior. Materials. 2017;10:623.

15. Roos-Jansaker AM, Renvert H, Lindahl C, Renvert S. Surgical treatment of peri-implantitis using a bone substitute with or without a resorbable membrane: a prospective cohort study. J Clin Periodontol. 2007;34:625.

16. Urban IA, Jovanovic SA, Lozada JL. Vertical ridge augmentation using guided bone regeneration (GBR) in three clinical scenarios prior to implant placement: a retrospective study of 35 patients 12 to 72 months after loading. Int J Oral Maxillofac Implants. 2009;24:502.

17. Sreedevi P, Varghese N, Varugheese JM. Prognosis of periapical surgery using bonegrafts: a clinical study. J Conserv Dent. 2011;14:68–72.

18. Depprich RA, Handschel JG, Naujoks C, Hahn T, Meyer U, Kubler NR. Sinus lifting before Le Fort I maxillary osteotomy: a suitable method for oral rehabilitation of edentulous patients with skeletal class-III conditions: review of the literature and report of a case. Head Face Med. 2007;3:2D.

19. Handschel J, Simonowska M, Naujoks C, Depprich RA, Ommerborn MA, Meyer U, Kübler NR. A histomorphometric meta-analysis of sinus elevation with various grafting materials. Head Face Med. 2009;5:12.

20. Catros S, Guillemot F, Lebraud E, Chanseau C, Perez S, Bareille R, Amédeé J, Fricain JC. Physico-chemical and biological properties of a nano-hydroxyapatite powder synthesized at room temperature. IRBM. 2010;31:226–33.

21. da Cruz AC, Pochapski MT, Daher JB, da Silva JC, Pilatti GL, Santos FA. Physico-chemical characterization and biocompatibility evaluation of hydroxyapatites. J Oral Sci. 2006;48(4):219–26.

22. Giannoudis PV, Dinopoulos H, Tsiridis E. Bone substitutes: an update. Injury. 2005;36(Suppl 3):S20–7.

23. Ilan DI, Ladd AL. Bone graft substitutes. Oper Tech Plast Reconstr Surg. 2022;9(4):151–60.

24. Masago H, Shibuya Y, Munemoto S, Takeuchi J, Umeda M, Komori T, Kuboki Y. Alveolar ridge augmentation using various bone substitutes - a web form of titanium fibers promotes rapid bone development. Kobe J Med Sci. 2007;53(5):257–63.

25. McAuliffe JA. Bone graft substitutes. J Hand Ther. 2003;16(2):180–7.

26. Parikh SN. Bone graft substitutes: past, present, future. J Postgrad Med. 2002;48(2):142–8. Review.

27. Tadic M. Epple. Biomaterials. 2004;25:987–94.

28. Trombelli L, Farina R, Marzola A, Itro A, et al. GBR and autogenous cortical bone particulate by bone scraper for alveolar ridge augmentation: a 2-case report. Int J Oral Maxillofac Implants. 2008;23:111.

29. Fretwurst T, Wanner L, Nahles S, Raguse JD, Stricker A, Metzger MC, Nelson K. J A prospective study of factors influencing morbidity after iliac crest harvesting for oral onlay grafting. Craniomaxillofac Surg. 2015;43(5):705–9. https://doi.org/10.1016/j.jcms.2015.03.023. Epub 2015 Apr 1. PMID: 25937474.

30. Becker S, Maissen O, Ponomarev I, Stoll T, et al. Osteopromotion with a plasmatransglutaminase on a beta-TCP ceramic. J Mater Sci Mater Med. 2008;19:659.

31. d'Aloja E, Santi E, Aprili G, Franchini M. Fresh frozen homologous bone in oral surgery: case reports. Cell Tissue Bank. 2008;9:41.

32. Dori S, Peleg M, Barnea E. Alveolar ridge augmentation with hip corticocancellous allogenic block graft prior to implant placement. Refuat Hapeh Vehashinayim. 2008;25:28.

33. Fretwurst T, Spanou A, Nelson K, Wein M, Steinberg T, Stricker A. Comparison of four different allogeneic bone grafts for alveolar ridge reconstruction: a preliminary histologic and biochemical analysis. Oral Surg Oral Med Oral Pathol Oral Radiol. 2014;118(4):424–31. https://doi.org/10.1016/j.oooo.2014.05.020. Epub 2014 Jun 13. PMID: 25183228.

34. Van der Stok J, Van Lieshout EM, El-Massoudi Y, Van Kralingen GH, Patka P. Bone substitutes in the Netherlands - a systematic literature review. Acta Biomater. 2011;7(2):739–50.

35. Diniz Oliveira HF, Weiner AA, Majumder A, Shastri VP. Non-covalent surface engineering of an alloplastic polymeric bone graft material for controlled protein release. J Control Release. 2008;126:237.

36. Gielkens PF, Bos RR, Raghoebar GM, Stegenga B. Is there evidence that barrier membranes prevent bone resorption in autologous bone graft during the healing period? A systematic review. Int J Oral Maxillofac Implants. 2007;22:390.

37. Camargo PM, Lekovic V, Weinlaender M, Nedic M, et al. A controlled re-entry study on the effectiveness of bovine porous bone mineral used in combination with a collagen membranes of porcine origin in the treatment of introbony defects in humans. J Clin Periodontol. 2000;27:889.

38. Hartman GA, Arnold RM, Mills MP, Cochran DL, et al. Clinical and histologic evaluation of anorganic bovine bone collagen with or without a collagen barrier. Int J Periodontics Restorative Dent. 2004;24:127.

39. Lee DW, Pi SH, Lee SK, Kim EC. Comparative histomorphometric analysis of extraction sockets healing implanted with bovine xenografts, irradiated cancellous allografts, and solvent-dehydrated allografts in humans. Int J Oral Maxillofac Implants. 2009;24:609.

40. Mardas N, Chadha V, Donos N. Alveolar ridge preservation with guided bone regeneration and a synthetic bone substitute or a bovine-derived xenograft: a randomized, controlled clinical trial. Clin Oral Implants Res. 2010;21(7):688–98.

41. Oltramari PV, de Lima Navarro R, Henriques JF, Taga R, et al. Orthodontic movement in bone defects filled with xenogenic graft: an experimental study in minipigs. Am J Orthod Dentofac Orthop. 2007;131:310.

42. Angermair J, Bosshardt DD, Nelson K, Flügge TV, Stricker A, Fretwurst T. Horizontal bone grafting using equine-derived cancellous bone blocks is associated with severe complications: a prospective clinical and histological pilot study. Clin Oral Implants Res. 2020;31(11):1149–58. https://doi.org/10.1111/clr.13661. Epub 2020 Sep 17. PMID: 32881075.

43. Cestari TM, Granjeiro JM, de Assis GF, Garlet GP, et al. Bone repair and augmentation using block of sintered bovine-derived anorganic bone graft in cranial bone defect model. Clin Oral Implants Res. 2009;20:340.

44. Fontana F, Rocchietta I, Dellavia C, Nevins M, et al. Biocompatibility and manageability of a new fixable bone graft for the treatment of localized bone defects: preliminary study in a dog model. Int J Periodontics Restorative Dent. 2008;28:601.

45. Hammerle CH, Lang NP. Single stage surgery combining transmucosal implant placement with guided bone regeneration and bioresorbable materials. Clin Oral Implants Res. 2001;12:9.

46. Hammerle CH, Jung RE, Yaman D, Lang NP. Ridge augmentation by applying bioresosrbable membranes and deproteinized bovine bone mineral: a report of twelve consecutive cases. Clin Oral Implants Res. 2008;19:19.

47. Hurzeler MB, Kohal RJ, Naghshbandi J, Mota LF, et al. Evaluation of a new bioresorbable barrier to facilitate guided bone regeneration around exposed implant threads. An experimental study in the monkey. Int J Oral Maxillofac Surg. 1998;27:315.

48. Zitzmann NU, Naef R, Schupbach P, Schaerer P. Immediate or delayed immediate implantation versus late implantation when using the principles of guided bone regeneration. Implantologie. 1997;27:49.

49. Johannes FH. Risk of trasmission of agents associated with Creutzfeldt-Jakob and bovine spongiform encephalopathy. Plast Reconstr Surg. 1999;103:1324.

50. Wenz B, Oesch B, Horst M. Analysis of the risk of transmitting bovine spongiform encephalopathy through bone grafts derived from bovine bone. Biomaterials. 2001;22:1599.

51. Hallman M, Lundgren S, Sennerby L. Histologic analysis of clinical biopsies taken 6 months and 3 years after maxillary sinus floor augmentation with 80% bovine hidroxyapatite and 20% autogenous bone mixed with fibren glue. Clin Implant Dent Relat Res. 2001;3:87.

52. Fazan F, Besar I, Osman A, Samsudin AR, et al. Successful commercialisation of locally fabricated bioceramics for clinical applications. Med J Malaysia. 2008;63:49.

53. Li J, Zuo Y, Cheng X, Yang W, et al. Preparation and characterization of nano-hydroxyapatite/polyamide 66 composite GBR membrane with asymmetric porous structure. J Mater Sci Mater Med. 2009;20:1031.

54. Pinheiro AL, Martinez Gerbi ME, de Assis Limeira F Jr, Carneiro Ponzi EA, et al. Bone repair following bone grafting hydroxyapatite guided bone regeneration and infra-red laser photobiomodulation: a histological study in rodent model. Lasers Med Sci. 2009;24:234.

55. Piattelli A. Biomateriali utilizzati in rigenerazione ossea: risultati istologici. Implantol Orale. 2003;4:77.

56. Hirota M, Matsui Y, Mizuki N, Kishi T, et al. Combination with allogenic bone reduces early absorption of beta-tricalcium phosphate (beta-TCP) and enhances the role as a bone regeneration scaffold. Experimental animal study in rat mandibular bone defects. Dent Mater J. 2009;28:153.

57. Irigaray JL, Oudadesse H, Blondiaux G, Collangettes D. Kinetics of the diffusion of some elements evaluated by neutron activation in a coral implanted in vivo. J Radioanal Nuvlear Chem. 1993;169:339.

58. Kucukkolbasi H, Mutlu N, Isik K, Celik I, et al. Histological evaluation of the effects of bioglass, hydroxyapatite, or demineralized freeze-dried bone, grafted alone or as composites, on the healing of tibial defects in rabbits. Saudi Med J. 2009;30:329.

59. Zhukauskas R, Dodds RA, Hartill C, Arola T, et al. Histological and radiographic evaluations of demineralized bone matrix and coralline hydroxyapatite in the rabbit tibia. J Biomater Appl. 2009;24(7):639.

60. Martin RB, Chapman MW, Holmes RE, Sartoris DJ, et al. Effects of bone ingrowth on the strength and non invasive assessment of a coralline hydroxyapatite material. Biomaterials. 1989;10:481.

61. Cauwels RG, Martens LC. Use of osteoconductive materials in pediatric dental medicine. Rev Belg Med Dent. 2004;59:203.

62. Geurs NC, Korostoff JM, Vassilopoulos PJ, Kang TH, et al. Clinical and histologic assessment of lateral alveolar ridge augmentation using a synthetic long-term bioabsorbable membrane and an allograft. J Periodontol. 2008;79:1133.

63. Lundgren D, Nyman S, Mathsen T, Isaksson S, et al. Guided bone regeneration of cranial defect, using biodegradable barriers: an experimental pilot study in the rabbit. J Craniomaxillofac Surg. 1992;20:257.

64. Miyamoto S, Takoaka K, Ono K. Bone induction and bone repair by composites of bone morphogenetic protein and biodegradable synthetic polymers. Ann Chir Gynaecol Suppl. 1993;207:69.

65. Winet H, Hollinger JO. Incorporation of polylactide-plyglycolide in a cortical defect: neoosteogenesis in a bone chamber. J Biomed Mater Res. 1993;27:667.

66. Beaman FD, Bancroft LW, Peterson JJ, Kransdorf MJ, Menke DM, DeOrio JK. Imaging characteristics of bone graft materials. Radiographics. 2006;26(2):373–88.

67. Song YD, Jun SH, Kwon JJ. Correlation between bone quality evaluated by cone-beam computerized tomography and implant primary stability. Int J Oral Maxillofac Implants. 2009;24:59–64.

68. Turkyilmaz I, Tözüm TF, Tumer MC. Bone density assessments of oral implant sites using computerized tomography. J Oral Rehabil. 2007;34(4):267–72.

69. Corpas Ldos S, Jacobs R, Quirynen M, Huang Y, Naert I, Duyck J. Peri-implant bone tissue assessment by comparing the outcome of intra-oral radiograph and cone beam computed tomography analyses to the histological standard. Clin Oral Implants Res. 2011;22(5):492–9. https://doi.org/10.1111/j.1600-0501.2010.02029.x.

70. Tyndall DA, Brooks SL. Selection criteria for dental implant site imaging: a position paper of the American Academy of Oral and Maxillofacial Radiology. Oral Surg Oral Med Oral Pathol Oral Radiol Endod. 2000;89:630–7.

71. Dahlin C, Johansson A. Iliac crest autogenous bone graft versus alloplastic graft and guided bone regeneration in the reconstruction of atrophic maxillae: a 5-year retrospective study on cost-effectiveness and clinical outcome. Clin Implant Dent Relat Res. 2010;13:305.

72. Bedini R, et al. 3D microtomography characterization of dental implantology bone substitutes used in vivo. Key Eng Mater. 2013;541:97–113.

73. Meleo D, Bedini R, Pecci R, Mangione F, Pacifici L. Microtomographic and morphometric characterization of a bioceramic bone substitute in dental implantology. Ann Ist Super Sanita. 2012;48(1):59–64.

74. Martín-Badosa E, Amblard D, Nuzzo S, Elmoutaouakkil A, Vico L, Peyrin F. Excised bone structures in mice: imaging at three-dimensional synchrotron radiation micro CT. Radiology. 2004;229:921–8. https://doi.org/10.1148/radiol.2293020558.

75. Odgaard A. Three-dimensional methods for quantification of cancellous bone architecture. Bone. 1997;20(4):315–28.

76. Fang L, Ding X, Wang HM, Zhu XH. Chronological changes in the microstructure of bone during peri-implant healing: a microcomputed tomographic evaluation. Br J Oral Maxillofac Surg. 2014;52(9):816–21. https://doi.org/10.1016/j.bjoms.2014.07.097. Epub 2014 Aug 15.

77. González-García R, Monje F. The reliability of cone-beam computed tomography to assess bone density at dental implant recipient sites: a histomorphometric analysis by micro-CT. Clin Oral Implants Res. 2013a;24(8):871–9. https://doi.org/10.1111/j.1600-0501.2011.02390.x. Epub 2012 Jan 17.

78. González-García R, Monje F. Is micro-computed tomography reliable to determine the microstructure of the maxillary alveolar bone? Clin Oral Implants

Res. 2013b;24(7):730–7. https://doi.org/10.1111/j.1600-0501.2012.02478.x. Epub 2012 Apr 30.

79. González-Martín O, Lee EA, Veltri M. CBCT fractal dimension changes at the apex of immediate implants placed using undersized drilling. Clin Oral Implants Res. 2012;23(8):954–7. https://doi.org/10.1111/j.1600-0501.2011.02246.x.

80. Iezzi G, Aprile G, Tripodi D, Scarano A, Piattelli A, Perrotti V. Implant surface topographies analyzed using fractal dimension. Implant Dent. 2011;20(2):131–8. https://doi.org/10.1097/ID.0b013e31820fb171.

81. Jeong KI, Kim SG, Oh JS, Jeong MA. Consideration of various bone quality evaluation methods. Implant Dent. 2013;22(1):55–9. https://doi.org/10.1097/ID.0b013e31827778d9.

82. Monje A, Monje F, González-García R, Galindo-Moreno P, Rodriguez-Salvanes F, Wang HL. Comparison between microcomputed tomography and cone-beam computed tomography radiologic bone to assess atrophic posterior maxilla density and microarchitecture. Clin Oral Implants Res. 2014;25(6):723–8. https://doi.org/10.1111/clr.12133. Epub 2013 Feb 26.

83. Kim JE, Yi WJ, Heo MS, Lee SS, Choi SC, Huh KH. Three-dimensional evaluation of human jaw bone microarchitecture: correlation between the microarchitectural parameters of cone beam computed tomography and micro-computer tomography. Oral Surg Oral Med Oral Pathol Oral Radiol. 2015;120(6):762–70. https://doi.org/10.1016/j.oooo.2015.08.022. Epub 2015 Sep 9.

84. Van Dessel J, Huang Y, Depypere M, Rubira-Bullen I, Maes F, Jacobs R. A comparative evaluation of cone beam CT and micro-CT on trabecular bone structures in the human mandible. Dentomaxillofac Radiol. 2013;42(8):20130145. https://doi.org/10.1259/dmfr.20130145. Epub 2013 Jul 5.

85. Mohagheghi S, Ahmadian A, Yaghoobee S. Accuracy assessment of a marker-free method for registration of CT and stereo images applied in image-guided implantology: a phantom study. J Craniomaxillofac Surg. 2014;42(8):1977–84. https://doi.org/10.1016/j.jcms.2014.09.002.

86. Parnia F, Fard EM, Mahboub F, Hafezeqoran A, Gavgani FE. Tomographic volume evaluation of submandibular fossa in patients requiring dental implants. Oral Surg Oral Med Oral Pathol Oral Radiol Endod. 2010;109(1):e32–6. https://doi.org/10.1016/j.tripleo.2009.08.035.

87. Al-Ekrish AA, Ekram M. A comparative study of the accuracy and reliability of multidetector computed tomography and cone beam computed tomography in the assessment of dental implant site dimensions. Dentomaxillofac Radiol. 2011;40(2):67–75. https://doi.org/10.1259/dmfr/27546065.

88. Al-Ekrish AA, Al-Shawaf R, Schullian P, Al-Sadhan R, Hörmann R, Widmann G. Validity of linear measurements of the jaws using ultralow-dose MDCT and the iterative techniques of ASIR and MBIR. Int J Comput Assist Radiol Surg. 2016;11(10):1791–801. https://doi.org/10.1007/s11548-016-1419-y. Epub 2016 Jun 2.

89. Kamiyama Y, Nakamura S, Abe T, Munakata M, Nomura Y, Watanabe H, Akiyama M, Kurabayashi T. Linear measurement accuracy of dental CT images obtained by 64-slice multidetector row CT: the effects of mandibular positioning and pitch factor at CT scanning. Implant Dent. 2012;21(6):496–501. https://doi.org/10.1097/ID.0b013e3182703387.

90. Saavedra-Abril JA, Balhen-Martin C, Zaragoza-Velasco K, Kimura-Hayama ET, Saavedra S, Stoopen ME. Dental multisection CT for the placement of oral implants: technique and applications. Radiographics. 2010;30(7):1975–91. https://doi.org/10.1148/rg.307105026.

91. Silva IM, Freitas DQ, Ambrosano GM, Bóscolo FN, Almeida SM. Bone density: comparative evaluation of Hounsfield units in multislice and cone-beam computed tomography. Braz Oral Res. 2012;26(6):550–6.

92. Nackaerts O, Maes F, Yan H, Couto Souza P, Pauwels R, Jacobs R. Analysis of intensity variability in multislice and cone beam computed tomography. Clin Oral Implants Res. 2011;22(8):873–9.

93. Aksoy U, Eratalay K, Tözüm TF. The possible association among bone density values, resonance frequency measurements, tactile sense, and histomorphometric evaluations of dental implant osteotomy sites: a preliminary study. Implant Dent. 2009;18(4):316–25.

94. Widmann G, Bischel A, Stratis A, Kakar A, Bosmans H, Jacobs R, Gassner E-M, Puelacher W, Pauwels R. Ultralow dose dentomaxillofacial CT imaging and iterative reconstruction techniques: variability of Hounsfield units and contrast-to-noise ratio. Br J Radiol. 2016;89:1060.

95. De Vos W, Casselman J, Swennen GR. Cone-beam computerized tomography (CBCT) imaging of the oral and maxillofacial region: a systematic review of the literature. Int J Oral Maxillofac Surg. 2009;38(6):609–25. https://doi.org/10.1016/j.ijom.2009.02.028.

96. Parsa A, Ibrahim N, Hassan B, van der Stelt P, Wismeijer D. Bone quality evaluation at dental implant site using multislice CT, micro-CT, and cone beam CT. Clin Oral Implants Res. 2015;26(1):e1–7. https://doi.org/10.1111/clr.12315. Epub 2013 Dec 11.

97. Van Dessel J, Nicolielo LF, Huang Y, Coudyzer W, Salmon B, Lambrichts I, Jacobs R. Accuracy and reliability of different cone beam computed tomography (CBCT) devices for structural analysis of alveolar bone in comparison with multislice CT and micro-CT. Eur J Oral Implantol. 2017;10(1):95–105.

98. Carrafiello G, Dizonno M, Colli V, Strocchi S, Pozzi Taubert S, Leonardi A, Giorgianni A, Barresi M, Macchi A, Bracchi E, Conte L, Fugazzola

C. Comparative study of jaws with multislice computed tomography and cone-beam computed tomography. Radiol Med. 2010;115(4):600–11. https://doi.org/10.1007/s11547-010-0520-5. Epub 2010 Feb 22.

99. Cremonini CC, Dumas M, Pannuti CM, Neto JB, Cavalcanti MG, Lima LA. Assessment of linear measurements of bone for implant sites in the presence of metallic artefacts using cone beam computed tomography and multislice computed tomography. Int J Oral Maxillofac Surg. 2011;40(8):845–50. https://doi.org/10.1016/j.ijom.2011.04.015.

100. Kamburoglu K, Yüksel S. A comparative study of the accuracy and reliability of multidetector CT and cone beam CT in the assessment of dental implant site dimensions. Dentomaxillofac Radiol. 2011;40(7):466–7. https://doi.org/10.1259/dmfr/30789406; author reply 468–9.

101. Naitoh M, Hirukawa A, Katsumata A, Ariji E. Evaluation of voxel values in mandibular cancellous bone: relationship between cone-beam computed tomography and multislice helical computed tomography. Clin Oral Implants Res. 2009;20(5):503–6. https://doi.org/10.1111/j.1600-0501.2008.01672.x.

102. Poeschl PW, Schmidt N, Guevara-Rojas G, Seemann R, Ewers R, Zipko HT, Schicho K. Comparison of cone-beam and conventional multislice computed tomography for image-guided dental implant planning. Clin Oral Investig. 2013;17(1):317–24. https://doi.org/10.1007/s00784-012-0704-6. Epub 2012 Mar 14.

103. Suomalainen A, Vehmas T, Kortesniemi M, Robinson S, Peltola J. Accuracy of linear measurements using dental cone beam and conventional multislice computed tomography. Dentomaxillofac Radiol. 2008;37(1):10–7. https://doi.org/10.1259/dmfr/14140281.

104. Schulze R, Heil U, Groβ D, et al. Artefacts in CBCT: a review. Dentomaxillofac Radiol. 2011;40(5):265–73. https://doi.org/10.1259/dmfr/30642039.

105. Barone A, Covani U, Cornelini R, Gherlone E. Radiographic bone density around immediately loaded oral implants. Clin Oral Implants Res. 2003;14:610–5.

106. Brosh T, Yekaterina BE, Pilo R, Shpack N, Geron S. Can cone beam CT predict the hardness of interradicular cortical bone? Head Face Med. 2014;10:12. https://doi.org/10.1186/1746-160X-10-12.

107. Fuster-Torres MÁ, Peñarrocha-Diago M, Peñarrocha-Oltra D, Peñarrocha-Diago M. Relationships between bone density values from cone beam computed tomography, maximum insertion torque, and resonance frequency analysis at implant placement: a pilot study. Int J Oral Maxillofac Implants. 2011;26:1051–6.

108. Harris D, Horner K, Gröndahl K, Jacobs R, Helmrot E, Benic GI, et al. E.A.O. guidelines for the use of diagnostic imaging in implant dentistry 2011. A consensus workshop organized by the European Association for Osseointegration at the Medical University of Warsaw. Clin Oral Implants Res. 2012;23:1243–53. https://doi.org/10.1111/j.1600-0501.2012.02441.x.

109. Sennerby L, Andersson P, Pagliani L, Giani C, Moretti G, Molinari M, et al. Evaluation of a novel cone beam computed tomography scanner for bone density examinations in preoperative 3D reconstructions and correlation with primary implant stability. Clin Implant Dent Relat Res. 2013;17:844. https://doi.org/10.1111/cid.12193.

110. Spin-Neto R, Gotfredsen E, Wenzel A. Variation in voxel value distribution and effect of time between exposures in six CBCT units. Dentomaxillofac Radiol. 2014;43:20130376. https://doi.org/10.1259/dmfr.20130376.

111. Tatli U, Salimov F, Kürkcü M, Akoğlan M, Kurtoğlu C. Does cone beam computed tomography-derived bone density give predictable data about stability changes of immediately loaded implants?: a 1-year resonance frequency follow-up study. J Craniofac Surg. 2014;25:e293–9. https://doi.org/10.1097/SCS.0000000000000727.

112. Tyndall DA, Price JB, Tetradis S, Ganz SD, Hildebolt C, Scarfe WC, American Academy of Oral and Maxillofacial Radiology. Position statement of the American Academy of Oral and Maxillofacial Radiology on selection criteria for the use of radiology in dental implantology with emphasis on cone beam computed tomography. Oral Surg Oral Med Oral Pathol Oral Radiol. 2012;113:817–26. https://doi.org/10.1016/j.oooo.2012.03.005.

113. Valiyaparambil JV, Yamany I, Ortiz D, Shafer DM, Pendrys D, Freilich M, et al. Bone quality evaluation: comparison of cone beam computed tomography and subjective surgical assessment. Int J Oral Maxillofac Implants. 2012;27:1271–7.

114. Liang X, Jacobs R, Hassan B, et al. A comparative evaluation of cone beam computed tomography and multislice CT. Part I. On subjective image quality. Eur J Radiol. 2010;75:265–9.

115. Nackaerts O, Depypere M, Zhang G, Vandenberghe B, Maes F, Jacobs R, SEDENTEXCT Consortium. Segmentation of trabecular jaw bone on cone beam CT datasets. Clin Implant Dent Relat Res. 2015;17(6):1082–91. https://doi.org/10.1111/cid.12217. Epub 2014 Mar 14.

116. Pauwels R, Nackaerts O, Bellaiche N, et al. Variability of dental cone beam computed tomography grey values for density estimations. Br J Radiol. 2013;86:20120135.

117. Pauwels R, Jacobs R, Singer SR, Mupparapu M. CBCT-based bone quality assessment: are Hounsfield units applicable? Dentomaxillofac Radiol. 2015a;44(1):20140238. https://doi.org/10.1259/dmfr.20140238.

118. Pauwels R, Faruangsaeng T, Charoenkarn T, Ngonphloy N, Panmekiate S. Effect of exposure parameters and voxel size on bone structure analysis in CBCT. Dentomaxillofac Radiol. 2015b;44:8.

119. Pauwels R, Araki K, Siewerdsen JH, Thongvigitmanee SS. Technical aspects of dental CBCT: state of the art. Dentomaxillofac Radiol. 2015c;44:1.

120. Vandenberghe B, Luchsinger S, Hostens J, Dhoore E, Jacobs R, SEDENTEXCT Project Consortium. The influence of exposure parameters on jawbone model accuracy using cone beam CT and multislice CT. Dentomaxillofac Radiol. 2012;41(6):466–74.

121. Guerra ENS, Almeida FT, Bezerra FV, Figueiredo PTDS, Silva MAG, Canto GDL, Pachêco-Pereira C, Leite AF. Capability of CBCT to identify patients with low bone mineral density: a systematic review. Dentomaxillofac Radiol. 2017;46:20160475.

122. Magill D, Beckmann N, Felice MA, Yoo T, Luo M, Mupparapu M. Investigation of dental cone-beam CT pixel data and a modified method for conversion to Hounsfield unit (HU). Dentomaxillofac Radiol. 2017;47:20170321.

123. Van Dessel J, Nicolielo LF, Huang Y, Slagmolen P, Politis C, Lambrichts I, Jacobs R. Quantification of bone quality using different cone beam computed tomography devices: accuracy assessment for edentulous human mandibles. Eur J Oral Implantol. 2016;9(4):411–24.

124. Stricker A, Jacobs R, Maes F, Fluegge T, Vach K, Fleiner J. Resorption of retromolar bone grafts after alveolar ridge augmentation-volumetric changes after 12 months assessed by CBCT analysis. Int J Implant Dent. 2021;7(1):7. https://doi.org/10.1186/s40729-020-00285-9. PMID: 33474648.

125. Damstra J, Fourie Z, Huddleston Slater JJ, Ren Y. Accuracy of linear measurements from cone-beam computed tomography derived surface models of different voxel sizes. Am J Orthod Dentofac Orthop. 2010;137(1):16.e11–6. https://doi.org/10.1016/j.ajodo.2009.06.016; discussion 16–17.

126. Fatemitabar SA, Nikgoo A. Multichannel computed tomography versus cone-beam computed tomography: linear accuracy of in vitro measurements of the maxilla for implant placement. Int J Oral Maxillofac Implants. 2010;25(3):499–505.

127. Fienitz T, Schwarz F, Ritter L, Dreiseidler T, Becker J, Rothamel D. Accuracy of cone beam computed tomography in assessing peri-implant bone defect regeneration: a histologically controlled study in dogs. Clin Oral Implants Res. 2011;23:882. https://doi.org/10.1111/j.1600-0501.2011.02232.x.

128. Jacobs R, Salmon B, Codari M, Hassan B, Bornstein MM. Cone beam computed tomography in implant dentistry: recommendations for clinical use. BMC Oral Health. 2018;18(1):88. https://doi.org/10.1186/s12903-018-0523-5. PMID: 29764458.

129. Ludlow JB, Laster WS, See M, Bailey LJ, Hershey HG. Accuracy of measurements of mandibular anatomy in cone beam computed tomography images. Oral Surg Oral Med Oral Pathol Oral Radiol Endod. 2007;103(4):534–42. https://doi.org/10.1016/j.tripleo.2006.04.008.

130. Razavi T, Palmer RM, Davies J, Wilson R, Palmer PJ. Accuracy of measuring the cortical bone thickness adjacent to dental implants using cone beam computed tomography. Clin Oral Implants Res. 2010;21(7):718–25. https://doi.org/10.1111/j.1600-0501.2009.01905.x.

131. Song D, Shujaat S, de Faria Vasconcelos K, Huang Y, Politis C, Lambrichts I, Jacobs R. Diagnostic accuracy of CBCT versus intraoral imaging for assessment of peri-implant bone defects. BMC Med Imaging. 2021;21(1):23. https://doi.org/10.1186/s12880-021-00557-9. PMID: 33568085.

132. Suphanantachat S, Tantikul K, Tamsailom S, Kosalagood P, Nisapakultorn K, Tavedhikul K. Comparison of clinical values between cone beam computed tomography and conventional intraoral radiography in periodontal and infrabony defect assessment. Dentomaxillofac Radiol. 2017;46(6):20160461.

133. Tomasi C, Bressan E, Corazza B, Mazzoleni S, Stellini E, Lith A. Reliability and reproducibility of linear mandible measurements with the use of a cone-beam computed tomography and two object inclinations. Dentomaxillofac Radiol. 2011;40(4):244–50. https://doi.org/10.1259/dmfr/1742330.

134. Tsutsumi K, Chikui T, Okamura K, Yoshiura K. Accuracy of linear measurement and the measurement limits of thin objects with cone beam computed tomography: effects of measurement directions and of phantom locations in the fields of view. Int J Oral Maxillofac Implants. 2011;26(1):91–100.

135. Vandenberghe B, Jacobs R, Yang J. Detection of periodontal bone loss using digital intraoral and cone beam computed tomography images: an in vitro assessment of bony and/or infrabony defects. Dentomaxillofac Radiol. 2008;37(5):252–60. https://doi.org/10.1259/dmfr/57711133.

136. Abrahams JJ. Dental CT imaging: a look at the jaw. Radiology. 2001;219:334–45.

137. Cohnen M, Kemper J, Möbes O, Pawelzik J, Mödder U. Radiation dose in dental radiology. Eur Radiol. 2002;12:634–7.

138. Liang X, Zhang Z, Gu J, Wang Z, Vandenberghe B, Jacobs R, Yang J, Ma G, Ling H, Ma X. Comparison of micro-CT and cone beam CT on the feasibility of assessing trabecular structures in mandibular condyle. Dentomaxillofac Radiol. 2017;46(5):20160435. https://doi.org/10.1259/dmfr.20160435. Epub 2017 Apr 26.

139. Panmekiate S, Ngonphloy N, Charoenkarn T, Faruangsaeng T, Pauwels R. Comparison of mandibular bone microarchitecture between micro-CT and CBCT images. Dentomaxillofac Radiol. 2015;44(5):20140322. https://doi.org/10.1259/dmfr.20140322.

140. Wang D, Künzel A, Golubovic V, Mihatovic I, John G, Chen Z, Becker J, Schwarz F. Accuracy of peri-implant bone thickness and validity of assessing bone

augmentation material using cone beam computed tomography. Clin Oral Investig. 2013a;17(6):1601–9. https://doi.org/10.1007/s00784-012-0841-y. Epub 2012 Oct 12.

141. Wang D, Künzel A, Golubovic V, Mihatovic I, John G, Chen Z, Becker J, Schwarz F. More about accuracy of peri-implant bone thickness and validity of assessing bone augmentation material using cone

beam computed tomography. Clin Oral Investig. 2013b;17(7):1787–8. https://doi.org/10.1007/s00784-013-0946-y. Epub 2013 Feb 21.

142. Schulze RKW, Berndt D, D'Hoedt B. On cone-beam computed tomography artifacts induced by titanium implants. Clin Oral Implants Res. 2010;21:100–7. https://doi.org/10.1111/j.1600-0501.2009.01817.x.

Biology of Low-Substitution Bone Substitutes

15

Richard J. Miron, Yufeng Zhang,
and Dieter D. Bosshardt

15.1 Introduction

In order to develop optimal implant sites either prior to or during implant surgery, a sufficient quantity of bone volume in the vertical and horizontal dimensions of the alveolar ridge is mandatory [1]. For these reasons, bone grafting materials have played both a pivotal and crucial role in modern-day implant dentistry. The concept of utilizing bone grafts in 'Guided Tissue/Bone Regeneration' (GTR/GBR) procedures dates back over 30 years when it was introduced to the field of periodontology and implant dentistry [2–5]. It is hard to imagine a modern implant dentistry textbook without mentioning the drastic impact of such procedures in everyday practice.

Today, an extensive array of bone grafts exists on the market. These range from autografts (derived from the same patient), allografts (derived from another human being), xenografts (derived from other animal species and plants), and synthetically fabricated alloplasts [6]. Each of these classes of bone grafts comes with vari-

ous handling properties, biocompatibility, surface geometry and chemistry, mechanical properties and degradation properties (Table 15.1). While autogenous bone has long been considered the gold standard due to its excellent combination of features including osteoconduction, osteoinduction, and osteogenesis [7, 8], alternative bone grafting materials available in higher supply with less patient morbidity have always been a desired end-goal of the clinician.

Allografts demonstrate an excellent replacement option with good osteoconductive properties and certain classes are known to be osteoinductive attributed to their release of bone morphogenetic proteins (BMPs) in demineralized grafts [9]. Furthermore, xenografts are a highly-utilized bone grafting material in many countries, especially in countries where the use of allografts is not permitted. It has since been revealed that, unlike allografts, xenografts typically do not undergo extensive resorption over time, and particularly the highly-investigated deproteinized bovine bone mineral (DBBM, Bio-Oss®, Geistlich, Switzerland) has been characterized as a slow-resorbing material due in large part to the material's non-resorbing properties over time even years after its implantation. The literature has often described these 'slow-resorbing' biomaterials as either non-resorbing, minimally-resorbing, slowly-resorbing, or low-substitution biomaterials. Below we highlight the widespread

R. J. Miron (✉) · D. D. Bosshardt
Department of Periodontology, University of Bern, Bern, Switzerland
e-mail: richard.miron@zmk.unibe.ch

Y. Zhang
Department of Oral Implantology, University of Wuhan, Wuhan, China

Table 15.1 Classification of bone grafting materials used for the regeneration of periodontal intrabony defects

Material characteristic	Ideal	Autograft	Allograft	Xenograft	Alloplast
Biocompatibility	+	+	+	+	+
Safety	+	+	+	+	+
Surface characteristics	+	+	+	+	+
Geometry	+	+	+	+	+
Handling	+	+	+/−	+	+
Mechanical characteristics	+	+	+/−	+	−
Osteogenic	+	+	−	−	−
Osteoinductivity	+	+	+/−	−	−
Osteoconductivity	+	+	+	+	+
Degradation Properties	+	+	+	+/−	+/−

use of slow-resorbing bone grafts in regenerative implant dentistry and discuss their impact on implant dentistry.

## 15.2 Use of Low-Substitution Materials in Contour Augmentation

While it was first relatively unknown to what extent bone resorption would occur following bone augmentation procedures with xenografts, the most prominent advantage of these biomaterials remains that augmented bone can be maintained years following their surgical implantation. Unlike allografts that are prone to dimensional ridge loss over time, xenografts tend to maintain their volume owing to their low-substitution properties. For these reasons, a variety of procedures in dentistry have since been adapted to take advantage of low-substitution rate materials; namely DBBM.

Implant placement in the esthetic zone has had many controversies relating to implant size, three-dimensional implant location, use of platform switching, and use of temporary crowns, among other things. The main concern has been the risk of a mucogingival recession occurring years after implant placement (typically found 5–6 years following immediate implant placement). For these reasons, Buser et al. [10] demonstrated high implant stability and bone volume on the facial aspect of implant surfaces years after placement when contour augmentation was performed with the slow-resorbing DBBM. In some of the most well-documented clinical studies on this topic, the likelihood of peri-implant soft tissue recession has been markedly reduced by following these protocols and by primarily utilizing slowly resorbing, particulate bone substitutes (Fig. 15.1).

Similarly, vertical bone augmentation has been one of the most difficult regenerative procedures to obtain predictable results. Several groups have further shown that the additional use of xenografts in combination with autografts is a way of preserving ideal bone volume years following regeneration when compared to the utilizing of autografts alone or allografts (Fig. 15.2). For these reasons, xenografts and low-substitution synthetic materials have also been utilized in such cases. Below, we highlight the experimental design and processing of typical histological parameters for the investigation of sections embedded in resin and paraffin and later investigate the nature of cells around low-substitution biomaterials and how to characterize them accordingly.
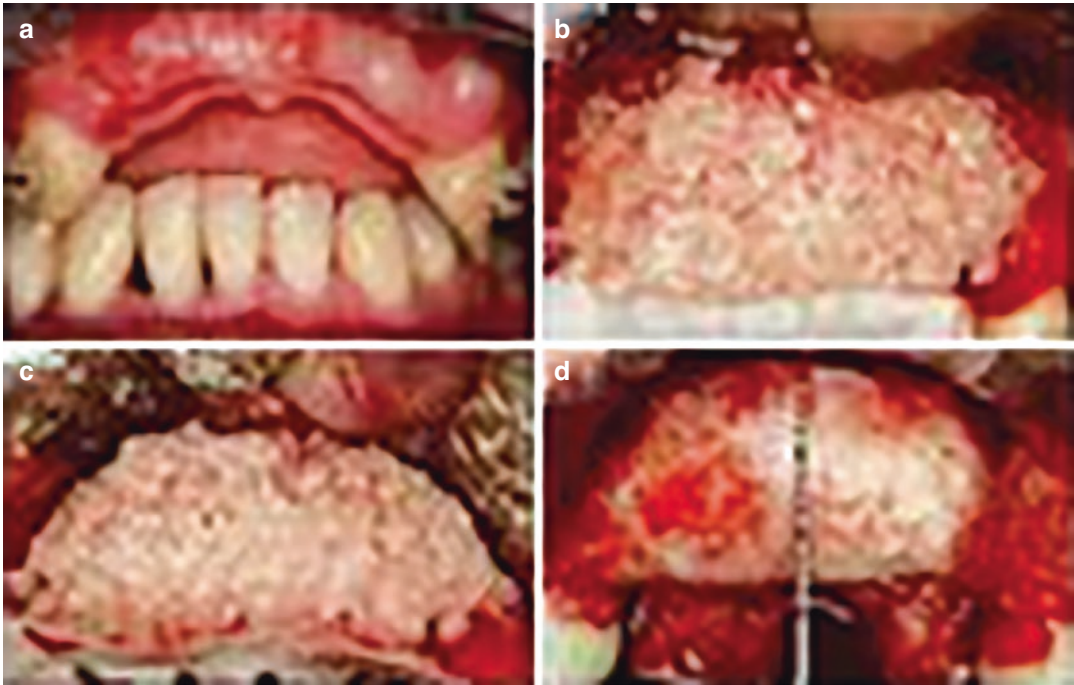
Fig. 15.1 (**a**) The bone-level implant is inserted in an appropriate three-dimensional position, leaving a crater-like defect on the facial aspect of the implant. The implant platform is located 2–3 mm apical to the midfacial cemen-toenamel junction of the adjacent central incisor. (**b**) The implant is positioned slightly to the palatal aspect with the exposed implant surface clearly inside the alveolar crest. (**c**) The endosseous portion of the defect is filled with autogenous bone chips, which were harvested at the nasal spine. (**d**) The site is overcontoured with a second layer of DBBM granules for contour augmentation. (**e**) The augmentation material is covered with a non-crosslinked collagen membrane applied with a double-layer technique. (**f**) After an incision is made in the periosteum, tension-free primary wound closure is achieved with fine, non-resorbable suture material. (Reprinted with permission from [10])
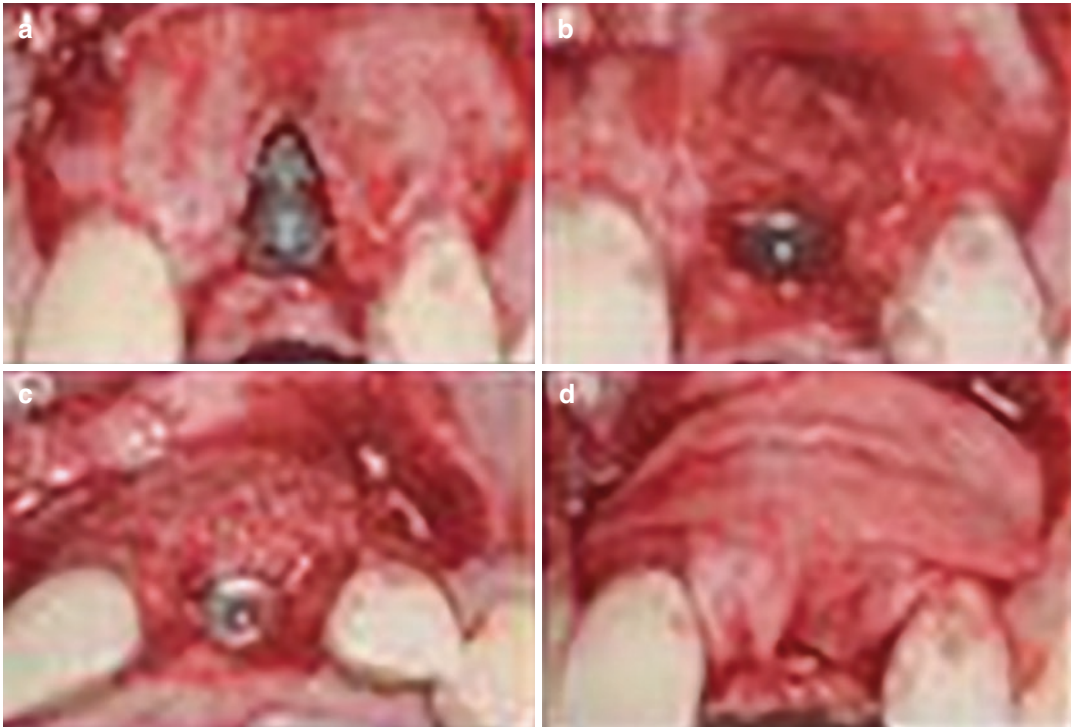
Fig. 15.2 (**a**) Labial view demonstrating a vertical defect after extraction of four incisors. (**b**, **c**) Labial and occlusal view of the particulate composite bone graft with autoge- nous bone and DBBM xenograft. (**d**) Labial view of the regenerated ridge after 9 months of healing. (Reprinted with permission from [11])

15.3   Typical Resin and Paraffin Embedding

Though the purpose of this chapter is not designed to elaborate on technical aspects of histology such as embedding and histological assessment of typical bone grafts, it is important to note that the majority of experimental designs investigating bone grafts are intended to quantify new bone formation and material resorption utilizing hard tissue resin sections due to their superior accuracy (Figs. 15.3, 15.4, and 15.5). While paraffin embedding has not been utilized as frequently to quantify new bone formation, it does however offer the advantage that sections can then be utilized to perform immunohistochemistry via different methods later discussed in this chapter. Below we showcase the specific protocols adapted for low-substitution bone grafts, with an emphasis placed on understanding how and why resorption occurs around bone biomaterials at both the cellular, molecular, and genetic levels.
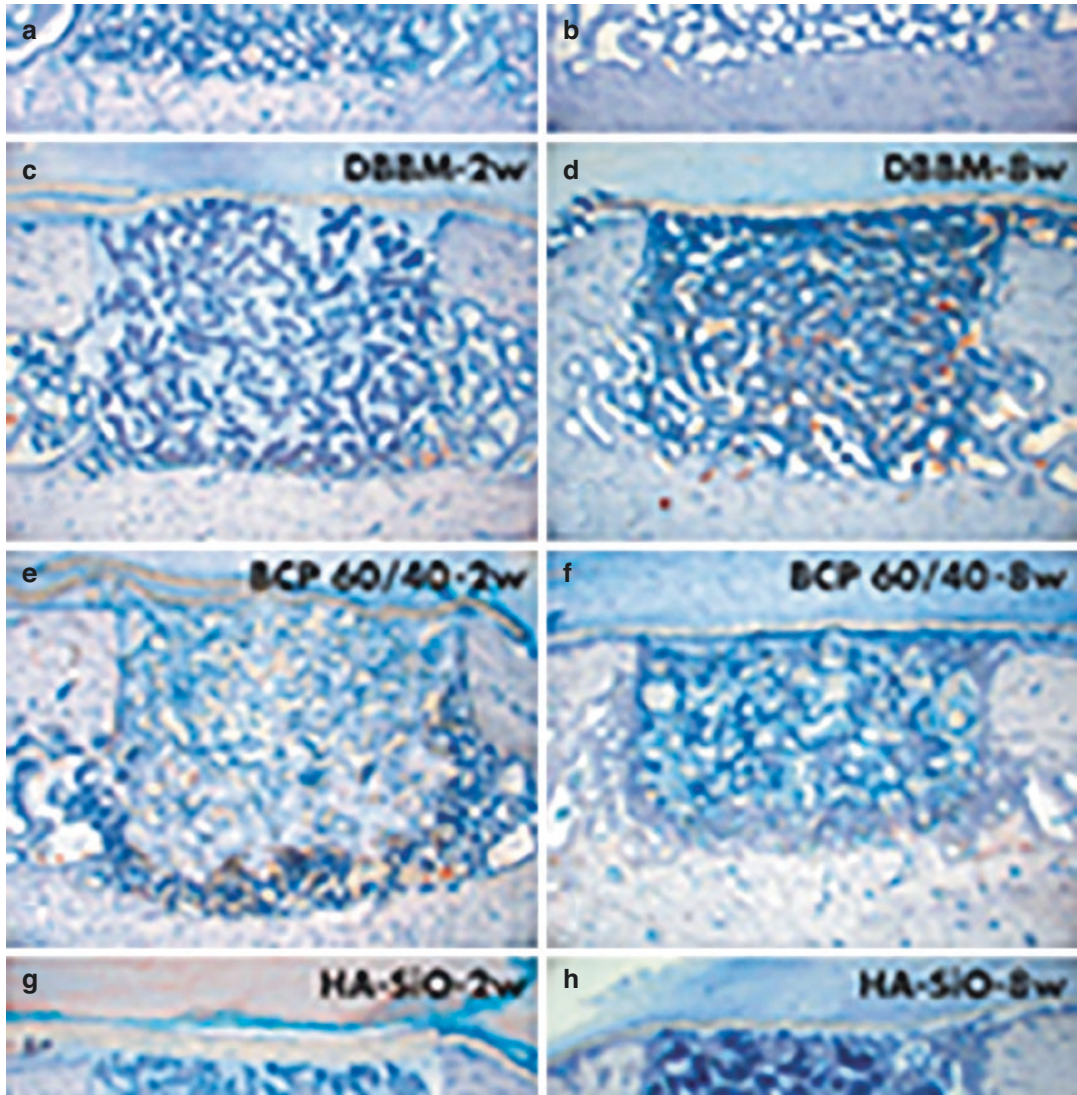
Fig. 15.3 Histological overview sections showing bone defects grafted with (**a**, **b**) autogenous bone, (**c**, **d**) DBBM, (**e**, **f**) BCP 60/40, and (**g**, **h**) HA-SiO, after (**a**, **c**, **e**, **g**) 2 and (**b**, **d**, **f**, **h**) 8 weeks of healing. In all defects, the bone fillers provide sufficient mechanical support for the barrier membrane. For all grafting materials, bone formation starts at the defect margins. However, penetration of the defect area with new bone occurs at different rates. (Reprinted with permission from [12])
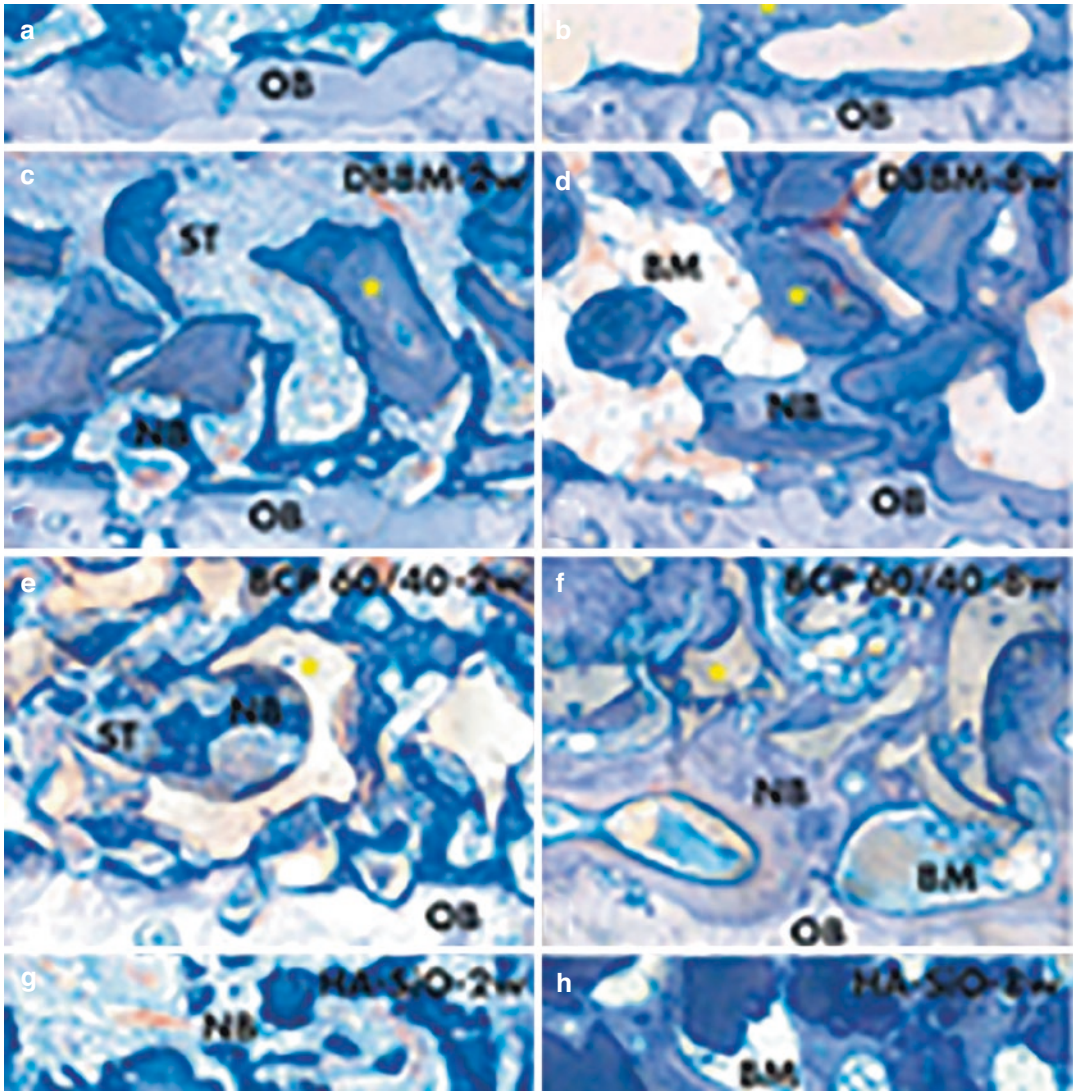
Fig. 15.4 Higher magnifications of the defect margins at the bottom of the defects grafted with (**a**, **b**) autogenous bone, (**c**, **d**) DBBM, (**e**, **f**) BCP 60/40, and (**g**, **h**) HA-SiO, after (**a**, **c**, **e**, **g**) 2 and (**b**, **d**, **f**, **h**) 8 weeks of healing. For all bone fillers, new bone (NB) is present in contact with old bone (OB) and interconnecting bone filler particles (*). Note that after 2 weeks, bone formation is most advanced for the autogenous bone group. In all groups, the soft tissue (ST) does not resemble bone marrow (BM). Most new bone is woven bone. However, conversion from woven bone to parallel-fibered bone formation is first observed in the autogenous bone group. After 8 weeks, dense and mature bone (i.e., woven bone reinforced by parallel-fibered bone) is observed in all groups. However, maturation of the bone marrow is most advanced in the autogenous bone group, as indicated by the presence of large bone marrow cavities and trabecular bone (**b**), followed by the DBBM (**d**), the HA-SiO (**h**), and the BCP 60/40 (**f**) groups. (Reprinted with permission from [12])
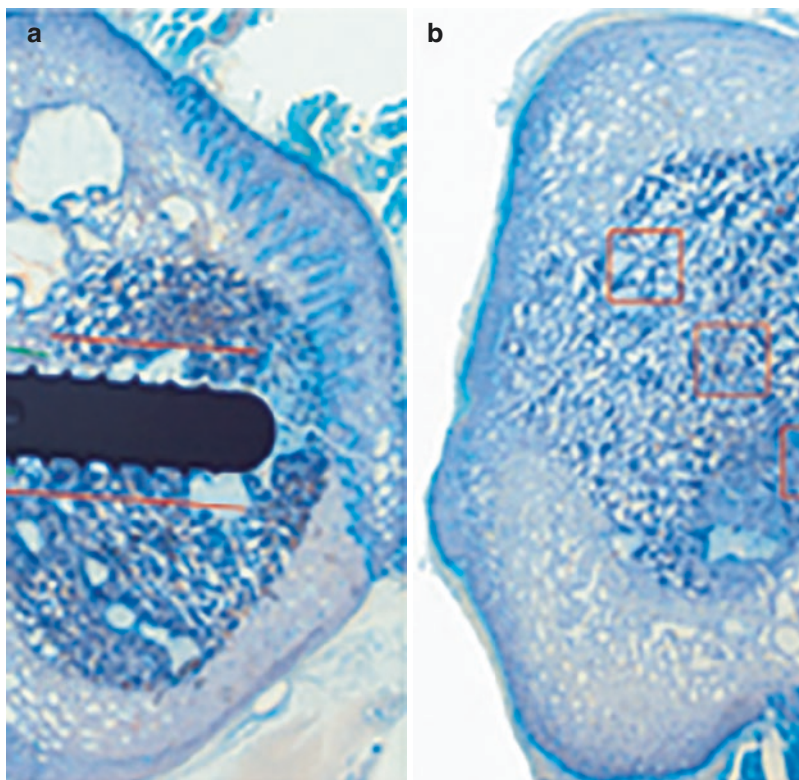
Fig. 15.5 Histologic overview sections showing regions of interest for the histomorphometric evaluation. (**a**) Overview, central section through the dental implant. The thickness of the original sinus wall is recorded as the average between the thickness on the mesial and on the distal aspect (green lines). In this case, the sinus wall around the implant is unusually thick due to the fact that the implant was placed in the area of a former sinus septum. The red lines delineate the area where the histomorphometric analysis of bone volume, DBBM volume, and osteocon-

duction was performed on the two central sections including the dental implant. (**b**) Overview section 5 mm mesial to the dental implant in the area of the former lateral window. The red squares indicate the areas where the histomorphometric evaluations were performed: a caudal-medial square, a central square, and a craniolateral square. In every other section, the order was shifted: a cranio-medial square, a central square, and a caudal-lateral square. (Reprinted with permission from [13])

15.4   Understanding Monocyte/ Macrophage Lineage Differentiation to Osteoclasts and Multi-Nucleated Giant Cells

Monocytes and macrophages are one of the most abundant cell types found in the body and represent the first cells that interact with implanted biomaterials such as bone grafts. Interestingly, while they are rapidly recruited to freshly implanted bone biomaterials, they also represent

the ability to polarize towards M1 pro-inflammatory macrophages or be associated with biomaterial tissue integration via M2 polarization [14]. Based on their crucial and distinct roles in tissue homeostasis and immunity, they have been deemed attractive therapeutic targets, and strategies in the biomaterial field are currently exploring their impact on tissue integration of various bone biomaterials [15]. It is now understood that macrophages are the major effector cells in bone tissue development and re(modeling) as well as biomaterial integration [15, 16]. Knockout ani-

mal models have clearly demonstrated that their loss around bone biomaterials is associated with a reduction in osteoinductivity [17].

This special subset of osteal macrophages (also referred to as "OsteoMacs") resides within the bone [18] and acts as the main driving force behind biomaterial integration (or non-integration). Interestingly, macrophages have also been known to fuse into large multi-nucleated giant cells that may polarize similarly to macrophages. Although it was once believed that all MNGCs around biomaterials were a sign of foreign body reaction and material rejection, more recently they have also been found associated with M2-related cytokines, growth factor expression, and material integration [19]. These cells have also more recently been identified to be distinctively different from osteoclasts [20]. While it is now well understood that MNGCs around certain classes of slow-resorbing bone grafts are distinctive from osteoclasts, their fusion from precursor cells including monocytes and macrophages, as well as their direct role in bone biomaterial integration remain extremely poorly understood. Furthermore, factors affecting their development and phenotypes towards more specialized cell types are also poorly understood.

Human histological samples derived from bone augmentation procedures performed within our dental clinics have shown that slow-resorption bone grafts are routinely surrounded by large MNGCs even years after their implantation [21] (Fig. 15.6). This led our research team to question the precise role of MNGCs, especially in this special subclass of bone biomaterials, as previously MNGCs have routinely been associated with a foreign body reaction [15]. In line with this same research direction, a group of studies in the cardiovascular field began to realize that calcified atherosclerotic plaque, which was once thought to be an inflammation-driven process, was shown to be associated with M2-macrophage polarization (not M1) with fusion towards MNGCs during the bone-forming process taking place [23–27]. While it is known that mineralized tissue formation found around arteries certainly represents a grave pathological state, our research team questioned whether such a situation would be advantageous around bone biomaterials. It
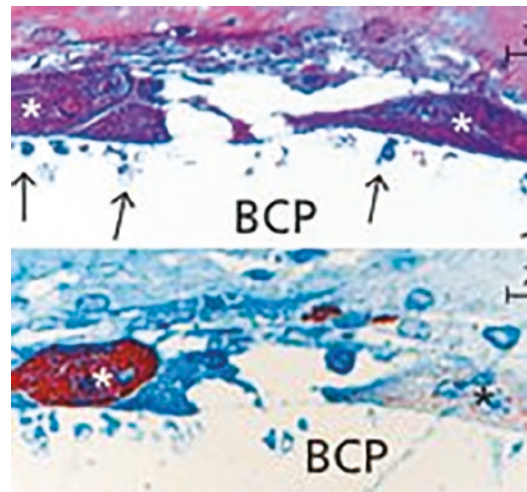
Fig. 15.6 MNGCs on Straumann® BoneCeramic (BCP). (Reprinted with permission from [22])

thus became clear that a substantial amount of additional research was needed to better understand this special class of cells including macrophage polarization and fusion towards MNGCs. For this reason, an entire chapter is dedicated to the necessary research protocols to better answer these important questions. Below we begin by elucidating the key monocyte differentiation pathways towards many cell types. While the focus is not to extensively review these pathways, it is important that clinicians/investigators alike understand the individual role and markers of these specific subsets of monocyte-derived cells in order to accurately identify them around bone biomaterials.

15.5 Monocyte to Macrophage Polarization Around Bone Biomaterials

The role of monocyte-derived macrophages has experienced a key shift in understanding. While it was once believed that the majority of macrophages were derived from monocytes, more recent evidence has in fact shown that monocytes do not substantially contribute to macrophage populations in the steady state [28]. More recent data from a number of studies opposed these initial viewpoints and found that the majority of

tissue-resident macrophages including OsteoMacs are self-renewing within host tissues [29–32].

Colony-stimulating factor 1 (CSF1, also known as M-CSF) is the most important growth factor for monocyte development. Knockout animal models where mice are deficient in CSF1 or its receptor CSF1R (CD115) exhibit severe malformations and monocytopenia [33–35]. In the late 1980s, two main subpopulations of monocytes were described either CD14+ monocytes (which can be further subdivided into distinct populations of CD14+CD16+ and CD14+CD16− monocytes) and CD14lowCD16+ monocytes [36]. It has been shown that under certain settings, IL-4 has been identified as a major modulator of macrophage proliferation [37] whereas CSF1 promotes both their proliferation and monocyte recruitment [38]. Macrophages are further known to secrete an entire range of growth factors and cytokines both owing to their role in either pro- or anti-inflammation [33, 39, 40]. For the detection of macrophages, the F4/80 monoclonal antibody has been most widespread and its expression is rapidly downregulated in osteoclasts [41].

Interestingly, more research over the past decade has pointed to the fact that macrophages may further be subdivided based on their polarization into classical M1 pro-inflammatory macrophages or M2 inflammation-resolution/wound healing macrophages (Fig. 15.7). Pro-inflammatory macrophages (M1) are created in response to LPS and TNF-alpha [42, 43], IL-6 [44, 45] and IL-1β [43, 46]. M2 macrophages are typically characterized based on their ability to secrete TGF-β and arginase, both implicators in tissue repair [47–50]. Table 15.2 summarizes some of the common M1 and M2 macrophage markers. M1 macrophages are produced in vitro with IFN-γ+ + LPS and TNF-α, whereas M2 macrophages have been subdivided into various classifications (Fig. 15.7) [52]. While it is known that IL-4 is the main cytokine responsible for M2 macrophage polarization [47–50, 52], subclasses including M2a, M2b, and M2c can be produced with IL-4 + IL-13 [49, 53–56], IgG-immune complexes and IL-1R ligands [57, 58] and IL-10 [58], respectively (Fig. 15.7). While macrophages and osteoclasts are both derived from the
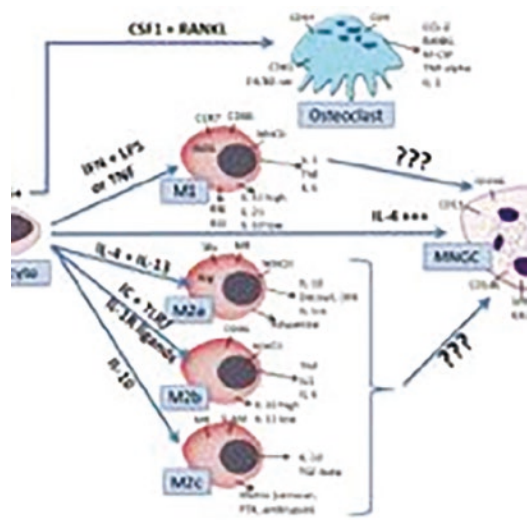
Fig. 15.7 Monocyte differentiation including expression markers into Osteoclasts, M1, M2a, M2b, M2c macrophages, and MNGCs. (Reprinted with permission from [15])

Table 15.2 Markers of macrophages of M1 and M2 phenotypes

M1	M2
B7 (CD80)	**M130 (CD163)**
B7.2 (CD86)	**CD206 (MRC1, mannose receptor)**
CCR7 (MCP-3)	**FceRII (CD23)**
CCL22 (MDC1)	**CD36**
CD64	
CXCL10 (IP-10)	IL-1 Ra
SOCS1	
TLR-2	Nucleotide receptors (GPR86, GPR105, P2Y8, P2Y11, P2Y12)
TLR-4	
FcyRIII (CD16)	C-type lectin-like receptor dectin-1
FcyRII (CD32)	DC-SIGN (CD209)
LAM-1 (CD62)	DCIR (CLECSF6)
IL-1 R1	CLACSF13
IL-7R (CD127)	FIZZ1, ST2 (mouse)
IL-2R (α chain)	Phagocyte receptors (SR-A, M60)
IL-15R (α chain)	CXCR4, fusin (CD184)
IL-17R (CTLA8) (CDw217)	TRAIL

Adapted from Novoselov et al. [51]
Highlighted bold markers present the most common

monocyte lineage, they can be clearly distinguished based on the presence of additional nuclei in osteoclasts as well as morphological features and expression markers presented later in this chapter [59, 60].

15.6 Multi-Nucleated Giant Cells as Previously Described: The Foreign Body Giant Cell

When original research began to notice the presence of MNGCs around either biomaterials or located throughout the human body, they were often characterized as being 'bad' cells associated with a foreign body reaction. As a result, original experiments focused on investigating their effects primarily in response to bacterial pathogens [61]. Since then, this field has expanded considerably with a number of synonyms including foreign-body giant cell (FBGC), foreign body cell (FBC), multinucleated cell (MNC), multinucleated giant cell (MNGC), or giant-body foreign cell (GBFC). These first experiments demonstrated how macrophages, in response to pathogens, formed large MNGCs (described as having 15 nuclei or more), whereas those found in response to low-virulence mycobacterium consistently produced MNGCs with seven or fewer nuclei [61]. It was therefore assumed that the larger the MNGC, the more serious the infection/inflammatory state.

To this day, when large MNGCs are found either around a biomaterial, they are routinely characterized as a foreign body reaction (which may not necessarily be the case in all scenarios) [62, 63]. Since no characteristic differences exist between FBGCs and MNGCs, our group recently proposed that the classical M1-macrophage fusion towards MNGCs be characterized as M1-MNGCs versus M2-MNGCs due to the ability for macrophages from both polarization states to form MNGCs.

15.7 Osteoclasts

Osteoclasts are by far the most characterized and well-researched multi-nucleated cells of the body. In fact, until recently, it was believed that all multi-nucleated cells around bone grafts were osteoclasts with no characterization possible differentiating between MNGCs and osteoclasts.

Osteoclasts produce a number of binding domains specific to osteoclasts including alpha$_v$beta$_3$ integrins which are absent from macrophage precursors [64]. These integrins bind through RGD peptide domains to bone matrix proteins to make podosome rings [65, 66]. One key differentiation factor needed for osteoclasts is the receptor activator of nuclear factor kappa-B ligand (RANKL) [34, 67–70]. Osteoprotegerin (OPG) is the antagonist of RANKL and binds to it to prevent osteoclast formation [71]. Over the past decade, more focused research has better-characterized osteoclasts specifically using expression profiles and surface marker recognition tools. Osteoclasts most commonly express calcitonin receptor (CTR or CT-R), tartrate-resistant acid phosphatase (TRAP), and RANK, as well as surface markers CD1a, CD40, CD83, and CD95/fas later discussed (Table 15.3).

Table 15.3 Expression of key cell surface markers in osteoclast and MNGCs

Cell surface marker	Osteoclast expression	MNGCs expression
Calcitonin receptor	+++	−
TRAP	+++	+
RANK	+++	−
Cathepsin K	+++	+/−
CD9	+	+
CD13	+	+
CD14	−	+/−
CD40	+/−	−
CD44	+	+
CD51	+	+/−
CD68	+	+++
CD86 (B7-2)	−	+++
CD98	+	+++
CD147	+	+
CD206	−	+
MMP9	+++	+
HLA-DR	−	+++
EMR1 (F4/80)	−	+/?
B7-H1 (PD-L1)	?	+++

For table purposes, + = expressed in cell-type, +++ = highly expressed in cell-type, − = not expressed in cell, +/− = expressed in certain studies, yet not expressed in others, ? = no study to date has investigated its expression

15.8   Recent Understanding of Multi-Nucleated Giant Cells

More recently, the expression patterns, binding motifs, fusion patterns, and surface markers of MNGCs have been studied; most notably around soft tissue biomaterials [72]. While MNGCs are not found abundantly in normal human tissues, they have commonly been reported in failing soft tissue implanted devices (from here forward referred to as M1-MNGCs) [73–77]. One hypothesis was that 'frustrated' macrophages would fuse in response to foreign particles too large in size in an attempt to better phagocytose the foreign biomaterial [75]. Some have in fact hypothesized that MNGCs found in soft tissues are the equivalent of bone-resorbing osteoclasts responsible for the degradation of biomaterials [78]. While this viewpoint is not opposed, it remains interesting to point out that MNGCs are also found around bone samples vastly different from osteoclasts [15].

Basic studies on MNGCs found that beta 1 and beta 2 integrins were the predominant binding domains of monocytes and macrophages induced by IL-4 cell-cell fusion during MNGC formation [79]. Furthermore, a variety of surface receptors during fusion include CD44, CD47, CD200, signal regulatory protein 1a, IL-4r, E-cadherin, and mannose receptors [72]. Other molecules found implicated in MNGC fusion, function or survival include STAT6, P2X7 receptor, and connexin 43 [80–83]. Interestingly, more recent basic in vitro work confirmed that IL-4 and IL-13 (both M2-polarization of macrophages) can induce the fusion and formation of MNGCs [84].

Other markers strongly expressed in MNGCs are HLA-DR, CD98, B7-2 (CD86), and B7-H1 (PD-L1), but not B7-1 (CD80) or B7-H2 (B7RP-1). In contrast, markers commonly expressed in osteoclasts include CTR or CT-R, TRAP, and RANK (Table 15.3). Furthermore, surface markers including CD1a, CD40, CD83, and CD95/fas are expressed highly in osteoclasts but found undetectable in soft tissue MNGCs [85]. Table 15.3 categorizes previous findings comparing expression profiles of osteoclasts and MNGCs.

15.9   Atherosclerotic 'Foam' Cells

One of the most interesting pieces of information regarding the ability of macrophages and MGNCs to induce new bone formation came from research conducted investigating atherosclerotic plaque around arteries. It has been well described in the literature that high levels of INF-gamma, a T-helper1 cytokine is one of the known inducers of M1 macrophage polarization in atherosclerosis [86]. During this pathology, macrophages ingest modified lipoproteins and secrete M1 pro-inflammatory mediators characterized as 'lipid-rich macrophages' or 'foam cells' contributing to lipid core buildup [87]. While it was originally thought that the build-up of macrophages involved classical M1 pro-inflammatory macrophages, in 2012 Oh et al. made the breakthrough discovery demonstrating that in fact these cells were M2-polarized [88]. For reasons still poorly understood, a transient shift in M1 macrophages towards M2 macrophages and even MNGC formation is done prior to their change from an inflammatory state towards one that induces ectopic mineralization of arteries. Current strategies in the cardiovascular field aim to in fact suppress M2 macrophage polarization to prevent calcification of arteries, a highly dangerous scenario and potentially life-threatening [88]. While it is interesting to point out how devastating this pathological situation may be, our research group also questioned whether such a situation would be bad around bone grafting materials. In summary, it remains interesting to point out how under one clinical situation, MNGC-producing bone around arteries is considered highly pathological, whereas in the context around bone, biomaterials may potentially be greatly therapeutic. Below we highlight key experimental designs to further investigate their role around low-substitution bone grafts.

15.9.1 Study Designs: Materials Related to Specific Procedures and Expected Outcomes—In Vitro Analysis

Perhaps the most well-performed study to date investigating the differences between macrophages, MNGCs, and osteoclasts was work conducted by ten Harkel et al. [89]. In their study, it was clearly shown that MNGCs cannot resorb bone. Following the isolation of CD14+ cells, cells were seeded on bovine cortical bone in 96-well plates to investigate the ability of each cell type to resorb bone. A cell concentration of 1.5×10^5 cells per 0.32 cm^2 (surface of one well) was utilized. The cells were cultured for 3 days with 25 ng/mL human recombinant M-CSF to produce macrophages. After 3 days, the concentration of M-CSF was reduced to 10 ng/mL for both MNGCs and osteoclast cultures until the end of the culture period. To produce MNGCs, 5 ng/mL human recombinant IL-4 and 5 ng/mL human recombinant IL-13 were added to the cultures for the duration of experiments. For the generation of osteoclasts, 2 ng/mL mouse recombinant RANK-L was added. Thereafter, a series of experiments were conducted utilizing histological staining, immunohistochemistry, transmission electron microscopy, confocal microscopy, and quantitative PCR. It was found that bone resorption occurred by osteoclasts but not macrophages or MNGCs (Fig. 15.8). While it was shown that MNGCs still formed actin rings similar to osteoclasts (Fig. 15.9), they did not form a ruffled border and neither were able to resorb bone. It was found that MNGCs dissolved parts of a biomimetic hydroxyapatite coating, very similar to what is observed clinically by several reports that find that MNGCs appear to degrade a very small portion of bone grafts in humans years after implantation but not further (Figs. 15.10 and 15.11).

This research clearly showed that IL-4 (an M2-macrophage marker) could sufficiently produce MNGCs on the bone that was non-resorbable. Therefore, future experiments now seek to investigate how macrophages/MNGCs/osteoclasts form and polarize on various bone grafting material surfaces. A series of three model sets of experiments have been proposed to achieve adequate testing to further evaluate bone grafts in vitro.

Summary Experimental Design 15.1 (Fig. 15.12): Investigation of Macrophage Behavior on Various Bone Grafts Including the Release of Cytokines and Growth Factors
The first set of experiments aims to investigate macrophage polarization on various bone grafts when compared to tissue culture plastic (TCP). Furthermore, macrophages cultured on TCP with LPS and IFN-gamma should be used as a negative control (M1 pro-inflammatory macrophages) or with IL4 and IL13 as a positive control (M2 tissue-healing macrophages). Thereafter macrophage polarization should be investigated via three methods including (1) surface marker recognition, (2) mRNA levels of various M1 and M2 macrophage markers via real-time PCR, and (3) cytokine expression via ELISA. Furthermore, the influence of bone graft surfaces should be investigated on macrophage attachment, cell morphology as well as fusion into MNGCs/osteoclasts over time as well as their ability to resorb the bone graft.

Proposed Summary of In Vitro Experimental Design: Part 1
1. Cell adhesion via an MTS assay at 4 and 8 h and cell shape via F-actin staining at 4 and 8 h
2. Cell numbers, shape, and multi-nucleated giant cell formation at 1, 3, and 7 days via F-actin staining
3. Expression of antibodies for M1 macrophage polarization including B7 (CD80), B7.2 (CD86), CCR7, CD64, and CCL22. Expression of antibody markers of M2 macrophage polarization including M2 macrophage polarization including M130 (CD163), CD206, CD23, and CD36 at 3 and 7 days post seeding according to Table 15.2.
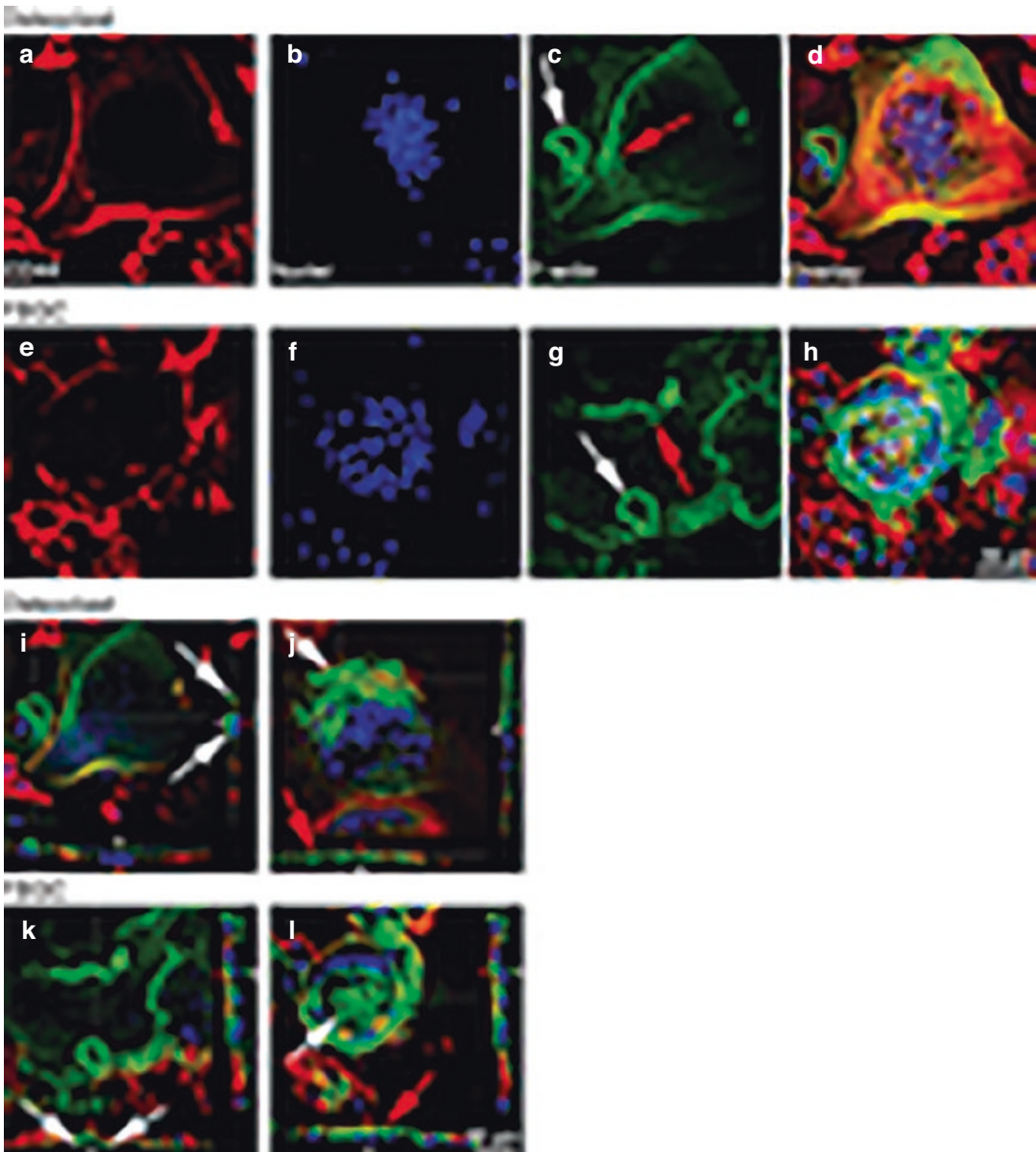
Fig. 15.8 Bone resorption by osteoclasts and FBGCs. After 25 days, cells were stained with Richardson's staining solution (**a**–**e**), and resorption pits were visualized (**c**–**f**) and quantified (**g**) using coomassie brilliant blue (CBB). Osteoclasts created resorption pits (Howship's lacunae) (**a**; black arrow) and formed a ruffled border (white arrow). No resorption pits nor ruffled borders were visible in the FBGC cultures (**d**, **e**). In the resorption pits, collagen fibrils were visible (**b**; black arrow). Numerous resorption pits were seen in the osteoclast culture (**c**; black arrow), but no signs of resorption were apparent in the FBGC cultures. Osteoclasts resorbed more than 20% of the bone surface (**g**). The percent bone resorption graph represents the mean area ± S.D. per 0.25 cm^2 bone surface. The scale bar is 10 μm for Panels (**a**), (**b**), (**d**), and (**e**). The scale bar is 100 μm for Panels (**c**) and (**f**). Red asterisk = bone. *$p < 0.05$, **$p < 0.01$. (Reprinted with permission from [89])
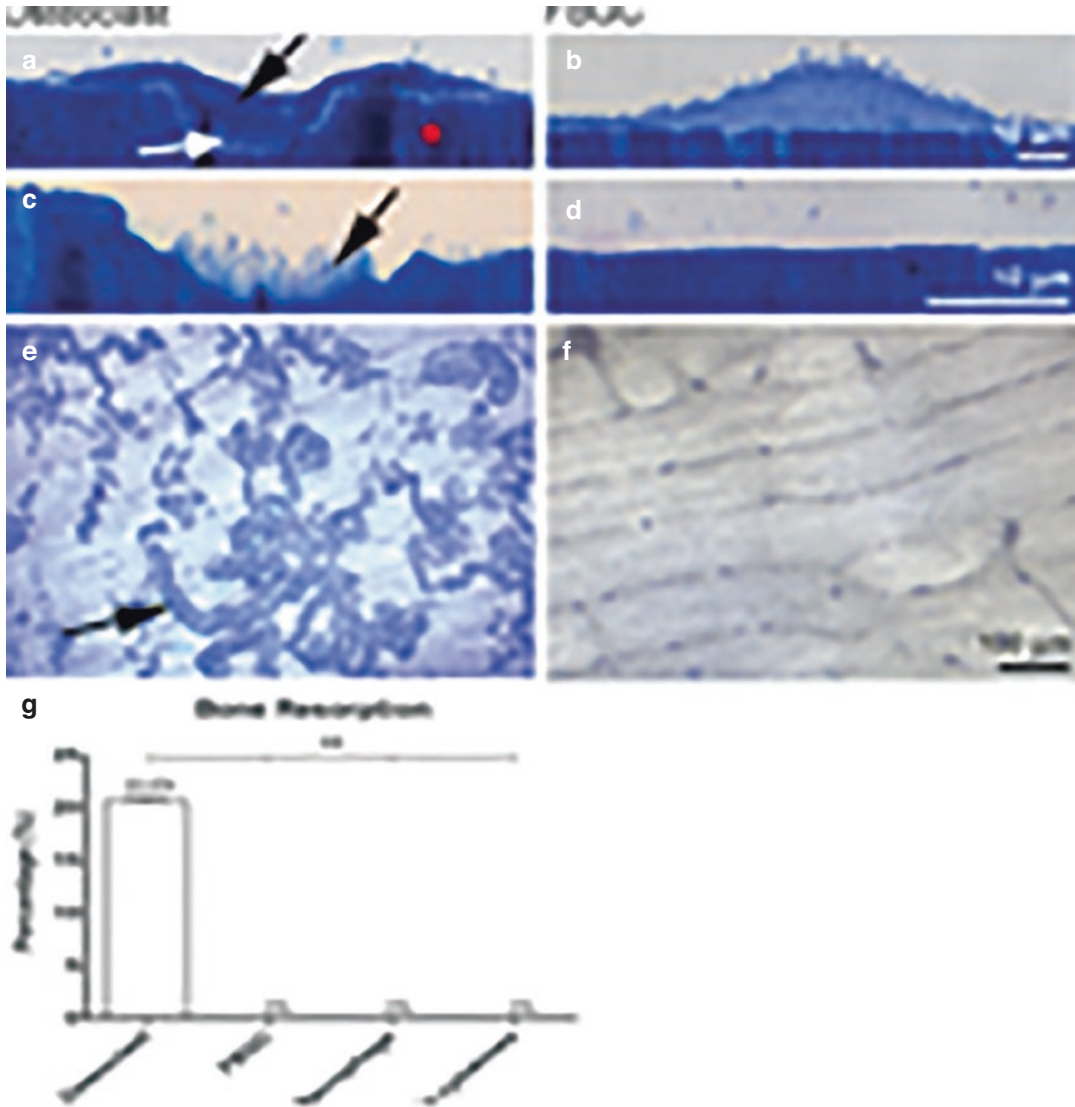
Fig. 15.9 Confocal microscopy of osteoclasts and FBGCs. Plasma membrane (red: CD44 antibody), nuclei (blue: Hoechst nuclei staining), and actin rings (green: phalloidin staining of F-actin) were fluorescently labeled after 25 days of culture on bone. Both cell types contained numerous nuclei (**a**, **b**, **e**, **f**), actin rings (**c**, **g**; white arrow), and podosome belts (**c**, **g**; red arrow). Sagittal views of both cell types composed from the apical side (white asterisk) showed actin structures resembling sealing zones (**i**, **k**; white arrows). Sagittal views composed from the basolateral side (red asterisk) of the cells showed round structures composed of actin (**j**, **i**; white arrow, red arrow). Scale bar = 50 μm. (Reprinted with permission from [89])

4. Expression of antibodies differentiating between osteoclasts and MNGCs (Table 15.3).
5. Real-time PCR is employed for genes including M1 macrophage polarization markers including TNF-alpha, IL-1beta, CCR7, IL-6, MMP2, MMP9, IFN-gamma, IL1-alpha, IL-12, and TLR4. M2 macrophage polarization markers will include CCL18, MDC, CD206, IL-10, CD36, Arg1, IL-4, and IL-1Ra at 3 and 7 days.
6. ELISA protein quantification is furthermore performed for genes including TNF-alpha, IL-1Beta, IL-6, IL-12, MMP2, and MMP9 for M1 macrophage polarization. Furthermore,
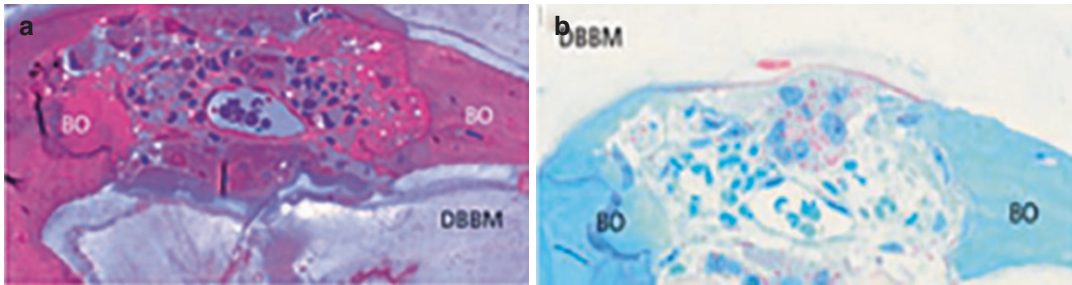
Fig. 15.10 (**a**) High magnification of a central part of a biopsy harvested from the anterior maxilla region of augmented bone with DBBM. MNGCs are observed on the surface of two DBBM particles otherwise covered with bone (BO). (**b**) TRAP staining of the neighboring section to (**a**). Discretely red-colored granules within the cyto-plasm of the MNGCs on the surface of the DBBM confirm them to be vaguely TRAP-positive. (**a**) and (**b**) panels were both stained with toluidine blue and basic fuchsin stains. The scale bar represent the same magnification in each panel. (Reprinted with permission from Jensen et al. 2014)
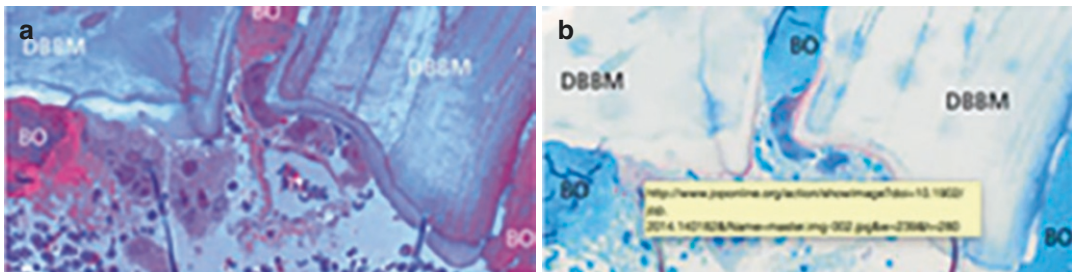
Fig. 15.11 (**a**) MNGCs observed on two DBBM particles facing periosteum after 29 months of healing. One of the MNGCs is located in a shallow concavity. (**b**) TRAP staining of the neighboring section to (**a**). No difference in TRAP staining intensity can be recognized between the MNGCs within this section compared with the ones in (**b**). BO = bone. (**a**) and (**b**) panels were both stained with toluidine blue and basic fuchsin stains. The scale bar represents the same magnification in each panel. (Reprinted with permission from Jensen et al. 2014)

IL-4, IL-10, CCL18, PDGF-BB, and TGFbeta1 will be investigated for M2 macrophage polarization at 3 and 7 days post-seeding.

The aim of Part 1 is to determine what bone grafts induce MNGC formation and determine which bone grafts are non-resorbable as previously described by ten Harkel et al. [89].

Summary Experimental Design 15.2 (Fig. 15.13): Effect of Released Cytokines from Macrophages on Osteoblast Cell Behavior

The first set of experiments aims to reveal the influence of the bone graft's surface topography/chemistry/composition on macrophage polarization and MNGC/osteoclast formation when com-pared to tissue culture plastic (TCP). Thereafter, macrophage-conditioned media (MCM) including all the cytokines released from macrophages will then be collected after 3 days and applied to human osteoblasts seeded on their corresponding bone grafts and investigated for cell wound-healing and tissue regrowth on various bone grafts. The experimental design will be investigated as follows.

Proposed Summary of In Vitro Experimental Design: Part 2

1. Effect of MCM on osteoblast attachment and cell shape at 4 and 8 h
2. Effect of MCM on osteoblast cell proliferation at 1, 3, and 7 days
3. Effect of MCM on osteoblast gene expression of collagen 1, fibronectin, vinculin, RUNX2,

Fig. 15.12 In vitro Model 1. Investigation of how macrophages interact with various bone grafting materials and their potential fusion towards osteoclasts and MNGCs

Fig. 15.13 In vitro Model 2: Investigation of culture media (CM) collected from macrophages/osteoclasts/MNGCs and their effect on bone-forming osteoblasts. This experimental design explores how released cytokines and growth factors from immune cells affect the bone formation of bone grafting materials
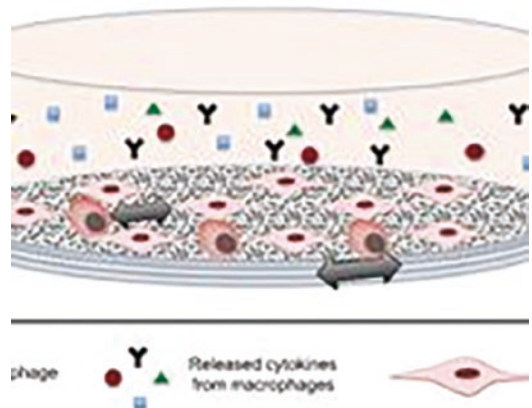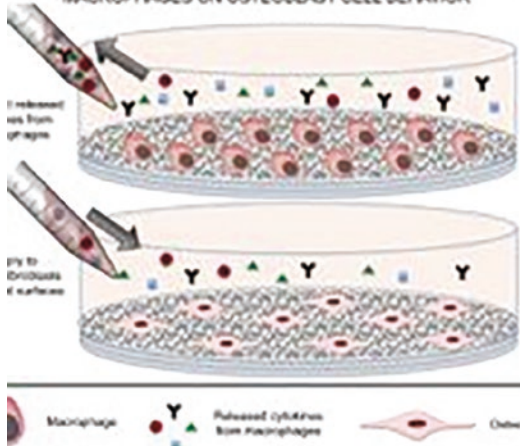
osteocalcin, and bone sialoprotein via real-time PCR at 3 and 14 days.

4. Effect of MCM on collagen 1 deposition, alkaline phosphatase, and alizarin red staining on bone grafts at 7 and 14 days

Fig. 15.14 In vitro Model 3: Investigation of how immune cells (macrophages) interact directly with bone-forming osteoblasts in a culture system with bone grafting materials. The ratio of macrophages and osteoblasts should be studied in a 1:6 ratio, proportional to what is found in the human body

Summary Experimental Design 15.3 (Fig. 15.14): Investigation of Osteoblast Behavior on Various Bone Grafts Co-cultured with Macrophages in a 6:1 Ratio (Human Ratio)

This set of experiments will culture macrophages directly with osteoblasts in a co-culture system in a 1:6 ratio as previously described [90]. Similar protocols from Experimental Designs 15.1 and 15.2 will be adapted accordingly.

The aim of model 3 is to determine if cell-cell contacts between macrophages and osteoblasts influence in vitro differentiation of osteoblasts and mineral deposition.

15.10 Conclusion from In Vitro Experiments

The totality of these experiments will reveal the prominent effects of immune cells (macrophages) on osteoblast behavior and further contribute to our understanding of the biological events taking place on different non-resorbable materials versus resorbable materials.

15.10.1 Study Designs: Materials-Related Specific Procedures and Expected Outcomes—In Vivo Analysis and Clinical Findings

To date, investigation of the expression patterns and markers of large MNGCs around bone grafting materials has been virtually omitted. The majority of tissue sections routinely analyzed for new bone formation are unfortunately embedded in hard sections (resin) complicating or even making impossible any potential immunohistochemical analysis. For these reasons, paraffin embedding is critical to further understanding differences between macrophage polarization, osteoclasts, and MNGCs around particles. Thus far, several studies have located MNGCs around slow-degrading bone grafting materials.

Jensen et al. [13] investigated the degradation of DBBM in a minipig model with bilateral sinus floor elevation (SFE) and simultaneous implant placement [13]. The two sides were randomized to receive large or small particle-size DBBM. Standard protocols investigating two time points (6 and 12 weeks) were utilized in five minipigs. ISQ values were recorded immediately after implant placement and at sacrifice. Qualitative histological differences were described and bone formation, DBBM degradation, bone-to-implant contact (BIC), and bone-to-DBBM contact (osteoconduction) were quantified histomorphometrically [13]. At 6 weeks, it was observed that three DBBM (*) particles in an area with early fibrous ingrowth showed signs of pronounced particle resorption (Fig. 15.15a). By 12 weeks it was found that DBBM particles were well integrated into bone and mature bone marrow with multiple MNGCs situated on a flat surface or in shallow concavities (arrows, Fig. 15.15b), unlike in Fig. 15.15a [13]. This potentially highlights the impact and importance of MNGCs originating from soft tissues versus bone tissues.

In a similar study performed by the same group, light and transmission electron micros-

copy was utilized to visualize MNGCs around slow-degrading DBBM and BCP particles [22]. Six defects were prepared bilaterally in the mandibular body of three mini-pigs. The defects were randomly grafted with either DBBM or BCP. After a healing period of 4 weeks, bone blocks were embedded in LR White resin. Three consecutive sections per defect were analyzed as follows: two with light microscopy using toluidine blue and tartrate-resistant acid phosphatase (TRAP) staining and one with transmission electron microscopy. MNGCs (*) situated on a DBBM surface of a particle demonstrated a surface beneath the MNGCs appearing unaffected or with only very shallow concavities (Fig. 15.16a, arrows). These cells stained positive for tartrate-resistant acid phosphatase (TRAP, Fig. 15.16b). TEM magnification of MNGC on DBBM reveals a sealing zone (SZ) and ruffled border (RB) (Fig. 15.16c, d) [22].

In one of the only human clinical studies investigating MNGCs around slow-degrading DBBM particles, Jensen et al. investigated in a case series various biopsies harvested from bone samples found in the esthetic zone augmented with DBBM [21]. Figure 15.17 demonstrates the cross-section overview of the biopsy after 74 months of healing [21]. In these samples, it was clearly observed that high magnification imaging of either the central part or DBBM particles facing the periosteum showed MNGCs around DBBM particles which were vaguely TRAP-positive, with little to no observable resorption of the bone grafting particles.

While it has since been concluded that MNGCs exist around certain classes of slow-degrading bone biomaterials and that their phenotype seems at least in part to be different from osteoclasts, little attempt has been made to further characterize them more accordingly using molecular and genetic means. In a recent review article titled: "Giant Cells around Bone Biomaterials: Osteoclasts or Multi-Nucleated Giant Cells?", our group characterized the markers that specifically differentiate between osteoblasts and MNGCs [91]. In this study, a specific
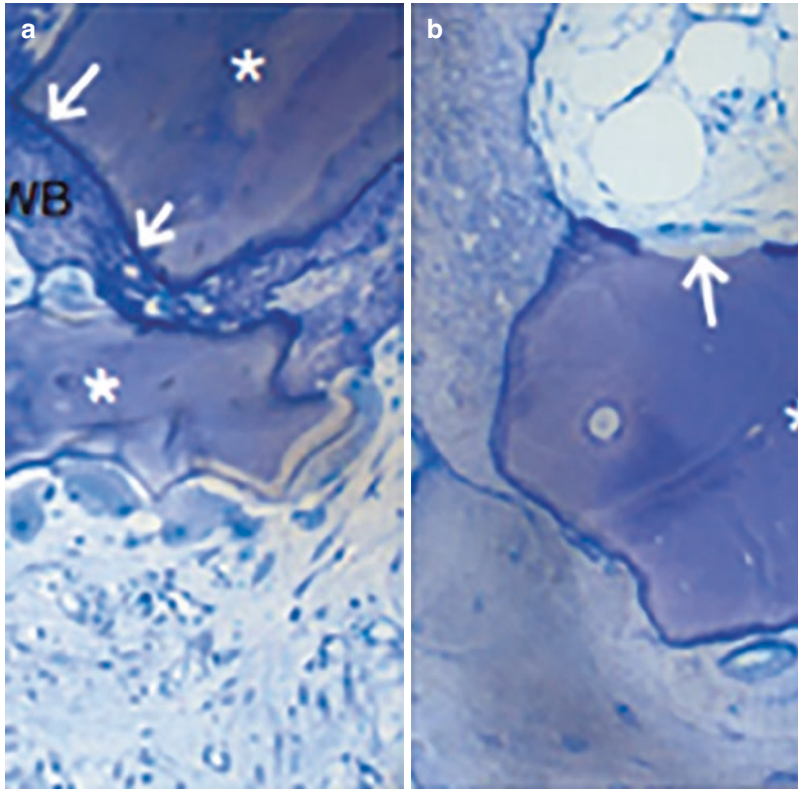
Fig. 15.15 Degradation of DBBM. (**a**) 6 weeks. Three DBBM (*) particles in an area with early fibrous ingrowth. One is covered with newly formed woven bone (WB), with what appears to be an intact particle surface (arrows). The two others, however, are captured in a cell-rich soft tissue, showing signs of pronounced resorption through multiple multinucleated osteoclast-like cells (OC). (**b**) 12 weeks. DBBM (*) particles are well integrated into bone and mature bone marrow. Where the DBBM surface is exposed to the bone marrow, multiple multinucleated osteoclast-like cells (OC) are observed. However, they are situated on a flat surface or in shallow concavities (arrows), unlike in (**a**). (Reprinted with permission from [13])

subset of markers can be utilized to characterize the difference between MNGCs and osteoclasts (Table 15.3). Furthermore, since the precursor cells of MNGCs are thought to be macrophages, MNGCs can further be investigated for their ability to polarize towards M1-MNGCs versus M2-MNGCs [91]. This allows future characterization potential to determine whether MNGCs around certain classes of non-resorbable bone grafts are either in a pro-inflammatory state (M1-MNGC) or tissue-resolving (M2-MNGC) state and may further aid in the future development of non-resorbable bone substitute materials. Figure 15.18 demonstrates one of the first documented cases whereby a large multi-nucleated cell around a bone biomaterial may be characterized as an MNGC and not an osteoclast based on its expression of CD86 and HLA-DR, both markers for MNGCs and non-expressed in osteoclasts [91].
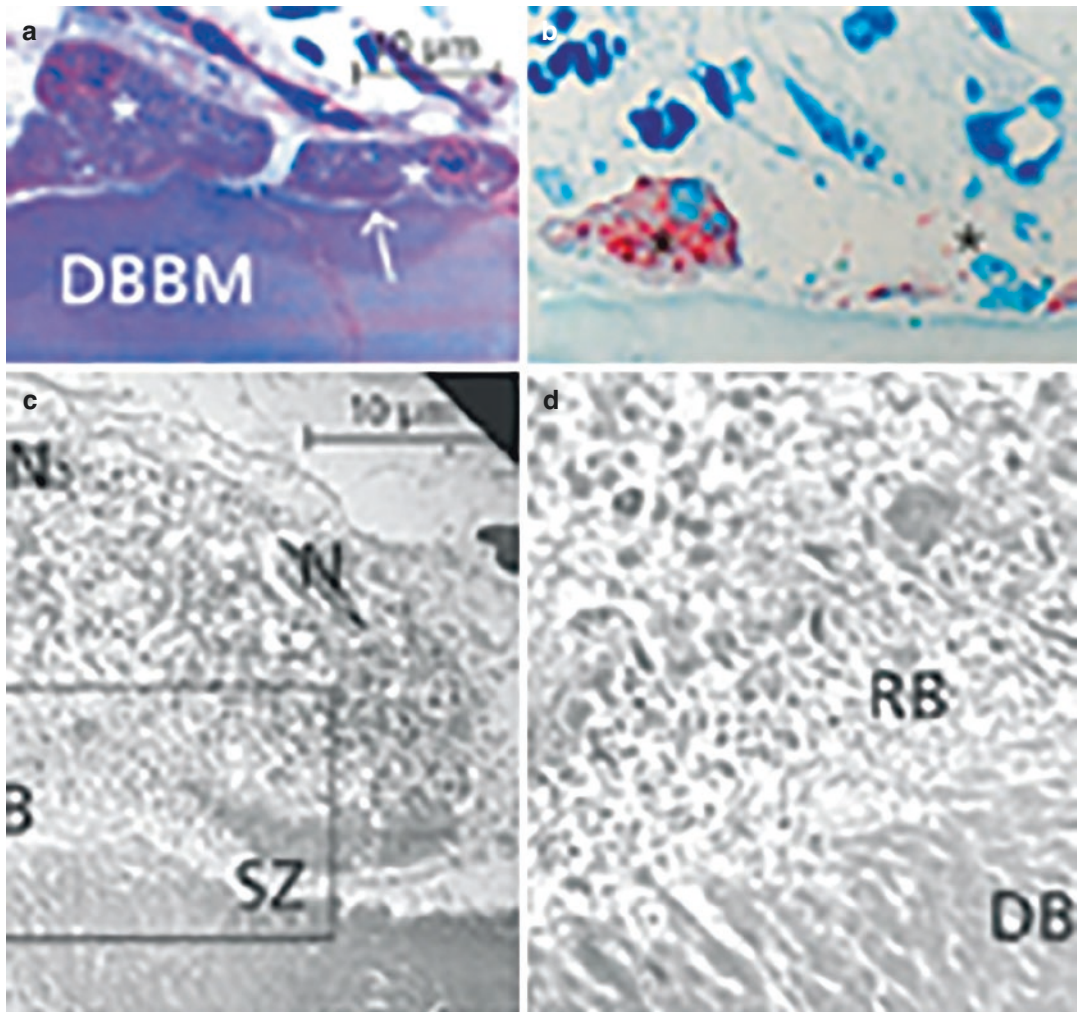
Fig. 15.16 (**a**) Multinucleated giant cells (MNGCs) (*) situated on a deproteinized bovine bone mineral (DBBM) surface of a particle placed inside the bone defect. The surface beneath the MNGCs appears unaffected or with only very shallow concavities (arrows). (**b**) A neighboring section demonstrates the multinucleated giant cells (*) on the surface of DBBM staining positive for tartrate-resistant acid phosphatase. However, the staining varies in intensity. (**c**) TEM magnification of MNGC on DBBM containing two nuclei. A sealing zone (SZ) and ruffled border (RB) are observed. (**d**) Higher magnification of the sealing zone (SZ) and ruffled border (RB). (Reprinted with permission from [22])

Fig. 15.17 Clinical pictures from harvesting of a biopsy (**a**) and the retrieved specimen (**b**). (**c**) Cross-section overview of biopsy after 74 months of healing. The convex side represents the central part of the biopsy, whereas the straight side faced the periosteum. Panel (**c**) was stained with toluidine blue and basic fuchsin stains. (Reprinted with permission from Jensen et al. 2014)
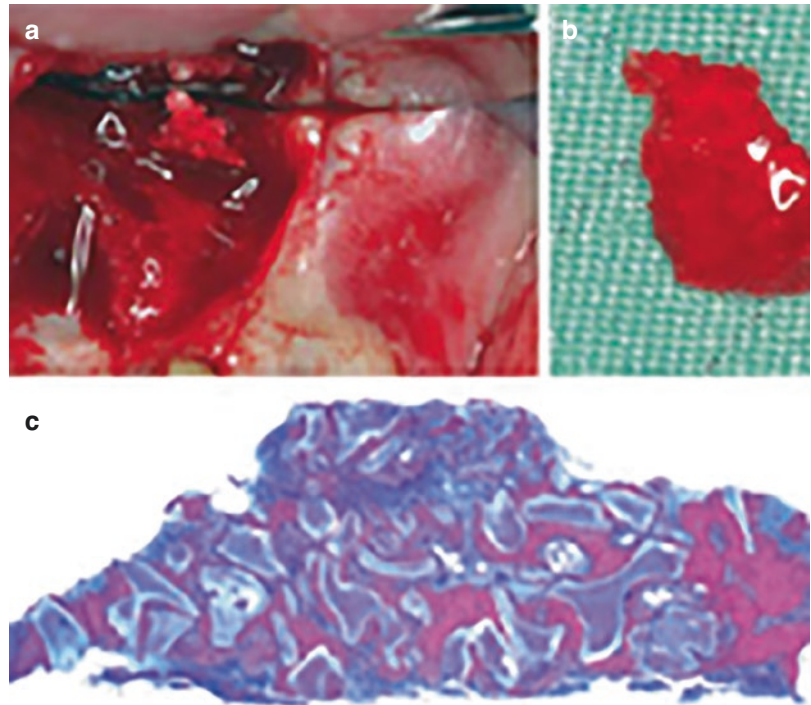
Fig. 15.18 Evidence of MNGC highly expressing CD86 and HLA-DR around a synthetic bone grafting material. Both CD86 and HLA-DR are exclusively expressed in MNGCs and are not expressed in osteoclasts. These cells also express TRAP (scale bar = 50 μm). (Reprinted with permission from [91])
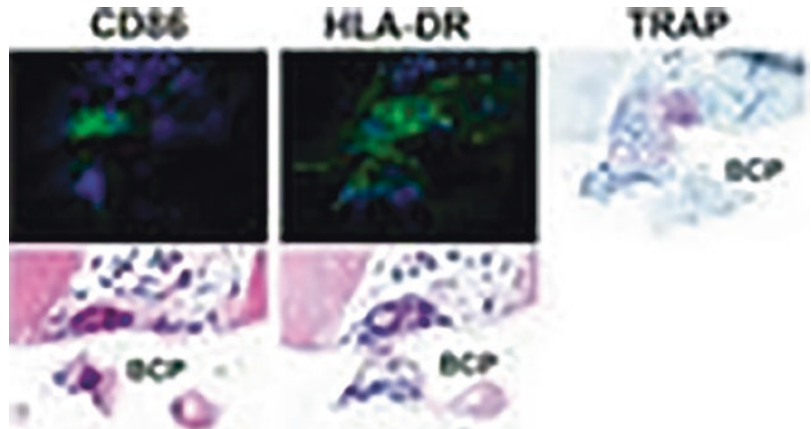
15.11 Expert Opinion

The comparison of slowly resorbable versus resorbable materials is certainly still in its infancy. About a decade ago, macrophage phenotyping around bone biomaterials was typically carried out using cell surface markers CD11b, CD68, macrophage antigen-2, and F4/80. More recently, an array of research has shown the marked impact of macrophages and their ability to either polarize into tissue-inflammatory M1 macrophages or tissue-resolving M2 macrophages or to further fuse into osteoclasts or MGNCs [58, 92–94]. As a result, gene expression profiles will surely be an avenue of future research to further investigate macrophage behavior in response to various bone biomaterials. Despite the presented summary of experimental designs to further advance the field, it remains clear that future studies to further investigate potential genes/tar-

gets that may be responsible for MNGC versus osteoclast formation remain necessary. These findings may further lead to reasons to explain why certain bone grafts are simply non-resorbable or minimally resorbed.

It may also be considered that specifically for bone biomaterials, the complexity to analyze tissue sections is exponentially more difficult since the majority of sections (whether old or new) were routinely embedded in resins, as opposed to paraffin. Therefore, immunohistochemistry is difficult (or even impossible) and new animal samples are therefore required as a result. Further complicating the situation is the fact that within the last decade, a major apparent difference has been reported with respect to the immune system between various animal species [95, 96]. This resulted in major difficulties in interpreting data generated in various animal models including rodents, canines, and minipigs when compared to humans. It remains therefore essential to better implement better protocols to investigate cells surrounding slowly resorbable materials utilizing new molecular strategies to better characterize them as opposed to only utilizing structural analysis. This has been a major focus of this book chapter and Tables 15.2 and 15.3 should aid the future study of non-resorbable materials to more accurately characterize macrophages, osteoclasts, and MNGCs around these special bone grafts. Future research by our group has already begun investigating various specific markers as highlighted in Table 15.4 either associated with osteoclasts or MNGCs. The future understanding of how monocytes and macrophages polarize and become non-resorbing giant cells remains completely unstudied with many open questions remaining.

Table 15.4 Advanced characterization of MNGCs around various non-resorbable bone grafting materials

	OC	MNGCs	M1φ	M2φ	DBBM_1	DBBM_2	DBBM_3	BCP_1	BCP_2	BCP_3
TRAP	++	+			++	++	++	++	++	++
CT-R	++	−			+/−	+/−	−	+/−	+	+/−
RANK	++	−			++	+	+/−	+	++	+/−
CTSK	++	+/−			++	++	+/−	+	++	+
MMP9	++	+	+	+	++	+/−	−	+/−	+/−	+
CD86	++	++	++	+	+	++	+	+/−	++	+/−
CD98	+	++			++	++	+	+/−	++	+
HLA-DR	−	++	+	+	++	+	++	+/−	++	+
B7-H1		++			++	++	+	+	+	+
EMR1 (F4/80)	+/−	+			+	+	+/−	−	++	+/−
CD68	+	++			++	++	++	++	++	++
CD13	+	+			++	+/−	+/−	+/−	+	−
CD80			++	+/−	++	+	+/−	+	++	+/−
CD197	−		++	−	+	−	+	+/−	+/−	+
CXCL10			+		+/−	+/−	−	−	−	−
CD64			++		++	+/−	+/−	+/−	++	+
CCL22		+		+	+	+/−	−	+/−	++	+
CD163				++	++	++	+/−	+/−	+	+
CD206	−	+	+/−	++	+	+	+/−	+/−	+	−
CD36	−	+		+	+	+/−	+	−	+	+
IL-1ra			+/−	+	+/−	+	−	+	+	+
SOCS1			+	+	+/−	+	−	+/−	+	+/−
CD23				+	+/−	+	−	−	−	+/−

Various surface markers (left column) were utilized to investigate the surface marker expression of either osteoclasts (OC), multi-nucleated giant cells (MNGCs), or M1 and M2 macrophages. Three bone biopsies of either DBBM or BCP were utilized and expression patterns were identified in their according table columns

References

1. Jung RE, Fenner N, Hammerle CH, Zitzmann NU. Long-term outcome of implants placed with guided bone regeneration (gbr) using resorbable and non-resorbable membranes after 12-14 years. Clin Oral Implants Res. 2013;24(10):1065–73.

2. Buser D, Dahlin C, Schenk R. Guided bone regeneration. Chicago, IL: Quintessence; 1994.

3. Buser D, Dula K, Belser U, Hirt HP, Berthold H. Localized ridge augmentation using guided bone regeneration. 1. Surgical procedure in the maxilla. Int J Periodont Restor Dent. 1993;13(1):29–45.

4. Dahlin C, Linde A, Gottlow J, Nyman S. Healing of bone defects by guided tissue regeneration. Plast Reconstr Surg. 1988;81(5):672–6.

5. Hardwick R, Dahlin C. Healing pattern of bone regeneration in membrane-protected defects: a histologic study in the canine mandible. Int J Oral Maxillofac Implants. 1994;9(1):13–29.

6. Miron RJ, Sculean A, Shuang Y, Bosshardt DD, Gruber R, Buser D, Chandad F, Zhang Y. Osteoinductive potential of a novel biphasic calcium phosphate bone graft in comparison with autographs, xenografts, and dfdba. Clin Oral Implants Res. 2016a;27(6):668–75.

7. Miron RJ, Gruber R, Hedbom E, Saulacic N, Zhang Y, Sculean A, Bosshardt DD, Buser D. Impact of bone harvesting techniques on cell viability and the release of growth factors of autografts. Clin Implant Dent Relat Res. 2013;15(4):481–9.

8. Miron RJ, Hedbom E, Saulacic N, Zhang Y, Sculean A, Bosshardt DD, Buser D. Osteogenic potential of autogenous bone grafts harvested with four different surgical techniques. J Dent Res. 2011;90(12):1428–33.

9. Sanz M, Vignoletti F. Key aspects on the use of bone substitutes for bone regeneration of edentulous ridges. Dent Mater. 2015;31(6):640–7.

10. Buser D, Chen ST, Weber HP, Belser UC. Early implant placement following single-tooth extraction in the esthetic zone: biologic rationale and surgical procedures. Int J Periodont Restor Dent. 2008;28(5):441.

11. Istvan A, Monje A, Wang DH-L. Vertical ridge augmentation and soft tissue reconstruction of the anterior atrophic maxillae: a case series. Int J Periodont Restor Dent. 2015;35:613–23.

12. Broggini N, Bosshardt DD, Jensen SS, Bornstein MM, Wang CC, Buser D. Bone healing around nanocrystalline hydroxyapatite, deproteinized bovine bone mineral, biphasic calcium phosphate, and autogenous bone in mandibular bone defects. J Biomed Mater Res B Appl Biomater. 2015;103(7):1478–87.

13. Jensen SS, Aaboe M, Janner SF, Saulacic N, Bornstein MM, Bosshardt DD, Buser D. Influence of particle size of deproteinized bovine bone mineral on new bone formation and implant stability after simultaneous sinus floor elevation: a histomorphometric study in minipigs. Clin Implant Dent Relat Res. 2015a;17(2):274–85.

14. Martinez FO, Gordon S. The m1 and m2 paradigm of macrophage activation: time for reassessment. F1000prime Rep. 2014;6:13.

15. Miron RJ, Bosshardt DD. Osteomacs: key players around bone biomaterials. Biomaterials. 2016;82:1–19.

16. Batoon L, Millard SM, Raggatt LJ, Pettit AR. Osteomacs and bone regeneration. Curr Osteopor Rep. 2017;15(4):385–95.

17. Davison NL, Gamblin AL, Layrolle P, Yuan H, de Bruijn JD, Barrere-de Groot F. Liposomal clodronate inhibition of osteoclastogenesis and osteoinduction by submicrostructured beta-tricalcium phosphate. Biomaterials. 2014;35(19):5088–97.

18. Chang MK, Raggatt LJ, Alexander KA, Kuliwaba JS, Fazzalari NL, Schroder K, Maylin ER, Ripoll VM, Hume DA, Pettit AR. Osteal tissue macrophages are intercalated throughout human and mouse bone lining tissues and regulate osteoblast function in vitro and in vivo. J Immunol. 2008;181(2):1232–44.

19. Vasconcelos DP, Costa M, Amaral IF, Barbosa MA, Aguas AP, Barbosa JN. Modulation of the inflammatory response to chitosan through m2 macrophage polarization using pro-resolution mediators. Biomaterials. 2015;37:116–23.

20. Barbeck M, Booms P, Unger R, Hoffmann V, Sader R, Kirkpatrick CJ, Ghanaati S. Multinucleated giant cells in the implant bed of bone substitutes are foreign body giant cells-new insights into the material-mediated healing process. J Biomed Mater Res A. 2017;105(4):1105–11.

21. Jensen SS, Bosshardt DD, Gruber R, Buser D. Long-term stability of contour augmentation in the esthetic zone: histologic and histomorphometric evaluation of 12 human biopsies 14 to 80 months after augmentation. J Periodontol. 2014;85(11):1549–56.

22. Jensen SS, Gruber R, Buser D, Bosshardt DD. Osteoclast-like cells on deproteinized bovine bone mineral and biphasic calcium phosphate: light and transmission electron microscopical observations. Clin Oral Implants Res. 2015b;26(8):859–64.

23. Chistiakov DA, Bobryshev YV, Nikiforov NG, Elizova NV, Sobenin IA, Orekhov AN. Macrophage phenotypic plasticity in atherosclerosis: the associated features and the peculiarities of the expression of inflammatory genes. Int J Cardiol. 2015a;184:436–45.

24. Chistiakov DA, Bobryshev YV, Orekhov AN. Changes in transcriptome of macrophages in atherosclerosis. J Cell Mol Med. 2015b;19(6):1163–73.

25. Mills CD, Lenz LL, Ley K. Macrophages at the fork in the road to health or disease. Front Immunol. 2015;6:59.

26. Roma-Lavisse C, Tagzirt M, Zawadzki C, Lorenzi R, Vincentelli A, Haulon S, Juthier F, Rauch A, Corseaux D, Staels B, et al. M1 and m2 macrophage proteolytic and angiogenic profile analysis in atherosclerotic patients reveals a distinctive profile in type 2 diabetes. Diab Vasc Dis Res. 2015;12(4):279–89.

27. Swier VJ, Tang L, Radwan MM, Hunter WJ III, Agrawal DK. The role of high cholesterol-high fructose diet on coronary arteriosclerosis. Histol Histopathol. 2015;31:167.

28. Wynn TA, Chawla A, Pollard JW. Macrophage biology in development, homeostasis and disease. Nature. 2013;496(7446):445–55.

29. Davies LC, Jenkins SJ, Allen JE, Taylor PR. Tissue-resident macrophages. Nat Immunol. 2013a;14(10):986–95.

30. Davies LC, Rosas M, Jenkins SJ, Liao CT, Scurr MJ, Brombacher F, Fraser DJ, Allen JE, Jones SA, Taylor PR. Distinct bone marrow-derived and tissue-resident macrophage lineages proliferate at key stages during inflammation. Nat Commun. 2013b;4:1886.

31. Hashimoto D, Chow A, Noizat C, Teo P, Beasley MB, Leboeuf M, Becker CD, See P, Price J, Lucas D, et al. Tissue-resident macrophages self-maintain locally throughout adult life with minimal contribution from circulating monocytes. Immunity. 2013;38(4):792–804.

32. Winkler IG, Sims NA, Pettit AR, Barbier V, Nowlan B, Helwani F, Poulton IJ, van Rooijen N, Alexander KA, Raggatt LJ, et al. Bone marrow macrophages maintain hematopoietic stem cell (hsc) niches and their depletion mobilizes hscs. Blood. 2010;116(23):4815–28.

33. Cecchini MG, Dominguez MG, Mocci S, Wetterwald A, Felix R, Fleisch H, Chisholm O, Hofstetter W, Pollard JW, Stanley ER. Role of colony stimulating factor-1 in the establishment and regulation of tissue macrophages during postnatal development of the mouse. Development. 1994;120(6):1357–72.

34. Dai XM, Ryan GR, Hapel AJ, Dominguez MG, Russell RG, Kapp S, Sylvestre V, Stanley ER. Targeted disruption of the mouse colony-stimulating factor 1 receptor gene results in osteopetrosis, mononuclear phagocyte deficiency, increased primitive progenitor cell frequencies, and reproductive defects. Blood. 2002;99(1):111–20.

35. Wiktor-Jedrzejczak W, Gordon S. Cytokine regulation of the macrophage (m phi) system studied using the colony stimulating factor-1-deficient op/op mouse. Physiol Rev. 1996;76(4):927–47.

36. Passlick B, Flieger D, Ziegler-Heitbrock HW. Identification and characterization of a novel monocyte subpopulation in human peripheral blood. Blood. 1989;74(7):2527–34.

37. Jenkins SJ, Ruckerl D, Cook PC, Jones LH, Finkelman FD, van Rooijen N, MacDonald AS, Allen JE. Local macrophage proliferation, rather than recruitment from the blood, is a signature of th2 inflammation. Science. 2011;332(6035):1284–8.

38. Jenkins SJ, Ruckerl D, Thomas GD, Hewitson JP, Duncan S, Brombacher F, Maizels RM, Hume DA, Allen JE. Il-4 directly signals tissue-resident macrophages to proliferate beyond homeostatic levels controlled by csf-1. J Exp Med. 2013;210(11):2477–91.

39. Hume DA, Ross IL, Himes SR, Sasmono RT, Wells CA, Ravasi T. The mononuclear phagocyte system revisited. J Leukoc Biol. 2002;72(4):621–7.

40. Theurl I, Fritsche G, Ludwiczek S, Garimorth K, Bellmann-Weiler R, Weiss G. The macrophage: a cellular factory at the interphase between iron and immunity for the control of infections. Biometals. 2005;18(4):359–67.

41. Austyn JM, Gordon S. F4/80, a monoclonal antibody directed specifically against the mouse macrophage. Eur J Immunol. 1981;11(10):805–15.

42. Kobayashi K, Takahashi N, Jimi E, Udagawa N, Takami M, Kotake S, Nakagawa N, Kinosaki M, Yamaguchi K, Shima N, et al. Tumor necrosis factor alpha stimulates osteoclast differentiation by a mechanism independent of the odf/rankl-rank interaction. J Exp Med. 2000;191(2):275–86.

43. Stacey KJ, Sweet MJ, Hume DA. Macrophages ingest and are activated by bacterial DNA. J Immunol. 1996;157(5):2116–22.

44. Lipford GB, Sparwasser T, Bauer M, Zimmermann S, Koch ES, Heeg K, Wagner H. Immunostimulatory DNA: sequence-dependent production of potentially harmful or useful cytokines. Eur J Immunol. 1997;27(12):3420–6.

45. Sparwasser T, Miethke T, Lipford G, Erdmann A, Hacker H, Heeg K, Wagner H. Macrophages sense pathogens via DNA motifs: induction of tumor necrosis factor-alpha-mediated shock. Eur J Immunol. 1997;27(7):1671–9.

46. Jimi E, Nakamura I, Duong LT, Ikebe T, Takahashi N, Rodan GA, Suda T. Interleukin 1 induces multinucleation and bone-resorbing activity of osteoclasts in the absence of osteoblasts/stromal cells. Exp Cell Res. 1999;247(1):84–93.

47. Heymann F, Trautwein C, Tacke F. Monocytes and macrophages as cellular targets in liver fibrosis. Inflamm Allergy Drug Targets. 2009;8(4):307–18.

48. Moreira AP, Hogaboam CM. Macrophages in allergic asthma: fine-tuning their pro- and anti-inflammatory actions for disease resolution. J Interf Cytokine Res. 2011;31(6):485–91.

49. Mosser DM, Edwards JP. Exploring the full spectrum of macrophage activation. Nat Rev Immunol. 2008;8(12):958–69.

50. Ricardo SD, van Goor H, Eddy AA. Macrophage diversity in renal injury and repair. J Clin Invest. 2008;118(11):3522–30.

51. Novoselov VV, Sazonova MA, Ivanova EA, Orekhov AN. Study of the activated macrophage transcriptome. Exp Mol Pathol. 2015;99(3):575–80.

52. Novak ML, Koh TJ. Macrophage phenotypes during tissue repair. J Leukoc Biol. 2013;93(6):875–81.

53. Gordon S. Alternative activation of macrophages. Nat Rev Immunol. 2003;3(1):23–35.

54. Louis CA, Mody V, Henry WL Jr, Reichner JS, Albina JE. Regulation of arginase isoforms i and ii by il-4 in cultured murine peritoneal macrophages. Am J Physiol. 1999;276(1 Pt 2):R237–42.

55. Mosser DM. The many faces of macrophage activation. J Leukoc Biol. 2003;73(2):209–12.

56. Song E, Ouyang N, Horbelt M, Antus B, Wang M, Exton MS. Influence of alternatively and classically

activated macrophages on fibrogenic activities of human fibroblasts. Cell Immunol. 2000;204(1):19–28.

57. Anderson CF, Gerber JS, Mosser DM. Modulating macrophage function with igg immune complexes. J Endotoxin Res. 2002;8(6):477–81.

58. Stout RD, Jiang C, Matta B, Tietzel I, Watkins SK, Suttles J. Macrophages sequentially change their functional phenotype in response to changes in microenvironmental influences. J Immunol. 2005;175(1):342–9.

59. Boyle WJ, Simonet WS, Lacey DL. Osteoclast differentiation and activation. Nature. 2003;423(6937):337–42.

60. Gordon S, Taylor PR. Monocyte and macrophage heterogeneity. Nat Rev Immunol. 2005;5(12):953–64.

61. Lay G, Poquet Y, Salek-Peyron P, Puissegur MP, Botanch C, Bon H, Levillain F, Duteyrat JL, Emile JF, Altare F. Langhans giant cells from m. Tuberculosis-induced human granulomas cannot mediate mycobacterial uptake. J Pathol. 2007;211(1):76–85.

62. Lorenz J, Kubesch A, Korzinskas T, Barbeck M, Landes C, Sader RA, Kirkpatrick CJ, Ghanaati S. Trap-positive multinucleated giant cells are foreign body giant cells rather than osteoclasts: results from a split-mouth study in humans. J Oral Implantol. 2015;41(6):e257–66.

63. Trindade R, Albrektsson T, Tengvall P, Wennerberg A. Foreign body reaction to biomaterials: on mechanisms for buildup and breakdown of osseointegration. Clin Implant Dent Relat Res. 2014;18:192.

64. Teitelbaum SL. Osteoporosis and integrins. J Clin Endocrinol Metab. 2005;90(4):2466–8.

65. McNally AK, Anderson JM. Beta1 and beta2 integrins mediate adhesion during macrophage fusion and multinucleated foreign body giant cell formation. Am J Pathol. 2002;160(2):621–30.

66. McNally AK, Macewan SR, Anderson JM. Alpha subunit partners to beta1 and beta2 integrins during il-4-induced foreign body giant cell formation. J Biomed Mater Res A. 2007;82(3):568–74.

67. Kong YY, Yoshida H, Sarosi I, Tan HL, Timms E, Capparelli C, Morony S, Oliveira-dos-Santos AJ, Van G, Itie A, et al. Opgl is a key regulator of osteoclastogenesis, lymphocyte development and lymph-node organogenesis. Nature. 1999;397(6717):315–23.

68. Raggatt LJ, Partridge NC. Cellular and molecular mechanisms of bone remodeling. J Biol Chem. 2010;285(33):25103–8.

69. Van Wesenbeeck L, Odgren PR, MacKay CA, D'Angelo M, Safadi FF, Popoff SN, Van Hul W, Marks SC Jr. The osteopetrotic mutation toothless (tl) is a loss-of-function frameshift mutation in the rat csf1 gene: evidence of a crucial role for csf-1 in osteoclastogenesis and endochondral ossification. Proc Natl Acad Sci U S A. 2002;99(22):14303–8.

70. Wiktor-Jedrzejczak W, Bartocci A, Ferrante AW Jr, Ahmed-Ansari A, Sell KW, Pollard JW, Stanley ER. Total absence of colony-stimulating factor 1 in the macrophage-deficient osteopetrotic (op/op) mouse. Proc Natl Acad Sci U S A. 1990;87(12):4828–32.

71. Simonet WS, Lacey DL, Dunstan CR, Kelley M, Chang MS, Luthy R, Nguyen HQ, Wooden S, Bennett L, Boone T, et al. Osteoprotegerin: a novel secreted protein involved in the regulation of bone density. Cell. 1997;89(2):309–19.

72. Anderson JM, Rodriguez A, Chang DT. Foreign body reaction to biomaterials. Semin Immunol. 2008;20(2):86–100.

73. Ingham E, Fisher J. The role of macrophages in osteolysis of total joint replacement. Biomaterials. 2005;26(11):1271–86.

74. Nich C, Takakubo Y, Pajarinen J, Ainola M, Salem A, Sillat T, Rao AJ, Raska M, Tamaki Y, Takagi M, et al. Macrophages-key cells in the response to wear debris from joint replacements. J Biomed Mater Res A. 2013;101(10):3033–45.

75. Rao AJ, Gibon E, Ma T, Yao Z, Smith RL, Goodman SB. Revision joint replacement, wear particles, and macrophage polarization. Acta Biomater. 2012;8(7):2815–23.

76. Santerre J, Woodhouse K, Laroche G, Labow R. Understanding the biodegradation of polyurethanes: from classical implants to tissue engineering materials. Biomaterials. 2005;26(35):7457–70.

77. Yang SY, Yu H, Gong W, Wu B, Mayton L, Costello R, Wooley PH. Murine model of prosthesis failure for the long-term study of aseptic loosening. J Orthop Res. 2007;25(5):603–11.

78. Brodbeck WG, Anderson JM. Giant cell formation and function. Curr Opin Hematol. 2009;16(1):53–7.

79. McNally AK, Anderson JM. Interleukin-4 induces foreign body giant cells from human monocytes/macrophages. Differential lymphokine regulation of macrophage fusion leads to morphological variants of multinucleated giant cells. Am J Pathol. 1995;147(5):1487–99.

80. Helming L, Gordon S. Macrophage fusion induced by il-4 alternative activation is a multistage process involving multiple target molecules. Eur J Immunol. 2007;37(1):33–42.

81. Lemaire I, Falzoni S, Leduc N, Zhang B, Pellegatti P, Adinolfi E, Chiozzi P, Di Virgilio F. Involvement of the purinergic p2x7 receptor in the formation of multinucleated giant cells. J Immunol. 2006;177(10):7257–65.

82. McNally AK, Anderson JM. Multinucleated giant cell formation exhibits features of phagocytosis with participation of the endoplasmic reticulum. Exp Mol Pathol. 2005;79(2):126–35.

83. Moreno JL, Mikhailenko I, Tondravi MM, Keegan AD. Il-4 promotes the formation of multinucleated giant cells from macrophage precursors by a stat6-dependent, homotypic mechanism: contribution of e-cadherin. J Leukoc Biol. 2007;82(6):1542–53.

84. Rodriguez A, Macewan SR, Meyerson H, Kirk JT, Anderson JM. The foreign body reaction in

t-cell-deficient mice. J Biomed Mater Res A. 2009;90(1):106–13.

85. McNally AK, Anderson JM. Foreign body-type multi-nucleated giant cells induced by interleukin-4 express select lymphocyte co-stimulatory molecules and are phenotypically distinct from osteoclasts and dendritic cells. Exp Mol Pathol. 2011;91(3):673–81.

86. Tintut Y, Patel J, Territo M, Saini T, Parhami F, Demer LL. Monocyte/macrophage regulation of vascular calcification in vitro. Circulation. 2002;105(5):650–5.

87. Landsman L, Bar-On L, Zernecke A, Kim KW, Krauthgamer R, Shagdarsuren E, Lira SA, Weissman IL, Weber C, Jung S. Cx3cr1 is required for monocyte homeostasis and atherogenesis by promoting cell survival. Blood. 2009;113(4):963–72.

88. Oh J, Riek AE, Weng S, Petty M, Kim D, Colonna M, Cella M, Bernal-Mizrachi C. Endoplasmic reticulum stress controls m2 macrophage differentiation and foam cell formation. J Biol Chem. 2012;287(15):11629–41.

89. ten Harkel B, Schoenmaker T, Picavet DI, Davison NL, de Vries TJ, Everts V. The foreign body giant cell cannot resorb bone, but dissolves hydroxyapatite like osteoclasts. PLoS One. 2015;10(10):e0139564.

90. Jonitz-Heincke A, Lochner K, Schulze C, Pohle D, Pustlauk W, Hansmann D, Bader R. Contribution of human osteoblasts and macrophages to bone matrix degradation and proinflammatory cytokine release after exposure to abrasive endoprosthetic wear particles. Mol Med Rep. 2016;14(2):1491–500.

91. Miron RJ, Zohdi H, Fujioka-Kobayashi M, Bosshardt DD. Giant cells around bone biomaterials: osteoclasts or multi-nucleated giant cells? Acta Biomater. 2016b;46:15–28.

92. Modolell M, Corraliza IM, Link F, Soler G, Eichmann K. Reciprocal regulation of the nitric oxide synthase/arginase balance in mouse bone marrow-derived macrophages by th1 and th2 cytokines. Eur J Immunol. 1995;25(4):1101–4.

93. Mylonas KJ, Nair MG, Prieto-Lafuente L, Paape D, Allen JE. Alternatively activated macrophages elicited by helminth infection can be reprogrammed to enable microbial killing. J Immunol. 2009;182(5):3084–94.

94. Rutschman R, Lang R, Hesse M, Ihle JN, Wynn TA, Murray PJ. Cutting edge: Stat6-dependent substrate depletion regulates nitric oxide production. J Immunol. 2001;166(4):2173–7.

95. Schneemann M, Schoeden G. Macrophage biology and immunology: man is not a mouse. J Leukoc Biol. 2007;81(3):579; discussion 580.

96. Schneemann M, Schoedon G. Species differences in macrophage no production are important. Nat Immunol. 2002;3(2):102.

Imaging of Resorbable Bone Substitute Materials

16

Patrick Rider, Željka Perić Kačarević,
Imke A. K. Fiedler, Said Alkildani, Björn Busse,
and Mike Barbeck

16.1 Introduction

Bone is a dynamic tissue that is constantly being remodeled [1]. Our entire skeleton is renewed every 5–10 years. The old bone is resorbed by the action of osteoclasts, whilst new bone is laid down by osteoblasts [2]. This is a responsive process, whereby bone is able to shift the balance between osteoblastic and osteoclastic activity according to external stimuli [2].

Bone is a metabolically active tissue, containing several cell types in a unique extracellular matrix. A distinctive feature of the extracellular matrix of bone is its composite nature, as it is made of a network of collagen fibers reinforced with a mineral phase, i.e., calcium phosphate (CaP) crystals. The mineral phase, composed of hydroxyapatite (HA) represents approximately 65% of the weight of bone tissue [3]. However, the properties of bone are not explained simply by its composition, but also by its complex structure.

Bone tissue defects can occur as a consequence of trauma or disease. When there is significant bone loss, the remodeling process may be unable to restore the integrity of the bone [4]. For instances where bone loss has reached a critical size, an intervention in the regeneration process is required. Biomaterials are used to replace lost bone and aid restoration by promoting tissue integration and regeneration.

Biomaterials are resorbable or non-resorbable materials that can be safely implanted into the human body. Once implanted, they invoke a tissue response similar to that caused by an injury. Resorbable bone grafts are used to support and repair bony defects by filling in voids and enhancing bone repair functions [5]. Autograft, allograft, xenograft, and alloplastic materials have all been used in the field of oral surgery to provide these functions, however, the ideal bone graft material has not yet been found and investigations continue to study these materials in an in vivo setting.

P. Rider
Botiss Biomaterials GmbH, Zossen, Germany

Ž. P. Kačarević
Botiss Biomaterials GmbH, Zossen, Germany

Department of Anatomy, Histology and Embryology,
Faculty of Dental Medicine and Health, Josip Juraj
Strossmayer University of Osijek, Osijek, Croatia

I. A. K. Fiedler · B. Busse
Department of Osteology and Biomechanics,
University Medical Centre Hamburg-Eppendorf,
Hamburg, Germany

S. Alkildani
Clinic and Policlinic for Dermatology and
Venereology, University Medical Center Rostock,
Rostock, Germany

M. Barbeck (✉)
Clinic and Policlinic for Dermatology and
Venereology, University Medical Center Rostock,
Rostock, Germany

BerlinAnalytix GmbH, Berlin, Germany
e-mail: mike.barbeck@med.uni-rostock.de

Autografts are the gold standard in the regeneration of bone tissue; however, due to donor site morbidity, low quality of geriatric/pathological sources, or the need for two invasive surgeries, alternative bone grafting scaffolds are needed. An idealized scaffold should be replaced by the host bone tissue through osteoinductive and osteoconductive material properties [6–8]. The main types of degradable bone graft materials are natural polymers, synthetic polymers, and bioceramics.

An idealized bone tissue scaffold must fulfill specific criteria: be biocompatible, match the physical properties of the bone tissue to be replaced, not elicit a chronic immune response, and fully integrate with the bone [9]. The tissue response to biomaterials includes a long remodeling phase due to the persistence of pro-inflammatory cells, such as macrophages. The interaction of osteogenic cells with the implant material can be influenced by aspects such as porosity, pore size, scaffold interconnectivity, and mechanical strength [10].

The development of different radiographical techniques and ultrasonography has provided a viable method for imaging bone graft materials in situ and observing the regeneration process. This chapter will discuss each of these techniques and their application to monitoring the healing process of different bone graft materials used in dentistry.

16.2 Radiography

Radiography is an important diagnostic tool used in dentistry that alongside clinical examination, which enables the dental practitioner to assess the bone and its surrounding structures. It can also be used to monitor the healing of bone grafts by providing information such as increases in mineral opacity, bridging of the margins, and the confluence of segments [11].

Bone formation and density can be assessed as the penetration of radiation, which depends upon the thickness and density of tissue or material. It is possible to determine densities by way of a comparison to an object with a known density. Radiographic absorptiometry is performed using a standardized radiograph with an aluminum step wedge that has defined optical densities. Using a visual overlay, densities are measured as aluminum equivalent values or as arbitrary units [12, 13]. However, the technique is unable to provide a true representation of bone density due to overlying soft tissues that will contribute to the recorded optical density.

Radiopacity over time is useful for assessing the absorption of material into the surrounding bone. When the materials are highly radiopaque, their resorption can be more easily monitored [14]. It has been shown that commonly used bovine bone grafts, as well as synthetic hydroxyapatite and β-TCP materials, generally have a higher optical density than that of cortical bone [15]. Although the technique is low cost and produces a low radiation dosage [16], problems include; overlying soft tissue obscuring the region of interest, fluctuations in beam quality affecting image quality, instability of X-ray source, film response, processing conditions, radiation scattering, and beam hardening effects [15].

16.2.1 Rotational Panoramic Radiography (OPG/OPT/ PAN/ DPR)

Panoramic radiography, otherwise known as orthopantomography (OPG), is an extraoral technique that provides a panoramic image of the lower face, teeth, jaw joints, and maxillary sinuses. The produced radiograph displays the teeth in a long flat line that is useful to demonstrate the number of teeth as well as their position, and growth. It is particularly useful to assess the integration of bone grafts with the surrounding bone. Figure 16.1 demonstrates OPG radiographic images showing the resorption of particulate xenograft over a 1-year period. The low dosage of radiation required to perform this technique, along with the large amount of information it provides, make it a very popular technique in dentistry [16]. However, the technique does have its limitations. The OPG scans distort the horizontal plane whilst magnifying the verti-
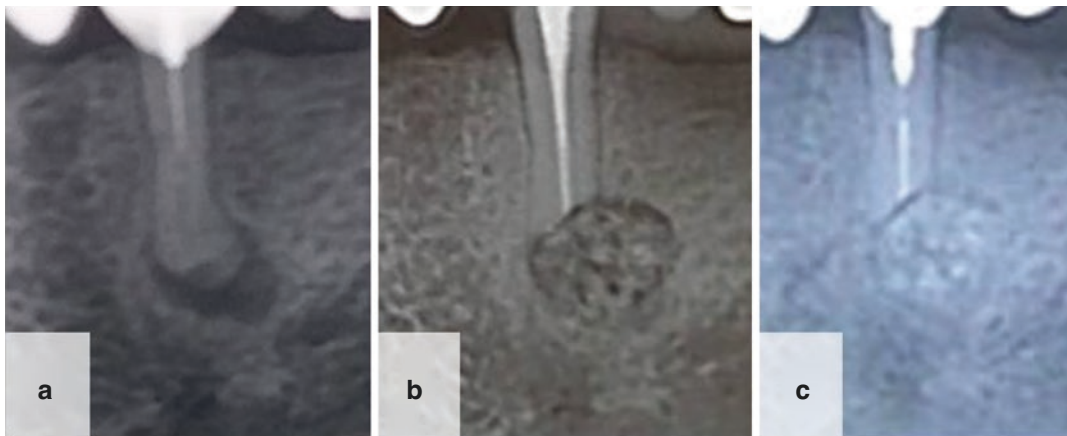
Fig. 16.1 Abscess around endodontically treated pre-molar, treated with a granular xenograft (Cerabone). OPG scan taken; (**a**) before the operation, (**b**) 2 weeks post-surgery, (**c**) 1-year post-surgery

cal plane. This prevents the establishment of true relationships between individual structures. The accuracy of the technique is also largely based on the skill of the operator. As it is a 2D image, it is difficult to assess the availability of the bone width, and the presence of soft tissue shadowing and ghost images can interfere with the interpretation of images [16].

OPGs can be used to record bone graft resorption of ridge augmentations by measuring the bone graft height over different treatment time points. Using OPG in a study comparing two different xenogeneic bone grafts that had different particle sizes (Bio-Oss with an average 1 mm diameter compared to Cerabone with an average 2.7 mm diameter), it was found that the larger particle sizes had a lower volumetric loss in relation to the height of the ridge over a 4-year period (33.4 ± 3.1% compared to 23.4 ± 3.6%) [17].

To determine the accuracy of OPG panoramic X-rays to reality, OPG scans were compared to (cone-beam computer tomography) CBCT scans [18]. Measurements were made and compared along the horizontal and vertical axis. It was shown that in the pre-molar and molar regions of the mouth the measurements were quite similar. However, in the frontal areas of the mouth, the varying inclination of the teeth and their positioning (e.g., rotation) meant that measurements of the teeth made with the OPG scans were shorter and thinner than those made using CBCT data.

16.2.2 Computer Tomography (CT)

Clinical computed tomography (CT) is employed in vast medical applications, ranging from traumatology to pneumology. A great advantage of this technique is rapid image acquisition facilitating a quick diagnosis (e.g., a total body scan can be acquired within less than a minute, depending on the resolution). While the patient is linearly moved through the CT unit via a motorized table, an X-ray source-detector assembly rotates around the patient. Set-ups utilizing this simultaneous movement of source-detector assembly and patient are termed spiral/helical CTs, which are nowadays the most often used CT systems in clinics.

Image reconstruction is, depending on detector size and manufacturer, done by filtered backprojection or iterative algorithms. With respect to resorbable bone substitutes, this CT technique is most commonly applied in orthopedics and trauma surgery. Surgery planning as well as the evaluation of operational success are commonly performed using CT imaging with sub-millimeter resolutions. To display in detail the location and interaction between bone and bone substitutes, a resolution of less than 200 µm is needed. Achieving this resolution requires the use of advanced imaging techniques, such as High-resolution peripheral quantitative CT (HR-pQCT).

### 16.2.2.1 High-Resolution Peripheral Quantitative CT (HR-pQCT)

High-resolution peripheral quantitative computed tomography facilitates in vivo imaging of the extremities of patients down to a spatial resolution of 58 μm at 68 kVp and 100 W using a cone beam. This enables physicians to image the bone microstructure of patients at the trabecular level with high precision to provide information on bone mineral density. Typical parameters used for bone quality and structure appraisal using HR-pQCT are bone volume per total volume (BV/TV), cortical thickness (Ct.Th), cortical porosity (Ct.Po), trabecular thickness (Tb.Th), trabecular number (Tb.N), and trabecular separation (Tb.Sp). In contrast to standard clinical (helical) CT imaging, the X-ray source in HR-pQCT rotates around extremities which are in a fixed position.

It is possible to use this technique for ex vivo imaging of bone substitutes, implant mounting, and cements, with high-precision scan volumes of up to 17 cm in diameter. Quantification of mineral density, resorption as well as the volume of different elements is feasible. An example is the spatial integration of cement into a material, a process that is dependent on the viscosity of the cement. Volumetric integration of the cement can be determined using HR-pQCT, as depicted in Fig. 16.2.

16.2.2.2 Micro-CT and Nano-CT

Three-dimensional (3D) imaging of bone tissue, bone substitutes, and the integration of biomaterials can be achieved from micro- to nanoscale using several X-ray-based techniques including micro-CT (μCT), nano-CT, and X-ray microscopy (XRM).

Micro-computed tomography is the most commonly applied imaging technique to acquire 3D information about internal architectural and structural properties of ex vivo bone biopsies and scaffolds of substitute materials [19, 20]. In contrast to clinical CT scanners, both micro- and nano-CT as well as XRM systems generate two-dimensional (2D) projections from different angles that are required for 3D reconstruction through a fine-tuned rotating sample stage posi-
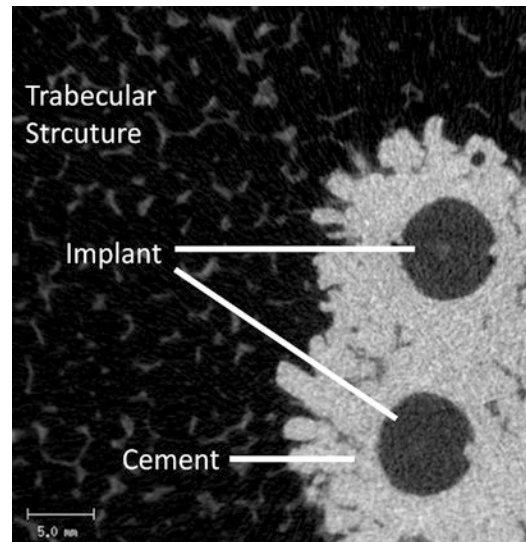
Fig. 16.2 HR-pQCT image of a cemented implant within a trabecular bone structure. The implant-surrounding cement is displayed in bright pixels and its integration can be quantified

tioned between the X-ray source and a detector arranged at a fixed distance.

After reconstruction of the images, 2D and 3D parameters are gained from micro-/nano-CT and XRM image stacks through the assessment of differences in image contrast, i.e., gray values. Based on thresholding procedures during post-processing, as illustrated in Fig. 16.3, materials with similar attenuation coefficients can be identified and their morphology and internal architecture displayed [21].

In μCT, voxel sizes of less than 30 μm are commonly applied to investigate the internal morphology of biomaterials, whereby scanning at smaller voxel sizes requires longer acquisition times and introduces higher radiation doses, which can be harmful to biological materials [22]. To resolve trabecular features on bone, 5–20 μm are commonly used [19]. Typical acquisition parameters for mineralized tissues are in the range of 50–100 kV X-ray voltage and 100–300 μA X-ray tube current, whereby samples can be measured while immersed in a fluid (e.g., fixative or saline solutions). Typical parameters indicative for bone quality and architecture assessed in bone specimens using μCT are bone
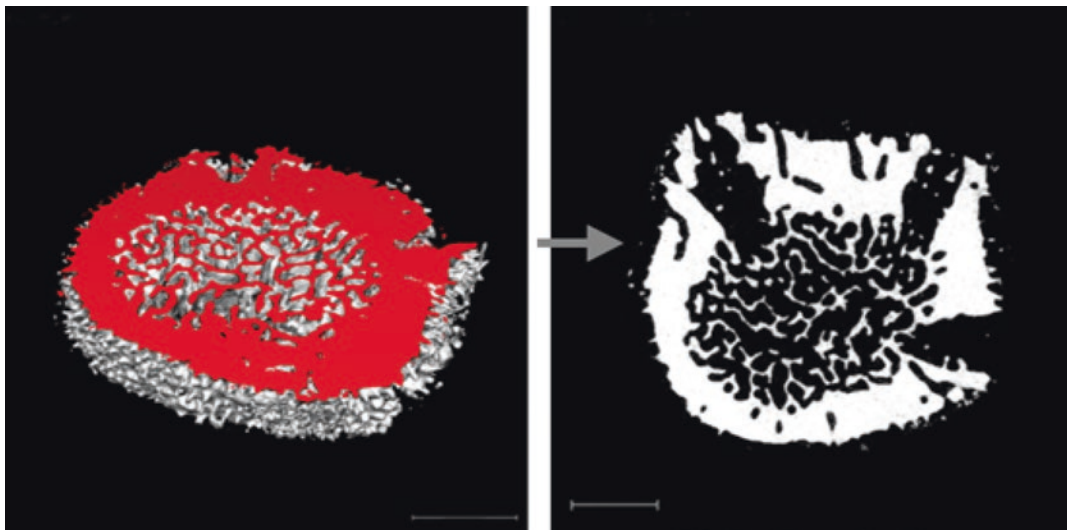
Fig. 16.3 Virtual cut through a 3D reconstruction of coral biomaterial showing internal trabecular-like structures. The inset displays the image threshold corresponding to the red-colored plane in the overview image (scale bar: 100 μm)

volume per total volume (BV/TV), cortical thickness (Ct.Th.), trabecular thickness (Tb.Th), and porosity (Po) [23, 24]. As displayed in Fig. 16.4, in reconstructed images from porous biomaterial scaffolds or grafts, dark pixels usually correspond to non-mineralized voids (e.g., channels filled with liquid or soft tissue), gray pixels to native mineralized tissue, and bright regions usually too highly mineralized materials, e.g., grafts based on hydroxyapatite. In this context, the ratio of biomaterial volume per bone volume can be gained from ex vivo scanning of bone biopsies after implantation of mineral-based biomaterial scaffolds to assess their integration into the host tissue.

Due to smaller X-ray focus spot sizes in nano-CT and XRM compared to μCT systems, these imaging techniques can display features at smaller length scales than classical μCT systems [19]. As the voxel size decreases and the spatial resolution increases, the field of view, i.e., the size of the observable volume, is generally decreased. Consequently, small specimens such as tissue biopsies are required for imaging at the micro-scale, while much smaller volumes of below 1 mm^3 are usually required for imaging of biomaterials at the nanoscale, where voxel sizes can reach <100 nm in advanced commercial

desktop nano-CT systems and XRM systems [25]. In tomographic applications at the nanoscale, image results are increased when specimens are dried and glued to a sample holder. In the scope of advanced synchrotron X-ray radiation techniques, nano-CT imaging can reach down to 20 nm voxel size, which enables the depiction of tissue heterogeneity, integrity, and porosity of materials far beyond the resolution capabilities of desktop systems [19].

16.2.2.3 Synchrotron Radiation Micro-computed Tomography (SR μCT)

Synchrotron radiation micro-computed tomography (SR μCT) provides a highly detailed 3D image of ex vivo samples, far superior to those attainable via standard μCT. A synchrotron source creates a high-flux, high-intensity, and monochromatic X-ray beam, enabling the capture of quantitative high-resolution 3D images with a high signal-to-noise ratio. Samples are placed on a high-precision sample stage that rotates the sample perpendicular to the beam [26]. The mechanical stability of the rotation, the quality of the scintillator material, and the number of recorded angular projections all contribute to the quality of the final high-precision image.

Fig. 16.4 Reconstructed µCT image of sinus biopsy showing trabecular bone structures (gray), soft tissue, and liquid (black) as well as biomaterial integrated into the host tissue (white) at 10 µm voxel size
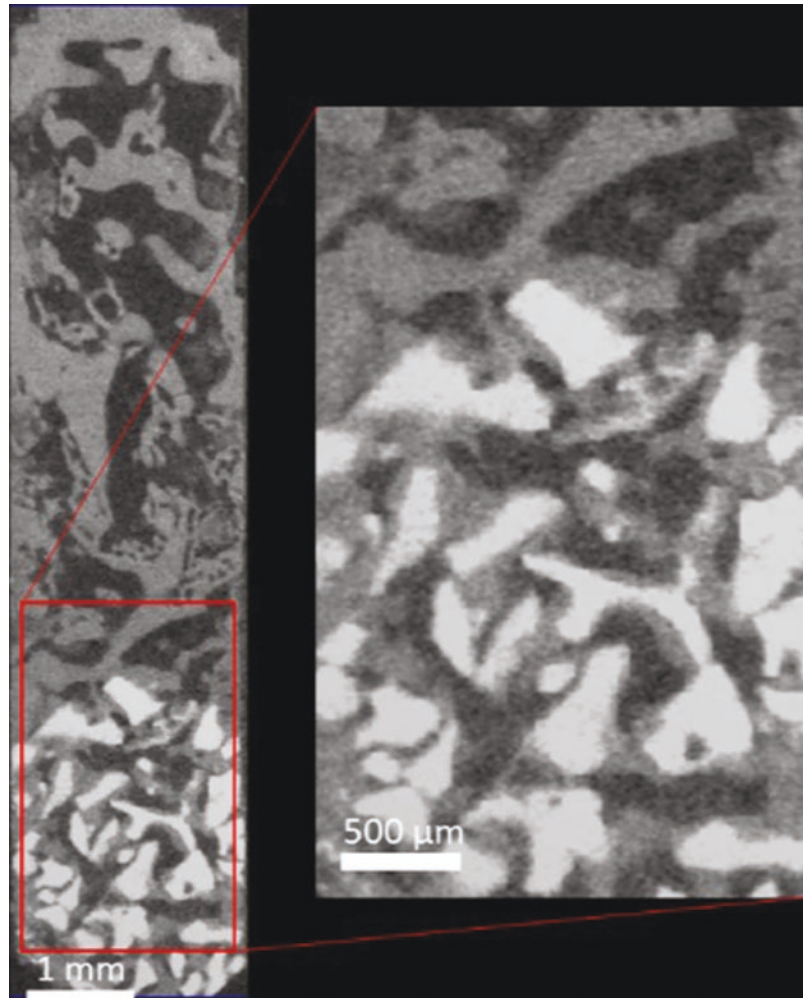
A voxel size of 300 nm is achievable [27], which enables unprecedented three-dimensional imaging of the bone lacunar network as well as the extracellular matrix [27, 28]. Most research has so far concentrated on the tissue structure itself, however, the potential for the technique to be used for monitoring bone graft integration has been demonstrated by its use to monitor degradable magnesium dental devices and their replacement by bone [29–31], as demonstrated in Fig. 16.5.

16.2.2.4 Cone-Beam Computed Tomography (CBCT)

Cone-beam computed tomography (CBCT) is an alternative to CT that uses a lower radiation dos-age whilst providing a high spatial resolution of bone and teeth and is commonly performed in the dental clinic. Although it uses a lower radiation exposure, CBCT provides an improved resolution in comparison to conventional CT as well as offers multiplanar reformatting of both 2D and 3D images in any plane. Another benefit of CBCT over CT is that it does not require a mechanism to move the patient during the scan in order to obtain a 3D image.

Cone-beam computed tomography (CBCT) has been commercially available since the year 2000 [16]. Ionizing radiation is projected and collected onto a rotating 2D plate that accumulates multiple sequential acquisitions [32]. A round or rectangular cone-shaped X-ray beam
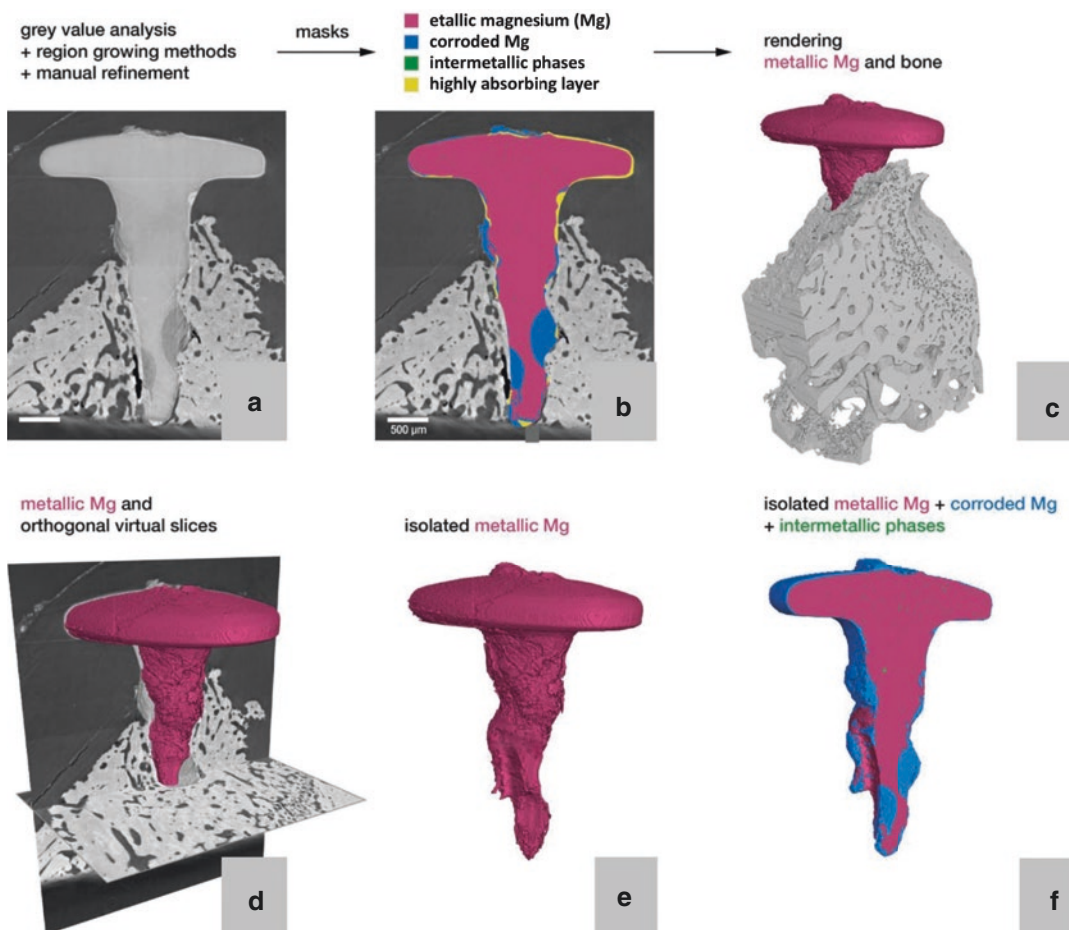
Fig. 16.5 Synchrotron μCT imaging of degrading Mg-alloy dental fixation pins. (*Adapted from Jung* et al. [29]. *Creative Commons Attribution (CC BY) license*). red color = etallic magnesium (Mg), blue color = corroded Mg, green color = intermetallic phases, yellow color = highly absorbing layer

with either an image intensifier or a flat panel detector is used for volumetric image acquisition [16].

3D images are reconstructed with software using a modified version of the cone-beam algorithm, developed by Aboudara et al. [11]. The software then enables the clinician to format the data in any plane; provides multiple views: standard axial, coronal, sagittal, and panoramic, as well as cross-sectional cuts of varying thickness (as demonstrated in Fig. 16.6); and can calculate 3D volumes from rendered images. Due to the creation of complete 3D structures, the clinician can perform accurate measurements within specialized software, such as linear and angular measurements of bony morphologies.

Morphological analysis of CBCT scans provides the spatial relationships between neighboring structures enabling the evaluation of growth, development, and function.

However, the imaging technique has its limitations, these include the cost of the equipment and a lack of training in the interpretation of the images. As with all radiographic techniques, a compromise must be made between patient radiation dosage and the detail of the CBCT dataset. Acquisition time affects the resolution of the image such as the voxel size, noise defects, and definition of the tissue structures. Fast acquisition times will reduce the radiation dosage as well as limit the risk of motion artifacts from occurring, as any slight movement can render an image

Fig. 16.6 CBCT scan showing a severe defect of the right mandible
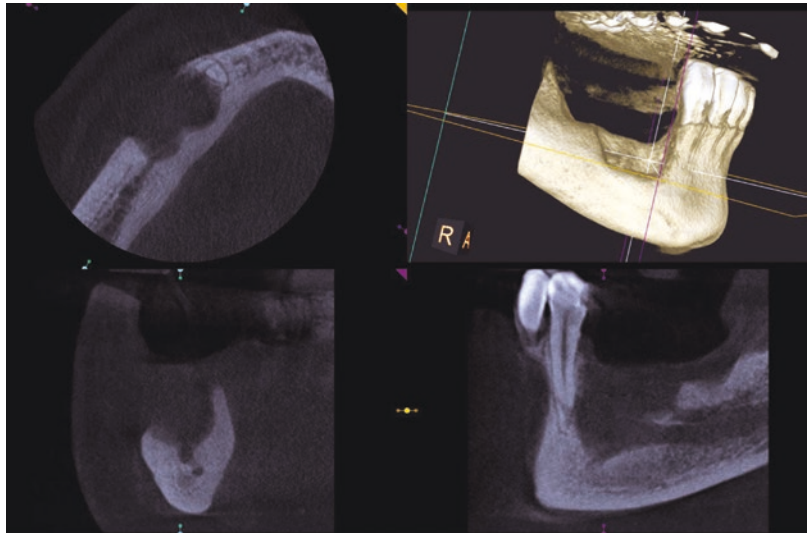
unusable for diagnostics. However, with a reduced acquisition time the level of detail is reduced, voxel size increases (reducing the definition), and there will be a greater interference from radiodense restorations.

One of the benefits of CBCT is the ability to justify multiple scans due to the low risks associated with modern CBCT scanners. A low radiation dose during CBCT scans with an extended field of view (FOV) scan ranges between 82 and 182.1 μSv for a Classic i-CAT scanner, however, this can still vary significantly between the device and is still several times higher than that used during panoramic scans, which range between 6.3 and 13.3 μSv [33]. Nevertheless, the radiation dosage is similar to that of traditional non-digital radiography and is significantly lower than that of a standard CT, which ranges between 569 and 1073 μSv [16, 33, 34].

CBCT scanners are categorized into large, medium, and limited volume units depending on the FOV, which determines the volume of the scan. The FOV can be adjusted according to the region of interest. Smaller scan volumes have a higher resolution due to reduced scatter and decrease radiation exposure to the patient. CBCT scans with a small FOV can give a radiation dosage between 11 and 674 μSv, compared to a large FOV that can give an exposure between 30 and 1073 μSv [35].

The lower radiation exposure in comparison to CT means that there is a lower resolution of the soft tissues. However, CBCT can offer more favorable resolutions of the hard tissues than that achievable with multi-slice CT machines. A resolution between 0.1 and 0.2 mm^2 can be obtained with a CBCT machine, in comparison to a resolution between 0.35 and 0.5 mm^2 with multi-slice CT machines [16].

By obtaining radiographic information at different time points, it is possible to compare the biomaterial's response in vivo over time. HU values obtained from CT scans, are commonly used by clinicians for determining bone quality and can be used to monitor changes in bone graft density. Although both CT and CBCT produce grayscale images, the method by which they are obtained differs. Therefore, the HU units calculated using CT grayscales are not necessarily reproduced using CBCT datasets.

Shokri et al. compared two CBCT systems for their ability to determine HU in comparison to those calculated using multidetector computed tomography (MDCT), which is the gold standard [34]. The CBCT systems used were the Cranex 3D (Sordex, Finland) and the Newtom 3G (QR srl., Italy). These were compared to the MDCT system Somatom Spirit System (Siemens, Germany). As the gray scaling produced by CBCT machines is influenced by the FOV, both

large and small FOVs were used when acquiring CBCT datasets. Each machine was used to scan three different bone graft materials: NanoBone® (Artoss GmbH, Germany), CenoBone® (Tissue Regeneration Corporation, Iran), and cerabone® (botiss biomaterials GmbH, Germany). The MDCT-derived HU units for the bone graft materials from the lowest to the highest were: NanoBone® (578–610), CenoBone® (876–928) and cerabone® (1374–1882). For each CBCT machine, the recorded HU unit was dependent upon the FOV used, with smaller FOVs producing a lower HU value than the larger FOV. The Cranex 3D CBCT scanner gave HU values similar to that of the MDCT machine when using a small FOV, however, the obtained HU values for cerabone® were not statistically different from the MDCT values for both small and large FOVs.

Another way for comparing the CBCT dataset is to perform image registration. Registration of CBCT datasets is the process of aligning two or more datasets for their direct comparison. The datasets can be rotated, translated, and scaled until pairs of identifying landmarks are aligned. Using CBCT datasets there are two main methods for image superimposition: surface-based and voxel-based. Surface-based superimposition requires a 3D model to be rendered before superimposition. However, the process of rendering the 3D model can create errors in the model, such as partial volume averaging and under-sampling, and has the potential for small details and sharp edges to be rendered smooth or completely lost [36]. Voxel-based superimposition is a much more accurate method for superimposition, although requires a large amount of computational power. The superimposed datasets can then be evaluated by being turned into color maps for visual assessment, or by digital subtraction.

Volumetric measurements calculated using CBCT are influenced by the resolution of the images, as it is the gray scaling of the rendered voxels that provide the definition of the individual tissues. Therefore, fewer voxels due to lower resolutions will affect the measured volumes. Some investigators have reported a risk of overestimating graft volumes when using CBCT in comparison to high-resolution images produced via μCT [37].

16.2.3 Scanning Electron Microscopy (SEM)

An electron-based imaging technique commonly used to assess the morphology of biomaterials and their tissue integration is electron microscopy (EM). The electron beam interacts with the surface of the specimen, which leads to the emission of several particles including secondary electrons (SE) and backscattered electrons (BSE). While SE is emitted from close to the surface, BSE is generated at higher depths of the specimen.

Imaging in SE mode is one of the most established techniques for the visualization of topographical and structural information at the micro- and sub-microscale of mineralized tissues and biomaterials [38]. It is thus particularly suitable to image the surface morphology of both unseeded biomaterials and grafts in their granular form [39], and of the osseous cellular integration and adhesion on seeded biomaterials in the scope of in vitro experiments [40]. A typical image of a seeded biomaterial is depicted in the first picture of Fig. 16.7, where the topography and morphology of the material and adhering cells can be analyzed. Commonly used magnifications of up to 50,000 times, enables the visualization of grain boundaries and interfaces. Cellular components with the typical depth of field provided by SEM are also visible, providing a 3D impression of their morphological features.

Imaging in BSE mode, also referred to as backscattered electron imaging (BEI), detects high-energy electrons and is the state-of-the-art technique to perform analytical EM in 2D as it allows to display differences in the composition of specimens. Hereby, differences in electron mass of the specimens' constituents are leading to differences in contrast of the resulting image plane and allow to display the integration of biomaterials into host tissue [41]. As shown in a BSE image of a biopsy that was embedded in plastic and ground coplanar as shown in the second picture of Fig. 16.7, the integration of biomaterials can be examined in situ and displayed in 2D. In the resulting BSE images, bright regions correspond to the biomaterial and darker regions correspond to bony tissue. With regard to quanti-
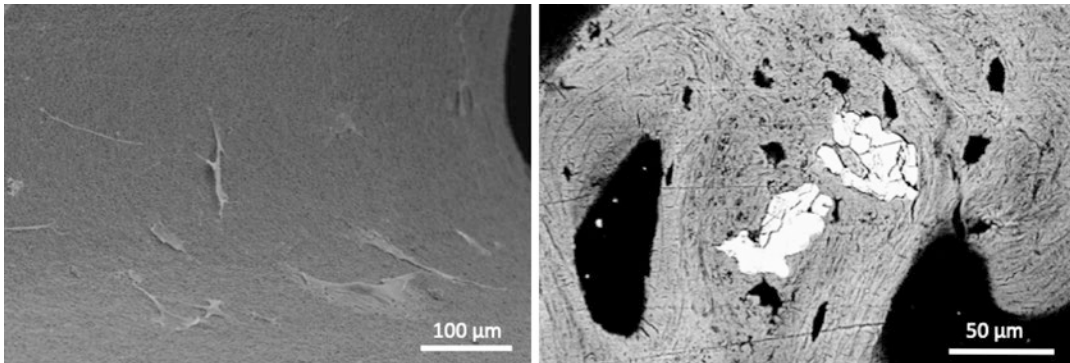
Fig. 16.7 (First picture) Secondary electron image of cement-based biomaterial in vitro, showing topography and morphology of material and seeded cells. (Second picture) Backscattered electron image of a biopsy embed- ded in plastic and ground coplanar, displaying the incor- poration of cement-based biomaterial (bright pixels) into native bone tissue (gray pixels)

fying the degree of calcification of biomaterials, established calibration procedures are commonly employed to determine parameters such as cal- cium weight percentage and the heterogeneity of the mineral distribution in 2D [42, 43].

In combination with a detector for energy- dispersive X-ray spectroscopy (EDX, EDAX, or EDS), additional spectroscopic information can be gained from the specimen surface during EM (e.g., the presence of strontium or other trace ele- ments), thus facilitating the site-matched, multi- modal investigation of osseous cell interaction and integration into graft materials [44, 45].

One commonly occurring issue in EM of bio- materials with low electron density (e.g., colla- gen foams, polymer membranes, hydroxyapatite scaffolds) is the effect of charging built up. Low electron beam voltages of less than 10 kV are commonly used in EM imaging of biological materials but can lead to a negative charge on the specimen surface. This in turn provokes artifacts in the detected image. To overcome this issue, dried specimens are commonly sputter-coated with conductive material (e.g., gold, gold- palladium, or carbon) in thin layers of around 10 nm thickness. In order to maintain the cellular features of non-embedded explants or biopsies, critical point-drying is often performed prior to coating [46]. In more recent EM systems, imag- ing can be performed at low vacuum, thus reduc- ing charging effects, however at the cost of resolution.

16.3　Ultrasonography

The application of ultrasound to diagnostic medi- cine has continued to grow through its develop- ment. Unlike the radiological and computed tomographic techniques, ultrasonography does not use ionizing radiation and therefore is not limited by the number of times that a patient can be examined using the technique. It is also a low- cost technique in comparison to the other imag- ing techniques and is therefore widely available. It is also more portable and has been tested for wearable devices that monitor healing progress over a sustained period of time [47].

Modern ultrasound units can be used to moni- tor the healing process. They can produce 3D images in real-time and visualize moving struc- tures. Ultrasonography can be performed rou- tinely to measure the rate of flow in blood vessels and tissue [48] as well as provide an assessment of bone graft quality (mechanical suitability) [49]. However, the immediate visualization of implanted grafts can be an issue due to the presence of air at the surgical site that causes arti- facts in the acquired image [13]. Another issue is that the accuracy of mechanical and flow mea-

surements will be affected by overlying soft tissues.

B-mode (brightness mode) imaging produces a cross-section of the desired tissue by displaying the boundaries between tissues and organs. Ultrasound waves are produced using a piezo-electric transducer that emits short bursts or pulses when in contact with the skin. Unlike ionizing radiation, ultrasound waves require a medium from transmission, with the presence of air between the transducer and the skin having a detrimental effect on image acquisition.

Images are produced by emitting ultrasound waves via a transducer that are directed along narrow-shaped beam paths into the patient. Once the transducer has emitted a burst or pulse of ultrasound waves, the transducer turns into a receiver to collect reflected waves and display them on a computer screen. As the beam travels through the patient, it then gets reflected and scattered at the boundaries of tissues and by tissue irregularities. The reflected waves (or echoes) travel back towards the transducer where they are recorded by a receiver.

Once the ultrasound waves have been emitted, they immediately begin to produce echoes as they pass through the tissue. Echoes that occur closer to the transducer return faster than those created at a greater depth. The delay between echoes made close to the transducer than those from further away enables an image to be formed. Each echo is represented as an individual point on an image, relative to its physiological position which is determined by the time difference between the ultrasound wave emission and receiving the echo. The brightness of each point relates to the strength of the echo, hence its name "brightness mode".

Using the B-mode ultrasound it is possible to produce real-time imaging, a prospect not attainable via radiography or CT scans. Compared to CBCT, ultrasonography has been shown to have a high accuracy for determining the level of alveolar bone, demonstrating a slight difference amounting to 1.6–8.8% [50].

Ultrasonography can be used to detect the bridging of bone defects and fractures earlier than radiography and CT [13]. In a study com-

paring the healing of tibial tuberosity defects in dogs using two different scaffolds of either a gelatinous matrix (GM) or demineralized bone matrix (DBM), the use of B-mode ultrasound was able to detect bony union from an early stage of the healing process. In comparison to two other imaging modalities used; OPG radiographs and CT scans, the detection of a bony union was observed significantly earlier with the B-mode ultrasound. For DBM, osseous bridging was diagnosed at 5.6 weeks, 10.4 weeks, and 9.6 weeks using either ultrasound, OPG, and CT, respectively. In comparison, the GM scaffold was diagnosed as providing a bony union after 4.0 weeks, 9.6 weeks, and 7.2 weeks using either ultrasound, OPG, and CT, respectively. Overall, it was shown that the radiographs had overestimated the time required for the bony union to occur and that the use of ultrasonography was more sensitive to early osseous formation. The study also demonstrated that the information collected by the sonogram regarding mineralization and shape of the regenerating bone was similar to that determined by the CT scans.

Ultrasonography can be used for determining the quality of bone, as well as assessing the phases of the healing process [47]. The velocity of the ultrasound waves through defect or fracture sites can indicate the presence of an inflammatory reaction as well as information on the mechanical and mineral density of the callus. Ultrasound waves traveling through healed bone have been shown to have a velocity around 80% of the velocity when traveling through healthy bone [47].

Noviana et al. used ultrasonography to identify the early stages of bone regeneration after implanting either hydroxyapatite-chitosan (HA-C) or hydroxyapatite-tricalcium phosphate (HA-TCP) composite scaffolds into sheep radial defects [51]. Using ultrasound within the first 30 days of the study, the level of inflammation was able to be compared for the initial phases of healing, as well as the formation of primary and secondary calluses. Radiological and histomorphometric assessments were performed in the later stages of the study. Sham surgery sites (used as controls) were shown to have a decreased

level of inflammation in comparison to the HA-C and HA-TCP scaffolds. The study showed that the HA-TCP scaffold began morphological changes after 30 days compared to 90 days with the HA-C scaffold.

Another study combined the use of ultrasonography with radiography throughout the healing process to gain a more detailed evaluation of bone regeneration. Monitoring radial bone defects in rabbits either treated with or without nano-hydroxyapatite coated cancellous bone scaffolds [52], radiographs were used to assess the formation of a callus, whereas doppler ultrasonography was used to evaluate the osseous tissue and the formation of a blood vascular network. For the sites treated with the nano-hydroxyapatite scaffold, a newly formed callus filled the defect site 60 days earlier than with the control, and a vascular network was observed to develop within half the time (15 days).

Ultrasonography can be used as an alternative to radiographic and CT techniques for monitoring the early regenerative processes of bone grafts without exposing the patient to a high dosage of ionizing radiation. Due to its low cost and lack of hazardous ionizing radiation, ultrasonography can be used for regular evaluation. It is particularly useful for the early phases of healing as it is able to visualize the soft tissue, enabling the initial inflammation reaction, development of a vascular network, and formation of a primary and secondary callus to be visualized.

16.4 Comparison of Bone Graft Materials Using Different Imaging Techniques in Dentistry

16.4.1 Autogenous Grafts

Autogenous bone is often used by itself or in combination with other materials for bone augmentations. Volumetric CBCT comparisons have shown that the location from which the autologous bone block is harvested will influence its resorption behavior. Autogenous bone blocks harvested from the iliac crest have shown that

after 3 months, the bone blocks can resorb by $36.50 \pm 5.04\%$, or by $31.69 \pm 5.50\%$ when an acellular dermal matrix membrane was used [53]. In comparison, bone blocks harvested from the mandibular body has been reported to resorb by $74.6 \pm 8.4\%$ over a 4–6 month period when using volumetric CBCT comparisons [54]. Graft resorption is also influenced by the form of the autogenous bone, whether it is used as a bone block or in a particulate form. For the reconstruction of the atrophic maxilla, a comparison of augmentations using autologous bone in a block or particulate form showed that after 6 months, the particulate graft had maintained a volume of $81.1 \pm 8.3\%$ whilst the bone block had maintained a volume of $77.8 \pm 5.2\%$ [55].

16.4.2 Allogeneic Grafts

Allogenic bone grafts offer an alternative to autologous bone, as they present similar properties to the native bone, yet do not require a second surgical site for the patient [5]. With CBCT, it is possible to compare the efficiency of allogeneic to autologous bone grafts. Using CBCT planimetric measurements, fresh-frozen allogeneic bone blocks (source not mentioned) were compared to autologous bone blocks harvested from the mandibular ramus, for their stability in horizontal alveolar ridge augmentation [56]. The total area of alveolar bone and bone block in planar segments were calculated and compared between time points. After 6 months, the total bone volume (alveolar bone and bone block within planar segments) had increased by $2.57 \pm 14.62\%$ for patients receiving autologous bone, however, had reduced by $9.33 \pm 9.57\%$ for patients receiving allogeneic bone.

However, the efficiency of the allogeneic bone block can be determined by its sourcing. In another study, the use of a commercially available fresh-frozen allogeneic bone block harvested from cancellous bone in the femoral head and sourced from living donors was shown to offer a promising alternative to autologous bone [57]. In the study, alveolar ridge augmentation was performed either with autologous bone

blocks harvested from the retromolar region or with an allogeneic bone block (Maxgraft®, botiss biomaterials GmbH, Germany). Similar resorption rates were observed in sagittal and cross-sectional CBCT images, and at all time points, the vertical and horizontal dimensions were not significantly different between the two block types. At 6 months the allogenic bone block had resorbed by 11.4 ± 9.7% in comparison to 9.1 ± 7.3% for the autogenous block. At 12 months, the allogeneic bone had resorbed by 14.4 ± 9.8% in comparison to 12.5 ± 7.8% for the autogenous bone block.

OPG radiography was used to monitor atrophic alveolar ridges with a low residual height, which underwent a sinus lift procedure using allogeneic bone with simultaneous implant placement [58]. Bone resorption was measured by a change in the height of the bone at the apex of the implant after 1 and 5 years. Before the implant placement bone height was measured to be 14.8 ± 0.694 mm high. After 1 year, this had reduced to 13.04 ± 1.038 mm, and then to 11.62 ± 1.023 mm after 5 years. Although bone resorption was not compared to a control, a 94% implant survival after a period between 3 and 8 years is a high success rate for immediate loading of the atrophic alveolar ridge with a low residual height.

CBCT can also be used to evaluate graft resorption for augmentations with immediate implant placement. Simonpieri et al. performed a 4-year follow-up on full arch rehabilitations made with immediate implant placement and loading [59]. Buccal plate augmentations were performed with allograft particles (Maxgraft®, botiss biomaterials GmbH, Germany) covered with a prepared L-PRF membrane. 4 years after implant loading, measurements of CBCT scans were made on the distal, mesial, vestibular and oral sides of each implant (Fig. 16.8 is a representative CBCT image of a defect site repaired with the same bone graft material before augmentation and 18 months post-augmentation and implant placement). Bone loss was calculated by subtracting the measured bone level from that recorded at the time of implant insertion. Using this method, it was possible to demonstrate that there was no statistical difference between the mean bone loss for sites with immediate compared to delayed implant loading, as well as between anterior and posterior positions.

16.4.3 Xenogeneic Grafts

Xenogeneic bone grafts offer a more widely available source or bone graft material and are most commonly sourced from bovine bone [60]. A comparison study using autologous and deproteinized bovine bone blocks for alveolar ridge augmentation was made using volumetric CBCT analysis [61]. After 3 months, the autologous bone, harvested from the iliac crest, had reduced in volume by 35.94 ± 2.35%, however in comparison, the bovine bone block (Bio-Oss®,
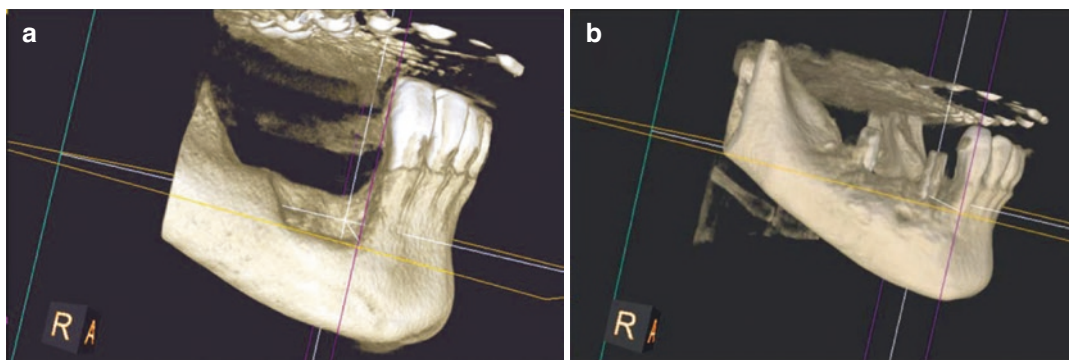
Fig. 16.8 CBCT of (**a**) a severe bone defect of the right mandible and (**b**) 18 months post-augmentation using Maxgraft® bone builder block and implant placement

Geistlich, Switzerland) had only reduced by an average of 12.26 ± 2.35% after a period of 6–9 months.

Different resorption rates have also been demonstrated between allogeneic and xenogeneic bovine bone. Allogeneic particulate bone (MinerOss, BioHorizons, USA) was compared to xenogeneic particulate bone (Bio-Oss, Geistlich biomaterials, Switzerland), via volumetric measurements made using CBCT over a 6-month period [62]. The allogeneic particulate bone graft had reduced in volume by 19.38 ± 9.22% compared to the xenogeneic bone, which reduced by 8.14 ± 3.76% over the same period. Augmentations were also made with a combination of both allogeneic and xenogeneic particles, however, these had resorbed by 24.66 ± 4.68%.

To evaluate the stability of bovine bone blocks for buccal bony defects with immediate implant insertion, CBCT scans were made before implant insertion and 1 year later [63]. It was shown that there was uniform resorption of the cerabone® block (botiss biomaterials, Germany) when the bone thickness was measured: one-third coronally, in the middle, or apically of the implant on the buccal plate using CBCT images.

The way the xenogeneic bone is treated before implantation will also influence its bone regenerative abilities [64]. In the comparison of com-mercially available bovine xenografts, bilateral sinus augmentation procedures were performed with either cerabone® (botiss biomaterials, Germany) or Bio-Oss® (Geistlich, Switzerland) granules. Measurements made using CBCT scans pre-operatively, immediately post-operatively, and after 8 months, showed that for all augmentations, the alveolar height had increased by similar amounts, and had remained stable over an 8-month period. However, histomorphometrical analysis showed that there was a 29.13 ± 13.81% increase in new bone for the cerabone® graft in comparison to 24.63 ± 19.76% for Bio-Oss®.

Another sinus floor augmentation procedure compared four different augmentation materials: xenogeneic bone material (Cerabone®, botiss biomaterials, Germany) (representative image provided in Fig. 16.9), alloplastic biphasic calcium phosphate with a 60:40 hydroxyapatite to tricalcium phosphate ratio (BoneCeramic®, Straumann, Switzerland), an alloplastic paste composed of an 80% nano-hydroxyapatite aqua gel and 20% biphasic calcium granules (Maxresorb® inject, botiss biomaterials, Germany), and a xenogeneic collagen fleece [65]. After 36 months, CBCT was used to evaluate the volume loss of each of the grafting materials. It was found that each material volume had reduced over the time period. Cerabone® and
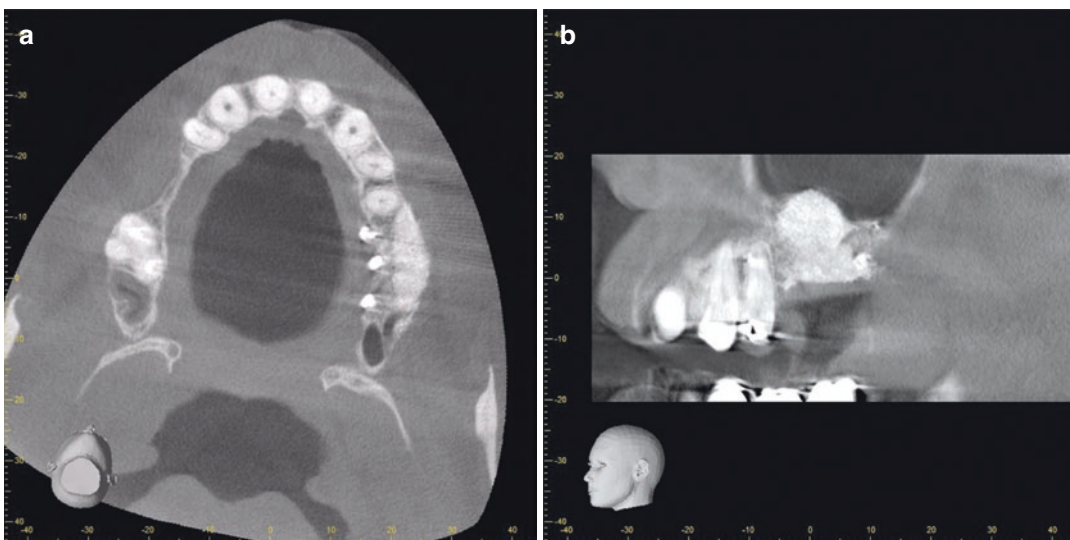
Fig. 16.9 CBCT scan taken 8 months post-surgery of a two-stage sinus floor elevation and horizontal GBR using cerabone® and autologous bone

BoneCeramic® lost around 20% of their immediate graft volume, which was between 1.65 and 1.7 cm^3. Maxresorb® inject lost around 38% of its initial volume of an average of 1.36 cm^3, whilst the collagen fleece lost the largest volume, losing around 70% of its initial volume of around 0.59 cm^3.

16.4.4 Alloplastic Grafts

Alloplastic materials present the advantage that they do not present the risk of disease transmission and that their properties can be easily developed to suit the application. An example of material adaptation to meet regenerative needs is the use of biphasic calcium phosphates. These are composed of a slow degrading HA and a faster degrading β-TCP for resorption rates and biological response.

A comparison study was performed that compared a monophasic calcium phosphate (Bioresorb®, Sybron Implant Solutions, Germany), composed of β-TCP, and a biphasic calcium phosphate (Maxresorb®, Botiss Biomaterials, Germany), composed of 60% HA and 40% β-TCP [66]. Each material was used for sinus floor augmentations and monitored over a 6-month period. Although histomorphometric analysis showed comparable results regarding the volume of new bone, residual graft, and nonmineralized tissue; radiographical analysis demonstrated that there were differences between the two materials used. CBCT datasets, used to determine the volume and homogeneity of the graft, indicated that the biphasic calcium phosphate graft was more stable than that of the monophasic. After 6 months, the volume of the Bioresorb® graft had reduced by 22.2%, whilst the Maxresorb® graft had resorbed by as little as 6.66%. Although immediately after the augmentation procedure both grafting materials demonstrated a high level of homogeneity, after 6 months, this level of homogeneity was only maintained by the Maxresorb® graft.

Another synthetic material that can be used for bone augmentation is calcium sulfate [67]. To compare the effect of graft resorption rate on sinus floor augmentations, augmentations were performed using either particulate calcium sulfate (BondBone, MIS Implants, Germany) with autologous bone or deproteinized bovine bone (Bio-Oss®, Geistlich, Switzerland). Calcium sulfate is a fast-resorbing material that was combined with the slow-resorbing autologous bone. Volumetric CBCT data showed that, after 6 months, the Bio-Oss® volume had reduced by 9.39 ± 3.01% whilst the CS composite graft had reduced by 17.65 ± 4.15%. Therefore, indicating the greater stability of sinus floor augmentation procedures when using a bovine bone graft in comparison to a fast-resorbing material.

Not all materials used for bone augmentations are radiopaque. Some materials are radiolucent at the time of surgery, radiographic analysis can still be performed over different time points, as new bone should penetrate the graft causing the site to become more radiopaque as the site regenerates. Using this reasoning, a gelatin sponge (Abgel, SURGISPON®, India) was compared to β-TCP for sinus augmentation [68]. CBCT was used to make linear measurements of the bone height for grafts with and without immediate implant placement. Although the Abgel material is relatively radiopaque, the baseline measurements (done immediately after the augmentation procedure) were measured from the crest of the ridge until the absence of apical hyperdensity. In the 5-month follow-up, the measurements were made of the new bone that had been maintained. After a 5-month period, the mean gain in bone height between the two groups was not statistically significant, and both groups measured a larger loss in height for grafts inserted without the immediate placement of an implant.

16.5 Conclusion

For the measurement of resorbable bone grafts in situ, OPGs are easily accessible and relatively inexpensive to perform; however, the collection of information obtained can be unsatisfactory for accurate assessment. The overlapping and superimposition of images produce background noise that reduces image sharpness and resolution,

thereby restricting the anatomical information of the region. Unequal magnification leads to distortions of geometric and anatomic accuracies that are also influenced by changes to the angulation of the performed OPG. All these factors limit the use of OPG for comparing biomaterial responses between treatment time points.

CT is able to overcome many of the limitations of OPG, as a 3D multiplanar image is created with high contrast and resolution without the superimposition of acquired data images. However, CT uses high radiation exposure, has a high cost, as well as has a huge laboratory footprint. CBCT offers an alternative to CT and provides a high spatial resolution whilst reducing radiation exposure. It can also provide multiplanar reformatting of both 2D and 3D images in any plane. However, image quality can be influenced by slight movements of the patient and the acquired image is not as detailed as that achieved through CT.

Ultrasonography can be used for assessment of the early stages of regeneration. Unlike radiological techniques that find it difficult to visualize new bone formation until the early stages of calcification of the callus, ultrasonography can provide information on the initial inflammation reaction and the formation of a primary and secondary callus. The technique can also be used for observing the development of a vascular network.

Overall, there are a variety of different imaging techniques that can be used for evaluating bone healing using bone grafts. The choice of technique used will depend on the situation, as the level of information required should be considered in relation to the invasiveness, frequency of evaluation, and radiation dosage of the technique.

References

1. Milovanovic P, et al. Osteocytic canalicular networks: morphological implications for altered mechanosensitivity. ACS Nano. 2013;7(9):7542–51. https://doi.org/10.1021/nn401360u.
2. Busse B, et al. Decrease in the osteocyte lacunar density accompanied by hypermineralized lacunar occlu-sion reveals failure and delay of remodeling in aged human bone. Aging Cell. 2010;9(6):1065–75. https://doi.org/10.1111/j.1474-9726.2010.00633.x.
3. Zimmermann EA, Busse B, Ritchie RO. The fracture mechanics of human bone: influence of disease and treatment. Bonekey Rep. 2015;4:743. https://doi.org/10.1038/bonekey.2015.112.
4. Roddy E, DeBaun MR, Daoud-Gray A, Yang YP, Gardner MJ. Treatment of critical-sized bone defects: clinical and tissue engineering perspectives. Eur J Orthop Surg Traumatol. 2018;28(3):351–62. https://doi.org/10.1007/s00590-017-2063-0.
5. Perić Kačarević Ž, et al. An introduction to bone tissue engineering. Int J Artif Organs. 2020;43(2):69–86. https://doi.org/10.1177/0391398819876286.
6. Polo-Corrales L, Latorre-Esteves M, Ramirez-Vick JE. Scaffold design for bone regeneration. J Nanosci Nanotechnol. 2014;14(1):15–56. https://doi.org/10.1166/jnn.2014.9127.
7. Albrektsson T, Johansson C. Osteoinduction, osteoconduction and osseointegration. Eur Spine J. 2001;10(Suppl 2):S96–101. https://doi.org/10.1007/s005860100282.
8. Rider P, Kačarević ŽP, Alkildani S, Retnasingh S, Schnettler R, Barbeck M. Additive manufacturing for guided bone regeneration: a perspective for alveolar ridge augmentation. Int J Mol Sci. 2018;19(11):3308. https://doi.org/10.3390/ijms19113308.
9. Bouet G, Cruel M, Laurent C, Vico L, Malaval L, Marchat D. Validation of an in vitro 3D bone culture model with perfused and mechanically stressed ceramic scaffold. Eur Cells Mater. 2015;29:250–67. https://doi.org/10.22203/eCM.v029a19.
10. Kasten P, Beyen I, Niemeyer P, Luginbühl R, Bohner M, Richter W. Porosity and pore size of β-tricalcium phosphate scaffold can influence protein production and osteogenic differentiation of human mesenchymal stem cells: an in vitro and in vivo study. Acta Biomater. 2008;4(6):1904–15. https://doi.org/10.1016/j.actbio.2008.05.017.
11. Shah N. Recent advances in imaging technologies in dentistry. World J Radiol. 2014;6(10):794. https://doi.org/10.4329/wjr.v6.i10.794.
12. Versluis RGJA, Vismans FJFE, Van De Ven CM, Springer MP, Petri H. Radiographic absorptiometry of the phalanges as a screening instrument to detect osteoporosis of the hip. Acta Radiol. 1999;40(4):418–21. https://doi.org/10.3109/02841859909177757.
13. Risselada M, Winter MD, Lewis DD, Griffith E, Pozzi A. Comparison of three imaging modalities used to evaluate bone healing after tibial tuberosity advancement in cranial cruciate ligament-deficient dogs and comparison of the effect of a gelatinous matrix and a demineralized bone matrix mix on bone healing - a pilot study. BMC Vet Res. 2018;14(1):164. https://doi.org/10.1186/s12917-018-1490-4.
14. Pekkan G. Radiopacity of dental materials: an overview. Avicenna J Dent Res. 2016;8(2):8. https://doi.org/10.17795/ajdr-36,847.

15. Pekkan G, Aktas A, Pekkan K. Comparative radiopacity of bone graft materials. J Craniomaxillofac Surg. 2012;40(1):e1. https://doi.org/10.1016/j.jcms.2011.01.018.

16. Monsour PA, Dudhia R. Implant radiography and radiology. Aust Dent J. 2008;53(Suppl 1):S11–25. https://doi.org/10.1111/j.1834-7819.2008.00037.x.

17. Riachi F, et al. Influence of material properties on rate of resorption of two bone graft materials after sinus lift using radiographic assessment. Int J Dent. 2012;2012:737262. https://doi.org/10.1155/2012/737262.

18. Tonea M, et al. Comparative dimensional study between panoramic X-ray (OPG) and cone beam CT (CBCT). ARS Medica Tomitana. 2016;22(3):196–202. https://doi.org/10.1515/arsm-2016-0033.

19. Peyrin F, Dong P, Pacureanu A, Langer M. Micro- and nano-CT for the study of bone ultrastructure. Curr Osteoporos Rep. 2014;12(4):465–74. https://doi.org/10.1007/s11914-014-0233-0.

20. De Lange GL, et al. A histomorphometric and micro-computed tomography study of bone regeneration in the maxillary sinus comparing biphasic calcium phosphate and deproteinized cancellous bovine bone in a human split-mouth model. Oral Surg Oral Med Oral Pathol Oral Radiol. 2014;117(1):8–22. https://doi.org/10.1016/j.oooo.2013.08.008.

21. Palacio-Mancheno PE, Larriera AI, Doty SB, Cardoso L, Fritton SP. 3D assessment of cortical bone porosity and tissue mineral density using high-resolution µCT: effects of resolution and threshold method. J Bone Miner Res. 2014;29(1):142–50. https://doi.org/10.1002/jbmr.2012.

22. Barth HD, Zimmermann EA, Schaible E, Tang SY, Alliston T, Ritchie RO. Characterization of the effects of x-ray irradiation on the hierarchical structure and mechanical properties of human cortical bone. Biomaterials. 2011;32(34):8892–904. https://doi.org/10.1016/j.biomaterials.2011.08.013.

23. Janovic A, et al. Association between regional heterogeneity in the mid-facial bone micro-architecture and increased fragility along Le Fort lines. Dent Traumatol. 2017;33(4):300–6. https://doi.org/10.1111/edt.12333.

24. Bouxsein ML, Boyd SK, Christiansen BA, Guldberg RE, Jepsen KJ, Müller R. Guidelines for assessment of bone microstructure in rodents using micro-computed tomography. J Bone Miner Res. 2010;25(7):1468–86. https://doi.org/10.1002/jbmr.141.

25. Hahn M, Bale H, Lavery L, Busse B. Detection of osteogenesis in explanted synthetic hydroxyapatite-silicone orbital implants using 3D X-ray microscopy. Microsc Microanal. 2016;22(S3):116–7. https://doi.org/10.1017/s1431927616001434.

26. Zehbe R, et al. Going beyond histology. Synchrotron micro-computed tomography as a methodology for biological tissue characterization: from tissue morphology to individual cells. J R Soc Interface. 2009;7(42):49–59. https://doi.org/10.1098/rsif.2008.0539.

27. Hesse B, et al. Accessing osteocyte lacunar geometrical properties in human jaw bone on the submicron length scale using synchrotron radiation µCT. J Microsc. 2014;255(3):158–68. https://doi.org/10.1111/jmi.12147.

28. Rothweiler RM, et al. Comparative quantification of the 3D microarchitecture of human alveolar bone and anterior iliac crest in autologous bone transplants – a synchrotron radiation µ-CT study. Clin Oral Implants Res. 2020;31(S20):16. https://doi.org/10.1111/clr.12_13643.

29. Jung O, et al. Biocompatibility analyses of HF-passivated magnesium screws for guided bone regeneration (GBR). Int J Mol Sci. 2021;22(22):12567. https://doi.org/10.3390/ijms222212567.

30. Rider P, et al. Biodegradable magnesium barrier membrane used for guided bone regeneration in dental surgery. Bioact Mater. 2021;14:152–68. https://doi.org/10.1016/j.bioactmat.2021.11.018.

31. Kačarević ŽP, et al. Biodegradable magnesium fixation screw for barrier membranes used in guided bone regeneration. Bioact Mater. 2021;14:15–30. https://doi.org/10.1016/j.bioactmat.2021.10.036.

32. Kumar PT, YashodaDevi BK, Rakesh N. Basics of CBCT imaging. JDOR. 2017;13(1):49–55.

33. Ludlow JB, Davies-Ludlow LE, Brooks SL, Howerton WB. Dosimetry of 3 CBCT devices for oral and maxillofacial radiology: CB Mercuray, NewTom 3G and i-CAT. Dentomaxillofac Radiol. 2006;35(4):219–26. https://doi.org/10.1259/dmfr/14340323.

34. Shokri A, Ramezani L, Bidgoli M, Akbarzadeh M, Ghazikhanlu-Sani K, Fallahi-Sichani H. Effect of field-of-view size on gray values derived from cone-beam computed tomography compared with the Hounsfield unit values from multidetector computed tomography scans. Imaging Sci Dent. 2018;48(1):31–9. https://doi.org/10.5624/isd.2018.48.1.31.

35. American Dental Association Council on Scientific Affairs. The use of cone-beam computed tomography in dentistry. J Am Dent Assoc. 2012;143(8):899–902. https://doi.org/10.14219/jada.archive.2012.0295.

36. Periago DR, Scarfe WC, Moshiri M, Scheetz JP, Silveira AM, Farman AG. Linear accuracy and reliability of cone beam CT derived 3-dimensional images constructed using an orthodontic volumetric rendering program. Angle Orthod. 2008;78(3):387–95. https://doi.org/10.2319/122106-52.1.

37. Umanjec-Korac S, Parsa A, Nikoozad AD, Wismeijer D, Hassan B. Accuracy of cone beam computed tomography in following simulated autogenous graft resorption in maxillary sinus augmentation procedure: an ex vivo study. Dentomaxillofac Radiol. 2016;45(6):20160092. https://doi.org/10.1259/dmfr.20160092.

38. Liljensten E, Adolfsson E, Strid KG, Thomsen P. Resorbable and nonresorbable hydroxyapatite granules as bone graft substitutes in rabbit cortical defects. Clin Implant Dent Relat Res. 2003;5(2):95–102. https://doi.org/10.1111/j.1708-8208.2003.tb00190.x.

39. Antonijević D, et al. Application of reference point indentation for micro-mechanical surface characterization of calcium silicate based dental materials. Biomed Microdevices. 2016;18(2):1–12. https://doi.org/10.1007/s10544-016-0047-1.

40. Antonijevic D, et al. Addition of a fluoride-containing radiopacifier improves micromechanical and biological characteristics of modified calcium silicate cements. J Endod. 2015;41(12):2050–7. https://doi.org/10.1016/j.joen.2015.09.008.

41. Rolvien T, et al. ß-TCP bone substitutes in tibial plateau depression fractures. Knee. 2017;24(5):1138–45. https://doi.org/10.1016/j.knee.2017.06.010.

42. Roschger P, Fratzl P, Eschberger J, Klaushofer K. Validation of quantitative backscattered electron imaging for the measurement of mineral density distribution in human bone biopsies. Bone. 1998;23(4):319–26. https://doi.org/10.1016/S8756-3282(98)00112-4.

43. Antonijevic D, et al. Microstructure and wettability of root canal dentine and root canal filling materials after different chemical irrigation. Appl Surf Sci. 2015;355:369–78. https://doi.org/10.1016/j.apsusc.2015.07.023.

44. Busse B, Jobke B, Werner M, Fürst M, Rüther W, Delling G. Fluoridosteopathie - Eine vergessene entität. Gleichzeitiges auftreten von coxarthrose und bis dahin unbekannter fluoridosteopathie bei einer 73-jährigen patientin. Pathologe. 2006;27(1):73–9. https://doi.org/10.1007/s00292-005-0799-5.

45. Busse B, et al. Effects of strontium ranelate administration on bisphosphonate-altered hydroxyapatite: matrix incorporation of strontium is accompanied by changes in mineralization and microstructure. Acta Biomater. 2010;6(12):4513–21. https://doi.org/10.1016/j.actbio.2010.07.019.

46. Langstaff S, Sayer M, Smith TJN, Pugh SM. Resorbable bioceramics based on stabilized calcium phosphates. Part II: evaluation of biological response. Biomaterials. 2001;22(2):135–50. https://doi.org/10.1016/S0142-9612(00)00139-3.

47. Protopappas VC, Baga DA, Fotiadis DI, Likas AC, Papachristos AA, Malizos KN. An ultrasound wearable system for the monitoring and acceleration of fracture healing in long bones. IEEE Trans Biomed Eng. 2005;52(9):1597–608. https://doi.org/10.1109/TBME.2005.851507.

48. Yang WP, Wang Z, Feng NQ, Wang CM, Du SL. Application of real-time B-mode ultrasound in posterior decompression and reduction for thoracolumbar burst fracture. Exp Ther Med. 2013;6(4):1005–9. https://doi.org/10.3892/etm.2013.1257.

49. Vastel L, Meunier A, Siney H, Sedel L, Courpied JP. Effect of different sterilization processing methods on the mechanical properties of human cancellous bone allografts. Biomaterials. 2004;25(11):2105–10. https://doi.org/10.1016/j.biomaterials.2003.08.067.

50. Nguyen KCT, Pachêco-Pereira C, Kaipatur NR, Cheung J, Major PW, Le LH. Comparison of ultrasound imaging and conebeam computed tomography for examination of the alveolar bone level: a systematic review. PLoS One. 2018;13(10):e0200596. https://doi.org/10.1371/journal.pone.0200596.

51. Noviana D, et al. In vivo study of hydroxyapatite-chitosan and hydroxyapatite-tricalcium phosphate bone graft in sheep's bone as animal model. In: Proceedings - international conference on instrumentation, communication, information technology and biomedical engineering 2011, ICICI-BME 2011, 2011. pp. 403–408. https://doi.org/10.1109/ICICI-BME.2011.6108636.

52. Rahimzadeh R, Veshkini A, Sharifi D, Hesaraki S. Value of color Doppler ultrasonography and radiography for the assessment of the cancellous bone scaffold coated with nano-hydroxyapatite in repair of radial bone in rabbit. Acta Cir Bras. 2012;27(2):148–54. https://doi.org/10.1590/s0102-86,502,012,000,200,009.

53. Xiao WL, Zhang DZ, Chen XJ, Yuan C, Xue LF. Osteogenesis effect of guided bone regeneration combined with alveolar cleft grafting: assessment by cone beam computed tomography. Int J Oral Maxillofac Surg. 2016;45(6):683–7. https://doi.org/10.1016/j.ijom.2016.01.013.

54. Lee H-G, Kim Y-D. Volumetric stability of autogenous bone graft with mandibular body bone: cone-beam computed tomography and three-dimensional reconstruction analysis. J Korean Assoc Oral Maxillofac Surg. 2015;41(5):232. https://doi.org/10.5125/jkaoms.2015.41.5.232.

55. Dasmah A, Thor A, Ekestubbe A, Sennerby L, Rasmusson L. Particulate vs. block bone grafts: three-dimensional changes in graft volume after reconstruction of the atrophic maxilla, a 2-year radiographic follow-up. J Craniomaxillofac Surg. 2012;40(8):654–9. https://doi.org/10.1016/j.jcms.2011.10.032.

56. Spin-Neto R, Stavropoulos A, Pereira LAVD, Marcantonio E, Wenzel A. Fate of autologous and fresh-frozen allogeneic block bone grafts used for ridge augmentation. A CBCT-based analysis. Clin Oral Implants Res. 2013;24(2):167–73. https://doi.org/10.1111/j.1600-0501.2011.02324.x.

57. Kloss FR, Offermanns V, Kloss-Brandstätter A. Comparison of allogeneic and autogenous bone grafts for augmentation of alveolar ridge defects—a 12-month retrospective radiographic evaluation. Clin Oral Implants Res. 2018;29(11):1163–75. https://doi.org/10.1111/clr.13380.

58. Tilaveridis I, Lazaridou M, Zouloumis L, Dimitrakopoulos I, Tilaveridis V, Tilaveridou S. The use of mineralized bone allograft as a single grafting material in maxillary sinus lifting with severely atrophied alveolar ridge (1–3 mm) and immediately inserted dental implants. A 3- up to 8-year retrospective study. Oral Maxillofac Surg. 2018;22(3):267–73. https://doi.org/10.1007/s10006-018-0698-6.

59. Simonpieri A, Gasparro R, Pantaleo G, Mignogna J, Riccitiello F, Sammartino G. Four-year post-loading results of full-arch rehabilitation with immedi-

ate placement and immediate loading implants: a retrospective controlled study. Quintessence Int. 2017;48(4):315–24. https://doi.org/10.3290/j.qi.a37894.

60. Zhao R, Yang R, Cooper PR, Khurshid Z, Shavandi A, Ratnayake J. Bone grafts and substitutes in dentistry: a review of current trends and developments. Molecules. 2021;26(10):1–27. https://doi.org/10.3390/molecules26103007.

61. Gultekin BA, Cansiz E, Borahan MO. Clinical and 3-dimensional radiographic evaluation of autogenous iliac block bone grafting and guided bone regeneration in patients with atrophic maxilla. J Oral Maxillofac Surg. 2017;75(4):709–22. https://doi.org/10.1016/j.joms.2016.11.019.

62. Alper Gultekin B, et al. Evaluation of volumetric changes of augmented maxillary sinus with different bone grafting biomaterials. J Craniofac Surg. 2016;27(2):e144–8. https://doi.org/10.1097/SCS.0000000000002393.

63. Tabrizi R, Mir H, Sadeghi M, Hashemzadeh H, Jafari S. Evaluation of demineralized freeze-dried bone in augmentation of buccal defects during implant placement. Regen Reconstr Restor. 2016;1(2):75–8. https://doi.org/10.22037/rrr.v1i2.10524.

64. Kacarevic ZP, et al. Purification processes of xenogeneic bone substitutes and their impact on tissue reactions and regeneration. Int J Artif Organs. 2018;41(11):789–800. https://doi.org/10.1177/0391398818771530.

65. Georgiev T, Peev S, Arnautska H, Gencheva A, Gerdzhikov I. An evaluation of three-dimensional scans of the time-dependent volume changes in bone grafting materials. Int J Sci Res ISSN. 2015;6. https://doi.org/10.21275/ART20164039.

66. Jelusic D, Zirk ML, Fienitz T, Plancak D, Puhar I, Rothamel D. Monophasic ß-TCP vs. biphasic HA/ß-TCP in two-stage sinus floor augmentation procedures – a prospective randomized clinical trial. Clin Oral Implants Res. 2017;28(10):e175–83. https://doi.org/10.1111/clr.12983.

67. Gultekin BA, Borahan O, Sirali A, Karabuda ZC, Mijiritsky E. Three-dimensional assessment of volumetric changes in sinuses augmented with two different bone substitutes. Biomed Res Int. 2016;2016:4085079. https://doi.org/10.1155/2016/4085079.

68. Sushma Sonale MN, et al. Absorbable gelatin sponge versus alloplastic graft material as adjuvants in direct sinus lift procedures—a comparative study. J Dent Orofac Res. 2018;14(1):7–17.

Biology of Resorbable Bone Substitutes: CaP-Based and Polymers

Mike Barbeck, Jens Pissarek, Said Alkildani, Ole Jung, and Ronald E. Unger

17.1 Introduction

Regeneration of bone defects or sites of augmentation often requires the application of so-called bone substitute materials combined with or without autologous bone; this is still considered as a regenerative gold standard [1–3]. A bone substitute is defined as "a synthetic, inorganic, or biologically organic combination, which can be inserted for the treatment of a bone defect instead of autogenous or allogenous bone" [4]. The principle behind the application of resorbable bone substitutes is called "creeping substitution" [5].

This term was created by Phemister, referring to a previous analysis by Axhausen, and defines the repair of osteonecrotic bone [6]. Axhausen described the repair process as "simultaneous absorption of dead bone and incomplete, irregular replacement by new bone" [6]. However, this explanation was expanded by Phemister, as he described the process of creeping substitution as "gradual absorption of the old bone and replacement by new bone, so that in the course of months or occasionally years, the necrotic area is more or less completely transformed into living bone" [6]. Phemister related this principle to the application of autologous bone transplants [7]. This term survives today and is used to describe the simultaneous process of bone regeneration up to the final condition of *restitution ad integrum* in concert with the degradation of a resorbable bone substitute.

For this, a broad variety of bone-substitute materials is commercially available. In particular, materials of "natural" origin, i.e., human- or animal-derived materials (allo- or xenografts), are supposed to allow for bone regeneration comparable to that allowed by autologous bone grafts, or at least to the regenerative potential of their calcified bone matrix serving as an osseoconductive scaffold structure [8]. This assumption is based on the similarity of their chemical composition, which mainly contains hydroxyapatite (HA), and their (macro-, micro-, and nano-) structure that is more or less preserved after the

M. Barbeck (✉)
Clinic and Policlinic for Dermatology and Venereology, University Medical Center Rostock, Rostock, Germany

BerlinAnalytix GmbH, Berlin, Germany
e-mail: mike.barbeck@med.uni-rostock.de

J. Pissarek
Biotrics Bioimplants AG, Berlin, Germany

S. Alkildani
Clinic and Policlinic for Dermatology and Venereology, University Medical Center Rostock, Rostock, Germany

O. Jung
BerlinAnalytix GmbH, Berlin, Germany

R. E. Unger
Repair-Lab, Institute of Pathology, University Medical Center of the Johannes Gutenberg University, Mainz, Germany
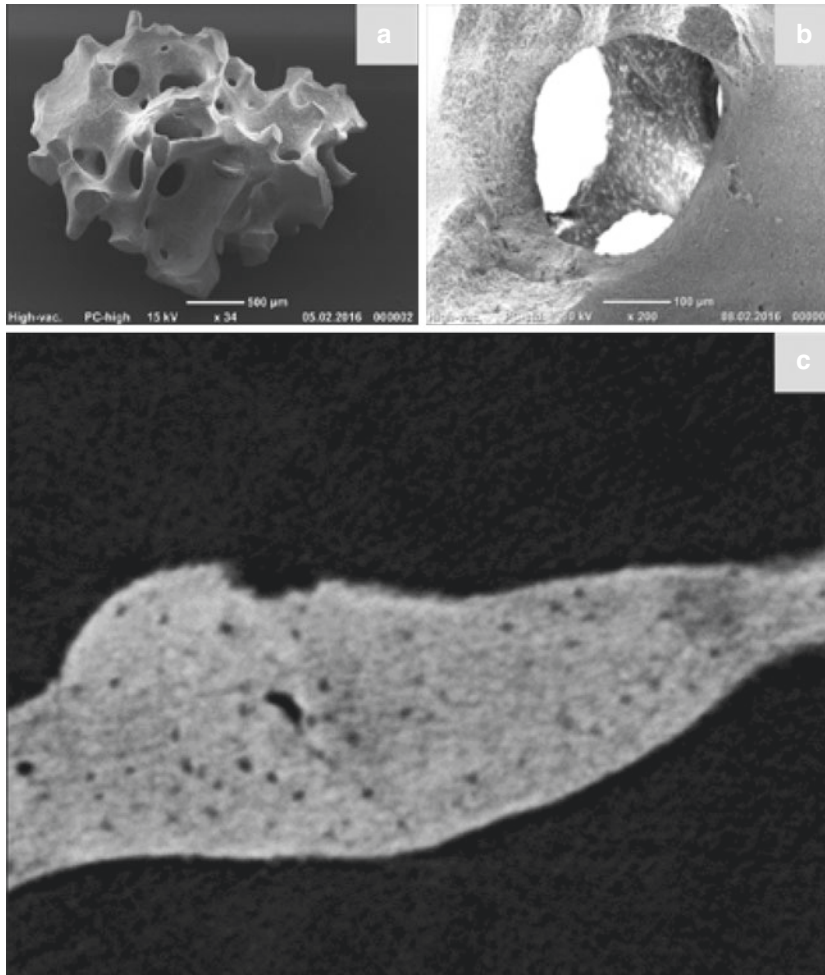
Fig. 17.1 Shows scanning electron microscopy (SEM) images of a xenogeneic bone substitute derived from bovine femoral heads. The typical structure of the bone matrix, including trabeculae and macro- and micropores (**a**, **b**), as well as osteocyte lacunae and the lamellar substructure, (**c**) is preserved

application of different purification methods (Fig. 17.1) [8, 9].

Interestingly, both allo- and xenogeneic materials are customizable via a milling process, allowing for the manufacturing of patient-individual scaffolds and, thus, for optimized bone healing [10–12]. In this context, computer-tomographical data can be used as bases for the milling process via computer-aided design and computer-aided manufacturing (CAD/CAM) [11]. However, the size of the donor tissue, which most often originates from cancellous bone obtained from femoral heads of living human donors or animals, restricts the final size of the implant. Furthermore, the dimensions of patient-individualized implants having these origins are limited by the milling tools and process parameters.

Many different synthetic or alloplastic bone substitutes are also clinically used [10, 12]. Most of these materials are based on HA and beta-tricalcium phosphate (β-TCP), which belong to the calcium phosphate (CaP) ceramics group and bear chemical similarities to the natural bone matrix [12]. CaP-based alloplastic bone substitutes are supposed to permit comparable regenerative possibilities; this has been shown in a broad variety of studies [13, 14]. Most CaP-based materials on the market are mixtures of both compounds, the so-called biphasic bone substi-

tutes containing different proportions of HA and β-TCP [8, 9, 12]. Materials such as bioglasses, or those based on calcium sulfate, are also available [15, 16].

Many different synthetic polymeric materials have been developed for bone regeneration [17–19]. The most investigated group of polymers contains aliphatic polyesters including polycaprolactone (PCL), polylactic acid (PLA), polyglycolic acid (PGA), and poly(lactic-*co*-glycolic) acid (PLGA) [17–19]. This special class of bone substitute materials allows for the manufacturing of patient-individualized scaffolds using techniques such as 3D printing or selective laser sintering (SLS) [19]. Moreover, metallic bone-substitute materials are also currently in focus for bone regeneration. Magnesium-based materials are of special interest because this metal has been shown to be highly biocompatible [20]. This raw material also allows for the preparation of 3D scaffolds, which can be customized for individual defect conditions [21].

These different classes of bone substitute materials provide regenerative bone growth via the process of osseoconduction, allowing the growth of osteoblasts onto their surfaces and subsequent synthesis of the bone matrix [22]. In contrast, autologous bone grafts promote bone healing via three different pathways: osseoconduction, osseoinduction, and osseogenesis [23]. The regenerative capacities of autologous bone grafts are based on the different elements of autologous bone tissue, which does not have to be purified from potentially immunogenic components such as allo- or xenografts [22, 24, 25]. Thus, an autologous bone graft contains different bone-cell types such as osteoblasts, osteocytes, and osteoclasts, combined with the calcified bone matrix [24, 25]. Matrix-associated proteins, such as bone morphogenetic proteins (BMPs), osteopontin, osteonectin, osteocalcin, and matrix- and cell-related metal ions are important components of autografts [23]. Furthermore, bone tissue-related connective tissue, including the vasculature and endothelial cells, is a key component of bone grafts [24, 26, 27]. Other cell types, including the so-called osteomacs, which represent a special subtype of macrophages residing in bony tissue, are also components of autografts and

have been shown to contribute to the healing process [28]. Altogether, an autograft more or less represents a physiologically active transplant that can support the process of bone regeneration via different pathways. In contrast, no bone substitute material possessing comparable regenerative capacities has been developed thus far. However, different approaches have been developed to overcome this issue.

The influence of different physical characteristics of bone substitutes, such as porosity or (nano-) topography, has been extensively analyzed, particularly in synthetic bone substitutes [29–31]. Certain material properties may allow such materials to mimic even the characteristics of the extracellular and calcified bone matrix, enabling inductive bone growth [32]. Although many materials used in different bone substitutes allow for osseoinduction, their regenerative properties have never been revealed in clinical studies, indicating that this concept is still not tenable [33].

Furthermore, different natural polymers or compounds, such as collagen or hyaluronic acid (HY), have been added to bone substitute materials to enhance their regenerative capacities [34–36]. Even various components of the extracellular matrix have been used to influence healing factors such as integration behavior, vascularization of the implant bed, and osteoblastic growth and differentiation (Fig. 17.2) [34–36]. Water-binding polymers, such as HY, enable the production of so-called bone pastes, which allow for minimally invasive application and insertion of bone substitute materials into borders of defects, allowing for improved bone healing [37].

Combining bone-substitute materials with osseoinductive agents, such as different BMPs, has also been reported [33, 35]. However, the underlying regenerative mechanisms of BMPs are not yet completely understood and, thus, possible side effects are still unknown. Moreover, such molecules are usually administered in nonphysiological doses, i.e., thousands to millions of times higher than the physiological amount [37]. Finally, osseoinductive substances, such as BMPs, remain very costly, which further limits their clinical application [37].

Various tissue-engineering concepts have been described for bone tissue regeneration [38,
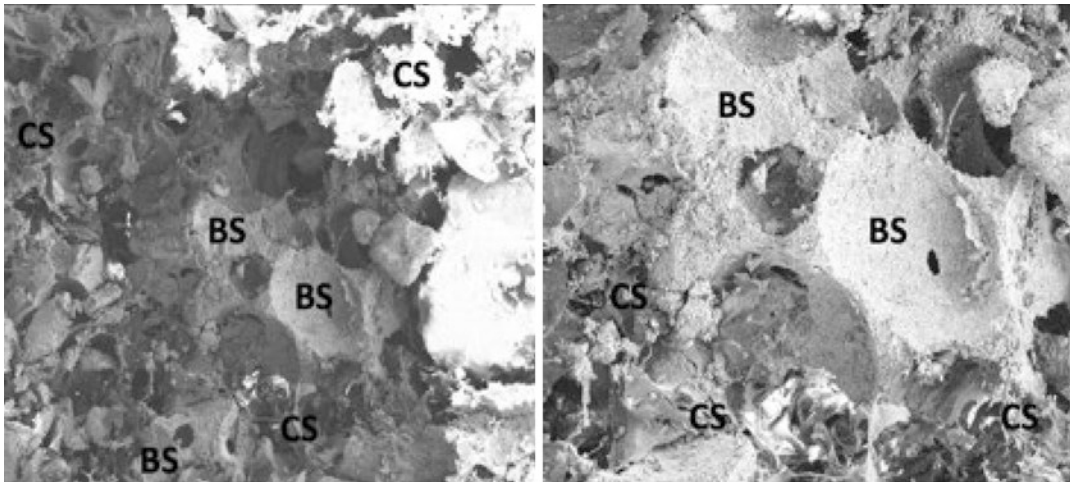
Fig. 17.2 Shows SEM images of a newly developed bone-substitute material composed of bone-substitute granules (BS) based on biphasic calcium phosphate embedded within a collagen scaffold (CS) (left images: ×100 magnification, right image: ×200 magnification)

39]. These concepts include the addition of different cell types to bone-substitute materials, such as osteoblasts and their precursor cells (i.e., mesenchymal stem cells) [39]. Combining bone substitutes with different other cell types that directly or indirectly support the process of bone growth has also been analyzed. For example, the influence of different endothelial cell types in mono- or co-culture with osteoblasts has been examined, because sufficient vascularization is an important factor for bone-tissue regeneration [39–42]. Blood cells or "inflammatory" cells, such as macrophages, have also been used to increase the regenerative properties of bone substitutes because these cell types can express different molecules that are involved in bone-tissue healing [43, 44]. However, most of these concepts are still not clinically applicable because they are not applicable in acute clinical situations, due to such factors as long-time spans needed for cell isolation and co-cultivation with bone substitutes [38, 45].

Combining different metal ions with bone-substitute materials has also been analyzed [15, 46]. This combination is based on the fact that different metal ions are both essential components of the extracellular calcified bone matrix and of cells or proteins that regulate essential

cellular processes such as proliferation and differentiation [15]. Thus, different metal ions play functional roles in the physiological cellular environment and in the course of bone healing. This brought the application of metal ions, in combination with the above-mentioned bone substitutes, into focus for bone regeneration [15].

Although numerous studies have analyzed the bone healing capacities of various materials, no bone substitute yet allows for regenerative capacities comparable to the healing pathways of autologous bone transplants described above. Thus, a variety of new bone substitute materials is still under development. Preclinical in vitro and in vivo, as well as clinical, testing of these newly developed materials is greatly important for evaluating their regenerative properties and securing their future clinical application. The preclinical and clinical analyses can be divided into three different major parts:

(a) Analysis of the regenerative effects of bone substitutes
(b) Analysis of the inflammatory tissue response to bone substitutes
(c) Analysis of the degradation pathways of bone substitutes

These three analyses are directly or indirectly connected [47, 48]. On the one hand, osteoblasts and their precursors need to migrate into a bone defect and thereby require a scaffold structure for their osteoconductive ingrowth, which should be provided by a bone substitute. Their growth and differentiation behavior are dependent on different material factors such as material geometry, pore size and distribution, pore structure, surface structure, and chemical composition [13, 15–18, 29, 30, 33, 35, 49]. On the other hand, every bone substitute is initially embedded within connective tissue within its implantation bed before its integration into bone tissue [8, 29, 30]. Interestingly, bone tissue is a special type of connective tissue and, thus, it could be supposed that this initial connective tissue within an implantation bed of a bone substitute is the further basis for bone growth. Thus, the tissue distribution of this material-associated connective tissue is dependent on the respective physicochemical characteristics of the bone substitute [29, 30, 47, 48]. Moreover, material characteristics, such as (nano-) topography or surface chemistry, as well as porosity and granule size, have been shown to regulate tissue integration of bone substitutes [13, 15–18, 29, 30, 33, 35, 49–51].

In this context, every bone substitute induces an inflammatory response and inflammatory tissue response cascade, the so-called "foreign body reaction to biomaterials" [47, 48, 52, 53]. This cascade starts with an accumulation of proteins at the surfaces of the implanted material; this is known as the "Vroman effect" [52, 53]. This process of protein accumulation is extremely specific for every bone substitute because it depends on the respective physicochemical characteristics of the substitute; these characteristics can cause the accumulation of specific types of proteins and influence their amounts and conformational changes [52, 53]. Interestingly, even this initial step of the foreign body reaction cascade appears to dictate the ensuing pattern of integration, as the protein layer leads to the binding of the first generation of cells [52, 53]. This cell binding at different binding sites of the accumulated proteins, with bonding capacity dependent on the respective protein and its special conformation at

the material surface, induces the later cellular responses by influencing a variety of signaling pathways [52, 53]. These primary cell populations guide further processes within the implantation bed, including the invasion of other cell types such as granulocytes, fibroblasts, and endothelial cells [52, 53]. In this inflammatory cascade, macrophages are key cellular components because they regulate different processes in the implantation bed [47, 48, 52, 53]. Moreover, their fused end stage, the multinucleated giant cell (MNGC), is regularly found within the implantation beds of most bone substitutes [47, 48, 52, 53]. Interestingly, the MNGCs in the implant beds of both natural-based bone-substitute materials and synthetic materials appear to possess the phenotype of foreign body giant cells (FBGCs) [47]. It has been long supposed that MNGCs in the implant beds of bone substitutes, based on calcium phosphates such as the calcified bone matrix, are osteoclasts, i.e., physiologically derived cells involved in bone metabolism. However, the newest results have shown that this cell type is of inflammatory origin [47]. Both macrophages and MNGCs express pro- and anti-inflammatory molecules, such as the vascular endothelial growth factor (VEGF) and heme oxygenase (HO), which have a major influence on the vascularization of the implant bed of a bone substitute material [48, 54]. Vascularization is a key factor for bone-tissue regeneration and the process of osteoconduction (Fig. 17.3); thus, the inflammatory response to a material is connected with the bone healing process and other various pathways [47, 48].

The different relationships between these two processes have already been revealed. For example, in addition to its other pathways and molecular interactions, VEGF also influences differentiation, proliferation, and bone formation [29, 47, 48]. Altogether, connective tissue is the basis for the subsequent process of bone growth and deposition of bone matrix.

The inflammatory reaction is also connected with the process of bone substitute degradation. Macrophages and their fused end stages, the multinucleated giant cells (MNGCs), are mainly involved in phagocytosis—besides the process of
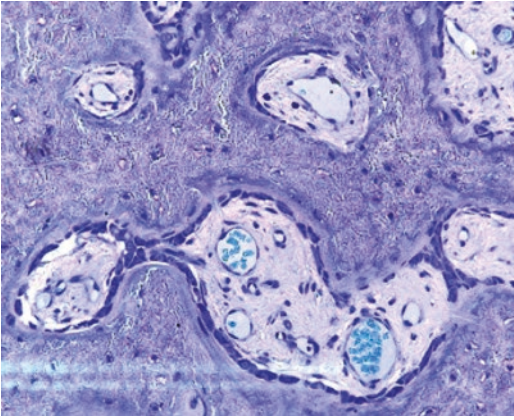
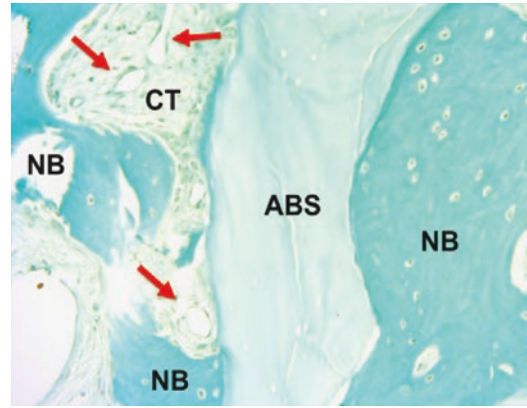**Fig. 17.3** Shows newly generated bone tissue within an implantation bed of a bone-substitute material. Within the interspaces of the calcified bone matrix, connective tissue islands are regularly observable and contain high numbers of blood vessels, indicating their importance in tissue regeneration

Fig. 17.5 Shows the integration behavior of an allogeneic bone substitute (ABS) within newly generated bone tissue (NB). The ABPS granule is completely embedded within the newly generated bone tissue, and histological signs of its cellular degradation, such as material-adherent macrophages or MNGCs, are not observable

Fig. 17.4 Shows an MNGC at the surface of a psychogenic bone-substitute granule phagocytizing fragments of the material (red staining = TRAP-containing phagosome)

dissolution that occurs in bone substitutes with higher solubility (Fig. 17.4) [43, 47, 48, 50].

Different degradation patterns have already been shown for the above-described materials, indicating their different clinical use for various indications [18, 30, 50, 55]. Although bone substitute materials of allo- and xenogeneic origin allow for sufficient bone regeneration, it is still questionable whether these substitute materials are resorbable [51, 56]. Allo- and xenografts have been found within their implantation beds years

or decades after their application [56]. This resorption behavior may result from their chemical composition, amongst other material factors; it has already been shown that hydroxyapatite-based bone substitutes are hardly or not resorbable (Fig. 17.5) [55]. Low numbers of phagocytizing cells, especially those of MNGCs, are often observed in the implantation beds of such bone substitutes [51, 55]. Altogether, a bone substitute with such a degradation behavior may not be suitable for defect sites that can heal up completely to the condition of *restitution ad integrum*. The application of such materials may be more suitable for defect sites that need material maintenance for long-term bone integration, such as in the case of sinus elevations.

Most often, synthetic bone-substitute materials based on HA mostly show resorption behaviors comparable to those of allo- and xenogeneic materials. In contrast, β-TCP-based bone substitutes have often been shown to be rapidly degraded via macrophage and MNGC phagocytosis and dissolution [29, 55]. Based on their opposing degradation behaviors, the two compounds are most often available in the form of biphasic bone substitutes as it has been revealed that mixtures of HA and β-TCP also induce a moderate inflammatory response [55]. That means a combination of their both degradation

patterns, i.e., the cellular degradation pattern via phagocytes such as MNGCs, and the solubility behavior [55]. Finally, the balanced overall degradation of biphasic bone substitutes may, in many cases, comply with the process of creeping substitution [50, 55]. The degradation of bioglasses is of special interest as it leads to the release of the ions such as magnesium or copper [15, 57]. These integrated ions also influence the process of bone healing and vascularization of the implant bed [57].

Degradation processes of synthetic polymers have also been elucidated within the last decades and remain partially controversial [58–62]. In the case of PCL, degradation is mainly based on random hydrolysis of ester bonds; this occurs within a span of 2–3 years [63–67]. While PLA, PGA, and PLA/PGA copolymers, used for bone regeneration, are mainly considered biocompatible, nontoxic, and non-inflammatory, different studies have shown that their degradation products may cause adverse tissue reactions [58, 59, 68]. Although PLA degrades to form lactic acid, which is normally present in the body and is excreted as water and carbon dioxide, the local release of acidic byproducts may decrease the biocompatibility of these materials [69]. Also, the release of small fragments during degradation can trigger local inflammatory tissue responses, even though these fragments are phagocytized by macrophages and multinucleated giant cells [70]. In the case of PGA, its cellular degradation via different enzymes with esterase activity occurs in addition to hydrolysis, with glycolic acid as the locally released product [71]. Copolymerization of PLA and PGA allows for the synthesis of PLGA, which is the most investigated degradable polymer for biomedical applications. Thus, PLGA has already been applied for suture materials, drug-delivery devices, and in tissue-engineering scaffolds [72, 73]. PLGA degrades via hydrolysis of its ester linkages in the presence of water to produce the original monomers, lactic and glycolic acids [72]. Combining both compounds can influence the time of degradation [65]. The time required for the degradation of PLGA is related to the monomer ratio. In general, an increase in glycolide units decreases the time

required for degradation [73]. However, materials based on the above-mentioned polymers, and many other related compounds, may not exhibit suitable biocompatibility or tissue response, which is required for bone tissue regeneration [18, 74]. Different strategies for overcoming these issues, such as combinations using ceramic bone-substitute materials, have been developed [18, 74]. Combining different classes of bone-substitute materials, such as allogeneic, xenogeneic, and synthetic materials, may produce optimal scaffolds for the regeneration of bone defects in different clinical situations; thus, this technology is of special interest for the development of new bone-substitute materials.

The application of metal-based bone substitutes for bone regeneration, with a special focus on magnesium-based scaffolds, remains in focus for regenerative medicine [57, 75, 76]. The degradation of magnesium is mainly based on the process of corrosion, which is one of the greatest limitations of its use in orthopedic applications [77, 78]. Although pure magnesium-based materials develop an oxide film of magnesium hydroxide ($Mg(OH)_2$), which slows corrosion, severe corrosion occurs under the release of hydrogen (H_2) [79]. Two different concepts have been established to prevent premature degradation. Alloying has been shown to improve the corrosion resistance of magnesium [77]. Different coatings and surface treatments have also been developed to prevent premature corrosion, allowing for the application of magnesium-based implants in bone regeneration [80]. For example, alloys containing a mixture of rare earth elements, in combination with another metal such as yttrium, have been shown to decrease the corrosion of such implants [77, 81]. Coating techniques often include the deposition of CaP onto the surfaces of magnesium-based materials [80].

Altogether, this summary shows that different material classes, having different regenerative properties, have been developed within the last decades. However, an optimal bone-substitute material, which would allow for bone regeneration in the context of different indications, has still not been found. Thus, further development in the field of bone substitutes is necessary to create

materials that are more adaptive to the respective (micro-) milieu. Such development requires evaluation of the three different processes of material-mediated bone regeneration: regenerative effects of bone substitutes, the analysis of material-induced inflammatory tissue response, and the analysis of material degradation. Different in vitro and in vivo analyses must be conducted for every new bone substitute material in order to evaluate its regenerative effects. Thus, different preclinical in vitro and in vivo, as well as clinical, methodologies were presented in this chapter.

17.2 Methods

17.2.1 Ex Situ Methodologies

17.2.1.1 Analyses of Physical and Chemical Properties of Bone Substitutes

Many different methods are used to analyze the physical and chemical characteristics of bone substitutes. The obtained data are often used to correlate material properties with respective cell or tissue responses [29, 35, 50, 55]. Most often, scanning electron microscopy (SEM) is used for visualization of the overall or surface morphology of bone substitutes; however, SEM can also be used for different material analyses such as measurement of pore size [29, 50, 55, 82, 83]. Thus, SEM is especially useful for comparing different materials [29, 50, 55, 83].

Data obtained by micro-computed tomography (μCT) allows for visualization of properties of bone substitute materials such as the inner structure (Fig. 17.1c) [84]. This method, which is based on X-ray imaging, allows for measurement of material properties such as pore distribution, and for 3D visualization of bone substitutes [84, 85]. X-ray diffractometry (XRD) and high-resolution X-ray diffractometry (HRXRD) are applied for the physical analysis of bone substitutes [86, 87]. In the case of CaP-based materials, both methods allow for the analysis of crystallinity [86].

Different methods are used for the determination of the chemical composition of bone substi-

tutes, depending on their components. In the case of crystalline biomaterials, such as CaP-based bone substitutes, infrared spectroscopy (IR spectroscopy or vibrational spectroscopy), thermogravimetry, or XRD are used to identify the chemical composition of bone substitute materials [86, 88].

The analysis of bone substitutes based on polymers is often an elaborate process as the characterization of macromolecules or polymers in biomaterials is complex and, thus, requires several methods to generate the necessary data. The molecular mass of a macromolecule is often the deciding factor when choosing an analytical method because many methods require the molecule to be in solution; this is more challenging to achieve if the molecular weight is high. Infrared spectroscopy (IR) delivers important data on functional groups in macromolecules and can be used even for poorly soluble macromolecules [89]. However, compared to nuclear magnetic resonance (NMR) spectroscopy, the data can lack resolution. NMR can provide detailed information on the structure, dynamics, reaction state, and chemical environment of molecules [90, 91]. The intramolecular magnetic field around an atom in a molecule changes resonance frequency, thus providing details on the electronic structure of a molecule and its individual functional groups [91, 92]. Important parameters in the characterization of macromolecules are molecular weight and molecular weight distribution, which influence mechanical properties and degradation behavior [93, 94]. Gel permeation chromatography (GPC) and size-exclusion chromatography (SEC) is dependent on the hydrodynamic volume of macromolecules, which correlates with their molecular weight [95, 96]. The data show the distribution of the molecular weight of the macromolecule blend. By adding a standard with a known molecular weight, it is possible to determine the relative molecular weight of each fraction. Mass spectroscopy is state-of-the-art for obtaining absolute molecular weight values [97]. Matrix-assisted laser-deionization time-of-flight mass spectroscopy (MALDI-TOF-MS) and electron-spray ionization mass spectroscopy (ESI-MS) can detect macromolecules having

large molecular weight [97, 98]. They overcome the problem of early decomposition of macromolecules during MS analysis and deliver structural data by tracing the fragmentation pathways.

In addition to molecular parameters, material characteristics such as tensile strength, elongation, and elasticity are among other important factors used to describe a biomaterial. For instance, aging or molecular degradation strongly influences the mechanical properties of a biomaterial and, therefore, may be used to quantify the degradation state [99, 100].

17.2.1.2 Methods for Analysis of Ex Situ Degradation of Bone Substitutes

Although the aforementioned techniques allow a basic insight into the resorption behavior of bone substitute materials, more exact methods can measure this factor both ex situ and in vivo. Even the degradation behavior of bone substitute materials known to be (partially) degraded via dissolution and corrosion, in addition to their cellular resorption, is often examined by different ex situ methods [18, 99, 101]. This is because material degradation based on dissolution or corrosion cannot be precisely analyzed by in vitro or in vivo analyses, as the distinction from phagocytic degradation is most often not possible. In this context, special solutions, such as simulated body fluid (SBF) and specialized cell culture media, have to be used for the immersion of bone substitutes to mimic the physiological environment [18, 99, 101]. To enhance the mimicry of a localized microenvironment of an implantation bed, bio-reactor systems with a specified flow rate are used as test systems for degradation studies [102, 103].

The first step in the analysis of the degradation behavior of bone substitutes is based on microscopic observations. Light microscopy is often used, but SEM is also often utilized to visualize the degradation processes of a biomaterial [18, 104]. Different quantitative methods for different types of bone substitutes have been described. In general, a simple method for analyzing degradation via dissolution or corrosion is to measure the initial weight of a bone substitute material and compare it with its weight after incubation in a degradation solution after a defined time span [105]. However, other more sensitive methods are often applied, including measuring the products of degradation [106–108]. In the case of CaP-based materials, the concentrations of calcium and phosphate ions eluted into the surrounding medium are measurable via methods such as complexometry, titration, and energy-dispersive X-ray spectroscopy (EDX) [109–111].

Effective separation of different degradation species and their characterization is mandatory for understanding the degradation mechanisms and pathways of polymeric bone substitutes. A reliable, convenient, and versatile method for assessing the fraction of degradation products is high-pressure liquid chromatography (HPLC), which may be combined, even inline, with ESI-MS [98, 112]. In addition to performing separation and characterization, HPLC can quantify the different species in the same run and, therefore, is a convenient and broadly used analysis tool [113].

Specialized methods are applied to analyze the degradation behavior of bone substitutes based on raw materials, such as magnesium, which undergo corrosion [114]. The low corrosion resistance of magnesium-based biomaterials leads to an overall degradation of these materials in physiological solutions. To detect the degradation kinetics, two major approaches are used: (a) unpolarized: loss of mass, pH monitoring, and hydrogen evolution; and (b) polarized: potentiodynamic polarization (PDP) and electrochemical impedance spectroscopy (EIS) [115]. Overall, degradation should be measured as physiologically, quickly, and validly as possible. This is currently not reflected by any of the methods. Both polarized and unpolarized methods have respective advantages and disadvantages; these are reviewed in detail by Kirkland et al. [115]. All the methods provide a relatively quick impression of the possible degradation. General disadvantages involve the accuracy and applicability in an in vivo environment. Usually, a combination of polarized and unpolarized methods (e.g., hydro-

gen evolution and potentiodynamic polarization) leads to a more precise assessment of corrosion and degradation. In the future, fluid-dynamic degradation test benches may reflect the in vivo environment far more closely.

17.2.2 In Vitro Methodologies

Biomaterials need to meet the basic requirements for biocompatibility outlined by the ISO 10993 standards [116–118]. Thus, biomaterials should be nontoxic, non-thrombogenic, non-carcinogenic, non-antigenic, and non-mutagenic [116–118]. Based on ISO protocols, the analyses of the biocompatibility of biomaterials include a series of steps and offer different starting points, allowing for application in most developed and developing medical devices. The first step is the in vitro assessment of a biomaterial including analysis of cytocompatibility. This biological evaluation, which includes standardized protocols to generate quantitative and comparable data, allows for rapid biological evaluation [116–118]. This analysis step enables a biological evaluation early in product development; it also allows for regular testing of marketed materials with regard to the efficiency of production and sterilization procedures. Moreover, the analysis of the cytocompatibility of a biomaterial via in vitro tests is required for its registration. Basic cytocompatibility analysis includes the test of (a) metabolic activity, and (b) cell viability and proliferation [117, 118]. Different methods are used for these analyses (Table 17.1) [118, 119].

Following adequate cell staining, analysis of cell morphology is also included in the evaluation of cytocompatibility via light microscopy, SEM, or confocal laser scanning microscopy [119–122]. For basic cytocompatibility analysis, using cell lines is preferable because it generates reproducible data [123, 124]. Cell lines maintain their genetic, metabolic, and morphological characteristics, making these cells reliable test objects for such kind of analysis [123]. Fibroblasts are used most often, because this cell type is essential in the healing process, having rapid contact with implanted materials [123, 124]. Moreover,

Table 17.1 shows testing methods for the analysis of cytocompatibility of biomaterials

Test object	Test method
Metabolic activity	MTT, Alamar blue assay
Cell viability	Neutral red uptake, propidium iodine staining
Cell proliferation	Cell counting, total protein content, DNA assay, 3H-TDR uptake

fibroblasts are cellular elements of nearly all tissues in the body. Thus, L-929 mouse fibroblasts are most often used for biomaterial testing because of their easy maintenance in culture [125]. Different methods for cytocompatibility testing are described with respect to material contact. Thus, cytocompatibility can be analyzed via direct or indirect contact of the cells with the biomaterial, depending on the nature of the material [124, 125].

After initial cytocompatibility tests using fibroblasts, more detailed tests are used to analyze the responses of specific cell types to a specific bone substitute. Thus, depending on the bone substitute, the responses of osteoblasts, osteoclasts, and endothelial cells are most often assessed [126–128]. Cell lines may generally be used for these tests, although primary or precursor cell populations in bone tissue are often selected [116–118].

17.2.2.1 Methods for Analyzing Regenerative Effects of Bone Substitutes

For the in vitro analysis of regenerative effects mediated by bone substitute materials, it is necessary to cultivate these materials with respective anabolic cells such as osteoblasts and precursor cells; this is done to analyze cellular growth patterns and proliferation [126, 128]. Most often, so-called "osteoblast-like cells," which are osteosarcoma cells from different origins such as mouse, rat, or humans, are used for these analyses; these cell lines include MG-63, MC3T3, UMR-106, SAOS-2, and HOS [116–121, 123–126, 128–130]. Osteosarcoma cells express a variety of osteoblastic marker molecules, but their overall phenotype differs from physiologi-

cal bone cells in functional activity, responsiveness to external agents, and expression of surface molecules; this has to be taken into consideration when planning experiments [129]. However, these cell types allow for an initial comparison of the osteogenic capacity of bone substitutes [124, 125, 129].

Primary osteoblasts are also used for analyzing the biocompatibility of bone substitutes, although these cells have to be isolated from bone samples. These osteoblasts can be isolated from animal and human bone tissue via enzymatic digestion and/or outgrowth from bone samples [131, 132]. Bone cells express different marker molecules such as collagen type I, bone sialoprotein, osteocalcin, osteonectin, osteocalcin, and alkaline phosphatase [133–135]. The expression level of these marker molecules is dependent on osteoblastic maturation [133, 134, 136]. The expression or secretion of marker molecules is measured to test the biocompatibility or regenerative effects of bone substitutes via methods such as enzyme-linked immunosorbent assays (ELISA) or polymerase chain reaction (PCR) [137]. Furthermore, osteoblastic cells can show signs of mineralization of the extracellular matrix in the form of mineralized nodules; these can be visualized by histological and histochemical methods such as Giemsa, Kossa, or Alizarin Red S stain, and by X-ray mapping for calcium and phosphate via SEM [138, 139].

Cells expressing an osteoblastic phenotype can be differentiated from different precursors [108]. One source is bone marrow cells derived from a single cell or colony forming unit-fibroblastic (CFU-F), which initially form fibroblastic colonies [115]. These cells can be differentiated into osteoblastic cells if cultured with osteogenic substances such as fetal calf serum (FCS) or glucocorticoids [115]. Mesenchymal stem cells (MSCs) can be differentiated into osteoblasts; thus, their differentiation is used as a benchmark for assessing the osteogenic capacity of bone substitutes [140, 141]. However, MSCs have to be characterized initially via methods such as flow cytometry [142]. This analysis has also shown that MSCs express a variety of surface markers, indicating that these cells express characteristic molecules of fibroblasts, endothelial cells, smooth muscle cells, and osteoblasts [142].

Furthermore, endothelial cells and their precursors are used for evaluating the biocompatibility of bone substitutes [143]. Both primary endothelial cells and cell lines are used to analyze the angiogenic potential of bone substitutes, which reflects their bone healing capacity [143]. The bone healing capacity and implant-bed vascularization of a bone substitute are directly and indirectly connected via molecules such as VEGF [29, 52, 144]. While VEGF expression by osteoblasts is often measured, the ability of endothelial cells to build vessel-like structures is also analyzed [145, 146]. Immunohistochemical staining can detect specific molecules such as CD31 or the von Willebrand factor (vWF) [146]. Moreover, the morphology and extent of vessel-like structures built on bone substitutes are histomorphometrically measured to compare their angiogenic properties [42]. A further approach to analyze the interaction of osteoblasts and endothelial cells with bone substitutes is their co-culture onto materials [42].

17.2.2.2   Methods for Analysis of Resorbability of Bone Substitutes

Macrophages are the main regulatory cells within the framework of inflammatory tissue reactions and healing events related to biomaterials and bone substitutes [44, 47, 52]. In vitro analyses by co-culturing bone substitutes with macrophages are used to analyze the cytotoxicity, growth behavior, degradation, and inflammatory potential of bone substitutes [147–150]. To analyze the interaction of macrophages with bone substitutes, different monocytic cell lines, such as THP-1 or U-937, are used most often [151, 152]. Both are model cell lines used in biomedical research [147, 151, 152]. The THP-1 cell line was derived from the peripheral blood of a 1-year-old human male with an acute monocytic leukemia, while the cells of the U-937 line were isolated from the histiocytic lymphoma of a 37-year-old male patient [153, 154]. Monocytes from other sources, such as cells from the peripheral blood of both

animals and humans, are often used for this kind of research [155, 156]. There is an important difference between cells from the two cell lines and primary cells: While THP-1 and U-937 cells have the capacity for further cell division and reproduction, primary monocytes or macrophages lose this ability after differentiation [157–159]. Thus, results from studies using different monocyte sources may not be comparable.

Analyses of resorbability include measuring the rate of adhesion and viability and examining the morphology of monocytic cells, macrophages, and multinucleated giant cells (MNGCs) on the surfaces of bone substitutes [160–164]. These methods include fluorescence, histochemical stainings such as DAPI, phalloidin, or Giemsa staining, and evaluation via light or electron microscopy [160, 165–167]. The data from such studies provide first insights into the resorption pattern of bone substitutes based on their interaction with phagocytic cell types. In vitro detection of tartrate-resistant acid phosphatase (TRAP), a lytic enzyme involved in the degradation of different biomaterials and bone substitutes, is of special interest for assessing material degradation even of CaP-based bone substitutes [48]. However, the number of TRAP-positive cells may not be easily measurable via histomorphometry due to the different microscopic planes in the 3D structure of bone substitutes. Therefore, more sensitive methods are for example based on direct TRAP detection and its quantitative measure via photometry [168].

Different methods are used to observe and quantitate the process of phagocytosis in human-mouse macrophages and MNGCs by following the internalization of (parts of) bone substitutes. These measurements are based on fluorescent dyes used to visualize phagocytized particles and trypan-blue staining to quench the fluorescence from particles that are not internalized [169, 170]. Finally, measurements could be performed using a fluorescence microplate reader. This methodology can also be used with cells from different adherent cell types. Furthermore, different other methods for quantification of the cellular resorption of bone substitutes have been described. One of the most interesting methods is based on culturing MNGCs on bone substitutes and measuring their respiration lacunae via SEM [160]. This method allows for quantification of the lacunae profiles, depths, diameters, and volumes.

17.2.2.3 Methods for the Analysis of Inflammatory Cell Responses to Bone Substitutes

On the one hand, it has been revealed that macrophages are mainly involved in the inflammatory responses to bone substitutes, depending on different physicochemical material characteristics [47, 48, 52–54]. Furthermore, it has been thought that MNGCs in the implant beds of bone-substitute materials are osteoclasts, based on their expression of TRAP, an osteoclastic marker, and multinucleation [47]. However, the newest data has shown that MNGCs in the implantation beds of both a synthetic and xenogeneic bone substitute appear to possess the foreign body giant cell (FBGC) phenotype [47]. Although being of inflammatory origin, both cell types express simultaneously pro- and anti-inflammatory molecules, even within the implant bed of a bone-substitute scaffold [48]. In this context, it has been revealed that the numbers of the above-mentioned cells and also the amounts of expressed cytokines are dependent on the physicochemical characteristics of a bone substitute [18, 29, 30, 43, 50, 51]. Altogether, these data show that analyses of differentiation and expression of pro- and inflammatory molecules expressed by both macrophages and MNGCs are important to evaluate the severity of material-dependent inflammatory cell responses. It has to be evaluated which combination of physicochemical material characteristics leads to which expression patterns; this can optimize and promote the bone healing process. Thus, many different studies have focused on the detection and measurements of inflammatory molecules, expressed by macrophages and MNGCs after their cultivation on different materials [48, 52, 54, 147]. To evaluate differentiation, different approaches such as immunohistochemical detection methods, fluorescence staining, microscopic
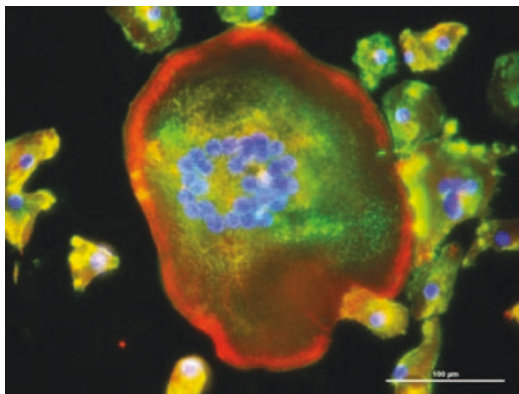
Fig. 17.6 Shows an example of an MNGC after immunohistochemical detection of integrin beta-2 (green staining)

visualization, SEM, TEM, and confocal microscopy can be used (Fig. 17.6) [47, 50, 171–175].

To measure pro- and anti-inflammatory molecules, including both cell-associated and secreted molecules, different techniques are suitable. In addition to immunohistochemical detection, ELISA, PCR, and fluorescence-activated cell sorting (FACS) can be employed [54, 168, 176, 177]. Especially, Luminex xMAP technology uses a bead-based flow cytometric platform, which permits the multiplexing of up to 100 different assays within a single sample [178]. For this system, different assays are available for many classes of biomolecules and species, including cytokines and growth factors. Alternatively, assays based on single antibodies and COOH beads can be developed by individual laboratories.

17.2.3 Preclinical In Vivo Studies

17.2.3.1 Experimental Animals and Implantation Models

Various preclinical in vivo studies are conducted to test material-induced tissue responses and the regenerative effects of bone substitute materials. Thus, different animals and implantation models play an important role in this research field [179–181]. Choosing the appropriate species and combining it with a correct implantation model is complicated, and a variety of factors need to be

taken into consideration [179–181]. First of all, the correct animal model should show the bone healing capacity of a bone substitute with the highest extent of comparability to that in human organism. Different factors involved in the selection of experimental animals include the ability to conduct surgical procedures, animal availability, size of the implant, number of implants per animal, intended duration of the test, potential differences between species with regard to biological responses, cost to acquire and care for the animals, availability, acceptability to society, resistance to infection and disease, biological characteristics analogous to humans, tolerance to surgery, adequate housing facilities and support staff, and lifespan of the experimental animals [179]. Implantations are normally conducted in mice, rats, rabbits, canines, sheep, goats, and pigs to simulate the human in vivo environment [179–181]. The animal model and site of implantation are dependent on the issue being investigated. Typical implantation sites are subcutaneous connective tissue, muscle tissue, calvaria, maxilla, mandible, femora, and ulna, depending on the aims of the respective study [179–181].

Ectopic implantation of bone substitutes is mainly used to analyze cytocompatibility, inflammatory tissue responses, cellular degradability, and vascularization of the implantation bed [18, 29, 30, 37, 41–44, 50, 51, 55]. Furthermore, such implantation sites are also widely used to examine the osteoinductive properties of bone substitute materials [182]. Such studies mostly use small animals, such as mice or rats, to test the tissue compatibility of medical devices [18, 29, 30, 37, 41–44, 50, 51, 55, 179–181]. In vivo tests of medical devices implanted subcutaneously in mice are also an integral part of the respective ISO norm 10993 [181].

Different testing models are used to analyze the interactions of tissue engineering constructs, which combine bone substitute materials or scaffolds with (human) cells; the testing models include the use of immunodeficient animals [40–44]. These mice exhibit a "severe combined immunodeficiency" (SCID), which causes a deficiency in the maturation of the immune system [183]. In particular, the development of B- and

T-lymphocytes and activation of the complement system are impaired in these mice; this affects the immune defense against infections, tumors, and transplants [183]. This particular knockout mouse model is of special interest for analyzing different clinical concepts. These include the implantation of different cell types, such as osteoblasts and/or endothelial cells, and subcutaneous implantation of material-cell combinations. Such studies allow for the distinction between implanted human cells and the surrounding cells of the host organism and are conducted by using mouse- or human-specific antibodies [41–44]. Not only SCID mice are available for this type of implantation study. Other knockout models include small experimental animals, such as rats, and larger animals, such as dogs [184].

In bone substitute research, bony implantation sites enable to analysis of the regenerative effects of bone substitutes, as well as cytocompatibility, inflammatory tissue reactions, cellular degradability, and material-induced vascularization of the implantation bed [179, 181, 185–187]. Studies on material-mediated bone regeneration have been conducted in species ranging from mice to larger animals [181]. The selection of correct experimental animals and understanding species-specific bone properties, such as bone microstructure, composition, and remodeling characteristics are important factors for later in vivo comparison to the human physiological environment [179–181]. For the evaluation of bone substitutes intended for dental applications, studies examine two bone types based on their differential embryonic development in the organism [188, 189]. While the cranium grows out of the ectoderm, the rest of the skeleton is derived from the mesoderm [188, 189]. Thus, differences in the processes of bone healing might exist between the two types of bone. Furthermore, the different implant locations have to be chosen on the basis of conditions, such as mechanical loading, which include different microenvironments in different parts of an organism [179–181]. Altogether, it is necessary to test bone substitutes for dental regeneration in the appropriate environment; this includes implantation sites such as the maxilla, mandible, or the calvaria. Most often, mice are not usable for bony implantation due to their thin or small bones in their skull region; this does not allow for implantation of most bone substitutes just because of their size. Rats are one of the most commonly used experimental animals for the analysis of bone substitutes, although different limitations have been described for this model [179–181]. For example, the bones of rats (and mice) show the least similarity to human bone [181]. Rabbits, canines, and pigs show minor differences in bone composition compared with that of humans [181]. Dogs, sheep, and goats demonstrate good comparability with human bone, which makes them suitable animals for the testing of bone-implant materials [181].

Choosing an adequate implantation model is very important for the analysis of material-induced tissue reactions and the regenerative effects of bone substitute materials. As mentioned above, the subcutaneous implantation model is suitable for the analysis of tissue compatibility, inflammatory tissue reactions, cellular degradability, and material-induced vascularization of the implantation bed [18, 29, 30, 37, 43, 44, 47, 48, 50, 51, 55]. However, predicting the healing capacities of a bone substitute is limited. The limitation is based on the fact that a bone substitute, depending on its physicochemical properties, becomes integrated into bone tissue at the bony implantation site while being only covered by connective tissue at a site of subcutaneous implantation. This different embedding behavior in different anatomical regions (orthotropic and ectopic regions) leads to differences in the attachment of phagocytizing cells such as macrophages and MNGCs. However, this implantation model is optimally suitable for a first assessment of the overall tissue reactions to bone substitutes. Combined with immunodeficient animal models, such as SCID mice, this implantation model has been widely shown useful for bone-regeneration research [40–42, 44, 183, 184].

For research on craniofacial regeneration, critical-size defect models in the calvaria and mandibula are the most used implantation sites for bone substitutes. The main prerequisite for all

bone implantation models is the creation of "critical size defects", which are defined as "the smallest osseous wound that does not heal spontaneously over an extended period of time" [179]. This means that no spontaneous complete bone regeneration of the created defects is possible. Such an implantation model allows for the analysis of bone healing capacity mediated by a bone substitute material.

The calvarial critical size defect (CSD) model is one of the most frequently used implantation models, particularly in rodents, for analyzing material-mediated bone healing. Small animals allow for easy handling and rapid testing procedures [179]. Different defect sizes in different species have been described [179]. In mice, the age of the animal is an important point to consider with respect to experimental planning because juvenile mice show increased healing capacity of calvarial defects in contrast to that in older animals [179, 190]. Calvarian defects up to 5 mm in diameter showed spontaneous healing in the calvarial bone of juvenile (6-day-old) mice, while such defect sizes were found critical in adult (60-day-old) mice, making older animals preferable for calvarial CSDs [179, 190–192]. In rats, controversial data on the minimal size of calvarial CSDs have been described, because both 5 and 8 mm defects can be of critical size [191]. Interestingly, CSDs 5 mm in diameter allow for the creation of two defects per animal without touching the sagittal suture; this is in contrast to 8-mm CSDs, which can prevent substance diffusion and impair local repair/regeneration due to the close vicinity of adjacent defects [191]. Furthermore, CSDs in the calvaria of rabbits should have a minimal diameter of 11 mm, which also allows for creation of two defects in a single cranium without involving a sagittal suture line [193]. Four 8-mm defects can be used to investigate the bone healing process for up to 4 weeks [193]. Furthermore, calvarial CSDs have also been described in dogs, sheep, and pigs, with minimal CSD diameters of 20, 22, and 10 mm, respectively [193]. The defects required to induce CSDs in the mandibles of dogs and sheep should minimally have a length of 8–9 mm, while lengths around 30 mm have also been reported in

many studies [194, 195]. Furthermore, minimal sizes for CSDs in the minipig mandible were determined as 6 and 2 cm, with and without periosteal involvement; the minimal size for mandibular CSDs in pigs was determined to have a length of 10 mm [179, 196].

In summary, testing bone substitutes for cranial and maxillofacial surgery via critical size defects (CSDs) involves a hierarchy of animal models. The testing started with implantations in the calvaria of mice, rats, and rabbits, followed by studies on implantation in the mandibles of larger animals such as dogs [197].

17.2.3.2   (Pre-)Treatment of Tissue Explants and Biopsies

Preclinical tissue explants and clinical biopsies allow for the analysis of different parameters. These include tissue fractions within a bone implantation bed of a bone substitute, the extent of newly generated bone, and the remaining bone substitute and connective tissue. These parameters also include material-related factors such as implant-bed vascularization and inflammatory cell types. Different technologies, such as histochemical and immunohistochemical staining, are used for this analysis [18, 29, 30, 37, 43, 44, 47, 48, 50, 51, 55, 198]. The workup of tissue samples is greatly important for analyzing these respective factors.

The first vital step is the fixation of tissue samples, which prevents autolysis or putrefaction. It is important to determine which components within a biopsy will be analyzed because this impacts the choice of the fixation reagent [199–201]. The fixation process has to terminate biochemical reactions within a biopsy sample while preserving the cells or tissues close as possible to their natural state [199–201]. Different fixation techniques exist for further detection of respective tissue components (Table 17.2) [199–201].

The most common fixative in histology is formaldehyde, which is normally used as neutral buffered formalin, i.e., 3.7–4.0% formaldehyde in phosphate-buffered saline [199, 200]. Formaldehyde fixates tissue via cross-linking of proteins, which may lead to issues with further detection of epitopes via immunohistochemistry

Table 17.2 shows different fixatives and related target structures

Fixation method	Target structure
Neutral buffered formalin, paraformaldehyde	Proteins
Frozen sections	Enzymes
Frozen sections, glutaraldehyde	Lipids
Alcoholic fixatives, HOPE fixation	Nucleic acids
Frozen sections	Polysaccharides
Bouin solution, neutral buffered formalin	Biogenic amines

[200]. This process can be mostly reversed using a simple water treatment. Special retrieval methods, such as ultrasonic, enzymatic, or heat treatments, among others, can also be applied to recover the natural state of epitopes [199, 200]. In general, using formaldehyde allows for good fixation of the tissue sample and is usable for the preparation of many stains in the field of bone regeneration. For tissue specimens that are to undergo immunohistochemical staining, different special fixative solutions are available, which might be more favorable as no treatment due to cross-linking processes is necessary for immunohistochemistry [199, 200, 202].

After this initial fixation step, the embedding technique is important for the sectioning of tissue samples. The hardness of the tissue "dictates" the embedding technique, because the embedding medium should optimally have the same or similar hardness as the specimen to enable sectioning. For hard tissue samples, including hard materials such as bone substitutes, and for soft tissue samples, embedding in plastic is preferable; this can maintain the bone substitutes within the subsequent histological slides. Paraffin embedding is an option for both kinds of biopsies, because an initial decalcification process might also allow for the sectioning of hard tissue samples or samples including bone substitute materials [198, 203]. However, most often the bone substitute material is eluted during the decalcification process. In most cases, the tissue interface at the surfaces of former bone substitute material can be histologically examined. Additionally, different decalcification media can be used. Three main types of decalcifying agents are used: (a) strong mineral acids, (b) weaker organic acids, or (c) chelating agents [203]. Strong acids, such as hydrochloric or nitric acid, provide the most rapid methods; however, these decalcifiers have to be used carefully to prevent tissue damage that may interfere with immunohistochemical detection [203]. Decalcifiers based on weak acids, such as formic acid or trichloroacetic acid (TCA), can be directly combined with formalin [203]. Their application leads to slower decalcification, compared with agents based on strong acids, but decreases tissue damage [203]. Decalcifiers based on chelating agents, such as ethylenediaminetetraacetic acid (EDTA), are preferable because they decalcify via capturing calcium ions from both bone tissue and bone substitutes [203]. EDTA used as a calcium chelating agent, allows for mild decalcification of biopsies without damaging the tissue [203]. However, using this medium requires a considerable amount of time, i.e., weeks to months, for sufficient decalcification. Also, the sectioning of the biopsy sample is dependent on components such as bone and different bone substitutes. The process of paraffin embedding is preceded by tissue processing [203]. This processing includes dehydration, clearing, and final infiltration by wax. The waxes used for histological preparation are mixtures of purified paraffin wax and various additives such as resins. Different wax formulations allow for different types of embedding, depending on the properties of the respective biopsy sample [204]. The optimal wax formulation should possess physical properties comparable to those of embedded tissue or bone substitute [204]. This issue can be circumvented using plastic embedding; however, how the tissue samples are subsequently treated or examined is important [205, 206]. Epoxy and acrylic resins are usable as embedding media. Acrylic resins in particular should be used for samples meant to undergo immunohistochemistry [207, 208]. For both paraffin and plastic-embedded specimens, further processing includes sectioning on a microtome using different specimen holders and different profiles of microtome blades.

Other techniques include tissue freezing for cryostat sectioning [209]. This technique includes an initial rapid freezing step (generally using liq-

uid nitrogen) as the fixation method [209]. This is the fastest and easiest of all fixation methods and is well-suited for immunohistochemistry and other analyses without requiring antigen retrieval [209, 210]. However, it shows the poorest morphology, depending on the tissue being used, and is prone to freezing artifacts caused by delays in the freezing process [211]. An additional example of a fixative is 4% PFA, combined with using sucrose as a cryoprotectant [212]. This results in excellent tissue morphology is suitable for immunohistochemistry and can be combined with a slower freeze in crushed-powder dry ice alone, slush of dry ice and 100% alcohol, or in a beaker of isopentane surrounded by dry ice. This method does not tend to incur freezing artifacts or cause cracked blocks [212]. However, this technique is very time-consuming and requires antigen retrieval due to cross-linking before applying immunohistochemical procedures [213].

Altogether, the respective choice of workup methods is dependent on the technical equipment of the institution or department, and the preferences of the researchers; it also depends on special analysis methods that may require further fixation or embedding techniques.

17.2.3.3 (Immuno-)Histochemical Staining Methods

There is a variety of histochemical stains and antibodies for immunohistochemical detection of different cell types. The field of biomaterial and bone substitute research uses a special range of histochemical stains whose application allows to highlight of different important features within the biopsies and enhance tissue contrast. Microscopically separating implanted bone-substitute materials and the surrounding (newly generated) bone or connective tissue, and distinguishing between different cell types and tissue elements, can provide a wealth of information.

Initial staining of a biopsy is most often conducted via hematoxylin and eosin (H&E), which is one of the principal stains in histology and is widely used in medical diagnosis [214]. Although H&E is a useful all-purpose stain that is quick and easy to apply, its disadvantages include low differentiation between newly-generated and

local bone tissue, or between vital bone tissue and implanted allo- or xenogeneic bone substitute [215]. For more detailed separation, specialized stains are used in this research field. Some of these methods are listed in the table below [216, 217] (Table 17.3).

While these stains partially allow us to separate different cell types, such as macrophages, granulocytes, or mast cells, involved in regeneration or inflammatory processes, other specialized stains, such as Giemsa, are used for the microscopic separation of cells [218]. Enzyme-detection techniques, such as the detection of alkaline phosphatase, are used for the visualization of osteoblasts involved in bone growth and regeneration [219, 220]. A special staining method, based on the detection of the enzyme

Table 17.3 Shows different histochemical stains and their advantages

Staining method	Advantages
Masson-Goldner trichrome stain	– Differentiation between mature bone, newly formed bone, fibrous tissue, cartilage tissue, and bone substitutes
	– Detection of blood vessels based on the color of erythrocytes
Modified Masson-Goldner trichrome stain	– Differentiation between mature bone, newly formed bone, fibrous tissue, cartilage tissue, and bone substitutes
Movat's pentachrome stain	– One of the most differentiating methods for the analysis of bone healing
	– Differentiation between mature bone, newly formed bone, fibrous tissue, cartilage tissue, and bone substitutes
	– Visualization of bone accumulation within the scaffold
Alcian blue stain	– Visualization of endochondral ossification
	– Labeling of glycosaminoglycans in a bright blue color
	– Detection of chondrocytes
Toluidine blue stain	– Differentiation between mature bone, newly formed bone, and fibrous tissue
Von Kossa stain	– Visualization of mineralization
Gomori's trichrome	– Visualization of collagen
Alizarin red/ Alcian blue stain	– Visualization of mineralization

tartrate-resistant acid phosphatase (TRAP), is used to detect cells that are involved in bone matrix resorption and degradation of biomaterials such as bone substitutes [221].

The processes within an implantation bed of a bone substitute can be discerned in more detail via immunohistochemistry, which allows for the detection of molecules or cell (sub-) types involved in bone regeneration, inflammatory tissue reactions to a bone substitute, and its degradation. Many different factors have to be considered for successful immunohistochemical detection; these are not discussed in detail in this chapter. However, different guides for conducting immunohistochemistry experiments are available from antibody manufacturers, books, and publications [222]. The variables that must be considered and optimized for successful immunohistochemical detection include the respective antigens (species, expression level, sample type), epitopes, appropriate controls, sample preparation, fixation methods and fixatives, blocking steps, antigen retrieval methods, detection methods, primary and secondary antibodies, labeling methods and labels, counterstains, and mounting reagents.

Some of the molecules listed below are important in visualizing bone growth and detecting regeneration processes (Table 17.4). Indirect processes, such as vascularization of the implanta-

Table 17.4 Shows different molecules available for immunohistochemical detection of bone growth, material-induced inflammation, and material degradation

Molecules	Involvement
Runt-related transcription factor 2 (RUNX2) [224]	– Osteoblast marker
	– A protein essential for osteoblastic differentiation
Alkaline phosphatase (ALP) [225–228]	– Surface protein of osteoblasts reflecting their activity
	– A sensitive and reliable indicator of bone metabolism
	– Bone-specific isoform of alkaline phosphatase
Collagen type 1 [229]	– The main constituent of the bone matrix (~90%)
Bone Sialoprotein (BSP) [230, 231]	– Osteoblast marker
	– Required for hydroxyapatite nucleation
	– Involved in osteoclast differentiation and function
Decorin [232]	– A marker of osteoblast differentiation
Core-binding factor alpha 1 (Cbfa1) [233]	– Osteoblast marker
	– Essential transcription factor for osteoblastic differentiation and osteogenesis
Osteonectin [133, 234]	– Bone matrix marker
	– Serves as a nucleus for mineralization and regulates the formation and growth of hydroxyapatite crystals
Osteocalcin [133, 234]	– Bone matrix marker
	– Differentiation between mature bone, newly-formed bone, and fibrous tissue
Osteopontin [133, 234]	– Bone matrix marker
	– Osteopontin physically blocks the mineral formation
	– Involved in osteoclast differentiation and function
Tartrate-resistant acid phosphatase (TRAP), TRAP5b [133, 234, 235]	– Osteoclast marker
	– TRAP5b = bone-specific isoform (in contrast to TRAP 5a, which is expressed by inflammatory cells)
	– Role in skeletal development, collagen synthesis, and degradation, mineralization of bonedegradation of skeletal phosphoproteins such as osteopontin
Calcitonin receptor (CTR) [236]	– Osteoclast marker
	– A specific marker of osteoclast differentiation
	– The degree of surface expression increases as osteoclasts undergo fusion and activation
	– Differentiation markers for distinguishing mammalian osteoclasts from macrophage polykaryons

Table 17.4 (continued)

Molecules	Involvement
Cathepsin K [237, 238]	– Osteoclast marker
	– Contributes cooperatively to the process of osteoclastic bone resorption
	– Cleaves key bone-matrix proteins and is believed to play an important role in degrading the organic phase of bone during bone resorption
Receptor Activator of Nuclear Factor κ B (RANK) [239]	– Osteoclast marker
	– RANKL/RANK signaling regulates osteoclast formation, activation, and survival in normal bone modeling
Vacuolar-Type Proton Pump (E11) [240]	– Osteoclast marker
	– Osteoclast proton pump/vacuolar H(+)-ATPase
Vitronectin Receptor (VR, VNR) [241, 242]	– Osteoclast marker
	– Alpha v beta 3 integrin
	– Highly expressed in osteoclasts
	– VR-mediated osteoclast adhesion and bone resorption
Cluster of differentiation 31 (CD31), platelet endothelial cell-adhesion molecule (PECAM-1) [18, 40–44, 243]	– Vessel marker
	– Expressed at high levels on early and mature endothelial cells
Vascular endothelial growth factor (VEGF) [29, 244]	– A marker for pro-angiogenic cells including osteoblasts, macrophages, and MNGCs
Cluster of differentiation 68 (CD68), macrosialin [245, 246]	– Marker for various cells of the macrophage lineage including monocytes, histiocytes, giant cells, Kupffer cells, and osteoclasts
	– "Pan-macrophage marker" because both M1- and M2-macrophages are detected
	– Cell-adhesion molecule
Cluster of differentiation 80 (CD80) [247]	– M1 macrophage marker
	– Protein found at monocyte surfaces, co-stimulates T-cell activation and survival
Cluster of differentiation 86 (CD86) [248]	– M1 macrophage marker
	– Protein found at monocyte surfaces, co-stimulates T-cell activation and survival
Interleukin-1 receptor (IL-1R) [249]	– M1 macrophage marker
	– Cytokine receptor that binds interleukin 1
	– Primarily responsible for transmitting the inflammatory effects of interleukin-1
Cluster of differentiation 163 (CD163) [250]	– M2 macrophage marker
	– Macrophage-specific protein; upregulated expression of this receptor is one of the major signals in macrophage switch to alternatively-activated phenotypes in inflammation
Scavenger receptor-AI (SR-AI) [251]	– M2 macrophage marker
	– Crucial for promoting M2-like M/activation and polarization during hepatic inflammation
Mannose receptor/cluster of differentiation 206 (CD206) [252]	– M2 macrophage marker
	– Functions in endocytosis and phagocytosis
	– Plays an important role in immune homeostasis

tion bed, can also be visualized via immunohistochemistry [18, 40–44]. Inflammatory processes can be detected using macrophage antibodies, and techniques for differentiating between the different pro- and anti-inflammatory subtypes have already been published [222, 223]. Different antibodies for visualization of the degradation processes of bone substitutes are used in this research field (Table 17.4). In this chapter, it was not possible to display the broad variety of marker molecules used for immunohistochemical detection; therefore, some of the most important marker molecules for the processes described above are listed below (Table 17.4).

In implantation models that use immunodeficient animals for analyzing the interactions of cell-scaffold-combinations with the host tissue,

species-specific antibodies allow for the separation of human and murine cells [40–44]. Implanted human osteoblasts, endothelial cells, and monocytes/macrophages are immunohistochemically detectable within implantation beds via the detection of cell-specific markers and overall markers, such as vimentin, an intermediate filament expressed in mesenchymal cells [40–44, 253].

17.2.4 Analysis Methods for Preclinical Tissue Explants and Clinical Biopsies

17.2.4.1 Methods for Analysis of Bone Healing Mediated by Bone Substitutes

The first step in the analysis of material-mediated bone healing includes microscopic analysis of the implantation bed of a bone substitute [11, 18, 29, 30, 37, 40–44]. Different methods allow for the quantitative determination of the healing processes within the implantation beds of bone substitutes. However, a qualitative description of bony integration is very important, because factors such as interactions with the bone matrix, or osteoblastic growth that is reflected by osteoblastic hems, can only be described based on observations. Therefore, it is useful to follow a specific protocol that defines monitoring parameters; such a procedure facilitates the comparison of different bone substitutes analyzed in the same study and allows cross-study comparisons. Parameters that are mainly analyzed qualitatively within the framework of bone healing, and depending on the bone substitute, are: bone growth within the different regions of an implantation bed (i.e., the depth of penetration of bone tissue within a scaffold or implantation bed of granular materials); material-bone contact or extent of osteoconductivity; vascularization of the implantation bed; bone matrix maturation (mineralized vs. precalcified bone matrix, lamellar vs. woven bone matrix); and state of bone growth (e.g., bone matrix or osteoid hems including active osteoblasts and number of osteocytes) [11, 18, 29, 30, 37, 40–44]. Finally, representative microphotographs are acquired with a light microscope combined with a digital camera; these are generally used for publication.

Furthermore, scoring systems for material-mediated bone healing represents a semi-quantitative approach [254, 255]. Examination is generally performed by two or more experts in histology, based on an evaluation form containing different parameters. In most cases, a score for each subject is obtained individually, and the overall healing score represents the sum of all evaluated parameters. The obtained data can be used for statistical analysis.

Histomorphometric analyses of the different factors involved in bone healing are used as a more exact method [11, 18, 29, 30, 37, 40–44, 256, 257]. However, this kind of analysis requires a microscope equipped with a digital camera and a computer running analytical software. Microscopic images from different regions of an implantation bed can be used for histomorphometry. Combined microscope systems, including motorized components such as a scanning table for digitization of histological slides, are available from different companies (Figs. 17.7 and 17.8).

The costs of appropriate microscopes, digital cameras, and related computer programs vary widely. The costs of programs vary from open-source software, such as ImageJ [258], a suitable tool for different histomorphometric analyses, to special software packages that can cost thousands of euros. However, costly software packages from certain manufacturers are optimally adapted for components such as a digital camera or scanning table. In contrast, such components are only occasionally compatible with open-source programs.

Histomorphometric analysis includes the following morphometric indices for the calculation of newly formed bone in sites of regeneration [258–261]

1. Total area (TA) or total volume (TV) of a biopsy/implantation site, including both new bone, remaining bone substitute, and soft-tissue cavities (in mm^2 or mm^3)

Fig. 17.7 (**a**) Shows an overview of a computer-based microscope system for histomorphometry, consisting of a light microscope (Eclipse 80i, Nikon, Japan) with a connected digital camera (Nikon DS-Fi1, Nikon, Japan) (**b**), an automated scanning table (ProScan III, Prior, USA) (**c**) and its control unit (**d**), and a controller for the manual control of the scanning table (**e**)

500 μm
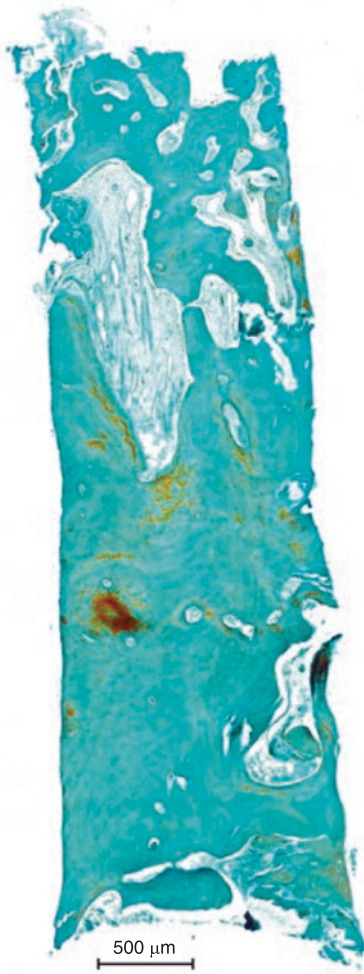
Fig. 17.8 Shows an overview of a clinical biopsy sample, called a "total scan," composed of single images used for histomorphometric analysis (Masson-Goldner stain, ×100 magnification)

2. Areas or volumes of newly formed bone tissue (BA or BV), of remaining bone-substitute material (MA or MV), or of connective tissue (CA or CV) (in mm^2 or mm^3)
3. Fractions of bone tissue (BA/TA or BV/TV), remaining bone substitute (MA/TA or MV/TV) or connective tissue (CA/MA or CV/TV), also described as the percentage or ratio (hence, no unit of measure is used)
4. Average bone thickness (B.Th) (in mm)
5. Average bone separation, which is the thickness of soft-tissue cavities (B.Sp) (in mm)

Various other factors, such as vascularization of the implantation bed (as percentage fraction of the implantation area and numbers of vessels/mm^2 of the implantation bed) or numbers of different cell types, such as MNGCs, within the implantation bed (cells/mm^2 of the implantation bed), can be measured, counted, and related to the respective implantation area via histomorphometry [11, 18, 29, 30, 37, 40–44]. Altogether, histomorphometric analyses are an appropriate method for analyzing the bone healing process and related factors. Interestingly, the manual marking of the areas of tissue fractions is most often still necessary for measurements of these parameters (Fig. 17.9).

Most histomorphometric programs currently offer automatic or semi-automatic analyses of the described parameters. However, conducting these analyses is strongly dependent on factors such as the quality of the histological slides and digitization quality, which, in turn, is based on the quality of components used for digitization (e.g., resolution of the digital camera); most of all, the contrast of the respective staining is the most important factor in these assessments. Immunohistochemical stains may provide the highest contrast, while many histochemical stains do not enable sufficient separation of different tissue fractions or cell types. However, some histochemical stains, such as Movat's Pentachrome or Masson Goldner, have already been shown suitable for (semi-) automatic histomorphometry [259, 260].

Other techniques, such as X-ray imaging, micro-computed tomography (μ-CT), high-resolution magnetic resonance imaging (MRI), or synchrotron X-ray microtomography, are also used for the analysis of regenerative bone growth [262–264]. X-ray imaging is most often used in clinical studies, evaluating the height of bone growth, because only anatomic structures such as bones and bone substitutes absorb the X-rays; based on their high signal attenuation, they appear bright [265]. However, structures such as soft tissues have low signal attenuation and, hence, appear dark in an image without the application of contrast agents [266]. Thus, this visual-
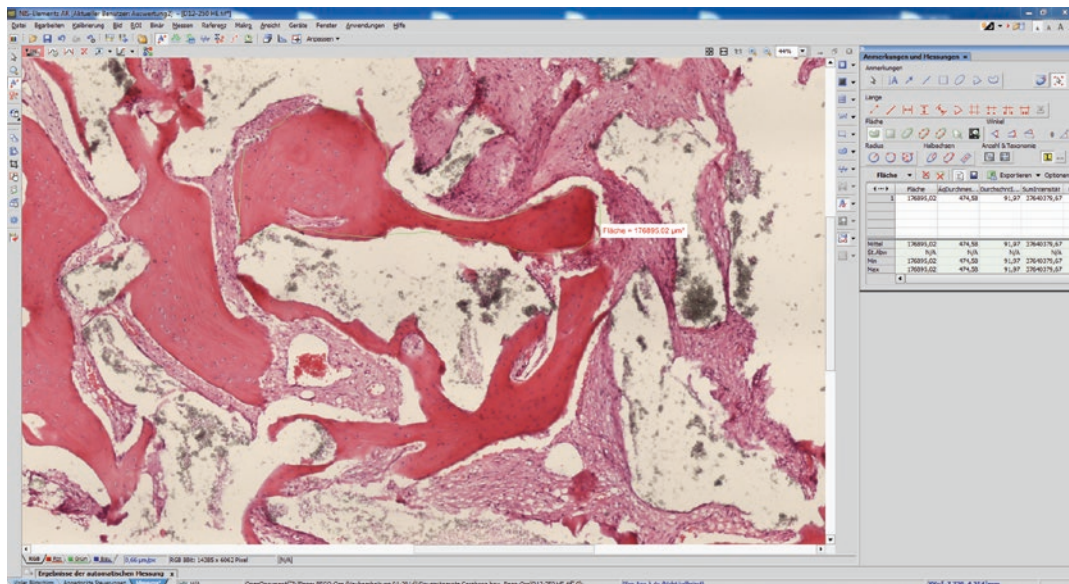
Fig. 17.9 Shows the manual marking (green line) of newly formed bone within the implantation bed of a xenogeneic bone-substitute material using Nikon NIS Elements software
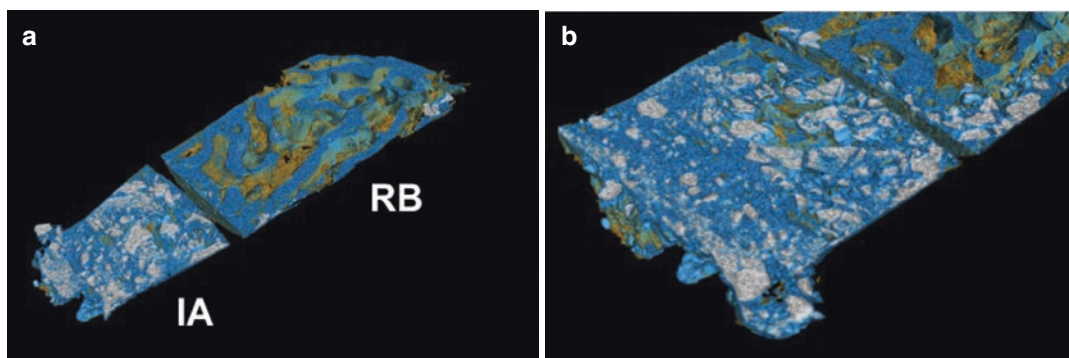
Fig. 17.10 Shows a μ-CT scan of a sinus biopsy acquired 6 months after bone augmentation with a xenogeneic bone substitute. RB = residual bone, IA = implantation area, orange color = connective tissue, blue color = bone tissue/ matrix, white color = xenogeneic bone substitute granules. (Images were generated with the kind assistance of Prof. Dr. Rothamel and Dr. Andre Beerlink from Yxlon)

ization method is not suitable for evaluating the integration behavior of a bone substitute or material-induced tissue reactions in close detail. μ-CT scanning is an important tool in bone research. It allows for bone histomorphometry based on 3D data, obtained for the whole implantation bed of a bone substitute, without destroying tissue or impeding volumetric measurements (Fig. 17.10) [264, 265]. Different protocols for μ-CT enable us to visualize the nature of the bone structure and to quantitatively analyze numerous bone structural parameters with a high degree of accuracy [266–268]. The morphometric indices described above can also be measured via μ-CT in all implantations models, i.e., ectopic and orthotropic implantation sides (long bone defects and cranial bone defects) [269].

This analytical method can be used for the dynamic measurement of bone-growth processes because μ-CT can also be used for in vivo

measurements; this avoids the sacrifice of the experimental animals at the respective study time points [270]. Altogether, these advantages render μ-CT a powerful tool for bone regeneration studies. However, it does not allow for the analysis of soft tissues due to their relatively poor μ-CT contrast; thus, it cannot be used to evaluate cellular reactions to a bone substitute. Combining μ-CT with histological or histomorphometric methods may, therefore, be a very useful approach.

Synchrotron radiation X-ray microtomography (SR-μCT) is another powerful tool for the analysis of bone regeneration, allowing nondestructive observation of bone and its internal structure without any sample preparation [262]. In the context of bone research, this overcomes the issues of other techniques that do not allow for discrimination of different tissue fractions, such as mineralized bone matrix and the surrounding connective tissue [271]. Thus, SR-μCT enables high resolution of a specimen, allowing for differentiation between tissues with similar absorption coefficients [272]. SR-μCT can be used to measure newly formed bone and other tissue fractions, as well as bone indices. Moreover, SR-μCT facilitates sufficient detection of fine structures, such as blood vessels, which can be used to measure vascularization of the implantation bed or tissue response among other structures [271].

Interestingly, all of these methods only allow for the measurement of the different tissue fractions and quality of the regenerated bone tissue. No quantification of the cellular responses or levels of gene expression is yet available. Measurements of serum markers of bone turnover, such as bone-specific alkaline phosphatase, osteocalcin, or type 1 procollagen, can be suitable for the determination of bone growth; however, such methods do not allow quantifying the expression of involved factors within the defect or implantation site [273]. In material-mediated bone regeneration, it is important to evaluate the gene expression of different cell types, such as osteoblasts, endothelial cells, or osteoclasts, and their precursors; this expression may vary with different bone substitute materials [274, 275]. Different methods have been

developed for this. One of the most powerful analytical tools is high-resolution magnetic resonance imaging (MRI) because it overcomes the various restrictions of the methods described above. MRI can be optimally used in the field of tissue-engineering research by generating spatial maps of tissue relaxation times, and the stiffness or shear moduli of growing or developing tissues such as bone; additionally, it can be used to visualize the integration of biomaterials within the surrounding tissues [276]. Moreover, MRI enables quantification of cell death, inflammatory processes, and visualization of cell trafficking and gene expression via application of (super-) paramagnetic contrast agents [276]. Other specially tailored measurement techniques, based on fluorescence-activated cell sorting (FACS) and laser capture microdissection (LCM) are used [277, 278]. These allow for immunophenotyping of different cell types within a biopsy, or isolation of specific cell populations from a biopsy, and are used to quantify gene expression.

17.2.4.2 Methods for Analysis of Resorbability of Bone Substitutes

The analysis of the degradation behavior of bone substitutes generally includes qualitative and quantitative methods. Qualitative methods encompass a microscopic analysis of biopsies or radiological data. While radiological data may only provide an overview of an implanted bone-substitute material, histological analysis of the degradation can provide details about the implanted material and specific processes of its cellular resorption [18, 29, 30, 37, 44, 50, 51]. Simple histochemical stains, such as H&E, can be used to analyze both parameters, as this staining method also shows the different cell types involved in the resorption process [214]. However, specialized histochemical staining methods, such as the Von Kossa/Safranin-O stain, allow for visualization of the calcium content in bone substitutes, within the surrounding connective tissue, and especially within phagocytizing cells such as macrophages and MNGCs [37].

The histochemical detection of the TRAP enzyme, which is mainly expressed by phagocytes within the implantation beds of various bone substitutes, can provide a first impression of the degradability of a material [18, 29, 43, 235]. However, it is still questionable whether the overall expression pattern of TRAP within the implantation bed of a bone substitute correlates with its degradation course; this is because, in its histochemical detection, both TRAP isoforms are labeled [48, 235]. The TRAP5a isoform is linked with inflammatory processes, while TRAP5b is involved in osteoclastic reposition processes of the bone matrix [235]. Until now, it has not been revealed which isoform is expressed in the cells degrading the bone substitutes, which are recognized as foreign body materials.

It is, therefore, important, to detect the cells involved in the degradation processes of bone substitutes and expression of molecules involved in cellular digestion. One of the most common analyses is immunohistochemical detection of the CD68 molecule, which is a pan-macrophage marker and is expressed by most of the phagocytes within an implantation bed of a bone substitute. Moreover, antibodies against TRAP, and

recently against TRAP5a and other molecules involved in the degradation or phagocytosis of bone-substitute materials, are also used [47]. Methods offering higher resolution, such as trans-electron microscopy (TEM), are useful for the analysis of phagocytosis and analyzing subcellular processes (Fig. 17.11) [50]. It is also possible to detect specific molecules via TEM based on immunogold labeling, which can lead to further information about intracellular pathways of bone substitute digestion or processing [279].

Based on these described detection methods, different parameters can be measured using histomorphometry to quantitatively analyze the resorbability of bone substitutes. For example, histological slides can be used to measure the numbers of different phagocytizing cells, such as MNGCs and their TRAP-positive and TRAP-negative subforms, or macrophages. Furthermore, by using TEM images, the sizes of engulfed particles can be measured, allowing a fundamental prediction of the resorption of a bone substitute (Fig. 17.11) [18, 29, 30, 37, 44, 50, 51]. However, these methods are generally not used to measure the exact degradation rate of a material because most of the bone-substitute materials (especially
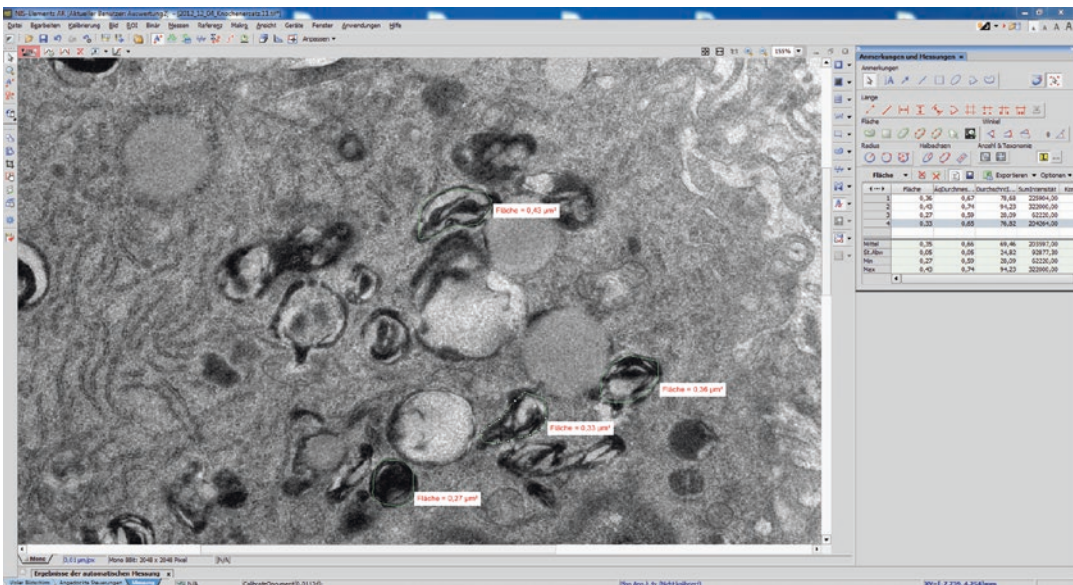
Fig. 17.11 Shows the histomorphometric measurement of bone-substitute fragments within a material-adherent macrophage, obtained using the Nikon NIS Elements software

in the form of granules) have a polygonal form; therefore, 2D slides do not provide an overview of the overall surfaces and, thus, no analysis of overall degradation. In many cases, the degradation of a material is not uniform because of irregularities in material composition; such is the case with biphasic bone substitutes, which show an irregular distribution of HA and β-TCP, among others. Thus, histomorphometric analyses can only be applied if a bone-substitute material possesses a consistent diameter or form.

While μ-CT, SR-μCT, and MRI allow for qualitative analysis of material resorption, these methods are also ideally suited for measurements [262–272]. These imaging techniques also allow for non-destructive observation of bone substitutes without any sample preparation, whereby the whole material structure and form are displayable. These techniques do not overcome the problem of analyzing resorbability of irregularly formed materials. However, even studies including different time points that normally require the sacrifice of many experimental animals, these techniques enable for dynamic in vivo measurements at respective study time points and help to decrease the number of experimental animals [270]. Altogether, the resorption behavior of a bone substitute can only be completely analyzed by a combination of different imaging techniques such as histology and μ-CT.

17.2.4.3 Methods for the Analysis of Inflammatory Tissue Responses to Bone Substitutes

The most conventional method for the analysis of inflammatory tissue response to a bone substitute is based on histochemical staining and qualitative microscopic analysis of preclinical and clinical biopsies. H&E or Giemsa stains are used often, allowing for the differentiation of different cell types involved in tissue reaction to a material [18, 29, 30, 37, 50, 51, 214–216]. These simple stains provide only a general insight into the inflammatory events, with no effective distinction between most of the relevant cell types such as macro-

phages and fibroblasts. However, this technique can be used to measure inflammatory tissue responses to bone substitutes using semi-quantitative scoring systems and histomorphometric measurements (such as the thickness of a wall of reactive tissue or fibrotic capsule around a bone substitute) [18, 29, 30, 37, 50, 51, 255]. For more detailed insights into the inflammatory events within an implantation bed of a bone substitute are achievable via immunohistochemical labeling, which enables differentiation of different cell types and inflammatory subtypes, such as M1- and M2-macrophages [216, 222, 223].

An enormous number of antibodies directed against a broad variety of animal and human-specific antigens are available. Finally, the numbers of cells, and other parameters such as vascularization of the implantation bed, are measurable via manual and automatic histomorphometric analysis [18, 29, 30, 37, 50, 51]. Furthermore, FACS methodology is also usable for quantification of the number of (inflammatory) cell types within the implantation beds of biomaterials and bone substitutes [277].

These methods allow us to analyze the severity of the inflammatory response to bone substitutes on a cellular level. However, they do not assess the gene expression of different cell types with respect to a particular bone substitute or its physicochemical characteristics. Different techniques are suitable for quantifying gene expression of inflammatory cells within biopsies and bone substitutes. MRI allows us to quantify inflammatory processes and gene expression based on (super-) paramagnetic contrast agents. LCM or directly applied real-time quantitative PCR (*qPCR*) helps measure gene expression of a certain cell type or that within the whole biopsy [276]. New molecular biological methods, such as NIR nanoprobes, bind to defined molecules, such as the folate receptor on activated macrophages. Bioluminescence-based assays detect cells tagged with the luciferase gene reporter. These novel techniques can be used to detect and quantify the extent of biomaterial-mediated inflammatory responses in vivo [280].

References

1. Sakkas A, Wilde F, Heufelder M, Winter K, Schramm A. Autogenous bone grafts in oral implantology—is it still a "gold standard"? A consecutive review of 279 patients with 456 clinical procedures. Int J Implant Dentistry. 2017;3(1):23.

2. Moses O, Nemcovsky CE, Langer Y, Tal H. Severely resorbed mandible treated with iliac crest autogenous bone graft and dental implants: 17-year follow-up. Int J Oral Maxillofac Implants. 2007;22(6):1017–21.

3. Zizelmann C, Schoen R, Metzger MC, Schmelzeisen R, Schramm A, Dott B, et al. Bone formation after sinus augmentation with engineered bone. Clin Oral Implants Res. 2007;18(1):69–73.

4. Schlickewei W, Schlickewei C, editors. The use of bone substitutes in the treatment of bone defects–the clinical view and history. In: Macromolecular symposia. Wiley Online Library; 2007.

5. Roberts TT, Rosenbaum AJ. Bone grafts, bone substitutes and orthobiologics. Organogenesis. 2012;8(4):114–24.

6. Phemister DB. The classic: repair of bone in the presence of aseptic necrosis resulting from fractures, transplantations, and vascular obstruction. Clin Orthop Relat Res. 2008;466(5):1021–33.

7. Phemister D. The fate of transplanted bone and regenerative power of its various constituents. Surg Gynecol Obstet. 1914;19:303–14.

8. Roberts TT, Rosenbaum AJ. Bone grafts, bone substitutes and orthobiologics: the bridge between basic science and clinical advancements in fracture healing. Organogenesis. 2012;8(4):114–24.

9. Bohner M. Resorbable biomaterials as bone graft substitutes. Mater Today. 2010;13(1–2):24–30.

10. Eppley BL, Pietrzak WS, Blanton MW. Allograft and alloplastic bone substitutes: a review of science and technology for the craniomaxillofacial surgeon. J Craniofac Surg. 2005;16(6):981–9.

11. Blume O, Hoffmann L, Donkiewicz P, Wenisch S, Back M, Franke J, et al. Treatment of severely resorbed maxilla due to peri-implantitis by guided bone regeneration using a customized allogenic bone block: a case report. Materials (Basel). 2017;10(10):1213.

12. Sheikh Z, Hamdan N, Ikeda Y, Grynpas M, Ganss B, Glogauer M. Natural graft tissues and synthetic biomaterials for periodontal and alveolar bone reconstructive applications: a review. Biomater Res. 2017;21:9.

13. Betz RR. Limitations of autograft and allograft: new synthetic solutions. Orthopedics. 2002;25(5 Suppl):s561–70.

14. Kurien T, Pearson RG, Scammell BE. Bone graft substitutes currently available in orthopaedic practice: the evidence for their use. Bone Joint J. 2013;95-B(5):583–97.

15. Gerhardt LC, Boccaccini AR. Bioactive glass and glass-ceramic scaffolds for bone tissue engineering. Materials (Basel). 2010;3(7):3867–910.

16. Tay BK, Patel VV, Bradford DS. Calcium sulfate- and calcium phosphate-based bone substitutes. Mimicry of the mineral phase of bone. Orthop Clin North Am. 1999;30(4):615–23.

17. Bose S, Vahabzadeh S, Bandyopadhyay A. Bone tissue engineering using 3D printing. Mater Today. 2013;16(12):496–504.

18. Barbeck M, Serra T, Booms P, Stojanovic S, Najman S, Engel E, et al. Analysis of the in vitro degradation and the in vivo tissue response to bi-layered 3D-printed scaffolds combining PLA and biphasic PLA/bioglass components–guidance of the inflammatory response as basis for osteochondral regeneration. Bioact Mater. 2017;2(4):208–23.

19. Do A-V, Smith R, Acri TM, Geary SM, Salem AK. 3D printing technologies for 3D scaffold engineering. Functional 3D tissue engineering scaffolds. Amsterdam: Elsevier; 2018. p. 203–34.

20. Yang J, Koons GL, Cheng G, Zhao L, Mikos AG, Cui F. A review on the exploitation of biodegradable magnesium-based composites for medical applications. Biomed Mater. 2018;13(2):022001.

21. Singh S, Bhatnagar N. A novel approach to fabricate 3D open cellular structure of Mg10Zn alloy with controlled morphology. Mater Lett. 2018;212:62–4.

22. Greenwald AS, Boden SD, Goldberg VM, Khan Y, Laurencin CT, Rosier RN, et al. Bone-graft substitutes: facts, fictions, and applications. J Bone Joint Surg Am. 2001;83-A(Suppl 2 Pt 2):98–103.

23. Albrektsson T, Johansson C. Osteoinduction, osteoconduction and osseointegration. Eur Spine J. 2001;10(Suppl 2):S96–101.

24. Burchardt H. The biology of bone graft repair. Clin Orthop Relat Res. 1983;174:28–42.

25. Campana V, Milano G, Pagano E, Barba M, Cicione C, Salonna G, et al. Bone substitutes in orthopaedic surgery: from basic science to clinical practice. J Mater Sci Mater Med. 2014;25(10):2445–61.

26. Trueta J. The role of the vessels in osteogenesis. Bone Joint J. 1963;45(2):402–18.

27. Weiland AJ, Moore JR, Daniel RK. Vascularized bone autografts. Experience with 41 cases. Clin Orthop Relat Res. 1983;174:87–95.

28. Raggatt L, Chang M, Alexander K, Maylin E, Walsh N, Gravallese E, et al. Osteomacs: osteoclast precursors during inflammatory bone disease but regulators of physiologic bone remodeling. Bone. 2009;44:S136–S7.

29. Ghanaati S, Barbeck M, Orth C, Willershausen I, Thimm BW, Hoffmann C, et al. Influence of beta-tricalcium phosphate granule size and morphology on tissue reaction in vivo. Acta Biomater. 2010;6(12):4476–87.

30. Barbeck M, Udeabor S, Lorenz J, Schlee M, Holthaus MG, Raetscho N, et al. High-temperature

sintering of xenogeneic bone substitutes leads to increased multinucleated giant cell formation: in vivo and preliminary clinical results. J Oral Implantol. 2015;41(5):e212–22.

31. Brydone AS, Meek D, Maclaine S. Bone grafting, orthopaedic biomaterials, and the clinical need for bone engineering. Proc Inst Mech Eng H. 2010;224(12):1329–43.

32. Yuan H, Fernandes H, Habibovic P, de Boer J, Barradas AM, de Ruiter A, et al. Osteoinductive ceramics as a synthetic alternative to autologous bone grafting. Proc Natl Acad Sci. 2010;107(31):13614–9.

33. Blokhuis TJ, Arts JJ. Bioactive and osteoinductive bone graft substitutes: definitions, facts and myths. Injury. 2011;42(Suppl 2):S26–9.

34. Badylak SF, Freytes DO, Gilbert TW. Extracellular matrix as a biological scaffold material: structure and function. Acta Biomater. 2009;5(1):1–13.

35. Wang W, Yeung KW. Bone grafts and biomaterials substitutes for bone defect repair: a review. Bioact Mater. 2017;2(4):224–47.

36. Benders KE, van Weeren PR, Badylak SF, Saris DB, Dhert WJ, Malda J. Extracellular matrix scaffolds for cartilage and bone regeneration. Trends Biotechnol. 2013;31(3):169–76.

37. Ghanaati S, Barbeck M, Hilbig U, Hoffmann C, Unger RE, Sader RA, et al. An injectable bone substitute composed of beta-tricalcium phosphate granules, methylcellulose and hyaluronic acid inhibits connective tissue influx into its implantation bed in vivo. Acta Biomater. 2011;7(11):4018–28.

38. Schroeder JE, Mosheiff R. Tissue engineering approaches for bone repair: concepts and evidence. Injury. 2011;42(6):609–13.

39. Florencio-Silva R, Sasso GR, Sasso-Cerri E, Simoes MJ, Cerri PS. Biology of bone tissue: structure, function, and factors that influence bone cells. Biomed Res Int. 2015;2015:421746.

40. Unger RE, Ghanaati S, Orth C, Sartoris A, Barbeck M, Halstenberg S, et al. The rapid anastomosis between prevascularized networks on silk fibroin scaffolds generated in vitro with cocultures of human microvascular endothelial and osteoblast cells and the host vasculature. Biomaterials. 2010;31(27):6959–67.

41. Fuchs S, Ghanaati S, Orth C, Barbeck M, Kolbe M, Hofmann A, et al. Contribution of outgrowth endothelial cells from human peripheral blood on in vivo vascularization of bone tissue engineered constructs based on starch polycaprolactone scaffolds. Biomaterials. 2009;30(4):526–34.

42. Ghanaati S, Fuchs S, Webber MJ, Orth C, Barbeck M, Gomes ME, et al. Rapid vascularization of starch–poly (caprolactone) in vivo by outgrowth endothelial cells in co-culture with primary osteoblasts. J Tissue Eng Regen Med. 2011;5(6):e136–43.

43. Barbeck M, Najman S, Stojanovic S, Mitic Z, Zivkovic JM, Choukroun J, et al. Addition of blood to a phycogenic bone substitute leads to increased in vivo vascularization. Biomed Mater. 2015;10(5):055007.

44. Barbeck M, Unger RE, Booms P, Dohle E, Sader RA, Kirkpatrick CJ, et al. Monocyte preseeding leads to an increased implant bed vascularization of biphasic calcium phosphate bone substitutes via vessel maturation. J Biomed Mater Res A. 2016;104(12):2928–35.

45. Rose FR, Oreffo RO. Bone tissue engineering: hope vs hype. Biochem Biophys Res Commun. 2002;292(1):1–7.

46. Bose S, Roy M, Bandyopadhyay A. Recent advances in bone tissue engineering scaffolds. Trends Biotechnol. 2012;30(10):546–54.

47. Barbeck M, Booms P, Unger R, Hoffmann V, Sader R, Kirkpatrick CJ, et al. Multinucleated giant cells in the implant bed of bone substitutes are foreign body giant cells-new insights into the material-mediated healing process. J Biomed Mater Res A. 2017;105(4):1105–11.

48. Barbeck M, Motta A, Migliaresi C, Sader R, Kirkpatrick CJ, Ghanaati S. Heterogeneity of biomaterial-induced multinucleated giant cells: possible importance for the regeneration process? J Biomed Mater Res A. 2016;104(2):413–8.

49. Bobbert FSL, Zadpoor AA. Effects of bone substitute architecture and surface properties on cell response, angiogenesis, and structure of new bone. J Mater Chem B. 2017;5(31):6175–92.

50. Barbeck M, Dard M, Kokkinopoulou M, Markl J, Booms P, Sader RA, et al. Small-sized granules of biphasic bone substitutes support fast implant bed vascularization. Biomatter. 2015;5:e1056943.

51. Barbeck M, Udeabor SE, Lorenz J, Kubesch A, Choukroun J, Sader RA, et al. Induction of multinucleated giant cells in response to small sized bovine bone substitute (Bio-Oss) results in an enhanced early implantation bed vascularization. Ann Maxillofac Surg. 2014;4(2):150–7.

52. Anderson JM, Rodriguez A, Chang DT. Foreign body reaction to biomaterials. Semin Immunol. 2008;20(2):86–100.

53. Hu WJ, Eaton JW, Ugarova TP, Tang L. Molecular basis of biomaterial-mediated foreign body reactions. Blood. 2001;98(4):1231–8.

54. Anderson JM, Jones JA. Phenotypic dichotomies in the foreign body reaction. Biomaterials. 2007;28(34):5114–20.

55. Ghanaati S, Barbeck M, Detsch R, Deisinger U, Hilbig U, Rausch V, et al. The chemical composition of synthetic bone substitutes influences tissue reactions in vivo: histological and histomorphometrical analysis of the cellular inflammatory response to hydroxyapatite, beta-tricalcium phosphate and biphasic calcium phosphate ceramics. Biomed Mater. 2012;7(1):015005.

56. Schlegel AK, Donath K. BIO-OSS--a resorbable bone substitute? J Long Term Eff Med Implants. 1998;8(3–4):201–9.

57. Glenske K, Donkiewicz P, Kowitsch A, Milosevic-Oljaca N, Rider P, Rofall S, et al. Applications of metals for bone regeneration. Int J Mol Sci. 2018;19(3):826.

58. Nelson JF, Stanford HG, Cutright DE. Evaluation and comparisons of biodegradable substances as osteogenic agents. Oral Surg Oral Med Oral Pathol. 1977;43(6):836–43.

59. Hollinger JO. Preliminary report on the osteogenic potential of a biodegradable copolymer of polyactide (PLA) and polyglycolide (PGA). J Biomed Mater Res. 1983;17(1):71–82.

60. Schakenraad JM, Nieuwenhuis P, Molenaar I, Helder J, Dijkstra PJ, Feijen J. In vivo and in vitro degradation of glycine/DL-lactic acid copolymers. J Biomed Mater Res. 1989;23(11):1271–88.

61. Van Sliedregt A, van Blitterswijk C, Hesseling S, Grote J, de Groot K. The effect of the molecular weight of polylactic acid on in vitro biocompatibility. Adv Biomater. 1990;9:207–11.

62. Verheyen CC, de Wijn JR, van Blitterswijk CA, Rozing PM, de Groot K. Examination of efferent lymph nodes after 2 years of transcortical implantation of poly(L-lactide) containing plugs: a case report. J Biomed Mater Res. 1993;27(8):1115–8.

63. Kronenthal RL. Biodegradable polymers in medicine and surgery. Polymers in medicine and surgery. Berlin: Springer; 1975. p. 119–37.

64. Holland S, Tighe B. Biodegradable polymers. Adv Pharm Sci. 1992;6:101–64.

65. Middleton JC, Tipton AJ. Synthetic biodegradable polymers as orthopedic devices. Biomaterials. 2000;21(23):2335–46.

66. Gabelnick H. Advances in human fertility and reproductive endocrinology. Long acting steroid contraception, vol. 2. New York: Raven Press; 1983. p. 149.

67. Zong C, Qian X, Tang Z, Hu Q, Chen J, Gao C, et al. Biocompatibility and bone-repairing effects: comparison between porous poly-lactic-co-glycolic acid and nano-hydroxyapatite/poly(lactic acid) scaffolds. J Biomed Nanotechnol. 2014;10(6):1091–104.

68. Ramot Y, Haim-Zada M, Domb AJ, Nyska A. Biocompatibility and safety of PLA and its copolymers. Adv Drug Deliv Rev. 2016;107:153–62.

69. Taylor M, Daniels A, Andriano K, Heller J. Six bioabsorbable polymers: in vitro acute toxicity of accumulated degradation products. J Appl Biomater. 1994;5(2):151–7.

70. Gibbons D. Tissue response to resorbable synthetic polymers. Degradation phenomena on polymeric biomaterials. Berlin: Springer; 1992. p. 97–105.

71. Williams D, Mort E. Enzyme-accelerated hydrolysis of polyglycolic acid. J Bioeng. 1977;1(3):231–8.

72. Gunatillake PA, Adhikari R. Biodegradable synthetic polymers for tissue engineering. Eur Cell Mater. 2003;5:1–16; discussion.

73. Ulery BD, Nair LS, Laurencin CT. Biomedical applications of biodegradable polymers. J Polym Sci B Polym Phys. 2011;49(12):832–64.

74. Li J, Baker B, Mou X, Ren N, Qiu J, Boughton RI, et al. Biopolymer/calcium phosphate scaffolds for bone tissue engineering. Adv Healthcare Mater. 2014;3(4):469–84.

75. Kokubo T, Kim HM, Kawashita M, Nakamura T. Bioactive metals: preparation and properties. J Mater Sci Mater Med. 2004;15(2):99–107.

76. Xiao M, Chen YM, Biao MN, Zhang XD, Yang BC. Bio-functionalization of biomedical metals. Mater Sci Eng C Mater Biol Appl. 2017;70(Pt 2):1057–70.

77. Staiger MP, Pietak AM, Huadmai J, Dias G. Magnesium and its alloys as orthopedic biomaterials: a review. Biomaterials. 2006;27(9):1728–34.

78. Kamrani S, Fleck C. Biodegradable magnesium alloys as temporary orthopaedic implants: a review. Biometals. 2019;32(2):185–93.

79. Noviana D, Paramitha D, Ulum MF, Hermawan H. The effect of hydrogen gas evolution of magnesium implant on the postimplantation mortality of rats. J Orthop Transl. 2016;5:9–15.

80. Hornberger H, Virtanen S, Boccaccini A. Biomedical coatings on magnesium alloys—a review. Acta Biomater. 2012;8(7):2442–55.

81. Johnson I, Liu H. A study on factors affecting the degradation of magnesium and a magnesium-yttrium alloy for biomedical applications. PLoS One. 2013;8(6):e65603.

82. Diamond S, Leeman ME, editors. Pore size distributions in hardened cement paste by SEM image analsysis. In: Materials research society symposium proceedings. Materials Research Society; 1995.

83. Bartoš M, Suchý T, Foltán R. Note on the use of different approaches to determine the pore sizes of tissue engineering scaffolds: what do we measure? Biomed Eng Online. 2018;17(1):110.

84. Van Cleynenbreugel T, Schrooten J, Van Oosterwyck H, Vander SJ. Micro-CT-based screening of biomechanical and structural properties of bone tissue engineering scaffolds. Med Biol Eng Comput. 2006;44(7):517–25.

85. Peyrin F. Evaluation of bone scaffolds by micro-CT. Osteoporos Int. 2011;22(6):2043–8.

86. Kim G-W, Yeo I-S, Kim S-G, Um I-W, Kim Y-K. Analysis of crystalline structure of autogenous tooth bone graft material: X-Ray diffraction analysis. J Korean Assoc Oral Maxillofac Surgeons. 2011;37(3):225–8.

87. Berberi A, Samarani A, Nader N, Noujeim Z, Dagher M, Kanj W, et al. Physicochemical characteristics of bone substitutes used in oral surgery in comparison to autogenous bone. BioMed Res Int. 2014;2014:320790.

88. Tadic D, Epple M. A thorough physicochemical characterisation of 14 calcium phosphate-based bone substitution materials in comparison to natural bone. Biomaterials. 2004;25(6):987–94.

89. Stuart B. Infrared spectroscopy. New York: Wiley Online Library; 2005.

90. Wen JL, Sun SL, Xue BL, Sun RC. Recent advances in characterization of lignin polymer by solution-state nuclear magnetic resonance (NMR) methodology. Materials (Basel). 2013;6(1):359–91.

91. Carman C, Wilkes C. Monomer sequence distribution in ethylene propylene elastomers. I. Measurement by carbon-13 nuclear magnetic resonance spectroscopy. Rubber Chem Technol. 1971;44(3):781–804.

92. Hajduk PJ, Bures M, Praestgaard J, Fesik SW. Privileged molecules for protein binding identified from NMR-based screening. J Med Chem. 2000;43(18):3443–7.

93. Tayal A, Khan SA. Degradation of a water-soluble polymer: molecular weight changes and chain scission characteristics. Macromolecules. 2000;33(26):9488–93.

94. Nunes RW, Martin JR, Johnson JF. Influence of molecular weight and molecular weight distribution on mechanical properties of polymers. Polym Eng Sci. 1982;22(4):205–28.

95. Gaborieau M, Castignolles P. Size-exclusion chromatography (SEC) of branched polymers and polysaccharides. Ann Bioanal Chem. 2011;399(4):1413–23.

96. Spatorico A, Coulter B. Molecular weight determinations by gel-permeation chromatography and viscometry. J Polym Sci Part B Polym Phys. 1973;11(6):1139–50.

97. Caprioli RM, Farmer TB, Gile J. Molecular imaging of biological samples: localization of peptides and proteins using MALDI-TOF MS. Anal Chem. 1997;69(23):4751–60.

98. Loo JA. Studying noncovalent protein complexes by electrospray ionization mass spectrometry. Mass Spectrom Rev. 1997;16(1):1–23.

99. Yaszemski MJ, Payne RG, Hayes WC, Langer R, Mikos AG. In vitro degradation of a poly (propylene fumarate)-based composite material. Biomaterials. 1996;17(22):2127–30.

100. Cai ZY, Yang DA, Zhang N, Ji CG, Zhu L, Zhang T. Poly(propylene fumarate)/(calcium sulphate/beta-tricalcium phosphate) composites: preparation, characterization and in vitro degradation. Acta Biomater. 2009;5(2):628–35.

101. Horan RL, Antle K, Collette AL, Wang Y, Huang J, Moreau JE, et al. In vitro degradation of silk fibroin. Biomaterials. 2005;26(17):3385–93.

102. Agrawal CM, Ray RB. Biodegradable polymeric scaffolds for musculoskeletal tissue engineering. J Biomed Mater Res. 2001;55(2):141–50.

103. Chen Q, Efthymiou A, Salih V, Boccaccini A. Bioglass®-derived glass–ceramic scaffolds: study of cell proliferation and scaffold degradation in vitro. J Biomed Mater Res A. 2008;84(4):1049–60.

104. Pilliar R, Filiaggi M, Wells J, Grynpas M, Kandel R. Porous calcium polyphosphate scaffolds for bone substitute applications—in vitro characterization. Biomaterials. 2001;22(9):963–72.

105. Marra KG, Szem JW, Kumta PN, DiMilla PA, Weiss LE. In vitro analysis of biodegradable polymer blend/ hydroxyapatite composites for bone tissue engineering. J Biomed Mater Res. 1999;47(3):324–35.

106. Danoux CB, Barbieri D, Yuan H, de Bruijn JD, van Blitterswijk CA, Habibovic P. In vitro and in vivo bioactivity assessment of a polylactic acid/hydroxyapatite composite for bone regeneration. Biomatter. 2014;4:e27664.

107. Schaefer S, Detsch R, Uhl F, Deisinger U, Ziegler G. How degradation of calcium phosphate bone substitute materials is influenced by phase composition and porosity. Adv Eng Mater. 2011;13(4):342–50.

108. Gorna K, Gogolewski S. In vitro degradation of novel medical biodegradable aliphatic polyurethanes based on ε-caprolactone and Pluronics® with various hydrophilicities. Polym Degrad Stab. 2002;75(1):113–22.

109. Salma-Ancane K, Stipniece L, Putnins A, Berzina-Cimdina L. Development of Mg-containing porous β-tricalcium phosphate scaffolds for bone repair. Ceram Int. 2015;41(3):4996–5004.

110. Fredholm YC, Karpukhina N, Brauer DS, Jones JR, Law RV, Hill RG. Influence of strontium for calcium substitution in bioactive glasses on degradation, ion release and apatite formation. J R Soc Interface. 2012;9(70):880–9.

111. Wang Q, Wang Q, Wang J, Zhang X, Yu X, Wan C. Degradation kinetics of calcium polyphosphate bioceramic: an experimental and theoretical study. Mater Res. 2009;12(4):495–501.

112. Martínez-Vázquez F, Cabañas M, Paris J, Lozano D, Vallet-Regí M. Fabrication of novel Si-doped hydroxyapatite/gelatine scaffolds by rapid prototyping for drug delivery and bone regeneration. Acta Biomater. 2015;15:200–9.

113. Lee J-Y, Nam S-H, Im S-Y, Park Y-J, Lee Y-M, Seol Y-J, et al. Enhanced bone formation by controlled growth factor delivery from chitosan-based biomaterials. J Controlled Release. 2002;78(1–3):187–97.

114. Kirkland N, Lespagnol J, Birbilis N, Staiger M. A survey of bio-corrosion rates of magnesium alloys. Corrosion Sci. 2010;52(2):287–91.

115. Kirkland NT, Birbilis N, Staiger M. Assessing the corrosion of biodegradable magnesium implants: a critical review of current methodologies and their limitations. Acta Biomater. 2012;8(3):925–36.

116. Anderson JM. Future challenges in the in vitro and in vivo evaluation of biomaterial biocompatibility. Regen Biomater. 2016;3(2):73–7.

117. Müller U. In vitro biocompatibility testing of biomaterials and medical devices. Med Device Technol. 2008;19(2):30, 2–4.

118. Schmalz G. Concepts in biocompatibility testing of dental restorative materials. Clin Oral Investig. 1998;1(4):154–62.

119. De Groot CJ, Van Luyn MJ, Van Dijk-Wolthuis WN, Cadée JA, Plantinga JA, Den Otter W, et al. In vitro biocompatibility of biodegradable dextran-based hydrogels tested with human fibroblasts. Biomaterials. 2001;22(11):1197–203.

120. Macnair R, Wilkinson R, MacDonald C, Goldie I, Jones D, Grant M. Application of confocal laser scanning microscopy to cytocompatibility testing of potential orthopaedic materials in immortalised osteoblast-like cell lines. Cells Mater. 1996;6(1):8.

121. Marques A, Reis R, Hunt J. The biocompatibility of novel starch-based polymers and composites: in vitro studies. Biomaterials. 2002;23(6):1471–8.

122. Park JH, Lee H, Kim JW, Kim JH. Cytocompatibility of 3D printed dental materials for temporary restorations on fibroblasts. BMC Oral Health. 2020;20(1):157.

123. Schmalz G. Use of cell cultures for toxicity testing of dental materials—advantages and limitations. J Dentistry. 1994;22:S6–11.

124. Pizzoferrato A, Ciapetti G, Stea S, Cenni E, Arciola CR, Granchi D. Cell culture methods for testing biocompatibility. Clin Mater. 1994;15(3):173–90.

125. Hanks CT, Wataha JC, Sun Z. In vitro models of biocompatibility: a review. Dent Mater. 1996;12(3):186–93.

126. Heinemann C, Heinemann S, Worch H, Hanke T. Development of an osteoblast/osteoclast co-culture derived by human bone marrow stromal cells and human monocytes for biomaterials testing. Eur Cell Mater. 2011;21:80–93.

127. Kirkpatrick C, Bittinger F, Wagner M, Köhler H, Van Kooten T, Klein C, et al. Current trends in biocompatibility testing. Proc Inst Mech Eng Part H J Eng Med. 1998;212(2):75–84.

128. Morrison C, Macnair R, MacDonald C, Wykman A, Goldie I, Grant M. In vitro biocompatibility testing of polymers for orthopaedic implants using cultured fibroblasts and osteoblasts. Biomaterials. 1995;16(13):987–92.

129. Czekanska EM, Stoddart MJ, Ralphs JR, Richards R, Hayes J. A phenotypic comparison of osteoblast cell lines versus human primary osteoblasts for biomaterials testing. J Biomed Mater Res A. 2014;102(8):2636–43.

130. Murray PE, García Godoy C, García GF. How is the biocompatibilty of dental biomaterials evaluated? Med Oral Patol Oral Cir Bucal. 2007;12(3):E258–66.

131. Macnair R, Rodgers E, Macdonald C, Wykman A, Goldie I, Grant M. The response of primary rat and human osteoblasts and an immortalized rat osteoblast cell line to orthopaedic materials: comparative sensitivity of several toxicity indices. J Mater Sci Mater Med. 1997;8(2):105–11.

132. Czekanska EM, Stoddart MJ, Richards RG, Hayes JS. In search of an osteoblast cell model for in vitro research. Eur Cell Mater. 2012;24:1–17.

133. Clarke B. Normal bone anatomy and physiology. Clin J Am Soc Nephrol. 2008;3(Suppl 3):S131–9.

134. Malaval L, Modrowski D, Gupta AK, Aubin JE. Cellular expression of bone-related proteins during in vitro osteogenesis in rat bone marrow stromal cell cultures. J Cell Physiol. 1994;158(3):555–72.

135. Qi MC, Zou SJ, Han LC, Zhou HX, Hu J. Expression of bone-related genes in bone marrow MSCs after cyclic mechanical strain: implications for distraction osteogenesis. Int J Oral Sci. 2009;1(3):143–50.

136. Aubin JE. Regulation of osteoblast formation and function. Rev Endocr Metab Disord. 2001;2(1):81–94.

137. Granéli C, Thorfve A, Ruetschi U, Brisby H, Thomsen P, Lindahl A, et al. Novel markers of osteogenic and adipogenic differentiation of human bone marrow stromal cells identified using a quantitative proteomics approach. Stem Cell Res. 2014;12(1):153–65.

138. Bellows C, Aubin J, Heersche J, Antosz M. Mineralized bone nodules formedin vitro from enzymatically released rat calvaria cell populations. Calcif Tissue Int. 1986;38(3):143–54.

139. Querido W, Farina M, Balduino A. Giemsa as a fluorescent dye for mineralizing bone-like nodules in vitro. Biomed Mater. 2012;7(1):011001.

140. Kasten P, Beyen I, Niemeyer P, Luginbühl R, Bohner M, Richter W. Porosity and pore size of β-tricalcium phosphate scaffold can influence protein production and osteogenic differentiation of human mesenchymal stem cells: an in vitro and in vivo study. Acta Biomater. 2008;4(6):1904–15.

141. Kulterer B, Friedl G, Jandrositz A, Sanchez-Cabo F, Prokesch A, Paar C, et al. Gene expression profiling of human mesenchymal stem cells derived from bone marrow during expansion and osteoblast differentiation. BMC Genomics. 2007;8(1):70.

142. Romanov YA, Darevskaya A, Merzlikina N, Buravkova L. Mesenchymal stem cells from human bone marrow and adipose tissue: isolation, characterization, and differentiation potentialities. Bull Exp Biol Med. 2005;140(1):138–43.

143. Thimm BW, Unger RE, Neumann H-G, Kirkpatrick CJ. Biocompatibility studies of endothelial cells on a novel calcium phosphate/SiO2-xerogel composite for bone tissue engineering. Biomed Mater. 2008;3(1):015007.

144. Carano RA, Filvaroff EH. Angiogenesis and bone repair. Drug Discov Today. 2003;8(21):980–9.

145. Panseri S, Cunha C, D'Alessandro T, Sandri M, Russo A, Giavaresi G, et al. Magnetic hydroxyapatite bone substitutes to enhance tissue regeneration: evaluation in vitro using osteoblast-like cells and in vivo in a bone defect. PLoS One. 2012;7(6):e38710.

146. Hofmann A, Ritz U, Verrier S, Eglin D, Alini M, Fuchs S, et al. The effect of human osteoblasts on proliferation and neo-vessel formation of human umbilical vein endothelial cells in a long-term 3D co-culture on polyurethane scaffolds. Biomaterials. 2008;29(31):4217–26.

147. Jones JA, Chang DT, Meyerson H, Colton E, Kwon IK, Matsuda T, et al. Proteomic analysis and quantification of cytokines and chemokines from biomaterial surface-adherent macrophages and foreign body giant cells. J Biomed Mater Res A. 2007;83(3):585–96.

148. Pamula E, Dobrzynski P, Szot B, Kretek M, Krawciow J, Plytycz B, et al. Cytocompatibility

of aliphatic polyesters—in vitro study on fibroblasts and macrophages. J Biomed Mater Res A. 2008;87(2):524–35.

149. Borciani G, Montalbano G, Baldini N, Cerqueni G, Vitale-Brovarone C, Ciapetti G. Co-culture systems of osteoblasts and osteoclasts: simulating in vitro bone remodeling in regenerative approaches. Acta Biomater. 2020;108:22–45.

150. Battiston KG, Cheung JW, Jain D, Santerre JP. Biomaterials in co-culture systems: towards optimizing tissue integration and cell signaling within scaffolds. Biomaterials. 2014;35(15):4465–76.

151. Heil T, Volkmann K, Wataha J, Lockwood P. Human peripheral blood monocytes versus THP-1 monocytes for in vitro biocompatibility testing of dental material components. J Oral Rehabil. 2002;29(5):401–7.

152. Sylvie J, Sylvie T-D, Pascal P-M, Fabienne P, Hassane O, Guy C. Effect of hydroxyapatite and beta-tricalcium phosphate nanoparticles on promonocytic U937 cells. J Biomed Nanotechnol. 2010;6(2):158–65.

153. Chanput W, Mes JJ, Wichers HJ. THP-1 cell line: an in vitro cell model for immune modulation approach. Int Immunopharmacol. 2014;23(1):37–45.

154. Sundström C, Nilsson K. Establishment and characterization of a human histiocytic lymphoma cell line (U-937). Int J Cancer. 1976;17(5):565–77.

155. Huang J, Best S, Bonfield W, Brooks R, Rushton N, Jayasinghe S, et al. In vitro assessment of the biological response to nano-sized hydroxyapatite. J Mater Sci Mater Med. 2004;15(4):441–5.

156. Mouline CC, Quincey D, Laugier J-P, Carle GF, Bouler J-M, Rochet N, et al. Osteoclastic differentiation of mouse and human monocytes in a plasma clot/biphasic calcium phosphate microparticles composite. Eur Cell Mater. 2010;20:379–92.

157. Bohbot A, Eischen A, Felden C, Vincent F, Oberling F. U937 cell line: impact of CSFs, IL-6 and IFN-gamma on the differentiation and the Leu-CAM proteins expression. Exp Hematol. 1993;21(4):564–72.

158. Lopez-Berestein G, Klostergaard J. Mononuclear phagocytes in cell biology. Boca Raton: CRC Press; 1992.

159. van Furth R, Raeburn JA, van Zwet TL. Characteristics of human mononuclear phagocytes. Blood. 1979;54(2):485–500.

160. Detsch R, Mayr H, Ziegler G. Formation of osteoclast-like cells on HA and TCP ceramics. Acta Biomater. 2008;4(1):139–48.

161. Detsch R, Schaefer S, Deisinger U, Ziegler G, Seitz H, Leukers B. In vitro-osteoclastic activity studies on surfaces of 3D printed calcium phosphate scaffolds. J Biomater Appl. 2011;26(3):359–80.

162. Herten M, Rothamel D, Schwarz F, Friesen K, Koegler G, Becker J. Surface-and nonsurface-dependent in vitro effects of bone substitutes on cell viability. Clin Oral Investig. 2009;13(2):149–55.

163. Nordsletten L, Høgåsen AKM, Konttinen Y, Santavirta S, Aspenberg P, Aasen AO. Human monocytes stimulation by particles of hydroxy-

apatite, silicon carbide and diamond: in vitro studies of new prosthesis coatings. Biomaterials. 1996;17(15):1521–7.

164. Simon JL, Michna S, Lewis JA, Rekow ED, Thompson VP, Smay JE, et al. In vivo bone response to 3D periodic hydroxyapatite scaffolds assembled by direct ink writing. J Biomed Mater Res A. 2007;83(3):747–58.

165. Blottière H, Daculsi G, Anegon I, Pouezat JA, Nelson PN, Passuti N. Utilization of activated U937 monocytic cells as a model to evaluate biocompatibility and biodegradation of synthetic calcium phosphate. Biomaterials. 1995;16(6):497–503.

166. Arbez B, Libouban H. Behavior of macrophage and osteoblast cell lines in contact with the β-TCP biomaterial (beta-tricalcium phosphate). Morphologie. 2017;101(334):154–63.

167. Beuvelot J, Pascaretti-Grizon F, Filmon R, Moreau MF, Baslé MF, Chappard D. In vitro assessment of osteoblast and macrophage mobility in presence of β-TCP particles by videomicroscopy. J Biomed Mater Res A. 2011;96(1):108–15.

168. Lange T, Schilling AF, Peters F, Haag F, Morlock MM, Rueger JM, et al. Proinflammatory and osteoclastogenic effects of beta-tricalciumphosphate and hydroxyapatite particles on human mononuclear cells in vitro. Biomaterials. 2009;30(29):5312–8.

169. Wiltfang J, Merten H, Schlegel K, Schultze-Mosgau S, Kloss F, Rupprecht S, et al. Degradation characteristics of α and β tri-calcium-phosphate (TCP) in minipigs. J Biomed Mater Res A. 2002;63(2):115–21.

170. Bosetti M, Hench L, Cannas M. Interaction of bioactive glasses with peritoneal macrophages and monocytes in vitro. J Biomed Mater Res A. 2002;60(1):79–85.

171. Davison NL, ten Harkel B, Schoenmaker T, Luo X, Yuan H, Everts V, et al. Osteoclast resorption of beta-tricalcium phosphate controlled by surface architecture. Biomaterials. 2014;35(26):7441–51.

172. Sato M, Grasser W. Effects of bisphosphonates on isolated rat osteoclasts as examined by reflected light microscopy. J Bone Miner Res. 1990;5(1):31–40.

173. Rittling SR, Matsumoto HN, Mckee MD, Nanci A, An XR, Novick KE, et al. Mice lacking osteopontin show normal development and bone structure but display altered osteoclast formation in vitro. J Bone Miner Res. 1998;13(7):1101–11.

174. Gomi K, Lowenberg B, Shapiro G, Davies J. Resorption of sintered synthetic hydroxyapatite by osteoclasts in vitro. Biomaterials. 1993;14(2):91–6.

175. Filgueira L. Fluorescence-based staining for tartrate-resistant acidic phosphatase (TRAP) in osteoclasts combined with other fluorescent dyes and protocols. J Histochem Cytochem. 2004;52(3):411–4.

176. Schilling AF, Linhart W, Filke S, Gebauer M, Schinke T, Rueger JM, et al. Resorbability of bone substitute biomaterials by human osteoclasts. Biomaterials. 2004;25(18):3963–72.

177. Cool S, Kenny B, Wu A, Nurcombe V, Trau M, Cassady A, et al. Poly (3-hydroxybutyrate-co-

3-hydroxyvalerate) composite biomaterials for bone tissue regeneration: in vitro performance assessed by osteoblast proliferation, osteoclast adhesion and resorption, and macrophage pro-inflammatory response. J Biomed Mater Res A. 2007;82(3):599–610.

178. Skogstrand K, Thorsen P, Nørgaard-Pedersen B, Schendel DE, Sørensen LC, Hougaard DM. Simultaneous measurement of 25 inflammatory markers and neurotrophins in neonatal dried blood spots by immunoassay with xMAP technology. Clin Chem. 2005;51(10):1854–66.

179. Li Y, Chen S-K, Li L, Qin L, Wang X-L, Lai Y-X. Bone defect animal models for testing efficacy of bone substitute biomaterials. J Orthop Transl. 2015;3(3):95–104.

180. Bigham-Sadegh A, Oryan A. Selection of animal models for pre-clinical strategies in evaluating the fracture healing, bone graft substitutes and bone tissue regeneration and engineering. Connect Tissue Res. 2015;56(3):175–94.

181. Pearce A, Richards R, Milz S, Schneider E, Pearce S. Animal models for implant biomaterial research in bone: a review. Eur Cell Mater. 2007;13(1):1–10.

182. Ghanaati S, Udeabor SE, Barbeck M, Willershausen I, Kuenzel O, Sader RA, et al. Implantation of silicon dioxide-based nanocrystalline hydroxyapatite and pure phase beta-tricalciumphosphate bone substitute granules in caprine muscle tissue does not induce new bone formation. Head Face Med. 2013;9(1):1.

183. Fulop G, Phillips R. The scid mutation in mice causes a general defect in DNA repair. Nature. 1990;347(6292):479.

184. Felsburg PJ, Somberg RL, Perryman L. Domestic animal models of severe combined immunodeficiency: canine X-linked severe combined immunodeficiency and severe combined immunodeficiency in horses. Immunodefic Rev. 1992;3(4):277–303.

185. Yao CH, Liu BS, Hsu SH, Chen YS, Tsai CC. Biocompatibility and biodegradation of a bone composite containing tricalcium phosphate and genipin crosslinked gelatin. J Biomed Mater Res A. 2004;69(4):709–17.

186. Koob S, Torio-Padron N, Stark GB, Hannig C, Stankovic Z, Finkenzeller G. Bone formation and neovascularization mediated by mesenchymal stem cells and endothelial cells in critical-sized calvarial defects. Tissue Eng Part A. 2010;17(3–4):311–21.

187. Khoshzaban A, Mehrzad S, Tavakoli V, Keshel SH, Behrouzi GR, Bashtar M. The comparative effectiveness of demineralized bone matrix, beta-tricalcium phosphate, and bovine-derived anorganic bone matrix on inflammation and bone formation using a paired calvarial defect model in rats. Clin Cosmet Investig Dent. 2011;3:69.

188. Hall BK. Developmental and cellular skeletal biology. New York: Academic Press; 2013.

189. Hall BK. Bones and cartilage: developmental and evolutionary skeletal biology. New York: Academic Press; 2005.

190. Neyt J, Buckwalter JA, Carroll N. Use of animal models in musculoskeletal research. Iowa Orthop J. 1998;18:118.

191. Gomes P, Fernandes M. Rodent models in bone-related research: the relevance of calvarial defects in the assessment of bone regeneration strategies. Lab Anim. 2011;45(1):14–24.

192. Aalami OO, Nacamuli RP, Lenton KA, Cowan CM, Fang TD, Fong KD, et al. Applications of a mouse model of calvarial healing: differences in regenerative abilities of juveniles and adults. Plast Reconstr Surg. 2004;114(3):713–20.

193. Sohn J-Y, Park J-C, Um Y-J, Jung U-W, Kim C-S, Cho K-S, et al. Spontaneous healing capacity of rabbit cranial defects of various sizes. J Periodontal Implant Sci. 2010;40(4):180–7.

194. Leake DL, Rappoport M. Mandibular reconstruction: bone induction in an alloplastic tray. Surgery. 1972;72(2):332–6.

195. Hjørting-Hansen E, Andreasen J. Incomplete bone healing of experimental cavities in dog mandibles. Br J Oral Surg. 1971;9(1):33–40.

196. Ma JL, Pan JL, Tan BS, Cui FZ. Determination of critical size defect of minipig mandible. J Tissue Eng Regen Med. 2009;3(8):615–22.

197. Schmitz JP, Hollinger JO. The critical size defect as an experimental model for craniomandibulofacial non-unions. Clin Orthop Relat Res. 1986;205:299–308.

198. Iwaniec UT, Wronski TJ, Turner RT. Histological analysis of bone. Alcohol. Berlin: Springer; 2008. p. 325–41.

199. Hopwood D. Fixatives and fixation: a review. Histochem J. 1969;1(4):323–60.

200. Buesa RJ. Histology without formalin? Ann Diagn Pathol. 2008;12(6):387–96.

201. Wolman M. Problems of fixation in cytology, histology, and histochemistry. Int Review Cytol. 1955;4:79–102.

202. Olert J, Wiedorn K-H, Goldmann T, Kühl H, Mehraein Y, Scherthan H, et al. HOPE fixation: a novel fixing method and paraffin-embedding technique for human soft tissues. Pathol Res Pract. 2001;197(12):823–6.

203. Skinner RA. Decalcification of bone tissue. Handbook of histology methods for bone and cartilage. Berlin: Springer; 2003. p. 167–84.

204. Hornbeck C, Emmanual J, Bloebaum RD. A comparative study of three paraffin media for preparing large decalcified bone sections. J Histotechnol. 1986;9(4):227–9.

205. Yaeger JA. Methacrylate embedding and sectioning of calcified bone. Stain Technol. 1958;33(5):229–39.

206. Emmanual J, Hornbeck C, Bloebaum RD. A polymethyl methacrylate method for large specimens of mineralized bone with implants. Stain Technol. 1987;62(6):401–10.

207. Newman GR, Hobot J. Modern acrylics for post-embedding immunostaining techniques. J Histochem Cytol. 1987;35(9):971–81.

208. Osamura RY, Itoh Y, Matsuno A. Applications of plastic embedding to electron microscopic immunocytochemistry and in situ hybridization in observations of production and secretion of peptide hormones. J Histochem Cytochem. 2000;48(7):885–91.

209. Plattner H, Bachmann L. Cryofixation: a tool in biological ultrastructural research. Int Rev Cytol. 1982;79:237–304.

210. Baskin T, Miller D, Vos J, Wilson J, Hepler P. Cryofixing single cells and multicellular specimens enhances structure and immunocytochemistry for light microscopy. J Microsc. 1996;182(2):149–61.

211. Meng H, Janssen PM, Grange RW, Yang L, Beggs AH, Swanson LC, et al. Tissue triage and freezing for models of skeletal muscle disease. J Vis Exp. 2014;(89):51586.

212. Santos RR, Tharasanit T, Figueiredo JR, Van Haeften T, Van den Hurk R. Preservation of caprine preantral follicle viability after cryopreservation in sucrose and ethylene glycol. Cell Tissue Res. 2006;325(3):523–31.

213. Hewitson TD, Wigg B, Becker GJ. Tissue preparation for histochemistry: fixation, embedding, and antigen retrieval for light microscopy. Methods Mol Biol. 2010;611:3–18.

214. Fischer AH, Jacobson KA, Rose J, Zeller R. Hematoxylin and eosin staining of tissue and cell sections. CSH Protoc. 2008;2008(5):pdb.prot4986.

215. Wittekind D. Traditional staining for routine diagnostic pathology including the role of tannic acid. 1. Value and limitations of the hematoxylin-eosin stain. Biotech Histochem. 2003;78(5):261–70.

216. Gruber HE, Ingram JA. Basic staining and histochemical techniques and immunohistochemical localizations using bone sections. In: Handbook of histology methods for bone and cartilage. Berlin: Springer; 2003. p. 281–6.

217. Rentsch C, Schneiders W, Manthey S, Rentsch B, Rammelt S. Comprehensive histological evaluation of bone implants. Biomatter. 2014;4(1):e27993.

218. Kavati E, Hosada T, Szulczewski V, Leão E, Borelli P, Cianciarullo A. A simple, fast, inexpensive and efficient method for leukocytes separation with preservation of morphology and cell viability for use in education and research. In: Méndez-Vilas A, editor. Microscopy and imaging science: practical approaches to applied research and education. Badajoz: Formatex Research Center.

219. Nilsen R, Magnusson B. Enzyme histochemistry of induced heterotropic bone formation in guinea-pigs. Arch Oral Biol. 1979;24(10):833–41.

220. Gomori G. The study of enzymes in tissue sections. Am J Clin Pathol. 1946;16(6):347–52.

221. Solberg LB. Experimental studies on bone with focus on tartrate-resistant acid phosphatase and bone remodeling; 2014.

222. Badylak SF, Valentin JE, Ravindra AK, McCabe GP, Stewart-Akers AM. Macrophage phenotype as a determinant of biologic scaffold remodeling. Tissue Eng Part A. 2008;14(11):1835–42.

223. Brown BN, Valentin JE, Stewart-Akers AM, McCabe GP, Badylak SF. Macrophage phenotype and remodeling outcomes in response to biologic scaffolds with and without a cellular component. Biomaterials. 2009;30(8):1482–91.

224. Komori T. Runx2, a multifunctional transcription factor in skeletal development. J Cell Biochem. 2002;87(1):1–8.

225. Magnusson P, Larsson L, Magnusson M, Davie MW, Sharp CA. Isoforms of bone alkaline phosphatase: characterization and origin in human trabecular and cortical bone. J Bone Miner Res. 1999;14(11):1926–33.

226. Kini U, Nandeesh B. Physiology of bone formation, remodeling, and metabolism. Radionuclide and hybrid bone imaging. Berlin: Springer; 2012. p. 29–57.

227. Allen M. Biochemical markers of bone metabolism in animals: uses and limitations. Vet Clin Pathol. 2003;32(3):101–13.

228. Magnusson P, Sharp CA, Farley JR. Different distributions of human bone alkaline phosphatase isoforms in serum and bone tissue extracts. Clin Chim Acta. 2002;325(1–2):59–70.

229. Gelse K, Pöschl E, Aigner T. Collagens—structure, function, and biosynthesis. Adv Drug Deliv Rev. 2003;55(12):1531–46.

230. Malaval L, Wade-Guéye NM, Boudiffa M, Fei J, Zirngibl R, Chen F, et al. Bone sialoprotein plays a functional role in bone formation and osteoclastogenesis. J Exp Med. 2008;205(5):1145–53.

231. Gordon JA, Tye CE, Sampaio AV, Underhill TM, Hunter GK, Goldberg HA. Bone sialoprotein expression enhances osteoblast differentiation and matrix mineralization in vitro. Bone. 2007;41(3):462–73.

232. Gutierrez J, Osses N, Brandan E. Changes in secreted and cell associated proteoglycan synthesis during conversion of myoblasts to osteoblasts in response to bone morphogenetic protein-2: role of decorin in cell response to BMP-2. J Cell Physiol. 2006;206(1):58–67.

233. Nishimura R, Hata K, Harris S, Ikeda F, Yoneda T. Core-binding factor α1 (Cbfa1) induces osteoblastic differentiation of C2C12 cells without interactions with Smad1 and Smad5. Bone. 2002;31(2):303–12.

234. Boskey AL, Robey PG. The regulatory role of matrix proteins in mineralization of bone. Osteoporosis (Fourth Edition). Amsterdam: Elsevier; 2013. p. 235–55.

235. Hayman AR. Tartrate-resistant acid phosphatase (TRAP) and the osteoclast/immune cell dichotomy. Autoimmunity. 2008;41(3):218–23.

236. Galson DL, Roodman GD. Origins of osteoclasts. In: Osteoimmunology. Amsterdam: Elsevier; 2011. p. 7–41.

237. Saftig P, Hunziker E, Everts V, Jones S, Boyde A, Wehmeyer O, et al. Functions of cathepsin K in bone resorption. In: Cellular peptidases in immune functions and diseases 2. Berlin: Springer; 2002. p. 293–303.

238. Goto T, Yamaza T, Tanaka T. Cathepsins in the osteoclast. J Electron Microsc. 2003;52(6):551–8.
239. Boyce BF, Xing L. Functions of RANKL/RANK/OPG in bone modeling and remodeling. Arch Biochem Biophys. 2008;473(2):139–46.
240. Bastani B, Ross F, Kopito R, Gluck S. Immunocytochemical localization of vacuolar H+-ATPase and Cl−-HCO3− anion exchanger (erythrocyte band-3 protein) in avian osteoclasts: effect of calcium-deficient diet on polar expression of the H+-ATPase pump. Calcif Tissue Int. 1996;58(5):332–6.
241. Rodan S, Rodan G. Integrin function in osteoclasts. J Endocrinol. 1997;154(3 Suppl):S47–56.
242. Harton M. Modulation of vitronectin receptor-mediated osteoclast adhesion to Arg-Gly-Asp peptide analogs: a structure-functional analysis. J Bone Miner Res. 1993;8:239–47.
243. Liu L, Shi G-P. CD31: beyond a marker for endothelial cells. Oxford: Oxford University Press; 2012.
244. Yang Y-Q, Tan Y-Y, Wong R, Wenden A, Zhang L-K, Rabie ABM. The role of vascular endothelial growth factor in ossification. Int J Oral Sci. 2012;4(2):64.
245. Stöger JL, Gijbels MJ, van der Velden S, Manca M, van der Loos CM, Biessen EA, et al. Distribution of macrophage polarization markers in human atherosclerosis. Atherosclerosis. 2012;225(2):461–8.
246. Gordon S, Plüddemann A, Martinez EF. Macrophage heterogeneity in tissues: phenotypic diversity and functions. Immunol Rev. 2014;262(1):36–55.
247. Stout RD, Suttles J. T cell signaling of macrophage function in inflammatory. Front Biosci. 1997;2:d197–206.
248. Mosser DM. The many faces of macrophage activation. J Leukoc Biol. 2003;73(2):209–12.
249. Wang N, Liang H, Zen K. Molecular mechanisms that influence the macrophage M1–M2 polarization balance. Front Immunol. 2014;5:614.
250. Etzerodt A, Moestrup SK. CD163 and inflammation: biological, diagnostic, and therapeutic aspects. Antioxid Redox Signal. 2013;18(17):2352–63.
251. Labonte AC, Sung SSJ, Jennelle LT, Dandekar AP, Hahn YS. Expression of scavenger receptor-AI promotes alternative activation of murine macrophages to limit hepatic inflammation and fibrosis. Hepatology. 2017;65(1):32–43.
252. Azad AK, Rajaram MV, Schlesinger LS. Exploitation of the macrophage mannose receptor (CD206) in infectious disease diagnostics and therapeutics. J Cytol Mol Biol. 2014;1(1).
253. Ghanaati S, Unger RE, Webber MJ, Barbeck M, Orth C, Kirkpatrick JA, et al. Scaffold vascularization in vivo driven by primary human osteoblasts in concert with host inflammatory cells. Biomaterials. 2011;32(32):8150–60.
254. Solchaga LA, Yoo JU, Lundberg M, Dennis JE, Huibregtse BA, Goldberg VM, et al. Hyaluronan-based polymers in the treatment of osteochondral defects. J Orthop Res. 2000;18(5):773–80.
255. Lucaciu O, Gheban D, Soriţau O, Băciuţ M, Câmpian RS, Băciuţ G. Comparative assessment of bone regeneration by histometry and a histological scoring system/Evaluarea comparativă a regenerării osoase utilizând histometria şi un scor de vindecare histologică. Roman Rev Lab Med. 2015;23(1):31–45.
256. Parfitt AM, Drezner MK, Glorieux FH, Kanis JA, Malluche H, Meunier PJ, et al. Bone : standardization of nomenclature, symbols, and units: report of the ASBMR Histomorphometry Nomenclature Committee. J Bone Miner Res. 1987;2(6):595–610.
257. Eriksen EF, Axelrod DW, Melsen F. Bone histomorphometry. New York: Raven Press; 1994.
258. Doube M, Kłosowski MM, Arganda-Carreras I, Cordelières FP, Dougherty RP, Jackson JS, et al. BoneJ: free and extensible bone image analysis in ImageJ. Bone. 2010;47(6):1076–9.
259. Revell P. Histomorphometry of bone. J Clin Pathol. 1983;36(12):1323–31.
260. Malluche HH, Sherman D, Meyer W, Massry SG. A new semiautomatic method for quantitative static and dynamic bone histology. Calcif Tissue Int. 1982;34(1):439–48.
261. Vidal B, Pinto A, Galvão MJ, Santos AR, Rodrigues A, Cascão R, et al. Bone histomorphometry revisited. Acta Reumatol Port. 2012;37(4):294–300.
262. Kim Y-G, Bark CW. Quantification of bone regeneration by virtual slices using non-destructive synchrotron X-ray microtomography. Tissue Eng Regen Med. 2015;12(5):379–85.
263. Haffner-Luntzer M, Müller-Graf F, Matthys R, Hägele Y, Fischer V, Jonas R, et al. Evaluation of high-resolution in vivo MRI for longitudinal analysis of endochondral fracture healing in mice. PLoS One. 2017;12(3):e0174283.
264. de Lange GL, Overman JR, Farré-Guasch E, Korstjens CM, Hartman B, Langenbach GE, et al. A histomorphometric and micro–computed tomography study of bone regeneration in the maxillary sinus comparing biphasic calcium phosphate and deproteinized cancellous bovine bone in a human split-mouth model. Oral Surg Oral Med Oral Pathol Oral Radiol. 2014;117(1):8–22.
265. Miwa S, Otsuka T. Practical use of imaging technique for management of bone and soft tissue tumors. J Orthop Sci. 2017;22(3):391–400.
266. Wathen CA, Foje N, Tv A, Miramontes B, Chapaman SE, Sasser TA, et al. In vivo X-ray computed tomographic imaging of soft tissue with native, intravenous, or oral contrast. Sensors. 2013;13(6):6957–80.
267. Topoliński T, Mazurkiewicz A, Jung S, Cichański A, Nowicki K. Microarchitecture parameters describe bone structure and its strength better than BMD. Sci World J. 2012;2012:502781.
268. Ito M. Assessment of bone quality using micro-computed tomography (micro-CT) and synchrotron micro-CT. J Bone Miner Metab. 2005;23(1):115–21.
269. Kallai I, Mizrahi O, Tawackoli W, Gazit Z, Pelled G, Gazit D. Microcomputed tomography–based struc-

tural analysis of various bone tissue regeneration models. Nat Protoc. 2011;6(1):105.

270. Campbell GM, Sophocleous A. Quantitative analysis of bone and soft tissue by micro-computed tomography: applications to ex vivo and in vivo studies. BoneKEy Rep. 2014;3:564.

271. Bukreeva I, Fratini M, Campi G, Pelliccia D, Spanò R, Tromba G, et al. High-resolution X-ray techniques as new tool to investigate the 3D vascularization of engineered-bone tissue. Front Bioeng Biotechnol. 2015;3:133.

272. Schulz G, Weitkamp T, Zanette I, Pfeiffer F, Beckmann F, David C, et al. High-resolution tomographic imaging of a human cerebellum: comparison of absorption and grating-based phase contrast. J R Soc Interface. 2010;7(53):1665–76.

273. Shetty S, Kapoor N, Bondu JD, Thomas N, Paul TV. Bone turnover markers: emerging tool in the management of osteoporosis. Indian J Endocrinol Metab. 2016;20(6):846.

274. Wang C, Duan Y, Markovic B, Barbara J, Howlett CR, Zhang X, et al. Phenotypic expression of bone-related genes in osteoblasts grown on calcium phosphate ceramics with different phase compositions. Biomaterials. 2004;25(13):2507–14.

275. Glenske K, Donkiewicz P, Köwitsch A, Milosevic-Oljaca N, Rider P, Rofall S, et al. Applications of metals for bone regeneration. Int J Mol Sci. 2018;19(3):826.

276. Xu H, Othman SF, Magin RL. Monitoring tissue engineering using magnetic resonance imaging. J Biosci Bioeng. 2008;106(6):515–27.

277. Tuchin VV, Tárnok A, Zharov VP. In vivo flow cytometry: a horizon of opportunities. Cytometry A. 2011;79(10):737–45.

278. Nioi P, Taylor S, Hu R, Pacheco E, He YD, Hamadeh H, et al. Transcriptional profiling of laser capture microdissected subpopulations of the osteoblast lineage provides insight into the early response to sclerostin antibody in rats. J Bone Miner Res. 2015;30(8):1457–67.

279. Slater M, Patava J, Kingham K, Mason RS. Involvement of platelets in stimulating osteogenic activity. J Orthop Res. 1995;13(5):655–63.

280. Logeart-Avramoglou D, Oudina K, Bourguignon M, Delpierre L, Nicola M-A, Bensidhoum M, et al. In vitro and in vivo bioluminescent quantification of viable stem cells in engineered constructs. Tissue Eng Part C Methods. 2009;16(3):447–58.

Membranes and Soft Tissues Enhancers

18

A. Friedmann and A. Akcalı

18.1　Introduction

The continuously emerging number of biomaterials in the field of membranes, barriers, and soft tissue enhancers, and their advertising may misguide the user to an attitude the products are all compatible regarding their application and services.

De facto all devices possess diverse features and should be investigated and discussed groupwise, separated by the material origin and manufacturing process; accounting for the functions and qualities provided by the manufacturer.

One rationale discriminates the membranes which are presenting with a barrier function from the "remodeling" membranes. While the first group represents materials for the GBR/GTR procedures, the others are supposed to facilitate the soft tissue conditions. Enhancement of peri-implant soft tissue volume in single implant sites majorly plays a role in the establishment of the outcome [1]. Therefore, to maximize the longevity of treatment outcomes from aesthetic and functional point of view soft and hard tissues should be considered together.

Biologics such as Enamel Matrix Derivatives (EMD), Autologous platelet concentrates (APCs), Hyaluronic acid (HA), or Growth Factors (GF) may serve for enhancing cells and tissues in both, the hard and the soft tissue compartment.

18.2　Use of Membranes

The principle coined Guided Bone Regeneration (GBR) aims at regenerating missing bone volume by newly formed mineralized tissues within deficient sites, however, without necessarily grafting the room by substitutes or fillers. The bone formation de novo—also considered intramembranous ossification—is a result of osteoblast activity within condensed mesenchymal tissue. It occurs during the development of the maxilla, the body of the mandible, or the midshaft of long bones [2]. The nature of this mechanism hallmarks bones of the skull throughout the life span of the vertebrates. In the late 80s of the last century, several research groups demonstrated successfully achieved the formation of new bone by secluding the defect space from non-osteogenic tissue [3]. The room created as a secluded space underneath a physical barrier is sought to fill with the blood which emanates from surrounding bone marrow [4]. Once sufficiently stabilized, the blood clot matures, the cells of mesenchymal origin proliferate and pre-osteoblasts are shown to invade then differentiate into cells capable of mineralization and initiating thereby the cascade

A. Friedmann (✉) · A. Akcalı
Department of Periodontology, School of Dentistry, Faculty of Health, Witten/Herdecke University, Witten, Germany
e-mail: Anton.Friedmann@uni-wh.de

of events necessary to form new alveolar bone. First resulting in an immature woven bone, it will maturate under strain and load by remodeling into lamellar bone. The remodeling relates to the permanent bone turnover of the skeleton and is based upon the activity expressed in the basic multicellular units (BMU). Single BMU contains osteoblasts, osteoclasts, and their precursors, whereby the osteoblasts are activated by osteoclast activity, i.e., initiating the resorption process of the bone. The Receptor Activating Nf kappaB ligand (RANKL) binds to the RANK receptor of the membrane and activates the osteoclasts. The antagonistic soluble protein Osteoprotegerin (OPG) counteracts by binding the RANKL protein within the bloodstream deactivating the ligand [5]. The resorption activity in a BMU in adult human bone is estimated at approximately 3 weeks and the formation response lasts for 3–4 months. The annual remodeling replacement rate is calculated with about 5–10% of the skeleton each year, with the entire adult human skeleton being replaced in 10 years until the person reached 50 years of age [6].

18.2.1 Studies on Membrane Materials

The membranes are considered to contribute to the new bone formation being themselves biocompatible, osteoconductive, and either nonresorbable or degradable. Various membrane materials were proposed for a semipermeable barrier function physically secluding the soft tissues and the periosteum from the room underneath. Both, the non-degradable and degradable materials representing the two major barrier categories were studied in vitro, pre-clinically, and clinically since then. Numerous studies focused on biocompatibility, cell occlusivity, barrier function, permeability, bacteria adherence and penetration, longevity in the tissues, soft tissue reaction, mineralizing capacity, and immune response from the recipient tissues. The experimental setting for in vitro and preclinical studies should adequately address the material characteristics the study is focusing on. In this context, the

popular setup once proposed as the proof of biocompatibility among native vs. cross-linked collagen membranes appears under concern as the positioning of the biomaterials in the chick mucosa of rodents doesn't reflect conditions at the alveolar crest [7]. More recent reproduction of this experiment using newer developed collagen matrices placed subcutaneously still confuses by conception as the chosen allocation has nothing in common with the intra-oral condition at the alveolar crest [8].

The narrative review by Elgali et al. offers a comprehensive overview regarding material characteristics, the benefits and disadvantages of several materials, and the evaluation methods each material cited was exposed to. Table 18.1 lists the membrane materials which were extensively investigated for GBR application (reprinted with permission). The review included 231 publications figuring out that the assessment of the outcome in preclinical studies is mainly based upon histologic and histomorphometric analyses [9]. Although this approach requires the termination of the animal, it represents the standard protocol which sometimes is supplemented by immuno-histochemical observations. Histologic evaluation of tissue integration by means of IHC can elucidate the vascularization process at the interface between soft tissue and the membrane and within the body of the membrane. Antihuman antibodies such as van Willebrandt factor, endothelial cells proliferation, transglutaminase 1 and 2, etc. are suitable for specific staining of the specimens retrieved after a determined healing period [10].

The visualization and monitoring of such dynamic process as bone formation require various termination endpoints increasing the number of animals and raising the costs of the experiment. The termination of the experimental animal may be also considered the highest grade of invasivity and becomes critical in terms of GAP. The group von See et al. suggested a plausible way to follow the capillary changes in the periosteum by an in vivo vital microscopy [11]. The setup allows for periodical recording of capillary density, vessel diameter, and velocity in the healing phase of soft tissues. The capillary

Table 18.1 Classification of guided bone regeneration (GBR) membranes according to type of biomaterial (with permissions from Elgali et al. [9])

Membrane groups/materials	Main advantages	Main disadvantages
Synthetic polymers		
Polytetrafluoroethylene	Inert and stable polymer in the biological system	Non-resorbable
Aliphatic polyesters (e.g. PLA, PGA, and PCL)	Bioresorbability	Lack of rigidity and stability
	Good processability and manageability	
	Drug-encapsulating ability	
Natural polymers		
Collagen and extracellular matrices derived from bovine, porcine and human tissues	Bioresorbability	
Chitosan	Low immunogenicity	
Alginate	Drug-encapsulating ability	
	Incorporation of biological components	
Metals		
Titanium and titanium alloy	High toughness and plasticity	Non-resorbable
Cobalt–chromium alloy		
Inorganic compounds		
Calcium sulfate	Bioresorbability	Low toughness and plasticity
Calcium phosphate (e.g. hydroxyapatite)	Osteoconductivity	

PCL poly(ε-caprolactone), *PGA* poly(glycolic acid), *PLA* poly(lactic acid)

vessels in the periosteum were monitored after the application of a membrane or an expanding device subperiostally in a sculpt model in rats [12]. The Laser Doppler Flowmetry offers the chance to monitor the blood perfusion rate in soft tissues at various time points representing another non-invasive approach to indirectly follow the healing process (Fig. 18.1). Once positioned, any membrane material counts as a foreign body per se, nevertheless membranes are supposed to integrate into the tissues without complications. The soft tissue interacts with a high number of membrane characteristics, either in a positive or negative manner. Thus, the perfusion rate reflects the initial healing in the soft tissue in the long-term [13–15]. As a series of studies demonstrates, this parameter is predictive for dehiscence onset in soft tissues 14 days after the surgery. The calculations reveal that the perfusion rate is predictive for the onset of such complication with an area of 0.8 under the curve [13].

In a pre-clinical setup, the critical-size surgical defect represents an acute defect within the boundaries of the native bone lacking a chance for spontaneous osseous healing. This type of defect is supposed to be sufficient for approving

Fig. 18.1 Periflux probe at beagle's mandible. (Courtesy Dr. Kaner/Dr. Friedmann)

the space-maintaining properties of the membrane. The space-maintaining capacity relates to the physical properties and favors solid materials which are resistant to deformation and thereby withstanding the pressure from the soft tissues as

masticatory forces. On the contrary, the opposite aspect is the material plasticity, i.e. the ease of handling the membrane to merge with the shape of the defect. However, once inserted into the body there is a lack of methods feasible to monitor the fate of material traits non-invasively in an animal (Tables 18.2 and 18.3).

The use of grafting materials in the field of GBR basically points to the observation that many membranes lack the space-maintaining

Table 18.2 Experimental in vivo studies evaluating the performance of non-resorbable membranes after modifications of the physicochemical properties (with permissions from Elgali et al. [9])

Membrane type/ modification	Experimental model	Experimental groups (membrane and/or graft materials)	Main findings
e-PTFE/embedding of titanium framework in the membrane	Peri-implant defect in mandible (dog)	1. e-PTFE membrane	Ti reinforcement resulted in:
		2. Ti-reinforced e-PTFE membrane	• More rigid and malleable membrane
			• Large and protected defect space for better stabilization of blood clot and higher bone formation
e-PTFE or Ti/ changing the porosity of the membrane	Denuded calvarial site (rat)	1. Less porous e-PTFE dome (8 μm ID)	More porous membranes showed:
		2. More porous e-PTFE dome (20–25 μm or 100 μm ID)	• Better tissue integration and stability
			• More bone formation after 6 weeks
	Supra-alveolar defect (dog)	1. e-PTFE	Sites receiving the occlusive membrane showed greater bone regeneration compared with sites with a porous membrane
		2. e-PTFE with 300 μm laser-drilled pores	
	Mandibular ramus (rat)	1. Autogenous bone	Macroporous membrane facilitated greater bone regeneration compared with microporous and resorbable mesh (membrane)
		2. Resorbable PLDLLA mesh cube + autogenous bone	
		3. Microporous Ti mesh cube (0.6 mm pore size) + autogenous bone	
		4. Macroporous Ti mesh cube (1.2 mm pore size) + autogenous bone	
	Calvaria (rabbit)	1. Ti cylinder covered with e-PTFE (semipermeable)	New bone was observed in both cases. It was suggested that membrane permeability is unnecessary in GBR
		2. Ti cylinder sealed with cast titanium (impermeable)	
	Calvaria (rat)	1. e-PTFE dome (5 μm ID)	PTFE with 100–300 μm pores permits soft-tissue invasion, but also allows more bone formation at the healing site
		2. e-PTFE dome (8 μm ID)	
		3. e-PTFE dome (100–300 μm ID)	
		4. PLGA dome	
	Mandibular ramus (rat)	1. Permeable PTFE capsule + DBM	Comparable amount of bone formation was observed in the two groups
		2. Occlusive PTFE capsule + DBM	

Table 18.2 (continued)

Membrane type/ modification	Experimental model	Experimental groups (membrane and/or graft materials)	Main findings
PTFE/use of non-expanded material (d-PTFE)	Calvarial defect (rabbit)	1. Semipermeable e-PTFE 2. d-PTFE	Whereas the d-PTFE membrane was much easier to detach from the underlying bone, e-PTFE showed faster and higher levels of bone regeneration
	Mandibular defect (rat)	1. Sham 2. d-PTFE membrane	After 10 weeks of healing, whereas very little osseous regeneration was observed in sham sites, complete ossification was observed in the d-PTFE-treated sites
	Calvarial defect (rat)	1. Sham	d-PTFE showed more bone formation than both e-PTFE and PLA/citric acid ester membrane at 2 weeks and 4 weeks of healing, respectively
		2. PLA/citric acid ester base membrane	d-PTFE required less force to be removed from the soft tissues
		3. e-PTFE membrane	
		4. d-PTFE membrane (0.2 μm ID)	
Incorporation of calcium phosphate material (HA)	Calvarial defect (rat)	1. Sham 2. e-PTFE membrane 3. Nano HA-polyamide 66 composite membrane	Bone volume was higher in the membrane groups and no differences were observed between the two membrane types

DBM demineralized bone matrix, *d-PTFE* dense polytetrafluoroethylene, *e-PTFE* expanded polytetrafluoroethylene, *GBR* guided bone regeneration, *HA* hydroxyapatite, *ID* internodal distance, *Ti* titanium, *PLA* polylactic acid, *PLDLLA* copolymer of poly(L-lactide-*co*-D,L-lactide), *PLGA* poly(lactide-*co*-glycolide)

capacity. However, the bone substitutes mainly represent osteoconductive scaffolds which will be populated by cells invading the bone defect. The bone grafts are sought to enhance the cell proliferation and to prevent the blood clot shrinkage while setting. The concordance analysis between histomorphometric and radiographic outcomes following GBR in a minipig revealed a difference in visualizing the mineralization stage of the specimen and may have enlightened different sensitivity of both methods [16]. The group of Elgali et al. evaluated recently the effects of a resorbable membrane and three bone substitutes by looking at histology but also at the gene expression profile in the osteoclast-osteoblast coupling [17].

The non-resorbable membranes are supposed to be removed from the site while degradable materials will be resorbed by means of enzymatic, hydrolytic, or collagenous degradation.

The initial idea of a barrier kept in place in the wound area for a certain period has shifted towards different durability of degradable membranes along with the introduction of resorbable materials. There is no recommendation derivable from today's perspective regarding barrier lasting time required for new bone formation.

Currently, with the aid of nanotechnology and tissue engineering, bioactive multifunctional (multi-layered membranes) membranes started to be designed and investigated in laboratory settings. The functionalization of the resorbable membranes is enhanced once by either molecule, growth factors (GF), or cells which thereby are sought to act as a scaffold and a carrier delivering the substances into the wound area. The main purpose is to drive new tissue formation by using biomolecules such as growth factors and/or antimicrobials. The effect of loading a native collagen membrane by BMP-9 was demonstrated in a

Table 18.3 Experimental in vivo studies evaluating the performance of resorbable membranes after modifications of the physicochemical properties (with permissions from Elgali et al. [9])

Modification	Experimental model	Experimental groups (membrane and/or graft materials)	Main findings
Increasing molecular weight of the polymer	Calvarial defect (rabbit)	PLLA membrane with different molecular weights 1. mw 100,000 2. mw 380,000	PLLA mw 380,000 membrane showed: • Higher compressive strength • Lower amount of deformation and higher bone formation after 4 and 12 weeks of healing
Changing the pore size	Calvarial defect (rat)	1. Sham 2. Stiff polyoxymethylene plastic plate 3. Polyester meshes with different porosities (10, 25, 50, 75, 100, and 300 μm)	• Placement of polyester meshes with perforations exceeding 10 μm resulted in faster and higher bone augmentation than did 10 μm pores and stiff polyoxymethylene material • The defect group with stiff barrier did not show ingrowth of suprabony connective tissue as did the porous membrane but the bone augmentation was more evenly distributed in the defect
	Diaphyseal defect in the radius (rabbit)	PLLA membrane with various pore sizes: microporous (size was not provided), medium (10–20 μm) and large (20–200 μm) pore sizes	• Microporous membrane showed more predictable bone regeneration compared with the membranes with pores of medium and large size (10–20 or 20–200 μm)
	Segmental defect in mandible (dog)	1. Sham 2. Autogenous bone 3. Mi 4. PMi 5. Mi + autogenous bone 6. PMi + autogenous bone	• Combination of PMi and autogenous bone increased the bone formation compared with other treatment modalities • The use of Mi alone delivered the least bone formation • The Mi did not add any benefit when combined with autogenous bone
	Segmental large diaphyseal defect (sheep)	1. External microporous PLLA membrane (pore size: 50–70 μm) 2. Internal and external microporous PLLA membrane 3. External perforated PLLA membrane (pore size 800–900 μm) 4. External perforated PLLA membrane + autogenous bone 5. Internal and external perforated PLLA membrane 6. Internal and external perforated PLLA membrane + autogenous bone	• The bone defect healed only when the laser-perforated membrane was used in combination with the autogenous bone • Use of the internal and external perforated membrane (tube-in-tube implant) with autogenous bone allowed reconstitution of the 'neocortex' with well-defined thickness. This was suggested to enhance vascularization of the bone graft from the soft tissue

Increasing thickness of the membrane	Mandibular defect (dog)	1. RHDM (100 μm thick) 2. RHDM (200 μm thick)	• The 200-μm-thick membrane showed less soft-tissue ingrowth and better bone formation after 6 months of healing
	Calvarial site with onlay graft (rabbit)	1. Block bone grafts 2. Monolayer collagen membrane + block grafts 3. Double-layer collagen membrane + block grafts	• Placement of double-layer membrane showed less graft resorption and enhanced bone augmentation • Whereas the monolayer membrane was completely degraded by 4 months, the body of the double-layer membrane was retained up to 6 months
	Calvarial defect (rat)	1. Monolayer collagen membrane 2. Double-layer collagen membrane	• Use of a double-layer technique provided a thicker barrier after 4 and 9 weeks of healing. The effect on bone regeneration was not studied
Incorporation of calcium phosphate materials such as HA and TCP	Calvarial defect (rat)	1. Sham 2. Collagen membrane 3. HA-Chitosan/fibroin membrane	• Bone volume and density were higher in the membrane groups and no difference was observed between the two membrane types
	Calvarial defect (rabbit)	1. Sham 2. PCL/PLGA membrane 3. PCL/PLGA membrane combined with β-TCP	Presence of β-TCP enhanced: • The toughness and tensile strength of the membrane • The membrane mechanical stability and tissue integration in vivo • Bone formation at 4 and 6 weeks
	Calvarial defect (rat)	1. Sham 2. Collagen commercial membrane 3. Cross-linked collagen membrane (experimental) 4. Cross-linked collagen membrane (experimental) with different levels of mineralization (HA)	In comparison with the commercially available collagen membrane, the cross-linked experimental membrane with and without HA showed: • Higher level of bone formation after 4 weeks • Lower degradation rate • Decreased level of the inflammatory marker, TNF-α, in the soft tissue
	Calvarial defect (rabbit)	1. Sham 2. Collagen commercial membrane + DBB 3. Sr-HA-containing collagen membrane + DBB 4. Sr-HA-containing collagen membrane + BCP substitute	• Combination of Sr-HA-containing collagen and BCP substitute showed highest bone formation after 24 weeks • Comparable bone formation was observed with the Sr-HA collagen-containing membrane and the commercial membrane after combining each of them with the DBB bone substitute
	Calvarial defect (rat)	1. Sham 2. Collagen membrane 3. Sr-HA 10 mg mL^{-1} gelatin 4. Sr-HA 20 mg mL^{-1} gelatin	• Sr-HA 20 mg mL^{-1} group yielded significantly greater bone formation than the other groups
	Calvarial defect (rat)	1. Sham 2. Collagen membrane 3. Zinc HA-gelatin membrane 70 mg mL^{-1}	• Group of zinc HA-gelatin membrane showed the highest bone formation at early (2 weeks) and late (4 and 6 weeks) time periods

(continued)

Table 18.3 (continued)

Modification	Experimental model	Experimental groups (membrane and/or graft materials)	Main findings
Incorporation of BG	Maxillary defect (rabbit)	1. Sham + autogenous bone 2. PEOT/PBT copolymer membrane combined with BG + autogenous bone	• The membrane group showed higher osteogenic activity. The increase in bone quantity was not statistically significant compared with the control group

β-TCP beta-tricalcium phosphate, *BCP* biphasic calcium phosphate, *BG* bioactive glass, *DBB* deproteinized bovine bone, *HA* hydroxyapatite, *Mi* microporous poly-ʟ/ᴅʟ-lactide membrane, *PBT* polybutylene terephthalate, *PEOT* polyethylene oxide terephthalate, *PCL* polycaprolactone, *PLGA* poly(lactide-*co*-glycolide), *PLLA* poly-ʟ-lactic acid, *PMi* perforated poly-ʟ/ᴅʟ-lactide membrane, *RHDM* resorbable human demineralized calvarial bone membrane, *Sr* strontium

rabbit model histologically confirming the results radiographically by μCT [18].

The colonization of the surfaces by cells seeding the cells approves the biocompatibility of the membrane material in vitro in the medium. Alternatively, the "air-lift" set-up allowed for studying the membrane permeability for nutrients by allocating the cells on top of membranes with interrupted contact to the medium [19].

An intriguing recent observation regards the ossifying capability of membranes with certain qualities either being meanwhile commercially available or in development. The ossification of the membrane body or its residues represents at least partial integration of the material into the newly mineralized tissues. Such membrane capacity coined osteopromotive quality is highly appreciated compared to osteoconductive properties commonly known for the major number of commercially available membranes (Fig. 18.2) [20].

Studies using e-PTFE membranes indicated that this non-resorbable material had a positive activating effect on cells involved in bone formation. The evaluation of modern materials regarding ossification capabilities is complex. The collagen-based membranes either easily integrate into soft tissues or disappear completely within a few weeks as shown for native collagen membranes or, if cross-linked by non-toxic agents they rather undergo integration into the augmented tissues. These two divergent properties,

however, both make the labeling of the material in the experimental body difficult for later discrimination of the membrane residues.

The group of Moses et al. suggested an elaborated approach to follow the degradation of the inserted collagen structures such as the membrane body in a pre-clinical setting [21]. By binding the aminohexanoyl-biotin-*N*-hydroxy-succinimide ester complex to the proteins of the test collagen it was likely to place a pre-coated membrane body into an experimental animal [22]. The purpose was to label the biotin receptors with the streptavidin antibody in the retrieved tissues containing the collagen residues as the given healing period was completed. The biotin-streptavidin antibody reaction helped to visualize the residual collagen structure, furthermore, it opened the possibility to quantify the angiogenesis within the membrane body and gave access to the count of macrophages and other immune-responsible cells invaded the inserted structures [23] (Figs. 18.3 and 18.4). Moses and associates used this approach to visualize and quantify the colla-

Fig. 18.3 Collagen membrane labelled by biotin embedded into tissues (ex vivo). (Courtesy Dr. Eliezer/Dr. Moses)
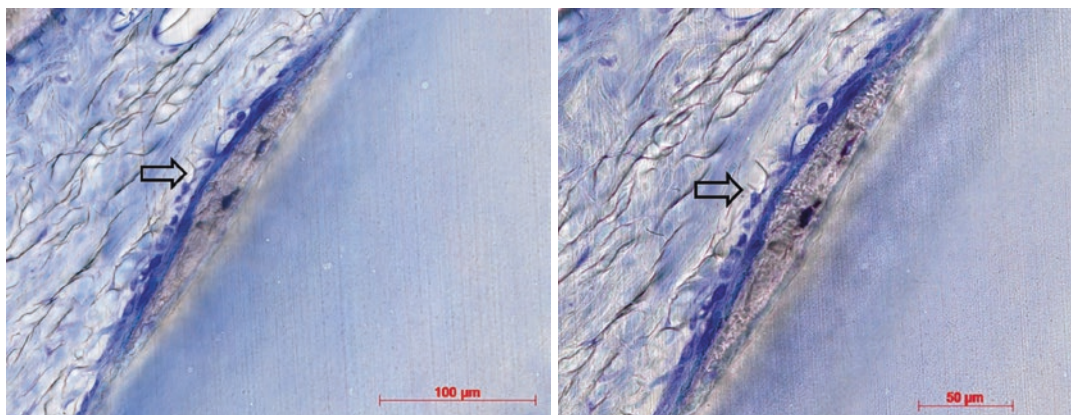
Fig. 18.2 Socket preservation study in beagle: ossifying residues of RCLC membrane in buccal tissues. (Courtesy Dr. Goetz/Dr. Friedmann)
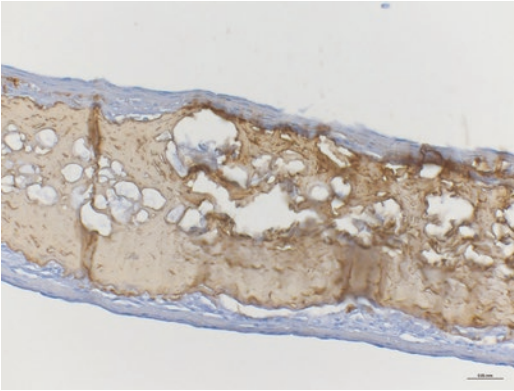
Fig. 18.4 Fragment from Fig. 18.3 at higher magnification. (Courtesy Dr. Eliezer/Dr. Moses)

gen degradation rate in diabetic rats compared to normoglycemic animals [24]. For any reasons, this approach hasn't been extended towards bigger animal models yet.

Turri et al. combined different pathways evaluating the ossification effect of the membrane applied in an animal experiment. Retrieved tissue samples were allocated either for the histologic and immunohistochemical processing or were homogenized and used for the PCR analysis to verify the transcription of the osteogenic proteins from the cells included in the sample to amplify the ossification effects recorded from microscopy [25].

In a clinical study, Friedmann et al. used the IHC technique to analyze the extension of inflammatory infiltrate and invasion of multinucleated giant cells into tissues associated with complications that occurred after a simultaneous bone augmentation procedure comparing ribose crosslinked collagen membrane with a native collagen membrane [10].

The group of Wang et al. developed a method to mineralize collagen membranes to enhance the surface stiffness during the manufacturing process to facilitate bone formation in the bone defect [26]. This new type of membrane was evaluated by several common methods including AFM, Instron tensile tests, the ultrastructural and FDXs analysis for estimation of element distribution and in vitro experiments. The microscopic analysis and RT-qPCR for ALP and immunohis-

tochemical staining for OCN evaluated tissue response to the membranes with varying stiffness degrees. After coating these membranes with MSC the researchers inserted this material subcutaneously to study the ectopic bone formation. Smeets et al. looked at the residues of ßTCP or HA modified, i.e., enhanced silk membranes after 5 and 10 weeks by µCT using a sculpt model in rabbits [27].

Monitoring the soft tissue healing process following a membrane placement favors noninvasive techniques.

The group of Retzepi et al. suggests a preclinical model for the evaluation of GBR under systemically compromised conditions. Particularly they developed an experimental setting for studying the bone formation process in diabetic rats using a subcutaneous pump to inflate the test animals with insulin to create hyperglycemia [28]. The methods implemented for analyzing the process at different time points were the histologic analysis and histomorphometric assessment in the retrieved specimens as a traditional approach and the microarray technology on the cRNA of the samples as a very recent methodology.

The same group under Mardas' first authorship introduced another animal model for estimating the effects of Bisphosphonates used for the treatment of ovarian ectomized and therefore osteoporotic rats on bone formation. The assessment method used was histologic analysis [29].

In a CCT chronologically harvested wound fluid samples after using Enamel matrix derivative in periodontal regeneration gave insights into the early steps of soft tissue healing by using a multiplex ELISA system [30]. However, even none invasive sampling of wound fluid and GCF, respectively, is unlikely to perform on a daily basis in an animal trial.

In summary, the clear majority of mentioned approaches are based upon ex vivo assessment of tissue quality, quantity, and composition. Thus, the key question remains how to assess the progress of collagen degradation or integration under vital conditions. In extension, the same is true for others, i.e., synthetic materials which are used for

GBR as well. Obviously, today we are still missing the ultimate tools and instruments feasible to evaluate the process of tissue formation and maturation in vivo. In terms of product evaluation, we are obliged to use a series of animals to determine various time points to terminate the experiment to get access to the biopsies for ex vivo analysis. The pre-clinical study protocols are missing a standardized timeline to assess the effects either initiated by placed biomaterials themselves or representing the response by the host to the intervention.

In conclusion, weighting the most recent approaches in membrane research the idea of pre-coating the collagen membranes and collagen matrices with the biotin complex appears as the one bearing tremendous potential in the context of studying the degradation and delivery properties in a pre-clinical study. The quantification of residual collagen, the grade of vascularization, and cell counts become accessible ex vivo after a certain period of healing and integration. The PCR methods for investigating the stimulating effects on adjacent cells from tissues, where the collagen materials were placed into membranes appear promising for future research [20] (Fig. 18.5).

18.2.2 Studies on Biologics

Biologics is used as a summary term describing several bioactive factors proposed to facilitate the local regenerative process in the deficient area. Pre-clinical studies have evaluated the added effect of bone morphogenetic proteins (such as BMP-2) and autologous platelet concentrates (APCs) in combination with biomaterial scaffolds on new bone formation. The BMPs were applied either as a single factor or as a mixture of different growth factors to enhance the effects in the wound area by reducing the dose of every single factor. Various carrier systems were suggested containing collagens, particulate xenogenic or synthetic substitutes as scaffolds favoring an easier control of the concentration and the delivery thereby upgrading the substantivity.

The pre-clinical studies were carried out in rodents and larger animals considering the effects of various biologically active materials on the bone healing process in cranio-facial surgery. The experimental set-up included intra-orally created deficient alveolar bone segments requiring vertical or horizontal ridge augmentation procedures, maxillary sinus grafting, extraction

Fig. 18.5 Schematic description of a membrane involvement into the process of new bone formation. (With permissions from Elgali et al. [9]) (© Thomsen/Elgali/Omar)
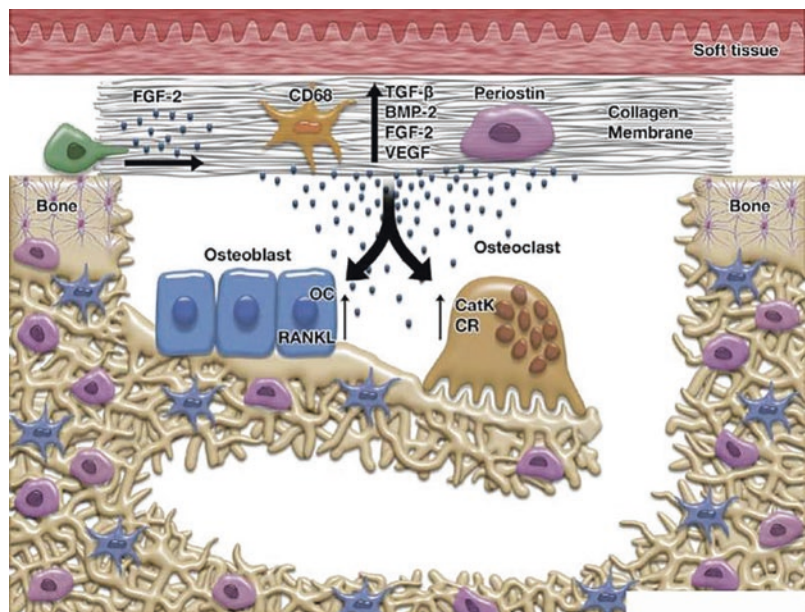
socket treatment, treatment at integrated but ailing implants with different surface characteristics but extra-orally created defects such as a calvaria model also. As claimed by the above-mentioned requests for the GBR protocols, a strong demand towards the use of critical size defects (CSD) in experiments evaluating the biologics pre-clinically is disposed of, likewise [31].

The pre-clinical trials estimating the impact of Amelogenins on bone healing have been carried out in both, subcritical size defects and CSDs as well. EMD was applied together with osteoconductive bone substitutes or a PEG hydrogel. Again, the main assessment strategy is to analyze the outcomes based on histology and histomorphometry [31].

The recent review by Calciolari and Donos focused on the future of experimental research in the field of bone healing and regenerative procedures. The authors claimed that omics approaches such as transcriptomics, proteomics, and epigenomics will dominate the research activities in the close future. The gene expression arrays, protein expression arrays, and maybe even "salivaomics" and "materiomics" 1 day will guide the decision-making process towards personalized and optimized choice of biomaterials and better-weighed strategies in treating a systemically compromised patient [32].

The combination between a growth factor (PRGF) and a particulate bone substitute (ß-TCP) has been applied alone to mandibular defects or is additionally covered by a resorbable collagen membrane in beagles [33]. Other groups used the calvaria model in rabbits to evaluate the same factor in combination with other carrier systems [34].

Autologous platelet concentrates are acquired by centrifugation of peripheral blood samples resulting either in a Platelet-Rich Fibrin (PRF) or Platelet-Rich Plasma (PRP) according to the applied centrifugation protocol [35]. A recent study compared the acceleration effect of PRF with that of hyaluronic acid (HA) in a fracture model using the mid-diaphyseal corticotomy in rats [36]. The outcomes were assessed histomorphometrically and by 3D-radiographic evaluation with a CBCT scan at two time points. The effects of HA on the degradability of the collagen membranes placed subcutaneously were assessed using an above-mentioned diabetic rat model. The histomorphometric counts of the membrane residues and the estimated number of voids inside each residual part of the collagen sample were the outcome parameters [37]. A Spanish group used customized hyaluronic acid scaffolds with and without adipose stem cells (ASCs) for treating vascular stroke lesions in rats [38]. Counting of immature (NF 160 kDa) and mature (NF 200 kDa) neurofilaments found in the ischemic zone in stroke controls, stroke animals after placement of biomaterials, and after placement of biomaterials with ASC was the primary parameter in this study.

The histomorphometric assessment of BIC (bone-to-implant contact) numbers was the most popular parameter in studying the effects of APCs combined with a carrier in maxillary sinus augmentation. Some authors compared the effect of PRP added to a xenogenic (bovine) bone mineral to that of rh-BMP 7 on DBBM [39] using the simultaneous approach for implant placement in the sinus cavities in minipigs.

In the field of dental regeneration, most popular one is probably the Enamel Matrix Derivative (EMD). The other group is represented by products based on the natural preparations of hyaluronic acid with different molecular sizes and available as non-cross-linked or cross-linked proteoglycans.

18.3 Use of Autogenous Soft Tissue Grafts and Soft Tissue Substitutes

The peri-implant mucosa assembly is supposed to be as sophisticated as it is around the natural teeth and should provide ideal coverage to the implant-supporting tissues [40]. The presence of healthy peri-implant soft tissue condition is crucial for long-term implant survival. Thus, the indications for peri-implant soft tissue augmentation intend to improve the plaque removal efficacy, facilitate peri-implant tissue stability, and enhance aesthetics. If the amount or quality of

the peri-implant soft tissue is diminished or limited, the soft tissue condition may be varied by using an autogenous soft tissue graft and/or soft tissue substitutes, fillers, and enhancers to support the healing and eventually improve the conditions. In this regard, free gingival grafts (FGG) and subepithelial connective tissue grafts (SCTG) have been widely recommended. The major rationale for developing soft tissue substitutes alternatively to the autogenous grafts was the limited amount and/or quality of the harvested autogenous tissues along with the patient morbidity because of an additional wound area at the donor site. Although the devices available today appear promising at first glance, meeting basic biologic criteria before their application to the planned surgical site can be recommended is critical. The soft tissue substitute is supposed to integrate well at the recipient site by allowing cell ingrowth while remaining mechanically and volumetrically stable itself as during and after the maturation phase. In the following section mostly investigated soft tissue enhancement devices and grafts along with their application methods are discussed.

18.3.1   Currently Available Concepts for Peri-implant Soft Tissue Enhancement

18.3.1.1   In Vitro Concepts

The in vitro proof of any new soft tissue device is crucial to understand its clinical application scope and to control the number of animals used in the next step of evaluation which is pre-clinical approval. Although the in vitro setting does not exactly reproduce the in vivo environment, it may serve as a basis for the clinical use of the tested materials. Different cell types were involved in cell culture studies, hence gingival fibroblasts, periodontal ligament fibroblasts, and epithelial cells were mostly investigated. The cell response to the prototype of a collagen sponge out of porcine collagen type I and III has been evaluated using an in vitro dynamic system. It replicated the natural forces in the oral cavity, i.e., pressure and shear forces [41]. By this system cell viability and activity on the collagen sponges have been analyzed under different cultivation and time conditions. Accordingly, the tested in vitro system could imitate the biological and mechanical conditions of the oral cavity to a certain extent. However, the investigation of soft tissue grafts requires setup that provides mechanical stimulations rather than just static conditions. Therefore, the adequate transition setting from in vitro to in vivo experiments for a better understanding of the complexity of wound healing events as a response to the applied soft tissue device is yet lacking.

18.3.1.2   Pre-clinical Concepts

As for today, the peri-implant soft tissue regeneration has mainly focused on increasing the peri-implant attached/keratinized mucosa in dimension and volume. Soft tissue manipulation for this purpose could be performed before or at the same time as the implant placement surgery or at the second stage surgery or even later when the implant has been uncovered already in the past. Regarding the outcome of interest, biomaterial characteristics in terms of tissue integration, cell growth, mechanical/volume stability, and wound healing events could be tested in a pre-clinical model. Pre-clinical models should be suitable to deliver valid information that thereafter can be translated and replicated when tested in human clinical trials. With this regard, histological and/or clinical outcome accessories were defined and evaluated. Thus, histological parameters for the keratinized tissue augmentation are so far, the absence of elastic fibers, the presence of rete peg formation, apparent keratin layer at the epithelium surface. As clinical parameters (i.e. macroscopic outcomes) the local tolerance of the material (signs or absence of local inflammation/intolerance), the monitoring of volume changes over time, the width (e.g. periodontal probe) and thickness (e.g. individual stents) of the graft, the contraction/shrinkage (e.g. master casts out of dental stone), re-epithelization and re-vascularization of the augmented soft tissue grafts and as final endpoint clinical performance of the graft/substitute were considered feasible for observation.

In current research on soft tissue enhancement, mostly larger animal models such as minipigs, pigs [42], and dogs [43–48] have been selected to investigate soft tissue related events. Since various pre-clinical models on soft tissue augmentation around teeth [42, 44, 49] were reported, in this chapter only models used for peri-implant sites were discussed. The earlier applied model in dogs [46, 47] had aimed at evaluating soft tissue augmentation of single tooth gaps with chronic ridge defects using a soft tissue device (collagen matrix). Tested grafting material was compared with autogenous SCTG as positive control and the sham-operated group as negative control. The outcome measures were volumetric analysis to assess the soft tissue volume changes by using master casts and histological and computer-assisted histomorphometric analyses. The possible advantage of this dog model was the intended similarity of the created chronic ridge defect to the single tooth gap experienced clinically. However, this model offered certain disadvantages, as there were differences in individual baseline defect shape and extension because of the different sizes of the extracted teeth. Thereby ridge defects thought to be chronic on the day of soft tissue augmentation represented individual healing patterns of non-standardized defects in each animal included.

The same research group modified their dog model for investigating soft tissue volume augmentation around dental implants [43, 48]. The model of choice aimed at the evaluation of linear and volumetric [43] histological and histomorphometric changes [48] after peri-implant soft tissue augmentation using a different soft tissue device (the volume-stable cross-linked collagen matrices). Corresponding groups received either the autogenous SCTG as positive control or a sham surgery as a negative control. Soft tissue augmentation was performed 3 months following implant placement with simultaneous GBR.

When these two dog models were compared, in the earlier design [46, 47] evaluation has been performed in single tooth gaps whereas in the newer design single tooth implant sites were evaluated and followed up to 6 months. Basically,

the more recent model assessed under chosen conditions the gain in tissue volume in both, the buccal and occlusal directions. Histological and histomorphometric parameters were biocompatibility and local tolerance of the material expressed by the horizontal tissue thickness of the augmented graft/device assessed at different time points of the evaluation period (4, 8, and 24 weeks). The most evident finding was that the desired clinical endpoint—the tissue thickness—was undergoing continuous volume decrease over the 6-month observation period. Hence, the hard and soft tissue remodeling process finally rendered limited changes in treated sites.

The search for a valid and reproducible evaluation method for peri-implant soft tissue is ongoing. The proposed three-dimensional analysis by using dental casts obtained at different time points of evaluation after surgical intervention has the potential for being a reliable non-invasive method. In principle, baseline (pre-augmentation) and post-augmentation impressions are obtained and master casts poured out of a scannable dental stone and then optically scanned with an industrial scanner and thereafter digitized as standard tessellation language files (STL files) [1]. The STL files of the casts are transferred into a specific digital software program to evaluate dimensional changes at the augmented site. Uploaded images representing different time points are superimposed and matched using the best-fit algorithm through tooth surfaces as references. Then, the region of interest (ROI) is defined manually in the relevant augmented area by mesial and distal papillary midline, the muco-gingival junction, and the alveolar ridge crest. By doing so, different sites could be directly compared in terms of volume changes irrespective of their size and the size of the measured area. However, measurement was only limited to the selected ROI on top of the keratinized mucosa which could be a maximum of 4 mm extended from the 0.5 mm apically from the transition between the buccal and occlusal plane. That means areas lack of or deficient keratinized mucosa did not allow accurate application of the selected methodology and eventually peri-implant mucosa in buccal sites could be partially evaluated. Thus, this method-

ological approach could only be performed under the experimental conditions with areas having enough keratinized mucosa and mucogingival junction without coronal displacement at surgical site.

18.3.2 Limitation of the Current Pre-clinical Models

Although reported findings from available experimental models especially from dogs were promising there are critical points that should be considered before conducting a pre-clinical trial. There are fundamental issues that are important for the correct interpretation of the findings. Integration of augmented soft tissue/substitute to the recipient site and replacement by host connective tissue and long-term stability with a natural color match and minimum amount of shrinkage are expected clinical endpoints. However, present models are less than ideal for measurements of clinical function and for evaluating the effects of various forces on tissues. For instance, the tested collagen matrix still seems not strong enough to resist compression forces even if it originated from suturing on top of the material. Moreover, unpredictable swelling of the surgical site during the first phases of the wound healing process originating from the physical characteristics of the substitute might cause wound dehiscence which thereafter ends up with volume loss of the augmented tissue. Another critical disadvantage is the possible growth of the animals during the study period resulting in difficulties in performing the clinical measurements, also markings serving as reference points may disappear.

Apart from these challenges, visualization of the defects in small animal models could also be accounted as a disadvantage. Also in these models, limited space of the surgical site is an important anatomical difficulty that might restrain the organization of the blood clot and the selective cells that are required for soft tissue regeneration [50]. Thus, the models used in the current literature may not necessarily represent the clinical scenario of the wound site after peri-implant surgery. Depending on the research objective the researcher should decide correct animal model and plan each step according to the intended surgical intervention.

18.3.3 Factors That Influence the Outcome

Today still knowledge gaps existed on the factors that potentially influence the outcome of peri-implant soft tissue augmentation procedures. Techniques used for soft tissue management including incision/flap design and suturing techniques are important elements that contribute to the outcome assessments either qualitative or quantitatively [51].

Figure 18.6 represents factors influencing the success of soft tissue volume augmentation (Fig. 18.6). Each factor including the location of the soft tissue augmentation (horizontal vs. vertical), flap preparation, the thickness of the flap, handling (trimming yes/no, wet vs. dry application) and thickness of the graft/substitute, the distance of the graft/substitute to the wound margins, the and environment which healing take place and wound closure should be carefully addressed before and during the procedure. Among all, the first factor is the location of the soft tissue augmentation. The surgical area of interest might involve soft tissue and/or bone. In other words, soft tissue volume augmentation could be performed limited to the buccal side of the implant (horizontal) or on the top of the implant (vertical). In horizontal soft tissue volume augmentation, soft tissue could be placed either supra-periosteal or sub-periosteal. Briefly, there could be two different clinical scenarios, first the buccal surface of the implant covered with bone or a biomaterial which means the soft tissue component includes the periosteum and the second scenario might be the lack of bone at the buccal surface of the implant which might be interpreted as insufficient bone support or unsuccessful guided bone regeneration. It is important to note that when there is bone dehiscence around the implant as presented second clinical scenario peri-implant recipient site might serve as "avascular implant

Fig. 18.6 Factors influencing the success of soft tissue volume augmentation. (*Figure courtesy of Kerem Odabaşı*)
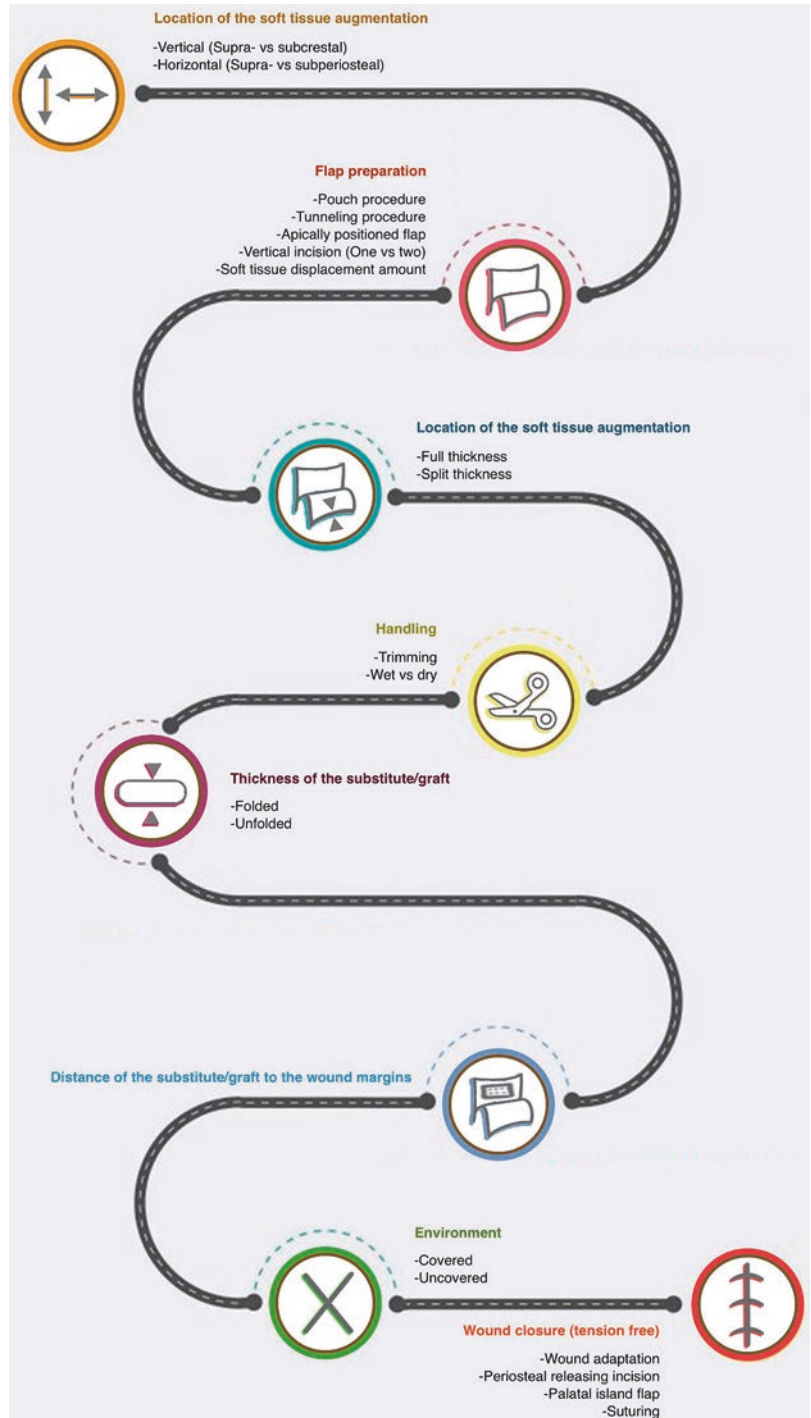
surface". In this situation, avascular implant surface area should be assessed and included in baseline site characteristics. In vertical soft tissue augmentation, soft tissue/substitute might be placed supra-crestal or sub-crestally. Sub-crestal placement of the soft tissue/substitute would be advantageous by its favorable vascular supply originating from the bone compared to its supra

placement. It is known that peri-implant tissues have lesser blood supply compared to the tissues surrounding the natural teeth. Therefore, the involvement of the periosteum and bone in the recipient site positively influences the vascular characteristics of the area. The second and third factors are the flap thickness and its preparation modality. Buccal pouch, tunneling, and apically positioned flap with or without realizing incision could be performed while preparing the recipient site. The decision should be given according to the presence/absence and dimension of keratinized mucosa which in turn affects the extension of soft tissue displacement. During the recipient site preparation split or full thickness flap elevation can be intended

The choice of flap preparation would further have attributed to the vascular supply of the recipient site. Basically, the full-thickness flap on top of the ridge and the lingual side and split-thickness flap leaving a limited amount of tissue at the recipient site is beneficial in maintaining a relatively thick soft tissue flap. This approach may provide the site with a sufficient vascular supply which is a preventive measure to avoid soft tissue dehiscence at the recipient site.

The fourth factor is related to the handling of the material. Trimming of a substitute/graft has mostly been preferred by the clinician to match the size of the tested material to the control material or to the recipient site. The application modality of a material either wet or dry should be decided according to the features of a material. This factor then will have an influence on the fifth factor which determines the thickness of the substitute/graft. Soft tissue graft can be placed in one layer (non-folded) or folded (fold into half) and the decision should be given according to the needs of the recipient site. But it should be kept in mind that thick substitutes (e.g., 2–3 mm) may initiate wound dehiscence due to the unpredictable post-operative swelling. The sixth factor is related to the distance of the substitute/graft to the wound margins ($\approx$1–1.5 mm is recommended) to avoid undesired wound dehiscence. The seventh factor influences the healing modality of the graft/substitute. Soft tissue could be covered by a flap or left uncovered. According to the material characteristics epithelial invagination and loss of soft tissue volume should be anticipated when the material is left uncovered. The last important factor is the mobilization of the mucosal flap in a tension-free manner by placement of muco-periostal-releasing incisions to provide close wound adaptation. A palatal island flap could also be preferable to allow tension-free closure. Correct and stable positioning of the soft tissue graft/substitute can be achieved by the selection of the correct suturing technique. It is recommended to place a horizontal matrix suture together with a single interrupted suture.

In a nutshell, it is desirable to plan the research protocol accounting for the conditions of the recipient site and in accordance with material characteristics.

18.3.4   Clinically Relevant Emerging Endpoints

Investigation of the materials for possible replacement of autogenous grafts goes back to the studies performed by Wainwright in 1995 [52]. So far, several prototypes have been tested and among them histologically evaluated soft tissue substitutes were acellular dermal matrix graft (ADMG), collagen matrices (CM), human fibroblast-derived dermal substitute (HF-DDS), and human skin equivalents (bilayered cell therapy). Autogenous SCTGs are still considered to be the gold standard because of their less shrinkage rates over time [53]. Also, most importantly when the autogenous graft is well adapted to the recipient site and the flap is well adapted above the graft and the healing process imposes the absence of hematoma at the graft-recipient site and graft-flap interface the outcome will be predicted as successful if finally, the elimination of the micro-movement in augmented tissue and flap was achieved. These rules are also valid for the tested biomaterials in the field of soft tissue regeneration to reach the gold standard. Future research should cover the following endpoints.

- Evaluation of volume changes in different time points allows clinicians to determine histological and volumetric changes over time.
- The follow-up period should be extended according to the required/predicted/anticipated period the complete maturation of the graft/substitute will last for.
- The extended follow-up protocol which covers the implant loading period may enable for monitoring the soft tissue response to the load, strain, and pressure.
- The long-term (up to 12 months) assessment of postoperative shrinkage in terms of substitute composition is emerging.
- The recipient site conditions should be standardized in terms of baseline defect characteristics, i.e. clearly either including or excluding the hard tissue deficiency. The presence of a bone deficiency determines the recipient site constitution bringing the substitute into direct contact with an implant surface.
- The size of the graft or material used in the control group should be standardized and matched in size to the tested material. Harvesting a standardized dimension of the autogenous graft should be possible by using a soft tissue punch with varying dimension ranges [54]. The same soft tissue punch could be also used to trim a substitute for standardized dimension. By following this proposal, dimensional variations of graft/substitutes originating from differences in their thickness can be avoided.
- It appears important to discriminate the localization of the augmented graft which either is placed buccal side of the implant (horizontal component) or on top of the implant extending over the occlusal side of the crest (horizontal and vertical component). This point is crucial while formulating the clinical question and focusing the research protocol on exactly the question raised by the investigator.
- The investigation of the real amount of connective tissue after grafting is emerging. Because the increase in thickness could not be attributed solely to the increase in soft tissue components but also to hard tissue components by new bone formation.

According to today's evidence, data on soft tissue devices for similar indications are limited to pre-clinical data [55] and yet not widely used for volume increase around dental implants. Recently, a randomized controlled clinical trial has been conducted to compare volume-stable collagen matrix with autogenous SCTG after peri-implant soft tissue augmentation but the outcomes were unfortunately followed up to 3 months only [56].

18.3.5 Future Perspectives

Future pre-clinical studies should be adequately powered and consider valid primary outcome assessments that are relevant for clinical situations (e.g. use of non-histological surrogate measures that can be measured clinically) [57]. Animal models should be selected according to the study design and clear/targeted/refined endpoints should be chosen before the initiation of the study.

Comparison of the findings from different settings with similarly focused clinical questions and later conveying the best established basic soft tissue model to the clinical setting is emerging. The rationale to have a basic model which has a standard gingival defect is to minimize bone regeneration in deficient sites because of tooth extraction and allow volume changes mainly through augmented soft tissue.

Although the innovation is ongoing in ex vivo models, still pre-clinical testing for new materials is needed in biomedical science before testing them clinically. Therefore, the key question of any pre-clinical animal study must include the most possible way to transfer the pre-clinical results to the human circumstances. There is still a need to find the most reliable, objective, and reproducible method to measure soft tissue thickness in both two- and three-dimensional. Because the understanding of the peri-implant mucosa in a dimensional manner may guide clinicians to predict critical physiological requirements and aesthetic demands of the restoration [58]. It is forthcoming that with the aid of emerging technologies techniques used for evaluating and com-

paring the soft tissue augmentation outcomes will develop in order to meet valid and predictable measure goals.

References

1. Schneider D, Grunder U, Ender A, Hämmerle CH, Jung RE. Volume gain and stability of peri-implant tissue following bone and soft tissue augmentation: 1-year results from a prospective cohort study. Clin Oral Implants Res. 2011;22:28–37.

2. Ten Cate AR. Oral histology: development, structure, and function. 5th ed. St. Louis: Mosby, Inc.; 1998.

3. Dahlin C, Linde A, Gottlow J, Nyman S. Healing of bone defects by guided tissue regeneration. Plast Reconstr Surg. 1988;81(5):672–6.

4. Schmid J, Hammerle CH, Fluckiger L, Winkler JR, Olah AJ, Gogolewski S, et al. Blood-filled spaces with and without filler materials in guided bone regeneration. A comparative experimental study in the rabbit using bioresorbable membranes. Clin Oral Implants Res. 1997;8(2):75–81.

5. Lossdorfer S, Gotz W, Jager A. Immunohistochemical localization of receptor activator of nuclear factor kappaB (RANK) and its ligand (RANKL) in human deciduous teeth. Calcif Tissue Int. 2002;71(1):45–52.

6. Martin TJ. Bone biology and anabolic therapies for bone: current status and future prospects. J Bone Metab. 2014;21(1):8–20.

7. Rothamel D, Schwarz F, Sager M, Herten M, Sculean A, Becker J. Biodegradation of differently cross-linked collagen membranes: an experimental study in the rat. Clin Oral Implants Res. 2005;16(3):369–78.

8. Rothamel D, Benner M, Fienitz T, Happe A, Kreppel M, Nickenig HJ, et al. Biodegradation pattern and tissue integration of native and cross-linked porcine collagen soft tissue augmentation matrices - an experimental study in the rat. Head Face Med. 2014;10:10.

9. Elgali I, Omar O, Dahlin C, Thomsen P. Guided bone regeneration: materials and biological mechanisms revisited. Eur J Oral Sci. 2017;125(5):315–37.

10. Friedmann A, Gissel K, Konermann A, Gotz W. Tissue reactions after simultaneous alveolar ridge augmentation with biphasic calcium phosphate and implant insertion--histological and immunohistochemical evaluation in humans. Clin Oral Investig. 2015;19(7):1595–603.

11. von See C, Gellrich NC, Bormann KH, Rahmann A, Rucker M. Microvascular response to the subperiosteal implantation of self-inflating hydrogel expanders. Int J Oral Maxillofac Implants. 2010;25(5):979–84.

12. von See C, Gellrich NC, Jachmann U, Laschke MW, Bormann KH, Rucker M. Bone augmentation after soft-tissue expansion using hydrogel expanders: effects on microcirculation and osseointegration. Clin Oral Implants Res. 2010;21(8):842–7.

13. Kaner D, Zhao H, Arnold W, Terheyden H, Friedmann A. Pre-augmentation soft tissue expansion improves scaffold-based vertical bone regeneration - a randomized study in dogs. Clin Oral Implants Res. 2016;28:640.

14. Kaner D, Zhao H, Terheyden H, Friedmann A. Submucosal implantation of soft tissue expanders does not affect microcirculation. Clin Oral Implants Res. 2014;25(7):867–70.

15. Kaner D, Zhao H, Terheyden H, Friedmann A. Improvement of microcirculation and wound healing in vertical ridge augmentation after pretreatment with self-inflating soft tissue expanders - a randomized study in dogs. Clin Oral Implants Res. 2015;26(6):720–4.

16. Friedmann A, Friedmann A, Grize L, Obrecht M, Dard M. Convergent methods assessing bone growth in an experimental model at dental implants in the minipig. Ann Anat. 2014;196(2–3):100–7.

17. Elgali I, Turri A, Xia W, Norlindh B, Johansson A, Dahlin C, et al. Guided bone regeneration using resorbable membrane and different bone substitutes: early histological and molecular events. Acta Biomater. 2016;29:409–23.

18. Saulacic N, Fujioka-Kobayashi M, Kobayashi E, Schaller B, Miron RJ. Guided bone regeneration with recombinant human bone morphogenetic protein 9 loaded on either deproteinized bovine bone mineral or a collagen barrier membrane. Clin Implant Dent Relat Res. 2017;19(4):600–7.

19. Friedmann A, Dehnhardt J, Kleber BM, Bernimoulin JP. Cytobiocompatibility of collagen and ePTFE membranes on osteoblast-like cells in vitro. J Biomed Mater Res A. 2008;86(4):935–41.

20. Omar O, Dahlin A, Gasser A, Dahlin C. Tissue dynamics and regenerative outcome in two resorbable non-cross-linked collagen membranes for guided bone regeneration: a preclinical molecular and histological study in vivo. Clin Oral Implants Res. 2018;29(1):7–19.

21. Zohar R, Nemcovsky CE, Kebudi E, Artzi Z, Tal H, Moses O. Tetracycline impregnation delays collagen membrane degradation in vivo. J Periodontol. 2004;75(8):1096–101.

22. Eliezer M, Nemcovsky C, Romanos G, Kozlovsky A, Tal H, Kolerman R, et al. Opposing effects of diabetes and tetracycline on the degradation of collagen membranes in rats. J Periodontol. 2013;84(4):529–34.

23. Airenne KJ, Laitinen OH, Alenius H, Mikkola J, Kalkkinen N, Arif SA, et al. Avidin is a promising tag for fusion proteins produced in baculovirus-infected insect cells. Protein Expr Purif. 1999;17(1):139–45.

24. Moses O, Eliezer M, Nemcovsky C, Tal H, Weinreb M. Accelerated degradation of collagen membranes in diabetic rats is associated with increased infiltration

of macrophages and blood vessels. Clin Oral Investig. 2016;20(7):1589–96.

25. Turri A, Elgali I, Vazirisani F, Johansson A, Emanuelsson L, Dahlin C, et al. Guided bone regeneration is promoted by the molecular events in the membrane compartment. Biomaterials. 2016;84:167–83.

26. Wang Y, Papagerakis S, Faulk D, Badylak SF, Zhao Y, Ge L, et al. Extracellular matrix membrane induces cementoblastic/osteogenic properties of human periodontal ligament stem cells. Front Physiol. 2018;9:942.

27. Smeets R, Knabe C, Kolk A, Rheinnecker M, Grobe A, Heiland M, et al. Novel silk protein barrier membranes for guided bone regeneration. J Biomed Mater Res B Appl Biomater. 2017;105(8):2603–11.

28. Retzepi M, Calciolari E, Wall I, Lewis MP, Donos N. The effect of experimental diabetes and glycaemic control on guided bone regeneration: histology and gene expression analyses. Clin Oral Implants Res. 2018;29(2):139–54.

29. Mardas N, Busetti J, de Figueiredo JA, Mezzomo LA, Scarparo RK, Donos N. Guided bone regeneration in osteoporotic conditions following treatment with zoledronic acid. Clin Oral Implants Res. 2017;28(3):362–71.

30. Kaner D, Soudan M, Zhao H, Gassmann G, Schonhauser A, Friedmann A. Early healing events after periodontal surgery: observations on soft tissue healing, microcirculation, and wound fluid cytokine levels. Int J Mol Sci. 2017;18(2).

31. Donos N, Dereka X, Calciolari E. The use of bioactive factors to enhance bone regeneration: a narrative review. J Clin Periodontol. 2019;46(Suppl 21):124–61.

32. Calciolari E, Donos N. The use of omics profiling to improve outcomes of bone regeneration and osseointegration. How far are we from personalized medicine in dentistry? J Proteome. 2018;188:85–96.

33. Batas L, Stavropoulos A, Papadimitriou S, Nyengaard JR, Konstantinidis A. Evaluation of autogenous PRGF+beta-TCP with or without a collagen membrane on bone formation and implant osseointegration in large size bone defects. A preclinical in vivo study. Clin Oral Implants Res. 2016;27(8):981–7.

34. Behnia H, Khojasteh A, Kiani MT, Khoshzaban A, Mashhadi Abbas F, Bashtar M, et al. Bone regeneration with a combination of nanocrystalline hydroxyapatite silica gel, platelet-rich growth factor, and mesenchymal stem cells: a histologic study in rabbit calvaria. Oral Surg Oral Med Oral Pathol Oral Radiol. 2013;115(2):e7–15.

35. Sanz M, Dahlin C, Apatzidou D, Artzi Z, Bozic D, Calciolari E, et al. Biomaterials and regenerative technologies used in bone regeneration in the craniomaxillofacial region: consensus report of group 2 of the 15th European workshop on periodontology on bone regeneration. J Clin Periodontol. 2019;46(Suppl 21):82–91.

36. Akyildiz S, Soluk-Tekkesin M, Keskin-Yalcin B, Unsal G, Ozel Yildiz S, Ozcan I, et al. Acceleration of fracture healing in experimental model: platelet-rich fibrin or hyaluronic acid? J Craniofac Surg. 2018;29(7):1794–8.

37. Eliezer M, Sculean A, Miron RJ, Nemcovsky C, Weinberg E, Weinreb M, et al. Hyaluronic acid slows down collagen membrane degradation in uncontrolled diabetic rats. J Periodontal Res. 2019;54:644.

38. Sanchez-Rojas L, Gomez-Pinedo U, Benito-Martin MS, Leon-Espinosa G, Rascon-Ramirez F, Lendinez C, et al. Biohybrids of scaffolding hyaluronic acid biomaterials plus adipose stem cells home local neural stem and endothelial cells: implications for reconstruction of brain lesions after stroke. J Biomed Mater Res B Appl Biomater. 2019;107(5):1598–606.

39. Roldan JC, Jepsen S, Schmidt C, Knuppel H, Rueger DC, Acil Y, et al. Sinus floor augmentation with simultaneous placement of dental implants in the presence of platelet-rich plasma or recombinant human bone morphogenetic protein-7. Clin Oral Implants Res. 2004;15(6):716–23.

40. Bosshardt DD, Lang NP. The junctional epithelium: from health to disease. J Dent Res. 2005;84:9–20.

41. Mathes SH, et al. A bioreactor test system to mimic the biological and mechanical environment of oral soft tissues and to evaluate substitutes for connective tissue grafts. Biotechnol Bioeng. 2010;107:1029–39.

42. Jung RE, Hürzeler MB, Thoma DS, Khraisat A, Hämmerle CHF. Local tolerance and efficiency of two prototype collagen matrices to increase the width of keratinized tissue. J Clin Periodontol. 2011;38:173–9.

43. Naenni N, Bienz SP, Benic GI, Jung RE, Hämmerle CHF, Thoma DS. Volumetric and linear changes at dental implants following grafting with volume-stable three-dimensional collagen matrices or autogenous connective tissue grafts: 6-month data. Clin Oral Investig. 2017;22:1185. https://doi.org/10.1007/s00784-017-2210-3.

44. Schmitt CM, Matta RE, Moest T, Humann J, Gammel L, Neukam FW, Schlegel KA. Soft tissue volume alterations after connective tissue grafting at teeth: the subepithelial autologous connective tissue graft versus a porcine collagen matrix – a pre-clinical volumetric analysis. J Clin Periodontol. 2016;43:609–17.

45. Bengazi F, Lang NP, Caroprese M, Urbizo Velez J, Favero V, Botticelli D. Dimensional changes in soft tissues around dental implants following free gingival grafting: an experimental study in dogs. Clin Oral Implants Res. 2015;26:176–82.

46. Thoma DS, Jung RE, Schneider D, Cochran DL, Ender A, Jones AA, Görlach C, Uebersax L, Graf-Hausner U, Hämmerle CHF. Soft tissue volume augmentation by the use of collagen-based matrices: a volumetric analysis. J Clin Peridontol. 2010;37:659–66.

47. Thoma DS, Hämmerle CHF, Cochran DL, Jones AA, Görlach C, Uebersax L, Mathes S, Graf-Hausner U, Jung RE. Soft tissue volume augmentation by the use of collagen-based matrices in the dog mandible – a histological analysis. J Clin Peridontol. 2011;38:1063–70.

48. Thoma DS, Naenni N, Benic GI, Hämmerle CHF, Jung RE. Soft tissue volume augmentation at dental implant sites using a volume stable three-dimensional collagen matrix – histological outcomes of a preclinical study. J Clin Periodontol. 2017;44:185–94.

49. Vignoletti F, Nunez J, de Sanctis F, Lopez M, Caffesse R, Sanz M. Healing of a xenogeneic collagen matrix for keratinized tissue augmentation. Clin Oral Implants Res. 2015;26:545–52.

50. Vignoletti F, Nunez J, Sanz M. Soft tissue regeneration in the oral cavity: review of the current literature on scaffolds, cells and biologicals. J Clin Periodontol. 2014;41:23–35.

51. Vignoletti F, Abrahamsson I. Quality of reporting of experimental research in implant dentistry. Critical aspects in design, outcome assessment and model validation. J Clin Periodontol. 2012;39:6–27.

52. Wainwright DJ. Use of an acellular allograft dermal matrix (AlloDerm) in the management of full-thickness burns. Burns. 1995;21:243–8.

53. Akcalı A, Schneider D, Ünlü F, Bıcakcı N, Köse T, Hämmerle CH. Soft tissue augmentation of ridge defects in the maxillary anterior area using two different methods: a randomized controlled clinical trial. Clin Oral Implants Res. 2015;26:688–95.

54. Nizam N, Akcalı A. A novel connective tissue graft harvesting technique: the ring method. Int J Periodontics Restor Dent. 2018;39:422. https://doi.org/10.11607/prd.2736.

55. Thoma DS, Buranawat B, Hämmerle CH, Held U, Jung RE. Efficacy of soft tissue augmentation around dental implants and in partially edentulous areas: a systematic review. J Clin Periodontol. 2014;41:77–91.

56. Zeltner M, Jung RE, Hämmerle CHF, Hüsler J, Thoma DS. Randomized controlled clinical study comparing a volume-stable collagen matrix to autogenous connective tissue grafts for soft tissue augmentation at implant sites: linear volumetric soft tissue changes up to 3 months. J Clin Periodontol. 2017;44:446–53.

57. Kilkenny C, Browne W, Cuthill IC, Emerson M, Altman DG, NC3Rs Reporting Guidelines Working Group. Animal research: reporting in vivo experiments: the ARRIVE guidelines. Br J Pharmacol. 2010;160(7):1577–9.

58. Akcalı A, Trullenque-Eriksson A, Sun C, Petrie A, Nibali L, Donos N. What is the effect of soft tissue thickness on crestal bone loss around dental implants? A systematic review. Clin Oral Implants Res. 2017;28:1046–53.

Biomarkers for Implant Dentistry Studies

19

Troy McGowan, Pingping Han, and Sašo Ivanovski

19.1 Importance of Monitoring the Peri-implant Health

Modern implant therapy is a predictable treatment modality with high survival rates reported in the long term [1]. However, survival rates are no longer considered the gold-standard measure of implant outcomes, and implant success, defined as the absence of technical and biological complications, is more clinically relevant in contemporary clinical practice. Reported success rates are much lower than the figures quoted for implant survival [2] and peri-implant disease is a significant contributor to the discrepancy between these two outcome measures. Peri-implant mucositis and peri-implantitis are the two most common peri-implant diseases. Peri-implant mucositis is defined as Inflammation in the absence of progressive hard and soft tissue loss, and when the host immune response becomes dysregulated to the point that progressive hard and soft tissue destruction is clinically evident, a diagnosis of peri-implantitis can be made. The prevalence of peri-implant mucositis is reported to be between 19–65%, while figures of 0–47% have been reported for peri-implantitis [3]. Studies investigating the treatment of peri-implantitis report a wide range of clinical outcomes and a recent systematic review concluded that there is currently insufficient evidence to support one treatment modality over another [4]. The difficulty in predictably achieving favorable clinical outcomes when treating peri-implant diseases highlights a need for regular assessment of peri-implant health in order to prevent or reduce disease occurrence. The importance of clinical monitoring and accurate diagnostic markers becomes even more important when one considers that the infectious etiology of peri-implantitis is not the only way bone can be lost from around a loaded implant. Marginal bone loss has been reported around implants due to deep implant placement [5], the presence of a micro gap [6], inadequate surrounding bone [7], poor surgical technique, subgingival cement [8], macro and micro design features [9], foreign body reaction and adverse interfacial strain [10]. When monitoring implant health clinically, the presence of a deep pocket or marginal bone loss does not automatically equate with a diagnosis of peri-implantitis. Other diagnostic methods are required to ensure that the correct etiology for the bone loss is determined, in order to allow for the correct clinical management to be implemented.

T. McGowan
School of Dentistry, University of Queensland, Herston, QLD, Australia
e-mail: t.mcgowan@uq.edu.au

P. Han · S. Ivanovski (✉)
School of Dentistry, Centre for Orofacial Regeneration, Reconstruction and Rehabilitation (COR3), University of Queensland, Herston, QLD, Australia
e-mail: p.han@uq.edu.au; s.ivanovski@uq.edu.au

It has been shown that ongoing maintenance is able to significantly reduce the incidence of peri-implant disease [11], and although compliance rates are higher in implant patients than those with periodontitis [12], the literature is still reporting an increasing burden of peri-implant disease [3]. Low-cost, sensitive, specific, and easy-to-use diagnostic markers will be of the utmost importance for monitoring peri-implant health and in preventing peri-implant disease in an age where dental implants as a treatment modality are experiencing a meteoric rise in popularity. It is in this area that biomarkers of disease initiation, progression, and regression will have a critical role in the ongoing maintenance of osseo-integrated implants.

19.2   Looking Behind: Clinical Diagnostic Tools

The soft and hard tissues surrounding an osseointegrated implant have been described as "scar tissue resulting from healing after a surgical procedure" [13]. In the majority of cases, there are no inserting (perpendicular) collagen fibers, the vascularity of the tissue in the immediate vicinity of the implant surface is reduced when compared to teeth [14], and the bacteria are in close proximity to the connective tissue without the presence of an epithelial barrier [15]. For these reasons, traditional clinical markers of assessing the health of the gingiva, such as pocket depth and bleeding on probing, may not be as accurate in the diagnosis of peri-implant disease.

Currently, assessment of peri-implant health is accomplished through the use of a periodontal probe and consecutive radiographs, which allow assessment of the soft tissues and marginal bone heights over a defined time period. Around healthy implants, it has been shown that the periodontal probe will penetrate deeper (come to rest closer to the alveolar crest) than around a healthy tooth [16]. This discrepancy is greater in the presence of inflammation [17, 18]. Angulation has also been shown to affect the accuracy of probing around implants. This is especially the case in the presence of the prosthetic superstructure. Serino

et al. [19] showed that when diseased implants were probed with and without the prosthesis present, only 37% of measurements remained consistent. In the majority of cases, there was over or underestimation of the actual depth of the peri-implant sulcus. The authors did report that when an implant is probed upon removal of the superstructure, the pocket depth recorded was an accurate reflection of the bone loss experienced. Lang et al. [17] concluded that although the probe penetrated deeper into inflamed peri-implant tissues compared to health, probing was an accurate technique to assess the status of the peri-implant mucosa. With regards to bleeding on probing as a diagnostic tool, the literature is less clear. Jepsen [20] and Luterbacher et al. [21] stated that bleeding on probing was a reliable indicator of disease although these studies both had some shortcomings. Jepsen et al. [20] did not use radiographs to confirm peri-implantitis diagnosis and Luterbacher et al. [21] did not outline the number of healthy sites that also experienced bleeding on probing. Ericsson and Lindhe [16] evaluated bleeding on probing around implants in a dog model and concluded that almost all healthy implant sites bled. When this is combined with the knowledge that the probe penetrates further into the tissues around an implant, bleeding on probing could be seen as a less reliable indicator of inflammation around implants. This point would seem to be reinforced by treatment studies that evaluate the stability of the marginal bone after treatment. It has been shown that, although marginal bone levels remain constant for as long as 7 years post-treatment, if bleeding on probing is included in the success criteria the percentage of sites deemed to be successful is much lower [22].

Further to the shortcomings highlighted above, traditional forms of diagnosis suffer from an inability to detect disease prior to its occurrence and from being unable to quantify the severity of the disease or the response to treatment. Radiographic bone loss, pocket depth, and bleeding on probing are all linear measures of past or present disease and have very little clinical utility in determining future outcomes. Given that peri-implantitis has been shown to have a

spontaneous [23] and accelerated disease progression [24], and is more difficult to predictably achieve conventional clinical success regardless of the treatment modality employed, the importance of a useful diagnostic test prior to the establishment of disease is emphasized.

Notably, epidemiological, retrospective, and interventional studies evaluating peri-implant diseases all suffer from a lack of case definition, with some authors defining peri-implantitis as bone loss beyond that which is expected by physiological remodeling [25] while others, recognizing the limitation of current diagnostic tools, use the cutoff of ≥ 2 mm of bone loss from the expected bone crest [26]. This lack of consensus highlights the difficulty of traditional clinical diagnosis in determining the presence and severity of peri-implant disease and highlights a need for the exploration of alternative methods for the assessment of peri-implant tissue status.

Currently explored alternative methods of diagnosis include the evaluation of biomolecules or biomarkers present in the peri-implant sulcular fluid and saliva, which represent both local and systemic markers of disease [27]. These biomarkers can arise from a number of pathways in the pathogenic process of peri-implant diseases, such as the microbiota of the diseased or healthy site, the inflammatory process initiated in response to microbiota, or the destruction of the tissues caused by the immunoinflammatory lesion. In the literature biomarkers have been further separated into their "omics" constituents; microbiome, proteome, metabolome, transcriptome, exosome, genome, and epigenome (Table 19.1) accentuating the diversity of molecules that can potentially be examined for diagnostic applications. It is accepted that the probability of a single biomarker being both sensitive and specific enough to be used as a sole marker of disease is very low, and it is most likely that a combination of markers tested concurrently will provide a diagnostic test with the required fidelity. Also, although systemic markers of inflammation (such as C-reactive protein) have been used in the study of periodontitis, due to the localized rather than generalized nature of peri-implant disease, it is very unlikely that biomarkers extracted and analyzed from serum will provide any useful indication of disease initiation or progression, and therefore the majority of the focus from a scientific and clinical perspective has been on the oral biofluids of saliva and peri-implant crevicular fluid (PICF).

19.2.1 Saliva

Saliva is a biofluid that contains a multitude of biomolecules, both human and other species (i.e., bacteria, fungus, and virus [28]) and has been described as a "mirror" for both oral and systemic health [29]. It is composed of secretions from the parotid, submandibular, and sublingual major salivary glands as well as minor salivary glands and transudates from the oral mucosa, oropharynx, lingual and palatine tonsils, and the gingival/peri-implant fluid. Saliva harbors host-response and microbial molecules as potential biomarkers for peri-implantitis, including tissue breakdown products, SARS-CoV-2 virus [30, 31], inflammatory cytokines, leucocytes, genetic materials, circular RNA [32], extracellular vesicles [33–37] and proteins. The method of collection can therefore have a profound effect on the composition of the sampled saliva and unless harvested via cannulation of a specific duct can be expected to contain a variety of secretions and should be referred to as a whole mouth fluid [38, 39]. Saliva is simple, cheap, and easy to collect, and is, therefore, a highly desirable body fluid for the examination of biomarkers for use in a clinical context [40, 41]. Salivaomics was the term proposed in 2008 to describe the study of the "omics" constituents of saliva [42] and since then research has begun to explore the various molecules present (Table 19.2) [40, 43]. Validated tests using salivary diagnostics for the detection of certain forms of pancreatic, oral, breast cancer, and COVID-19 pandemics [28] have been reported highlighting the clinical potential of saliva as a diagnostic tool [40].

There are some limitations to using saliva that need to be considered when investigating its potential as a diagnostic tool. Firstly, saliva samples are taken distal to the disease site (compared

Table 19.1 Overview of potential areas of exploration regarding biomarkers in oral fluids

	Description	Testing methods
Epigenome	Epigenetics describes changes in gene expression that are not directly coded into a gene's DNA sequence and are usually a result of environmental changes resulting in DNA methylation or histone modification or non-coding RNAs [44]	• Methylation-specific PCR + pyrosequencing • Methylated DNA immunoprecipitation NGS • Genome-wide bisulfite sequencing • Microarray Chromatin ImmunoPrecipitation (ChIP) of histone
Exosome or small extracellular vesicles	Studies exosomes - nanoparticles (30–200 nm) secreted by various cells into the extracellular environment that is thought to act by transporting lipids, proteins, and other molecules to cells, where they affect changes in function and physiology [40]	• Ultra-filtration • Ultracentrifuge • Polymer-based precipitation • Immunological separation • Size- exclusion chromatography
Genome	Genome studies usually fall into one of two general types: Genome-wide association studies (GWAS) where the whole genome is investigated to determine if there are any genetic loci associated with the disease phenotype of interest and candidate genome association studies, where gene selection is done a priori and allele frequency is compared in cases and controls	• Sanger sequencing • Nanopore DNA sequencing • Sequencing by synthesis (Illumina) • Pyrosequencing (454) • Genome amplification and genotyping • PCR-RFLP
Metabolome	Evaluates endogenous and exogenous metabolites, potentially providing data on physiological and disease status	• Liquid chromatography-mass spectrometry • Raman spectroscopy • Capillary electrophoresis • Time of flight mass spectrometry
Microbiome	There are more than 700 bacteria in the oral cavity, 32% of which are uncultivatable [46]. With the completion of the Human Oral Microbiome Database (HOMD), high throughput techniques can now be used to determine the resident microflora in both health and disease	• 16S rRNA sequencing • Shotgun metagenomics sequencing • Light microscopy • Culture studies • DNA-DNA hybridisation • ELISA • Pyrosequencing • PCR
Proteome	Saliva has been shown to contain more than 2000 proteins which are thought to function in health to maintain homeostasis, and in disease to perpetuate/reduce or resolve inflammation. It has however been shown that proteins in saliva are degraded rapidly when compared to those in the serum [45] and therefore specialized techniques must be used during the collection of oral fluids for the use of proteome analysis.	• Liquid chromatography-mass spectrometry • ELISA • SDS-PAGE • Multiplex protein array • Flow cytometry • Cytokine array
Transcriptome	The transcriptome consists of RNA molecules (both micro and messenger) which are involved in a number of important biological processes both in health and disease. Recent data suggests that there are more than 3000 different mRNAs and 300 microRNAs present in saliva [40]	• RNA-sequencing • Microarray • RT-PCR

Table 19.2 Candidate biomarkers for the study of peri-implantitis reported by the literature

Pro-inflammatory cytokines	• IL-1β, IL-4, IL-6, IL-10, IL-12, IL-17, TNF-α
Anti-inflammatory cytokines	• IL-4, IL-10, IL1 receptor antagonist, IL-13
Chemokines	• IL-8, macrophage-derived chemoattractant, eotaxin, monocyte chemoattractant protein3, macrophage inflammatory protein 1
Growth factors	• VEGF, FGF-2, PDGF-BB, GM-CSF and FMs-like tyrosine kinase-3 ligand
Modulators of the immune response	• Soluble human CD40 ligand, IL-17, IL-12p40, IL-12p70, IL-2 and IL-15
Enzymes responsible for tissue degradation	• MMP-1, MMP-3, MMP-8, MMP-13, elastase, alkaline phosphatase, receptor activator of nuclear factor kappa-B ligand (RANKL), cathepsin-K
Other molecules	• C-telopeptide, α2-macroglobulin, osteocalcin, deoxypyridinoline, myeloperoxidase, nitrite, osteoprotegerin, sclerostin

to PISF which is proximal) and therefore have no relevance at the site level providing information only at the patient level. Resting saliva volume varies significantly among subjects, and secretion and composition can be affected by a variety of factors including diet and oral hygiene. Finally, although saliva is a reservoir of gingival or peri-implant sulcular fluid allowing easy collection of a sample of these fluids and their analytes, there is significant dilution (~1000 times diluted compared to blood) that occurs requiring the use of highly sensitive arrays [47].

19.2.1.1 Saliva Collection Methods, Preparation for Analysis

The whole saliva can be collected unstimulated or stimulated [48]. The collection of unstimulated whole saliva is preferred diagnostically since stimulated saliva is frequently more dilute which makes detection of biomarkers more difficult. Unstimulated saliva is however affected by numerous factors, such as the degree of hydration, body posture, the position of the head during collection, drug, and circadian rhythm [49].

Stimulated saliva can be obtained through either masticatory (paraffin wax, unflavoured chewing gum base, rubber bands, and cotton puff) or gustatory (citric acid and sour candy drops) stimulation. Stimulated saliva represents the secretion during food intake (in the mouth for up to 2 h), and is affected by various factors, such as gland size, food intake, gag reflex, and stimulation method [50]. Based on these merits and drawbacks, unstimulated whole saliva offers an accurate method for the analysis of salivary gland status, while stimulated saliva is useful for the study of the functional reserve [51].

Guidelines for Collection of Saliva
- Avoid high sugar/acidity, or high-caffeine foods immediately before sample collection, since they might compromise the assay by lowering saliva pH and increasing bacterial growth [52].
- The collection is preferably done between 8 to 11 am (if possible). The participant should preferably not eat a major meal or drink 1 h prior to saliva collection.
- Teeth cannot be brushed 45 min prior to sample collection.
- Rinse mouth with water to remove food debris and wait for at least 10 min after rinsing to avoid dilution of the collected sample.
- If visibly contaminated with blood, the sample should be discarded.
- The participants should avoid smoking for at least 2 h prior to collection.

Methods for Collection of the Whole Saliva
The methods available presently for the collection of the whole saliva include spitting, draining, suction, and swab methods [48, 53].

- *Spitting method*: The participant spits out into a sterile falcon tube and is encouraged to place the tube on ice while collecting more saliva. This method collects approximately 5 mL volume.
- *Draining method*: The participant sits quietly with the head bent down and allows passive saliva collection from the lower lip into a sterile falcon tube.

- *Suction method*: Saliva is allowed to accumulate in the mouth and then is collected via continuous aspiration using micropipettes, syringes, and an aspirator or saliva ejector.
- *Swabbing method*: The participant is asked to chew a synthetic gauze sponge, pre-weighed swab, or cotton pad into the mouth. Saliva-soaked sponge is removed and placed in a sterile test tube. This method is mainly used in the monitoring of drugs, hormones, or steroids.

Processing and Storage for Downstream Analysis

All the procedures must proceed on ice.

- Place the saliva sample into cryotubes with 500 μL per tube. Each 500 μL sample can be processed for storage according to the expected endpoint analysis (e.g., protein, RNA, or DNA analysis).
- Add the protease inhibitors (1 mM phenyl-methylsulfonyl fluoride) to the sample intended for protein analysis. Add RNase inhibitors (5–10 U) to each sample intended for RNA analysis.
- Store all samples at −80 °C.
- For some protocols that require cell-free supernatant fraction from the whole saliva, vortex the whole saliva and spin the entire sample at 300–2000 g for 15 min at 4 °C. Remove the supernatant and transfer the fractions to a new cryotube. Add the RNase inhibitor or protease inhibitors as described above. Then, store all fractions and the pellet at -80 °C.
- DNA analysis can be obtained from a 500 μL whole saliva sample. Do not discard the pellet if a DNA test is required. DNA is stable at room temperature for up to 5 days, or multiple freeze-thaw cycles, without compromising the quality of DNA [54].

19.2.2 Peri-implant Crevicular Fluid

Peri-implant sulcular fluid is a tissue-derived interstitial fluid in health and an inflammatory exudate in disease. PICF volume has been shown to increase with inflammation and has been suggested as a quantitative marker for peri-implant gingival inflammation [55, 56], and there are studies that report no difference in volume between sites diagnosed with mucositis and peri-implantitis [57]. A number of studies have evaluated the presence and concentration of biomarkers in the PICF and although the general consensus is that some biomarkers are upregulated at diseased compared to healthy sites, the reported data varies significantly [58]. Currently, there is no consensus on the biochemical constituents and their levels/concentrations in PICF in health [59] and more work needs to be done to establish the biochemical milieu and baseline levels of biomarkers in non-diseased sites. The limited flow of PICF and the variability of resting volume also present a problem for researchers. These shortcomings have resulted in a variety of measurements being reported and comparisons between studies are difficult. PICF is also the oral fluid with the lowest protein content [60] which means that assays with high amplified sensitivity and detection limits should be used, instead of commercial kits designed for testing media such as serum with significantly higher protein content.

Javed et al. [61] conducted a systematic review in order to assess the cytokine profile of PICF in patients with peri-implantitis. They concluded that although there is evidence to suggest that the levels of pro-inflammatory cytokines are elevated in the PICF of patients, further study was required to assess the diagnostic utility of biomarkers in the detection of early peri-implant changes.

19.2.2.1   Collection Methods, Preparation for Analysis

Similar to gingival crevicular fluid (GCF), the volume of PICF can be affected by numerous lifestyle factors, including mechanical factors (from chewing coarse foods, and vigorous brushing), smoking status, sex hormones, and circadian periodicity [62]. A variety of methods are available to collect PICF, including gingival washing techniques, microcapillary tubes or micropipettes, and absorption techniques (via absorbent filter paper strips or paper points) [63–65].

Guideline for the Collection of PICF

- PICF should be collected prior to probing, to avoid blood contamination.
- The collection is preferable in the morning, 2–3 h after breakfast.
- The sites to be sampled should be isolated with cotton rolls to avoid saliva contamination.
- Gently air dry the selected sites; supragingival plaque should be removed without touching the marginal gingiva.
- Collect PICF by carefully inserting the chosen collection device into the sulcus/pocket until mild resistance is reached (1–2 mm into the pocket) and hold in place for 30 s.
- Between samples, clean the jaws with an alcohol swab and allow them to dry.
- The PICF volume should be recorded (if possible), as well as whether the samples are analyzed individually or pooled.
- All samples containing blood should be discarded.

Collection Methods

- *Washing technique*: This method involves a device consisting of two injection needles placed one inside the other. During the sampling, the thinner "ejection needle" is at the bottom of the pocket and the "collection needle" is at the mucosal margin. The washing solution (0.9% sodium chloride) is manually ejected into the crevice and immediately drained through the collection needle into a sample tube by continuous suction [66].
- *Microcapillary Technique:* PICF can be obtained by placing a calibrated volumetric or non-calibrated microcapillary pipette at the entrance of the gingival sulcus and gently touching the gingival margin [67].
- *Absorption technique*: This technique is divided into extracrevicular and intracrevicular by using paper strips, or paper points. The first one is performed by placing paper strips over the gingival crevice to reduce trauma. The second method is the intracrevicular technique which is most commonly used and is subdivided into superficial and deep, depending on the depth of strip insertions into the gingival sulcus or periodontal pocket.

Sample Process and Storage

- The collected samples should be placed on ice prior to elution (immediately after collection), at 4 °C overnight into 50–500 μL phosphate-buffered saline (PBS).
- Gently vortex for 15 s and centrifuge the samples at 300–3, 000 g for 5 min at 4 °C; both paper points/strips and supernatant should be kept frozen at −80 °C prior to analysis.
- Add the protease inhibitors (1 mM phenyl-methylsulfonyl fluoride) to the sample intended for protein analysis. Add RNase inhibitors (5–10 U) to each sample intended for RNA analysis.

19.3 Proteins Biomarkers of Peri-implantitis

The anatomy of the PI tissues results in some distinct differences in the histological presentation of the PI lesion when compared to periodontal disease. Lack of epithelial barrier at the apical extension of the inflammatory cell infiltrates around implants [15] potentially results in greater infiltration of bacterial products resulting in a larger inflammatory response. Carcuac et al. [68] showed that the PI lesion is almost twice the size of a comparable periodontal lesion and that the infiltration of plasma cells, macrophages, and lymphocytes is significantly greater than in periodontal lesions. The same authors reported that the vascular density was much higher in the CT zone surrounding the PI lesion compared to the comparable periodontal lesion. They hypothesized that this resulted in a long distance for migrating lymphocytes to travel in order to reach the PI lesion. Despite these anatomical and histological differences, the underlying mechanism of tissue destruction is considered to be similar in both PI and periodontitis, meaning that protein biomarkers of inflammation, epithelial, connective tissue, and bone destruction as well as markers of bone remodeling have all been evaluated in the search for a more accurate and pre-emptive diagnostic test for peri-implant disease. Cytokines, chemokines, and biological mediators have all been shown to play a crucial role in the regulation of homeostasis and pathological states

around implants [57, 69]. Pro-inflammatory cytokines (IL-1β, IL-6, IL-12, IL-17, and TNF-α), anti-inflammatory cytokines (IL-4 and IL-10), osteoclastogenesis-related cytokines (RANKL and OPG), and chemokines (IL-8) are amongst the most studied of the protein biomarkers [70], although there have been a great many more proteins evaluated. For a full list of evaluated biomarkers see Table 19.2.

Recker et al. [59] conducted a study aiming to determine the presence of Il-1α, IL-1β, IL-6, IL-8, Il-10, IL-12, IL-17α, TNF-α, CRP, OPG, leptin, and adiponectin using multiplexed immunofluorescent bead assay in the gingival fluid and PICF at healthy sites. The authors concluded that the levels of measured cytokines were similar, except for IL-17α and TNF-α which were found to have significantly higher concentrations in PICF. Nowzari et al. [71] also found increased concentrations of TNF-α in PICF compared to gingival fluid. A recent systematic review [72] evaluated 18 studies that investigated the use of cytokine levels to distinguish between diseased and healthy sites. Nine studies reported a statistically significant increase in the levels of pro-inflammatory cytokines in the PICF of diseased implants compared to healthy sites, with IL-1β being the cytokine with the most evidence of association. Most studies evaluated by this review found no difference regarding anti-inflammatory cytokines or osteoclastogenesis-related cytokines and only two studies [73, 74] reported on the levels of IL-8, both finding no difference between healthy and diseased sites. The authors concluded that in terms of differentiating diseased and healthy peri-implant sites through the use of biomarkers, there is evidence for increased levels of pro-inflammatory cytokines, whereas there is no evidence to suggest that anti-inflammatory cytokines or chemokines are able to be used in a diagnostic capacity. They concluded that only 8 cytokines (IL-1β, IL-4, IL-6, IL-10, IL-12, IL-17, TNF-α, and RANKL) and one chemokine (IL-8) have been evaluated in comparative studies assessing both healthy and diseased implants. With regards to the biomarkers for bone loss (RANKL, OPG, and sRANKL) there is conflicting evidence, with some studies reporting lower concentrations [75] and others reporting higher concentrations but with no change to the overall ratio [76]. Rakic et al. [60] used more sensitive arrays than Arikan et al. [75] and found that sRANKL and OPG levels (as well as sclerostin) were clearly associated with peri-implantitis.

Enzymes such as matrix metalloproteinases, myeloperoxidase (MPO), cathepsin-K, and elastase have also been investigated as biomarkers of disease initiation and progression. Dursun et al. [77] reported in their systematic review that MMP-1, MMP-3, MMP-8, and MMP-13, as well as their various tissue inhibitors (TIMPs), were most frequently tested and that MMPs could be considered to be positively correlated with clinical inflammatory conditions around integrated implants. Ramseier et al. [78] demonstrated that MMP-1 bound to tissue inhibitor of MMP-1 complex (MMP-1/TIMP-1) correlated inversely with attachment loss at implants, and in the two cases of peri-implantitis included in the study population, MMP-1/TIMP-1 was below detectable concentration, showing a potential benefit to the evaluation of these complexes in future studies. Three studies [79–81] reported significantly higher levels of MPO in the PICF of inflamed peri-implant tissues and one study reported significantly higher amounts of elastase in the PICF of diseased implants [82]. Cathepsin-K has been suggested as a marker of peri-implant mucositis [60] and has been shown to correlate well with clinical markers such as pocket depth, bleeding on probing and plaque scores [83].

Other enzymes and markers of tissue degradation, such as alkaline phosphatase (ALP) and osteocalcin, have also been investigated with conflicting results reported for osteocalcin levels but an association between ALP/OPN/OCN and peri-implantitis reported by two studies [82, 84]. Zani et al. [85] evaluated 20 biomarkers in the PICF of diseased and healthy implants finding that diseased sites had elevated levels of 12/20 of the included analytes. The authors used a best-fit model to determine which combination of investigated markers had the best discriminatory capacity, concluding that IL-17, IL-1 receptor antagonist (IL-1ra), FMs-like tyrosine kinase-3 ligand (Flt-3L), IL-10, soluble human CD40

ligand (sCD40L), granulocyte macrophage colony-stimulating factor (GM-CSF), TNFa, PDGF-BB and IL-15 were present in 13% of the best fit models suggesting that further research into these specific biomarkers may be warranted. 6 analytes greatly increased the diagnostic properties of the model when compared to the analytes alone or in lower numbers, although increasing the number beyond this point resulted in only limited improvement. An interesting finding from this study was that elevated levels of various biomarkers were found at healthy sites of diseased implants suggesting that PICF collected from any point around a diseased implant may contain the markers of peri-implant disease potentially limiting the amount of sampling that is required.

19.4 Microbial Markers of Peri-implantitis

Peri-implantitis is a disease initiated by microorganisms and therefore involves the presence of bacteria as a biofilm which is responsible for the initial inflammatory response. Although the pellicle around teeth and implants varies [86] there seems to be minimal difference in the temporal sequence of colonization. While the majority of older studies have reported a mixed anaerobic infection dominated by gram-negative bacteria, newer studies using more accurate and higher throughput techniques such as pyrosequencing have shown that the microbiota present in peri-implantitis is more complex than that seen around teeth [87, 88] and that a large majority of the bacteria present are currently un-cultivatable. Furthermore, some studies have found high numbers of other microorganisms more commonly associated with extra-oral infections (e.g., *Staphylococcus aureus, Parvimonas micra*) [89, 90]. A recent meta-analysis review [91] showed that *Aggregatibacter actinomycetemcomitans* and *Prevotella intermedia* were detected in peri-implantitis biofilms compared with healthy implants. Another systematic review [92] concluded that the peri-implantitis-associated biofilm was significantly more heterogeneous and

complex when compared to healthy implants or diseased teeth and is comprised of putative periodontal pathogens, uncultivatable asaccharolytic gram-positive rods, anaerobic gram-negative rods and in some cases opportunistic microorganisms such as enteric rods. The authors also stated that there were significant differences between the results obtained from subgingival biofilm methods when compared to entire microbiome sequencing techniques, due to the high proportion of uncultivatable bacterial species present around diseased implants. The clinical ramifications of these findings are currently unknown but these differences may prove to be useful in the establishment of diagnostic techniques using microbial markers for the detection and quantification of disease around dental implants.

Wang et al. [93] examined microbial profiles via qPCR (*Aggregatibacter actinomycetemcomitans*, *Prevotella intermedia*, *Porphyromonas gingivalis*, *Tannerella forsythia*, and *Treponema denticola*) and combined these with the biomarker (Il-1β, VEGF, MMP-8, TIMP-2, and OPG) profile of PICF from healthy peri-implant tissues and those with diagnosed peri-implantitis. The PICF samples were harvested from the same site as the subgingival biofilm in order to establish a correlation between microbial profiles and inflammatory markers and to test the individual and combined diagnostic ability of each biomarker and bacterial species evaluated. The study found that *T.denticola* combined with IL-1β, TIMP-2, and VEGF levels had stronger diagnostic ability than the markers individually. This highlights the importance of a combined approach in the study of microbial and endogenous biomarkers in relation to peri-implantitis.

19.5 Biomarkers Beyond Proteins and Microbial Profiles

With the advent of more discriminatory testing methods, evaluation of the genome, epigenome, transcriptome, and exosome is now possible. This means that evaluation of gene polymorphisms, epigenetic changes caused by environ-

mental factors, extracellular vesicles, mRNA, and microRNA expression in health and disease is now a clinical reality and may serve to improve the clinical applicability of biomarker evaluations. Chaparro et al. [94] reported that increased EVs concentration and decreased miRNA-21-3p and miRNA-150-5p expression was found in PICF of patients with peri-implantitis in comparison with peri-implant mucositis. Rakic et al. [95] investigated CD14 and TNF-α single nucleotide polymorphisms (SNP) as candidate genetic biomarkers of peri-implantitis via PCR and ELISA from DNA extracted from peripheral blood. They found that patients with SNP at CD14–159 had increased RANKL expression compared to the regular allele and five times increased risk of peri-implantitis. Similar results were reported for SNP at the TNF-α allele, with a five-fold increase in the risk of peri-implantitis but with no correlation to a change in the evaluated biomarker level. Similar studies evaluating other SNPs in different populations have also reported associations between environmental risk factors such as smoking and putative genetic risk markers, highlighting the need for future studies in larger and more diverse patient populations [96] to determine the role of environmental influence on the genetic phenotype. Currently, there are limited studies evaluating epigenetic changes (i.e., DNA methylation and histone modification) in peri-implantitis although the preliminary data from the periodontitis literature would suggest that this is an area of biomarker research that should be explored [44].

The clinical utility of genetic markers is currently limited as they are only suitable for risk profiling but could potentially be used prior to disease initiation to tailor a preventative strategy aimed at reducing disease incidence. As has been shown in the periodontitis literature [97–99], patient susceptibility is critical in the pathogenesis of peri-implantitis, and therefore a test allowing risk stratification based on genetic risk markers would be useful clinically.

Becker et al. [100] evaluated the transcriptome profile of peri-implantitis lesions comparing it to control samples taken from periodontitis lesions. Although this study had only limited numbers, through quantitative transcriptome and gene ontology analysis the authors were able to report that the mRNA signatures of peri-implantitis and periodontitis differed significantly and that peri-implantitis represented a complex inflammatory disease due to the variety of pathophysiological pathways determined in their analysis. It was also reported that peri-implantitis transcript regulation was for the majority related to innate immune and host defense responses, while in the periodontitis lesions bacterial response systems predominated. This highlights the importance of transcriptome analysis in determining the pathophysiology of peri-implant diseases which can then be used to guide future scientific and clinical research.

19.6 Expert Opinion: Choice and Use of Biomarkers for Pre-clinical and Clinical Investigations

There has been significant research exploring the use of biomarkers for the purpose of diagnosing, quantifying, and evaluating peri-implantitis; however, there are still many questions that need to be answered before the recommendations and results can be translated into a clinically relevant treatment protocol. The state of the current literature is equivocal and although there are some biomarkers that have been repeatedly shown to have an association and limited diagnostic capacity, marked inconsistencies between study design, selection criteria, methodology, and reporting have resulted in highly heterogeneous data that very rarely can be compared.

A key issue in the study of peri-implantitis as a disease has been the lack of case definition and inconsistency regarding its diagnosis. This has resulted in a number of different clinical thresholds being used, which can have a significant impact on the results of studies evaluating biomarkers in both saliva and PICF for clinical applications. With the introduction of the new classification system and case definition for peri-implant disease, researchers will now be able to provide results that can be compared [101]. When

considering the effect of modifiable risk factors such as smoking, diabetes, and other systemic diseases [102] on the oral microbiome [103, 104], the host immune response [105, 106], and the ability of the body to heal, it does not seem unreasonable that patients with these confounders are excluded from analysis in order to achieve the best possible baseline data for future comparison. This has been highlighted by a recent systematic review [72].

The majority of studies evaluating biomarkers in peri-implantitis have been cross-sectional in nature and lack the ability to draw clinically relevant conclusions. Future studies evaluating biomarkers in peri-implantitis should focus on the determination of the biomolecular characteristics of the PICF and saliva in health, and then prospectively assess changes in these markers to determine relevant analytes for disease initiation, progression, and response to treatment. All tested biomarkers should be correlated to clinical parameters to ensure that findings can be translated into the clinical setting, as well as controlling for the effect of disease severity on biomarker levels in the oral fluids. The majority of studies fail to report the calculated concentration of evaluated biomarkers, choosing to only report total volume which could potentially be a mere consequence of the volume sampled rather than actual biological changes at experimental sites. With regards to methodology, the use of highly sensitive arrays is recommended as the expected levels of biomarkers in oral fluids are generally less than corresponding amounts found in serum or blood. This means that commercially available assays and arrays designed for evaluating biomarkers in other body fluids may not have the required fidelity to be used for analyzing oral fluids.

The potential of biomarkers in early diagnosis, determining patient susceptibility, quantifying the response to treatment, and guiding distinct and personalized treatment approaches determined by individual pathogenesis is indisputable. Systematic reviews have outlined that higher levels of pro-inflammatory cytokines are associated with peri-implantitis and that more work needs to be done on evaluating the relationship of chemo-kines, anti-inflammatory cytokines, innate and adaptive immune modulatory molecules, growth factors, and tissue degradation products [72, 77]. It is clear that a single analyte is unlikely to have the sensitivity and specificity required and therefore it is most likely that a group of biomarkers will be used to achieve the desired precision for future applications [93, 107]. In the absence of consistent, repeated and high-quality data the recommendation at this stage should be that as many biomarkers as possible should be evaluated in concert and that comparison of analytes from various "omics" constituents should be attempted in order to increase the accuracy of the reported model.

References

1. Jung ER, et al. Systematic review of the survival rate and the incidence of biological, technical, and aesthetic complications of single crowns on implants reported in longitudinal studies with a mean follow-up of 5 years. Clin Oral Implants Res. 2012;23(s6):2–21.
2. Pjetursson BE, et al. A systematic review of the survival and complication rates of implant-supported fixed dental prostheses (FDPs) after a mean observation period of at least 5 years. Clin Oral Implants Res. 2012;23(s6):22–38.
3. Derks J, Tomasi C. Peri-implant health and disease. A systematic review of current epidemiology. J Clin Periodontol. 2015;42(Suppl 16):S158–71.
4. Heitz-Mayfield LJ, Mombelli A. The therapy of peri-implantitis: a systematic review. Int J Oral Maxillofac Implants. 2014;29:325–45.
5. Hämmerle CH, et al. The effect of subcrestal placement of the polished surface of ITI® implants on marginal soft and hard tissues. Clin Oral Implants Res. 1996;7(2):111–9.
6. Hermann JS, et al. Biologic width around one-and two-piece titanium implants. Clin Oral Implants Res. 2001;12(6):559–71.
7. Tarnow D, Cho S, Wallace S. The effect of inter-implant distance on the height of inter-implant bone crest. J Periodontol. 2000;71(4):546–9.
8. Wilson TG Jr. The positive relationship between excess cement and peri-implant disease: a prospective clinical endoscopic study. J Periodontol. 2009;80(9):1388–92.
9. Ivanovski S. Group D. Initiator paper. Implants--peri-implant (hard and soft tissue) interactions in health and disease: the impact of explosion of implant manufacturers. J Int Acad Periodontol. 2015;17(1 Suppl):57–68.

10. Qian J, Wennerberg A, Albrektsson T. Reasons for marginal bone loss around oral implants. Clin Implant Dent Relat Res. 2012;14(6):792–807.
11. Costa FO, et al. Peri-implant disease in subjects with and without preventive maintenance: a 5-year follow-up. J Clin Periodontol. 2012;39(2):173–81.
12. Cardaropoli D, Gaveglio L. Supportive periodontal therapy and dental implants: an analysis of patients' compliance. Clin Oral Implants Res. 2012;23(12):1385–8.
13. Albrektsson T, et al. Initial and long-term crestal bone responses to modern dental implants. Periodontol 2000. 2017;73(1):41–50.
14. Cho M-I. Development and general structure of the periodontium. Periodontology. 2000;24(1):9–27.
15. Albouy JP, et al. Spontaneous progression of ligatured induced peri-implantitis at implants with different surface characteristics. An experimental study in dogs II: histological observations. Clin Oral Implants Res. 2009;20(4):366–71.
16. Ericsson I, Lindhe J. Probing depth at implants and teeth. J Clin Periodontol. 1993;20(9):623–7.
17. Lang NP, et al. Histologic probe penetration in healthy and inflamed peri-implant tissues. Clin Oral Implants Res. 1994;5(4):191–201.
18. Schou S, et al. Probing around implants and teeth with healthy or inflamed peri-implant mucosa/gingiva. Clin Oral Implants Res. 2002;13(2):113–26.
19. Serino G, Turri A, Lang NP. Probing at implants with peri-implantitis and its relation to clinical peri-implant bone loss. Clin Oral Implants Res. 2013;24(1):91–5.
20. Jepsen S, et al. Progressive peri-implantitis. Incidence and prediction of peri-implant attachment loss. Clin Oral Implants Res. 1996;7(2):133–42.
21. Luterbacher S, et al. Diagnostic characteristics of clinical and microbiological tests for monitoring periodontal and peri-implant mucosal tissue conditions during supportive periodontal therapy (SPT). Clin Oral Implants Res. 2000;11(6):521–9.
22. Roccuzzo M, et al. Surgical treatment of peri-implantitis intrabony lesions by means of deproteinized bovine bone mineral with 10% collagen: 7-year-results. Clin Oral Implants Res. 2017;28:1577.
23. Zitzmann N, et al. Spontaneous progression of experimentally induced periimplantitis. J Clin Periodontol. 2004;31(10):845–9.
24. Derks J, et al. Peri-implantitis–onset and pattern of progression. J Clin Periodontol. 2016;43(4):383–8.
25. Rosen P, et al. Peri-implant mucositis and peri-implantitis: a current understanding of their diagnoses and clinical implications. J Periodontol. 2013;84(4):436–43.
26. Sanz M, Chapple IL. Clinical research on peri-implant diseases: consensus report of Working Group 4. J Clin Periodontol. 2012;39(s12):202–6.
27. Kinney JS, Ramseier CA, Giannobile WV. Oral fluid–based biomarkers of alveolar bone loss in periodontitis. Ann N Y Acad Sci. 2007;1098(1):230–51.
28. Han P, Ivanovski S. Saliva—friend and foe in the COVID-19 outbreak. Diagnostics. 2020;10(5):290.
29. Giannobile WV, et al. Saliva as a diagnostic tool for periodontal disease: current state and future directions. Periodontol 2000. 2009;50(1):52–64.
30. Nicholls J. The management of periodontal and peri implant disease. BDJ Team. 2020;7(6):34–6.
31. Kadkhodazadeh M, Amid R, Moscowchi A. Does COVID-19 affect periodontal and Peri-implant diseases? J Long-Term Eff Med Implants. 2020;30(1):1–2.
32. Jiao K, et al. The emerging regulatory role of circular RNAs in periodontal tissues and cells. Int J Mol Sci. 2021;22(9):4636.
33. Han P, Bartold PM, Ivanovski S. The emerging role of small extracellular vesicles in saliva and gingival crevicular fluid as diagnostics for periodontitis. J Periodontal Res. 2022;57(1):219–31.
34. Hua S, et al. Periodontal and dental pulp cell-derived small extracellular vesicles: a review of the current status. Nanomaterials. 2021;11(7):1858.
35. Han P, et al. Salivary outer membrane vesicles and DNA methylation of small extracellular vesicles as biomarkers for periodontal status: a pilot study. Int J Mol Sci. 2021;22(5):2423.
36. Han P, et al. Detection of salivary small extracellular vesicles associated inflammatory cytokines gene methylation in gingivitis. Int J Mol Sci. 2020;21(15):5273.
37. Han P, et al. Salivary small extracellular vesicles associated miRNAs in periodontal status-a pilot study. Int J Mol Sci. 2020;21(8):5273.
38. Johnson N, et al. Mucosal fluids and biomarkers of clinical disease: workshop 3B. Adv Dent Res. 2011;23(1):137–41.
39. Han P, Ivanovski S. Effect of saliva collection methods on the detection of periodontium-related genetic and epigenetic biomarkers—a pilot study. Int J Mol Sci. 2019;20(19):4729.
40. Zhang Y, et al. The emerging landscape of salivary diagnostics. Periodontol 2000. 2016;70(1):38–52.
41. Dawes C, Wong DTW. Role of saliva and salivary diagnostics in the advancement of oral health. J Dent Res. 2019;98(2):133–41.
42. Yan W, et al. Salivaomics knowledge base (SKB) (abstract 1179). In: 37th annual meeting and exhibition of the American Association for Dental Research. 2008.
43. Wong DT. Salivaomics. J Am Dent Assoc. 2012;143:19S–24S.
44. Larsson L, Castilho RM, Giannobile WV. Epigenetics and its role in periodontal diseases: a state-of-the-art review. J Periodontol. 2015;86(4):556–68.
45. Helmerhorst EJ, Oppenheim FG. Saliva: a dynamic proteome. Journal of dental research, 2007;86(8):680–93.
46. Kilian M, Chapple ILC, Hannig M, Marsh P.D, Meuric V, Pedersen AML, Tonetti MS, Wade WG, Zaura E. The oral microbiome–an update for oral

healthcare professionals. British dental journal, 2016;221(10):657–66.

47. Teles R. Periodontal medicine—new diagnostic opportunities. Curr Oral Health Rep. 2017;4(2):158–66.

48. Yamuna Priya K, Muthu Prathibha K. Methods of collection of saliva-a review. Int J Oral Health Dent. 2017;3(3):149–53.

49. Rantonen P. Salivary flow and composition in healthy and diseased adults. Helsinki: Panu Rantonen; 2003.

50. Zimmermann BG, Park NJ, Wong DT. Genomic targets in saliva. Ann N Y Acad Sci. 2007;1098:184–91.

51. Fenoll-Palomares C, et al. Unstimulated salivary flow rate, pH and buffer capacity of saliva in healthy volunteers. Rev Esp Enferm Dig. 2004;96(11):773–83.

52. Klein LC, et al. Caffeine and stress alter salivary alpha-amylase activity in young men. Hum Psychopharmacol. 2010;25(5):359–67.

53. Henson BS, Wong DT. Collection, storage, and processing of saliva samples for downstream molecular applications. Methods Mol Biol. 2010;666:21–30.

54. Nemoda Z, et al. Assessing genetic polymorphisms using DNA extracted from cells present in saliva samples. BMC Med Res Methodol. 2011;11:170.

55. Niimi A, Ueda M. Crevicular fluid in the osseointegrated implant sulcus: a pilot study. Int J Oral Maxillofac Implant. 1995;10(4):434.

56. Bevilacqua L, et al. Volumetric analysis of gingival crevicular fluid and peri-implant sulcus fluid in healthy and diseased sites: a cross-sectional split-mouth pilot study. Open Dent J. 2016;10:131.

57. Fonseca FJPO, et al. Cytokines expression in saliva and peri-implant crevicular fluid of patients with peri-implant disease. Clin Oral Implants Res. 2014;25(2):e68.

58. Heitz-Mayfield LJ. Peri-implant diseases: diagnosis and risk indicators. J Clin Periodontol. 2008;35(s8):292–304.

59. Recker EN, et al. A cross-sectional assessment of biomarker levels around implants versus natural teeth in periodontal maintenance patients. J Periodontol. 2015;86(2):264–72.

60. Rakic M, et al. Estimation of bone loss biomarkers as a diagnostic tool for peri-implantitis. J Periodontol. 2014;85(11):1566–74.

61. Javed F, et al. Proinflammatory cytokines in the crevicular fluid of patients with peri-implantitis. Cytokine. 2011;53(1):8–12.

62. Khurshid Z, et al. Human gingival crevicular fluids (GCF) proteomics: an overview. Dent J (Basel). 2017;5(1):12.

63. Griffiths GS. Formation, collection and significance of gingival crevice fluid. Periodontology. 2000;2003(31):32–42.

64. Guentsch A, et al. Comparison of gingival crevicular fluid sampling methods in patients with severe chronic periodontitis. J Periodontol. 2011;82(7):1051–60.

65. Wassall RR, Preshaw PM. Clinical and technical considerations in the analysis of gingival crevicular fluid. Periodontology. 2000;70(1):65–79.

66. Salonen JI, Paunio KU. An intracrevicular washing method for collection of crevicular contents. Scand J Dent Res. 1991;99(5):406–12.

67. Pradeep AR, et al. Levels of pentraxin-3 in gingival crevicular fluid and plasma in periodontal health and disease. J Periodontol. 2011;82(5):734–41.

68. Carcuac O, Berglundh T. Composition of human peri-implantitis and periodontitis lesions. J Dent Res. 2014;93(11):1083–8.

69. Basegmez C, et al. Evaluation of periimplant crevicular fluid prostaglandin E2 and matrix metalloproteinase-8 levels from health to periimplant disease status: a prospective study. Implant Dent. 2012;21(4):306–10.

70. Hentenaar DFM, et al. Biomarker levels in peri-implant crevicular fluid of healthy implants, untreated and non-surgically treated implants with peri-implantitis. J Clin Periodontol. 2021;48(4):590–601.

71. Nowzari H, et al. The profile of inflammatory cytokines in gingival crevicular fluid around healthy osseointegrated implants. Clin Implant Dent Relat Res. 2012;14(4):546–52.

72. Duarte P, et al. Could cytokine levels in the peri-implant crevicular fluid be used to distinguish between healthy implants and implants with peri-implantitis? A systematic review. J Periodontal Res. 2016;51(6):689–98.

73. Severino VO, Napimoga MH, de Lima Pereira SA. Expression of IL-6, IL-10, IL-17 and IL-8 in the peri-implant crevicular fluid of patients with peri-implantitis. Arch Oral Biol. 2011;56(8):823–8.

74. Ata-Ali J, et al. Clinical, microbiological, and immunological aspects of healthy versus peri-implantitis tissue in full arch reconstruction patients: a prospective cross-sectional study. BMC Oral Health. 2015;15(1):43.

75. Arıkan F, Buduneli N, Lappin DF. C-telopeptide pyridinoline crosslinks of type I collagen, soluble RANKL, and osteoprotegerin levels in crevicular fluid of dental implants with peri-implantitis: a case-control study. Int J Oral Maxillofac Implants. 2011;26(2):282.

76. Rakic M, et al. Bone loss biomarkers associated with peri-implantitis. A cross-sectional study. Clin Oral Implants Res. 2013;24(10):1110–6.

77. Dursun E, Tözüm TF. Peri-implant crevicular fluid analysis, enzymes and biomarkers: a systemetic review. J Oral Maxillofac Res. 2016;7(3):e9.

78. Ramseier CA, et al. Host-derived biomarkers at teeth and implants in partially edentulous patients. A 10-year retrospective study. Clin Oral Implants Res. 2016;27(2):211–7.

79. Liskmann S, et al. Correlations between clinical parameters and lnterleukin-6 and lnterleukin-10 levels in saliva from totally edentulous patients with Peri-implant disease. Int J Oral Maxillofac Implants. 2006;21(4):543.

80. Tözüm TF, et al. Analysis of the inflammatory process around endosseous dental implants and natural teeth: myeloperoxidase level and nitric oxide metabolism. Int J Oral Maxillofac Implants. 2007;22(6):969–79.

81. Güncü GN, et al. Myeloperoxidase as a measure of polymorphonuclear leukocyte response in inflammatory status around immediately and delayed loaded dental implants: a randomized controlled clinical trial. Clin Implant Dent Relat Res. 2008;10(1):30–9.

82. Plagnat D, et al. Elastase, α2-macroglobulin and alkaline phosphatase in crevicular fluid from implants with and without periimplantitis. Clin Oral Implants Res. 2002;13(3):227–33.

83. Strbac GD, et al. Cathepsin K levels in the crevicular fluid of dental implants: a pilot study. J Clin Periodontol. 2006;33(4):302–8.

84. Cakal OT, Efeoglu C, Bozkurt E. The evaluation of peri-implant sulcus fluid osteocalcin, osteopontin, and osteonectin levels in peri-implant diseases. J Periodontol. 2018;89(4):418–23.

85. Zani SR, et al. Peri-implant crevicular fluid biomarkers as discriminants of peri-implant health and disease. J Clin Periodontol. 2016;43(10):825–32.

86. Edgerton M, Lo SE, Scannapieco FA. Experimental salivary pellicles formed on titanium surfaces mediate adhesion of streptococci. Int J Oral Maxillofac Implants. 1996;11(4):443–9.

87. Belibasakis GN, Manoil D. Microbial community-driven Etiopathogenesis of Peri-Implantitis. J Dent Res. 2021;100(1):21–8.

88. Koyanagi T, et al. Comprehensive microbiological findings in peri-implantitis and periodontitis. J Clin Periodontol. 2013;40(3):218–26.

89. Fürst MM, et al. Bacterial colonization immediately after installation on oral titanium implants. Clin Oral Implants Res. 2007;18(4):501–8.

90. Persson GR, et al. Mechanical non-surgical treatment of peri-implantitis: a single-blinded randomized longitudinal clinical study. II. Microbiological results. J Clin Periodontol. 2010;37(6):563–73.

91. Sahrmann P, et al. The microbiome of Peri-Implantitis: a systematic review and meta-analysis. Microorganisms. 2020;8(5):661.

92. Lafaurie GI, et al. Microbiome and microbial biofilm profiles of Peri-Implantitis: a systematic review. J Periodontol. 2017;0:1–26.

93. Wang HL, et al. Protein biomarkers and microbial profiles in peri-implantitis. Clin Oral Implants Res. 2016;27(9):1129–36.

94. Chaparro A, et al. Diagnostic potential of peri-implant crevicular fluid microRNA-21-3p and microRNA-150-5p and extracellular vesicles in peri-implant diseases. J Periodontol. 2021;92(6):11–21.

95. Rakic M, et al. CD14 and TNFα single nucleotide polymorphisms are candidates for genetic biomarkers of peri-implantitis. Clin Oral Investig. 2015;19(4):791–801.

96. Petkovic-Curcin A, et al. Association of cytokine gene polymorphism with peri-implantitis risk. Int J Oral Maxillofac Implants. 2017;32(5):e241.

97. Hirschfeld L, Wasserman B. A long-term survey of tooth loss in 600 treated periodontal patients. J Periodontol. 1978;49(5):225–37.

98. Löe H, et al. The natural history of periodontal disease in man. J Periodontal Res. 1978;13(6):563–72.

99. Ramseier C, et al. Natural history of periodontitis: disease progression and tooth loss over 40 years. J Clin Periodontol. 2017;44:1182.

100. Becker ST, et al. Peri-implantitis versus periodontitis: functional differences indicated by transcriptome profiling. Clin Implant Dent Relat Res. 2014;16(3):401–11.

101. Berglundh T, et al. Peri-implant diseases and conditions: consensus report of workgroup 4 of the 2017 world workshop on the classification of periodontal and Peri-implant diseases and conditions. J Clin Periodontol. 2018;45:S286–91.

102. Han P, Liu T, Vaquette C, Frazer D, Anderson G, Ivanovski S. Iron accumulation is associated with periodontal destruction in a mouse model of HFE-related hemochromatosis. J Periodontal Res. 2021;57:294. https://doi.org/10.1111/jre.12959.

103. Grossi S, et al. Assessment of risk for periodontal disease. II. Risk indicators for alveolar bone loss. J Periodontol. 1995;66(1):23–9.

104. Lalla E, Papapanou PN. Diabetes mellitus and periodontitis: a tale of two common interrelated diseases. Nat Rev Endocrinol. 2011;7(12):738–48.

105. Palmer RM, et al. Mechanisms of action of environmental factors–tobacco smoking. J Clin Periodontol. 2005;32(s6):180–95.

106. Taylor JJ, Preshaw PM, Lalla E. A review of the evidence for pathogenic mechanisms that may link periodontitis and diabetes. J Clin Periodontol. 2013;40:S113–34.

107. Ramseier CA, et al. Identification of pathogen and host-response markers correlated with periodontal disease. J Periodontol. 2009;80(3):436–46.

Computer-Assisted Implant Dentistry

20

João Manuel Mendez Caramês
and Duarte Nuno da Silva Marques

20.1 Precision Digital Technologies

Technological developments have accelerated in all fields of knowledge over recent decades, allowing dental professionals to work [1] inexorable, and the clinical practice of dentistry has followed suit, where a paradigm shift from manual and more classical dentistry practice to computer-assisted concepts and digital technologies is observed. The integration of these technological systems in the field of implant dentistry to improve the quality of care and patient-centered outcomes has led to several computerized advances such as three-dimensional imaging through CT scan images, intra and extra-oral scanners, implant-planning software, computer-aided-design, and manufacturing (Fig. 20.1) [2] technology through the fabrication of implant abutments, crowns and different types of super-
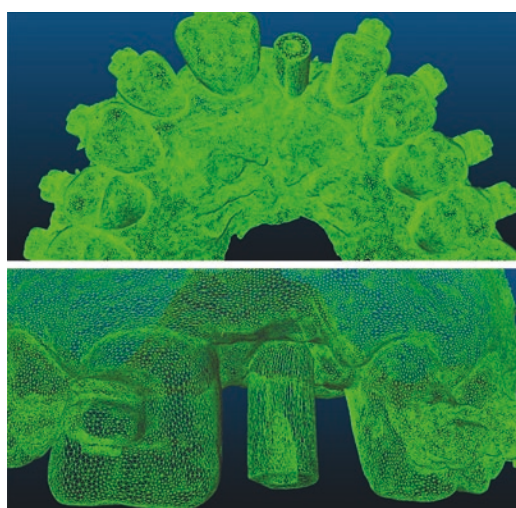

Fig. 20.1 STL file from intra-oral scanner with implant scan body for the provisional crown of #21 while a patient is undergoing orthodontic treatment

structures, static and dynamic computer-guided implant surgery to tracking technologies used to monitor occlusion and parafunctions (Fig. 20.2) [1, 3–7].

Digital technologies also allow for the merging of different digital files (STL, DICOM) resulting in new applications such as dental implant planning via merging of CT scan images (DICOM) and intra-oral digital scanning files [8] of patients thus creating surgical guidelines with improved accuracy when compared to non-guided conventional methods, thus enhancing the clinical outcome [7, 9]

J. M. M. Caramês (✉)
Oral Surgery and Implant Department, LIBPhys-FCT UID/FIS/04559/2013, Faculty of Dentistry, University of Lisbon, Lisbon, Portugal

Implantology Institute, Lisbon, Portugal

D. N. da Silva Marques
Implantology Institute, Lisbon, Portugal

Evidence Based Dentistry Centre, LIBPhys-FCT UID/FIS/04559/2013, Faculty of Dentistry, University of Lisbon, Lisbon, Portugal
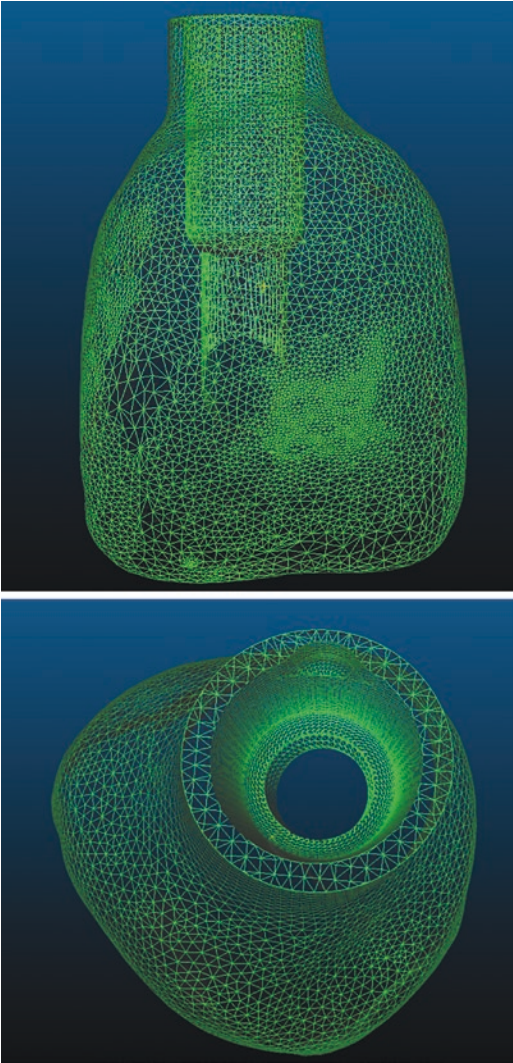
Fig. 20.2 Emergence profile of Provisional Crown designed in CAD software

At the educational level, these technologies will produce lasting effects on future generations of practitioners with a number of dental schools' curricula already embracing digital dentistry with enhanced learning objectives and specific outcome measures [10–12]

While the clinical discipline of implant dentistry focuses on the use of the available technology in providing patients with better quality of care, encompassing a range of rehabilitative procedures and systems [4, 13], the variety of different procedures makes it extremely difficult to

compare them. Although the International Organization for Standardization [2] specifies the test methods for assessing the accuracy of many of these digital technologies [2, 14, 15], the scientific literature presents different accuracy measurement techniques and terms making it more challenging for the users to conduct comparisons.

The aim of this chapter is to review the most frequently adopted methods for evaluating digital technologies used in implant dentistry. Moreover, the different methodological designs used in vitro, in vivo, and clinical studies will be discussed.

20.2 Methodological Designs in Computer-Assisted Implant Dentistry: Diagnostic Studies of Accuracy—In Vitro, In Vivo, and Clinical Studies

When assessing the methodological designs in computer-assisted implant dentistry, in the majority of these studies' accuracy is one of the primary outcomes to be determined. Placing a dental implant in a previously planned location or replacing bone and/or soft tissues requires highly accurate reproduction in the digital workflow.

Thus, several terms should be formulated correctly to allow the reader to compare different studies, technologies, or devices.

According to ISO standards [14, 16] the following terms should be taken into account (Fig. 20.3):

Accuracy—This is a qualitative concept, being the quantitative counterpart of the error of measurement that represents the closeness of agreement between an individual result and an accepted reference value. Depends on trueness and precision results.

Trueness—This is a qualitative concept, being the quantitative counterpart of systematic error, representing the deviation between the mean obtained from a large series of results of measurement and a true value or a conventional true value. In practice, the systematic error should be
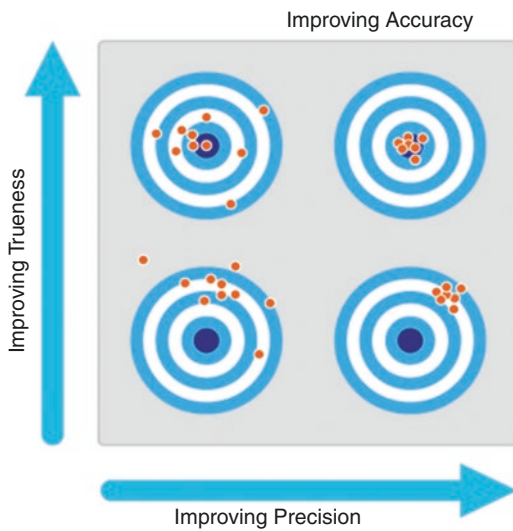
Fig. 20.3 Schematics representing the influence of trueness and precision in overall accuracy

estimated from 30 or more repeated measurements of an object under specified conditions

Precision—This is a qualitative concept, being the operational definition of the standard deviation, which represents the deviation between independent results of measurement obtained under stipulated conditions.

True and precise metrical outcomes are needed for almost every technology in the computer-assisted implant dentistry field. From cone beam computerized tomography (CBCT) exams to scanners and CAD/CAM technologies the evaluation of treatment success or validation of new treatment strategies are critically dependent on the methodological procedures and study designs used.

In many of these fields, validation procedures use linear distance measurements with microscopes or calipers which are compared between groups [17–21] These methods present limitations regarding three-dimensional changes and are reduced to only a few measuring points of the testing area. Newer measuring methods include radiographic or optical capturing of the entire surfaces or volumes, which can use superimposition models to measure volumetric changes, or deformations in all three coordinate axes [22–25].

Although providing more possibilities these new methods still depend precisely on the accuracy of the scanners used which is often a value given by the manufacturer derived from scanning small calibrated objects and are thus different when scanning large objects like a dental arch directly affecting the results due to scan errors [26–28].

20.2.1   Role of the Different Study Research Designs in Current Computer-Assisted Implant Dentistry

Most studies in the new digital technologies are designed so that new treatments can obtain regulatory approval, or to evaluate treatments under ideal conditions (i.e., efficacy), which often don't translate well into real-world circumstances (i.e., effectiveness).

Modern contemporary healthcare is patient-centered, effectiveness-focused and evidence-based, and by necessity and definition translational in nature [29].

For this purpose studies in new emerging digital technologies should satisfy the fundamental standards of methodology, design, and data analysis to decrease the risk of research bias with systematic, random, or inferential errors [30, 31].

The hierarchical structure of research designs has become increasingly popular today, positioning designs in terms of their clinical relevance in which the level of evidence can be expressed through different systems, being that the principle remains the same: to evaluate "what" was done.

Considerable confusion exists regarding study design and the research questions that can be best answered by each design.

Although the *in vitro* and animal studies belong to the lower levels in the evidence-based pyramid they should be considered fundamental to establishing the plausibility of a novel treatment modality thus yielding information critical to the development of clinical trials [32]. For that purpose, they should provide sufficient information to the reader to understand the procedures

	IN VITRO	IN VIVO (ANIMAL)	CLINICAL TRIAL
Advantages	• Standardization with improved internal validity • Ethical Considerations	• Technique improvement • Step before clinical trials	• Clinical Significance
Disadvantages	• Biological Variability • External validity • Generalizability to clinical situation	• Biological difference with humans	• Confounding Factors

Fig. 20.4 Advantages and disadvantages according to study design

performed (material and methods), to assess the biological relevance of the study and the validity and reliability of the findings (outcomes) [33–35]. The reader should therefore be able to repeat the experiment in a similar way.

When comparing the different types of study designs used with these new technologies, one can consider the study-related pros and cons (Fig. 20.4):

Studies in the new digital technologies in dentistry should be designed according to guidelines that enable standardization of the assessed outcomes, thus improving the quality of the reported research.

20.2.2 Assessment Tools for Improving the Quality of Research Reporting

In recent years several assessment tools have been proposed with the intention of improving the quality of reporting. These include; CONSORT guidelines for clinical trials [36], STROBE guidelines for observational studies [37], GRADE for accuracy research [38], STARD guidelines for studies involving diagnostic tests [39], ARRIVE for reporting In Vivo studies [34], and PRISMA or ROBIS guidelines for meta-analysis and systematic reviews [40, 41].

These guidelines encourage the researcher to report the study in relation to an itemized checklist. The aim is not to improve the quality of the study but to help in setting standards that allow comparability across studies [36, 42]. There is convincing evidence that the use of such checklists has improved the quality of published articles [43–47].

Extrapolation of similar guidelines for in vitro studies would improve the quality of reporting, but still, there have been no validated guidelines for reporting in vitro studies. Some proposals have been published [48–50], but validation data is still lacking.

20.3 Guided Surgery

20.3.1 Diagnostics

#### 20.3.1.1 Three-Dimensional Computed Tomography Imaging

Imaging in one form or another, has been available to dentistry since 1896 [51], although in the last 30 years since the launch of digital imaging, several advanced imaging technologies like computed tomography, cone beam computed tomography, magnetic resonance imaging, and ultrasound have found a place in modern den-

tistry. These technologies have not only made the process simpler and faster but made it more accurate too.

Intraoral and extraoral radiographic examinations are the backbone of imaging for the dental practitioners to provide detailed information about the teeth and surrounding tissues. However, periapical and panoramic radiographs are subject to geometric distortion and only provide a two-dimensional image of a three-dimensional object. The relationship of the tooth to the surrounding anatomical structures cannot be assessed accurately thus limiting its diagnostic performance which is of major importance in implant dentistry [52, 53]

A number of different techniques have evolved in the recent past that have revolutionized the diagnosis and treatment planning in implant dentistry based on dental cone beam computed tomography (CBCT). CBCT is recommended for implant planning by several professional associations [54–57]. Although a strong improvement in dental implant treatment planning has been observed with the use of CBCT images, some limitations are still present. This is seen particularly in voxel definition, increased radiation dose to the patient when compared to panoramic imaging, scattering that decreases the available details regarding soft tissues, blood vessels, and lymph nodes or the presence of image artifacts, such as dental implants or dense restorations which can influence diagnostic or surgical guides manufacturing accuracy [58, 59] (Fig. 20.5).

Rapid advances in diagnostic imaging technology make a thorough assessment of new technology prior to its implementation a challenge. A hierarchical approach to the assessment of new diagnostic imaging technology has been advocated and used by technology assessors in the field [60–63]. This approach should entail an assessment of the technical performance; diagnostic performance (accuracy); diagnostic, therapeutic, and effect of prognosis; effectiveness (patient and societal outcomes); and cost-effectiveness. Although this approach is rigorous and scientifically sound when performed sequentially, it is time and resource consuming particu-
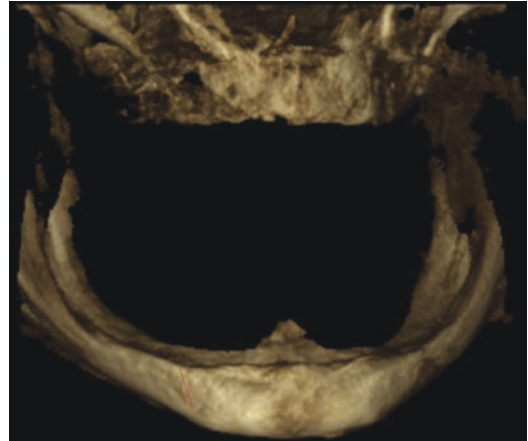
Fig. 20.5 CBCT with reduced bone volume in the maxilla and mandible

larly when evaluating new technological imaging developments in a timely fashion towards improving implant dentistry outcomes. For that purpose, some authors in the last years have proposed pragmatic designs in which the outcome measures reflect the clinical decision process [64].

At the core of the problem is the difficulty in connecting the performance of an imaging test to a health-related outcome. Patients rarely live or die based on the performance of a noninvasive test and in the field of implant dentistry, improper implant placement can be attributed to several different variables from poor diagnosis to poor implant placement technique. When assessing new imaging technologies in implant dentistry we should develop and implement standards for using imaging in clinical trials (ethical considerations regarding radiation exposure should be discussed), the imaging technique and quality better defined (voxel size, field of view, and image detection system), the methods to achieve it agreed on and implemented, and the impact on outcomes measured. In general, all these standards will help to improve imaging effectiveness and efficacy as well as efficiency in clinical practice.

In vitro and animal studies have a place in the initial steps towards comparing different imaging technologies. For example, animal studies can be performed as the initial step in comparing accu-

racy in different techniques for proximity to vital anatomical structures, since the different tests can be used in the same animals, thus increasing the efficiency of the study design.

CBCT for Diagnosis Outcome Assessment

CBCT studies could be used to assess pre-implant diagnostic value for the presence of occult pathology, foreign bodies, and/or defects and to determine the suitability of the site in terms of 3D morphology and proximity to vital anatomic structures. For this purpose, a hierarchical approach should be used with in vitro and animal studies performed for protocol validation prior to human studies. These studies could be designed to determine sensitivity and specificity (or a receiver characteristic operating curve) values in comparison to a reference standard. This entails the performance of both the new test and reference standard in all patients in a cohort study or in a diagnostic test-treatment trial and the determination of the probability of abnormal and normal findings conditional to diagnosis assessment [65, 66]. Although based on ethical grounds for radiation exposure, some cases could be left out, thus leading to biased estimates of sensitivity and specificity [67, 68]. Furthermore, although sensitivity and specificity may be useful performance parameters in the initial evaluation of a new test, when deciding if the new diagnostic strategy should be implemented, patient outcomes and costs should also be evaluated.

Taking into consideration the SEDENTEXCT guidelines [69] and the more recent pragmatic proposals for imaging studies [64], we could propose that an in vivo imaging study design in implant dentistry should comply with the following key features:

- *Randomization*—Random assignment to either group minimizes the bias from extrinsic factors and decreases the ethical considerations of double radiation exposure to patients (ALARA principle) [70]. However, if there are good reasons to believe that one diagnostic imaging modality is superior to another, then randomization should not be performed.

- *Pragmatic*—Patients are treated as close to daily clinical practice as possible thus increasing their ability to generalize. The results can also influence the recruitment rate.
- *Integration*—Additional exams may be requested or performed, thus integrating the clinical process into the clinical research.
- *Description of imaging techniques*—Authors should strive to clearly describe the scanning features of the imaging techniques used
- *Diagnostic and effectiveness-oriented outcome measures*—Outcome measures should be standardized according to the major outcomes to be assessed in diagnostic studies (accuracy for anatomical landmarks and/or receiver operator curve). Cost-effectiveness outcomes should be assessed too.
- *Treatment outcome measurements*—When determining geometric implant accuracy, outcomes such as linear and angular measurements are to be considered.
- *Patient outcomes*—Include measures that reflect the overall goal of health care, such as quality of life (dose optimization and exposure factor reduction), number of events, and crossovers to other diagnostic strategies during follow-up.

Before performing in vivo studies researchers should ascertain in vitro the sensitivity and specificity of the proposed technique when compared to the reference method by the use of standardized protocols taking into account the following key features:

- *Quality Control*—Researchers should consider the following quality parameters when assessing CBCT quality
  - Uniformity, Geometric Precision, Voxel density values, Noise, Low-contrast resolution, Spatial resolution
- *Image Quality Phantoms*—CBCT equipment should be evaluated by using image quality phantoms in a standardized, reproducible, and consistent way since performance interferes with accuracy results. The in vitro universal phantom requirements have already been

addressed [71, 72], with commercially available devices.

CBCT Treatment Outcome Assessment

Today CBCT imaging can be used for assessing treatment outcome measurements such as geometric implant accuracy or volumetric bone regeneration changes.

For that purpose animal models have been used to validate the concept of using CBCT imaging for bone measurements around titanium implants [73] or linear/ volumetric changes after bone regeneration techniques [74, 75].

When designing an animal study to assess bone changes or implant accuracy, researchers should consider the following key features:

- *Standardization of procedure*—The procedure should comply with animal welfare guidelines and the surgical and outcome assessment procedures should be described in such detail as to allow the reader to repeat the protocols described.
- *Validation*—Regardless of the outcomes to be assessed, investigators should perform comparative studies with those considered as the gold standard to assess the quality of the proposed new method.
- *Implant accuracy*—Linear measurements from the CBCT can be used to determine the accuracy of a specific surgical technique or guide, although results should be cross-checked with histological measurements to allow concept validation and accuracy determination [73, 76]. Outcomes such as the difference between programmed placements and real placement or distance to anatomical structures can be used in accuracy determination [77].
- *Bone regeneration*—A number of papers have been published assessing graft behavior in implant dentistry with CBCT imaging, although standardization of the methods is lacking [78–80], most likely due to different imaging devices and software use. Several studies have used the method proposed by Uchida et al. [81] which implies the 2D measurement of each slice and adding up all

areas for total volume determination. Nowadays, the use of specific software to convert and measure volumes from the DICOM files obtained from the CBCT imaging could allow for easier, quicker, and more accurate measurements [82–84]. Tomographic data can be exported by means of an internationally standardized file format known as DICOM (Digital Imaging and Communications in Medicine) and with appropriate software render a 3D model which could be used for volumetric measurements (Fig. 20.6). Nowadays several types of software are available free of charge and via a more or less sophisticated user interface perform image segmentation and export the data as a 3D surface format [4].

- *Bone quality*—This has been suggested as one of the main factors influencing implant therapy success and should be strongly recommended as one outcome to be assessed in implant therapy research. According to recent data, CBCT gray values offer poor correlation to Hounsfield units with data varying for other CBCT models or exposure conditions [85]. For this purpose, alternative methods redirecting bone evaluation from density to quality have been proposed. With increasingly improving image quality in CBCT characteristics such as 3D trabecular bone architecture, bone surface, (BS)/volume ratios expressing bone density, bulk or amount of bone, and spacing between trabeculae and marrow spaces have shown potential, although evidence regarding accuracy and stability is still limited [86].

When preparing an in vivo study to assess bone changes or implant accuracy, researchers should also consider the following key features:

- *As Low As Reasonably Achievable (ALARA) Principle*—Patient radiation exposure should be reduced, thus mitigating ethical considerations.
- *Evaluators*—Should be calibrated and Intra-class correlation coefficient (ICC) calculated between assessors.

Fig. 20.6 Bone volume assessment between CBCTs of the same patient before and after guided bone regeneration in the edentulous atrophic maxilla using demineralized bovine bone mineral (DBBM) combined with platelet-rich fibrin (PRF)
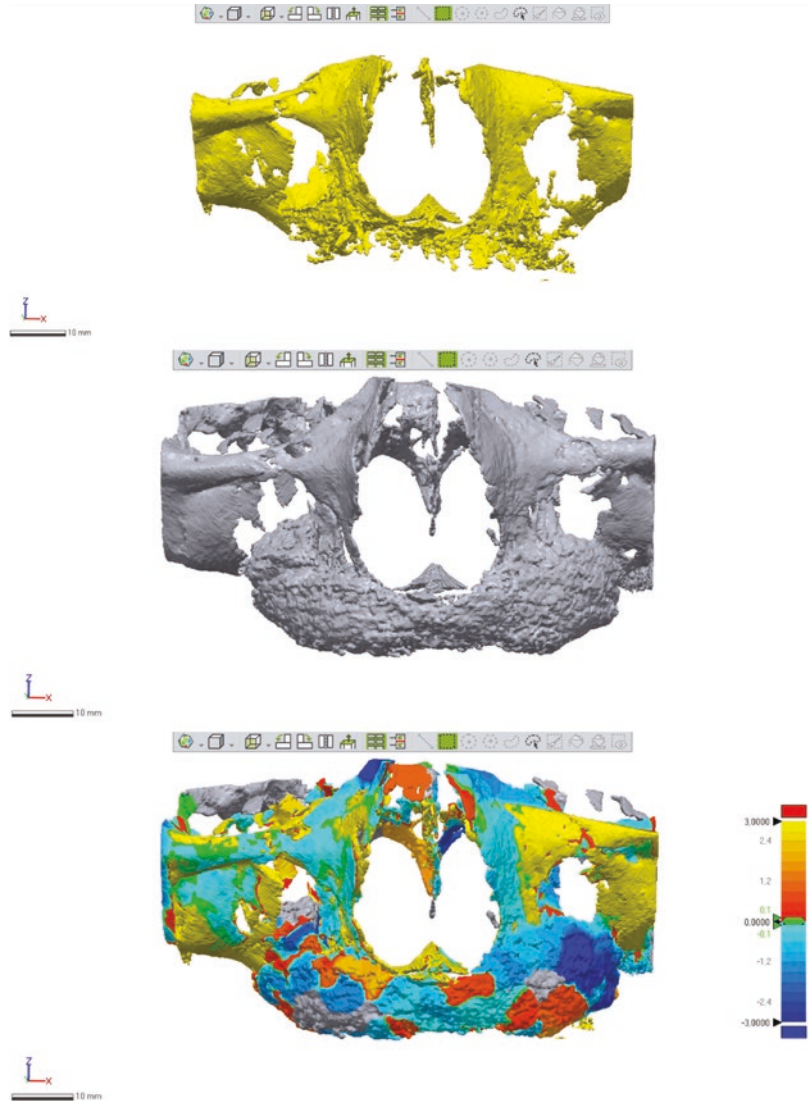
- *CBCT accuracy*—standardization and accuracy determination of CBCT devices should be determined and taken into account.
- *Sample size determination and Randomization*—according to the outcomes to be assessed.

20.3.1.2 Intra, Extra-Oral, and Facial Scanners

In computer-assisted implant dentistry, creating three-dimensional (3D) digital datasets has become the standard. Treatment has shifted towards a digital 3D approach where treatment can be planned in advance, making surgery more predictable and reducing the surgical time, thus improving patient-centred outcomes [87, 88].

Dental research has been focused on intraoral and facial scanning devices in order to minimize procedural errors during digital workflow increasing reliability and prognosis of medical therapies [89].

As previously stated, in the digital diagnostic phase, images derived from CBCT imaging are still lacking detail mainly due to the scanning

resolution and artifacts caused by radiopaque dental restorations, dental implants, or orthodontic brackets [90–92].

Digital workflow introduced a novel approach for a more predictable implant-supported rehabilitation using patient photos, facial scanning, virtual diagnostic wax mock-ups for the surgical models or guides, and provisional rehabilitation.

The initial step for a highly precise digital workflow is to obtain the digital dental models, and therefore two main types of dental CAD/CAM scanners exist: intraoral scanners that are used for chairside scanning of the patient's dental arches and extra-oral scanners that are used in the dental laboratory to scan casts. Both scanners develop a digital model of the patient's mouth using CAD software that can be used for implant planning along with the CBCT imaging or provisional/final implant rehabilitation with the use of 3D printers or milling machines [93, 94].

According to a number of studies, the acceptance level of fit for implant-supported prostheses range between 50–150 μm [95–97]. As these numbers also include errors in the final processing and production of the framework, the scanning deviation must be below this threshold.

Studies that evaluate the accuracy of scanning or misfit of fabrication are necessary for this purpose [98–102].

Accuracy Evaluation

Accuracy consists of precision and trueness [16], being that both components should be evaluated when assessing intra-, extra-oral, or facial scanner accuracy [103].

Several methodologies and study designs have been published and proposed without standardization which does not allow for inter-studies comparisons.

Two approaches in vitro and in vivo are possible. It has to be noted that these two types of study can and should be complementary.

When preparing an in vitro study, researchers should take into consideration the following key features:

- *Outcomes definition*—Precision and trueness should comply with ISO definitions when

evaluating the diagnostic accuracy of intra- and extra-oral scanners. Depending on study objectives, repeatability, reproducibility, and dispersion measures could also be considered [104].

- *Methods standardization*—The methods should describe how the reference model was obtained, the scanner characteristics, calibration procedures, and a standardized method of measurement. One of the main purposes of standardization is to eliminate differences between users or between identical pieces of equipment. According to some authors, the preferred statistic is known as the Root Mean Square Error (RMS) [105–107], but alternatives can be x standard deviation (also known as Sigma) or, for example, 50%-, 75%- or 95%-percentile values relative to what can be considered as clinically or technologically relevant accuracy [108].

- *Validation of Accuracy Method*—Researchers using digital technologies should validate and evaluate the reliability of the method used for accuracy determination.

- *Master Die*—Should be prepared in a material that represents those applied in normal use and presents high dimensional stability and optical properties that allow an unhindered scan of the surface.

- *CAD reference model*—Should be obtained in a measuring device with an accuracy of ±2 μm [2], being that nowadays a coordinate measuring machine (CMM) is still considered as reference [2], although professional industrial scanners with more than 12 Megapixels resolution offer a viable alternative [109, 110]. More recently, a new method has been proposed with the use of a metal reference bar while performing in vitro intra- and extra-oral scanning [111], although the clinical application of this scanning methodology has to be questioned.

- *Operator and equipment variance*—Most studies consider operator variance but very few address the possibility of variance between identical pieces of equipment.

- *Digital models superimposition*—Volumetric changes or three-dimensional divergences can
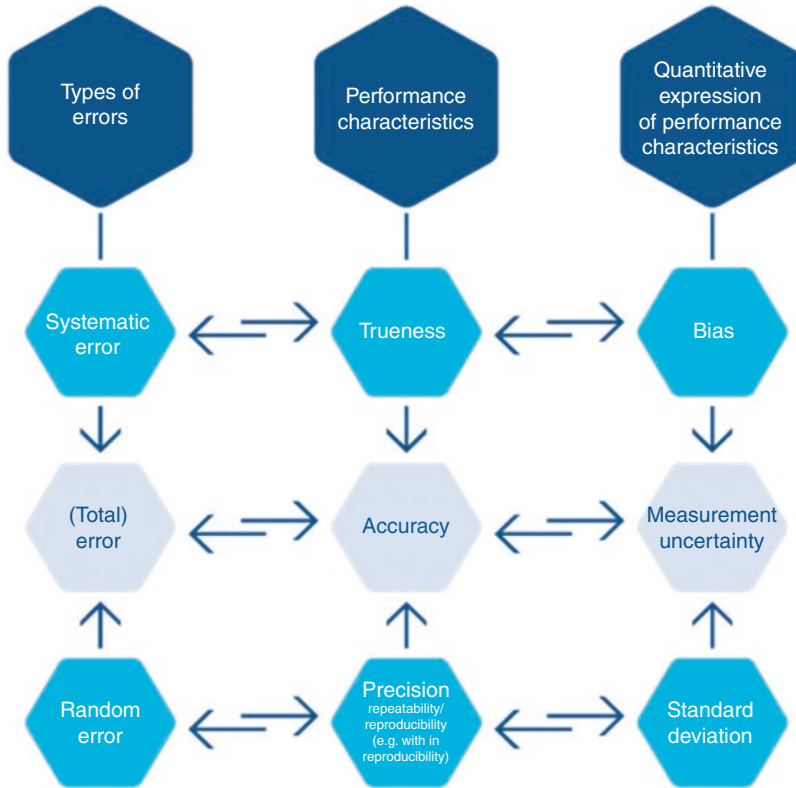
Fig. 20.7 Interrelations between error types, performance characteristics, and expression of estimates. Adapted from Menditto et al. [114]

be calculated with software that allows for three-dimensional superimposition for quality control comparison such as Geomagic or Gominspect [112, 113] (Fig. 20.7).

When preparing an in vivo study, researchers should consider the following key features:

- *Pragmatic*—studies should compare the accuracy of these new devices/technologies with a gold standard within values that can have clinical significance.
- *Outcomes definition*—When assessing in vivo accuracy, researchers should clearly define the study objectives and outcomes. Endpoints such as accuracy between conventional and digital implant impressions, between intra-oral scanners, or even between different inter-implant positions, angulations, or distances should be defined.

- *Material and Methods description*—A clear description regarding subject characteristics (partially or totally edentulous), implant characteristics and position, scan bodies and scanners used, reference models, and accuracy method determination should be present in the material and methods section thus allowing for inter-studies comparisons.
- *Inter and intra-operator variability*—While using the intra-oral scanners there is a learning curve that could interact with the accuracy determination and researchers should ideally evaluate not only one operator-one scanner accuracy but the several operators-several identical scanners accuracy. The main problem with this type of design is the associated economic costs, although it would mitigate the operator or device bias.
- *Biological variability*—confusing factors such as jaw opening, saliva, blood, or other

factors are present in clinical situations, thus these parameters shall be taken into account when performing sample size determination.

- *Sample Size*—To draw reliable conclusions studies should include a large number of patients based on a statistical sample size determination taking into account possible attrition bias.

Photogrammetry: A New Tool for Full-Arch Implant Impressions?

Although in single and short-span implant-supported prostheses the use of intra-oral scanners offers a predictable alternative to conventional impressions, nowadays in full-arch implant-supported prostheses the conventional silicone impressions still present higher accuracy when compared to IOS systems.

Factors such as saliva, movable mucosa, reflective restorations, ambient light, handling, and scanning protocols among others have been found to influence the IOS accuracy [115–118].

In the last years, photogrammetry (PG) has been reported as a digitizing technology that allows the use of screw-retained optical markers to virtually transfer the implant location from the patient's mouth to the computer-aided software program, thus allowing the fabrication of implant-supported prostheses.

However, the assessment of the PG accuracy for implant position is scarce, mostly from in vitro studies and with contradictory results [113, 119, 120].

Previously mentioned criteria for in vitro and in vivo studies with intra-oral scanners should be used to evaluate PG with digital and conventional impressions regarding accuracy, efficiency, and patient-related outcomes.

Intraoral and Facial Scanners: Powerful Tools for Diagnostic Studies

Effective clinical management is facilitated by early detection and differential diagnosis. Moreover, it is essential to be able to reliably assess the outcome of hard or soft tissue procedures to meet the right clinical decisions. Some examples where scanners were used in different study designs are:

- *Volumetric determination of soft tissue procedures* [26, 121, 122]—Intra-oral scanners appear to be useful to determine soft tissue stability when performing surgical or prosthodontic procedures. In addition, software that allows for the merging of CBCT and intra-oral scanners will enable researchers to correlate hard and soft tissue changes after regenerative procedures. (Fig. 20.8)
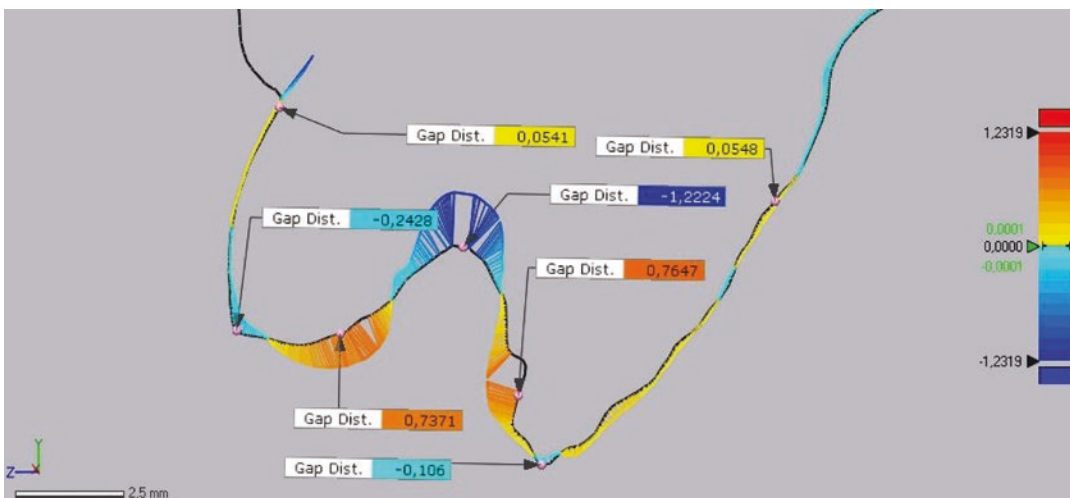
Fig. 20.8 Soft tissue emergence profile comparison in single unit implant impression between intra-oral scanner with scan body and custom-impression coping and conventional impression technique
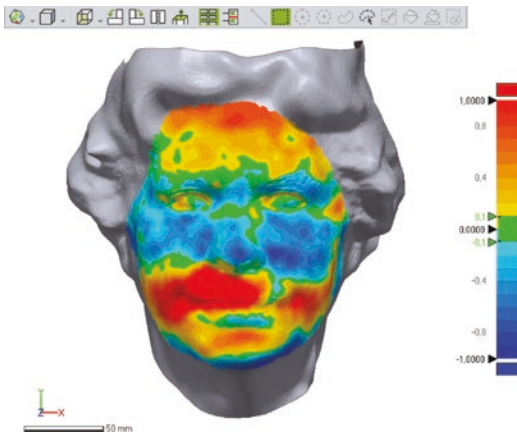
Fig. 20.9 Facial profile comparison between facial scanners of the same patient with and without full arch implant-supported maxillary prosthesis for lip support analysis

- *Tooth and Prosthesis Wear evaluation* [123, 124]—In vitro or In vivo wear measurement by the means of digital models and quality control software shows promising results and are cost-effective tools when comparing with the gold standard.
- *Orthodontics*—curvilinear measurements for diagnostic purposes (da Silva [25, 116, 125]) or assessing tooth movement and soft tissue changes during orthodontic procedures [126] (Fig. 20.9).
- *New technologies in 3D intraoral scanning*—Technologies such as CBCT, Magnetic Resonance Imaging, Ultrasound, or Stereophotogrammetry have been described as possibilities for mitigating the limitations of optical scanners with promising results [127–130]

20.3.2 Planning

20.3.2.1 CT-Based Implant-Planning Software

For virtual planning implant placement, anatomical data of the patient is required. CBCT or CT displays a three-dimensional image of the jaw for the identification of 3D ridge topography and proximity to vital anatomic structures [54].

CBCT data imported into third-party interactive software platforms that simulate virtual implants as precursors to the fabrication of templates that will be used in the actual surgery have been widely studied and applied in clinical practice [7, 56, 131, 132]

In addition, intra-oral scanning devices have recently begun to contribute considerably to these novel treatment modalities with respect to treatment planning [133], by superposing images of recognizable structures obtained from CBCT and intra-oral scanning, thus creating a more realistic view of the hard and soft dental tissues of a patient. However, apart from the benefits of a more rapid procedure, reduced perioperative bleeding, and decreased postoperative patient discomfort, there are still some major issues that need to be addressed. Researchers have described multiple ways of measuring accuracy errors by means of direct measurement in sagittal, coronal, or frontal slices; percentage of 3D superimpositions of reconstructed implant images, or in vitro direct measurements with caliper or other image software. Because of the use of a wide array of CT or CBCT machines, guided implant surgical systems, types of accuracy definitions, and study designs (retrospective or prospective), it is difficult to make comparisons, thus making it difficult to draw conclusions that can be extrapolated to all clinical scenarios.

For this, in vitro, ex vivo e in vivo studies and appropriate validation procedures need to be developed for evaluating the accuracy of navigated implant systems [131, 134–136], thus increasing their predictability.

In Vitro and Ex Vivo Experiments

As in any other automated system, guided implant surgery is not entirely perfect and is prone to minimal errors that can be magnified when protocols are not strictly followed [137]. Sources of these minimal errors can result in a total error, which can ultimately influence the final position of the implants and potentially cause surgical or prosthetic complications [138]. Separate presentation and quantification of technical and application-related implementation errors within

the process sequence appear to be difficult, and for that purpose, appropriate study designs shall be performed according to the key features:

- *Validation Procedures*—Serve for the illustration and quantification of deviations from the preoperatively planned to the postoperatively achieved implant positions. Angular and linear (coronal, apical, and depth) accuracy should be assessed as direct measurements or 3D superimposition software [56, 139–141].
- *Accuracy determination of digital planning procedure* [131]
  - *Image acquisition errors*—can be introduced with poor image quality, motion, or metal artifacts, thus the number of artifacts and deviation between models should be assessed.
  - *Image processing*—Data manipulation and merging procedures such as default or manual in different implant planning software can lead to underestimation or overestimation of direct measurements. Overall, maximum, and minimum deviation between CBCT and the digital model should be determined.
  - *Operator experience*—It could lead to accuracy differences when identifying anatomical landmarks. Inter- and Intra-operator variability must be performed to assess the experience factor when registration procedures occur.
  - *Edentulism type*—Total edentulism could result in different accuracy results during digital planning procedures due to a smaller number of recognizable structures (e.g., teeth) during superimposing protocols.
  - *Level of guidance*—Different levels of guided surgery protocols have been described from fully guided to guided osteotomy which in turn could interfere with the outcome. The type of guided surgery is determined during the digital planning procedure. The study design will be discussed in the guided surgery chapter.

In Vivo Studies
- *Clinical significance*—is related to the identification of safe distances from anatomical structures when inserting dental implants, to the category of patients who benefit the most from guided surgery and accuracy from computer-assisted planning to implant placement.
- *Outcomes definition*—When assessing in vivo accuracy, researchers should clearly define the study objectives and outcomes. Endpoints such as accuracy between navigated surgery, implant planning software, and free-hand implant placement or accuracy between different implant planning software or registration accuracy between virtual and CBCT models are some of the different clinically significant outcomes that could be evaluated.
- *Quality of Life and Effectiveness outcomes*—Future research should also aim at assessing stress reduction in the operating theatre, time-cost analysis, patient acceptance, and other quality of life or effectiveness outcomes.
- *Material and Methods description*—A clear description regarding subject characteristics (partially or totally edentulous), implant planning software surgical template manufacture, and accuracy method determination should be present in the material and methods section thus allowing for inter-study comparison.
- *Inter and intra-operator variability*—Since guided implant placement, accuracy depends on the cumulative errors of the different steps, researchers should try to avoid as many potentially confusing factors as possible, and thus operator variability should be assessed. The main problem for this type of design is the associated economic cost due to increased sample size, although it would mitigate the operator bias.
- *Biological variability*—confounding factors such as type of edentulism, jaw opening, saliva, blood, or other factors in clinical situations are present and must be taken into

account when performing sample size determination.

- *Sample Size*—To draw reliable conclusions studies should include a large number of patients based on a statistical sample size determination based on the cumulative possible errors and their magnitude in each procedural step.

20.3.2.2 Computer-Aided Design/ Computer-Aided Manufacturing (CAD/CAM) Technology

The growing development of additive/subtractive manufacturing technologies has opened up different applications in implant dentistry encompassing the "Scan, Plan, and Manufacture" principle of the digital workflow paradigm. Each part of this workflow is based on distinct technologies that should be evaluated regarding their accuracy-quality-effectiveness when compared with the current gold standard.

Even with the most optimal preoperative planning software, transfer to the surgical field still needs to achieve clinical and medico-legal acceptable accuracy. Several options are available for such a transfer: computer-guided surgery (static) surgery; or computer-navigated (dynamic) surgery [142]. For computer-guided surgery, a static surgical guide is used that transfers the virtual implant position from computed tomography data to the surgical site.

Additive manufacturing has been commercially available for nearly 30 years when the process known as stereolithography was patented. Since then, several manufacturing options have been proposed leading to the development of digital manufacturing of models, guides, and medical devices.

More recently, the application of CAD/CAM technology in bone regeneration for implant dentistry has been proposed with the use of customized bone blocks based on the pre-surgical planning stage [143–148]. According to these authors, the precise fitting manufacture would allow enhanced physical contact between graft and recipient site, a decrease in time spent in sur-

gery associated with a reduction in the risk of graft infection by a smaller number of manual interactions.

Since bone regeneration study design assessment is addressed in a different chapter, from the digital approach we maintain that outcomes such as fitting between graft and recipient site, surgery duration, and patient quality of life outcomes should be assessed upon validation of the proposed CAD-CAM procedure.

In Vitro Studies
They are important for validation purposes and to assess the role of collateral events.

Validation Procedures—Serve to illustrate and quantify deviations from different additive or subtractive manufacturing procedures. Angular and linear (coronal, apical, and depth) accuracy should be assessed as direct measurements or 3D superimposition software [56, 134, 140, 141].

Confounding factors—error sources from CBCT scans, intraoral scans, software or human manipulation should be reduced or eliminated in order to properly assess manufacturing differences [149].

Manufacturing precision assessment—when determining manufacturing accuracy, researchers should use in vitro and animal studies before human studies in order to reduce human exposure to intervention studies. As such, different guides should be manufactured from the index model and deviations in the internal geometry of the implant sleeves evaluated [150].

20.3.3 Guided Implant Surgery

Prosthetically driven implant surgery has been a subject of fundamental interest in the implant dentistry field. Correct implant positioning highlights obvious advantages, such as favorable aesthetic, prosthetic, and biomechanical outcomes with the long-term stability of peri-implant hard and soft tissues [151, 152].

The introduction of CBCT and surgical planning software strongly supports the justification for three-dimensional-based pre-surgical plan-

ning [7, 56, 77]. When a planned prosthesis is incorporated into these computed tomography images, the planning can take into account both the bone anatomy and the planned superstructure.

In recent years, several options have been proposed to transfer planning to the surgical field, although studies regarding clinical and medico-legal acceptable accuracy are still lacking [9, 142]. Two major techniques can be considered: Static and dynamic guidance, which present different technological principles although with the same objective which is to increase implant placement accuracy with high levels of reproducibility.

20.3.3.1 Static Guidance

For computer-guided surgery, a static surgical guide is used that transfers the virtual implant position from the surgical planning software to the surgical site. The templates can be produced by computer-aided design/computer-assisted manufacturing technology by additive methods such as 3D printing or subtractive methods such as milling or, manually, in a dental laboratory (using mechanical positioning devices or drilling machines) (Fig. 20.10) [18, 150, 153].

Several methods for identifying ideal tooth position have been proposed, from copying the prosthesis in radiopaque resin, to double-scan

Fig. 20.10 Fully guided surgery for full arch rehabilitation

procedures, or from 3D images obtained from an intra-oral scanner.

Regardless of the described method, accuracy and reproducibility outcomes should be assessed, mainly angular and linear deviations between planned and placed implants.

In addition, from a pragmatic perspective, a comparison with the currently most used techniques (implant software planning and free-hand placement) should be addressed when performing accuracy studies, since deviations between the preoperative and the post-operative implant location may lead to important clinical consequences [154–159].

20.3.3.2 Dynamic Implant Guidance

Dynamic navigation systems have been developed to guide the placement of dental implants in real time by the computer, based on information generated from the patient cone beam scan and the surgeon's virtual implant planning. This can overcome some of the above-mentioned limitations of static implant guidance, such as the reduced ability to change implant selection, placement, angulation, or depth during the intra-operative procedure to achieve a clinically better implant position [139, 160, 161]. The physical dimensions of the static guide may also prevent use in the second molar regions or in patients with restricted openings. Thus, a real-time system that coordinates the surgeon's hands and eyes by means of 3-dimensional visualization of the preparation with high magnification could be considered a promising technology, although certain challenges, such as cost and accuracy, remain to be addressed.

20.3.3.3 Study Design to Evaluate Accuracy in Guided Implant Placement

When assessing accuracy in guided implant placement, deviations between the planned and actual implant position which might occur at any stage in the treatment should be taken into account: in CBCT and/or intra-oral scanning, in the transfer of the planning data, in the manufacturing of the surgical template, in positioning the surgical guide [158, 162, 163], and while implant placement [18,

164–166]. In addition, depending on whether researchers want to address a specific topic or the clinical objective (implant placement), in vitro, ex vivo, or clinical trials are of value.

In Vitro

These studies can constitute the first step when assessing a new surgical template or a new dynamic guidance system since they enable the best control of confounding factors such as operator experience, CBCT quality, or manufacturing distortion.

When preparing for an in vitro study, researchers should consider the following key features:

Validation Procedures—They serve to illustrate and quantify deviations between the clinical and software-planned position of dental implants. Angular and linear (coronal, apical, and depth) accuracy should be assessed as direct measurements or 3D superimposition software with root mean square values (Fig. 20.11) [56, 134, 140, 141, 167].
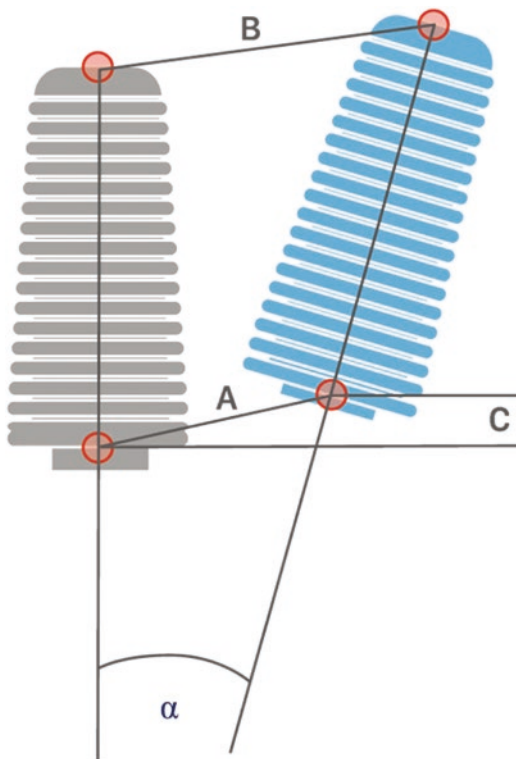
Fig. 20.11 Three-dimensional evaluation of the virtual planned and the placed implants. A= coronal; B= apical; C= depth; α= angle

Confounding factors—Depending on the study objective, and to be able to mitigate confounding factors, such as manufacturing interference, different templates shall be manufactured from the index implant planning model and deviations in the internal geometry of the implant sleeves evaluated [150, 168].

Inter-groups comparisons—When using in vitro studies to compare different systems, an index model appears to be helpful, and inter-group variability must be assessed.

Inter and intra-operator assessment—Researchers should evaluate the operator influence in the implant placement, and for that, intra- and inter-operator variability should be assessed since it is a known factor for result interference [169, 170].

In Vivo

When preparing an in vivo study, researchers shall consider the following key features:

- *Pragmatic*—studies should compare the accuracy of Guided Implant placement with the implant placement gold standard (CBCT planning and freehand placement) within values that can are clinically significant [171, 172]. Safe distances from vital anatomical structures should also be checked as well as implant survival, bone loss, and clinical complications (surgical and prosthetic) [94].
- *Outcomes definition*—When assessing in vivo accuracy, researchers should clearly define the study objectives and outcomes. Endpoints such as accuracy can be defined as angular and linear deviations between planned and placed implants and assessed by superimposition methods with as dicom or stl files [161, 173–177].
- *Material and Methods description*—A clear description regarding subject characteristics, template support, implant placement, type of manufacturing, implant characteristics and position, reference model, and accuracy method determination should be present in the material and methods section, thus allowing for inter studies comparisons.
- *Inter and intra-operator variability*—While using digital systems for implant placement

there is a learning curve that could interact with the implant placement accuracy and because of this the intra and inter-operator variability should be evaluated. The main problem for this type of design is the associated economic cost although it would mitigate the operator or device bias.

• *Biological variability*—confounding factors such as jaw opening, saliva, blood or other factors in clinical situations are present and should thus be taken into account when performing sample size determination [178].

20.4   Computer-Assisted Rehabilitation

20.4.1 CAD-CAM Restorations, Abutments, and Superstructures

Digital implant prosthodontics in routine dental practice is seldom with a fully digital workflow, being some of the individual work steps mostly undertaken by conventional procedures [179–181].

Nowadays the growing field of implant-impression procedures is related to the use of intraoral optical scanners and computer-assisted design/computer-assisted manufacturing of superstructures, restorations, or/and abutments [179, 182, 183].

For implant-supported restorations due to reduced mobility of dental implants [184], the passive fit is critical when compared to teeth-supported rehabilitations [185].

Although the passive fit is difficult to describe we could consider it as an accuracy parameter that does not cause long-term clinical complications which according to some authors corresponds to discrepancies below 150 μm [96, 186].

In contrast, others put this threshold, between 50 and 75 μm [95, 97, 187], although there is a consensus among several authors that marginal openings below 120 μm are clinically acceptable [188–193]. As these numbers include the cumulative errors of the different working steps in the final implant-supported restoration, when performing studies regarding an individual step, the discrepancies should be lower than the overall threshold.

Different means of fabrication are applicable for treatment with implant-supported fixed dental prostheses: a conventional, a mixed conventional-digital approach, using a technical concept of framework plus veneering, or, in contrast, full-contour, monolithic restorations which in some cases can be performed fully digitally (Fig. 20.12) [179, 180, 182, 194–197].

Like CAD/CAM crown fabrication, there are two digital workflows used in fabricating a custom abutment. In the first, a conventional impression is made to fabricate a master cast which in turn is scanned using a desktop scanner and in the second, a digital impression is made using scan bodies to obtain the digital master cast [198].

When evaluating study design in CAD-CAM restorations we should consider the two major steps where discrepancies might take place: Data acquisition and computer-assisted milling.

20.4.1.1 Data Acquisition in Computer-Assisted Restorations

Digital implant impressions are challenging, with multiple implant scanning presenting accuracy problems when compared to single units, arising from error accumulation throughout the digital workflow. Factors such as lack of landmarks, scan body design, scanned surface characteristics, sensor size, scanning strategy, software, and other variables can affect accuracy. Although, the clinically acceptable level of misfit of the implant-supported restoration according to previous studies should not exceed 120 μm, we maintain that the acceptable level of misfit relates to the extent of the implant-supported restorations, thus creating additional problems when wanting to standardize the cut-off point of clinical significance [117].

Study design for data acquisition should follow the principles previously stated in Sect. 20.3.1.2.
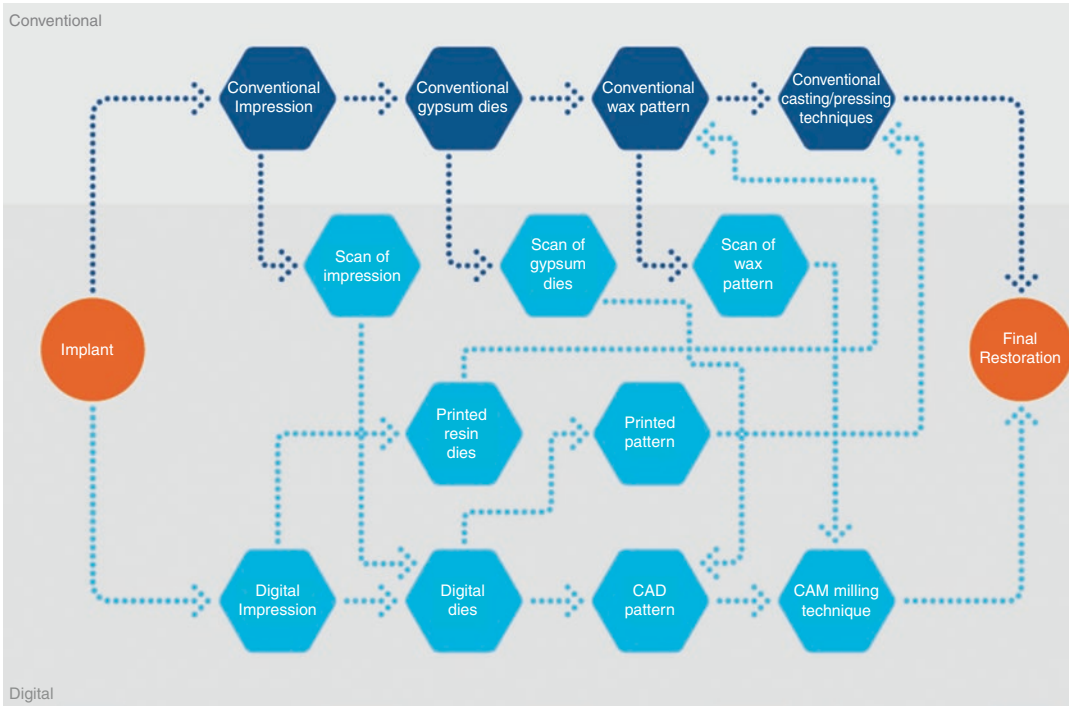
Fig. 20.12 Workflow combinations between digital and conventional manufacture of implant-supported rehabilitations

20.4.1.2 Computer-Assisted Milling

CAD/CAM of implant abutment and/or framework is much simpler and requires less technical time and involvement in comparison to the lost wax/casting protocol.

When performing studies in this area it is decisive to follow a standardized technical approach and comply with the ISO 12836 [2], assessing the accuracy of the milling devices used according to standard protocols, or following a clinical perspective of accuracy utilizing the 120 μm discrepancy threshold for different manufacturing technologies and durability of different materials.

20.4.1.3 In Vitro Study Design

As stated earlier, milling is anticipated to eliminate the lost wax and casting of prostheses, which is assumed will improve the overall precision. However, milling accuracy is not only dictated by the milling process itself but also by materials properties, with higher material hardness corre-

sponding to lower machinability and more uncontrolled forces [199–201]. As such, milling is a process with different intervening factors that can influence the clinical accuracy outcome of implant restorations and should be assessed according to specific study designs [202].

In vitro studies must be considered as the first step in assessing a new implant restoration manufacturing process since they allow for the control of most confounding factors.

When preparing for an in vitro study, researchers shall consider the following key features:

- *Outcomes to assess*—depending on the objective, researchers can propose the evaluation of the accuracy, dimensional distortions, durability, and wear of different milled materials
  - *Accuracy (precision of fit)*—Vertical, horizontal, and occlusal misfit should be determined by a proven method such as stereomicroscopy, X-ray micro-computed tomography, coordinate measuring or by

means of a video measurement machine or even a scanning electron microscope.

- *Dimensional distortions*—implant framework misfit is a result of accumulated distortions that occurred during the clinical and laboratory steps. While performing in vitro studies dimensional distortion between a digitally planned implant framework or restoration and the obtained physical analog can be assessed with the help of calibrated industrial computed tomography or scanner, conversion to STL files, and volumetric quality assessment software.
- *Materials load and Wear behaviors*—milled materials behavior should be determined by standardized methods. Specific methodology regarding material proprieties will not be discussed here as this is not the chapter's objective.
- *Stress distribution*—load distribution over bone tissue from different framework materials could influence implant survival rate. For this, in vitro finite element analysis can be used.

- *Material and Methods description*—Depending on the variables to assess a clear description regarding the reference model, scanner specifications, type of manufacturing and intrinsic accuracy, implant characteristics and position, and accuracy method determination should be present thus allowing inter studies comparison. Additionally, sample size determination and power analysis should be reported.
- *Confounding factors*—Depending on the study objective, and in order to mitigate confounding factors, such as impression interference, different frameworks should be manufactured from the index implant model and deviations evaluated.
- *Intra- and Inter-groups comparisons*—When comparing different manufacturing systems or materials intra- and inter-group variability should be assessed.

20.4.1.4 In Vivo Study Design

In vivo study design should focus on important clinical outcomes such as long-term biological and prosthetic complications, patient-centered and cost-effective outcomes.

When preparing an in vivo study, researchers should take into account the following key features:

- *Pragmatic vs Explanatory Trial*—Clinical trials design could have a different focus depending on the study objectives.
  - *Pragmatic design*—randomized trials that aim to compare the effectiveness of two or more interventions in real-world settings [203]. Trials should be designed to inform clinicians regarding the comparative balance of benefits, burdens, and risks of the intervention at the level of the individual or general population [204]. Outcomes such as long-term biological or prosthetic complications and patient-centered or cost-effective outcomes should be addressed [205]. This type of trial requires a more complex design and is not suitable for early trials that aim to explore the accuracy of a new manufacturing technique or material [206].
  - *Explanatory design*—The use of standardized protocols according to previously described checklists decreases the risk of selection, performance, detection, and attrition bias, thus increasing internal validity by allowing for an unbiased distribution of confounding factors between groups. This type of design aims to investigate whether a manufacturing technique or material could work under ideal conditions.
- *Outcomes definition*—When assessing in vivo clinical performance, researchers should clearly define the study objectives and outcomes. Endpoints such as biological complications (implant survival/success, peri-implantitis, marginal bone loss, etc.), mechanical complications (prostheses survival/success, ceramic chipping, decementation, framework fracture, etc.), peri-implant mucosa, and aesthetic assessment should be determined by proven methods.
- *Material and Methods description*—A clear description regarding subject characteristics (partially or totally edentulous, parafunctional

habits), implant characteristics and position, impression technique and materials (conventional or digital), type of prostheses manufacturing, prostheses type (screw or cement-retained), materials (metal ceramic, zirconia-ceramic, monolithic zirconia, full ceramic, etc.), and outcomes determination should be present in the material and methods section thus allowing for inter studies comparison.

- *Survival/Success analysis*—For survival/success rate analysis a Kaplan-Meier approach should be used, as well as the Cox proportional hazards model for analysis of predictor variables. Sample size determination should be addressed in this section [207–209].
- *Inter and intra-operator variability*—Clinical and laboratory procedures, even following a standardized protocol, have an intrinsic operator variability and for this purpose, the intra and inter-operator variability should be evaluated. The main problem for this type of design is the associated economic cost although it would mitigate the operator or device bias.

20.4.2 Monitoring Occlusion, Parafunction, and Orthofunction

Dental occlusion is an important aspect of implant dentistry since the biomechanics in implant-supported prostheses differ from tooth-supported occlusion. Nowadays with the increase of available clinical digital technologies, we can track the kinetics of the mandible and the condyles with digital models, thus allowing for control of the occlusal function.

Recent attempts to establish guidelines for the use of digital devices for studying occlusion functions have been published in terms of examination protocol [210] and for diagnosis of parafunction [211].

It is expected that in the following years studies of these new devices in relation to occlusion accuracy, parafunctional diagnostic potential, and ability to assess wear will be needed.

20.4.2.1 Digital Articulators, Facebows, and Jaw-Tracking Devices

Although the evolution of digital technology continues to improve patient data acquisition, the ability to both standardize the recording of the maxillary occlusal plane and capture the necessary dynamic data for dento-facial analysis remains elusive. In the last years, several devices have been described, mostly in case reports [212–218] where by the use of different methods the maxillary surface model is located in its skull-related position in a virtual dental space and in this coordinate system, electronically recorded mandibular movements can be used for dynamic occlusal analysis [212, 219–225].

Currently, most of the commercially available CAD/CAM systems provide a virtual articulator simulator, being the main problem in transferring the data from the patient to the simulator.

Studies that compare the accuracy of digital articulators' occlusion and dynamic movements with conventional methods are necessary to develop standard methodologies to be part of everyday clinical practice [210, 226].

In vitro studies are the first step in assessing new digital technologies since they allow for the control of most confounding factors.

In Vitro Study Design
Key features to be considered when designing an in vitro study to evaluate digital articulators' accuracy:

- *Outcomes definition*—Precision and trueness should comply with ISO definitions when evaluating the diagnostic accuracy of digital articulators. Depending on study objectives, repeatability, reproducibility, and dispersion measures could also be considered [104].
- *Methods standardization*—The methods should describe how the outcomes were measured, the reference models and scanner characteristics and the conventional and digital methods for occlusion acquisition and comparison. Several methodologies have been proposed from a comparison of spatial dis-

tances in occlusion points between methods [225], agreement of interocclusal contacts [227], areas of occlusion [228], receiver-operator curves [228] or condylar inclination and bennet angles [229].

- *Validation of Accuracy Method*—Researchers using digital technologies should validate and evaluate the reliability of the method used for accuracy determination.
- *Operator and equipment variance*—Most studies consider operator variance but very few address the possibility of variance between identical pieces of equipment.

In Vivo Study Design

In vivo study design should focus on important clinical outcomes such as long-term biological and prosthetic complications, and patient-centered and cost-effective outcomes.

When preparing an in vivo study, researchers should take into account the following key features:

- *Pragmatic*—Studies should compare the accuracy of these new devices/technologies with a gold standard within values that can have clinical significance.
- *Outcomes definition*—When assessing in vivo accuracy, researchers should clearly define the study objectives and outcomes. Endpoints such as accuracy between conventional and digital articulators should be defined.
- *Material and Methods description*—A clear description regarding subject characteristics (partially or totally edentulous), analogic and digital acquisition method and accuracy method determination should be present in the material and methods section thus allowing for inter studies comparisons.
- *Inter and intra-operator variability*—While using the jaw tracking devices and digital articulators presents a learning curve that could interact with accuracy determination. When performing in vivo studies, we should take into account patient intra-variability and researchers should ideally evaluate at least three different records per patient per method to mitigate patient confounding factors.

- *Sample Size*—To draw reliable conclusions studies should include a large number of patients based on a statistical sample size determination taking into account possible attrition bias.

20.4.3 Virtual Dental Patients: Digital Superimposition Techniques

For more than a century, analogic and digital techniques have been developed to analyze facial characteristics [230–232]. Facial scanning in association with intraoral scan and bone anatomy imaging allows the reproduction of the static 3D virtual patient and it is expectable that in the forthcoming years, we will be able to bring together the additional technologies to create the 4D dynamic virtual patient. Healthcare providers, patients, and educators will benefit from this further development in dental medicine, but for that, the successful fusion of intraoral and facial surfaces with dynamic occlusion movements combined with skeletal anatomy imaging is necessary [215, 233].

The first step while developing groundbreaking technologies or methodologies should be by developing feasibility studies to assess the practicality of the proposed method or system. They should be used to estimate important parameters that are needed to design the main study, mainly [234]:

- *Outcomes definition*—feasibility studies might involve designing a suitable outcome measure or characteristics of the proposed outcome. Endpoints such as accuracy between planned and obtained results should be defined.
- *Sample size*—standard deviation of the outcome measured to be able in some cases to estimate sample size.
- *Participants*—estimate the number of eligible participants and willingness of clinicians to recruit participants and of participants to be randomized.
- *Time*—needed to collect and analyze data.

- *Methodology*—methods to superimpose and fuse files from different technologies should be evaluated for repeatability and accuracy.

20.5 Critical Appraisal of Flagship Results from the Literature Related to Specific Methodologies and Outcomes

20.5.1 Computer-Guided Implant Placement

Historically, freehand implant placement is still the technique most often used amongst clinicians, where execution of the treatment plan is guided by mental navigation [170] which inevitably leads to inaccuracies in implant positioning. Several factors can intervene in the accuracy level such as operator experience, single- or multiple implant placement, and angulated implants between others. With the increasing demand over recent years for more appropriate implant positioning, tools for computer-guided implant placement have been regularly reported in the literature: robots, static and dynamic guidance. Although robots are accurate tools in the transfer of the treatment plan to patients, due to their high cost and low availability they are still in the research phase and not in standard clinical use. In relation to static and dynamic guidance, considering all the possible confounding factors and limited scientific evidence, the results suggest:

- *Guided surgery vs freehand implant placement*—Guided surgery leads to similar implant survival rates to conventional freehand protocols in single implant placement with reliable implant positioning, favorable clinical outcomes, and asthetics. A tooth-supported template for the treatment of single missing teeth results in greater accuracy of implant positioning than with mucosa-supported or bone-supported templates. Long-term clinical trials are needed in partially edentate patients for clinical perfor-

mance, patient-centered and cost-effective outcomes [235].
- *Static vs dynamic guidance*—Initial data suggests similar accuracy between systems and higher accuracy than freehand placement [164].
- *Full-guided surgery vs. half-guided surgery*—full-guided implant surgery showed significantly less horizontal coronal deviation for cadaver studies, significantly less horizontal apical deviation for clinical studies, and significantly less angular deviation for both clinical and cadaver studies [236].
- *Tissue support*—The bone-supported guides presented a statistically greater significant deviation in angle, entry point, and apex when compared to the tooth-supported guides. Between the mucosa- and tooth-supported guides, there were no statistically significant differences for any of the outcome measures, although with a favorable trend in the tooth-supported guides with minor deviations [162].
- *Patient-reported outcome measures and experiences*—Conventional and guided surgery obtained a similar post-operative level of patient satisfaction, analgesic intake, edema, and pain. Nevertheless, the economic effects in terms of time efficiency and treatment costs need well-designed RCTs with standardized parameters [237, 238].

20.5.2 Digital Implant Impression Procedures

Implant-supported prostheses fit relies on several factors, one of the most important being the accuracy of the impressions. Several systematic reviews addressing the accuracy of conventional techniques have been published in recent years with results favoring direct to indirect impressions and splinted over non-splinted techniques, particularly with an increased number of implants [239–241]. To reduce some of the disadvantages of the conventional techniques (patient discomfort, uncontrolled variables during the different individual variables, and expensive laboratory

and chair time), digital impressions have been proposed as a viable alternative for tooth- and implant-impressions. Additionally, in the last years, the use of photogrammetry for complete-arch implant impression has been proposed as a viable option although with contradictory results between studies [242–245].

To date, there is scarce evidence available regarding digital implant impressions with several case reports but few published in vivo studies. Based on the limited evidence available, results suggest [116–118, 246].

- *Outcomes definition*—Trueness and precision definitions should be standardized according to ISO requirements.
- *Digital vs conventional impressions*—Digital implant impressions may offer a valid alternative with accuracy within the clinically accepted values for single- and multi-unit implant-supported restorations.
- *In vivo vs In vitro conditions*—Clinical factors such as operator experience, patient movement, saliva, blood, soft tissues, scanning location, size of edentulous area, implant angulation, distance, and depth are factors that could interfere with in vivo accuracy studies.
- *Edentulous Area*—Based on the available data, and while presenting promising in vitro results in single and short-span implant restorations, in vivo studies should be performed to evaluate the clinical accuracy of these devices. For full-arch implant restorations, it seems that nowadays the conventional impressions are still more predictable when compared to intra-oral scanners acquisition.
- *Fast-paced technology*—Due to constant changes in the software and hardware, reliable, and standardized methodology should be used to compare accuracies and provide guidelines.
- *Patient-centered and time-effectiveness outcomes*—Based on preliminary data it seems as if digital techniques emerge as the most favored according to patient-centered outcomes and are more time-effective compared to conventional impressions [179, 247–252].

20.5.3 CAD/CAM Implant Dental Restorations

20.5.3.1 Milling

The CAD/CAM production process uses either direct or indirect digitalization, enabling the design, analysis, and manufacture (additive or subtractive) of crowns by means of a computer. Considering the variety of restorative materials and CAD and/or CAM systems studied and that the vast majority of available studies are in vitro, results suggest [202, 253]:

- The performance of a CAD-CAM system relative to marginal adaptation is influenced by the restorative material.
- Most of the comparative studies involving CAD/CAM dental restorations or infrastructure showed results within the clinically acceptable range.
- No clear conclusions can be drawn relative to marginal adaptation on the superiority of CAD/CAM milling technology as opposed to the casting technique and direct metal laser sintering processes.
- CAD-CAM implant restorations have shown promising results in the short-term, although with limited quality studies and the paucity of data on long-term clinical outcomes of 5 years or more [254, 255].

20.6 Expert Opinion: Main Outcomes to Assess/Achieve in the Next Years—Expected Breakthroughs

A technological revolution in the implant dentistry field has been brought about in recent decades with the introduction of a new concept in clinical practice known as "digital workflow". It is foreseen that with the increasing accuracy of these digital systems, we will achieve a full digital workflow from planning through to prosthesis placement in all types of implant-supported rehabilitations (single, partial, or full arch) in the near future.

However, there is still room for improvement in some areas where further breakthroughs are expected. For example, the diagnostic ability of 3D systems to integrate CBCT exams and intra-oral scanners still lack the quality to provide clinically predictable outcomes in full arch implant-supported rehabilitations.

We also expect in forthcoming years to witness major breakthroughs in algorithm software for CBCT scans and intraoral scanners, thus improving digital implant placement accuracy. The use of infrared or ultrasound systems in intra-oral scanners has also been described in the scientific literature with promising results, thus overcoming one of the major disadvantages of intra-oral scanners (infragengival preparations). The use of photogrammetry for full-arch is expectable to overcome conventional impression accuracy being the superimposition with intra-oral scanner soft tissue relationship an advantage. In the last years, some systems have been described to render the patient's functional dynamic occlusion in the virtual world, and we expect that following method validation we could have the final missing component to a fully predictable digital workflow.

When comparing static and dynamic guided surgery, both systems have already provided results with clinical significance with the expectation that in forthcoming years we will see affordable systems with a higher degree of accuracy.

In prosthesis manufacture the degree of accuracy for the milling systems is already comparable or even better than the conventional methods. We believe that the future will be centered on additive methods such as 3D printing, not only because of efficient material usage but also layering control in the range of microns, thus providing much higher degrees of accuracy.

We are convinced that the digital world has now arrived in the field of implant dentistry and that the next decade will see a paradigm shift in the way treatment is planned and executed with digital technologies bringing in a new era of quality, precision, and predictability.

References

1. Joda T, Bornstein MM, Jung RE, Ferrari M, Waltimo T, Zitzmann NU. Recent trends and future direction of dental research in the digital era. Int J Environ Res Public Health. 2020;17(6):1987. https://doi.org/10.3390/ijerph17061987.
2. ISO 12836:2015: dentistry—Digitizing devices for CAD/CAM systems for indirect dental restorations—Test methods for assessing accuracy. Switzerland: ISO Copyright Office; 2015.
3. Alghazzawi TF. Advancements in CAD/CAM technology: options for practical implementation. J Prosthodont Res. 2016;60(2):72–84. https://doi.org/10.1016/j.jpor.2016.01.003.
4. Jokstad A. Computer-assisted technologies used in oral rehabilitation and the clinical documentation of alleged advantages - a systematic review. J Oral Rehabil. 2017;44(4):261–90. https://doi.org/10.1111/joor.12483.
5. Tahmaseb A, Wismeijer D, Coucke W, Derksen W. Computer technology applications in surgical implant dentistry: a systematic review. Int J Oral Maxillofac Implants. 2014;29(Suppl):25–42. https://doi.org/10.11607/jomi.2014suppl.g1.2.
6. Unkovskiy A, Unkovskiy N, Spintzyk S. A virtual patient concept for esthetic and functional rehabilitation in a fully digital workflow. Int J Comput Dent. 2021;24(4):405–17. Retrieved from https://www.ncbi.nlm.nih.gov/pubmed/34931776.
7. Vercruyssen M, Laleman I, Jacobs R, Quirynen M. Computer-supported implant planning and guided surgery: a narrative review. Clin Oral Implants Res. 2015;26(Suppl 11):69–76. https://doi.org/10.1111/clr.12638.
8. Khachatryan V, Sirunyan AM, Tumasyan A, Adam W, Bergauer T, Dragicevic M, et al. Search for displaced supersymmetry in events with an electron and a muon with large impact parameters. Phys Rev Lett. 2015;114(6):061801. https://doi.org/10.1103/PhysRevLett.114.061801.
9. Vercruyssen M, Hultin M, Van Assche N, Svensson K, Naert I, Quirynen M. Guided surgery: accuracy and efficacy. Periodontol 2000. 2014;66(1):228–46. https://doi.org/10.1111/prd.12046.
10. Afshari FS, Sukotjo C, Alfaro MF, McCombs J, Campbell SD, Knoernschild KL, Yuan JC. Integration of digital dentistry into a predoctoral implant program: program description, rationale, and utilization trends. J Dent Educ. 2017;81(8):986–94. https://doi.org/10.21815/JDE.017.050.
11. Brownstein SA, Murad A, Hunt RJ. Implementation of new technologies in U.S. dental school curricula. J Dent Educ. 2015;79(3):259–64. Retrieved from http://www.ncbi.nlm.nih.gov/pubmed/25729019.
12. Douglas RD, Hopp CD, Augustin MA. Dental students' preferences and performance in crown design:

conventional wax-added versus CAD. J Dent Educ. 2014;78(12):1663–72. Retrieved from http://www.ncbi.nlm.nih.gov/pubmed/25480282.

13. Papaspyridakos P, Chen CJ, Chuang SK, Weber HP. Implant loading protocols for edentulous patients with fixed prostheses: a systematic review and meta-analysis. Int J Oral Maxillofac Implants. 2014;29(Suppl):256–70. https://doi.org/10.11607/jomi.2014suppl.g4.3.

14. ISO 18739: dentistry — Vocabulary of process chain for CAD/CAM systems.. Switzerland: ISO Copyright Office; 2016.

15. ISO/TR 18845 : dentistry — Test methods for machining accuracy of computer- aided milling machines. Switzerland: ISO Copyright Office; 2017.

16. ISO 5725-1: accuracy (trueness and precision) of measurement methods and results — Part 1: general principles and definitions. Switzerland: ISO Copyright Office; 1994.

17. Aragon ML, Pontes LF, Bichara LM, Flores-Mir C, Normando D. Validity and reliability of intraoral scanners compared to conventional gypsum models measurements: a systematic review. Eur J Orthod. 2016;38(4):429–34. https://doi.org/10.1093/ejo/cjw033.

18. D'Haese J, Van De Velde T, Komiyama A, Hultin M, De Bruyn H. Accuracy and complications using computer-designed stereolithographic surgical guides for oral rehabilitation by means of dental implants: a review of the literature. Clin Implant Dent Relat Res. 2012;14(3):321–35. https://doi.org/10.1111/j.1708-8208.2010.00275.x.

19. Haralur SB, Saad Toman M, Ali Al-Shahrani A, Ali Al-Qarni A. Accuracy of multiple pour cast from various elastomer impression methods. Int J Dent. 2016;2016:7414737. https://doi.org/10.1155/2016/7414737.

20. Hoyos A, Soderholm KJ. Influence of tray rigidity and impression technique on accuracy of polyvinyl siloxane impressions. Int J Prosthodont. 2011;24(1):49–54. Retrieved from http://www.ncbi.nlm.nih.gov/pubmed/21210004.

21. Jamshidy L, Mozaffari HR, Faraji P, Sharifi R. Accuracy of the one-stage and two-stage impression techniques: a comparative analysis. Int J Dent. 2016;2016:7256496. https://doi.org/10.1155/2016/7256496.

22. Amin S, Weber HP, Finkelman M, El Rafie K, Kudara Y, Papaspyridakos P. Digital vs. conventional full-arch implant impressions: a comparative study. Clin Oral Implants Res. 2016. https://doi.org/10.1111/clr.12994

23. da Silva Marques DN, Aparicio Aguiar Alves RV, Marques Pinto RJ, Bartolo Carames JR, de Oliveira Francisco HC, Mendez Carames JM. Facial scanner accuracy with different superimposition methods - In vivo study. Int J Prosthodont. 2021;34(5):578–84. https://doi.org/10.11607/ijp.7253.

24. Ender A, Mehl A. Accuracy in dental medicine, a new way to measure trueness and precision. J Vis Exp. 2014;(86):51374. https://doi.org/10.3791/51374.

25. Mack S, Bonilla T, English JD, Cozad B, Akyalcin S. Accuracy of 3-dimensional curvilinear measurements on digital models with intraoral scanners. Am J Orthod Dentofacial Orthop. 2017;152(3):420–5. https://doi.org/10.1016/j.ajodo.2017.05.011.

26. da Silva Marques DN, Marques Pinto RJ, Alves R, Baratieri LN, da Mata A, Carames JMM. Soft tissue replication in single unit implant impressions- A three dimensional clinical study. J Esthet Restor Dent. 2019;31(4):359–68. https://doi.org/10.1111/jerd.12481.

27. Goracci C, Franchi L, Vichi A, Ferrari M. Accuracy, reliability, and efficiency of intraoral scanners for full-arch impressions: a systematic review of the clinical evidence. Eur J Orthod. 2016;38(4):422–8. https://doi.org/10.1093/ejo/cjv077.

28. Kuhr F, Schmidt A, Rehmann P, Wostmann B. A new method for assessing the accuracy of full arch impressions in patients. J Dent. 2016;55:68–74. https://doi.org/10.1016/j.jdent.2016.10.002.

29. Chiappelli F. Fundamentals of evidence-based health care and translational science. Heidelberg: Springer-Verlag; 2014.

30. Barkhordarian A, Pellionisz P, Dousti M, Lam V, Gleason L, Dousti M, et al. Assessment of risk of bias in translational science. J Transl Med. 2013;11:184. https://doi.org/10.1186/1479-5876-11-184.

31. Lohr KN, Carey TS. Assessing "best evidence": issues in grading the quality of studies for systematic reviews. Jt Comm J Qual Improv. 1999;25(9):470–9. Retrieved from http://www.ncbi.nlm.nih.gov/pubmed/10481816.

32. Faggion CM Jr. Animal research as a basis for clinical trials. Eur J Oral Sci. 2015;123(2):61–4. https://doi.org/10.1111/eos.12175.

33. Festing MF, Altman DG. Guidelines for the design and statistical analysis of experiments using laboratory animals. ILAR J. 2002;43(4):244–58. Retrieved from https://www.ncbi.nlm.nih.gov/pubmed/12391400.

34. Kilkenny C, Browne WJ, Cuthill IC, Emerson M, Altman DG. Improving bioscience research reporting: the ARRIVE guidelines for reporting animal research. PLoS Biol. 2010;8(6):e1000412. https://doi.org/10.1371/journal.pbio.1000412.

35. Thoma DS, Martin IS, Muhlemann S, Jung RE. Systematic review of pre-clinical models assessing implant integration in locally compromised sites and/or systemically compromised animals. J Clin Periodontol. 2012;39(Suppl 12):37–62. https://doi.org/10.1111/j.1600-051X.2011.01833.x.

36. Moher D, Hopewell S, Schulz KF, Montori V, Gotzsche PC, Devereaux PJ, et al. CONSORT 2010 explanation and elaboration: updated guidelines for

reporting parallel group randomised trials. BMJ. 2010;340:c869. https://doi.org/10.1136/bmj.c869.

37. Noah N. The STROBE initiative: STrengthening the Reporting of OBservational studies in Epidemiology (STROBE). Epidemiol Infect. 2008;136(7):865. https://doi.org/10.1017/S0950268808000733.

38. Rogozinska E, Khan K. Grading evidence from test accuracy studies: what makes it challenging compared with the grading of effectiveness studies? Evid Based Med. 2017;22(3):81–4. https://doi.org/10.1136/ebmed-2017-110717.

39. Bossuyt PM, Reitsma JB, Bruns DE, Gatsonis CA, Glasziou PP, Irwig L, et al. STARD 2015: an updated list of essential items for reporting diagnostic accuracy studies. BMJ. 2015;351:h5527. https://doi.org/10.1136/bmj.h5527.

40. Moher D, Liberati A, Tetzlaff J, Altman DG, PRISMA Group. Preferred reporting items for systematic reviews and meta-analyses: the PRISMA statement. BMJ. 2009;339:b2535. https://doi.org/10.1136/bmj.b2535.

41. Whiting P, Savovic J, Higgins JP, Caldwell DM, Reeves BC, Shea B, et al. ROBIS: a new tool to assess risk of bias in systematic reviews was developed. J Clin Epidemiol. 2016;69:225–34. https://doi.org/10.1016/j.jclinepi.2015.06.005.

42. Sarkis-Onofre R, Cenci MS, Demarco FF, Lynch CD, Fleming PS, Pereira-Cenci T, Moher D. Use of guidelines to improve the quality and transparency of reporting oral health research. J Dent. 2015;43(4):397–404. https://doi.org/10.1016/j.jdent.2015.01.006.

43. Han S, Olonisakin TF, Pribis JP, Zupetic J, Yoon JH, Holleran KM, et al. A checklist is associated with increased quality of reporting preclinical biomedical research: a systematic review. PLoS One. 2017;12(9):e0183591. https://doi.org/10.1371/journal.pone.0183591.

44. Hopewell S, Dutton S, Yu LM, Chan AW, Altman DG. The quality of reports of randomised trials in 2000 and 2006: comparative study of articles indexed in PubMed. BMJ. 2010;340:c723. https://doi.org/10.1136/bmj.c723.

45. Leow NM, Hussain Z, Petrie A, Donos N, Needleman IG. Has the quality of reporting in periodontology changed in 14 years? A systematic review. J Clin Periodontol. 2016;43(10):833–8. https://doi.org/10.1111/jcpe.12572.

46. Tonetti M, Palmer R, Working Group 2 of the VIII European Workshop on Periodontology. Clinical research in implant dentistry: study design, reporting and outcome measurements: consensus report of Working Group 2 of the VIII European Workshop on Periodontology. J Clin Periodontol. 2012;39(Suppl 12):73–80. https://doi.org/10.1111/j.1600-051X.2011.01843.x.

47. Turner L, Shamseer L, Altman DG, Weeks L, Peters J, Kober T, et al. Consolidated standards of reporting trials (CONSORT) and the completeness of reporting of randomised controlled trials (RCTs) published in medical journals. Cochrane Database Syst Rev. 2012;11:MR000030. https://doi.org/10.1002/14651858.MR000030.pub2.

48. Faggion CM Jr. Guidelines for reporting preclinical in vitro studies on dental materials. J Evid Based Dent Pract. 2012;12(4):182–9. https://doi.org/10.1016/j.jebdp.2012.10.001.

49. Krithikadatta J, Gopikrishna V, Datta M. CRIS Guidelines (Checklist for Reporting In-vitro Studies): a concept note on the need for standardized guidelines for improving quality and transparency in reporting in-vitro studies in experimental dental research. J Conserv Dent. 2014;17(4):301–4. https://doi.org/10.4103/0972-0707.136338.

50. Nagendrababu V, Murray PE, Ordinola-Zapata R, Peters OA, Rocas IN, Siqueira JF Jr, et al. PRILE 2021 guidelines for reporting laboratory studies in Endodontology: a consensus-based development. Int Endod J. 2021;54(9):1482–90. https://doi.org/10.1111/iej.13542.

51. Langland OE, Langlasis R, Preece JW. Principles of dental imaging, In: Goucher J, editor, 2nd ed. Lippincott Williams & Wilkins; 2002.

52. Cotti E, Vargiu P, Dettori C, Mallarini G. Computerized tomography in the management and follow-up of extensive periapical lesion. Endod Dent Traumatol. 1999;15(4):186–9. Retrieved from https://www.ncbi.nlm.nih.gov/pubmed/10815569.

53. Patel S, Dawood A, Whaites E, Pitt Ford T. New dimensions in endodontic imaging: part 1. Conventional and alternative radiographic systems. Int Endod J. 2009;42(6):447–62. https://doi.org/10.1111/j.1365-2591.2008.01530.x.

54. Benavides E, Rios HF, Ganz SD, An CH, Resnik R, Reardon GT, et al. Use of cone beam computed tomography in implant dentistry: the International Congress of Oral Implantologists consensus report. Implant Dent. 2012;21(2):78–86. https://doi.org/10.1097/ID.0b013e31824885b5.

55. Harris D, Horner K, Grondahl K, Jacobs R, Helmrot E, Benic GI, et al. E.A.O. guidelines for the use of diagnostic imaging in implant dentistry 2011. A consensus workshop organized by the European Association for Osseointegration at the Medical University of Warsaw. Clin Oral Implants Res. 2012;23(11):1243–53. https://doi.org/10.1111/j.1600-0501.2012.02441.x.

56. Rios HF, Borgnakke WS, Benavides E. The use of cone-beam computed tomography in management of patients requiring dental implants: an american academy of periodontology best evidence review. J Periodontol. 2017;88(10):946–59. https://doi.org/10.1902/jop.2017.160548.

57. Tyndall DA, Price JB, Tetradis S, Ganz SD, Hildebolt C, Scarfe WC, et al. Position statement of the American Academy of Oral and Maxillofacial Radiology on selection criteria for the use of radiology in dental implantology with emphasis on

cone beam computed tomography. Oral Surg Oral Med Oral Pathol Oral Radiol. 2012;113(6):817–26. https://doi.org/10.1016/j.oooo.2012.03.005.

58. Al-Rawi B, Hassan B, Vandenberge B, Jacobs R. Accuracy assessment of three-dimensional surface reconstructions of teeth from cone beam computed tomography scans. J Oral Rehabil. 2010;37(5):352–8. https://doi.org/10.1111/j.1365-2842.2010.02065.x.

59. Spin-Neto R, Gotfredsen E, Wenzel A. Impact of voxel size variation on CBCT-based diagnostic outcome in dentistry: a systematic review. J Digit Imaging. 2013;26(4):813–20. https://doi.org/10.1007/s10278-012-9562-7.

60. Freedman LS. Evaluating and comparing imaging techniques: a review and classification of study designs. Br J Radiol. 1987;60(719):1071–81. https://doi.org/10.1259/0007-1285-60-719-1071.

61. Guyatt GH, Tugwell PX, Feeny DH, Haynes RB, Drummond M. A framework for clinical evaluation of diagnostic technologies. CMAJ. 1986;134(6):587–94. Retrieved from https://www.ncbi.nlm.nih.gov/pubmed/3512062.

62. Hunink MG. Outcomes research and cost-effectiveness analysis in radiology. Eur J Radiol. 1998;27(2):85–7. Retrieved from https://www.ncbi.nlm.nih.gov/pubmed/9639132.

63. van der Schouw YT, Verbeek AL, Ruijs SH. Guidelines for the assessment of new diagnostic tests. Invest Radiol. 1995;30(6):334–40. Retrieved from https://www.ncbi.nlm.nih.gov/pubmed/7490184.

64. Hunink MG, Krestin GP. Study design for concurrent development, assessment, and implementation of new diagnostic imaging technology. Radiology. 2002;222(3):604–14. https://doi.org/10.1148/radiol.2223010335.

65. Ferrante di Ruffano L, Dinnes J, Taylor-Phillips S, Davenport C, Hyde C, Deeks JJ. Research waste in diagnostic trials: a methods review evaluating the reporting of test-treatment interventions. BMC Med Res Methodol. 2017;17(1):32. https://doi.org/10.1186/s12874-016-0286-0.

66. Hot A, Bossuyt PM, Gerke O, Wahl S, Vach W, Zapf A. Randomized test-treatment studies with an outlook on adaptive designs. BMC Med Res Methodol. 2021;21(1):110. https://doi.org/10.1186/s12874-021-01293-y.

67. Begg CB. Biases in the assessment of diagnostic tests. Stat Med. 1987;6(4):411–23. Retrieved from https://www.ncbi.nlm.nih.gov/pubmed/3114858.

68. Begg CB, McNeil BJ. Assessment of radiologic tests: control of bias and other design considerations. Radiology. 1988;167(2):565–9. https://doi.org/10.1148/radiology.167.2.3357976.

69. SEDENTEXCT. Radiation protection: cone beam CT for dental and maxillofacial radiology (Evidence Based Guidelines). 2012.

70. The 2007 Recommendations of the International Commission on Radiological Protection. ICRP publication 103. Ann ICRP. 2007;37(2–4):1–332. https://doi.org/10.1016/j.icrp.2007.10.003.

71. de Las Heras Gala H, Torresin A, Dasu A, Rampado O, Delis H, Hernández Girón I, Theodorakou C, Andersson J, Holroyd J, Nilsson M, Edyvean S, Gershan V, Hadid-Beurrier L, Hoog C, Delpon G, Sancho Kolster I, Peterlin P, Garayoa Roca J, Caprile P, Zervides C. Quality control in cone-bem computed tomography (CBCT). In: E-E-I. protocol, editor. 2017.

72. de Las Heras Gala H, Torresin A, Dasu A, Rampado O, Delis H, Hernandez Giron I, et al. Quality control in cone-beam computed tomography (CBCT) EFOMP-ESTRO-IAEA protocol (summary report). Phys Med. 2017;39:67–72. https://doi.org/10.1016/j.ejmp.2017.05.069.

73. Grobe A, Semmusch J, Schollchen M, Hanken H, Hahn M, Eichhorn W, et al. Accuracy of bone measurements in the vicinity of titanium implants in CBCT data sets: a comparison of radiological and histological findings in minipigs. Biomed Res Int. 2017;2017:3848207. https://doi.org/10.1155/2017/3848207.

74. Min S, Kim T, Kim O, Goncalo C, Utsunomiya T, Matsumoto T, et al. Functionalized scaffold and barrier membrane with anti-BMP-2 monoclonal antibodies for alveolar ridge preservation in a canine model. Biomed Res Int. 2020;2020:6153724. https://doi.org/10.1155/2020/6153724.

75. Omran M, Min S, Abdelhamid A, Liu Y, Zadeh HH. Alveolar ridge dimensional changes following ridge preservation procedure: part-2 - CBCT 3D analysis in non-human primate model. Clin Oral Implants Res. 2016;27(7):859–66. https://doi.org/10.1111/clr.12701.

76. Ritter L, Elger MC, Rothamel D, Fienitz T, Zinser M, Schwarz F, Zoller JE. Accuracy of peri-implant bone evaluation using cone beam CT, digital intra-oral radiographs and histology. Dentomaxillofac Radiol. 2014;43(6):20130088. https://doi.org/10.1259/dmfr.20130088.

77. Stimmelmayr M, Denk K, Erdelt K, Krennmair G, Mansour S, Beuer F, Guth JF. Accuracy and reproducibility of four cone beam computed tomography devices using 3D implant-planning software. Int J Comput Dent. 2017;20(1):21–34. Retrieved from https://www.ncbi.nlm.nih.gov/pubmed/28294203.

78. Faria PE, Okamoto R, Bonilha-Neto RM, Xavier SP, Santos AC, Salata LA. Immunohistochemical, tomographic and histological study on onlay iliac grafts remodeling. Clin Oral Implants Res. 2008;19(4):393–401. https://doi.org/10.1111/j.1600-0501.2007.01485.x.

79. Min S, Liu Y, Tang J, Xie Y, Xiong J, You HK, Zadeh HH. Alveolar ridge dimensional changes following

ridge preservation procedure with novel devices: part 1--CBCT linear analysis in non-human primate model. Clin Oral Implants Res. 2016;27(1):97–105. https://doi.org/10.1111/clr.12521.

80. Sbordone C, Sbordone L, Toti P, Martuscelli R, Califano L, Guidetti F. Volume changes of grafted autogenous bone in sinus augmentation procedure. J Oral Maxillofac Surg. 2011;69(6):1633–41. https://doi.org/10.1016/j.joms.2010.12.004.

81. Uchida Y, Goto M, Katsuki T, Soejima Y. Measurement of maxillary sinus volume using computerized tomographic images. Int J Oral Maxillofac Implants. 1998;13(6):811–8. Retrieved from https://www.ncbi.nlm.nih.gov/pubmed/9857592.

82. Deluiz D, Oliveira LS, Fletcher P, Pires FR, Tinoco JM, Tinoco EM. Histologic and tomographic findings of bone block allografts in a 4 years follow-up: a case series. Braz Dent J. 2016;27(6):775–80. https://doi.org/10.1590/0103-6440201601100.

83. Shi JY, Li Y, Zhuang LF, Zhang X, Fan LF, Lai HC. Accuracy assessment of a novel semiautomatic method evaluating bone grafts around the dental implant: an in vitro and ex vivo study. Sci Rep. 2020;10(1):14902. https://doi.org/10.1038/s41598-020-71651-1.

84. Xie Y, Su Y, Min S, Tang J, Goh BT, Saigo L, et al. Collagen sponge functionalized with chimeric anti-BMP-2 monoclonal antibody mediates repair of critical-size mandibular continuity defects in a nonhuman primate model. Biomed Res Int. 2017;2017:8094152. https://doi.org/10.1155/2017/8094152.

85. Pauwels R, Jacobs R, Singer SR, Mupparapu M. CBCT-based bone quality assessment: are Hounsfield units applicable? Dentomaxillofac Radiol. 2015;44(1):20140238. https://doi.org/10.1259/dmfr.20140238.

86. de Oliveira MA, Asahi DA, Silveira CA, Lima LA, Glick M, Gallottini M. The effects of zoledronic acid and dexamethasone on osseointegration of endosseous implants: histological and histomorphometrical evaluation in rats. Clin Oral Implants Res. 2015;26(4):e17–21. https://doi.org/10.1111/clr.12335.

87. Vercruyssen M, van de Wiele G, Teughels W, Naert I, Jacobs R, Quirynen M. Implant- and patient-centred outcomes of guided surgery, a 1-year follow-up: an RCT comparing guided surgery with conventional implant placement. J Clin Periodontol. 2014;41(12):1154–60. https://doi.org/10.1111/jcpe.12305.

88. Vercruyssen M, Cox C, Naert I, Jacobs R, Teughels W, Quirynen M. Accuracy and patient-centered outcome variables in guided implant surgery: a RCT comparing immediate with delayed loading. Clin Oral Implants Res. 2016;27(4):427–32. https://doi.org/10.1111/clr.12583.

89. Li Q, Bi M, Yang K, Liu W. The creation of a virtual dental patient with dynamic occlusion and its application in esthetic dentistry. J Prosthet Dent. 2021;126(1):14–8. https://doi.org/10.1016/j.prosdent.2020.08.026.

90. Benic GI, Sancho-Puchades M, Jung RE, Deyhle H, Hammerle CH. In vitro assessment of artifacts induced by titanium dental implants in cone beam computed tomography. Clin Oral Implants Res. 2013;24(4):378–83. https://doi.org/10.1111/clr.12048.

91. Bohner LOL, Tortamano P, Marotti J. Accuracy of linear measurements around dental implants by means of cone beam computed tomography with different exposure parameters. Dentomaxillofac Radiol. 2017;46(5):20160377. https://doi.org/10.1259/dmfr.20160377.

92. Schulze R, Heil U, Gross D, Bruellmann DD, Dranischnikow E, Schwanecke U, Schoemer E. Artefacts in CBCT: a review. Dentomaxillofac Radiol. 2011;40(5):265–73. https://doi.org/10.1259/dmfr/30642039.

93. Baan F, Bruggink R, Nijsink J, Maal TJJ, Ongkosuwito EM. Fusion of intra-oral scans in cone-beam computed tomography scans. Clin Oral Investig. 2021;25(1):77–85. https://doi.org/10.1007/s00784-020-03336-y.

94. Hammerle CH, Cordaro L, van Assche N, Benic GI, Bornstein M, Gamper F, et al. Digital technologies to support planning, treatment, and fabrication processes and outcome assessments in implant dentistry. Summary and consensus statements. The 4th EAO consensus conference 2015. Clin Oral Implants Res. 2015;26(Suppl 11):97–101. https://doi.org/10.1111/clr.12648.

95. Denissen H, Dozic A, van der Zel J, van Waas M. Marginal fit and short-term clinical performance of porcelain-veneered CICERO, CEREC, and Procera onlays. J Prosthet Dent. 2000;84(5):506–13. https://doi.org/10.1067/mpr.2000.110258.

96. Jemt T, Lie A. Accuracy of implant-supported prostheses in the edentulous jaw: analysis of precision of fit between cast gold-alloy frameworks and master casts by means of a three-dimensional photogrammetric technique. Clin Oral Implants Res. 1995;6(3):172–80. Retrieved from https://www.ncbi.nlm.nih.gov/pubmed/7578793.

97. van der Zel JM, Vlaar S, de Ruiter WJ, Davidson C. The CICERO system for CAD/CAM fabrication of full-ceramic crowns. J Prosthet Dent. 2001;85(3):261–7. https://doi.org/10.1067/mpr.2001.114399.

98. Gomes RS, Souza CMC, Bergamo ETP, Bordin D, Del Bel Cury AA. Misfit and fracture load of implant-supported monolithic crowns in zirconia-reinforced lithium silicate. J Appl Oral Sci. 2017;25(3):282–9. https://doi.org/10.1590/1678-7757-2016-0233.

99. Kim TG, Kim S, Choi H, Lee JH, Kim JH, Moon HS. Clinical acceptability of the internal gap of CAD/CAM PD-AG crowns using intraoral digital impressions. Biomed Res Int. 2016;2016:7065454. https://doi.org/10.1155/2016/7065454.

100. Park JS, Lim YJ, Kim B, Kim MJ, Kwon HB. Clinical evaluation of time efficiency and fit accuracy of lithium disilicate single crowns between conventional and digital impression. Materials (Basel). 2020;13(23). https://doi.org/10.3390/ma13235467

101. Ramalho IS, Bergamo ETP, Witek L, Coelho PG, Lopes ACO, Bonfante EA. Implant-abutment fit influences the mechanical performance of single-crown prostheses. J Mech Behav Biomed Mater. 2020;102:103506. https://doi.org/10.1016/j.jmbbm.2019.103506.

102. Schlenz MA, Vogler J, Schmidt A, Rehmann P, Wostmann B. New intraoral scanner-based chairside measurement method to investigate the internal fit of crowns: a clinical trial. Int J Environ Res Public Health. 2020;17(7):2182. https://doi.org/10.3390/ijerph17072182.

103. Ender A, Mehl A. Full arch scans: conventional versus digital impressions--an in-vitro study. Int J Comput Dent. 2011;14(1):11–21. Retrieved from https://www.ncbi.nlm.nih.gov/pubmed/21657122.

104. ISO 5725-2: accuracy (trueness and precision) of measurement methods and results — Part 2: basic method for the determination of repeatability and reproducibility of a standard measurement method. Switzerland: ISO Copyright Office; 1994.

105. Amin S, Weber HP, Finkelman M, El Rafie K, Kudara Y, Papaspyridakos P. Digital vs. conventional full-arch implant impressions: a comparative study. Clin Oral Implants Res. 2017;28(11):1360–7. https://doi.org/10.1111/clr.12994.

106. Kim MK, Kim JM, Lee YM, Lim YJ, Lee SP. The effect of scanning distance on the accuracy of intra-oral scanners used in dentistry. Clin Anat. 2019;32(3):430–8. https://doi.org/10.1002/ca.23334.

107. Sim JY, Jang Y, Kim WC, Kim HY, Lee DH, Kim JH. Comparing the accuracy (trueness and precision) of models of fixed dental prostheses fabricated by digital and conventional workflows. J Prosthodont Res. 2019;63(1):25–30. https://doi.org/10.1016/j.jpor.2018.02.002.

108. Jokstad A. Accuracy of digital appliances for use in dentistry for dummies. Clin Exp Dent Res. 2017;3:43–4.

109. Fernandes MP, Pinto R, Almeida P, Marques D, Fernandes J, Figueiral M. Determinação da exatidão da aquisição de impressões dentárias com um scanner extraoral. Rev Port Estomatol Med Dent Cir Maxilofac. 2019;60. https://doi.org/10.24873/j.rpemd.2019.12.609.

110. Mendricky R. Determination of measurement accuracy of optical 3D scanners. MM Sci J. 2016;2016(06):1565–72. https://doi.org/10.17973/MMSJ.2016_12_2016183.

111. Guth JF, Edelhoff D, Schweiger J, Keul C. A new method for the evaluation of the accuracy of full-arch digital impressions in vitro. Clin Oral Investig. 2016;20(7):1487–94. https://doi.org/10.1007/s00784-015-1626-x.

112. Ender A, Mehl A. Accuracy of complete-arch dental impressions: a new method of measuring trueness and precision. J Prosthet Dent. 2013;109(2):121–8. https://doi.org/10.1016/S0022-3913(13)60028-1.

113. Rey-Joly Maura C, Godinho J, Amorim M, Pinto R, Marques D, Jardim L. Precision and trueness of maxillary crowded models produced by 2 vat photopolymerization 3-dimensional printing techniques. Am J Orthod Dentofacial Orthop. 2021;160(1):124–31. https://doi.org/10.1016/j.ajodo.2020.06.033.

114. Menditto A, Patriarca M, Magnusson B. Understanding the meaning of accuracy, trueness and precision. Accred Qual Assur. 2007;12:45. https://doi.org/10.1007/s00769-006-0191-z.

115. Ahlholm P, Sipila K, Vallittu P, Jakonen M, Kotiranta U. Digital versus conventional impressions in fixed prosthodontics: a review. J Prosthodont. 2018;27(1):35–41. https://doi.org/10.1111/jopr.12527.

116. Marques S, Ribeiro P, Falcao C, Lemos BF, Rios-Carrasco B, Rios-Santos JV, Herrero-Climent M. Digital impressions in implant dentistry: a literature review. Int J Environ Res Public Health. 2021;18(3). https://doi.org/10.3390/ijerph18031020.

117. Rutkunas V, Geciauskaite A, Jegelevicius D, Vaitiekunas M. Accuracy of digital implant impressions with intraoral scanners. A systematic review. Eur. J Oral Implantol. 2017;10 Suppl 1:101–20. Retrieved from https://www.ncbi.nlm.nih.gov/pubmed/28944372.

118. Zhang YJ, Shi JY, Qian SJ, Qiao SC, Lai HC. Accuracy of full-arch digital implant impressions taken using intraoral scanners and related variables: a systematic review. Int J Oral Implantol (Berl). 2021;14(2):157–79. Retrieved from https://www.ncbi.nlm.nih.gov/pubmed/34006079.

119. Bergin JM, Rubenstein JE, Mancl L, Brudvik JS, Raigrodski AJ. An in vitro comparison of photogrammetric and conventional complete-arch implant impression techniques. J Prosthet Dent. 2013;110(4):243–51. https://doi.org/10.1016/S0022-3913(13)60370-4.

120. Penarrocha-Diago M, Balaguer-Marti JC, Penarrocha-Oltra D, Balaguer-Martinez JF, Penarrocha-Diago M, Agustin-Panadero R. A combined digital and stereophotogrammetric technique for rehabilitation with immediate loading of complete-arch, implant-supported prostheses: a randomized controlled pilot clinical trial. J Prosthet Dent. 2017;118(5):596–603. https://doi.org/10.1016/j.prosdent.2016.12.015.

121. Lehmann KM, Kasaj A, Ross A, Kammerer PW, Wagner W, Scheller H. A new method for volumetric evaluation of gingival recessions: a feasibility

study. J Periodontol. 2012;83(1):50–4. https://doi.org/10.1902/jop.2011.110143.

122. Schneider D, Ender A, Truninger T, Leutert C, Sahrmann P, Roos M, Schmidlin P. Comparison between clinical and digital soft tissue measurements. J Esthet Restor Dent. 2014;26(3):191–9. https://doi.org/10.1111/jerd.12084.

123. Hartkamp O, Lohbauer U, Reich S. Antagonist wear by polished zirconia crowns. Int J Comput Dent. 2017;20(3):263–74. Retrieved from https://www.ncbi.nlm.nih.gov/pubmed/28852744.

124. Hartkamp O, Peters F, Bothung H, Lohbauer U, Reich S. Optical profilometry versus intraoral (handheld) scanning. Int J Comput Dent. 2017;20(2):165–76. Retrieved from https://www.ncbi.nlm.nih.gov/pubmed/28630957.

125. Ferreira JB, Christovam IO, Alencar DS, da Motta AFJ, Mattos CT, Cury-Saramago A. Accuracy and reproducibility of dental measurements on tomographic digital models: a systematic review and meta-analysis. Dentomaxillofac Radiol. 2017;46(7):20160455. https://doi.org/10.1259/dmfr.20160455.

126. Ahn HW, Chang YJ, Kim KA, Joo SH, Park YG, Park KH. Measurement of three-dimensional perioral soft tissue changes in dentoalveolar protrusion patients after orthodontic treatment using a structured light scanner. Angle Orthod. 2014;84(5):795–802. https://doi.org/10.2319/112913-877.1.

127. Agustin-Panadero R, Penarrocha-Oltra D, Gomar-Vercher S, Penarrocha-Diago M. Stereophotogrammetry for recording the position of multiple implants: technical description. Int J Prosthodont. 2015;28(6):631–6. https://doi.org/10.11607/ijp.4146.

128. Boldt J, Rottner K, Schmitter M, Hopfgartner A, Jakob P, Richter EJ, Tymofiyeva O. High-resolution MR imaging for dental impressions: a feasibility study. Clin Oral Investig. 2017. https://doi.org/10.1007/s00784-017-2204-1

129. Vollborn T, Habor D, Pekam FC, Heger S, Marotti J, Reich S, et al. Soft tissue-preserving computer-aided impression: a novel concept using ultrasonic 3D-scanning. Int J Comput Dent. 2014;17(4):277–96. Retrieved from https://www.ncbi.nlm.nih.gov/pubmed/25643460.

130. Wesemann C, Muallah J, Mah J, Bumann A. Accuracy and efficiency of full-arch digitalization and 3D printing: a comparison between desktop model scanners, an intraoral scanner, a CBCT model scan, and stereolithographic 3D printing. Quintessence Int. 2017;48(1):41–50. https://doi.org/10.3290/j.qi.a37130.

131. Flugge T, Derksen W, Te Poel J, Hassan B, Nelson K, Wismeijer D. Registration of cone beam computed tomography data and intraoral surface scans - a prerequisite for guided implant surgery with CAD/CAM drilling guides. Clin Oral Implants Res. 2017;28(9):1113–8. https://doi.org/10.1111/clr.12925.

132. Ritter L, Reiz SD, Rothamel D, Dreiseidler T, Karapetian V, Scheer M, Zoller JE. Registration accuracy of three-dimensional surface and cone beam computed tomography data for virtual implant planning. Clin Oral Implants Res. 2012;23(4):447–52. https://doi.org/10.1111/j.1600-0501.2011.02159.x.

133. Joda T, Gallucci GO. The virtual patient in dental medicine. Clin Oral Implants Res. 2015;26(6):725–6. https://doi.org/10.1111/clr.12379.

134. Vasak C, Strbac GD, Huber CD, Lettner S, Gahleitner A, Zechner W. Evaluation of three different validation procedures regarding the accuracy of template-guided implant placement: an in vitro study. Clin Implant Dent Relat Res. 2015;17(1):142–9. https://doi.org/10.1111/cid.12085.

135. Wang F, Wang Q, Zhang J. Role of dynamic navigation systems in enhancing the accuracy of implant placement: a systematic review and meta-analysis of clinical studies. J Oral Maxillofac Surg. 2021;79(10):2061–70. https://doi.org/10.1016/j.joms.2021.06.005.

136. Wei SM, Shi JY, Qiao SC, Zhang X, Lai HC, Zhang XM. Accuracy and primary stability of tapered or straight implants placed into fresh extraction socket using dynamic navigation: a randomized controlled clinical trial. Clin Oral Investig. 2022;26(3):2733–41. https://doi.org/10.1007/s00784-021-04247-2.

137. Hinckfuss S, Conrad HJ, Lin L, Lunos S, Seong WJ. Effect of surgical guide design and surgeon's experience on the accuracy of implant placement. J Oral Implantol. 2012;38(4):311–23. https://doi.org/10.1563/AAID-JOI-D-10-00046.

138. Cassetta M, Di Mambro A, Giansanti M, Stefanelli LV, Barbato E. How does an error in positioning the template affect the accuracy of implants inserted using a single fixed mucosa-supported stereolithographic surgical guide? Int J Oral Maxillofac Surg. 2014;43(1):85–92. https://doi.org/10.1016/j.ijom.2013.06.012.

139. Jorba-Garcia A, Gonzalez-Barnadas A, Camps-Font O, Figueiredo R, Valmaseda-Castellon E. Accuracy assessment of dynamic computer-aided implant placement: a systematic review and meta-analysis. Clin Oral Investig. 2021;25(5):2479–94. https://doi.org/10.1007/s00784-021-03833-8.

140. Rivara F, Lumetti S, Calciolari E, Toffoli A, Forlani G, Manfredi E. Photogrammetric method to measure the discrepancy between clinical and software-designed positions of implants. J Prosthet Dent. 2016;115(6):703–11. https://doi.org/10.1016/j.prosdent.2015.10.017.

141. Verhamme LM, Meijer GJ, Boumans T, Schutyser F, Berge SJ, Maal TJ. A clinically relevant validation method for implant placement after virtual planning. Clin Oral Implants Res. 2013;24(11):1265–72. https://doi.org/10.1111/j.1600-0501.2012.02565.x.

142. Vercruyssen M, Fortin T, Widmann G, Jacobs R, Quirynen M. Different techniques of static/dynamic guided implant surgery: modalities and indications.

Periodontol 2000. 2014;66(1):214–27. https://doi.org/10.1111/prd.12056.

143. Ambrosio F, Azimi K, Lopez-Torres A, Notice T, Khoshneviszadeh A, Neely A, Kinaia B. Custom allogeneic block graft for ridge augmentation: case series. Clin Adv Periodontics. 2021;13(2):94–101. https://doi.org/10.1002/cap.10183.

144. Blume O, Hoffmann L, Donkiewicz P, Wenisch S, Back M, Franke J, et al. Treatment of severely resorbed maxilla due to peri-implantitis by guided bone regeneration using a customized allogenic bone block: a case report. Materials (Basel). 2017;10(10):1213. https://doi.org/10.3390/ma10101213.

145. Jacotti M, Barausse C, Felice P. Posterior atrophic mandible rehabilitation with onlay allograft created with CAD-CAM procedure: a case report. Implant Dent. 2014;23(1):22–8. https://doi.org/10.1097/ID.0000000000000023.

146. Landsberg C, Moses O. Ridge augmentation using customized allogeneic bone block: a 3-year follow-up of two case reports. Int J Periodontics Restorative Dent. 2020;40(6):881–9. https://doi.org/10.11607/prd.3354.

147. Ryu JI, Yang BE, Yi SM, Choi HG, On SW, Hong SJ, et al. Bone regeneration of a 3D-printed alloplastic and particulate xenogenic graft with rhBMP-2. Int J Mol Sci. 2021;22(22):12518. https://doi.org/10.3390/ijms222212518.

148. Tamimi F, Torres J, Al-Abedalla K, Lopez-Cabarcos E, Alkhraisat MH, Bassett DC, et al. Osseointegration of dental implants in 3D-printed synthetic onlay grafts customized according to bone metabolic activity in recipient site. Biomaterials. 2014;35(21):5436–45. https://doi.org/10.1016/j.biomaterials.2014.03.050.

149. Neumeister A, Schulz L, Glodecki C. Investigations on the accuracy of 3D-printed drill guides for dental implantology. Int J Comput Dent. 2017;20(1):35–51. Retrieved from https://www.ncbi.nlm.nih.gov/pubmed/28294204.

150. Matta RE, Bergauer B, Adler W, Wichmann M, Nickenig HJ. The impact of the fabrication method on the three-dimensional accuracy of an implant surgery template. J Craniomaxillofac Surg. 2017;45(6):804–8. https://doi.org/10.1016/j.jcms.2017.02.015.

151. Buser D, Bornstein MM, Weber HP, Grutter L, Schmid B, Belser UC. Early implant placement with simultaneous guided bone regeneration following single-tooth extraction in the esthetic zone: a cross-sectional, retrospective study in 45 subjects with a 2- to 4-year follow-up. J Periodontol. 2008;79(9):1773–81. https://doi.org/10.1902/jop.2008.080071.

152. Buser D, Halbritter S, Hart C, Bornstein MM, Grutter L, Chappuis V, Belser UC. Early implant placement with simultaneous guided bone regeneration following single-tooth extraction in the esthetic zone: 12-month results of a prospective study with 20 consecutive patients. J Periodontol. 2009;80(1):152–62. https://doi.org/10.1902/jop.2009.080360.

153. Van Assche N, Vercruyssen M, Coucke W, Teughels W, Jacobs R, Quirynen M. Accuracy of computer-aided implant placement. Clin Oral Implants Res. 2012;23(Suppl 6):112–23. https://doi.org/10.1111/j.1600-0501.2012.02552.x.

154. Van de Velde T, Glor F, De Bruyn H. A model study on flapless implant placement by clinicians with a different experience level in implant surgery. Clin Oral Implants Res. 2008;19(1):66–72. https://doi.org/10.1111/j.1600-0501.2007.01423.x.

155. Abdelhay N, Prasad S, Gibson MP. Failure rates associated with guided versus non-guided dental implant placement: a systematic review and meta-analysis. BDJ Open. 2021;7(1):31. https://doi.org/10.1038/s41405-021-00086-1.

156. Cristache CM, Burlibasa M, Tudor I, Totu EE, Di Francesco F, Moraru L. Accuracy, labor-time and patient-reported outcomes with partially versus fully digital workflow for flapless guided dental implants insertion-a randomized clinical trial with one-year follow-up. J Clin Med. 2021;10(5):1102. https://doi.org/10.3390/jcm10051102.

157. Gargallo-Albiol J, Barootchi S, Marques-Guasch J, Wang HL. Fully guided versus half-guided and freehand implant placement: systematic review and meta-analysis. Int J Oral Maxillofac Implants. 2020;35(6):1159–69. https://doi.org/10.11607/jomi.7942.

158. Matsumura A, Nakano T, Ono S, Kaminaka A, Yatani H, Kabata D. Multivariate analysis of causal factors influencing accuracy of guided implant surgery for partial edentulism: a retrospective clinical study. Int J Implant Dent. 2021;7(1):28. https://doi.org/10.1186/s40729-021-00313-2.

159. Nickenig HJ, Wichmann M, Hamel J, Schlegel KA, Eitner S. Evaluation of the difference in accuracy between implant placement by virtual planning data and surgical guide templates versus the conventional free-hand method - a combined in vivo - in vitro technique using cone-beam CT (Part II). J Craniomaxillofac Surg. 2010;38(7):488–93. https://doi.org/10.1016/j.jcms.2009.10.023.

160. Pellegrino G, Ferri A, Del Fabbro M, Prati C, Gandolfi MG, Marchetti C. Dynamic navigation in implant dentistry: a systematic review and meta-analysis. Int J Oral Maxillofac Implants. 2021;36(5):e121–40. https://doi.org/10.11607/jomi.8770.

161. Wang ZY, Chao JR, Zheng JW, You M, Liu Y, Shen JF. The influence of crown coverage on the accuracy of static guided implant surgery in partially edentulous models: an in vitro study. J Dent. 2021;115:103882. https://doi.org/10.1016/j.jdent.2021.103882.

162. Raico Gallardo YN, da Silva-Olivio IRT, Mukai E, Morimoto S, Sesma N, Cordaro L. Accuracy comparison of guided surgery for dental implants according to the tissue of support: a systematic review and meta-analysis. Clin Oral Implants

Res. 2017;28(5):602–12. https://doi.org/10.1111/clr.12841.

163. Widmann G, Fischer B, Berggren JP, Dennhardt A, Schullian P, Reto B, Puelacher W. Cone beam computed tomography vs multislice computed tomography in computer-aided design/computer-assisted manufacture guided implant surgery based on three-dimensional optical scanning and stereolithographic guides: does image modality matter? Int J Oral Maxillofac Implants. 2016;31(3):527–33. https://doi.org/10.11607/jomi.4222.

164. Block MS, Emery RW, Cullum DR, Sheikh A. Implant placement is more accurate using dynamic navigation. J Oral Maxillofac Surg. 2017;75(7):1377–86. https://doi.org/10.1016/j.joms.2017.02.026.

165. Cunha RM, Souza FA, Hadad H, Poli PP, Maiorana C, Carvalho PSP. Accuracy evaluation of computer-guided implant surgery associated with prototyped surgical guides. J Prosthet Dent. 2021;125(2):266–72. https://doi.org/10.1016/j.prosdent.2019.07.010.

166. Zhou W, Liu Z, Song L, Kuo C-L, Shafer DM. Clinical factors affecting the accuracy of guided implant surgery—a systematic review and meta-analysis. J Evid Based Dental Pract. 2017. https://doi.org/10.1016/j.jebdp.2017.07.007.

167. Guentsch A, Sukhtankar L, An H, Luepke PG. Precision and trueness of implant placement with and without static surgical guides: an in vitro study. J Prosthet Dent. 2021;126(3):398–404. https://doi.org/10.1016/j.prosdent.2020.06.015.

168. Kuhl S, Payer M, Zitzmann NU, Lambrecht JT, Filippi A. Technical accuracy of printed surgical templates for guided implant surgery with the coDiagnostiX software. Clin Implant Dent Relat Res. 2015;17(Suppl 1):e177–82. https://doi.org/10.1111/cid.12152.

169. Marei HF, Abdel-Hady A, Al-Khalifa K, Al-Mahalawy H. Influence of surgeon experience on the accuracy of implant placement via a partially computer-guided surgical protocol. Int J Oral Maxillofac Implants. 2019;34(5):1177–83. https://doi.org/10.11607/jomi.7480.

170. Vermeulen J. The accuracy of implant placement by experienced surgeons: guided vs freehand approach in a simulated plastic model. Int J Oral Maxillofac Implants. 2017;32(3):617–24. https://doi.org/10.11607/jomi.5065.

171. Behneke A, Burwinkel M, Behneke N. Factors influencing transfer accuracy of cone beam CT-derived template-based implant placement. Clin Oral Implants Res. 2012;23(4):416–23. https://doi.org/10.1111/j.1600-0501.2011.02337.x.

172. Noharet R, Pettersson A, Bourgeois D. Accuracy of implant placement in the posterior maxilla as related to 2 types of surgical guides: a pilot study in the human cadaver. J Prosthet Dent. 2014;112(3):526–32. https://doi.org/10.1016/j.prosdent.2013.12.013.

173. Beretta M, Poli PP, Maiorana C. Accuracy of computer-aided template-guided oral implant placement: a prospective clinical study. J Periodontal Implant Sci. 2014;44(4):184–93. https://doi.org/10.5051/jpis.2014.44.4.184.

174. El Kholy K, Lazarin R, Janner SFM, Faerber K, Buser R, Buser D. Influence of surgical guide support and implant site location on accuracy of static Computer-Assisted Implant Surgery. Clin Oral Implants Res. 2019;30(11):1067–75. https://doi.org/10.1111/clr.13520.

175. Geng W, Liu C, Su Y, Li J, Zhou Y. Accuracy of different types of computer-aided design/computer-aided manufacturing surgical guides for dental implant placement. Int J Clin Exp Med. 2015;8(6):8442–9. Retrieved from https://www.ncbi.nlm.nih.gov/pubmed/26309497.

176. Nickenig HJ, Eitner S. An alternative method to match planned and achieved positions of implants, after virtual planning using cone-beam CT data and surgical guide templates--a method reducing patient radiation exposure (part I). J Craniomaxillofac Surg. 2010;38(6):436–40. https://doi.org/10.1016/j.jcms.2009.10.025.

177. Song YW, Kim J, Kim JH, Park JM, Jung UW, Cha JK. Accuracy of dental implant placement by a novel in-house model-free and zero-setup fully guided surgical template made of a light-cured composite resin (VARO Guide((R))): a comparative in vitro study. Materials (Basel). 2021;14(14):4023. https://doi.org/10.3390/ma14144023.

178. Pettersson A, Komiyama A, Hultin M, Nasstrom K, Klinge B. Accuracy of virtually planned and template guided implant surgery on edentate patients. Clin Implant Dent Relat Res. 2012;14(4):527–37. https://doi.org/10.1111/j.1708-8208.2010.00285.x.

179. Joda T, Bragger U. Time-efficiency analysis of the treatment with monolithic implant crowns in a digital workflow: a randomized controlled trial. Clin Oral Implants Res. 2016;27(11):1401–6. https://doi.org/10.1111/clr.12753.

180. Joda T, Ferrari M, Gallucci GO, Wittneben JG, Bragger U. Digital technology in fixed implant prosthodontics. Periodontol 2000. 2017;73(1):178–92. https://doi.org/10.1111/prd.12164.

181. Kapos T, Evans C. CAD/CAM technology for implant abutments, crowns, and superstructures. Int J Oral Maxillofac Implants. 2014;29(Suppl):117–36. https://doi.org/10.11607/jomi.2014suppl.g2.3.

182. Joda T, Bragger U. Complete digital workflow for the production of implant-supported single-unit monolithic crowns. Clin Oral Implants Res. 2014;25(11):1304–6. https://doi.org/10.1111/clr.12270.

183. van Noort R. The future of dental devices is digital. Dent Mater. 2012;28(1):3–12. https://doi.org/10.1016/j.dental.2011.10.014.

184. Kim Y, Oh TJ, Misch CE, Wang HL. Occlusal considerations in implant therapy: clinical guide-

lines with biomechanical rationale. Clin Oral Implants Res. 2005;16(1):26–35. https://doi.org/10.1111/j.1600-0501.2004.01067.x.

185. Abduo J, Lyons K, Bennani V, Waddell N, Swain M. Fit of screw-retained fixed implant frameworks fabricated by different methods: a systematic review. Int J Prosthodont. 2011;24(3):207–20. Retrieved from https://www.ncbi.nlm.nih.gov/pubmed/21519567.

186. Heckmann SM, Karl M, Wichmann MG, Winter W, Graef F, Taylor TD. Cement fixation and screw retention: parameters of passive fit. An in vitro study of three-unit implant-supported fixed partial dentures. Clin Oral Implants Res. 2004;15(4):466–73. https://doi.org/10.1111/j.1600-0501.2004.01027.x.

187. Millington ND, Leung T. Inaccurate fit of implant superstructures. Part 1: stresses generated on the superstructure relative to the size of fit discrepancy. Int J Prosthodont. 1995;8(6):511–6. Retrieved from https://www.ncbi.nlm.nih.gov/pubmed/8595110.

188. Att W, Komine F, Gerds T, Strub JR. Marginal adaptation of three different zirconium dioxide three-unit fixed dental prostheses. J Prosthet Dent. 2009;101(4):239–47. https://doi.org/10.1016/S0022-3913(09)60047-0.

189. Beuer F, Aggstaller H, Edelhoff D, Gernet W, Sorensen J. Marginal and internal fits of fixed dental prostheses zirconia retainers. Dent Mater. 2009;25(1):94–102. https://doi.org/10.1016/j.dental.2008.04.018.

190. Bragger U, Karoussis I, Persson R, Pjetursson B, Salvi G, Lang N. Technical and biological complications/failures with single crowns and fixed partial dentures on implants: a 10-year prospective cohort study. Clin Oral Implants Res. 2005;16(3):326–34. https://doi.org/10.1111/j.1600-0501.2005.01105.x.

191. Katsoulis J, Mericske-Stern R, Rotkina L, Zbaren C, Enkling N, Blatz MB. Precision of fit of implant-supported screw-retained 10-unit computer-aided-designed and computer-aided-manufactured frameworks made from zirconium dioxide and titanium: an in vitro study. Clin Oral Implants Res. 2014;25(2):165–74. https://doi.org/10.1111/clr.12039.

192. Kunii J, Hotta Y, Tamaki Y, Ozawa A, Kobayashi Y, Fujishima A, et al. Effect of sintering on the marginal and internal fit of CAD/CAM-fabricated zirconia frameworks. Dent Mater J. 2007;26(6):820–6. Retrieved from https://www.ncbi.nlm.nih.gov/pubmed/18203487.

193. McLean JW, von Fraunhofer JA. The estimation of cement film thickness by an in vivo technique. Br Dent J. 1971;131(3):107–11. Retrieved from https://www.ncbi.nlm.nih.gov/pubmed/5283545.

194. Carames J, Marques D, Malta Barbosa J, Moreira A, Crispim P, Chen A. Full-arch implant-supported rehabilitations: a prospective study comparing porcelain-veneered zirconia frameworks to monolithic zirconia. Clin Oral Implants Res. 2019;30(1):68–78. https://doi.org/10.1111/clr.13393.

195. Carames J, Tovar Suinaga L, Yu YC, Perez A, Kang M. Clinical advantages and limitations of monolithic zirconia restorations full arch implant supported reconstruction: case series. Int J Dent. 2015;2015:392496. https://doi.org/10.1155/2015/392496.

196. Kim JH, Lee SJ, Park JS, Ryu JJ. Fracture load of monolithic CAD/CAM lithium disilicate ceramic crowns and veneered zirconia crowns as a posterior implant restoration. Implant Dent. 2013;22(1):66–70. https://doi.org/10.1097/ID.0b013e318278a576.

197. Mendez Carames JM, Pereira S, da Mata AD, da Silva Marques DN, de Oliveira Francisco HC. Ceramic-veneered zirconia frameworks in full-arch implant rehabilitations: a 6-month to 5-year retrospective cohort study. Int J Oral Maxillofac Implants. 2016;31(6):1407–14. https://doi.org/10.11607/jomi.4675.

198. Masri R, Kempler J, Driscoll CF. Digital design and manufacture of implant abutments. In: Clinical applications of digital dental technology. Wiley; 2015. p. 167–76.

199. Abduo J, Lyons K, Bennamoun M. Trends in computer-aided manufacturing in prosthodontics: a review of the available streams. Int J Dent. 2014;2014:783948. https://doi.org/10.1155/2014/783948.

200. Kikuchi M, Okuno O. Machinability evaluation of titanium alloys. Dent Mater J. 2004;23(1):37–45. Retrieved from https://www.ncbi.nlm.nih.gov/pubmed/15164923

201. Koch GK, Gallucci GO, Lee SJ. Accuracy in the digital workflow: from data acquisition to the digitally milled cast. J Prosthet Dent. 2016;115(6):749–54. https://doi.org/10.1016/j.prosdent.2015.12.004.

202. Papadiochou S, Pissiotis AL. Marginal adaptation and CAD-CAM technology: a systematic review of restorative material and fabrication techniques. J Prosthet Dent. 2017;119(4):545–51. https://doi.org/10.1016/j.prosdent.2017.07.001.

203. Whicher DM, Miller JE, Dunham KM, Joffe S. Gatekeepers for pragmatic clinical trials. Clin Trials. 2015;12(5):442–8. https://doi.org/10.1177/1740774515597699.

204. Califf RM, Sugarman J. Exploring the ethical and regulatory issues in pragmatic clinical trials. Clin Trials. 2015;12(5):436–41. https://doi.org/10.1177/1740774515598334.

205. Siqueira R, Galli M, Chen Z, Mendonca G, Meirelles L, Wang HL, Chan HL. Intraoral scanning reduces procedure time and improves patient comfort in fixed prosthodontics and implant dentistry: a systematic review. Clin Oral Investig. 2021;25(12):6517–31. https://doi.org/10.1007/s00784-021-04157-3.

206. Williams HC, Burden-Teh E, Nunn AJ. What is a pragmatic clinical trial? J Invest Dermatol. 2015;135(6):1–3. https://doi.org/10.1038/jid.2015.134.

207. Chuang SK, Tian L, Wei LJ, Dodson TB. Kaplan-Meier analysis of dental implant survival: a strategy for estimating survival with clustered observations. J Dent Res. 2001;80(11):2016–20. https://doi.org/10.1177/00220345010800111301.

208. Collett D. Sample size determination in survival analysis. In: Encyclopedia of biostatistics. Wiley; 2005.

209. Hannigan A, Lynch CD. Statistical methodology in oral and dental research: pitfalls and recommendations. J Dent. 2013;41(5):385–92. https://doi.org/10.1016/j.jdent.2013.02.013.

210. Ahlers MO, Bernhardt O, Jakstat HA, Kordass B, Turp JC, Schindler HJ, Hugger A. Motion analysis of the mandible: guidelines for standardized analysis of computer-assisted recording of condylar movements. Int J Comput Dent. 2015;18(3):201–23. Retrieved from https://www.ncbi.nlm.nih.gov/pubmed/26389133.

211. Hugger A, Hugger S, Ahlers MO, Schindler HJ, Türp JC, Kordass B. Movement function of the mandible: a concept for structuring criteria for analysis and for standardizing computer-assisted recordings. J Craniomand Funct. 2013;5:41–53.

212. Amezua X, Iturrate M, Garikano X, Solaberrieta E. Analysis of the impact of the facial scanning method on the precision of a virtual facebow record technique: an in vivo study. J Prosthet Dent. 2021. https://doi.org/10.1016/j.prosdent.2021.10.025

213. Bapelle M, Dubromez J, Savoldelli C, Tillier Y, Ehrmann E. Modjaw(R) device: analysis of mandibular kinematics recorded for a group of asymptomatic subjects. Cranio. 2021:1–7. https://doi.org/10.1080/08869634.2021.2000790.

214. Kois JC, Kois DE, Zeitler JM, Martin J. Digital to analog facially generated interchangeable facebow transfer: capturing a standardized reference position. J Prosthodont. 2021;31(S1):13–22. https://doi.org/10.1111/jopr.13437.

215. Li J, Att W, Chen Z, Lepidi L, Wang HL, Joda T. Prosthetic articulator-based implant rehabilitation virtual patient: a technique bridging implant surgery and reconstructive dentistry. J Prosthet Dent. 2021. https://doi.org/10.1016/j.prosdent.2021.09.013

216. Manazza F, La Rocca S, Nagni M, Chirico L, Cattoni F. A simplified digital workflow for the prosthetic finishing of implant rehabilitations: a case report. J Biol Regul Homeost Agents. 2021;35(4 Suppl. 1):87–97. https://doi.org/10.23812/21-4supp1-8.

217. Park JH, Lee GH, Moon DN, Kim JC, Park M, Lee KM. A digital approach to the evaluation of mandibular position by using a virtual articulator. J Prosthet Dent. 2021;125(6):849–53. https://doi.org/10.1016/j.prosdent.2020.04.002.

218. Yang S, Feng N, Li D, Wu Y, Yue L, Yuan Q. A novel technique to align the intraoral scans to the virtual articulator and set the patient-specific sagittal condylar inclination. J Prosthodont. 2021;31(1):79–84. https://doi.org/10.1111/jopr.13403.

219. Amezua X, Iturrate M, Garikano X, Solaberrieta E. Analysis of the influence of the facial scanning method on the transfer accuracy of a maxillary digital scan to a 3D face scan for a virtual facebow technique: an in vitro study. J Prosthet Dent. 2021. https://doi.org/10.1016/j.prosdent.2021.02.007

220. Kordass B, Behrendt C, Ruge S. Computerized occlusal analysis - innovative approaches for a practice-oriented procedure. Int J Comput Dent. 2020;23(4):363–75. Retrieved from https://www.ncbi.nlm.nih.gov/pubmed/33491932.

221. Petre A, Drafta S, Stefanescu C, Oancea L. Virtual facebow technique using standardized background images. J Prosthet Dent. 2019;121(5):724–8. https://doi.org/10.1016/j.prosdent.2018.07.008.

222. Solaberrieta E, Garmendia A, Minguez R, Brizuela A, Pradies G. Virtual facebow technique. J Prosthet Dent. 2015;114(6):751–5. https://doi.org/10.1016/j.prosdent.2015.06.012.

223. Solaberrieta E, Minguez R, Barrenetxea L, Etxaniz O. Direct transfer of the position of digitized casts to a virtual articulator. J Prosthet Dent. 2013;109(6):411–4. https://doi.org/10.1016/S0022-3913(13)60330-3.

224. Solaberrieta E, Otegi JR, Minguez R, Etxaniz O. Improved digital transfer of the maxillary cast to a virtual articulator. J Prosthet Dent. 2014;112(4):921–4. https://doi.org/10.1016/j.prosdent.2014.03.021.

225. Ury E, Fornai C, Weber GW. Accuracy of transferring analog dental casts to a virtual articulator. J Prosthet Dent. 2020;123(2):305–13. https://doi.org/10.1016/j.prosdent.2018.12.019.

226. Lepidi L, Galli M, Mastrangelo F, Venezia P, Joda T, Wang HL, Li J. Virtual articulators and virtual mounting procedures: where do we stand? J Prosthodont. 2021;30(1):24–35. https://doi.org/10.1111/jopr.13240.

227. Fraile C, Ferreiroa A, Romeo M, Alonso R, Pradies G. Clinical study comparing the accuracy of interocclusal records, digitally obtained by three different devices. Clin Oral Investig. 2021. https://doi.org/10.1007/s00784-021-04174-2.

228. Fraile C, Ferreiroa A, Solaberrieta E, Pradies G. Intraoral versus extraoral digital occlusal records: a pilot study. Int J Comput Dent. 2018;21(4):329–33. Retrieved from https://www.ncbi.nlm.nih.gov/pubmed/30539175.

229. Goob J, Erdelt K, Schweiger J, Pho Duc JM, Schubert O, Guth JF. Reproducibility of a magnet-based jaw motion analysis system. Int J Comput Dent. 2020;23(1):39–48. Retrieved from https://www.ncbi.nlm.nih.gov/pubmed/32207460.

230. Conejo J, Dayo AF, Syed AZ, Mupparapu M. The digital clone: intraoral scanning, face scans and cone beam computed tomography integration for diagnosis and treatment planning. Dent Clin North Am. 2021;65(3):529–53. https://doi.org/10.1016/j.cden.2021.02.011.

231. Hong SJ, Noh K. Setting the sagittal condylar inclination on a virtual articulator by using a facial

and intraoral scan of the protrusive interocclusal position: a dental technique. J Prosthet Dent. 2021;125(3):392–5. https://doi.org/10.1016/j.prosdent.2020.01.031.

232. Joda T, Bragger U, Gallucci G. Systematic literature review of digital three-dimensional superimposition techniques to create virtual dental patients. Int J Oral Maxillofac Implants. 2015;30(2):330–7. https://doi.org/10.11607/jomi.3852.

233. Mangano C, Luongo F, Migliario M, Mortellaro C, Mangano FG. Combining intraoral scans, cone beam computed tomography and face scans: the virtual patient. J Craniofac Surg. 2018;29(8):2241–6. https://doi.org/10.1097/SCS.0000000000004485.

234. Eldridge SM, Lancaster GA, Campbell MJ, Thabane L, Hopewell S, Coleman CL, Bond CM. Defining feasibility and pilot studies in preparation for randomised controlled trials: development of a conceptual framework. PLoS One. 2016;11(3):e0150205. https://doi.org/10.1371/journal.pone.0150205.

235. Pozzi A, Polizzi G, Moy PK. Guided surgery with tooth-supported templates for single missing teeth: a critical review. Eur J Oral Implantol. 2016;9(Suppl 1):S135–53. Retrieved from https://www.ncbi.nlm.nih.gov/pubmed/27314119.

236. Bover-Ramos F, Vina-Almunia J, Cervera-Ballester J, Penarrocha-Diago M, Garcia-Mira B. Accuracy of implant placement with computer-guided surgery: a systematic review and meta-analysis comparing cadaver, clinical, and in vitro studies. Int J Oral Maxillofac Implants. 2017. https://doi.org/10.11607/jomi.5556

237. Afrashtehfar KI. Conventional free-hand, dynamic navigation and static guided implant surgery produce similar short-term patient-reported outcome measures and experiences. Evid Based Dent. 2021;22(4):143–5. https://doi.org/10.1038/s41432-021-0216-9.

238. Joda T, Derksen W, Wittneben JG, Kuehl S. Static computer-aided implant surgery (s-CAIS) analysing patient-reported outcome measures (PROMs), economics and surgical complications: a systematic review. Clin Oral Implants Res. 2018;29(Suppl 16):359–73. https://doi.org/10.1111/clr.13136.

239. Baig MR. Accuracy of impressions of multiple implants in the edentulous arch: a systematic review. Int J Oral Maxillofac Implants. 2014;29(4):869–80. https://doi.org/10.11607/jomi.3233.

240. Kim JH, Kim KR, Kim S. Critical appraisal of implant impression accuracies: a systematic review. J Prosthet Dent. 2015;114(2):185–92. e181. https://doi.org/10.1016/j.prosdent.2015.02.005.

241. Papaspyridakos P, Chen CJ, Gallucci GO, Doukoudakis A, Weber HP, Chronopoulos V. Accuracy of implant impressions for partially and completely edentulous patients: a systematic review. Int J Oral Maxillofac Implants. 2014;29(4):836–45. https://doi.org/10.11607/jomi.3625.

242. Hussein MO. Photogrammetry technology in implant dentistry: a systematic review. J Prosthet Dent. 2021. https://doi.org/10.1016/j.prosdent.2021.09.015.

243. Ma B, Yue X, Sun Y, Peng L, Geng W. Accuracy of photogrammetry, intraoral scanning, and conventional impression techniques for complete-arch implant rehabilitation: an in vitro comparative study. BMC Oral Health. 2021;21(1):636. https://doi.org/10.1186/s12903-021-02005-0.

244. Revilla-Leon M, Att W, Ozcan M, Rubenstein J. Comparison of conventional, photogrammetry, and intraoral scanning accuracy of complete-arch implant impression procedures evaluated with a coordinate measuring machine. J Prosthet Dent. 2021;125(3):470–8. https://doi.org/10.1016/j.prosdent.2020.03.005.

245. Revilla-Leon M, Rubenstein J, Methani MM, Piedra-Cascon W, Ozcan M, Att W. Trueness and precision of complete-arch photogrammetry implant scanning assessed with a coordinate-measuring machine. J Prosthet Dent. 2021. https://doi.org/10.1016/j.prosdent.2021.05.019.

246. Papaspyridakos P, Gallucci GO, Chen CJ, Hanssen S, Naert I, Vandenberghe B. Digital versus conventional implant impressions for edentulous patients: accuracy outcomes. Clin Oral Implants Res. 2016;27(4):465–72. https://doi.org/10.1111/clr.12567.

247. Bishti S, Tuna T, Rittich A, Wolfart S. Patient-reported outcome measures (PROMs) of implant-supported reconstructions using digital workflows: a systematic review and meta-analysis. Clin Oral Implants Res. 2021;32(Suppl 21):318–35. https://doi.org/10.1111/clr.13846.

248. Delize V, Bouhy A, Lambert F, Lamy M. Intrasubject comparison of digital vs. conventional workflow for screw-retained single-implant crowns: prosthodontic and patient-centered outcomes. Clin Oral Implants Res. 2019;30(9):892–902. https://doi.org/10.1111/clr.13494.

249. Joda T, Bragger U. Time-efficiency analysis comparing digital and conventional workflows for implant crowns: a prospective clinical crossover trial. Int J Oral Maxillofac Implants. 2015;30(5):1047–53. https://doi.org/10.11607/jomi.3963.

250. Joda T, Bragger U. Patient-centered outcomes comparing digital and conventional implant impression procedures: a randomized crossover trial. Clin Oral Implants Res. 2016;27(12):e185–9. https://doi.org/10.1111/clr.12600.

251. Joda T, Ferrari M, Bragger U, Zitzmann NU. Patient Reported Outcome Measures (PROMs) of posterior single-implant crowns using digital workflows: a randomized controlled trial with a three-year follow-up. Clin Oral Implants Res. 2018;29(9):954–61. https://doi.org/10.1111/clr.13360.

252. Kunavisarut C, Jarangkul W, Pornprasertsuk-Damrongsri S, Joda T. Patient-reported outcome measures (PROMs) comparing digital and con-

ventional workflows for treatment with posterior single-unit implant restorations: a randomized controlled trial. J Dent. 2021;117:103875. https://doi.org/10.1016/j.jdent.2021.103875.

253. Mello CC, Lemos CAA, de Luna Gomes JM, Verri FR, Pellizzer EP. CAD/CAM vs conventional technique for fabrication of implant-supported frameworks: a systematic review and meta-analysis of in vitro studies. Int J Prosthodont. 2019;32(2):182–92. https://doi.org/10.11607/ijp.5616.

254. Patzelt SB, Spies BC, Kohal RJ. CAD/CAM-fabricated implant-supported restorations: a systematic review. Clin Oral Implants Res. 2015;26(Suppl 11):77–85. https://doi.org/10.1111/clr.12633.

255. Spies BC, Pieralli S, Vach K, Kohal RJ. CAD/CAM-fabricated ceramic implant-supported single crowns made from lithium disilicate: final results of a 5-year prospective cohort study. Clin Implant Dent Relat Res. 2017;19(5):876–83. https://doi.org/10.1111/cid.12508.

Insight into the Statistical Procedure

21

Leticia Grize

Bright ideas are those brought efficiently to reality and translated into benefits. These ideas often start with assumptions which are developed as hypotheses, and in turn, evaluated and tested. The evaluation of ideas requires the collection of data and its use for inference testing.

Statistics, a branch of applied mathematics, ensures the appropriate collection, description, and analysis of data. It warrants an inference of the posed hypotheses and the right interpretation of the obtained results. The terms biostatistics, industrial statistics, federal statistics, and others refer to statistics as a science applied to specific fields.

Data are usually collected at the sample level and sometimes at the population level. A population is the entire set of items or individuals for which or decisions are to be made. A sample is a representative subset of a population. Since rarely a population is used as a whole, inferences or testing of hypotheses are performed when using information from a sample. The sample should contain enough study individuals or items to assure hypothesis testing with a certain statistical power.

The hypothesis of the investigation describes what is to be proven is true or not. Therefore, there are always two mutually exclusive statements. The first one is the baseline hypothesis or null hypothesis which is usually of the form 'there is no difference' or 'there is no association'. The opposite is the alternative hypothesis of the form 'there is a difference' or 'there is an association'. A measure for or against a hypothesis is provided by a P value (probability).

The proper statement of a hypothesis is very important, it should be expressed first in words and then in statistical terms.

Data are facts and figures collected in the process of an investigation and can be quantitative or qualitative. Quantitative data arise from measurements (how much or how many) and qualitative data, strictly speaking, from the classification of narrative information.

Data collection is organized and recorded in terms called variables, variables are of the following nature:

Categorical
- Ordinal which indicates an order in the categorization of its values (e.g., always, sometimes, never).
– Nominal if the categorization of its values cannot be ordered (e.g., gender: female, male).
– Numerical.

L. Grize (✉)
Swiss Tropical and Public Health Institute, Basel, Switzerland

University of Basel, Basel, Switzerland
e-mail: leticia.grize@swisstph.ch; leticia.grize@unibas.ch

– Continuous if there is an infinite number of collected values or measurements.
– Discrete if it is countable, values are integers or whole numbers.

21.1 Statistical Analysis

The analysis should start with the visualization of the data. This can be achieved by summarizing the data in tables or graphs. Categorical variables can be summarized as counts and proportions or percentages and numerical values by calculating parameters such as means, standard deviations, median, and ranges. These parameters are usually set in tables for easy examination. There are many graph types with which one can easily visualize the obtained information. Histograms or bar plots are used to present the frequencies or percentages of categorical variables, box plots show the distribution of continuous variables, scatter plots show the association between two continuous variables, and so on.

Data visualization helps to determine if the data values are feasible or were caused by errors in data entry. Outliers are values which seem to be out of the feasible range, usually solitary points in the visualization graphs. The cause of an outlier should be investigated because not all outliers are errors or non-feasible values, such outliers can be or not influencers in the analysis results.

After controlling the data values, the following step is to calculate descriptive statistics which characterize and describe the sample used for the investigation. This allows the comparison to samples for which information already exists in published form or for other investigators to confirm the findings of the present investigation.

Obviously, the next step would be to confirm inferences and perform comparisons. There are many statistical techniques or methods, but those used depend on the type of the collected data and the hypothesis to be tested.

The last step is the presentation and interpretation of the results. The report of the results should include the used sample size, the obtained size of the effect (usually reported as difference, ratio, risk, or other), a measure of deviation (standard deviation, standard error, or a confidence interval), and/or a P value. Scientists and experts knowledgeable in the matter in conjunction with the statistician or person who performed the analysis should interpret the results.

The following lists terms which should be in mind when planning an investigation (a study):

Study types:
Observational studies—the conditions of interest are observed in the sample or population (there is no treatment or intervention). Usually, there are comparisons performed among groups with certain characteristics.
• Cross-sectional studies—information is collected at only one time.
• Longitudinal studies—information is collected at different points in time.
• Case-control studies—Individuals with a certain outcome or disease and an appropriate group of appropriate and matched controls are selected and then compared.
Experimental studies—a treatment is given or an intervention performed on a part of the sample and its effect compared to the untreated part of that sample.
  – Randomized control trials—individuals in the sample are allocated to treatment/intervention or no treatment (placebo)/control randomly.
  – Crossover design studies—control trials in which each individual in the sample is exposed to two treatments or therapies. Individuals are randomized first to treatment and in a second step to the other treatment.
  – Cohort studies—data are obtained from groups exposed/not exposed to a technology or factor of interest. No allocation of the exposure is made by the researcher, but data or information is already given (e.g., patient records or databases).

21.2   Sample Size Determination

Sample size refers to the number of observations or experimental units necessary to be included in a study to assure inference testing with a certain statistical power. There are three factors required to determine the sample size: the effect size, the wished statistical power to detect the difference, and the level of significance [1].

- Effect size is the difference in measurement (size and deviation) or difference in proportions between the comparison groups.
- Statistical power is the likelihood/probability that a study will yield a statistically significant effect (the ability to detect a difference).
- The level of significance or the alpha level is the probability of making the wrong decision with the null hypothesis. The most used value is alpha level of 0.05 (5% probability), but other values could be used (an alpha level of 0.001 could be used in cases of detrimental effects or a level of 0.10 when the effects are not of much importance).

Some measures of central tendency and dispersion [2]

- Mean is the simple average of all the data (sum of all values divided by the number of values).
- Standard deviation is a measure of the average difference between the mean and each data value. It indicates how dispersed the data are.
- Standard error is the uncertainty of the sample mean.
- Median is the middle value when the values are arranged in ascending order of size.
- Percentiles are points which divide the distribution of the data into sets of percentages above or below a certain value (the median and quartiles are examples of percentiles, respectively, the 50%, 25%, and 75%iles).
- Interquartile range is the range of values that includes the 50% of values bounded by the lower (25%) and upper (75%) quartiles.

- Range is the difference between the smallest and largest value usually expressed as minimum and maximum.
- Confidence intervals are a range of values that is likely to include the estimate (mean, ratio, risk) with a certain degree of confidence [3]. A 95% confidence interval mean that 95 out of 100 times, the created interval will include the population parameter.

21.3   Probability Distributions

Every variable has a unique corresponding distribution. To draw precise conclusions about a population based on a sample taken from that population it is necessary to understand the probability distribution corresponding to the population [4]. Of all the distribution types, three are mostly used in biomedical and health science research:

- Binomial distribution is the discrete probability distribution of the number of successes in a sequence of a determinate number of independent experiments.
- Poisson distribution is the discrete distribution when the number of events which occur over a period of time, area, volume, or space is small in a large sample.
- Normal distribution is the most used distribution of continuous random variables. The graph of a normal distribution is a symmetric bell-shaped curve centered at its mean with a certain dispersion.

Which statistical tests to use to test inferences (described in a simplistic manner)

- One sample *t*-test: used to test whether a sample mean, from a normally distributed variable, differs from a hypothesized value.
- One sample median test (signed test or signed rank test): used to test if a sample median differs significantly from a hypothesized value. This is a non-parametric test and is used when

sample sizes are small or the distribution of the variable is non-normal [5].

– One sample binomial test allows to test if the proportion of successes on a two-level categorical variable differs from the hypothesized value.

– The Chi-square goodness of fit test allows to test whether the observed proportions for a categorical variable differ from hypothesized proportions.

– Two independent samples *t*-test: is used to compare means of normally distributed dependent variables for two independent groups.

– Mann-Whitney *U*-test, a non-parametric test analog to the independent samples *t*-test, is used when the distribution cannot be assumed to be normal.

– Chi-square test: is used to examine the relationship between two categorical variables, this compares the proportions of a characteristic in different groups. This test assumed that the counts in the different levels are 5 or more. If the counts for any level is less than five, the test to use is the Fisher exact test.

– One-way ANOVA: is used when the means of a measured, dependent variable, is to be compared among different groups (a categorical independent variable).

– Kruskal Wallis test: is the non-parametric version of the one-way ANOVA.

– Paired *t*-test: is used when two observations are made in the same subject and it is wished to know if the means of the two normally distributed variables differ from one another.

– Wilcoxon signed rank sum test; is the non-parametric version of a paired *t*-test.

– McNemar's test: used to compare binary outcomes on dependent samples (paired or matched).

– Correlation and regression are used to investigate the association between two variables. Pearson correlation and regression analysis are used when the variables are continuous and the Spearman correlation and logistic regression when the variables are categorical.

– Regression analysis examines or evaluates the association between outcome or dependent

variables and predictors or independent variables [6]. The associations between dependent and independent variables in regression analysis are expressed in equations or models.

A simple linear regression allows to look at the linear relationship between one predictor and a normally distributed outcome.

A simple logistic regression assumes that the outcome is binary (two-category variable) and a predictor or independent variable (Hosmer and [7]).

Multiple regression, linear or logistic, is similar to simple linear logistic regressions, but there more than one predictor variable is involved.

Mixed regression models are used when in addition to the predictors are of fixed (the usual independent variables) or random character (e.g., the effect of the individuals in the sample). These are used when there is more than one measurement per individual but there are not repeated. Repeated measurements should be declared as such.

– Kaplan-Meier method and Cox regressions are used to evaluate the survival or probabilities of an event in time. The Kaplan-Meier allows visualization of the probability with time and Cox-regressions provide a measure of the risk of non-survival or the occurrence of an event [8].

There are many other statistical techniques such as those to evaluate agreement between measurement methods, those to perform quality control, multivariate multiple regressions for cases when there would be two or more dependent variables, and many others which were not cited.

The statistical tests described above, if not referenced are described in Kim and Daily [4].

21.4 The Role of a Statistician

It is only advantageous when a statistician is part of the investigation team. A statistician has the mathematical and statistical knowledge and the

ability to use appropriate computing facilities to support scientists who carry out an investigation. The statistician must be willing to acquire the required knowledge for a full understanding of the study matter and to communicate with other members of the team in clear and understandable terms.

The scientists or clinical experts should make sure that the statistician understands the purpose of the study and gets to know the basics of the 'science' involved to help with the design and hypothesis statement. They should also provide the statistician with the numbers (own assumptions or based on published literature) necessary to calculate sample sizes. It is the responsibility of a statistician to provide an analysis plan describing the techniques to be used in data quality assurance, description of the characteristics of experimental units, and inference testing. Nevertheless, the analysis plan should be written in partnership with the scientists and should be included in the study protocol [9].

In a few words, the statistician should participate in all stages of a project, from the design and study protocol development, through measurement, data control, and statistical analysis to interpretation of results and statement of the study conclusions [10]. A study well planned assures its success.

References

1. Borenstein M, et al. Power and precision. Engelwood: Biostat; 2001. ISBN 0–9709662–0-2.
2. Peacock JL, Peacock PJ. Oxford handbook of medical statistics. Oxford: Oxford University Press; 2011.
3. Altman DG, et al. Statistics with confidence: confidence intervals and statistical guidelines. 2nd ed. Bristol: BMJ Books; 2000.
4. Kim JS, Dailey RJ. Biostatistics for oral healthcare. 1st ed. Berlin: Blackwell Munksgaard; 2008.
5. Hollander M, Wolfe DA. Nonparametric statistical methods. 2nd ed. New York: Wiley; 1999.
6. Armitage P, et al. Statistical methods in medical research. 4th ed. Oxford: Blackwell Science; 2002.
7. Hosmer DW, Lemeshow S. Applied logistic regression. New York: Wiley; 1989.
8. Keinbaum DG, Klein M. Survival analysis: a self-learning text. 3rd ed. New York: Springer; 2012.
9. Adams-Huet B, Ahn C. Bridging clinical investigators and statisticians: writing the statistical methodology for a research proposal. J Invest Med. 2009;57(8):818–24.
10. Dobson AJ. The role of the statistician. Int J Epidemiol. 1983;12(3):274–5.